UCLA
UCLA Electronic Theses and Dissertations

Title
Development of Nickel-Catalyzed Cross-Coupling Reactions

Permalink
https://escholarship.org/uc/item/9zg7z83s

Author
Hie, Liana

Publication Date
2016

Peer reviewed|Thesis/dissertation

eScholarship.org Powered by the California Digital Library
University of California

UNIVERSITY OF CALIFORNIA

Los Angeles

Development of Nickel-Catalyzed Cross-Coupling Reactions

A dissertation submitted in partial satisfaction of the

requirements for the degree Doctor of Philosophy

in Chemistry

by

Liana Hie

2016

© Copyright by

Liana Hie

2016

ABSTRACT OF THE DISSERTATION

Development of Nickel-Catalyzed Cross-Coupling Reactions

by

Liana Hie

Doctor of Philosophy in Chemistry

University of California, Los Angeles, 2016

Professor Neil Kamal Garg, Chair

Transition metal-catalyzed cross-couplings provide a powerful means to assemble carbon–carbon (C–C) and carbon–heteroatom (C–X) bonds. Although Pd catalysis is most commonly used in these transformations, Ni catalysis offers a valuable alternative due to the low cost and high reactivity of Ni. More importantly, Ni catalysis has proven effective for the activation of traditionally inert carbon–heteroatom bonds and therefore provides exciting opportunities with regard to chemical reactivity and synthetic applications.

Chapter one, two, and three describe the development of practical cross-coupling methodologies. Chapter one explains the amination of aryl sulfamates and carbamates that relies on an air-stable Ni(II) precatalyst. Chapter two introduces the development of green cross-couplings of phenolic derivatives and aryl halides to form biaryls. Subsequently, the couplings of heterocycles, which are commonly encountered in natural product synthesis and in the

pharmaceutical sector, are described. Chapter three describes the development of green cross-couplings of aryl sulfamates and chlorides to form aryl amines.

Chapter four and seven concern the utility of amides as electrophilic cross-coupling partners. These traditionally unreactive moieties are activated by nickel and coupled to alcohols to form acyl C–O bonds. This study suggests that amides may serve as useful building blocks to construct carbon–carbon and carbon–heteroatom bonds. Chapter four describes the development of nickel-catalyzed activation of benzamides and chapter seven introduces the development of nickel-catalyzed activation of aliphatic amide derivatives.

Chapter five describes the nickel-catalyzed activation of the acyl carbon–oxygen bonds of methyl esters through an oxidative addition process. The oxidative addition adducts, formed using nickel catalysis, undergo in situ trapping to provide anilide products. DFT calculations are used to support the proposed reaction mechanism, understand why decarbonylation does not occur competitively, and to elucidate the beneficial role of the substrate structure and $Al(O\textit{t}Bu)_3$ additive on the kinetics and thermodynamics of the reaction.

Chapter six focus on the nickel-catalyzed Heck cyclization for the construction of quaternary stereocenters. This transformation is demonstrated in the synthesis of 3,3-disubstituted oxindoles, which are prevalent motifs seen in bioactive molecules.

The dissertation of Liana Hie is approved.

Kendall N. Houk

Robert Michael van Dam

Neil Kamal Garg, Committee Chair

University of California, Los Angeles

2016

For Hie Nita, Liauw Iwan, Lufiliyana, Selvie Oktovia, and Joyce Pham.

"Family isn't always blood. It's the people in your life who want you in theirs. The ones you accept you for who you are. The ones who would do anything to see you smile, and who love you no matter what."

TABLE OF CONTENTS

Abstract ii

Committee Page iv

Dedication Page v

Table of Contents vi

List of Figures xiv

List of Tables xxxiv

List of Abbreviations xxxvii

Acknowledgements xl

Biographical Sketch xlv

CHAPTER ONE: Nickel-Catalyzed Amination of Aryl Sulfamates and Carbamates Using an Air-Stable Precatalyst……...…...……..1

1.1 Abstract 1

1.2 Introduction 1

1.3 Optimization of Amination Conditions 2

1.4 Substrate Scope 4

1.5 Amination with Various Electrophiles 7

1.6 Conclusion 7

1.7 Experimental Section 8

1.7.1 Materials and Methods 8

1.7.2 Experimental Procedures 8

1.7.2.1 Synthesis of Aryl Sulfamate and Carbamate Substrates 9

1.7.2.2 Amination of Aryl Sulfamates and Carbamates 9

Appendix One: Spectra Relevant to Chapter One 25

1.8 Notes and References.....48

CHAPTER TWO: Nickel-Catalyzed Suzuki–Miyaura Couplings in Green Solvents……..53

2.1 Abstract 53

2.2 Introduction.....53

2.3 Optimization of Conditions.....54

2.4 Substrate Scope 56

2.5 Heterocycle–Heterocycle Couplings 59

2.6 Gram Scale Couplings 61

2.7 Conclusion 61

2.8 Experimental Section 62

2.8.1 Materials and Methods.....62

2.8.2 Experimental Procedures 63

2.8.2.1. Synthesis of Aryl Carbamate, Sulfamate, and Mesylate Substrates 63

2.8.2.2. Screening of Green Solvents.....65

2.8.2.3. Screening of Arylboron-Based Nucleophiles 70

2.8.2.4. Cross-coupling Reactions of Aryl Halides 75

2.8.2.5. Cross-coupling Reactions of Aryl Carbamates, Sulfamates, and Mesylates 78

2.8.2.6. Heterocycle-Heterocycle Cross-Couplings of Aryl Halides…….81

2.8.2.7. Heterocycle-Heterocycle Cross-Couplings of Aryl Carbamates, Sulfamates, and Mesylates 84
2.8.2.8. Isolation Experiments 88
2.8.2.9. Cross-coupling Reactions Utilizing Microwave Heating 90
Appendix Two: Spectra Relevant to Chapter Two 91
2.9 Notes and References 127

CHAPTER THREE: Nickel-Catalyzed Amination of Aryl Chlorides and Sulfamates in 2-Me-THF 134
3.1 Abstract 134
3.2 Introduction 134
3.3 Optimization and Substrate Scope 135
3.4 Gram-Scale Couplings 142
3.5 Conclusion 143
3.6 Experimental Section 144
3.6.1 Materials and Methods 144
3.6.2 Experimental Procedures 145
3.6.2.1 Syntheses of Aryl Pseudohalide Substrates 145
3.6.2.2 Solvent Optimization and Scope of Electrophile 145
3.6.2.3 Aminations of Aryl Sulfamates and Chlorides 146
3.6.2.4 Isolation Experiments 155
Appendix Three: Spectra Relevant to Chapter Three 159
3.7 Notes and References 181

CHAPTER FOUR: Conversion of Amides to Esters by the Nickel-Catalyzed Activation of Amide C–N Bonds 187
4.1 Abstract 187
4.2 Introduction 188
4.3 Optimization and Substrate Scope 191
4.4 Computational Study 196
4.5 Selective Amide Bond Activation 199
4.6 Conclusion 200
4.7 Experimental Section 201
4.7.1 Materials and Methods 201
4.7.2 Experimental Procedures 203
4.7.2.1 Syntheses of Amide Substrates 203
4.7.2.2 Methanolysis Control Experiments 208
4.7.2.3 Screening of Amide Substrates 209
4.7.2.4 Comparison of Ligands and Relevant Control Experiments 210
4.7.2.5 Scope of Methodology 212
4.7.2.6 Selective Cleavage of Tertiary over Secondary Amide 223
4.7.2.7 Selective Cleavage of Aryl Amide Over Alkyl Amide 225
4.7.2.8 Selective Cleavage of Aryl Amide in the Presence of an Ester 229
4.7.3 Verification of Enantiopurity 232
4.7.3.1 Racemic Compound Syntheses 232
4.7.3.2 Chiral SFC Assays 234
4.7.4 Computational Methods 240

4.7.4.1 Complete Reference of Gaussian 09.....240

4.7.4.2 Transition State Structures for Decarbonylation Pathway.....241

4.7.4.3 Comparison of Acyl C–N and Aryl C–N Bond Activation Pathway 241

4.7.4.4 Analysis of Amides Derived from Alkyl Carboxylic Acids.....242

4.7.4.5 Analysis of *N*-Me,Boc Amide Esterification.....243

4.7.4.6 Free Energy and Enthalpy of Amide and Ester Formation.....245

4.7.4.7 Energies, Enthalpies, and Free Energy of the Calculated Structures. …… ……....248

4.7.4.8 Cartesian Coordinates for the Optimized Structures……..…249

Appendix Four: Spectra Relevant to Chapter Four.....251

4.8 Notes and References.....303

CHAPTER FIVE: Nickel-Catalyzed Activation of Acyl C–O Bonds of Methyl Ester.....308

5.1 Abstract 308

5.2 Introduction.....308

5.3 Optimization and Substrate Scope.....310

5.4 Computational Studies on Decarbonylation Pathways.....313

5.5 Effects of Additives on the Nickel-Catalyzed Amidation …….316

5.6 Effects of Distortion on the Thermodynamics.....317

5.7 Sequential Site-Selective C–N Bond Forming Processes……..318

5.8 Conclusion ……...…….....320

5.9 Experimental Section ……320

5.9.1 Materials and Methods……..…….320

5.9.2 Experimental Procedures……..…….321

5.9.2.1 Syntheses of Starting Materials……...321

5.9.2.2 Scope of Methodology ……...….325

5.9.2.3 Sequential Site-Selective C–N Bond Forming Processes ……..…….....333

5.9.2.4 Gram Scale Coupling……...…..…..337

5.9.3 Computational Method……..……..……..……..….338

5.9.3.1 Complete Reference of Gaussian 09……..……..338

5.9.3.2 Computed Catalytic Cycle…….……..……339

5.9.3.3 Transition States for Decarbonylation Pathways…...……...…339

5.9.3.4 Effects of Additive on Ester Complexation……..……...…340

5.9.3.5 Dihedral Angles and Bond Lengths of Selected Esters and Amides……..…….……..….342

5.9.3.6 Dihedral Angles and Bond Lengths of Selected Esters and Amides with Additive…….……...…..….343

5.9.3.7 Energies and Cartesian Coordinates of the Structures ……343

Appendix Five: Spectra Relevant to chapter Five…….……..….344

5.10 Notes and References ……...…….……...….388

CHAPTER SIX: Construction of Quaternary Stereocenters via Nickel-Catalyzed Heck Cyclizations.....393

6.1 Abstract.....393

6.2 Introduction.....393

6.3 Optimization and Substrate Scope.....395

6.4 Conclusion.....404

6.5 Experimental Section.....404

6.5.1. Materials and Methods.....404

6.5.2. Experimental Procedure.....406

6.5.2.1. Synthesis of Starting Materials (General Procedure A).....406

6.5.2.2. Synthesis of Starting Materials (General Procedure B).....411

6.5.2.3. Synthesis of Starting Materials (Miscellaneous).....416

6.5.2.4. Nickel-Catalyzed Heck Cyclization for the Synthesis of Spirooxindoles.....418

6.5.2.5. Enantioselective Nickel-Catalyzed Heck Cyclization.....426

6.5.2.6. Robustness Screening.....427

6.5.2.7. Glove-box Free Procedure.....428

Appendix Six: Spectra Relevant to Chapter Six.....429

6.6 Notes and References.....472

CHAPTER SEVEN: Nickel-Catalyzed Esterification of Aliphatic Amides …….....476

7.1 Abstract 476

7.2 Introduction 476

7.3 Optimization and Substrate Scope 478

7.4 Conclusion 483

7.5. Experimental Section 483

7.5.1. Materials and Methods ……....……..…483

7.5.2. Experimental Procedure ……....……..485

7.5.2.1. Synthesis of Starting Materials …….....485

7.5.2.2. Reaction Discovery ……..…….....497

7.5.2.3. Survey of Amide Substrates ……..……...…….499

7.5.2.4. Optimization or Reaction Conditions and Relevant Control Experiments ……..……...……..500

7.5.2.5. Scope of Methodology …...……..……...….…….501

Appendix Seven: Spectra Relevant to Chapter Seven. .....…513

7.6 Notes and References.....…571

LIST OF FIGURES

CHAPTER ONE

Figure 1.1. Amination of aryl carbamates and sulfamates using Ni(II) precatalyst 2

Figure 1.2. Amination of aryl sulfamates and carbamates using morpholine 5

Figure 1.3. Amination of various amines.....6

APPENDIX ONE

Figure A1.1 ^{1}H NMR (500 MHz, $CDCl_3$) of compound **1.5** 26

Figure A1.2 ^{1}H NMR (500 MHz, $CDCl_3$) of compound **1.6** 27

Figure A1.3 ^{1}H NMR (500 MHz, $CDCl_3$) of compound **1.7** 28

Figure A1.4 ^{1}H NMR (500 MHz, $CDCl_3$) of compound **1.8** 29

Figure A1.5 ^{1}H NMR (500 MHz, $CDCl_3$) of compound **1.9** 30

Figure A1.6 ^{1}H NMR (500 MHz, $CDCl_3$) of compound **1.10** 31

Figure A1.7 ^{1}H NMR (500 MHz, $CDCl_3$) of compound **1.11** 32

Figure A1.8 ^{1}H NMR (500 MHz, $CDCl_3$) of compound **1.12** 33

Figure A1.9 ^{1}H NMR (500 MHz, $CDCl_3$) of compound **1.13** 34

Figure A1.10 ^{1}H NMR (500 MHz, $CDCl_3$) of compound **1.14** 35

Figure A1.11 ^{1}H NMR (300 MHz, $CDCl_3$) of compound **1.15** 36

Figure A1.12 ^{1}H NMR (500 MHz, $CDCl_3$) of compound **1.16** 37

Figure A1.13 ^{1}H NMR (600 MHz, $CDCl_3$) of compound **1.17** 38

Figure A1.14 ^{1}H NMR (600 MHz, $CDCl_3$) of compound **1.18** 39

Figure A1.15 ^{1}H NMR (300 MHz, C_6D_6) of compound **1.4** 40

Figure A1.16 ^{1}H NMR (500 MHz, $CDCl_3$) of compound **1.19** 41

Figure A1.17 ^{1}H NMR (500 MHz, $CDCl_3$) of compound **1.20** 42

Figure A1.18 ^{1}H NMR (600 MHz, $CDCl_3$) of compound **1.21** 43

Figure A1.19 ^{1}H NMR (600 MHz, $CDCl_3$) of compound **1.22** 44

Figure A1.20 ^{1}H NMR (300 MHz, $CDCl_3$) of compound **1.23** 45

Figure A1.21 ^{1}H NMR (600 MHz, $CDCl_3$) of compound **1.24** 46

Figure A1.22 ^{1}H NMR (500 MHz, $CDCl_3$) of compound **1.25** 47

CHAPTER TWO

Figure 2.1. Suzuki–Miyaura cross-coupling of aryl halides and phenol derivatives in green solvents.....54

Figure 2.2. Coupling of Heterocyclic Halides with Aryl Boronic Acids.....57

Figure 2.3. Coupling of Heterocyclic Phenolic Derivatives with Aryl Boronic Acids 58

Figure 2.4. Coupling of Heterocyclic Substrates with Heterocyclic Aryl Boronic Acids 60

Figure 2.5. Gram Scale Couplings 61

APPENDIX TWO

Figure A2.1 ^{1}H NMR (300 MHz, $CDCl_3$) of compound **2.3** 92

Figure A2.2 ^{1}H NMR (300 MHz, $CDCl_3$) of compound **2.4** 93

Figure A2.3 ^{1}H NMR (300 MHz, $CDCl_3$) of compound **2.5** 94

Figure A2.4 ^{1}H NMR (400 MHz, DMSO-d_6) of compound **2.6** 95

Figure A2.5 ^{1}H NMR (500 MHz, $CDCl_3$) of compound **2.7** 96

Figure A2.6 ^{1}H NMR (300 MHz, $CDCl_3$) of compound **2.8** 97

Figure A2.7 ^{1}H NMR (500 MHz, C_6D_6) of compound **2.9** 98

Figure A2.8 ^{1}H NMR (500 MHz, $CDCl_3$) of compound **2.10** 99

Figure A2.9 ^{1}H NMR (600 MHz, $CDCl_3$) of compound **2.11** 100

Figure A2.10 ^{1}H NMR (600 MHz, $CDCl_3$) of compound **2.12** 101

Figure A2.11 ^{1}H NMR (600 MHz, $CDCl_3$) of compound **2.13** 102

Figure A2.12 ^{1}H NMR (600 MHz, $CDCl_3$) of compound **2.14** 103

Figure A2.13 ^{1}H NMR (600 MHz, $CDCl_3$) of compound **2.15** 104

Figure A2.14 Infrared spectrum of compound **2.15** 105

Figure A2.15 ^{13}C NMR (125 MHz, $CDCl_3$) of compound **2.15** 105

Figure A2.16 ^{1}H NMR (300 MHz, $CDCl_3$) of compound **2.16** 106

Figure A2.17 ^{1}H NMR (400 MHz, $CDCl_3$) of compound **2.17** 107

Figure A2.18 ^{1}H NMR (500 MHz, $CDCl_3$) of compound **2.18** 108

Figure A2.19 ^{1}H NMR (500 MHz, $CDCl_3$) of compound **2.19** 109

Figure A2.20 Infrared spectrum of compound **2.19** 110

Figure A2.21 ^{13}C NMR (125 MHz, $CDCl_3$) of compound **2.19** 110

Figure A2.22 ^{1}H NMR (500 MHz, $CDCl_3$) of compound **2.20** 111

Figure A2.23 ^{1}H NMR (300 MHz, $CDCl_3$) of compound **2.21** 112

Figure A2.24 ^{1}H NMR (600 MHz, $CDCl_3$) of compound **2.22** 113

Figure A2.25 Infrared spectrum of compound **2.22** 114

Figure A2.26 ^{13}C NMR (125 MHz, $CDCl_3$) of compound **2.22** 114

Figure A2.27 ^{1}H NMR (600 MHz, $CDCl_3$) of compound **2.23** 115

Figure A2.28 ^{1}H NMR (600 MHz, $CDCl_3$) of compound **2.24** 116

Figure A2.29 Infrared spectrum of compound **2.24** 117

Figure A2.30 ^{13}C NMR (125 MHz, $CDCl_3$) of compound **2.24** 117

Figure A2.31 ^{1}H NMR (400 MHz, $CDCl_3$) of compound **2.25** 118

Figure A2.32 Infrared spectrum of compound **2.25** 119

Figure A2.33 ^{13}C NMR (125 MHz, $CDCl_3$) of compound **2.25** 119

Figure A2.34 ^{1}H NMR (600 MHz, $CDCl_3$) of compound **2.26** 120

Figure A2.35 Infrared spectrum of compound **2.26** 121

Figure A2.36 ^{13}C NMR (125 MHz, $CDCl_3$) of compound **2.26** 121

Figure A2.37 ^{1}H NMR (600 MHz, $CDCl_3$) of compound **2.27** 122

Figure A2.38 Infrared spectrum of compound **2.27** 123

Figure A2.39 ^{13}C NMR (125 MHz, $CDCl_3$) of compound **2.27** 123

Figure A2.40 ^{1}H NMR (600 MHz, $CDCl_3$) of compound **2.34** 124

Figure A2.41 Infrared spectrum of compound **2.34** 125

Figure A2.42 ^{13}C NMR (125 MHz, $CDCl_3$) of compound **2.34** 125

Figure A2.43 ^{1}H NMR (500 MHz, $CDCl_3$) of compound **2.35** 126

CHAPTER THREE

Figure 3.1. Amination of (Hetero)aryl Chlorides and Sulfamates in a Green Solvent Using Nickel 135

Figure 3.2. Coupling of (Hetero)aryl Sulfamates with Morpholine in 2-Me-THF.....139

Figure 3.3. Coupling of (Hetero)aryl Chlorides with Morpholine in 2-Me-THF.....140

Figure 3.4. Scope of Amine Component in the Coupling Reaction 141

Figure 3.5. Gram-Scale Couplings of Trifluoromethyl-Containing Substrates.....142

Figure 3.6. Gram-Scale Couplings of Heterocyclic Substrates 143

APPENDIX THREE

Figure A3.1 ^{1}H NMR (400 MHz, $CDCl_3$) of compound **3.4** 160

Figure A3.2 ^{1}H NMR (500 MHz, $CDCl_3$) of compound **3.6** 161

Figure A3.3 ^{1}H NMR (500 MHz, $CDCl_3$) of compound **3.7** 162

Figure A3.4 ^{1}H NMR (400 MHz, $CDCl_3$) of compound **3.8** 163

Figure A3.5 ^{1}H NMR (400 MHz, $CDCl_3$) of compound **3.9** 164

Figure A3.6 ^{1}H NMR (400 MHz, $CDCl_3$) of compound **3.10** 165

Figure A3.7 ^{1}H NMR (600 MHz, $CDCl_3$) of compound **3.11** 166

Figure A3.8 ^{1}H NMR (400 MHz, $CDCl_3$) of compound **3.12** 167

Figure A3.9 ^{1}H NMR (600 MHz, $CDCl_3$) of compound **3.13** 168

Figure A3.10 ^{1}H NMR (400 MHz, $CDCl_3$) of compound **3.14** 169

Figure A3.11 Infrared spectrum of compound **3.14** 170

Figure A3.12 ^{13}C NMR (125 MHz, $CDCl_3$) of compound **3.14** 170

Figure A3.13 ^{1}H NMR (400 MHz, $CDCl_3$) of compound **3.15** 171

Figure A3.14 Infrared spectrum of compound **3.15** 172

Figure A3.15 ^{13}C NMR (125 MHz, $CDCl_3$) of compound **3.15** 172

Figure A3.16 ^{1}H NMR (400 MHz, $CDCl_3$) of compound **3.16** 173

Figure A3.17 ^{1}H NMR (400 MHz, $CDCl_3$) of compound **3.17** 174

Figure A3.18 Infrared spectrum of compound **3.17** 175

Figure A3.19 ^{13}C NMR (125 MHz, $CDCl_3$) of compound **3.17** 175

Figure A3.20 ^{1}H NMR (600 MHz, $CDCl_3$) of compound **3.18** 176

Figure A3.21 ^{1}H NMR (500 MHz, $CDCl_3$) of compound **3.19** 177

Figure A3.22 ^{1}H NMR (600 MHz, $CDCl_3$) of compound **3.20** 178

Figure A3.23 ^{1}H NMR (500 MHz, $CDCl_3$) of compound **3.21** 179

Figure A3.24 ^{1}H NMR (500 MHz, $CDCl_3$) of compound **3.26** 180

CHAPTER FOUR

Figure 4.1. Amide-bond cleavage using transition-metal catalysis ……...…..…..... 190

Figure 4.2. Computational study of catalytic cycle ……..……...…..… 196

Figure 4.3. Selective amide-bond cleavage processes...……..…….…. 200

Figure 4.4. Analysis of Competing Pathways for Esterification of *N*-Me,Boc Substrate **4.95**...……...……...……..244

Figure 4.5. Substitution Effects on Equilibrium of Amide Esterification...……..…..247

APPENDIX FOUR

Figure A4.1 ^{1}H NMR (500 MHz, $CDCl_3$) of compound **4.31** 252

Figure A4.2 Infrared spectrum of compound **4.31** 253

Figure A4.3 ^{13}C NMR (125 MHz, $CDCl_3$) of compound **4.31** 253

Figure A4.4 ^{1}H NMR (500 MHz, $CDCl_3$) of compound **4.33** 254

Figure A4.5 Infrared spectrum of compound **4.33** 255

Figure A4.6 ^{13}C NMR (125 MHz, $CDCl_3$) of compound **4.33** 255

Figure A4.7 ^{1}H NMR (300 MHz, $CDCl_3$) of compound **4.35** 256

Figure A4.8 Infrared spectrum of compound **4.35** 257

Figure A4.9 ^{13}C NMR (125 MHz, $CDCl_3$) of compound **4.35** 257

Figure A4.10 ^{1}H NMR (300 MHz, $CDCl_3$) of compound **4.37** 258

Figure A4.11 Infrared spectrum of compound **4.37** 259

Figure A4.12 ^{13}C NMR (125 MHz, $CDCl_3$) of compound **4.37** 259

Figure A4.13 ^{1}H NMR (300 MHz, $CDCl_3$) of compound **4.39** 260

Figure A4.14 Infrared spectrum of compound **4.39** 261

Figure A4.15 ^{13}C NMR (125 MHz, $CDCl_3$) of compound **4.39** 261

Figure A4.16 ^{1}H NMR (300 MHz, $CDCl_3$) of compound **4.8** 262

Figure A4.17 ^{1}H NMR (400 MHz, $CDCl_3$) of compound **4.40** 263

Figure A4.18 ^{1}H NMR (300 MHz, $CDCl_3$) of compound **4.42** 264

Figure A4.19 ^{1}H NMR (400 MHz, $CDCl_3$) of compound **4.44** 265

Figure A4.20 ^{1}H NMR (400 MHz, $CDCl_3$) of compound **4.46** 266

Figure A4.21 ^{1}H NMR (500 MHz, $CDCl_3$) of compound **4.48** 267

Figure A4.22 ^{1}H NMR (500 MHz, $CDCl_3$) of compound **4.49** 268

Figure A4.23 ^{1}H NMR (500 MHz, $CDCl_3$) of compound **4.51** 269

Figure A4.24 ^{1}H NMR (500 MHz, $CDCl_3$) of compound **4.53** 270

Figure A4.25 ^{1}H NMR (300 MHz, $CDCl_3$) of compound **4.54** 271

Figure A4.26 ^{1}H NMR (400 MHz, $CDCl_3$) of compound **4.55** 272

Figure A4.27 ^{1}H NMR (300 MHz, $CDCl_3$) of compound **4.56** 273

Figure A4.28 ^{1}H NMR (500 MHz, $CDCl_3$) of compound **4.64** 274

Figure A4.29 ^{1}H NMR (500 MHz, $CDCl_3$) of compound **4.66** 275

Figure A4.30 ^{1}H NMR (500 MHz, $CDCl_3$) of compound **4.68** 276

Figure A4.31 ^{1}H NMR (600 MHz, $CDCl_3$) of compound **4.70** 277

Figure A4.32 Infrared spectrum of compound **4.70** 278

Figure A4.33 ^{13}C NMR (150 MHz, $CDCl_3$) of compound **4.70** 278

Figure A4.34 ^{1}H NMR (500 MHz, $CDCl_3$) of compound **4.72** 279

Figure A4.35 ^{1}H NMR (500 MHz, $CDCl_3$) of compound **4.21** 280

Figure A4.36 ^{1}H NMR (500 MHz, $CDCl_3$) of compound **4.74** 281

Figure A4.37 ^{1}H NMR (500 MHz, $CDCl_3$) of compound **4.76** 282

Figure A4.38 Infrared spectrum of compound **4.76** 283

Figure A4.39 ^{13}C NMR (125 MHz, $CDCl_3$) of compound **4.76** 283

Figure A4.40 ^{1}H NMR (500 MHz, $CDCl_3$) of compound **4.78** 284

Figure A4.41 Infrared spectrum of compound **4.78** 285

Figure A4.42 ^{13}C NMR (125 MHz, $CDCl_3$) of compound **4.78** 285

Figure A4.43 ^{1}H NMR (500 MHz, $CDCl_3$) of compound **4.80** 286

Figure A4.44 Infrared spectrum of compound **4.80** 287

Figure A4.45 ^{13}C NMR (125 MHz, $CDCl_3$) of compound **4.80** 287

Figure A4.46 ^{1}H NMR (400 MHz, $CDCl_3$) of compound **4.19** 288

Figure A4.47 Infrared spectrum of compound **4.19** 289

Figure A4.48 ^{13}C NMR (125 MHz, $CDCl_3$) of compound **4.19** 289

Figure A4.49 ^{1}H NMR (500 MHz, $(CD_3)_2SO$) of compound **4.22** 290

Figure A4.50 Infrared spectrum of compound **4.22** 291

Figure A4.51 ^{13}C NMR (125 MHz, $(CD_3)_2SO$) of compound **4.22** 291

Figure A4.52 ^{1}H NMR (500 MHz, $CDCl_3$) of compound **4.83** 292

Figure A4.53 ^{1}H NMR (500 MHz, $CDCl_3$) of compound **4.85** 293

Figure A4.54 Infrared spectrum of compound **4.85** 294

Figure A4.55 ^{13}C NMR (125 MHz, $CDCl_3$) of compound **4.85** 294

Figure A4.56 ^{1}H NMR (500 MHz, $CDCl_3$) of compound **4.23** 295

Figure A4.57 Infrared spectrum of compound **4.23** 296

Figure A4.58 ^{13}C NMR (125 MHz, $CDCl_3$) of compound **4.23** 296

Figure A4.59 ^{1}H NMR (500 MHz, $CDCl_3$) of compound **4.24** 297

Figure A4.60 Infrared spectrum of compound **4.24** 298

Figure A4.61 ^{13}C NMR (125 MHz, $CDCl_3$) of compound **4.24** 298

Figure A4.62 ^{1}H NMR (500 MHz, $CDCl_3$) of compound **4.26** 299

Figure A4.63 Infrared spectrum of compound **4.26** 300

Figure A4.64 ^{13}C NMR (125 MHz, $CDCl_3$) of compound **4.26** 300

Figure A4.65 ^{1}H NMR (500 MHz, $CDCl_3$) of compound **4.25** 301

Figure A4.66 Infrared spectrum of compound **4.25** 302

Figure A4.67 ^{13}C NMR (125 MHz, $CDCl_3$) of compound **4.25** 302

CHAPTER FIVE

Figure 5.1. Known catalytic activation of esters and our approach for the activation of methyl esters (without decarbonylation)……..332

Figure 5.2 Conversion of ester **5.5** to amide **5.7**...……..309

Figure 5.3 Scope of methodology ……..……...……...311

Figure 5.4.a DFT calculations show the relative ease of ligand exchange and reductive elimination compared to disfavorable decarbonylation pathways……...312

Figure 5.4.b The transition states for oxidative addition (TS1), ligand exchange (TS2), and reductive elimination (TS3).…….…..…….……..……..…..313

Figure 5.5 Effect of the additive on the thermodynamics of amidation and kinetic barrier for oxidative addition using DFT calculations..……..……...…..314

Figure 5.6 Effects of distortion of the ester-aluminum additive complex on the thermodynamics of the amidation based on substrate……..……..…..316

Figure 5.7 Multistep synthesis using mild catalytic ester activation and sequential site-selective C–N bond forming processes…….....……..……..…...317

Figure 5.8 Gibbs free energy changes of the full catalytic cycle of nickel-catalyzed amidation of methyl 1-naphthoate …...…….....…..……..…..337

Figure 5.9 Gibbs free energy changes of possible decarbonylation transition states, the free energies are compared to [Ni(SIPr)$_2$]. …...……...……..……...337

Figure 5.10 Distortion/interaction analysis of the complexation energy between Ni(SIPr) and ester or ester-aluminium complex …...……...……..……...…..339

Figure 5.11 Dihedral angles and bond lengths of selected esters and amides …...……...……..……..……..…...…340

Figure 5.12 Dihedral angle and bond length of selected esters and amides with Lewis acid …...……...……..……341

APPENDIX FIVE

Figure A5.1 ^{1}H NMR (400 MHz, $CDCl_3$) of compound **5.37** 345

Figure A5.2 Infrared spectrum of compound **5.37** 346

Figure A5.3 ^{13}C NMR (125 MHz, $CDCl_3$) of compound **5.37** 346

Figure A5.4 ^{1}H NMR (500 MHz, $CDCl_3$) of compound **5.39** 347

Figure A5.5 Infrared spectrum of compound **5.39** 348

Figure A5.6 ^{13}C NMR (125 MHz, $CDCl_3$) of compound **5.39** 348

Figure A5.7 ^{1}H NMR (500 MHz, $CDCl_3$) of compound **5.42** 349

Figure A5.8 Infrared spectrum of compound **5.42** 350

Figure A5.9 ^{13}C NMR (125 MHz, $CDCl_3$) of compound **5.42** 350

Figure A5.10 ^{1}H NMR (400 MHz, $CDCl_3$) of compound **5.7** 351

Figure A5.11 ^{1}H NMR (300 MHz, $CDCl_3$) of compound **5.8** 352

Figure A5.12 Infrared spectrum of compound **5.8** 353

Figure A5.13 ^{13}C NMR (125 MHz, $CDCl_3$) of compound **5.8** 353

Figure A5.14 ^{1}H NMR (300 MHz, $CDCl_3$) of compound **5.9** 354

Figure A5.15 Infrared spectrum of compound **5.9** 355

Figure A5.16 ^{13}C NMR (125 MHz, $CDCl_3$) of compound **5.9** 355

Figure A5.17 ^{1}H NMR (300 MHz, $CDCl_3$) of compound **5.10** 356

Figure A5.18 Infrared spectrum of compound **5.10** 357

Figure A5.19 ^{13}C NMR (125 MHz, $CDCl_3$) of compound **5.10** 357

Figure A5.20 ^{1}H NMR (500 MHz, $CDCl_3$) of compound **5.11** 358

Figure A5.21 Infrared spectrum of compound **5.11** 359

Figure A5.22 ^{13}C NMR (125 MHz, $CDCl_3$) of compound **5.11** 359

Figure A5.23 ^{1}H NMR (500 MHz, $CDCl_3$) of compound **5.12** 360

Figure A5.24 Infrared spectrum of compound **5.12** 361

Figure A5.25 ^{13}C NMR (125 MHz, $CDCl_3$) of compound **5.12** 361

Figure A5.26 ^{1}H NMR (500 MHz, $CDCl_3$) of compound **5.13** 362

Figure A5.27 Infrared spectrum of compound **5.13** 363

Figure A5.28 ^{13}C NMR (125 MHz, $CDCl_3$) of compound **5.13** 363

Figure A5.29 ^{1}H NMR (500 MHz, $CDCl_3$) of compound **5.14** 364

Figure A5.30 ^{1}H NMR (500 MHz, $CDCl_3$) of compound **5.15** 365

Figure A5.31 Infrared spectrum of compound **5.15** 366

Figure A5.32 ^{13}C NMR (125 MHz, $CDCl_3$) of compound **5.15** 366

Figure A5.33 ^{1}H NMR (500 MHz, $CDCl_3$) of compound **5.16** 367

Figure A5.34 Infrared spectrum of compound **5.16** 368

Figure A5.35 ^{13}C NMR (125 MHz, $CDCl_3$) of compound **5.16** 368

Figure A5.36 ^{1}H NMR (500 MHz, $CDCl_3$) of compound **5.17** 369

Figure A5.37 Infrared spectrum of compound **5.17** 370

Figure A5.38 ^{13}C NMR (125 MHz, $CDCl_3$) of compound **5.17** 370

Figure A5.39 ^{1}H NMR (500 MHz, $CDCl_3$) of compound **5.18** 371

Figure A5.40 Infrared spectrum of compound **5.18** 372

Figure A5.41 ^{13}C NMR (125 MHz, $CDCl_3$) of compound **5.18** 372

Figure A5.42 ^{1}H NMR (500 MHz, $CDCl_3$) of compound **5.19** 373

Figure A5.43 Infrared spectrum of compound **5.19** 374

Figure A5.44 ^{13}C NMR (125 MHz, $CDCl_3$) of compound **5.19** 374

Figure A5.45 ^{1}H NMR (500 MHz, $CDCl_3$) of compound **5.20** 375

Figure A5.46 Infrared spectrum of compound **5.20** 376

Figure A5.47 ^{13}C NMR (125 MHz, $CDCl_3$) of compound **5.20** 376

Figure A5.48 ^{1}H NMR (500 MHz, $CDCl_3$) of compound **5.21** 377

Figure A5.49 Infrared spectrum of compound **5.21** 378

Figure A5.50 ^{13}C NMR (125 MHz, $CDCl_3$) of compound **5.21** 378

Figure A5.51 ^{1}H NMR (500 MHz, $CDCl_3$) of compound **5.55** 379

Figure A5.52 ^{1}H NMR (500 MHz, $CDCl_3$) of compound **5.56** 380

Figure A5.53 Infrared spectrum of compound **5.56** 381

Figure A5.54 ^{13}C NMR (125 MHz, $CDCl_3$) of compound **5.56** 381

Figure A5.55 ^{1}H NMR (500 MHz, $CDCl_3$) of compound **5.32** 382

Figure A5.56 Infrared spectrum of compound **5.32** 383

Figure A5.57 ^{13}C NMR (125 MHz, $CDCl_3$) of compound **5.32** 383

Figure A5.58 ^{1}H NMR (500 MHz, $CDCl_3$) of compound **5.34** 384

Figure A5.59 Infrared spectrum of compound **5.34** 385

Figure A5.60 ^{13}C NMR (125 MHz, $CDCl_3$) of compound **5.34** 385

Figure A5.61 ^{1}H NMR (500 MHz, $CDCl_3$) of compound **5.35** 386

Figure A5.62 Infrared spectrum of compound **5.35** 387

Figure A5.63 ^{13}C NMR (125 MHz, $CDCl_3$) of compound **5.35** 387

CHAPTER SIX

Figure 6.1.a Common Ni-Catalyzed Couplings …….....…..…..…..... 416

Figure 6.1.b Present Study of Ni-Catalyzed Heck Cyclization for Quaternary Stereocenter Formation …….... 416

Figure 6.2 Survey of Ligands …….. ……...…..…..... 421

Figure 6.3 Influence of the Source of Aryl Halides ……...….422

Figure 6.4 Effect of Substituents on the Aryl Ring……....423

Figure 6.5 Effects of Alkene Geometry……...……424

Figure 6.6 Evaluation of Alkene Substituents and Protecting Groups ……..……..…425

Figure 6.7 Preliminary Data on the Asymmetric Variant …….……..……426

APPENDIX SIX

Figure A6.1 ^{1}H NMR (500 MHz, $CDCl_3$) of compound **6.1** 430

Figure A6.2 Infrared spectrum of compound **6.1** 431

Figure A6.3 ^{13}C NMR (125 MHz, $CDCl_3$) of compound **6.1** 431

Figure A6.4 ^{1}H NMR (500 MHz, $CDCl_3$) of compound **6.4** 432

Figure A6.5 Infrared spectrum of compound **6.4** 433

Figure A6.6 ^{13}C NMR (125 MHz, $CDCl_3$) of compound **6.4** 433

Figure A6.7 ^{1}H NMR (500 MHz, $CDCl_3$) of compound **6.5** 434

Figure A6.8 Infrared spectrum of compound **6.5** 435

Figure A6.9 ^{13}C NMR (125 MHz, $CDCl_3$) of compound **6.5** 435

Figure A6.10 ^{1}H NMR (500 MHz, $CDCl_3$) of compound **6.6** 436

Figure A6.11 Infrared spectrum of compound **6.6** 437

Figure A6.12 ^{13}C NMR (125 MHz, $CDCl_3$) of compound **6.6** 437

Figure A6.13 ^{1}H NMR (500 MHz, $CDCl_3$) of compound **6.23** 438

Figure A6.14 Infrared spectrum of compound **6.23** 439

Figure A6.15 ^{13}C NMR (125 MHz, $CDCl_3$) of compound **6.23** 439

Figure A6.16 ^{1}H NMR (500 MHz, $CDCl_3$) of compound **6.26** 440

Figure A6.17 Infrared spectrum of compound **6.26** 441

Figure A6.18 ^{13}C NMR (125 MHz, $CDCl_3$) of compound **6.26** 441

Figure A6.19 ^{1}H NMR (500 MHz, $CDCl_3$) of compound **6.27** 442

Figure A6.20 Infrared spectrum of compound **6.27** 443

Figure A6.21 ^{13}C NMR (125 MHz, $CDCl_3$) of compound **6.27** 443

Figure A6.22 ^{1}H NMR (500 MHz, $CDCl_3$) of compound **6.29** 444

Figure A6.23 Infrared spectrum of compound **6.29** 445

Figure A6.24 ^{13}C NMR (125 MHz, $CDCl_3$) of compound **6.29** 445

Figure A6.25 ^{1}H NMR (500 MHz, $CDCl_3$) of compound **6.35** 446

Figure A6.26 Infrared spectrum of compound **6.35** 447

Figure A6.27 ^{13}C NMR (125 MHz, $CDCl_3$) of compound **6.35** 447

Figure A6.28 ^{1}H NMR (500 MHz, $CDCl_3$) of compound **6.37** 448

Figure A6.29 Infrared spectrum of compound **6.37** 449

Figure A6.30 ^{13}C NMR (125 MHz, $CDCl_3$) of compound **6.37** 449

Figure A6.31 ^{1}H NMR (500 MHz, $CDCl_3$) of compound **6.39** 450

Figure A6.32 Infrared spectrum of compound **6.39** 451

Figure A6.33 ^{13}C NMR (125 MHz, $CDCl_3$) of compound **6.39** 451

Figure A6.34 ^{1}H NMR (500 MHz, $CDCl_3$) of compound **6.40** 452

Figure A6.35 Infrared spectrum of compound **6.40** 453

Figure A6.36 ^{13}C NMR (125 MHz, $CDCl_3$) of compound **6.40** 453

Figure A6.37 ^{1}H NMR (500 MHz, $CDCl_3$) of compound **6.2** 454

Figure A6.38 Infrared spectrum of compound **6.2** 455

Figure A6.39 ^{13}C NMR (125 MHz, $CDCl_3$) of compound **6.2** 455

Figure A6.40 ^{1}H NMR (500 MHz, $CDCl_3$) of compound **6.7** 456

Figure A6.41 Infrared spectrum of compound **6.7** 457

Figure A6.42 ^{13}C NMR (125 MHz, $CDCl_3$) of compound **6.7** 457

Figure A6.43 ^{1}H NMR (500 MHz, $CDCl_3$) of compound **6.8** 468

Figure A6.44 Infrared spectrum of compound **6.8** 459

Figure A6.45 ^{13}C NMR (125 MHz, $CDCl_3$) of compound **6.8** 459

Figure A6.46 ^{1}H NMR (500 MHz, $CDCl_3$) of compound **6.9** 460

Figure A6.47 Infrared spectrum of compound **6.9** 461

Figure A6.48 ^{13}C NMR (125 MHz, $CDCl_3$) of compound **6.9** 461

Figure A6.49 ^{1}H NMR (500 MHz, $CDCl_3$) of compound **6.10** 462

Figure A6.50 Infrared spectrum of compound **6.10** 463

Figure A6.51 ^{13}C NMR (125 MHz, $CDCl_3$) of compound **6.10** 463

Figure A6.52 ^{1}H NMR (500 MHz, $CDCl_3$) of compound **6.13** 464

Figure A6.53 ^{1}H NMR (500 MHz, $CDCl_3$) of compound **6.14** 465

Figure A6.54 Infrared spectrum of compound **6.14** 466

Figure A6.55 ^{13}C NMR (125 MHz, $CDCl_3$) of compound **6.14** 466

Figure A6.56 ^{1}H NMR (500 MHz, $CDCl_3$) of compound **6.15** 467

Figure A6.57 ^{1}H NMR (500 MHz, $CDCl_3$) of compound **6.16** 468

Figure A6.58 ^{1}H NMR (500 MHz, $CDCl_3$) of compound **6.17** 469

Figure A6.59 ^{1}H NMR (500 MHz, $CDCl_3$) of compound **6.18** 470

Figure A6.60 Infrared spectrum of compound **6.18** 471

Figure A6.61 ^{13}C NMR (125 MHz, $CDCl_3$) of compound **6.18** 471

CHAPTER SEVEN

Figure 7.1 Nickel-Catalyzed Activation of Benzamides and Derivatives (prior studies) and Nickel-Catalyzed Conversion of Aliphatic Amides to Esters (present study).……...…..….....476

Figure 7.2. Evaluation of Amide Substrate…….478

Figure 7.3. Scope of Alcohol Coupling Partner …….480

Figure 7.4. Scope Coupling of Proline-Derived Substrates……..…….481

APPENIDIX SEVEN

Figure A7.1 ^{1}H NMR (500 MHz, $CDCl_3$) of compound **7.1** 514

Figure A7.2 Infrared spectrum of compound **7.1** 515

Figure A7.3 ^{13}C NMR (125 MHz, $CDCl_3$) of compound **7.1** 516

Figure A7.4 ^{1}H NMR (500 MHz, $CDCl_3$) of compound **7.15** 516

Figure A7.5 Infrared spectrum of compound **7.15** 517

Figure A7.6 ^{13}C NMR (125 MHz, $CDCl_3$) of compound **7.15** 517

Figure A7.7 ^{1}H NMR (500 MHz, $CDCl_3$) of compound **7.37** 518

Figure A7.8 Infrared spectrum of compound **7.37** 519

Figure A7.9 ^{13}C NMR (125 MHz, $CDCl_3$) of compound **7.37** 519

Figure A7.10 ^{1}H NMR (500 MHz, $CDCl_3$) of compound **7.39** 520

Figure A7.11 Infrared spectrum of compound **7.39** 521

Figure A7.12 ^{13}C NMR (125 MHz, $CDCl_3$) of compound **7.39** 521

Figure A7.13 ^{1}H NMR (500 MHz, $CDCl_3$) of compound **7.41** 522

Figure A7.14 Infrared spectrum of compound **7.41** 523

Figure A7.15 ^{13}C NMR (125 MHz, $CDCl_3$) of compound **7.41** 523

Figure A7.16 ^{1}H NMR (500 MHz, $CDCl_3$) of compound **7.43** 523

Figure A7.17 Infrared spectrum of compound **7.43** 524

Figure A7.18 ^{13}C NMR (125 MHz, $CDCl_3$) of compound **7.43** 525

Figure A7.19 ^{1}H NMR (500 MHz, $CDCl_3$) of compound **7.45** 526

Figure A7.20 Infrared spectrum of compound **7.45** 527

Figure A7.21 ^{13}C NMR (125 MHz, $CDCl_3$) of compound **7.45** 527

Figure A7.22 ^{1}H NMR (500 MHz, $CDCl_3$) of compound **7.47** 528

Figure A7.23 Infrared spectrum of compound **7.47** 529

Figure A7.24 ^{13}C NMR (125 MHz, $CDCl_3$) of compound **7.47** 529

Figure A7.25 ^{1}H NMR (500 MHz, $CDCl_3$) of compound **7.30** 530

Figure A7.26 Infrared spectrum of compound **7.30** 531

Figure A7.27 ^{13}C NMR (125 MHz, $CDCl_3$) of compound **7.30** 531

Figure A7.28 ^{1}H NMR (500 MHz, $CDCl_3$) of compound **7.31** 532

Figure A7.29 Infrared spectrum of compound **7.31** 533

Figure A7.30 ^{13}C NMR (125 MHz, $CDCl_3$) of compound **7.31** 533

Figure A7.31 ^{1}H NMR (500 MHz, $CDCl_3$) of compound **7.7** 534

Figure A7.32 ^{1}H NMR (500 MHz, $CDCl_3$) of compound **7.8** 535

Figure A7.33 ^{1}H NMR (500 MHz, $CDCl_3$) of compound **7.9** 536

Figure A7.34 Infrared spectrum of compound **7.9** 537

Figure A7.35 ^{13}C NMR (125 MHz, $CDCl_3$) of compound **7.9** 537

Figure A7.36 ^{1}H NMR (500 MHz, $CDCl_3$) of compound **7.10** 538

Figure A7.37 ^{1}H NMR (500 MHz, $CDCl_3$) of compound **7.11** 539

Figure A7.38 Infrared spectrum of compound **7.11** 540

Figure A7.39 ^{13}C NMR (125 MHz, $CDCl_3$) of compound **7.11** 540

Figure A7.40 ^{1}H NMR (500 MHz, $CDCl_3$) of compound **7.12** 541

Figure A7.41 ^{1}H NMR (500 MHz, $CDCl_3$) of compound **7.13** 542

Figure A7.42 Infrared spectrum of compound **7.13** 543

Figure A7.43 ^{13}C NMR (125 MHz, $CDCl_3$) of compound **7.13** 543

Figure A7.44 ^{1}H NMR (500 MHz, $CDCl_3$) of compound **7.14** 544

Figure A7.45 Infrared spectrum of compound **7.14** 545

Figure A7.46 ^{13}C NMR (125 MHz, $CDCl_3$) of compound **7.14** 545

Figure A7.47 ^{1}H NMR (500 MHz, $CDCl_3$) of compound **7.18** 546

Figure A7.48 Infrared spectrum of compound **7.18** 547

Figure A7.49 ^{13}C NMR (125 MHz, $CDCl_3$) of compound **7.18** 547

Figure A7.50 ^{1}H NMR (500 MHz, $CDCl_3$) of compound **7.19** 548

Figure A7.51 Infrared spectrum of compound **7.19** 549

Figure A7.52 ^{13}C NMR (125 MHz, $CDCl_3$) of compound **7.19** 549

Figure A7.53 ^{1}H NMR (500 MHz, $CDCl_3$) of compound **7.20** 550

Figure A7.54 Infrared spectrum of compound **7.20** 551

Figure A7.55 ^{13}C NMR (125 MHz, $CDCl_3$) of compound **7.20** 551

Figure A7.56 ^{1}H NMR (500 MHz, $CDCl_3$) of compound **7.21** 552

Figure A7.57 Infrared spectrum of compound **7.21** 553

Figure A7.58 ^{13}C NMR (125 MHz, $CDCl_3$) of compound **7.21** 553

Figure A7.59 ^{1}H NMR (500 MHz, $CDCl_3$) of compound **7.22** 554

Figure A7.60 Infrared spectrum of compound **7.22** 555

Figure A7.61 ^{13}C NMR (125 MHz, $CDCl_3$) of compound **7.22** 555

Figure A7.62 ^{1}H NMR (500 MHz, $CDCl_3$) of compound **7.23** 556

Figure A7.63 Infrared spectrum of compound **7.23** 557

Figure A7.64 ^{13}C NMR (125 MHz, $CDCl_3$) of compound **7.23** 557

Figure A7.65 ^{1}H NMR (500 MHz, $CDCl_3$) of compound **7.24** 558

Figure A7.66 Infrared spectrum of compound **7.24** 559

Figure A7.67 ^{13}C NMR (125 MHz, $CDCl_3$) of compound **7.24** 559

Figure A7.68 ^{1}H NMR (500 MHz, $CDCl_3$) of compound **7.25** 560

Figure A7.69 Infrared spectrum of compound **7.25** 561

Figure A7.70 ^{13}C NMR (125 MHz, $CDCl_3$) of compound **7.25** 561

Figure A7.71 ^{1}H NMR (500 MHz, $CDCl_3$) of compound **7.26** 562

Figure A7.72 Infrared spectrum of compound **7.26** 563

Figure A7.73 ^{13}C NMR (125 MHz, $CDCl_3$) of compound **7.26** 563

Figure A7.74 ^{1}H NMR (500 MHz, $CDCl_3$) of compound **7.27** 564

Figure A7.75 ^{1}H NMR (500 MHz, $CDCl_3$) of compound **7.28** 565

Figure A7.76 ^{1}H NMR (500 MHz, $CDCl_3$) of compound **7.29** 566

Figure A7.77 ^{1}H NMR (500 MHz, $CDCl_3$) of compound **7.32** 567

Figure A7.78 Infrared spectrum of compound **7.32** 568

Figure A7.79 ^{13}C NMR (125 MHz, $CDCl_3$) of compound **7.32** 568

Figure A7.80 ^{1}H NMR (500 MHz, $CDCl_3$) of compound **7.33** 569

Figure A7.81 Infrared spectrum of compound **7.33** 570

Figure A7.82 ^{13}C NMR (125 MHz, $CDCl_3$) of compound **7.33** 570

LIST OF TABLES

CHAPTER ONE

Table 1.1. Optimization of Amination Using Ni(II) Precatalyst 4

Table 1.2. Survey of Halide and Pseudohalide Substrates.....7

CHAPTER TWO

Table 2.1. Survey of Solvents in the Suzuki–Miyaura Coupling .....…55

Table 2.2. Survey of Cross-Coupling Partners .....…56

Table 2.3. Cross-Coupling Reactions of Naphthyl Halides in Various Solvents .....…66

Table 2.4. Cross-Coupling Reactions of Tolyl Halides in Selected Solvents.....…67

Table 2.5. Cross-Coupling Reactions of Naphthol Derivatives in Various Solvents ....…67

Table 2.6. Cross-Coupling Reactions of Naphthyl Mesylate, Tosylate, and Pivalates in Selected Green Solvents .....…69

Table 2.7. Cross-Coupling Reactions of *o*-Methylphenyl Sulfamate and Carbamate in Selected Solvents .....…69

Table 2.8. Arylboron-Based Nucleophile Phenylboronic Acid .....…72

Table 2.9. Arylboron-Based Nucleophile Pinacol Ester 73

Table 2.10. Arylboron-Based Nucleophile MIDA (*N*-Methyliminodiacetic Acid).....74

Table 2.11. Arylboron-Based Nucleophile Potassium Aryl Trifluoroborate.....…74

CHAPTER THREE

Table 3.1. Examination of Solvents in the Amination of 1-Chloronaphthalene 136

Table 3.2. Evaluation of Various Electrophiles 137

CHAPTER FOUR

Table 4.1. Experimental and computational study of amide-bond activation during the conversion of benzamides **4.7** to methyl benzoate **4.8a**..... 193

Table 4.2. Scope of our methodology.....196

Table 4.3. Attempted Conversion of Amide **4.7g** to Methyl Benzoate **4.8a** Under Various Reaction Conditions.....208

Table 4.4. Survey of Amide Substrates.....209

Table 4.5. Comparison of Aryl vs. Alkyl Amide Substrates.....242

Table 4.6. Energies, Enthalpies, and Free Energy of the Calculated Structures.....248

CHAPTER FIVE

N/A

CHAPTER SIX

Table 6.1. Optimization of Reaction Conditions.....397

CHAPTER SEVEN

Table 7.1. Optimization of Reaction Conditions.....479

Table 7.2. Evaluation of Pyridine-Type Ligands.....498

Table 7.3. Survey of Amide Substrates Under the Optimized Reaction Conditions…...499

Table 7.4. Optimization of Reaction Conditions.....500

LIST OF ABBREVIATIONS

$[a]_D$	specific rotation at wavelength of sodium D line
Å	ångström
Ac	acetyl, acetate
acac	acetylacetonate
ACS	American Chemical Society
aq.	aqueous
Ar	aryl
BINAP	2,2'-bis(diphenylphosphino)-1,1'-binaphthyl
Bn	benzyl
Boc	*tert*-butyloxycarbonyl
Bu	butyl
bs	broad singlet
c	concentration for specific rotation measurements
°C	degrees Celsius
ca	circa
calcd	calculated
celite	diatomaceous earth
cod	cyclooctadiene
cy	cyclohexyl
d	doublet, day(s)
dd	doublet of doublet
δ	chemical shift (ppm)
dba	dibenzylideneacetone
DFT	density functional theory
DMA	dimethylacetamide
DME	dimethoxyethane (glyme)
DMF	*N*,*N*-dimethylformamide
DMSO	dimethyl sulfoxide
dppe	diphenylphosphino ethane
equiv	equivalent
ESI	electrospray ionization

Et	ethyl
G	Gibbs free energy
g	gram(s)
h	hour(s)
η	hapticity
hex	hexyl
HRMS	high-resolution mass spectroscopy
i	iso
IMES	1,3-Bis(2,4,6-trimethylphenyl)imidazol-2-ylidene
IPr	1,3-Bis(2,6-di-i-propylphenyl)imidazol-2-ylidene,
IR	infrared (spectroscopy)
J	coupling constant
L	liter
M	metal, molar, mass
m	multiplet, milli, meter
m	meta
μ	micro
m/*z*	mass to charge ratio
Me	methyl
Mes	mesityl
MHz	megahertz
MIDA	*N*-Methyliminodiacetic Acid
min	minute(s)
mol	mole(s)
MOM	methoxymethyl
mp	melting point
MTBE	methyl *t*-butyl ether
n	normal
NHC	*N*-heterocyclic carbene
NIS	*N*-Iodosuccinimide
NMP	*N*-methyl-2-pyrrolidone
NMR	nuclear magnetic resonance
o	ortho
p	para
p-TsOH	*p*-toluenesulfonic acid
Ph	phenyl
pH	hydrogen ion concentration in aqueous solution
pin	pinacol
Piv	pivaloyl

ppm	parts per million
Pr	propyl
q	quartet
rt	room temperature
R_f	retention factor
s	singlet
s	secondary
SIMES•HCl	1,3-Bis(2,4,6-trimethylphenyl)imidazolinium chloride
SIMES	1,3-Bis(2,4,6-trimethylphenyl)-4,5-dihydroimidazol-2-ylidene
IMES	1,3-Bis(2,4,6-trimethylphenyl)imidazol-2-ylidene
SIPr•HCl	1,3-Bis-(2,6-diisopropylphenyl)imidazolidinium chloride
SIPr	1,3-Bis(2,6-di-i-propylphenyl)-4,5-dihydroimidazol-2-ylidine
t	triplet
t	tertiary
tt	triplet of triplet
Tf	trifluoromethanesulfonyl (trifyl)
TFA	trifluoroacetic acid
THF	tetrahydrofuran
TLC	thin layer chromatography
TS	transition state
Ts	*p*-toluenesulfonyl (tosyl)
UV	ultraviolet
v	volume
X	leaving group

ACKNOWLEDGEMENTS

Foremost, I would like to express my sincere gratitude to my advisor, Professor Neil K. Garg. His guidance and patience have led me to grow as a scientist, and motivated me to keep challenging myself. I am very thankful that he did not give up on me during the difficult times, but instead he proactively provided me with sound advice and resources to get over the nightmares that I was dealing with in my first year. In the past five years, Neil's mentorship has been instrumental in my development, scientifically and professionally, and I will always be grateful for his 'specific' feedbacks.

The support from Professor Houk has been extremely helpful during my time at UCLA. Professor Houk not only served on my candidacy committee and taught me about physical organic and computational chemistry, but also has been a great collaborator and supporter. I would also like to acknowledge the other members of my thesis committee, Professors van Dam and Bouchard for taking time out of their busy schedule to serve on my committees.

Professor Xi Chen and Dr. Yi Chen, my graduate student mentor, introduced me to chemical biology and inspired me to be a scientist when I was an undergraduate student at UC Davis. I am highly indebted to them for mentoring me and motivating to pursue graduate level education. I am also obliged to Professor Dean Tantillo for encouraging me to join Neil's lab.

My 2015 summer internship at Boehringer Ingelheim has helped to confirm the future directions of my career. I had the opportunity to work alongside process chemists and truly enjoyed the experience. I am grateful to Drs. Nick Desrosiers and Chris Senanayake for hosting and mentoring me. Nick is incredibly kind and patient, and he always entertained my ideas.

The projects that contributed to my thesis would have not been possible without my amazing teammates: Stephen Ramgren, Tehetena Mesganaw, Emma Baker, Noah F. Fine Nathel,

Qi Liu, Yuxuan Ye, Xingyu Jiang, Junyong Kim, Tejas Shah, and Sarah Anthony. I also had the opportunity to collaborate with the Houk lab. I want to thank Xin Hong, Yun-Fang Yang, and Peng Liu for their expertise and their patience in answering my questions. I enjoyed working on the projects and learned a great deal from all of my coworkers.

I consider the Garg lab members like my own family. I think our lab is a bit unusual considering how frequent we hang out inside and outside of the lab. The lab will always have a special spot in my heart. The first few years of my graduate study were very challenging and I would not be able to get over the obstacles without the constant support of the lab members. They constantly offered and provided me with guidance and moral support. Despite their busy work schedule, they always answered all of my questions and helped me to improve.

When I joined the lab, I had the pleasure of overlapping with Neil's first few graduate students. They kindly shared their knowledge and experiences with me. I do not know a lot of people who are as adorable and inspirational as Kyle Quasdorf. Ben Boal is a free-spirited hipster. Sarah Bronner is a female version of Noah F. Fine Nathel. Tehetena Mesganaw is a perfectionist and I learned about producing high quality professional documents from her. I worked next to Alex Schammel during his last year. I enjoyed our conversations and thanks for sharing your lab techniques to me. Adam Goetz was the voice of reason in our lab. Grace Chiou and I share a lot of common interests. I am appreciative of her positivity and friendship. Amanda Silberstein is one of the most wise and mature people I know. She is an incredibly smart, caring, and wonderful person. Joel Smith helped me tremendously in the first few years of my graduate school career. I am fortunate to overlap with them even for a short duration of time.

Stephen Ramgren has been an amazing mentor and friend. I am very thankful to his active mentoring even until this present day. When I joined the lab, Amanda Silberstein was

assigned to be my mentor. However, it just happened that Stephen took over that position from Amanda. Since then, we spent a lot of time together as coworkers and friends. Stephen's help was crucial in my development as an independent thinker and to my survival in graduate school. Thanks for sharing your knowledge with me and pushing me out of my comfort zone.

The support and encouragement I have received from Noah F. Fine Nathel have been crucial in getting through challenging phases. Noah is a great friend and coworker. Besides his constant anxiousness and terrible perception of time, I appreciate the time we have had together exploring LA food scenes and enjoying high tea in Los Angeles. Noah is a really good listener and he has always been there when I need someone to talk to.

Evan Styduhar is a good friend. He is really generous with his time and supportive of me. Thanks for your help with my presentations and writings. Evan is also a considerate and warm person, and I am grateful for our friendship. I will cherish the conversations we had inside and outside of the lab.

Tejas Shah is my work husband. Thanks for surviving on the program with me. We have gone through a lot of challenges together and I appreciate his support over the past five years. I thought I would not like him so much after Neil moved his workspace next to mine, but I was wrong. Our friendship became better and stronger. We share a lot of common interests and values. We understand each other, like a married couple; hence we got to be work spouses. He is always willing to help me with personal and work troubles. I will treasure the three fancy dinners we have had to celebrate our last year as a graduate student.

The last two years have gone like the wind. I am fortunate to becoming friends with the occupants of MSB 5234: Lucas Morril, Junyong Kim, Robert Susick, Jesus Moreno (and Tejas Shah). Despite of their occasional obnoxiousness, they are terrific coworkers and friends. I am

always entertained by Lucas' goofiness, Jesus' sassiness, Tejas' saltiness, Robert's cheesiness, and Junyong for being himself. As an office, we love karaoke, cuties and Dunkin Donuts' munchkins. Lucas introduced me to some of the best beers I have ever tasted (Pliney and Alpine, delish!). Jesus is as sassy as me. He also has beautiful and thick dark luscious hair (jealous….). I enjoyed trying new restaurants and hiking with Junyong. Robert is very positive and he is always game to explore new things (except for his inability to enjoy raw seafood). He also thinks that I am very facetious (really??). They also have always been helpful and I appreciate their support.

Emma Baker is a lovely and thoughtful young lady. Thanks for cheering me up when I needed some TLC. She always brought me cookies and sweets. Emma is unique as she is a classy person, but can be really vulgar as well. I value her sense of humor. We have worked together on two projects and had great 'chemistry' together.

I also have the pleasure of knowing Elias Picazo, a silly and mischievous person. His optimism always brings a lively vibe to our lab. Joyann Barber is also really bright and cheerful and I appreciate her enthusiasms towards life. It was really nice to get to know Bryan Simmons and Jose Medina in the short time we overlapped. Nick Weires and Michael Corsello are gifted scientists, and I am excited to see their future independent research. Jacob Dander and Michael Yamano are talented first year students who know how to have fun with life. Michael, I am sorry I am too short on time to go to a rave with you. Jacob is eloquent funny, and weird. He reminds me of Noah.

It was nice to get to know undergraduate students in the lab. Sarah Anthony and JJ are talented young ladies with bright futures. They are always so positive and vibrant and make me feel younger (and older). I have to thank the postdocs in the lab, Travis McMahon and Marie Hoffmann, for sharing their knowledge with me.

Finally, this thesis would have not been possible without the support of my family, relatives, and friends. I want to thank my parents for believing in me and letting me pursue my dreams. I have known Daniel Sun from my first year of graduate school and I am very happy to be graduating together with him. I would not have been able to stay sane without the support of my best friend Joyce Pham. Even though we are a thousand miles apart, we have managed to stay as best friends and grow together over the past seven years. Thanks for listening to me babbling without complaining and motivating me throughout difficult times.

Chapter one is a version of Hie, L.; Ramgren, S. D.; Mesganaw, T.; Garg, N. K. *Org. Lett.* **2012**, *14*, 4182–4185. Hie, Ramgren, and Mesganaw are responsible for experimental work.

Chapter two is a version of Ramgren, S. D.; Hie, L.; Ye, Y.; Garg, N. K. *Org. Lett.* **2013**, *15*, 3950–3953. Ramgren, Hie, and Ye were responsible for experimental work.

Chapter three is a version of Fine Nathel, N. F.; Kim, J.; Hie, L.; Jiang, X.; Garg, N. K. *ACS Catal.* **2014**, *4*, 3289–3293. Fine Nathel, Kim, Hie, and Jiang were responsible for experimental work.

Chapter four is a version of Hie, L.; Fine Nathel, N. F.; Shah, T.; Baker, E. L.; Hong, X.; Yang, Y.-F.; Liu, P.; Houk, K. N.; Garg, N. K. *Nature* **2015**, *524*, 79–83. Hie, Fine Nathel, Shah, and Baker were responsible for experimental work. Hong, Yang, and Liu were responsible for computational work.

Chapter five is a version of Hie, L.; Fine Nathel, N. F.; Hong, X.; Yang, Y.-F.; Houk, K. N.; Garg, N. K. Garg. *Angew. Chem. Int. Ed.* **2016**, *55*, 2810–2814. Hie and Fine Nathel were responsible for experimental work. Hong and Yang were responsible for computational work.

Chapter six is a version of Desrosiers, J.-N.; Hie, L.; Lee, H.; Grinberg, N.; Haddad, N.; Yee, N. K.; Garg, N. K.; Senanayake, C. *Submitted.* Desrosiers, Hie, Lee, and Grinberg were responsible for experimental work.

Chapter seven is a version of Hie, L.; Baker, E. L; Anthony, S. M.; Desrosiers, J.-N.; Senanayake, C.; Garg, N. K. *Manuscript in preparation*. Hie, Baker, and Anthony were responsible for experimental work.

BIOGRAPHICAL SKETCH

Education

University of California, Los Angeles, CA

- Ph.D., Organic Chemistry, anticipated Spring 2016.
- Graduate Research Assistant, September 2011 to present.
- Current GPA: 3.89/4.00

University of California, Davis, CA

- Bachelor of Science, Chemistry, June 2011.
- Cumulative GPA: 3.67/4.00

Professional and Academic Experience

Graduate Research Assistant: University of California, Los Angeles, CA.

- September 2011 to present; Advisor: Prof. Neil K. Garg.
- Established the nickel-catalyzed activation of aryl and aliphatic amides to cleave carbon–nitrogen bonds and construct ester linkages (in collaboration with the Houk group).
- Discovered an efficient means for the formation of amide bonds from methyl esters using nickel catalysis (in collaboration with the Houk group).
- Developed a practical method for the catalytic amination of aryl sulfamates and carbamates to construct carbon–nitrogen bonds.
- Discovered 'greener' variant of the nickel-catalyzed Suzuki–Miyaura cross-coupling in collaboration with the ACS GCI Pharmaceutical Roundtable.
- Developed an undergraduate teaching laboratory experiment in collaboration with the ACS GCI Pharmaceutical Roundtable to introduce green chemistry and cross-coupling reactions to undergraduate students.

Graduate Student Intern: Boehringer Ingelheim, Ridgefield, CT.

- May 2015 to September 2015
- Discovered nickel-mediated bond forming methodologies in the catalysis branch of the company's chemical development group

Teaching Assistant: University of California at Los Angeles, CA.

- Taught discussion sections for undergraduate organic chemistry (Winter 2012, Spring 2012, Fall 2012, Spring 2014).
- Supervised and taught undergraduate students experimental organic chemistry and laboratory technique (Fall 2011).

Undergraduate Research Assistant: University of California, Davis, CA.

- December 2009 to June 2011; Advisor: Prof. Xi Chen.
- Investigated chemical and enzymatic synthesis of heparin sulfate oligosaccharides.

Awards and Honors

- UCLA Travel Grant for the ACS Spring National Meeting & Exposition, San Diego, CA, 2016.
- UCLA Majeti-Alapati Fellowship, 2015.
- Bristol-Myers Squibb Graduate Fellowship in Synthetic Organic Chemistry, 2015–2016.
- UCLA Dissertation Year Fellowship, 2015–2016.
- UCLA Dorothy Radcliffe Dee Fellowship, 2014.
- American Chemical Society Division of Organic Chemistry Graduate Fellowship, 2014–2015.
- UCLA Christopher S. Foote Graduate Fellowship, 2014–2016.
- UCLA Hanson–Dow Excellence in Teaching Award, 2014.
- UCLA Excellence in Second Year Academics and Research, 2013.
- UCLA Edwin W. Pauley Fellowship, 2012–2013.

Publications

9. **Nickel Catalyzed Esterification of Aliphatic Amides.** Liana Hie, Emma L. Baker, Sarah Anthony, and Neil K. Garg. *Manuscript in preparation.*

8. **Nickel-Catalyzed Suzuki–Miyaura Coupling in *t*-Amyl Alcohol for the Preparation of 5-(furan-3-yl)pyrimidine.** Liana Hie and Neil K. Garg. *Submitted.*

7. **Construction of Quaternary Stereocenters via Nickel-Catalyzed Heck Cyclizations.** Jean-Nicolas Desrosiers, Liana Hie, Heewon Lee, Nelu Grinberg, Nizar Haddad, Nathan K. Yee, Neil K. Garg, and Chris H. Senanayake. *Submitted.*

6. **Nickel-Catalyzed Activation of Acyl C–O Bonds of Methyl Esters.** Liana Hie, Noah F. Fine Nathel, Xin Hong, Yun-Fang Yang, K. N. Houk, and Neil K. Garg. *Angew. Chem. Int. Ed*. **2016**, *55*, 2810–2814.

5. **Conversion of Amides to Esters by the Nickel-Catalysed Activation of Amide C–N Bonds.** Liana Hie, Noah F. Fine Nathel, Tejas K. Shah, Emma L. Baker, Xin Hong, Yun-Fang Yang, Peng Liu, K. N. Houk, and Neil K. Garg. *Nature* **2015**, *524*, 79–83 (Highlighted in *Chem. & Eng. News.* **2015**, *93*, 9; *Nat. Chem*. **2015**, *7*, 682; *Angew. Chem. Int. Ed*. **2015**, *54*, 13856–13858; *Synform* **2016**, *01*, A3–A8).

4. **Nickel-Catalyzed Suzuki–Miyaura Cross-Coupling in a Green Solvent for an Undergraduate Organic Chemistry Laboratory.** Liana Hie, Jonah Chang, and Neil K. Garg. *J. Chem. Educ.* **2015**, *92*, 571–574.

3. **Nickel-Catalyzed Amination of Aryl Chlorides and Sulfamates in 2-Me-THF.** Noah F. Fine Nathel, Junyong Kim, Liana Hie, Xingyu Jiang, and Neil K. Garg. *ACS Catal.* **2014**, *4*, 3289–3293 (highlighted in *Chem. & Eng. News.* **2014**, *92*, 24).

2. **Nickel-Catalyzed Suzuki–Miyaura Coupling in Green Solvents.** Stephen D. Ramgren, Liana Hie, Yuxuan Ye, and Neil K. Garg. *Org. Lett.* **2013**, *15*, 3950–3953.

1. **Amination of Aryl Sulfamates and Carbamates Using a Ni (II) Precatalyst.** Liana Hie, Stephen D. Ramgren, Tehetena Mesganaw, and Neil K. Garg. *Org. Lett.* **2012**, *14*, 4182–4185.

CHAPTER ONE

Nickel-Catalyzed Amination of Aryl Sulfamates and Carbamates Using an Air-Stable Precatalyst

Liana Hie, Stephen D. Ramgren, Tehetena Mesganaw, and Neil K. Garg.

Org. Lett. **2012**, *14*, 4182–4185.

1.1 Abstract

A facile nickel-catalyzed method to achieve the amination of synthetically useful aryl sulfamates and carbamates is reported. Contrary to most Ni-catalyzed amination reactions, this user-friendly approach relies on an air-stable Ni(II) precatalyst, which, when employed with a mild reducing agent, efficiently delivers aminated products in good to excellent yields. The scope of the method is broad with respect to both coupling partners and includes heterocyclic substrates.

1.2 Introduction

Nickel-catalyzed cross-couplings of phenol-based electrophiles have received considerable attention in recent years.[1] Attractive aspects of such processes include the low cost of Ni and the many benefits that pertain to utilizing phenol derivatives. Of the substrates widely explored, aryl carbamates and sulfamates are particularly attractive because of their pronounced stability and capacity to direct the installation of functional groups onto an aromatic ring through directed ortho-metallation[1,2,3] or electrophilic aromatic substitution processes.[2d] Although carbon–carbon bond forming reactions using aryl sulfamates and carbamates have been most widely

studied,[4,5] several reports of carbon–nitrogen bond formation are available.[6,7,8,9] Aminations of aryl sulfamates and carbamates are facile and proceed in synthetically useful yields; however, the air sensitivity of the nickel precatalyst employed in all cases (i.e., $Ni(cod)_2$)[10] limits the widespread use of these C–N bond forming processes.

We report the development of sulfamate and carbamate aminations using an inexpensive air-stable nickel(II) precatalyst (Figure 1.1). When used in combination with phenylboronic acid pinacol ester (Ph–B(pin)) as a mild reducing agent, this procedure provides an efficient and user-friendly means to achieve amination reactions across a range of aryl substrates and amine coupling partners.

Figure 1.1. Amination of aryl carbamates and sulfamates using Ni(II) precatalyst.

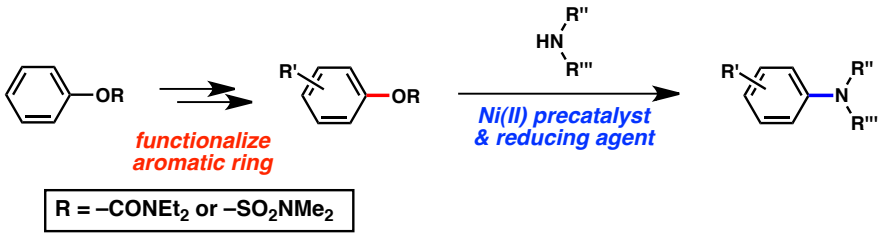

1.3 Optimization of Amination Conditions

A key challenge in developing the desired amination reaction using a Ni(II) precatalyst is the difficulty in reducing Ni(II) to Ni(0). Although Pd(II) precatalysts readily undergo in situ reduction with amines or phosphines in Pd-catalyzed Buchwald–Hartwig couplings, the corresponding reduction of Ni(II) is less facile. Ni-catalyzed amination methodologies that use Ni(II) precatalysts are only available for aryl halides, and typically use Zn or hydrides as reducing agents.[11]

We selected phenylcarbamate **1.1** and phenylsulfamate **1.2** as substrates for the desired amination and then surveyed Ni(II) complexes in the presence of the NHC ligand SIPr•HCl (**1.3**)[12] and various reducing agents. Key results are summarized in, where piperidine was employed as the amine coupling partner. Reaction conditions utilizing Zn dust proved ineffective (entries 1 and 2), while the use of triethylsilane gave either poor or modest results (entries 3 and 4). Inspired by Suzuki–Miyaura coupling methodologies of sulfamates and carbamates, where boronic acids serve to reduce Ni(II) to Ni(0) in situ,[4a,4b,4c,4e,4f] we tested the use of Ph–$B(OH)_2$ in the amination reaction. Gratifyingly, good to excellent yields could be obtained (entries 5 and 6), and $NiCl_2$(DME) complex[13] was identified as the optimal Ni precatalyst (entry 6). Although these results were promising, we found that the corresponding coupling of sulfamate **1.2** gave inconsistent results (entry 7). Nonetheless, it was observed that boronic esters could be used in place of Ph–$B(OH)_2$ or boroxines to give more consistent results (entries 8 and 9). By using Ph–B(pin) as reducing agent with $NiCl_2$(DME) as precatalyst, a 94% yield of the desired aminated product **1.4** was obtained. These conditions were also found to be useful for the coupling of carbamate **1.1** (entry 10).

Table 1.1. Optimization of Amination Using Ni(II) Precatalyst.[a]

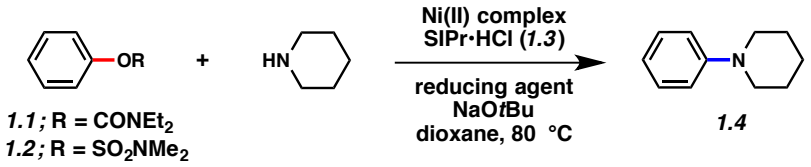

1.1; R = $CONEt_2$
1.2; R = SO_2NMe_2

1.4

entry	substrate	Ni source	reducing agent	yield[b]
1	*1.1*	$Ni(acac)_2$	Zn dust[c]	0%
2	*1.1*	$NiCl_2(DME)$	Zn dust[c]	0%
3	*1.1*	$Ni(acac)_2$	$H–SiEt_3$[c]	0%
4	*1.1*	$NiCl_2(DME)$	$H–SiEt_3$[c]	51%
5	*1.1*	$Ni(acac)_2$	$Ph–B(OH)_2$	57%
6	*1.1*	$NiCl_2(DME)$	$Ph–B(OH)_2$	98%
7	*1.2*	$NiCl_2(DME)$	$Ph–B(OH)_2$	variable
8	*1.2*	$NiCl_2(DME)$	$(Ph–BO)_3$	58%
9	*1.2*	$NiCl_2(DME)$	Ph–B(pin)	94%
10	*1.1*	$NiCl_2(DME)$	Ph–B(pin)	92%

[a] Conditions: Ni(II) complex (5 mol %), **1.3** (10 mol %), sulfamate/carbamate substrate (1 equiv), piperidine (1.2 equiv), reducing agent (0.55 equiv), NaO*t*Bu (1.85 equiv), hexamethylbenzene (0.1 equiv), 3 h. [b] Yield determined by ^{1}H NMR analysis of the crude reaction mixtures using hexamethylbenzene as an internal standard. [c] Reducing agent (0.8 equiv) and NaO*t*Bu (1.4 equiv).

1.4 Substrate Scope

Having identified optimal reaction conditions,[14] we examined the scope of aryl sulfamates and carbamates, using morpholine as the amine coupling partner (Figure 1.2). Fused arenes were tolerated, as demonstrated by the smooth formation of **1.5** and **1.6**. The ability to form **1.7**–**1.12** in good yields shows the methodology's tolerance to non-fused arenes with a variety of substituent patterns. It should also be noted that *ortho*-substituted substrates, which are readily accessible by *ortho*-functionalization of phenyl sulfamates or carbamates,[2,3] underwent the desired coupling to give **1.12**–**1.15**. Heterocycles such as indoles and pyridines were also tolerated, as revealed by the formation of products **1.16**–**1.18**. In many cases, sulfamates and carbamates perform equally well in this amination methodology.

Figure 1.2. Amination of Aryl Sulfamates and Carbamates Using Morpholine.

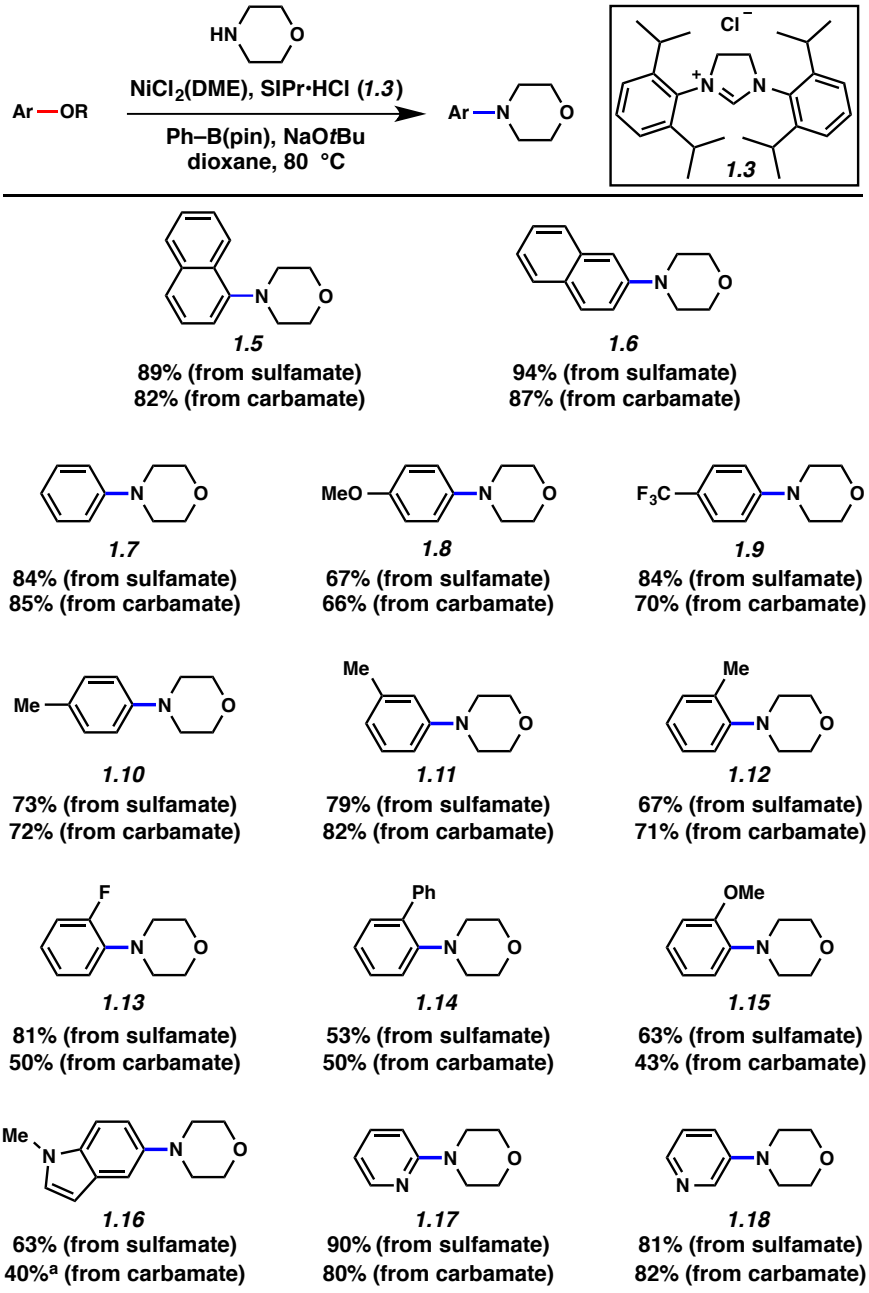

Reaction conditions: $NiCl_2$(DME) (5–20 mol %), **1.3** (10–40 mol %), sulfamate/carbamate substrate (1 equiv), morpholine (1.2–2.4 equiv), Ph–B(pin) (0.15–1.4 equiv), NaO*t*Bu (1.4–3.75 equiv), 3 h. Unless otherwise noted, yields reflect those of isolated product. [a]Yield determined by ^{1}H NMR analysis with hexamethylbenzene as the internal standard.

The scope with respect to the amine coupling partner is provided in Figure 1.3. In addition to morpholine, the cyclic amines piperidine and pyrrolidine underwent the desired coupling to furnish **1.4** and **1.19**. Acyclic secondary amines and anilines reacted successfully, as shown by the formation of **1.20**–**1.23**. Finally, amines with appended heterocycles were also tolerated, thus giving rise to **1.24**–**1.25**.

Figure 1.3. Amination of Various Amines.

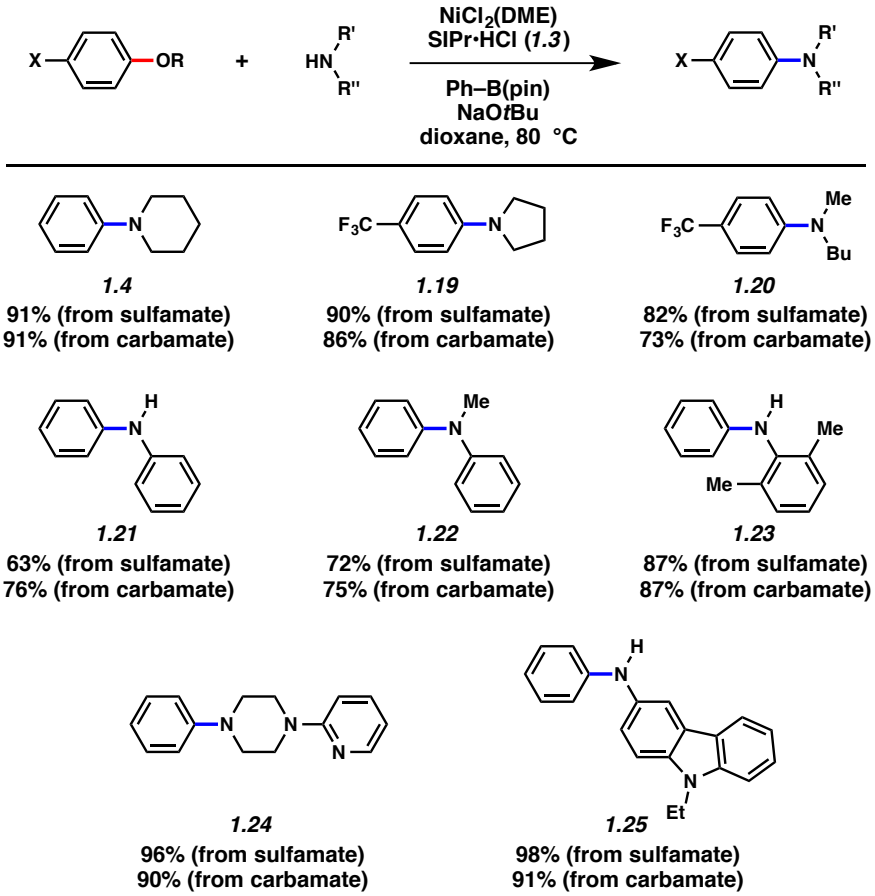

Reaction conditions: $NiCl_2$(DME) (5–20 mol %), **1.3** (10–40 mol %), sulfamate/carbamate substrate (1 equiv), amine (1.2–2.4 equiv), Ph–B(pin) (0.15–1.05 equiv), NaO*t*Bu (1.4–3.75 equiv), 3 h. Unless otherwise noted, yields reflect those of isolated product.

1.5 Amination with Various Electrophiles

Given that most Ni-catalyzed amination reactions employ Ni(0) precatalysts, we tested the generality of our optimal reaction conditions on other electrophilic substrate classes using morpholine as the coupling partner (Table 1.2). Although modest results were obtained using phenyl *tert*-Bu-carbonate and phenyl pivalate (entries 1 and 2), the use of phenyl tosylate was more promising, giving a 63% yield of product (entry 3). Phenyl triflate was not a suitable coupling partner (entry 4), and low yields were observed using iodobenzene or bromobenzene as substrate (entries 5 and 6). On the other hand, chlorobenzene coupled smoothly under our reaction conditions to furnish the desired aminated product in 98% yield (entry 7).

Table 1.2. Survey of Halide and Pseudohalide Substrates.[a]

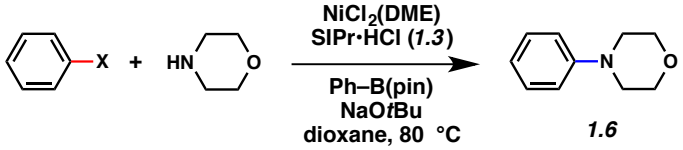

entry	X	yield[b]
1	OCO_2tBu	15%
2	OPiv	44%
3	OTs	63%
4	OTf	4%
5	I	25%
6	Br	33%
7	Cl	98%

[a] Conditions: $NiCl_2$(DME) (5 mol %), **1.3** (10 mol %), substrate (1 equiv), morpholine (1.8 equiv), Ph–B(pin) (0.35 equiv), NaO*t*Bu (2.25 equiv), hexamethylbenzene (0.1 equiv), 3 h. [b] Yield determined by ^{1}H NMR analysis with hexamethylbenzene as the internal standard.

1.6 Conclusion

In summary, we have developed a facile nickel-catalyzed method to achieve the amination of synthetically useful aryl sulfamates and carbamates. Our user-friendly approach

employs $NiCl_2$(DME) as a bench-stable Ni(II) precatalyst, in addition to the mild reducing agent Ph–B(pin), to furnish aminated products in good to excellent yields. Given the attractive features of aryl sulfamates and carbamates, coupled with the transformation's broad scope, this Ni(II)-based methodology is expected to find use in various applications that require C–N bond construction.

1.7 Experimental Section

1.7.1 Materials and Methods

Unless stated otherwise, reactions were conducted in flame-dried glassware under an atmosphere of nitrogen using anhydrous solvents (either freshly distilled or passed through activated alumina columns). Unless otherwise stated, commercially obtained reagents were used as received. Amines were purified by filtration over basic Brockman Grade I 58 Å Al_2O_3 (Activity 1), followed by distillation over calcium hydride, prior to use. $NiCl_2$(DME) was obtained from Strem Chemicals. NaO*t*Bu was obtained from Alfa Aesar. The amines, SIPr•HCl, and Ph–B(pin) were obtained from Sigma Aldrich and Alfa Aesar. Dioxane was purified by distillation over sodium benzophenone ketyl. Reaction temperatures were controlled using an IKAmag temperature modulator, and unless stated otherwise, reactions were performed at room temperature (rt, approximately 23 °C). Thin-layer chromatography (TLC) was conducted with EMD gel 60 F254 pre-coated plates (0.25 mm) and visualized using a combination of UV, anisaldehyde, ceric ammonium molybdate, iodine, vanillin, and potassium permanganate staining. Silicycle Siliaflash P60 (particle size 0.040–0.063 mm) was used for flash column chromatography. ^{1}H NMR spectra were recorded on Bruker spectrometers (at 300, 400, 500, 600

MHz) and are reported relative to deuterated solvent signals. Data for ^{1}H NMR spectra are reported as follows: chemical shift (δ ppm), multiplicity, coupling constant (Hz) and integration.

1.7.2 Experimental Procedures

1.7.2.1 Synthesis of Aryl Sulfamate and Carbamate Substrates

Note: Supporting information for the synthesis of the aryl sulfamates and carbamates shown in Tables 1.1–1.2 and Figures 1.2–1.3 have previously been reported.[15]

1.7.2.2 Amination of Aryl Sulfamates and Carbamates

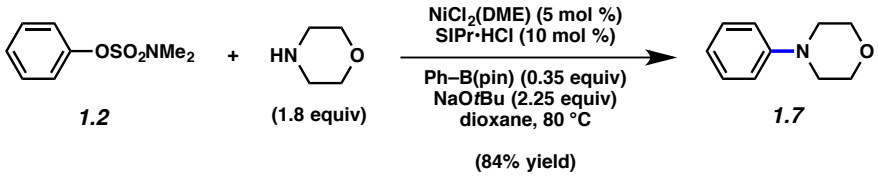

Representative Procedure (coupling of phenylsulfamate 1.2 is used as an example). 1.7 (Figure 1.2). A 4 mL reaction vial was charged with a magnetic stir bar, flame-dried under reduced pressure, and allowed to cool under N_2. The vial was then charged with Ph–B(pin) (35.71 mg, 0.175 mmol, 35 mol%), anhydrous powdered NaO*t*Bu (108.1 mg, 1.125 mmol, 2.25 equiv), $NiCl_2$(DME) (5.5 mg, 0.025 mmol, 5 mol%), and SIPr•HCl (21.3 mg, 0.05 mmol, 10 mol%). Subsequently, dioxane (2.5 ml), phenylsulfamate **1.2** (100.6 mg, 0.50 mmol, 1.0 equiv), and morpholine (87.1 mL, 0.9 mmol, 1.8 equiv) were added, sequentially. The resulting heterogenous mixture was stirred for 1 min while purging with N_2, and the vial was sealed with a Teflon-lined screw cap. The mixture was stirred at 23 °C for 1 h, and then at 80 °C for 3 h in a preheated aluminum heating block. After cooling the reaction vessel to 23 °C and concentrating the mixture under reduced pressure, the crude residue was purified by flash chromatography (9:1

Hexanes:EtOAc) to yield aminated product **1.7** (68.3 mg, 84% yield) as a white solid. R_f 0.28 (9:1 Hexanes:EtOAc). Spectral data match those previously reported.[16]

Any modifications of the conditions shown in this representative procedure are specified in the following schemes, which depict all of the results shown in Figures 1.2–1.3.

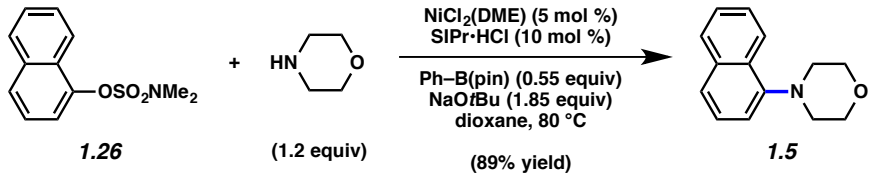

1.5 (Figure 1.2). Purification by flash chromatography (9:1 Hexanes:EtOAc) yielded aminated product **1.5** (89% yield) as a white solid. R_f 0.41 (9:1 Hexanes:EtOAc). Spectral data match those previously reported.[17]

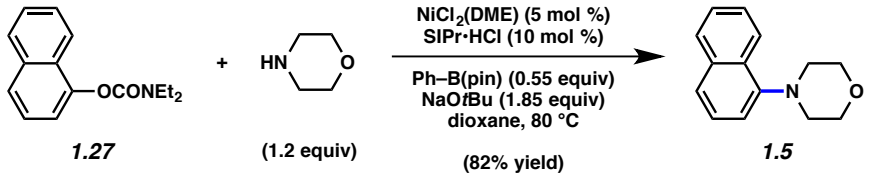

1.5 (Figure 1.2). Purification by flash chromatography (9:1 Hexanes:EtOAc) afforded aminated product **1.5** (82% yield) as a white solid. R_f 0.41 (9:1 Hexanes:EtOAc). Spectral data match those previously reported.[17]

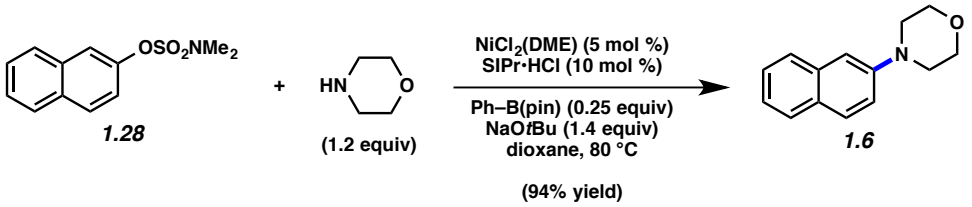

1.6 (Figure 1.2). Purification by flash chromatography (9:1 Hexanes:EtOAc) produced aminated product **1.6** (94% yield) as a white solid. R_f 0.23 (9:1 Hexanes:EtOAc). Spectral data match those previously reported.[18]

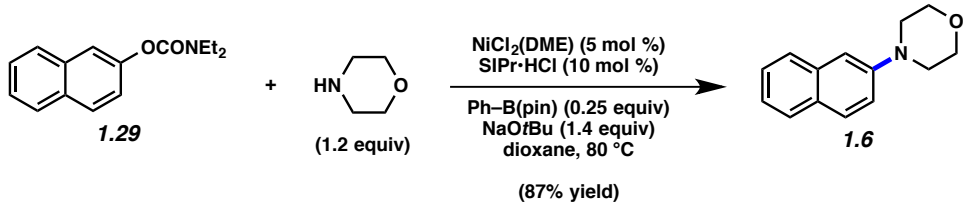

1.6 (Figure 1.2). Purification by flash chromatography (9:1 Hexanes:EtOAc) generated aminated product **1.6** (87% yield) as a white solid. R_f 0.23 (9:1 Hexanes:EtOAc). Spectral data match those previously reported.[18]

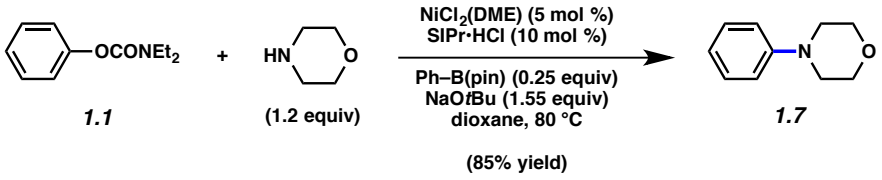

1.7 (Figure 1.2). Purification by flash chromatography (9:1 Hexanes:EtOAc) supplied aminated product **1.7** (85% yield) as a white solid. R_f 0.28 (9:1 Hexanes:EtOAc). Spectral data match those previously reported.[16]

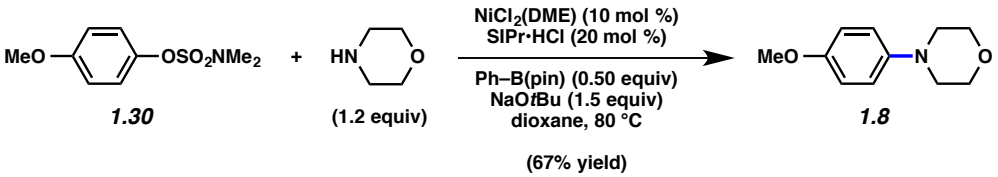

1.8 (Figure 1.2). Purification by flash chromatography (10:1:1 Benzene:Et_2O:CH_2Cl_2) afforded aminated product **1.8** (67% yield) as a white solid. R_f 0.16 (10:1:1 Benzene:Et_2O:CH_2Cl_2). Spectral data match those previously reported.[19]

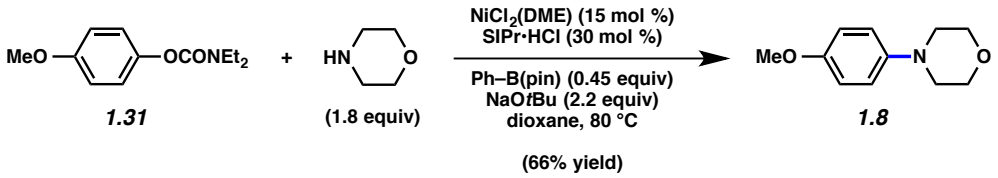

1.8 (Figure 1.2). Purification by flash chromatography (10:1:1 Benzene:Et_2O:CH_2Cl_2) afforded aminated product **1.8** (66% yield) as a white solid. R_f 0.16 (10:1:1 Benzene:Et_2O:CH_2Cl_2). Spectral data match those previously reported.[19]

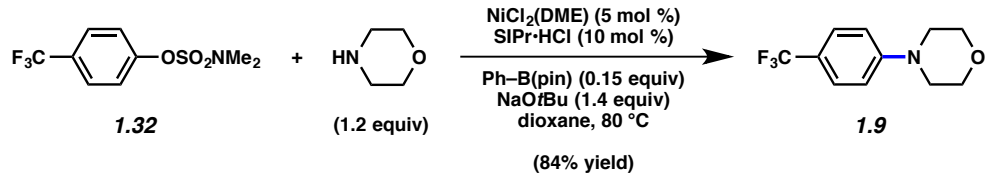

1.9 (Figure 1.2). Purification by flash chromatography (30:1 Benzene:Et_2O) generated aminated product **1.9** (84% yield) as a white solid. R_f 0.38 (30:1 Benzene:Et_2O). Spectral data match those previously reported.[20]

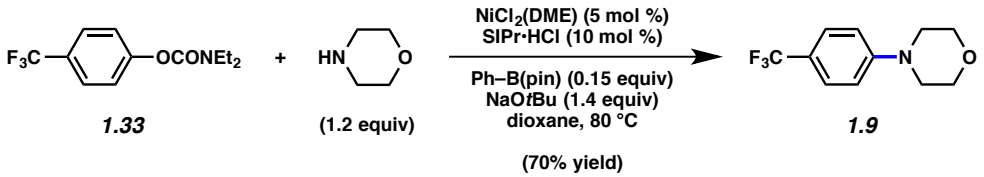

1.9 (Figure 1.2). Purification by flash chromatography (30:1 Benzene:Et_2O) generated aminated product **1.9** (84% yield) as a white solid. R_f 0.38 (30:1 Benzene:Et_2O). Spectral data match those previously reported.[20]

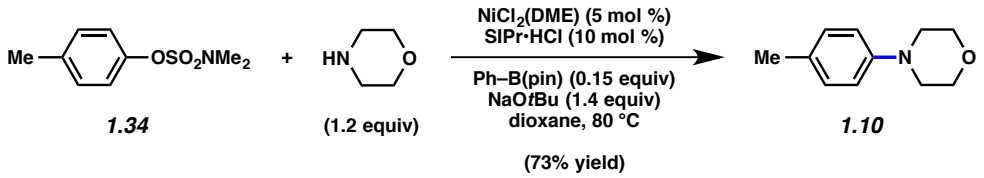

1.10 (Figure 1.2). Purification by flash chromatography (19:1 Benzene:Et_2O) afforded aminated product **1.10** (73% yield) as a white solid. R_f 0.29 (19:1 Benzene:Et_2O). Spectral data match those previously reported.[21]

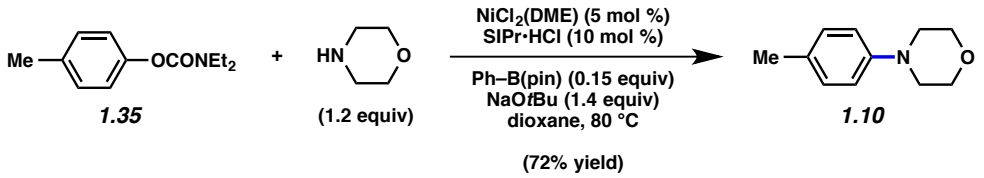

1.10 (Figure 1.2). Purification by flash chromatography (19:1 Benzene:Et_2O) yielded aminated product **1.10** (72% yield) as a white solid. R_f 0.29 (19:1 Benzene:Et_2O). Spectral data match those previously reported.[21]

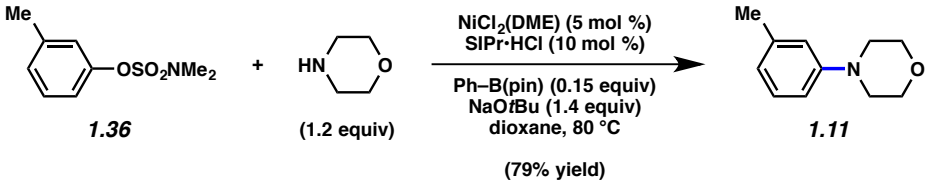

1.11 (Figure 1.2). Purification by flash chromatography (19:1 Benzene:Et_2O) generated aminated product **1.11** (79% yield) as a yellow oil. R_f 0.34 (19:1 Benzene:Et_2O). Spectral data match those previously reported.[21]

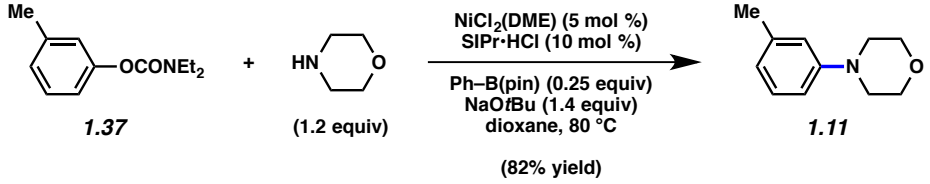

1.11 (Figure 1.2). Purification by flash chromatography (19:1 Benzene:Et_2O) afforded aminated product **1.11** (82% yield) as a yellow oil. R_f 0.34 (19:1 Benzene:Et_2O). Spectral data match those previously reported.[21]

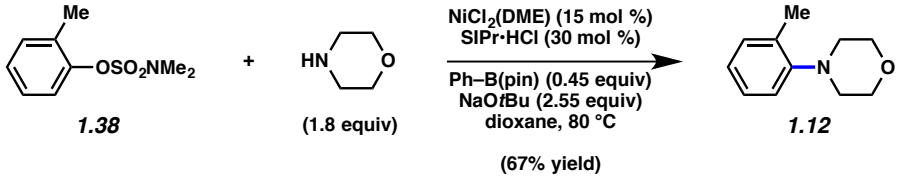

1.12 (Figure 1.2). Purification by flash chromatography (20:1 Hexanes:EtOAc) produced aminated product **1.12** (67% yield) as a yellow oil. R_f 0.30 (20:1 Hexanes:EtOAc). Spectral data match those previously reported.[21]

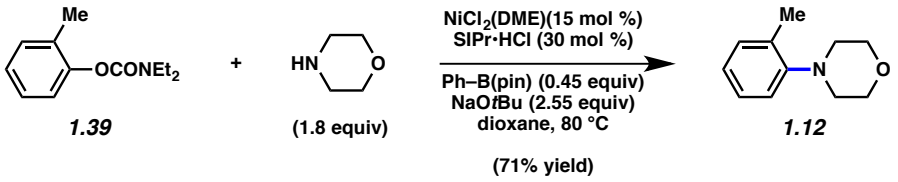

1.12 (Figure 1.2). Purification by flash chromatography (20:1 Hexanes:EtOAc) supplied aminated product **1.12** (71% yield) as a yellow oil. R_f 0.30 (20:1 Hexanes:EtOAc). Spectral data match those previously reported.[21]

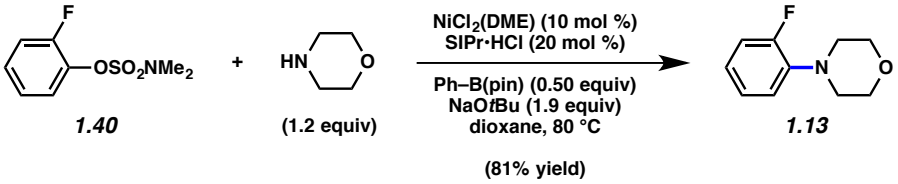

1.13 (Figure 1.2). Purification by flash chromatography (60:1:1 Benzene:Et_2O:CH_2Cl_2) afforded aminated product **1.13** (81% yield) as an off-white solid. R_f 0.45 (60:1:1 Benzene:Et_2O:CH_2Cl_2). Spectral data match those previously reported.[22]

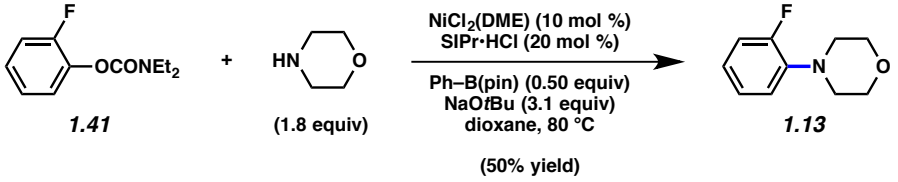

1.13 (Figure 1.2). Purification by flash chromatography (60:1:1 Benzene:Et_2O:CH_2Cl_2) supplied aminated product **1.13** (50% yield) as an off-white solid. R_f 0.45 (60:1:1 Benzene:Et_2O:CH_2Cl_2). Spectral data match those previously reported.[22]

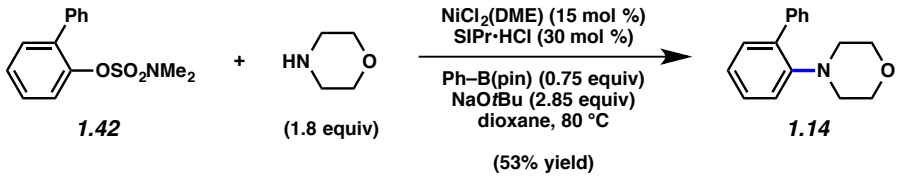

1.14 (Figure 1.2). Purification by flash chromatography (100% Benzene) yielded aminated product **1.14** (53% yield) as a yellow oil. R_f 0.50 (100% Benzene). Spectral data match those previously reported.[23]

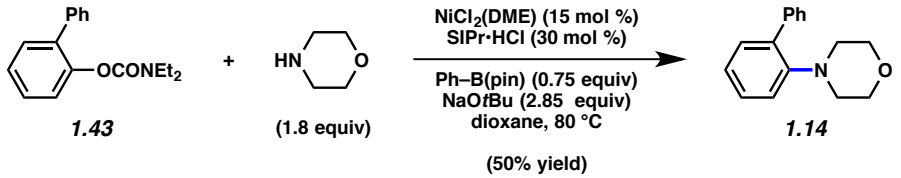

1.14 (Figure 1.2). Purification by flash chromatography (100% Benzene) afforded aminated product **1.14** (50% yield) as a yellow oil. R_f 0.50 (100% Benzene). Spectral data match those previously reported.[23]

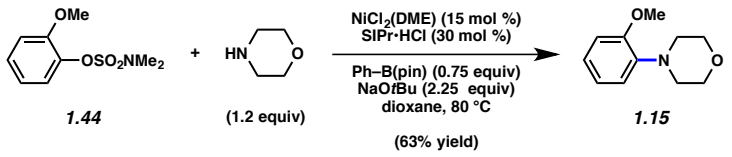

1.15 (Figure 1.2). Purification by flash chromatography (20:1 Hexanes:EtOAc) supplied aminated product **1.15** (63% yield) as a yellow oil. R_f 0.26 (20:1 Hexanes:EtOAc). Spectral data match those previously reported.[23]

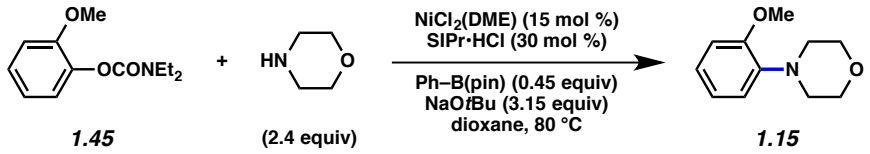

1.15 (Figure 1.2). Purification by flash chromatography (9:1 Benzene:Et_2O) generated aminated product **1.15** (43% yield) as a yellow oil. R_f 0.27 (9:1 Benzene:Et_2O). Spectral data match those previously reported.[23]

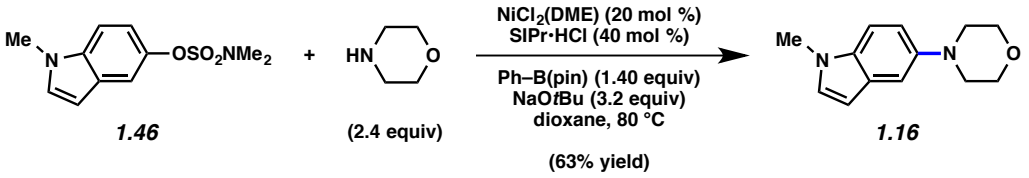

1.16 (Figure 1.2). Purification by flash chromatography (6:1:1 Benzene:Et_2O:CH_2Cl_2) yielded aminated product **1.16** (63% yield) as an off-white solid. R_f 0.36 (6:1:1 Benzene:Et_2O:CH_2Cl_2). Spectral data match those previously reported.[23]

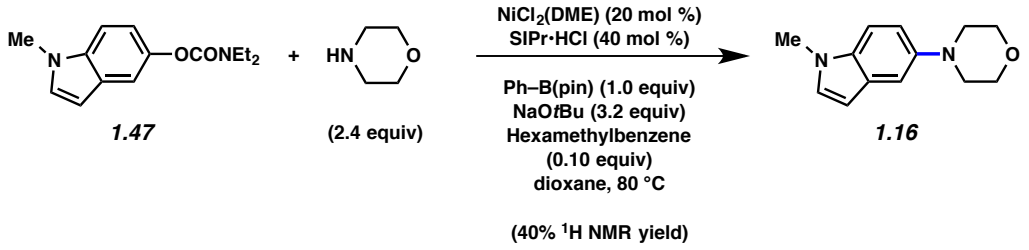

1.16 (Figure 1.2). The reaction mixture was filtered over a short plug of silica gel (eluted with EtOAc (10 mL)), then volatiles were removed in in vacuo and evaporated to dryness. The yield was determined by ^1H NMR analysis with hexamethylbenzene as an internal standard.

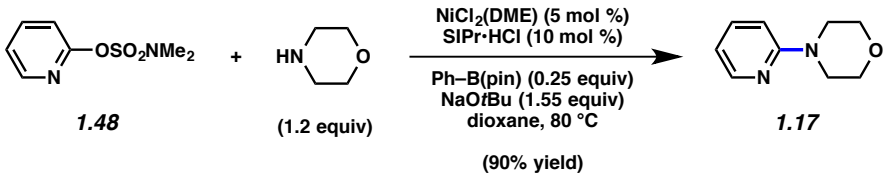

1.17 (Figure 1.2). Purification by flash chromatography (2:1 Hexanes:EtOAc) afforded aminated product **1.17** (90% yield) as a pale yellow oil. R_f 0.23 (2:1 Hexanes:EtOAc. Spectral data match those previously reported.[24]

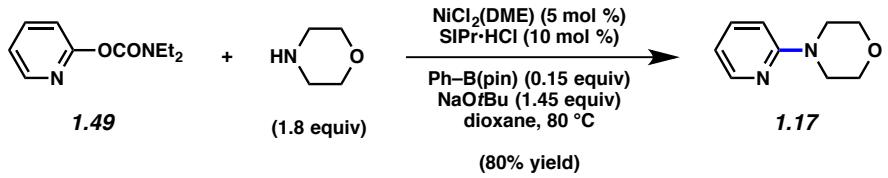

1.17 (Figure 1.2). Purification by flash chromatography (2:1 Hexanes:EtOAc) produced aminated product **1.17** (80% yield) as a pale yellow oil. R_f 0.27 (2:1 Hexanes:EtOAc. Spectral data match those previously reported.[24]

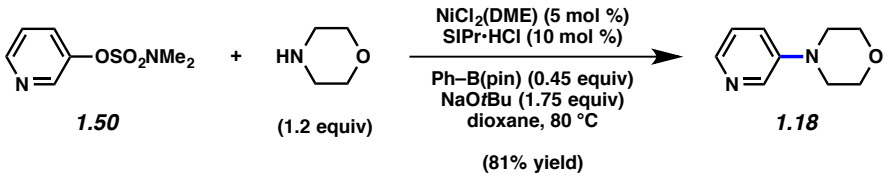

1.18 (Figure 1.2). Purification by flash chromatography (100% EtOAc) afforded aminated product **1.18** (81% yield) as a pale yellow oil. R_f 0.14 (100% EtOAc). Spectral data match those previously reported.[25]

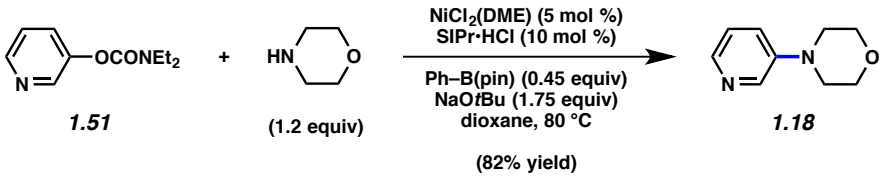

1.18 (Figure 4.2). Purification by flash chromatography (100% EtOAc) generated aminated product **1.18** (82% yield) as a pale yellow oil. R_f 0.14 (100% EtOAc). Spectral data match those previously reported.[25]

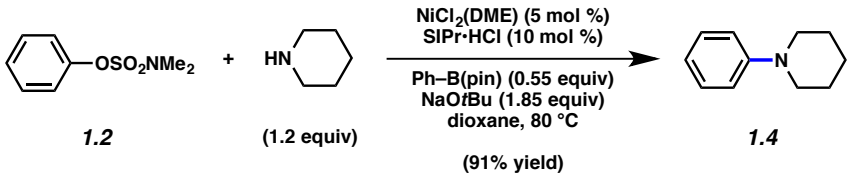

1.4 (Figure 1.3). Purification by flash chromatography (50:1 Hexanes:EtOAc) afforded aminated product **1.4** (91% yield) as a clear oil. R_f 0.39 (50:1 Hexanes:EtOAc). Spectral data match those previously reported.[9]

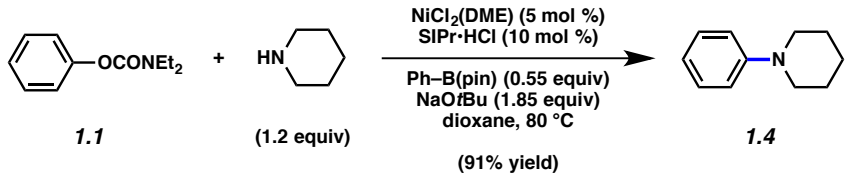

1.4 (Figure 1.3). Purification by flash chromatography (50:1 Hexanes:EtOAc) supplied aminated product **1.4** (91% yield) as a clear oil. R_f 0.39 (50:1 Hexanes:EtOAc). Spectral data match those previously reported.[9]

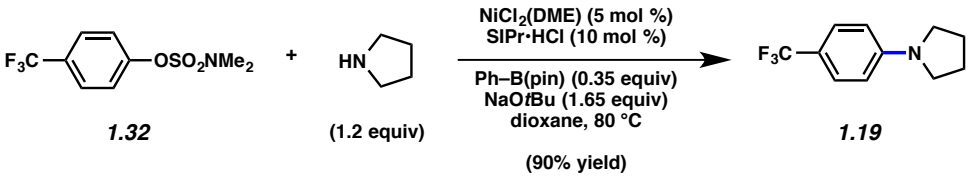

1.19 (Figure 1.3). Purification by flash chromatography (50:1 Hexanes:Et_2O) generated aminated product **1.19** (90% yield) as a white solid. R_f 0.34 (50:1 Hexanes:Et_2O). Spectral data match those previously reported.[26]

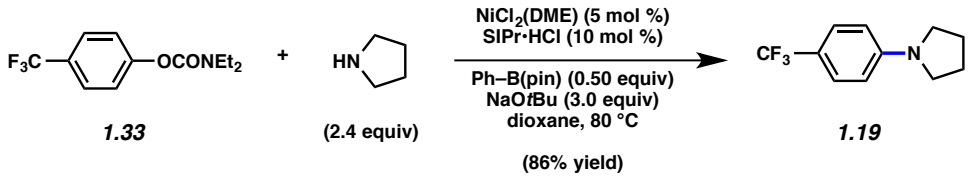

1.19 (Figure 1.3). Purification by flash chromatography (50:1 Hexanes:Et_2O) produced aminated product **1.19** (86% yield) as a white solid. R_f 0.34 (50:1 Hexanes:Et_2O). Spectral data match those previously reported.[26]

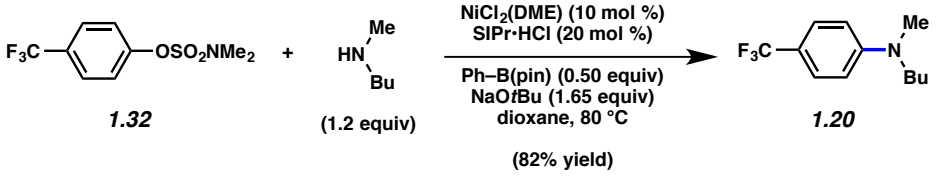

1.20 (Figure 1.3). Purification by flash chromatography (90:1 Hexanes:Et_2O) afforded aminated product **1.20** (82% yield) as a clear oil. R_f 0.37 (90:1 Hexanes:Et_2O). Spectral data match those previously reported.[23]

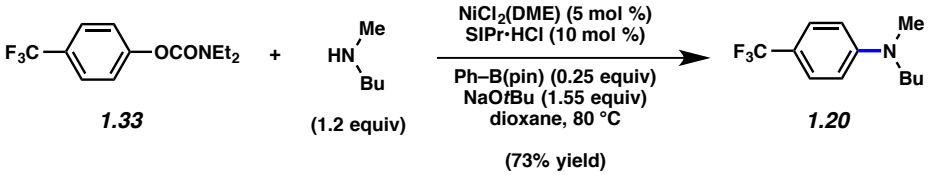

1.20 (Figure 1.3). Purification by flash chromatography (90:1 Hexanes:Et_2O) generated aminated product **1.20** (73% yield) as a clear oil. R_f 0.37 (90:1 Hexanes:Et_2O). Spectral data match those previously reported.[23]

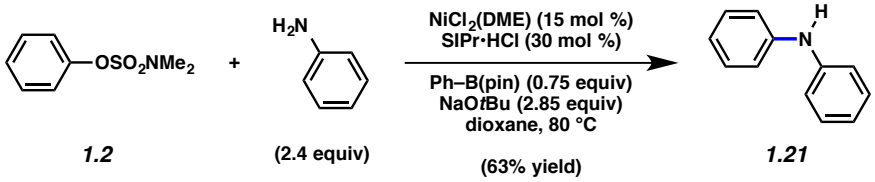

1.21 (Figure 1.3). Purification by flash chromatography (4:1 Hexanes:CH_2Cl_2) afforded aminated product **1.21** (63% yield) as a yellow solid. R_f 0.20 (4:1 Hexanes:CH_2Cl_2). Spectral data match those previously reported.[11e]

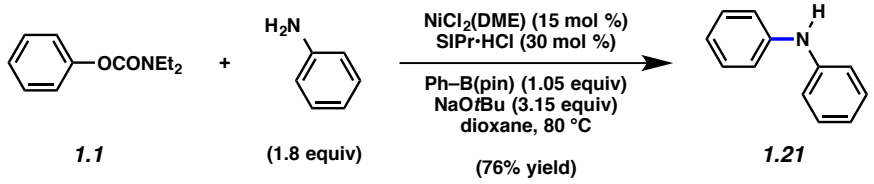

1.21 (Figure 1.3). Purification by flash chromatography (4:1 Hexanes:CH_2Cl_2) yielded aminated product **1.21** (76% yield) as a yellow solid. R_f 0.20 (4:1 Hexanes:CH_2Cl_2). Spectral data match those previously reported.[11e]

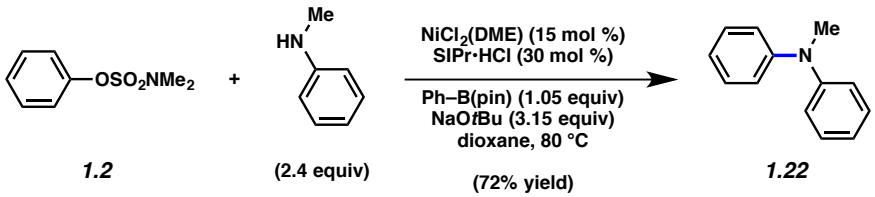

1.22 (Figure 1.3). Purification by flash chromatography (100% Hexanes) afforded aminated product **1.22** (72% yield) as a yellow oil. R_f 0.15 (100% Hexanes). Spectral data match those previously reported.[11e]

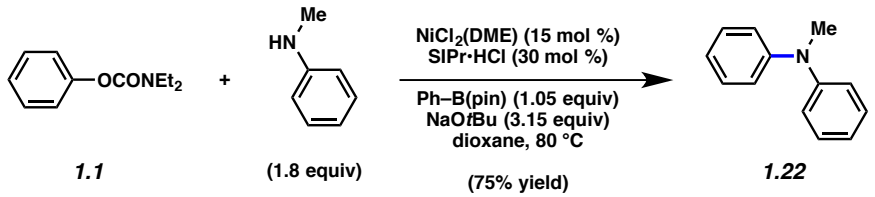

1.22 (Figure 1.3). Purification by flash chromatography (100% Hexanes) generated aminated product **1.22** (75% yield) as a yellow oil. R_f 0.15 (100% Hexanes). Spectral data match those previously reported.[11e]

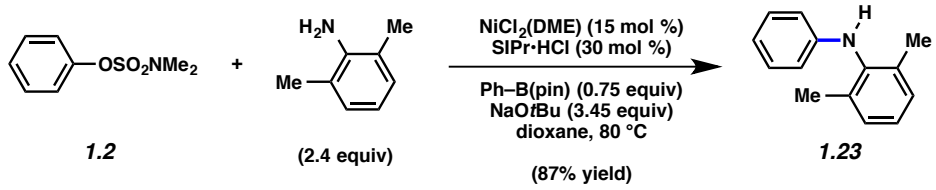

1.23 (Figure 1.3). Purification by flash chromatography (20:1 Hexanes:Et_2O) yielded aminated product **1.23** (87% yield) as a clear oil. R_f 0.45 (40:1 Hexanes:Et_2O). Spectral data match those previously reported.[11e]

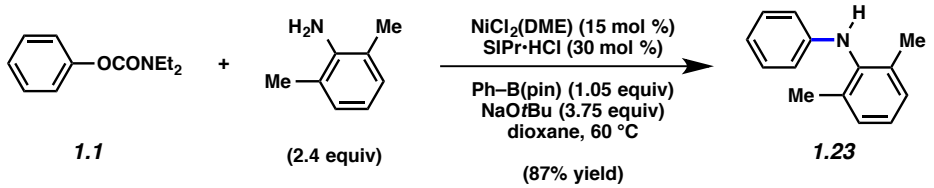

1.23 (Figure 1.3). Purification by flash chromatography (20:1 Hexanes:Et_2O) produced aminated product **1.23** (87% yield) as a clear oil. R_f 0.45 (40:1 Hexanes:Et_2O). Spectral data match those previously reported.[11e]

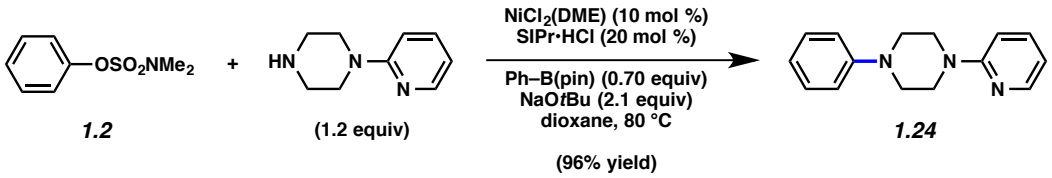

1.24 (Figure 1.3). Purification by flash chromatography (8:1 Hexanes:EtOAc) supplied aminated product **1.24** (96% yield) as a white solid. R_f 0.18 (8:1 Hexanes:EtOAc). Spectral data match those previously reported.[9]

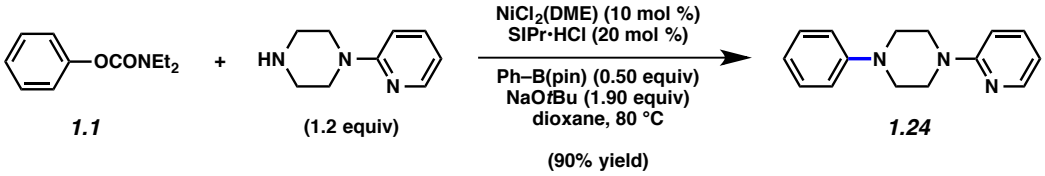

1.24 (Figure 1.3). Purification by flash chromatography (8:1 Hexanes:EtOAc) afforded aminated product **1.24** (90% yield) as a white solid. R_f 0.18 (8:1 Hexanes:EtOAc). Spectral data match those previously reported.[9]

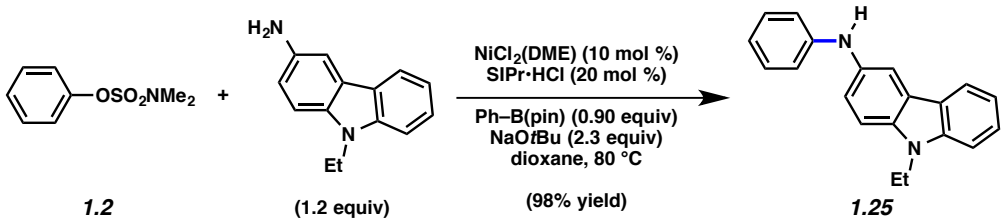

1.2 (1.2 equiv) (98% yield) *1.25*

1.25 (Figure 1.3). Purification by flash chromatography (300:150:1 Hexanes:CH_2Cl_2:Et_3N) yielded aminated product **1.25** (98% yield) as a white solid. R_f 0.19 (300:150:1 Hexanes:CH_2Cl_2:Et_3N). Spectral data match those previously reported.[23]

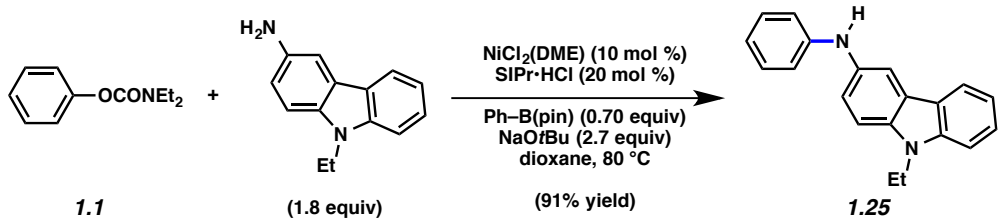

1.1 (1.8 equiv) (91% yield) *1.25*

1.25 (Figure 1.3). Purification by flash chromatography (300:150:1 Hexanes:CH_2Cl_2:Et_3N) afforded aminated product **1.25** (91% yield) as a white solid. R_f 0.19 (300:150:1 Hexanes:CH_2Cl_2:Et_3N). Spectral data match those previously reported.[23]

Appendix One: Spectra Relevant to Chapter One

Nickel-Catalyzed Amination of Aryl Sulfamates and Carbamates Using an Air-Stable Precatalyst

Liana Hie, Stephen D. Ramgren, Tehetena Mesganaw, and Neil K. Garg.

Org. Lett. **2012**, *14*, 4182–4185.

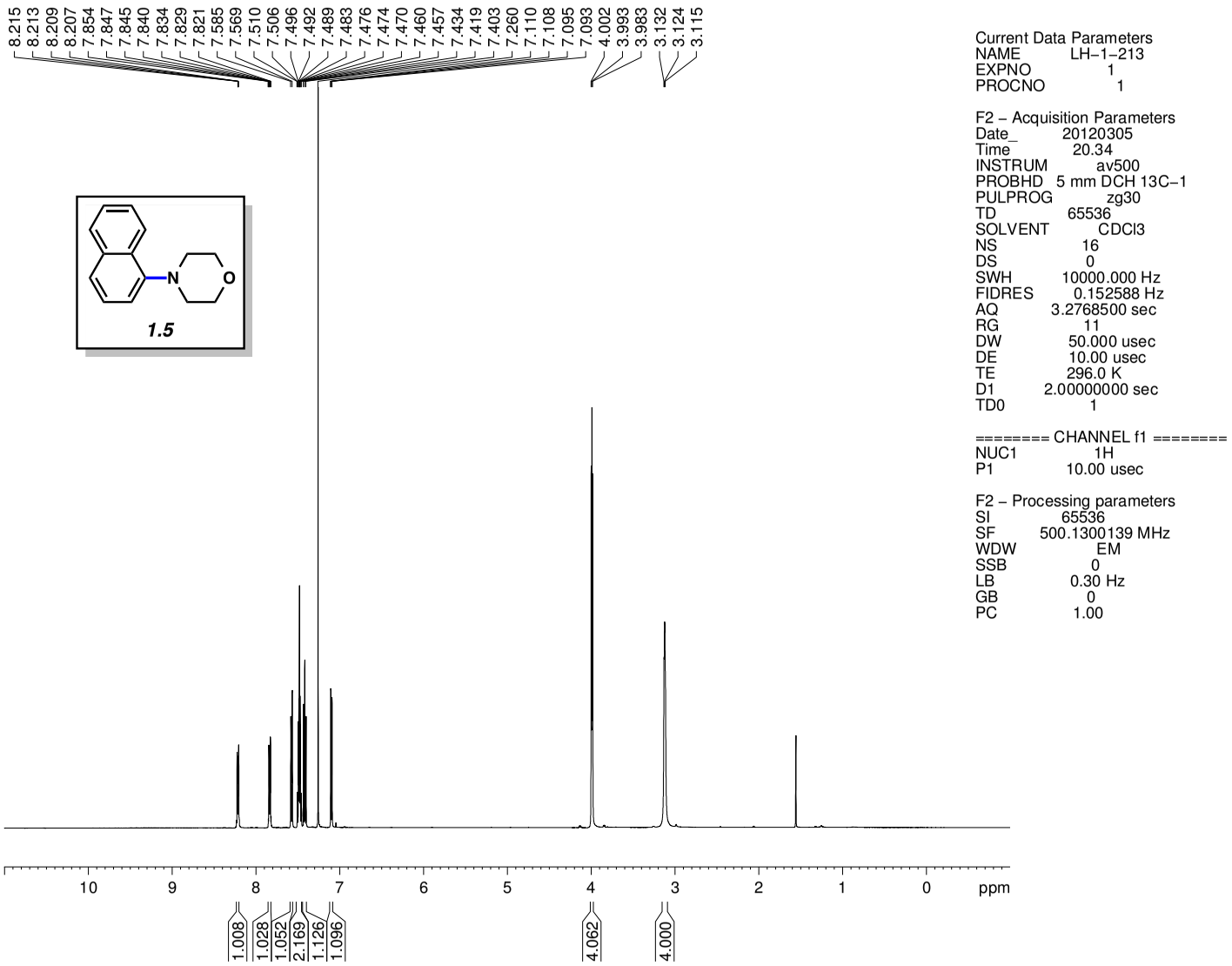

Figure A1.1 ^{1}H NMR (500 MHz, $CDCl_3$) of compound **1.5**.

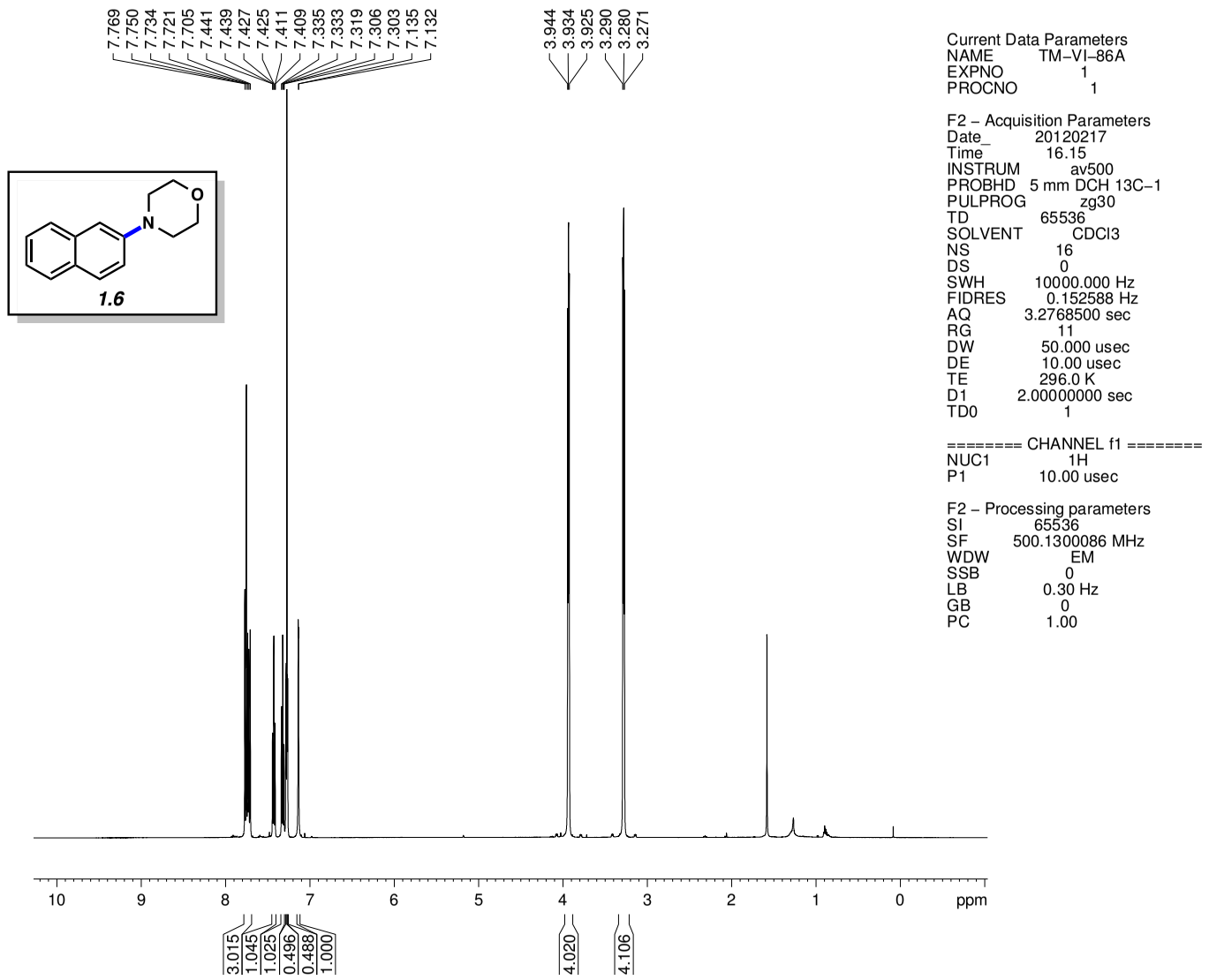

Figure A1.2 ^{1}H NMR (500 MHz, $CDCl_3$) of compound **1.6**.

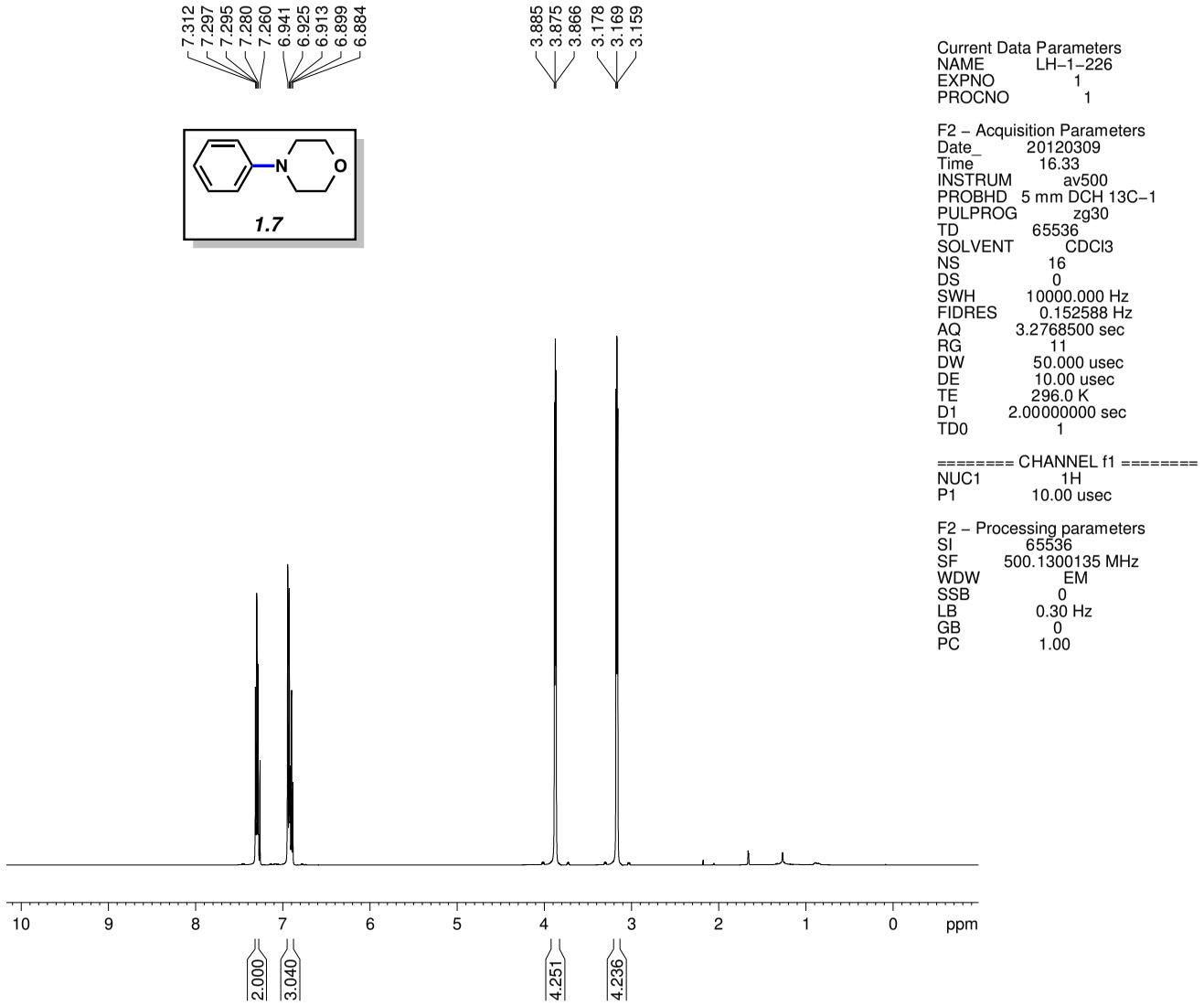

Figure A1.3 ^{1}H NMR (500 MHz, $CDCl_3$) of compound **1.7**.

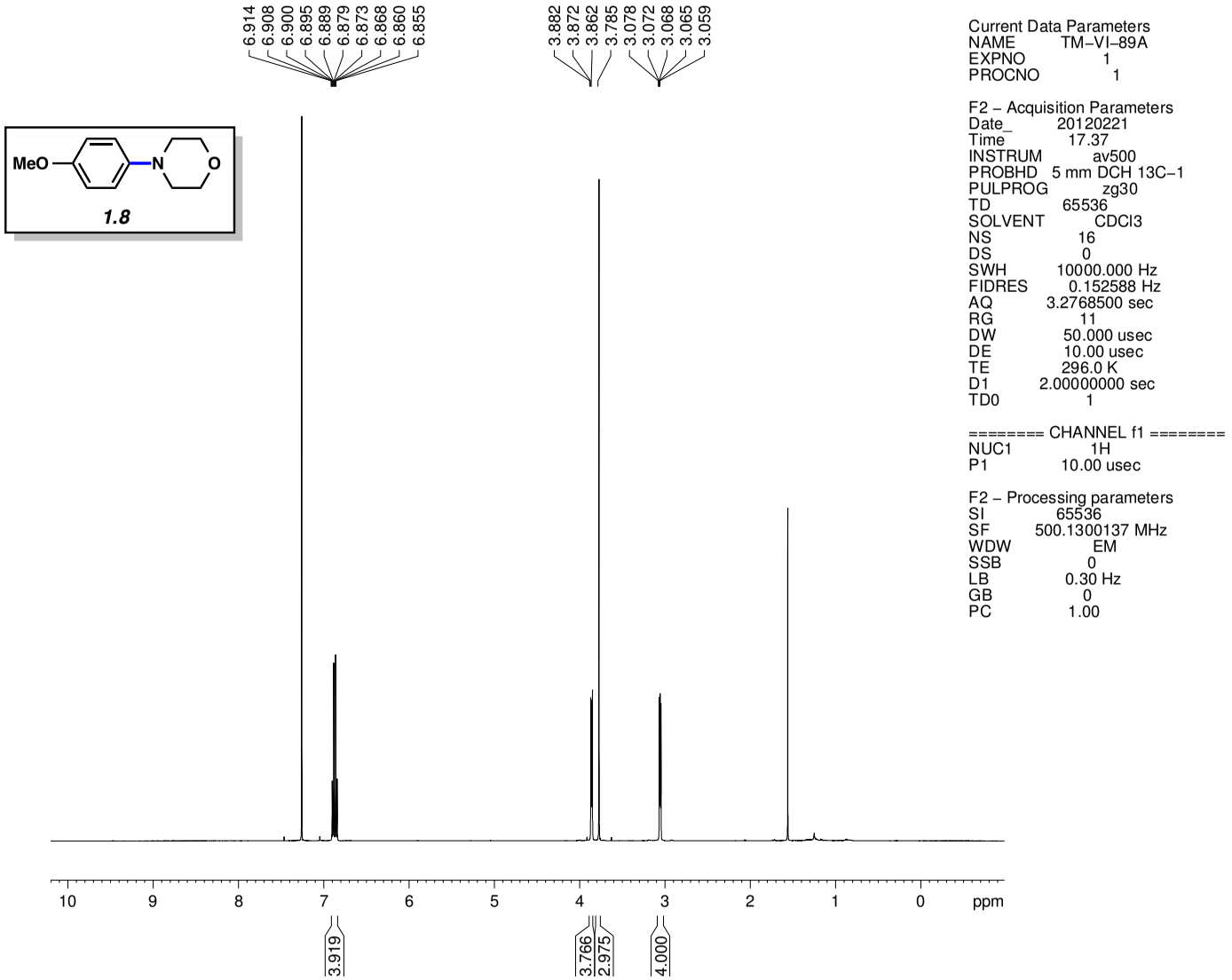

Figure A1.4 ^{1}H NMR (500 MHz, $CDCl_3$) of compound **1.8**.

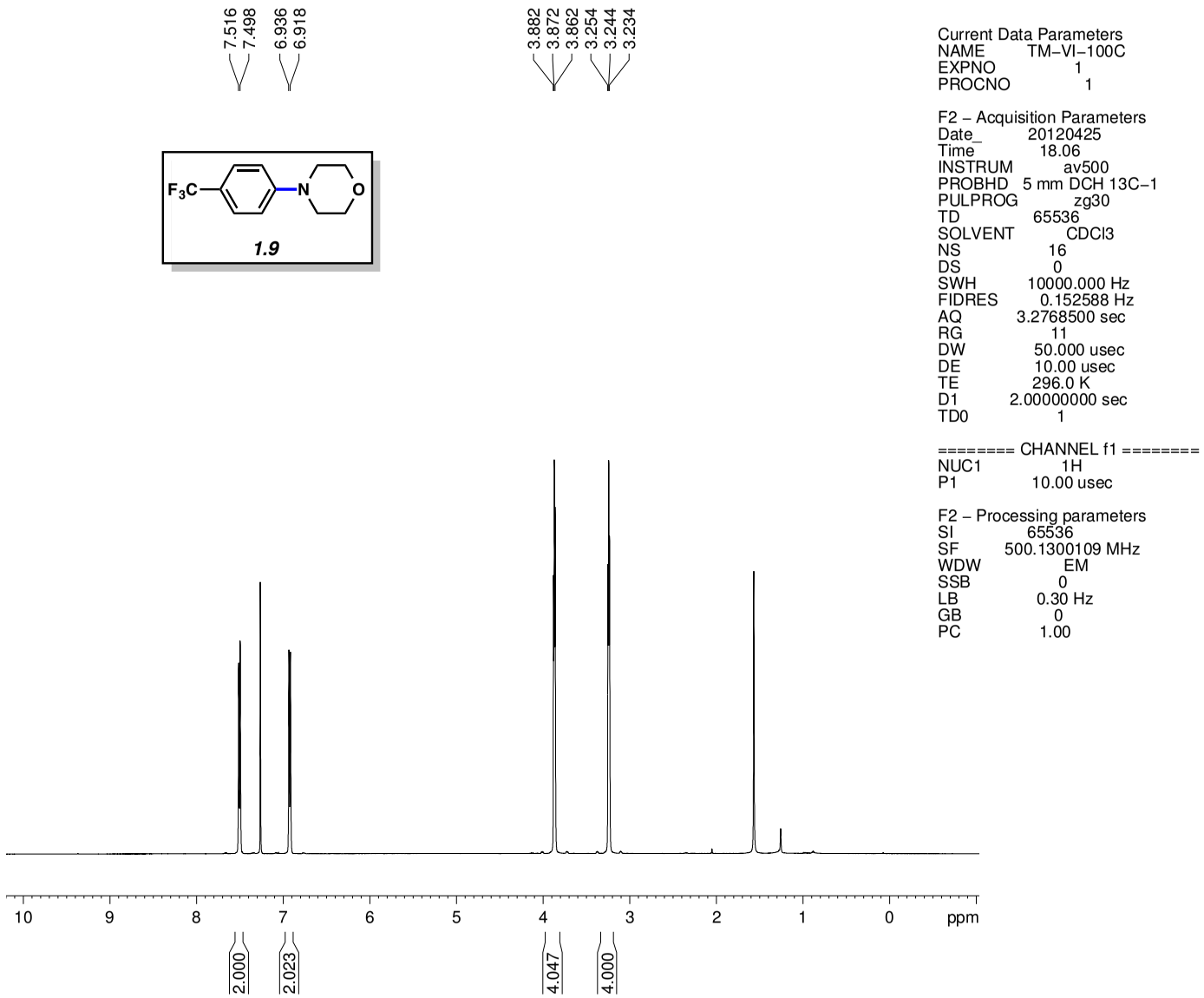

Figure A1.5 ^{1}H NMR (500 MHz, $CDCl_3$) of compound **1.9**.

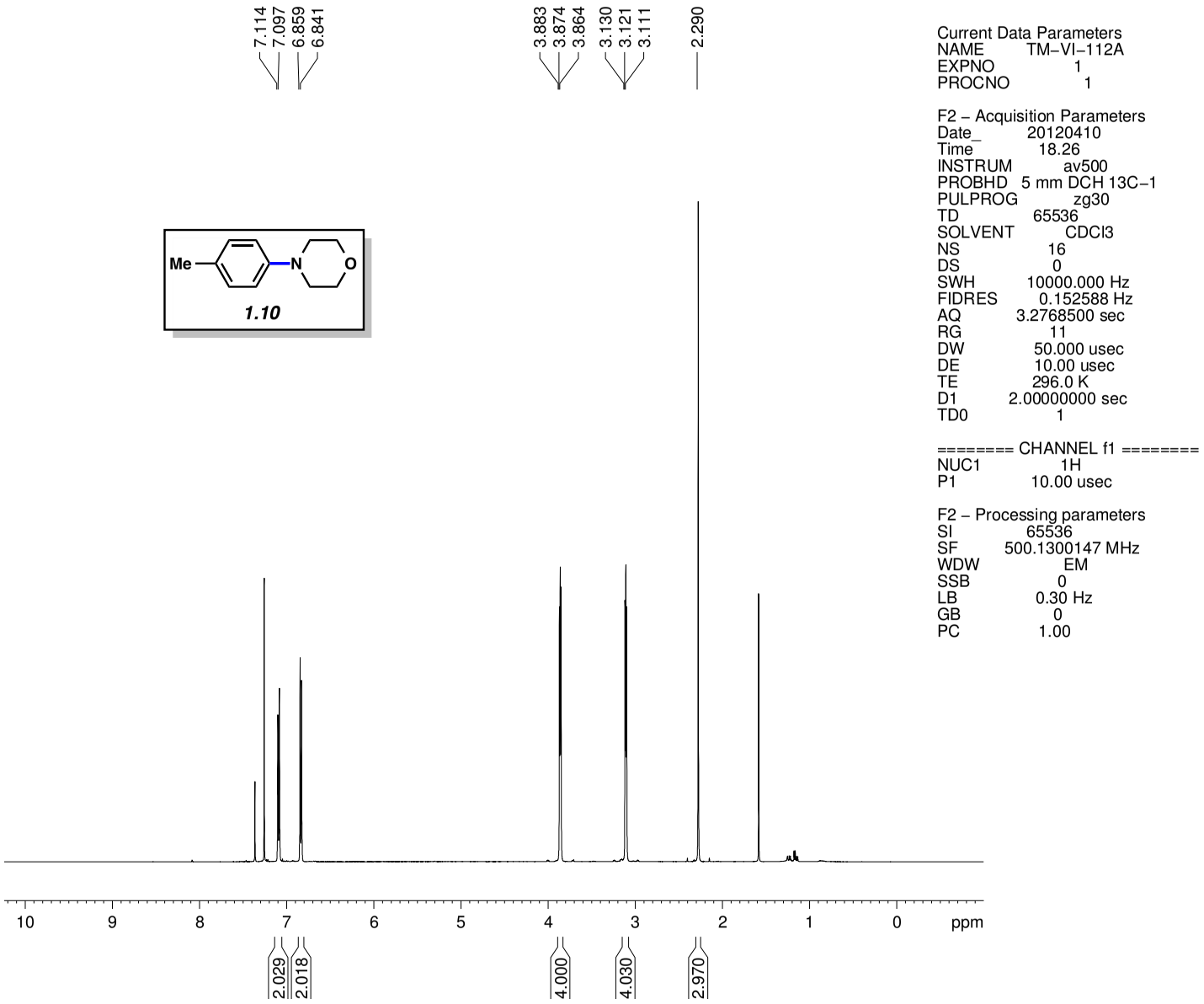

Figure A1.6 ^{1}H NMR (500 MHz, $CDCl_3$) of compound **1.10**.

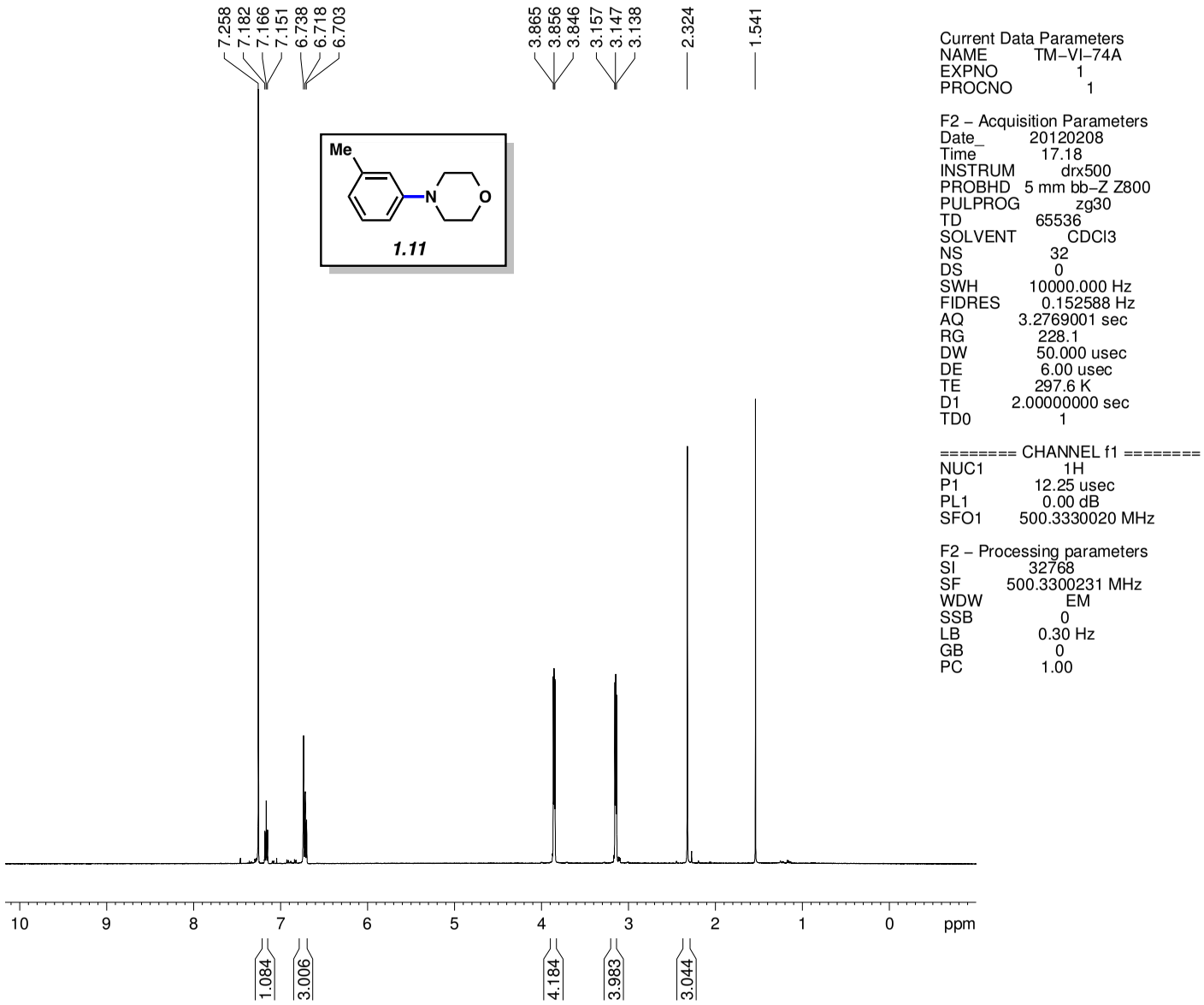

Figure A1.7 ^{1}H NMR (500 MHz, $CDCl_3$) of compound **1.11**.

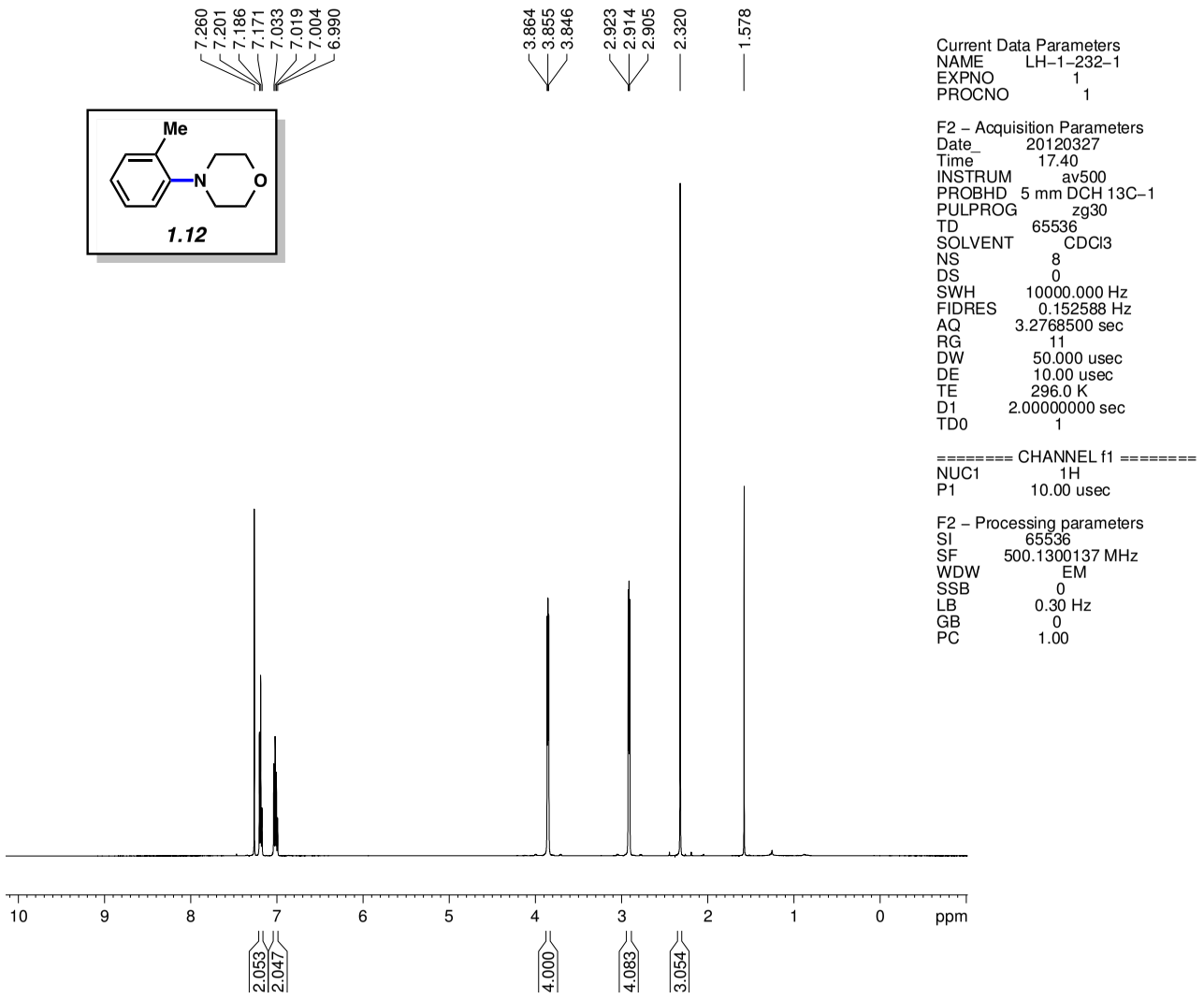

Figure A1.8 ^{1}H NMR (500 MHz, $CDCl_3$) of compound **1.12**.

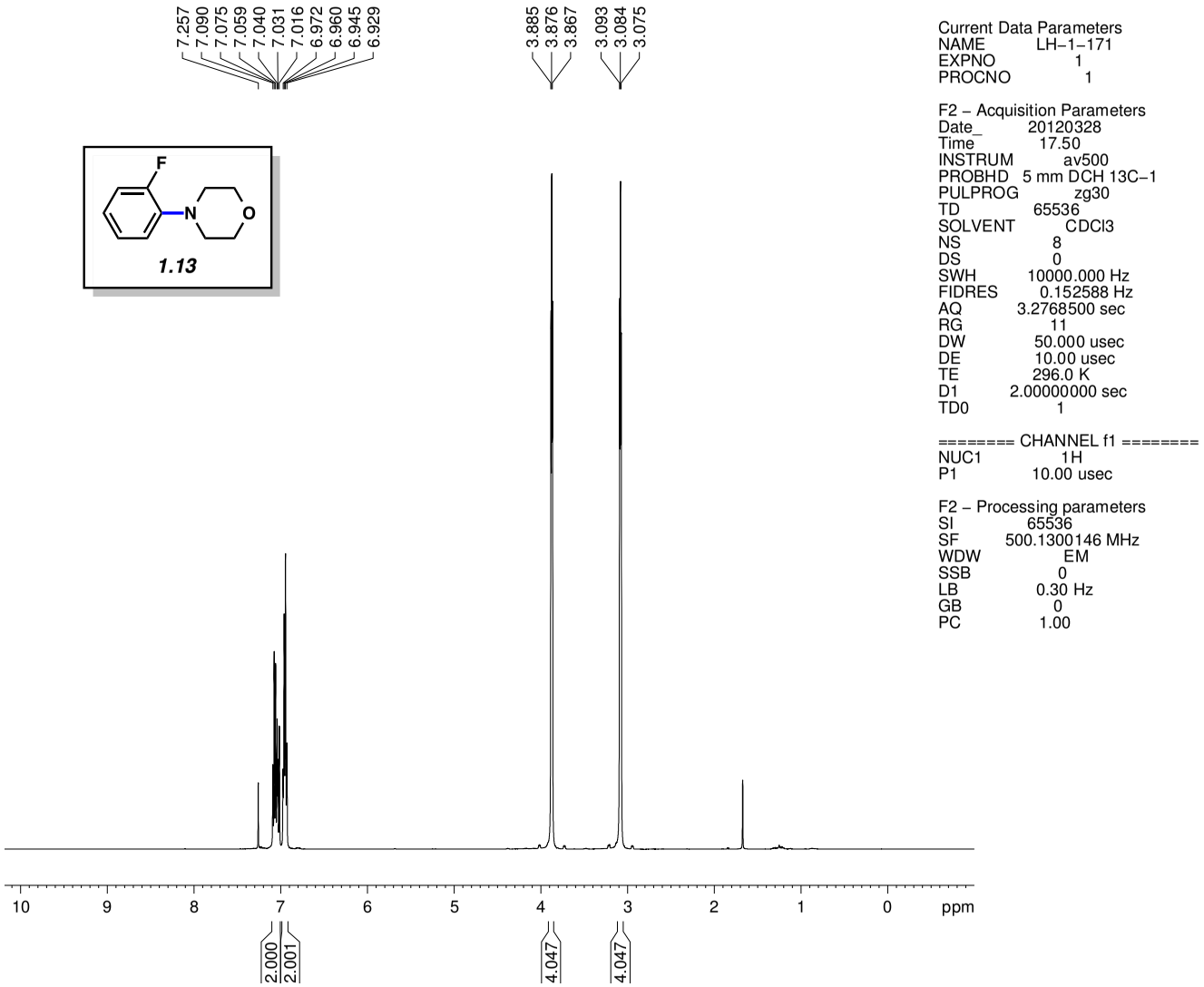

Figure A1.9 ^{1}H NMR (500 MHz, $CDCl_3$) of compound **1.13**.

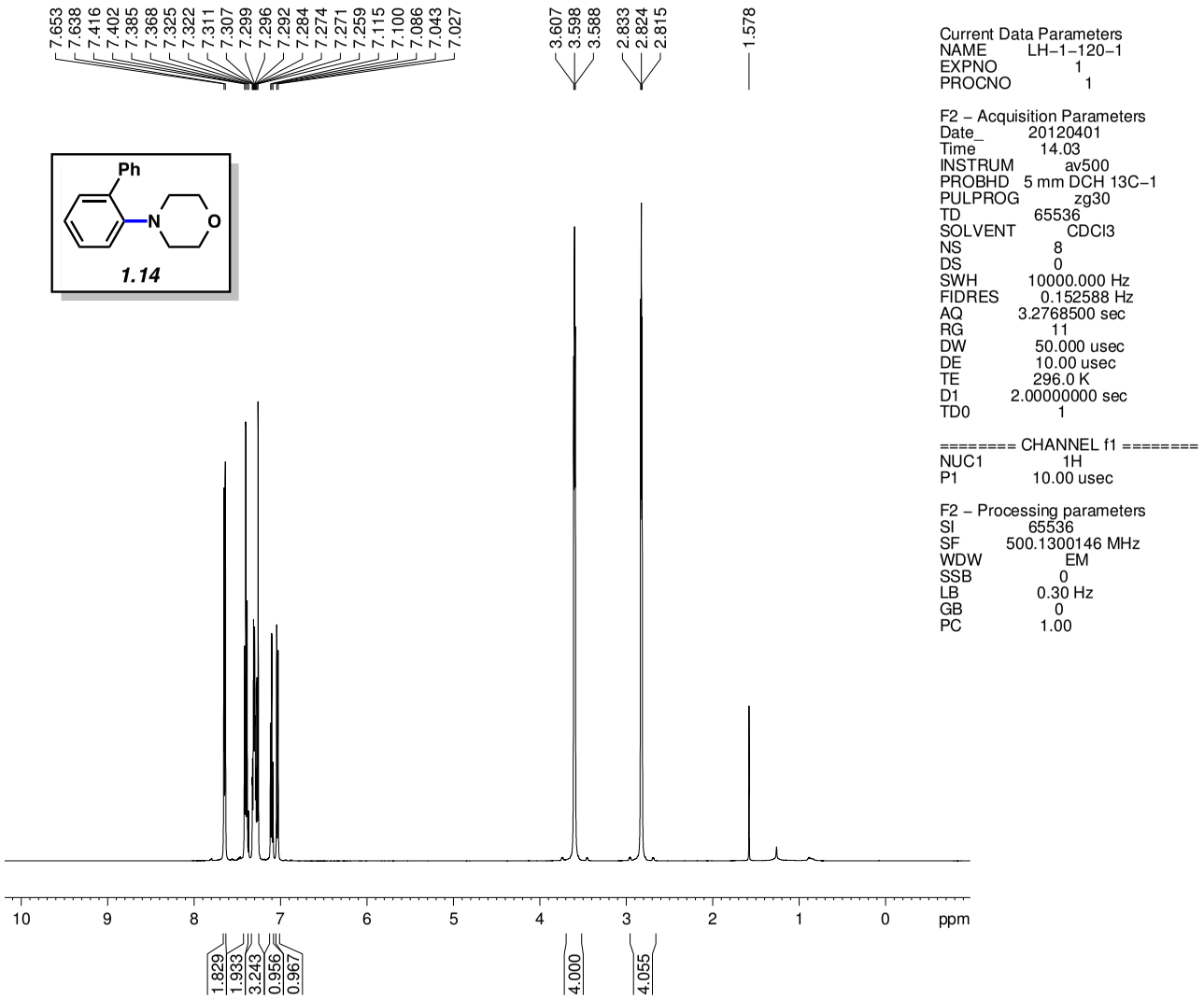

Figure A1.10 ^{1}H NMR (500 MHz, $CDCl_3$) of compound **1.14**.

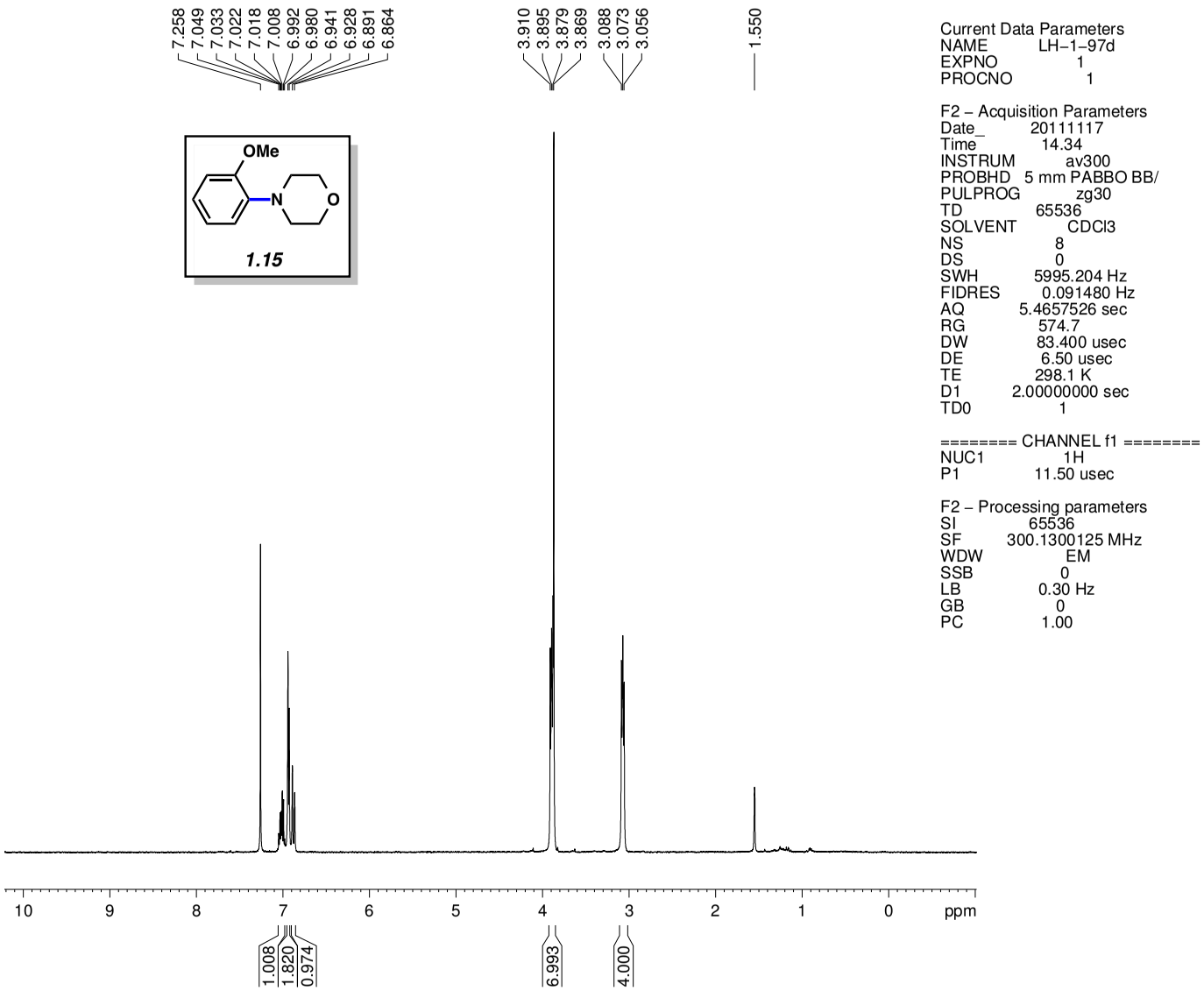

Figure A1.11 ^{1}H NMR (300 MHz, $CDCl_3$) of compound **1.15**.

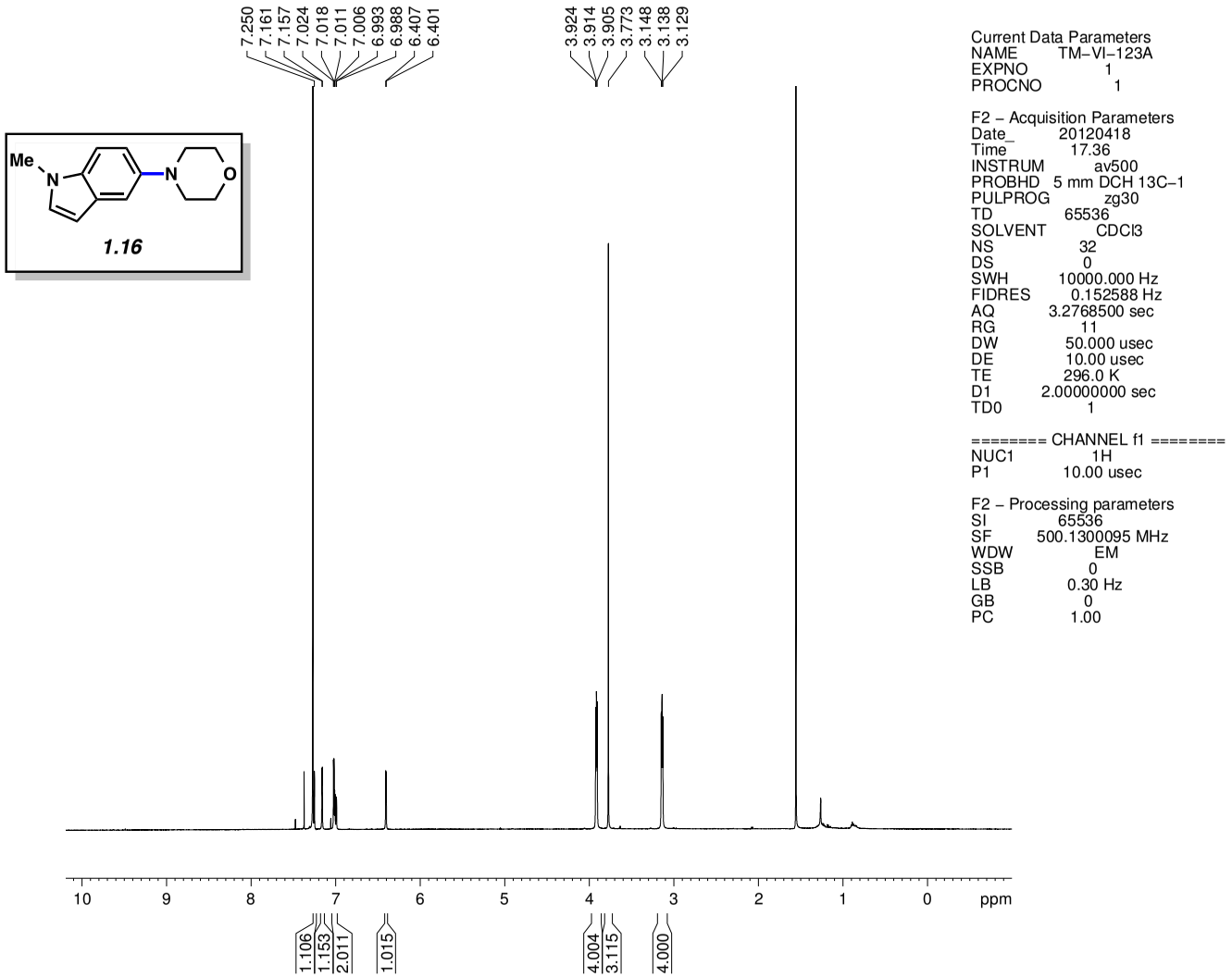

Figure A1.12 ^{1}H NMR (500 MHz, $CDCl_3$) of compound **1.16**.

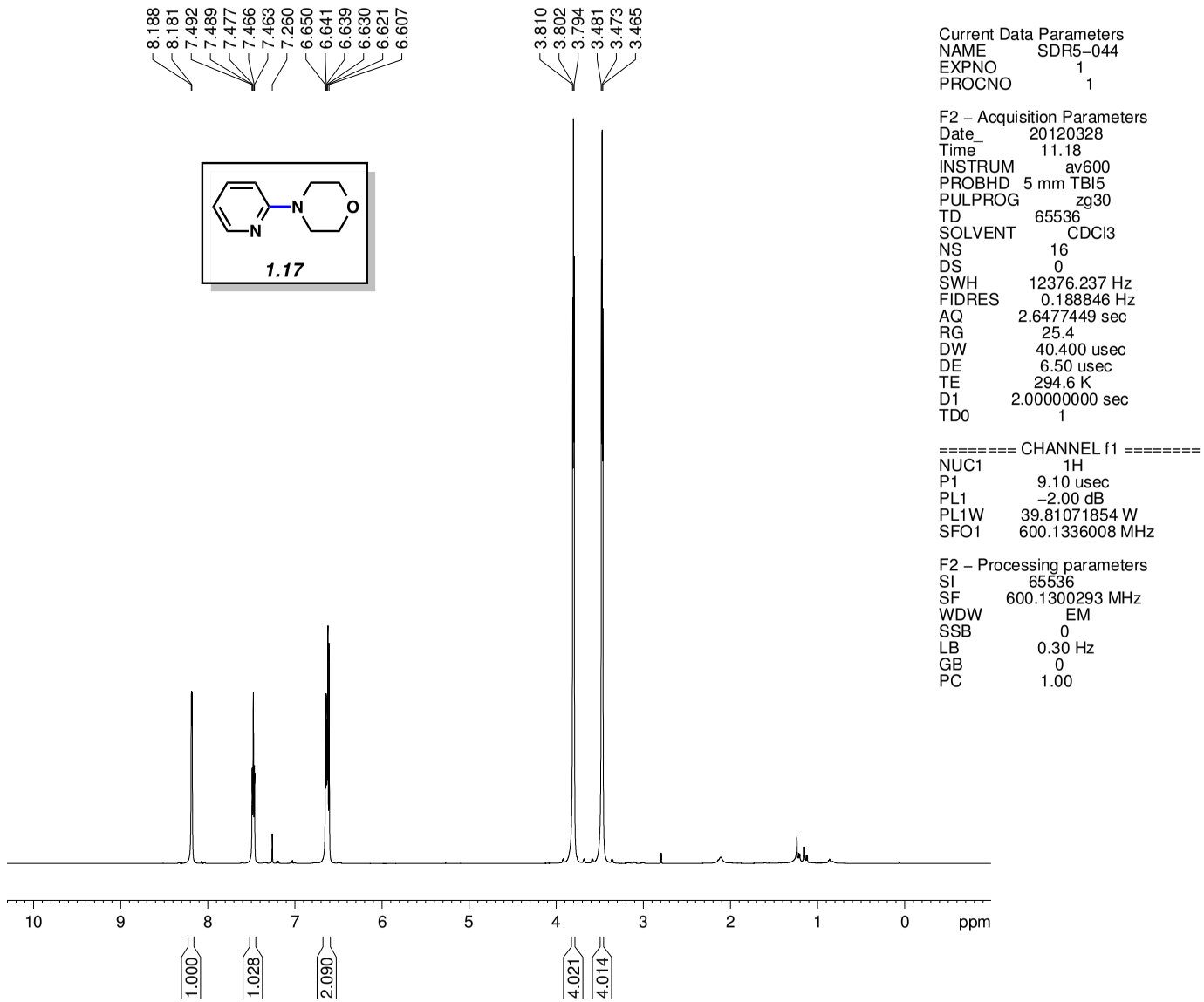

Figure A1.13 ^{1}H NMR (600 MHz, $CDCl_3$) of compound **1.17**.

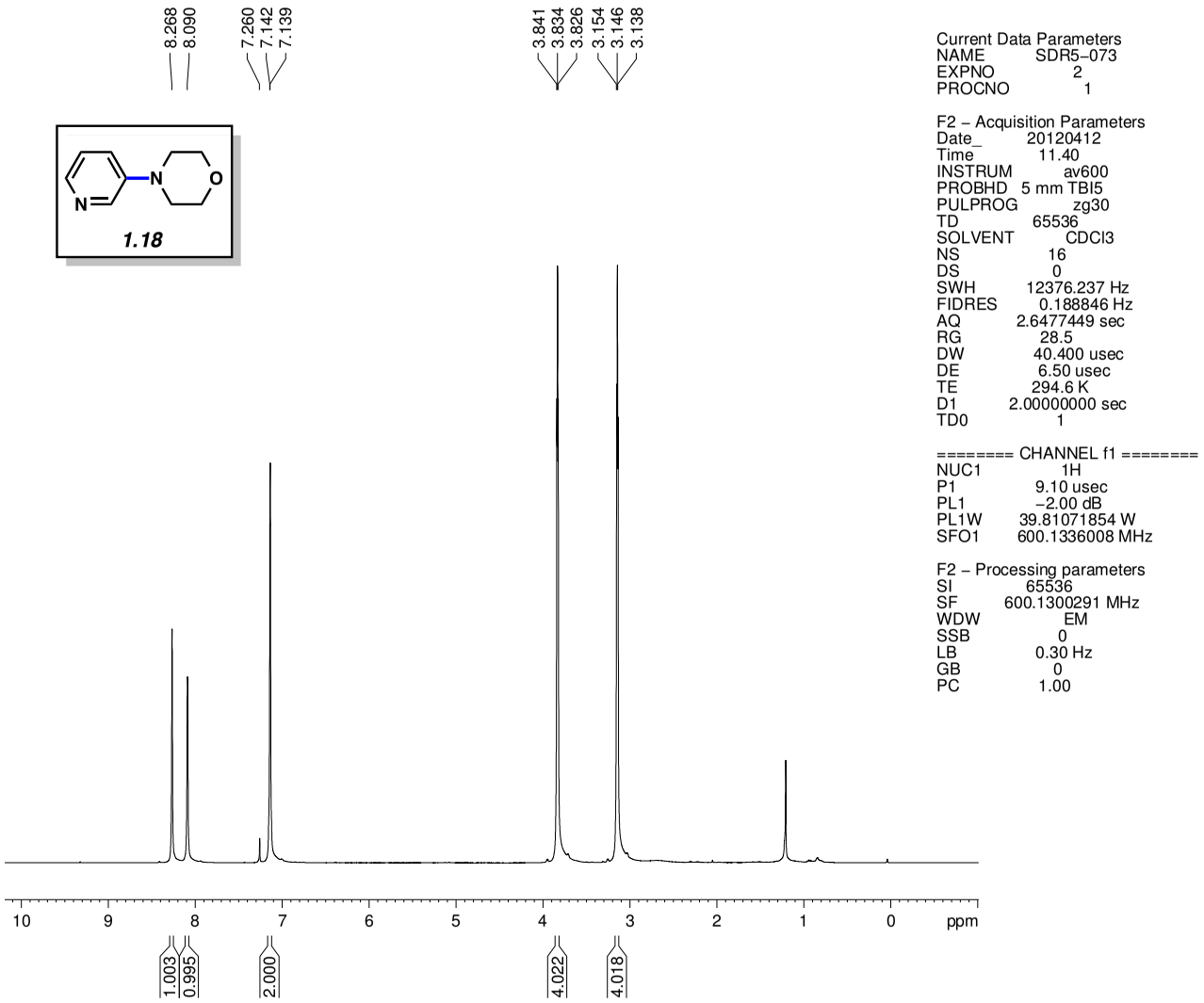

Figure A1.14 ^{1}H NMR (600 MHz, $CDCl_3$) of compound **1.18**.

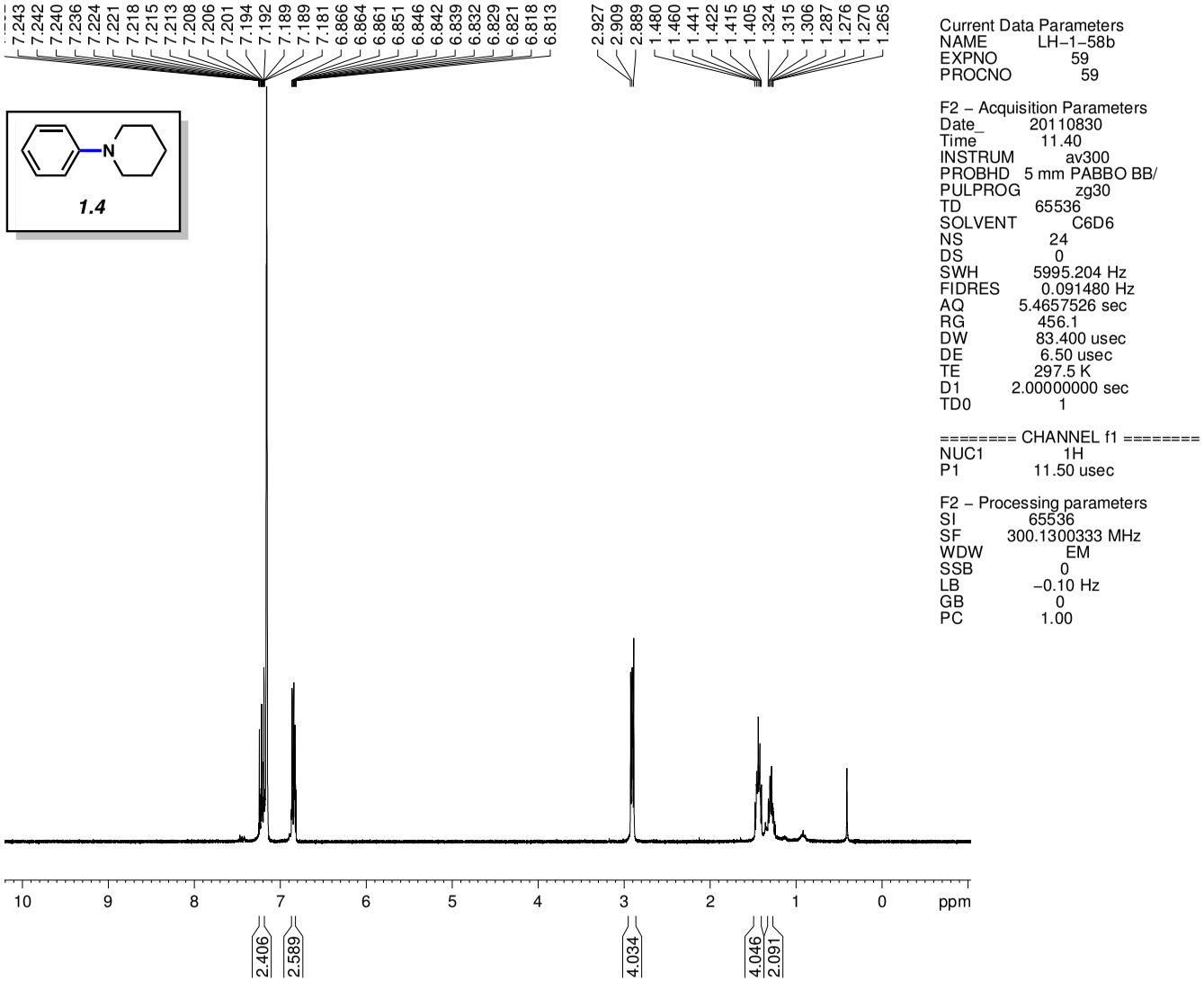

Figure A1.15 ^{1}H NMR (300 MHz, C_6D_6) of compound **1.4**.

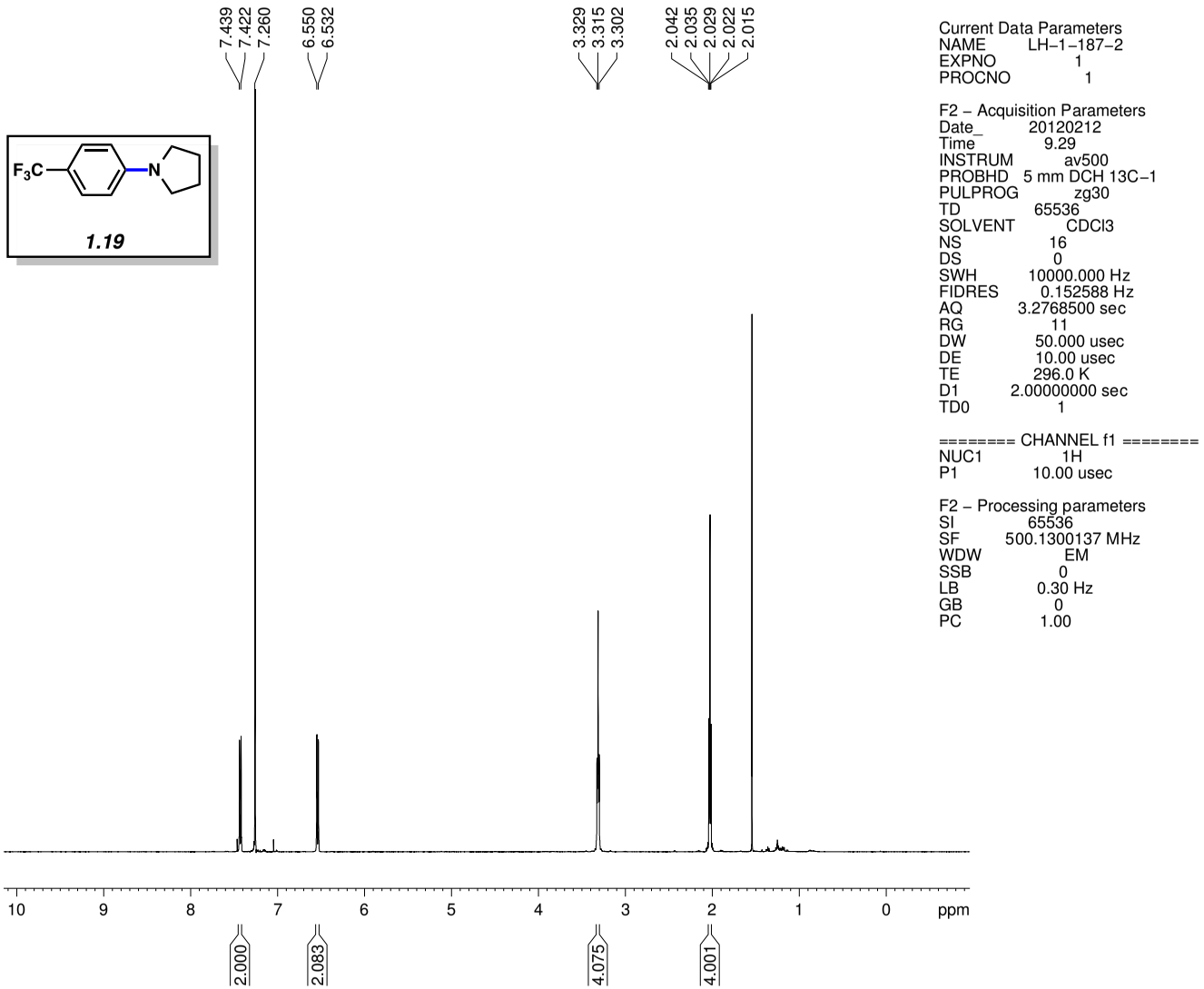

Figure A1.16 ^{1}H NMR (500 MHz, $CDCl_3$) of compound **1.19**.

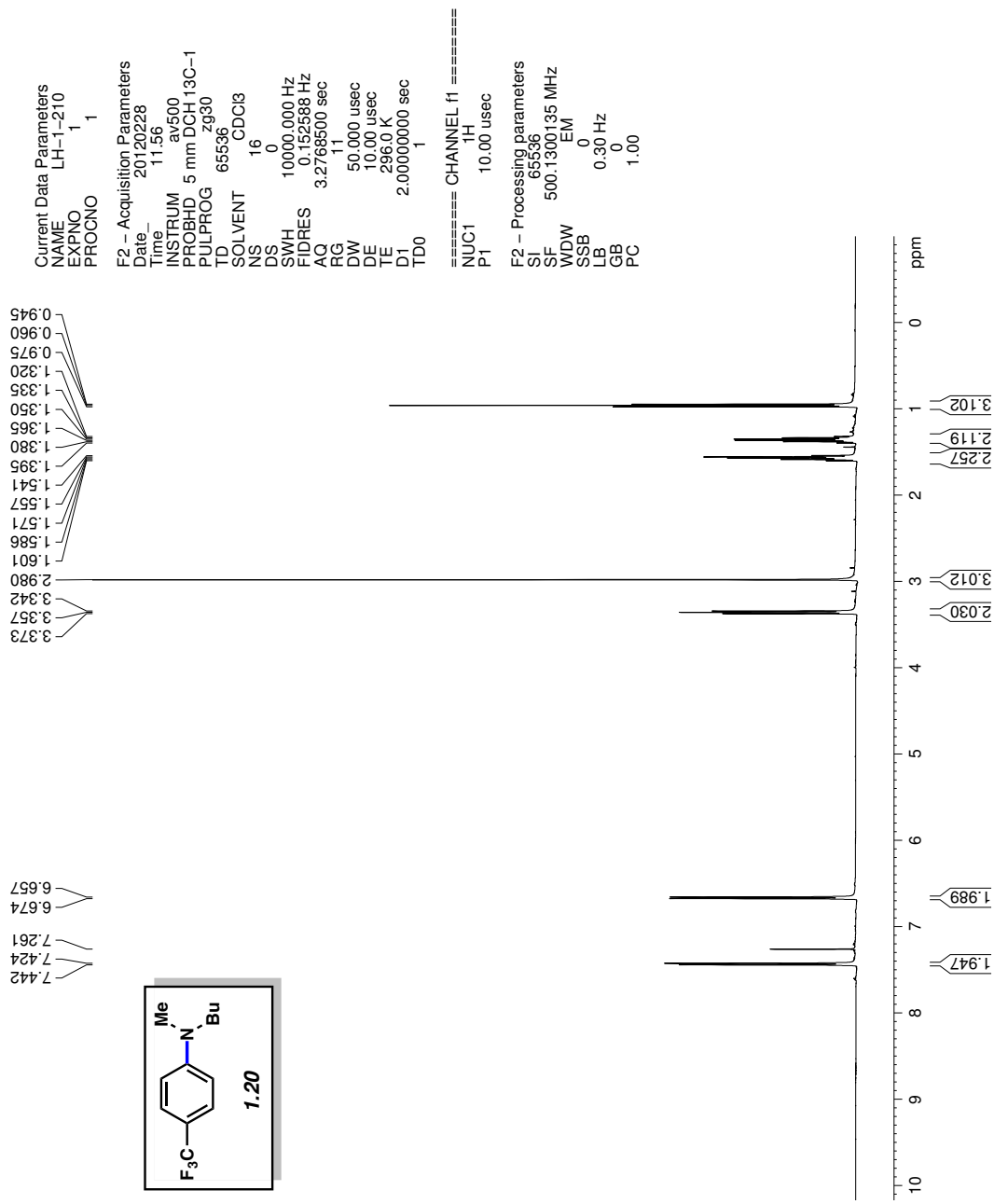

Figure A1.17 ^{1}H NMR (500 MHz, $CDCl_3$) of compound **1.20**.

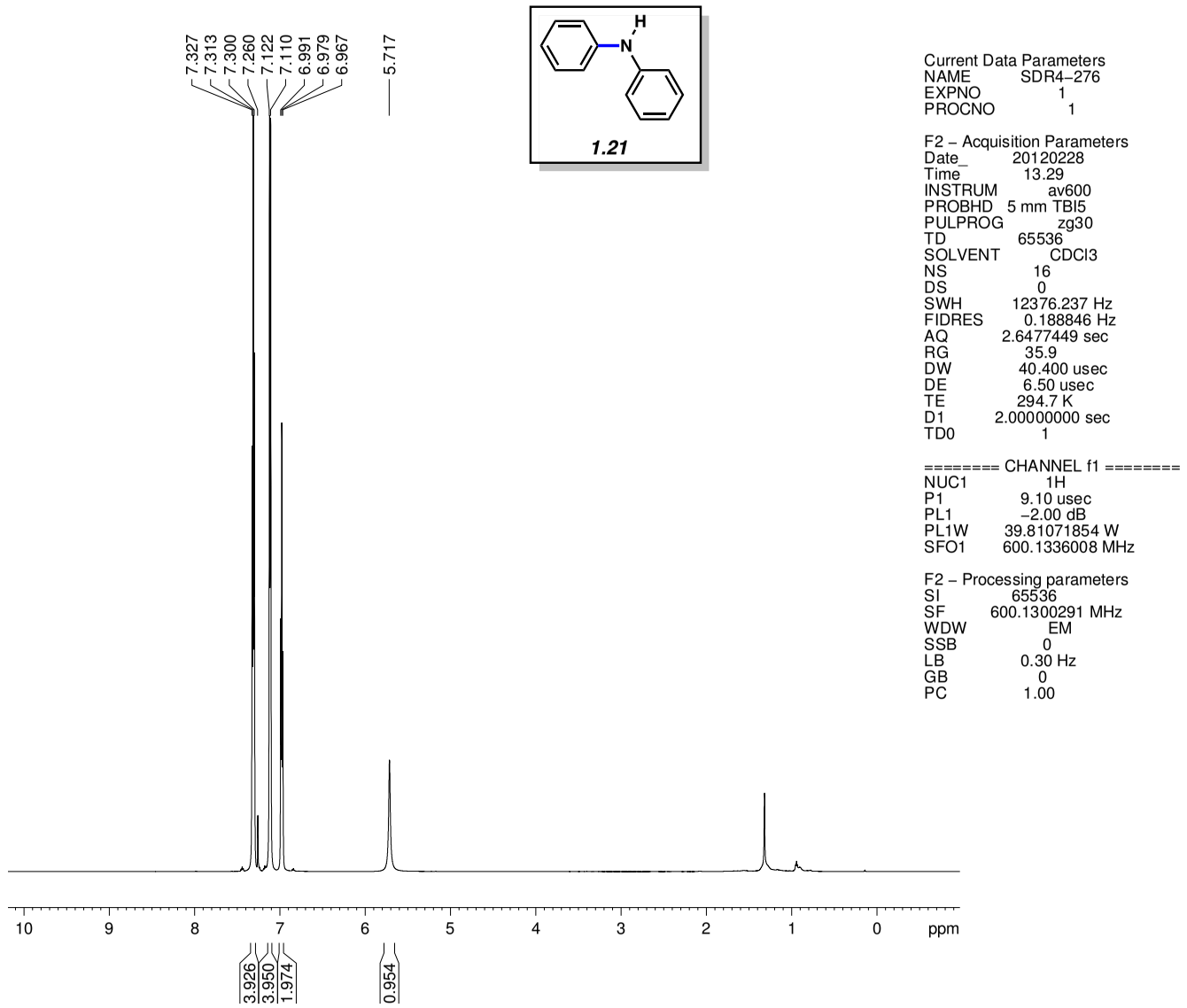

Figure A1.18 ^{1}H NMR (600 MHz, $CDCl_3$) of compound **1.21**.

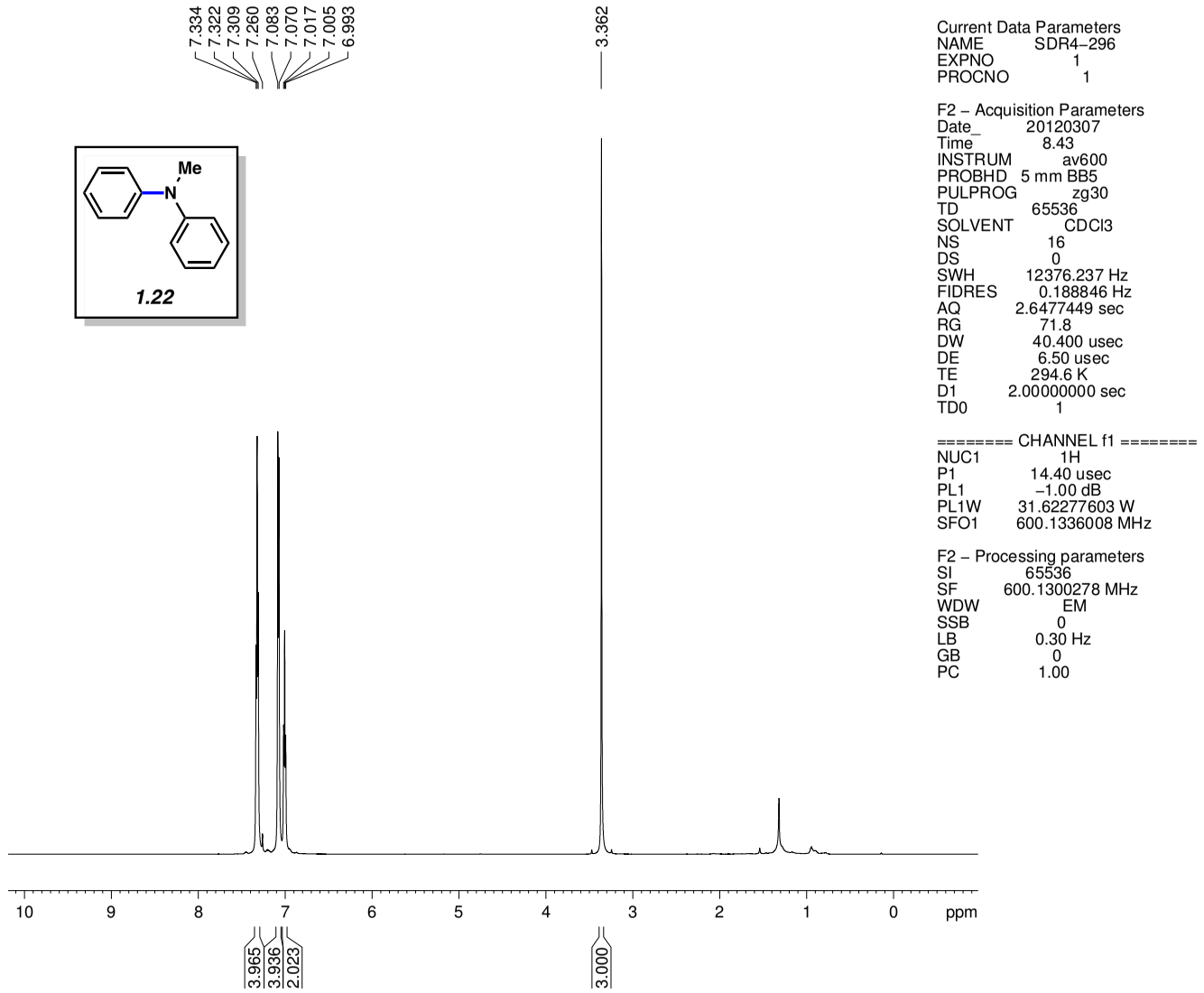

Figure A1.19 ^{1}H NMR (600 MHz, $CDCl_3$) of compound **1.22**.

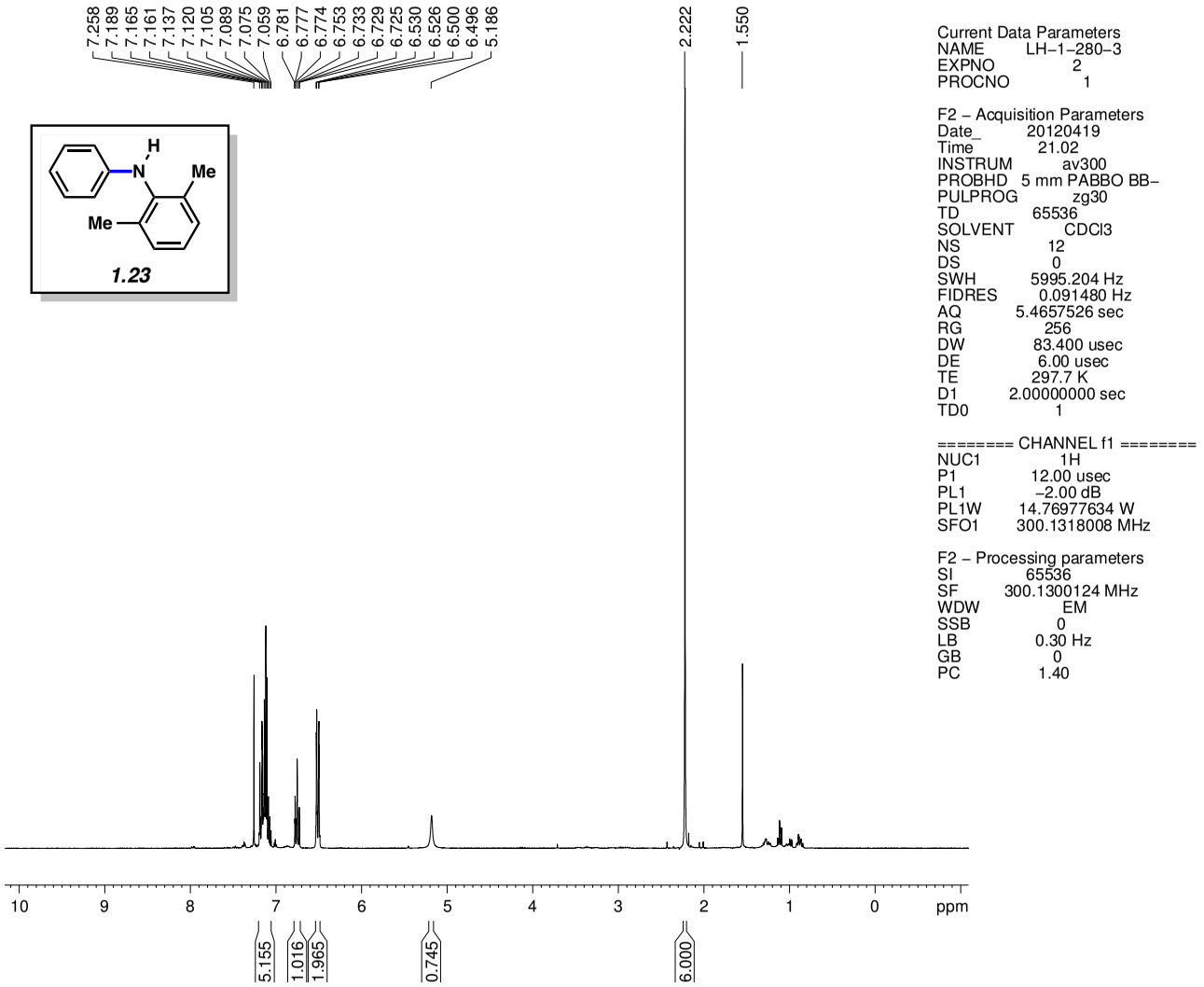

Figure A1.20 ^{1}H NMR (300 MHz, $CDCl_3$) of compound **1.23**.

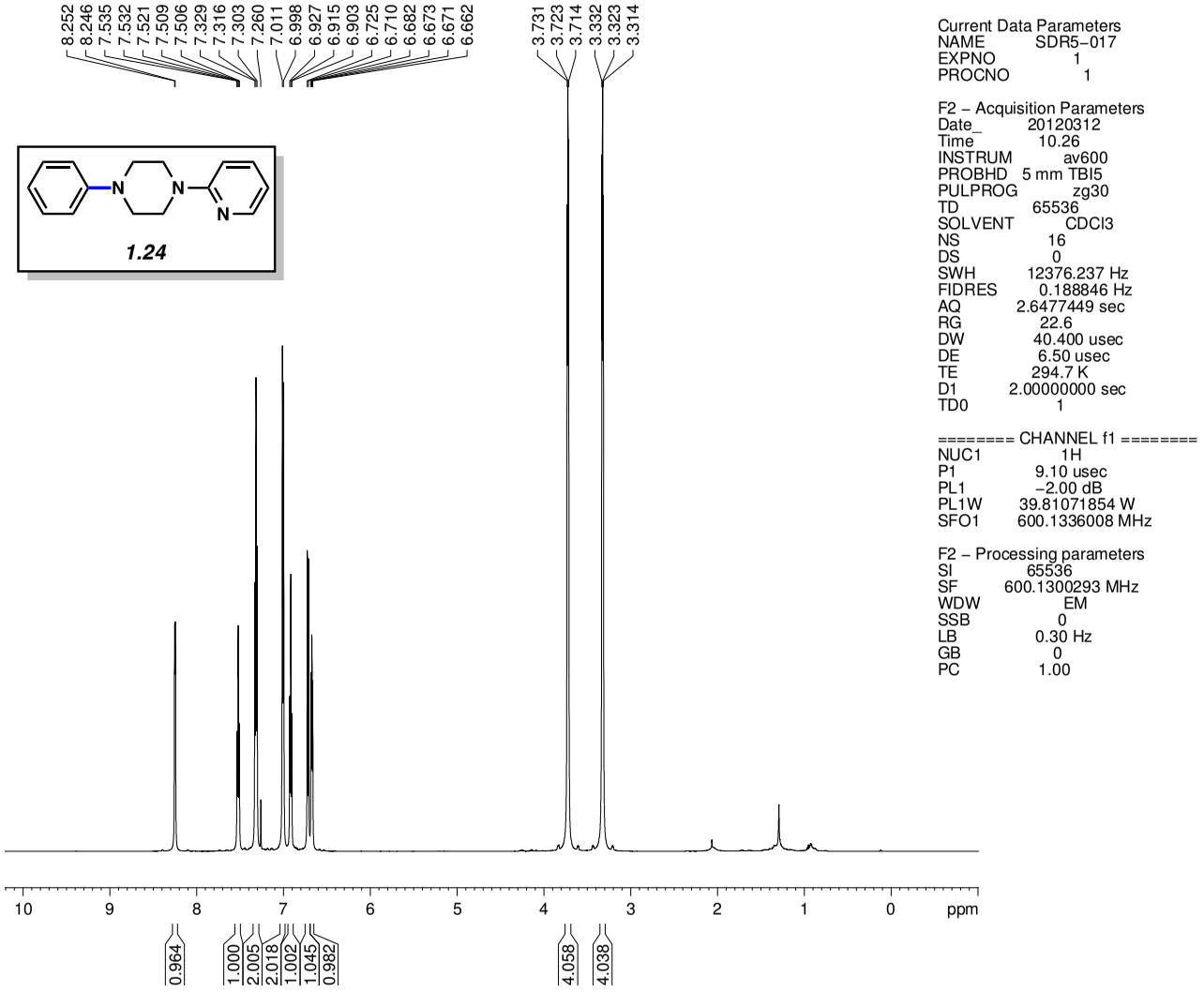

Figure A1.21 ^{1}H NMR (600 MHz, $CDCl_3$) of compound **1.24**.

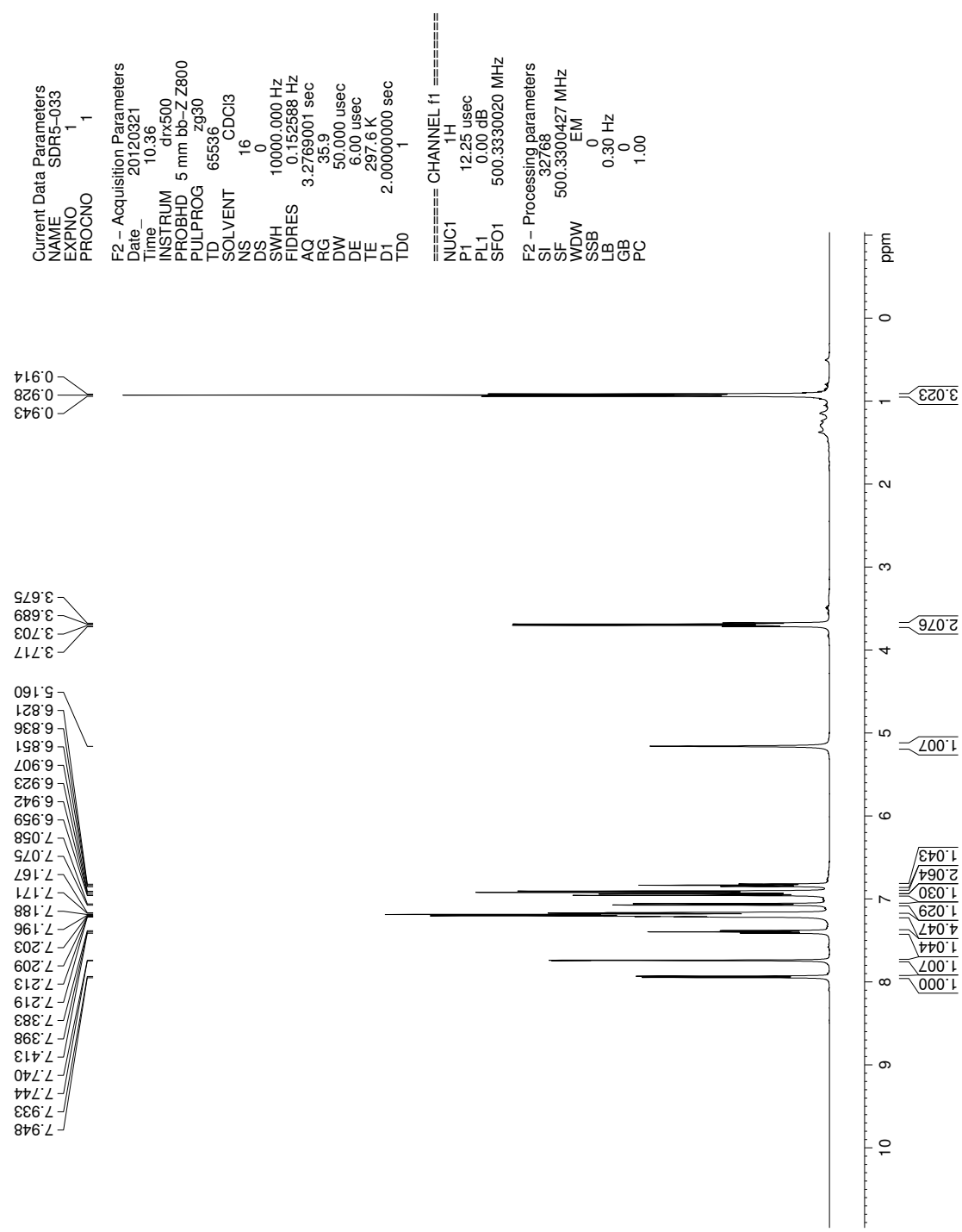

Figure A1.22 ^{1}H NMR (500 MHz, $CDCl_3$) of compound **1.25**.

1.8. Notes and References

(1) For recent reviews regarding the cross-coupling of phenolic derivatives, see: (a) Rosen, B. M.; Quasdorf, K. W.; Wilson, D. A.; Zhang, N.; Resmerita, A.-M.; Garg, N. K.; Percec, V. *Chem. Rev.* **2011**, *111*, 1346–1416. (b) Li, B.-J.; Yu, D.-G.; Sun, C.-L.; Shi, Z.-J. *Chem. Eur. J.* **2011**, *17*, 1728–1759. (c) Yu, D.-G.; Li, B.-J.; Shi, Z.-J. *Acc. Chem. Res.* **2010**, *43*, 1486–1495. (d) Knappke, C. E. I.; Jacobi von Wangelin, A. *Angew. Chem. Int. Ed.* **2010**, *49*, 3568–3570. (e) Gooßen, L. J.; Gooßen, K.; Stanciu, C. *Angew. Chem. Int. Ed.* **2009**, *48*, 3569–3571.

(2) (a) Snieckus, V. *Chem. Rev.* **1990**, *90*, 879–933. (b) Hartung, C. G.; Snieckus, V. In *Modern Arene Chemistry;* Astruc, D., Ed.; Wiley–VCH: New York, 2002; pp 330–367. (c) Macklin, T.; Snieckus, V. In *Handbook of C–H Transformations*; Dyker, G., Ed.; Wiley–VCH: New York, 2005; pp 106–119. (d) Smith, M. B.; March, J. In *March's Advanced Organic Chemistry;* 6th ed.; John Wiley & Sons, Inc.; New Jersey; 2007; pp 670. (e) Macklin, T. K.; Snieckus, V. *Org. Lett.* **2005**, *7*, 2519–2522.

(3) Aryl carbamates may also be *ortho*-functionalized through transition metal-catalyzed processes; see: (a) Bedford, R. B.; Webster, R. L.; Mitchell, C. J. *Org. Biomol. Chem.* **2009**, *7*, 4853–4857. (b) Zhao, X.; Yeung, C. S.; Dong, V. M. *J. Am. Chem. Soc.* **2010**, *132*, 5837–5844. (c) Nishikata, T.; Abela, A. R.; Huang, S.; Lipshutz, B. H. *J. Am. Chem. Soc.* **2010**, *132*, 4978–4979. (d) Yamazaki, K.; Kawamorita, K.; Ohmiya, H.; Sawamura, M. *Org. Lett.* **2010**, *12*, 3978–3981. (e) Feng, C.; Loh, T.-P. *Chem. Commun.* **2011**, *47*, 10458–10460. (f) Gong, T.-J.; Xiao, B.; Liu, Z.-J.; Wan, J.; Xu, J.; Luo, D.-F.; Fu, Y.; Liu, L. *Org. Lett.* **2011**, *13*, 3235–3237.

(4) For the use of aryl carbamates in C–C bond forming processes, see: (a) Quasdorf, K. W.; Riener, M.; Petrova, K. V.; Garg, N. K. *J. Am. Chem. Soc.* **2009**, *131*, 17748–17749. (b) Antoft-Finch, A.; Blackburn, T.; Snieckus, V. *J. Am. Chem. Soc.* **2009**, *131*, 17750–17752. (c) Xi, L.; Li, B.-J.; Wu, Z.-H.; Lu, X.-Y.; Guan, B.-T.; Wang, B.-Q.; Zhao, K.-Q.; Shi, Z.-J. *Org. Lett.* **2010**, *12*, 884–887. (d) Yoshikai, N.; Matsuda, H.; Nakamura, E. *J. Am. Chem. Soc.* **2009**, *131*, 9590–9599. (e) Quasdorf, K. W.; Antoft-Finch, A.; Liu, P.; Silberstein, A. L.; Komaromi, A.; Blackburn, T.; Ramgren, S. D.; Houk, K. N.; Snieckus, V.; Garg, N. K. *J. Am. Chem. Soc.* **2011**, *133*, 6352–6363. (f) Baghbanzadeh, M.; Pilger, C.; Kappe, C. O. *J. Org. Chem.* **2011**, *76*, 1507–1510. (g) Dallaire, C.; Kolber, I.; Gingras, M. *Org. Synth.* **2002**, *78*, 42. (h) Sengupta, S.; Leite, M.; Raslan, D. S.; Quesnelle, C.; Snieckus, V. *J. Org. Chem.* **1992**, *57*, 4066–4068.

(5) For the use of aryl sulfamates in C–C bond forming processes, see: (a) Civicos, J. F.; Gholinejad, M.; Alonso, D. A.; Najera, C. *Chem. Lett.* **2011**, *40*, 907–909. (b) Shirbin, S. J.; Boughton, B. A.; Zammit, S. C.; Zanatta, S. D.; Marcuccio, S. M.; Hutton, C. A.; Williams, S. J. *Tetrahedron Lett.* **2010**, *51*, 2971–2974. (c) Albaneze-Walker, J.; Raju, R.; Vance, J. A.; Goodman, A. J.; Reeder, M. R.; Liao, J.; Maust, M. T.; Irish, P. A.; Espino, P.; Andrews, D. R. *Org. Lett.* **2009**, *11*, 1463–1466. (d) Ackermann, L.; Barfüsser, S.; Pospech, J. *Org. Lett.* **2010**, *12*, 724–726. (e) Leowanawat, P.; Zhang, N.; Resmerita, A.-M.; Rosen, B. M.; Percec, V. *J. Org. Chem.* **2011**, *76*, 9946–9955. (f) When, P. M.; Du Bois, J. *Org. Lett.* **2005**, *7*, 4685–4688. (g) Chen, G.-J.; Han, F.-S. *Eur. J. Org. Chem.* **2012**, 3575–3579; (h) Zhang, N.; Hoffman, D. J.; Gutsche, N.; Gupta, J.; Percec, V. *J. Org. Chem.* **2012**, *77*, 5956–5964; see also references 2e, 4a, 4e, and 4f.

(6) For examples of sulfamate and carbamate amination, see: (a) Mesganaw, T.; Silberstein, A. L.; Ramgren, S. D.; Fine Nathel, N. F.; Hong, X.; Liu, P.; Garg, N. K. *Chem. Sci.* **2011**, *2*, 1766–1771. (b) Ramgren, S. D.; Silberstein, A. L.; Yang, Y.; Garg, N. K. *Angew. Chem. Int. Ed.* **2011**, *50*, 2171–2173. (c) Ackermann, L.; Sandmann, R.; Song, W. *Org. Lett.* **2011**, *13*, 1784–1786.

(7) For examples of the amination of aryl sulfonates, see: (a) Hamann, B. C.; Hartwig, J. F. *J. Am. Chem. Soc.* **1998**, *120*, 7369–7370. (b) Roy, A. H.; Hartwig, J. F. *J. Am. Chem. Soc.* **2003**, *125*, 8704–8705. (c) Ogata, T.; Hartwig, J. F. *J. Am. Chem. Soc.* **2008**, *130*, 13848–13849. (d) Gao, C.-Y.; Yang, L.-M. *J. Org. Chem.* **2008**, *73*, 1624–1627. (e) Fors, B. P.; Watson, D. A.; Biscoe, M. R.; Buchwald, S. L. *J. Am. Chem. Soc.* **2008**, *130*, 13552–13554. (f) So, C. M.; Zhou, Z.; Lau, C. P.; Kwong, F. Y. *Angew. Chem. Int. Ed.* **2008**, *47*, 6402–6406.

(8) For the amination of aryl methyl ethers, see: Tobisu, M.; Shimasaki, T.; Chatani, N. *Chem. Lett.* **2009**, *38*, 710–711.

(9) For the amination of aryl pivalates, see: Shimasaki, T.; Tobisu, M.; Chatani, N. *Angew. Chem. Int. Ed.* **2010**, *49*, 2929–2932.

(10) $Ni(cod)_2$ is commercially available from Strem Chemicals Inc. or Sigma-Aldrich (CAS # 1295-35-8). For more information on this precatalyst, see: Wender, P. A.; Smith, T. E.; Zuo, G.; Duong, H. A.; Louie, J. *Encyclopedia of Reagents for Organic Synthesis* **2006**, DOI 10.1002/047084289X.rb118.pub2

(11) (a) Fan, X.-H.; Li, G.; Yang, L. M. *J. Organomet. Chem.* **2011**, *696*, 2482–2484. (b) Gao, C.-Y.; Cao, X.; Yang, L.-M. *Org. Biomol. Chem.* **2009**, *7*, 3922–3925. (c) Manolikakes, G.; Gavryushin, A.; Knochel, P. *J. Org. Chem.* **2008**, *73*, 1429–1434. (d) Amrani, R. O.; Thomas, A.; Brenner, E.; Schneider, R.; Fort, Y. *Org. Lett.* **2003**, *5*, 2311–2314. (e) Desmarets, C.; Schneider, R.; Fort, Y. *J. Org. Chem.* **2002**, *67*, 3029–3036. (f) Gradel, B.; Brenner, E.; Schneider, R.; Fort, Y. *Tetrahedron Lett.* **2001**, *42*, 5689–5692; see also ref 8.

(12) NHC ligand **1.3** has been employed in the Ni-catalyzed amination of sulfamates and carbamates; see refs 6a and 6b.

(13) $NiCl_2$(DME) is commercially available from Strem Chemicals Inc. (CAS #29046-78-4) at an approximate cost of $32 USD/gram.

(14) Although the optimal reaction conditions shown in Table 1.1 (entries 9 and 10) are generally useful across a range of substrates, further optimization of reaction conditions for individual substrates led to improved yields. The optimized conditions and results are shown in Figures 1.2 and 1.3.

(15) (a) Yamazaki, K.; Kawamorita, S.; Ohmiya, H.; Sawamura, M. *Org. Lett.* **2010**, *12*, 3978–3981. (b) Quasdorf, K. W.; Riener, M.; Petrova, K.; Garg, N. K. *J. Am. Chem. Soc.* **2009**, *131*, 17748–17749. (c) Sengupta, S.; Leite, M.; Raslan, D. S.; Quenelle, C.; Snieckus, V. *J. Org. Chem.* **1992**, *57*, 4066–4068. (d) Zhao, Z.; Snieckus, V. *Org. Lett.* **2005**, *7*, 2523–2526. (e) Kamila, S.; Mukherjee, C.; Mondal, S. S.; De, A. *Tetrahedron* **2003**, *59* 1339–1348. (f) Bedford, R. B.; Webster, R. L.; Mitchell, C. J. *Org. Biomol. Chem.* **2009**, *7*, 4853–4857. (g) Azzena, U.; Pisano, L.; Pittalis, M. *Appl. Organomet. Chem.* **2008**, *22*, 523–528. (h) Mesganaw, T.; Silberstein, A. L.; Ramgren, S. D.; Fine Nathel, N. F.; Hong, X.; Liu, P.;

Garg, N. K. *Chem. Sci.* **2011**, *2*, 1766–1771. (i) Ramgren, S. D.; Silberstein, A. L.; Yang, Y.; Garg, N. K. *Angew. Chem. Int. Ed.* **2011**, *50*, 2171–2173.

(16) Barker, T. J.; Jarvo, E. R. *J. Am. Chem. Soc.* **2009**, *131*, 15598–15599.

(17) Desmarets, C.; Champagne, B.; Walcarius, A.; Bellouard, C.; Omar-Amrani, R.; Ahajji, A.; Fort, Y.; Schneider, R. *J. Org. Chem.* **2006**, *71*, 1351–1361.

(18) Gao, C.; Yang, L. *J. Org. Chem.* **2008**, *73*, 1624–1627.

(19) Wolfe, J. P.; Buchwald, S. L. *J. Org. Chem.* **1996**, *61*, 1133–1135.

(20) Guo, D.; Huang, H.; Xu, J.; Jiang, H.; Liu, H. *Org. Lett.* **2008**, *10*, 4513–4516.

(21) Desmarets, C.; Schneider, R.; Fort, Y. *J. Org. Chem.* **2002**, *67*, 3029–3036.

(22) Fasani, E.; Tilocca, F.; Protti, S.; Merli, D.; Albini, A. *Org. Biomol. Chem.* **2008**, ***6***, 4634–4642.

(23) Ramgren, S. D.; Silberstein, A. L.; Yang, Y.; Garg, N. K. *Angew. Chem. Int. Ed.* **2011**, *123*, 2219–2221.

(24) Wagaw, S.; Buchwald, S. L. *J. Org. Chem.* **1996**, *61*, 7240–7241.

(25) Tobisu, M.; Yasutome, A.; Yamakawa, K.; Shimasaki, T.; Chatani, N. *Tetrahedron* **2012**, *68*, 5157–5161.

(26) Brenner, E.; Schneider, R.; Fort, Y. *Tetrahedron* **1999**, *55*, 12829–12842.

CHAPTER TWO

Nickel-Catalyzed Suzuki–Miyaura Couplings in Green Solvents

Stephen D. Ramgren, Liana Hie, Yuxuan, Ye, and Neil K. Garg.

Org. Lett. **2013**, *15*, 3950–3953.

2.1 Abstract

The nickel-catalyzed Suzuki–Miyaura coupling of aryl halides and phenol-derived substrates with aryl boronic acids using green solvents, such as 2-Me-THF and *tert*-amyl alcohol, is reported. This methodology employs the commercially available and air-stable precatalyst, $NiCl_2(PCy_3)_2$, and gives biaryl products in synthetically useful to excellent yields. Using this protocol, bis(heterocylic) frameworks can be assembled efficiently.

2.2 Introduction

Transition-metal-catalyzed cross-coupling reactions are widely used in the pharmaceutical industry in both medicinal chemistry and drug manufacturing.[1] Although the use of Pd catalysis is most common, complementary approaches are highly sought after. Specifically, cost effective catalyst systems that allow for unconventional couplings to take place smoothly are of great value. Additionally, the ability to efficiently carry out cross-coupling reactions in more environmentally friendly solvents[2,3] remains an important goal of green chemistry research.[4] It should be noted that organic solvents comprise up to 85% of the waste produced from a drug synthesis.[5]

Recently, the field of nickel-catalyzed cross-coupling reactions has gained considerable attention. The low cost and high reactivity of nickel is attractive, and a range of substrates have been shown to undergo nickel-catalyzed carbon–carbon and carbon–heteroatom bond forming reactions, including halides[6] and a variety of oxygen-based electrophiles (e.g., aryl-esters,[7] -ethers,[8] -carbamates,[9] -sulfamates[10]).[11,12] Considering the promise of nickel-catalyzed couplings and the need to make industrial processes more environmentally friendly, we explored coupling reactions in green solvents. Herein, we demonstrate that a range of substrates, including heterocycles, participate in the nickel-catalyzed Suzuki–Miyaura coupling in solvents that are attractive for industrial applications (Figure 2.1).

Figure 2.1. Suzuki–Miyaura cross-coupling of aryl halides and phenol derivatives in green solvents.

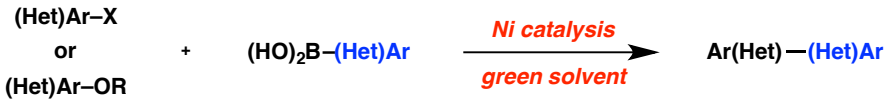

2.3 Optimization of Conditions

We initiated our efforts by examining the cross-coupling of naphthyl sulfamate **2.1** and phenylboronic acid (**2.2**) using the commercially available $NiCl_2(PCy_3)_2$ precatalyst (Table 2.1). Although solvents such as 1,4-dioxane and *N*-methyl-2-pyrrolidone (NMP), which have been deemed as enviromentally unfriendly solvents,[2] are commonly used in nickel-catalyzed cross-couplings, we were delighted to find that many other solvents may be employed in the coupling to give biaryl **2.3**. Of the >30 solvents that were surveyed, more than half gave quantitative yields of **2.3**, while many others also showed promise.[13] A subset of our findings are summarized in Table 2.1. The solvent used in our previous studies,[7c,9b,9d] toluene, gave biaryl **2.3** in

quantitative yield (entry 1). Acetone, ethyl acetate, and isopropyl acetate (entries 2–4, respectively) also gave product in comparable yields. In addition, alcohol solvents were examined. Whereas the use of *n*-BuOH proved ineffective (entry 5), *tert*-amyl alcohol was found to be an excellent solvent for the cross-coupling (entry 6). Ethereal solvents also provided biaryl **2.3** in quantitative yield (entries 7–8). Mixed results were observed for highly coordinating solvents; for example, the use of DMSO was unsuccessful (entry 9), but the use of acetonitrile led to the desired coupling. Although many solvents could be employed, we opted to pursue *tert*-amyl alcohol and 2-Me-THF (entries 6 and 8, respectively) for further studies.[3,14]

Table 2.1. Survey of Solvents in the Suzuki–Miyaura Coupling.[a]

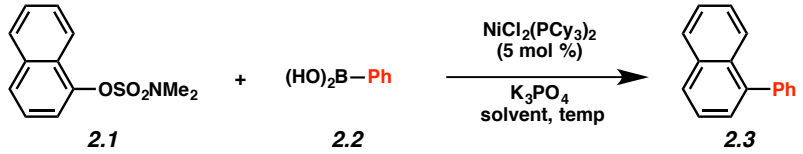

2.1 *2.2* *2.3*

entry	solvent, temp	yield[b]	entry	solvent, temp	yield[b]
1	toluene, 110 °C	100%	6	*t*-amyl alcohol, 100 °C	100%
2	acetone, 75 °C	96%	7	MTBE, 80 °C	100%
3	EtOAc, 100 °C	100%	8	2-Me-THF, 80 °C	100%
4	*i*-PrOAc, 110 °C	100%	9	DMSO, 110 °C	0%
5	*n*-BuOH, 110 °C	0%	10	acetonitrile, 100 °C	99%

[a] Conditions: $NiCl_2(PCy_3)_2$ complex (5 mol %), sulfamate substrate **2.1** (1.00 equiv), **2.2** (2.50 equiv), K_3PO_4 (4.50 equiv), hexamethylbenzene (0.10 equiv), 12 h. [b] Yield of **2.3** determined by ^1H NMR analysis of crude reaction mixtures using hexamethylbenzene as an internal standard.

With promising results in hand, we tested the analogous cross-coupling of several other electrophilic partners (Table 2.2). In addition to the naphthyl sulfamate (entry 1), the corresponding carbamate15 and pivalate ester were deemed competent substrates (entries 2–3). Furthermore, sulfonate derivatives of 1-naphthol also gave high yields of coupled product

(entries 4–6). Moreover, the use of 1-naphthyl chloride, bromide, and iodide each delivered the desired product under our optimized conditions (entries 7–9, respectively).

Table 2.2. Survey of Cross-Coupling Partners.[a]

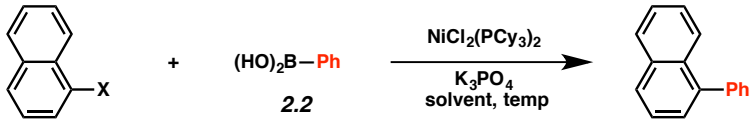

entry	X	yield (*tert*-amyl alcohol)[b]	yield (2-Me-THF)[b,c]
1	OSO_2NMe_2	100	100
2	$OCONEt_2$	57	50
3	OPiv	94	100
4	OMs	97	95
5	OTs	100	98
6	OTf	100	100
7	Cl	100	94
8	Br	97	92
9	I	100	97

[a] Conditions: $NiCl_2(PCy_3)_2$ complex (5 mol %), substrate (1.00 equiv), **2.2** (2.50 equiv), K_3PO_4 (4.50 equiv), hexamethylbenzene (0.10 equiv), 100 °C, 12 h. [b] Yield of **2.3** determined by ^1H NMR analysis of the crude reaction mixtures using hexamethylbenzene as an internal standard. [c] 66 °C

2.4 Substrate Scope

An array of heterocyclic aryl halide substrates underwent the desired cross-coupling with aryl boronic acids in *tert*-amyl alcohol and 2-Me-THF (Figure 2.2). Nitrogen-containing heterocycles such as indole and pyridine, were tolerated to give products **2.4**–**2.6**, respectively. 3-Bromofuran also underwent the desired coupling to give cross-coupled product **2.7**. In addition, the methodology was found to be tolerant of substrates that contain multiple heteroatoms, as demonstrated by the formation of products **2.8**–**2.10**.

Figure 2.2. Coupling of heterocyclic halides with aryl boronic acids.[a,b]

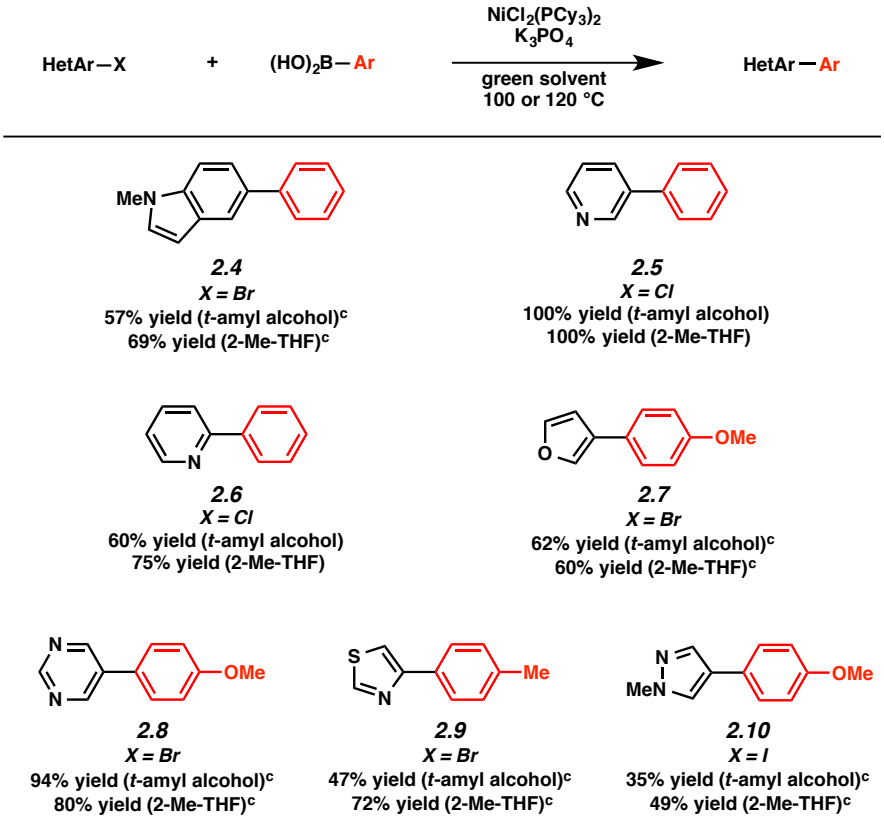

[a] Conditions: $NiCl_2(PCy_3)_2$ complex (5 mol %), halide substrate (1.00 equiv), aryl boronic acid (2.50 equiv), K_3PO_4 (4.50 equiv), hexamethylbenzene (0.10 equiv), 100 or 120 °C, 12 h. [b] Yield of product determined by ^1H NMR analysis of the crude reaction mixtures using hexamethylbenzene as an internal standard. [c] Conditions: $NiCl_2(PCy_3)_2$ complex (10 mol %), halide substrate (1.00 equiv), aryl boronic acid (4.00 equiv), K_3PO_4 (7.20 equiv), hexamethylbenzene (0.10 equiv), 100 or 120 °C, 12 h.

As shown in Figure 2.3, heterocyclic phenol-derived electrophiles participate in the Suzuki–Miyaura coupling in green solvents.16 Both the carbamate and ester derivatives of 2-hydroxy-*N*-Me-carbazole coupled smoothly with phenyl boronic acid to give **2.11** in good yields. Quinoline, isoquinoline, and pyridine derivatives were also tolerated, as demonstrated by the formation of **2.12**, **2.13**, and **2.6**, respectively. Dihydrobenzofuran- and pyrazole-based sulfamate substrates gave excellent yields of products **2.14** and **2.15**, respectively.

Figure 2.3. Coupling of heterocyclic phenolic derivatives with aryl boronic acids.[a,b]

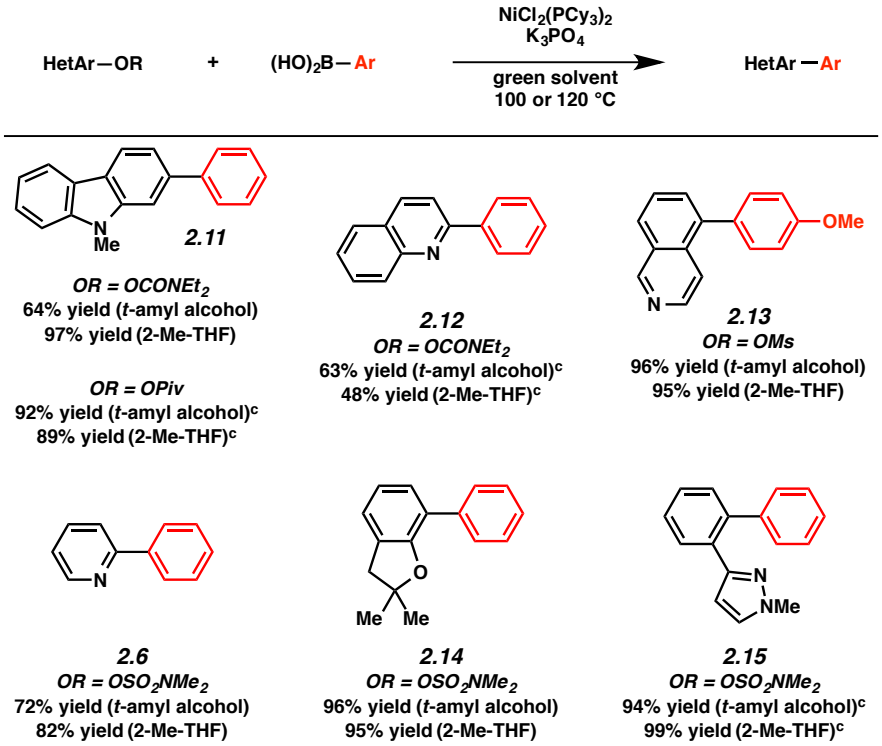

[a] Conditions: $NiCl_2(PCy_3)_2$ complex (5 mol %), phenolic-substrate (1.00 equiv), aryl boronic acid (2.50 equiv), K_3PO_4 (4.50 equiv), hexamethylbenzene (0.10 equiv), 100 or 120 °C, 12 h. [b] Yield of product determined by ^1H NMR analysis of the crude reaction mixtures using hexamethylbenzene as an internal standard. [c] Conditions: $NiCl_2(PCy_3)_2$ complex (10 mol %), phenolic substrate (1.00 equiv), aryl boronic acid (4.00 equiv), K_3PO_4 (7.20 equiv), hexamethylbenzene (0.10 equiv), 100 or 120 °C, 12 h.

2.5 Heterocycle–Heterocycle Couplings

We also tested our cross-coupling procedure for the assembly of bis(heterocyclic) scaffolds (Figure 2.4), which are prevalent in numerous drugs and natural products, but are sometimes difficult to access using Pd-catalyzed methods.[17] 3-Cl-pyridine readily underwent coupling with pyridyl-,[18] furyl-, and thiophenyl-boronic acid derivatives to provide bis(heterocyclic) compounds **2.16**–**2.18**. Likewise, 5-Br-pyrimidine was coupled to deliver compounds **2.19**–**2.21**.[19] The mesylate derived from 5-hydroxyisoquinoline also underwent facile coupling, thus affording **2.22**–**2.24** in excellent yields. Additionally, the coupling of a benzofuranyl sulfamate was explored to give bis(heterocycles) **2.25** and **2.26**.[20] We also tested the coupling of a pyrazole derived sulfamate with 3-furanyl boronic acid, which afforded **2.27** in moderate yield. Our methodology complements the recently disclosed Ni-catalyzed cross-couplings to form bis(heterocycles) reported by Hartwig.[6e]

Figure 2.4. Coupling of heterocyclic substrates with heterocyclic aryl boronic acids.[a,b]

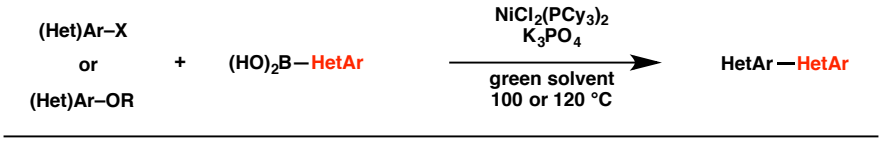

2.16
X = Cl
98% yield (*t*-amyl alcohol)
91% yield (2-Me-THF)

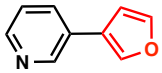

2.17
X = Cl
81% yield (*t*-amyl alcohol)
87% yield (2-Me-THF)

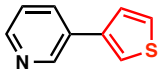

2.18
X = Cl
86% yield (*t*-amyl alcohol)[c]
93% yield (2-Me-THF)[c]

2.19
X = Br
100% yield (*t*-amyl alcohol)
96% yield (2-Me-THF)

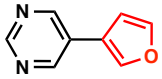

2.20
X = Br
100% yield (*t*-amyl alcohol)
99% yield (2-Me-THF)

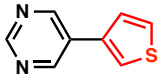

2.21
X = Br
86% yield (*t*-amyl alcohol)
93% yield (2-Me-THF)

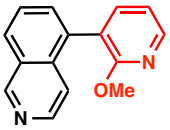

2.22
OR = OMs
100% yield (*t*-amyl alcohol)[c]
96% yield (2-Me-THF)[c]

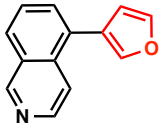

2.23
OR = OMs
90% yield (*t*-amyl alcohol)[c]
95% yield (2-Me-THF)[c]

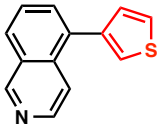

2.24
OR = OMs
99% yield (*t*-amyl alcohol)[c]
93% yield (2-Me-THF)[c]

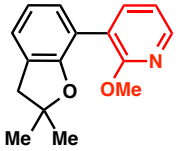

2.25
OR = OSO_2NMe_2
100% yield (*t*-amyl alcohol)[d]
100% yield (2-Me-THF)[d]

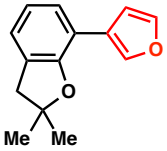

2.26
OR = OSO_2NMe_2
100% yield (*t*-amyl alcohol)[d]
100% yield (2-Me-THF)[d]

2.27
OR = OSO_2NMe_2
49% yield (*t*-amyl alcohol)[d]
33% yield (2-Me-THF)[d]

[a] Conditions: $NiCl_2(PCy_3)_2$ complex (1 mol %), substrate (1.00 equiv), aryl boronic acid (2.50 equiv), K_3PO_4 (4.50 equiv), hexamethylbenzene (0.10 equiv), 100 or 120 °C, 12 h. [b] Yield of product determined by ^1H NMR analysis of the crude reaction mixtures using hexamethylbenzene as an internal standard. [c] Conditions: $NiCl_2(PCy_3)_2$ complex (5 mol %), substrate (1.00 equiv), aryl boronic acid (2.50 equiv), K_3PO_4 (4.50 equiv), hexamethylbenzene (0.10 equiv), 100 or 120 °C, 12 h. [d] Conditions: $NiCl_2(PCy_3)_2$ complex (10 mol %), substrate (1.00 equiv), aryl boronic acid (4.00 equiv), K_3PO_4 (7.20 equiv), hexamethylbenzene (0.10 equiv), 100 or 120 °C, 12 h.

2.6 Gram Scale Couplings

The nickel-catalyzed Suzuki–Miyaura coupling shows promise for the assembly of bis(heterocyclic) frameworks on preparative scale (Figure 2.5).[21] Using 1 mol% Ni catalyst, isoquinoline **2.28** was coupled with pyridylboronic acid **2.29** to provide adduct **2.22** in quantitative yield on gram scale. Additionally, bromopyrimidine **2.30** underwent Ni-catalyzed cross-coupling with furanylboronic acid **2.31** using 0.5 mol% catalyst. This transformation, which was performed on 5 g scale, delivered **2.20** in 97% yield.

Figure 2.5. Gram scale couplings.[a,b]

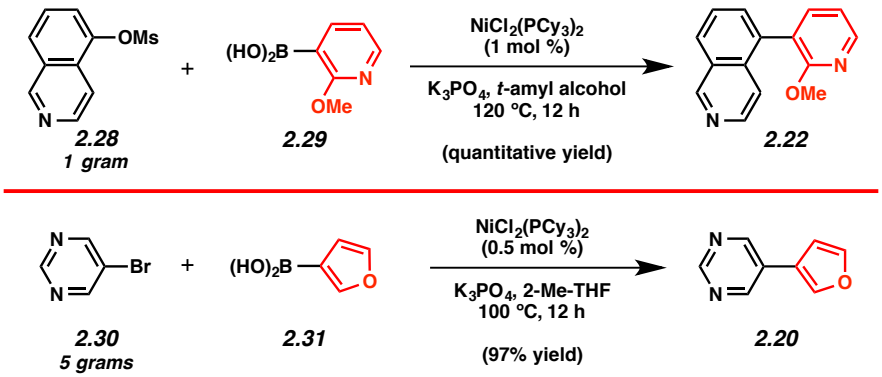

[a] Conditions: $NiCl_2(PCy_3)_2$ complex (1 or 5 mol %), substrate (1.00 equiv), aryl boronic acid (2.50 equiv), K_3PO_4 (4.50 equiv), reflux, 12 h. [b] Isolated yields.

2.7 Conclusion

In summary, we have demonstrated the efficient Ni-catalyzed Suzuki–Miyaura cross-coupling of aryl halides and phenolic derivatives in green solvents. The scope of these reactions is broad with respect to both coupling partners and heterocycles are well-tolerated. Additionally, the potential for these couplings to be performed on preparative scale has been demonstrated by the gram scale assembly of bis(heterocycles) using low catalyst loadings (i.e., 0.5–1 mol% Ni).

Given the appeal of Ni catalysis and that favorable green solvents that may be employed, we expect the methodology presented will find utility in academic and industrial applications.

2.8 Experimental Section

2.8.1 Materials and Methods

Materials and Methods. Unless stated otherwise, reactions were conducted in flame-dried glassware under an atmosphere of nitrogen using anhydrous solvents (either freshly distilled, purchased from a commercial source, or passed through activated alumina columns). DriSolv® anhydrous solvents were purchased from Acros Organics and used without further purification. Non-commercially available substrates were synthesized following protocols specified in Section 2.8.2. Unless otherwise stated, commercially obtained reagents were used as received. Halogenated substrates were obtained from Combi-Blocks, Sigma-Aldrich, and Oakwood Products, Inc. $NiCl_2(PCy_3)_2$ was obtained from Strem Chemicals and Sigma-Aldrich. Finely powdered anhydrous K_3PO_4 was obtained from Acros Organics. Boronic acids were obtained from Oakwood Products, Inc., Frontier Scientific, Inc. and Combi-Blocks. 2-Methyltetrahydrofuran (2-Me-THF), anhydrous, was obtained from Acros Organics (the water content was measured to be 0.035–0.13% using the Karl Fischer titration; water content of unopened bottle is reported to be 0.005%). *Tert*-amyl alcohol (*t*-amyl alcohol) was obtained from Sigma-Aldrich and used as received (the water content was measured to be 0.0053–0.25% using the Karl Fischer titration). Reaction temperatures were controlled using an IKAmag temperature modulator, and unless stated otherwise, reactions were performed at room temperature (rt, approximately 23 °C). Thin-layer chromatography (TLC) was conducted with EMD gel 60 F254 pre-coated plates (0.25 mm) and visualized using a combination of UV, anisaldehyde, ceric

ammonium molybdate, iodine, vanillin, and potassium permanganate staining techniques. Silicycle Siliaflash P60 (particle size 0.040–0.063 mm) was used for flash column chromatography. ^{1}H NMR spectra were recorded on Bruker spectrometers (at 300, 400, 500, 600 MHz) and are reported relative to deuterated solvent signals. Data for ^{1}H NMR spectra are reported as follows: chemical shift (δ ppm), multiplicity, coupling constant (Hz) and integration. ^{13}C NMR spectra were recorded on Bruker Spectrometers (at 125 MHz). Data for ^{13}C NMR spectra are reported in terms of chemical shift. IR spectra were recorded on a Perkin-Elmer 100 spectrometer and are reported in terms of frequency of absorption (cm^{-1}). High resolution mass spectra were obtained from the UC Irvine Mass Spectrometry Facility.

For more information about the ACS Green Chemistry Institute Pharmaceutical Roundtable Solvent Selection Guide, see:

http://portal.acs.org/portal/PublicWebSite/greenchemistry/industriainnovation/roundtable/index.htm

2.8.2 Experimental Procedures

A. Synthesis of Aryl Carbamate, Sulfamate, and Mesylate Substrates

Note: Supporting information for the synthesis of the aryl sulfamates, carbamates, and mesylates shown in Tables 2.1–2 and Figures 2.2–2.5 have previously been reported,[22] with the exception of pyrazole **2.34**.

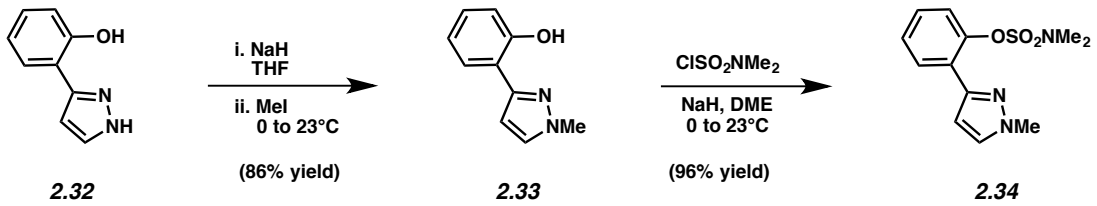

2.32 *2.33* *2.34*

Pyrazole 2.33. To a round bottom flask charged with NaH (0.15 g, 3.74 mmol, 2.00 equiv, 60% dispersion in oil) was added a solution of pyrazole **2.32** (0.30 g, 1.88 mmol, 1.00 equiv) in THF (11.1 mL) dropwise via cannula over several minutes at 0 °C. After stirring for 2 h, methyl iodide (0.12 mL, 1.88 mmol, 1.00 equiv) in THF (7.2 mL) was added dropwise over 1 min and the resulting mixture was stirred for 12 h while warming to rt. The volatiles were removed under reduced pressure and then, H_2O (10 mL) and Et_2O (10 mL) were added. The layers were separated, and the aqueous layer was extracted with Et_2O (10 mL). The combined organic layers were washed successively with 1 M aqueous $NaHCO_3$ (10 mL) and brine (10 mL), dried over $MgSO_4$, and concentrated under reduced pressure. The crude residue was purified by flash chromatography (3:1 Hexanes:EtOAc) to give pyrazole **2.33** (0.22 g, 86% yield) as a yellow solid . R_f 0.36 (3:1 Hexanes:EtOAc). Spectral data match those previously reported.[23]

Sulfamate 2.34. To a round bottom flask charged with NaH (0.78 g, 1.94 mmol, 1.20 equiv, 60% dispersion in oil) was added a solution of pyrazole **2.33** (0.28 g, 1.62 mmol, 1.00 equiv) in DME (6.5 mL) dropwise via cannula over several minutes at 0 °C. Dimethylsulfamoyl chloride (0.17 mL, 1.56 mmol, 0.95 equiv) was added dropwise to the reaction vessel. The reaction was allowed to stir for 12 h while warming to rt. The reaction was quenched with H_2O (0.3 mL) and the volatiles were removed under reduced pressure. Et_2O (45 mL) and H_2O (15 mL) were added and the layers were separated. The organic layer was washed with 1 M aqueous KOH (2 x 15 mL). The combined aqueous layers were extracted with Et_2O (3 x 30 mL). The combined organic

layers were then washed with brine (30 mL), dried over $MgSO_4$, and concentrated under reduced pressure. The crude residue was purified by flash chromatography (3:1 Hexanes:Acetone) to yield sulfamate **2.34** as a yellow oil (0.42 g, 96% yield). R_f 0.12 (1:1 Hexanes: EtOAc); ^{1}H NMR (600 MHz, $CDCl_3$): δ 7.85 (dd, *J* = 7.2, 2.0, 1H), 7.54 (dd, *J* = 8.1, 1.5, 1H), 7.35 (d, *J* = 2.1, 1H), 7.32-7.27 (m, 2H), 6.69 (d, *J* = 2.2, 1H), 3.93 (s, 3H), 2.68 (s, 6H); ^{13}C NMR (150 MHz, $CDCl_3$): δ 147.6, 147.0, 130.9, 129.7, 128.6, 127.1, 126.7, 122.5, 107.2, 39.1, 38.4; IR (film): 2941, 1460, 1366, 1191, 1156, 973, 740 cm^{-1}; HRMS-ESI (*m/z*) $[M+H]^+$ calcd for $C_{12}H_{15}N_3O_3S$, 282.0912; found 282.0912.

B. Screening of Green Solvents

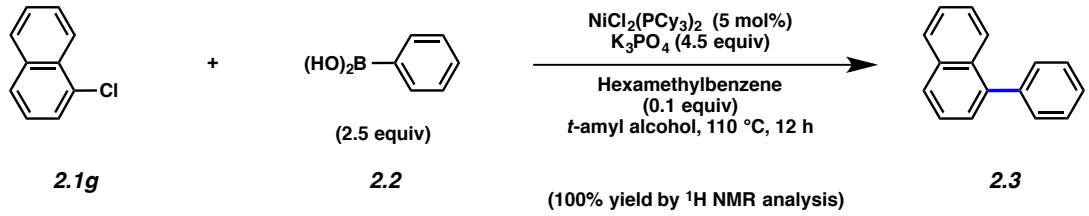

Representative Procedure (coupling of 2.1g is used as an example). 2.3 (Table 2.2). A 1-dram vial was charged with anhydrous powdered K_3PO_4 (419.3 mg, 1.98 mmol, 4.50 equiv) and a magnetic stir bar. The vial and contents were flame-dried under reduced pressure, then allowed to cool under N_2. Hexamethylbenzene (7.1 mg, 0.044 mmol, 0.10 equiv), boronic acid **2.2** (134.1 mg, 1.1 mmol, 2.50 equiv), $NiCl_2(PCy_3)_2$ (15.2 mg, 0.022 mmol, 5 mol%), and substrate **2.1g** (71.3 mg, 0.44 mmol, 1.00 equiv) were added. The vial was then evacuated and backfilled with N_2. To the vial, *t*-amyl alcohol (1.5 mL) was added and then the vial was sealed with a Teflon-lined screw cap. The mixture was allowed to stir rapidly at 23 °C for 1 h, and then heated to 110 °C for 12 h. After cooling the reaction vessel to 23 °C, the reaction was transferred to a test tube

containing 1 M aqueous HCl (2 mL). The layers were separated; the aqueous layer was extracted with EtOAc (3 x 2 mL). The combined organic layers were then washed with brine (2 mL), dried over $MgSO_4$, and passed through a SiO_2 plug. The pad was washed with EtOAc (10 mL) and the organic layers were concentrated under reduced pressure. The yield was determined by ^1H NMR analysis with hexamethylbenzene as an internal standard. Spectral data match those previously reported.[22e]

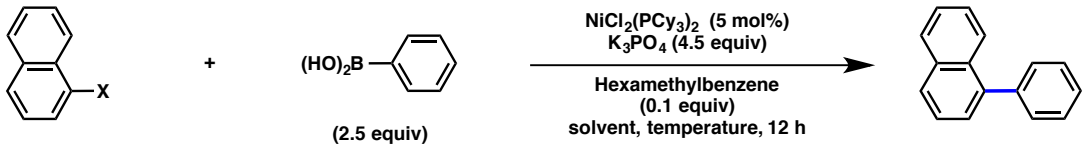

X = Cl, Br, I — ***2.2*** — ***2.3***

Table 2.3. Cross-Coupling Reactions of Naphthyl Halides in Various Solvents.[a]

Solvent Name (temperature (°C))	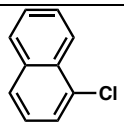 ***2.1g***	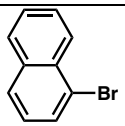 ***2.1h***	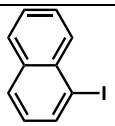 ***2.1i***
	^1H NMR yield of desired product (%) determined by hexamethylbenzene as an internal standard		
t-butanol (83)	88[b]	100[b], 87[c]	90[b], 82[c]
t-amyl alcohol (110)	100[b]	97[b]	100[b]
2-Me-THF (66)	94[d]	92[d]	97[d]
CPME (106)	100[d]	90[d]	100[d]
dimethyl isosorbide (110)	40[c]	42[c]	44[c]
i-PrOAc (89)	90[c]	90[c]	95[c]
DMSO (110)	100[b]	91[b]	86[b]
DMF (106)	100[b]	90[b]	97[b]
DMA (110)	0[b]	0[b]	0[b]
NMP (110)	100[b]	69[b]	54[b]
sulfolane (110)	100[b]	98[b]	96[b]

[a] Reaction conditions, unless otherwise noted, the reaction was carried out with $NiCl_2(PCy_3)_2$ complex (5 mol %), substrate **2.1g–2.1i** (1.00 equiv), **2.2** (2.50 equiv), K_3PO_4 (4.50 equiv), hexamethylbenzene (0.10 equiv), 12 h. [b] Distilled from desiccant. [c] Used without purification. [d] Drysolv®.

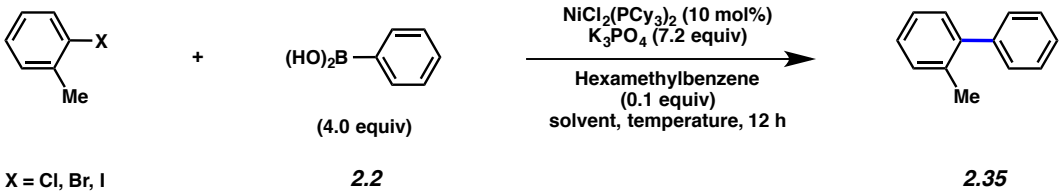

Table 2.4. Cross-Coupling Reactions of Tolyl Halides in Selected Solvents.[a]

Solvent Name (temperature (°C))	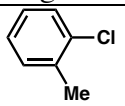 **2.36**	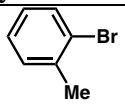 **2.37**	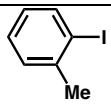 **2.38**
	^{1}H NMR yield of desired product (%) determined by hexamethylbenzene as an internal standard		
t-butanol (83)	98[b], 92[c]	99[b], 100[c]	97[b], 95[c]
2-Me-THF (80)	93[d]	99[d]	99[d]
CPME (106)	96[d]	96[d]	100[d]
i-PrOAc (89)	90[c]	91[c]	85[c]

[a] Reaction conditions, unless otherwise noted, the reaction was carried out with $NiCl_2(PCy_3)_2$ complex (10 mol %), substrate **2.36–2.38** (1.00 equiv), **2.2** (4.00 equiv), K_3PO_4 (7.20 equiv), hexamethylbenzene (0.1 equiv), 12 h. [b] Distilled from desiccant. [c] Used without purification. [d] Drysolv®.

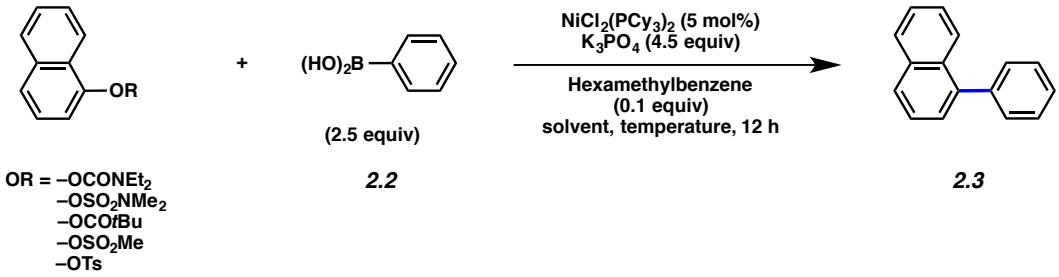

Table 2.5. Cross-Coupling Reactions of Naphthol Derivatives in Various Solvents.[a]

Solvent Name (temperature (°C))	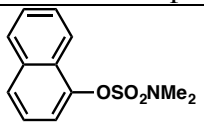 **2.1a**	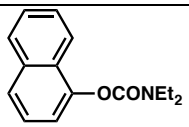 **2.1b**
	^{1}H NMR yield of desired product (%) determined by hexamethylbenzene as an internal standard	
t-butanol (100)	100[c,d]	100[b,c,d]
n-butanol (110)	0[c,d]	0[b,c,d]

Table 2.5. Cross-Coupling Reactions of Naphthol Derivatives in Various Solvents (Continued).[a]

Solvent Name (temperature (°C))	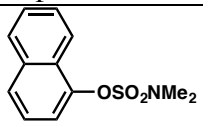 **2.1a**	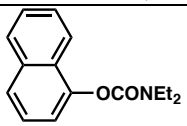 **2.1b**
	^{1}H NMR yield of desired product (%) determined by hexamethylbenzene as an internal standard	
2-butanol (110)	0[c,d]	0[b,c,d,f]
i-butanol (110)	3[c], 2[d]	0[b,c,d,g]
t-amyl alcohol (100)	100[c]	88[b,c]
toluene (110)	100[b]	100[b]
xylenes (110)	100[c,d]	100[b,c,d,g]
triethylamine (110)	99[c], 100[d]	91[b,c], 76[b,d]
pyridine (110)	70[c], 67[d]	0[b,c,g], 0[b,d,g]
2-Me-THF (100)	100[e]	97[b,e]
CPME (110)	100[e]	100[b,e,g]
MTBE (80)	100[e]	100[b,e]
1,2-dimethoxyethane (110)	100[b]	92[b]
1,4-dioxane (110)	100[c,d]	58[b,c], 75[b,d]
diglyme	100[c], 54[d]	93[b,c], 16[b,d]
EtOAc (100)	100[c,d]	100[b,c,d]
n-butyl acetate (110)	100[d]	97[b,d]
i-PrOAc (110)	100[d]	99[b,d]
n-amyl acetate (110)	0[d]	0[b,d]
acetone (75)	96[c], 99[d]	68[b,c], 54[b,d]
2-butanone (79)	99[c]	69[b,c]
methyl *i*-butyl ketone (110)	97[c,d]	97[b,c], 71[b,d]
cyclohexanone (110)	100[c]	100[b,c]
acetonitrile (100)	99[b]	0[b]
DMSO (110)	0[c]	0[b,c]
DMA (110)	0[c]	0[b,c]
DMF (106)	97[b]	86[b]
NMP (110)	100[c]	43[b,c]
sulfolane (110)	100[c]	64[b,c]
i-octane (95)	86[c], 95[d]	69[b,c], 73[b,d]
n-heptane (98)	100[c,d]	76[b,c], 77[b,d]
cyclohexane (80)	96[c], 90[d]	78[b,c], 50[b,d]
1,2-dichloroethane (100)	0[c]	0[b,c]

[a] Reaction conditions, unless otherwise noted, the reaction was carried out with $NiCl_2(PCy_3)_2$ complex (5 mol %), substrate **2.1a–2.1b** (1.00 equiv), **2.2** (2.50 equiv), K_3PO_4 (4.50 equiv), hexamethylbenzene (0.10 equiv), 12 h. [b] The reaction was carried out with $NiCl_2(PCy_3)_2$ complex (10 mol %), substrate **2.1a–b** (1.00 equiv), **2.2** (4.00 equiv), K_3PO_4 (7.20 equiv), hexamethylbenzene (0.10 equiv), 12 h. [c] Distilled from desiccant. [d] Used without purification. [e] Drysolv®. [f] The reaction was performed at 120 °C. [g] The reaction was performed at 130 °C.

Table 2.6. Cross-Coupling Reactions of Naphthyl Mesylate, Tosylate, and Pivalates in Selected Green Solvents.[a]

Solvent Name (temperature (°C))	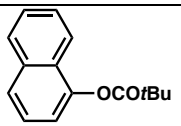 **2.1c**	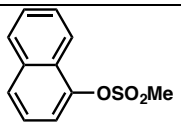 **2.1d**	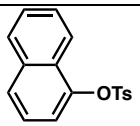 **2.1e**
	^{1}H NMR yield of desired product (%) determined by hexamethylbenzene as an internal standard		
t-butanol (82)	100[b,c], 53[b,d]	90[c], 90[d]	100[c], 95[d]
2-Me-THF (66)	99[b,e]	95[e]	96[e]
CPME (106)	100[b,e]	100[e]	84[e]
i-PrOAc (89)	92[b,d]	95[d]	100[d]

[a] Reaction conditions, unless otherwise noted, the reaction was carried out with $NiCl_2(PCy_3)_2$ complex (5 mol %), substrate **2.1c–2.1e** (1.00 equiv), **2.2** (2.50 equiv), K_3PO_4 (4.50 equiv), hexamethylbenzene (0.10 equiv), 12 h. [b] The reaction was carried out with $NiCl_2(PCy_3)_2$ complex (10 mol %), substrate **2.1c–2.1e** (1.00 equiv), **2.2** (4.00 equiv), K_3PO_4 (7.20 equiv), hexamethylbenzene (0.10 equiv), 12 h. [c] Distilled from desiccant. [d] Used without purification. [e] Drysolv®.

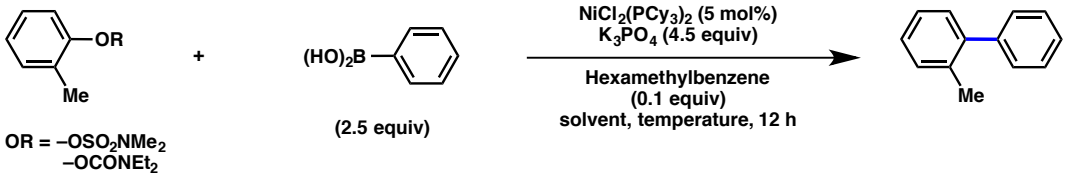

2.2 **2.35**

Table 2.7. Cross-Coupling Reactions of *o*-Methylphenyl Sulfamate and Carbamate in Selected Solvents.[a]

Solvent Name (temperature (°C))	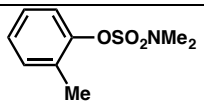 **2.39**	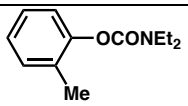 **2.40**
	^{1}H NMR yield of desired product (%) determined by hexamethylbenzene as an internal standard	
t-butanol (100)	78[c], 68[d]	45[b,c], 50[b,d]
t-amyl alcohol (120)	100[d]	45[b,d]
toluene (110)	92[b]	61[b]
xylenes (110)	100[c]	69[b,c,f]

Table 2.7. Cross-Coupling Reactions of *o*-Methylphenyl Sulfamate and Carbamate in Selected Solvents (Continued).[a]

Solvent Name (temperature (°C))	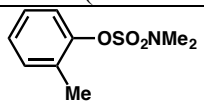 **2.39**	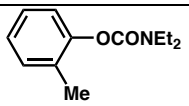 **2.40**
	^{1}H NMR yield of desired product (%) determined by hexamethylbenzene as an internal standard	
triethylamine (110)	52[c]	29[b,c]
2-Me-THF (100)	97[e]	88[b,e]
CPME (110)	96[e]	58[b,e,f]
MTBE (80)	99[e]	60[b,e]
1,2-dimethoxyethane (110)	99[b]	65[b]
1,4-dioxane (110)	99[c], 90[d]	57[b,c], 34[b,d]
EtOAc (100)	33[c], 26[d]	17[b,c], 16[b,d]
n-butyl acetate (110)	20[d]	15[b,d,f]
i-PrOAc (110)	78[d]	70[b,d]
acetone (75)	98[c]	5[b,c]

[a] Reaction conditions, unless otherwise noted, the reaction was carried out with $NiCl_2(PCy_3)_2$ complex (5 mol %), substrate **2.39–2.40** (1.00 equiv), **2.2** (2.50 equiv), K_3PO_4 (4.50 equiv), hexamethylbenzene (0.10 equiv), 12 h. [b] The reaction was carried out with $NiCl_2(PCy_3)_2$ complex (10 mol %), substrate **2.39–2.40** (1.00 equiv), **2.2** (4.00 equiv), K_3PO_4 (7.20 equiv), hexamethylbenzene (0.10 equiv), 12 h. [c] Distilled from desiccant. [d] Used without purification.
[e] Drysolv®.

2.8.2.3 Screening of Arylboron-Based Nucleophiles

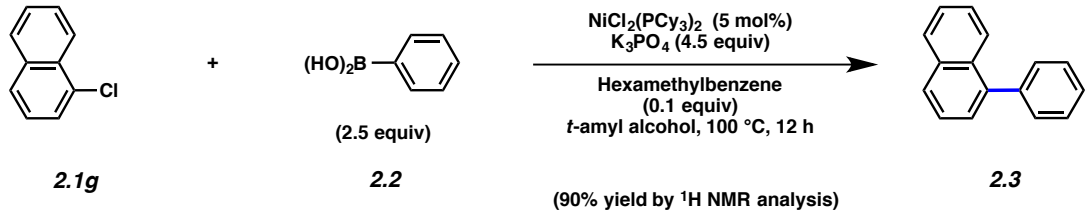

Representative Procedure (coupling of 2.1g is used as an example). 2.3 (Table 2.2). A 1-dram vial was charged with anhydrous powdered K_3PO_4 (419.3 mg, 1.98 mmol, 4.50 equiv) and a magnetic stir bar. The vial and contents were flame-dried under reduced pressure, then allowed to cool under N_2. Hexamethylbenzene (7.1 mg, 0.044 mmol, 0.10 equiv), boronic acid **2.2** (134.1

mg, 1.1 mmol, 2.50 equiv), $NiCl_2(PCy_3)_2$ (15.2 mg, 0.022 mmol, 5 mol%), and substrate **2.1g** (71.3 mg, 0.44 mmol, 1.00 equiv) were added. The vial was then evacuated and backfilled with N_2. To the vial, *t*-amyl alcohol (1.5 mL) was added and then the vial was sealed with a Teflon-lined screw cap. The mixture was allowed to stir rapidly at 23 °C for 1 h, and then heated to 100 °C for 12 h. The reaction vessel was cooled to 23 °C, then transferred to a test tube containing 1 M aqueous HCl (2 mL). The layers were separated; the aqueous layer was extracted with EtOAc (3 x 2 mL). The combined organic layers were then washed with brine (2 mL), dried over $MgSO_4$, and passed through a SiO_2 plug. The pad was washed with EtOAc (10 mL) and the organic layers were concentrated under reduced pressure. The yield was determined by ^1H NMR analysis with hexamethylbenzene as an internal standard. Spectral data match those previously reported.[22e]

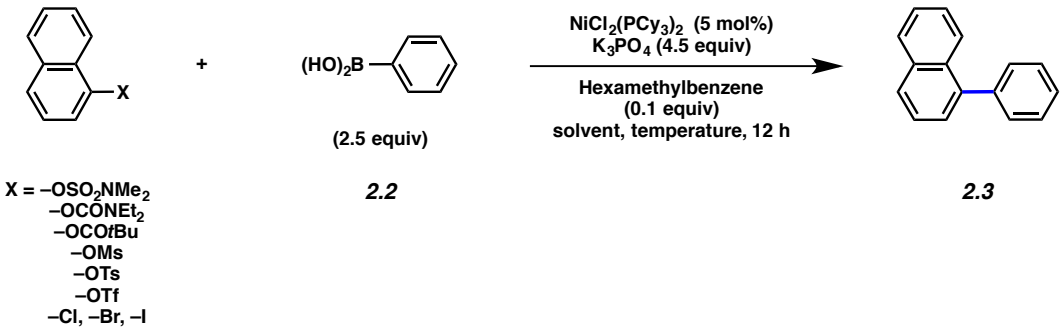

Table 2.8. Arylboron-Based Nucleophile Phenylboronic Acid.[a]

X	^{1}H NMR yield of desired product (%) determined by hexamethylbenzene as an internal standard	
	t-amyl alcohol[b] (100 °C)	2-Me-THF[c] (66 °C)
OSO_2NMe_2 (**2.1a**)	100	100
$OCONEt_2$ (**2.1b**)	57	50
OCO*t*Bu (**2.1c**)	94	100
OMs (**2.1d**)	97	95
OTs (**2.1e**)	100	98
OTf (**2.1f**)	100	100
Cl (**2.1g**)	100	94
Br (**2.1h**)	97	92
I (**2.1i**)	100	97

[a] Reaction conditions, unless otherwise noted, the reaction was carried out with $NiCl_2(PCy_3)_2$ complex (5 mol %), substrate **2.1a–i** (1.00 equiv), **2.2** (2.50 equiv), K_3PO_4 (4.50 equiv), hexamethylbenzene (0.10 equiv), 12 h. [b] Used without purification. [c] Drysolv®.

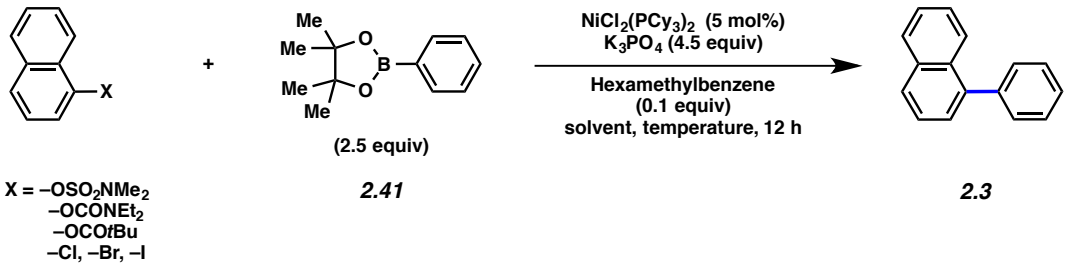

Table 2.9. Arylboron-Based Nucleophile Pinacol Ester.[a]

X	^{1}H NMR yield of desired product (%) determined by hexamethylbenzene as an internal standard	
	t-amyl alcohol[b] (120 °C)	2-Me-THF[c] (100 °C)
OSO_2NMe_2 (**2.1a**)	100	0
$OCONEt_2$ (**2.1b**)	97	0
OCO*t*Bu (**2.1c**)	99	75
Cl (**2.1g**)	96	0
Br (**2.1h**)	98	0
I (**2.1i**)	93	0

[a] Reaction conditions, unless otherwise noted, the reaction was carried out with $NiCl_2(PCy_3)_2$ complex (5 mol %), substrate **2.1a–2.1c**, **2.1g–2.1i** (1.00 equiv), **2.2** (2.50 equiv), K_3PO_4 (4.50 equiv), hexamethylbenzene (0.10 equiv), 12 h. [b] Used without purification. [c] Drysolv®.

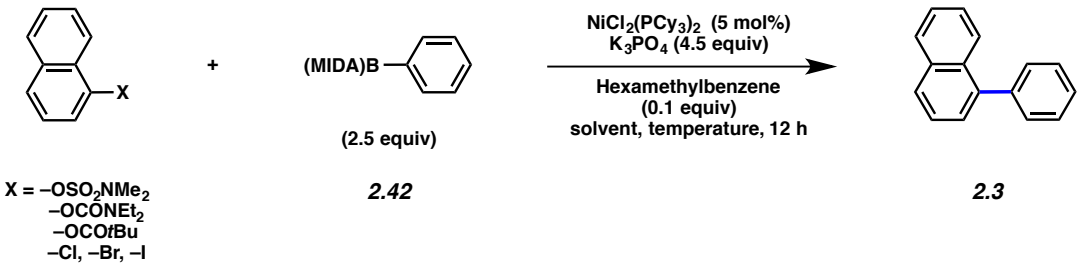

Table 2.10. Arylboron-Based Nucleophile MIDA (*N*-Methyliminodiacetic Acid).[a]

X	^{1}H NMR yield of desired product (%) determined by hexamethylbenzene as an internal standard	
	t-amyl alcohol[b] (100 °C)	2-Me-THF[c] (66 °C)
OSO_2NMe_2 (**2.1a**)	0	0
$OCONEt_2$ (**2.1b**)	0	0
OCO*t*Bu (**2.1c**)	0	0
Cl (**2.1g**)	0	0
Br (**2.1h**)	0	0
I (**2.1i**)	0	0

[a] Reaction conditions, unless otherwise noted, the reaction was carried out with $NiCl_2(PCy_3)_2$ complex (5 mol %), substrate **2.1a–2.1c**, **2.1g–2.1i** (1.00 equiv), **2.2** (2.50 equiv), K_3PO_4 (4.50 equiv), hexamethylbenzene (0.10 equiv), 12 h. [b] Used without purification. [c] Drysolv®.

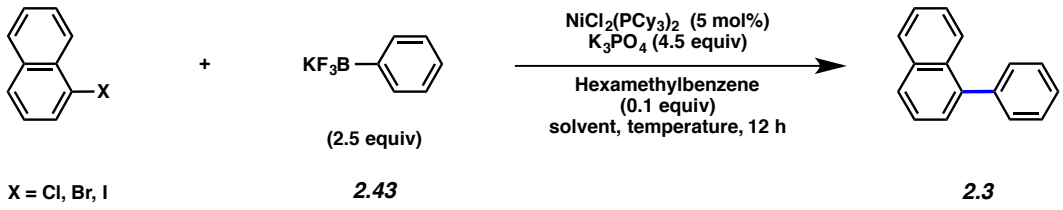

Table 2.11. Arylboron-Based Nucleophile Potassium Aryl Trifluoroborate.[a]

X	^{1}H NMR yield of desired product (%) determined by hexamethylbenzene as an internal standard	
	t-amyl alcohol[b] (100 °C)	2-Me-THF[c] (66 °C)
Cl (**2.1g**)	0	0
Br (**2.1h**)	0	0
I (**2.1i**)	0	0

[a] Reaction conditions, unless otherwise noted, the reaction was carried out with $NiCl_2(PCy_3)_2$ complex (5 mol %), substrate **2.1g–2.1i** (1.00 equiv), **2.2** (2.50 equiv), K_3PO_4 (4.50 equiv), hexamethylbenzene (0.10 equiv), 12 h. [b] Used without purification. [c] Drysolv®.

2.8.2.4 Cross-coupling Reactions of Aryl Halides

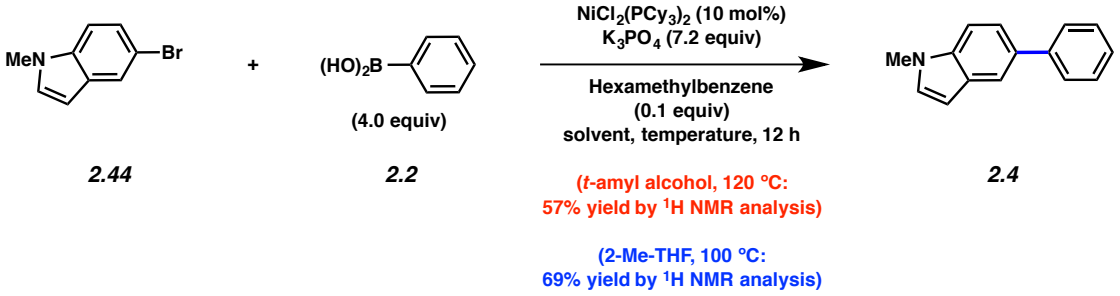

2.44 *2.2* *2.4*

Representative Procedure (coupling of 2.44 is used as an example). 2.4 (Figure 2.2). A 1-dram vial was charged with anhydrous powdered K_3PO_4 (831.4 mg, 7.20 mmol, 7.20 equiv) and a magnetic stir bar. The vial and contents were flame-dried under reduced pressure, then allowed to cool under N_2. Hexamethylbenzene (8.8 mg, 0.054 mmol, 0.10 equiv), boronic acid **2.2** (265.3 mg, 2.20 mmol, 4.0 equiv), $NiCl_2(PCy_3)_2$ (37.5 mg, 0.054 mmol, 10 mol%), and indole **2.44** (112.8 mg, 0.54 mmol, 1.00 equiv) were added. The vial was then evacuated and backfilled with N_2. To the vial, solvent (1.5 mL) was added and then the vial was sealed with a Teflon-lined screw cap. The mixture was allowed to stir rapidly at 23 °C for 1 h, and then heated to 100 °C (2-Me-THF) or 120 °C (*t*-amyl alcohol) for 12 h. After cooling the reaction to 23 °C, the reaction was transferred to a test tube containing 1 M aqueous HCl (2 mL). The layers were separated; the aqueous layer was extracted with EtOAc (3 x 2 mL). The combined organic layers were then washed with brine (2 mL), dried over $MgSO_4$, passed through a SiO_2 plug. The pad was washed with EtOAc (10 mL) and the organic layers were concentrated under reduced pressure. The yield was determined by ^1H NMR analysis with hexamethylbenzene as an internal standard. Spectral data match those previously reported.[22b]

Any modifications of the conditions shown in this representative procedure are specified in the following schemes, which depict all of the results shown in Figure 2.2.

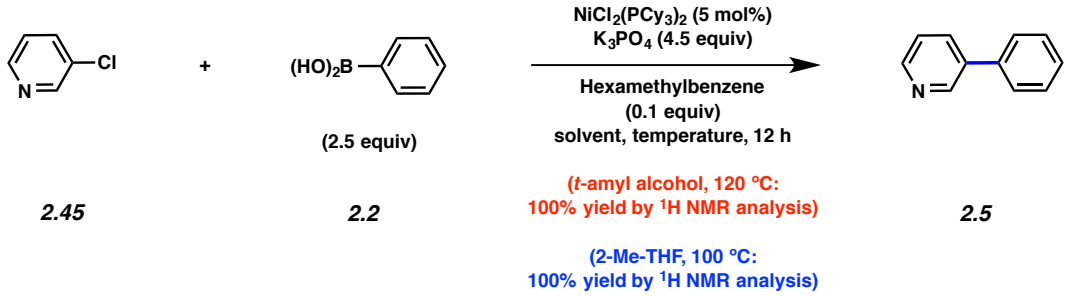

2.5 (Figure 2.2). The yield was determined by ^{1}H NMR analysis with hexamethylbenzene as an internal standard. Spectral data match those previously reported.[24]

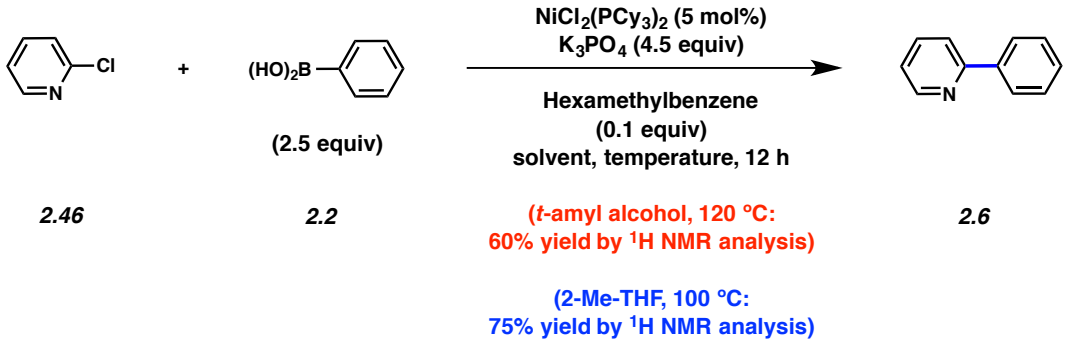

2.6 (Figure 2.2). The yield was determined by ^{1}H NMR analysis with hexamethylbenzene as an internal standard. Spectral data match those previously reported.[25]

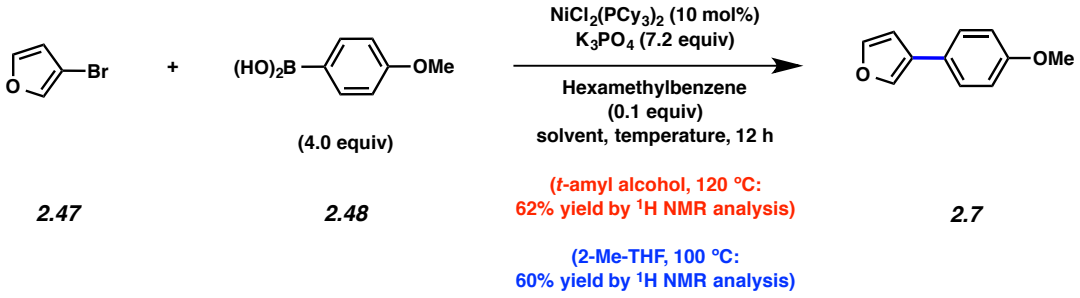

2.7 (Figure 2.2). The yield was determined by ^{1}H NMR analysis with hexamethylbenzene as an internal standard. Spectral data match those previously reported.[26]

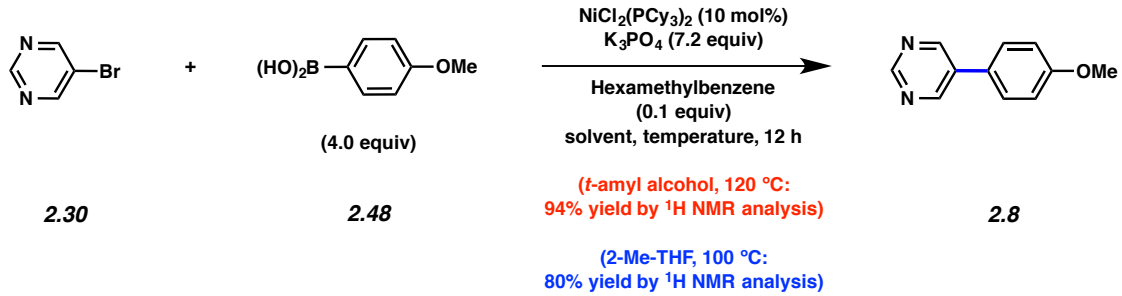

2.8 (Figure 2.2). The yield was determined by ^{1}H NMR analysis with hexamethylbenzene as an internal standard. Spectral data match those previously reported.[26]

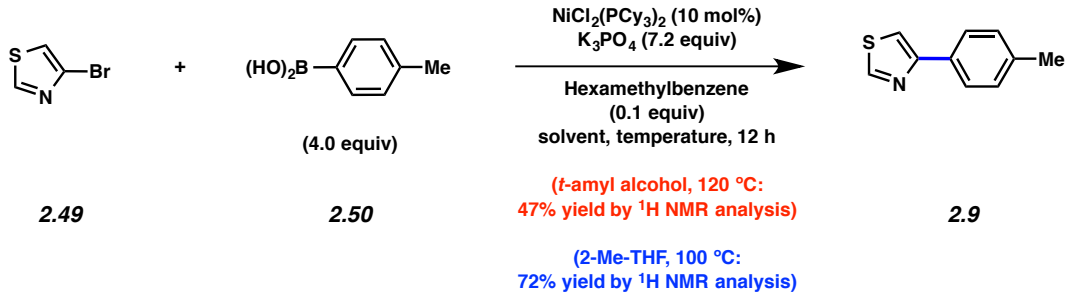

2.9 (Figure 2.2). The yield was determined by ^{1}H NMR analysis with hexamethylbenzene as an internal standard. Spectral data match those previously reported.[27]

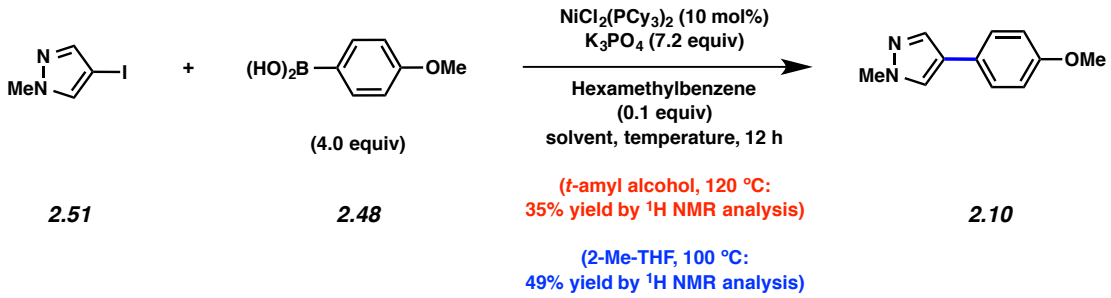

2.10 (Figure 2.2). The yield was determined by ^{1}H NMR analysis with hexamethylbenzene as an internal standard. Spectral data match those previously reported.[28]

2.8.2.5 Cross-coupling Reactions of Aryl Carbamates, Sulfamates, and Mesylates.

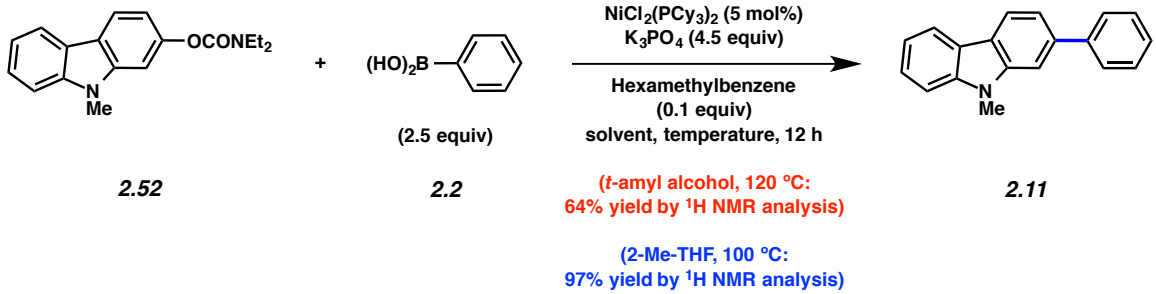

2.52 *2.2* *2.11*

Representative Procedure (coupling of 2.52 is used as an example). 2.11 (Figure 2.3). A 1-dram vial was charged with anhydrous powdered K_3PO_4 (429.8 mg, 2.03 mmol, 4.50 equiv) and a magnetic stir bar. The vial and contents were flame-dried under reduced pressure, then allowed to cool under N_2. Hexamethylbenzene (7.3 mg, 0.045 mmol, 0.10 equiv), boronic acid **2.2** (171.0 mg, 1.125 mmol, 2.50 equiv), $NiCl_2(PCy_3)_2$ (15.5 mg, 0.023 mmol, 5 mol%), and substrate **2.52** (104.9 mg, 0.45 mmol, 1.00 equiv) were added. The vial was then evacuated and backfilled with N_2. To the vial, solvent (1.5 mL) was added and then the vial was sealed with a Teflon-lined screw cap. The mixture was allowed to stir rapidly at 23 °C for 1 h, and then heated to 100 °C (2-Me-THF) or 120 °C (*t*-amyl alcohol) for 12 h. After cooling the reaction vessel to 23 °C, the reaction was transferred to a test tube containing 1 M aqueous HCl (4 mL). The layers were separated; the aqueous layer was extracted with EtOAc (3 x 2 mL). The combined organic layers were then washed with brine (2 mL), dried over Na_2SO_4, and passed through a SiO_2 plug. The pad was washed with EtOAc (10 mL) and the organic layers were concentrated under reduced pressure. The yield was determined by ^1H NMR analysis with hexamethylbenzene as an internal standard. Spectral data match those previously reported.[22a]

Any modifications of the conditions shown in this representative procedure are specified in the following schemes, which depict all of the results shown in Figure 2.3.

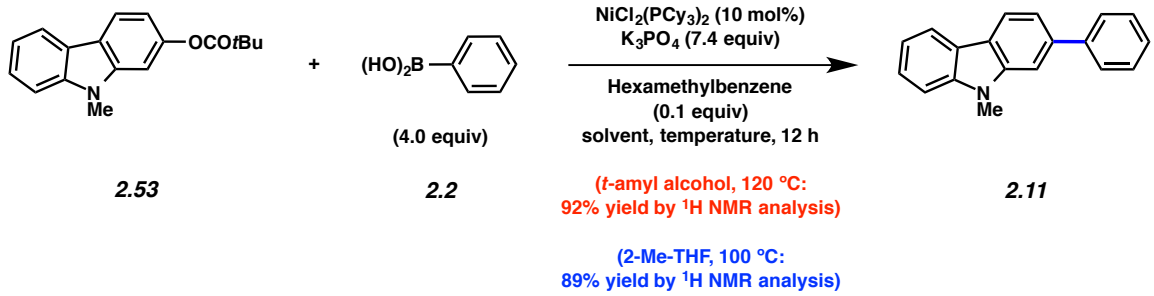

2.53 *2.2* *2.11*

2.11 (Figure 2.3). The yield was determined by ^{1}H NMR analysis with hexamethylbenzene as an internal standard. Spectral data match those previously reported.[22a]

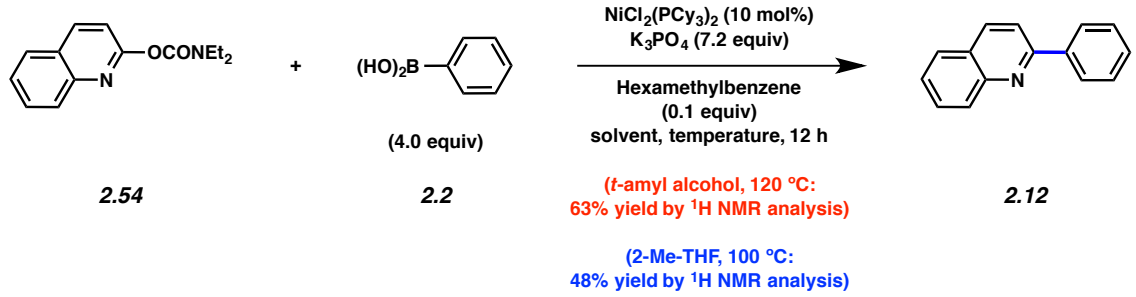

2.54 *2.2* *2.12*

2.12 (Figure 2.3). The yield was determined by ^{1}H NMR analysis with hexamethylbenzene as an internal standard. Spectral data match those previously reported.[29]

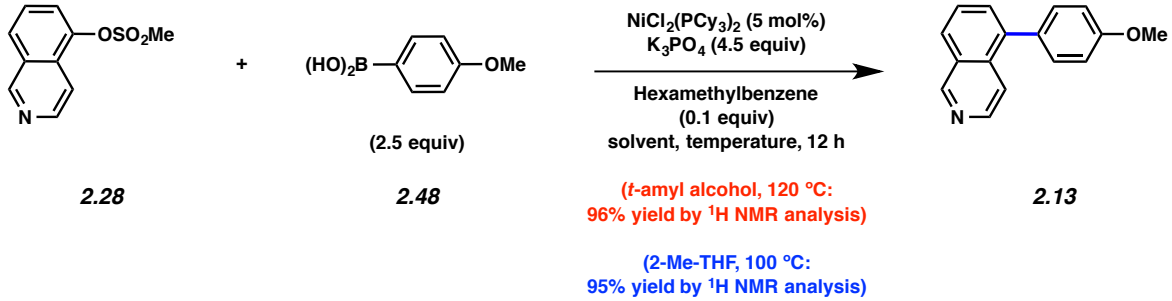

2.28 *2.48* *2.13*

2.13 (Figure 2.3). The yield was determined by ^{1}H NMR analysis with hexamethylbenzene as an internal standard. Spectral data match those previously reported[30]

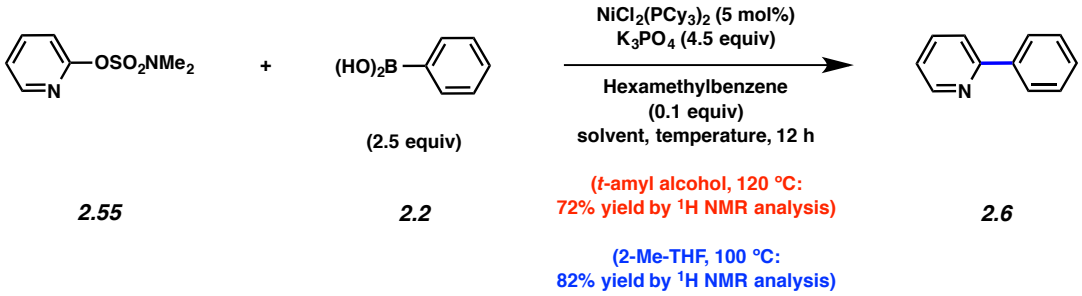

2.6 (Figure 2.3). The yield was determined by ^{1}H NMR analysis with hexamethylbenzene as an internal standard. Spectral data match those previously reported.[29]

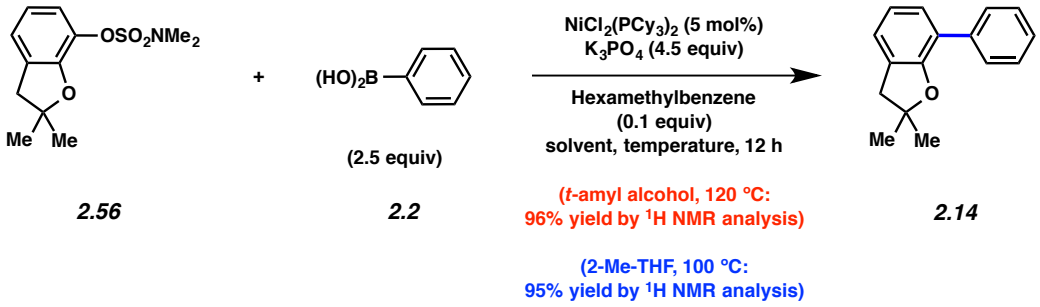

2.14 (Figure 2.3). The yield was determined by ^{1}H NMR analysis with hexamethylbenzene as an internal standard. Spectral data match those previously reported.[22e]

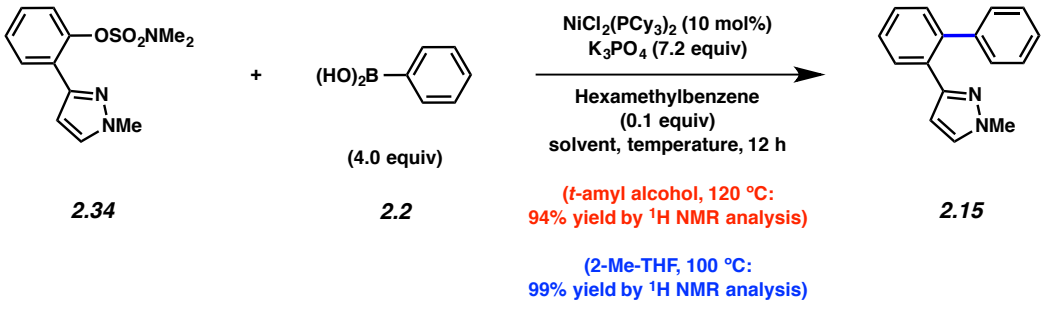

2.15 (Figure 2.3). The yield was determined by ^{1}H NMR analysis with hexamethylbenzene as an internal standard. R*f* 0.24 (3:1 Hexanes:EtOAc); ^{1}H NMR: (600 MHz, $CDCl_3$): δ 7.82 (dd, *J* =

7.6, 1.4, 1H), 7.41–7.35 (m, 2H), 7.33–7.26 (m, 6H), 7.08 (d, J = 2.1, 1H), 5.45 (d, J = 2.1, 1H), 3.89 (s, 3H);^{13}C NMR (125 MHz, $CDCl_3$): δ 151.3, 142.2, 140.7, 132.5, 130.5, 130.1, 129.7, 129.3, 128.0, 127.7, 127.6, 126.8, 106.7, 39.0; IR (film): 3055, 2934, 1597, 1501, 1461, 1392, 1221, 751, 699 cm^{-1}; HRMS-ESI (m/z) [M+H]$^+$ calcd for $C_{16}H_{14}N_2$, 235.1235; found 235.1236.

2.8.2.6 Heterocycle-Heterocycle Cross-Couplings of Aryl Halides

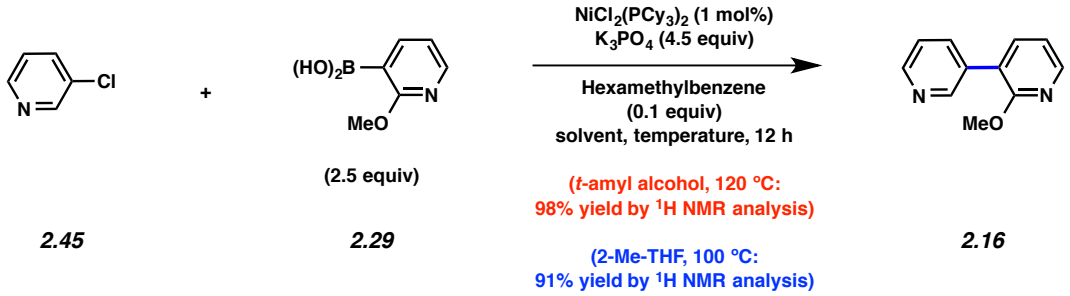

2.45 *2.29* *2.16*

Representative Procedure (coupling of 2.45 is used as an example). 2.16 (Figure 2.4). A 1-dram vial was charged with anhydrous powdered K_3PO_4 (859.7 mg, 4.1 mmol, 4.50 equiv) and a magnetic stir bar. The vial and contents were flame-dried under reduced pressure, then allowed to cool under N_2. Hexamethylbenzene (14.6 mg, 0.09 mmol, 0.10 equiv), boronic acid **2.29** (344.1 mg, 2.25 mmol, 2.5 equiv), $NiCl_2(PCy_3)_2$ (6.2 mg, 0.009 mmol, 1 mol%), and substrate **2.45** (102.2 mg, 0.9 mmol, 1.00 equiv) were added. The vial was then evacuated and backfilled with N_2. To the vial, solvent (1.5 mL) was added and then the vial was sealed with a Teflon-lined screw cap. The mixture was allowed to stir rapidly at 23 °C for 1 h, and then heated to 100 °C (2-Me-THF) or 120 °C (*t*-amyl alcohol) for 12 h. The reaction vessel was cooled to 23 °C and then transferred to a test tube containing 1 M aqueous HCl (2 mL). The layers were separated; the aqueous layer was extracted with EtOAc (3 x 2 mL). The combined organic layers were then washed with brine (2 mL), dried over $MgSO_4$, and passed through a SiO_2 plug. The pad was washed with EtOAc (10 mL) and the organic layers were concentrated under reduced pressure.

The yield was determined by ^{1}H NMR analysis with hexamethylbenzene as an internal standard. Spectral data match those previously reported.31

Any modifications of the conditions shown in this representative procedure are specified in the following schemes, which depict all of the results shown in Figure 2.4.

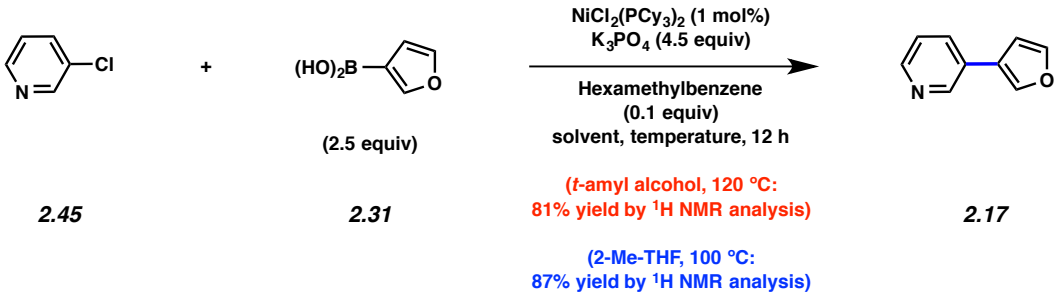

2.45 ***2.31*** ***2.17***

2.17 (Figure 2.4). The yield was determined by ^{1}H NMR analysis with hexamethylbenzene as an internal standard. Spectral data match those previously reported.[32]

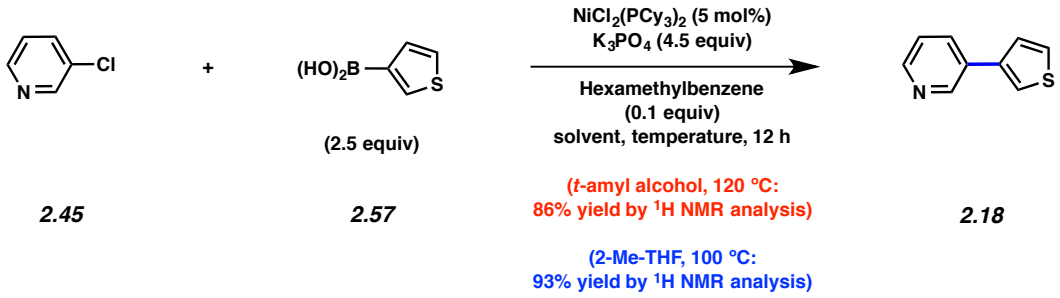

2.45 ***2.57*** ***2.18***

2.18 (Figure 2.4). The yield was determined by ^{1}H NMR analysis with hexamethylbenzene as an internal standard. Spectral data match those previously reported.[22f]

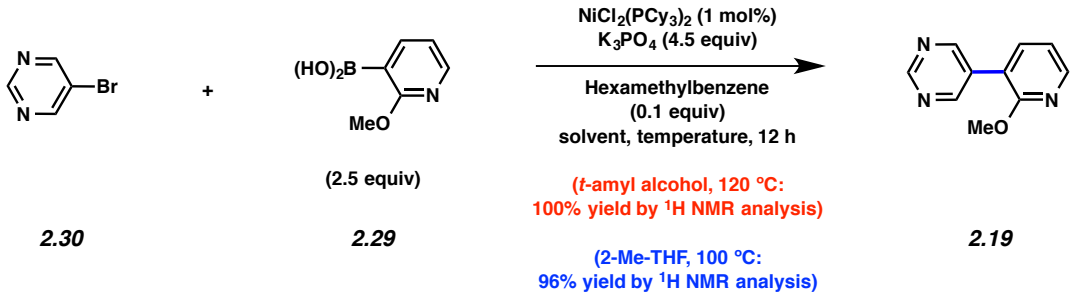

2.19 (Figure 2.4). The yield was determined by ^{1}H NMR analysis with hexamethylbenzene as an internal standard. R_f 0.24 (1:1 Hexanes:EtOAc); ^{1}H NMR: (500 MHz, $CDCl_3$): δ 9.15 (s, 1H), 8.92 (s, 2H), 8.23 (dd, J = 4.9, 1.8, 1H), 7.63 (dd, J = 7.3, 1.8, 1H), 7.02 (dd, J = 7.3, 4.9, 1H), 3.97 (s, 3H); ^{13}C NMR (125 MHz, $CDCl_3$): δ 160.8, 157.4, 156.5, 147.7, 138.2, 130.6, 117.6, 117.3, 53.7; IR (film): 3020, 2956, 1578, 1551, 1460, 1395, 1015, 798, 726 cm^{-1}; HRMS-ESI (*m*/*z*) $[M+H]^+$ calcd for $C_{10}H_9N_3O$, 188.0824; found 188.0831.

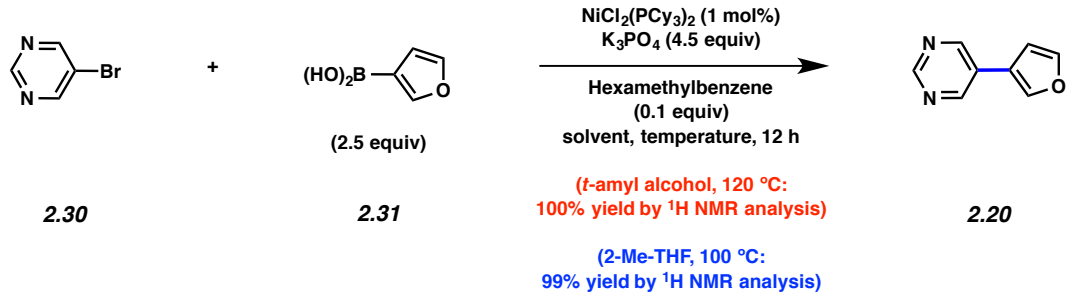

2.20 (Figure 2.4). The yield was determined by ^{1}H NMR analysis with hexamethylbenzene as an internal standard. Spectral data match those previously reported.[33]

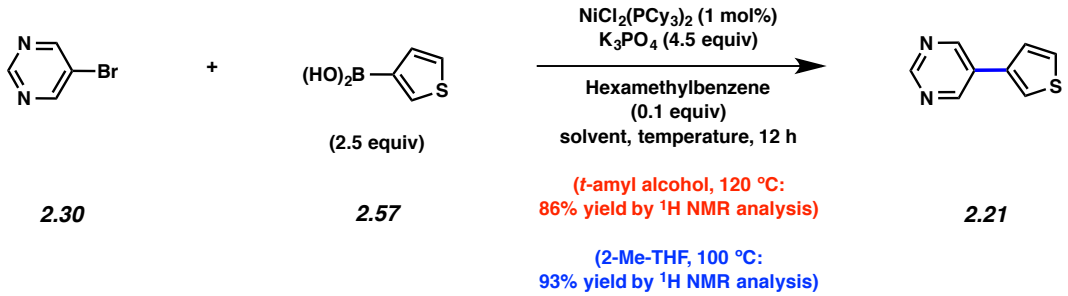

2.21 (Figure 2.4). The yield was determined by ^{1}H NMR analysis with hexamethylbenzene as an internal standard. Spectral data match those previously reported.[34]

2.8.2.7 Heterocycle-Heterocycle Cross-Couplings of Aryl Carbamates, Sulfamates, and Mesylates

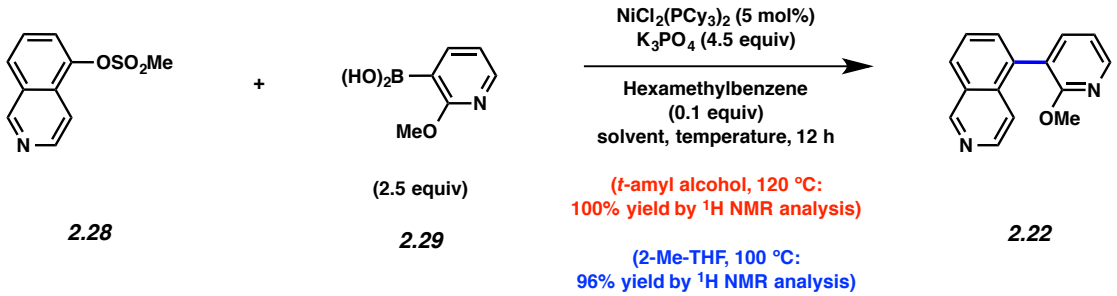

Representative Procedure (coupling of 2.28 is used as an example). 2.22 (Figure 2.4). A 1-dram vial was charged with anhydrous powdered K_3PO_4 (429.9 mg, 2.03 mmol, 4.50 equiv) and a magnetic stir bar. The vial and contents were flame-dried under reduced pressure, then allowed to cool under N_2. Hexamethylbenzene (7.3 mg, 0.045 mmol, 0.10 equiv), boronic acid **2.29** (125.9 mg, 1.125 mmol, 2.50 equiv), $NiCl_2(PCy_3)_2$ (15.5 mg, 0.023 mmol, 5 mol%), and substrate **2.28** (104.9 mg, 0.45 mmol, 1.00 equiv) were added. The vial was then evacuated and backfilled with N_2. To the vial, solvent (1.5 mL) was added and then the vial was sealed with a Teflon-lined screw cap. The mixture was allowed to stir rapidly at 23 °C for 1 h, and then heated to 100 °C (2-Me-THF) or 120 °C (*t*-amyl alcohol) for 12 h. The reaction vessel was cooled to 23 °C and then transferred to a test tube containing 1 M aqueous HCl (4 mL). The layers were

separated; the aqueous layer was extracted with EtOAc (3 x 2 mL). The combined organic layers were then washed with brine (2 mL), dried over Na_2SO_4, and passed through a SiO_2 plug. The pad was washed with EtOAc (10 mL) and the organic layers were concentrated under reduced pressure. The yield was determined by ^{1}H NMR analysis with hexamethylbenzene as an internal standard. R_f 0.40 (1:1 Hexanes:Acetone); ^{1}H NMR: (600 MHz, $CDCl_3$): δ 9.30 (d, J = 0.9, 1H), 8.46 (d, J = 6.0, 1H), 8.31 (dd, J = 5.0, 1.9, 1H), 8.01 (dt, J = 8.0, 0.9, 1H), 7.67 (dd, J = 7.0, 0.9, 1H), 7.63 (dd, J = 7.0, 1.3, 1H), 7.58 (dd, J = 7.2, 1.9, 1H), 7.35 (dt, J = 5.9, 0.9, 1H), 7.05 (dd, J = 7.2, 5.0, 1H), 3.87 (s, 3H); ^{13}C NMR (125 MHz, $CDCl_3$): 161.5, 153.0, 147.0, 143.3, 140.2, 134.5, 134.2, 131.7, 128.8, 127.8, 126.9, 122.0, 118.6, 116.9, 53.6; IR (film): 3404, 2931, 1618, 1574, 1459, 1400, 1015, 776 cm^{-1}; HRMS-ESI (m/z) $[M+H]^+$ calcd for $HC_{15}H_{21}N_2O$, 237.1025; found 237.1028.

Any modifications of the conditions shown in this representative procedure are specified in the following schemes, which depict all of the results shown in Figure 2.4.

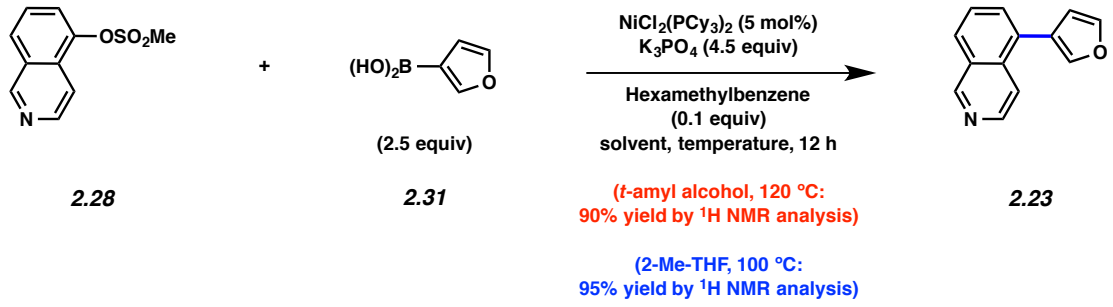

2.28 ***2.31*** ***2.23***

2.23 (Figure 2.4). The yield was determined by ^{1}H NMR analysis with hexamethylbenzene as an internal standard. Spectral data match those previously reported.[32]

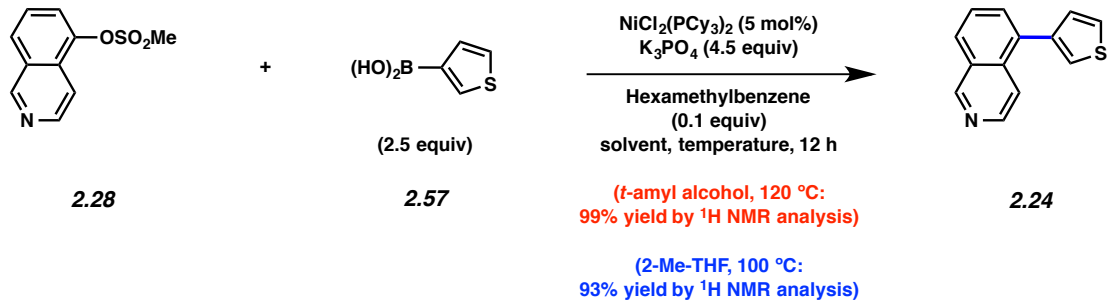

2.28 *2.57* *2.24*

2.24 (Figure 2.4). The yield was determined by ^{1}H NMR analysis with hexamethylbenzene as an internal standard. R_f 0.43(1:1 Hexanes:EtOAc); ^{1}H NMR: (600 MHz, $CDCl_3$): δ 9.29 (s, 1H), 8.51 (d, *J* = 6.0, 1H), 7.96 (d, *J* = 8.2, 1H), 7.85 (d, *J* = 6.0, 1H), 7.71 (dd, *J* = 7.2, 1.2, 1H), 7.63 (t, *J* = 7.2, 1H), 7.50 (dd, *J* = 4.9, 3.0, 1H), 7.42 (dd, *J* = 3.0, 1.2, 1H), 7.30 (dd, J = 4.9, 1.2, 1H); ^{13}C NMR (150 MHz, $CDCl_3$): δ 151.9, 148.6, 142.5, 138.6, 133.4, 133.1, 129.9, 128.2, 128.1, 126.3, 125.9, 125.1, 123.0, 117.5; IR (film): 3072, 1938, 1721, 1615, 1585, 1370, 829, 787, 663 cm^{-1}; HRMS-ESI (*m/z*) $[M+H]^+$ calcd for $C_{13}H_9NS$, 212.0534; found 212.0530.

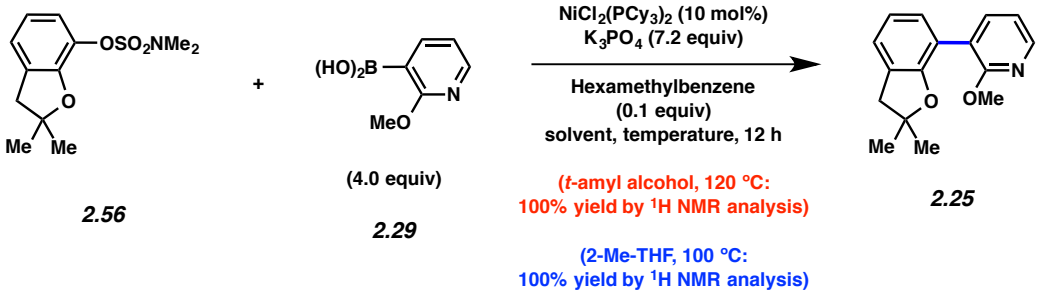

2.56 *2.29* *2.25*

2.25 (Figure 2.4). The yield was determined by ^{1}H NMR analysis with hexamethylbenzene as an internal standard. R_f 0.59 (3:1 Hexanes:EtOAc); ^{1}H NMR: (400 MHz, $CDCl_3$): δ 8.13 (dd, *J* = 4.9, 1.9, 1H), 7.70 (dd, *J* = 7.4, 1.9, 1H), 7.23 (d, *J* = 7.7, 1H), 7.12 (d, *J* = 7.2, 1H), 6.94 (dd, *J* = 7.2, 4.9, 1H), 6.87 (t, *J* = 7.4, 1H), 3.95 (s, 3H), 3.05 (s, 2H), 1.46 (s, 6H); ^{13}C NMR (125 MHz, $CDCl_3$): δ 161.2, 156.7, 145.7, 145.6, 139.5, 129.4, 127.7, 124.7, 120.9, 119.7, 118.8, 116.7,

86.6, 53.5, 43.1, 28.3; IR (film): 2927, 1577, 1439, 1397, 1297, 1257 cm^{-1}; HRMS-ESI (*m/z*) $[M+H]^+$ calcd for $C_{16}H_{17}NO_2$, 256.1338; found 256.1335.

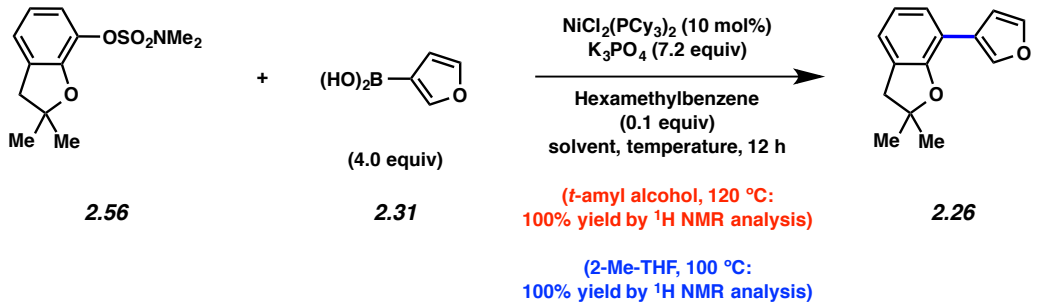

2.56 ***2.31*** ***2.26***

2.26 (Figure 2.4). The yield was determined by ^1H NMR analysis with hexamethylbenzene as an internal standard. R_f 0.38 (4:1 Hexanes:Benzene); ^1H NMR: (600 MHz, $CDCl_3$): δ 8.06 (s, 1H), 7.46 (t, *J* = 1.5, 1H), 7.30 (d, *J* = 7.5, 1H), 7.04 (dd, *J* = 7.2, 0.8, 1H), 6.86 (t, *J* = 7.5, 1H), 6.83 (d, *J* = 1.3, 1H), 3.06 (s, 2H), 1.53 (s, 6H); ^{13}C NMR (125 MHz, $CDCl_3$): 155.8, 142.7, 141.3, 127.6, 125.1, 123.3, 121.7, 120.2, 114.9, 108.5, 86.9, 42.9, 28.6; IR (film): 2972, 1599, 1510, 1449, 1295, 1246, 1160, 1024 cm^{-1}; HRMS-ESI (*m/z*) $[M+H]^+$ calcd for $C_{14}H_{14}O_2$, 215.1072; found 215.1065.

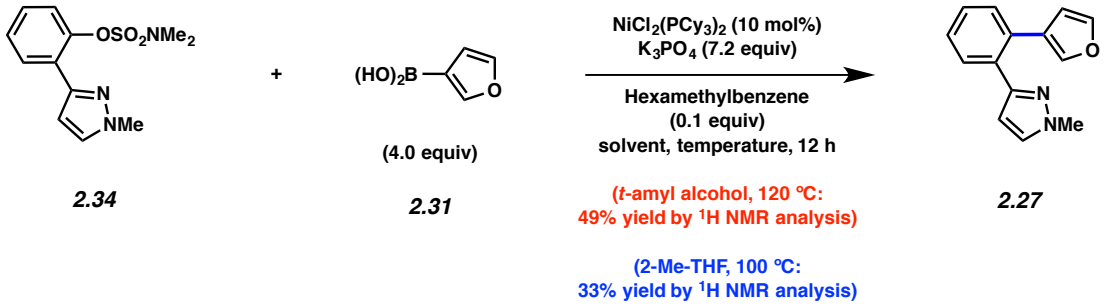

2.34 ***2.31*** ***2.27***

2.27 (Figure 2.4). The yield was determined by ^1H NMR analysis with hexamethylbenzene as an internal standard. R_f 0.54 (1:1 Hexanes:EtOAc); ^1H NMR: (600 MHz, $CDCl_3$): δ 7.64-7.62 (m, 1H), 7.39-7.37 (m, 1H), 7.35-7.33 (m, 4H), 7.26-7.25 (m, 1H), 6.28 (d, J = 0.9, 1H), 5.99 (d, J =

2.2, 1H), 3.93 (s, 3H); ^{13}C NMR (125 MHz, $CDCl_3$): δ 151.5, 142.2, 140.1, 133.0, 131.6, 130.3, 130.1, 129.9, 127.9, 127.4, 125.9, 111.9, 106.6, 39.0; IR (film): 2930, 1460, 1368, 1161, 850, 742 cm^{-1}.

2.8.2.8 Isolation Experiments

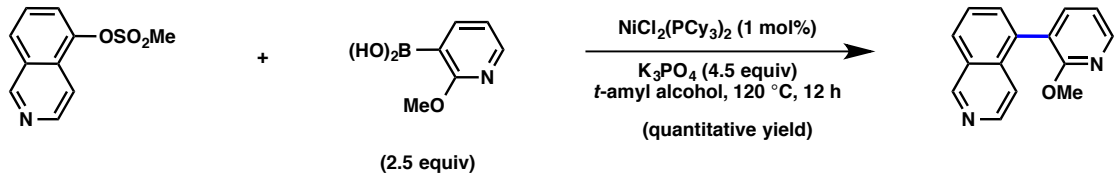

2.28 ***2.29*** ***2.22***

A 100 mL round bottom flask was charged with anhydrous powdered K_3PO_4 (4.28 g, 20.16 mmol, 4.50 equiv) and a magnetic stir bar. The flask and contents were flame-dried under reduced pressure, then allowed to cool under N_2. Boronic acid **2.29** (1.71 g, 11.20 mmol, 2.50 equiv), $NiCl_2(PCy_3)_2$ (31.1 mg, 0.045 mmol, 1 mol%), and isoquinoline **2.28** (1.00 g, 4.48 mmol, 1.00 equiv) were added. The flask was then evacuated and backfilled with N_2. *Tert*-amyl alcohol (14.93 mL) was added and the flask was equipped with a water-cooled condenser. The heterogeneous mixture was allowed to stir at 23 °C for 1 h, then heated to 120 °C for 12 h. The reaction vessel was cooled to 23 °C and then transferred to a round bottom flask containing CH_2Cl_2 (45 mL), EtOAc (15 mL), and MeOH (3 mL). Silica gel (24 mL) was added and the solvent was removed under reduced pressure to afford a free-flowing powder. This powder was then dry-loaded onto a silica gel column (7 cm x 15 cm) and purified by flash chromatography (6:1 Hexanes:Acetone) to yield hetero-biaryl product **2.22** (1.06 g, 100% yield) as a white solid. R_f 0.40 (1:1 Hexanes:Acetone); ^{1}H NMR: (600 MHz, $CDCl_3$): δ 9.30 (d, J = 0.9, 1H), 8.46 (d, J = 6.0, 1H), 8.31 (dd, J = 5.0, 1.9, 1H), 8.01 (dt, J = 8.0, 0.9, 1H), 7.67 (dd, J = 7.0, 0.9, 1H), 7.63

(dd, J = 7.0, 1.3, 1H), 7.58 (dd, J = 7.2, 1.9, 1H), 7.35 (dt, J = 5.9, 0.9, 1H), 7.05 (dd, J = 7.2, 5.0, 1H), 3.87 (s, 3H); ^{13}C NMR (125 MHz, $CDCl_3$): 161.5, 153.0, 147.0, 143.3, 140.2, 134.5, 134.2, 131.7, 128.8, 127.8, 126.9, 122.0, 118.6, 116.9, 53.6; IR (film): 3404, 2931, 1618, 1574, 1459, 1400, 1015, 776 cm^{-1}; HRMS-ESI (m/z) $[M+H]^+$ calcd for $HC_{15}H_{12}N_2O$, 237.1025; found 237.1028.

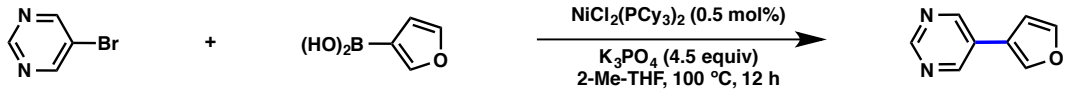

A 250 mL round-bottom flask was charged with anhydrous powdered K_3PO_4 (30.04 g, 141.53 mmol, 4.50 equiv) and a magnetic stir bar. The flask and contents were flame-dried under reduced pressure, then allowed to cool under N_2. Boronic acid **2.31** (8.80 g, 78.63 mmol, 2.50 equiv), $NiCl_2(PCy_3)_2$ (110.47 mg, 0.16 mmol, 0.5 mol%), and pyrimidine **2.30** (5.00 g, 31.45 mmol, 1.00 equiv) were added. The flask was then evacuated and backfilled with N_2. 2-Me-THF (104.83 mL) was added and the flask was equipped with a water-cooled condenser. The heterogeneous mixture was allowed to stir at 23 °C for 1 h, then heated to 100 °C for 12 h. The reaction vessel was cooled to 23 °C and was quenched with 1 M HCl (20 mL). The layers were separated; the aqueous layer was extracted with EtOAc (3 x 100 mL). The combined organic layers were then washed with brine (50 mL), dried over $MgSO_4$, and concentrated under reduced pressure. The crude residue was purified by flash chromatography (3:1 Hexanes:EtOAc) to yield bis(heterocyclic) compound **2.20** as a yellow solid (4.46 g, 97% yield). R_f 0.25 (3:1 Hexanes:EtOAc). Spectral data match those previously reported.[33]

2.8.2.9 Cross-coupling Reactions Utilizing Microwave Heating

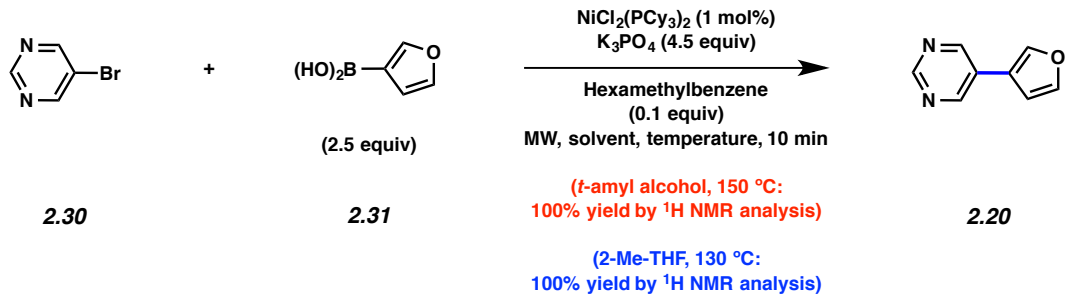

2.30 ***2.31*** ***2.20***

A 10 mL microwave vial was charged with anhydrous powdered K_3PO_4 (620.9 mg, 2.93 mmol, 4.50 equiv) and a magnetic stir bar. The vial and contents were flame-dried under reduced pressure, then allowed to cool under N_2. Boronic acid **2.31** (181.8 mg, 1.63 mmol, 2.50 equiv), $NiCl_2(PCy_3)_2$ (4.5 mg, 0.033 mmol, 1 mol%), and pyrimidine **2.30** (103.3 mg, 0.65 mmol, 1.00 equiv) were added. The flask was then evacuated and backfilled with N_2. The solvent (2.2 mL) was added and the heterogeneous mixture was subsequently placed in the microwave cavity and irradiated at the temperature indicated for 10 min (hold time). The reaction vessel was cooled to 23 °C and was quenched with 1 M HCl (2 mL). The layers were separated; the aqueous layer was extracted with EtOAc (3 x 2 mL). The combined organic layers were then washed with brine (2 mL), dried over $MgSO_4$, and passed through a SiO_2 plug. The pad was washed with EtOAc (10 mL) and the organic layers were concentrated under reduced pressure. The yield was determined by ^1H NMR analysis with hexamethylbenzene as an internal standard. R_f 0.25 (3:1 Hexanes:EtOAc). Spectral data match those previously reported.[34]

Appendix Two: Spectra Relevant to Chapter Two

Nickel-Catalyzed Suzuki–Miyaura Couplings in Green Solvents

Stephen D. Ramgren, Liana Hie, Yuxuan Ye, and Neil K. Garg.

Org. Lett. **2013**, *15*, 3950–3953.

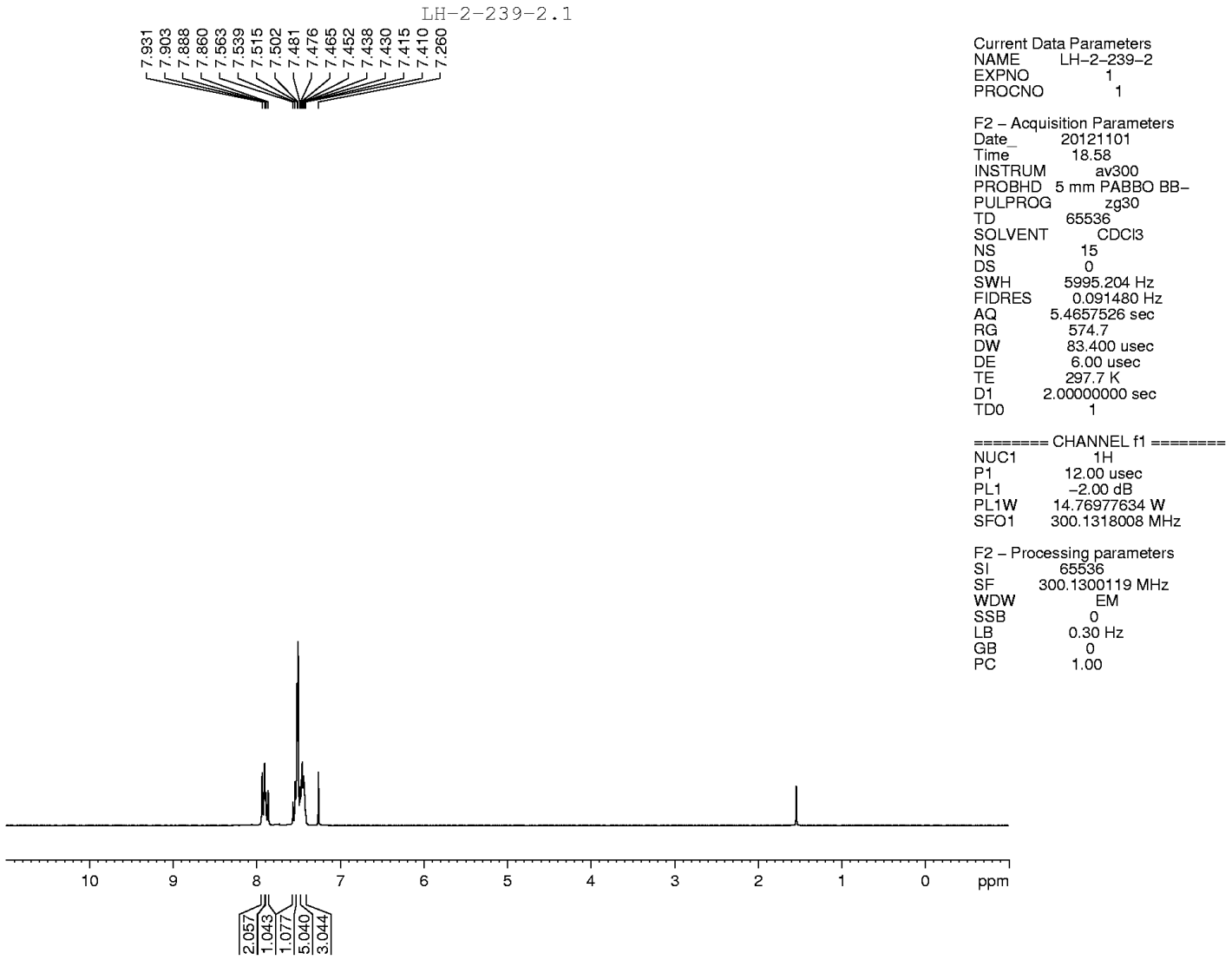

Figure A2.1 ^{1}H NMR (300 MHz, $CDCl_3$) of compound **2.3**.

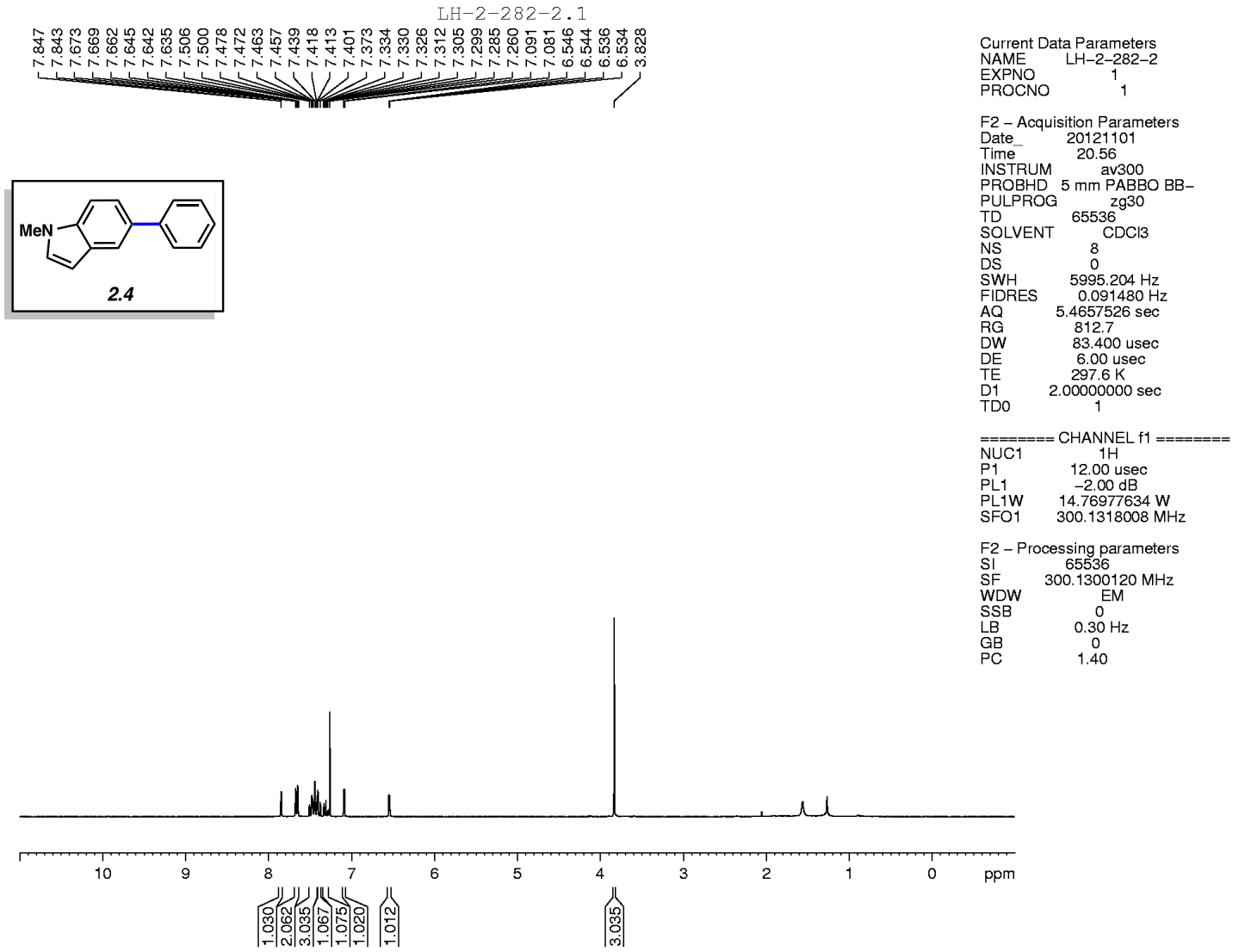

Figure A2.2 ^{1}H NMR (300 MHz, $CDCl_3$) of compound **2.4**.

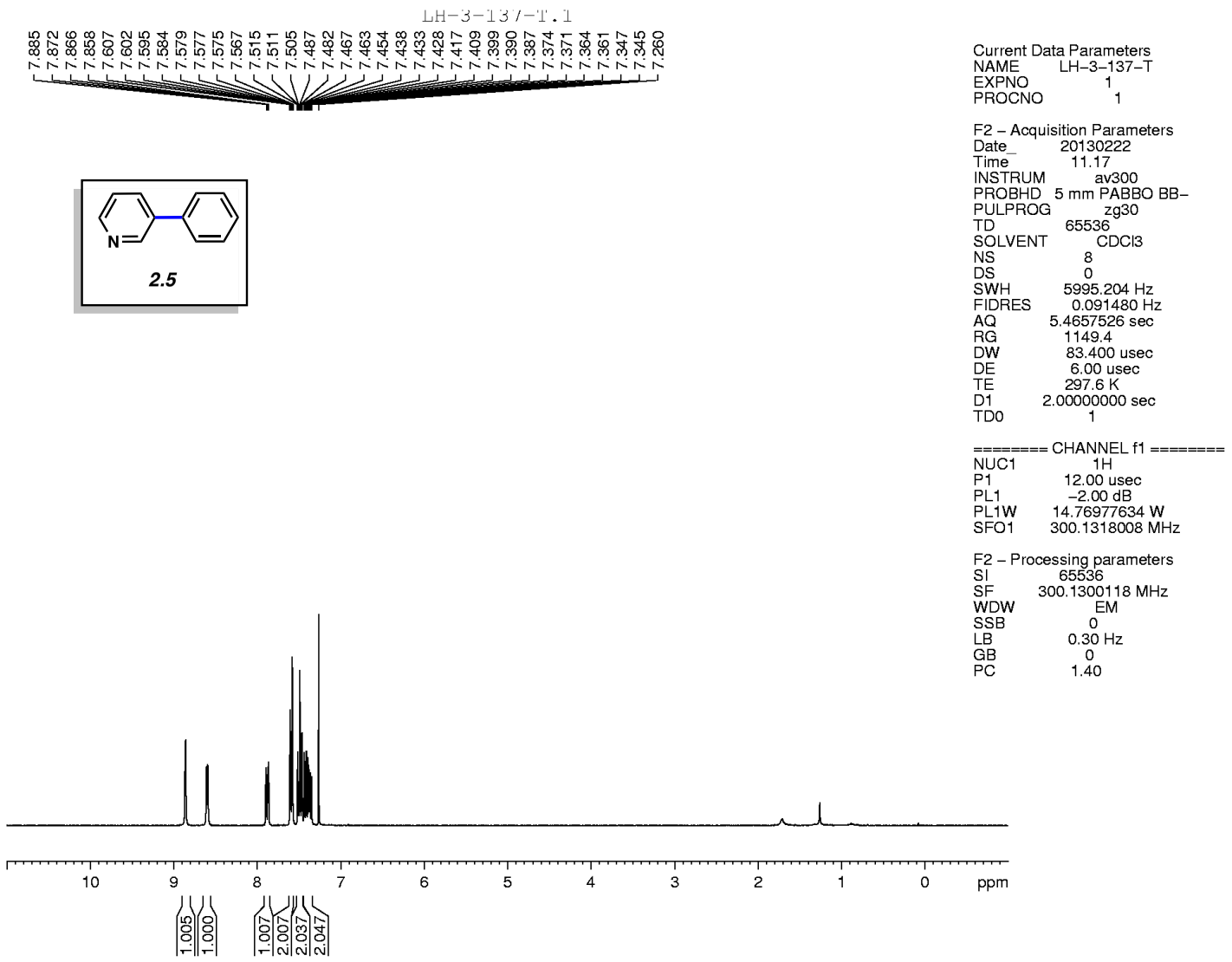

Figure A2.3 ^{1}H NMR (300 MHz, $CDCl_3$) of compound **2.5**.

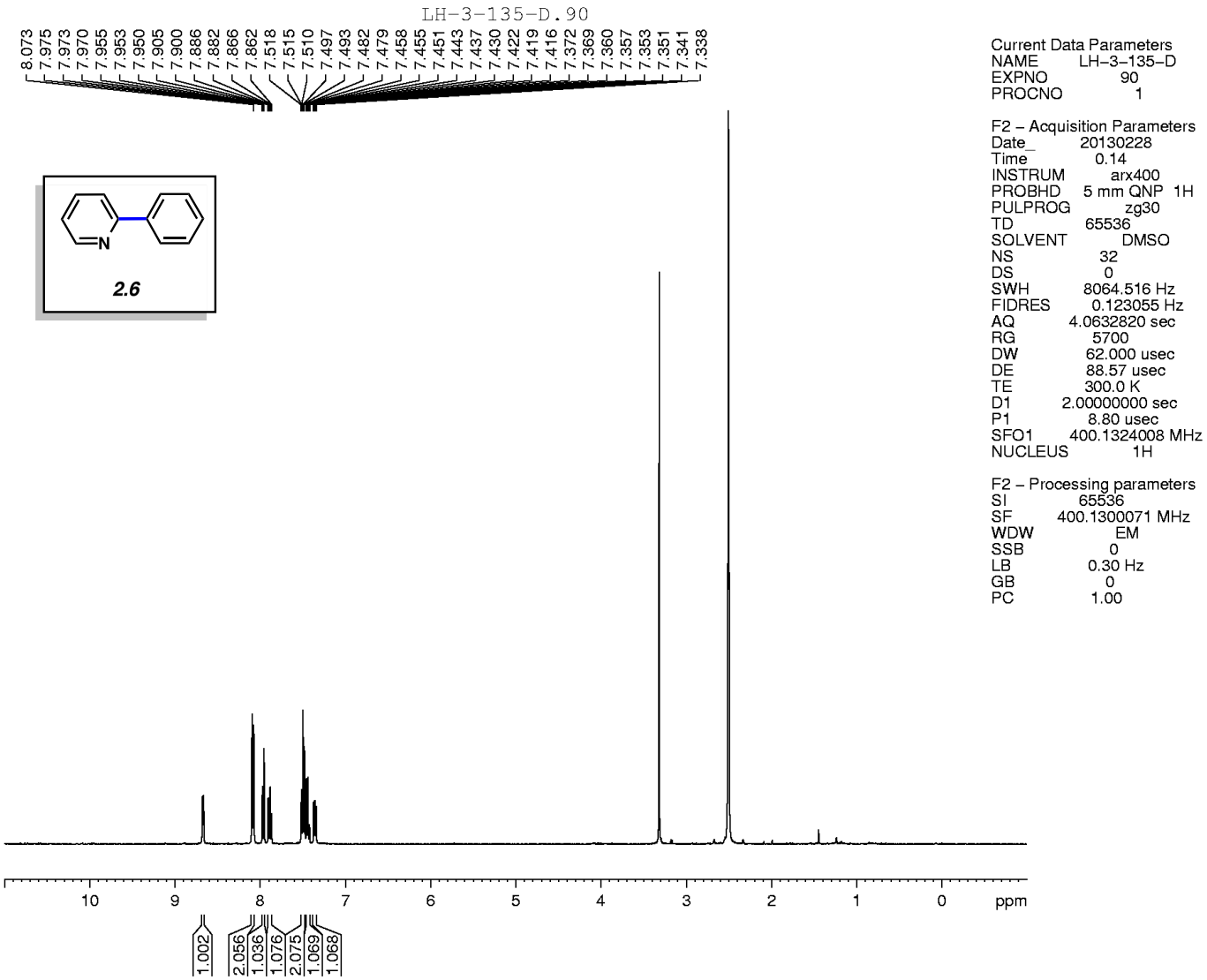

Figure A2.4 ^{1}H NMR (400 MHz, DMSO-d_6) of compound **2.6**.

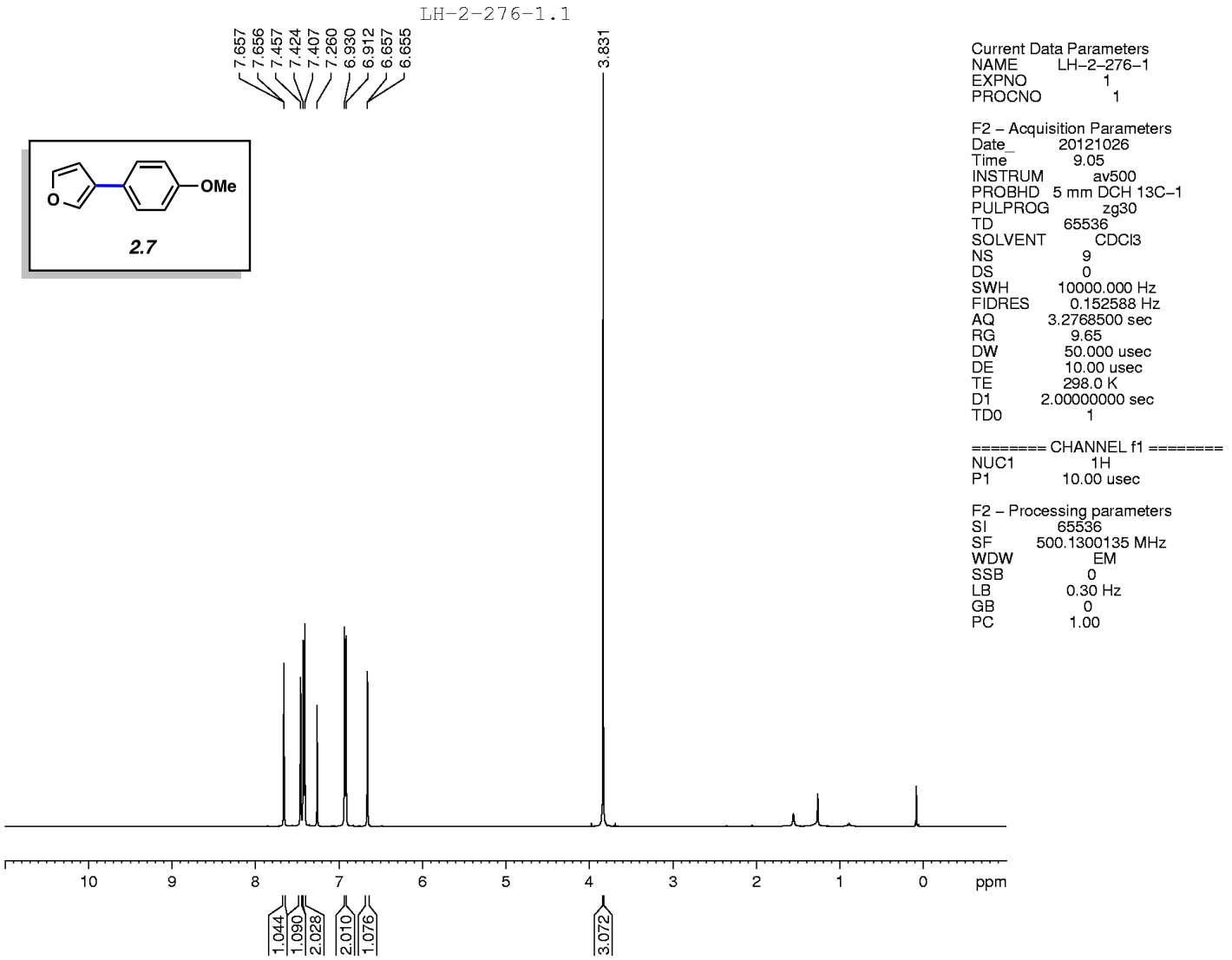

Figure A2.5 ^{1}H NMR (500 MHz, $CDCl_3$) of compound **2.7**.

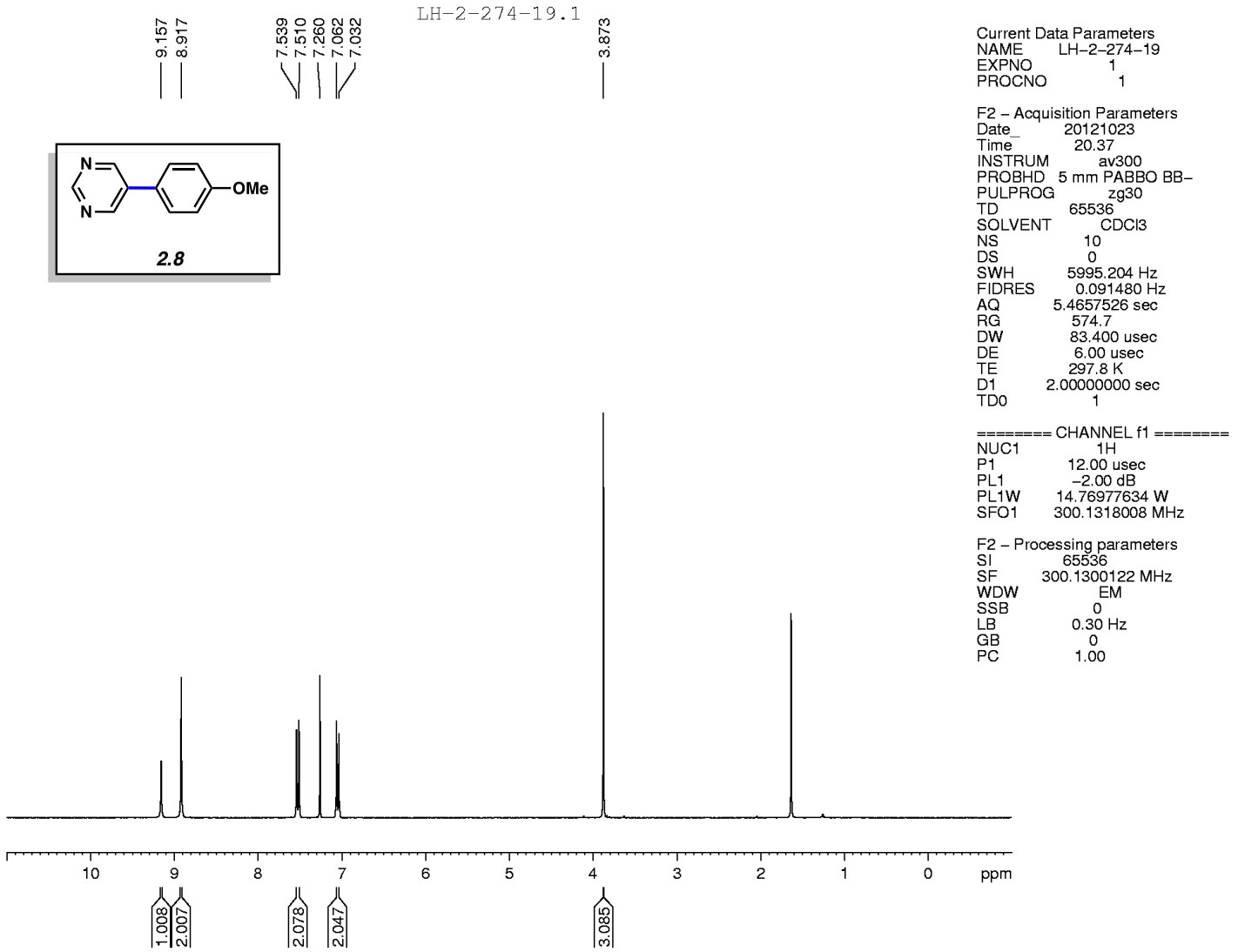

Figure A2.6 ^{1}H NMR (300 MHz, $CDCl_3$) of compound **2.8**.

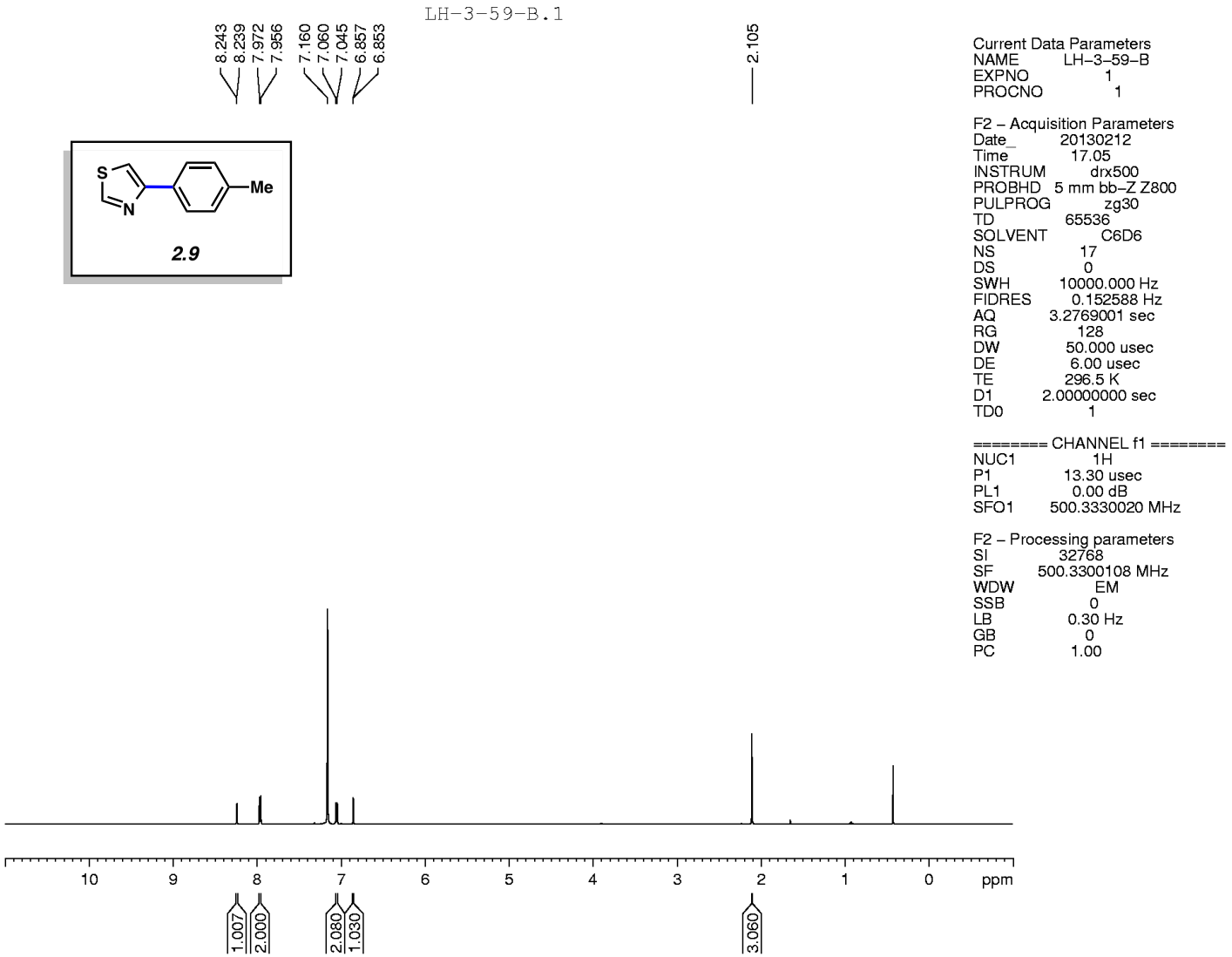

Figure A2.7 ^{1}H NMR (500 MHz, C_6D_6) of compound **2.9**.

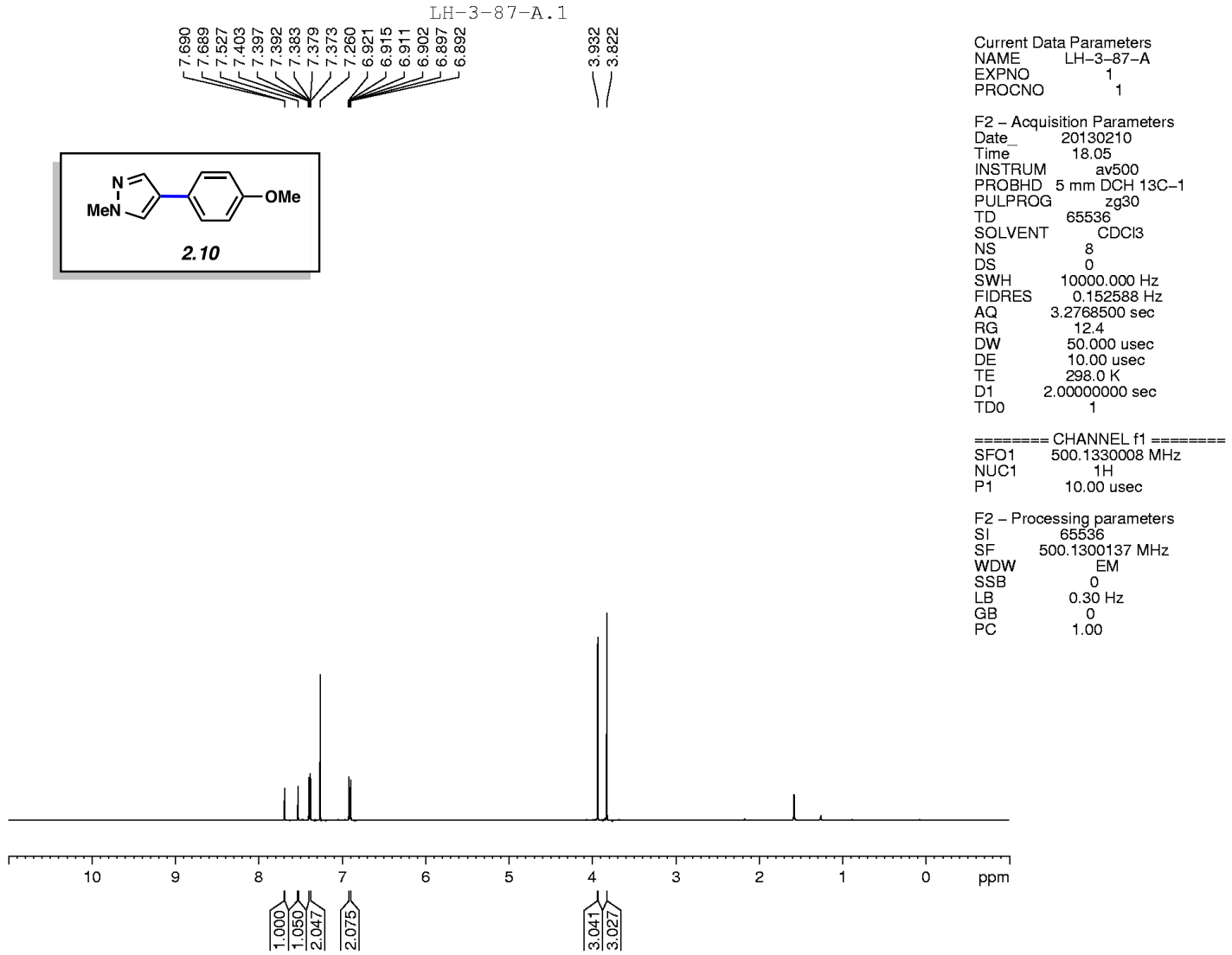

Figure A2.8 ^{1}H NMR (500 MHz, $CDCl_3$) of compound **2.10**.

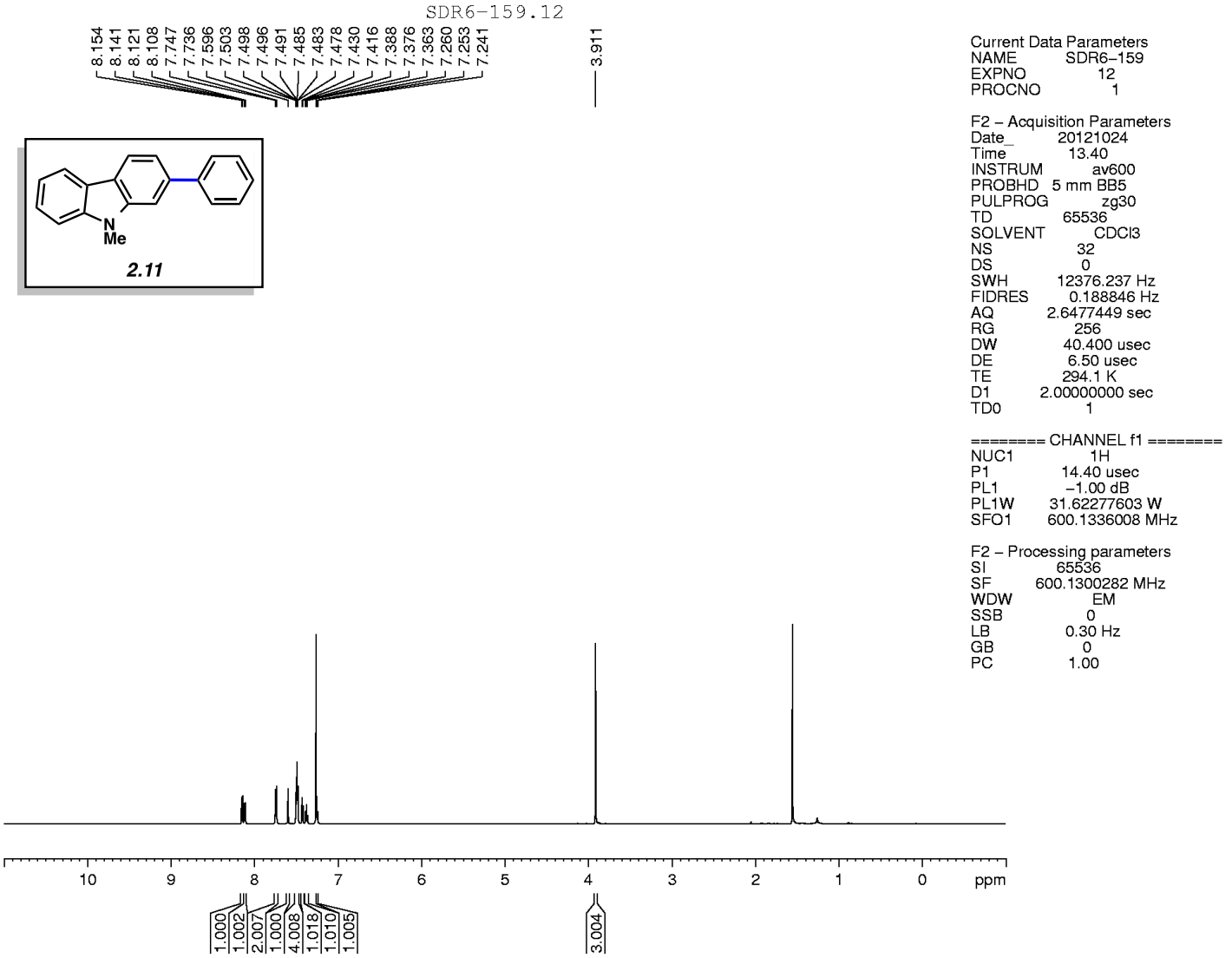

Figure A2.9 ^{1}H NMR (600 MHz, $CDCl_3$) of compound **2.11**.

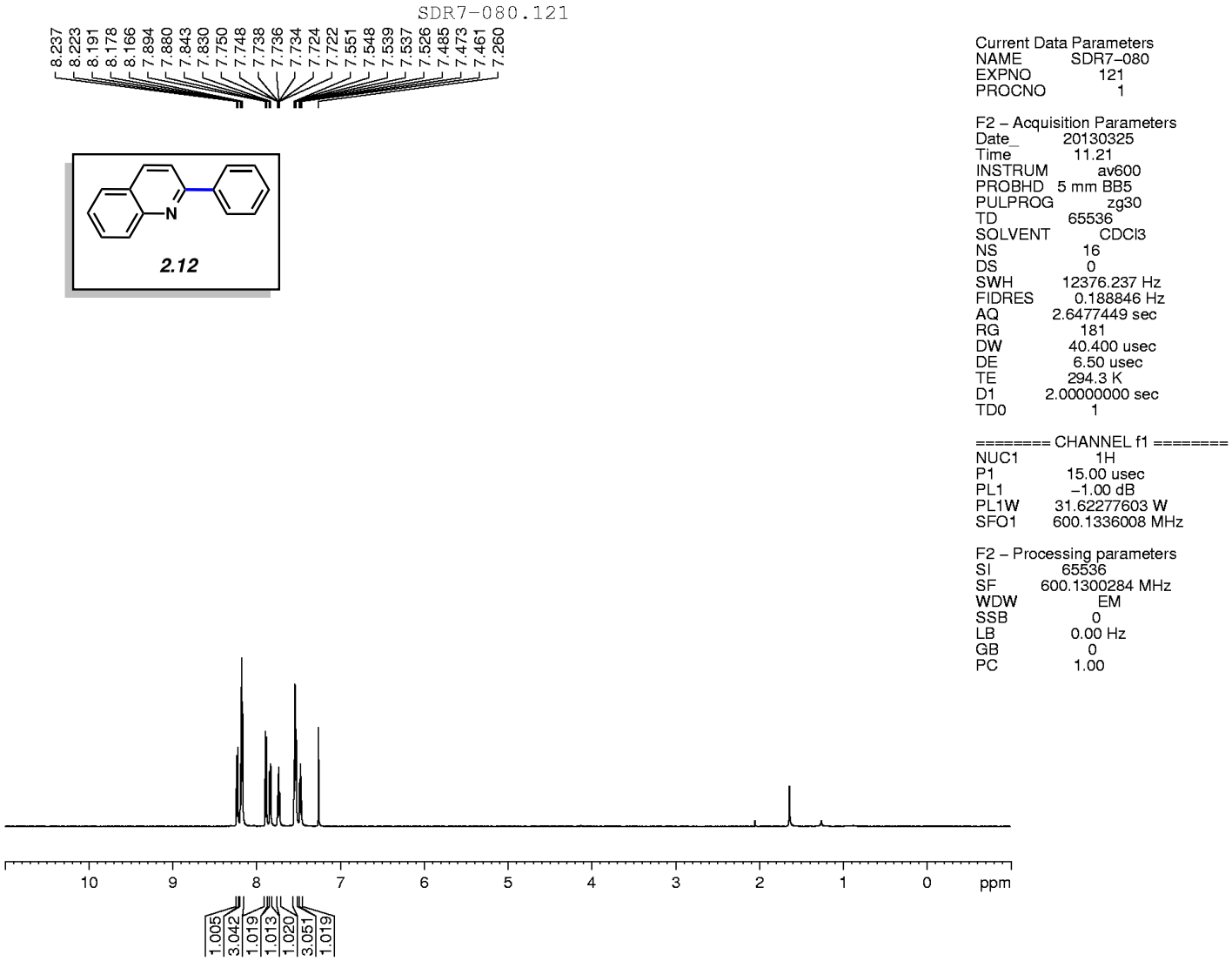

Figure A2.10 ^{1}H NMR (600 MHz, $CDCl_3$) of compound **2.12**.

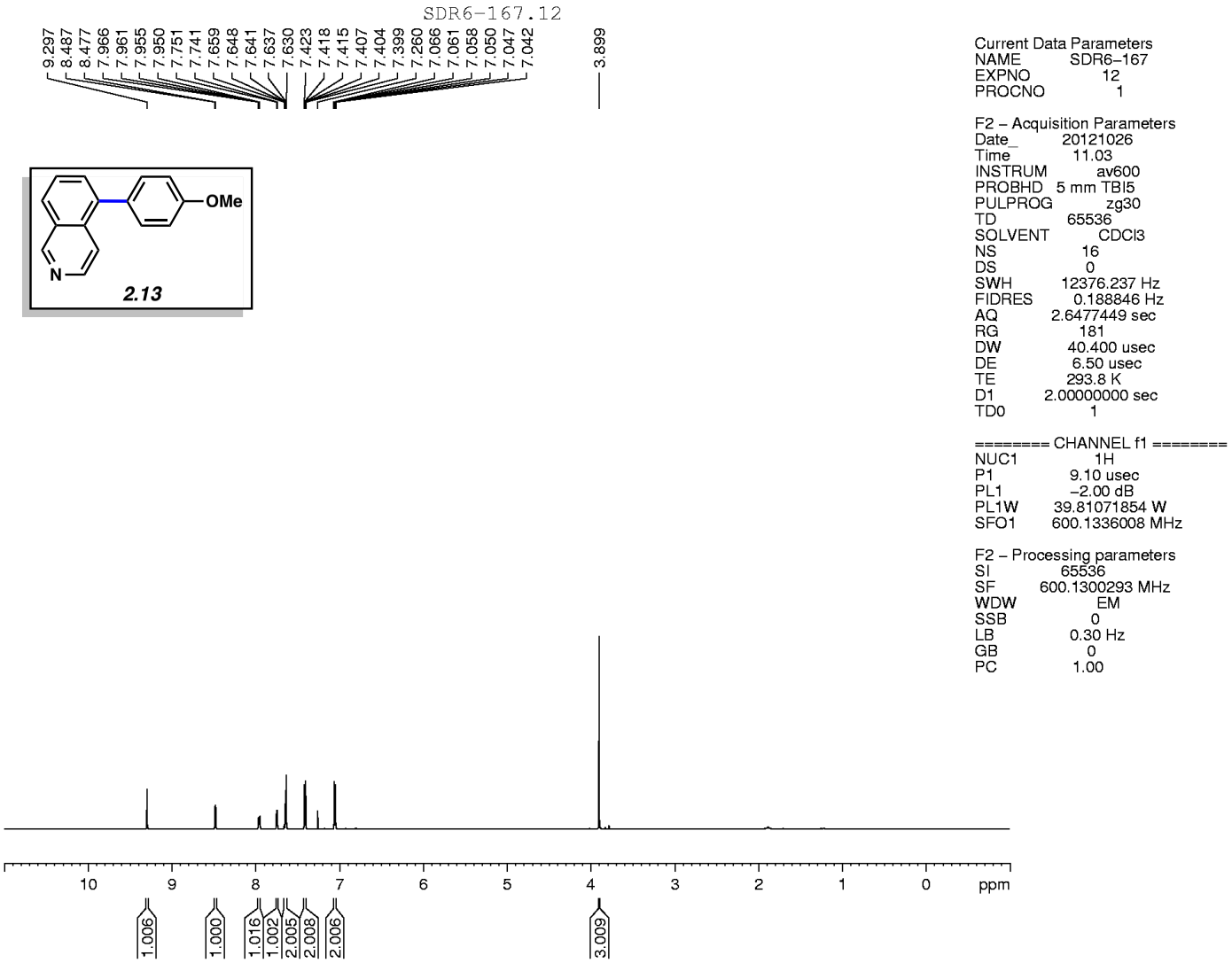

Figure A2.11 ^{1}H NMR (600 MHz, $CDCl_3$) of compound **2.13**.

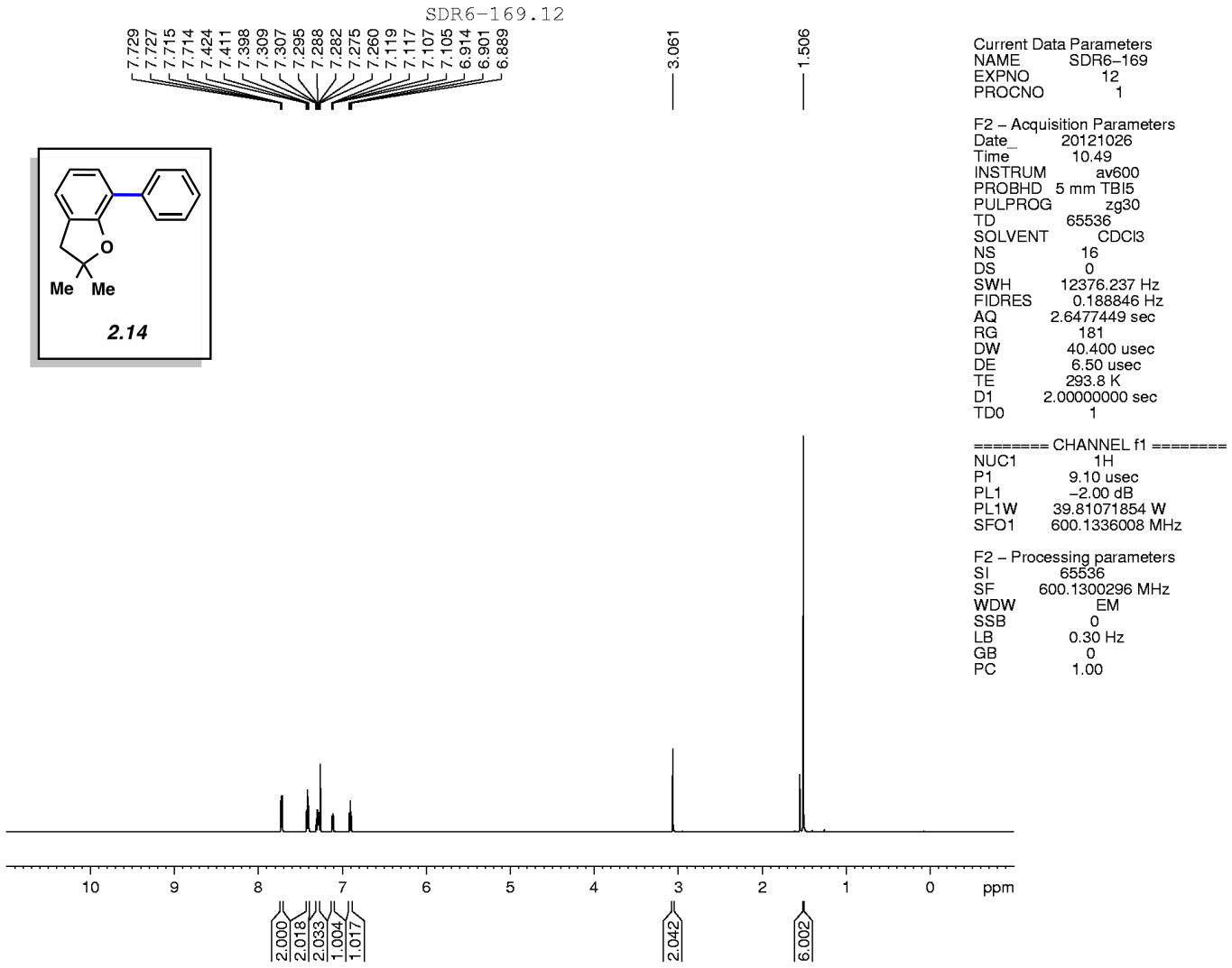

Figure A2.12 ^{1}H NMR (600 MHz, $CDCl_3$) of compound **2.14**.

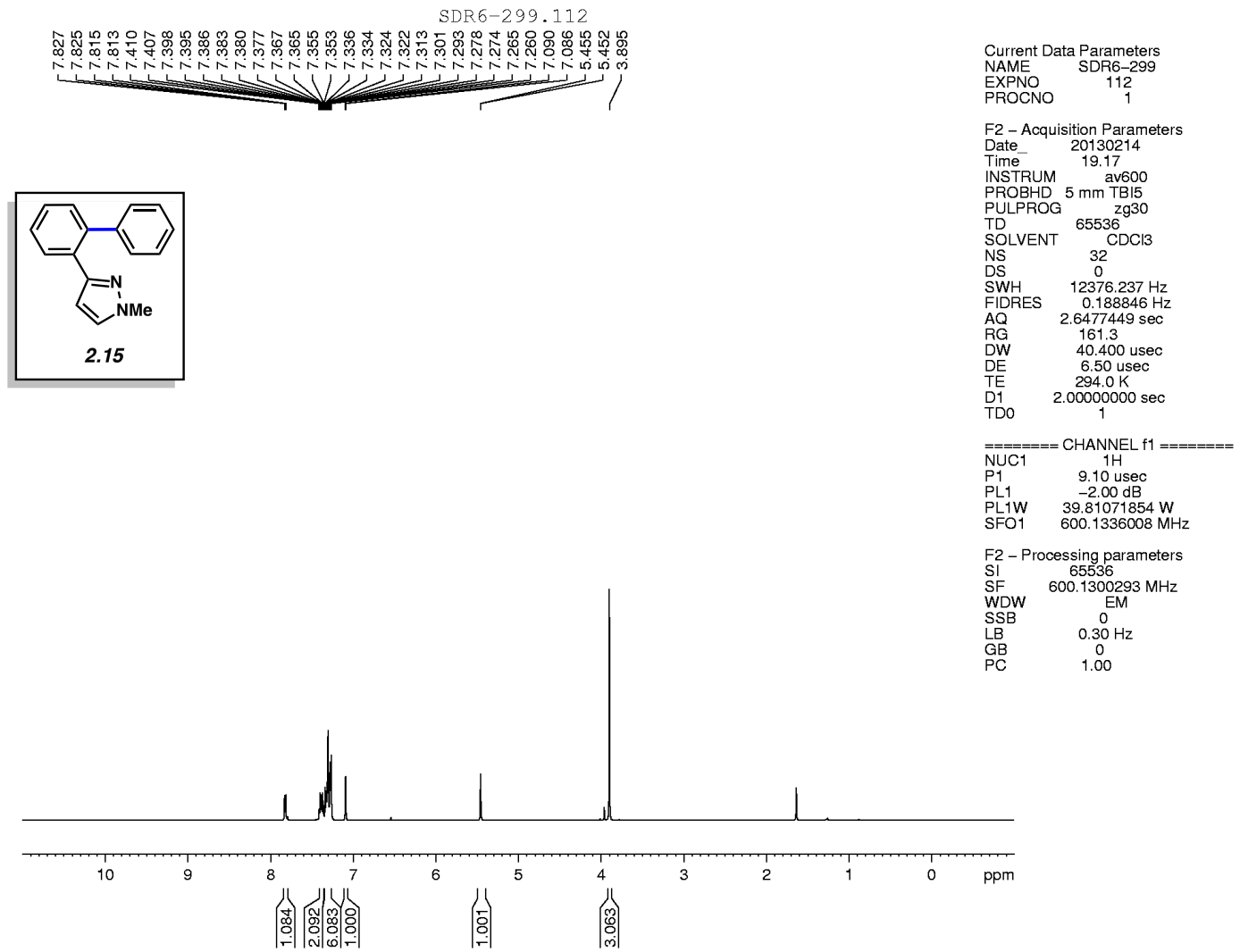

Figure A2.13 ^{1}H NMR (600 MHz, $CDCl_3$) of compound **2.15**.

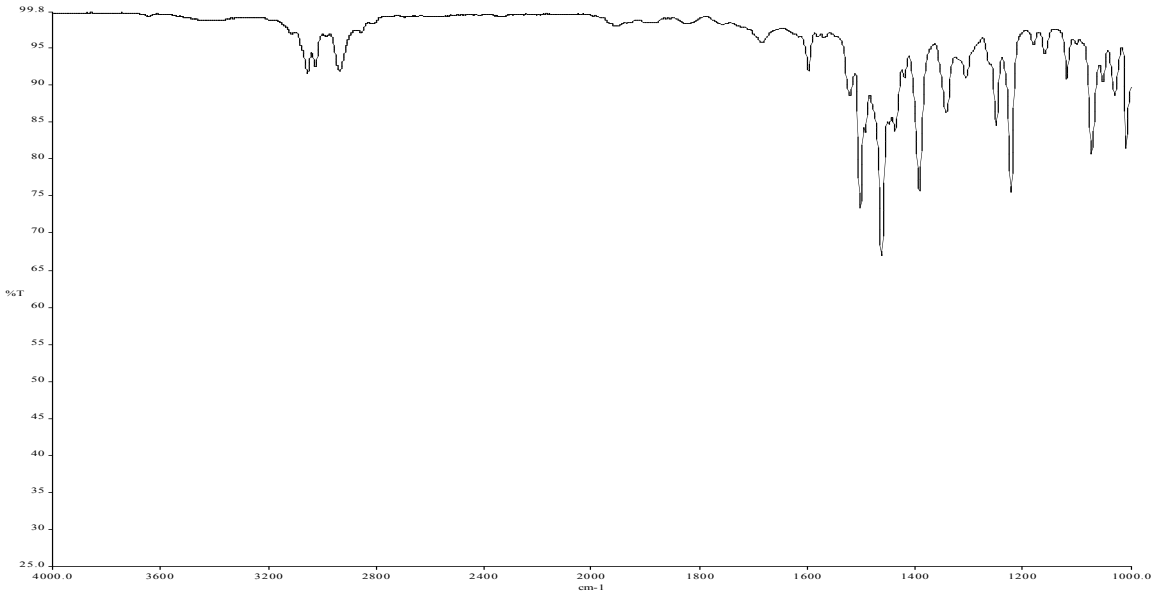

Figure A2.14 Infrared spectrum of compound **2.15**.

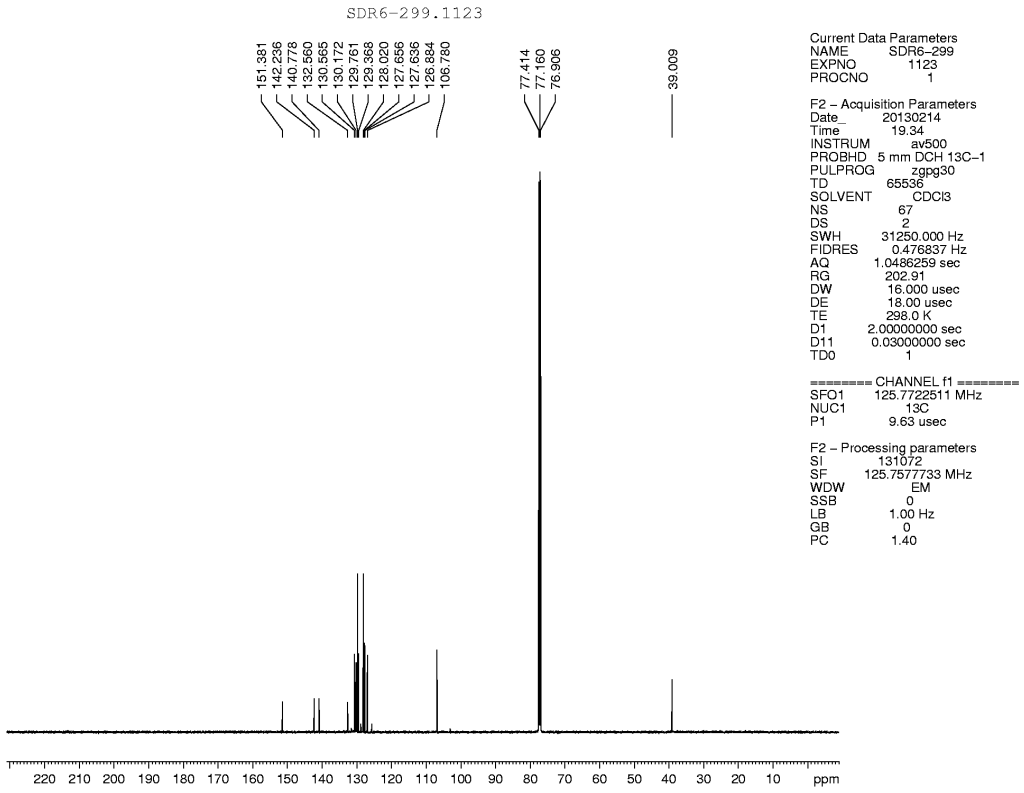

Figure A2.15 ^{13}C NMR (125 MHz, $CDCl_3$) of compound **2.15**.

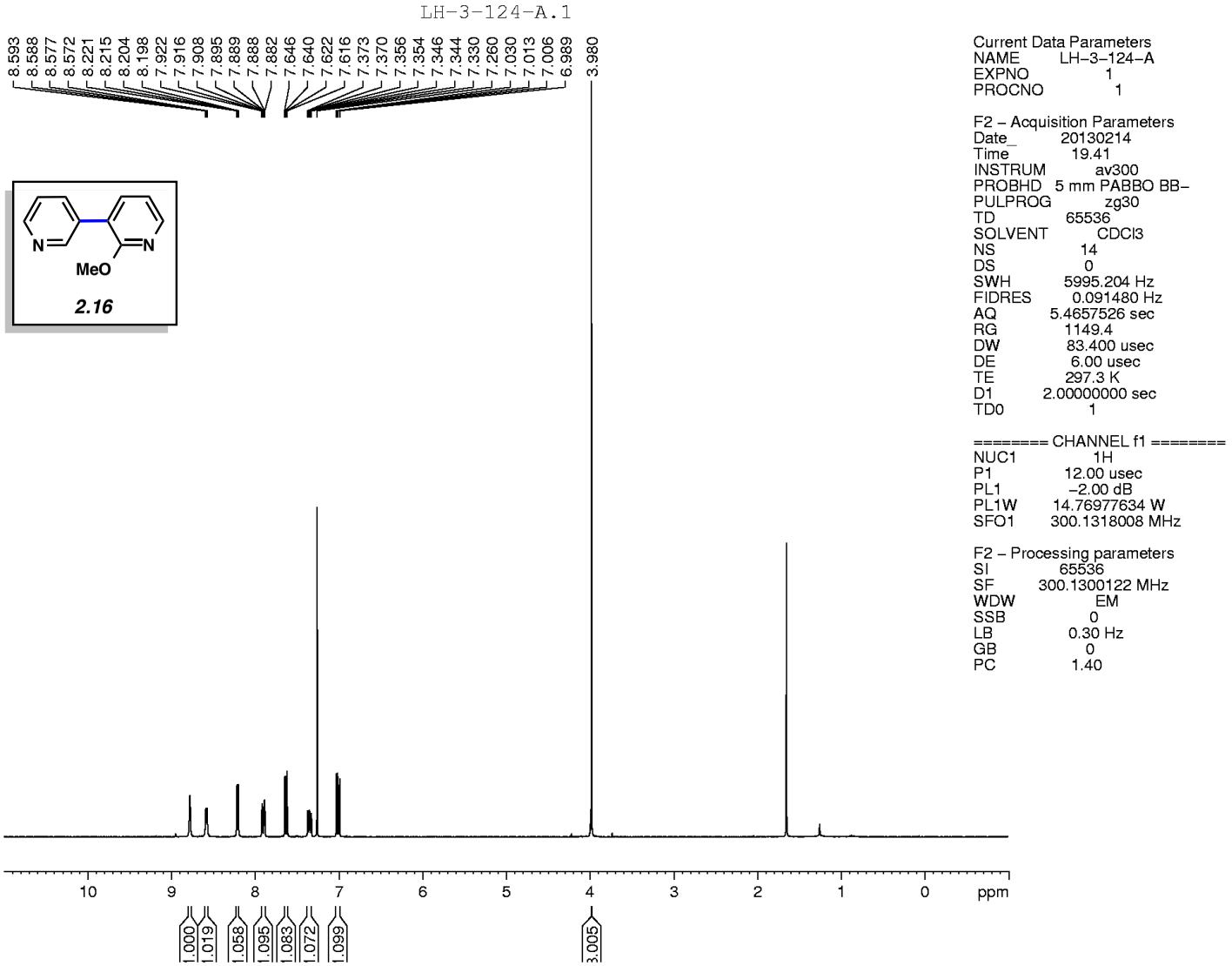

Figure A2.16 ^{1}H NMR (300 MHz, $CDCl_3$) of compound **2.16**.

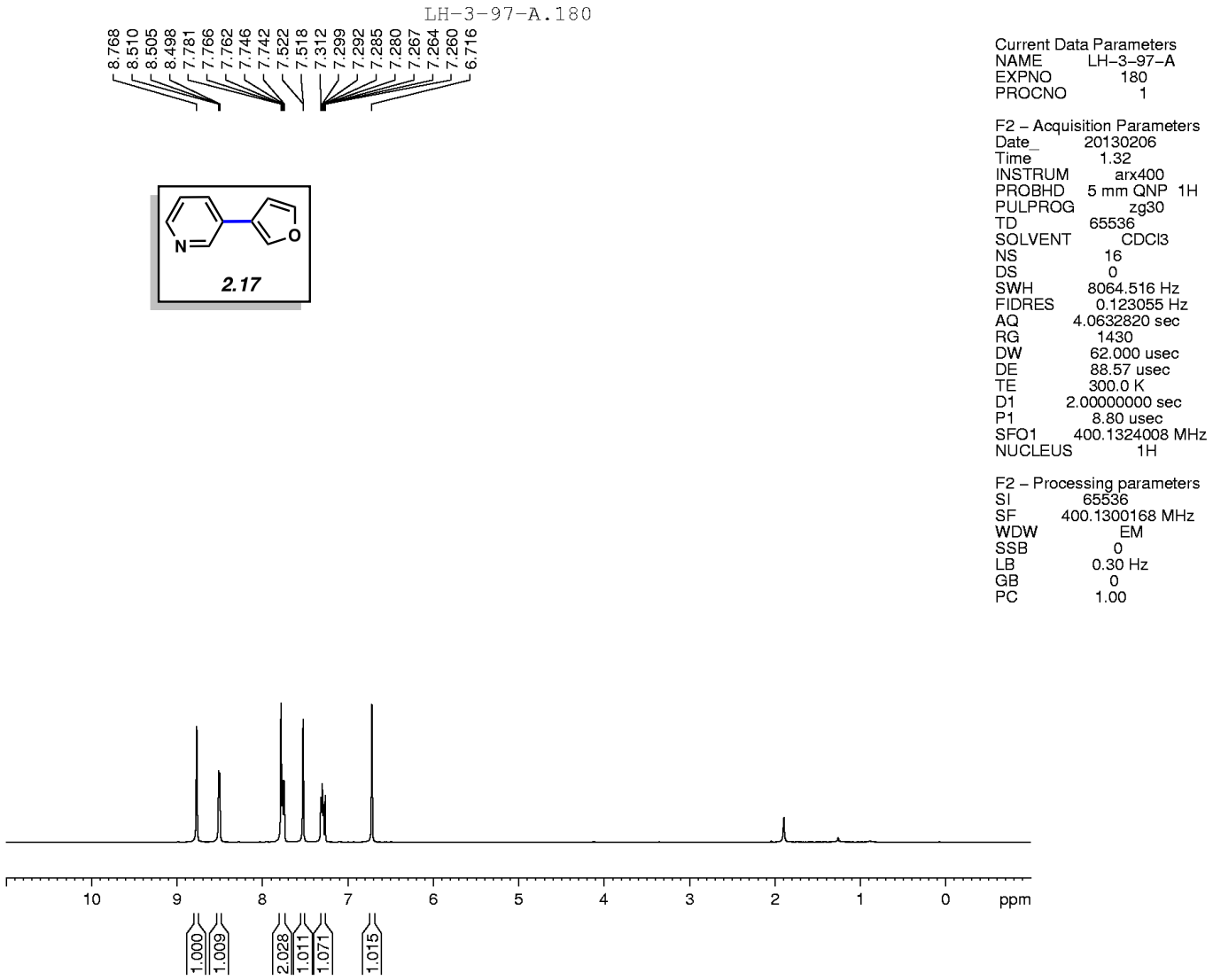

Figure A2.17 ^{1}H NMR (400 MHz, $CDCl_3$) of compound **2.17**.

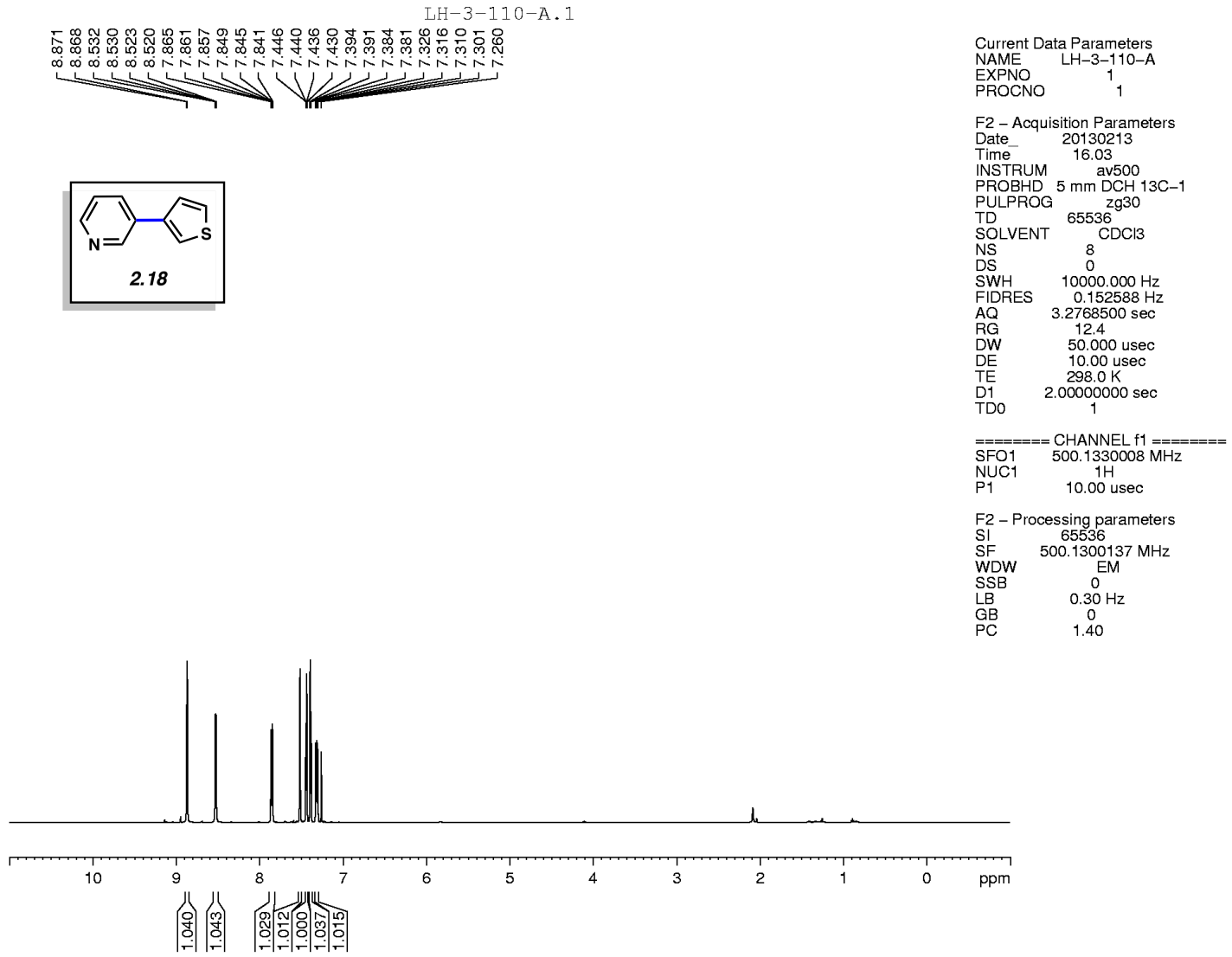

Figure A2.18 ^{1}H NMR (500 MHz, $CDCl_3$) of compound **2.18**.

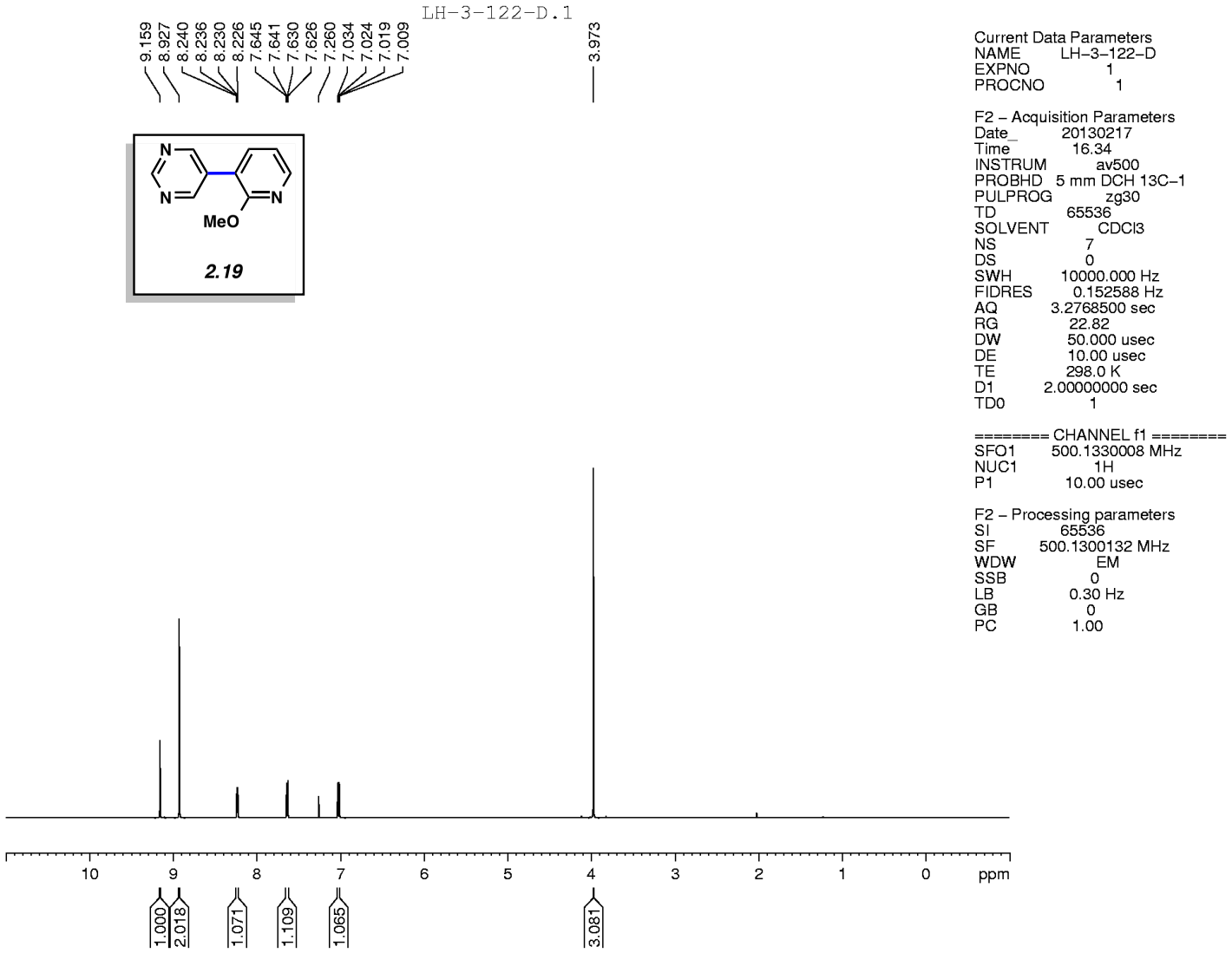

Figure A2.19 ^{1}H NMR (500 MHz, $CDCl_3$) of compound **2.19**.

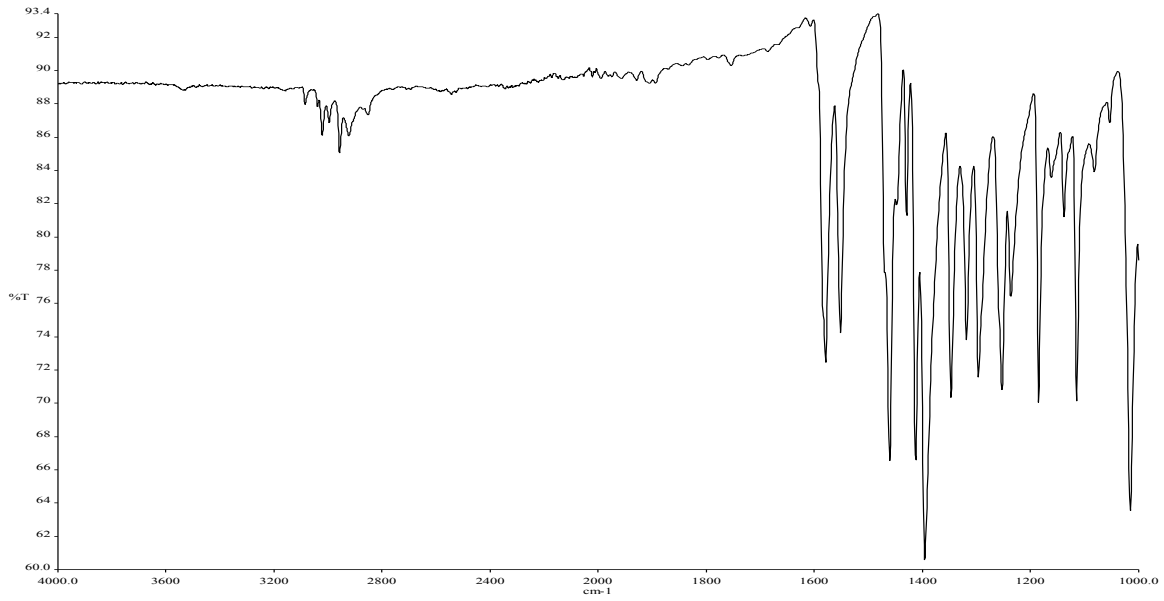

Figure A2.20 Infrared spectrum of compound **2.19**.

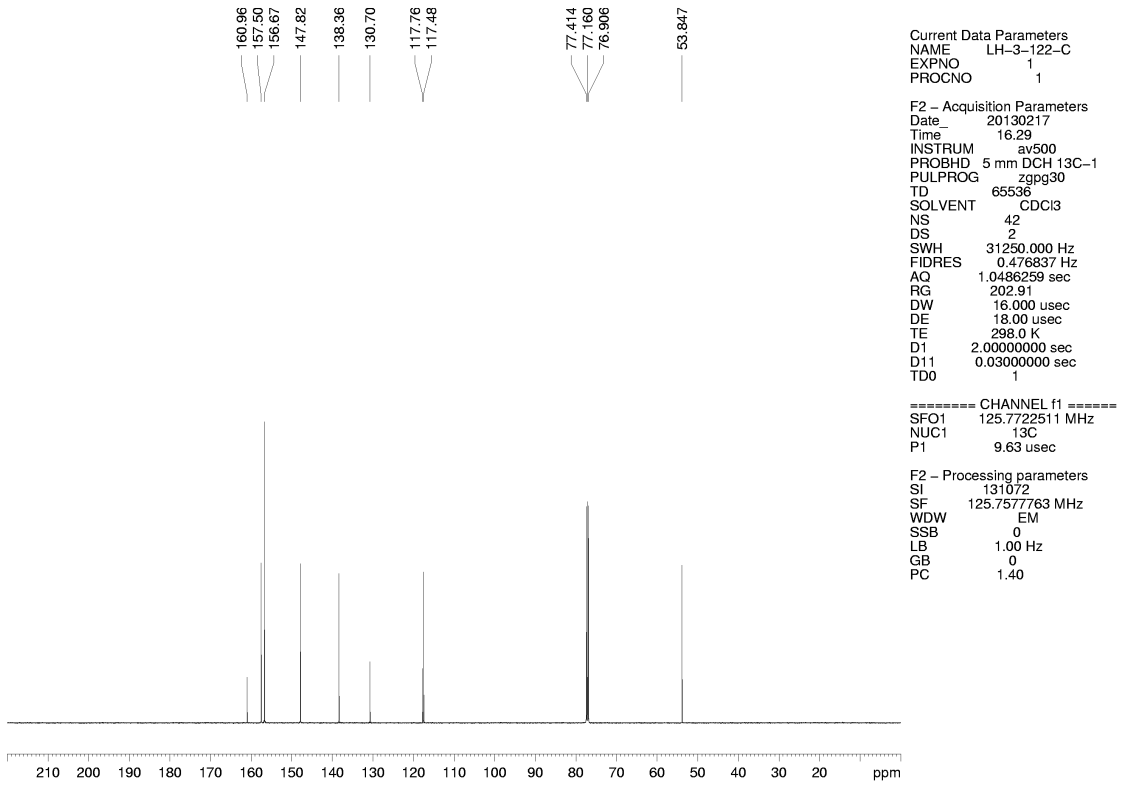

Figure A2.21 ^{13}C NMR (125 MHz, $CDCl_3$) of compound **2.19**.

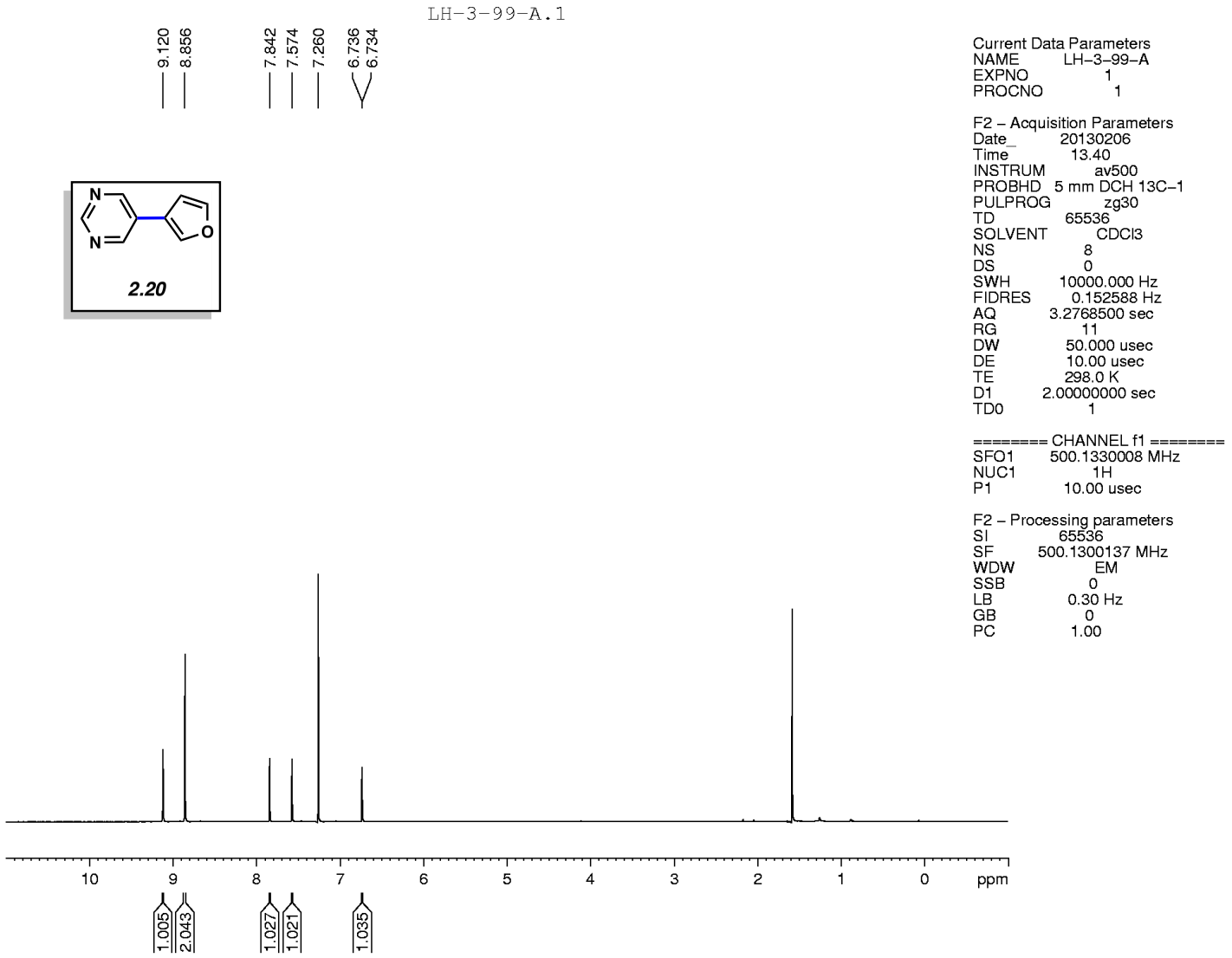

Figure A2.22 ^{1}H NMR (500 MHz, $CDCl_3$) of compound **2.20**.

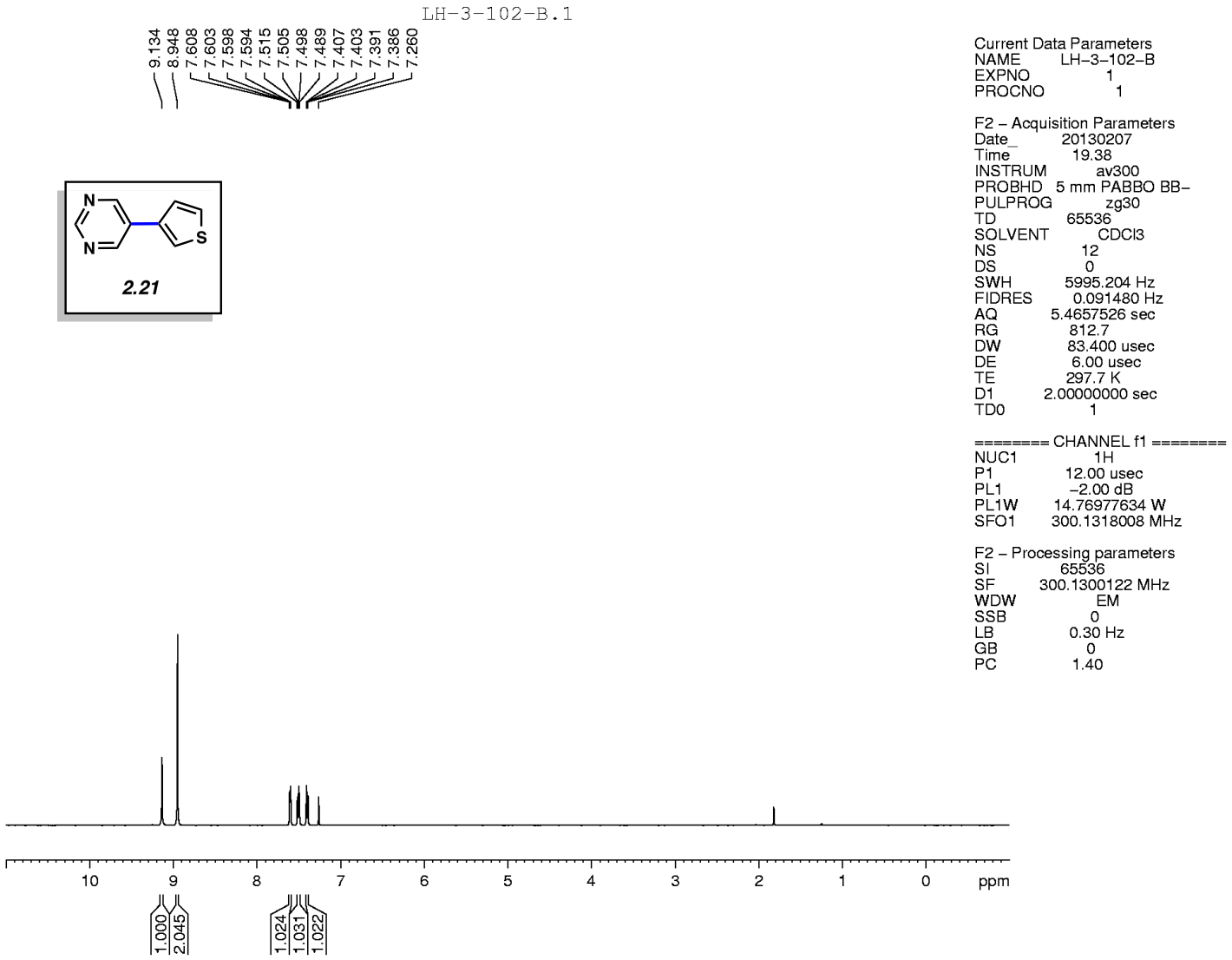

Figure A2.23 ^{1}H NMR (300 MHz, $CDCl_3$) of compound **2.21**.

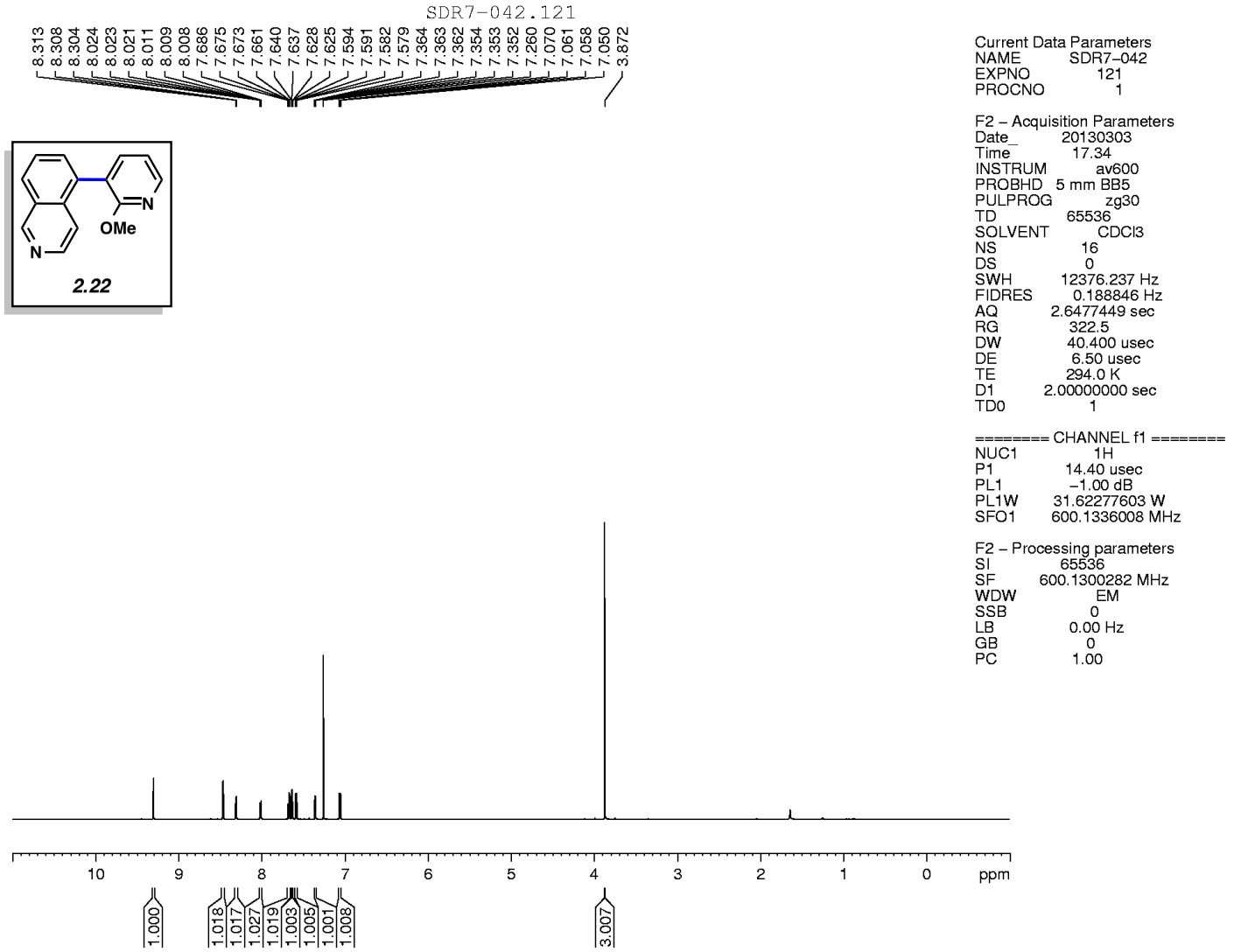

Figure A2.24 ^{1}H NMR (600 MHz, $CDCl_3$) of compound **2.22**.

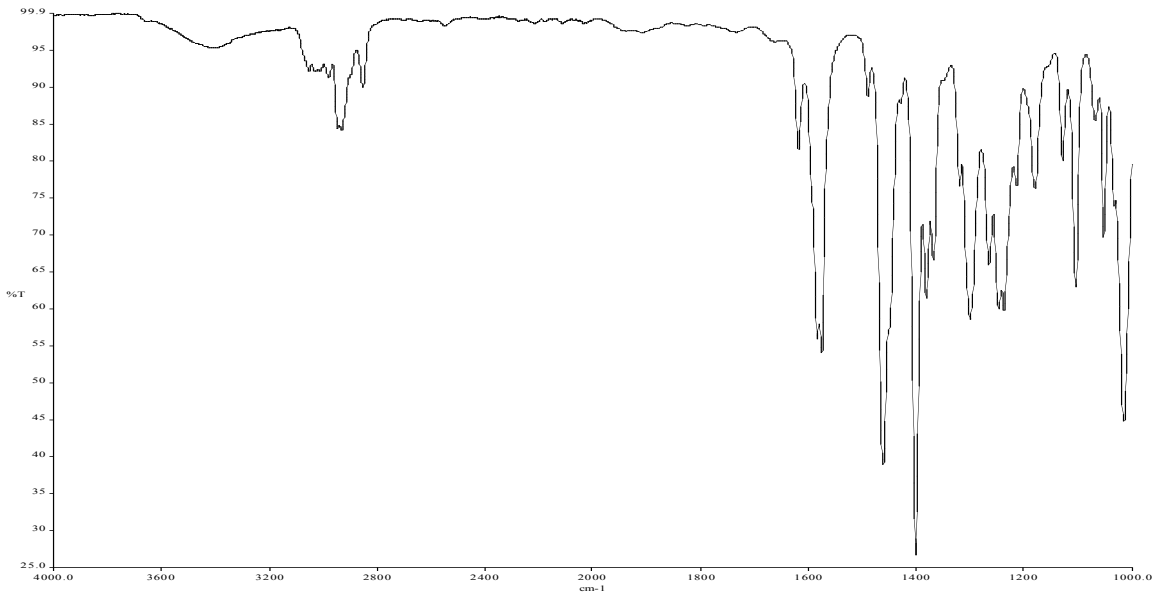

Figure A2.25 Infrared spectrum of compound **2.22**.

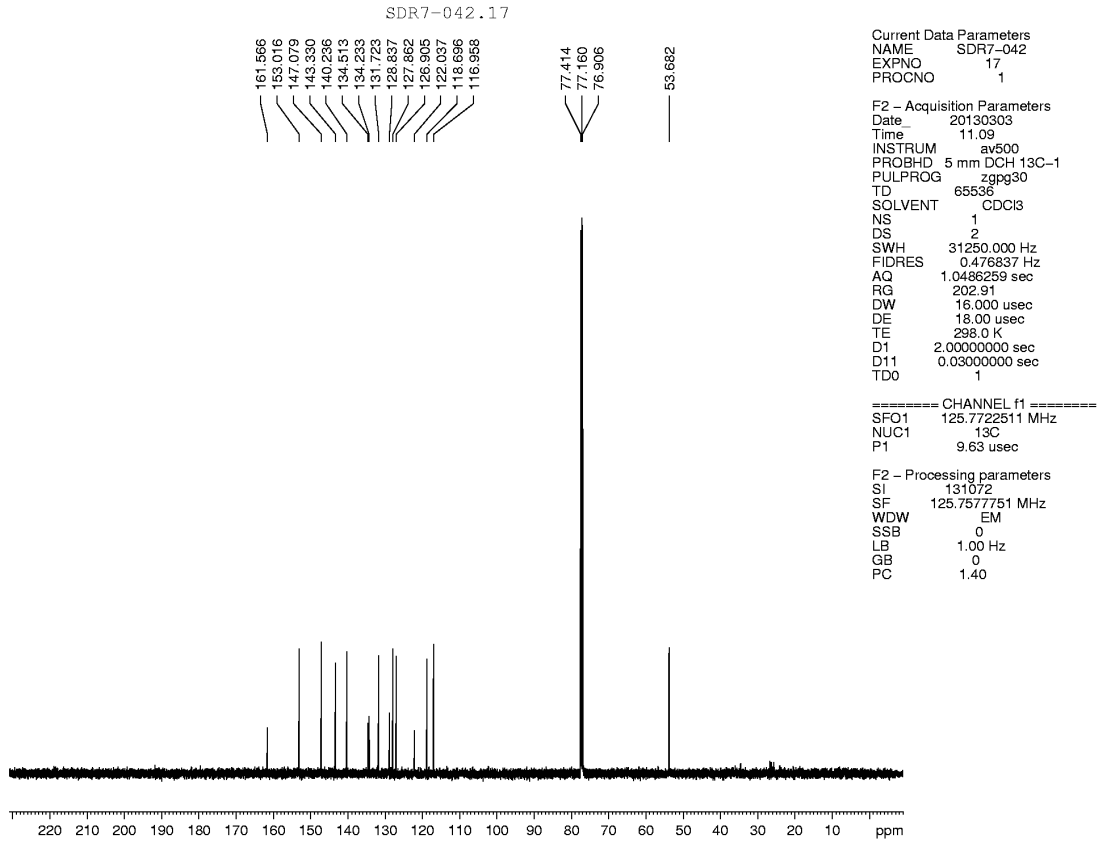

Figure A2.26 ^{13}C NMR (125 MHz, $CDCl_3$) of compound **2.22**.

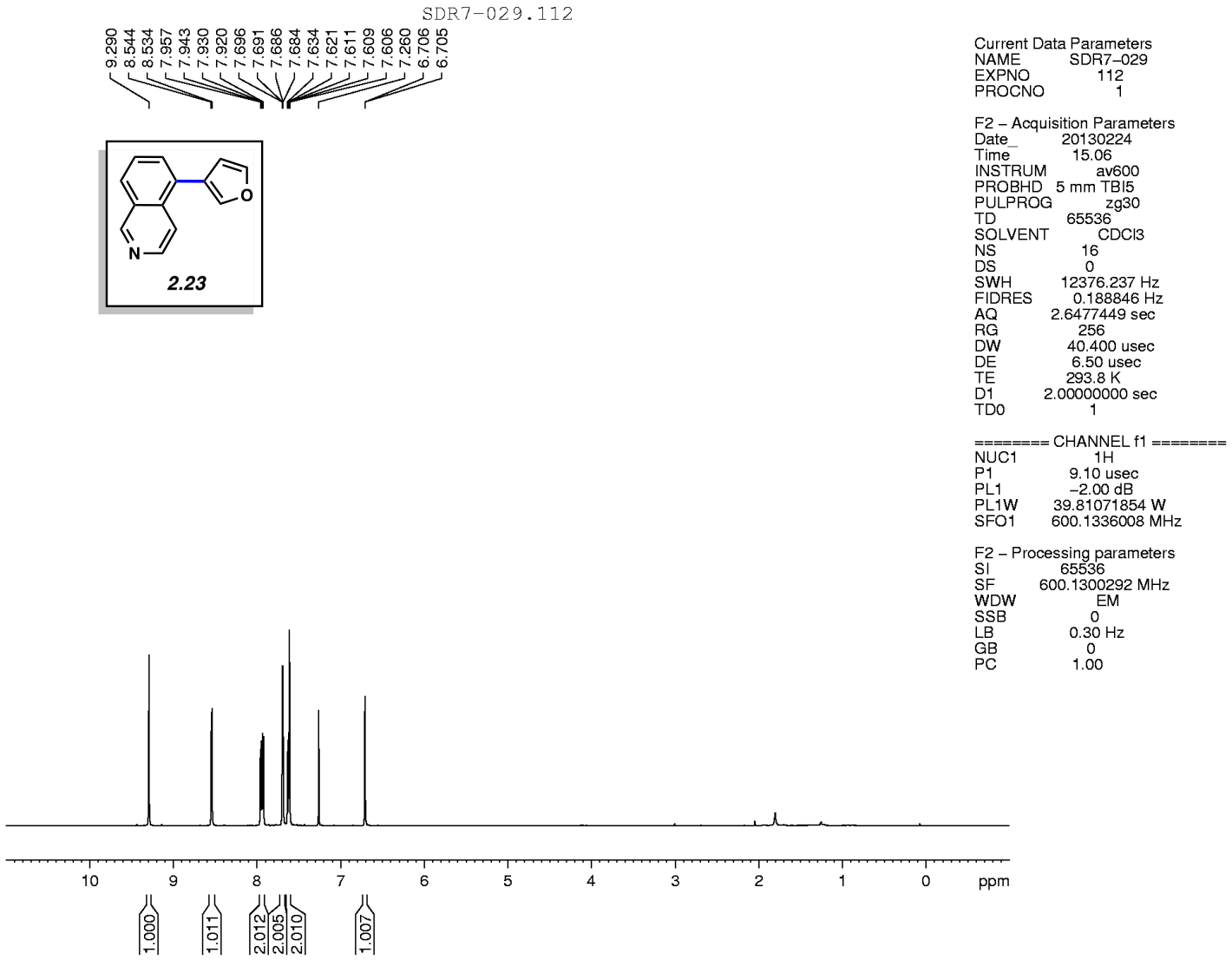

Figure A2.27 ^{1}H NMR (600 MHz, $CDCl_3$) of compound **2.23**.

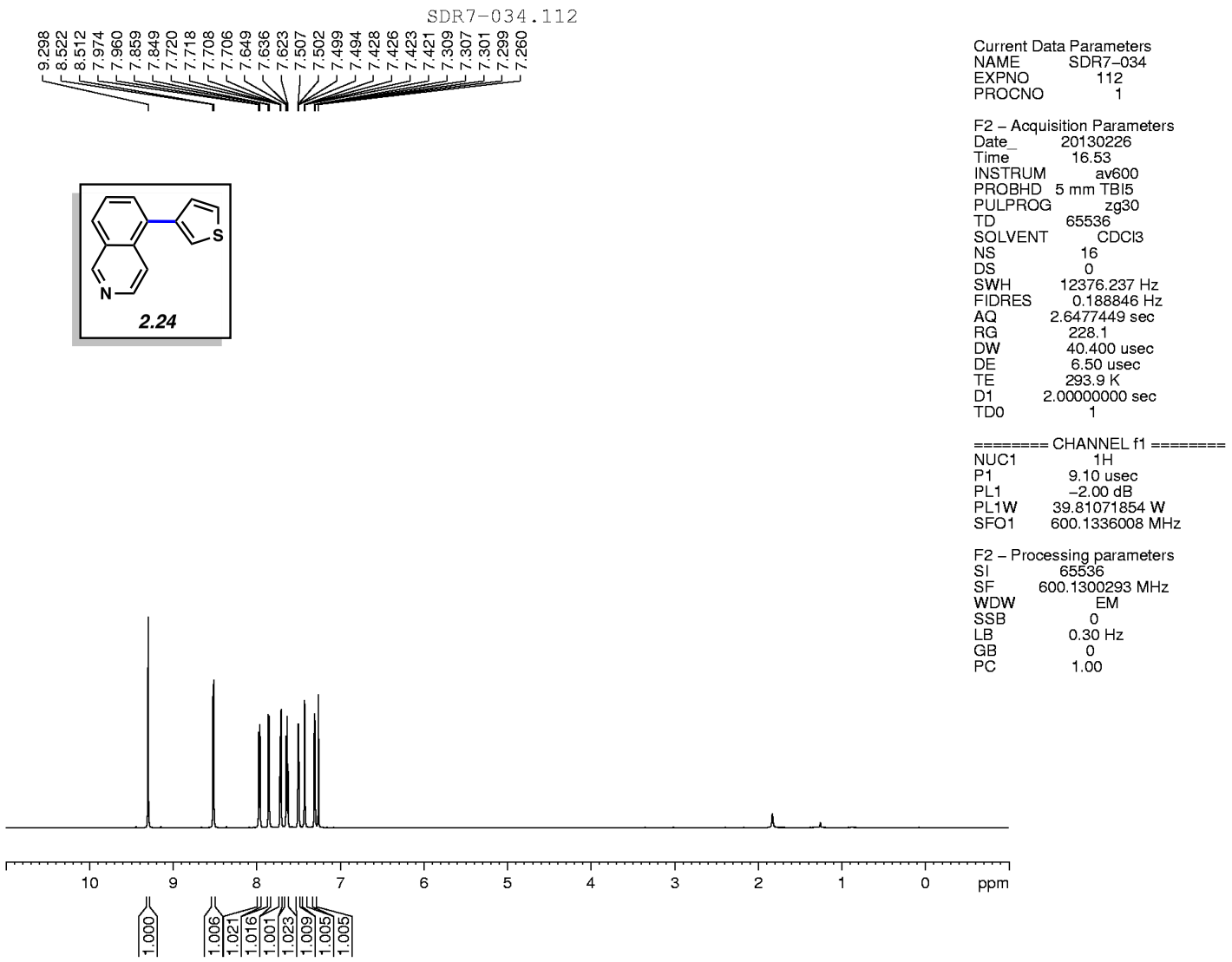

Figure A2.28 ^{1}H NMR (600 MHz, $CDCl_3$) of compound **2.24**.

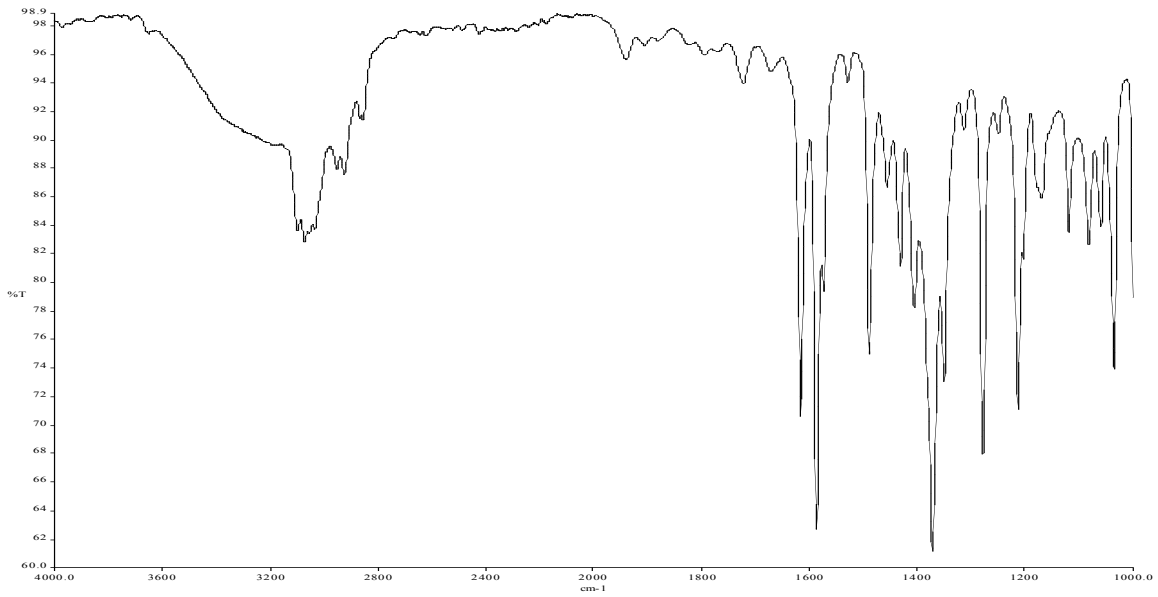

Figure A2.29 Infrared spectrum of compound **2.24**.

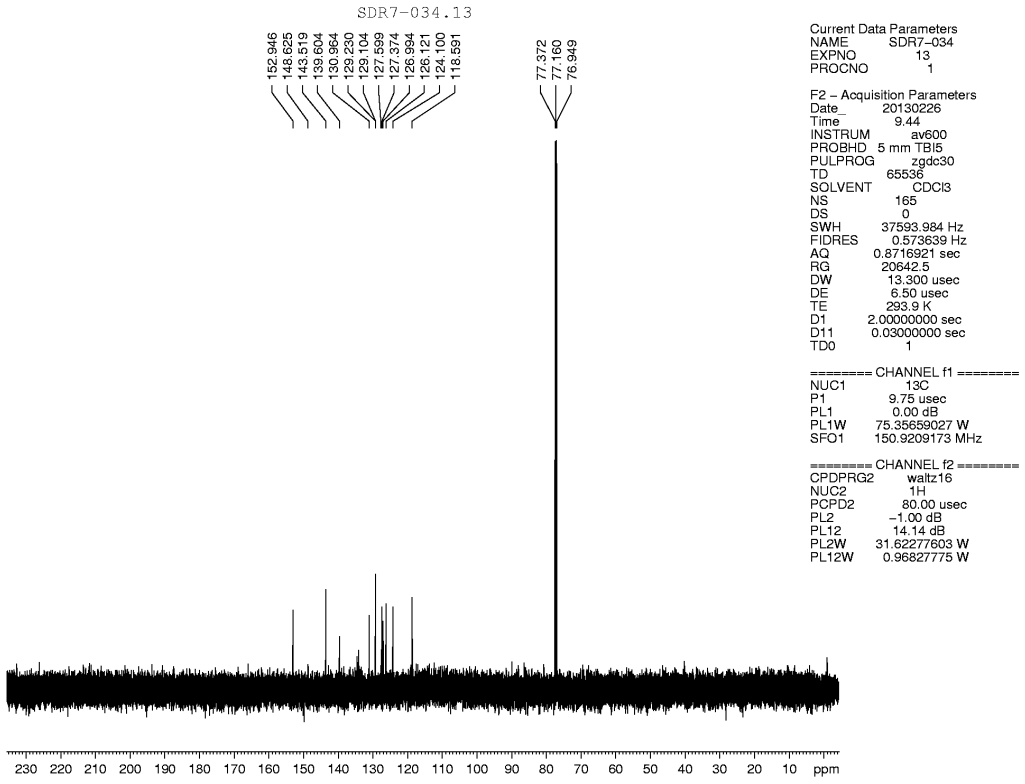

Figure A2.30 ^{13}C NMR (150 MHz, $CDCl_3$) of compound **2.24**.

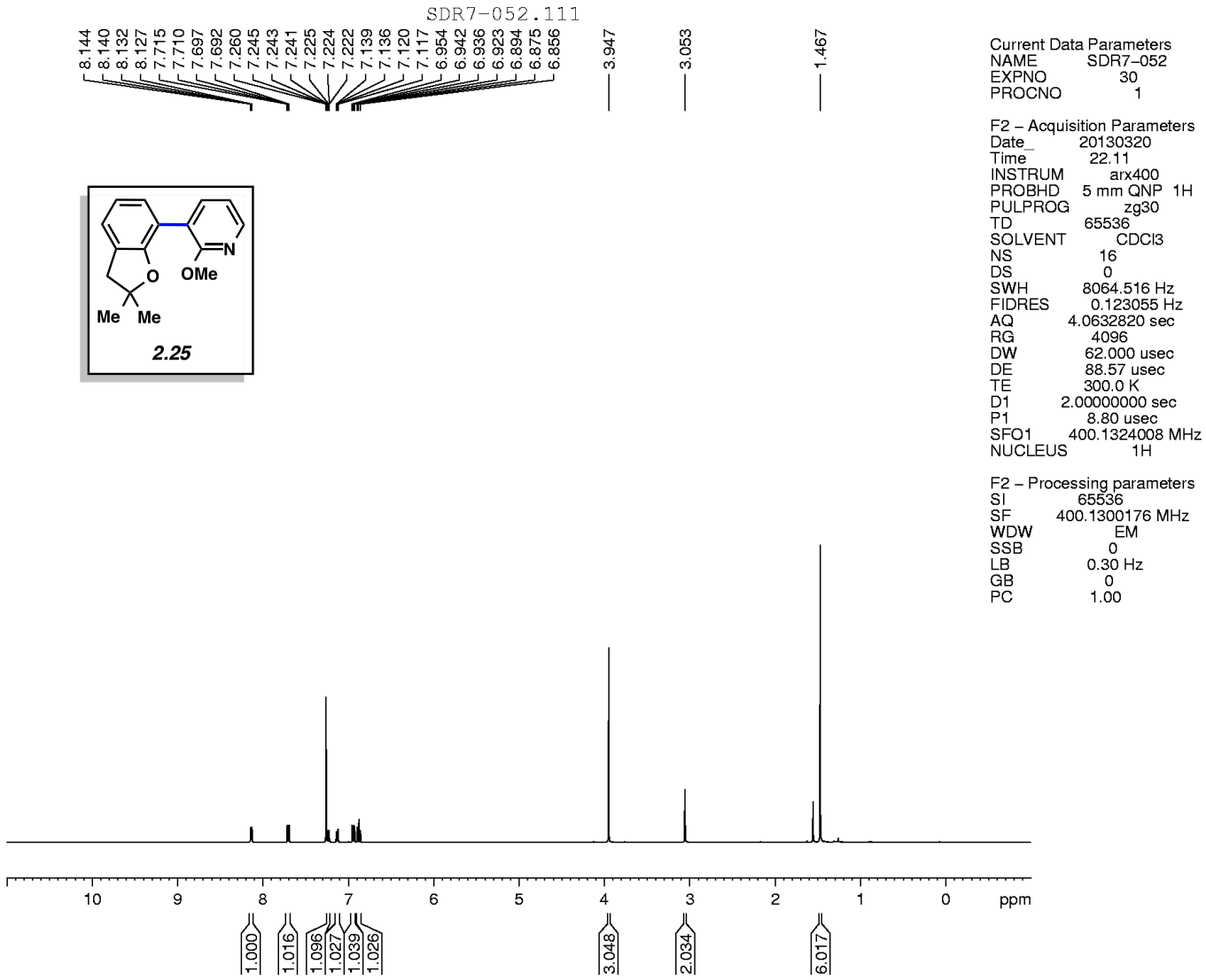

Figure A2.31 ^{1}H NMR (400 MHz, $CDCl_3$) of compound **2.25**.

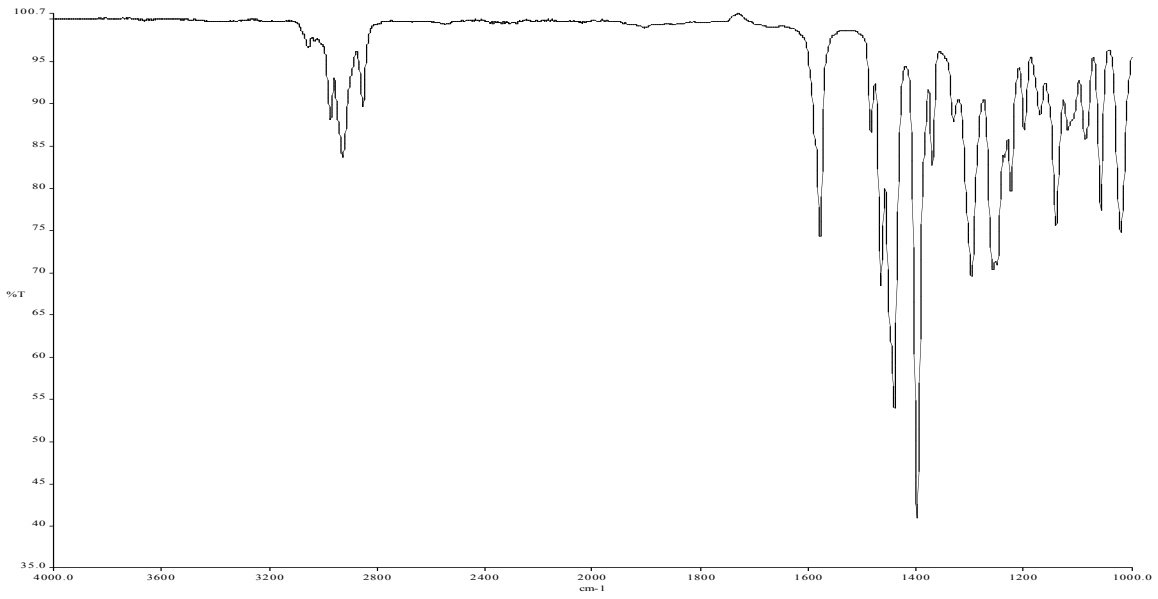

Figure A2.32 Infrared spectrum of compound **2.25**.

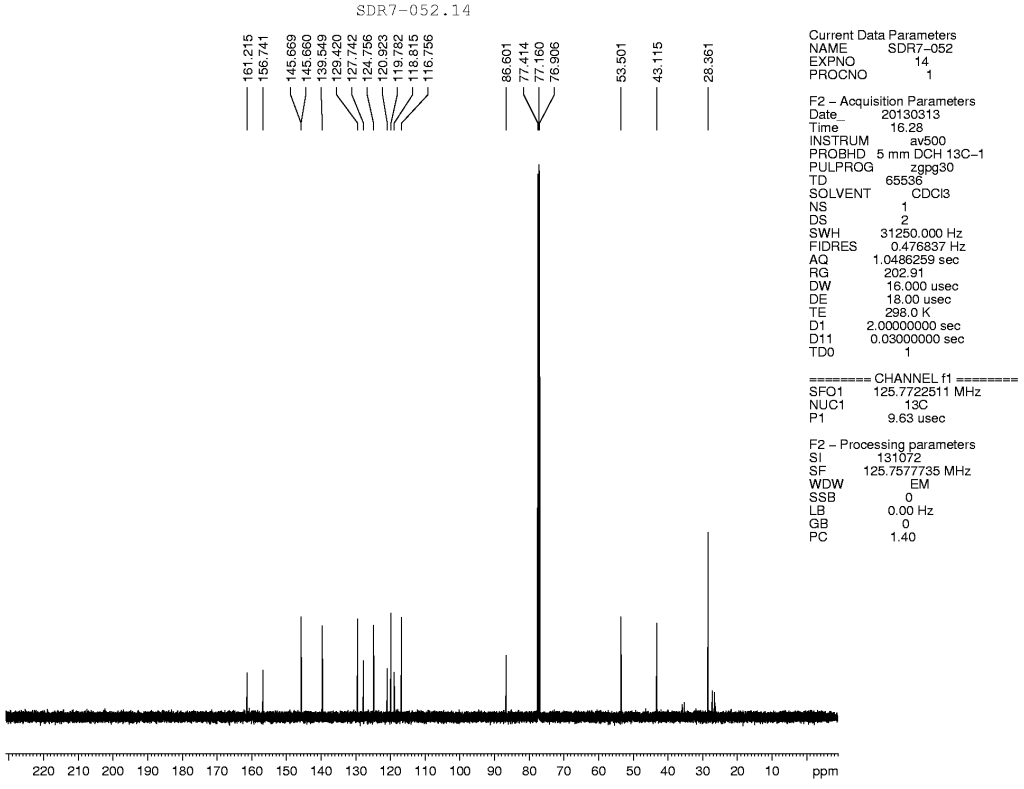

Figure A2.33 ^{13}C NMR (125 MHz, $CDCl_3$) of compound **2.25**.

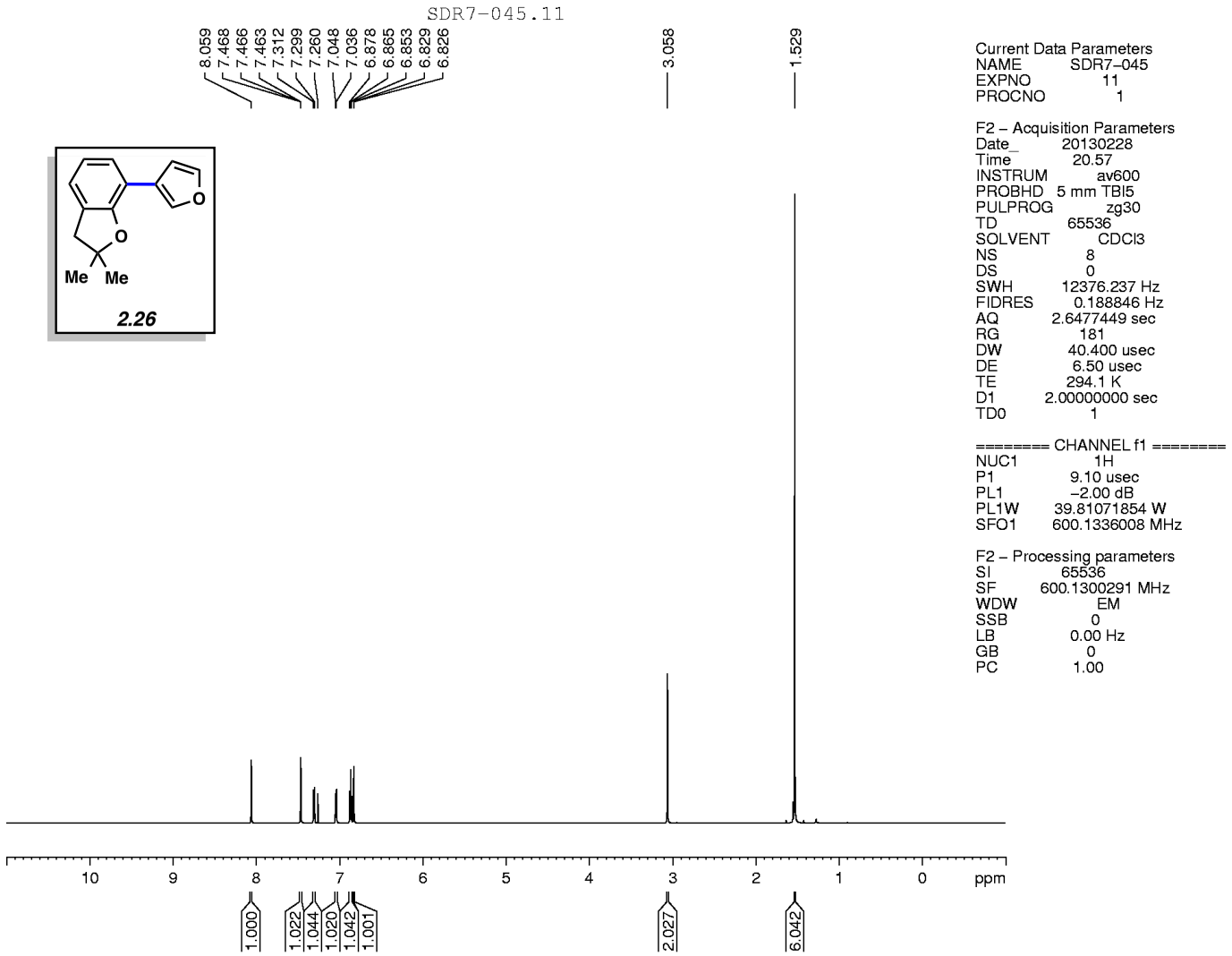

Figure A2.34 ^{1}H NMR (600 MHz, $CDCl_3$) of compound **2.26**.

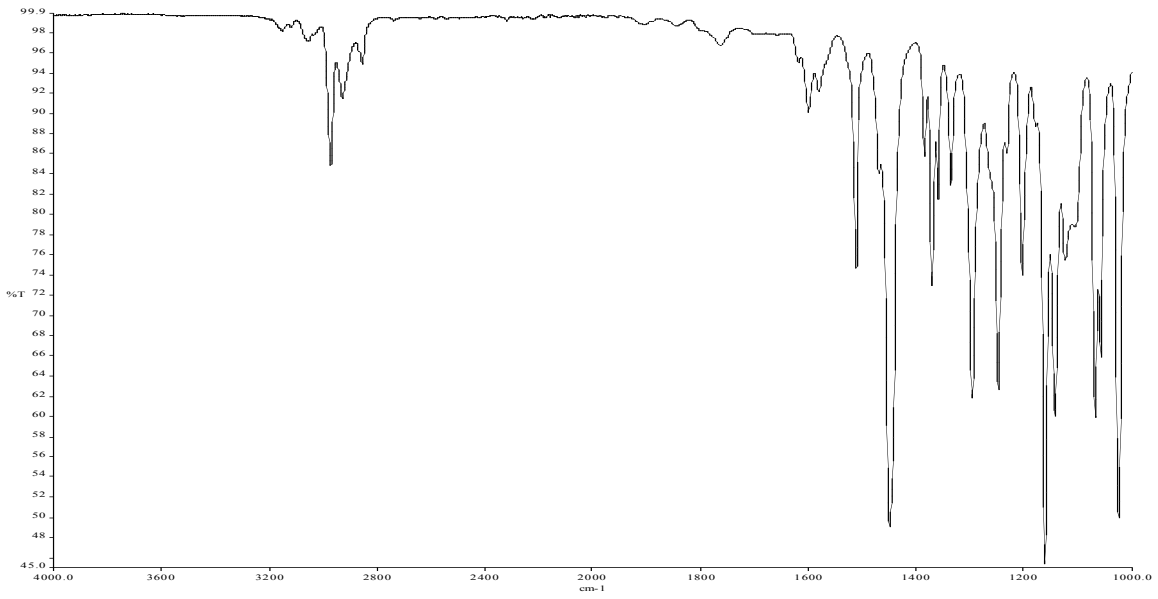

Figure A2.35 Infrared spectrum of compound **2.26**.

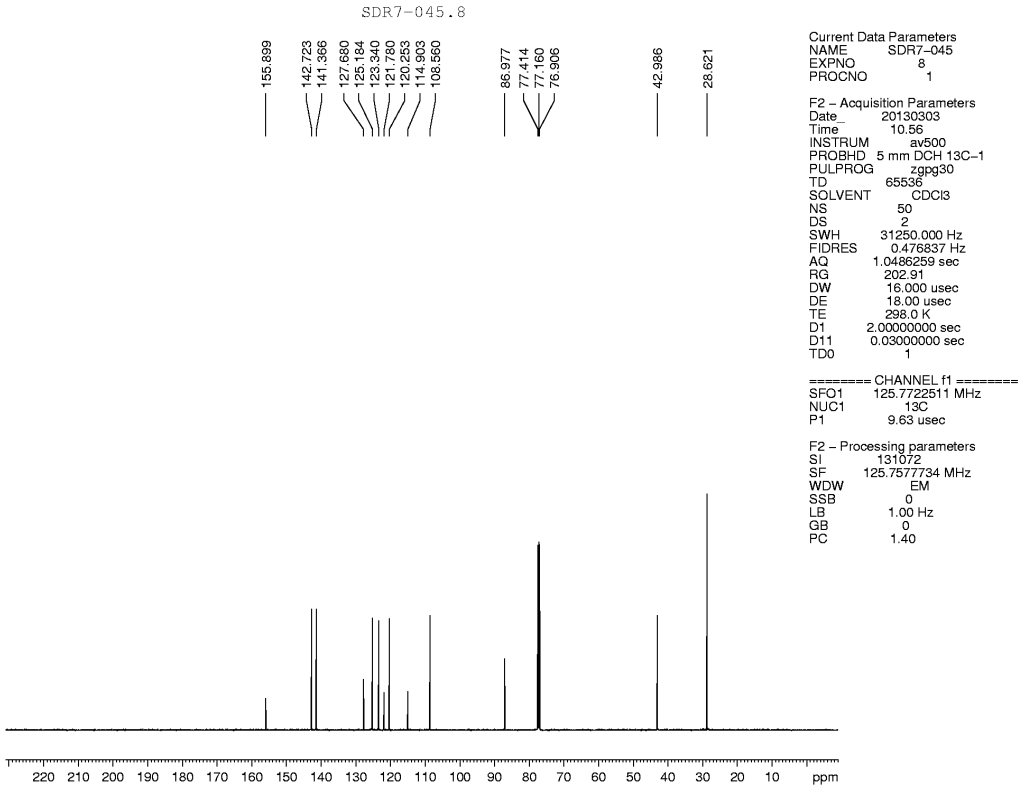

Figure A2.36 ^{13}C NMR (125 MHz, $CDCl_3$) of compound **2.26**.

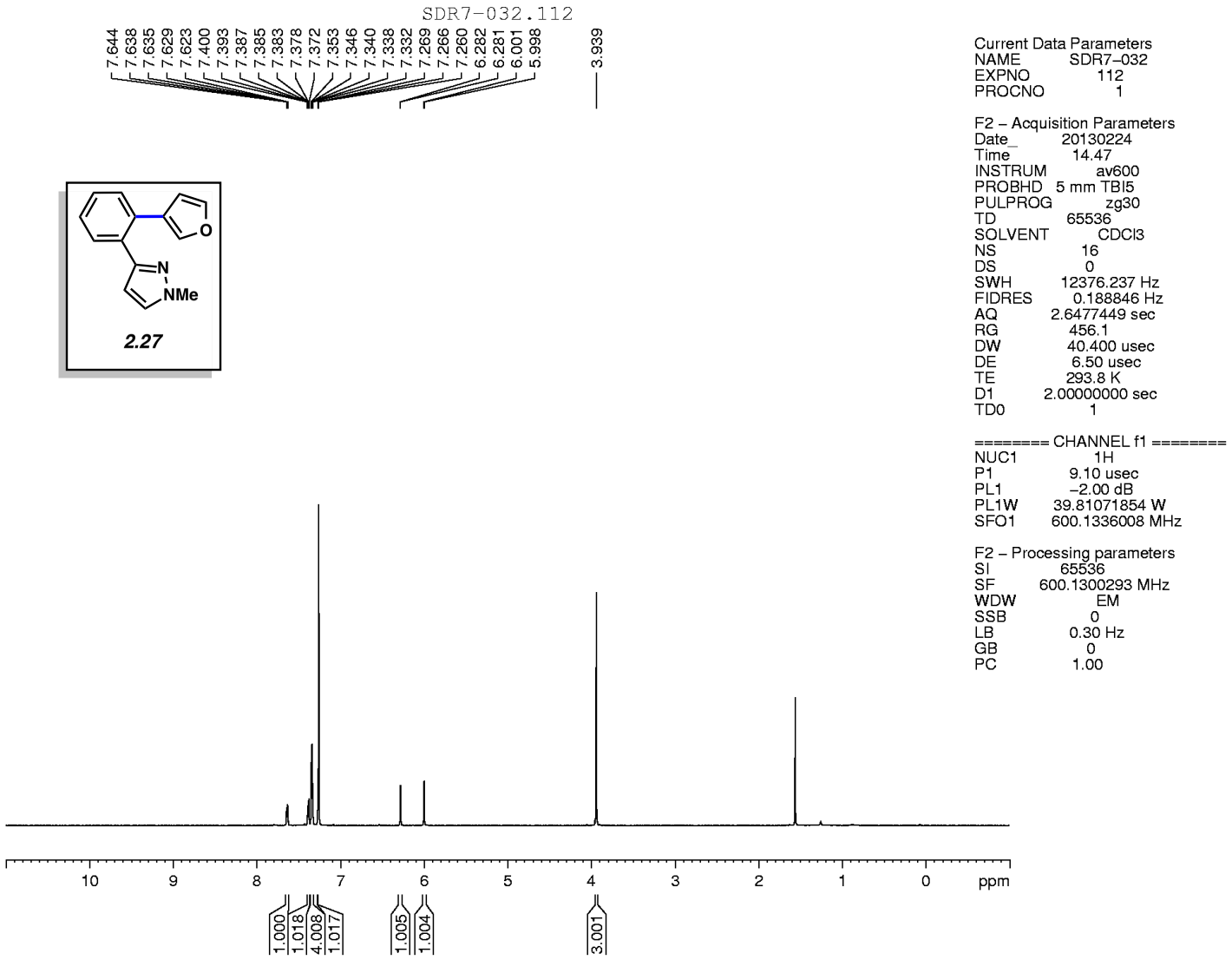

Figure A2.37 ^{1}H NMR (600 MHz, $CDCl_3$) of compound **2.27**.

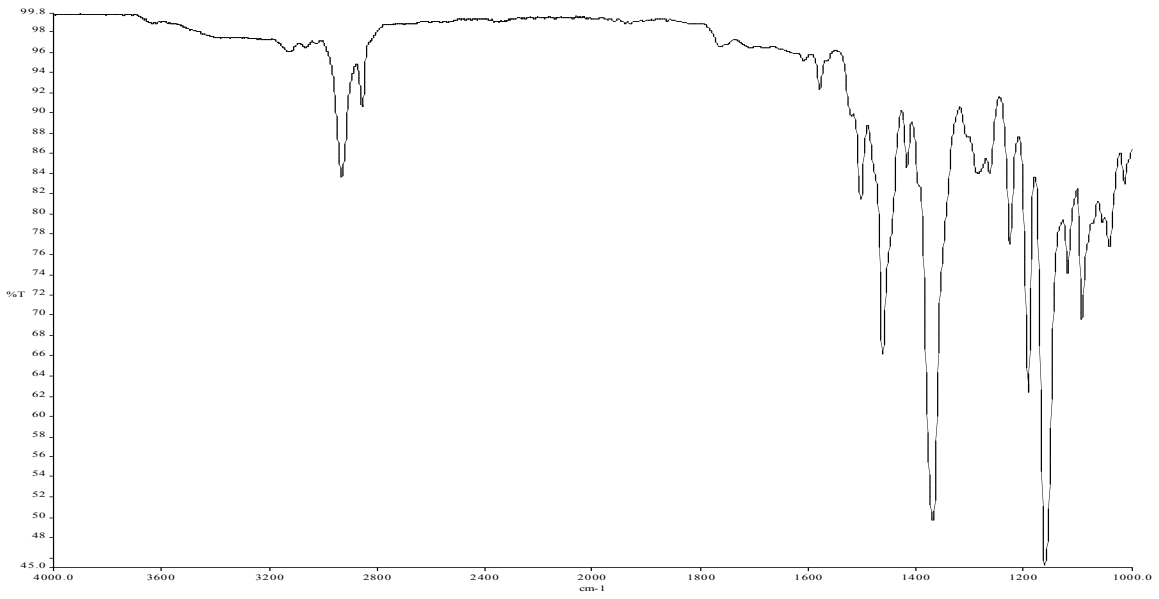

Figure A2.38 Infrared spectrum of compound **2.27**.

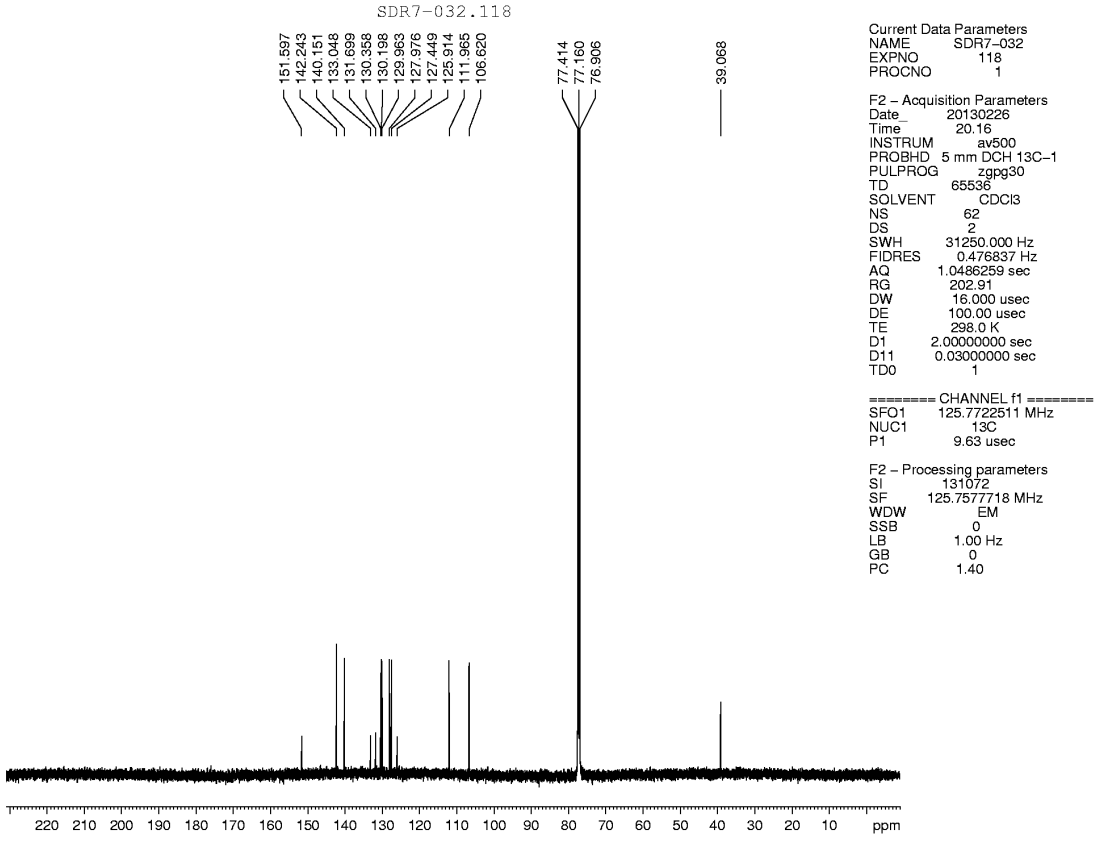

Figure A2.39 ^{13}C NMR (125 MHz, $CDCl_3$) of compound **2.27**.

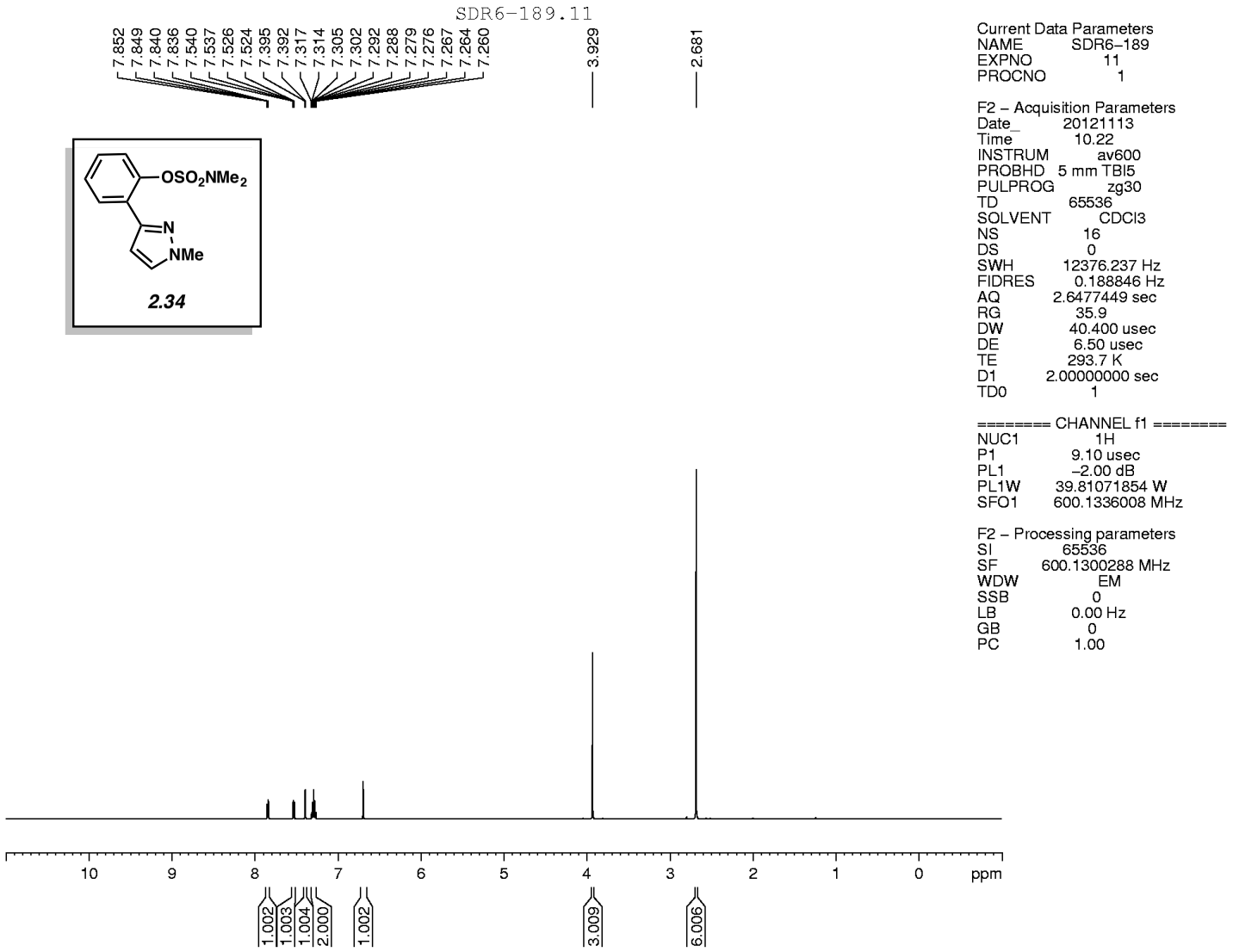

Figure A2.40 ^{1}H NMR (600 MHz, $CDCl_3$) of compound **2.34**.

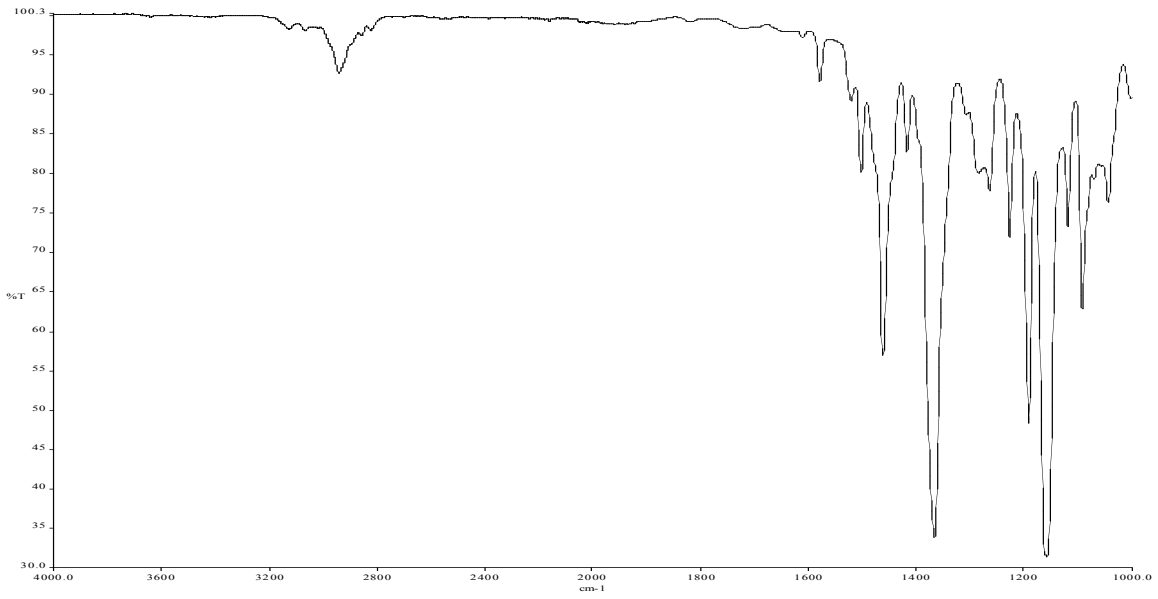

Figure A2.41 Infrared spectrum of compound **2.34**.

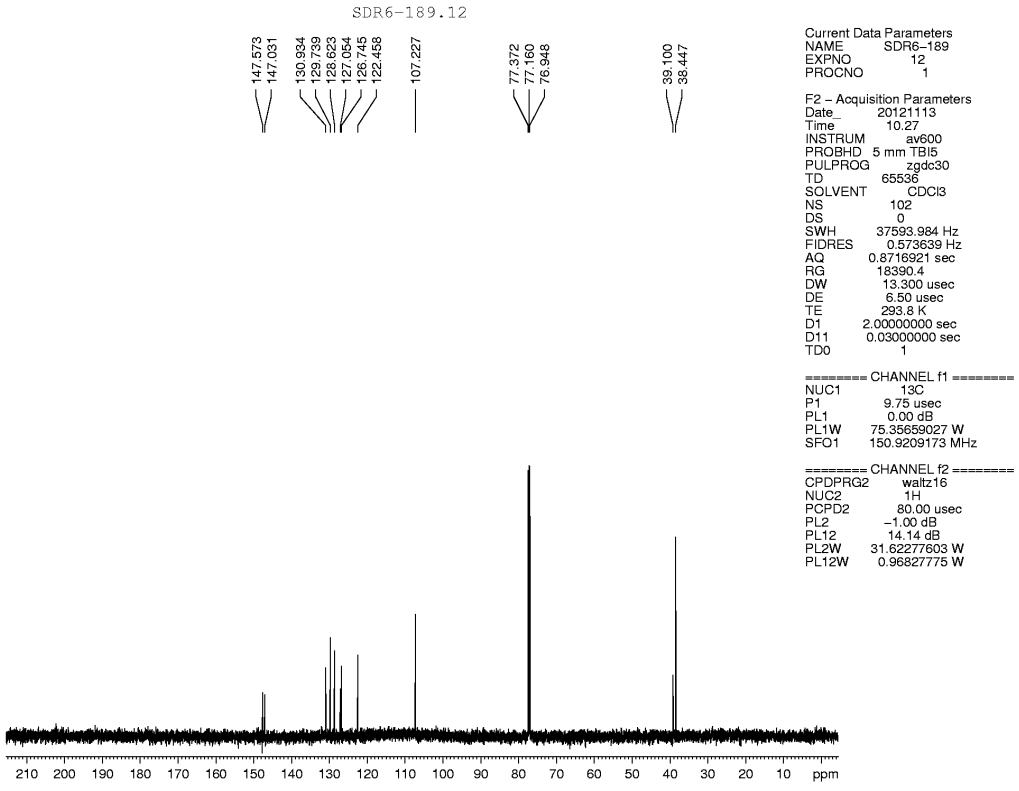

Figure A2.42 ^{13}C NMR (150 MHz, $CDCl_3$) of compound **2.34**.

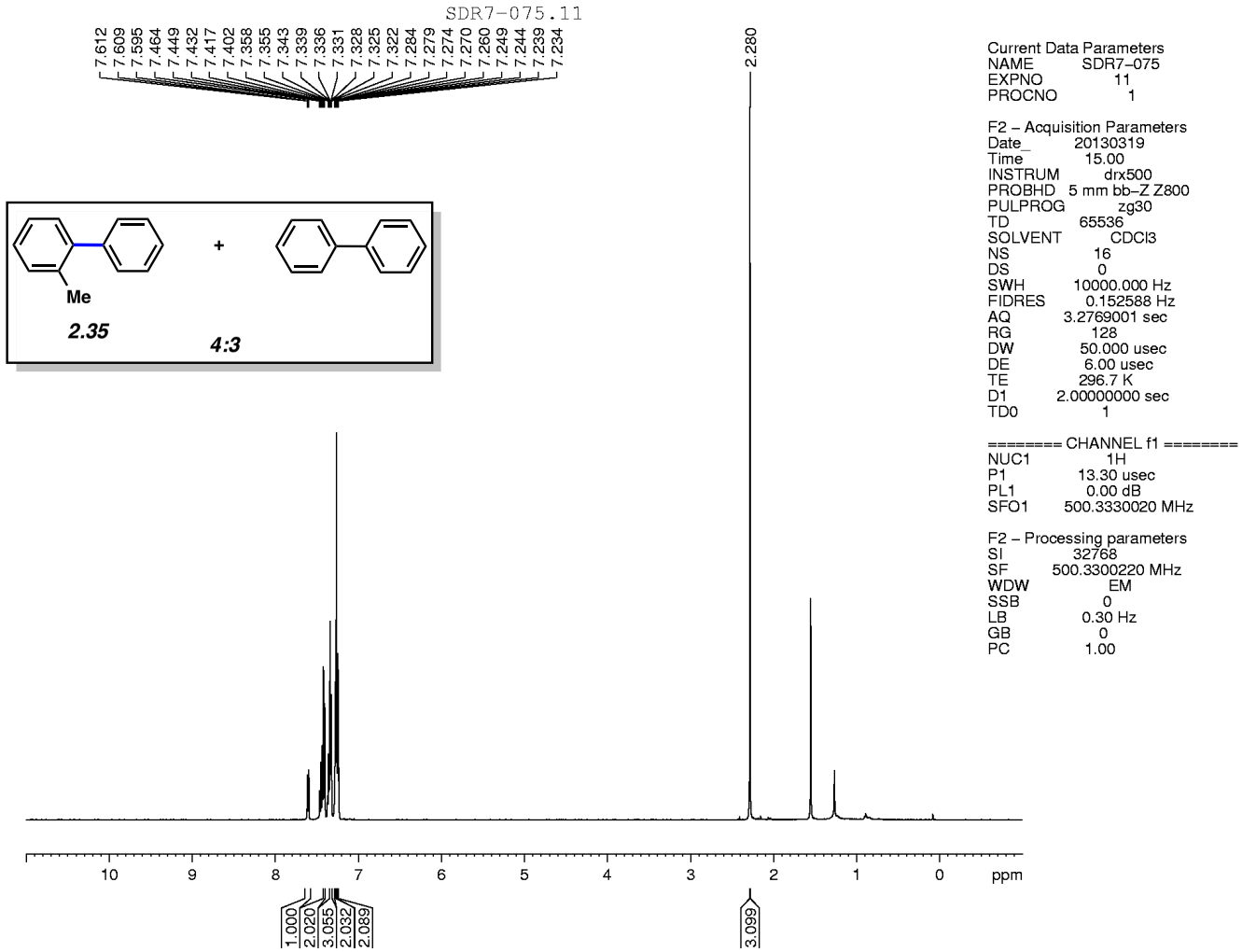

Figure A2.43 ^{1}H NMR (500 MHz, $CDCl_3$) of compound **2.35**.

2.9. Notes and References

(1) (a) *Metal-Catalyzed Cross-Coupling Reactions*; Diederich, F.; Meijere, A., Eds.; Wiley-VCH: Weinheim, 2004. (b) Hassan, J.; Sevignon, M.; Gozzi, C.; Schulz, E.; Lemaire, M. *Chem. Rev.* **2002**, *102*, 1359–1469. (c) *Topics in Current Chemistry*, Vol. 219; Miyaura, N., Ed.; Springer-Verlag: New York, 2002. (d) Corbet, J.; Mignani, G. *Chem. Rev.* **2006**, *106*, 2651–2710. (e) Negishi, E. *Bull. Chem. Soc. Jpn.* **2007**, *80*, 233–257. (f) *Application of Transition Metal Catalysis in Drug Discovery and Development: An Industrial Perspective*; Shen, H. C.; Crawley, M. L., Trost, B. M., Eds.; John Wiley & Sons, Inc.: Hoboken, NJ, 2012.

(2) For solvent selection guide in medicinal chemistry, see: (a) Alfonsi, K.; Colberg, J.; Dunn, P. J.; Fevig, T.; Jennings, S.; Johnson, T. A.; Kleine, H. P.; Knight, C.; Nagy, M. A.; Perry, D. A.; Stefaniak, M. *Green Chem.* **2008**, *10*, 31–36. (b) Henderson, R. K.; Jiménez-Gonález, C.; Constable, D. J. C.; Alston, S. R.; Inglis, G. G. A.; Fisher, G.; Sherwood, J.; Binks, S. P.; Curzons, A. D. *Green Chem.* **2011**, *13*, 854–862.

(3) For examples of cross-coupling reactions in aqueous media, see (a) Bussolari, J. C.; Rehborn, D. C. *Org. Lett.* **1999**, *1*, 965–967. (b) Hesse, S.; Kirsch, G. *Synthesis* **2001**, 755–759. (c) Anderson, K. W.; Buchwald, S. L. *Angew. Chem. Int. Ed.* **2005**, *44*, 6173–6177. (d) Lipshutz, B. H.; Ghorai, S. *Aldrichimica. Acta*, **2008**, *41*, 59–72. (e) Alacid, E.; Nájera, C. *J. Org. Chem.* **2009**, *74*, 2321–2327. (f) Han, J.; Liu, Y.; Guo, R. *J. Am. Chem. Soc.* **2009**, *131*, 2060–2061. (g) Chalker, J. M.; Wood, C. S.; Davis, B. G. *J. Am. Chem. Soc.* **2009**, *131*, 16346–16347.

(4) (a) *Green Chemistry: Theory and Practice;* Anastas, P. T.; Warner, J. C., Eds.; Oxford University Press: New York, 1998. (b) Anastas, P. T.; Kirchhoff, M. M. *Acc. Chem. Res.* **2002**, *35*, 686–694.

(5) Fortunak, J. M. *Future Med. Chem.* **2009**, *1*, 571–575.

(6) For selected examples involving aryl halides, see: (a) Semmelhack, M. F.; Helquist, P. M.; Jones, L. D. *J. Am. Chem. Soc.* **1971**, *93*, 5908–5910. (b) Klein, A.; Budnikova, Y. H.; Sinyashin, O. G. *J. Organomet. Chem.* **2007**, *692*, 3156–3166. (c) Jennings, P. W.; Pillsbury, D. G.; Hall, J. L.; Brice, V. T. *J. Org. Chem.* **1976**, *41*, 719–722. (d) Zembayashi, M.; Tamao, K.; Yoshida, J.; Kumada, M. *Tetrahedron Lett.* **1977**, 4089–4092. (e) Ge, S.; Hartwig, J. F. *Angew. Chem. Int. Ed.* **2012**, *51*, 12837–12841. (f) Wilson, D. A.; Wilson, C. J.; Rosen, B. M.; Percec, V. *Org. Lett.* **2008**, *10*, 4879–4882. (g) Golding, G. M.; Smidrkal, J.; Weichold, O.; Percec, V. *J. Org. Chem.* **2004**, *69*, 3442–3452. (h) Zhang, N.; Hoffman, D. J.; Gutsche, N.; Gupta, J.; Percec, V. *J. Org. Chem.* **2012**, *77*, 5956–5964. (i) Saito, S.; Sakai, M.; Miyaura, N. *Tetrahedron Lett.* **1996**, *37*, 2993–2996. (j) Indolese, A. F. *Tetrahedron Lett.* **1997**, *38*, 3513–3516. (k) Moldoveanu, C.; Wilson, D. A.; Wilson, C. J.; Leowanawat, P.; Resmerita, A.-M.; Liu, C.; Rosen, B. M.; Percec, P. *J. Org. Chem.* **2010**, *75*, 5438–5454. (l) Moldoveanu, C.; Wilson, D. A.; Wilson, C. J.; Corcoran, P.; Rosen, B.M.; Percec, V. *Org. Lett.* **2009**, *11*, 4974–4977. (m) Leowanawat, P.; Resmerita, A.-M.; Moldoveanu, C.; Liu, C.; Zhang, N.; Wilson, D. A.; Hoang, L. M.; Rosen, B. M.; Percec, V. *J. Org. Chem.* **2010**, *75*, 7822–7828. (n) Wolfe, J. P.; Buchwald, S. P. *J. Am. Chem. Soc.* **1997**, *119*, 6054–6058.

(7) For selected examples examples involving aryl esters, see: (a) Guan, B.-T.; Wang, Y.; Li, B.-J.; Yu, D.-G.; Shi, Z.-J. *J. Am. Chem. Soc.* **2008**, *130*, 14468–14470. (b) Li, B.-J.; Li, Y.-Z.;

Lu, X.-Y.; Liu, J.; Guan, B.-T.; Shi, Z.-J. *Angew. Chem. Int. Ed.* **2008**, *47*, 10124–10127. (c) Quasdorf, K. W.; Riener, M.; Petrova, K. V.; Garg, N. K. *J. Am. Chem. Soc.* **2009**, *131*, 17748–17749. (d) Zhou, Q.; Srinivas, H. D.; Dasgupta, S.; Watson, M. P. *J. Am. Chem. Soc.* **2013**, *135*, 3307–3310.

(8) For selected examples involving aryl ethers, see: (a) Tobisu, M.; Shimasaki, T.; Chatani, N. *Angew. Chem. Int. Ed.* **2008**, *47*, 4866–4869. (b) Shimasaki, T.; Konno, Y.; Tobisu, M.; Chatani, N. *Org. Lett.* **2009**, *11*, 4890–4892. (c) Shimasaki, T.; Tobisu, M.; Chatani, N. *Angew. Chem. Int. Ed.* **2010**, *49*, 2929–2932. (d) Li, X.-J.; Zhang, J.-L.; Geng, Y.; Jin, Z. *J. Org. Chem.* **2013**, *78*, 5078–5084.

(9) For selected examples involving aryl carbamates, see: (a) Sengupta, S.; Leite, M.; Raslan, D. S.; Quesnelle, C.; Snieckus, V. *J. Org. Chem.* **1992**, *57*, 4066–4068. (b) Quasdorf, K. W.; Tian, X.; Garg, N. K. *J. Am. Chem. Soc.* **2008**, *130*, 14422–14423. (c) Antoft-Finch, A.; Blackburn, T.; Snieckus, V. *J. Am. Chem. Soc.* **2009**, *131*, 17750–17752. (d) Quasdorf, K. W.; Antoft-Finch, A.; Liu, P.; Silberstein, A. L.; Komaromi, A.; Blackburn, T.; Ramgren, S. D.; Houk, K. N.; Snieckus, V.; Garg, N. K. *J. Am. Chem. Soc.* **2011**, *133*, 6352–6363. (e) Mesganaw, T.; Silberstein, A. L.; Ramgren, S. D.; Fine Nathel, N. F.; Hong, X.; Garg, N. K. *Chem. Sci.* **2011**, *2*, 1766–1771. (f) Hie, L.; Ramgren, S. D.; Mesganaw, T.; Garg, N. K. *Org. Lett.* **2012**, *14*, 4182–4185.

(10) For selected examples involving aryl sulfamates, see: (a) Macklin, T. K.; Snieckus, V. *Org. Lett.* **2005**, *7*, 2519–2522. (b) Baghbanzadeh, M.; Pilger, C.; Kappe, C. O. *J. Org. Chem.* **2011**, *76*, 1507–1510. (c) Ramgren, S. D.; Silberstein, A. L.; Yang, Y.; Garg, N. K. *Angew. Chem. Int. Ed.* **2011**, *50*, 2171–2173. (d) Ackerman, L.; Sandmann, R.; Song, W. *Org. Lett.*

2011, *13*, 1784–1786. (e) Zhang, N.; Hoffman, D. J.; Gutsche, N.; Gupta, J.; Percec, V. *J. Org. Chem.* **2012**, *77*, 5956–5964. (f) Chen, G.-J.; Han, F.-S. *Eur. J. Org. Chem.* **2012**, 3575–3579. (g) Wehn, P. M.; Du Bois, J. *Org. Lett.* **2005**, *7*, 4685–4688.

(11) For selected examples involving aryl sulfonates, see: (a) Wilson, D. A.; Wilson, C. J.; Moldoveanu, C.; Resmerita, A.-M.; Cororan, P.; Hoang, L. M.; Rosen, B. M.; Percec, V. *J. Am. Chem. Soc.* **2010**, *132*, 1800–1801. (b) Percec, V.; Bae, J.-Y.; Hill, D. H. *J. Org. Chem.* **1995**, *60*, 1060–1065. (c) Percec, V.; Bae, J.-Y.; Zhoa, M.; Hill, D. H.; Percec, V. *J. Org. Chem.* **1995**, *60*, 1066–1069. (d) Percec, V.; Bae, J.-Y.; Zhao, M.; Hill, D. H.; Percec, V. *J. Org. Chem.* **1995**, *60*, 176–185. (e) Fan, X.-H.; Yang, L.-M. *Eur. J. Org. Chem.* **2011**, 1467–1471. (f) Gao, C.-Y.; Yang, L. M. *J. Org. Chem.* **2008**, *73*, 1624–1627. (g) Percec, V. J.; Golding, G. M.; Smidrkal, J.; Weichold, O. *J. Org. Chem.* **2004**, *69*, 3447–3452. (h) Tang, Z.-Y.; Fu, Q.-S. *J. Am. Chem. Soc.* **2004**, *126*, 3058–3059. (i) Zim, D.; Lando, V. R.; Dupont, J.; Montero, A. L. *Org. Lett.* **2001**, *3*, 3049–3051; see also references 6e-g and 10d.

(12) For recent reviews, see: (a) Rosen, B. M.; Quasdorf, K. W.; Wilson, D. A.; Zhang, N.; Resmerita, A.-M.; Garg, N. K.; Percec, V. *Chem. Rev.* **2011**, *111*, 1346–1416. (b) Li, B.-J.; Yu, D.-G.; Sun, C.-L.; Shi, Z.-J. *Chem.—Eur. J.* **2011**, *17*, 1728–1759. (c) Mesganaw, T.; Garg, N. K. *Org. Process Res. Dev.* **2013**, *17*, 29–39. (d) Yamaguchi, J.; Muto, K.; Itami, K. *Eur. J. Org. Chem.* **2013**, 19–30.

(13) Solvents were selected from the ACS Green Chemistry Institute Roundtable Solvent Selection Guide. See Section 2.8.1.

(14) *tert*-Amyl alcohol and 2-Me-THF were selected in consultation with the ACS Green Chemistry Institute. *tert*-Amyl alcohol is attractive due to its safety profile, low freezing

point (in comparison to *t*-BuOH), and ability to solubilize polar compounds. 2-Me-THF is advantageous because it is obtained from renewable feedstocks and possesses many process advantages over THF. For a discussion of 2-Me-THF, see: Aycock, D. F. *Org. Process Res. Dev.* **2007**, *11*, 156–159.

(15) Under standard conditions using 5% Ni, 50–60% yields of **2.3** were obtained, with the remaining mass being unreacted carbamate substrate.

(16) The specific combination of heterocyclic framework and leaving group were chosen at random or based on substrate availability to span a broad range of coupling partners for this Letter. As such, the absence of a specific combination should not imply that such a combination would not lead to a successful Ni-catalyzed cross coupling.

(17) For examples of Pd-catalyzed cross-coupling to access bis-heterocycles, see: (a) Zhao, D.; You, J.; Hu, C. *Chem. Eur. J.* **2011**, *17*, 5466–5492. (b) Molander, G. A.; Shin, I. *Org. Lett.* **2013**, *15*, 2534–2537.

(18) The corresponding coupling between 2-chloropyridine and 2-methoxy-3-pyridinylboronic acid gave the desired bis(heteroaryl) in 60% yield (*tert*-amyl alcohol) and 71% yield (2-Me-THF).

(19) Microwave conditions were also tested for comparison. Cross-coupling of bromopyrimidine **2.30** with 3-furylboronic acid (**2.31**) using microwave conditions gave compound **2.20** in quantitative yield (*tert*-amyl alcohol) and 100% yield (2-Me-THF). For Suzuki–Miyaura couplings of aryl carbamates and sulfamates under microwave conditions, see: ref. 10b.

(20) Interestingly, the corresponding cross-coupling with thiophene-3-boronic acid resulted in no product formation.

(21) The choice of solvents for these transformations was arbitrary to showcase that either *tert*-amyl alcohol or 2-Me-THF can be employed on preparative scale. As shown in Figure 2.4, the couplings to prepare **2.22** and **2.20** readily proceed in either solvent.

(22) (a) Quasdorf, K. W.; Tian, X.; Garg, N. K. *J. Am. Chem. Soc.* **2008**, *130*, 14422–14423. (b) Mesganaw, T.; Fine Nathel, N. F.; Garg, N. K. *Org. Lett.* **2012**, *14*, 2918–2921. (c) Antoft-Finch, A.; Blackburn, T.; Snickus, V. *J. Am. Chem. Soc.* **2009**, *131*, 17750–17752. (d) Mesganaw, T.; Silberstein, A. L.; Ramgren, S. D.; Fine Nathel, N. F.; Hong, X.; Liu, P.; Garg, N. K. *Chem. Sci.* **2011**, *2*, 1766–1771. (e) Quasdorf, K. W.; Antoft-Finch, A.; Liu, P.; Silberstein, A. L.; Komaromi, A.; Blackburn, T.; Ramgren, S. D.; Houk, K. N.; Snieckus, V.; Garg, N. K. *J. Am. Chem. Soc.* **2011**, *133*, 6352–6363. (f) Leowanawat, P.; Zhang, N.; Resmerita, A.-M.; Rosen, B. M.; Percec, V. *J. Org. Chem.* **2011**, *76*, 9946–9955. (g) Silberstein, A. L.; Ramgren, S. D.; Garg, N. K. *Org. Lett.* **2012**, *14*, 3796–3799.

(23) Catalan, J.; Fabero, F.; Claramunt, R. M.; Santa Maria, M. D.; Foces-Foces, M. C.; Cano, F. H.; Martinez-Ripoll, M.; Elguero, J.; Sastre, R. *J. Am. Chem. Soc.* **1992**, *114*, 5039–5048.

(24) Lerebours, R.; Wolf, C. *Org. Lett.* **2004**, *6*, 1147–1150.

(25) Yannan, C.; Gu, X.; Li, P. *Org. Lett.* **2013**, *15*, 2664–2667.

(26) Trice, S. L.; Kennedy, S. M.; Molander, G. A. *J. Org. Chem.* **2012**, *77*, 8678–8688.

(27) Adam, W.; Hartung, J.; Okamoto, H.; Marquardt, S.; Nau, W. M.; Pischel, U.; Saha-Moeller, C. R.; Spehar, K. *J. Org. Chem.* **2002**, *67*, 6041–6049.

(28) Beladhria, A.; Beydoun, K.; Ben Ammar, H.; Ben Sallem, R.; Doucet, H. *Synthesis* **2011**, *16*, 2553–2560.

(29) Mahdi, T.; del Castillo, J. N.; Stephan, D. W. *Organometalllics* **2013**, *32*, 1971–1978.

(30) Bhayana, B.; Fors, B. P.; Buchwald, S. L. *Org Lett*. **2009**, *11*, 3954–3957.

(31) Pena, M. A.; Sestelo, J. P.; Sarandeses, L. A. *J. Org. Chem*. **2007**, *72*, 1271–1275.

(32) Beaumard, F.; Molander, G. A. *Org. Lett*. **2010**, *12*, 4022–4025.

(33) Biolatto, B.; Molander, G. A. *J. Org. Chem*. **2003**, *68*, 4302–4314.

(34) Oberli, M. A.; Buchwald, S. L. *Org. Lett*. **2012**, *14*, 4606–4609.

CHAPTER THREE

Nickel-Catalyzed Amination of Aryl Chlorides and Sulfamates in 2-Me-THF

Noah F. Fine Nathel, Junyong Kim, Liana Hie, Xingyu Jiang, and Neil K. Garg.

ACS Catal. **2014**, *4, 3289–3293.*

3.1 Abstract

The nickel-catalyzed amination of aryl *O*-sulfamates and chlorides using the green solvent 2-methyl-THF is reported. This methodology employs the commercially available and air-stable pre-catalyst $NiCl_2$(DME), is broad in scope, and provides access to aryl amines in synthetically useful yields. The utility of this methodology is underscored by examples of gram-scale couplings conducted with catalyst loadings as low as 1 mol % nickel. Moreover, the nickel-catalyzed amination described is tolerant of heterocycles and should prove useful in the synthesis of pharmaceutical candidates and other heteroatom-containing compounds.

3.2 Introduction

Transition metal-catalyzed cross-couplings have had a profound impact on chemical synthesis.[1] As mild and useful alternatives to classical fragment couplings, cross-couplings have become one of the most frequently employed transformations for the construction of carbon–carbon (C–C) and carbon–heteroatom (C–X) bonds in both academic and industrial settings.[1] Although palladium-catalyzed couplings dominate the field, there has been growing interest in the development of related couplings that employ non-precious metals.[2] Nickel, in particular, is very attractive in part due to its wide availability and low cost.[2d–h] Additionally, certain nickel

catalysts have the unique ability to activate a wide range of electrophilic coupling partners, well beyond the scope of traditional cross-couplings that use palladium catalysis.[2d–h] Moreover, in addition to cost and reactivity benefits, nickel catalysis has shown great promise for operating under green reaction conditions,[3] particularly in green solvents.[4]

Our research group and others have developed new protocols for aryl C–C and C–N bond formation[5] using nickel catalysis.[2d–h,4,6,7,8] These procedures not only enable the desired bond formations, but also utilize air and moisture stable Ni(II) precatalysts that do not require glove box handling. To render these transformations more practical, we have recently focused our efforts on developing greener variants. This has led to a general nickel-catalyzed Suzuki–Miyaura coupling procedure that takes place in a variety of green solvents, is scalable at low catalyst loadings, and possesses an unusually broad substrate scope.[4] Herein, we report a complementary procedure for the efficient formation of aryl C–N bonds that proceeds in a green solvent using nickel catalysis (Figure 3.1).

Figure 3.1. Amination of (hetero)aryl chlorides and sulfamates in a green solvent using nickel catalysis.

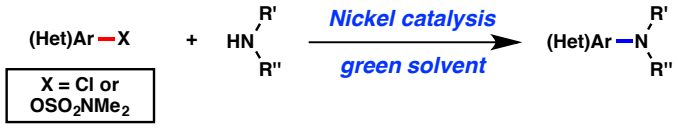

3.3 Optimization and Substrate Scope

Having previously established the nickel-catalyzed amination of aryl sulfamates,[7g,j] albeit not in a green solvent, we sought to first develop the corresponding coupling of aryl chlorides. We chose naphthyl chloride **3.1** for our studies and tested its coupling with morpholine (**3.2**)

using nickel catalysis (Table 2.1). Indeed, upon exposure of **3.1** and **3.2** to our previously disclosed sulfamate amination conditions,[7g,7j,9,10] product **3.4** was obtained when toluene was used as the solvent (entry 1). Other solvents that are considered environmentally attractive were also tested.[11,12] The use of DMF, which ranks favorably with regard to safety and some environmental considerations,[11] gave **3.4** in 50% yield (entry 2). We also examined alcohol solvents. Although the desired coupling did not take place when *n*-butanol was employed (entry 3), we found that the use of *t*-amyl alcohol gave the aminated product in good yield (entry 4). Ethereal solvents were also tested. Fortunately, the use of THF, MTBE, CPME,[13] or 2-Me-THF (entries 5–8, respectively) uniformly furnished **3.4** in excellent yield.

Table 3.1. Examination of Solvents in the Amination of 1-Chloronaphthalene.[a]

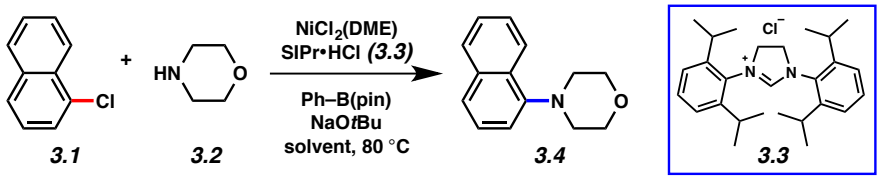

Entry	Solvent	Yield[b]	Entry	Solvent	Yield[b]
1	toluene	95%	5	THF	88%
2	DMF	50%	6	MTBE	96%
3	*n*-BuOH	0%	7	CPME	100%
4	*t*-amyl alcohol	78%	8	2-Me-THF	95%

[a] Reactions were carried out with $NiCl_2$(DME) (5 mol %), SIPr•HCl (10 mol %), Ph-B(pin) (0.55 equiv), substrate (0.5 mmol, 1.00 equiv), morpholine (1.80 equiv), NaOtBu (1.85 equiv), hexamethylbenzene (0.10 equiv), and solvent (used as received, 2.5 mL), for 3 h. [b] Yields were determine using hexamethylbenzene as an internal standard.

Of the solvents surveyed, we elected to focus on the use of 2-Me-THF for our subsequent studies.[14] 2-Me-THF has gained attention as a promising solvent for industrial applications[15] due to several salient features, including that: a) it is not easily oxidized; b) it readily phase-separates from aqueous layers (in contrast to THF); c) it is obtained from furfural, which, in turn comes

from renewable feedstock; d) it has a higher boiling point compared to THF, which can be advantageous in some instances; and e) it poses minimal health risks.

After establishing suitable reaction conditions for the amination of **3.1** with morpholine (**3.2**) we probed the use of other 1-naphthyl-based electrophilic coupling partners **3.5** in this methodology (Table 3.2). We were delighted to find that 1-bromonaphthalene could also be employed (entry 2). However, the corresponding iodide and triflate substrates gave only modest yields of **3.4** (entries 3 and 4). The use of a tosylate coupling partner, on the other hand, led to the desired product in 71% yield (entry 5). Finally, whereas the pivalate ester substrate failed (entry 6), we found that the corresponding carbamate and sulfamate substrates could be employed in the methodology (entries 7 and 8). Overall, the chloride and sulfamate substrates gave the best yields of product **3.4**; thus, we elected to evaluate the scope of the methodology for these two types of electrophiles.[16,17]

Table 3.2. Evaluation of Various Electrophiles.[a]

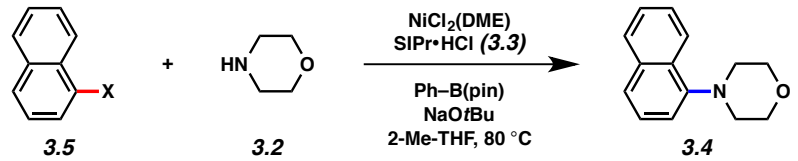

3.5 *3.2* *3.4*

Entry	*X*	*Yield*[b]	*Entry*	*X*	*Yield*[b]
1	Cl	95%	5	OTs	71%
2	Br	62%	6	OPiv	4%
3	I	27%	7	$OC(O)NEt_2$	76%
4	OTf	6%	8	OSO_2NMe_2	87%

[a] Reactions were carried out with $NiCl_2$(DME) (5 mol %), SIPr•HCl (10 mol %), Ph–B(pin) (0.55 equiv), substrate (0.5 mmol, 1.00 equiv), morpholine (1.80 equiv), NaOtBu (1.85 equiv), hexamethylbenzene (0.10 equiv), and solvent (used as received, 2.5 mL), for 3 h. [b] Yields were determine using hexamethylbenzene as an internal standard.

Figure 3.2 highlights the scope of the methodology with regard to the coupling of aryl sulfamate substrates using morpholine (**3.2**) as the amine partner and 2-Me-THF as solvent. Simple aryl hydrocarbon substrates, such as naphthyl and phenyl sulfamates, were readily aminated as demonstrated by the high yielding formation of **3.4** and **3.6**, respectively. Additionally, the generation of products **3.7**–**3.10** in good yields shows the methodology's tolerance of electron-donating, electron-withdrawing, and ortho substituents. Given the prevalence of heterocycles in pharmaceuticals, where amination reactions are widely employed, we also tested several heterocyclic sulfamate substrates. 2- and 3-substituted pyridines were well tolerated, as demonstrated by the formation of products **3.11** and **3.12**, respectively. Moreover, indole-, isoquinoline-, and dihydrobenzofuran-containing substrates were suitable coupling partners, as judged by the formation of **3.13**–**3.15** in synthetically useful yields.

Figure 3.2. Coupling of (hetero)aryl sulfamates with morpholine in 2-Me-THF.[a]

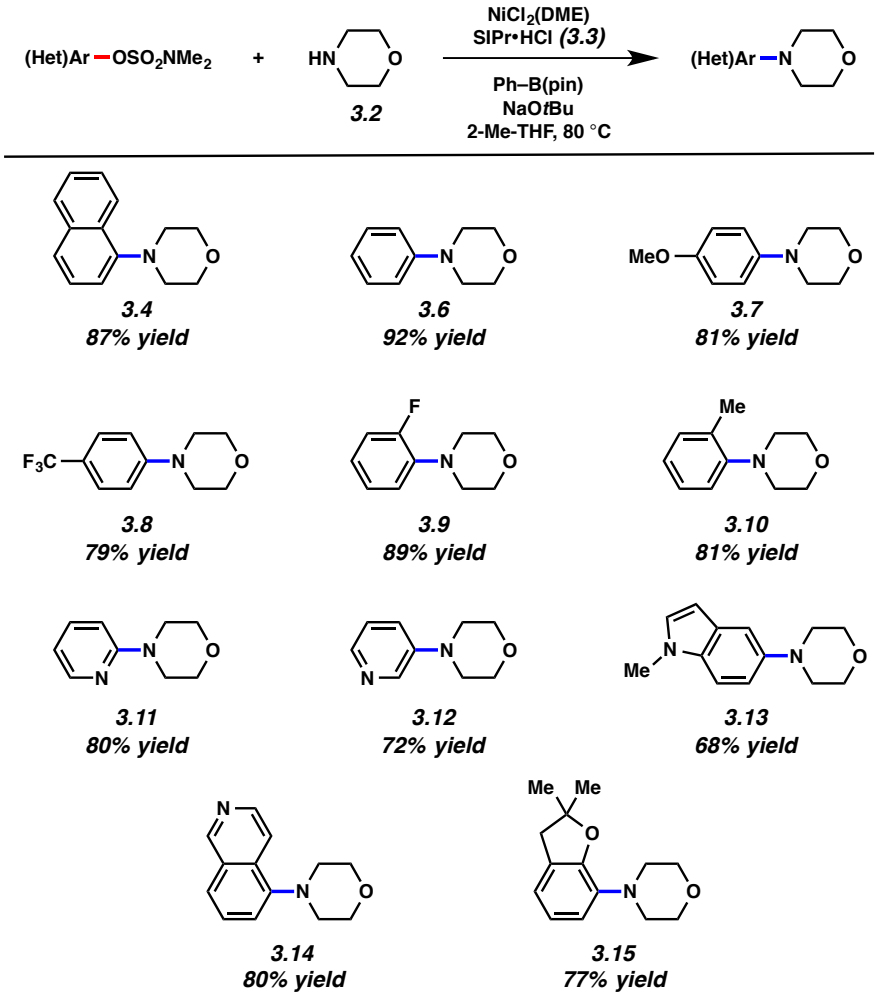

[a] Reactions were carried out with $NiCl_2$(DME) (5–15 mol %), SIPr•HCl (10–30 mol %), Ph–B(pin) (0.30–0.45 equiv), substrate (0.5 mmol, 1.00 equiv), morpholine (1.80 equiv), NaO*t*Bu (2.25–2.55 equiv), hexamethylbenzene (0.10 equiv), and solvent (used as received, 2.5 mL), for 3 h. Yields were determine using hexamethylbenzene as an internal standard.

Similarly, an array of aryl chlorides underwent the nickel-catalyzed amination reaction with morpholine (**3.2**) in 2-Me-THF (Figure 3.3). Non-heterocyclic substrates, including those containing electronically or sterically biasing substituents, coupled smoothly, as shown by the formation of adducts **3.4** and **3.7**–**3.10**. Of note, commercially available heterocyclic aryl chlorides could also be employed, thus giving rise to products **3.11**, **3.12**, **3.16**, and **3.17**. The

tolerance of the methodology to pyridines, quinolines, and benzothiophenes suggests the utility of our coupling conditions for applications in drug discovery.

Figure 3.3. Coupling of (hetero)aryl chlorides with morpholine in 2-Me-THF.[a]

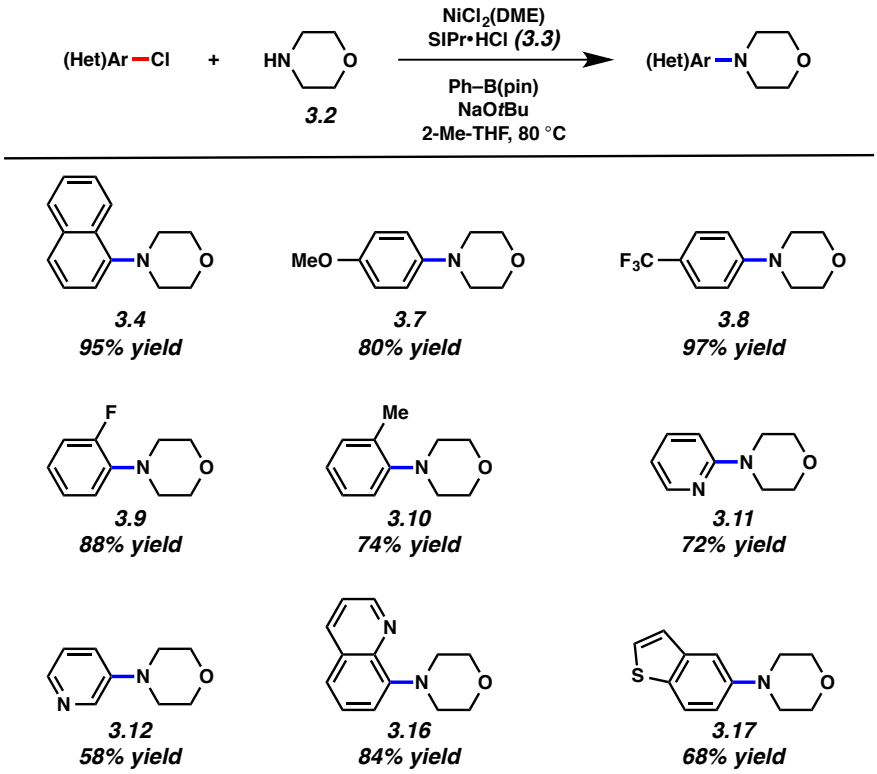

[a] Reactions were carried out with $NiCl_2$(DME) (5–15 mol %), SIPr•HCl (10–30 mol %), Ph–B(pin) (0.35–0.70 equiv), substrate (0.5 mmol, 1.00 equiv), morpholine (1.80 equiv), NaOtBu (2.25–2.70 equiv), hexamethylbenzene (0.10 equiv), and solvent (used as received, 2.5 mL), for 3 h. Yields were determine using hexamethylbenzene as an internal standard.

As shown in Figure 3.4, the scope of this amination methodology is not limited to the use of morpholine as the amine coupling partner. For example, pyrrolidine could be employed to give aminated product **3.18**. As demonstrated by the formation of **3.19**, the acyclic amine n-methylbutylamine was also tolerated in this methodology. Additionally, we found that 2,6-dimethylaniline, despite its steric hindrance, underwent the desired amination to give the

unsymmetrical biaryl amine product **3.20**. We were also delighted to find that a piperazine nucleophile bearing a pyridine ring coupled smoothly to give product **3.21** in 94% yield.

Figure 3.4. Scope of amine component in the coupling reaction.[a]

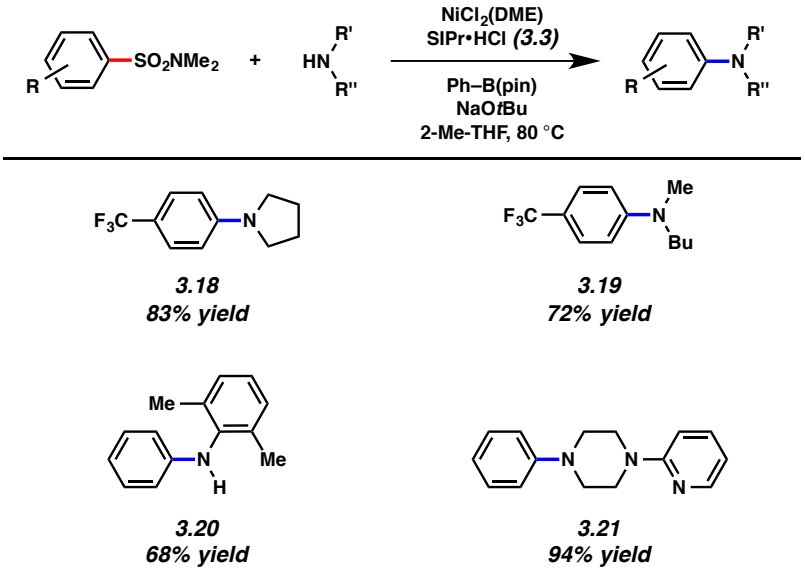

[a] Reactions were carried out with $NiCl_2$(DME) (5–15 mol %), SIPr•HCl (10–30 mol %), Ph–B(pin) (0.35–0.75 equiv), substrate (0.5 mmol, 1.00 equiv), morpholine (1.20–2.40 equiv), NaOtBu (2.10–3.45 equiv), hexamethylbenzene (0.10 equiv), and solvent (used as received, 2.5 mL), for 3 h. Yields were determined using hexamethylbenzene as an internal standard.

3.4 Gram-Scale Couplings

One general limitation pertaining to nickel-catalyzed cross-couplings is the frequent use of high catalyst loadings (i.e., often >10%).[2d–h] Whereas progress has been made in rendering nickel-catalyzed Suzuki–Miyaura couplings more efficient,[4,6i] corresponding achievements in nickel-mediated amination reactions have been lacking. To address this challenge, we tested the coupling of trifluoromethyl-containing sulfamate and chloride substrates **3.22** and **3.23**, respectively, in the amination reaction with **3.2** using 2-Me-THF as solvent (Figure 2.5). Using 3 and 1 mol% Ni, respectively, we found that gram-scale couplings could be achieved to give the arylated morpholine product **3.8** in excellent yields.

Figure 3.5. Gram-scale couplings of trifluoromethyl-containing substrates.

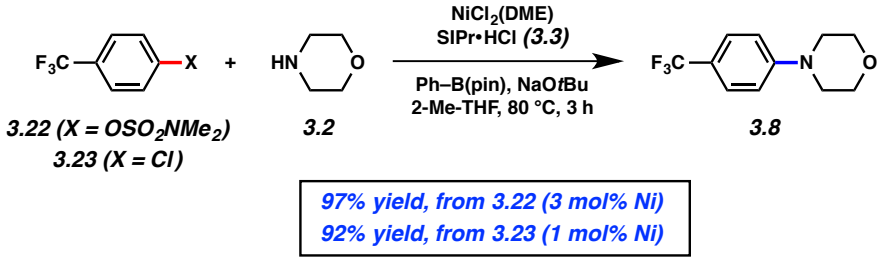

As noted earlier, the amination of heterocyclic substrates in 2-Me-THF provides a promising tool for the synthesis of pharmaceutical candidates. To further probe this notion, we tested the gram-scale couplings of heterocycle-containing substrates, as shown in Figure 2.6. Chloroquinoline **3.24** underwent facile coupling with morpholine (**3.2**) to generate aminated product **3.16** in 94% yield. This coupling was performed on gram-scale using 3 mol % Ni. Finally, we tested the gram-scale coupling of trifluoromethylated aryl chloride **3.23** with pyridyl piperazine derivative **3.25**. This reaction provided adduct **3.26** in 88% yield; of note, **3.26**

contains two heterocycles and a trifluoromethyl group, all of which are motifs commonly seen in pharmaceuticals.

Figure 3.6. Gram-scale couplings of heterocyclic substrates.

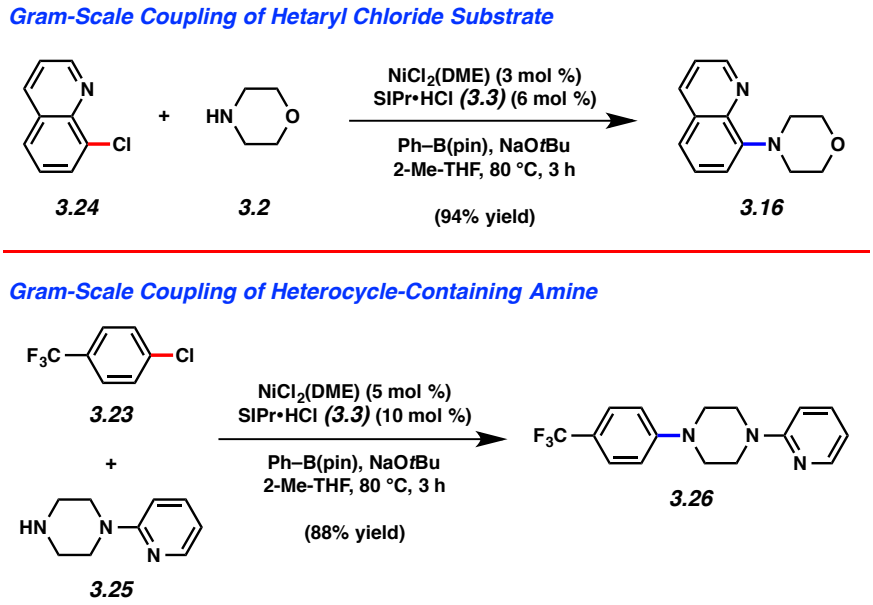

3.5 Conclusion

In summary, we have developed the nickel-catalyzed coupling of a variety of electrophilic substrates (e.g., halides and pseudohalides) with amines using the attractive, green solvent 2-Me-THF. The couplings of aryl *O*-sulfamates and aryl chlorides proceed in the highest yields, and may be achieved using an air-stable nickel precatalyst. The methodology has a broad scope and is tolerant of electronically biasing substituents, sterics, and even pharmaceutically-relevant heterocycles. The scalability of the nickel-catalyzed amination in 2-Me-THF using low catalyst loading bodes well for future synthetic applications in drug discovery and other arenas.

3.6 Experimental Section

3.6.1 Materials and Methods

Unless stated otherwise, reactions were conducted in flame-dried glassware under an atmosphere of nitrogen and commercially obtained reagents were used as received. Amines were purified by filtration over basic Brockman Grade I 58 Å Alumina (Activity 1), followed by distillation over calcium hydride prior to use. $NiCl_2$(DME) was obtained from Strem Chemicals. NaO*t*Bu, the amines, SIPr•HCl, and Ph–B(pin) were obtained from Sigma-Aldrich and Alfa Aesar. Halogenated substrates were obtained from Combi-Blocks, Sigma-Aldrich, and Oakwood Products, Inc. 2-Me-THF was obtained from Acros Organics [2-Methyltetrahydrofuran, 99+%, pure, stabilized] and used without further purification. Reaction temperatures were controlled using an IKAmag temperature modulator, and unless stated otherwise, reactions were performed at room temperature (rt, approximately 23 °C). Thin-layer chromatography (TLC) was conducted with EMD gel 60 F254 pre-coated plates (0.25 mm for analytical chromatography and 0.5 mm for preparative chromatography) and visualized using a combination of UV, anisaldehyde, ceric ammonium molybdate, iodine, vanillin, and potassium permanganate staining. Silicycle Siliaflash P60 (particle size 0.040–0.063 mm) was used for flash column chromatography. ^{1}H NMR spectra were recorded on Bruker spectrometers (at 400, 500, and 600 MHz) and are reported relative to residual solvent signals. Data for ^{1}H NMR spectra are reported as follows: chemical shift (δ ppm), multiplicity, coupling constant (Hz), integration and are referenced to the residual solvent peak 7.26 ppm for $CDCl_3$. Data for ^{13}C NMR are reported in terms of chemical shift (at 125 MHz) and are referenced to the residual solvent peak 77.16 for $CDCl_3$. IR spectra were recorded on a Perkin-Elmer 100 spectrometer and are reported in terms of frequency absorption (cm^{-1}). Uncorrected melting points were measured using a Digimelt MPA160 melting

point apparatus. High-resolution mass spectra were obtained from the UCLA Mass Spectrometry Facilities.

3.6.2 Experimental Procedures

3.6.2.1 Syntheses of Aryl Pseudohalide Substrates

Note: Experimental procedures for the syntheses of the aryl triflates,[18] tosylates,[19] pivalates,[20] carbamates,[21] and sulfamates[21a,22] shown in Table 3.2 and Figures 3.2, 3.4, and 3.5 have previously been reported.

3.6.2.2 Solvent Optimization and Scope of Electrophile

Representative Procedure for Amination of Electrophiles from Table 3.1 (coupling of naphthylchloride 3.1 is used as an example). A 4 mL reaction vial with a magnetic stir bar was charged with Ph–B(pin) (57.5 mg, 0.275 mmol, 0.55 equiv), anhydrous powdered NaO*t*Bu (88.9 mg, 0.925 mmol, 1.85 equiv), $NiCl_2$(DME) (5.5 mg, 0.025 mmol, 5 mol %), hexamethylbenzene (8.1 mg, 0.050 mmol, 0.1 equiv), and SIPr•HCl (21.7 mg, 0.0506 mmol, 10 mol %). Subsequently, toluene (2.5 ml), naphthylchloride **3.1** (81.3 mg, 0.500 mmol, 1.0 equiv), and morpholine (87.1 μL, 0.900 mmol, 1.8 equiv) were added sequentially. The resulting heterogenous mixture was stirred for 1 min while purging with N_2, and the vial was sealed with a Teflon-lined screw cap. The mixture was stirred at 23 °C for 1 h, and then at 80 °C for 3 h in a preheated aluminum block. The reaction vessel was allowed to cool to 23 °C and the mixture was filtered by passage through a plug of silica gel (EtOAC eluent, 5 mL), and then concentrated under reduced pressure. The yield was determined by ^{1}H NMR analysis with hexamethylbenzene as an internal standard. Spectral data match those previously reported.[23]

3.6.2.3 Aminations of Aryl Sulfamates and Chlorides

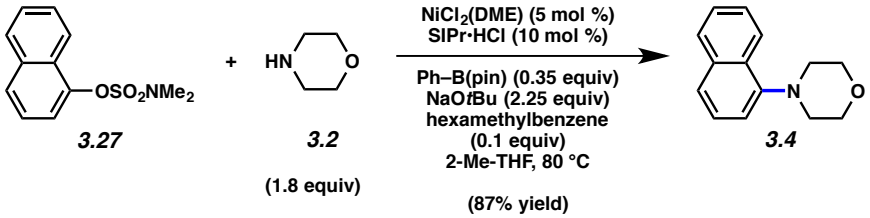

Representative Procedure (coupling of naphthylsulfamate 3.27 is used as an example). A 4 mL reaction vial with a magnetic stir bar was charged with Ph–B(pin) (36.6 mg, 0.175 mmol, 0.35 equiv), anhydrous powdered NaO*t*Bu (108.1 mg, 1.125 mmol, 2.25 equiv), $NiCl_2$(DME) (5.5 mg, 0.025 mmol, 5 mol %), hexamethylbenzene (8.1 mg, 0.050 mmol, 0.1 equiv), and SIPr•HCl (21.7 mg, 0.0506 mmol, 10 mol %). Subsequently, 2-Me-THF (2.5 ml), naphthylsulfamate **3.27** (125.7 mg, 0.5002 mmol, 1.0 equiv), and morpholine (87.1 μL, 0.900 mmol, 1.8 equiv) were added, sequentially. The resulting heterogenous mixture was stirred for 1 min while purging with N_2, and the vial was sealed with a Teflon-lined screw cap. The mixture was stirred at 23 °C for 1 h, and then at 80 °C for 3 h in a preheated aluminum heating block. The reaction vessel was allowed to cool to 23 °C and the mixture was filtered by passage over a plug of silica gel (EtOAC eluent, 5 mL), and then concentrated under reduced pressure. The yield was determined by ^{1}H NMR analysis with hexamethylbenzene as an internal standard. Spectral data match those previously reported.[23]

Any modifications of the conditions shown in the representative procedure above are specified in the following schemes, which depict all of the results shown in Figures 3.2–3.4.

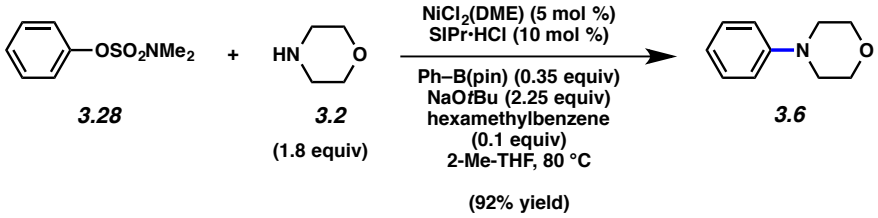

3.28 *3.2* (1.8 equiv) *3.6*

3.6 (Figure 3.2). The yield was determined by ^{1}H NMR analysis with hexamethylbenzene as an internal standard. Spectral data match those previously reported.[24]

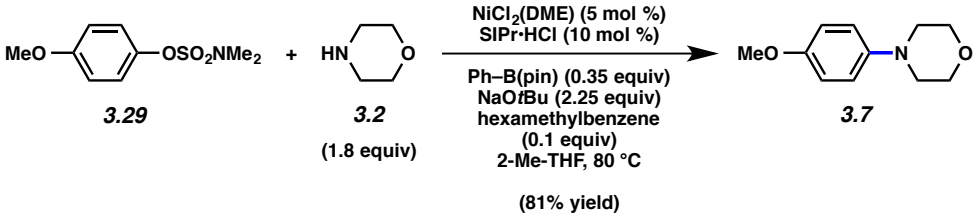

3.29 *3.2* (1.8 equiv) *3.7*

3.7 (Figure 3.2). The yield was determined by ^{1}H NMR analysis with hexamethylbezene as an internal standard. Spectral data match those previously reported.[25]

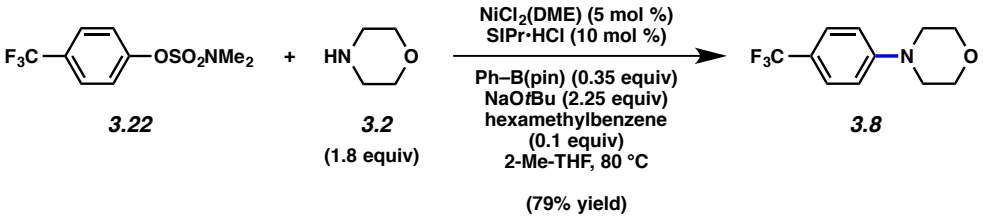

3.22 *3.2* (1.8 equiv) *3.8*

3.8 (Figure 3.2). The yield was determined by ^{1}H NMR analysis with hexamethylbenzene as an internal standard. Spectral data match those previously reported.[26]

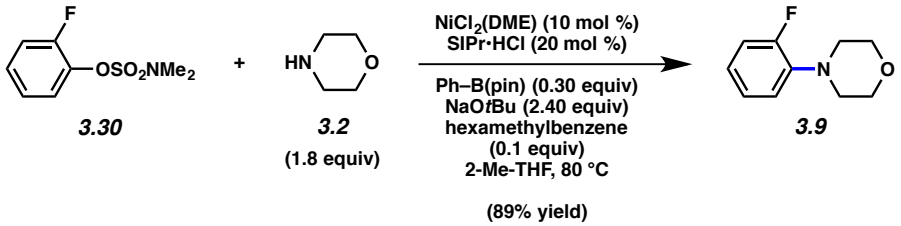

3.9 (Figure 3.2). The yield was determined by ^{1}H NMR analysis with hexamethylbenzene as an internal standard. Spectral data match those previously reported.[27]

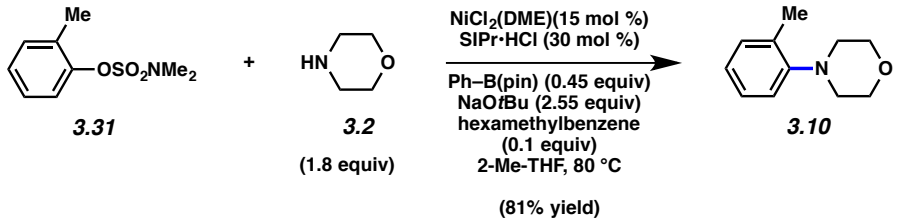

3.10 (Figure 3.2). The yield was determined by ^{1}H NMR analysis with hexamethylbenzene as an internal standard. Spectral data match those previously reported.[10e]

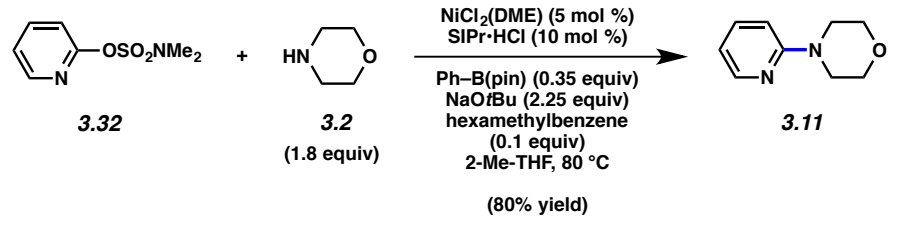

3.11 (Figure 3.2). The yield was determined by ^{1}H NMR analysis with hexamethylbenzene as an internal standard. Spectral data match those previously reported.[28]

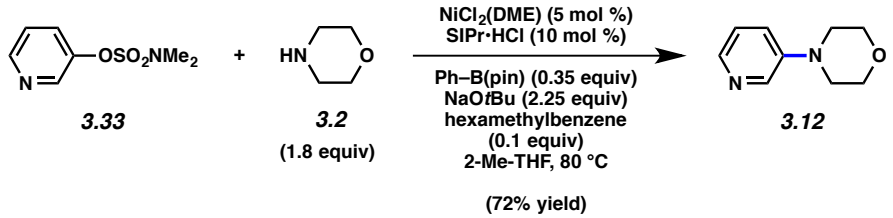

3.12 (Figure 3.2). The yield was determined by ^{1}H NMR analysis with hexamethylbenzene as an internal standard. Spectral data match those previously reported.[28]

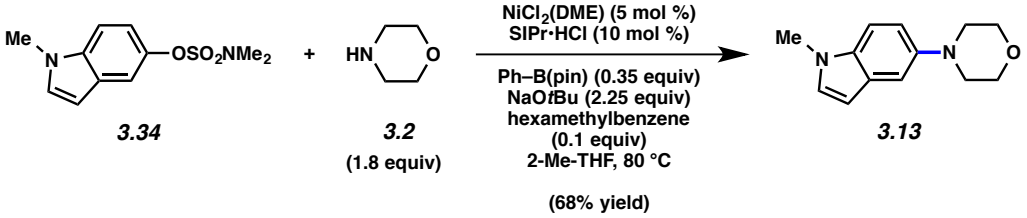

3.13 (Figure 3.2). The yield was determined by ^{1}H NMR analysis with hexamethylbenzene as an internal standard. Spectral data match those previously reported.[29]

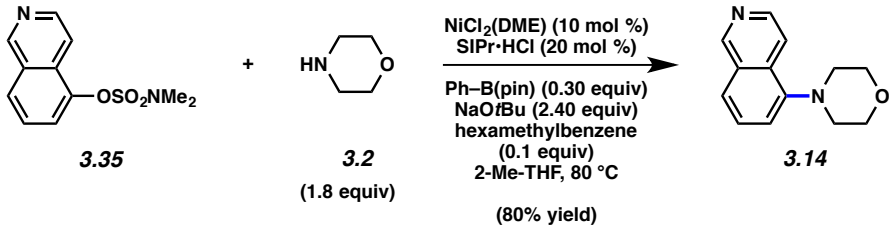

3.14 (Figure 3.2). The yield was determined by ^{1}H NMR analysis with hexamethylbenzene as an internal standard. An analytic sample of **3.14** was prepared by filtration of the reaction mixture through a plug of silica gel (EtOAc eluent, 5 mL), evaporation of the solvent under reduced pressure, and purification of an aliquot of the crude residue by preparative thin-layer chromatography (5:1 Hexanes:EtOAC, 20x20 cm). R_f 0.18 (1:1 Hexanes:EtOAc); ^{1}H NMR: (400 MHz, $CDCl_3$): δ 9.23 (s, 1H), 8.53 (d, J = 6.0, 1H), 7.93 (d, J = 6.0, 1H), 7.68 (d, J = 8.0,

1H), 7.54 (app t, J = 8.0, 1H), 7.27 (t, J = 7.5, 1H), 3.99 (t, J = 4.5, 4H), 3.11 (t, J = 4.5, 4H); ^{13}C NMR (125 MHz, $CDCl_3$): δ 152.1, 147.6, 141.8, 130.8, 129.1, 126.5, 122.0, 117.7, 115.5, 66.4, 52.4; IR (film): 2966, 2825, 1617, 1582, 1489, 1454, 1433, 1387, 1263, 1115, 1055, 1033 cm^{-1}; HRMS-ESI (*m/z*) $[M+H]^+$ calcd for $C_{13}H_{15}N_2O$, 215.11789; found 215.11741.

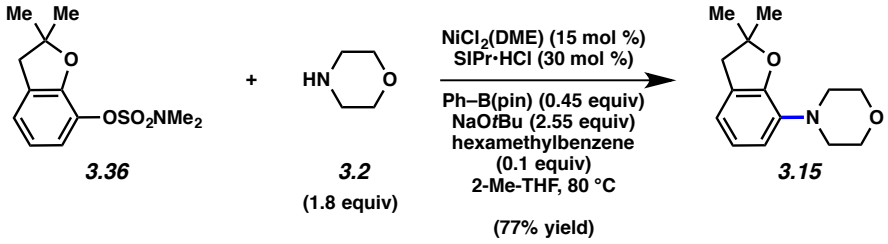

3.15 (Figure 3.2). The yield was determined by ^{1}H NMR analysis with hexamethylbenzene as an internal standard. An analytic sample of **3.15** was prepared by filtration of the reaction mixture through a plug of silica gel (EtOAc eluent, 5 mL), evaporation of the solvent under reduced pressure, and purification of an aliquot of the crude residue by preparative thin-layer chromatography (5:1 Hexanes:EtOAC, 20x20 cm). R_f 0.27 (9:1 Hexanes:EtOAc); ^{1}H NMR: (400 MHz, $CDCl_3$): δ 6.81–6.77 (m, 3H), 6.68 (dd, J = 6.7, 2.2, 1H), 3.88 (t, J = 4.5, 4H), 3.13 (t, J = 4.5, 4H), 2.99 (s, 2H), 1.49 (s, 6H); ^{13}C NMR (125 MHz, $CDCl_3$): δ 150.1, 136.4, 128.0, 120.7, 118.6, 115.3, 86.8, 67.1, 50.0, 43.2, 28.4; IR (film): 2968, 2854, 1608, 1455, 1269, 1119, 1006 cm^{-1}; HRMS-ESI (*m/z*) $[M+H]^+$ calcd for $C_{14}H_{20}NO_2$, 234.14886; found 234.14766.

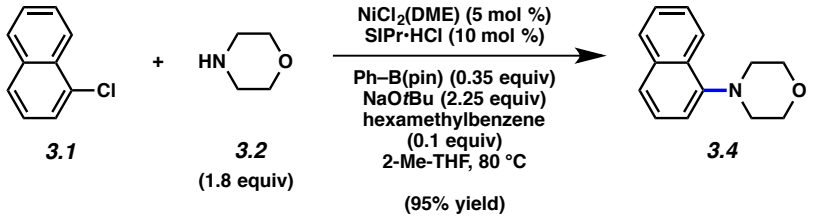

3.4 (Figure 3.3). The yield was determined by ^{1}H NMR analysis with hexamethylbenzene as an internal standard. Spectral data match those previously reported.[23]

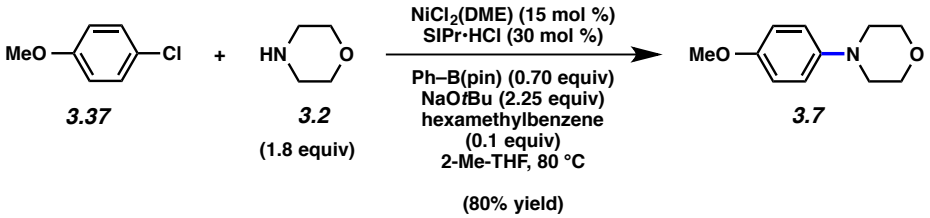

3.7 (Figure 3.3). The yield was determined by 1H NMR analysis with hexamethylbenzene as an internal standard. Spectral data match those previously reported.[25]

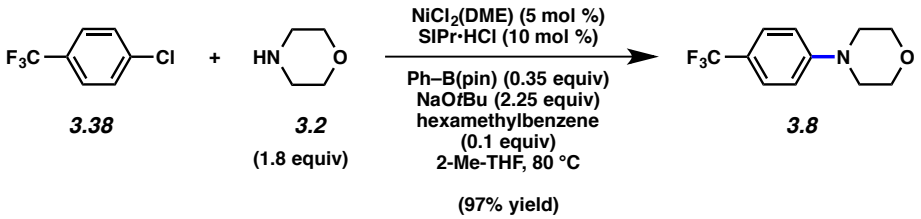

3.8 (Figure 3.3). The yield was determined by ^{1}H NMR analysis with hexamethylbenzene as an internal standard. Spectral data match those previously reported.[26]

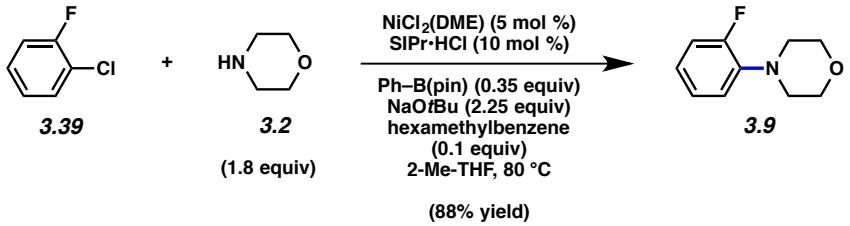

3.9 (Figure 3.3). The yield was determined by ^{1}H NMR analysis with hexamethylbenzene as an internal standard. Spectral data match those previously reported.[27]

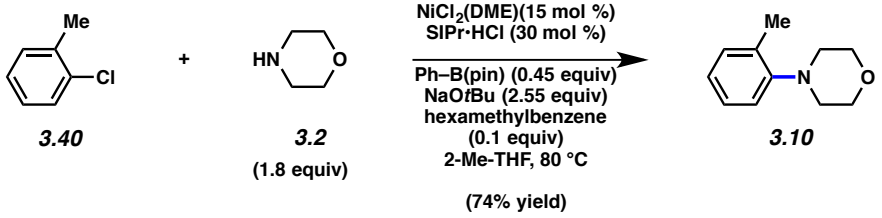

3.10 (Figure 3.3). The yield was determined by ^{1}H NMR analysis with hexamethylbenzene as an internal standard. Spectral data match those previously reported.[10e]

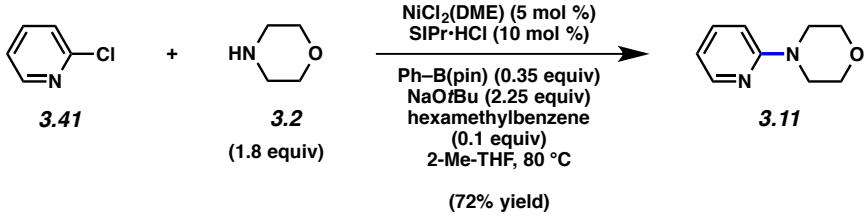

3.11 (Figure 3.3). The yield was determined by ^{1}H NMR analysis with hexamethylbenzene as an internal standard. Spectral data match those previously reported.[28]

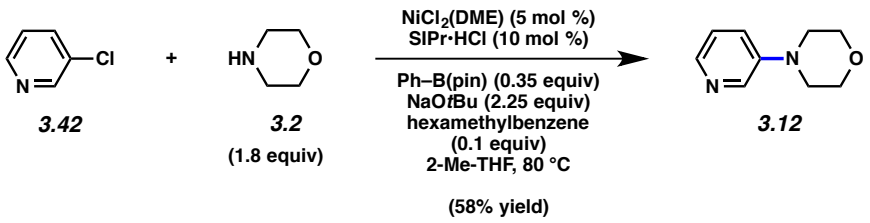

3.12 (Figure 3.3). The yield was determined by ^{1}H NMR analysis with hexamethylbenzene as an internal standard. Spectral data match those previously reported.[28]

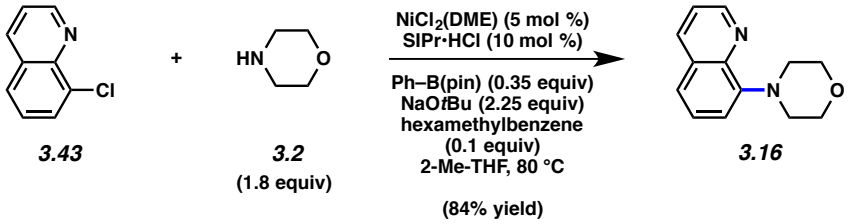

3.16 (Figure 3.3). The yield was determined by ^{1}H NMR analysis with hexamethylbenzene as an internal standard. Spectral data match those previously reported.[30]

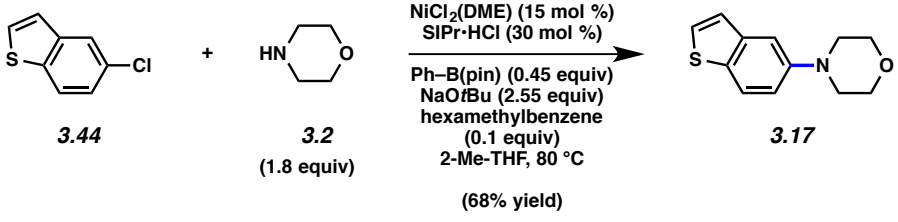

3.17 (Figure 3.3). The yield was determined by ^{1}H NMR analysis with hexamethylbenzene as an internal standard. An analytic sample of **3.17** was prepared by filtration of the reaction mixture through a plug of silica gel (EtOAc eluent, 5 mL), evaporation of the solvent under reduced pressure, and purification of an aliquot of the crude residue by preparative thin-layer chromatography (5:1 Hexanes:EtOAC, 20x20 cm). R_f 0.21 (9:1 Hexanes:EtOAc); ^{1}H NMR: (400 MHz, $CDCl_3$): δ 7.75 (d, J = 8.8, 1H), 7.41 (d, J = 5.4, 1H), 7.29 (br s, 1H), 7.24 (d, J = 5.4, 1H),

7.07 (dd, J = 8.8, 2.2, 1H), 3.90 (t, J = 4.5, 4H), 3.20 (t, J = 4.5, 4H); ^{13}C NMR (125 MHz, $CDCl_3$): δ 149.2, 140.8, 132.3, 127.3, 123.8, 123.0, 116.3, 109.7, 67.1, 50.8; IR (film): 2966, 2909, 2829, 1595, 1444, 1262, 1233, 1120 cm^{-1}; HRMS-ESI (*m/z*) $[M+H]^+$ calcd for $C_{12}H_{14}SNO$, 220.07906; found 220.07835.

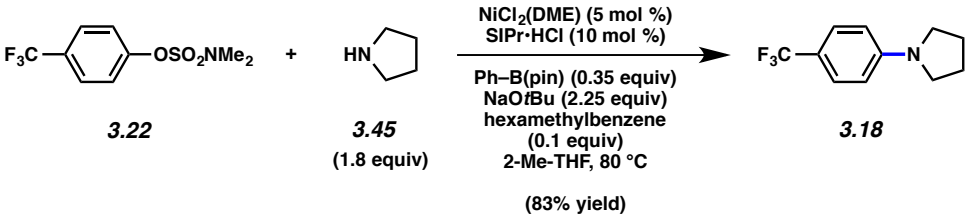

3.18 (Figure 3.4). The yield was determined by ^{1}H NMR analysis with hexamethylbenzene as an internal standard. Spectral data match those previously reported.[31]

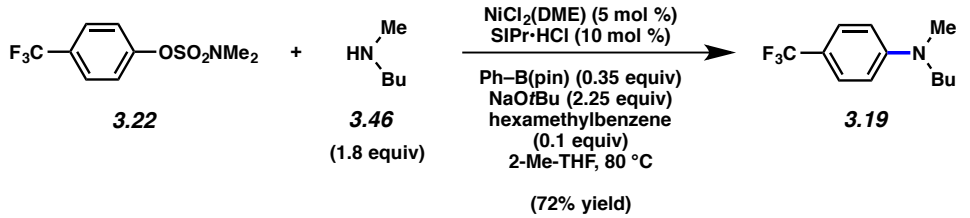

3.19 (Figure 3.4). The yield was determined by ^{1}H NMR analysis with hexamethylbenzene as an internal standard. Spectral data match those previously reported.[29]

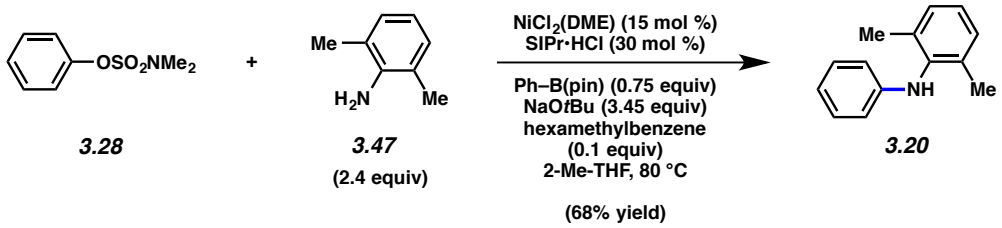

3.20 (Figure 3.4). The yield was determined by ^{1}H NMR analysis with hexamethylbenzene as an internal standard. Spectral data match those previously reported.[10e]

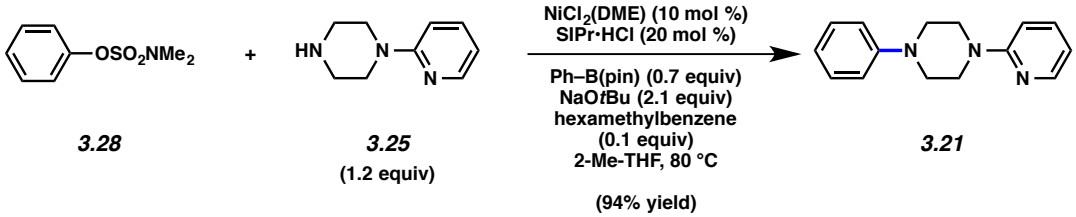

3.21 (Figure 3.4). The yield was determined by ^{1}H NMR analysis with hexamethylbenzene as an internal standard. Spectral data match those previously reported.[7e]

3.6.2.4 Isolation Experiments

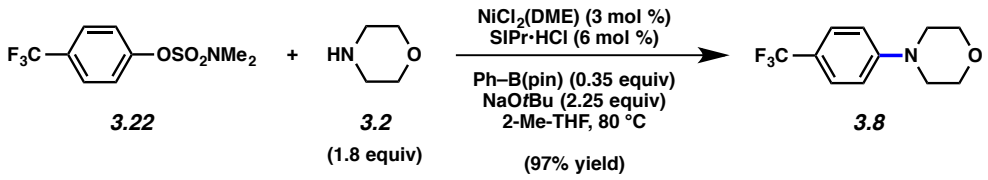

3.8 (Figure 3.5). A 100 mL round bottom flask with a magnetic stir bar was charged with Ph–B(pin) (271.5 mg, 1.30 mmol, 0.35 equiv), anhydrous powdered NaO*t*Bu (802.2 mg, 8.35 mmol, 2.25 equiv), $NiCl_2$(DME) (24.5 mg, 0.11 mmol, 3 mol %), and SIPr•HCl (95.5 mg, 0.22 mmol, 6 mol %). Subsequently, 2-Me-THF (18.6 ml), trifluorobenzosulfamate **3.22** (1.0 g, 3.71 mmol, 1.0 equiv), and morpholine (578 µL, 6.69 mmol, 1.8 equiv) were added, sequentially. The resulting

heterogenous mixture was stirred for 1 min while purging with N_2, and then under an atmosphere of N_2 for 1 h. The reaction was then equipped with a reflux condenser and placed in an oil bath, preheated to 80 °C, for 3 h. The reaction flask was allowed to cool to 23 °C and the mixture was filtered by passage over a plug of silica gel (EtOAC eluent, 5 mL). After concentration under reduced pressure, the crude residue was purified by flash chromatography (4:1 Hexanes:EtOAc) to yield amine **3.8** (832.1 mg, 97% yield) as a white solid. Spectral data match those previously reported.[26]

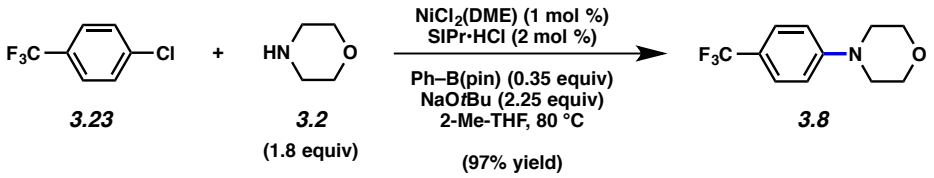

3.8 (Figure 3.5). A 100 mL round bottom flask with a magnetic stir bar was charged with Ph–B(pin) (405.4 mg, 1.94 mmol, 0.35 equiv), anhydrous powdered NaO*t*Bu (1.20 g, 12.47 mmol, 2.25 equiv), $NiCl_2$(DME) (12.2 mg, 0.06 mmol, 1 mol %), and SIPr•HCl (47.5 mg, 0.111 mmol, 2 mol %). Subsequently, 2-Me-THF (27.7 ml), trifluorobenzochloride **3.23** (1.0 g, 5.54 mmol, 1.0 equiv), and morpholine (863 μL, 9.97 mmol, 1.8 equiv) were added, sequentially. The resulting heterogenous mixture was stirred for 1 min while purging with N_2, and then under an atmosphere of N_2 at 23 °C for 1 h. The reaction was then equipped with a reflux condenser and placed in an oil bath, preheated to 80 °C, for 3 h. The reaction flask was allowed to cool to 23 °C and the mixture was filtered by passage through a plug of silica gel (EtOAC eluent, 5 mL). After concentration under reduced pressure, the crude residue was purified by flash chromatography (4:1 Hexanes:EtOAc) to yield amine **3.8** (1.18 g, 97% yield) as a white solid. Spectral data match those previously reported.[26]

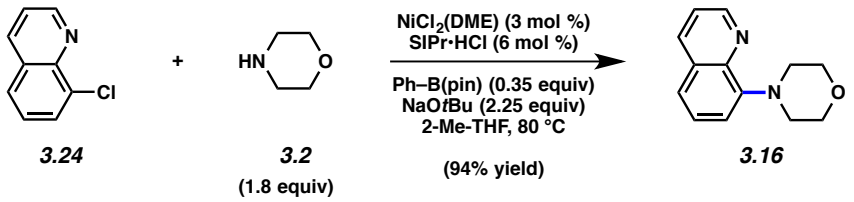

3.16 (Figure 3.6). A 100 mL round bottom flask was charged with a magnetic stir bar, flame-dried under reduced pressure, and allowed to cool under N_2. The flask was then charged with Ph–B(pin) (447.1 mg, 2.14 mmol, 0.35 mol), anhydrous powdered NaO*t*Bu (1.32 g, 13.8 mmol, 2.25 equiv), $NiCl_2$(DME) (40.2 mg, 0.183 mmol, 3 mol %), and SIPr•HCl (157.3 mg, 0.367 mmol, 6 mol %). Subsequently, 2-Me-THF (30.6 mL), chloroquinoline **3.24** (1.0 g, 6.11 mmol, 1.0 equiv), and morpholine (95.1 μL, 11.0 mmol, 1.8 equiv) were added, sequentially. The resulting heterogenous mixture was stirred for 1 min while purging with N_2, and then under an atmosphere for 1 h. The reaction was then equipped with a reflux condenser and placed in an oil bath, preheated to 80 °C, for 3 h. The reaction flask was allowed to cool to 23 °C and the mixture was filtered by passage through a plug of silica gel (EtOAC eluent, 5 mL). After concentration under reduced pressure, the crude residue was purified by flash chromatography (2:1 Hexanes:EtOAc) to yield morpholino quinoline **3.16** (1.23 g, 94% yield) as a clear viscous oil. Spectral data match those previously reported.[30]

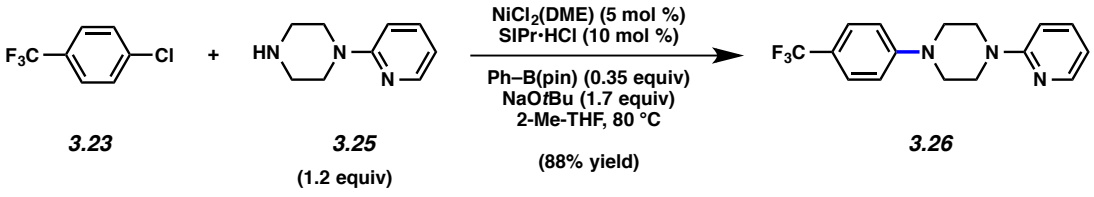

3.26 (Figure 3.6). A 100 mL round bottom flask was charged with a magnetic stir bar, flame-dried under reduced pressure, and allowed to cool under N_2. The flask was then charged with

Ph–B(pin) (426.0 mg, 1.94 mmol, 0.35 equiv), anhydrous powdered NaO*t*Bu (904.9 mg, 9.42 mmol, 1.7 equiv), $NiCl_2$(DME) (60.9 mg, 0.277 mmol, 5 mol %), and SIPr•HCl (237.7 mg, 0.554 mmol, 10 mol %). Subsequently, 2-Me-THF (27.7 ml), chloride **3.23** (1.0 g, 5.54 mmol, 1.0 equiv), and 1-(2-pyridyl)piperizine (1.01 mL, 6.65 mmol, 1.2 equiv) were added, sequentially. The resulting heterogenous mixture was stirred for 1 min while purging with N_2, and then under an atmosphere of N_2 for 1 h. The reaction was then equipped with a reflux condenser and placed in an oil bath, preheated to 80 °C, for 3 h. The reaction flask was allowed to cool to 23 °C and the mixture was filtered by passage through a plug of silica gel (EtOAC eluent, 5 mL). After concentration under reduced pressure, the crude residue was purified by flash chromatography (8:1 Hexanes:EtOAc) to yield piperizine **3.26** (1.49 g, 88% yield) as an off-white solid. Spectral data match those previously reported.[32]

Appendix Three: Spectra Relevant to Chapter Three

Nickel-Catalyzed Amination of Aryl Chlorides and Sulfamates in 2-Me-THF

Noah F. Fine Nathel, Junyong Kim, Liana Hie, Xingyu Jiang, and Neil K. Garg.

ACS Catal. **2014**, *4*, 3289–3293.

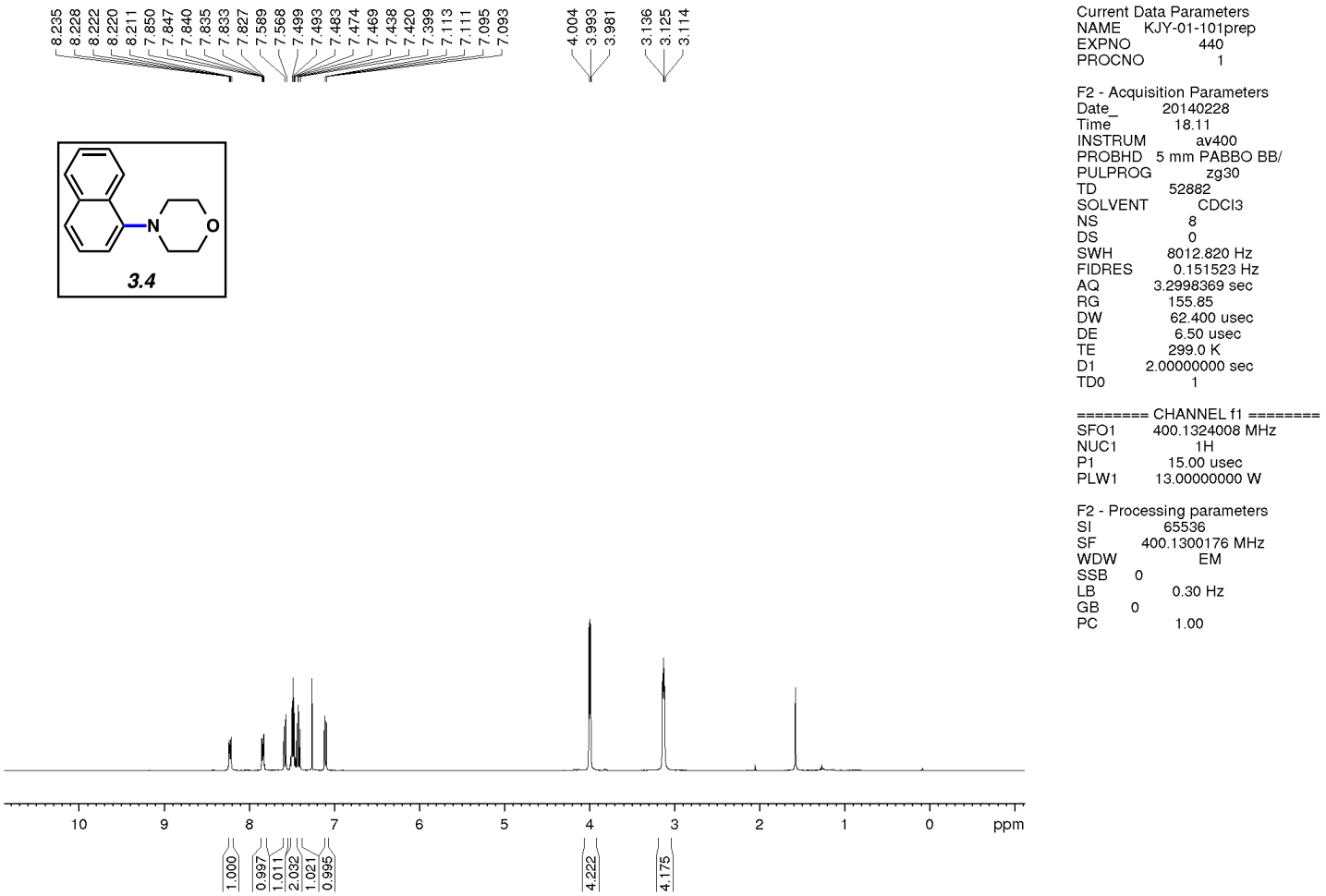

Figure A3.1 ^{1}H NMR (400 MHz, $CDCl_3$) of compound **3.4**.

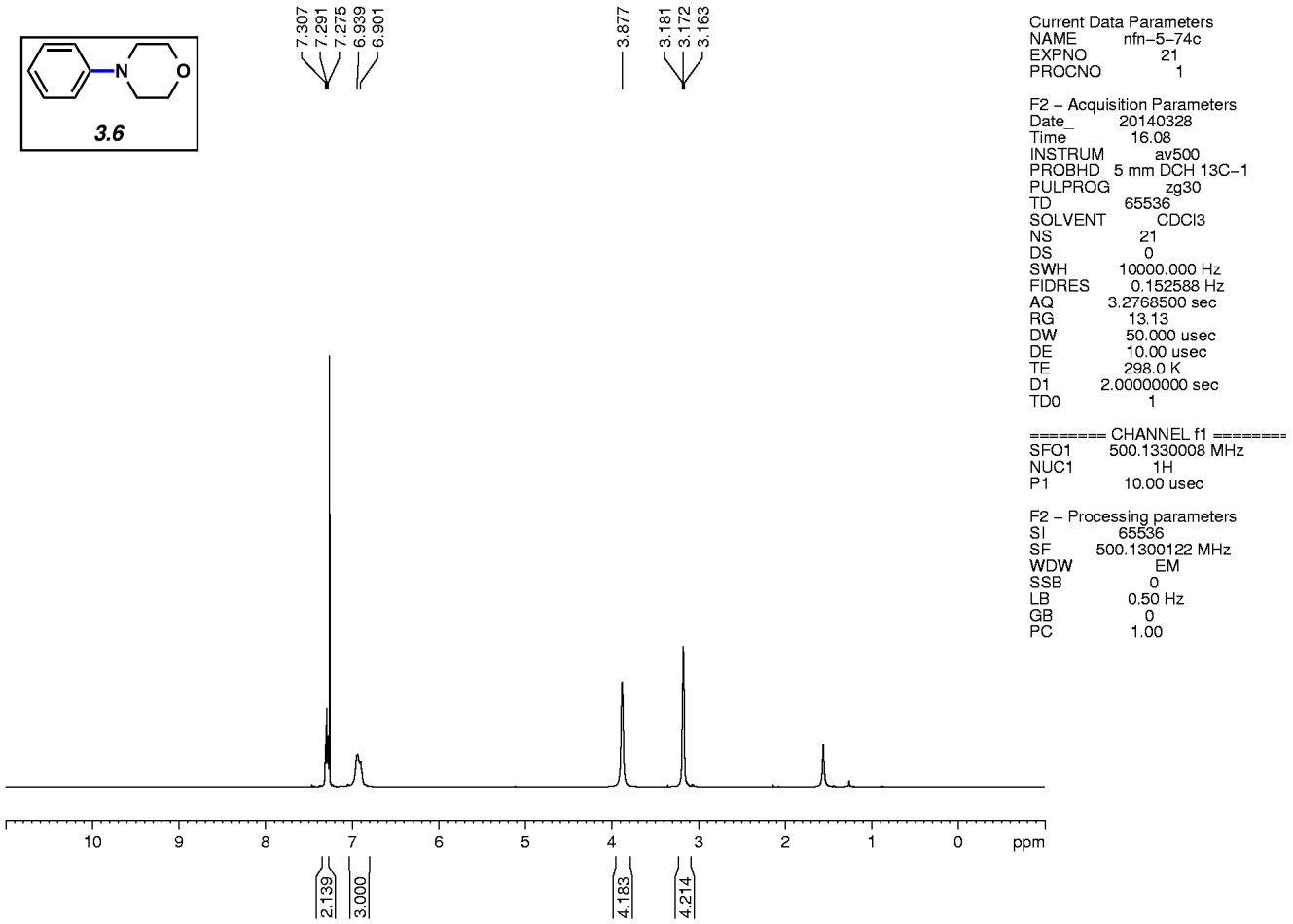

Figure A3.2 ^{1}H NMR (500 MHz, $CDCl_3$) of compound **3.6**.

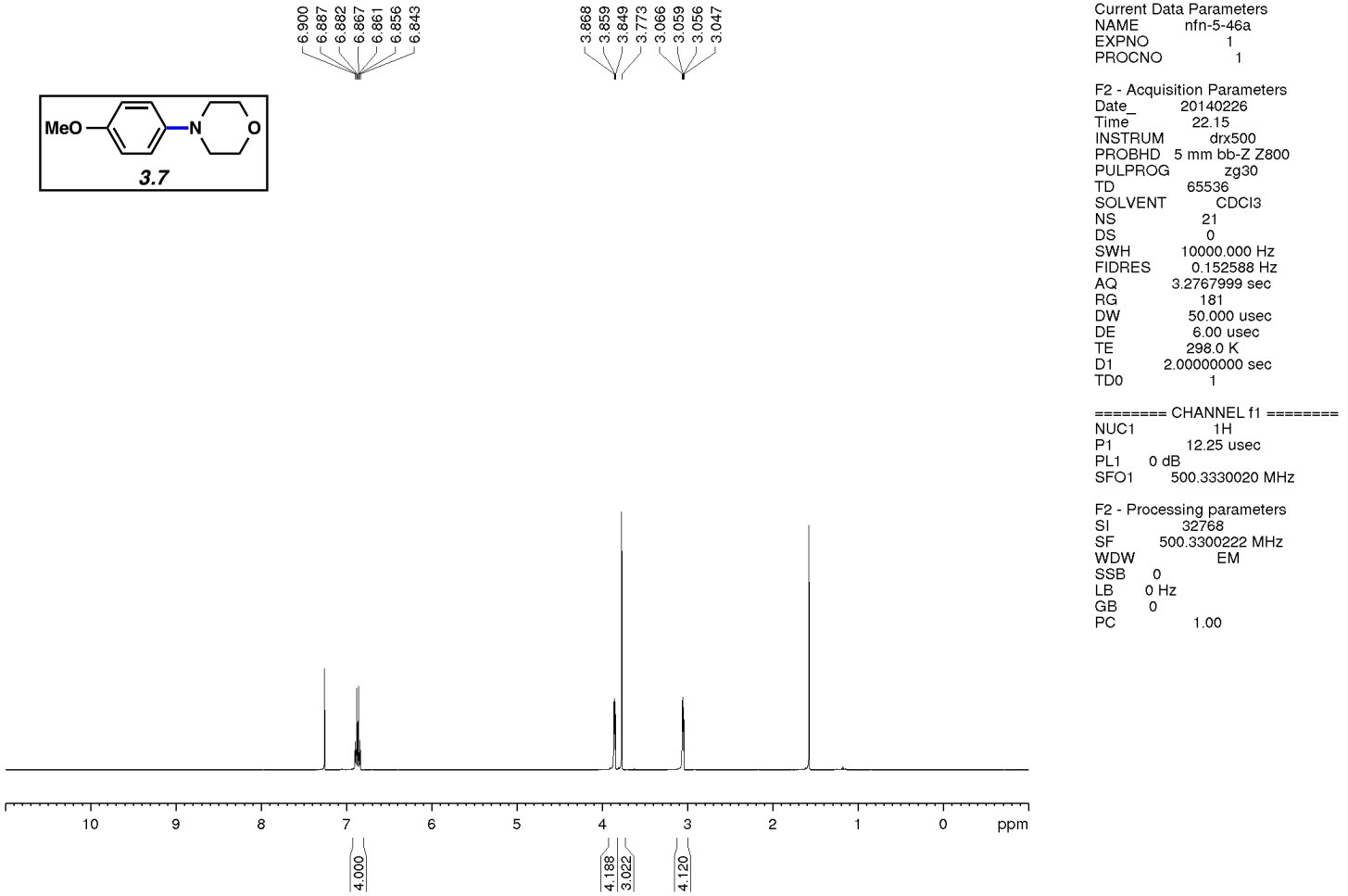

Figure A3.3 ^{1}H NMR (500 MHz, $CDCl_3$) of compound **3.7**.

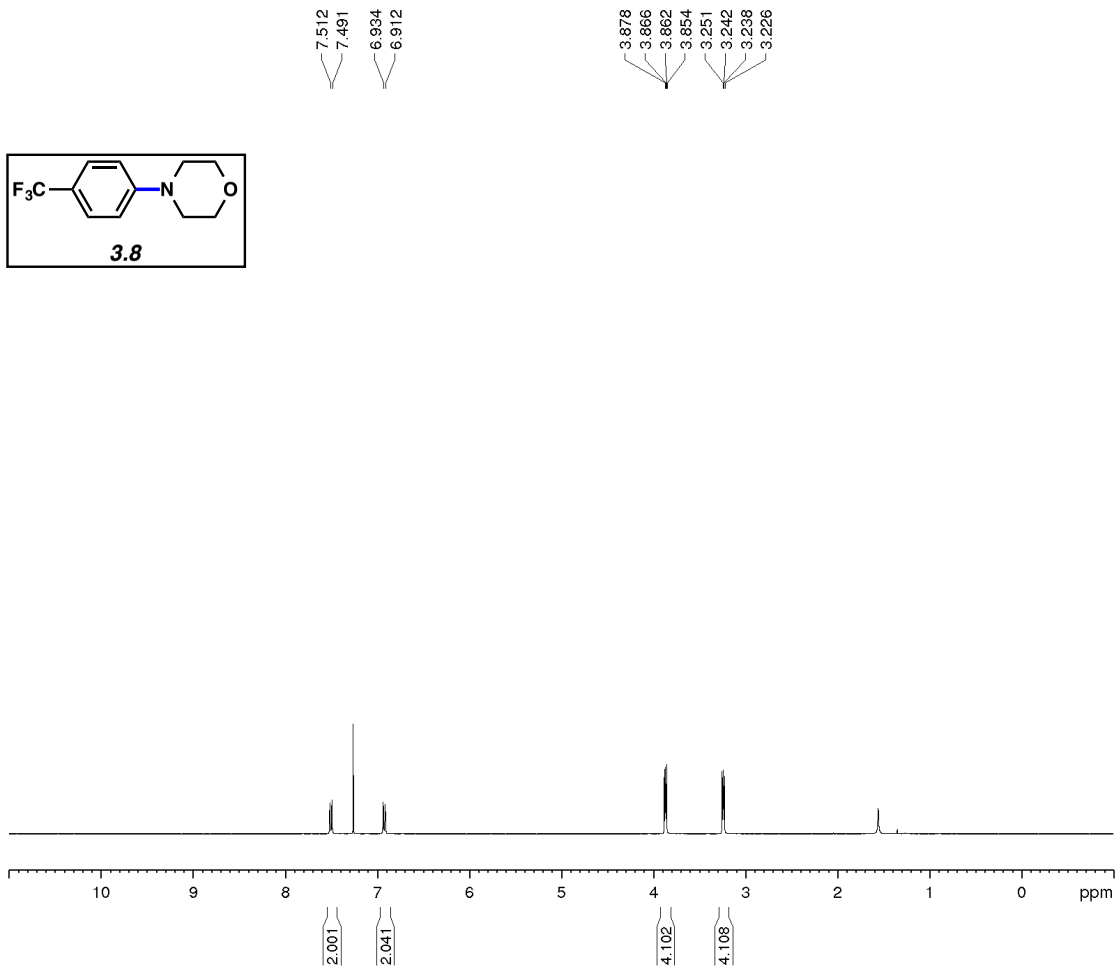

Current Data Parameters
NAME KJY-01-095
EXPNO 650
PROCNO 1

F2 - Acquisition Parameters
Date_ 20140227
Time 19.55
INSTRUM av400
PROBHD 5 mm PABBO BB/
PULPROG zg30
TD 52882
SOLVENT CDCl3
NS 8
DS 0
SWH 8012.820 Hz
FIDRES 0.151523 Hz
AQ 3.2998369 sec
RG 155.85
DW 62.400 usec
DE 6.50 usec
TE 299.0 K
D1 2.00000000 sec
TD0 1

======== CHANNEL f1 ========
SFO1 400.1324008 MHz
NUC1 1H
P1 15.00 usec
PLW1 13.00000000 W

F2 - Processing parameters
SI 65536
SF 400.1300176 MHz
WDW EM
SSB 0
LB 0.30 Hz
GB 0
PC 1.00

Figure A3.4 ^{1}H NMR (400 MHz, $CDCl_3$) of compound **3.8**.

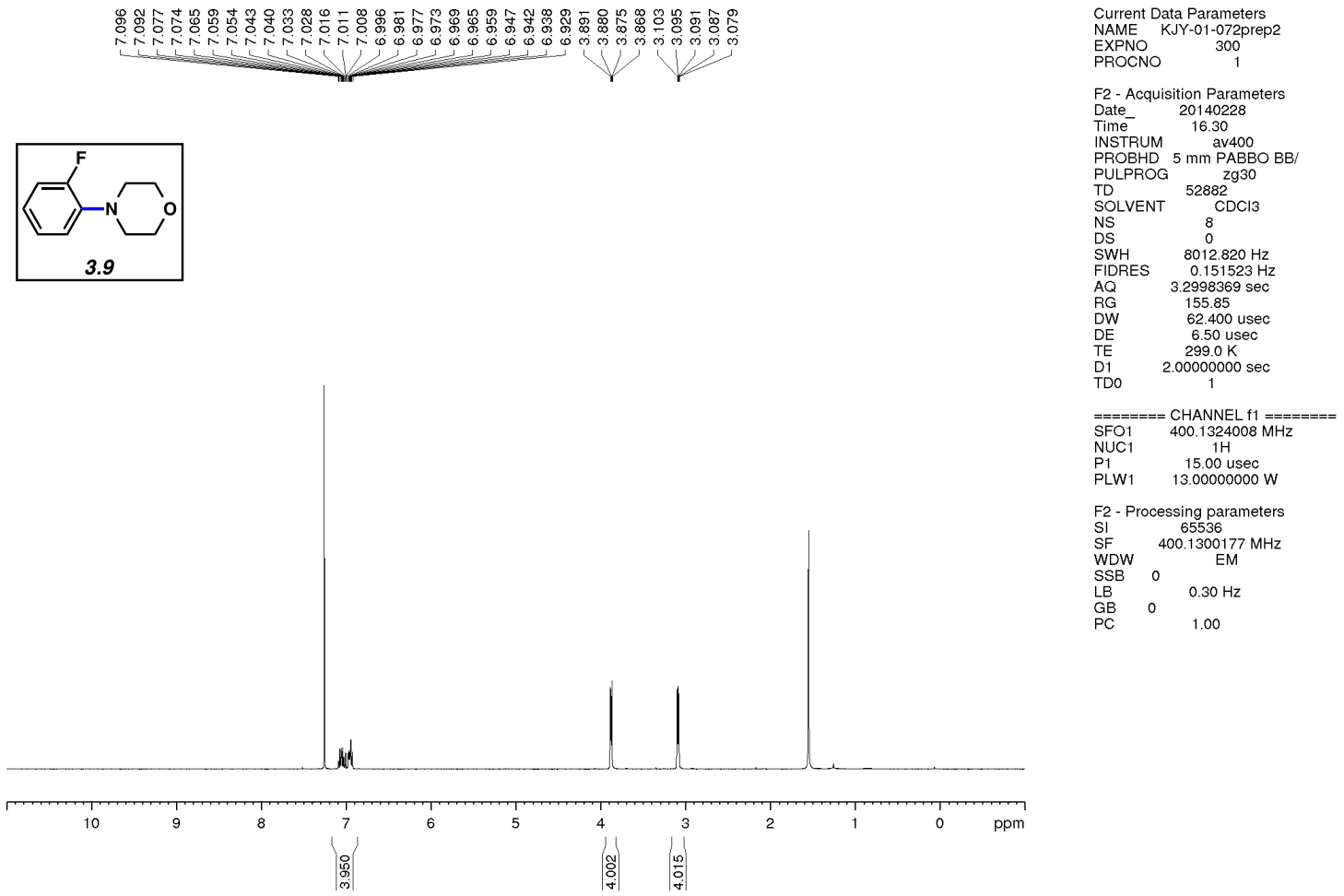

Figure A3.5 ^{1}H NMR (400 MHz, $CDCl_3$) of compound **3.9**.

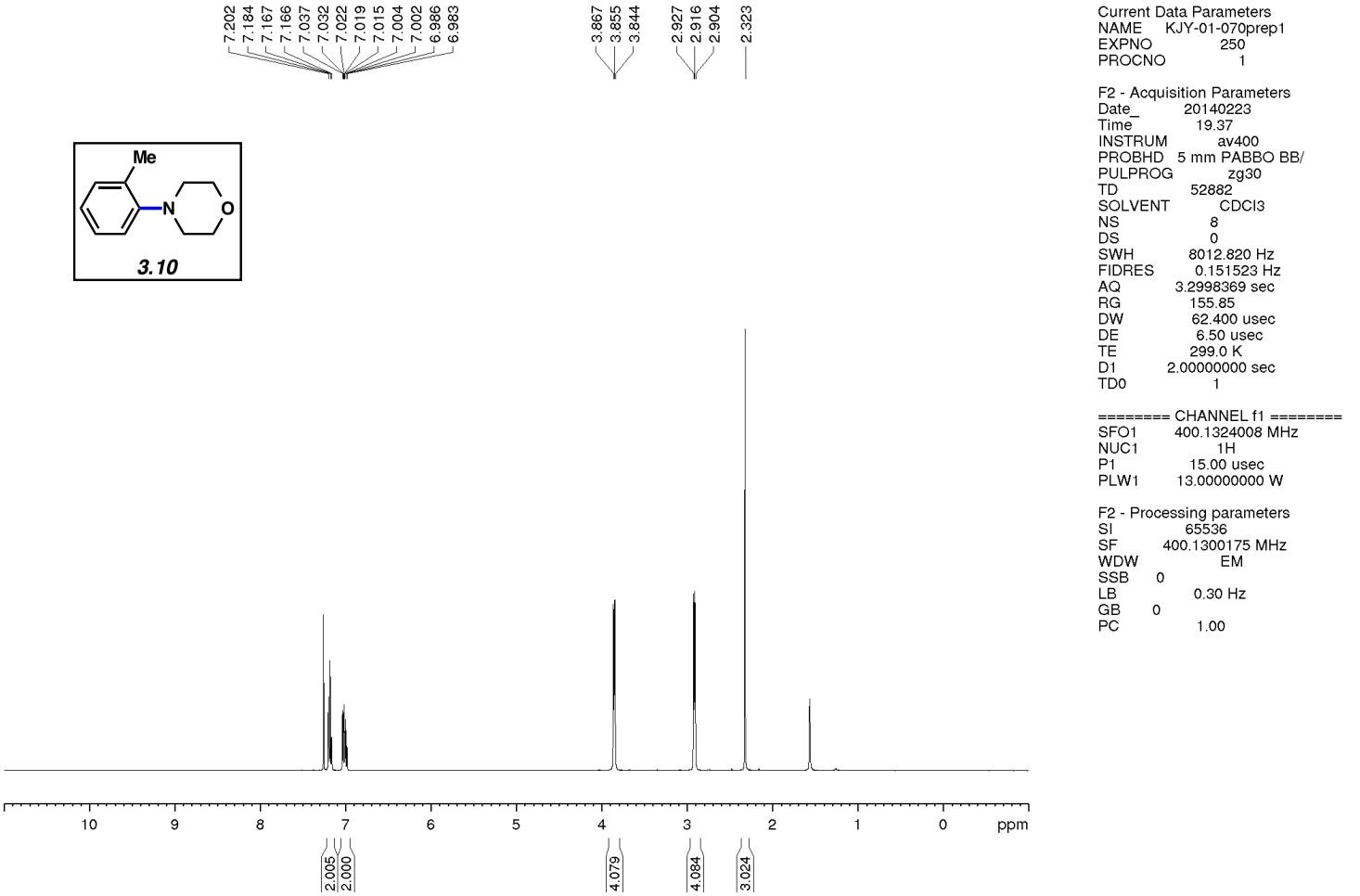

Figure A3.6 ^{1}H NMR (400 MHz, $CDCl_3$) of compound **3.10**.

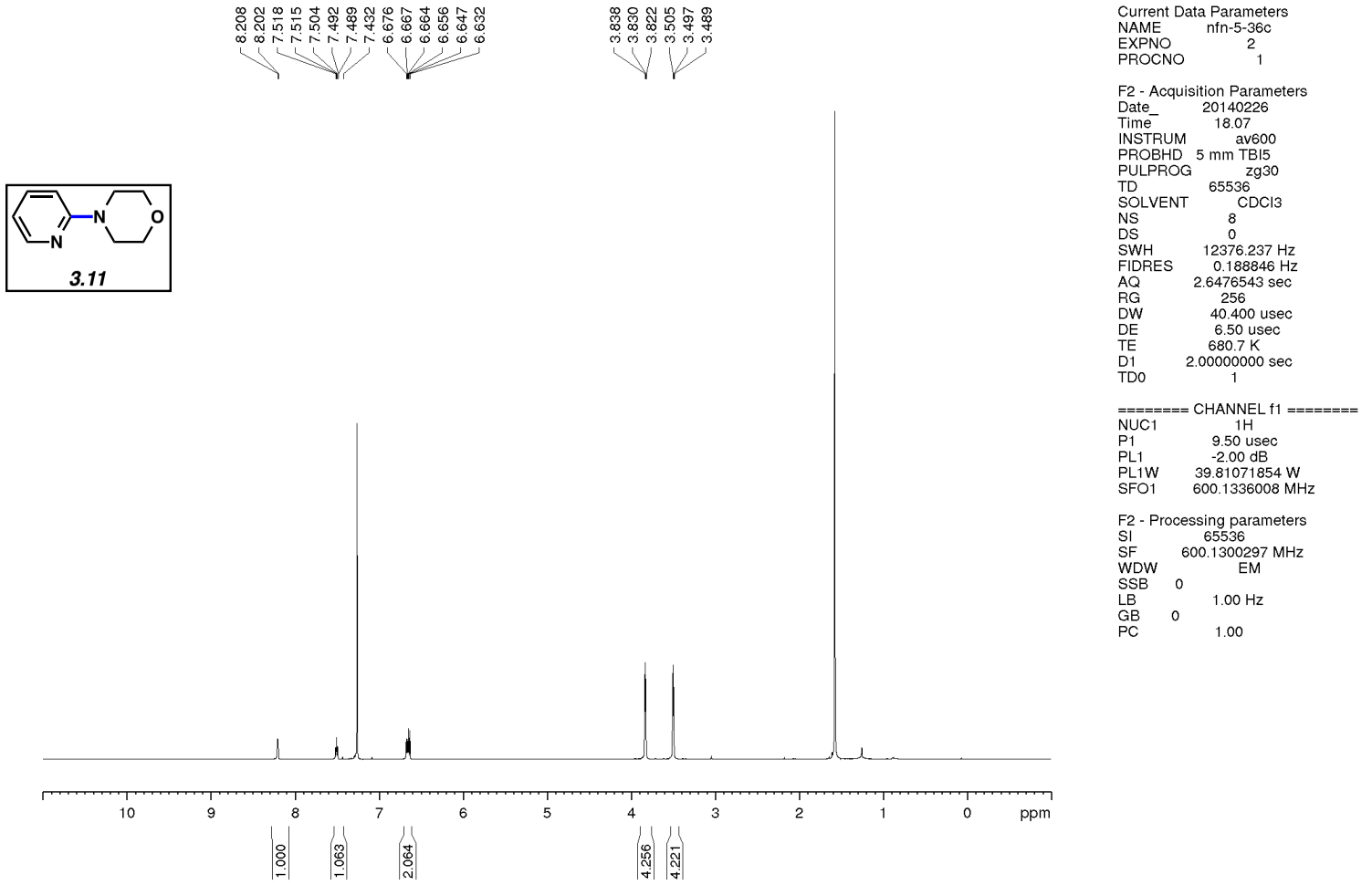

Figure A3.7 ^{1}H NMR (600 MHz, $CDCl_3$) of compound **3.11**.

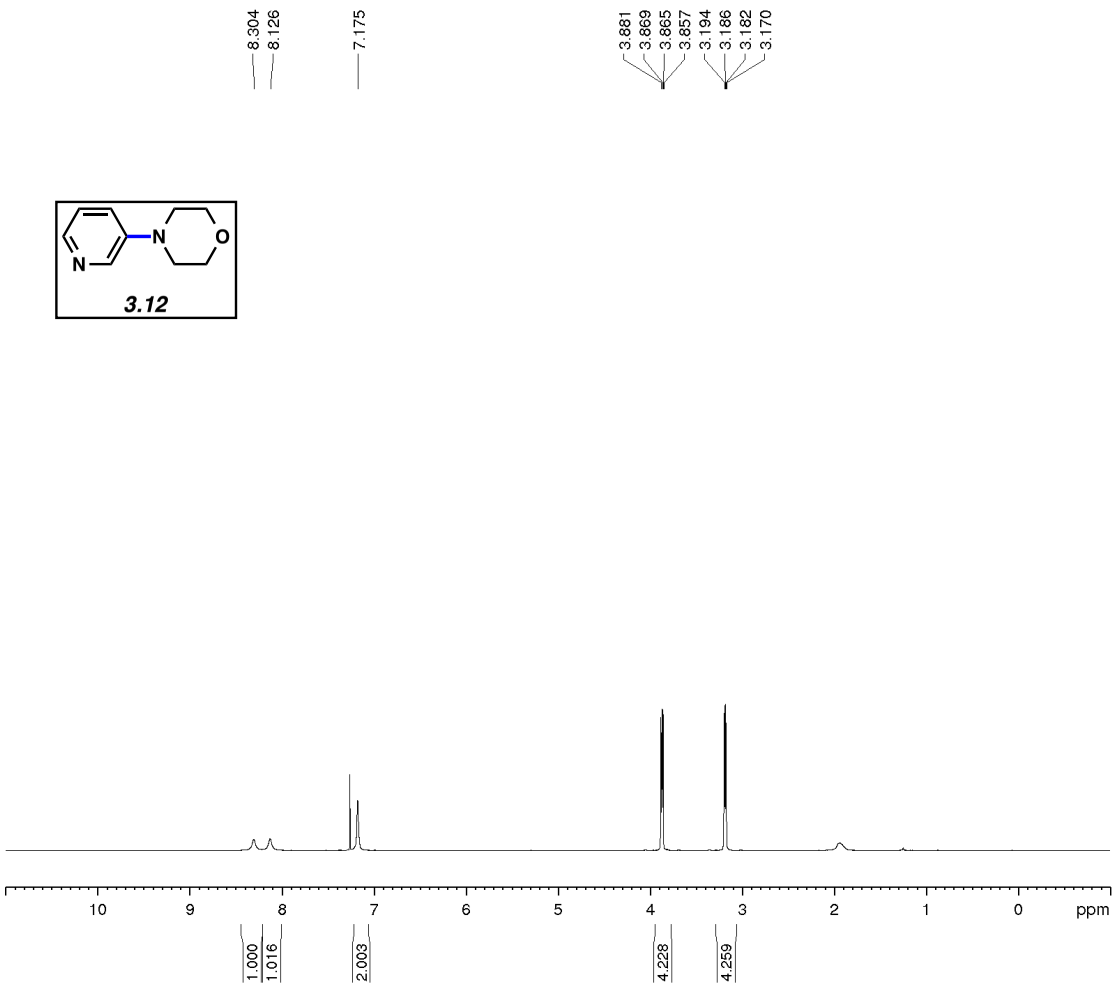

Current Data Parameters
NAME KJY-01-100prep
EXPNO 400
PROCNO 1

F2 - Acquisition Parameters
Date_ 20140304
Time 21.01
INSTRUM av400
PROBHD 5 mm PABBO BB/
PULPROG zg30
TD 52882
SOLVENT CDCl3
NS 8
DS 0
SWH 8012.820 Hz
FIDRES 0.151523 Hz
AQ 3.2998369 sec
RG 155.85
DW 62.400 usec
DE 6.50 usec
TE 299.0 K
D1 2.00000000 sec
TD0 1

======== CHANNEL f1 ========
SFO1 400.1324008 MHz
NUC1 1H
P1 15.00 usec
PLW1 13.00000000 W

F2 - Processing parameters
SI 65536
SF 400.1300174 MHz
WDW EM
SSB 0
LB 0.30 Hz
GB 0
PC 1.00

Figure A3.8 ^{1}H NMR (400 MHz, $CDCl_3$) of compound **3.12**.

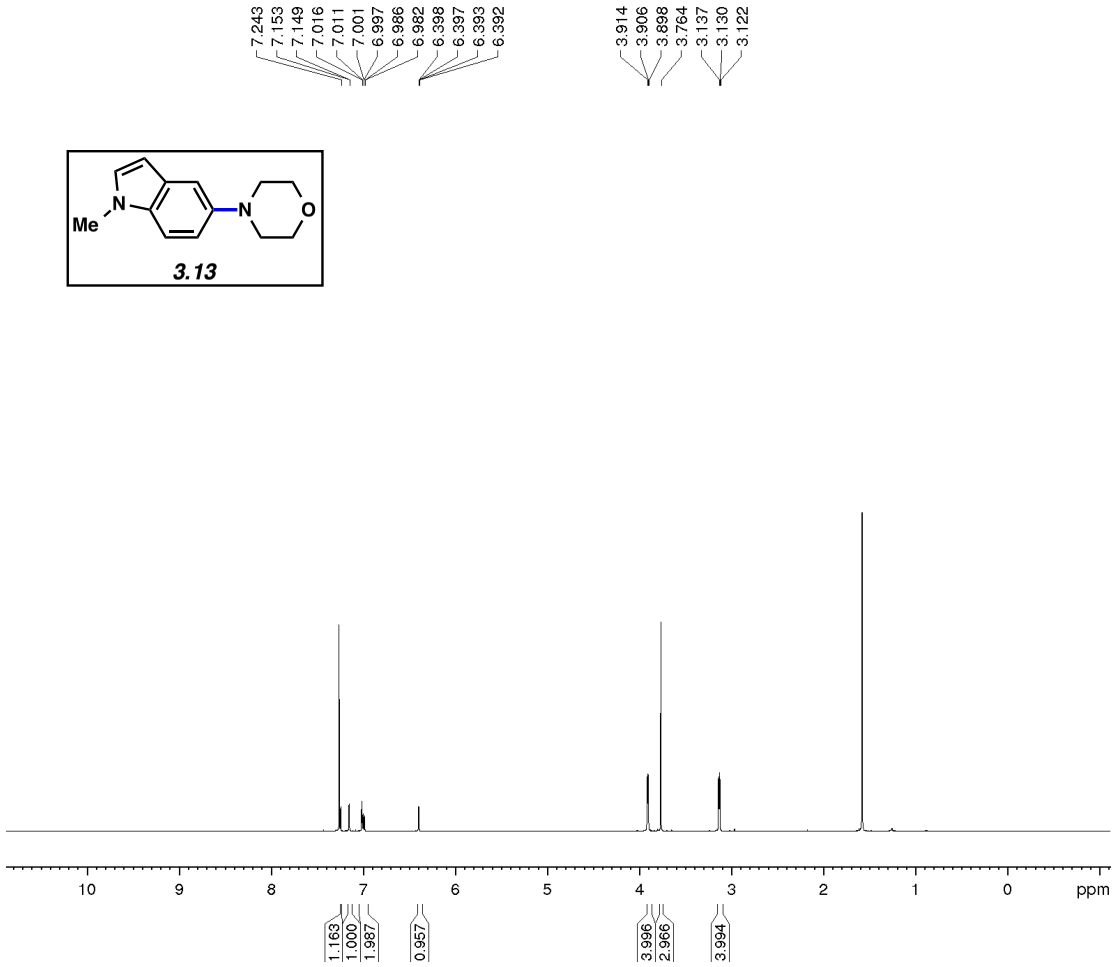

Current Data Parameters
NAME nfn-5-37c
EXPNO 2
PROCNO 1

F2 - Acquisition Parameters
Date_ 20140226
Time 17.44
INSTRUM av600
PROBHD 5 mm TBI5
PULPROG zg30
TD 65536
SOLVENT CDCl3
NS 8
DS 0
SWH 12376.237 Hz
FIDRES 0.188846 Hz
AQ 2.6476543 sec
RG 256
DW 40.400 usec
DE 6.50 usec
TE 680.7 K
D1 2.00000000 sec
TD0 1

======== CHANNEL f1 ========
NUC1 1H
P1 9.50 usec
PL1 -2.00 dB
PL1W 39.81071854 W
SFO1 600.1336008 MHz

F2 - Processing parameters
SI 65536
SF 600.1300297 MHz
WDW EM
SSB 0
LB 0.30 Hz
GB 0
PC 1.00

Figure A3.9 ^{1}H NMR (600 MHz, $CDCl_3$) of compound **3.13**.

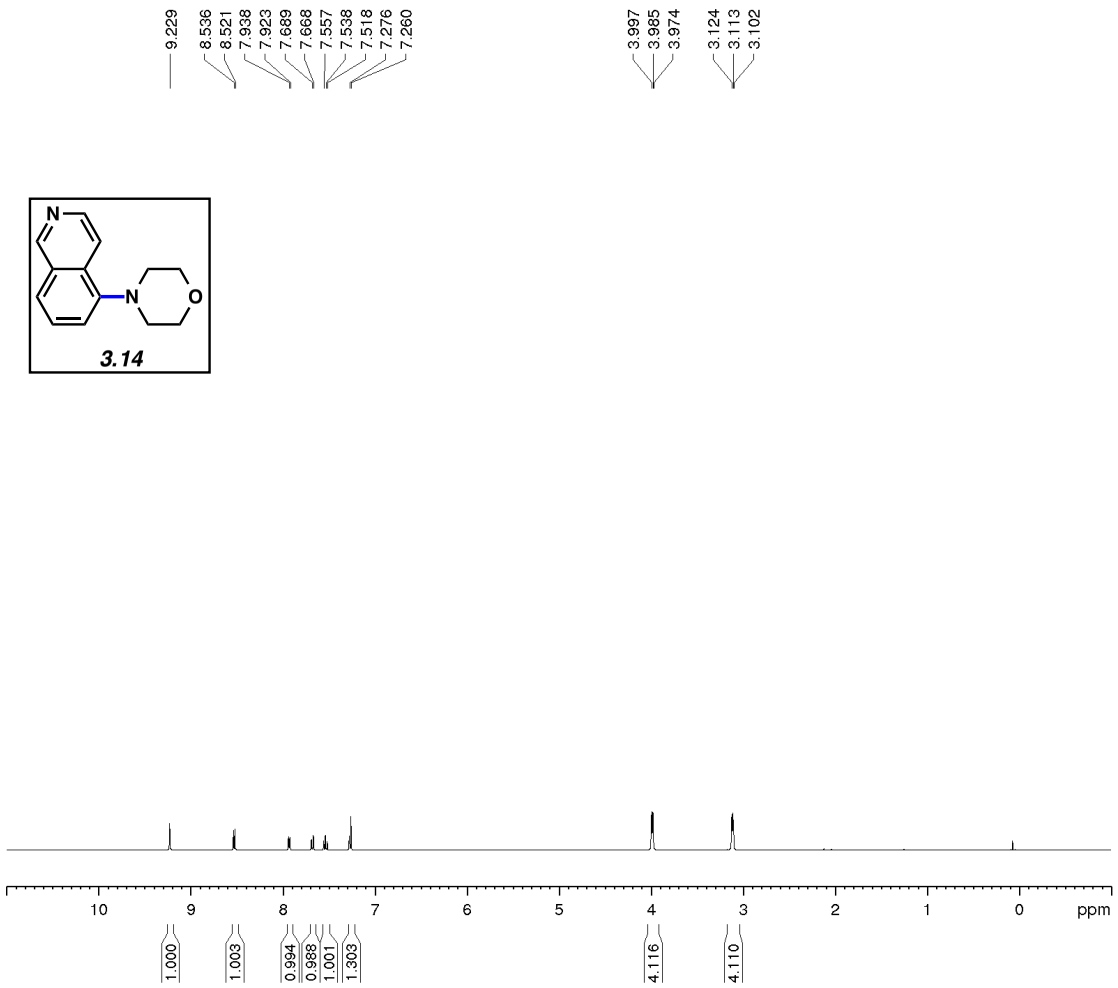

Figure A3.10 ^{1}H NMR (400 MHz, $CDCl_3$) of compound **3.14**.

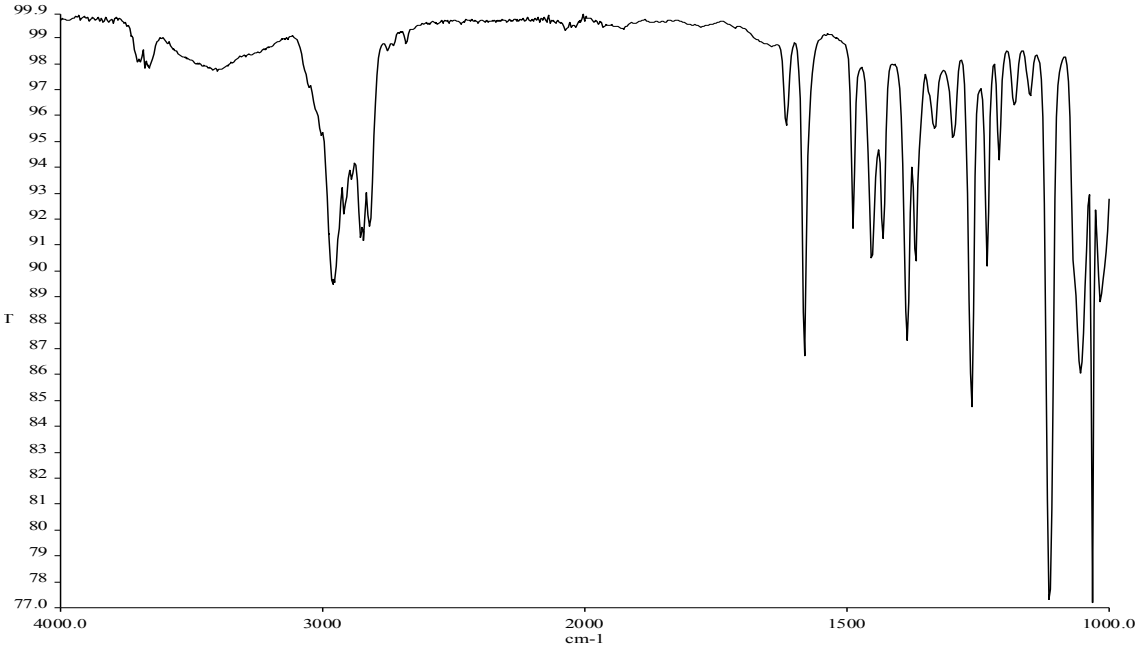

Figure A3.11 Infrared spectrum of compound **3**.**14**.

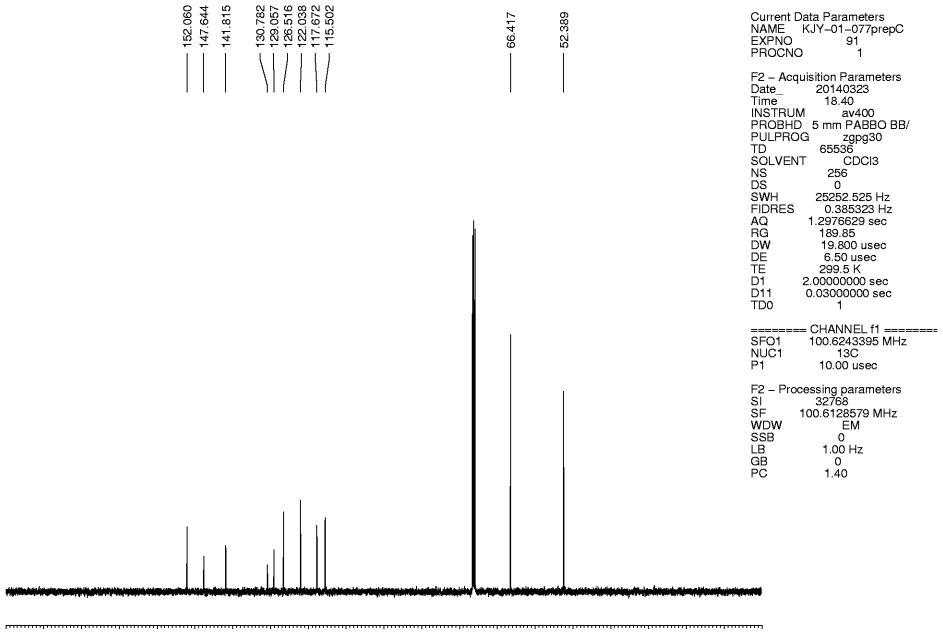

Figure A3.12 ^{13}C NMR (125 MHz, $CDCl_3$) of compound **3.14**.

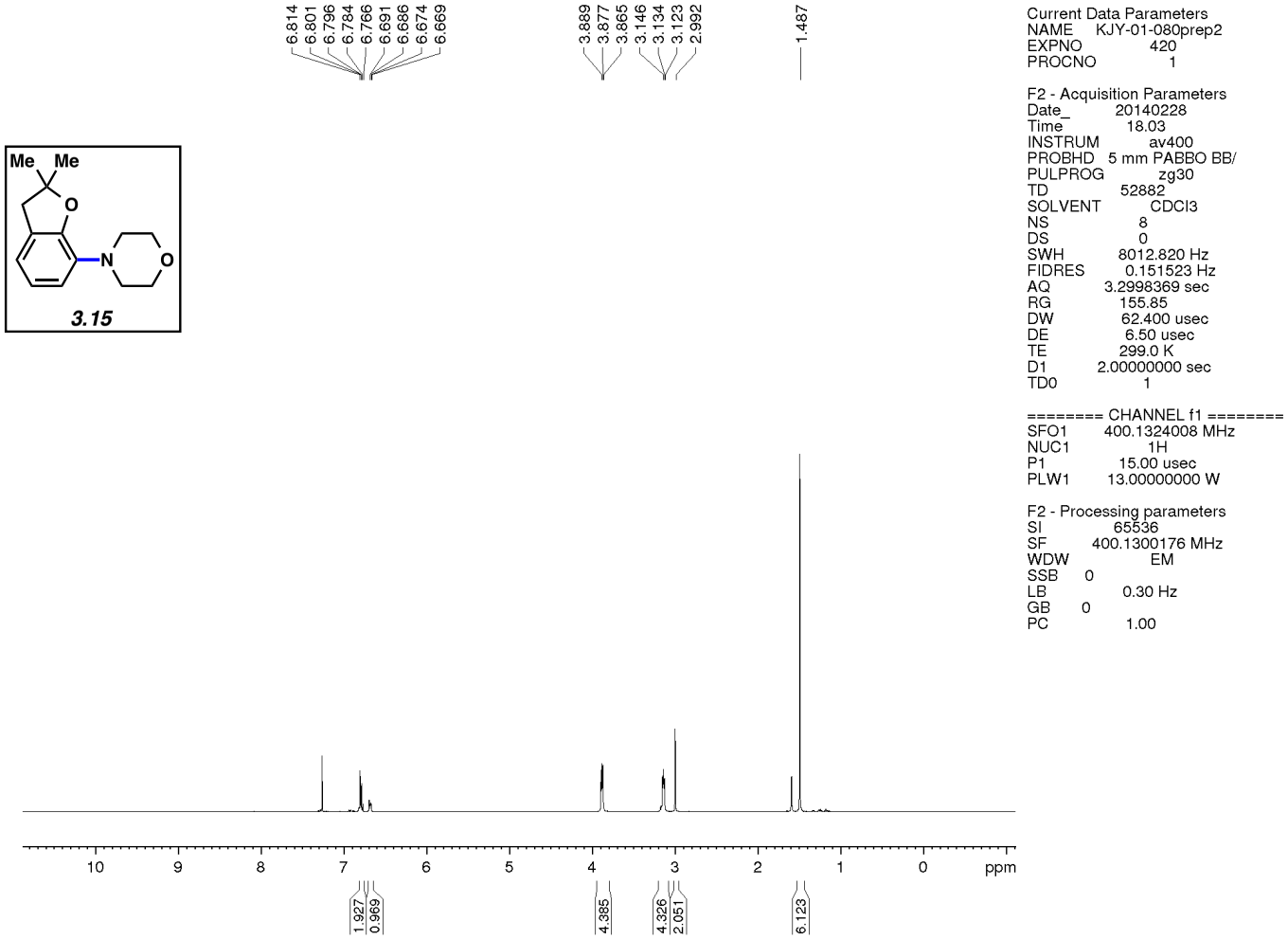

Figure A3.13 ^{1}H NMR (400 MHz, $CDCl_3$) of compound **3.15**.

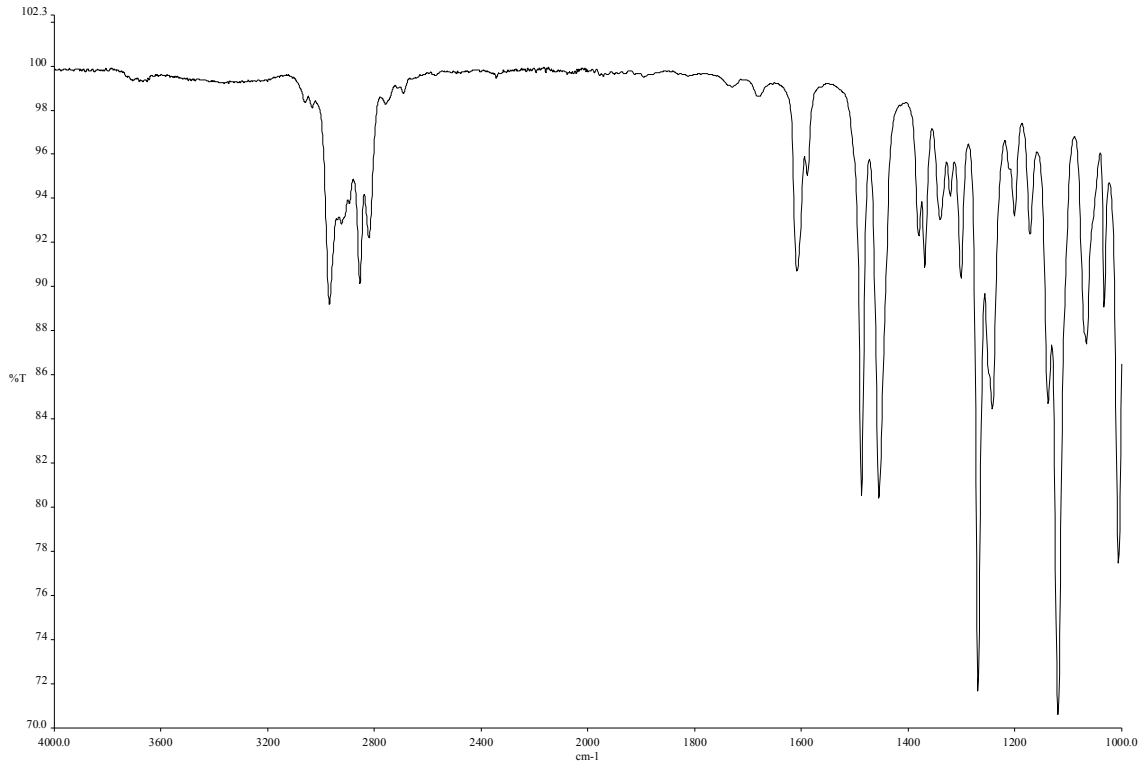

Figure A3.14 Infrared spectrum of compound **3.15**.

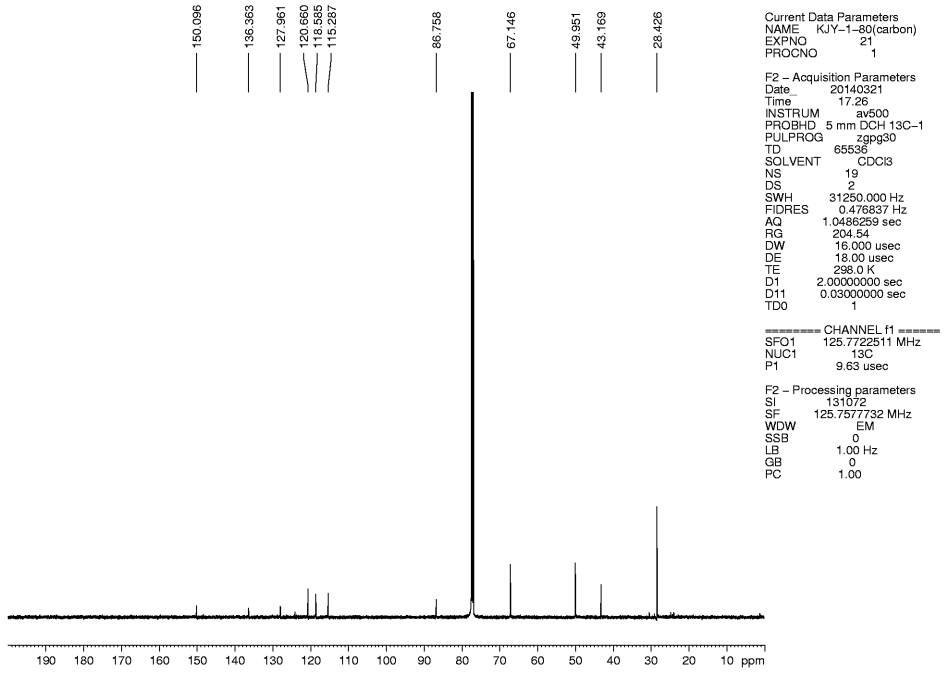

Figure A3.15 ^{13}C NMR (125 MHz, $CDCl_3$) of compound **3.15**.

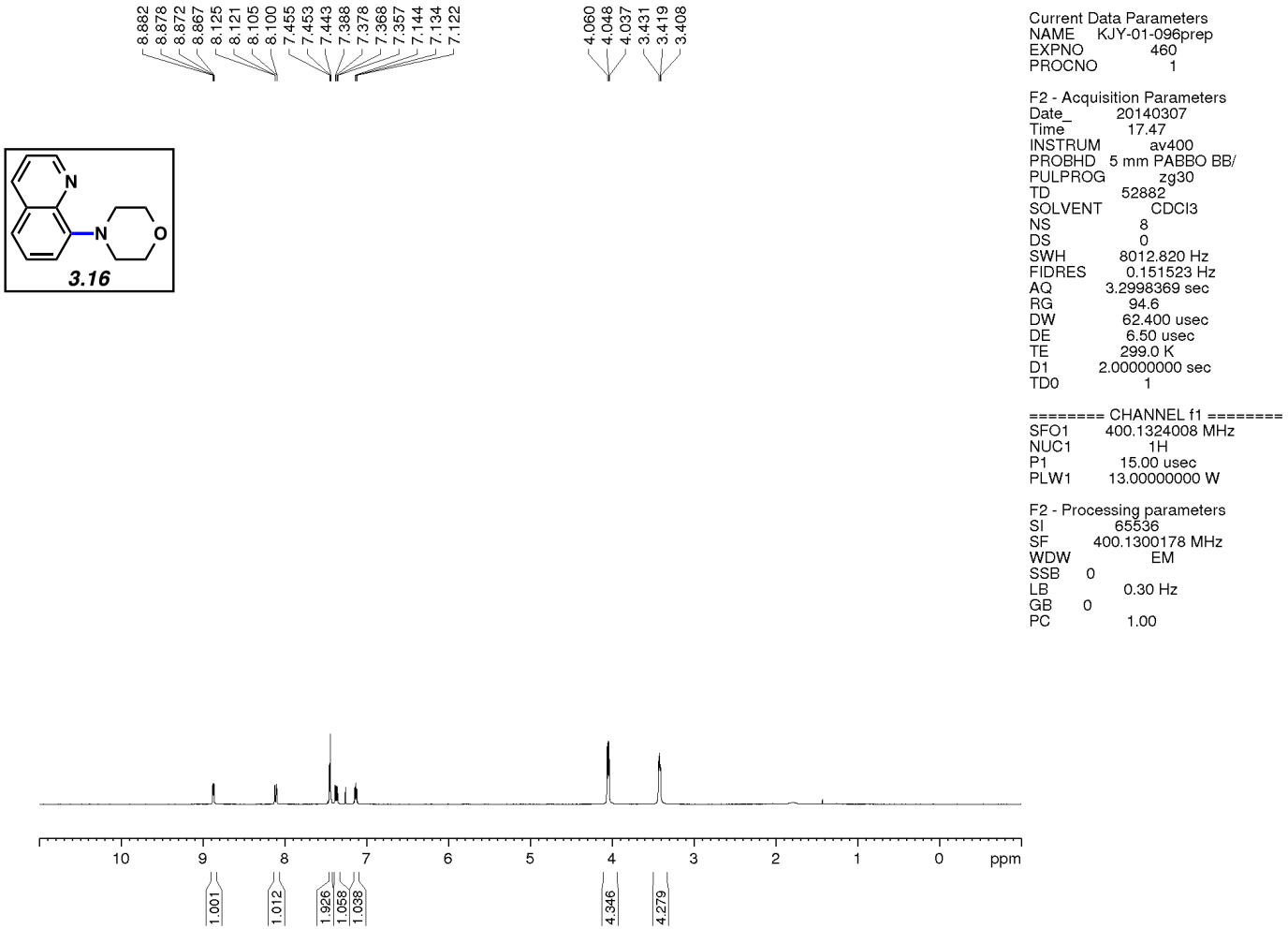

Figure A3.16 ^{1}H NMR (400 MHz, $CDCl_3$) of compound **3.16**.

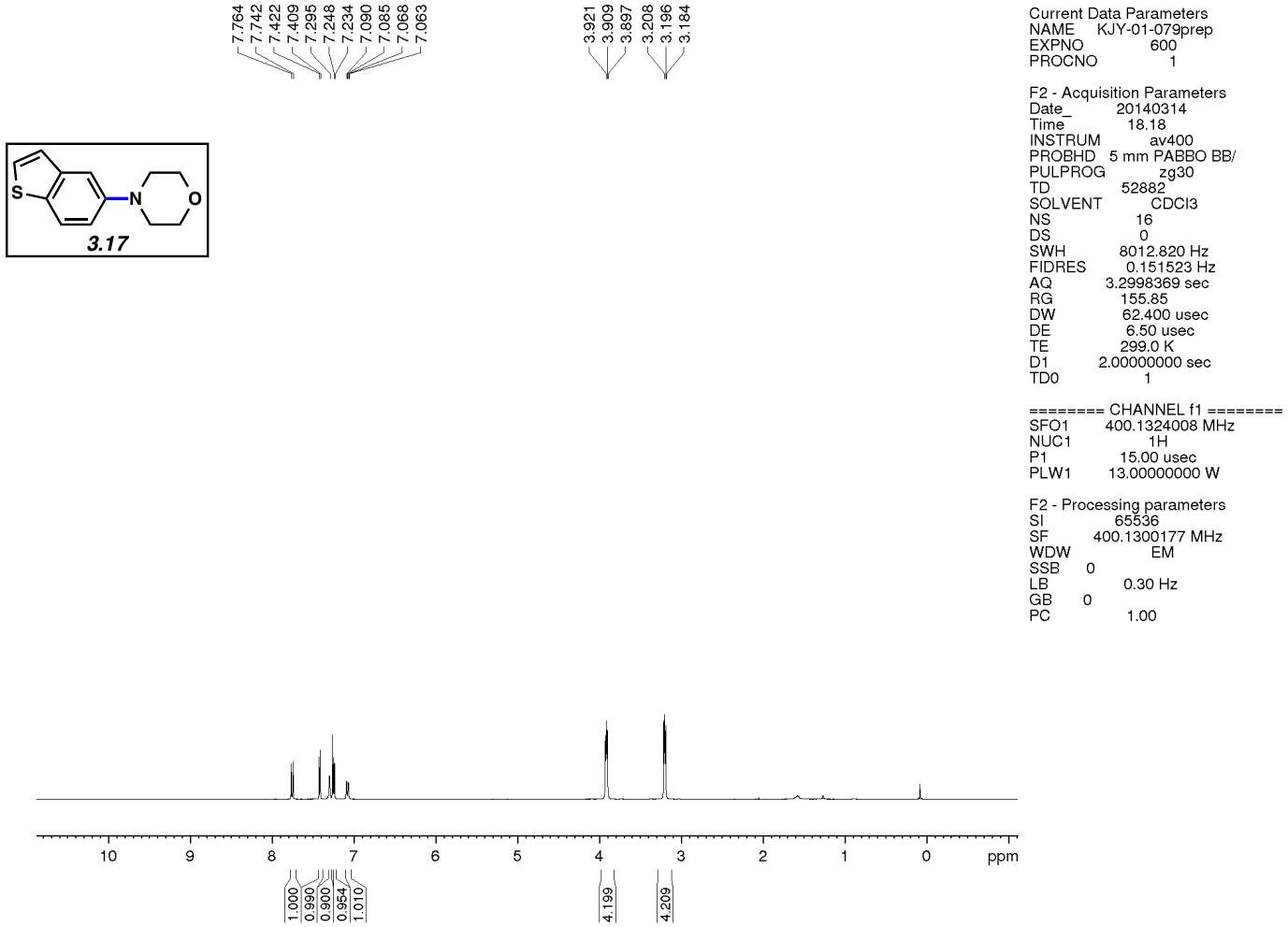

Figure A3.17 ^{1}H NMR (400 MHz, $CDCl_3$) of compound **3.17**.

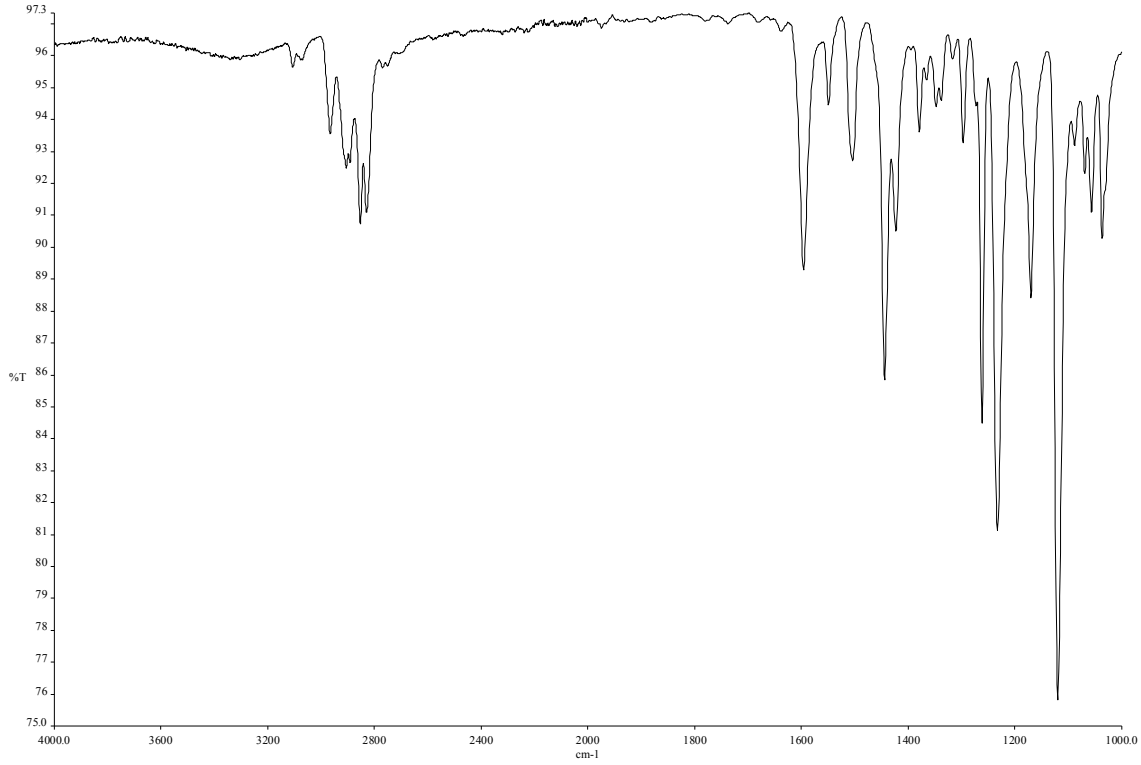

Figure A3.18 Infrared spectrum of compound **3.17**.

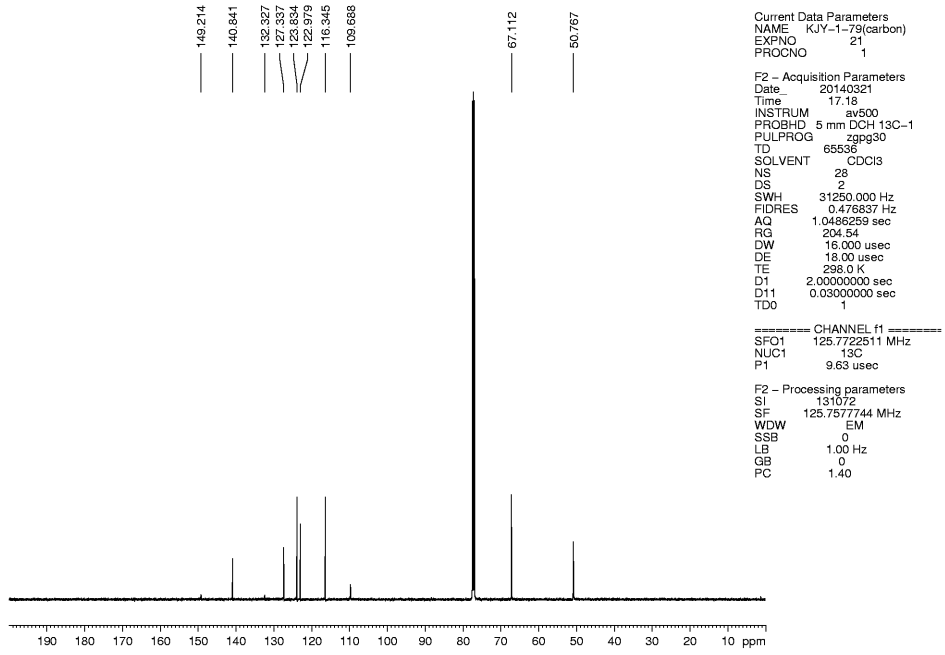

Figure A3.19 ^{13}C NMR (125 MHz, $CDCl_3$) of compound **3.17**.

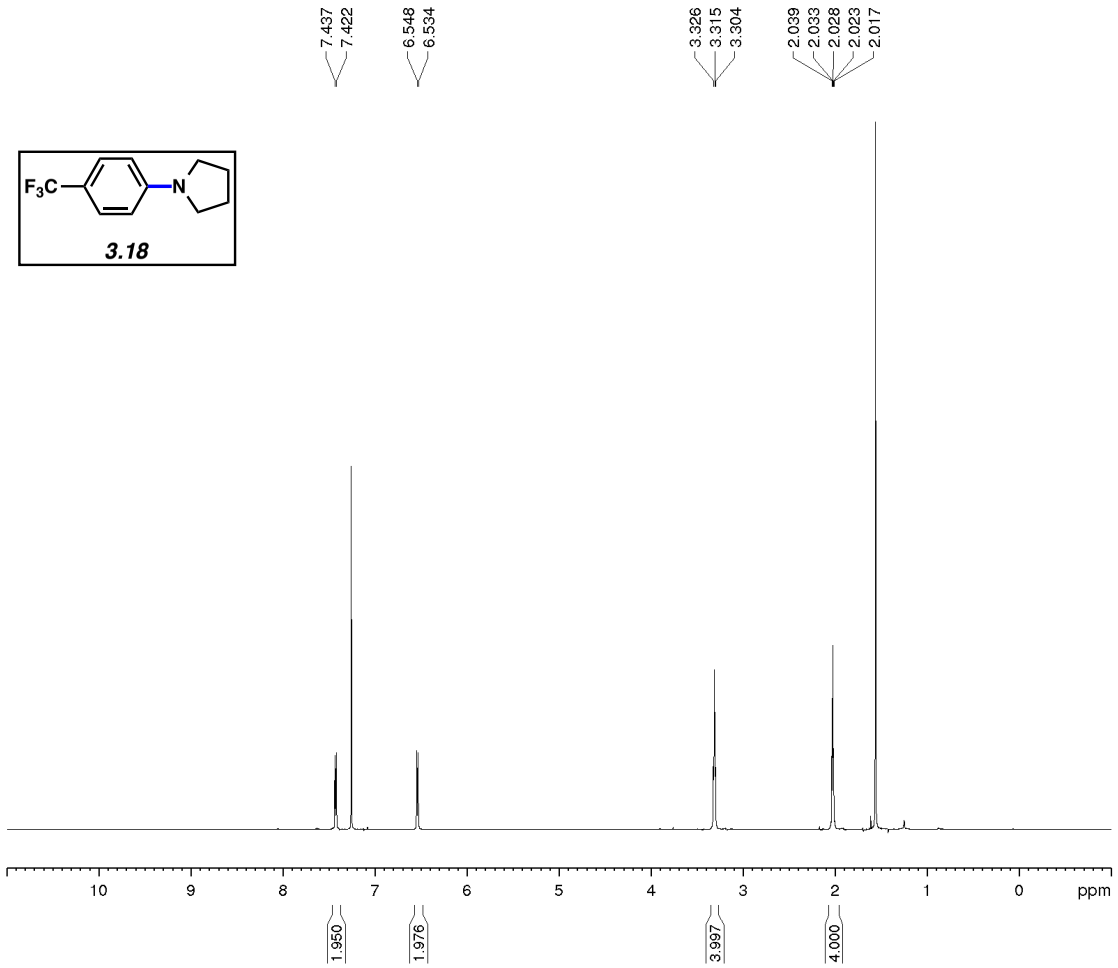

Current Data Parameters
NAME nfn-5-41c
EXPNO 2
PROCNO 1

F2 - Acquisition Parameters
Date_ 20140226
Time 17.59
INSTRUM av600
PROBHD 5 mm TBI5
PULPROG zg30
TD 65536
SOLVENT CDCl3
NS 8
DS 0
SWH 12376.237 Hz
FIDRES 0.188846 Hz
AQ 2.6476543 sec
RG 256
DW 40.400 usec
DE 6.50 usec
TE 680.7 K
D1 2.00000000 sec
TD0 1

======== CHANNEL f1 ========
NUC1 1H
P1 9.50 usec
PL1 -2.00 dB
PL1W 39.81071854 W
SFO1 600.1336008 MHz

F2 - Processing parameters
SI 65536
SF 600.1300297 MHz
WDW EM
SSB 0
LB 1.00 Hz
GB 0
PC 1.00

Figure A3.20 ^{1}H NMR (600 MHz, $CDCl_3$) of compound **3.18**.

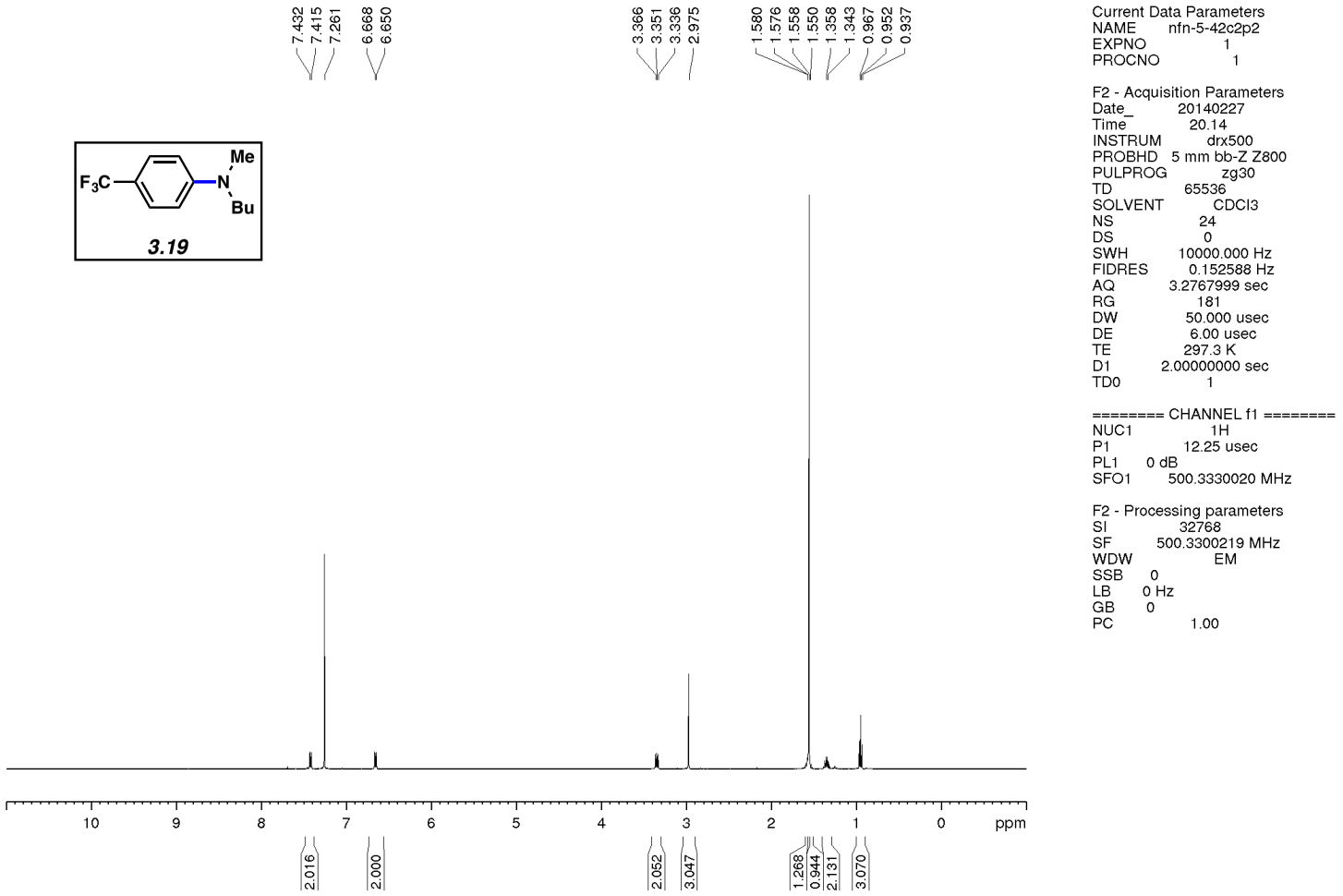

Figure A3.21 ^{1}H NMR (500 MHz, $CDCl_3$) of compound **3.19**.

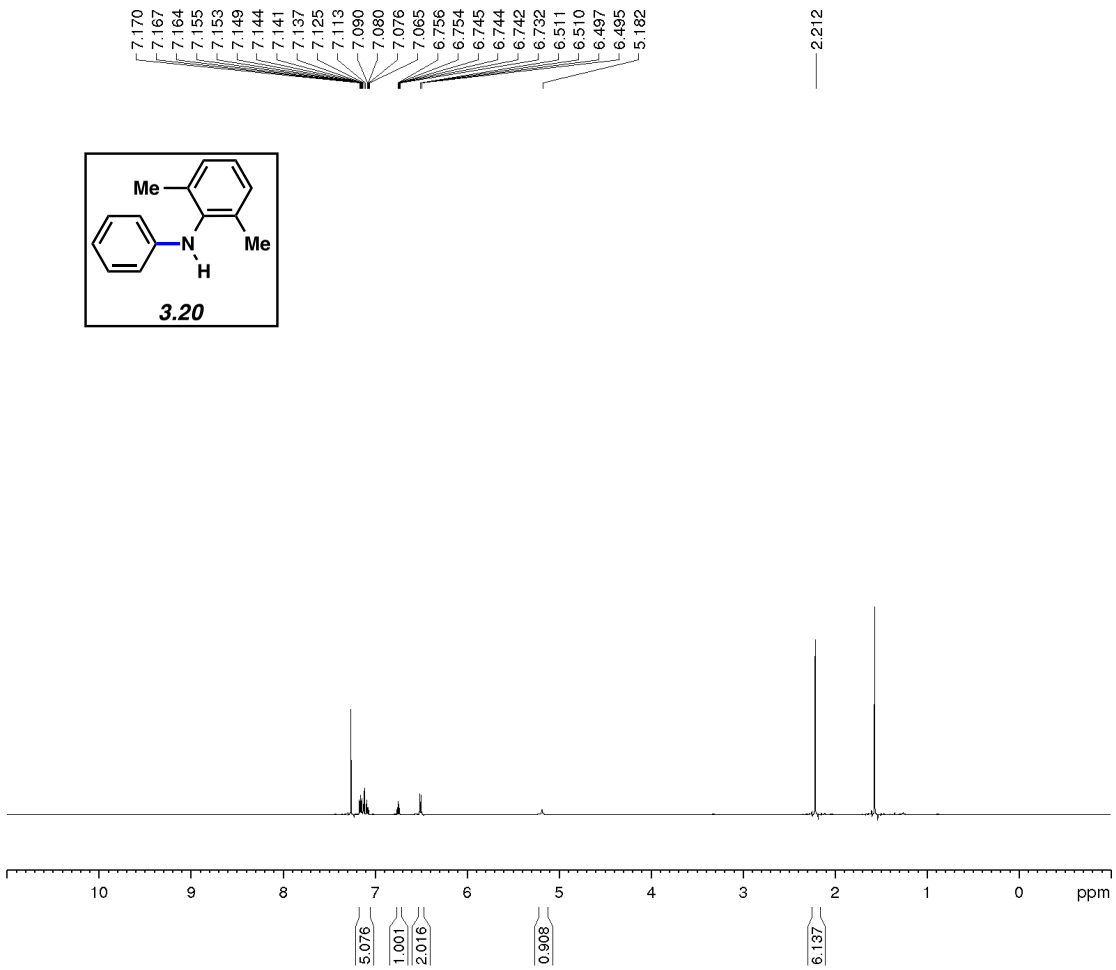

Current Data Parameters
NAME nfn-5-38c
EXPNO 2
PROCNO 1

F2 - Acquisition Parameters
Date_ 20140226
Time 17.37
INSTRUM av600
PROBHD 5 mm TBI5
PULPROG zg30
TD 65536
SOLVENT CDCl3
NS 8
DS 0
SWH 12376.237 Hz
FIDRES 0.188846 Hz
AQ 2.6476543 sec
RG 256
DW 40.400 usec
DE 6.50 usec
TE 680.9 K
D1 2.00000000 sec
TD0 1

======== CHANNEL f1 ========
NUC1 1H
P1 9.50 usec
PL1 -2.00 dB
PL1W 39.81071854 W
SFO1 600.1336008 MHz

F2 - Processing parameters
SI 65536
SF 600.1300297 MHz
WDW EM
SSB 0
LB 0.30 Hz
GB 0
PC 1.00

Figure A3.22 ^{1}H NMR (600 MHz, $CDCl_3$) of compound **3.20**.

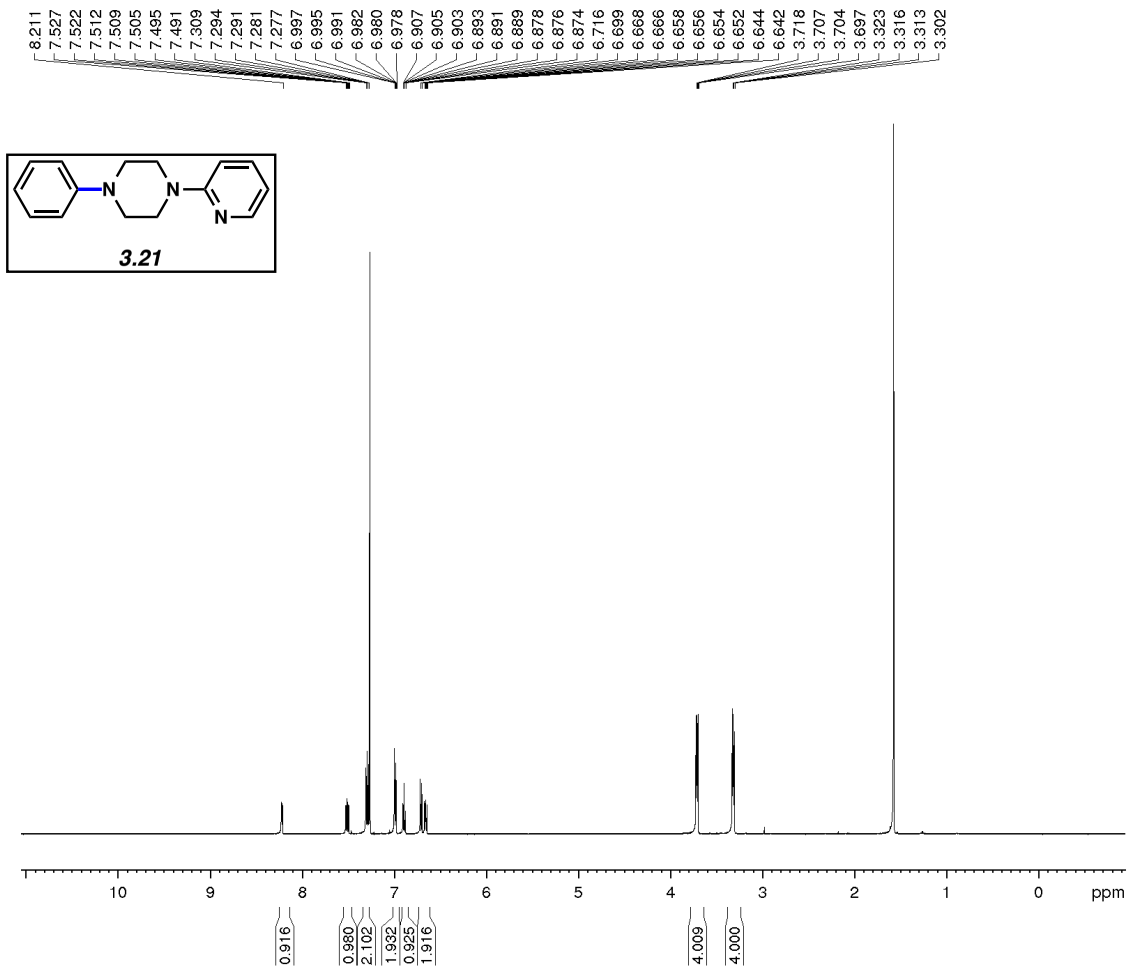

Current Data Parameters
NAME nfn-5-47a
EXPNO 1
PROCNO 1

F2 - Acquisition Parameters
Date_ 20140226
Time 22.31
INSTRUM drx500
PROBHD 5 mm bb-Z Z800
PULPROG zg30
TD 65536
SOLVENT CDCl3
NS 31
DS 0
SWH 10000.000 Hz
FIDRES 0.152588 Hz
AQ 3.2767999 sec
RG 181
DW 50.000 usec
DE 6.00 usec
TE 298.0 K
D1 2.00000000 sec
TD0 1

======== CHANNEL f1 ========
NUC1 1H
P1 12.25 usec
PL1 0 dB
SFO1 500.3330020 MHz

F2 - Processing parameters
SI 32768
SF 500.3300219 MHz
WDW EM
SSB 0
LB 0 Hz
GB 0
PC 1.00

Figure A3.23 ^{1}H NMR (500 MHz, $CDCl_3$) of compound **3.21**.

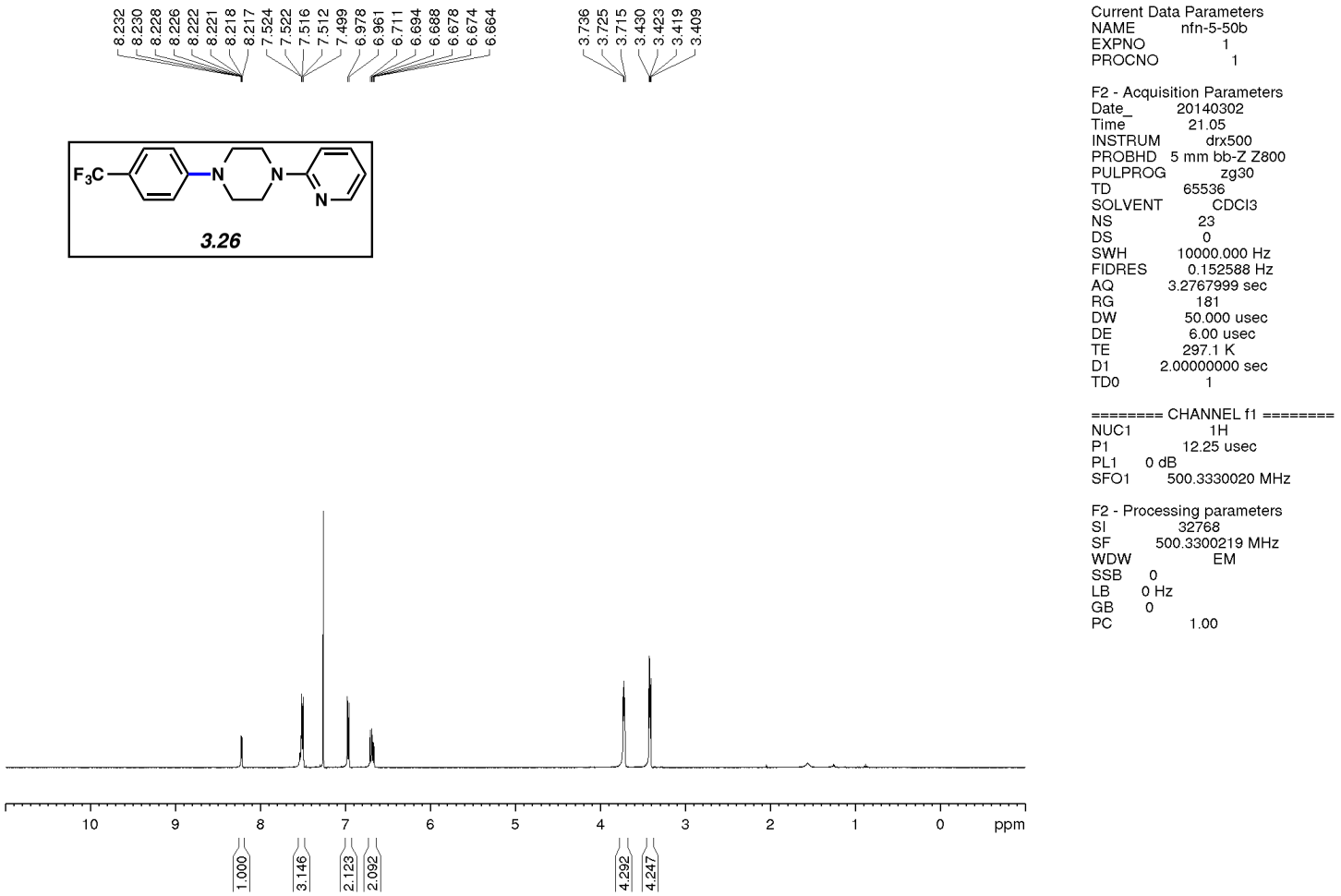

Current Data Parameters
NAME nfn-5-50b
EXPNO 1
PROCNO 1

F2 - Acquisition Parameters
Date_ 20140302
Time 21.05
INSTRUM drx500
PROBHD 5 mm bb-Z Z800
PULPROG zg30
TD 65536
SOLVENT CDCl3
NS 23
DS 0
SWH 10000.000 Hz
FIDRES 0.152588 Hz
AQ 3.2767999 sec
RG 181
DW 50.000 usec
DE 6.00 usec
TE 297.1 K
D1 2.00000000 sec
TD0 1

======== CHANNEL f1 ========
NUC1 1H
P1 12.25 usec
PL1 0 dB
SFO1 500.3330020 MHz

F2 - Processing parameters
SI 32768
SF 500.3300219 MHz
WDW EM
SSB 0
LB 0 Hz
GB 0
PC 1.00

Figure A3.24 ^{1}H NMR (500 MHz, $CDCl_3$) of compound **3.26**.

3.7. Notes and References

(1) (*a*) Hassan, J.; Sévignon, M.; Gozzi, C.; Schulz, E.; Lemaire, M. *Chem. Rev*. **2002**, *102*, 1359–1470. (*b*) Muci, A. R.; Buchwald, S. L. In *Topics in Current Chemistry*; Miyaura, N., Ed.; Springer Verlag: New York, 2002; Vol. 219, pp 131–209. (*c*) Jiang, L.; Buchwald, S. L. In *Metal-Catalyzed Cross-Coupling Reactions*, 2nd ed.; Meijere, A., Diederich, F., Eds.; Wiley-VCH: Weinheim, 2004; pp 699–760. (*d*) Corbet, J. P.; Mignani, G. *Chem. Rev*. **2006**, *106*, 2651–2710. (*e*) Negishi, E. *Bull. Chem. Soc. Jpn*. **2007**, *80*, 233–257. (*f*) Shen, H. C. In *Application of Transition Metal Catalysis in Drug Discovery and Development: An Industrial Perspective*; Crawley, M. L., Trost, B. M., Eds.; John Wiley & Sons, Inc.: Hoboken, NJ, 2012; pp 25–96.

(2) (*a*) Bolm, C.; Legros, J.; Le Paih, J.; Zani, L. *Chem. Rev*. **2004**, *104*, 6217–6254. (*b*) Enthaler, S.; Junge, K.; Beller, M. *Angew. Chem. Int. Ed*. **2008**, *47*, 3317–3321. (*c*) Bauer, E. B. *Curr. Org. Chem*. **2008**, *12*, 1341–1369. (*d*) Yu, D.-G.; Li, B.-J.; Shi, Z.-J. *Acc. Chem. Res*. **2010**, *43*, 1486–1495. (*e*) Rosen, B. M.; Quasdorf, K. W.; Wilson, D. A.; Zhang, N.; Resmerita, A.-M.; Garg, N. K.; Percec, V. *Chem. Rev*. **2011**, *111*, 1346–1416. (*f*) Li, B.-J.; Yu, D.-G.; Sun, C.-L.; Shi, Z.-J. *Chem. Eur. J*. **2011**, *17*, 1728–1759. (*g*) Mesganaw, T.; Garg, N. K. *Org. Process Res. Dev*. **2013**, *17*, 29–39. (*h*) Tasker, S. Z.; Standley, E. A.; Jamison, T. F. *Nature* **2014**, *509*, 299–309.

(3) (*a*) Anastas, P. T.; Warner, J. C. *Green Chemistry: Theory and Practice*; Oxford University Press: New York, 1998. (*b*) Anastas, P. T.; Kirchhoff, M. M. *Acc. Chem. Res*. **2002**, *35*, 686–694.

(4) (*a*) Ramgren, S. D.; Hie, L.; Ye, Y.; Garg, N. K. *Org. Lett*. **2013**, *15*, 3950–3953. (*b*) Hie, L.; Chang, J. J.; Garg, N. K. *J. Chem. Educ.* **2015**, *92*, 571–574.

(5) For reviews on Buchwald–Hartwig cross-couplings, see: (*a*) Wolfe, J. P.; Wagaw, S.; Marcoux, J.-F.; Buchwald, S. L. *Acc. Chem. Res*. **1998**, *31*, 805–818. (*b*) Hartwig, J. F. *Angew. Chem. Int. Ed*. **1998**, *37*, 2046–2067. (*c*) Anderson, K. W.; Tundel, R. E.; Ikawa, T.; Altman, R. A.; Buchwald, S. L. *Angew. Chem. Int. Ed*. **2006**, *45*, 6523–6527. (*d*) Kienle, M.; Dubbaka, S. R.; Brade, K.; Knochel, P. *Eur. J. Org. Chem*. **2007**, 4166–4176. (*e*) Surry, D. S.; Buchwald, S. L. *Angew. Chem. Int. Ed*. **2008**, *47*, 6338–6361. (*f*) Hartwig, J. F. *Acc. Chem. Res*. **2008**, *41*, 1534–1544; see also ref. 1b.

(6) For select recent examples of Ni-catalyzed aryl C–C bond couplings, see: (*a*) Guan, B.-T.; Wang, Y.; Li, B.-J.; Yu, D.; Shi, Z.-J. *J. Am. Chem. Soc*. **2008**, *130*, 14468–14470. (*b*) Quasdorf, K. W.; Tian, X.; Garg, N. K. *J. Am. Chem. Soc*. **2008**, *130*, 14422–14423. (*c*) Tobisu, M.; Shimasaki, T.; Chatani N. *Angew. Chem. Int. Ed*. **2008**, *47*, 4866–4869. (*d*) Quasdorf, K. W.; Riener, M.; Petrova, K. V.; Garg, N. K. *J. Am. Chem. Soc*. **2009**, *131*, 17748–17749. (*e*) Antoft-Finch, A.; Blackburn, T.; Snieckus, V. *J. Am. Chem. Soc*. **2009**, *131*, 17750–17752. (*f*) Xi, L.; Li, B.-J.; Wu, Z.-H.; Lu, X.-Y.; Guan, B.-T.; Wang, B.-Q.; Zhao, K.-Q.; Shi, Z.-J. *Org. Lett*. **2010**, *12*, 884–887. (*g*) Quasdorf, K. W.; Antoft-Finch, A.; Liu, P.; Silberstein, A. L.; Komaromi, A.; Blackburn, T.; Ramgren, S. D.; Houk, K. N.; Snieckus, V.; Garg, N. K. *J. Am. Chem. Soc*. **2011**, *133*, 6352–6363. (*h*) Zhang, N.; Hoffman, D. J.; Gutsche, N.; Gupta, J.; Percec, V. *J. Org. Chem*. **2012**, *77*, 5956–5964. (*i*) Ge, S.; Hartwig, J. F. *Angew. Chem. Int. Ed*. **2012**, *51*, 12837–12841; see also ref. 4.

(7) For select recent examples of Ni-catalyzed aryl C–N bond couplings, see: (*a*) Ogata, T.; Hartwig, J. F. *J. Am. Chem. Soc*. **2008**, *130*, 13848–13849. (*b*) Gao, C.-Y.; Yang, L.-M. *J. Org. Chem*. **2008**, *73*, 1624–1627. (*c*) Fors, B. P.; Watson, D. A.; Biscoe, M. R.; Buchwald, S. L. *J. Am. Chem. Soc*. **2008**, *130*, 13552–13554 (*d*) Tobisu, M.; Shimasaki, T.; Chatani, N. *Chem. Lett*. **2009**, *38*, 710–711. (*e*) Shimasaki, T.; Tobisu, M.; Chatani, N. *Angew. Chem. Int. Ed*. **2010**, *49*, 2929–2932. (*f*) Mesganaw, T.; Silberstein, A. L.; Ramgren, S. D.; Fine Nathel, N. F.; Hong, X.; Liu, P.; Garg, N. K. *Chem. Sci*. **2011**, *2*, 1766–1771. (*g*) Ramgren, S. D.; Silberstein, A. L.; Yang, Y.; Garg, N. K. *Angew. Chem. Int. Ed*. **2011**, *50*, 2171–2173. (*h*) Ackermann, L.; Sandmann, R.; Song, W. *Org. Lett*. **2011**, *13*, 1784–1786. (*i*) Huang, J.-H.; Yang L.-M. *Org. Lett*. **2011**, *13*, 3750–3753. (*j*) Hie, L.; Ramgren, S. D.; Mesganaw, T.; Garg, N. K. *Org. Lett*. **2012**, *14*, 4182–4185.

(8) For select seminal studies on aryl C–C and C–N bond coupling using Ni catalysis, see: (*a*) Sengupta, S.; Leite, M.; Raslan, D. S.; Quesnelle, C.; Snieckus, V. *J. Org. Chem*. **1992**, *57*, 4066–4068. (*b*) Wolfe, J. P.; Buchwald, S. L. *J. Am. Chem. Soc*. **1997**, *119*, 6054–6058. (*c*) Hamann, B. C.; Hartwig, J. F. *J. Am. Chem. Soc*. **1998**, *120*, 7369–7370. (*d*) Brenner, E.; Fort, Y. *Tetrahedron Lett*. **1998**, *39*, 5359–5362. (*e*) Wehn, P. M.; Du Bois, J. *Org. Lett*. **2005**, *7*, 4685–4688.

(9) The addition of Ph–B(pin) is believed to be instrumental in reducing the Ni(II) precatalyst to an active Ni(0) species.

(10) For nickel catalyzed amination methodologies that use Ni(II) precatalysts with Zn or hydrides as reducing agents, see: (*a*) Fan, X.-H.; Li, G.; Yang, L.-M. *J. Organomet. Chem*. **2011**, *696*, 2482–2484. (*b*) Gao, C.-Y.; Cao, X.; Yang, L.-M. *Org. Biomol. Chem*. **2009**, *7*,

3922–3925. (*c*) Manolikakes, G.; Gavryushin, A.; Knochel, P. *J. Org. Chem*. **2008**, *73*, 1429–1434. (*d*) Omar-Amrani, R.; Thomas, A.; Brenner, E.; Schneider, R.; Fort, Y. *Org. Lett*. **2003**, *5*, 2311–2314. (*e*) Desmarets, C.; Schneider, R.; Fort, Y. *J. Org. Chem*. **2002**, *67*, 3029–3036. (*f*) Gradel, B.; Brenner, E.; Schneider, R.; Fort, Y. *Tetrahedron Lett*. **2001**, *42*, 5689–5692.

(11) Solvents were selected from the ACS Green Chemistry Institute Roundtable Solvent Selection Guide. http://www.acs.org/content/dam/acsorg/greenchemistry/industriainnovation/roundtable/acs-gci-pr-solvent-selection-guide.pdf.

(12) For solvent selection guides in medicinal chemistry, see: (*a*) Alfonsi, K.; Colberg, J.; Dunn, P. J.; Fevig, T.; Jennings, S.; Johnson, T. A.; Kleine, H. P.; Knight, C.; Nagy, M. A.; Perry, D. A.; Stefaniak, M. *Green Chem*. **2008**, *10*, 31–36. (*b*) Henderson, R. K.; Jiménez-González, C.; Constable, D. J. C.; Alston, S. R.; Inglis, G. G. A.; Fisher, G.; Sherwood, J.; Binks, S. P.; Curzons, A. D. *Green Chem*. **2011**, *13*, 854– 862.

(13) For a discussion on CPME, see: (*a*) Watanabe, K.; Yamagiwa, N.; Torisawa, Y. *Org. Process Res. Dev*. **2007**, *11*, 251–258. (*b*) Antonucci, V.; Coleman, J.; Ferry, J. B.; Johnson, N.; Mathe, M.; Scott, J. P.; Xu, J. *Org. Process Res. Dev*. **2011**, *15*, 939–941.

(14) *Tert*-Amyl alcohol was also considered an especially promising solvent for the amination reaction; however, it was found to be less generally useful compared to 2-Me-THF in attempts to couple various other substrates.

(15) For discussion on 2-Me-THF, see: (*a*) Aycock, D. F. *Org. Process Res. Dev*. **2007**, *11*, 156–159. (*b*) Pace, V.; Hoyos, P.; Castoldi, L.; Domínguez de María, P.; Alcántara, A. R. *ChemSusChem* **2012**, *5*, 1369–1379; see also ref. 13b.

(16) Aryl chlorides are attractive substrates as they are often available commercially or are easily synthesized. Additionally, aryl chlorides are often robust enough to be carried through multiple synthetic operations.

(17) Aryl sulfamates bear many notable features. They are easily synthesized from their corresponding phenols, which are often commercially available, and are generally stable to acidic and basic reaction conditions. Moreover, aryl sulfamates may be used to direct arene functionalization through electrophilic aromatic substitution or *ortho*-lithiation processes. For a discussion of these features, see: (*a*) Snieckus, V. *Chem. Rev*. **1990**, *90*, 879–933. (*b*) Hartung, C. G.; Snieckus V. In *Modern Arene Chemistry*; Astruc, D., Ed.; Wiley-VCH: New York, 2002; pp. 330–367. (*c*) Macklin, T. K., Snieckus, V. *Org. Lett*. **2005**, *7*, 2519–2522. (*d*) Snieckus, V.; Macklin, T. In *Handbook of C-H Transformations*; Dyker G., Ed.; Wiley-VCH: New York, 2005; Vol. 1, pp 106–118; see also ref. 6d.

(18) Piel, I.; Steinmetz, M.; Hirano, K.; Frohlich, R.; Grimme, S.; Glorius, F. *Angew. Chem. Int. Ed.* **2011**, *50*, 4983–4987.

(19) Civicos, J. F.; Alonso, D. A.; Najera, C. *Adv. Synth. Catal.* **2012**, *354*, 2771–2776.

(20) Quasdorf, K. W.; Tian, X.; Garg, N. K. *J. Am. Chem. Soc.* **2008**, *130*, 14422–14423.

(21) (*a*) Quasdorf, K. W.; Riener, M.; Petrova, K. V.; Garg, N. K. *J. Am. Chem. Soc.* **2009**, *131*, 17748–17749. (*b*) Antoft-Finch, A.; Blackburn, T.; Snieckus, V. *J. Am. Chem. Soc.* **2009**, *131*, 17750–17752.

(22) (*a*) King, J. F.; Lee. T. M. *Can. J. Chem.* **1981**, *59*, 356–361. (*b*) Ramgren, S. D.; Silberstein, A. L.; Yang, Y.; Garg, N. K. *Angew. Chem. Int. Ed.* **2011**, *50*, 2171–2173. (*c*) Leowanawat, P.; Zhang, N.; Resmerita, A.-M.; Rosen, B. M.; Percec, V. *J. Org. Chem.* **2011**, *76*, 9946–9955. **(***d*) Quasdorf, K. W.; Antoft-Finch, A.; Liu, P.; Silberstein, A. L.; Komaromi, A.; Blackburn, T.; Ramgren, S. D.; Houk, K. N.; Snieckus, V.; Garg, N. K. *J. Am. Chem. Soc.* **2011**, *133*, 6352–6363. (*e*) Agrawal, T.; Cook, S. P. *Org. Lett.* **2013**, *15*, 96–99. (*f*) Molander, G. A.; Shin, I. *Org. Lett.* **2013**, *15*, 2534–2537.

(23) Desmarets, C.; Champagne, B.; Walcarius, A.; Bellouard, C.; Omar-Amrani, R.; Ahajji, A.; Fort, Y.; Schneider, R. *J. Org. Chem*. **2006**, *71*, 1351–1361.

(24) Barker, T. J.; Jarvo, E. R. *J. Am. Chem. Soc.* **2009**, *131*, 15598–15599.

(25) Wolfe, J. P.; Buchwald, S. L. *J. Org. Chem.* **1996**, *61*, 1133–1135.

(26) Guo, D.; Huang, H.; Xu, J.; Jiang, H.; Liu, H. *Org. Lett.* **2008**, *10*, 4513–4516.

(27) Fasani, E.; Tilocca, F.; Protti, S.; Merli, D.; Albini, A. *Org. Biomol. Chem.* **2008**, *6*, 4634–4642.

(28) Wagaw, S.; Buchwald, S. L. *J. Org. Chem.* **1996**, *61*, 7240–7241.

(29) Mesganaw, T.; Silberstein, A. L.; Ramgren, S. D.; Fine Nathel, N. F.; Hong, X.; Liu, P.; Garg, N. K. *Chem. Sci.* **2011**, *2*, 1766–1771.

(30) Tobisu, M.; Yasutome, A.; Yamakawa, K.; Shimasaki, T.; Chatani, N. *Tetrahedron* **2012**, *68*, 5157–5161.

(31) Brenner, E.; Schneider, R.; Fort, Y. *Tetrahedron* **1999**, *55*, 12829–12842.

(32) Zhu, F.; Wang, Z.-X. *Adv. Synth. Catal.* **2013**, *355*, 3694–3702.

CHAPTER FOUR

Conversion of Amides to Esters by the Nickel-Catalyzed Activation of Amide C–N Bonds

Liana Hie, Noah F. Fine Nathel, Tejas K. Shah, Emma L. Baker, Xin Hong, Yun-Fang Yang, Peng Liu, K. N. Houk, and Neil K. Garg

Nature **2015**, *524*, 79–83.

4.1 Abstract

Amides are common functional groups that have been studied for more than a century.[1] They are the key building blocks of proteins and are present in a broad range of other natural and synthetic compounds. Amides are known to be poor electrophiles, which is typically attributed to the resonance stability of the amide bond.[1,2] Although amides can readily be cleaved by enzymes such as proteases,[3] it is difficult to selectively break the carbon–nitrogen bond of an amide using synthetic chemistry. Here we demonstrate that amide carbon–nitrogen bonds can be activated and cleaved using nickel catalysts. We use this methodology to convert amides to esters, which is a challenging and underdeveloped transformation. The reaction methodology proceeds under exceptionally mild reaction conditions, and avoids the use of a large excess of an alcohol nucleophile. Density functional theory calculations provide insight into the thermodynamics and catalytic cycle of the amide-to-ester transformation. Our results provide a way to harness amide functional groups as synthons and are expected to lead to the further use of amides in the construction of carbon–heteroatom or carbon–carbon bonds using non-precious-metal catalysis.

4.2 Introduction

The ability to interconvert functional groups is important in synthetic chemistry and many biological processes. Methodologies[4,5] have been developed that enable chemists to strategically harness the reactivity of most functional groups. Likewise, breakthroughs in biochemistry have led to an understanding of how changes in functional groups regulate physiological processes.[6]

One particularly interesting dichotomy exists in considering the amide functional group,[1] which is the key component of all proteins (Figure 4.1a). Since Schwann's initial discovery of pepsin—the first enzyme to be discovered—in 1836, scientists have been intrigued by the ability of enzymes to break down amide linkages.[3,6] Such amide cleavage processes govern many cellular regulatory functions and are responsible for the degradation of proteins to amino acids.[1,3] In contrast, the synthetic chemistry of amide-bond cleavage has remained underdeveloped, even though amides are well suited for use in multistep synthesis because of their stability under a variety of reaction conditions. Commonly used methods to break amide carbon–nitrogen (C–N) bonds include the reductive conversion of amides to aldehydes using Schwartz's reagent[7] and the displacement of Weinreb's *N*-OMe-*N*-Me amides with organometallic reagents en route to ketones.[8] Following Pauling's seminal postulate regarding amide planarity,[2] the poor reactivity of amides is now well understood as being a result of the strength of the resonance-stabilized amide C–N bond.[1]

To circumvent the long-standing problem involving the low reactivity of amides and their modest synthetic use in C–N bond cleavage processes, we designed the general approach shown in Figure 4.1b. The C–N bond of amide **4.1** undergoes activation by a

transition-metal catalyst. Following oxidative addition, the resultant acyl metal species **4.2** is trapped by an appropriate nucleophile to furnish product **4.3**, with the release of amine **4.4**. This approach allows for the breakdown of amides, and renders amides useful synthetic building blocks. Although examples exist for the metal-catalyzed C–heteroatom bond activation of acid chlorides,[9] anhydrides,[9] and 2-pyridyl esters,[10] to our knowledge, the direct metal-catalyzed activation of C–N bonds of amides is unknown. This is notable given the widespread use of transition-metal catalysis in organic synthesis, where there exist many examples of catalytic transformations occurring smoothly in the presence of amide linkages. We validate the strategy outlined in Figure 4.1b through the conversion of amides to esters (Figure 4.1c).

Amide to ester conversion, much like transamidation,[11,12] remains a challenging and underdeveloped synthetic transformation. Amides are often stable enough that esterification is difficult and requires the use of harsh acidic or basic conditions, while employing a large excess of nucleophile (for example, using the alcohol nucleophile as a solvent).[1] Perhaps the most promising protocol to achieve amide-to-ester conversions is Keck's methylation/hydrolysis sequence,[13] although this methodology is limited to the synthesis of methyl esters. Esterifications using acyl aziridines[14] and *N*-methylamides (albeit with activation by nitrosation)[15] have also been reported. Here we demonstrate the nickel-catalyzed conversion of amides to esters, which proceeds under exceptionally mild reaction conditions. In addition to establishing the scope of this methodology, we use density functional theory (DFT) calculations to predict whether the amide-to-ester conversion, or the reverse, is thermodynamically favored. DFT calculations are also used to predict a plausible catalytic cycle. These experimental and computational studies not

only substantiate the notion of using non-precious-metal catalysis for the activation of amide C–N bonds, but also lay the foundation for further studies aimed at the strategic manipulation of amides as synthetic building blocks using catalysis.

Figure 4.1. Amide-bond Cleavage Using Transition-metal Catalysis. **a**. An illustration of the stability of amides and the contrast between how amides are used in nature and in chemical synthesis. **b**. Design of amide C–N bond activation to deconstruct amides and exploit them as synthetic building blocks **c**. Strategy for the conversion of amides to esters.

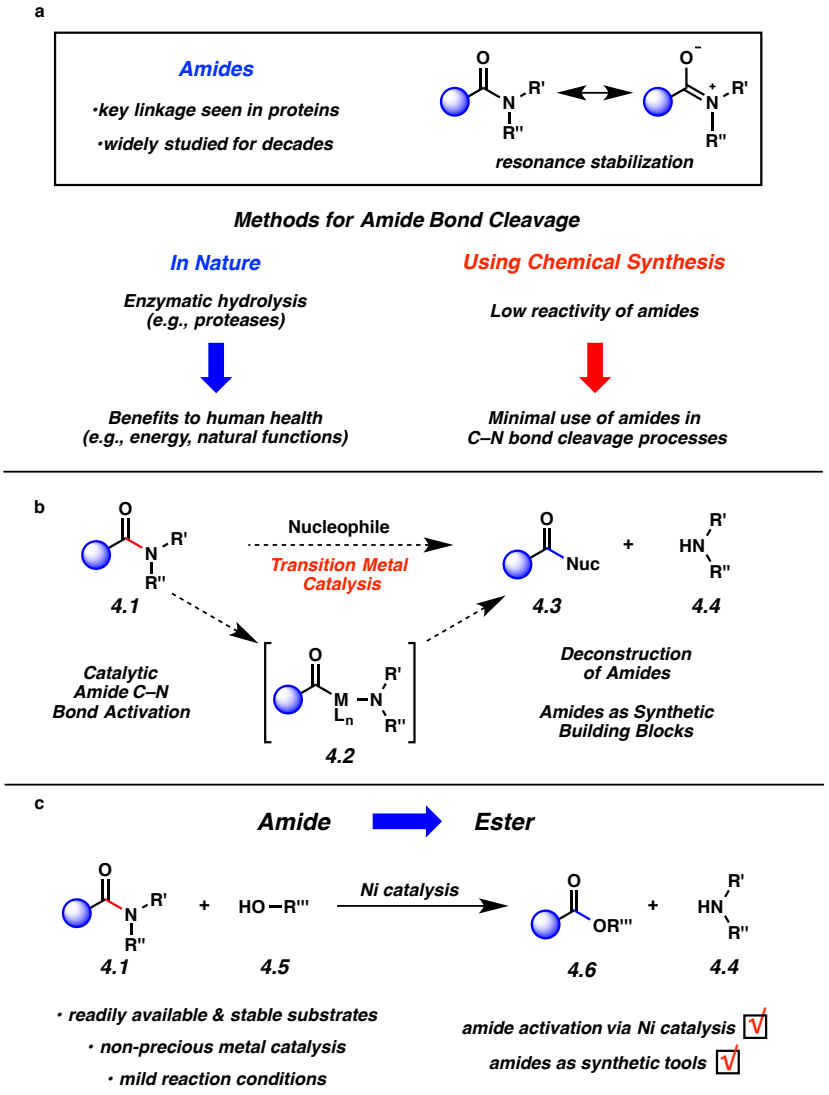

4.3 Optimization and Substrate Scope

We examined the conversion of benzamides **4.7** to methyl benzoate **4.8a** both computationally (using the Gaussian '09 software; see section 4.7.4.1 Complete Reference of Gaussian 09) and experimentally (Table 4.1). Because amides are known for their stability, we assessed whether the amide-to-ester conversion could be rendered thermodynamically favorable by the judicious choice of amide *N*-substituents. Using DFT methods, we calculated the change in Gibbs free energy (ΔG) for the reaction of amides **4.7** with methanol to give esters **4.8a** and amines **4.4**. Whether this transformation is favorable or not depends on the nature of the *N*-substituents (entries 1–8). Methanolysis of Weinreb amide **4.7d** (entry 4) and *N*-arylated substrates **4.7f** and **4.7g** (entries 6–8) were found to be the most energetically favorable. In contrast, esterifications of *N*-alkyl amides **4.7a**, **4.7b**, and **4.7e** were deemed thermodynamically unfavorable. This is in line with the experimentally measured equilibrium constant for the reaction of *N*,*N*-dimethylbenzamide **4.7b** and methanol (entry 2), in which the reverse reaction is thermodynamically favored (see section 4.7.4.6. Free Energy and Enthalpy of Amide and Ester Formation for further discussion).[16]

Encouraged by the unique ability of nickel to catalyze the activation of strong aryl–heteroatom bonds,[17–19] particularly those in phenol,[19] aniline,[20–22] and phthalimide[23] derivatives, we also calculated the activation free energies for acyl C–N bond oxidative addition of each amide substrate using nickel catalysis. The barriers calculated for commercially available *N*-heterocyclic carbene ligand SIPr (entries 1–8) reveal that the oxidative addition barriers are reasonable in some cases. We studied these reactions experimentally using 10 mol% $Ni(cod)_2$, 10 mol% SIPr, 2.0 equivalents of methanol, and

toluene as solvent at 110 °C for 12 h. There was good agreement between our observations and computational predictions. No reaction or low yields were seen for substrates **4.7a**–**4.7e** (entries 1–5). However, when the calculated ΔG and the oxidative addition barrier were favorable, substantial formation of product **4.8a** was observed (entries 6 and 7). Coupling of substrate **4.7g** gave a quantitative yield of product (entry 7), and further optimization showed that even with only 1.2 equivalents of methanol and a temperature of 80 °C, product formation occurred smoothly (entry 8) to give complete conversion to **4.8a**. Importantly, no reaction takes place if either the precatalyst or the ligand are omitted, whereas the use of alternative *N*-heterocyclic carbene or phosphine ligands typically leads to lower yields or no reaction. We conclude that nickel catalysis is indeed operative in the amide activation/esterification process.

Table 4.1. Experimental and Computational Study of Amide-bond Activation During the Conversion of Benzamides **4.7** to Methyl Benzoate **4.8a**.

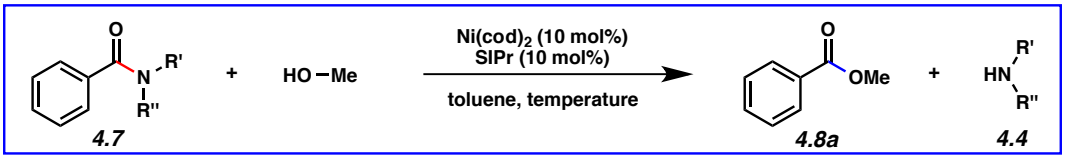

Entry		Calculated ΔG[a] (kcal/mol)	Calculated oxidative addition barrier with Ni /SIPr (kcal/mol)[b]	Temp	Equivalents of MeOH	Yield of ester[c]
1	4.7a	+2.4	36.8	110 °C	2.0	0%
2	4.7b	0.0	36.2	110 °C	2.0	0%
3	4.7c	–1.1	34.0	110 °C	2.0	23%
4	4.7d	–6.1	31.9	110 °C	2.0	22%
5	4.7e	+3.1	39.0	110 °C	2.0	0%
6	4.7f	–4.3	30.6	110 °C	2.0	55%
7	4.7g	–6.8	26.0	110 °C	2.0	>99%
8				80 °C	1.2	>99%

[a] The ΔG values for the overall reactions were obtained using DFT calculations (assuming a temperature of 298 K). [b] DFT methods were used to calculate oxidative addition barriers using Ni/SIPr as the metal/ligand combination.
[c] Reactions were carried out with bis(1,5-cyclooctadiene)nickel(0) ($Ni(cod)_2$, 10 mol%), SIPr (10 mol%), substrate (50.0 mg, 1.0 equiv), methanol (1.2 or 2.0 equiv), and toluene (1.0 M), for 12 h at the specified temperatures. Yields were determined by ^1H nuclear magnetic resonance (NMR) analysis using hexamethylbenzene as an internal standard. (Me, methyl; OMe, methoxy; Ph, phenyl).

Having determined the optimal reaction conditions, we examined the scope of the transformation with regard to the amide substrate (Table 4.2a). In addition to the parent

benzamide (entry 1), substrates containing the electron-withdrawing trifluoromethyl or fluoride substituents (entries 2 and 3) or the electron-donating methoxy or methyl substituents (entries 4 and 5) were well tolerated. The transformation also proceeded smoothly using *meta*- and *ortho*-methyl-substituted substrates to give the desired esters in excellent yields (entries 6 and 7). Beyond the use of phenyl derivatives, we examined naphthyl and heterocyclic substrates. Naphthyl compounds readily coupled (entries 8 and 9), as did furan, quinoline, and isoquinoline substrates (entries 10–12, respectively). However, amides derived from alkyl carboxylic acids did not undergo the nickel-catalyzed esterification under our reaction conditions. This attribute provides opportunities to realize selective amide C–N bond cleavages in more complex substrates (see section 4.5 Selective Amide Bond Activation).

A variety of *N*-substituents were also surveyed, as shown in Table 4.2a. In addition to the longer *N*-butyl (Bu) and the branched *N*-*iso*-propyl alkyl chains (entries 13 and 14, respectively), we found that a cyclic amide derived from indoline was tolerated by the methodology (entry 15). Lastly, protected *N*-alkyl benzamides were tested. Although use of the *N*-*p*-toluenesulfonyl (Ts) derivative gave the corresponding ester in modest yield (entry 16), the corresponding *N*-*tert*-butyloxycarbonyl (Boc) substrate more efficiently underwent conversion to ester **4.8a** (entry 17). The analogous *N*-benzyl, *N*-*tert*-butyloxycarbonyl (*N*-Bn,Boc) substrate was also evaluated and gave the desired ester in 89% yield (entry 18). These results show that the methodology is not restricted to anilide substrates, as long as the overall reaction energetics are thermodynamically favorable (see section 4.7.4.5 Analysis of *N*-Me,Boc Amide Esterification, for energetics involving the *N*-Boc,Me substrate). Moreover, secondary benzamides can be used

strategically as substrates for esterification, following a straightforward activation step (Boc-protection).

Using amide **4.7g** as the substrate, we evaluated the scope of the methodology with respect to the alcohol nucleophile (Table 4.2b). As shown, synthetically useful yields of product were obtained using only 1.2 equivalents of the alcohol, even when complex and hindered alcohols were used. Cyclohexanol, *tert*-butanol, and 1-adamantol coupled smoothly to give the corresponding esters (entries 19–21, respectively); *tert*-butyl esters can readily be hydrolyzed to carboxylic acids under acidic conditions. Similarly, we found that cyclopropyl carbinol and an oxetane-derived alcohol could be used in the esterification reaction (entries 22 and 23, respectively). The use of the hindered secondary alcohol (–)-menthol was also tested and the desired ester was obtained in 88% yield (entry 24). Furthermore, we found that *N*-Boc-L-prolinol was tolerated in the methodology (entry 25), in addition to an indole-containing alcohol (entry 26), which further demonstrates the promise our methodology holds for reactions of heterocyclic substrates. As shown in entries 27 and 28, a complex sugar-containing alcohol bearing two acetals and an estrone-derived steroidal alcohol, respectively, also underwent the desired esterification reaction.

Table 4.2. Scope of Our Methodology. The scope of the amide-to-ester transformation was evaluated with respect to the amide substrate (**a**), and with respect to the alcohol nucleophile, using **4.7g** as the amide substrate (**b**).

a

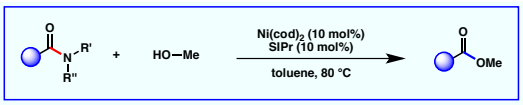

Entry	Amide Substrate	Yield of Methyl Ester[a]
1	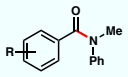	88% (R = H)
2		80% (R = *p*-CF_3)
3		92% (R = *p*-F)
4		90% (R = *p*-OMe)
5		90% (R = *p*-Me)
6		83% (R = *m*-Me)
7		89% (R = *o*-Me)
8	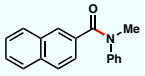	94%
9	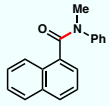	94%
10	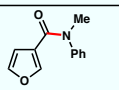	91%[b]
11	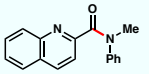	84%
12	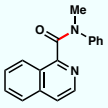	56%
13	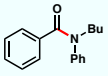	92%
14	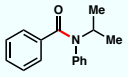	78%
15	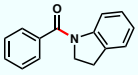	58%
16	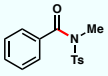	49%
17	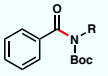	84% (R = Me)
18		89% (R = Bn)

b

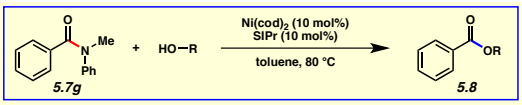

Entry	Ester Product	Yield of Ester[a]
19	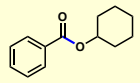	82%
20	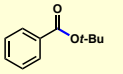	64%
21	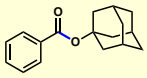	67%
22	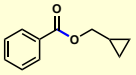	90%
23	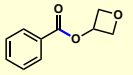	49%
24	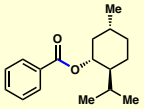	88%

Entry	Ester Product	Yield of Ester[a]
25	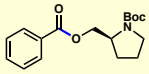	67%
26	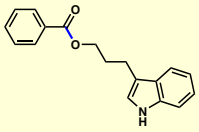	65%
27	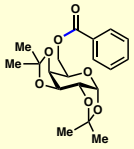	91%
28	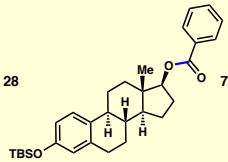	74%

[a] Reactions were carried out with $Ni(cod)_2$ (10 mol%), SIPr (10 mol%), substrate (100.0 mg, 1.00 equiv), alcohol (1.2 equiv), and toluene (1.0 M) at 80 °C for 12 h. Yields shown reflect the average of two isolated experiments.
[b] The yield for entry 10 was determined by ^{1}H NMR analysis using hexamethylbenzene as an internal standard, owing to the volatility of the ester product. (*t*-Bu, *tert*-butyl; *p*, para; *m*, meta; *o*, ortho).

4.4 Computational Studies

Although nickel-catalyzed aryl and acyl C–O bond activation processes have been previously studied computationally,[24–28] no analogous studies involving C–N bond activation have been reported. Thus, to shed light on the mechanism of the facile amide-to-ester conversion, the catalytic cycle was computed using DFT calculations. Figure 4.2

provides the free energy profile using amide substrate **4.7g**. The [Ni(SIPr)$_2$] complex, **4.9**, is believed to be the resting state of the catalytic cycle. Dissociation of one carbene ligand from complex **4.9** provides a coordination site for amide **4.7g**. Following coordination to give intermediate **4.10,** oxidative addition occurs via transition state **4.11**. This key event cleaves the amide C–N bond and produces acyl nickel species **4.12**. The next step of the catalytic cycle is ligand exchange, which proceeds by coordination of methanol to give intermediate **4.13**. Subsequent ligand exchange via transition state **4.14** facilitates the deprotonation of methanol, giving nickel complex **4.14.** Dissociation of *N*-Me-aniline produces acyl nickel species **4.16**, which in turn, undergoes reductive elimination via transition state **4.17** to deliver the ester-coordinated complex **4.18**. Finally, the ester product **4.8a** is released to regenerate catalyst **4.9**. The rate-determining step in the catalytic cycle is the oxidative addition (transition state **4.11**) with an overall barrier of 26.0 kcal mol^{-1} relative to the resting state **4.9**. The overall reaction is thermodynamically favored by −6.8 kcal mol^{-1}. Because decarbonylation of acyl nickel species have been observed,[29,30] we also calculated the kinetic barrier for decarbonylation events (see section 4.7.4.2 Transition State Structures for Decarbonylation Pathway). Consistent with experiments, decarbonylation pathways from acyl nickel species **4.12** or **4.16** were found to be less favorable than the product formation pathways.

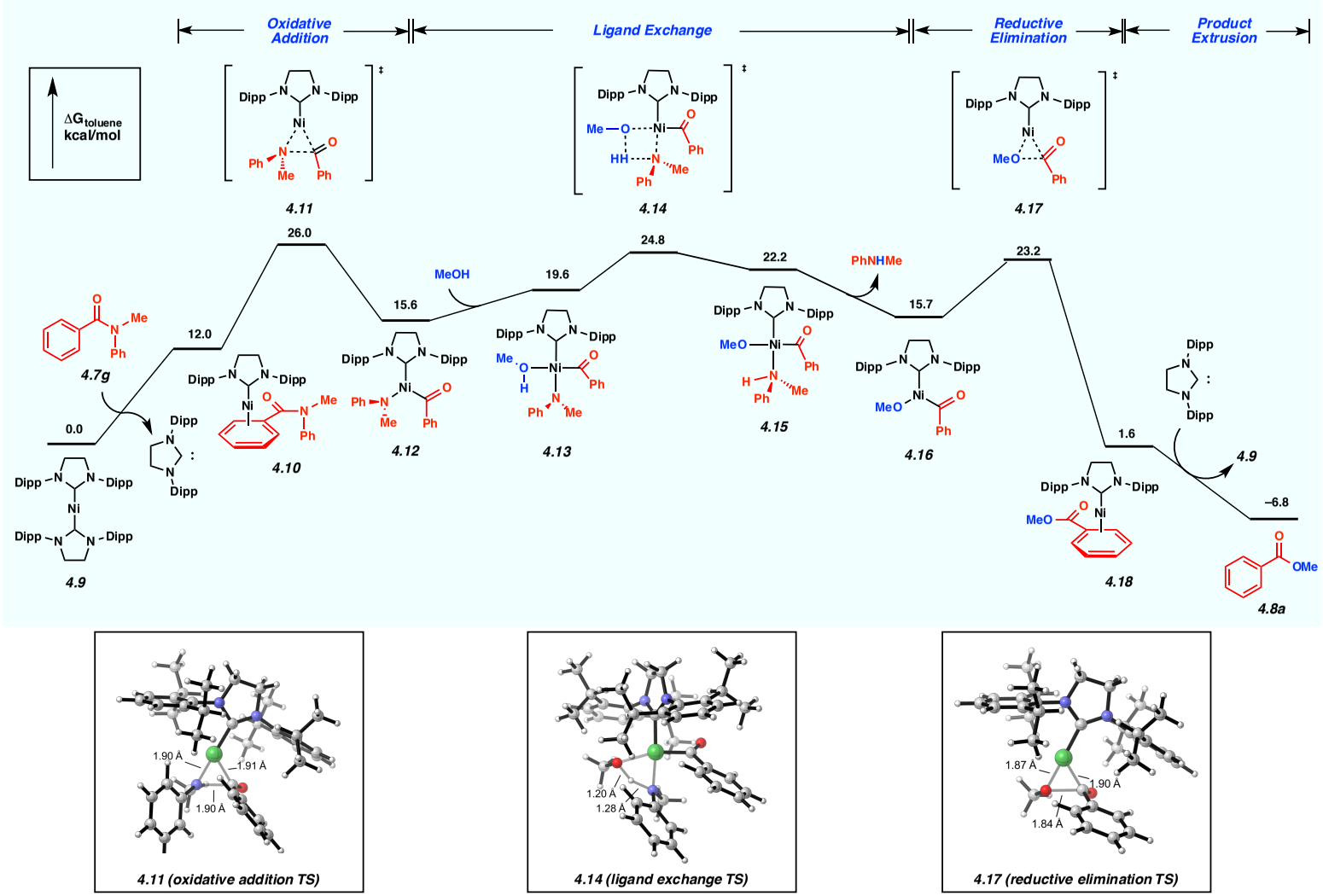

Figure 4.2. Computational Study of Catalytic Cycle. DFT methods were used to calculate the full catalytic cycle for the amide-to-ester conversion (assuming a temperature of 298 K). We propose that the reaction occurs by oxidative addition, ligand exchange, and reductive elimination. Key transition state structures (**4.11**, **4.14**, and **4.17**) are shown at the bottom. (Dipp, 2,6-diisopropylphenyl)

4.5 Selective Amide Bond Activation

As highlighted by the experiments shown in Figure 4.3, the nickel-catalyzed conversion of amides to esters can be used to achieve selective and mild amide-bond cleavages. First, we performed the esterification of bis(amide) substrate **4.19** using (–)-menthol (Figure 4.3a). Although both amides are *N*-arylated benzamides, only the tertiary amide was cleaved to give ester **4.21**, while also releasing aminoamide **4.22**. Second, bis(amide) **4.23**, which possesses two tertiary amides, was studied in the nickel-catalyzed esterification reaction (Figure 4.3b). In this case, the tertiary L-proline-derived alkyl amide was not disturbed, while the tertiary benzamide underwent cleavage to give ester **4.21** and aminoamide **4.24** in good yields. Lastly, we prepared L-valine derivative **4.25**, which also bears an ester (Figure 4.3c). Upon exposure of **4.25** to 1.2 equivalents of (–)-menthol and the nickel-catalyzed conditions, ester **4.21** and aminoester **4.26** were obtained in 70% and 79% yields, respectively. We believe that the ester functionality withstands the reaction conditions because it is not attached to an arene, analogous to the lack of reactivity seen in our attempts to esterify amides derived from alkyl carboxylic acids (for example, **4.23**). Compounds **4.24** and **4.26** were obtained in high enantiomeric excess, highlighting the mild nature of the reaction conditions, which avoid any substantial epimerization of the α stereocenters.

Figure 4.3. Selective Amide-bond Cleavage Processes. **a**. Cleavage of tertiary over secondary amide using menthol (1.2 equiv). **b**. Cleavage of benzamide over an alkyl prolinederived amide using menthol (1.2 equiv). **c**. Cleavage of valinederived amide in the presence of an ester using menthol (1.2 equiv).

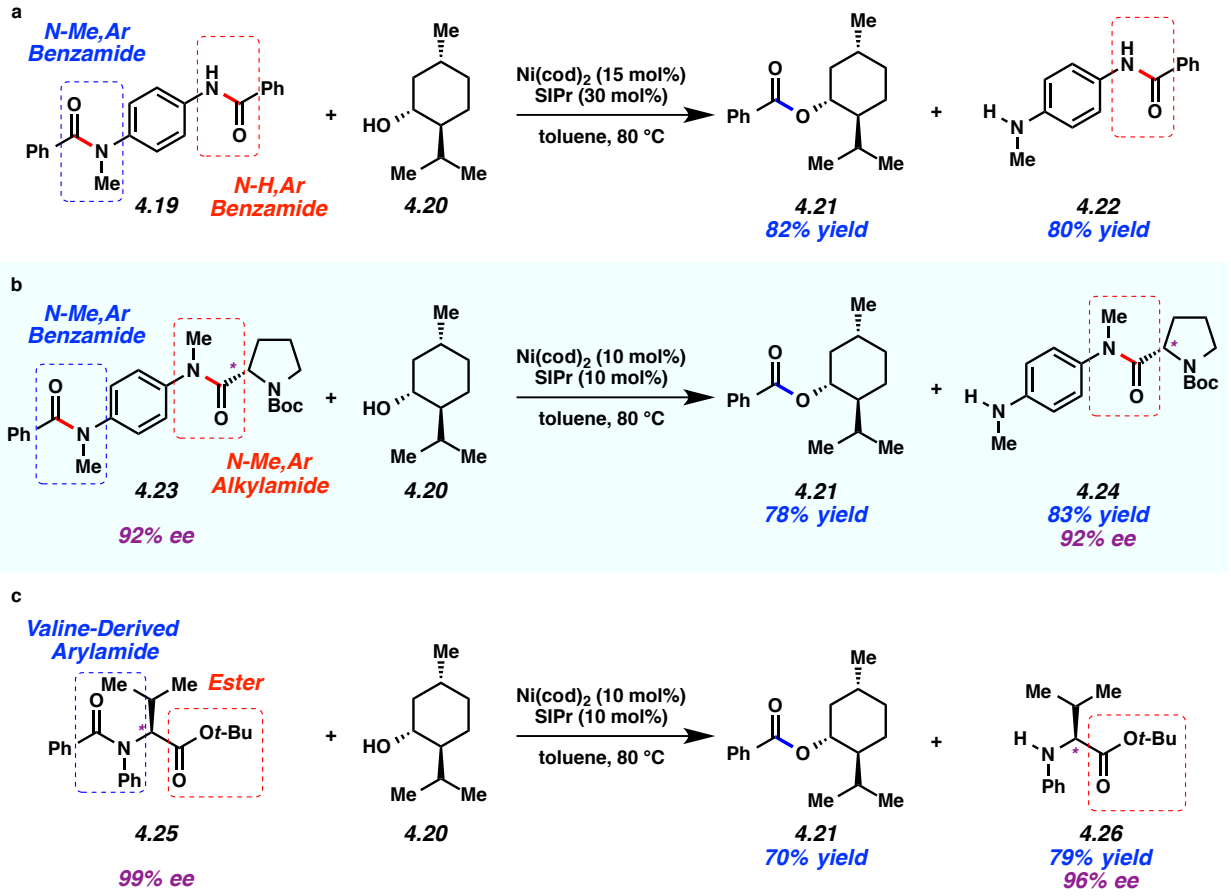

4.6 Conclusion

We have presented an efficient way to convert amides to esters. The methodology circumvents the classic problem of amides being poorly reactive functional groups by using nickel catalysis to achieve the previously unknown catalytic activation of amide C–N bonds. DFT calculations support a catalytic cycle that involves a rate-determining oxidative addition step, followed by ligand exchange and reductive elimination. The methodology is broad in scope, particularly with respect to the alcohol nucleophiles, and

proceeds under exceptionally mild reaction conditions using just 1.2 equivalents of the alcohol nucleophile. Moreover, selective amide-bond cleavage is achieved in the presence of other functional groups, including less reactive amides and esters, without the epimerization of α stereocenters. We envision that this methodology will lead to advances such as the catalytic esterification of primary amides, additional *N,N*-disubstituted amides, amides derived from alkyl or vinyl carboxylic acids, and perhaps even polyamide substrates bearing multiple stereocenters. This study may also lead to further harnessing of amides as valuable building blocks for the construction of C–heteroatom or C–C bonds using non-precious-metal catalysis.

4.7 Experimental Section

4.7.1 Materials and Methods

Unless stated otherwise, reactions were conducted in flame-dried glassware under an atmosphere of nitrogen and commercially obtained reagents were used as received. Alcohols and toluene were purified by distillation and taken through five freeze-pump-thaw cycles or recrystallized prior to use. Carboxylic acid **4.38**, amine **4.81**, and ester **4.87** were obtained from Combi-Blocks. Acid chlorides **4.27**, **4.29**, **4.32**, **4.34**, **4.36**, alcohols **4.63**, **4.65**, **4.67**, **4.69**, **4.71**, **4.73**, **4.75**, **4.77**, **4.79**, **4.20**, amines **4.28**, **4.30**, **4.82**, **4.84**, amide **4.7b**, benzamide and ligand SIMes were obtained from Sigma-Aldrich. Boronic acid **4.86** was obtained from Oakwood Products, Inc. $Ni(cod)_2$, SIPr, IMes, IPr, PCy_3, dppe, and dppf were obtained from Strem Chemicals. Amide **4.7e**, ligands PPh_3, PPh_2Cy, and PCy_2Ph were obtained from Alfa Aesar. Reaction temperatures were controlled using an IKAmag temperature modulator, and unless stated otherwise,

reactions were performed at room temperature (approximately 23 °C). Thin-layer chromatography (TLC) was conducted with EMD gel 60 F254 pre-coated plates (0.25 mm for analytical chromatography and 0.50 mm for preparative chromatography) and visualized using a combination of UV, anisaldehyde, ceric ammonium molybdate, iodine, vanillin, and potassium permanganate staining techniques. Silicycle Siliaflash P60 (particle size 0.040–0.063 mm) was used for flash column chromatography. ^{1}H NMR spectra were recorded on Bruker spectrometers (at 300, 400, 500, and 600 MHz) and are reported relative to residual solvent signals. Data for ^{1}H NMR spectra are reported as follows: chemical shift (δ ppm), multiplicity, coupling constant (Hz), integration. Data for ^{13}C NMR are reported in terms of chemical shift (at 75, 125, and 150 MHz). IR spectra were recorded on a Perkin-Elmer 100 spectrometer and are reported in terms of frequency absorption (cm^{-1}). High-resolution mass spectra were obtained on Thermo Scientific™ Exactive Mass Spectrometer with DART ID-CUBE. Determination of enantiopurity was carried out on a Mettler Toledo SFC (supercritical fluid chromatography) using a Daicel ChiralPak OJ-H column.

4.7.2 Experimental Procedures

4.7.2.1 Syntheses of Amide Substrates

Representative procedure for the synthesis of amide substrates from Table 4.1 and Table 4.2 (synthesis of amide 4.7a is used as an example).

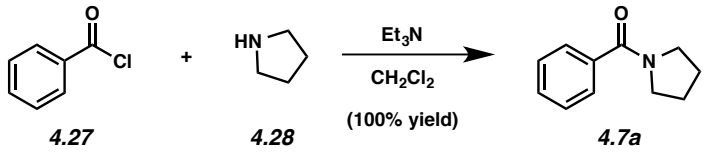

Amide 4.7a (Table 4.1). To a solution of pyrrolidine **4.28** (1.3 mL, 14.7 mmol, 1.1 equiv), triethylamine (2.5 mL, 17.8 mmol, 1.25 equiv), and dichloromethane (28.5 mL, 0.5 M) at 0 °C, was added acid chloride **4.27** (2.0 g, 14.2 mmol, 1.0 equiv). The reaction mixture was gradually warmed to 23 °C over 30 min and then stirred for 1 h. The reaction mixture was diluted with EtOAc (50 mL), and then washed successively with 1.0 M HCl (50 mL) and brine (50 mL). The organic layer was dried over Na_2SO_4 and concentrated under reduced pressure. The crude solid material was purified by flash chromatography (1:1 Hexanes:EtOAc) to yield amide product **4.7a** (2.5 g, 100% yield) as a white solid. Spectral data matched those previously reported.[31a]

Note: Experimental procedures for the syntheses of amides shown in Table 4.1 and Table 4.2 have previously been reported: **4.7a**,[31a] **4.7c**,[31b] **4.7d**,[31c] **4.7f**,[31d] **4.7g**,[31e] **4.41**,[31f] **4.43**,[31f] **4.45**,[31f] **4.47**,[31g] **4.50**,[31g] **4.52**,[31h] **4.57**,[31f] **4.58**,[31e] **4.59**,[31i] **4.60**,[31j] **4.61**,[31k] and **4.62**,[31l] with the exception of *p*-trifluoromethyl amide **4.31**, *o*-methyl amide **4.33**, furan **4.35,** quinoline **4.37**, and isoquinoline **4.39**. Syntheses for these latter compounds are as follows:

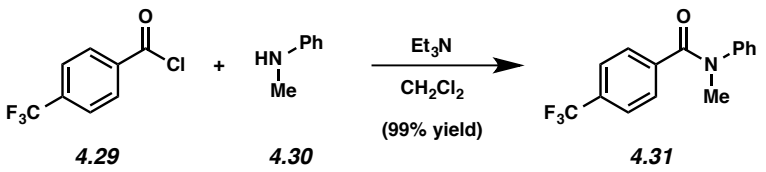

4.29 *4.30* *4.31*

Amide 4.31 (Table 4.2). To a solution of triethylamine (2.1 mL, 15 mmol, 1.25 equiv) and *N*-Me aniline (**4.30**) (1.43 mL, 13.2 mmol, 1.1 equiv) in dichloromethane (24.0 mL, 0.5 M) at 0 °C, was added acid chloride **4.29** (2.5 g, 12.0 mmol, 1.0 equiv). The resulting heterogeneous mixture was allowed to stir at 23 °C for 12 h. The mixture was then diluted with EtOAc (30 mL) and 1.0 M HCl (40 mL). The organic layer was washed with brine (2 x 40 mL) and then dried over Na_2SO_4. The volatiles were removed under reduced pressure, and the crude oil was purified by flash chromatography (5:1 Hexanes:EtOAc) to yield amide product **4.31** (3.3 g, 99% yield) as a white solid. Amide **4.31**: R_f 0.27 (5:1 Hexanes:EtOAc); ^{1}H NMR (500 MHz, $CDCl_3$): δ 7.44 (q, J = 8.4, 4H), 7.24–7.23 (m, 2H), 7.19 (t, J = 7.4, 1H), 7.03 (d, J = 7.55, 2H), 3.51 (s, 3H); ^{13}C NMR (125 MHz, $CDCl_3$): δ 169.3, 144.3, 139.6, 131.4 (q, J_{C-F} = 32.6 Hz), 129.5, 129.1, 127.2, 127.0, 124.9 (q, J_{C-F} = 3.8 Hz), 122.7, 120.5, 38.5; IR (film): 2971, 1738, 1639, 1596, 1496, 1371, 1322, 1165, 1122, 1108, 1065, 1019 cm^{-1}; HRMS-ESI (*m/z*) $[M+H]^+$ calcd for $C_{15}H_{13}F_3NO$, 280.09492; found 280.09339.

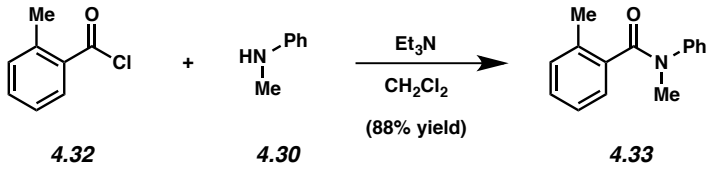

4.32 *4.30* *4.33*

Amide 4.33 (Table 4.2). To a solution of acid chloride **4.32** (2.5 g, 16.0 mmol, 1.0 equiv) and dichloromethane (10 mL) at 0 °C, was added a solution of triethylamine (2.1 mL, 15

mmol, 1.25 equiv) and *N*-Me aniline (**4.30**) (1.43 mL, 13.2 mmol, 1.1 equiv) in dichloromethane (22 mL). The resulting heterogeneous mixture was warmed to 23 °C and allowed to stir for 12 h. The mixture was then diluted with EtOAc (30 mL) and 1.0 M HCl (50 mL). The organic layer was washed with brine (50 mL) and then dried over Na_2SO_4. The volatiles were removed under reduced pressure, and the crude oil was purified by flash chromatography (5:1 Hexanes:EtOAc) to yield amide product **4.33** (3.2 g, 88% yield) as a white solid. Amide **4.33**: R_f 0.30 (5:1 Hexanes:EtOAc); ^{1}H NMR (400 MHz, $CDCl_3$): δ 7.18–7.03 (m, 9H), 3.49 (s, 3H), 2.33 (s, 3H); ^{13}C NMR (125 MHz, $CDCl_3$): δ 171.3, 143.9, 136.7, 134.8, 130.3, 129.0, 128.7, 127.6, 126.7, 126.6, 124.2, 37.4, 19.6; IR (film): 3062, 2924, 1643, 1594, 1494, 1456, 1417, 1364, 1303, 1280, 1180, 1121, 1097, 1028 cm^{-1}; HRMS-ESI (*m/z*) $[M+H]^+$ calcd for $C_{15}H_{16}NO$, 226.12319; found 226.12159.

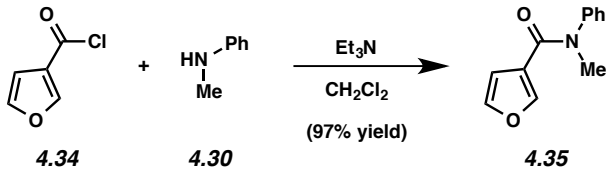

Amide 4.35 (Table 4.2). To a flask containing a solution of *N*-Me aniline (**4.30**) (1.3 mL, 12.3 mmol, 1.6 equiv) and triethylamine (1.1 mL, 7.7mmol, 1.0 equiv) in dichloromethane (11.5 mL, 0.67 M) at 0 °C, was added acid chloride **4.34** (1.0 g, 7.7 mmol, 1.0 equiv). The resulting heterogeneous mixture was warmed to 23 °C over 30 min and then heated to reflux for 1 h. After cooling to 23 °C, the reaction mixture was stirred for 12 h and then quenched with 1.0 M HCl (10 mL). The organic layer was washed with brine (30 mL) and then dried over Na_2SO_4. The volatiles were removed

under reduced pressure, and the crude solid was purified by flash chromatography (5:1 Hexanes:EtOAc) to yield amide product **4.35** (1.5 g, 97% yield) as a white solid. Amide **4.35**: R_f 0.24 (5:1 Hexanes:EtOAc); ^{1}H NMR (300 MHz, $CDCl_3$): δ 7.44–7.36 (m, 3H), 7.23–7.19 (m, 2H), 7.14 (t, J = 1.78, 1H), 6.89–6.87 (m, 1H), 6.11–6.10 (m, 1H), 3.41 (s, 3H); ^{13}C NMR (75 MHz, $CDCl_3$): δ 163.2, 144.7, 144.1, 141.9, 129.7, 128.1, 127.8, 121.9, 111.0, 38.2; IR (film): 3481, 3129, 2970, 1739, 1630, 1593, 1561, 1497, 1379, 1354, 1157, 1074, 1040 cm^{-1}; HRMS-ESI (*m/z*) $[M+H]^+$ calcd for $C_{12}H_{12}NO_2$, 202.08680; found 202.08580.

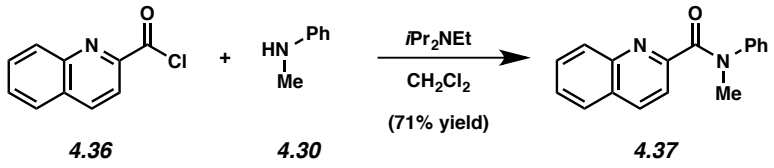

4.36 *4.30* *4.37*

Amide 4.37 (Table 4.2). To a solution of *N*-Me aniline (**4.30**) (1.2 mL, 11.5 mmol, 1.1 equiv) and *N*,*N*-diisopropylethylamine (9.1 mL, 52.2 mmol, 4.0 equiv) in dichloromethane (100 mL, 0.1 M) at 0 °C, was added acid chloride **4.36** (2.0 g, 10.4 mmol, 1.0 equiv). The resulting heterogeneous mixture was allowed to stir at 23 °C. After 17 h, additional *N*-Me aniline (1.2 mL, 11.5 mmol, 1.1 equiv) and *N*,*N*-diisopropylethylamine (6.0 mL, 34.4 mmol, 3.3 equiv) were added sequentially. After stirring at 23 °C for 6 h, the reaction mixture was quenched with 1.0 M HCl (50 mL). The organic layer was washed with brine (50 mL) and then dried over Na_2SO_4. The volatiles were removed under reduced pressure, and the crude oil was purified by flash chromatography (5:1 Hexanes:EtOAc) to yield amide product **4.37** (2.0 g, 71% yield) as a white solid. Amide **4.37**: R_f 0.40 (5:1 Hexanes:EtOAc); ^{1}H NMR (500 MHz, $CDCl_3$): δ

8.03 (br s, 1H), 7.85 (br s, 1H), 7.77–7.58 (m, 2H), 7.57–7.43 (m, 2H), 7.24–6.99 (m, 5H), 3.59 (s, 3H); ^{13}C NMR (125 MHz, $CDCl_3$): δ 168.9, 154.2, 146.9, 144.4, 136.4, 129.9, 129.8, 129.1, 127.7, 127.5, 127.5, 127.0, 126.7, 120.6, 38.2; IR (film): 3457, 2971, 1739, 1642, 1594, 1495, 1374.55, 1229, 1217, 1121, 1104 cm^{-1}; HRMS-ESI (*m/z*) $[M+H]^+$ calcd for $C_{17}H_{15}N_2O$, 263.11844; found 263.11718.

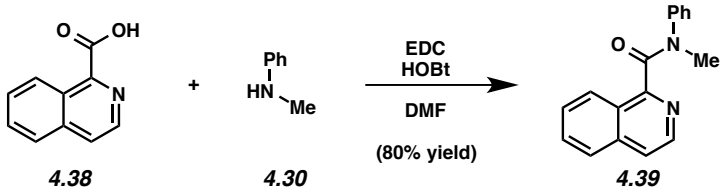

4.38 *4.30* *4.39*

Amide 4.39 (Table 4.2). To a mixture of carboxylic acid **4.38** (1.0 g, 4.0 mmol, 1.0 equiv), EDC (0.7 g, 4.4 mmol, 1.1 equiv), HOBt (0.6 g, 4.4 mmol, 1.1 equiv), and DMF (60.0 mL, 0.067 M) was added *N*-Me aniline (**4.30**) (0.5 mL, 4.4 mmol, 1.1 equiv). The resulting mixture was stirred at 23 °C for 12 h, and then diluted with deionized water (100 mL) and EtOAc (100 mL). The aqueous layer was separated and the organic layer was extracted with EtOAc (3 X 100 mL). The combined organic layer was washed with brine (150 mL), dried over Na_2SO_4, and concentrated under reduced pressure. The crude oil was purified by flash chromatography with (1:1 Hexanes:EtOAc) to yield amide product **4.39** (0.9 g, 80% yield) as a white solid. Amide **4.39**: R_f 0.50 (1:1 Hexanes:EtOAc); ^{1}H NMR (500 MHz, $CDCl_3$): (major rotamer) δ 8.25 (d, J = 4.8, 1H), 8.18–8.17 (m, 1H), 7.74–7.72 (m, 1H), 7.66–7.60 (m, 2H), 7.46 (d, J = 4.8, 1H), 7.04–6.97 (m, 5H), 3.65 (s, 3H); (minor rotamer) [10/14 protons were discernable] δ 8.60–8.58 (m, 1H), 7.96–7.84 (m, 1H), 7.59–7.49 (m, 5H), 3.23 (s, 3H); ^{13}C NMR (125 MHz,

$CDCl_3$): δ 168.4, 154.8, 143.4, 141.4, 136.2, 130.5, 128.9, 128.0, 127.1, 126.9, 126.7, 126.0, 124.9, 121.1, 37.3; IR (film): 3060, 2939, 1651, 1595, 1561, 1496, 1460, 1431, 1399 1372, 1119, 1054, 1033 cm^{-1}; HRMS-ESI (*m/z*) $[M+H]^+$ calcd for $C_{17}H_{15}N_2O$, 263.11844; found 263.11768.

Note: ***4.39*** *was obtained as a 7.5:1 mixture of rotamers. These data represent empirically observed chemical shifts and coupling constants from the* ^{1}*H NMR spectrum*

4.7.2.2 Methanolysis Control Experiments

Table 4.3. Attempted Conversion of Amide **4.7g** to Methyl Benzoate **4.8a** Under Various Reaction Conditions.[a]

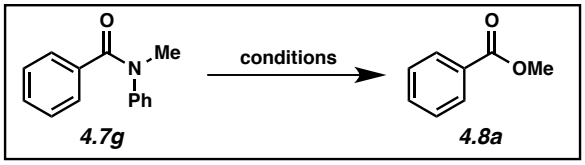

4.7g *4.8a*

Reaction Conditions	*Experimental Results* *Recovered 4.7g*	*4.8a*
Conc. HCl (5.13 equiv), MeOH (0.12 M) 23 °C (2 h) → 75 °C (2 h) → 100 °C (17 h)	100%	0%
NaOMe (2.0 equiv), MeOH (0.12 M) 23 °C (4 h) → 80 °C (4 h) → 110 °C (13.5 h)	93%	7%
NaOMe (10.0 equiv), MeOH (0.12 M) 23 °C (1.5 h) → 80 °C (4 h) → 110 °C (14 h)	94%	6%
K_2CO_3 (1.0 equiv), MeOH (0.12 M) 23 °C (7 h) → 110 °C (12 h)	95%	5%

[a] Yields were determined by ^{1}H NMR analysis using hexamethylbenzene as an internal standard.

4.7.2.3 Screening of Amide Substrates

Table 4.4. Survey of Amide Substrates[a]

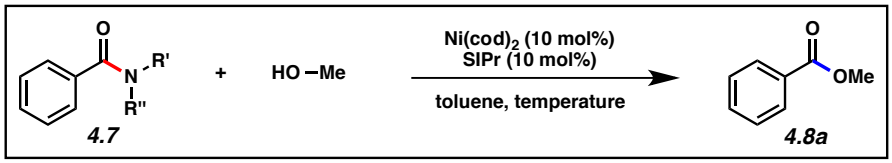

Entry		*Temp*	*Equivalents of MeOH*	*Yield of ester*	*Remainder of the mass*
1	*4.7a*	110 °C	2.0	0%	*4.7a* (100%)
2	*4.7b*	110 °C	2.0	0%	*4.7b* (100%)
3	*4.7c*	110 °C	2.0	23%	*4.7c* (77%)
4	*4.7d*	110 °C	2.0	22%	*4.7d* (72%) + *4.7e* (6%)
5	*4.7e*	110 °C	2.0	0%	*4.7e* (100%)
6	*4.7f*	110 °C	2.0	55%	*4.7f* (45%)
7	*4.7g*	110 °C	2.0	quant.	-
8		80 °C	1.2	quant.	-

[a] Yields were determined by ^{1}H NMR analysis using hexamethylbenzene as an internal standard.

Note: The attempted esterification of benzamide using MeOH (2.0 equiv), Ni(cod)$_2$ (10 mol%), SIPr (10 mol%), and toluene (1.0 M) at 110 °C led to no reaction.

4.7.2.4 Comparison of Ligands and Relevant Control Experiments

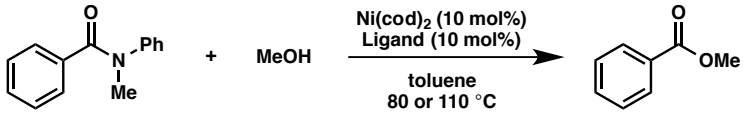

4.7g *4.8a*

Representative Procedure for Esterifications of Benzamides from Table 4.4 and Table 4. (coupling of amide 4.7g is used as an example). A 1-dram vial containing amide **4.7g** (50.0 mg, 0.24 mmol, 1.0 equiv), hexamethylbenzene (7.8 mg, 0.48 mmol, 0.2 equiv), and a magnetic stir bar was charged with $Ni(cod)_2$ (6.6 mg, 0.024 mmol, 10 mol%) and ligand (0.024 mmol, 10 mol%) in a glove box. Subsequently, toluene (0.24 mL, 1.0 M) and then methanol (19.4 μL, 0.48 mmol, 2.0 equiv) were added. The vial was sealed with a Teflon-lined screw cap, removed from the glove box, and stirred at 80 or 110 °C for 12 h. After cooling to 23 °C, the mixture was diluted with hexanes (0.5 mL) and filtered over a plug of silica gel (10 mL of EtOAc eluent). The volatiles were removed under reduced pressure, and the yield was determined by ^1H NMR analysis with hexamethylbenzene as an internal standard.

Any modifications of the conditions shown in the representative procedure above are specified in the following Tables 4.4 and 4.5

Table 4.4. Ligand Screening for Nickel-Catalyzed Esterification.[a]

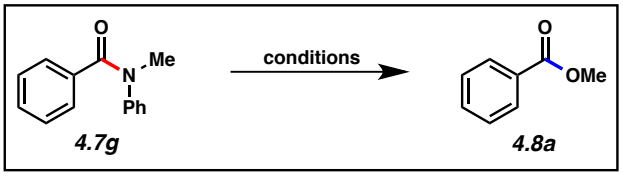

4.7g *4.8a*

Reaction Conditions	*Experimental Results* *Recovered 4.7g*	*4.8a*
MeOH (2.0 equiv), $Ni(cod)_2$ (10 mol%), SIPr (10 mol%) toluene (1.0 M), 110 °C, 12 h	0%	100%
MeOH (2.0 equiv), $Ni(cod)_2$ (10 mol%), IPr (10 mol%) toluene (1.0 M), 110 °C, 12 h	0%	100%
MeOH (2.0 equiv), $Ni(cod)_2$ (10 mol%), SIMes (10 mol%) toluene (1.0 M), 110 °C, 12 h	0%	0%
MeOH (2.0 equiv), $Ni(cod)_2$ (10 mol%), IMes (10 mol%) toluene (1.0 M), 110 °C, 12 h	63%	37%
MeOH (2.0 equiv), $Ni(cod)_2$ (10 mol%), PPh_3 (10 mol%) toluene (1.0 M), 110 °C, 12 h	100%	0%
MeOH (2.0 equiv), $Ni(cod)_2$ (10 mol%), PPh_2Cy (10 mol%) toluene (1.0 M), 110°C, 12 h	100%	0%
MeOH (2.0 equiv), $Ni(cod)_2$ (10 mol%), PCy_3 (10 mol%) toluene (1.0 M), 110 °C, 12 h	85%	15%
MeOH (2.0 equiv), $Ni(cod)_2$ (10 mol%), $PhPCy_2$ (10 mol%) toluene (1.0 M), 110 °C, 12 h	97%	3%
MeOH (2.0 equiv), $Ni(cod)_2$ (10 mol%), dppe 10 mol%) toluene (1.0 M), 110 °C, 12 h	100%	0%
MeOH (2.0 equiv), $Ni(cod)_2$ (10 mol%), dppf (10 mol%) toluene (1.0 M), 110 °C, 12 h	100%	0%
Control Experiments:		
MeOH (1.2 equiv), $Ni(cod)_2$ (10 mol%), SIPr (10 mol%) toluene (1.0 M), 80 °C, 12 h	0%	100%
MeOH (1.2 equiv), toluene (1.0 M), 80 °C, 12 h	100%	0%
MeOH (1.2 equiv), SIPr (10 mol%) toluene (1.0 M), 80 °C, 12 h	100%	0%
MeOH (1.2 equiv), $Ni(cod)_2$ (10 mol%) toluene (1.0 M), 80 °C, 12 h	100%	0%

[a] Yields were determined by ^1H NMR analysis using hexamethylbenzene as an internal standard.

4.7.2.5 Scope of Methodology

*Representative Procedure (coupling of amide **4.7g** and methanol is used as an example).*

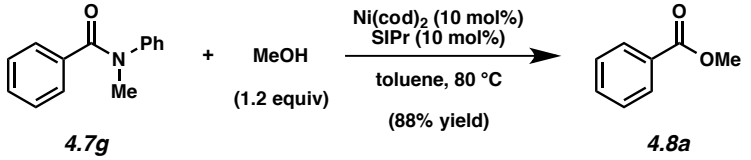

Ester 4.8a (Table 4.2a). A 1-dram vial containing amide **4.7g** (100.0 mg, 0.47 mmol, 1.0 equiv) and a magnetic stir bar was charged with $Ni(cod)_2$ (13.0 mg, 0.047 mmol, 10 mol%) and SIPr (18.4 mg, 0.047 mmol, 10 mol%) in a glove box. Subsequently, toluene (0.47 mL, 1.0 M) and then methanol (23.0 μL, 0.56 mmol, 1.2 equiv) were added. The vial was sealed with a Teflon-lined screw cap, removed from the glove box, and stirred at 80 °C for 12 h. After cooling to 23 °C, the mixture was diluted with hexanes (0.5 mL) and filtered over a plug of silica gel (10 mL of EtOAc eluent). The volatiles were removed under reduced pressure, and the crude residue was purified by flash chromatography (20:1 Hexanes:EtOAc) to yield ester product **4.8a** (88% yield, average of two experiments) as a clear oil. Ester **4.8a**: R_f 0.41 (20:1 Hexanes:EtOAc). Spectral data match those previously reported.[32]

Any modifications of the conditions shown in the representative procedure above are specified in the following schemes, which depict all of the results shown in Table 4.2.

For each of the nickel-catalyzed reactions described herein, control experiments were performed concurrently where $Ni(cod)_2$ and both $Ni(cod)_2$ and SIPr were omitted from

the reactions. In all cases, these control experiments led to the recovery of the amide substrates with no detectable conversion to the corresponding esters.

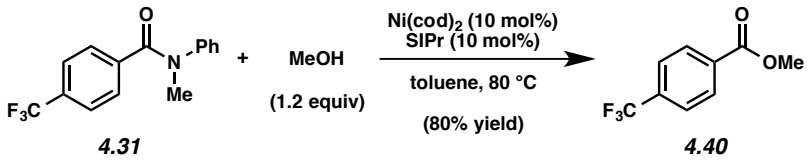

Ester 4.40 (Table 4.2a). Purification by flash chromatography (10:1 Hexanes:EtOAc) generated ester **4.40** (80% yield, average of two experiments) as a clear oil. Ester **4.40**: R_f 0.59 (10:1 Hexanes:EtOAc). Spectral data match those previously reported.[33]

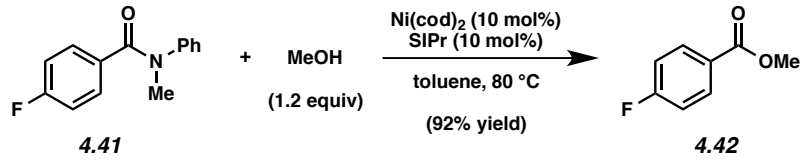

Ester 4.42 (Table 4.2a). Purification by flash chromatography (20:1 Hexanes:EtOAc) generated ester **4.42** (92% yield, average of two experiments) as a clear oil. Ester **4.42**: R_f 0.37 (20:1 Hexanes:EtOAc). Spectral data match those previously reported.[34]

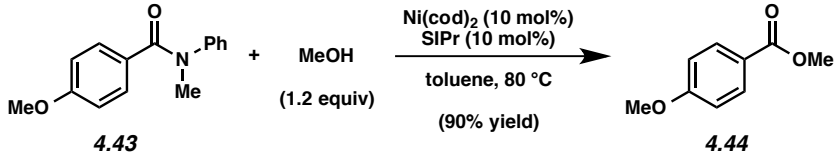

Ester 4.44 (Table 4.2a). Purification by flash chromatography (5:1 Hexanes:EtOAc) generated ester **4.44** (90% yield, average of two experiments) as a white solid. Ester **4.44**: R_f 0.59 (10:1 Hexanes:EtOAc). Spectral data match those previously reported.[35]

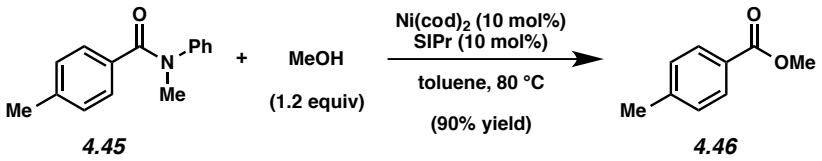

Ester 4.46 (Table 4.2a). Purification by flash chromatography (15:1 Hexanes:EtOAc) generated ester **4.46** (90% yield, average of two experiments) as a clear oil. Ester **4.46**: R_f 0.60 (20:1 Hexanes:EtOAc). Spectral data match those previously reported.[35]

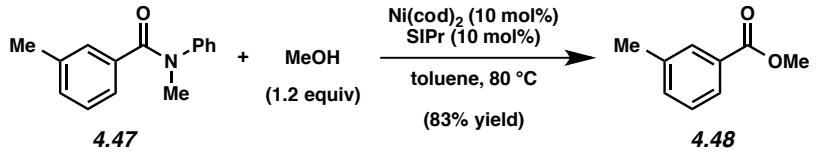

Ester 4.48 (Table 4.2a). Purification by flash chromatography (20:1 Hexanes:Et_2O) generated ester **4.48** (83% yield, average of two experiments) as a clear oil. Ester **4.48**: R_f 0.52 (15:1 Hexanes:EtOAc). Spectral data match those previously reported.[36]

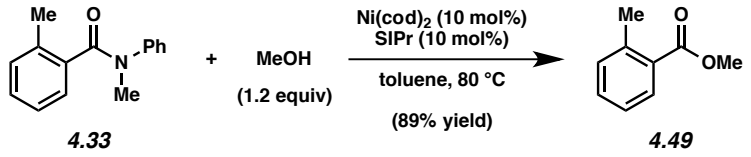

Ester 4.49 (Table 4.2a). Purification by flash chromatography (15:1 Hexanes:EtOAc) generated ester **4.49** (89% yield, average of two experiments) as a clear oil. Ester **4.49**: R_f 0.69 (15:1 Hexanes:EtOAc). Spectral data match those previously reported.[34]

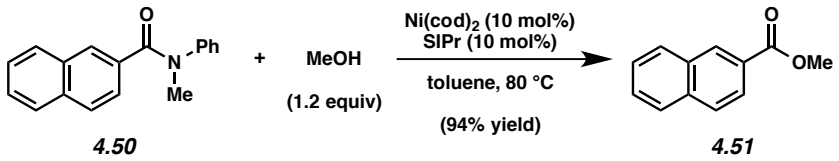

Ester 4.51 (Table 4.2a). Purification by flash chromatography (20:1 Hexanes:EtOAc) generated ester **4.51** (94% yield, average of two experiments) as a white solid. Ester **4.51**: R_f 0.69 (10:1 Hexanes:EtOAc). Spectral data match those previously reported.[37]

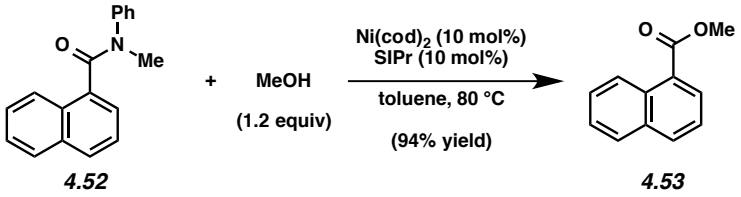

Ester 4.53 (Table 4.2a). Purification by flash chromatography (15:1 Hexanes:EtOAc) generated ester **4.53** (94% yield, average of two experiments) as a clear oil. Ester **4.53**: R_f 0.57 (15:1 Hexanes:EtOAc). Spectral data match those previously reported.[38]

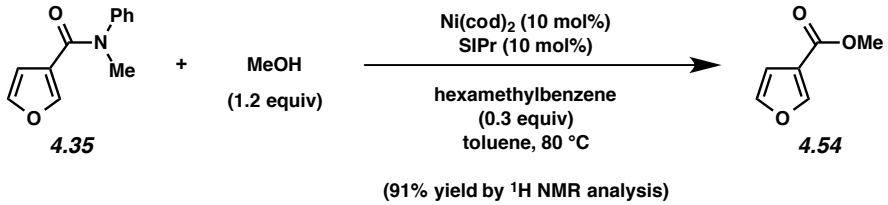

Ester 4.54 (Table 4.2a). The yield was determined by ^{1}H NMR analysis of the crude reaction mixture using hexamethylbenzene (0.3 equiv based on **4.35**) as an external standard (91% yield, average of two experiments). Ester **4.54**: ^{1}H NMR (300 MHz, $CDCl_3$): δ 8.02–8.01 (m, 1H), 7.43–7.42 (m, 1H), 6.76–6.74 (m, 1H), 3.85 (s, 3H). Spectral data of the crude mixture of ester **4.54** match those previously reported.[39]

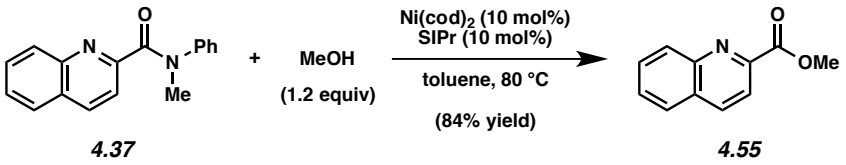

Ester 4.55 (Table 4.2a). Purification by flash chromatography (1:1 Hexanes:EtOAc) generated ester **4.55** (84% yield, average of two experiments) as a white solid. Ester **4.55**: R_f 0.39 (1:1 Hexanes:EtOAc). Spectral data match those previously reported.[40]

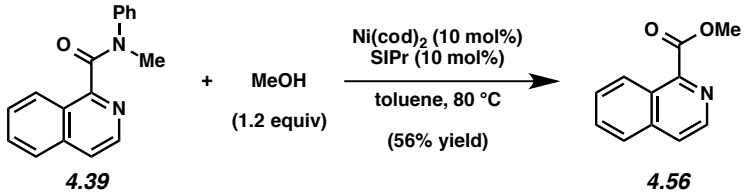

Ester 4.56 (Table 4.2a). Purification by flash chromatography (1:1 Hexanes:EtOAc) generated ester **4.56** (56% yield, average of two experiments) as a clear oil. Ester **4.56**: R_f 0.43 (1:1 Hexanes:EtOAc). Spectral data match those previously reported.[41]

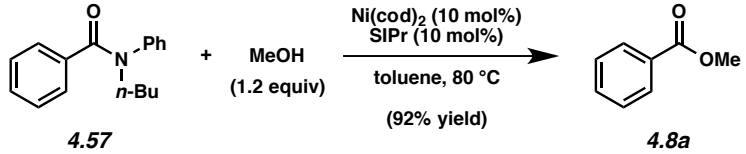

Ester 4.8a (Table 4.2a). Purification by flash chromatography (10:1 Hexanes:Et_2O) generated ester **4.8a** (92% yield, average of two experiments) as a clear oil. Ester **4.8a**: R_f 0.44 (5:1 Hexanes:EtOAc). Spectral data match those previously reported.[32]

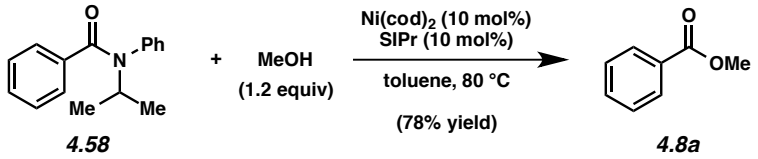

Ester 4.8a (Table 4.2a). Purification by flash chromatography (10:1 Hexanes:Et_2O) generated ester **4.8a** (78% yield, average of two experiments) as a clear oil. Ester **4.8a**: R_f 0.44 (5:1 Hexanes:EtOAc). Spectral data match those previously reported.[32]

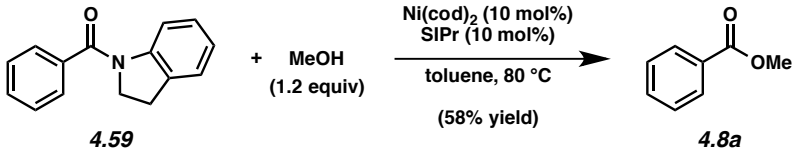

Ester 4.8a (Table 4.2a). Purification by flash chromatography (10:1 Hexanes:Et_2O) generated ester **4.8a** (58% yield, average of two experiments) as a clear oil. Ester **4.8a**: R_f 0.44 (5:1 Hexanes:EtOAc). Spectral data match those previously reported.[32]

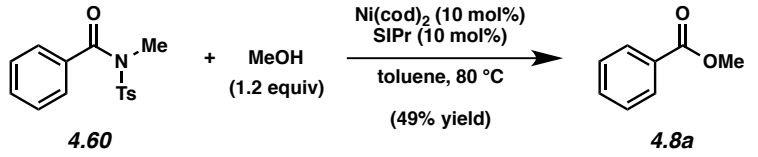

Ester 4.8a (Table 4.2a). Purification by flash chromatography (10:1 Hexanes:Et_2O) generated ester **4.8a** (49% yield, average of two experiments) as a clear oil. Ester **4.8a**: R_f 0.44 (5:1 Hexanes:EtOAc). Spectral data match those previously reported.[32]

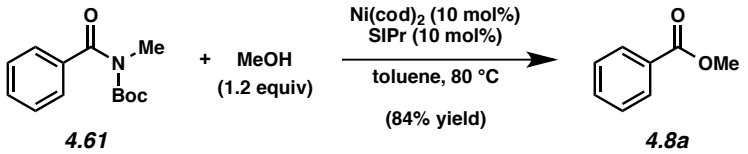

4.61 *4.8a*

Ester 4.8a (Table 4.2a). Purification by flash chromatography (10:1 Hexanes:Et_2O) generated ester **4.8a** (84% yield, average of two experiments) as a clear oil. Ester **4.8a**: R_f 0.44 (5:1 Hexanes:EtOAc). Spectral data match those previously reported.[32]

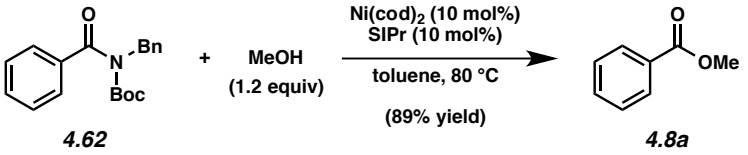

4.62 *4.8a*

Ester 4.8a (Table 4.2a). Purification by flash chromatography (10:1 Hexanes:Et_2O) generated ester **4.8a** (89% yield, average of two experiments) as a clear oil. Ester **4.8a**: R_f 0.44 (5:1 Hexanes:EtOAc). Spectral data match those previously reported.[32]

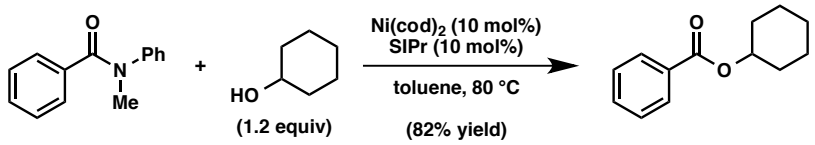

4.7g *4.63* *4.64*

Ester 4.64 (Table 4.2b). Purification by flash chromatography (100:1 Hexanes:EtOAc) generated ester **4.64** (82% yield, average of two experiments) as a clear oil. Ester **4.64**: R_f 0.59 (5:1 Hexanes:EtOAc). Spectral data match those previously reported.[42]

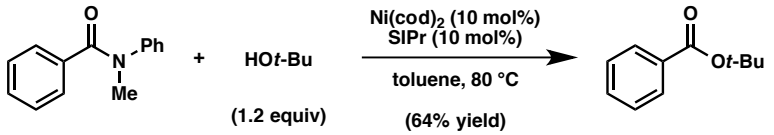

4.7g *4.65* *4.66*

Ester 4.66 (Table 4.2b). Purification by flash chromatography (100:1 Hexanes:EtOAc) generated ester **4.66** (64% yield, average of two experiments) as a clear oil. Ester **4.66**: R_f 0.71 (5:1 Hexanes:EtOAc). Spectral data match those previously reported.[43]

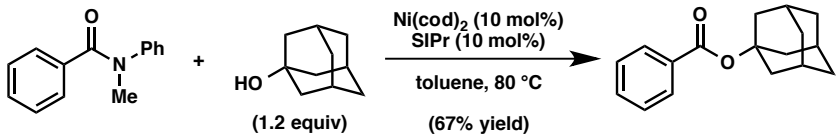

4.7g *4.67* *4.68*

Ester 4.68 (Table 4.2b). Purification by flash chromatography (100:1 Hexanes:EtOAc) generated ester **4.68** (67% yield, average of two experiments) as a clear oil. Ester **4.68**: R_f 0.76 (5:1 Hexanes:EtOAc). Spectral data match those previously reported.[44]

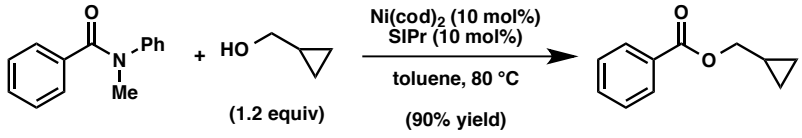

4.7g *4.69* *4.70*

Ester 4.70 (Table 4.2b). Purification by flash chromatography (20:1 Hexanes:Et_2O) generated ester **4.70** (90% yield, average of two experiments) as a clear oil. Ester **4.70**: R_f 0.88 (5:1 Hexanes:EtOAc); ^{1}H NMR (600 MHz, $CDCl_3$): δ 8.09–8.05 (m, 2H), 7.57–7.54 (m, 1H), 7.46–7.42 (m, 2H), 4.16 (d, J = 7.2, 2H), 1.30–1.23 (m, 1H), 0.64–0.57 (m, 2H), 0.41–0.32 (m, 2H), ^{13}C NMR (125 MHz, $CDCl_3$): δ 166.9, 132.9, 130.7, 129.7, 128.4,

69.8, 10.0, 3.4; IR (film): 3079, 1451, 1712, 1272, 1114 cm^{-1}; HRMS-ESI (*m/z*) $[M+H]^+$ calcd for $C_{11}H_{13}O2$, 177.09101; found 177.09057.

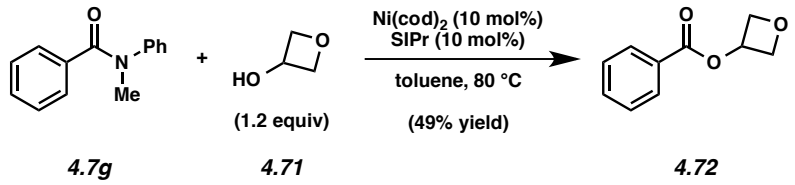

Ester 4.72 (Table 4.2b). Purification by flash chromatography (10:1 Hexanes:Et_2O) generated ester **4.72** (49% yield, average of two experiments) as a clear oil. Ester **4.72**: R_f 0.41 (5:1 Hexanes:EtOAc). Spectral data match those previously reported.[45]

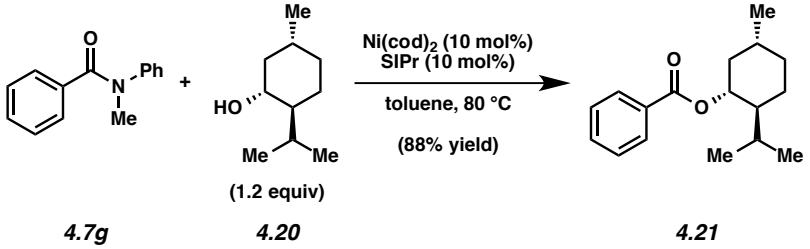

Ester 4.21 (Table 4.2b). Purification by flash chromatography (100:1 Hexanes:EtOAc) generated ester **4.21** (88% yield, average of two experiments) as a white solid. Ester **4.21**: R_f 0.59 (5:1 Hexanes:EtOAc). Spectral data match those previously reported.[46]

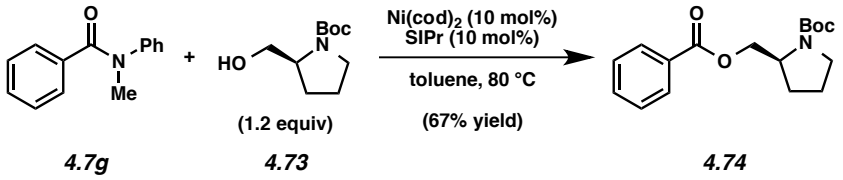

Ester 4.74 (Table 4.2b). Purification by flash chromatography (5:1 Hexanes:EtOAc) generated ester **4.74** (67% yield, average of two experiments) as a clear oil. Ester **4.74**: R_f 0.81 (5:1 Hexanes:EtOAc). Spectral data match those previously reported.[47]

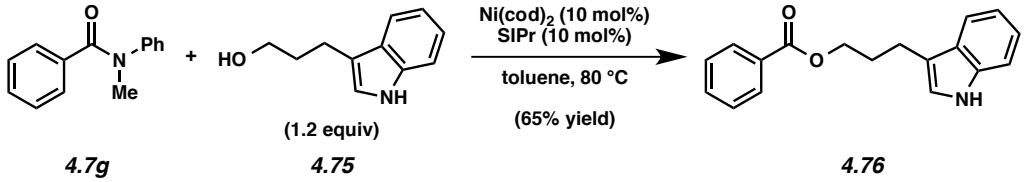

Ester 4.76 (Table 4.2b). Purification by flash chromatography (100:1 Benzene:Acetone) generated ester **4.76** (65% yield, average of two experiments) as a clear oil. Ester **4.76**: R_f 0.26 (5:1 Hexanes:EtOAc); ^{1}H NMR (500 MHz, $CDCl_3$): δ 8.06–8.03 (m, 2H), 8.00–7.90 (br s, 1H), 7.64–7.60 (m, 1H), 7.56 (tt, *J* = 7.3, 1.4, 1H), 7.48–7.42 (m, 2H), 7.37 (dt, *J* = 8.1, 0.9, 1H), 7.20 (ddd, *J* = 11.6, 7.5, 1.2, 1H), 7.12 (ddd, *J* = 11.6, 7.5, 1.2, 1H), 7.04–7.02 (m, 1H), 4.40 (t, *J* = 6.40, 2H), 2.98–2.92 (m, 2H) 2.24–2.17 (m, 2H); ^{13}C NMR (125 MHz, $CDCl_3$): δ 166.9, 136.5, 133.0, 130.6, 129.7, 128.5, 127.5, 122.2, 121.6, 119.4, 118.9. 114.5, 111.3, 64.7, 29.2, 21.8; IR (film): 3411, 2360, 1702, 1273, 1117 cm^{-1}; HRMS-ESI (*m/z*) $[M+H]^+$ calcd for $C_{18}H_{18}NO_2$, 280.13321; found 280.13204.

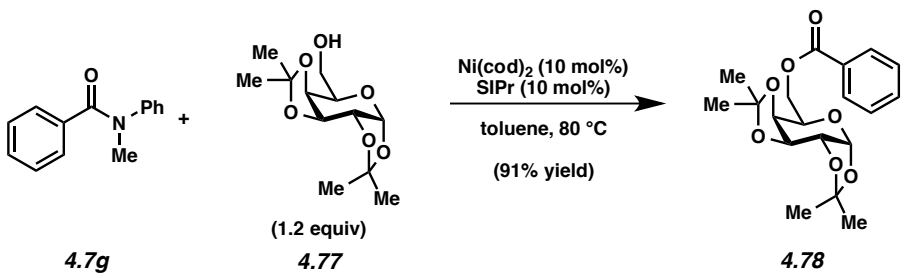

4.7g *4.77* *4.78*

Ester 4.78 (Table 4.2b). Purification by flash chromatography (10:1 Hexanes:Et_2O) generated ester **4.78** (91% yield, average of two experiments) as a clear oil. Ester **4.78**: R_f 0.25 (5:1 Hexanes:Et_2O); ^{1}H NMR (500 MHz, $CDCl_3$): δ 8.07–8.03 (m, 2H), 7.58–7.53 (m, 1H), 7.46–7.41 (m, 2H), 4.57 (d, *J* = 4.9, 1H), 4.65 (dd, *J* = 7.9, 2.5, 1H), 4.53 (dd, *J* = 11.5, 4.9, 1H), 4.43 (dd, *J* = 11.5, 7.5, 1H), 4.35 (dd, *J* = 4.0, 2.5, 1H), 4.33 (dd, *J* = 7.9, 2.0, 1H), 4.19 (ddd, *J* = 7.5, 4.0, 2.0, 1H), 1.52 (s, 3H), 1.48 (s, 3H), 1.36 (s, 3H), 1.34 (s, 3H); ^{13}C NMR (125 MHz, $CDCl_3$): δ 166.6, 133.1, 130.2, 129.9, 128.5, 109.9, 109.0, 96.5, 71.3, 70.9, 70.7, 66.3, 64.0, 26.2, 26.1, 24.1, 24.7; IR (film): 2989, 1720, 1276 1108, 1070 cm^{-1}; HRMS-ESI (*m/z*) $[M+H]^+$ calcd for $C_{19}H_{25}O_7$, 364.15948; found 364.15835; $[\alpha]^{22.0}_D$ –70.4° (*c* = 1.000, CH_2Cl_2).

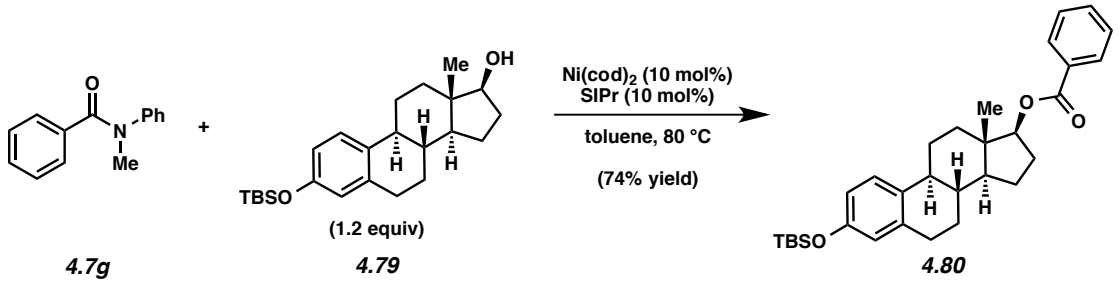

4.7g *4.79* *4.80*

Ester 4.80 (Table 4.2b). Purification by flash chromatography (100:1 Hexanes:EtOAc) generated ester **4.80** (74% yield, average of two experiments) as a clear oil. Ester **4.80**: R_f 0.67 (5:1 Hexanes:EtOAc); ^{1}H NMR (500 MHz, $CDCl_3$): δ 8.09–8.03 (m, 2H), 7.59–

7.53 (m, 1H), 7.49–7.41 (m, 2H), 7.15–7.10 (m, 1H), 6.64–6.59 (m, 1H), 6.58–6.54 (m, 1H), 4.13–4.90 (m, 1H), 2.90–2.76 (m, 2H), 2.48–2.17 (m, 3H), 2.02–1.63 (m, 5H), 1.60–1.28 (m, 6H), 0.99–0.86 (m, 11H), 0.19 (s, 6H); ^{13}C NMR (125 MHz, $CDCl_3$): δ 166.7, 166.3, 153.5, 153.5, 138.0, 137.9, 133.1, 133.1, 132.9, 131.0, 130.9, 129.7, 129.7, 128.5, 128.5, 126.3, 126.3, 120.1, 120.1, 117.3, 83.4, 82.8, 50.0, 49.7, 44.5, 44.0, 43.9, 43.5, 39.2, 38.7, 37.2, 32.3, 30.4, 29.9, 29.8, 28.2, 27.9, 27.4, 24.9, 24.6, 23.6, 18.3, 17.0, 12.5, -4.2; IR (film): 2928, 1717, 1496, 1274, 1256, 1116 cm^{-1}; HRMS-ESI (*m/z*) $[M+H]^+$ calcd for $C_{31}H_{43}O_3Si$, 491.28866; found 491.29615; $[\alpha]^{22.0}_D$ +56.2° (*c* = 1.000, CH_2Cl_2).

*Note: **4.80** was obtained as mixture of rotamers. These data represent empirically observed chemical shifts from the ^{13}C NMR spectrum.*

4.7.2.6 Selective Cleavage of Tertiary over Secondary Amide

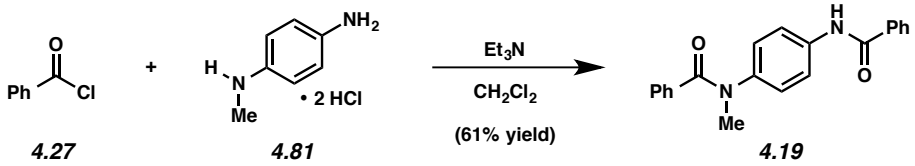

4.27 *4.81* *4.19*

Amide 4.19 (Figure 4.3a). A mixture of amine salt **4.81** (3.1 g, 16.0 mmol, 1.0 equiv), dichloromethane (96.0 mL, 0.5 M), and triethylamine (8.9 mL, 64.0 mmol, 8.9 mL) was stirred at 23 °C for 30 min. The reaction vessel was cooled to 0 °C and benzoyl chloride (**4.27**) (4.6 mL, 48.0 mmol, 3.0 equiv) was added dropwise over 15 min with stirring. The resulting heterogeneous mixture was warmed to 23 °C over 30 min and stirred for 18 h. The reaction mixture was then diluted with EtOAc (50 mL) and then washed sequentially with 1.0 M HCl (50 mL) and brine (50 mL). The organic layer was dried over Na_2SO_4

and concentrated under reduced pressure. The crude mixture was purified via flash chromatography (1:1 Hexanes:EtOAc) to give amide **4.19** (3.2 g, 61% yield) as a white solid. Amide **4.19**: R_f 0.34 (1:1 Hexanes:EtOAc); ^{1}H NMR (400 MHz, $CDCl_3$): δ 7.85–7.80 (m, 2H), 7.76 (br s, 1H), 7.58–7.44 (m, 5H), 7.34–7.30 (m, 2H), 7.25–7.22 (m, 1H), 7.21–7.15 (m, 2H), 7.05 (d, J = 8.9 Hz, 2H), 3.49 (s, 3H); ^{13}C NMR (125 MHz, $CDCl_3$): δ 170.9, 166.0, 141.0, 140.9, 136.7, 136.6, 136.0, 134.8, 132.1, 132.1, 129.8, 128.9, 128.8, 128.8, 128.0, 127.6, 127.5, 127.2, 127.2, 120.9, 120.8, 38.6; IR (film): 3299, 2971, 2245, 1737, 1625, 1602, 1578, 1509, 1372, 1316, 1292, 1244, 1101 cm^{-1}; HRMS-ESI (*m/z*) $[M+H]^+$ calcd for $C_{21}H_{19}N_2O_2$, 331.14465; found 331.14229.

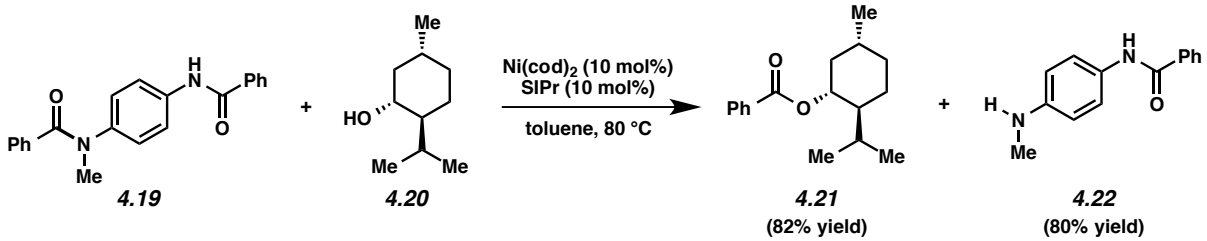

Ester 4.21 and Aminoamide 4.22 (Figure 4.3a). A 1-dram vial containing amide **4.19** (100.0 mg, 0.30 mmol, 1.0 equiv) and a magnetic stir bar was charged with $Ni(cod)_2$ (12.4 mg, 0.045 mmol, 15 mol%) and SIPr (34.2 mg, 0.045 mmol, 30 mol%) in a glove box. Subsequently, toluene (0.45 mL, 1.0 M) and then (–)-menthol (**4.20**) (56.0 mg, 0.36 mmol, 1.2 equiv) were added. The vial was sealed with a Teflon-lined screw cap, removed from the glove box, and stirred at 80 °C for 12 h. After cooling to 23 ºC, the mixture was diluted with hexanes (0.5 mL) and filtered over a plug of silica gel (10 mL of EtOAc eluent). The volatiles were removed under reduced pressure, and the crude residue was purified by flash chromatography (10:1 → 1:1 Hexanes:EtOAc) generated

ester **4.21** (82% yield, average of two experiments) as a white solid and aminoamide **4.22** (80% yield, average of two experiments) as a white solid. Ester **4.21**: R_f 0.90 (1:1 Hexanes:EtOAc). Spectral data matched those previously reported.[46] Aminoamide **4.22**: R_f 0.30 (1:1 Hexanes:EtOAc); ^{1}H NMR (500 MHz, DMSO): δ 9.89 (s, 1H), 7.93 (d, J = 7.6, 2H), 7.58–7.40 (m, 5H), 6.52 (d, J = 8.4, 2H), 4.50 (br s, 1H), 2.66 (d, J = 4.9, 3H); ^{13}C NMR (125 MHz, DMSO): δ 164.6, 146.7. 134.3, 131.1, 128.3, 128.0, 127.4, 122.2, 111.3, 30.0; IR (film): 3268, 1639, 1535, 1517, 1468, 1402, 1310, 1246, 1177, 1026 cm^{-1}; HRMS-ESI (*m/z*) $[M+H]^+$ calcd for $C_{14}H_{15}N_2O$, 227.11844; found 227.11649.

4.7.2.7 Selective Cleavage of Aryl Amide Over Alkyl Amide

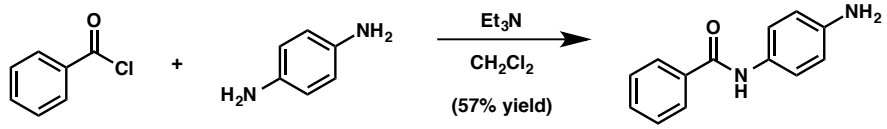

4.27 *4.82* *4.83*

Amide 4.83 (Figure 4.3b). To a solution of amine **4.82** (7.7g, 71.1 mmol, 2.0 equiv) and triethylamine (6.2 mL, 44.5 mmol, 1.25 equiv) in dichloromethane (356.0 mL, 0.1 M) was added benzoyl chloride **4.27** (4.0 g, 34.6 mL, 1.0 equiv) dropwise over 15 min. After stirring at 23 °C for 12 h, the reaction mixture was then diluted with deionized water (200 mL) and dichloromethane (200 mL). The organic layer was separated and the aqueous layer was extracted with EtOAc (3 x 500 mL). The combined organic layers were dried over $MgSO_4$ and concentrated under reduced pressure. The resulting red solid was purified by flash chromatography (1:1 Hexanes:EtOAc → 100% EtOAc) to give a white solid (4.3 g, 57% yield). Amide **4.83**: R_f 0.31 (1:1 Hexanes:EtOAc). Spectral data matched those previously reported.[48]

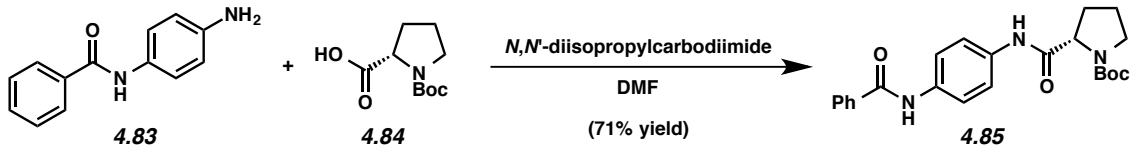

4.83 4.84 4.85

Amide 4.85 (Figure 4.3b). To a mixture of amide **4.83** (1.5 g, 7.1 mmol, 1.0 equiv) and carboxylic acid **4.84** (1.52 g, 7.1 mmol, 1.0 equiv) in dry DMF (2.7 mL, 2.6 M) at 0 °C was added *N*,*N*'-diisopropylcarbodiimide (1.3 mL, 8.5 mmol, 1.2 equiv) dropwise over 5 min. The reaction was then stirred at 0 °C for 10 min and 23 °C for 12 h. The crude reaction mixture was poured into 1:1 H_2O:MeOH solution (1 L). The resulting solid was collected to afford amide **4.85** (2.1 g, 71% yield) as a white solid. Amide **4.85**: R_f 0.69 (3:1 Acetone:Benzene); ^{1}H NMR (500 MHz, $CDCl_3$): δ 9.53 (m, 1H), 7.90–7.84 (m, 2H), 7.76 (br s, 1H), 7.65–7.52 (m, 5H), 7.52–7.46 (m, 2H), 4.59–3.18 (m, 3H), 2.68–1.74 (m, 4H), 1.50 (s, 9H), ^{13}C NMR (125 MHz, $CDCl_3$): δ 170.1, 164.7, 156.7, 134.4, 134.1, 133.8, 131.9, 128.9, 127.2, 121.2, 120.3, 81.1, 60.6, 47.4, 28.6, 27.4, 24.8; IR (film): 3295, 1668, 1515, 1405, 1308, 1162 cm^{-1}; HRMS-ESI (*m/z*) [M-H] calcd for $C_{23}H_{26}O_4N_3$, 408.19178; found 408.19340; $[\alpha]^{22.0}_D$ –50.0° (*c* = 0.100, $CHCl_3$).

*Note: **4.85** was obtained as mixture of rotamers. These data represent empirically observed chemical shifts and coupling constants from the ^{1}H NMR and ^{13}C NMR spectra.*

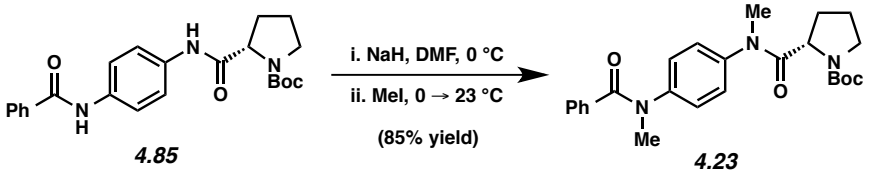

4.85 4.23

Amide 4.23 (Figure 4.3b). To a solution of amide **4.85** (300.0 mg, 0.73 mmol) in dry DMF (12.0 mL, 0.06 M) at 0 °C, was added NaH (60% in oil dispersion, 62.0 mg, 1.5 mmol, 2.1 equiv). The mixture was stirred at 0 °C for 1 h and then methyl iodide (91.0 mL, 1.5 mmol, 2.0 equiv) was added. The solution was stirred at 0 °C for an additional hour and then warmed to 23 °C over 30 min. After 14 h, the reaction was quenched with a solution of saturated aqueous NH_4Cl (5 mL) and diluted with deionized water (50 mL). The mixture was extracted with EtOAc (4 x 50 mL) and the combined organic layers were washed succesively with water (4 x 50 mL) and brine (50 mL), and then dried over $MgSO_4$. After concentration under reduced pressure, the crude residue was purified by flash chromatography (2:1 → 1:1 Hexanes:EtOAc) to provide amide **4.23** (272.0 mg, 85% yield) as a clear oil. Amide **4.23**: R_f 0.33 (1:1 Hexanes:EtOAc); ^{1}H NMR (500 MHz, $CDCl_3$): δ 7.91–7.37 (m, 1H), 7.33–7.24 (m, 2H), 7.24–7.14 (m, 6H), 4.25–3.98 (m, 1H), 3.59–3.48 (m, 3H), 3.52 (app d, J = 8.6, 1H), 3.48–3.33 (m, 1H), 3.29–3.17 (m, 3H), 2.02–1.59 (m, 4H), 1.45 (app d, J = 3.2, 9H) ^{13}C NMR (125 MHz, $CDCl_3$): δ 172.6, 172.5, 170.8, 154.5, 153.9, 144.6, 144.4, 141.7, 141.4, 134.9, 134.8, 130.1, 129.9, 128.8, 128.8, 128.5, 128.2, 127.9, 127.9, 127.2, 79.9, 79.5, 57.2, 56.9, 47.3, 47.2, 38.3, 37.8, 37.7, 31.6, 30.3, 28.8, 28.7, 24.4, 23.6, 1.2; IR (film): 2974, 2876, 1643, 1509, 1364, 1119 cm^{-1}; HRMS-ESI (*m/z*) $[M+H]^+$ calcd for $C_{25}H_{32}O_4N_3$, 438.23873; found 438.23824; $[\alpha]^{22.0}_D$ +76.0° (*c* = 0.100, $CHCl_3$).

*Note: **4.23** was obtained as mixture of rotamers. These data represent empirically observed chemical shifts and coupling constants from the ^{1}H NMR and ^{13}C NMR spectra.*

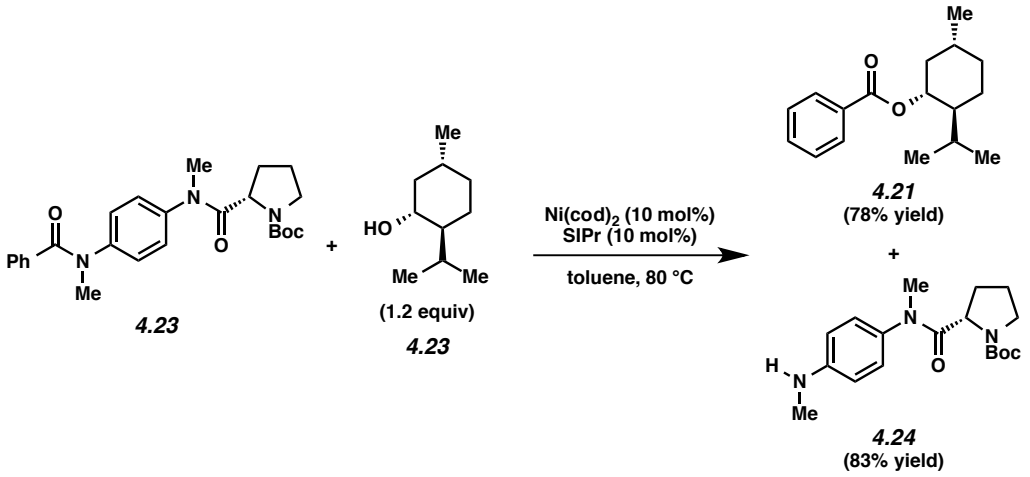

Ester 4.21 and Amine 4.24 (Figure 4.3b). A 1-dram vial containing amide **4.23** (100.0 mg, 0.23 mmol, 1.0 equiv) and a magnetic stir bar was charged with $Ni(cod)_2$ (6.3 mg, 0.023 mmol, 10 mol%) and SIPr (8.9 mg, 0.023 mmol, 10 mol%) in a glove box. Subsequently, toluene (0.23 mL, 1.0 M) and then (–)-menthol (**4.20**) (42.9 mg, 0.27 mmol, 1.2 equiv) were added. The vial was sealed with a Teflon-lined screw cap, removed from the glove box, and stirred at 80 °C for 12 h. After cooling to 23 °C, the mixture was diluted with hexanes (0.5 mL) and filtered over a plug of silica gel (10 mL of EtOAc eluent). The volatiles were removed under reduced pressure, and the crude residue was purified by flash chromatography (100:1 → 1:1 Hexanes:EtOAc) provided ester **4.21** (78% yield, average of two experiments) as a white solid and amine **4.24** (83% yield, average of two experiments) as a clear oil. Ester **4.21**: R_f 0.90 (1:1 Hexanes:EtOAc). Spectral data matched those previously reported.[46] Amine **4.24**: R_f 0.18 (1:1 Hexanes:EtOAc); ^{1}H NMR (500 MHz, $CDCl_3$): δ 7.16 (d, J = 7.5, 1H), 7.03 (d, J = 8.5, 1H), 6.63 (t, J = 8.5, 2H), 4.60–3.25 (m, 4H), 3.22 (s, 3H), 2.86 (app d, J = 7.3, 3H), 2.03–1.59 (m, 4H), 1.47 (app d, J = 14.4, 9H); ^{13}C NMR (125 MHz, $CDCl_3$): δ 128.9,

128.7, 79.6, 79.2, 57.3, 57.0, 47.4, 47.2, 38.0, 31.8, 30.9, 30.6, 28.8, 28.7, 24.4, 23.7; IR (film): 3368, 2976, 1649, 1524, 1390, 1160, 1119 cm^{-1}; HRMS-ESI (*m/z*) $[M+H]^+$ calcd for $C_{18}H_{28}N_3O_3$, 334.21252; found 334.21195; $[\alpha]^{22.0}_D$ +66.00° (*c* = 0.100, $CHCl_3$).

Note: **4.*24*** *was obtained as mixture of rotamers. These data represent empirically observed chemical shifts and coupling constants from the ^1H NMR and ^{13}C NMR spectra.*

4.7.2.8 Selective Cleavage of Aryl Amide in the Presence of an Ester

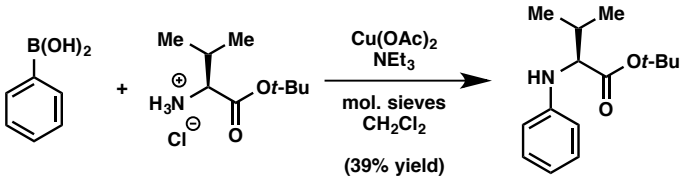

4.86 ***4.87*** ***4.26***

Amine 4.26 (Figure 4.3c). A round bottom flask was charged with 4Å molecular sieves (14.0 g, 2.0 equiv), ester **4.87** (7.0 g, 33.4 mmol, 1.0 equiv), boronic acid **4.86** (8.1 g, 66.8 mmol, 2.0 equiv), and $Cu(OAc)_2$ (6.7 g, 36.7 mmol, 1.1 equiv). The flask was evacuated by vacuum, backfilled with O_2, and then held under an O_2 atmosphere by balloon. Dichloromethane (333.0 mL, 0.1 M) and triethylamine (9.3 mL, 66.8 mmol, 2.0 equiv) were added sequentially, and the reaction mixture was stirred at 23 °C for 14 h. The reaction mixture was then quenched with a solution of ammonia in methanol (6N, 15 mL). After removing the volatiles under reduced pressure, the crude mixture was purified via flash chromatography (10:1 Hexanes:EtOAc) to give amine **4.26** as a white solid (3.2 g, 39% yield). Amide **4.26**: R_f 0.65 (5:1 Hexanes:EtOAc); ^1H NMR (500 MHz, $CDCl_3$): δ 7.18–7.13 (m, 2H), 6.71 (tt, *J* = 7.3, 1.0, 1H), 6.66–6.61 (m, 2H), 4.15 (br s, 1H), 3.75 (d,

J = 4.6, 1H), 2.15–2.05 (m, 1H), 1.42 (s, 9H), 1.03 (dd, J = 11.3, 7.0, 6H); ^{13}C NMR (125 MHz, $CDCl_3$): δ 172.9, 147.7, 129.4, 118.1, 113.8, 81.6, 63.0, 31.6, 28.2, 19.1, 18.8; IR (film): 3383, 2970, 1708, 1605, 1368, 1156 cm^{-1}; HRMS-ESI (m/z) $[M+H]^+$ calcd for $C_{15}H_{24}N_1O_2$, 250.18016; found 250.17955; $[\alpha]^{22.0}_D$ –26.00° (c = 0.100, $CHCl_3$)

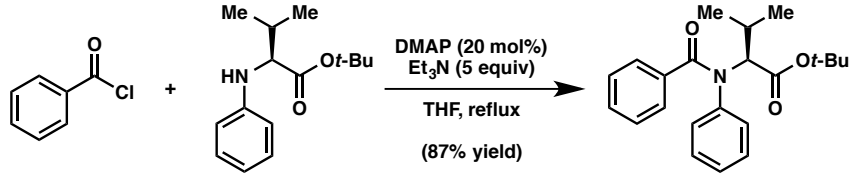

4.27 *4.26* *4.25*

Amide 4.25 (Figure 4.3c). To a solution of amine **4.26** (887 mg, 3.55 mmol) in THF (34.5 mL, 0.1 M) was added DMAP (86.7 mg, 0.71 mmol, 0.2 equiv) and triethylamine (2.46 mL, 17.75 mmol, 5 equiv). Then, benzoyl chloride (**4.27**) (2.05 mL, 17.75 mmol, 5 equiv) was added dropwise into the flask over 5 min and then refluxed. After 18 h, the reaction mixture was cooled to 23 °C, quenched with 1.0 M HCl (20 mL), extracted with EtOAc (3 X 50 mL), and dried over Na_2SO_4. The volatiles were removed under reduced pressure and the crude residue was purified via flash chromatography (30:1 Hexanes:EtOAc) to give amide **4.25** as a yellow solid (1.09 g, 87% yield). Amide **4.25**: R_f 0.43 (5:1 Hexanes:EtOAc); ^{1}H NMR (500 MHz, $CDCl_3$): δ 7.26–7.25 (m, 2H), 7.21–7.10 (m, 8H), 4.56 (d, J = 9.7, 1H), 2.59–2.56 (m, 1H), 1.43 (s, 9H), 1.09 (d, J = 6.9, 6H); ^{13}C NMR (125 MHz, $CDCl_3$): δ 170.8, 169.7, 143.2, 136.4, 129.6, 128.8, 128.7, 128.6, 127.8, 126.9, 81.6, 68.9, 28.8, 28.2, 21.4, 20.3; IR (film): 2973, 1734, 1649, 1493, 1368, 1153 cm^{-1}; HRMS-ESI (m/z) $[M+H]^+$ calcd for $C_{15}H_{24}NO_2$, 354.20692; found 354.20591; $[\alpha]^{22.0}_D$ –76.00° (c = 0.100, $CHCl_3$).

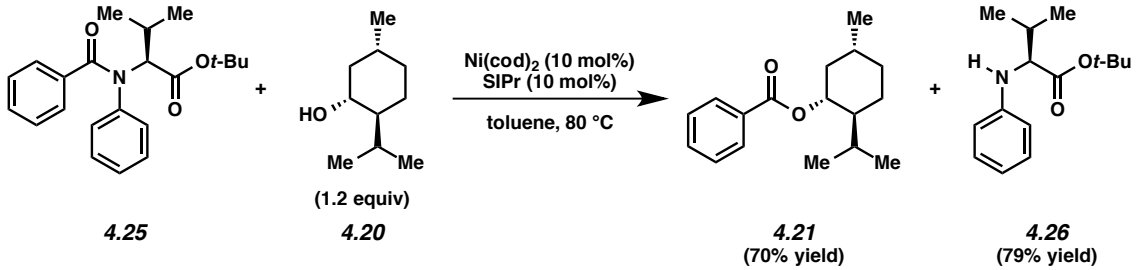

Ester 4.21 and Amide 4.26 (Figure 4.3c). A 1-dram vial containing amide **4.25** (100.0 mg, 0.28 mmol, 1.0 equiv) and a magnetic stir bar was charged with $Ni(cod)_2$ (7.8 mg, 0.028 mmol, 10 mol%) and SIPr (11.1 mg, 0.028 mmol, 10 mol%) in a glove box. Subsequently, toluene (0.28 mL, 1.0 M) and then (–)-menthol (**4.20**) (53.1 mg, 0.34 mmol, 1.2 equiv) were added. The vial was sealed with a Teflon-lined screw cap, removed from the glove box, and stirred at 80 °C for 12 h. After cooling to 23 °C, the mixture was diluted with hexanes (0.5 mL) and filtered over a plug of silica gel (10 mL of EtOAc eluent). The volatiles were removed under reduced pressure, and the crude residue was purified by flash chromatography (100:1 Hexanes:EtOAc) generated ester **4.21** (70% yield) as a white solid and amine **4.26** (79% yield) as a clear oil. Ester **4.21**: R_f 0.90 (1:1 Hexanes:EtOAc). Spectral data matched those previously reported.[46] Amide **4.26**: Spectral data of amide **4.26** matched the characterization data shown in page 229–230.

4.7.3 Verification of Enantiopurity

4.7.3.1 Racemic Compound Syntheses

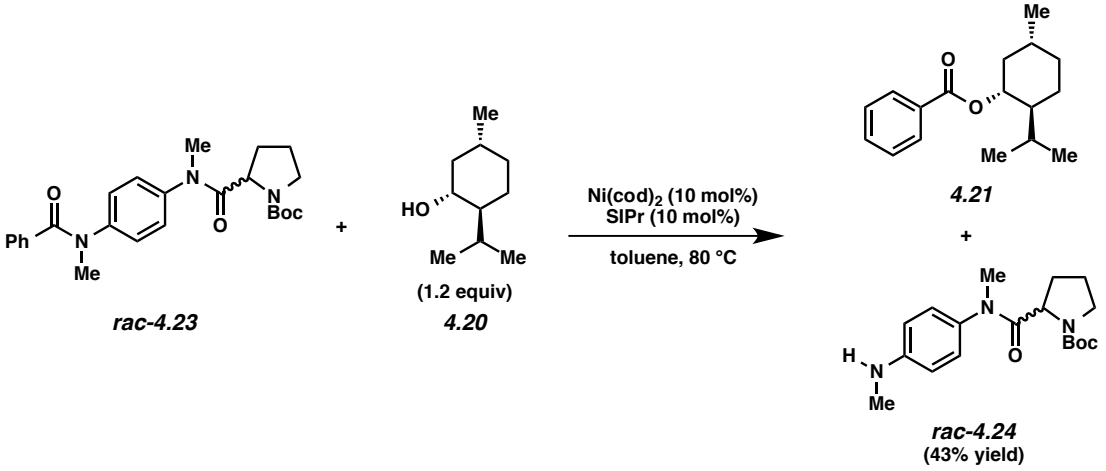

Amine rac-4.24 (Figure 4.3b). Rac-4.23 was prepared using the procedure described earlier to synthesize (+)-**4.23** (see section 4.7.2.7 Selective Cleavage of Aryl Amide Over Alkyl Amide, page 225), except using the racemic Boc-proline **4.84**. A 1-dram vial containing **rac-4.23** (40.0 mg, 0.09 mmol, 1.0 equiv) and a magnetic stir bar was charged with $Ni(cod)_2$ (3.1 mg, 0.011 mmol, 12.5 mol%) and SIPr (4.5 mg, 0.011 mmol, 12.5 mol%) in a glove box. Subsequently, toluene (0.11 mL, 0.8 M) and then (–)-menthol **4.20** (21.4 mg, 0.24 mmol, 1.5 equiv) were added. The vial was sealed with a Teflon-lined screw cap, removed from the glove box, and stirred at 80 °C for 12 h. After cooling to 23 °C, the mixture was diluted with hexanes (0.5 mL) and filtered over a plug of silica gel (10 mL of EtOAc eluent). The volatiles were removed under reduced pressure. The crude residue was purified by preparative thin-layer chromatography (1:1 Hexanes:EtOAc) to give amine **rac-4.24** (13.2 mg, 43% yield) as a clear oil. Spectral data matched those reported in the section 4.7.2.7 Selective Cleavage of Aryl Amide Over Alkyl Amide.

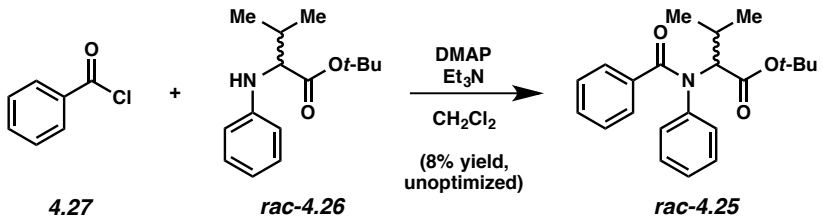

4.27 *rac-4.26* *rac-4.25*

Amide rac-4.25 (Figure 4.3c). Rac-4.26 was prepared using the procedure described earlier to synthesize (+)-**4.26** (see page 229), but using racemic ester **4.87**. A 1-dram vial containing a magnetic stir bar, aniline **rac-4.26** (20.0 mg, 0.080 mmol, 1.05 equiv), and CH_2Cl_2 (0.8 mL) was added Et_3N (14 μL, 0.10 mmol, 1.3 equiv) and benzoyl chloride (8.9 μL, 0.076 mmol). The mixture was stirred at 23 °C for 2 d and then diluted in water (25 mL). After extraction with EtOAc (4 x 25 mL), the combined organic layers were washed with brine (25 mL) and dried over $MgSO_4$. The solution was filtered and concentrated under reduced pressure. The crude residue was purified by preparative thin-layer chromatography (5:1 EtOAc:Hexanes) to give **rac-4.25** (2.2 mg, 8% yield, unoptimized) as a clear oil.

4.7.3.2 Chiral SFC Assays

Compound	Method Column /Temp	Polar Cosolvent	Method Flow Rate	Retention Times	Enantiomeric Ratio (er)
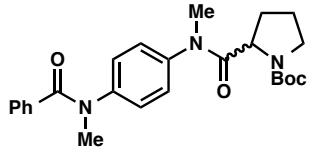 ***rac-4.23***	Daicel ChiralPak OJ-H / 35°C	7% MeOH	2.00 mL/min	4.00/4.67 min	52:48
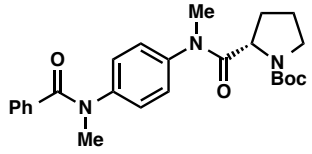 ***4.23***	Daicel ChiralPak OJ-H / 35°C	7% MeOH	2.00 mL/min	4.53/4.27 min	**96:4**
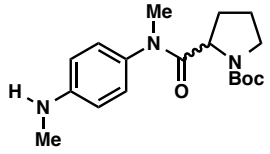 ***rac-4.25***	Daicel ChiralPak OJ-H / 35°C	15 % *i*-PrOH	1.00 mL/min	7.96/9.09 min	52:48
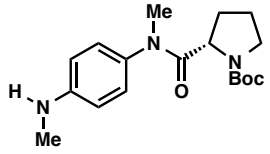 ***4.25***	Daicel ChiralPak OJ-H / 35°C	15 % *i*-PrOH	1.00 mL/min	7.60/8.78 min	**96:4**

No stereochemical erosion occurs during the nickel-catalyzed esterification.

Date:12/16/2014
Sample:nfn-6-199b-bbb1
Method Name:NOT DEFINED
Run Info:N.A.

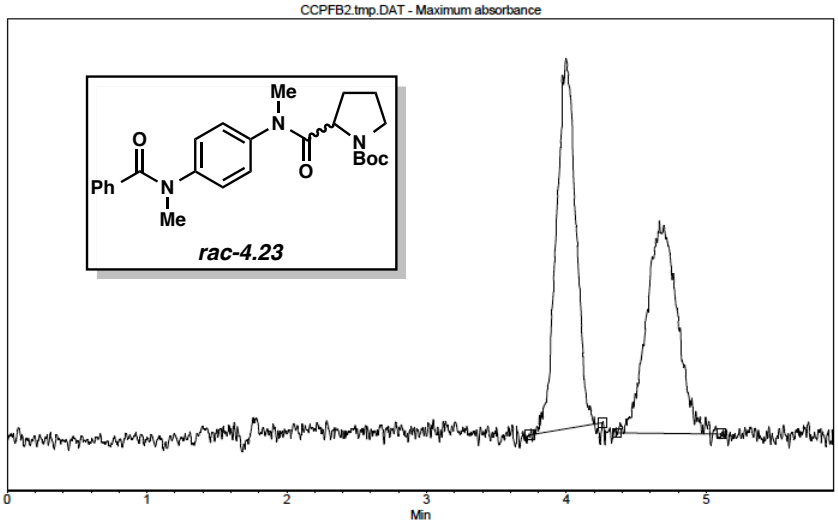

Index	Name	Start	Time	End	RT Offset	Quantity	Height	Area	Area
		[Min]	[Min]	[Min]	[Min]	[% Area]	[µV]	[µV.Min]	[%]
1	UNKNOWN	3.74	4.00	4.26	0.00	52.37	119.3	19.2	52.367
2	UNKNOWN	4.36	4.67	5.11	0.00	47.63	68.6	17.5	47.633
Total						100.00	187.9	36.7	100.000

Date:12/16/2014
Sample:nfn-6-107b1
Method Name:OJiso7%MeOH
Run Info:N.A.

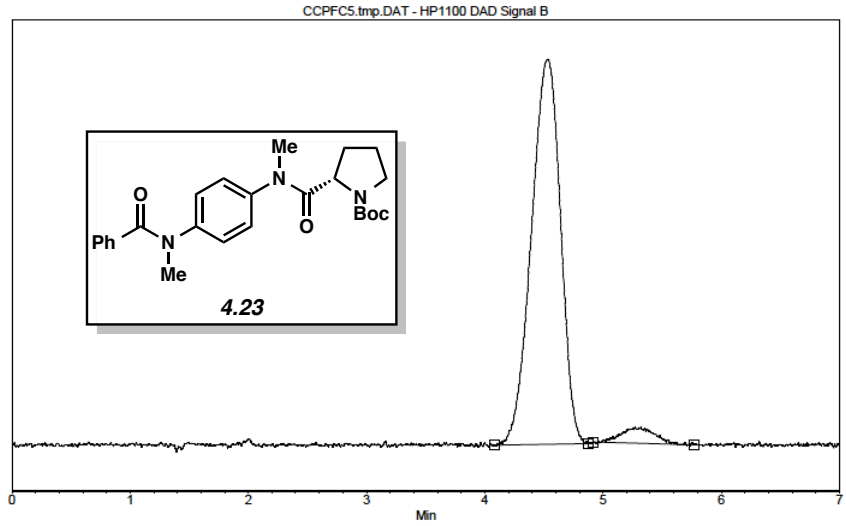

Index	Name	Start	Time	End	RT Offset	Quantity	Height	Area	Area
		[Min]	[Min]	[Min]	[Min]	[% Area]	[µV]	[µV.Min]	[%]
1	UNKNOWN	4.08	4.53	4.87	0.00	95.57	311.2	89.1	95.569
2	UNKNOWN	4.92	5.27	5.77	0.00	4.43	13.3	4.1	4.431
Total						100.00	324.5	93.2	100.000

Date:12/16/2014
Sample:nfn-6-197b-71
Method Name:OJiso15%iPrOH-A
Run Info:N.A.

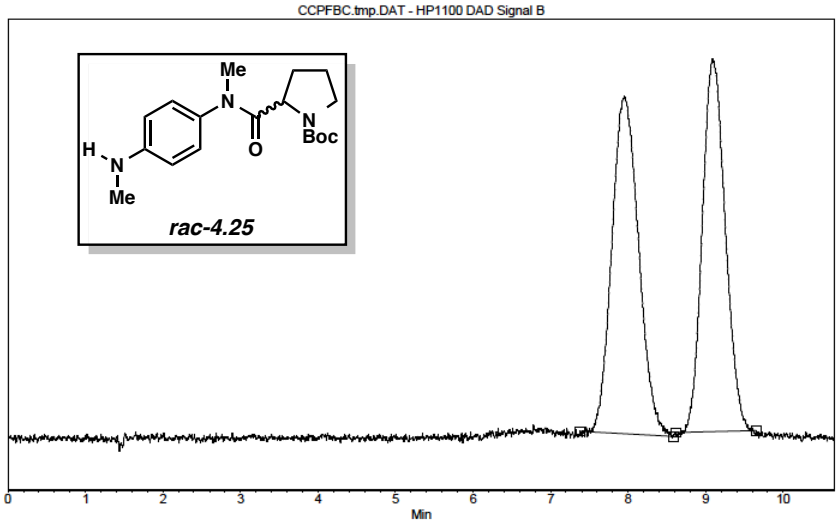

Index	Name	Start	Time	End	RT Offset	Quantity	Height	Area	Area
		[Min]	[Min]	[Min]	[Min]	[% Area]	[µV]	[µV.Min]	[%]
1	UNKNOWN	7.38	7.96	8.59	0.00	51.46	112.9	45.2	51.463
2	UNKNOWN	8.61	9.09	9.65	0.00	48.54	124.9	42.7	48.537
Total						100.00	237.8	87.9	100.000

Date:12/16/2014
Sample:nfn-6-197b-61
Method Name:OJiso15%iPrOH-A
Run Info:N.A.

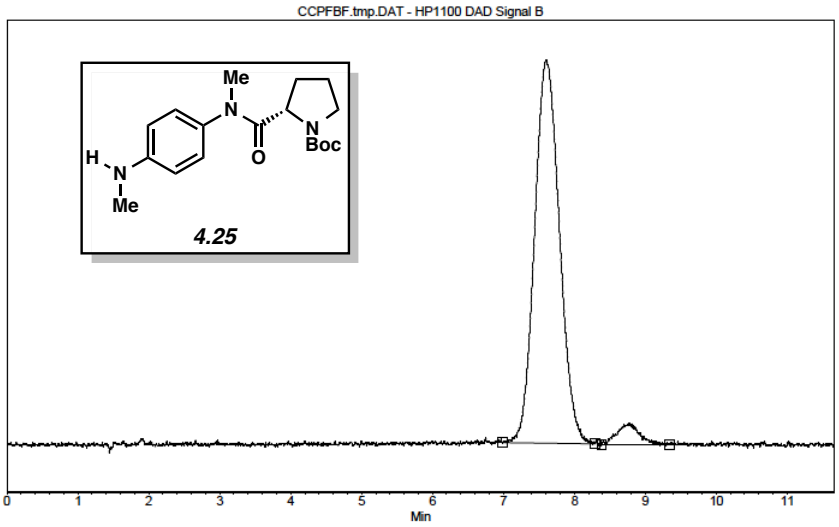

Index	Name	Start	Time	End	RT Offset	Quantity	Height	Area	Area
		[Min]	[Min]	[Min]	[Min]	[% Area]	[µV]	[µV.Min]	[%]
1	UNKNOWN	6.99	7.60	8.29	0.00	95.51	208.2	84.5	95.512
2	UNKNOWN	8.39	8.78	9.35	0.00	4.49	11.3	4.0	4.488
Total						100.00	219.5	88.5	100.000

Compound	Method Column /Temp	Polar Cosolvent	Method Flow Rate	Retention Times	Enantiomeric Ratio (er)
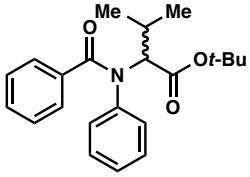 ***rac-4.26***	Daicel ChiralPak OJ-H / 35°C	0.5 % MeOH	0.5 mL/min	12.24/13.55 min	50:50
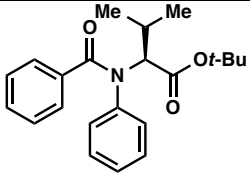 ***4.26***	Daicel ChiralPak OJ-H / 35°C	0.5 % MeOH	0.5 mL/min	12.23 min	**100:0**
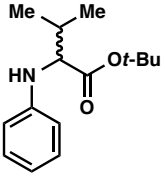 ***rac-4.27***	Daicel ChiralPak OJ-H / 35°C	5 % *i*-PrOH	2.00 mL/min	4.73/4.95 min	50:50
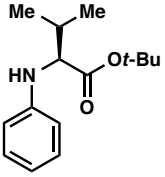 ***4.27***	Daicel ChiralPak OJ-H / 35°C	5 % *i*-PrOH	2.00 mL/min	4.77/4.99 min	**98:2**

Minimal stereochemical erosion during the nickel-catalyzed esterification was observed.

Date:12/16/2014
Sample:nfn-6-201f-bb1
Method Name:OJiso.5iPrOH
Run Info:N.A.

CCPFAB.tmp.DAT - HP1100 DAD Signal B

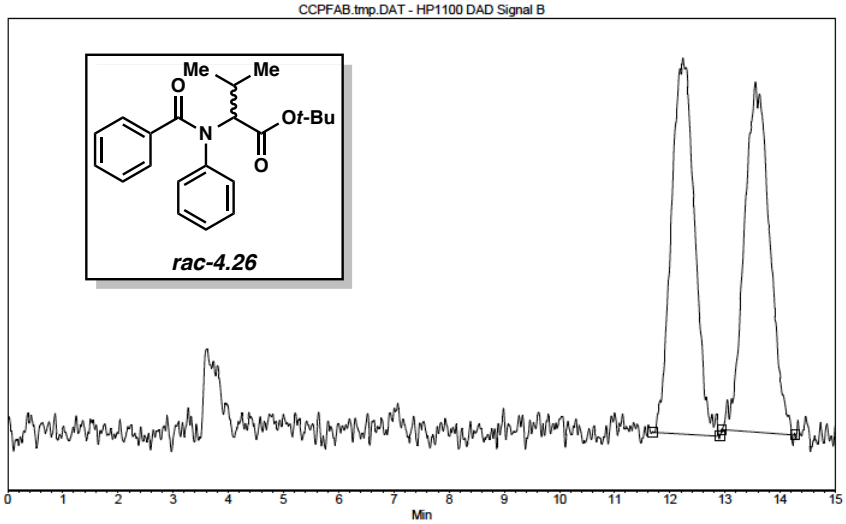

Index	Name	Start	Time	End	RT Offset	Quantity	Height	Area	Area
		[Min]	[Min]	[Min]	[Min]	[% Area]	[µV]	[µV.Min]	[%]
1	UNKNOWN	11.70	12.24	12.91	0.00	49.67	91.0	44.6	49.672
2	UNKNOWN	12.94	13.55	14.28	0.00	50.33	84.6	45.2	50.328
Total						100.00	175.6	89.8	100.000

Date:12/16/2014
Sample:nfn-6-171a-k0
Method Name:OJisopoint5flow1-3
Run Info:N.A.

CCPFAF.tmp.DAT - HP1100 DAD Signal B

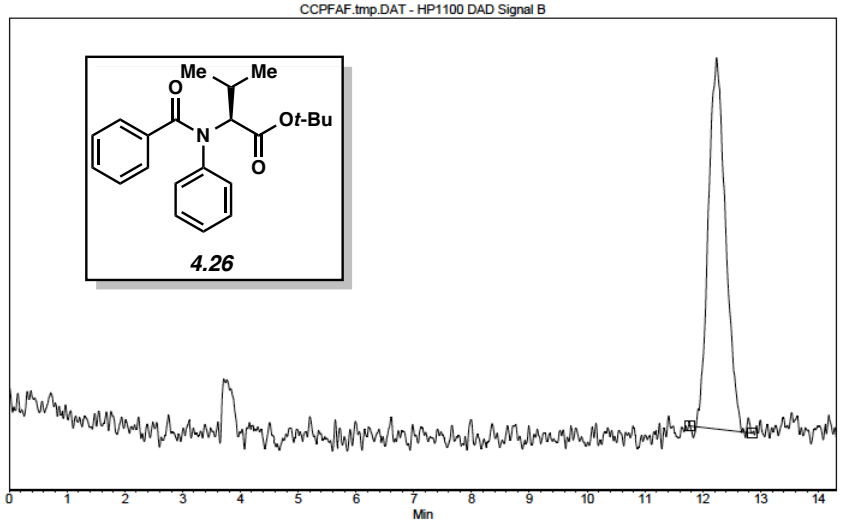

Index	Name	Start	Time	End	RT Offset	Quantity	Height	Area	Area
		[Min]	[Min]	[Min]	[Min]	[% Area]	[µV]	[µV.Min]	[%]
1	UNKNOWN	11.78	12.23	12.85	0.00	100.00	100.4	34.7	100.000
Total						100.00	100.4	34.7	100.000

Date:12/16/2014
Sample:NFN-6-195bb1
Method Name:NOT DEFINED
Run Info:N.A.

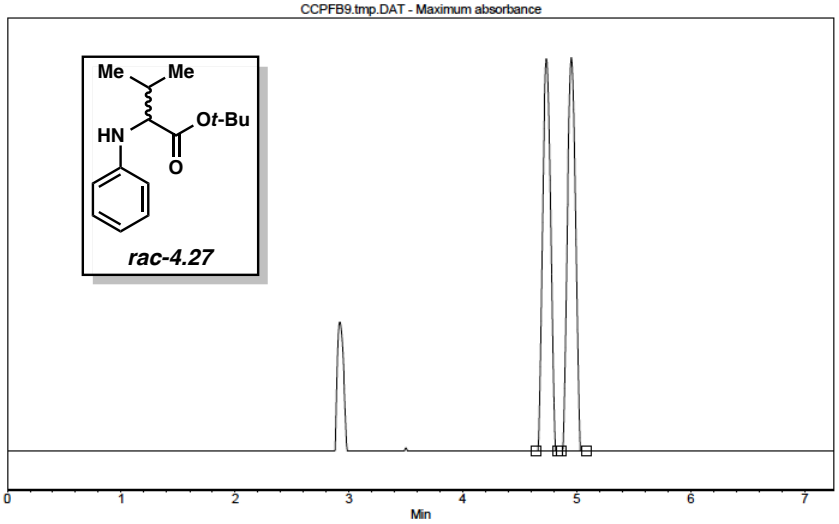

Index	Name	Start	Time	End	RT Offset	Quantity	Height	Area	Area
		[Min]	[Min]	[Min]	[Min]	[% Area]	[µV]	[µV.Min]	[%]
1	UNKNOWN	4.64	4.73	4.83	0.00	49.64	137.3	11.2	49.644
2	UNKNOWN	4.87	4.95	5.09	0.00	50.36	137.6	11.3	50.356
Total						100.00	274.9	22.5	100.000

Date:12/16/2014
Sample:nfn-6-195rrr1
Method Name:NOT DEFINED
Run Info:N.A.

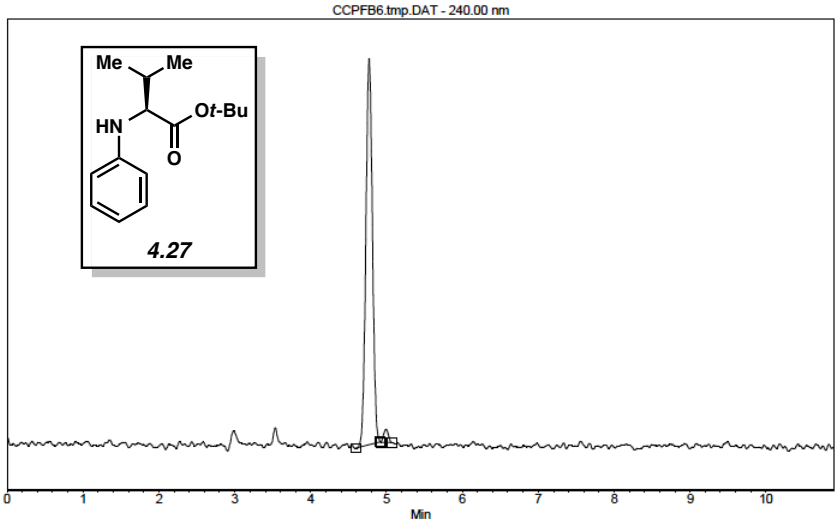

Index	Name	Start	Time	End	RT Offset	Quantity	Height	Area	Area
		[Min]	[Min]	[Min]	[Min]	[% Area]	[µV]	[µV.Min]	[%]
1	UNKNOWN	4.59	4.77	4.92	0.00	97.64	509.0	50.9	97.643
2	UNKNOWN	4.93	4.99	5.07	0.00	2.36	17.4	1.2	2.357
Total						100.00	526.4	52.2	100.000

4.7.4 Computational Methods

All the calculations were carried out with the Gaussian 09 package. Geometry optimizations were performed with B3LYP.[49] The LANL2DZ basis set[50] with ECP was used for Ni, and the 6-31G(d) basis set[51] was used for other atoms. Frequency analysis was conducted at the same level of theory to verify the stationary points to be minima or saddle points. The single-point energies and solvent effects in toluene were computed with M06[52]/SDD[53]-6-311+G(d,p) basis sets by using SMD solvation model.[54] Computed structures are illustrated using CYLView.[55]

4.7.4.1 Complete Reference of Gaussian 09

Frisch, M. J.; Trucks, G. W.; Schlegel, H. B.; Scuseria, G. E.; Robb, M. A.; Cheeseman, J. R.; Scalmani, G.; Barone, V.; Mennucci, B.; Petersson, G. A.; Nakatsuji, H.; Caricato, M.; Li, X.; Hratchian, H. P.; Izmaylov, A. F.; Bloino, J.; Zheng, G.; Sonnenberg, J. L.; Hada, M.; Ehara, M.; Toyota, K.; Fukuda, R.; Hasegawa, J.; Ishida, M.; Nakajima, T.; Honda, Y.; Kitao, O.; Nakai, H.; Vreven, T.; Montgomery, Jr., J. A.; Peralta, J. E.; Ogliaro, F.; Bearpark, M.; Heyd, J. J.; Brothers, E.; Kudin, K. N.; Staroverov, V. N.; Keith, T.; Kobayashi, R.; Normand, J.; Raghavachari, K.; Rendell, A.; Burant, J. C.; Iyengar, S. S.; Tomasi, J.; Cossi, M.; Rega, N.; Millam, J. M.; Klene, M.; Knox, J. E.; Cross, J. B.; Bakken, V.; Adamo, C.; Jaramillo, J.; Gomperts, R.; Stratmann, R. E.; Yazyev, O.; Austin, A. J.; Cammi, R.; Pomelli, C.; Ochterski, J. W.; Martin, R. L.; Morokuma, K.; Zakrzewski, V. G.; Voth, G. A.; Salvador, P.; Dannenberg, J. J.; Dapprich, S.; Daniels, A. D.; Farkas, O.; Foresman, J. B.; Ortiz, J. V.; Cioslowski, J.; Fox, D. J. *Gaussian 09, Rev. D.01*; Gaussian, Inc., Wallingford, CT, **2010**.

4.7.4.2 Transition State Structures for Decarbonylation Pathway

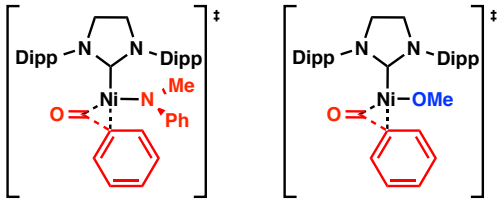

4.88
28.6 kcal/mol

4.89
24.1 kcal/mol

4.7.4.3 Comparison of Acyl C–N and Aryl C–N Bond Activation Pathway

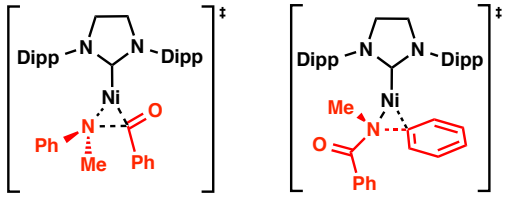

4.11
26.0 kcal/mol

4.90
35.3 kcal/mol

*Calculations were performed on the competing aryl C–N bond cleavage transition state. Transition state **4.90** was found to be 9.3 kcal/mol higher compared to the barrier for acyl C–N bond cleavage, via **4.11**.*

4.7.4.4 Analysis of Amides Derived from Alkyl Carboxylic Acids

We have performed computations involving two additional substrates (Table 4.5): *N*-Me-*N*-phenylacetamide (**4.91**) and *N*,*N*-dimethylacetamide (**4.93**). In the case of *N*-Me-*N*-phenylacetamide, the oxidative addition barrier (transition state **4.92**) was found to be 31.8 kcal/mol with respect to the $Ni(SIPr)_2$ resting state. Similarly, for *N*,*N*-dimethylacetamide, the oxidative addition barrier (transition state **4.94**) was found to be 36.7 kcal/mol with respect to the $Ni(SIPr)_2$ resting state. These high kinetic barriers are likely responsible for the inability of alkyl carboxylic acids to participate in our nickel-catalyzed esterifications. Also, in the case of substrate **4.93**, the amide to methyl ester conversion is not energetically favorable.

Table 4.5. Comparison of Aryl vs. Alkyl Amide Substrates.

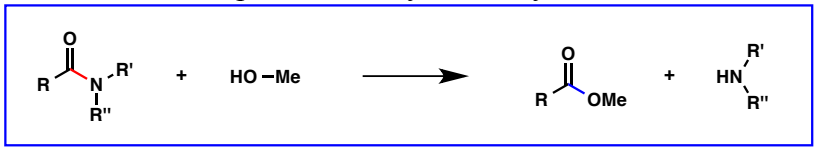

Entry	*Amide*		*Calculated ΔG (kcal/mol)*	*Calculated oxidative addition barrier with Ni /SIPr (kcal/mol)*
1	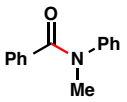	*4.7g*	–6.8	26.0 (see 5.11)
2	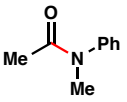	*4.91*	–3.6	31.8 (see 5.92)
3	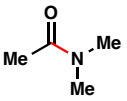	*4.93*	+2.3	36.7 (see 5.94)

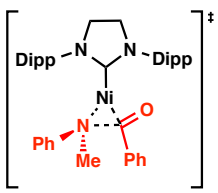

4.11
26.0 kcal/mol

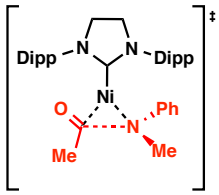

4.92
31.8 kcal/mol

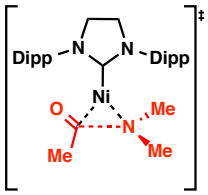

4.94
36.7 kcal/mol

4.7.4.5 Analysis of *N*-Me,Boc Amide Esterification

The calculations show that the desired esterification of substrate **4.95** with MeOH is thermodynamically favorable by 14.7 kcal/mol (Figure 4.4.). The oxidative addition transition state (transition state **4.97**) was found to be 29.0 kcal/mol with respect to the $Ni(SIPr)_2$ resting state. We have also performed computations of a plausible competitive process involving cleavage of the carbamate acyl C–N bond. This transformation is also thermodynamically favorable (11.5 kcal/mol). However, the oxidative addition barrier (transition state **4.99**) was found to be 36.9 kcal/mol with respect to the $Ni(SIPr)_2$ resting state. Accordingly, carbamate C–N bond cleavage is not observed and the desired esterification occurs smoothly.

Figure 4.4. Analysis of Competing Pathways for Esterification of *N*-Me,Boc Substrate **4.95**.

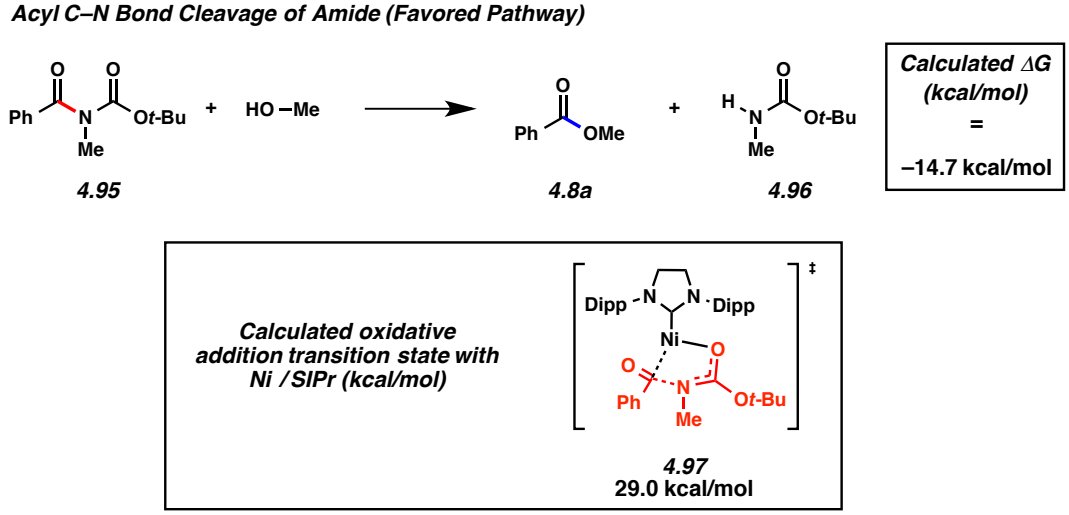

4.7.4.6 Free Energy and Enthalpy of Amide and Ester Formation

Figure 4.5 shows how substituents effect the equilibrium of amide esterification. We performed DFT calculations on the reaction enthalpies and free energies of the esterification of four amides, for which the experimental enthalpy of formation data are available. The enthalpies of reaction are also calculated using experimental enthalpy of formation data in the gas phase ($\Delta_r H$(gas)) and in the condensed phase ($\Delta_r H$(cond.)).[56] Interestingly, the esterification reaction is significantly more endothermic if condensed phase enthalpy of formation data were used. One of the major factors that contribute to this deviation is the greater intermolecular stabilizing forces in neat methanol liquid. The equilibrium of reaction (b) in methanol has been investigated by Guthrie *et al*.[57] The standard free energy of reaction derived from equilibrium constant ($\Delta_r G$(methanol)) and the standard enthalpy of reaction in methanol solution derived from enthalpies of solution data both indicate the amide esterification is less endothermic than the prediction by $\Delta_r H$(cond.). Based on these considerations, we postulate that the gas phase thermodynamic data ($\Delta_r H$(gas)) would better represent the experimental conditions with the non-polar toluene solvent. Unfortunately, the gas phase enthalpies of formation for amides **4.100** and **4.105** are not available, and were derived from liquid and solid phase enthalpies of formation and enthalpies of vaporization and sublimation, respectively. Thus, larger experimental errors are expected for $\Delta_r H$(gas) of reactions (a) and (d).

The DFT calculations with the SMD solvation model in toluene (1.0 M, 298 K) predicted very close reaction enthalpies compared to $\Delta_r H$(gas) for reactions (b) and (c). Larger deviations from $\Delta_r H$(gas) were obtained for (a) and (d), which may be attributed to the greater experimental error as described above. Thus, the DFT predicted enthalpies

of reactions ($\Delta_r H$(calc)) are used to analyze the substituent effects. Phenyl substitution at the carbonyl and N position significantly favors the esterification (a vs. b and c vs. d), while the esterification of *N*-methylacetamide is much less favorable than that of *N,N*-dimethylacetamide. This further confirms the expectation that mostly the reverse reaction (i.e. amidation) should be favorable, but the judicious use of varied substrates can perturb the equilibrium.

Figure 4.5. Substitution Effects on Equilibrium of Amide Esterification

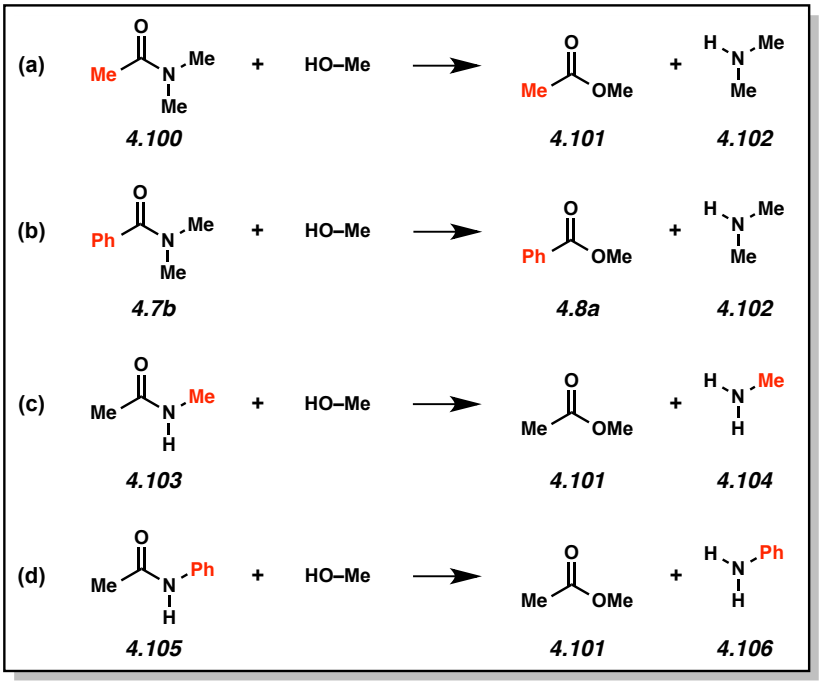

Reaction	$\Delta_r H$(gas)[a]	$\Delta_r H$(cond.)[d]	$\Delta_r H$(methanol)[e]	$\Delta_r G$(methanol)[f]	$\Delta_r H$(calc.)[g]	$\Delta_r G$(calc.)[g]
(a)	+4.3[b]	+11.4			+2.3	+2.3
(b)	-0.3	+10.6	+3.6	+3.3	0.0	0.0
(c)	+3.8	+14.0			+3.4	+3.9
(d)	+0.2[c]	+8.0			-3.0	-2.6

[a] Yields were determined by ^{1}H NMR analysis using hexamethylbenzene as an internal standard. [a] Reaction enthalpy calculated using gas phase standard enthalpy of formation data.[56] [b] Gas phase enthalpy of formation for the amide **4.100** is calculated from liquid phase standard enthalpy of formation and enthalpy of vaporization.[56] [c] Gas phase enthalpy of formation for the amide **4.105** is calculated from solid phase standard enthalpy of formation and enthalpy of sublimation.[56] [d] Reaction enthalpy calculated using condensed phase standard enthalpy of formation data. Solid phase enthalpies of formation were used for amides **4.7b** and **4.104.** Liquid phase enthalpies of formation were used for other compounds.[56] [e] Reaction enthalpy calculated from enthalpies of reaction and solution.[57] [f] Reaction free energy derived from the equilibrium constant of ester aminolysis in methanol.[57] [g] Energies are calculated with M06/6-311+G(d,p)/SMD(toluene)//B3LYP/6-31G(d). [h] All energies are in kcal/mol.

4.7.4.7 Energies, Enthalpies, and Free Energy of the Calculated Structures

Table 4.6. Energies, enthalpies, and free energies of the structures calculated at the M06/SDD, 6-311+G(d,p)(SMD^{toluene})//B3LYP/LANL2DZ,6-31G(d)

Structures	ZPE	DE	DH	DG	E	H	G	Imaginary	DDG
MeOH	0.051473	0.054761	0.055705	0.028756	-114.691065	-114.63536	-114.662309	—	—
4.4a	0.130353	0.135268	0.136212	0.102291	-212.479801	-212.343589	-212.377510	—	—
4.4b	0.093028	0.097390	0.098334	0.067601	-134.098988	-134.000654	-134.031387	—	—
4.4c	0.135967	0.141254	0.142199	0.107525	-287.686445	-287.544246	-287.578920	—	—
4.4d	0.097148	0.102641	0.103585	0.069012	-210.253121	-210.149536	-210.184109	—	—
4.4e	0.064450	0.067831	0.068775	0.041555	-94.816309	-94.747534	-94.774754	—	—
4.4f	0.117436	0.123214	0.124158	0.088289	-287.465710	-287.341552	-287.377421	—	—
4.4g	0.145946	0.153153	0.154097	0.114653	-326.747411	-326.593314	-326.632758	—	—
4.7a	0.221898	0.232888	0.233832	0.184277	-556.741196	-556.507364	-556.556919	—	—
4.7b	0.184539	0.195044	0.195988	0.148064	-479.354994	-479.159006	-479.206930	—	—
4.7c	0.227243	0.238874	0.239819	0.188374	-631.941051	-631.701232	-631.752677	—	—
4.7d	0.188279	0.199798	0.200742	0.150388	-554.500325	-554.299583	-554.349937	—	—
4.7e	0.156359	0.165575	0.166519	0.121160	-440.076464	-439.909945	-439.955304	—	—
4.7f	0.209470	0.221355	0.222299	0.169869	-631.715959	-631.493660	-631.546090	—	—
4.7g	0.237383	0.250756	0.2517	0.195805	-670.987803	-670.736103	-670.791998	—	—
4.7a_TS	0.817159	0.862147	0.863091	0.73669	-1888.379615	-1887.516524	-1887.642925	-221.285	**36.8**
4.7b_TS	0.779705	0.824113	0.825057	0.700324	-1810.994261	-1810.169204	-1810.293937	-243.236	**36.2**
4.7c_TS	0.822386	0.868066	0.869011	0.741075	-1963.584228	-1962.715217	-1962.843153	-192.983	**34.0**
4.7d_TS	0.78317	0.828976	0.82992	0.701265	-1886.145139	-1884.315219	-1884.443874	-144.322	**31.9**
4.7e_TS	0.751675	0.79476	0.795704	0.673483	-1771.711376	-1770.915672	-1771.037893	-264.940	**39.0**
4.7f_TS	0.805092	0.850906	0.85185	0.722942	-1963.364955	-1962.513105	-1962.642013	-234.989	**30.6**
4.7g_TS (4.11)	0.832519	0.880023	0.880968	0.749155	-2002.644449	-2001.763481	-2001.895294	-226.879	**26.0**
4.8a	0.144145	0.152933	0.153878	0.109776	-459.947621	-459.793743	-459.837845	—	—
4.9	1.194703	1.259623	1.260567	1.092339	-2492.357024	-2491.096457	-2491.264685	—	**0.0**
4.10	0.834665	0.882315	0.883259	0.750844	-2002.668552	-2001.785293	-2001.917708	—	**12.0**
4.11	0.832519	0.880023	0.880968	0.749155	-2002.644449	-2001.763481	-2001.895294	-226.879	**26.0**
4.12	0.833357	0.881423	0.882367	0.749078	-2002.661012	-2001.778645	-2001.911934	—	**14.6**
4.13	0.887528	0.939803	0.940747	0.797540	-2118.365280	-2117.424533	-2117.567740	—	**19.6**
4.14	0.884746	0.935623	0.936567	0.799931	-2118.359517	-2117.422950	-2117.559586	-880.974	**24.8**
4.15	0.890480	0.941197	0.942141	0.806427	-2118.370107	-2117.427966	-2117.563680	—	**22.2**
4.16	0.740176	0.783680	0.784625	0.661525	-1791.602890	-1790.818265	-1790.941365	—	**14.7**
4.17	0.740041	0.782667	0.783611	0.662388	-1791.591727	-1790.808116	-1790.929339	-178.698	**23.2**
4.18	0.741023	0.784452	0.785396	0.661905	-1791.625676	-1790.840280	-1790.963771	—	**1.6**
4.88	0.831324	0.878890	0.879834	0.749575	-2002.640735	-2001.760901	-2001.891160	24.100	**28.6**

4.89	0.738576	0.781652	0.782596	0.660871	-1791.588769	-1790.806173	-1790.927898	-141.606	**24.1**
4.90	0.832584	0.880133	0.881077	0.747983	-2000.935468	-2000.934524	-2001.067618	-284.50	**34.3**
4.92	0.780187	0.824315	0.825259	0.702244	-1810.187123	-1810.186179	-1810.309194	-262.54	**31.8**
4.94	0.726324	0.767748	0.768692	0.651647	-1617.596856	-1617.595911	-1617.712957	-261.49	**36.7**
4.95	0.283512	0.300766	0.30171	0.237711	-784.774018	-784.472308	-784.536307	—	—
4.96	0.192446	0.203738	0.204682	0.15551	-441.544868	-441.340186	-441.389358	—	—
4.97	0.878983	0.930354	0.931298	0.791429	-2117.431420	-2116.500122	-2116.639991	-127.940	**29.0**
4.98	0.180461	0.191201	0.192146	0.144843	-461.411697	-461.219551	-461.266854	—	—
4.99	0.879394	0.930259	0.931203	0.793358	-2117.420778	-2116.489575	-2116.627420	-181.425	**36.9**

4.7.4.8 Cartesian Coordinates for the Optimized Structures.

Cartesian coordinates for the optimized structures have been reported.[58]

Appendix Four: Spectra Relevant to Chapter Four

Conversion of Amides to Esters by the Nickel-Catalyzed Activation of Amide C–N Bonds

Liana Hie, Noah F. Fine Nathel, Tejas K. Shah, Emma L. Baker, Xin Hong, Yun-Fang Yang, Peng Liu, K. N. Houk & Neil K. Garg

Nature **2015**, *524*, 79–83.

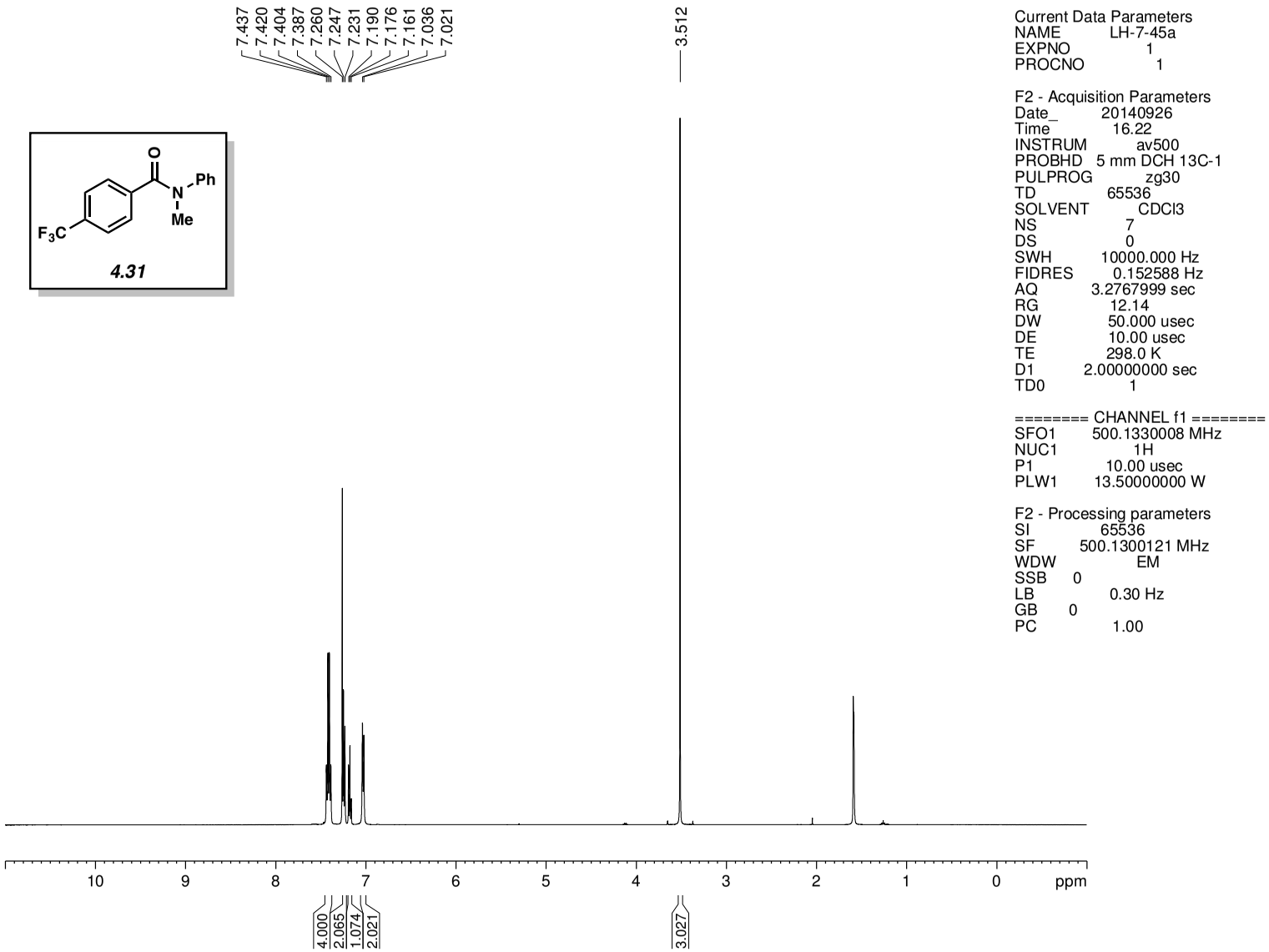

Figure A4.1 ^{1}H NMR (500 MHz, $CDCl_3$) of compound **4.31**

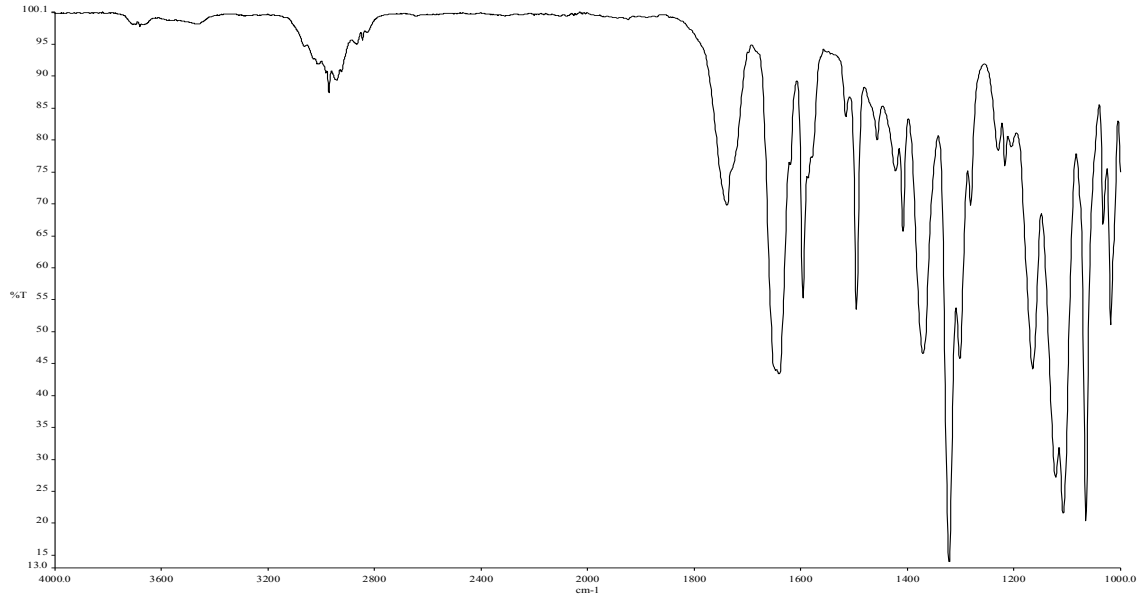

Figure A4.2 Infrared spectrum of compound **4.31**

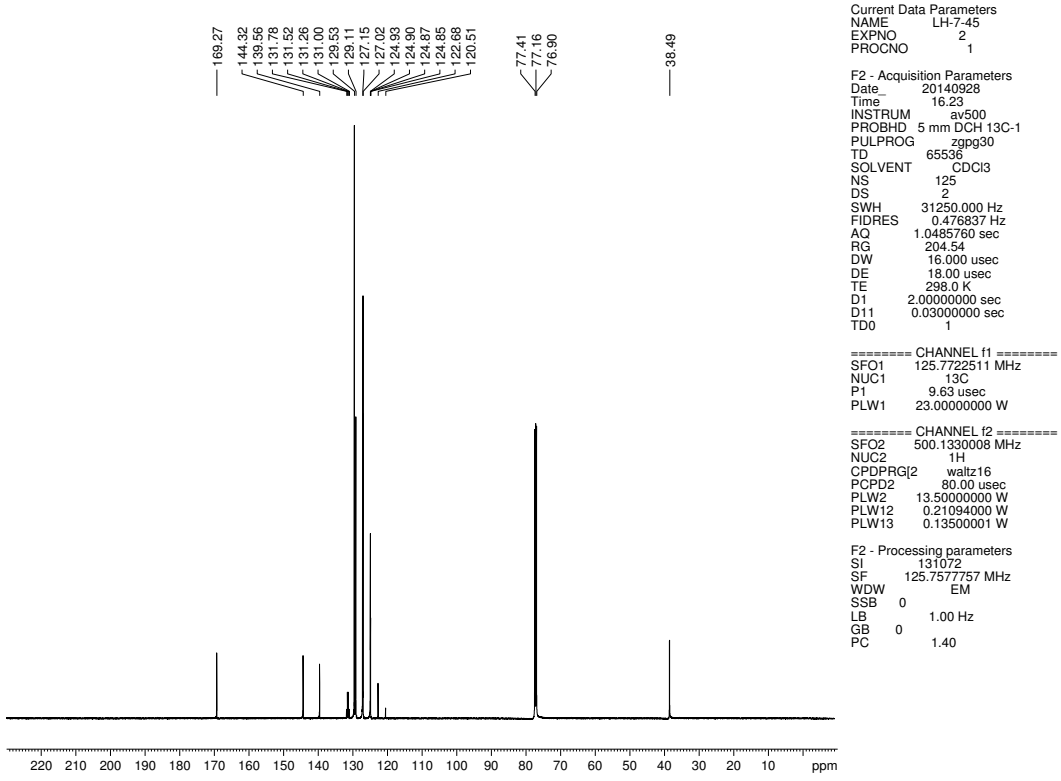

Figure A4.3 ^{13}C NMR (125 MHz, $CDCl_3$) of compound **4.31**

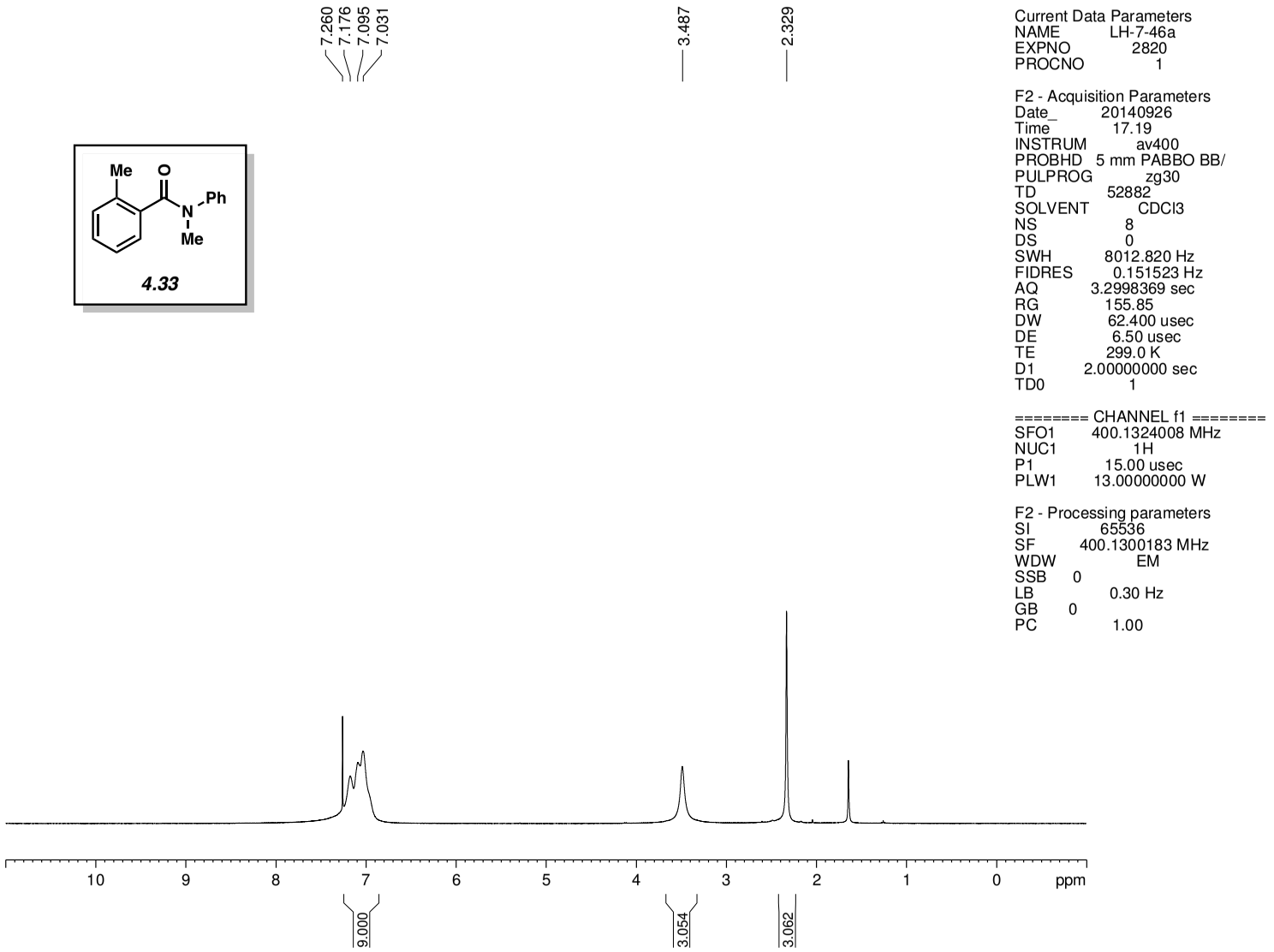

Figure A4.4. ^{1}H NMR (500 MHz, $CDCl_3$) of compound **4.33**

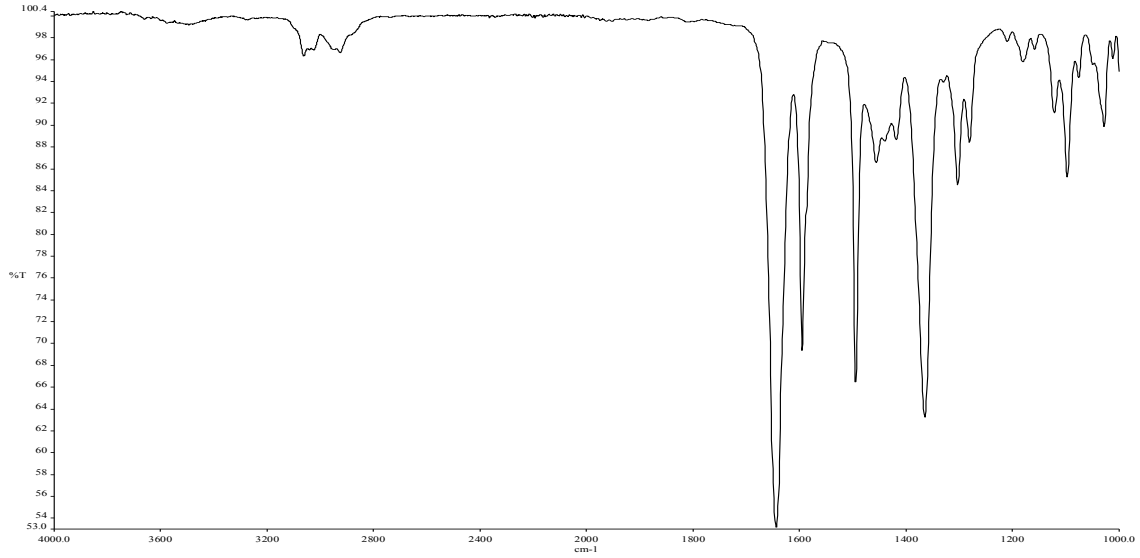

Figure A4.5. Infrared spectrum of compound **4.33**

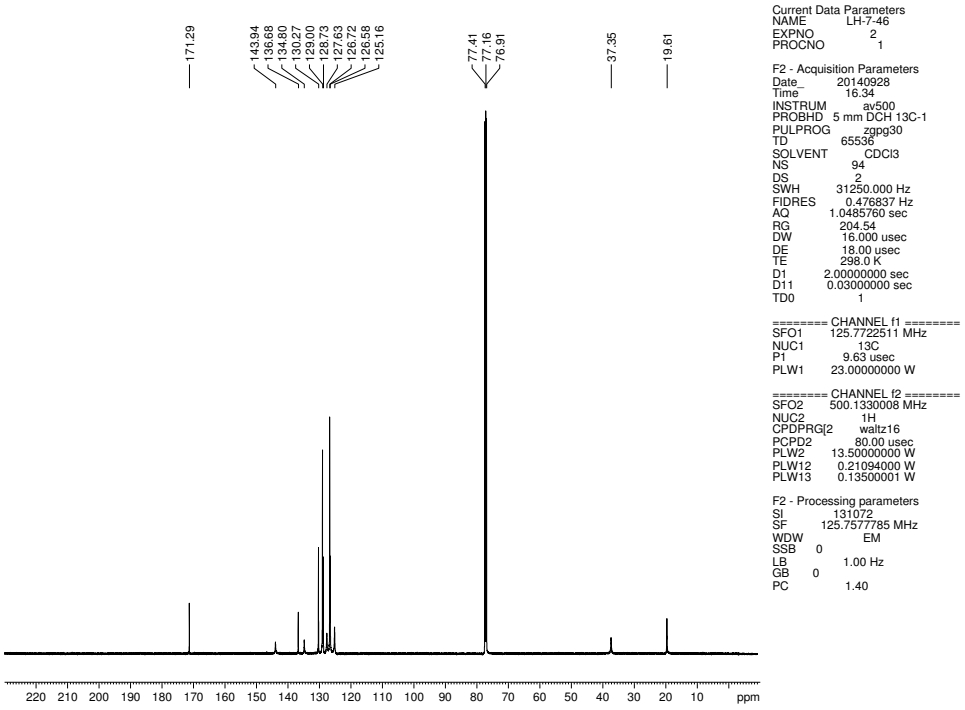

Figure A4.6 ^{13}C NMR (125 MHz, $CDCl_3$) of compound **4.33**

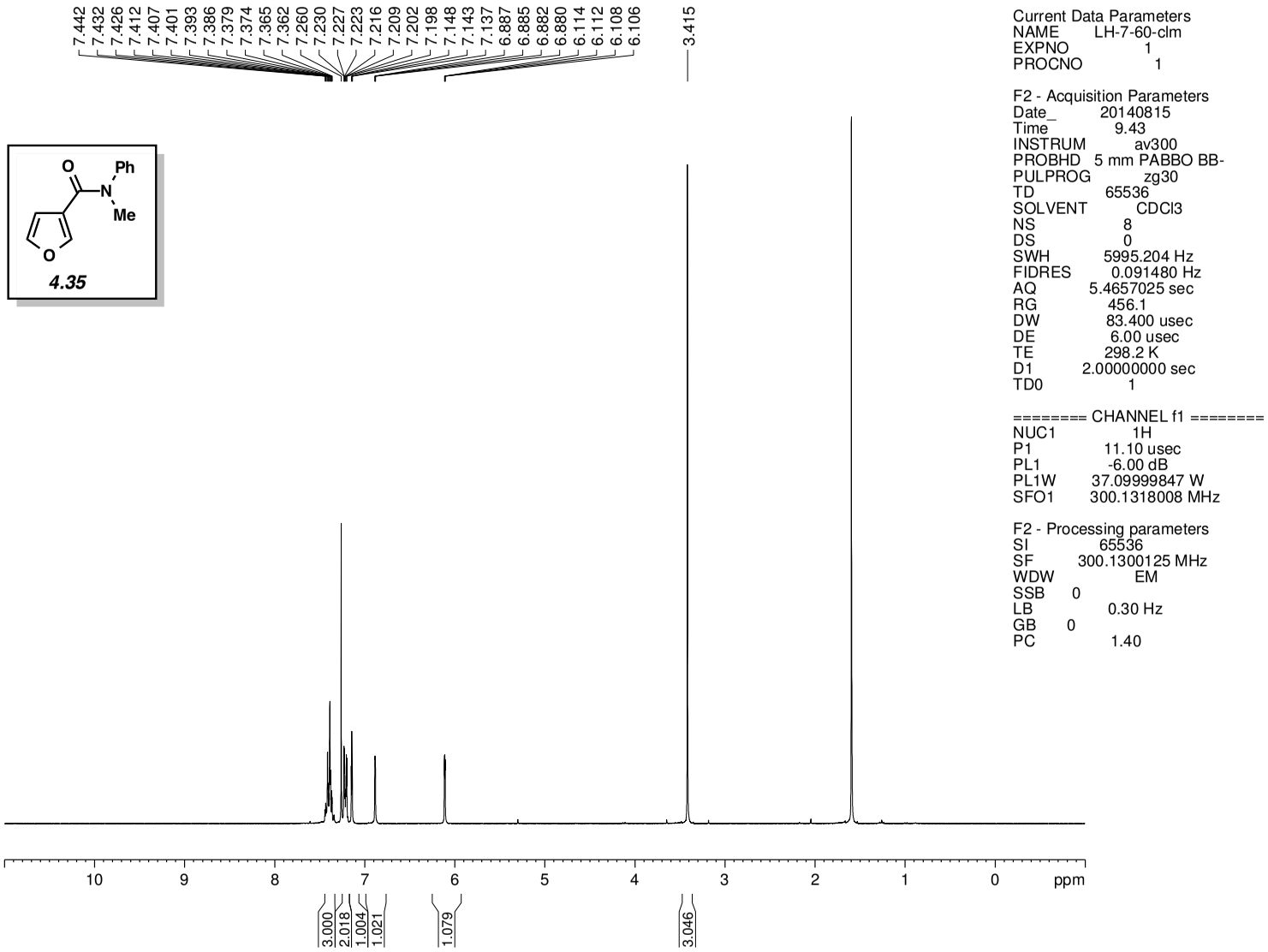

Figure A4.7 ^{1}H NMR (300 MHz, $CDCl_3$) of compound **4.35**

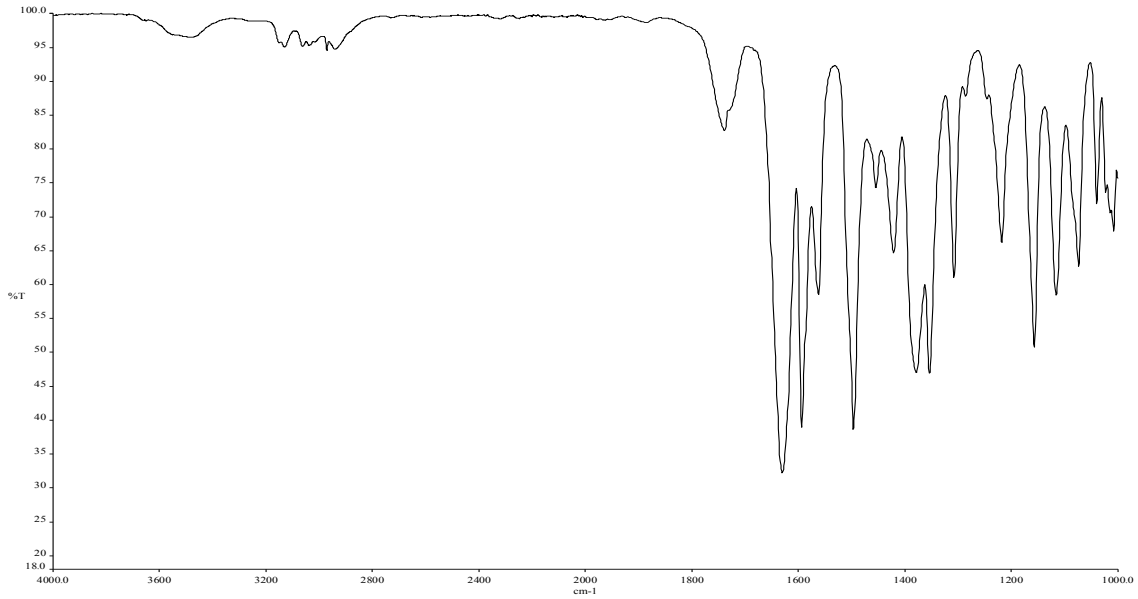

Figure A4.8 Infrared spectrum of compound **4.35**

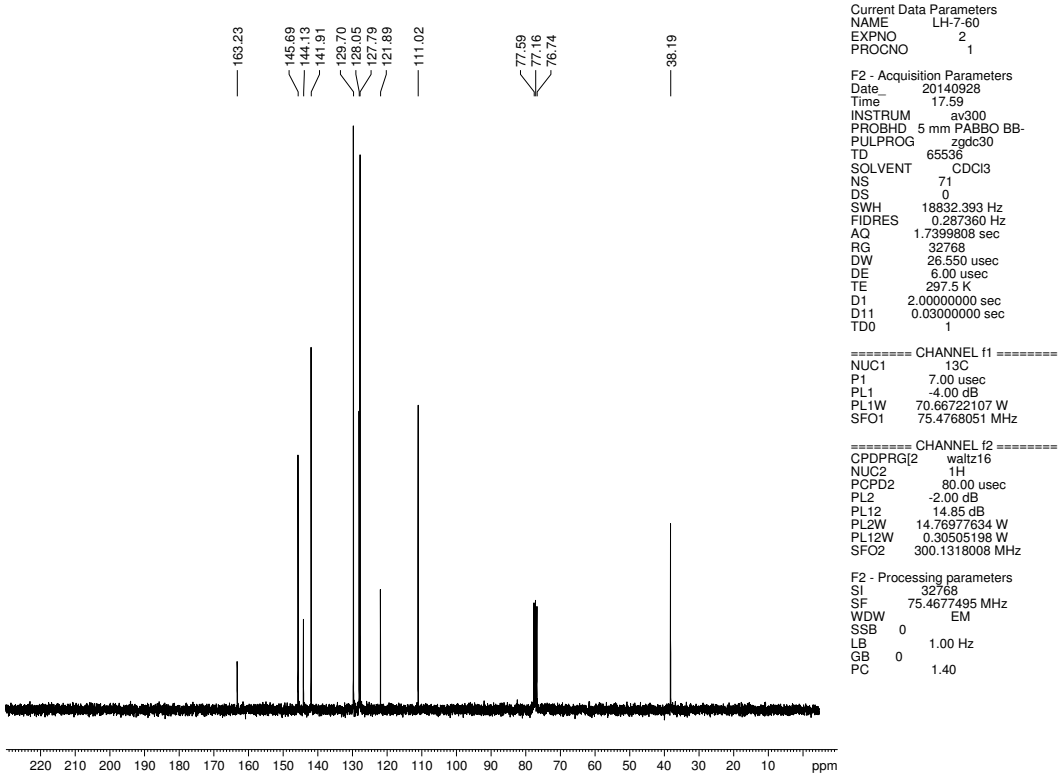

Figure A4.9 ^{13}C NMR (75 MHz, $CDCl_3$) of compound **4.35**

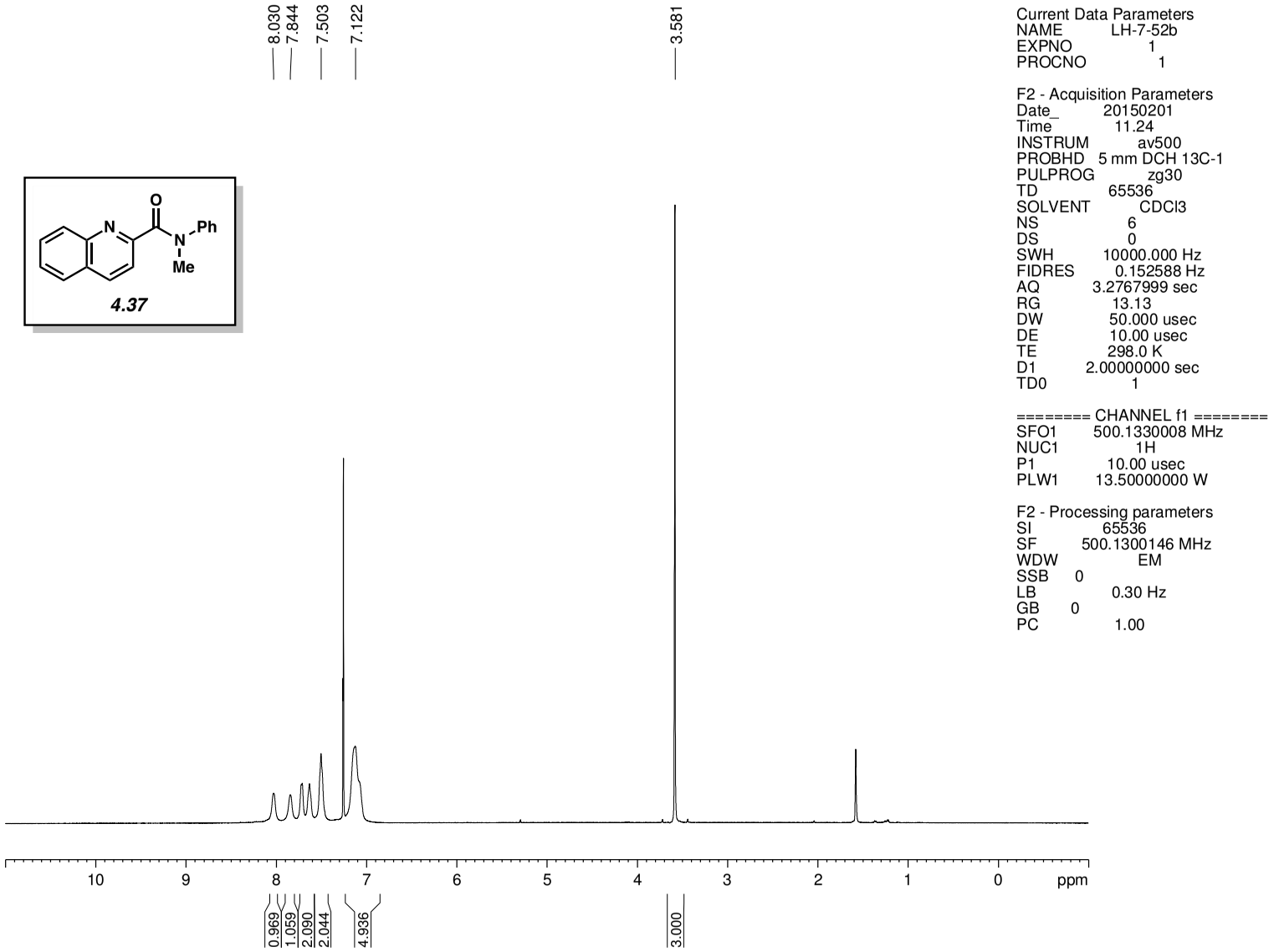

Figure A4.10 ^{1}H NMR (500 MHz, $CDCl_3$) of compound **4.37**

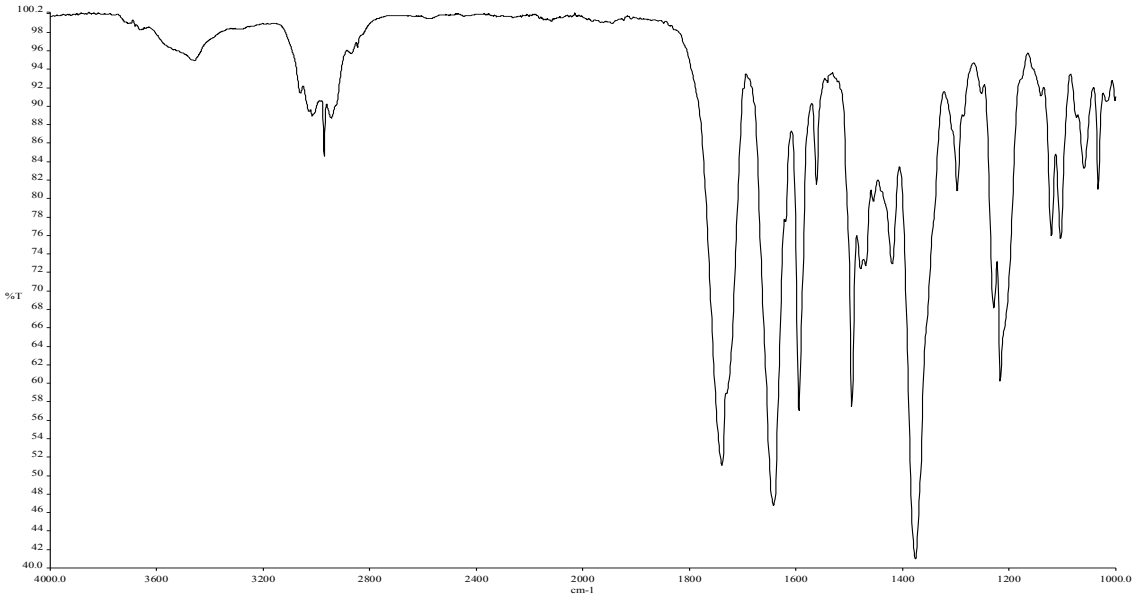

Figure A4.11 Infrared spectrum of compound **4.37**

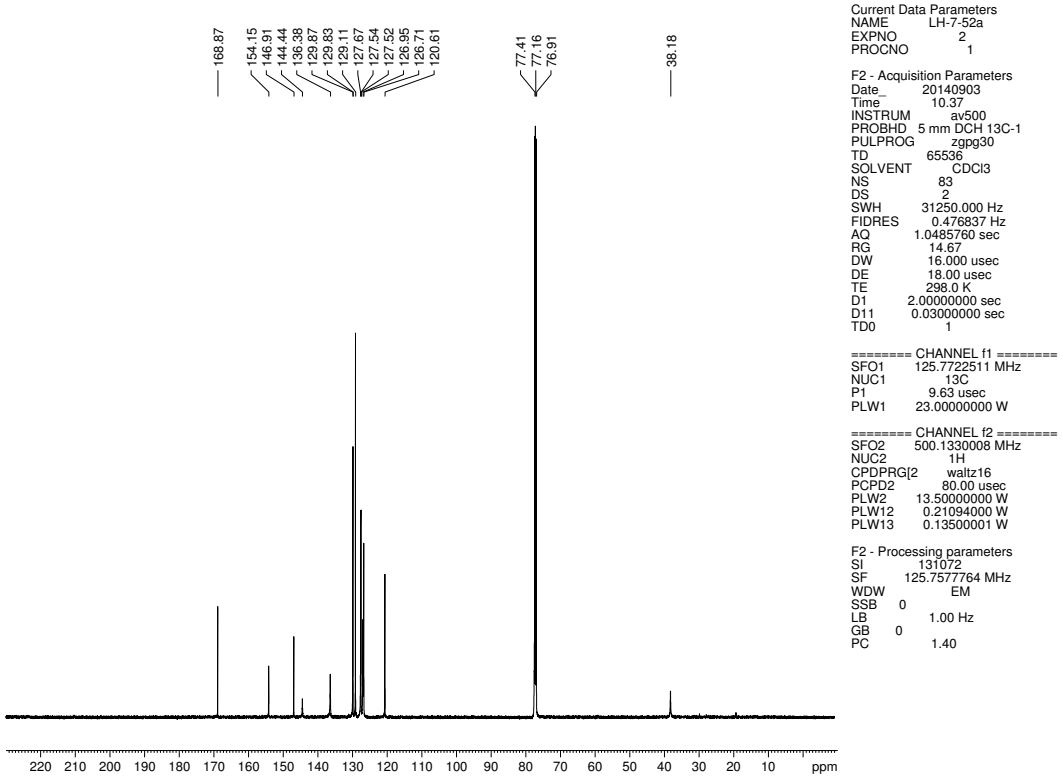

Figure A4.12 ^{13}C NMR (125 MHz, $CDCl_3$) of compound **4.37**

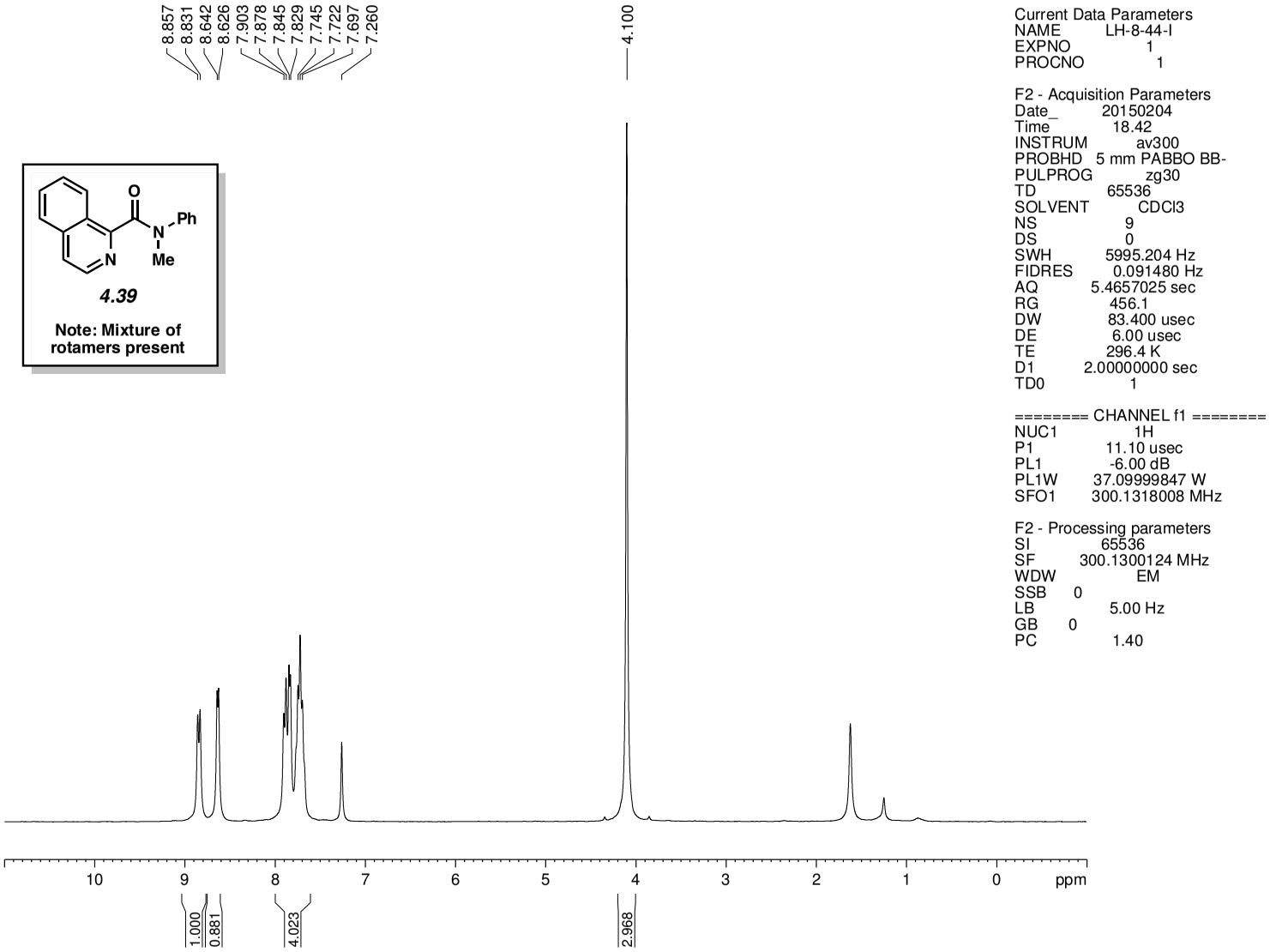

Figure A4.13. ^{1}H NMR (300 MHz, $CDCl_3$) of compound **4.39**

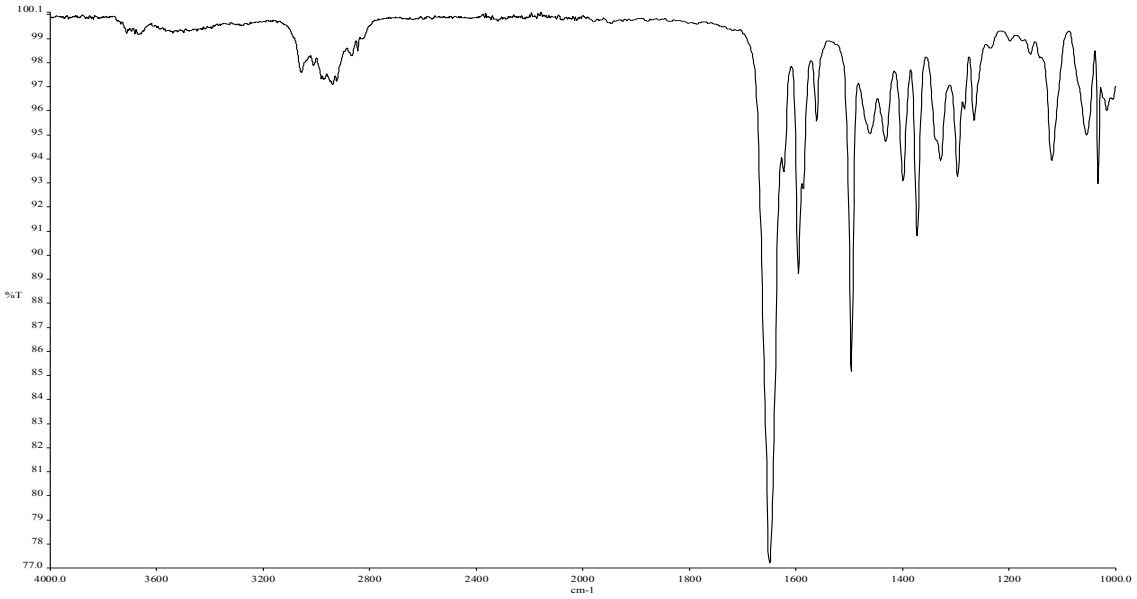

Figure A4.14. Infrared spectrum of compound **4.39**

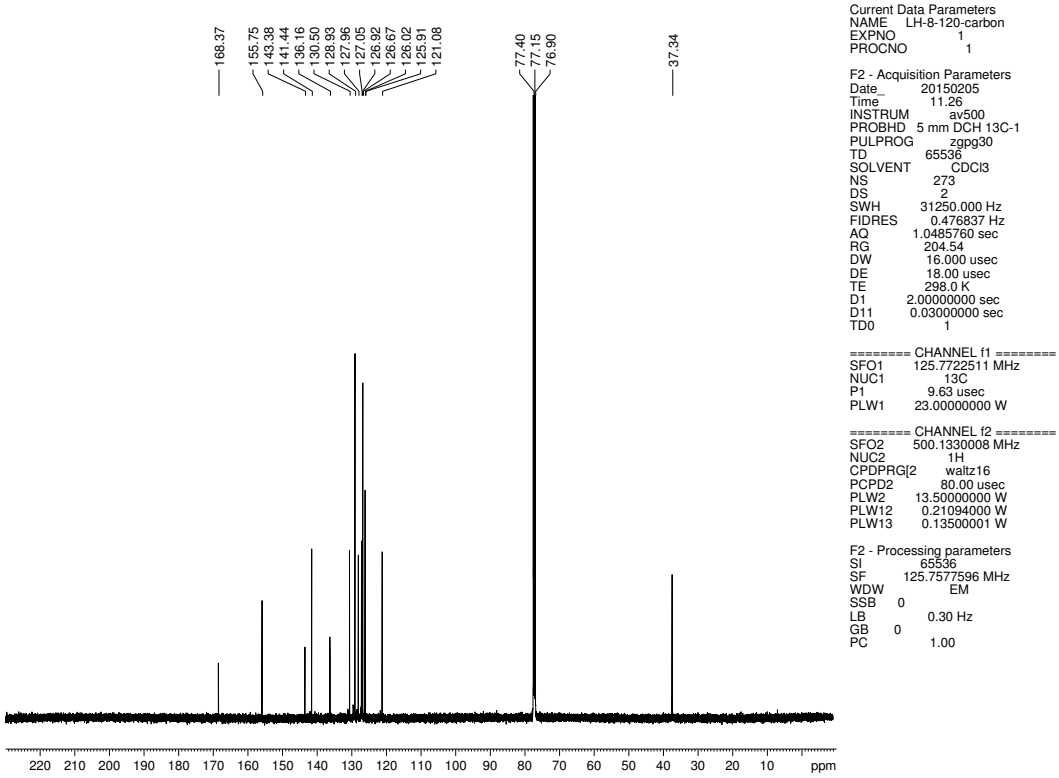

Figure A4.15 ^{13}C NMR (125 MHz, $CDCl_3$) of compound **4.39**

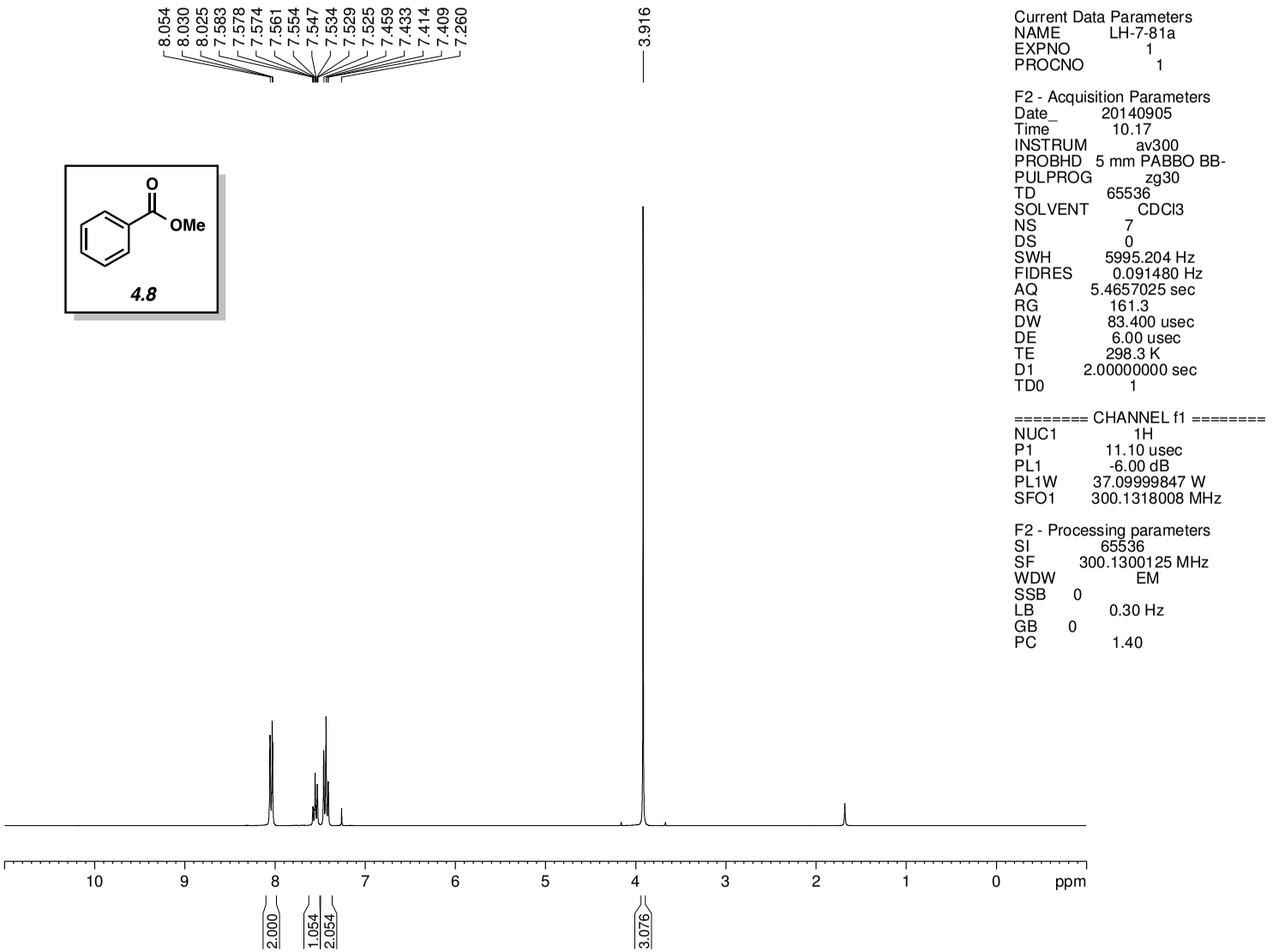

Figure A4.16 ^{1}H NMR (300 MHz, $CDCl_3$) of compound **4.8**

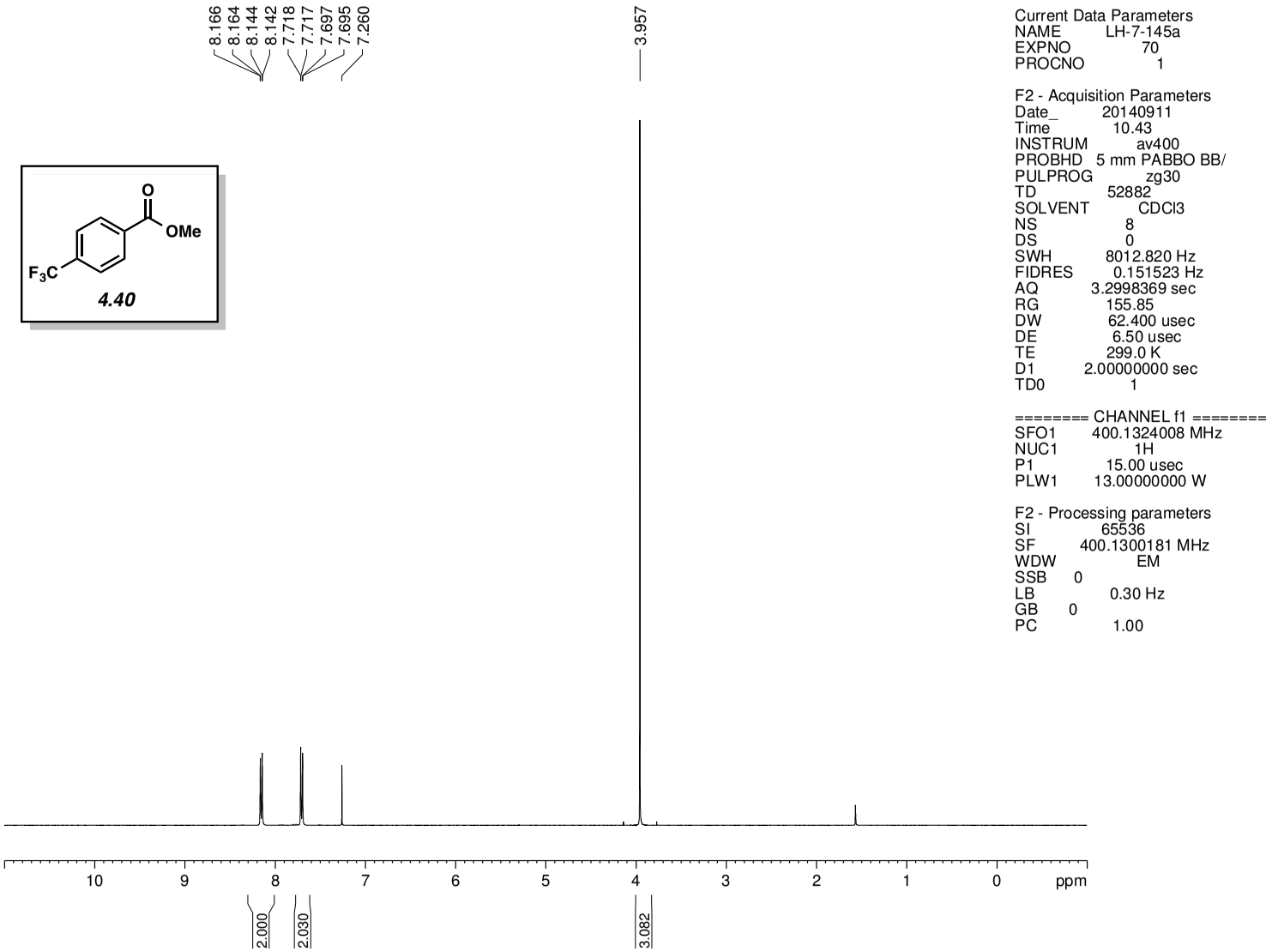

Figure A4.17 ^{1}H NMR (400 MHz, $CDCl_3$) of compound **4.40**

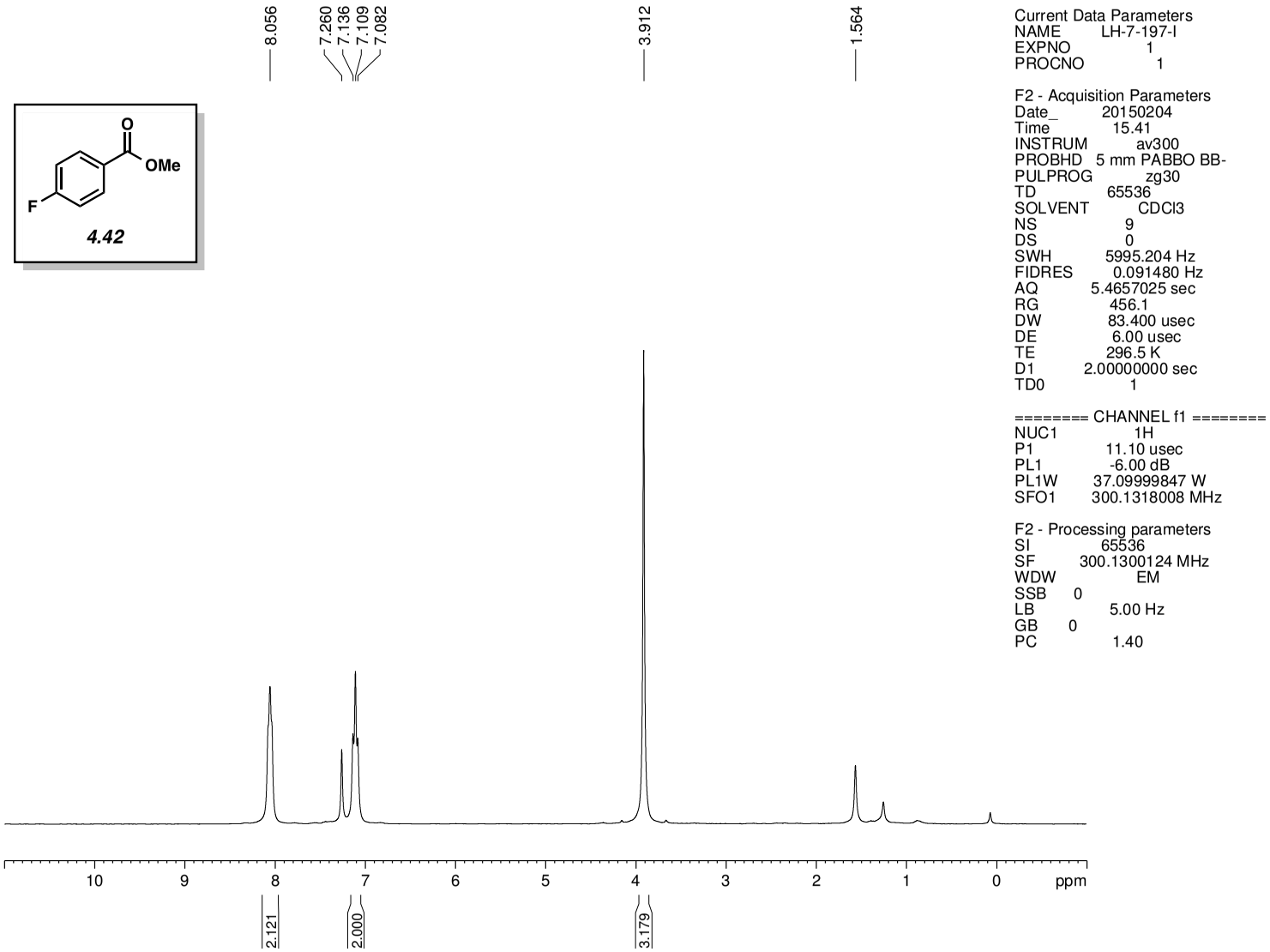

Figure A4.18 ^{1}H NMR (300 MHz, $CDCl_3$) of compound **4.42**

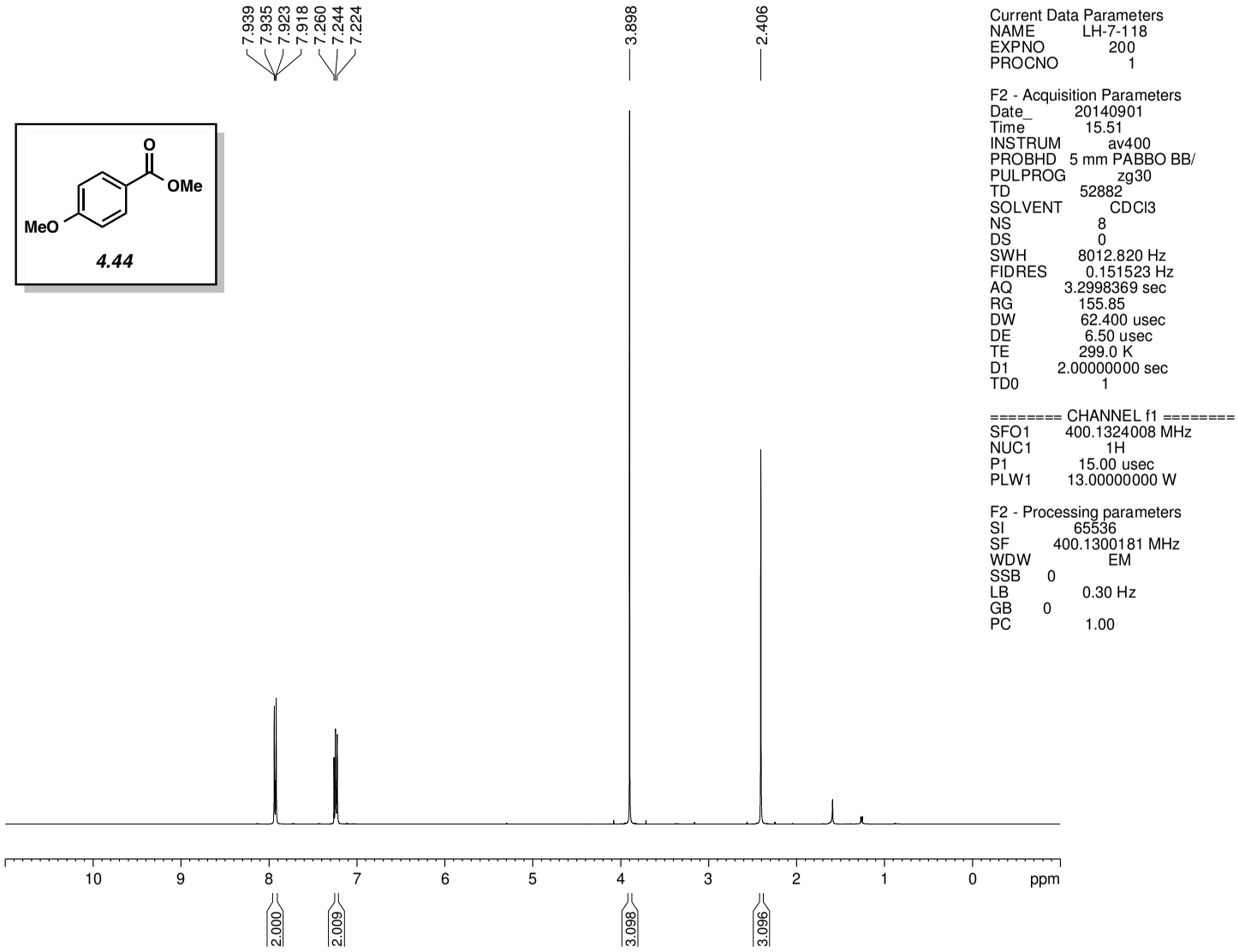

Figure A4.19 ^{1}H NMR (400 MHz, $CDCl_3$) of compound **4.44**

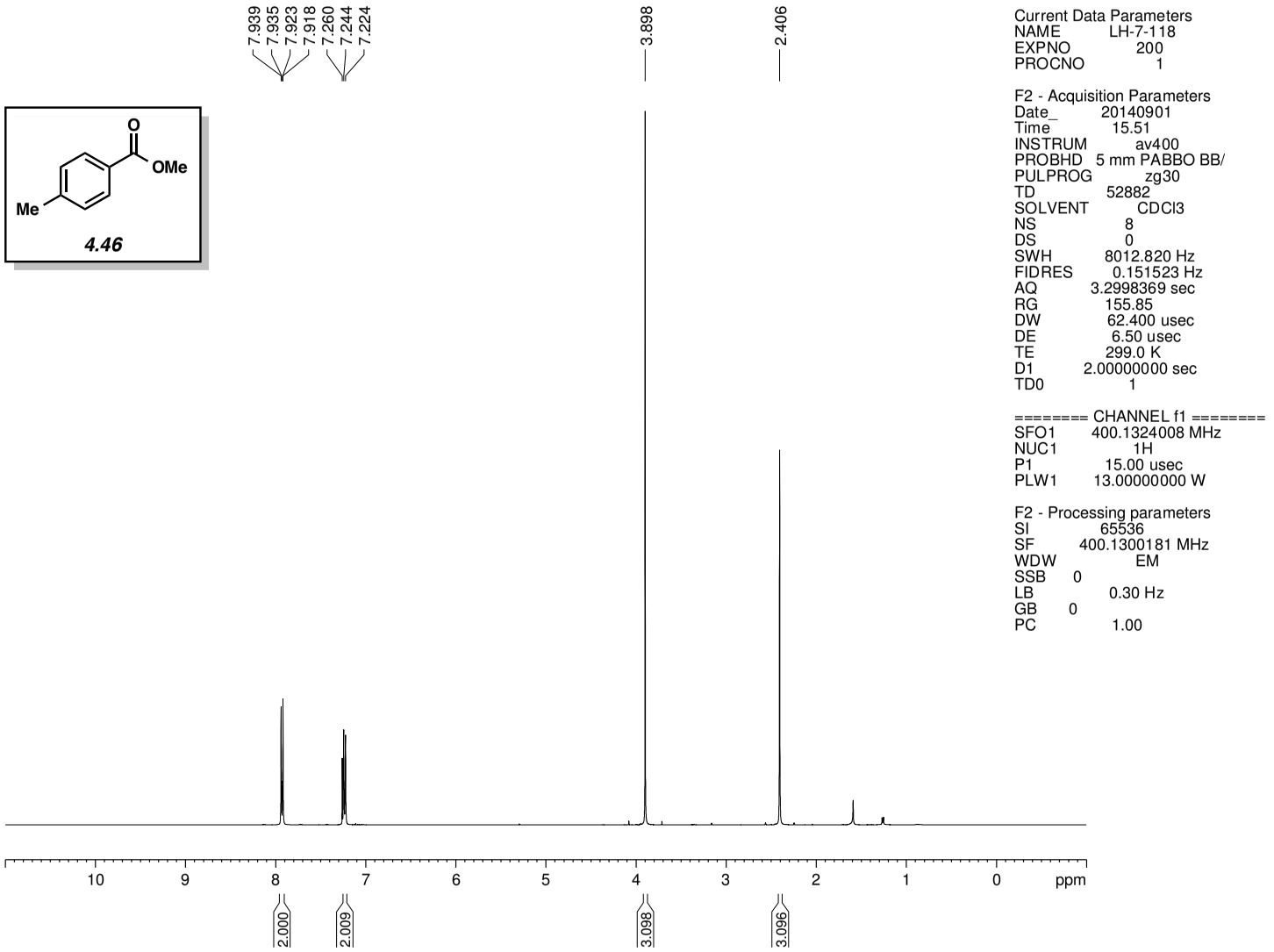

Figure A4.20 ^{1}H NMR (400 MHz, $CDCl_3$) of compound **4.46**

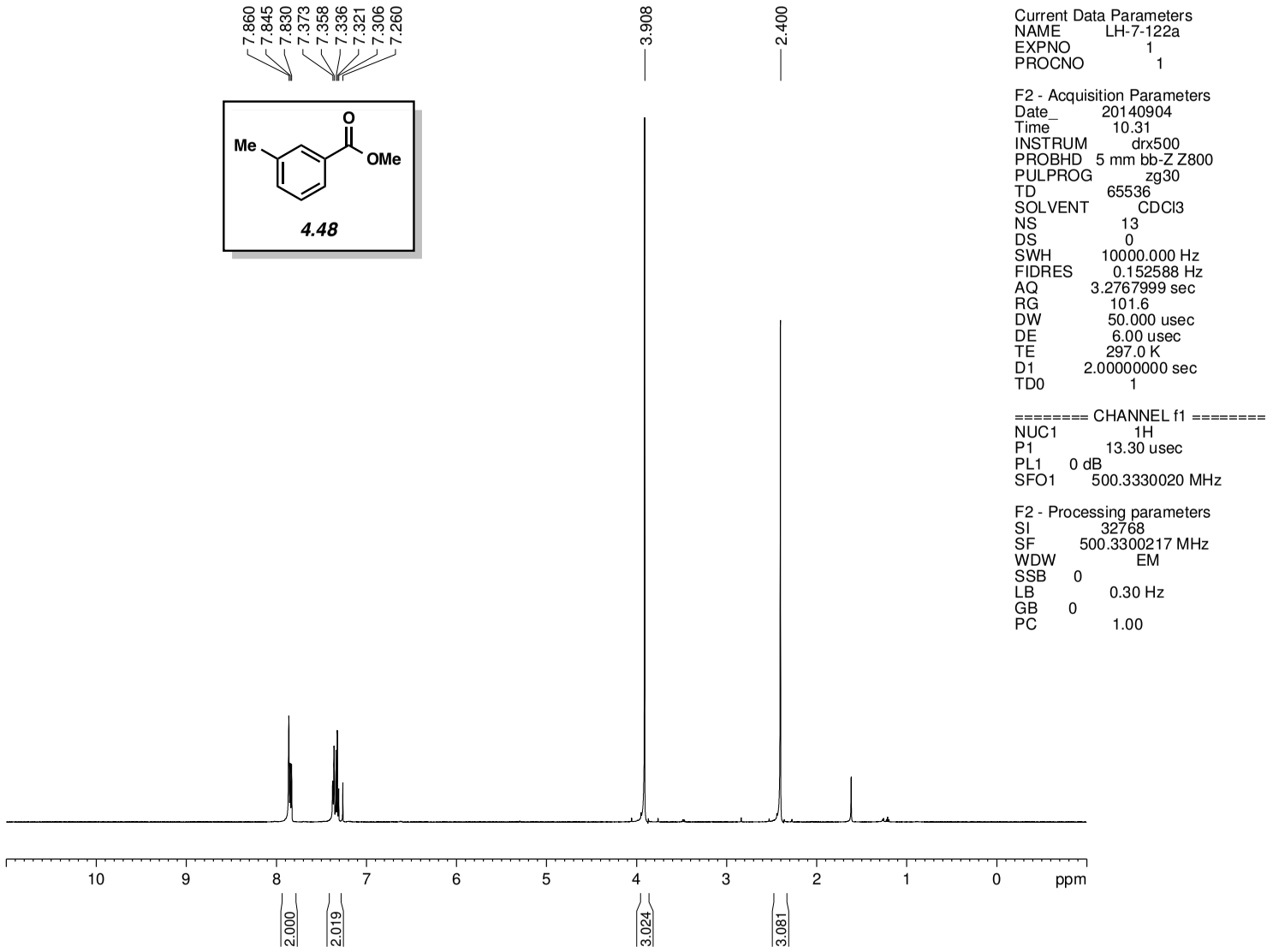

Figure A4.21 ^{1}H NMR (500 MHz, $CDCl_3$) of compound **4.48**

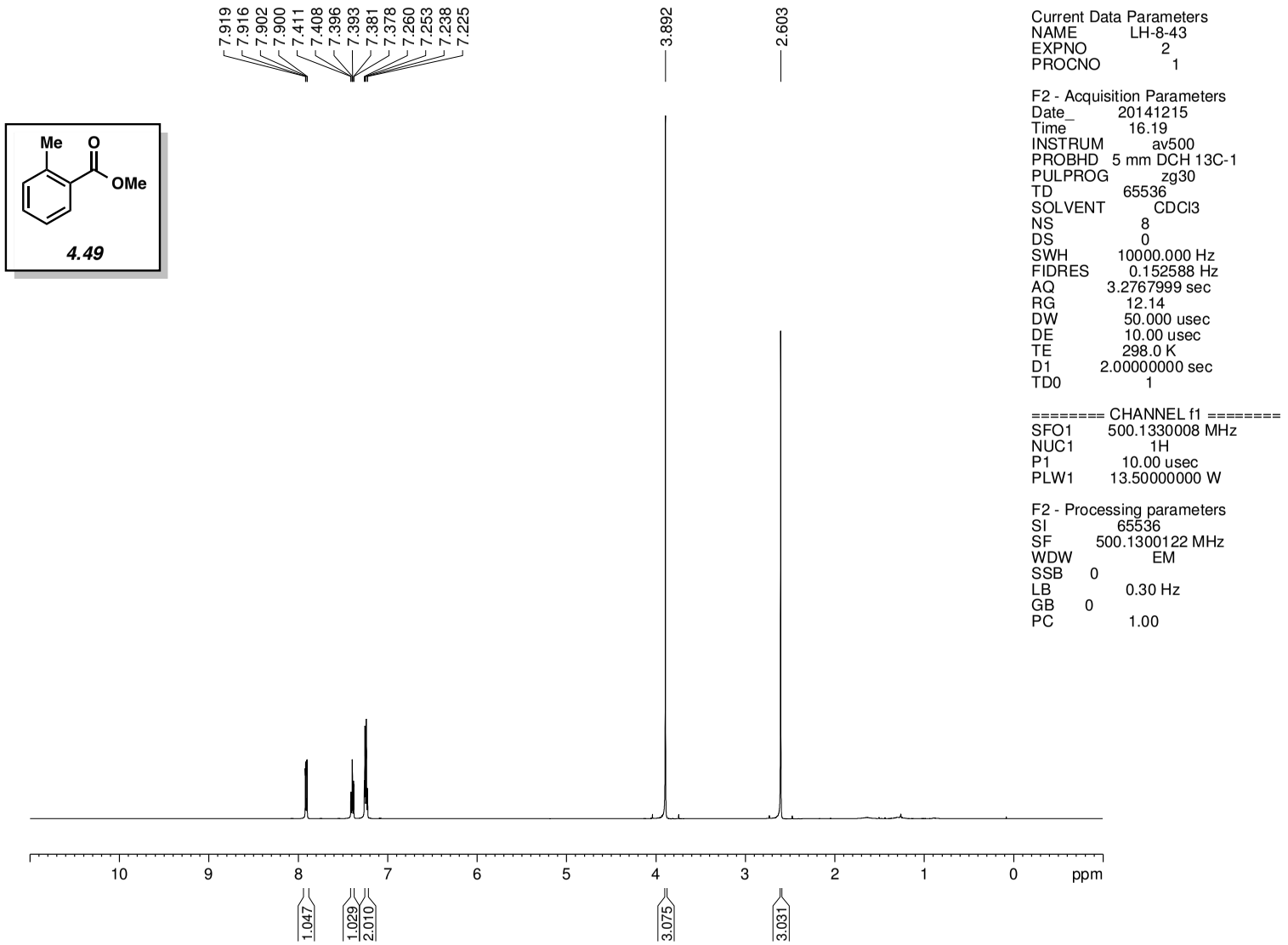

Figure A4.22 ^{1}H NMR (500 MHz, $CDCl_3$) of compound **4.49**

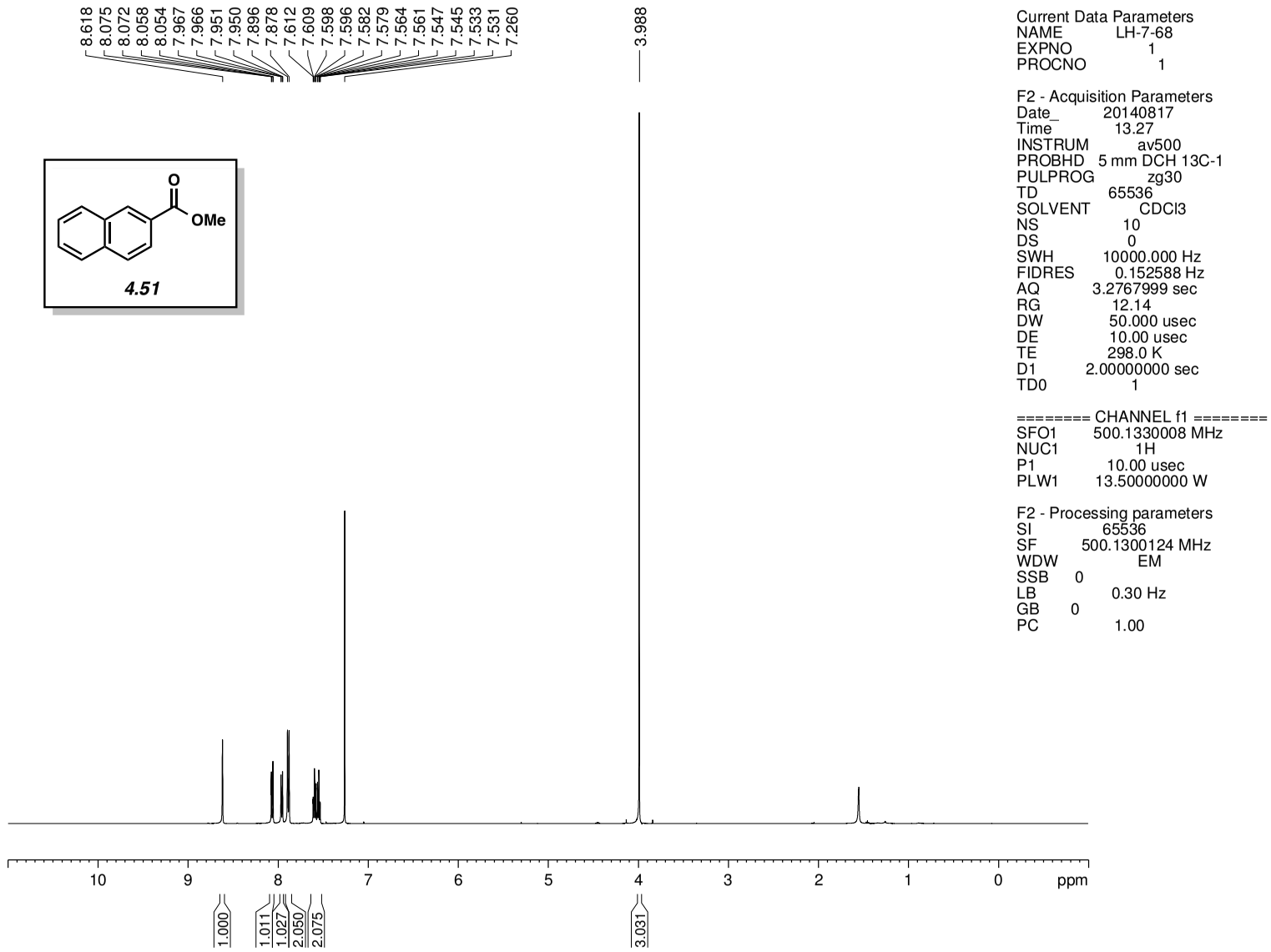

Figure A4.23 ^{1}H NMR (500 MHz, $CDCl_3$) of compound **4.51**

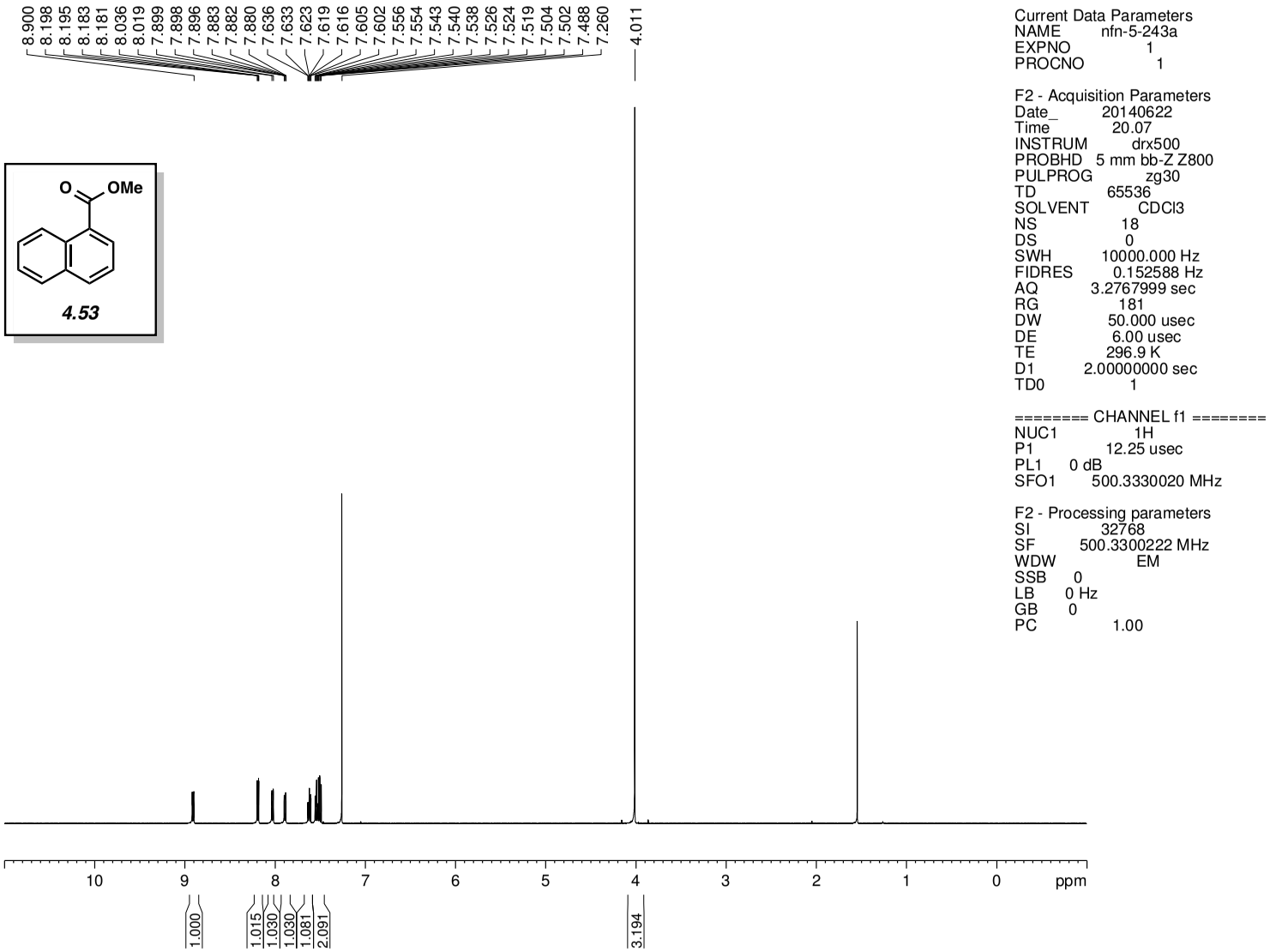

Figure A4.24 ^{1}H NMR (500 MHz, $CDCl_3$) of compound **4.53**

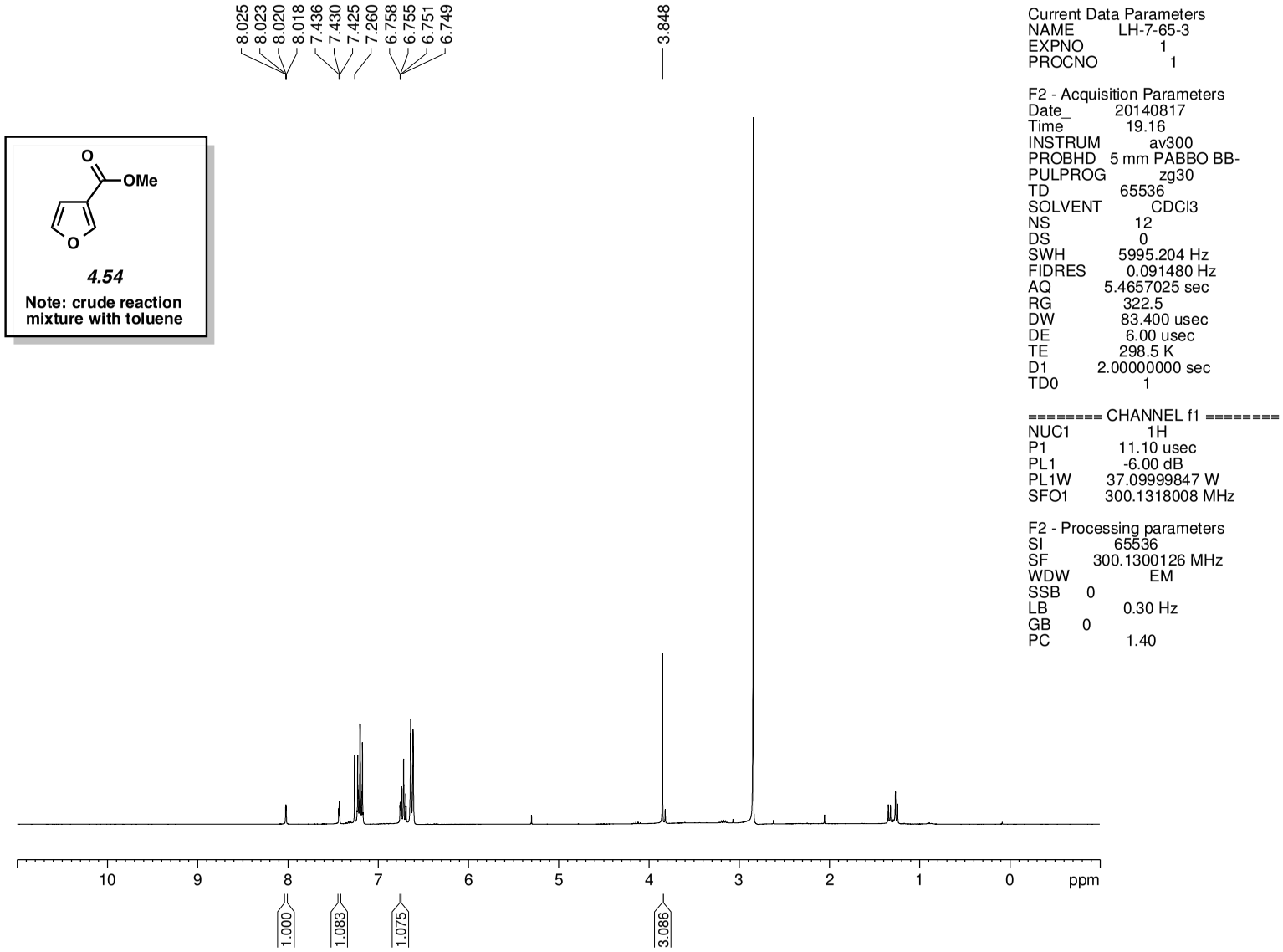

Figure A4.25 ^{1}H NMR (300 MHz, $CDCl_3$) of compound **4.54**

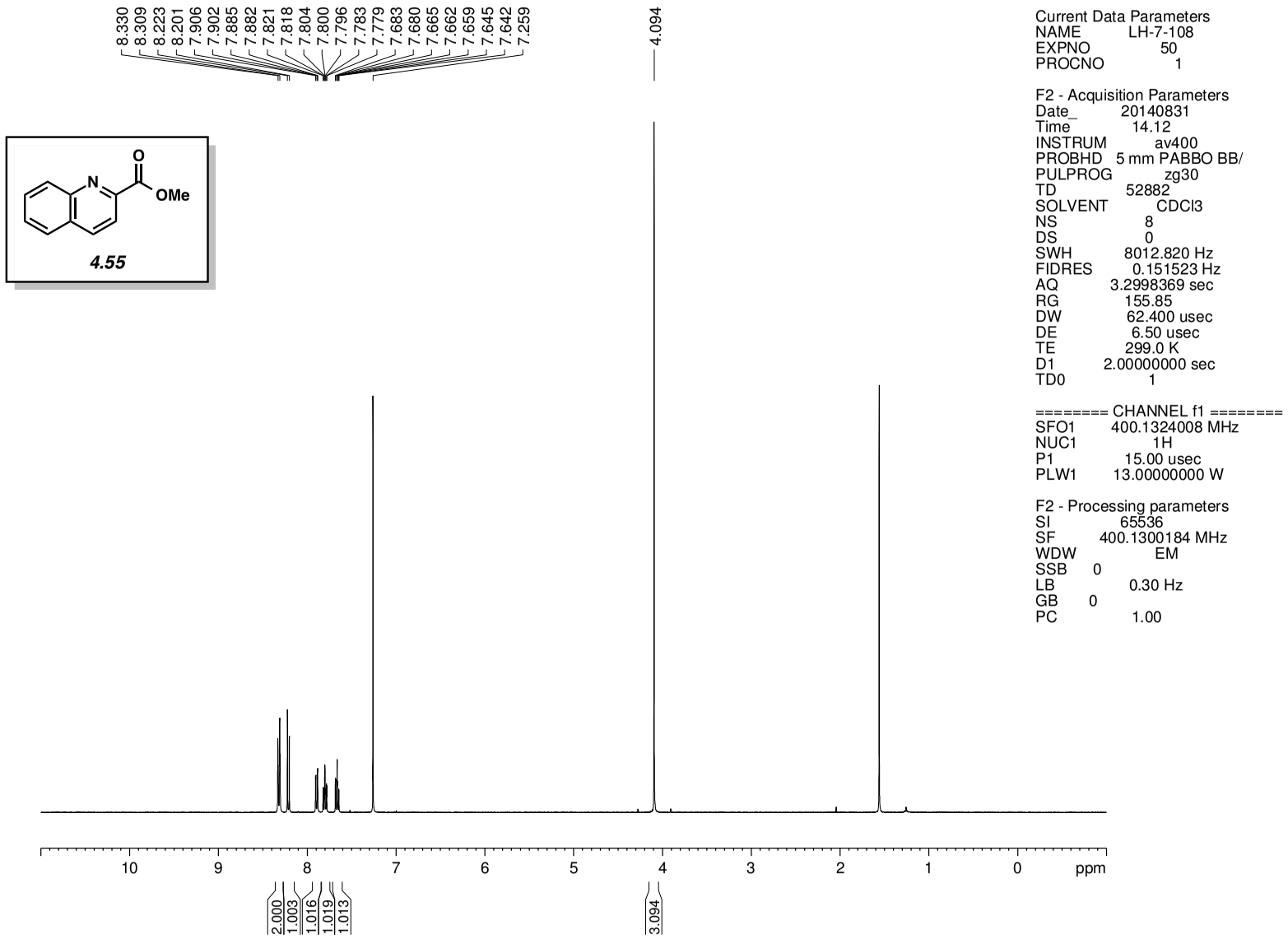

Figure A4.26 ^{1}H NMR (400 MHz, $CDCl_3$) of compound **4.55**

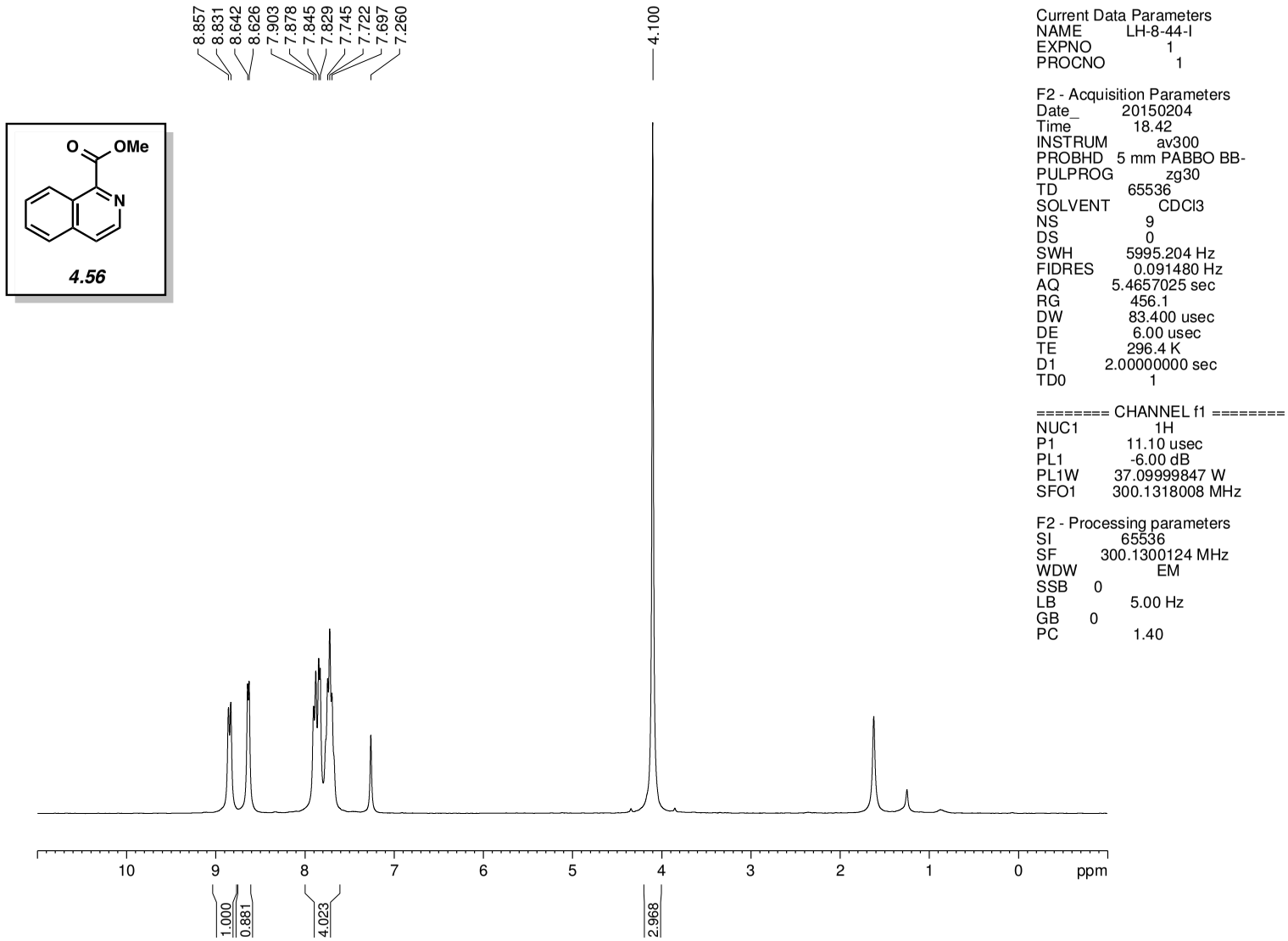

Figure A4.27 ^{1}H NMR (300 MHz, $CDCl_3$) of compound **4.56**

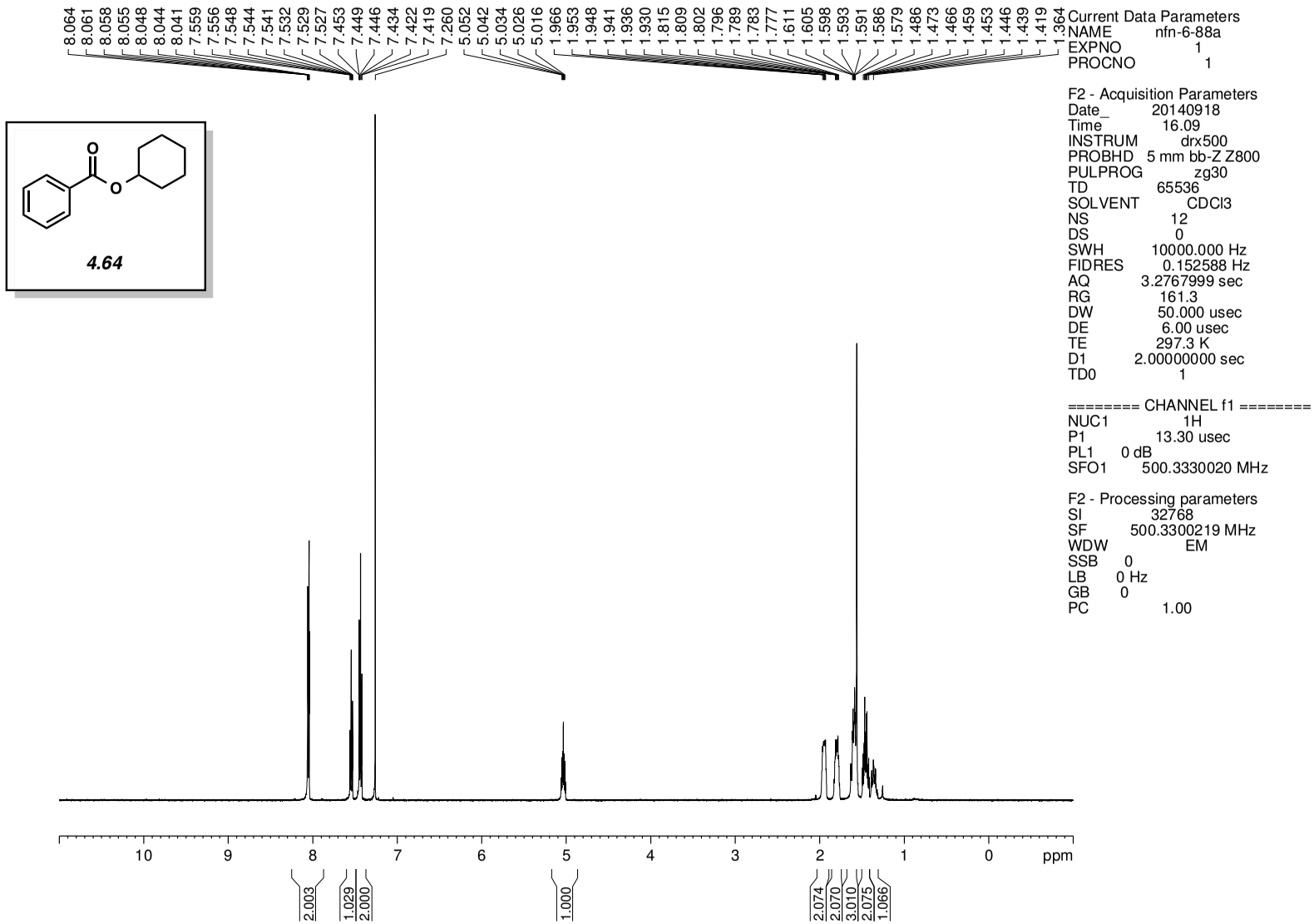

Figure A4.28 ^{1}H NMR (500 MHz, $CDCl_3$) of compound **4.64**

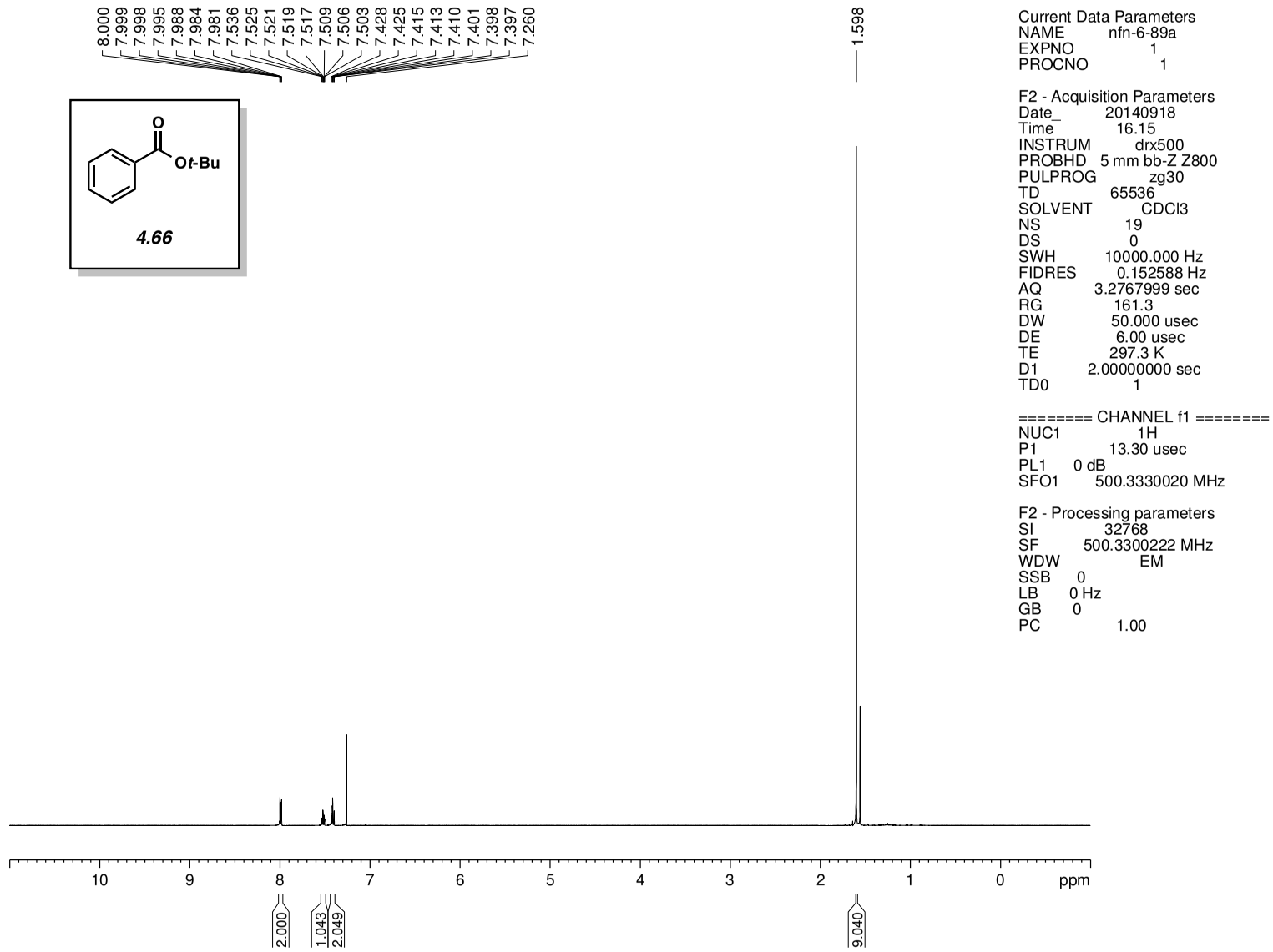

Figure A4.29 ^{1}H NMR (500 MHz, $CDCl_3$) of compound **4.66**

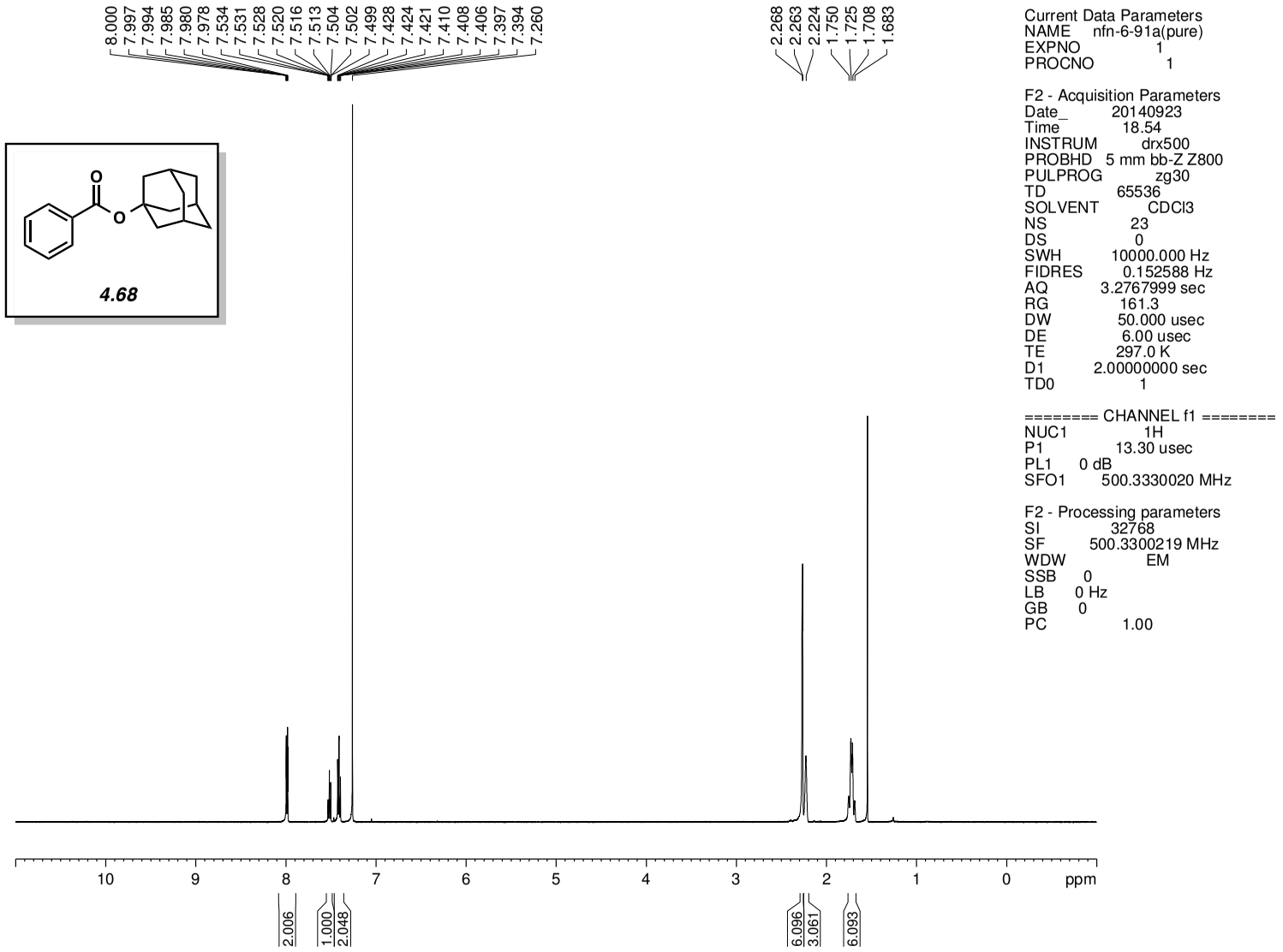

Figure A4.30 ^{1}H NMR (500 MHz, $CDCl_3$) of compound **4.68**

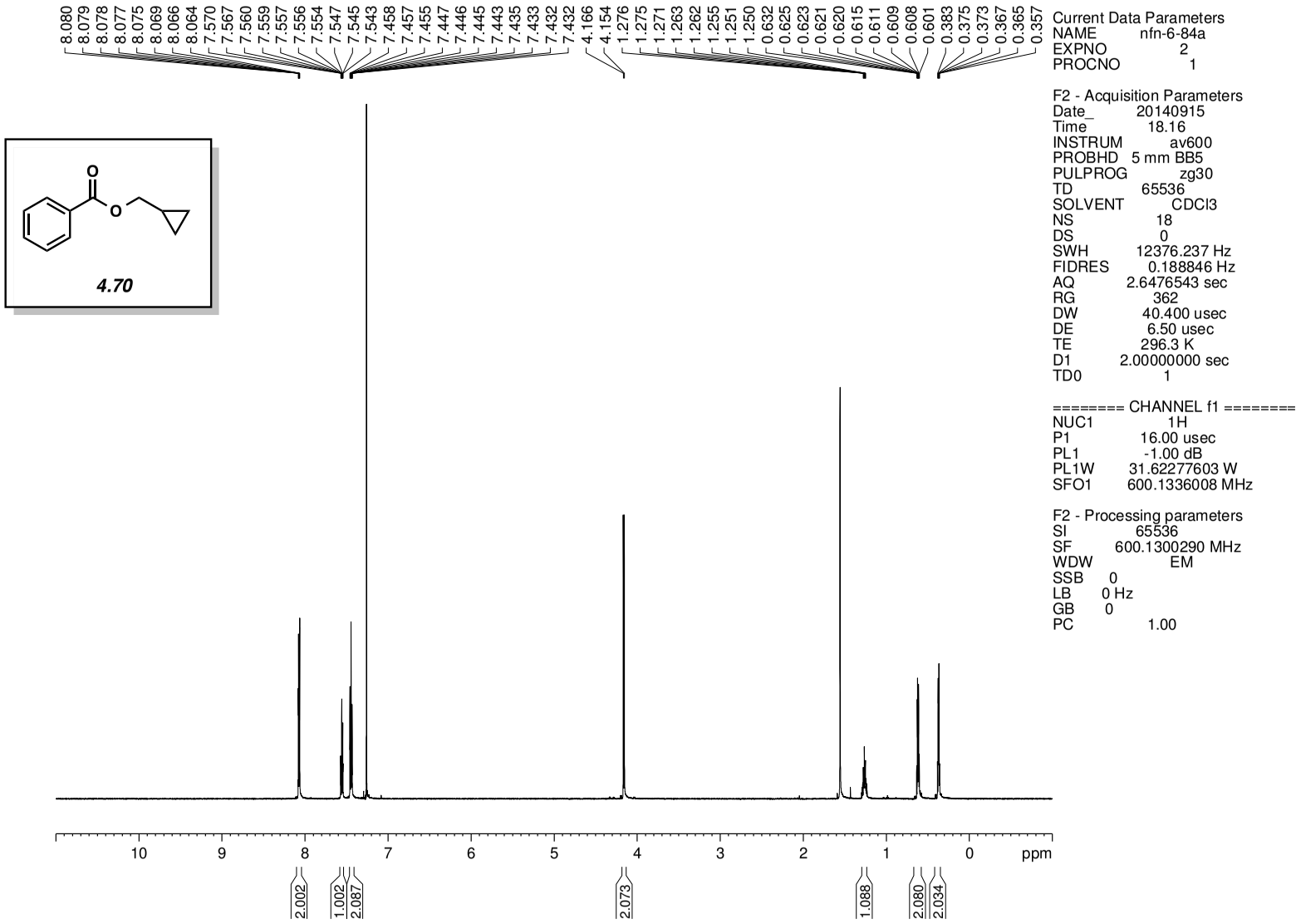

Figure A4.31 ^{1}H NMR (600 MHz, $CDCl_3$) of compound **4.70**

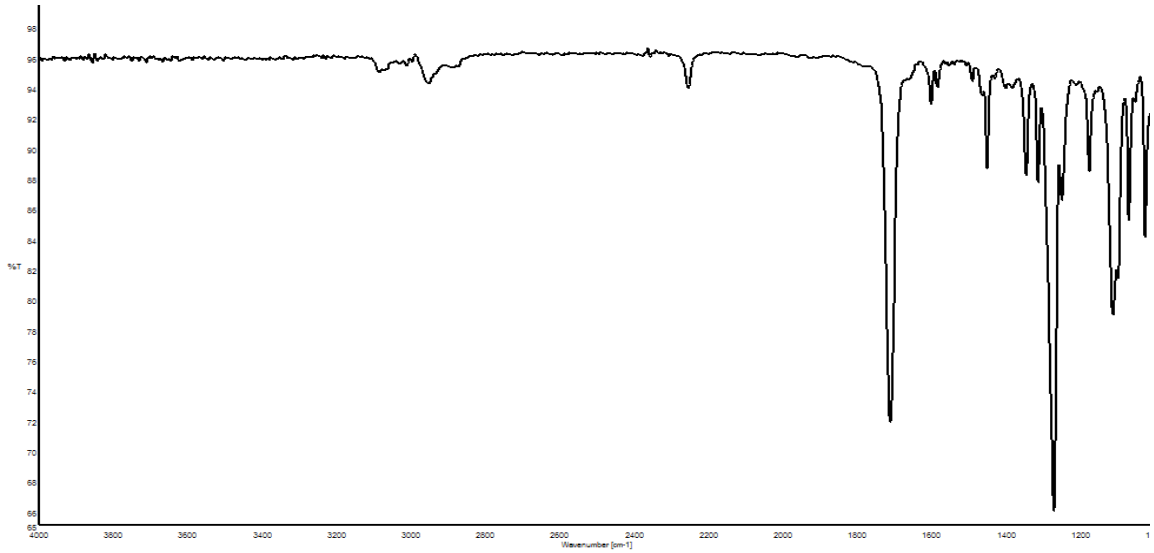

Figure A4.32 Infrared spectrum of compound **4.70**

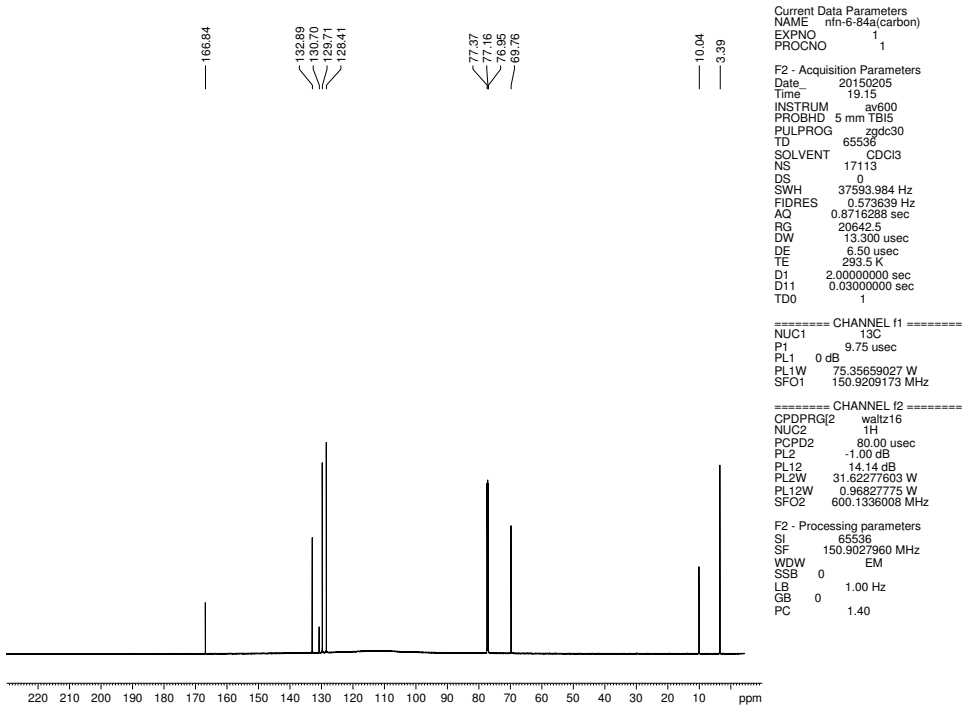

Figure A4.33 ^{13}C NMR (150 MHz, $CDCl_3$) of compound **4.70**

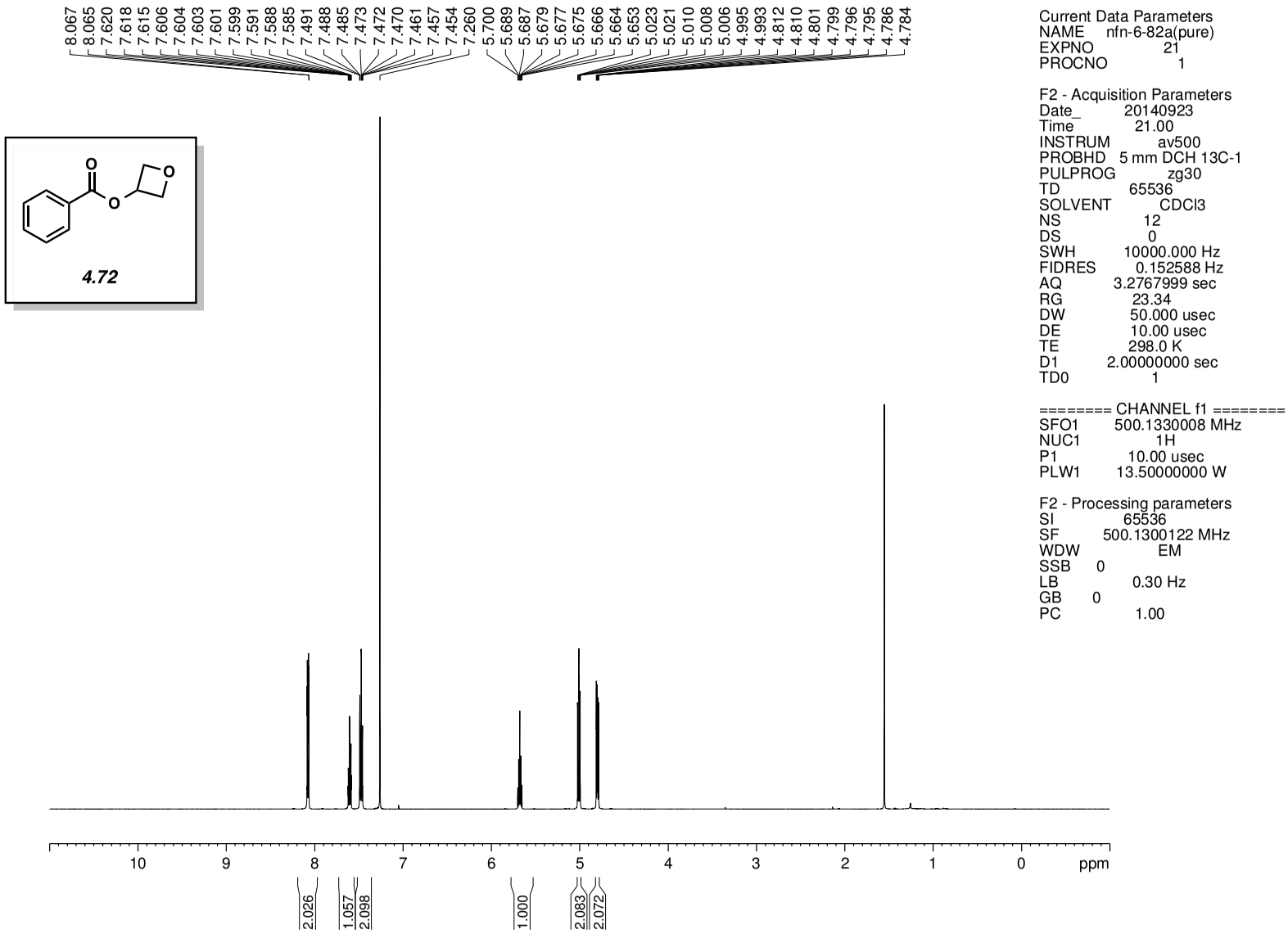

Figure A4.34. ^{1}H NMR (500 MHz, $CDCl_3$) of compound **4.72**

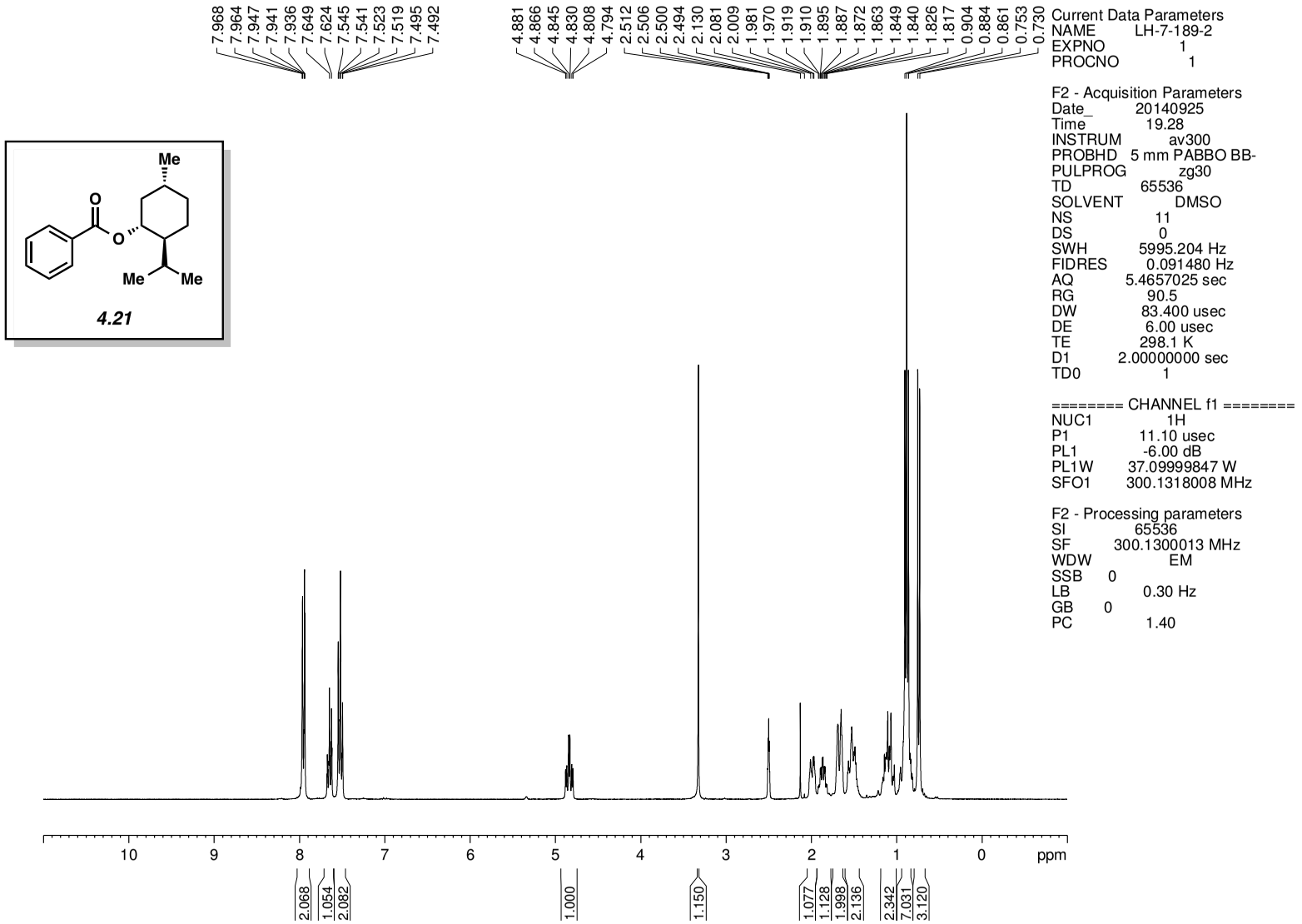

Figure A4.35 ^{1}H NMR (300 MHz, $(CD_3)_2SO$) of compound **4.21**

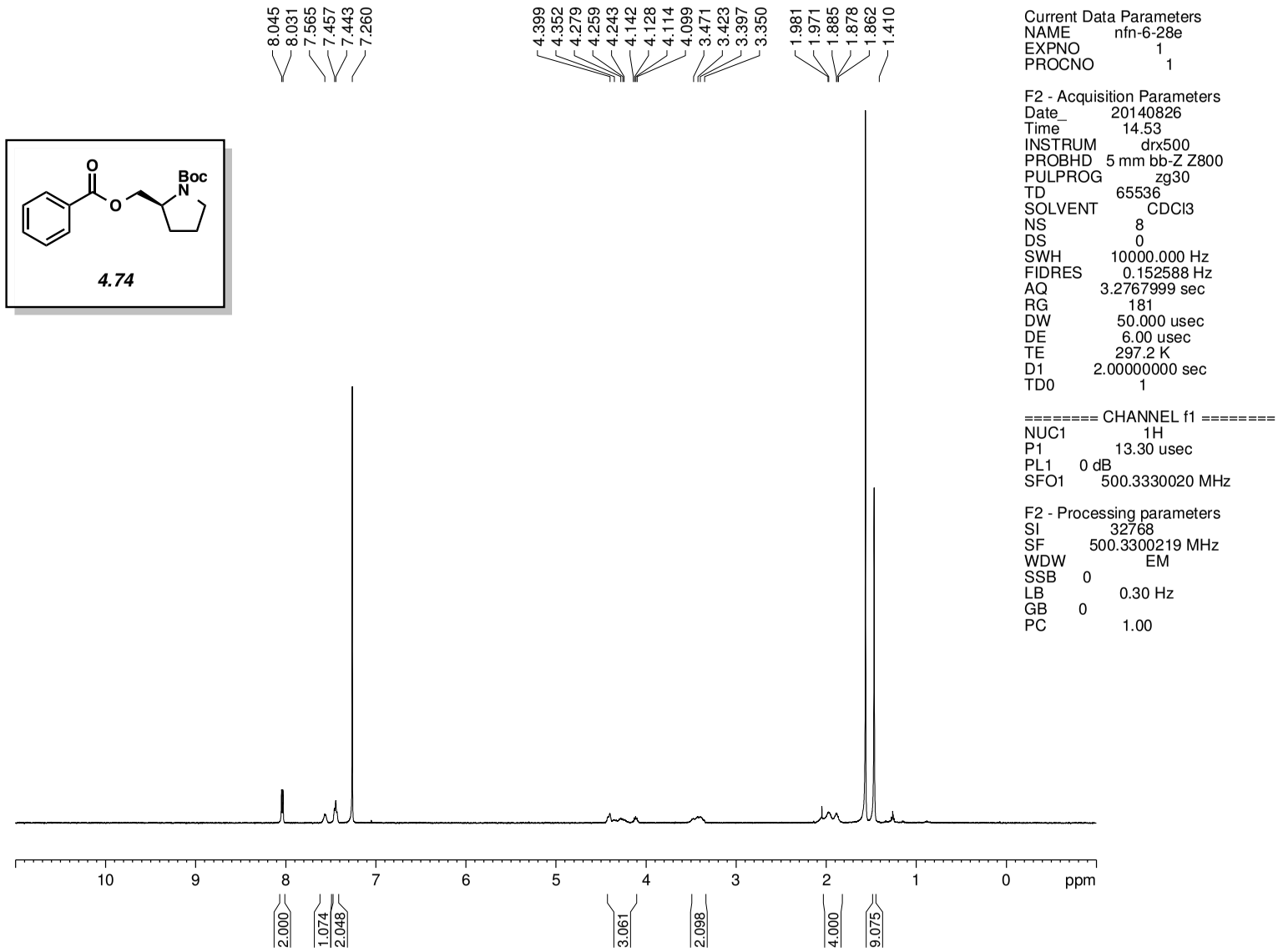

Figure A4.36 ^{1}H NMR (500 MHz, $CDCl_3$) of compound **4.74**

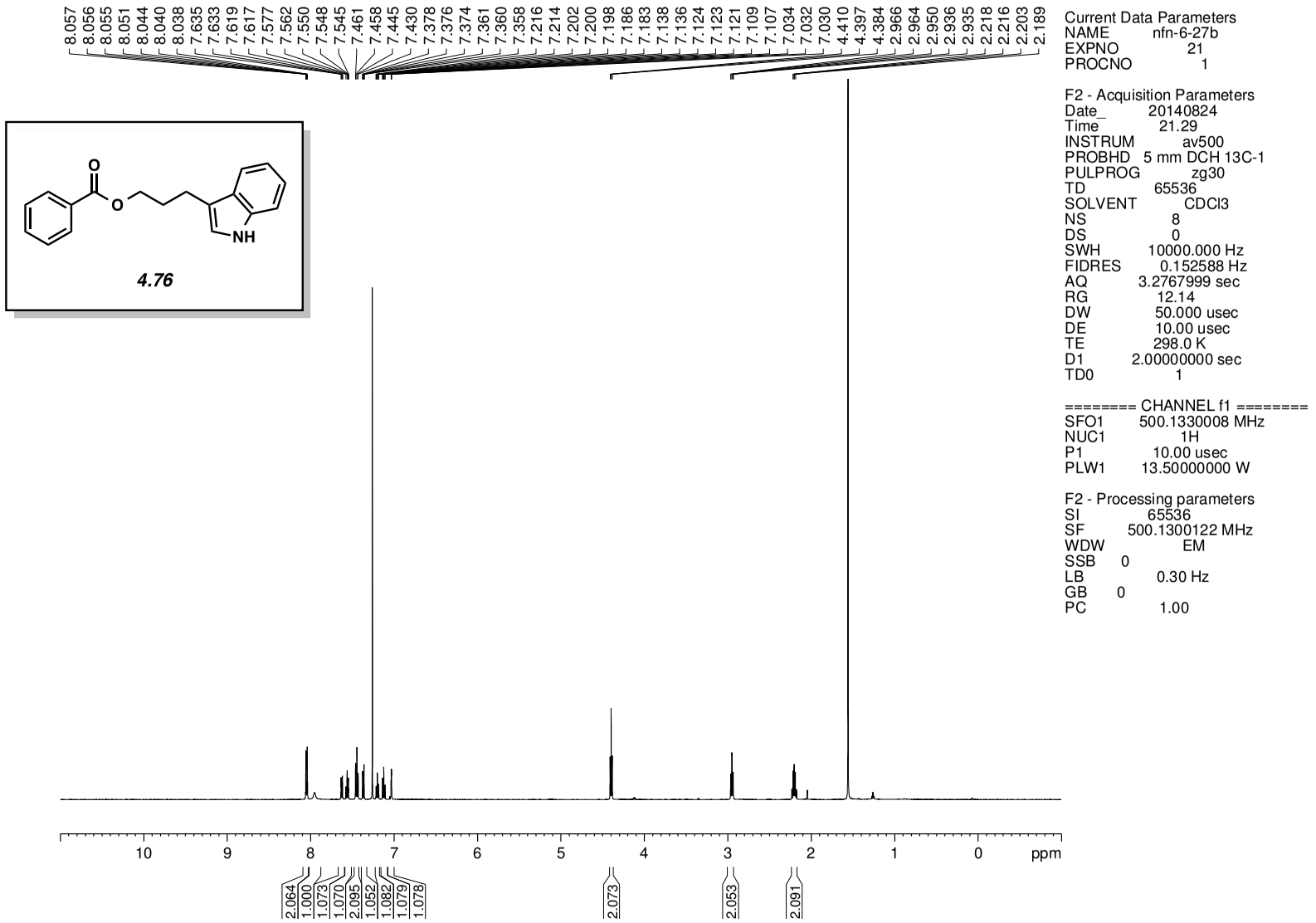

Figure A4.37 ^{1}H NMR (500 MHz, $CDCl_3$) of compound **4.76**

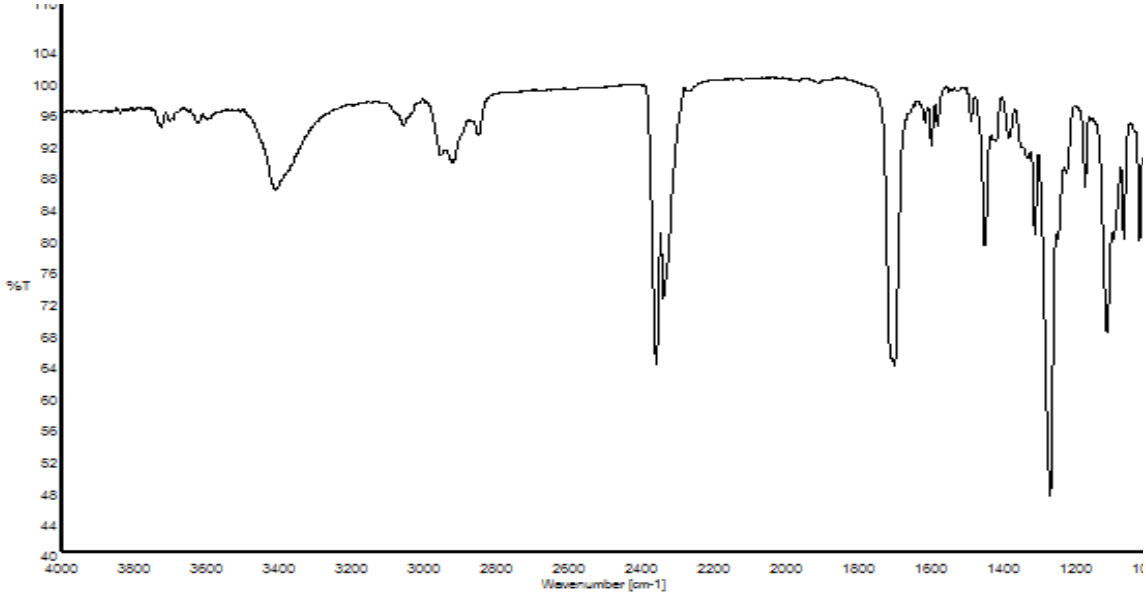

Figure A4.38. Infrared spectrum of compound **4.76**

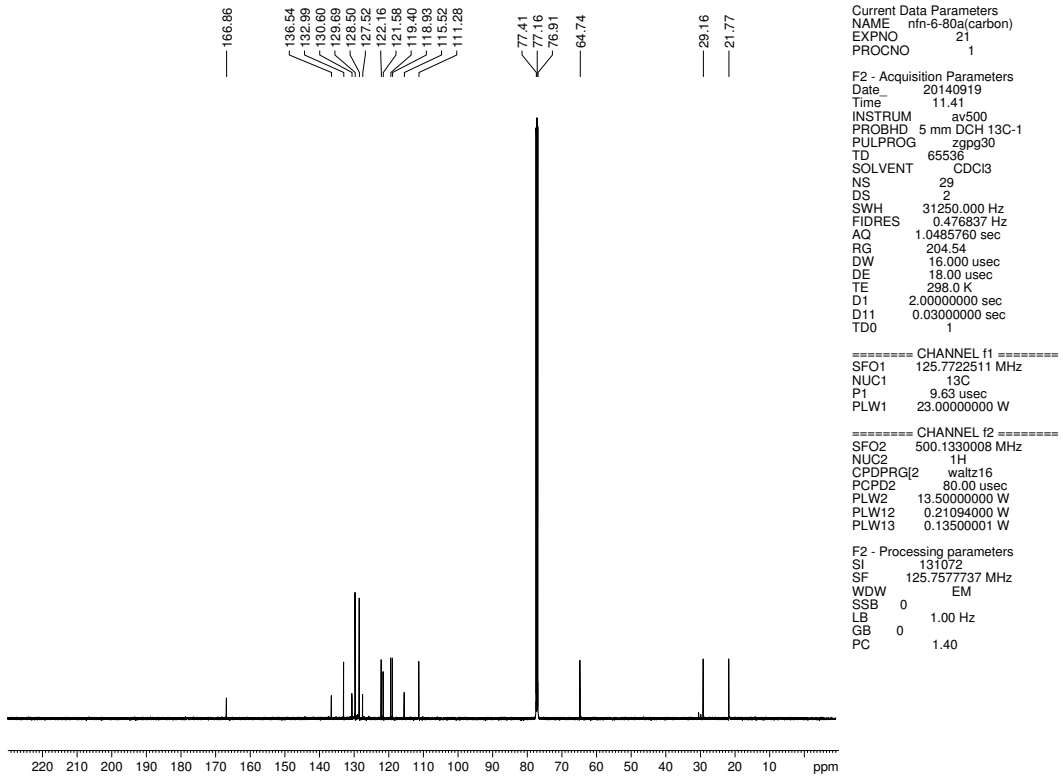

Figure A4.39. ^{13}C NMR (125 MHz, $CDCl_3$) of compound **4.76**

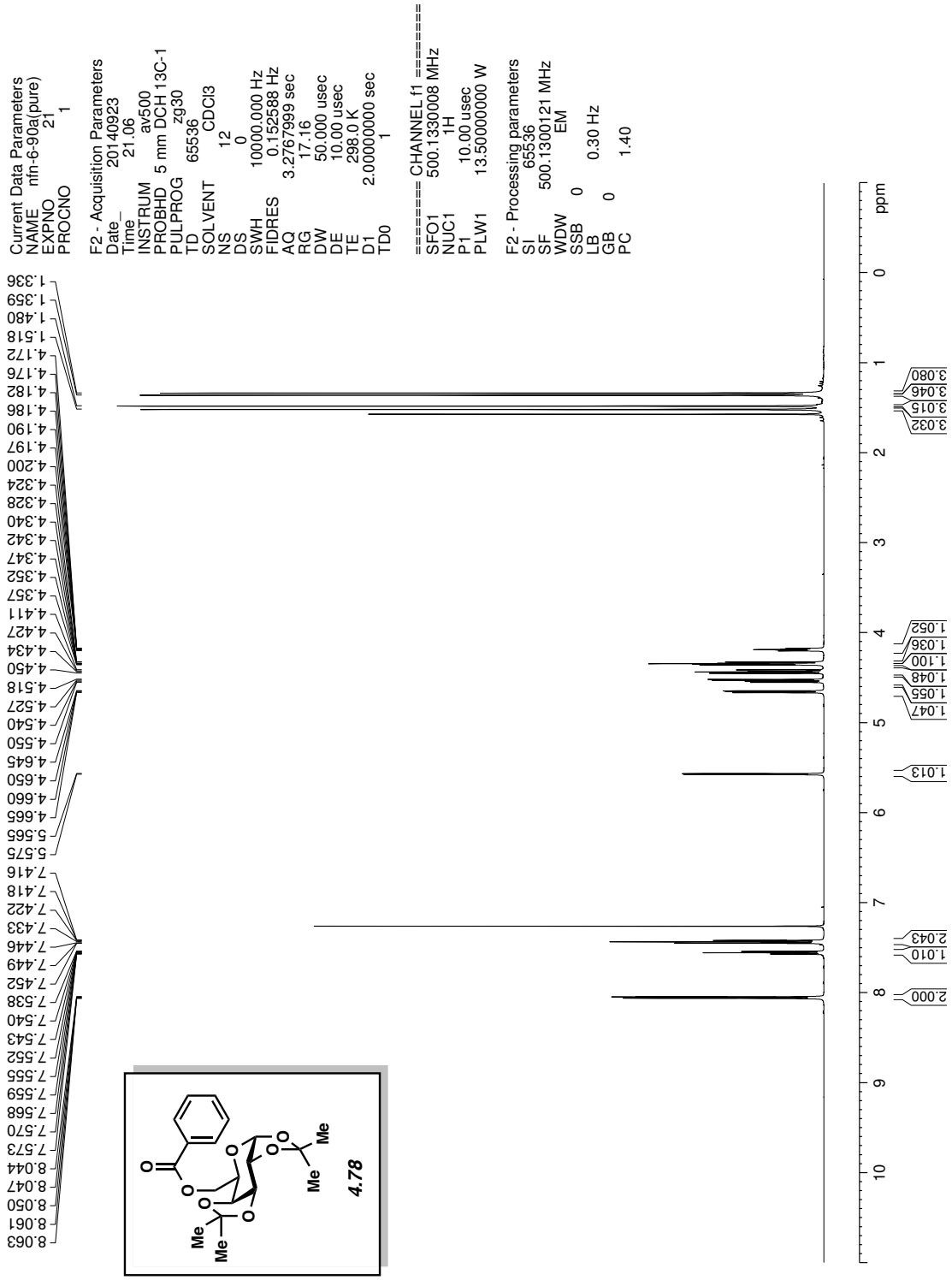

Figure A4.40 ^{1}H NMR (500 MHz, $CDCl_3$) of compound **4.78**

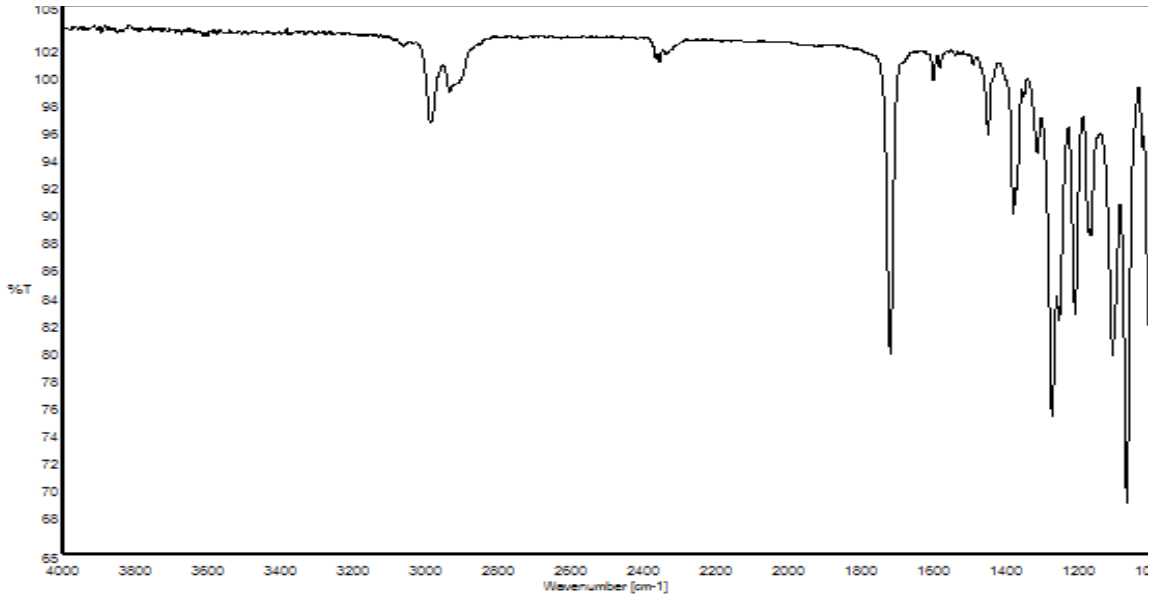

Figure A4.41 Infrared spectrum of compound **4.78**

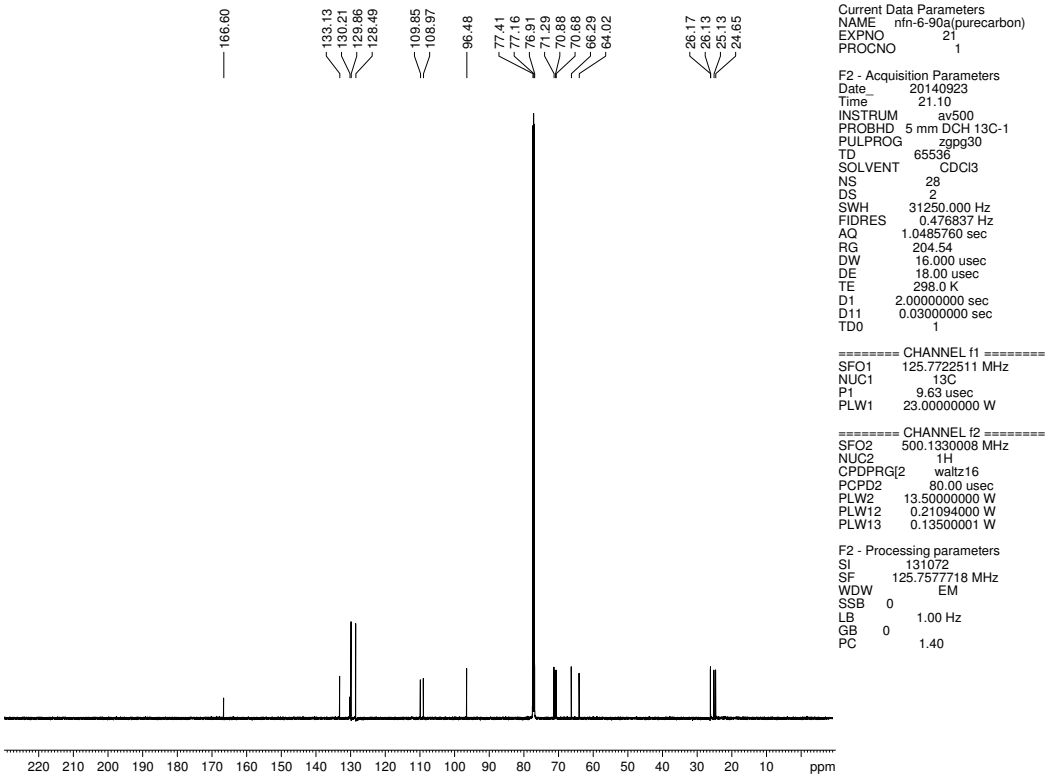

Figure A4.42 ^{13}C NMR (125 MHz, $CDCl_3$) of compound **4.78**

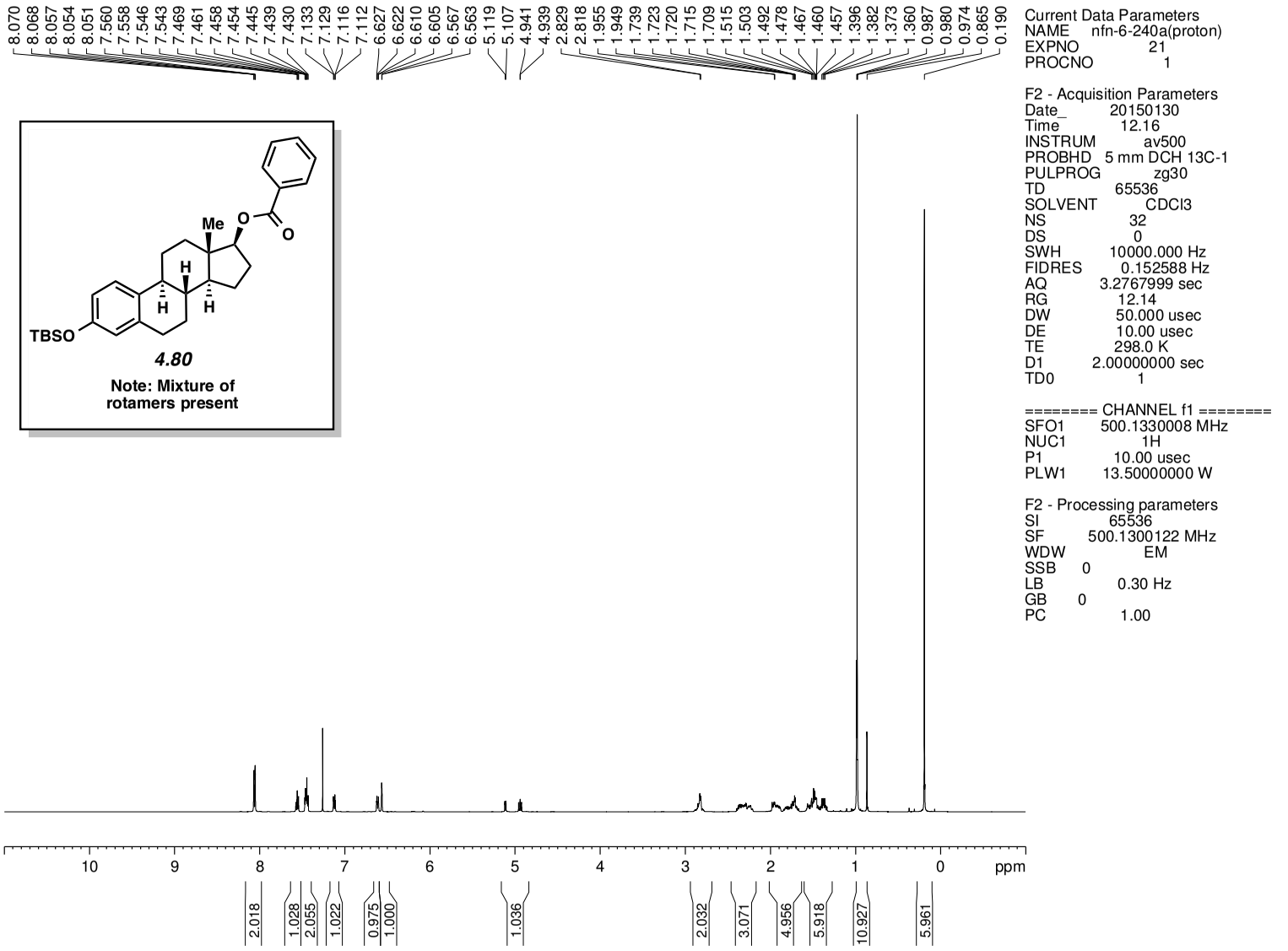

Figure A4.43 ^{1}H NMR (500 MHz, $CDCl_3$) of compound **4.80**

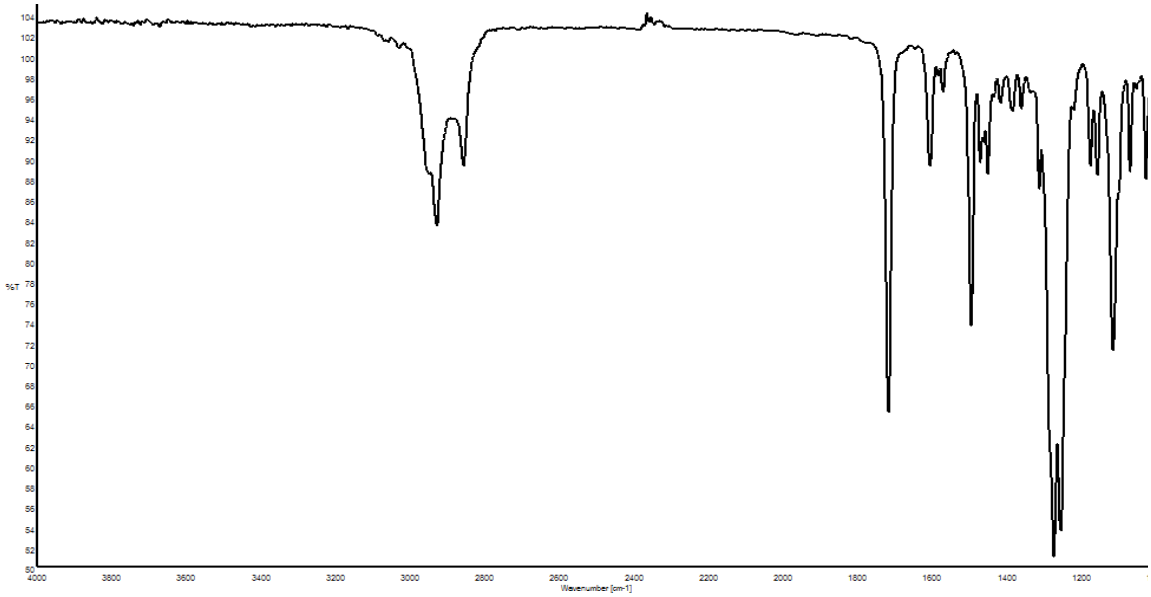

Figure A4.44. Infrared spectrum of compound **4.80**

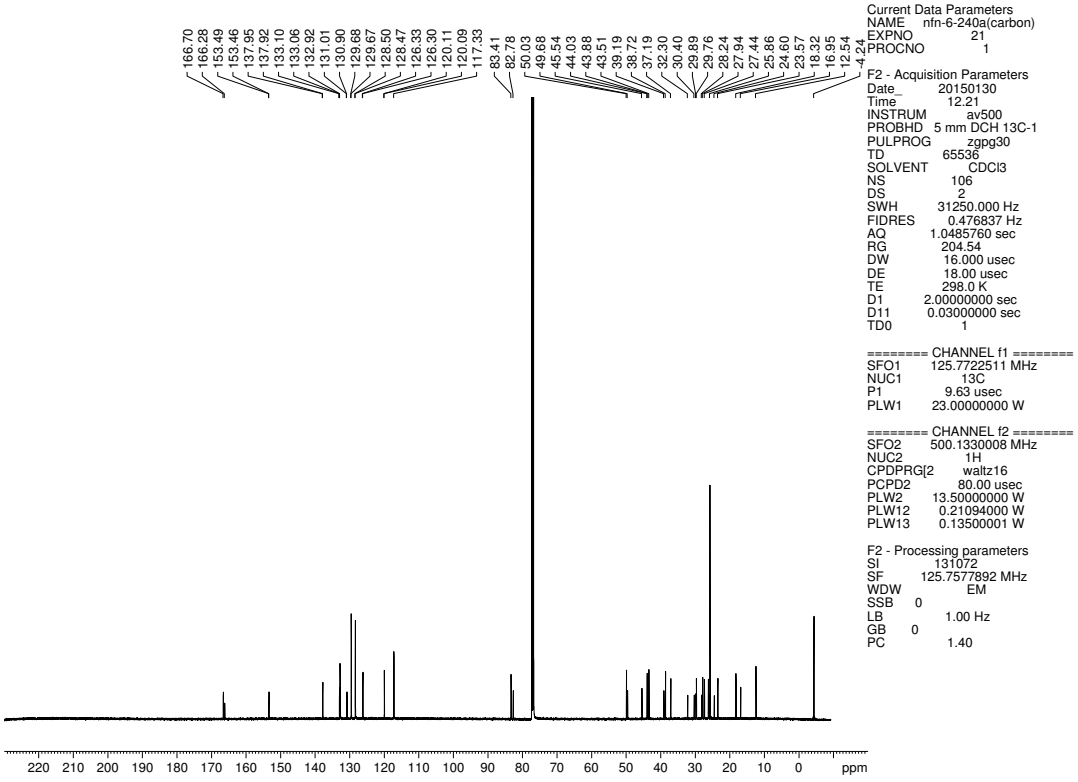

Figure A4.45 ^{13}C NMR (125 MHz, $CDCl_3$) of compound **4.80**

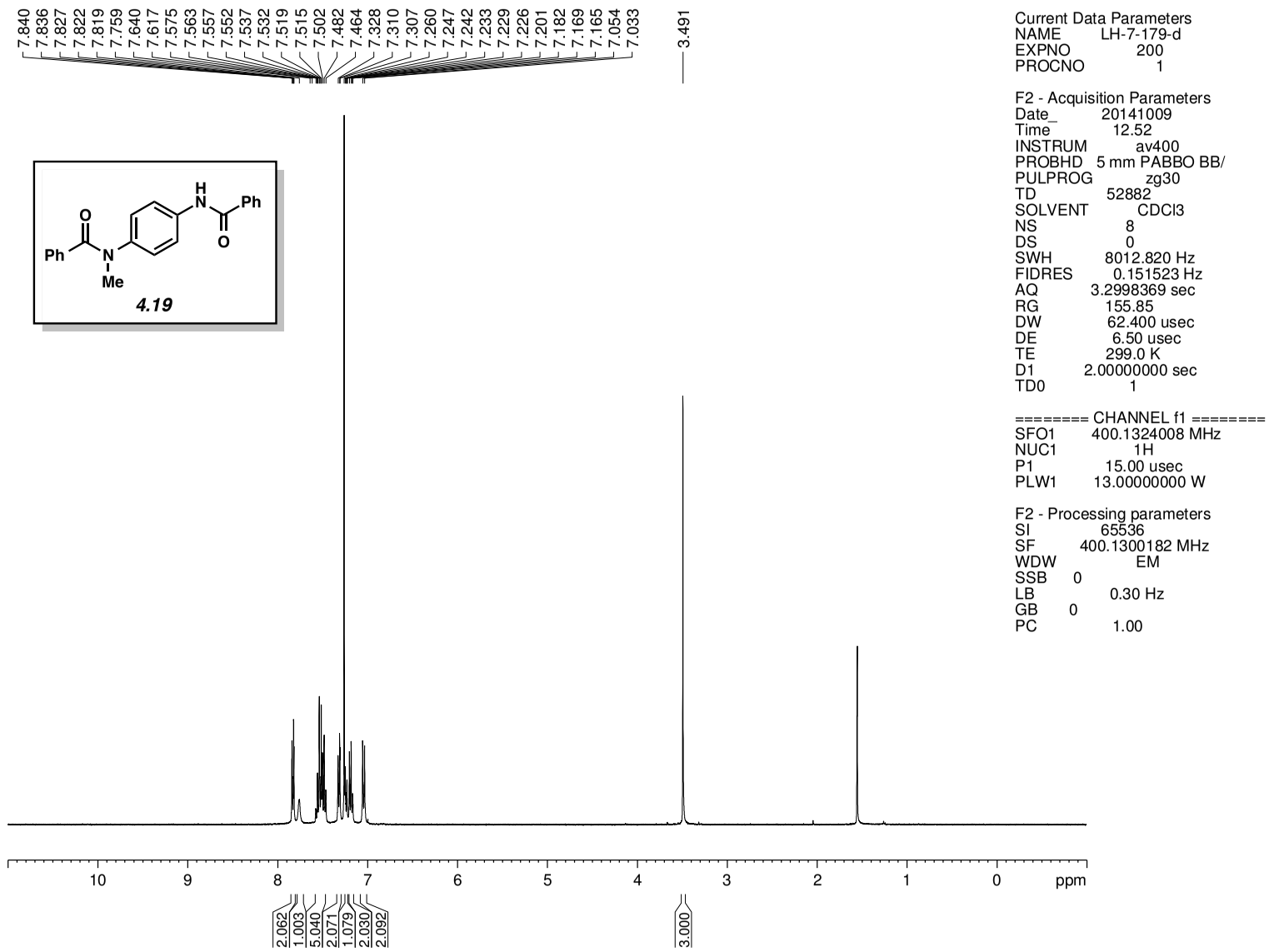

Figure A4.46 ^{1}H NMR (400 MHz, $CDCl_3$) of compound **4.19**

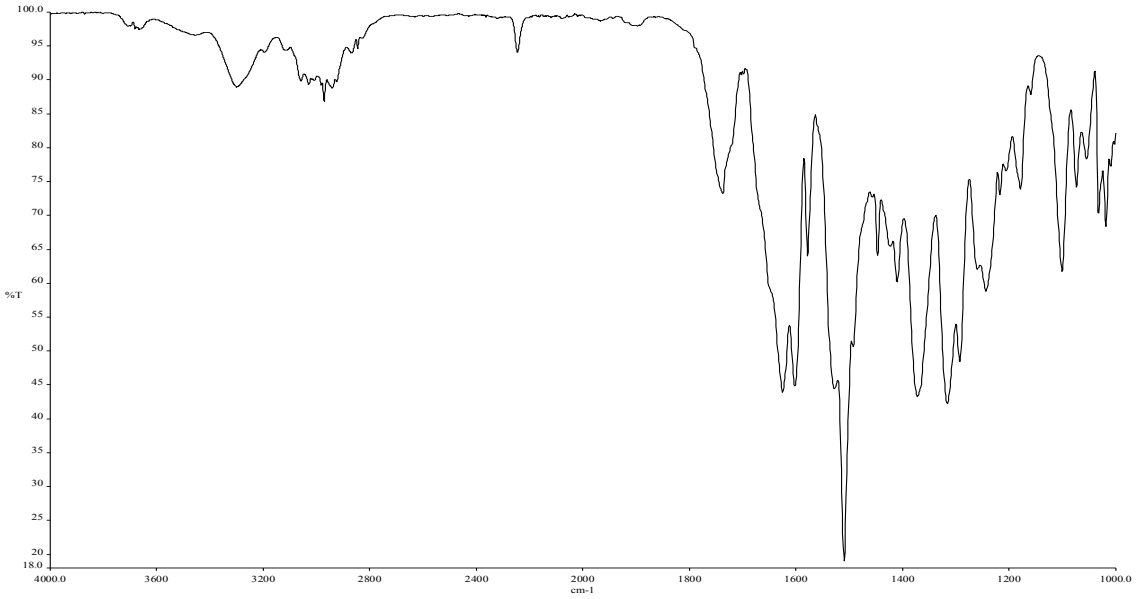

Figure A4.47 Infrared spectrum of compound **4.19**

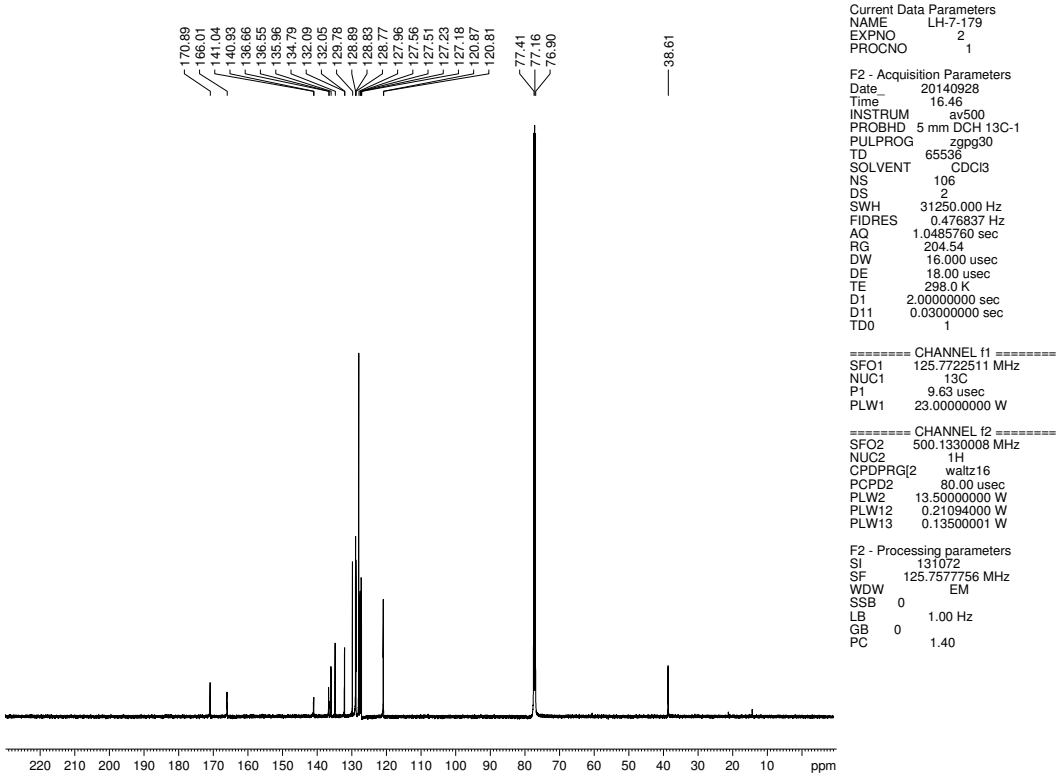

Figure A4.48 ^{13}C NMR (125 MHz, $CDCl_3$) of compound **4.19**

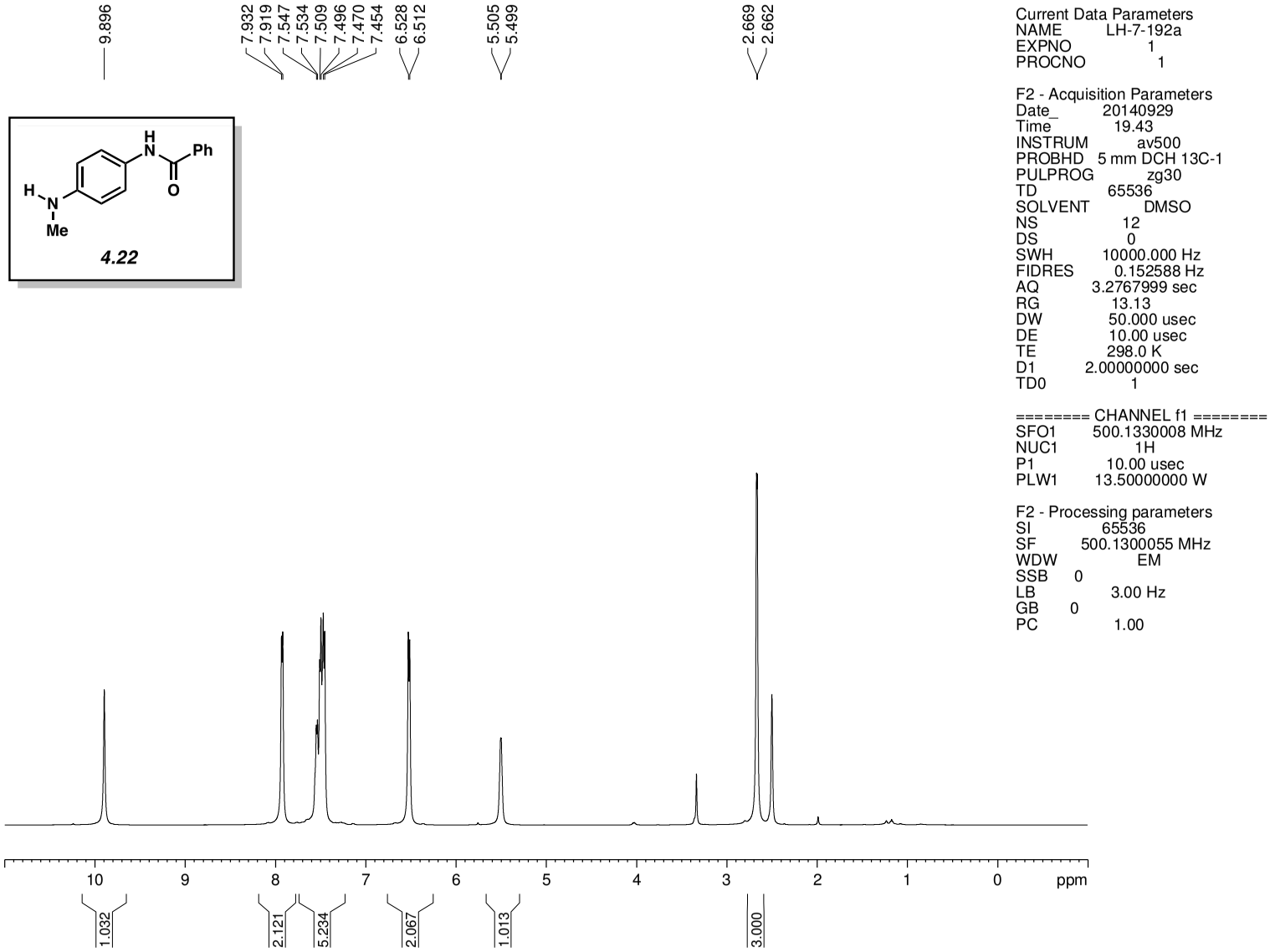

Figure A4.49. ^{1}H NMR (500 MHz, $(CD_3)_2SO$) of compound **4.22**

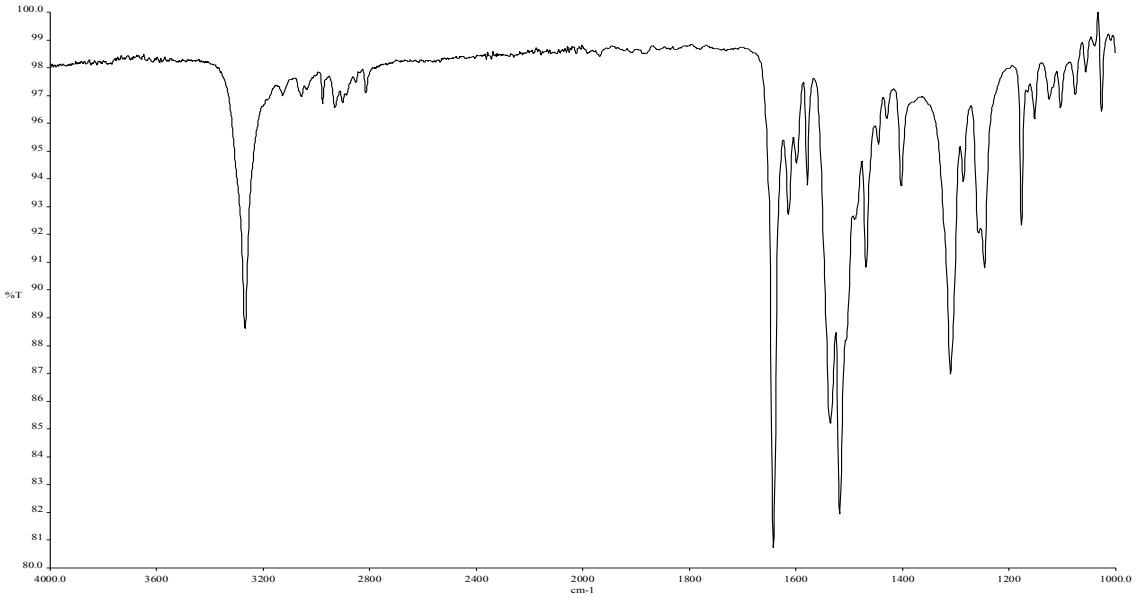

Figure A4.50. Infrared spectrum of compound **4.22**

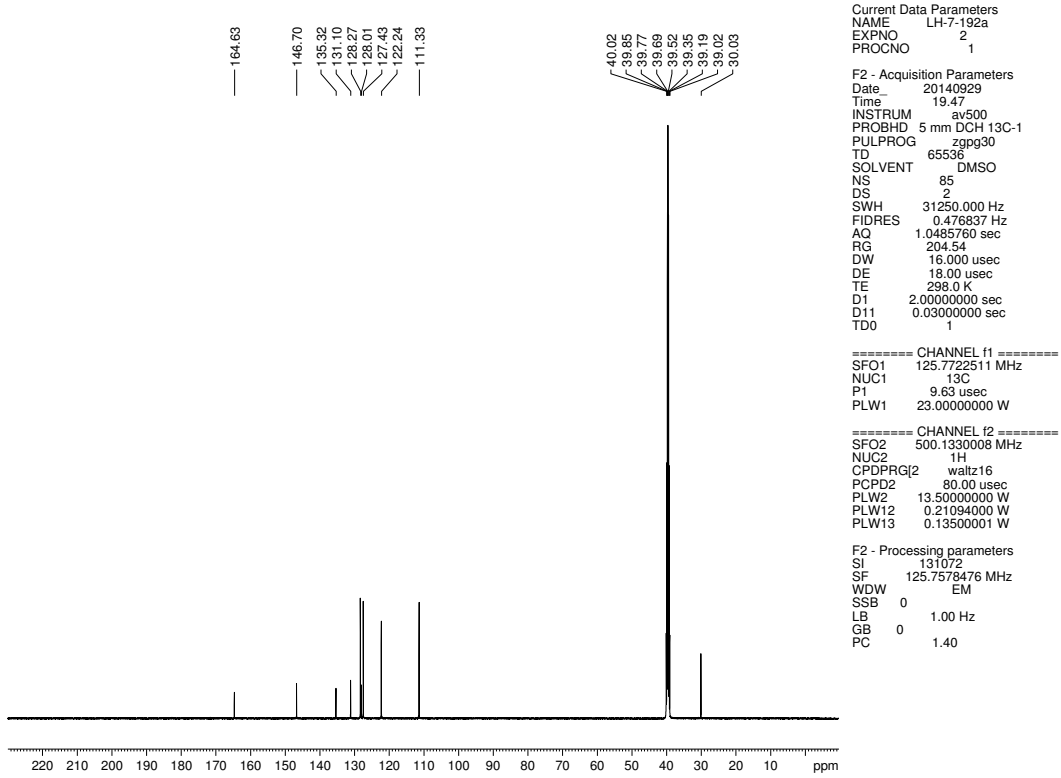

Figure A4.51 ^{13}C NMR (125 MHz, $(CD_3)_2SO$) of compound **4.22**

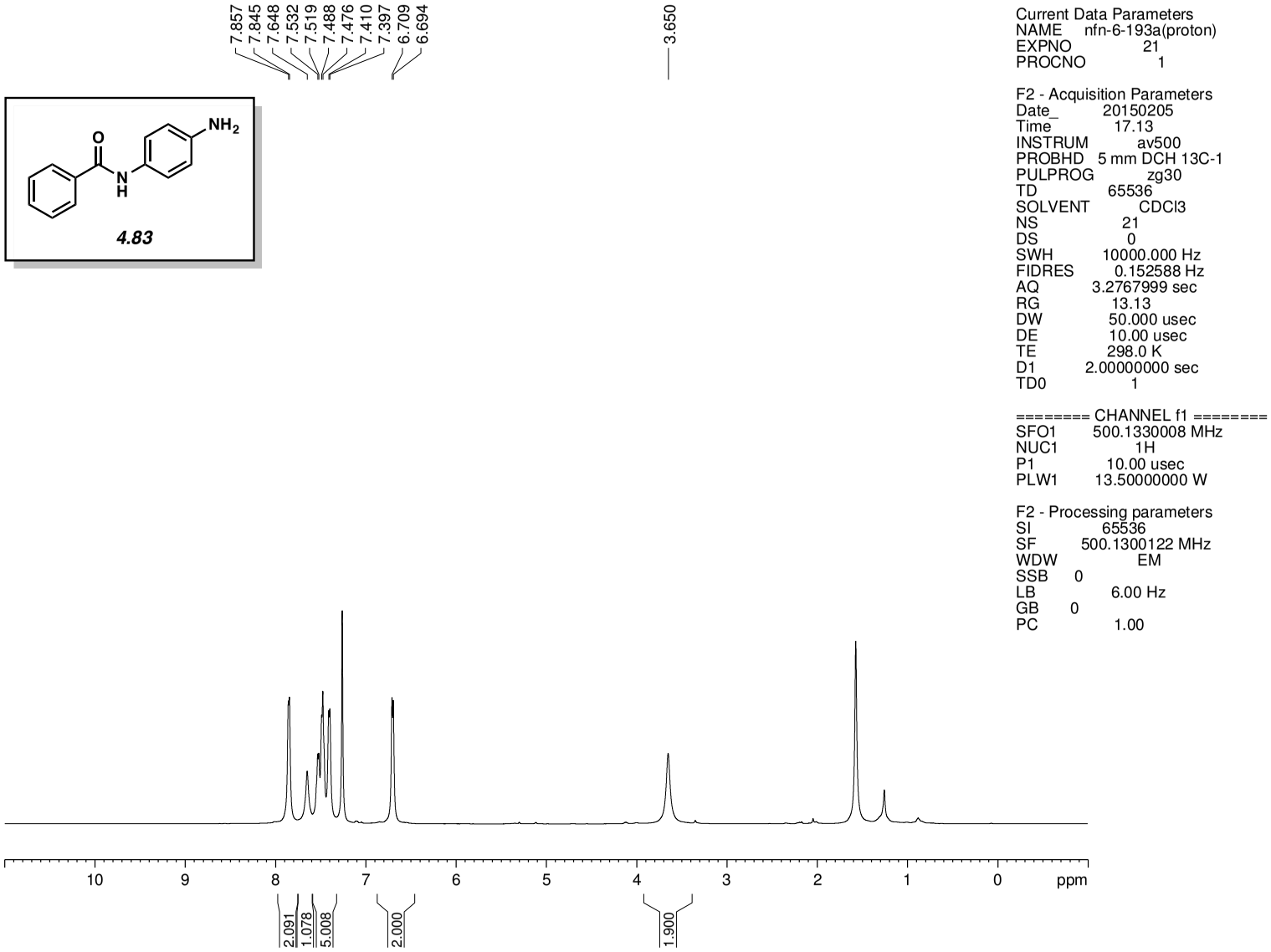

Figure A4.52 ^{1}H NMR (500 MHz, $CDCl_3$) of compound **4.83**

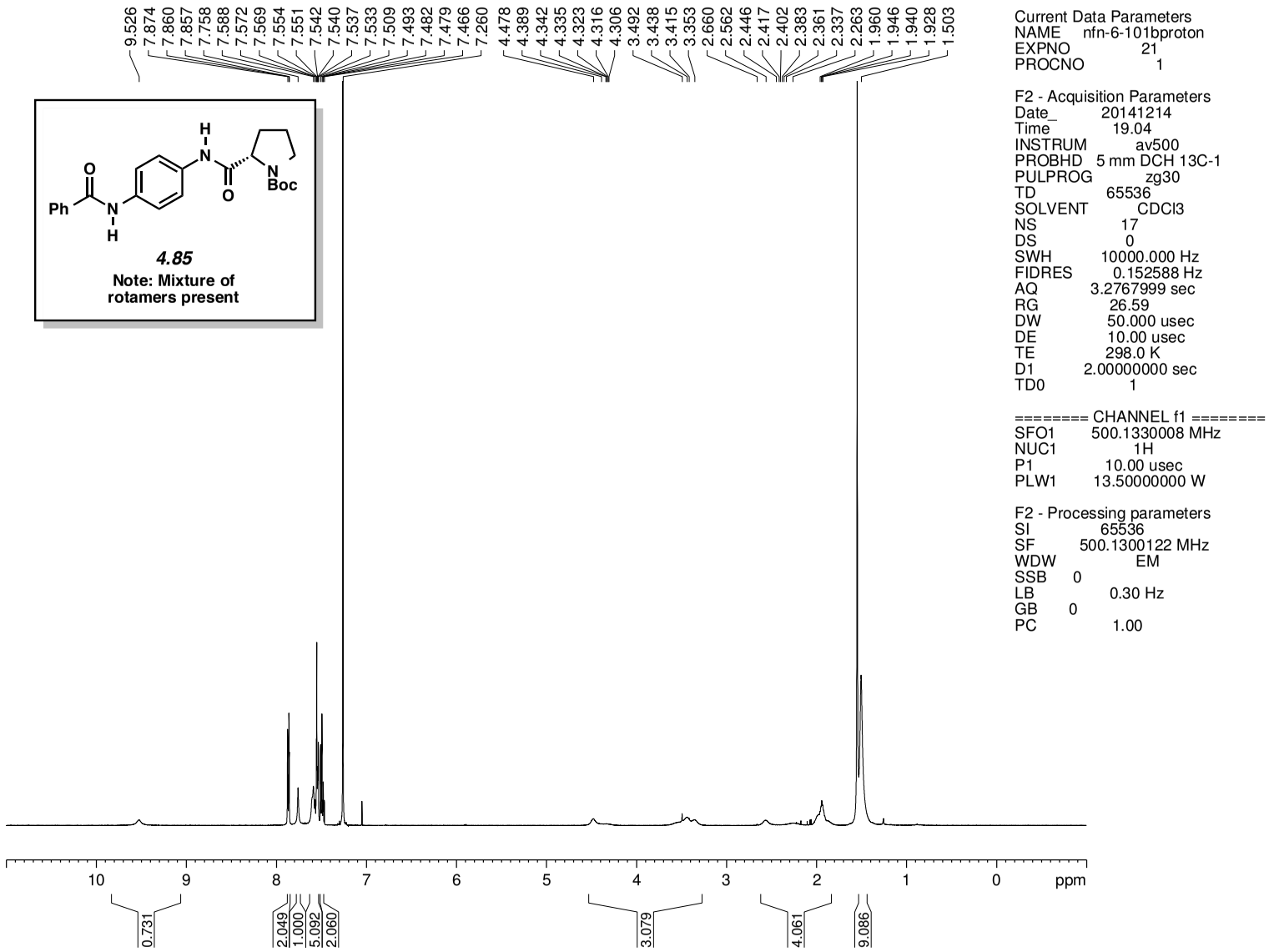

Figure A4.53 ^{1}H NMR (500 MHz, $CDCl_3$) of compound **4.85**

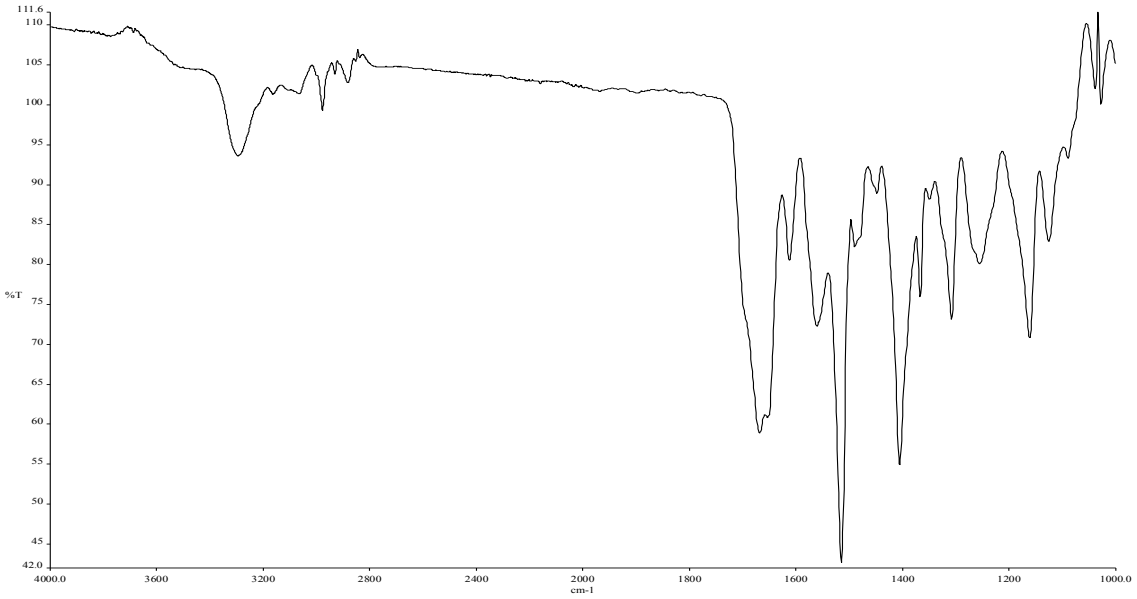

Figure A4.54 Infrared spectrum of compound **4.85**

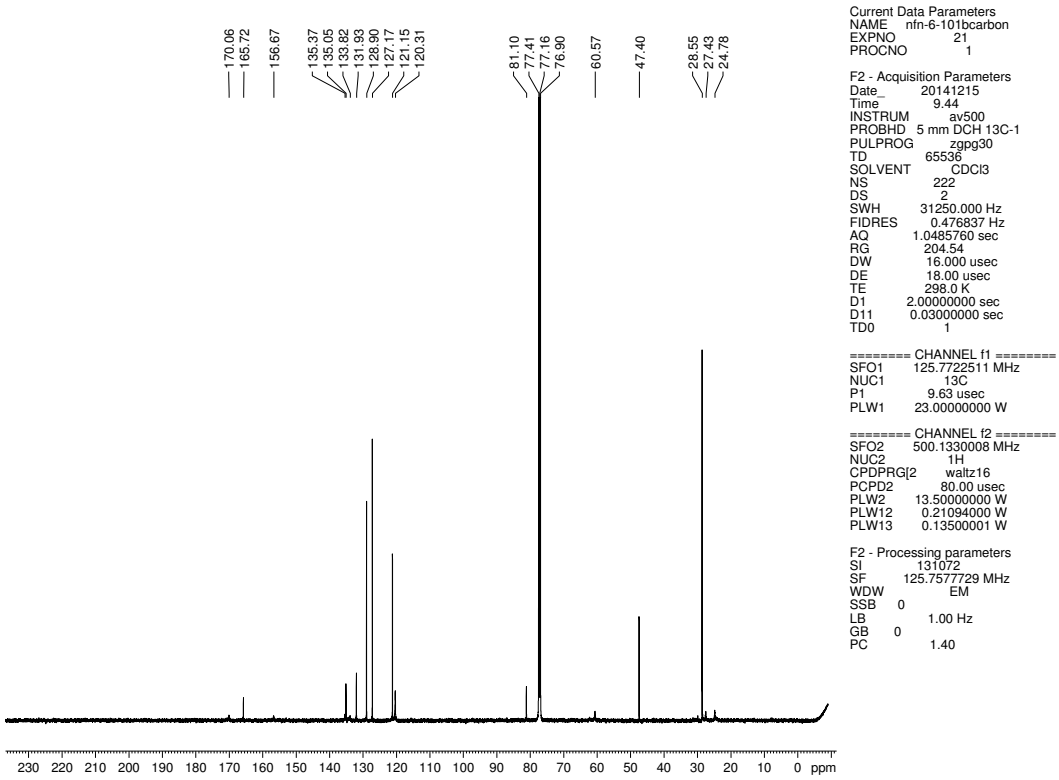

Figure A4.55 ^{13}C NMR (125 MHz, $CDCl_3$) of compound **4.85**

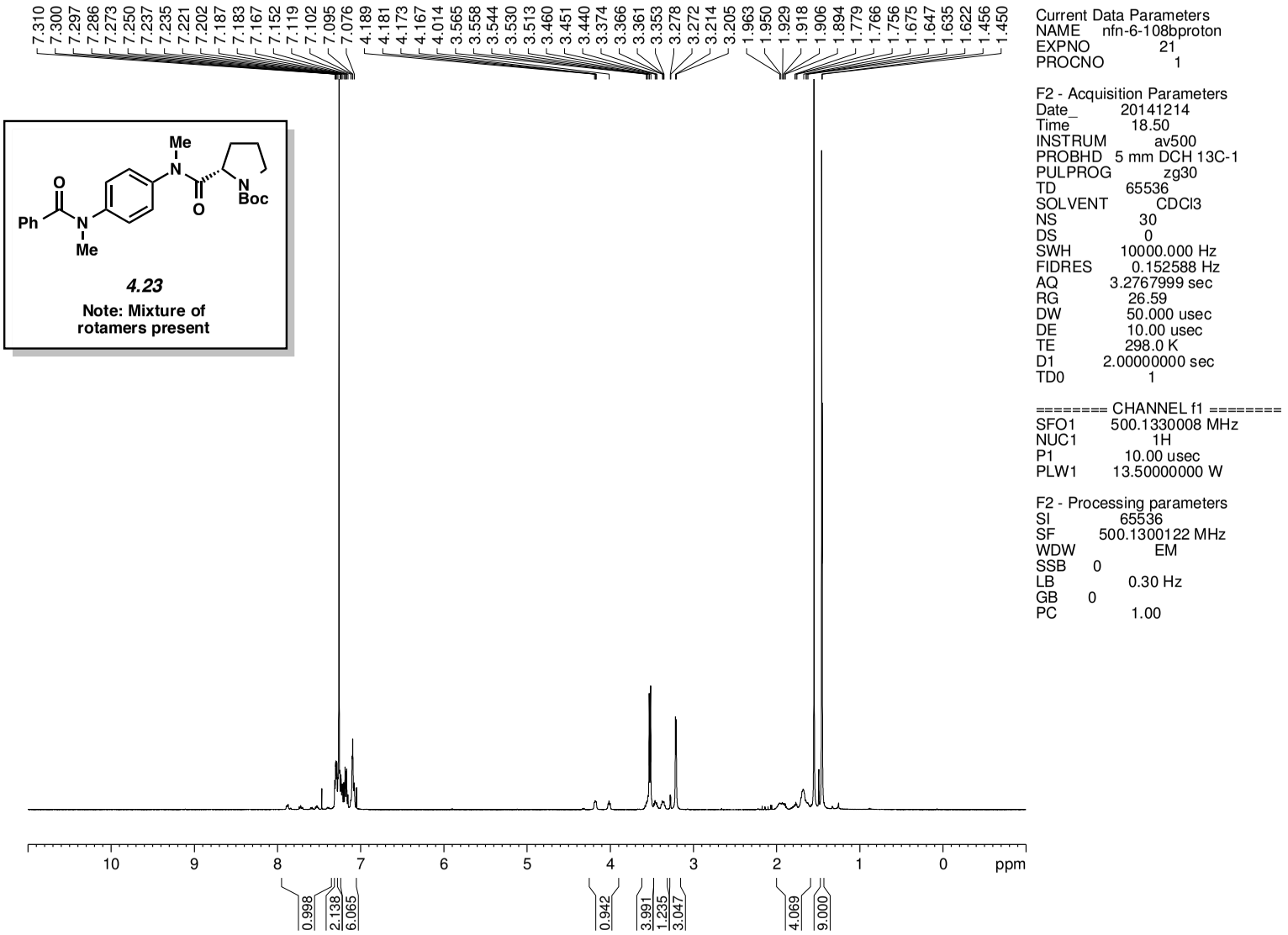

Figure A4.56 ^{1}H NMR (500 MHz, $CDCl_3$) of compound **4.23**

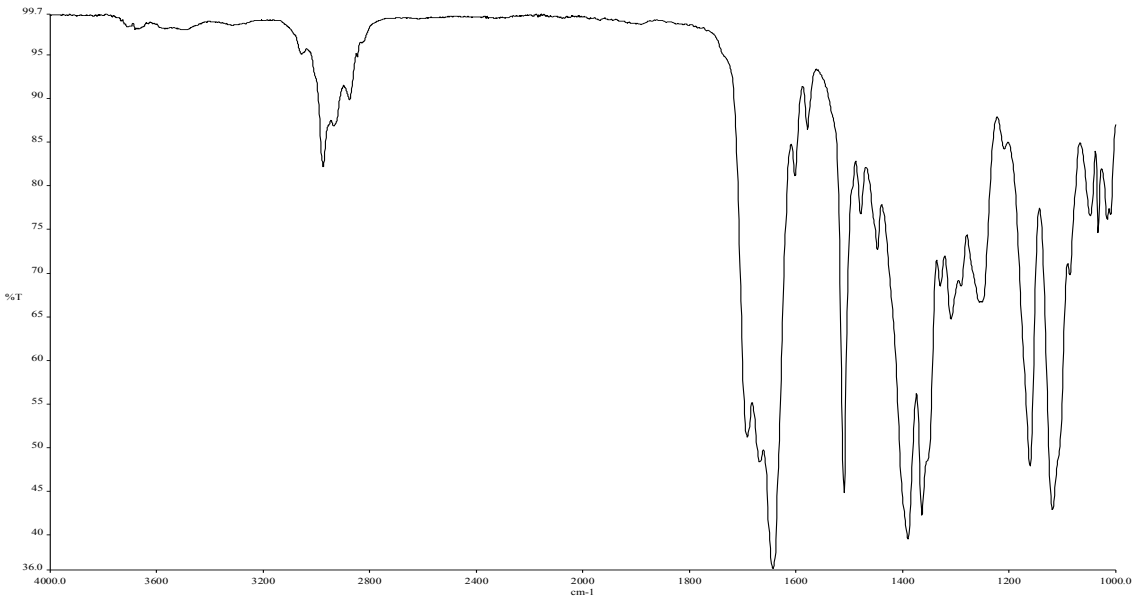

Figure A4.57 Infrared spectrum of compound **4.23**

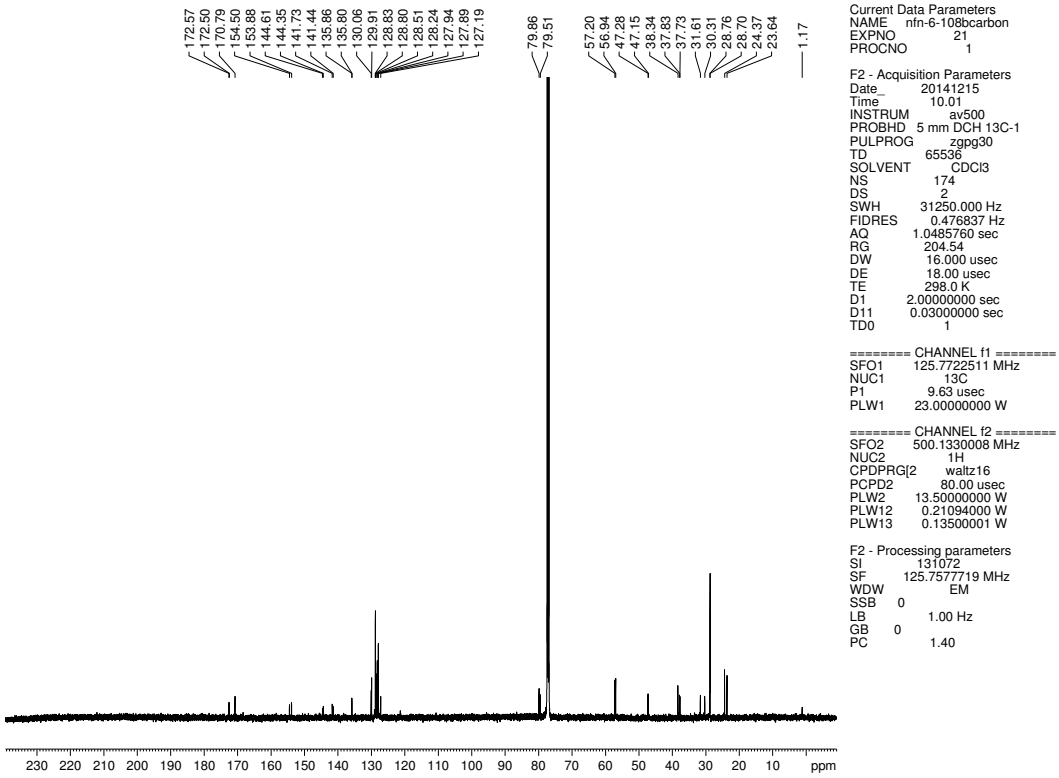

Figure A4.58. ^{13}C NMR (125 MHz, $CDCl_3$) of compound **4.23**

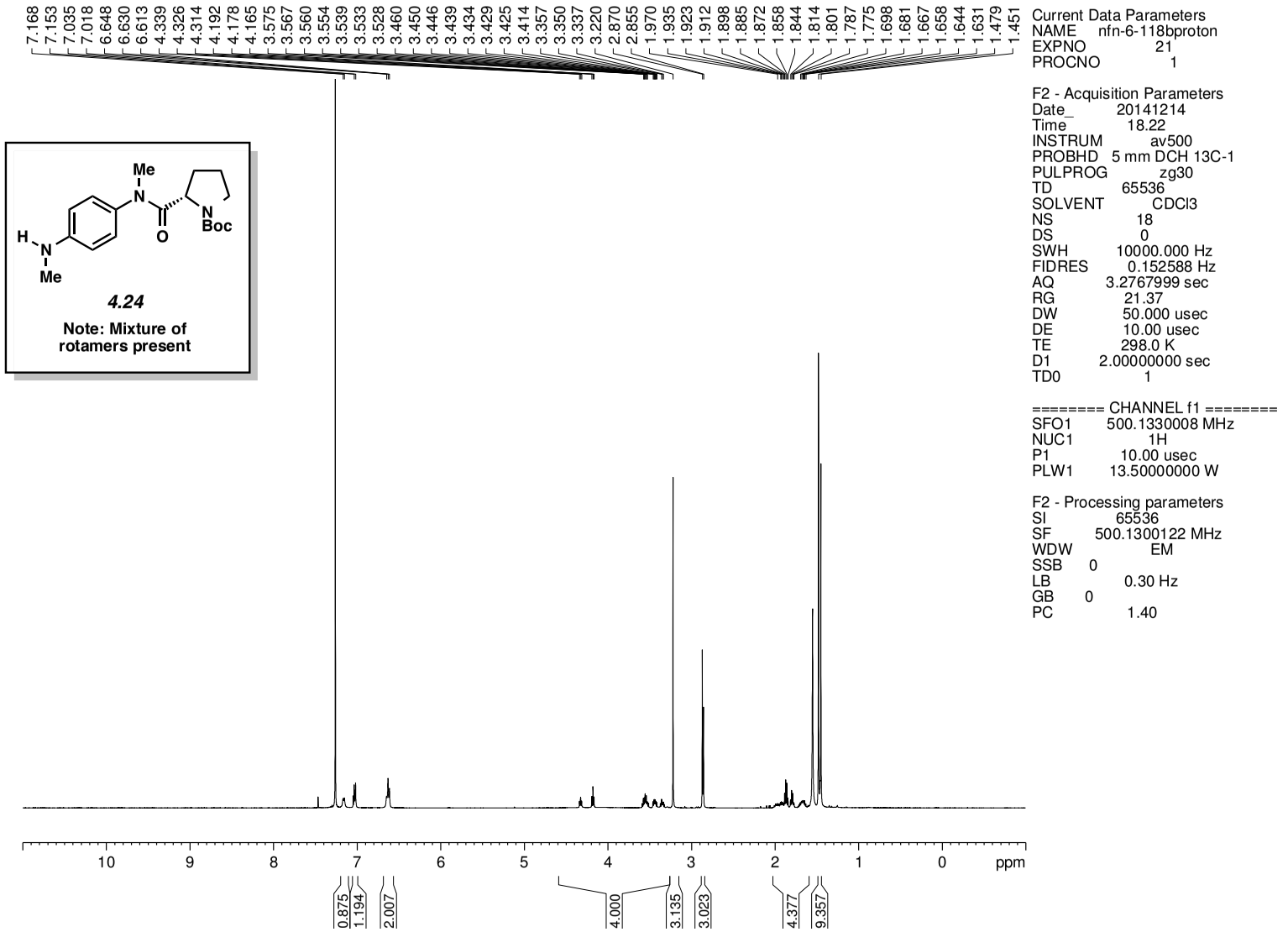

Figure A4.59 ^{1}H NMR (500 MHz, $CDCl_3$) of compound **4.24**

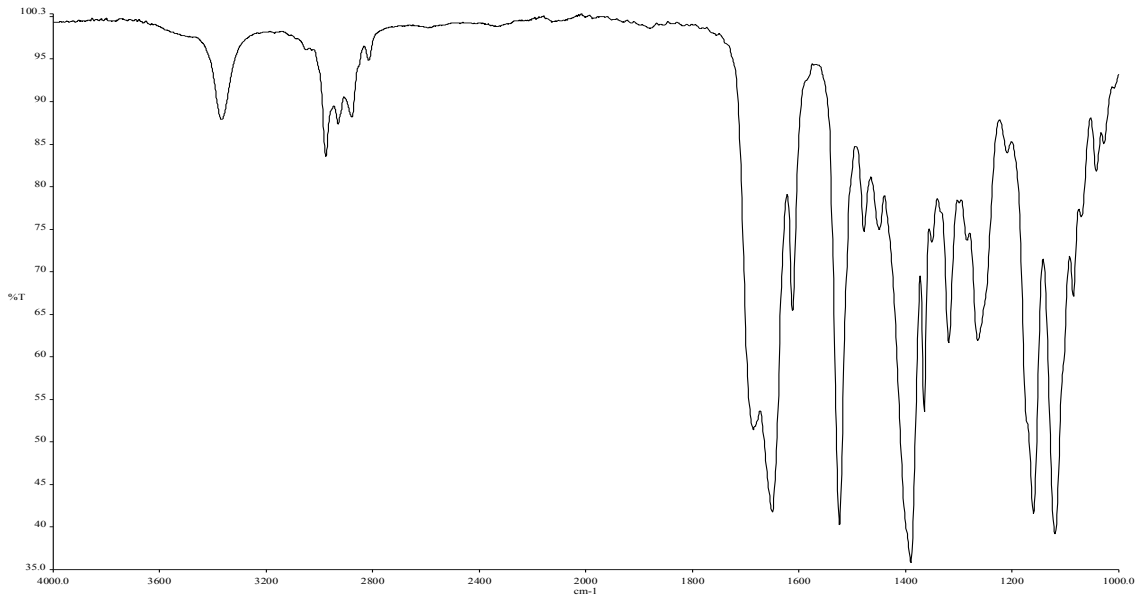

Figure A4.60. Infrared spectrum of compound **4.24**

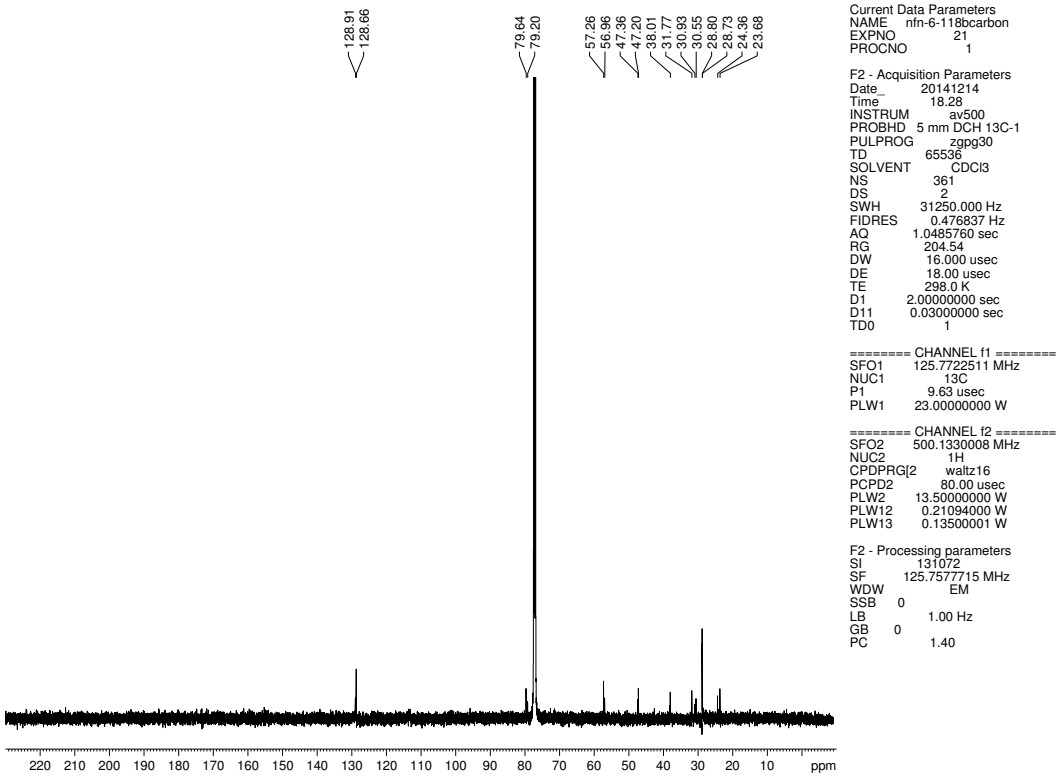

Figure A4.61 ^{13}C NMR (125 MHz, $CDCl_3$) of compound **4.24**

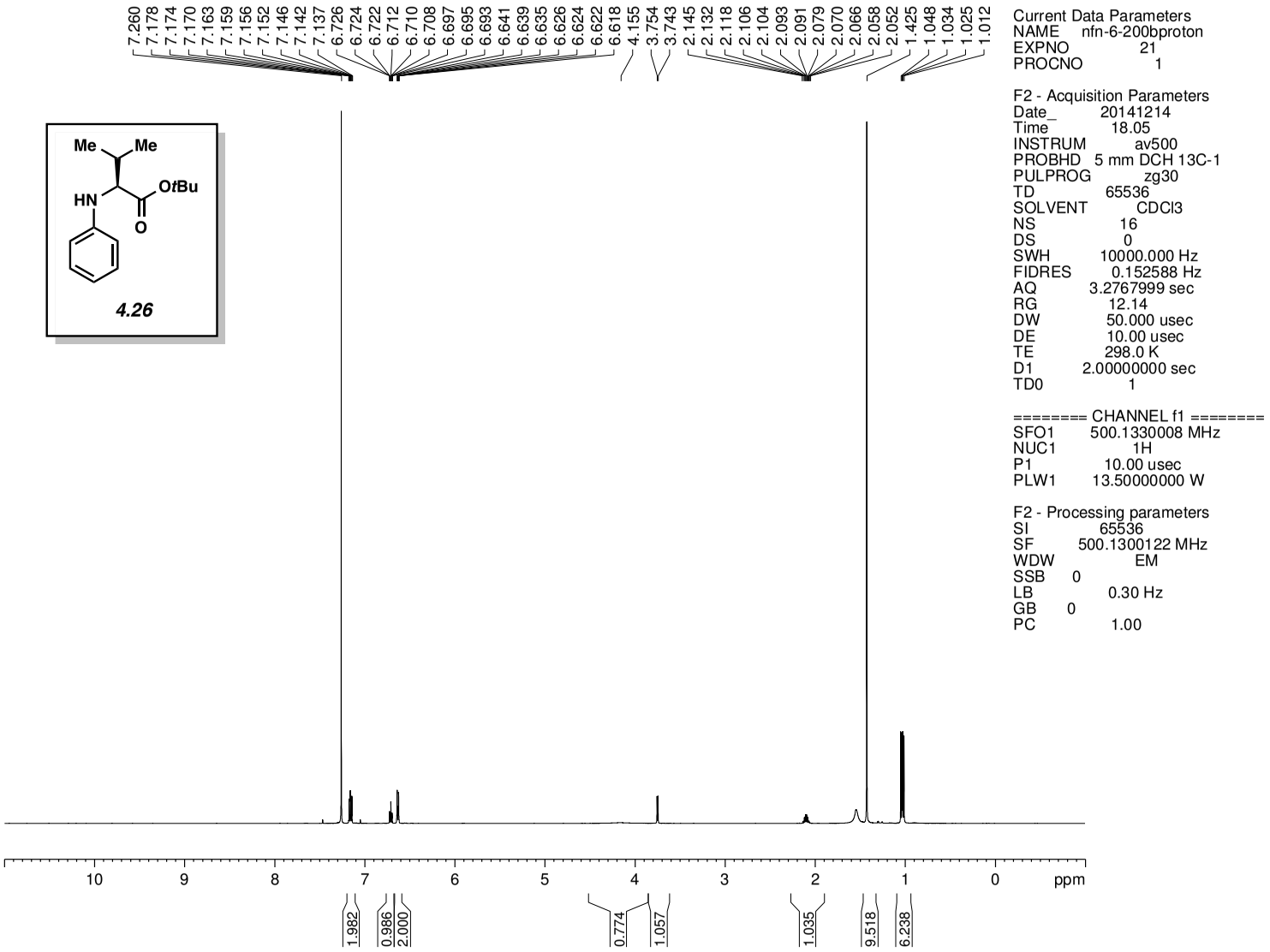

Figure A4.62 ^{1}H NMR (500 MHz, $CDCl_3$) of compound **4.26**

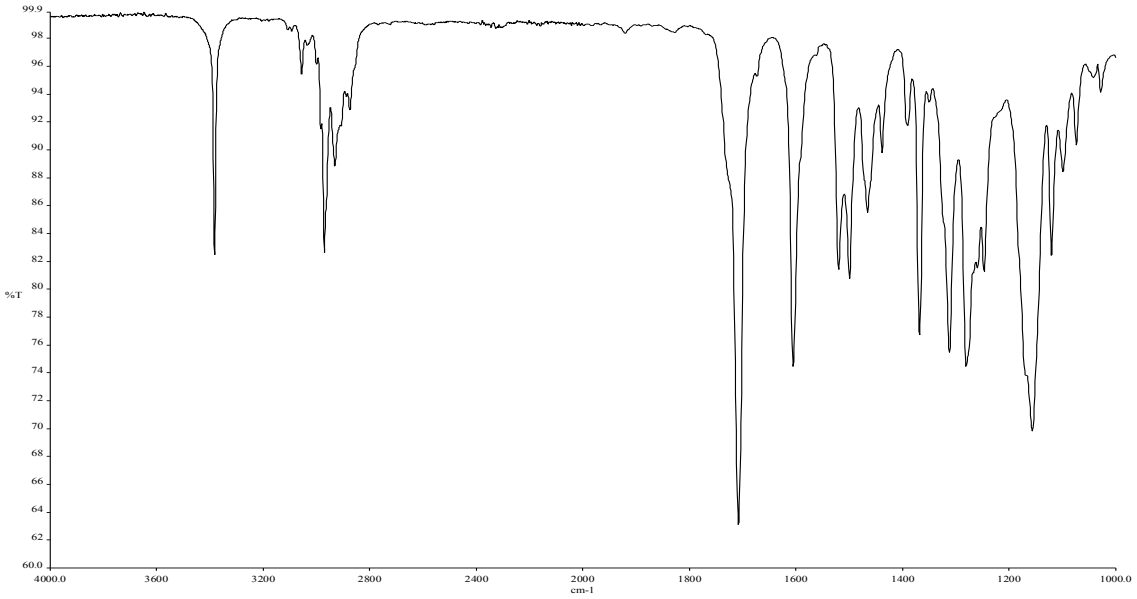

Figure A4.63 Infrared spectrum of compound **4.26**

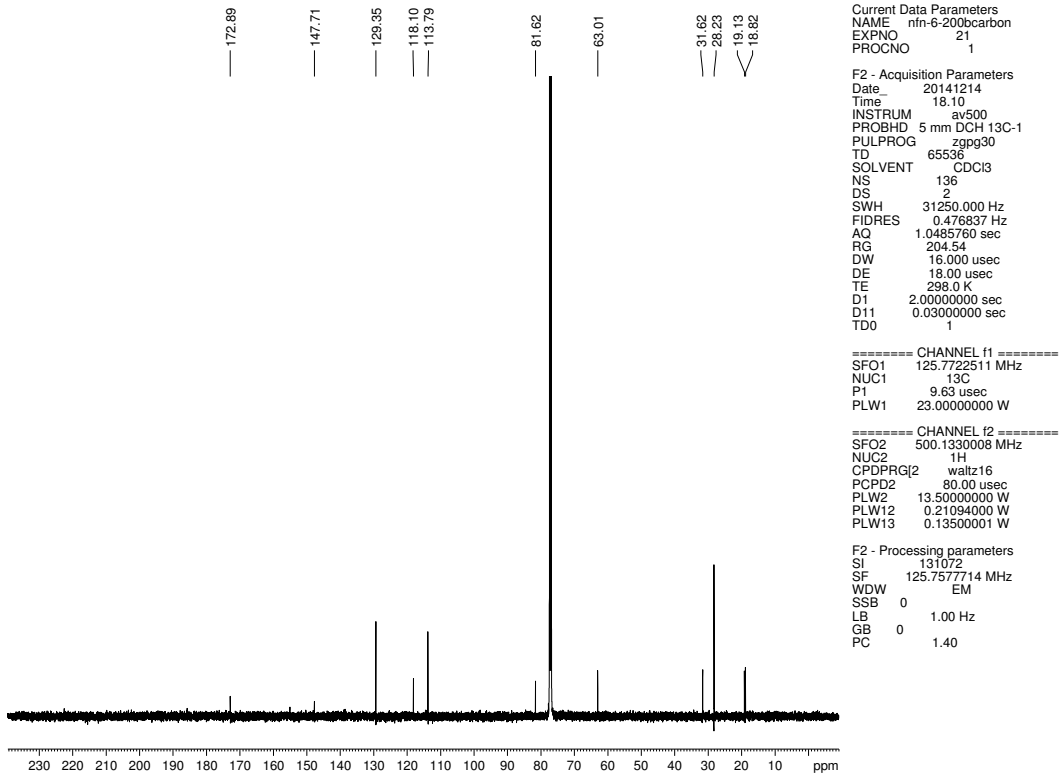

Figure A4.64 ^{13}C NMR (125 MHz, $CDCl_3$) of compound **4.26**

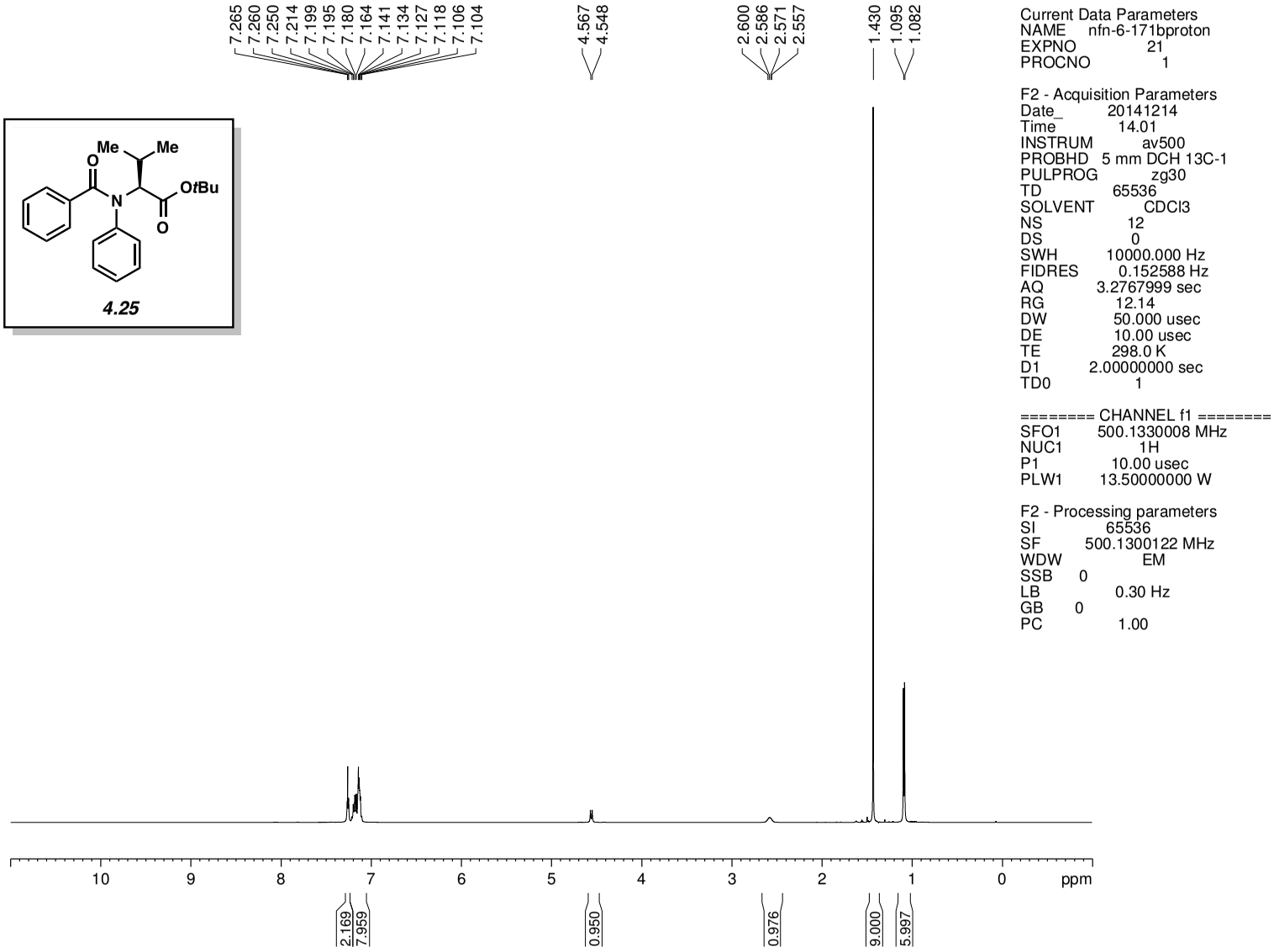

Figure A4.65 ^{1}H NMR (500 MHz, $CDCl_3$) of compound **4.25**

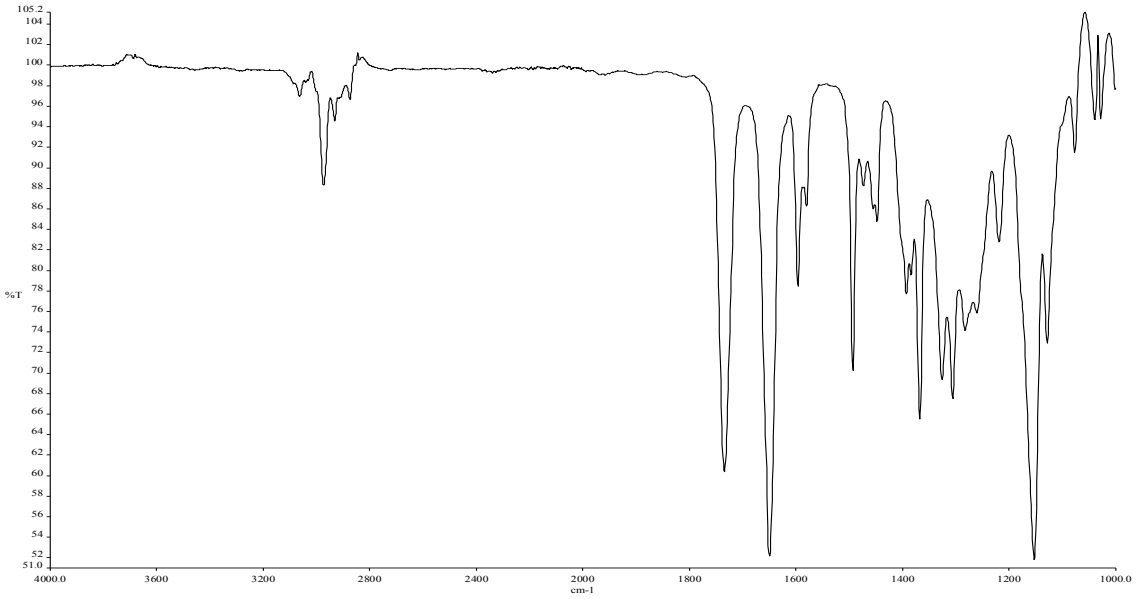

Figure A4.66 Infrared spectrum of compound **4.25**

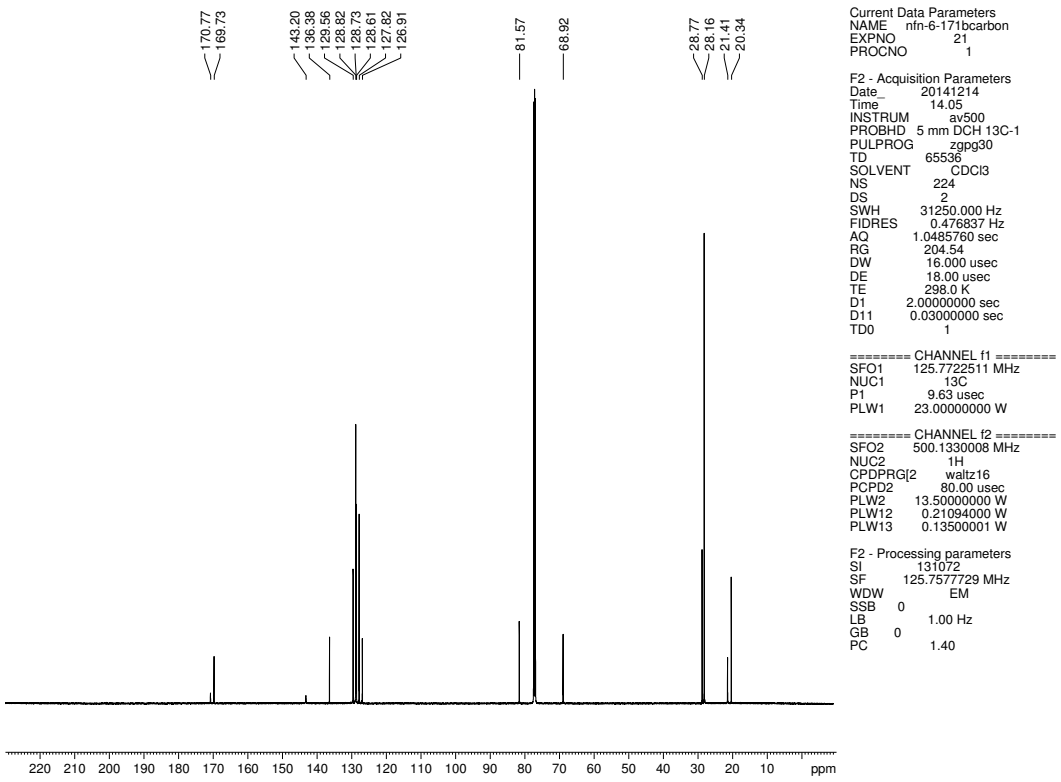

Figure A4.67 ^{13}C NMR (125 MHz, $CDCl_3$) of compound **4.**

4.8. Notes and References

[1] Greenberg, A., Breneman, C. M., Liebman, J. F., Eds. *The Amide Linkage: Structural Significance in Chemistry, Biochemistry, and Materials Science*; Wiley-Interscience, 2003.

[2] Pauling, L.; Corey, R. B.; Branson, H. R. *Proc. Natl Acad. Sci. USA* **1951**, *37*, 205–211.

[3] Brix, K., Stöcker, W., Eds. *Proteases: Structure and Function*; Springer, 2013.

[4] Corey, E. J.; Cheng, X.-M. *The Logic of Chemical Synthesis*; Wiley, 1994.

[5] Hudlicky, T.; Reed, J. W. *The Way of Synthesis: Evolution of Design and Methods for Natural Products*; Wiley, 2007.

[6] Van Vranken, D.L.; Weiss, G. A. *Introduction to Bioorganic Chemistry and Chemical Biology*; Garland Science, 2013.

[7] Spletstoser, J. T.; White, J. M.; Tunoori, A. R.; Georg, G. I. *J. Am. Chem. Soc.* **2007**, *129***,** 3408–3419.

[8] Nahm, S.; Weinreb, S. M. *Tetrahedron Lett.* **1981**, *22*, 3815–3818.

[9] Blangetti, M.; Rosso, H.; Prandi, C.; Deagostino, A.; Venturello, P. *Molecules* **2013**, *18*, 1188–1213.

[10] Tatamidani, H.; Kakiuchi, F.; Chatani, N. *Org. Lett.* **2004**, *6*, 3597–3599.

[11] Dineen, T. A.; Zajac, M. A.; Myers, A. G. *J. Am. Chem. Soc.* **2006**, *128*, 16406–16409.

[12] Stephenson, N. A.; Zhu, J.; Gellman, S. H.; Stahl, S. S. *J. Am. Chem. Soc.* **2009**, *131*, 10003–10008.

[13] Keck, G. E.; McLaws, M. D.; Wager, T. T. *Tetrahedron* **2000**, *56*, 9875–9883.

[14] Nishimoto, S.-i.; Izukawa, T.; Kagiya, T. *Bull. Chem. Soc. Jpn* **1982**, *55*, 1484–1488.

[15] White, E. H. *J. Am. Chem. Soc.* **1955**, *77*, 6011–6014.

[16] Guthrie, J. P.; Pike, D. C.; Lee, Y.-C. *Can. J. Chem.* **1992**, *70*, 1671–1683.

[17] Tasker, S. Z.; Standley, E. A.; Jamison, T. F. *Nature* **2014**, *509*, 299–309.

[18] Mesganaw, T.; Garg, N. K. *Org. Process Res. Dev.* **2013**, *17*, 29–39.

[19] Rosen, B. M. *et al. Chem. Rev.* **2011**, *111*, 1346–1416.

[20] Blakey, S. B.; MacMillan, D. W. C. *J. Am. Chem. Soc.* **2003**, *125*, 6046–6047.

[21] Zhang, X.-Q.; Wang, Z.-X. *Org. Biomol. Chem.* **2014**, *12*, 1448–1453.

[22] Tobisu, M.; Nakamura, K.; Chatani, N. *J. Am. Chem. Soc.* **2014**, *136*, 5587–5590.

[23] Shiba, T., Kurahashi, T. & Matsubara, S. *J. Am. Chem. Soc.* **2013**, *135*, 13636–13639.

[24] Quasdorf, K. W. *et al. J. Am. Chem. Soc.* **2011**, *133*, 6352–6363.

[25] Mesganaw, T. *et al. Chem. Sci.* **2011**, *2*, 1766–1771.

[26] Hong, X.; Liang, Y.; Houk, K. N. *J. Am. Chem. Soc.* **2014**, *136*, 2017–2024.

[27] Lu, Q.; Yu, H.; Fu, Y. *J. Am. Chem. Soc.* **2014**, *136*, 8252–8260.

[28] Xu, H. *et al. J. Am. Chem. Soc.* **2014**, *136*, 14834–14844.

[29] Yamamoto, T.; Ishizu, J.; Kohara, T.; Komiya, S.; Yamamoto, A. *J. Am. Chem. Soc.* **1980**, *102*, 3758–3764.

[30] Amaike, K.; Muto, K.; Yamaguchi, J.; Itami, K. *J. Am. Chem. Soc.* **2012**, *134*, 13573–13576.

[31] (a) Rao, Y.; Li, X.; Danishefsky, S. J. *J. Am. Chem. Soc*. **2009**, *131*, 12924–12926. (b) Oldenhuis, N. J.; Dong, V. M.; Guan, Az. *Tetrahedron* **2014**, *70*, 4213–4218. (c) Friel,

D. K.; Snapper, M. L.; Hoveyda, A. H. *J. Am. Chem. Soc*. **2008**, *130*, 9942–9951. (d) Ueda, S.; Nagasawa, H. *J. Org. Chem*. **2009**, *74*, 4272–4277. (e) Li, Y.; Jia, F.; Li, Z. *Chem. Eur. J*. **2013**, *19*, 82–86. (f) Wang, S.; Wang, J.; Guo, R.; Wang, G.; Chen, S.-Y.; Yu, X.-Q. *Tetrahedron Lett*. **2013**, *54*, 6233–6236. (h) Baroudi, A.; Alicea, J.; Flack, P.; Kirincich, J.; Alabugin, I. V. *J. Org. Chem*. **2011**, *76*, 1521–1537. (h) Fang, W.; Deng, Q.; Xu, M.; Tu, T. *Org. Lett*. **2013**, *15*, 3678–3681. (i) Ganton, M. D.; Kerr. M. A. *Org. Lett*. **2005**, *7*, 4777–4779. (j) Yates, M. H.; Kallman, N. J.; Ley, C. P.; Wei, J. N. *Org. Process. Rev. Dev*. **2009**, *13*, 255–262. (k) Oishi, S.; Saito, S. *Angew. Chem. Int. Ed*. **2012**, *51*, 5395–5399. (l) Johnson II, D. C.; Widlanski, T. S. *Tetrahedron Lett*. **2004**, *45*, 8483–8487.

[32] Zhang, C.; Feng, P.; Jiao, N. *J. Am. Chem. Soc*. **2013**, *135*, 15257–15262.

[33] Ye, Y.; Sanford, M. S. *J. Am. Chem. Soc*. **2012**, *134*, 9034–9037.

[34] Tschaen, B. A.; Schmink, J. R.; Molander, G. A. *Org. Lett*. **2013**, *15*, 500–503.

[35] Powell, A. B.; Stahl, S. S. *Org. Lett*. **2013**, *15*, 5072–5074.

[36] Dohi, S.; Moriyama, K.; Togo, H. *Eur. J. Org. Chem*. **2013**, *34*, 7815–7822.

[37] Correa, A.; Leon, T.; Martin, R. *J. Am. Chem. Soc*. **2014**, *136*, 1062–1069.

[38] Hirashima, S.-I.; Nobuta, T.; Tada, N.; Miura, T.; Itoh, A. *Org. Lett*. **2010**, *12*, 3645–3647.

[39] Harrar, K.; Reiser, O. *Chem. Commun*. **2013**, *48*, 3457–3459.

[40] Heller, S. T.; Sarpong, R. *Org. Lett*. **2010**, *12*, 4572–4574.

[41] Dong, J.; Shi, X.-X.; Yan, J.-J.; Xing, J.; Xhang, Q.; Xiao, S. *Eur. J. Org. Chem*. **2010**, *36*, 6987–6992.

[42] Hanato, M.; Furuya, Y.; Shimmura, T.; Moriyama, K.; Kamiya, S.; Maki, T.; Ishihara, K. *Org. Lett*. **2011**, *13*, 426–429.

[43] Zhou, W.; Li, H.; Wang, L. *Org. Lett*. **2012**, *14*, 4594–4597.

[44] Liu, Z.; Ma, Q.; Liu, Y.; Wang, Q. *Org. Lett*. **2014**, *16*, 236–239.

[45] Kanoh, S.; Naka, M.; Nishimura, T.; Motoi, M. *Tetrahedron* **2002**, *58*, 7049–7064.

[46] Ueda, T.; Konishi, H.; Manabe, K. *Org. Lett*. **2013**, *15*, 5370–5373.

[47] Holan, M.; Jahn, U. *Org. Lett*. **2014**, *16*, 58–61.

[48] Wang, J.; Yin, X.; Wu, J.; Wu, D.; Pan, Y. *Tetrahedron* **2013**, *69*, 10463–10469.

[49] (a) Becke, A. D. *J. Chem. Phys.* **1993**, *98*, 5648–5652. (b) Lee, C.; Yang W.; Parr, R. G. *Phys. Rev. B* **1988**, *37*, 785–789. (c) Becke, A. D. *J. Chem. Phys.* **1993**, *98*, 1372–1377. (d) Stephens, P. J.; Devlin, F. J.; Chabalowski, C. F.; Frisch, M. J. *J. Phys. Chem.* **1994**, *98*, 1623–1627.

[50] (a) Hay, P. J.; Wadt, W. R. *J. Chem. Phys.* **1985**, *82*, 299–310. (b) Roy, L. E.; Hay, P. J.; Martin, R. L. *J. Chem. Theory Comput.* **2008**, *4*, 1029–1031. (c) Ehlers, A. W.; Böhme, M.; Dapprich, S.; Gobbi, A.; Höllwarth, A.; Jonas, V.; Köhler, K. F.; Stegmann, R.; Veldkamp, A.; Frenking, G. *Chem. Phys. Lett.* **1993**, *208*, 111–114.

[51] (a) Ditchfield, R.; Hehre, W. J.; Pople, J. A. *J. Chem. Phys.* **1971**, *54*, 724–728. (b) Hehre, W. J.; Ditchfield, R.; Pople, J. A. *J. Chem. Phys.* **1971**, *54*, 2257–2261. (c) Hariharan, P. C.; Pople, J. A. *Theor. Chim. Acta.* **1973**, *28*, 213–222.

[52] Zhao, Y.; Truhlar, D. G. *Theor. Chem. Acc.* **2008**, *120*, 215–241.

[53] (a) Dolg, M.; Wedig, U.; Stoll, H.; Preuss, H. *J. Chem. Phys.* **1987**, *86*, 866–872. (b) Andrae, D.; Häußermann, U.; Dolg, M.; Stoll, H.; Preuß, H. *Theor. Chem. Acc.* **1990**, *77*, 123–141.

[54] Marenich, A. V.; Cramer, C. J.; Truhlar, D. G. *J. Phys. Chem. B* **2009**, *113*, 6378–6396.

[55] Legault, C. Y. CYLView, 1.0b; Université de Sherbrooke, Canada, **2009**; http://www.cylview.org.

[56] W.E. Acree, Jr., J.S. Chickos, "Phase Transition Enthalpy Measurements of Organic and Organometallic Compounds" in NIST Chemistry WebBook, **NIST Standard Reference Database Number 69**, Eds. P.J. Linstrom and W.G. Mallard, National Institute of Standards and Technology, Gaithersburg MD, 20899, http://webbook.nist.gov, (retrieved March 27, 2015).

[57] Guthrie, J. P.; Pike, D. C.; Lee, Y.-C. *Can. J. Chem.* **1992**, *70*, 1671–1683.

[58] Hie, L.; Fine Nathel, N. F.; Shah, T. K.; Hong, X.; Yang, Y.-F.; Liu, P.; Houk, K. N.; Garg, N. K. *Nature* **2015**, *524*, 79–83.

CHAPTER FIVE

Nickel-Catalyzed Activation of Acyl C–O Bonds of Methyl Esters

Liana Hie, Noah F. Fine Nathel, Xin Hong, Yun-Fang Yang,
Kendall N. Houk, and Neil K. Garg
Angew. Chem. Int. Ed. **2016**, *55*, 2810–2814.

5.1 Abstract

We report the first catalytic method for activating the acyl C–O bonds of methyl esters through an oxidative addition process. The oxidative addition adducts, formed using nickel catalysis, undergo in situ trapping to provide anilide products. DFT calculations are used to support the proposed reaction mechanism, understand why decarbonylation does not occur competitively, and to elucidate the beneficial role of the substrate structure and $Al(O\textit{t}Bu)_3$ additive on the kinetics and thermodynamics of the reaction.

5.2 Introduction

Catalytic methodologies that rely on the activation of C–heteroatom bonds have transformed the way chemists build molecules of importance.[1] Although decades of research have mainly focused on the coupling of halide and sulfonate derivatives, particularly on aryl systems, recent efforts have been put forth to catalytically activate functional groups that have traditionally been considered inert in cross-coupling reactions.[2] One such endeavor involves couplings of pivalate esters, which proceed by the nickel-mediated activation of aryl C–O bonds (Figure 5.1).[3] In contrast, the cleavage of the acyl C–O bond of esters remains underdeveloped.

Seminal efforts in ester acyl C–O bond cleavage include Yamamoto's stoichiometric studies of ester reactivity,[4] Itami's coupling of phenolic esters, which proceed with loss of the carbonyl in the form of CO,[5] and Chatani's Suzuki–Miyaura coupling of activated pyridyl esters.[6] To our knowledge, no transition-metal catalyzed couplings of simple esters, such as readily available methyl esters, have been reported.

With the aim of developing non-decarbonylative couplings of simple esters using non-precious metal catalysis, we considered the sequence outlined in Figure 5.1. Ni-catalyzed activation of the acyl C–O bond of ester **5.1** would furnish oxidative addition adduct **5.3**. Subsequent ligand exchange by trapping with a nucleophile would provide acyl nickel species **5.4**. Finally, reductive elimination would furnish product **5.2** and regenerate the requisite Ni(0) catalyst. Despite the simplicity of this strategy and the abundance of methyl esters, no such process has been discovered. In this manuscript, we report the validation of this approach, as demonstrated by the nickel-catalyzed conversion of aryl methyl esters to anilides,[7,8,9] in addition to computational insights.

Figure 5.1. Known Catalytic Activation of Esters and Our Approach for the Activation of Methyl Esters (without Decarbonylation).

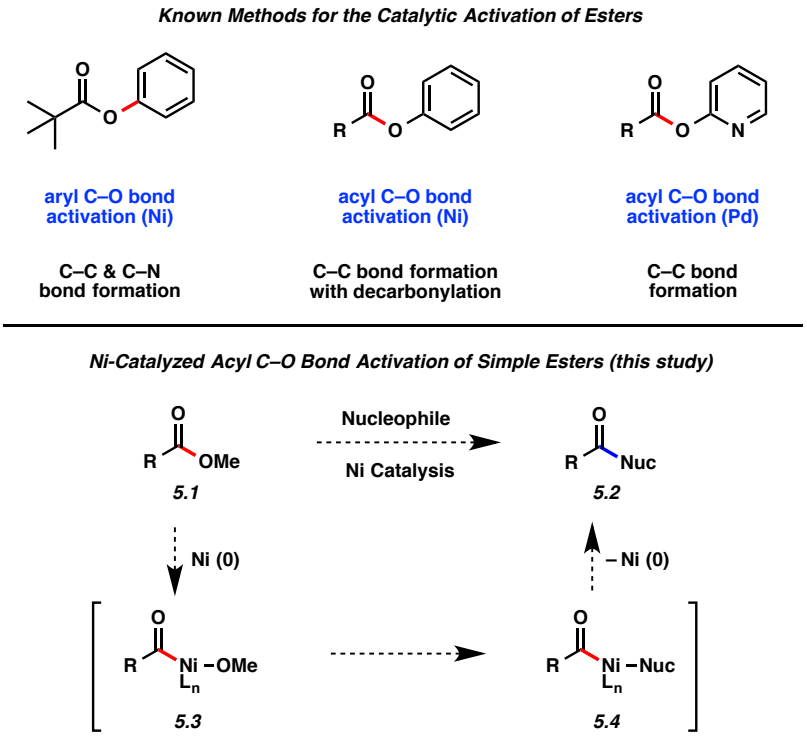

5.3 Optimization and Substrate Scope

Our decision to pursue ester to anilide conversion was in part driven by this transformation being the reverse of one that we recently reported[10] and was therefore considered to be both challenging and conceptually interesting. Methyl 1-naphthoate (**5.5**) was selected as the substrate for our initial studies (Figure 5.2).[11] We surveyed a range of reaction parameters, including the choice of amine coupling partner, ligand, solvent, temperature, concentration, and additives. By using *N*-methylaniline (**5.6**) as the coupling partner, in conjunction with Ni/SIPr in toluene at 60 °C, only trace amounts of amide product **5.7** was observed. This finding is consistent with the overall reaction (i.e., ester **5.5** + amine **5.6** → amide **5.7** + methanol) being

energetically uphill, which would be expected based on our recent studies.[10] However, the addition of Al(O*t*Bu)$_3$ was found to have a critical beneficial effect and led to the formation of amide **5.7** in 89% yield.[12] As described in the latter part of the manuscript, we propose that Al(O*t*Bu)$_3$ benefits the reaction both kinetically and thermodynamically. Also, it should be emphasized that the reaction does not proceed in the absence of Ni/SIPr.[13]

Figure 5.2. Conversion of Ester **5.5** to Amide **5.7**.

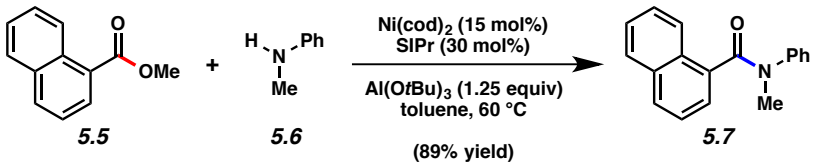

We next examined variations in both coupling partners (Figure 5.3).[14] 1- and 2-Naphthyl substrates bearing fluoride, methoxy, and morpholino substituents were tolerated, as shown by the formation of anilides **5.8–5.11**, respectively. It is notable that ortho-substitution did not hinder reactivity and that the methoxy group did not undergo activation by nickel under these reaction conditions. The methodology could also be performed in the presence of a furan heterocycle to give anilide **5.12**. The coupling of a phenanthrene derivative proceeded smoothly to furnish **5.13** in 74% yield. In contrast, attempts to employ non-extended aromatic substrates were less successful, as shown by the formation of **5.14** in only modest yield. Extended aromatic substrates are frequently necessary to enable nickel-mediated C–O bond cleavage,[2, 15] although this effect is still not well understood.[16] With regard to the aniline coupling partner,[17] *N*-Bn and *N*-Bu substituted anilines could be coupled, as shown by the formation of amides **5.15** and **5.16**, respectively. Substitution on the arene of the aniline was also well tolerated. For example,

methoxy- and fluoride-containing substrates underwent the coupling reaction to give amides **5.17**–**5.19**. An aniline bearing a furan moiety could also be used, as demonstrated by the formation of **5.20**. Finally, the use of the cyclic aniline derivative indoline gave the corresponding amide product **5.21** in 61% yield. Although this first-generation variation of this methodology requires the use of aryl esters and aniline coupling partners, as noted earlier, no reaction occurs in the absence of $Ni(cod)_2$, SIPr, or $Al(O\textit{t}Bu_3)$. Therefore, these results support the notion that nickel catalysis is indeed operative in the methyl ester acyl C–O bond cleavage process.

Figure 5.3. Scope of Methodology.[a]

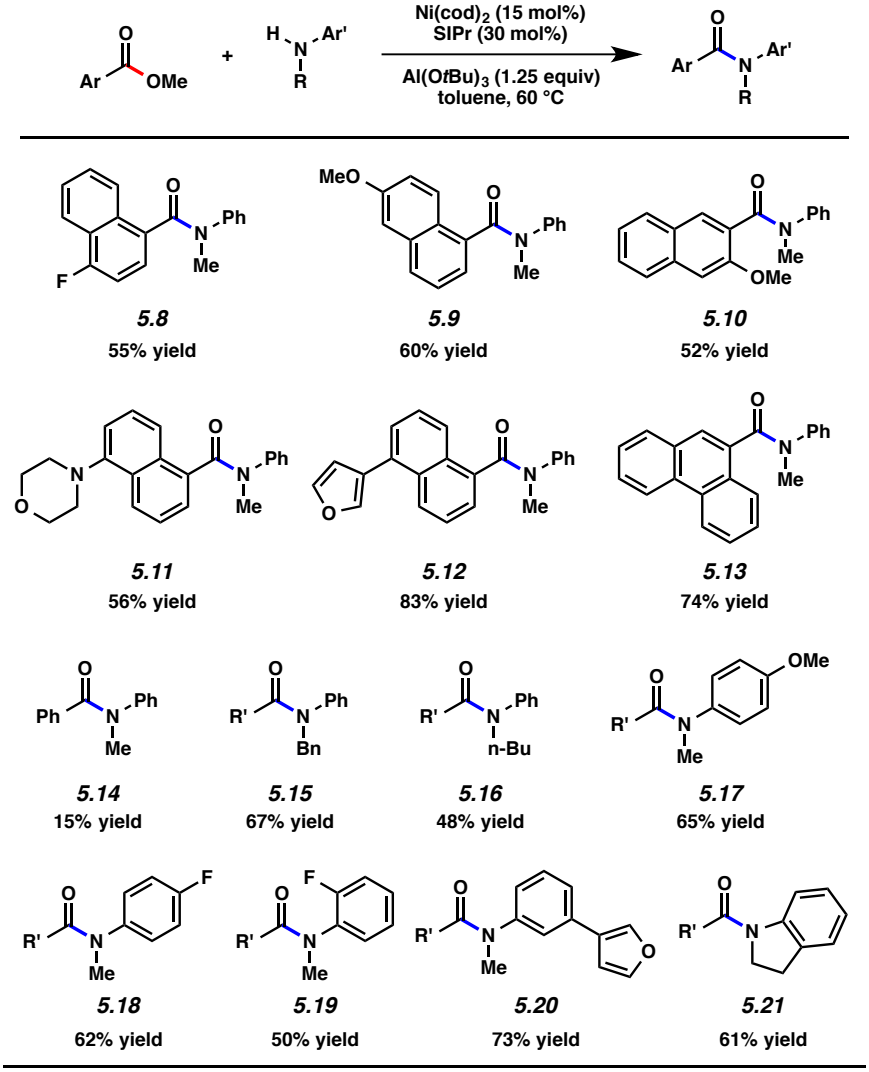

[a] Reaction conditions: substrate (100.0 mg), $Ni(cod)_2$ (15 mol%), SIPr (15 mol%), $Al(OtBu)_3$ (1.25 equiv), toluene (1.0 M), 60 °C, 12 h.

5.4 Computational Studies on Decarbonylation Pathways

Given that decarbonylation is not observed in the nickel-catalyzed conversion of esters to amides, we examined the competing pathways that would stem from the putative oxidative addition intermediate **5.22** using DFT methods (Figure 5.4a).[18] Ligand exchange[19] to give **5.23** is thought to occur through a two-step process, with a small barrier of 4.9 kcal/mol relative to oxidative addition intermediate **5.22**. In contrast, the barrier for decarbonylation of **5.22** to give

5.25 is calculated to be 17.0 kcal/mol relative to **5.22**. Additionally, we examined the activation barriers for reductive elimination and decarbonylation of **5.23**. The barrier for reductive elimination to give **5.24** is 15.4 kcal/mol more favorable compared to decarbonylation to give **5.26**, which is consistent with amide bond formation taking place. Moreover, the high barriers for decarbonylation are consistent with prior computational studies.[18c] The transition states for oxidative addition (**TS1**), ligand exchange (**TS2**), and reductive elimination (**TS3**) are depicted in Figure 5.4.b.

Figure 5.4.a. DFT Calculations Show the Relative Ease of Ligand Exchange and Reductive Elimination Compared to Disfavorable Decarbonylation Pathways. $Al(OMe)_3$ is used as a model for $Al(OtBu)_3$ and R = 1-naphthyl; Dipp=2,6-diisopropylphenyl.

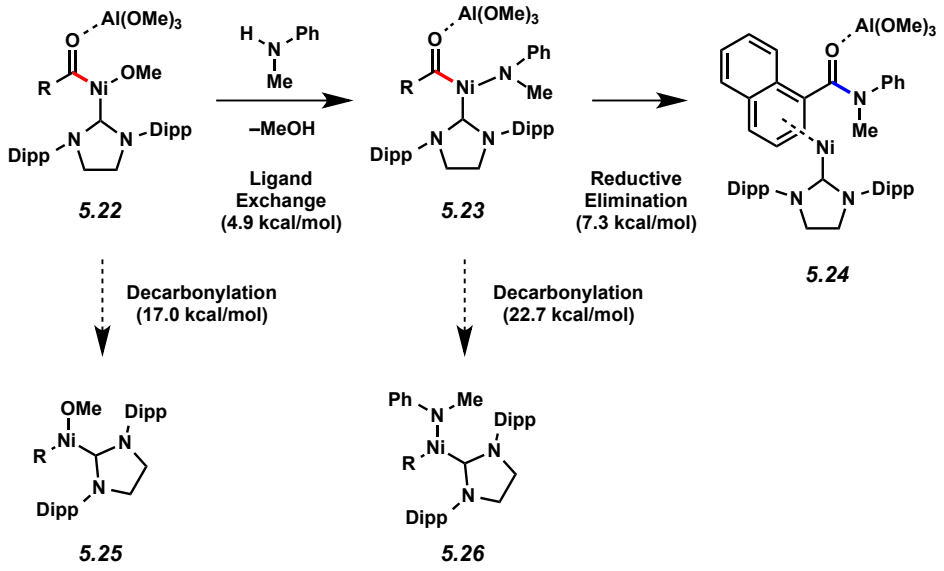

Figure 5.4.b. The Transition States for Oxidative Addition (**TS1**), Ligand Exchange (**TS2**), and Reductive Elimination (**TS3**).

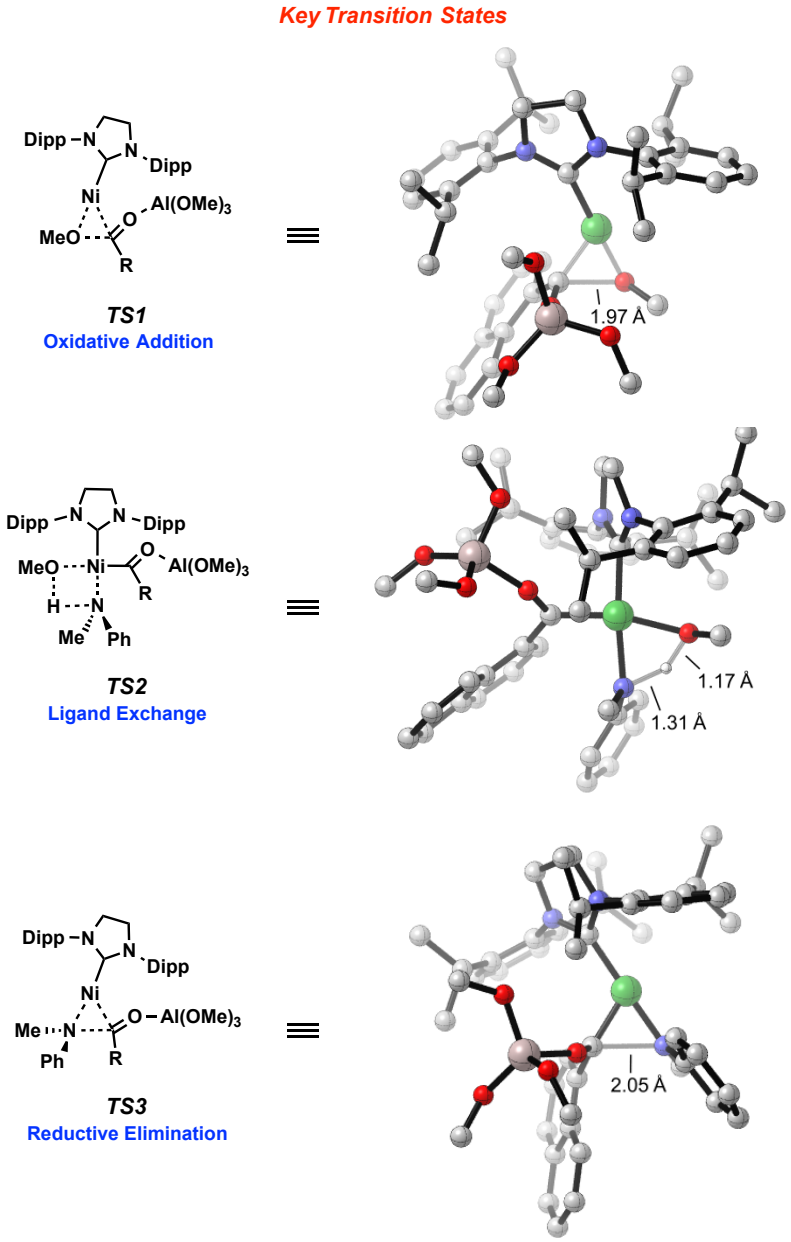

5.5 Effects of Additives on the Nickel-Catalyzed Amidation

DFT calculations were also used to probe the beneficial influence of the Al(O*t*Bu)$_3$ additive on the Ni-catalyzed ester to amide conversion (Figure 5.5). Without the additive, the amidation of ester **5.5** with aniline **5.6** is endergonic by 4.9 kcal/mol. However, with the addition of the aluminum additive, the amidation becomes almost thermoneutral.[20] This arises because of the greater Lewis basicity of the carbonyl oxygen of the amide compared to that of ester, which therefore drives the equilibrium towards amide complex **5.28**.[21] The additive is also thought to have a beneficial kinetic influence with regard to the rate-determining oxidative addition step. In the absence of the additive, the kinetic barrier for oxidative addition is computed to be 33.2 kcal/mol relative to [Ni(SIPr)$_2$] **5.29**.[22] With the additive, however, the oxidative addition becomes significantly more facile, with a kinetic barrier of 26.8 kcal/mol.

Figure 5.5. Effect of the Additive on the Thermodynamics of Amidation and Kinetic Barrier for Oxidative Addition using DFT Calculations. Al(OMe)$_3$ is used as a model for Al(O*t*Bu)$_3$ and R = 1-naphthyl; Dipp=2,6-diisopropylphenyl.

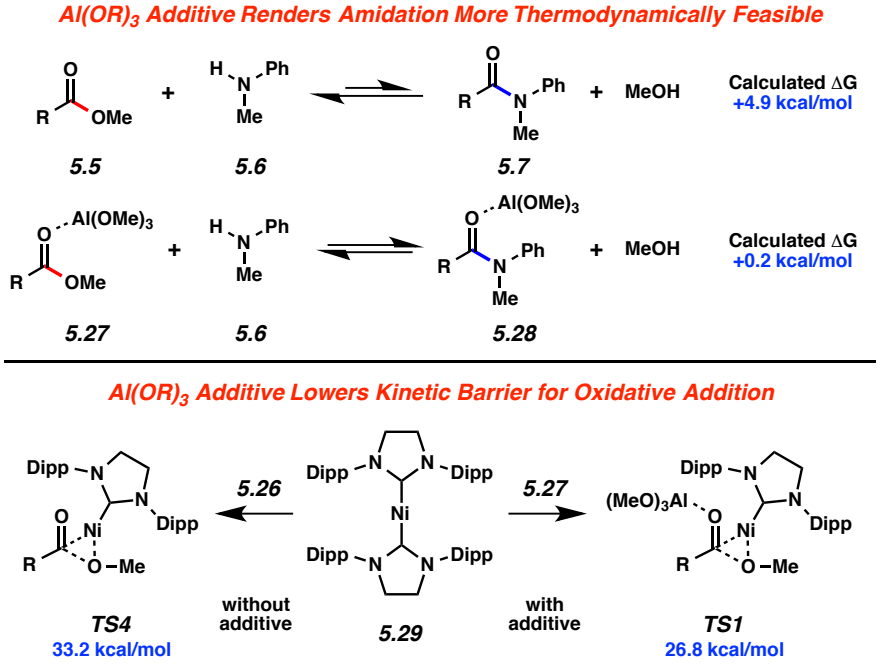

5.6 Effects of Distortion on the Thermodynamics

With insight into the beneficial role of the $Al(OtBu)_3$ additive, we questioned why certain substrates performed, while others proved more challenging in the nickel-catalyzed amidation. Key results are shown in Figure 5.6. Experimentally, methyl 1-naphthoate undergoes amidation in higher yields compared to methyl 2-naphthoate and methyl benzoate (89% yield, versus 53% or 15% yield, respectively). This agrees with the computed trends in the Gibbs free energy for the amidation of each substrate. Calculations reveal that the distortion of the ester–$Al(OR)_3$ complex from steric hindrance facilitates and controls the thermodynamics of the amidation. In the ester–$Al(OR)_3$ complexes, the carbonyl and arene are nearly co-planar in all cases (13° or 2°) to maintain conjugation. In the case of methyl 1-naphthoate, the steric repulsions between the naphthyl group and the acyl moiety distort the highlighted angle to 122.7°, which is about 4° larger than the corresponding angles of the complexes with methyl 2-naphthoate and methyl benzoate. This renders the $Al(OR)_3$ complex with methyl 1-naphthoate less stable than the other two complexes.[23] The amide–$Al(OR)_3$ complexes are all relatively nonplanar and each possesses a similar C–C–C(O) angle of 122.3–122.7°. This is because of lesser arene-carbonyl conjugation; amide conjugation prevails and the arenes and attached carbonyls are easily twisted out of planarity to minimize steric effects. Therefore, the stability of the amide–$Al(OR)_3$ complex is minimally effected by the identity of the arene attached to the carbonyl.[24] The steric repulsion seen in the ester–$Al(OR)_3$ complex of methyl 1-naphthoate makes reactions of these substrates most thermodynamically favorable. This insight into ester destabilization is expected to guide future reaction discovery efforts.

Figure 5.6. Effects of Distortion of the Ester-Aluminum Additive Complex on the Thermodynamics of the Amidation Based on Substrate. $Al(OMe)_3$ is used as a model for $Al(OtBu)_3$.

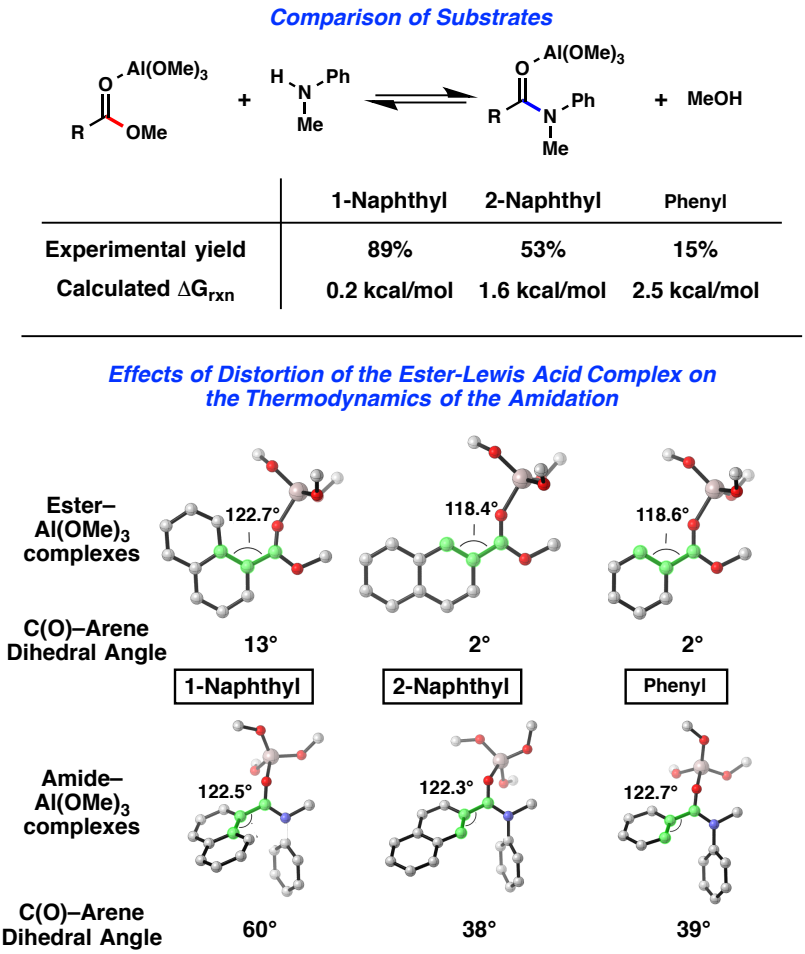

5.7. Sequential Site-Selective C–N Bond Forming Processes

An attractive aspect of employing simple methyl esters in this methodology is that esters are generally stable to a variety of reaction conditions. As such, they are well suited for use in multistep synthesis. To probe this feature, we conducted the reaction sequence shown in Figure 5.7. First, proline-derived ester **5.30** was united with **5.31** using a Buchwald–Hartwig coupling.[25] This C–N bond formation occurred smoothly, without disturbing either of the ester motifs. Treatment of the coupled product with TFA led to selective *t*-butyl ester cleavage to give **5.32**.

This set the stage for sequential amide bond forming reactions. The first involved a conventional DCC coupling with valine-derived amino ester **5.33**, and furnished peptide **5.34**. With the methyl ester again remaining intact, a nickel-catalyzed amidation was performed to deliver dipeptide **5.35**. The *t*-butyl ester was not disturbed in this process, and the stereochemical integrity was preserved at both epimerizable centers. In addition to highlighting the mildness of the acyl C–O bond activation and illustrating the potential of esters as cross-coupling partners, this sequence demonstrates that conventional and new C–N bond forming methodologies can be strategically merged to build linkages in a predictable and chemoselective manner.

Figure 5.7. Multistep Synthesis Using Mild Catalytic Ester Activation and Sequential Site-Selective C–N Bond Forming Processes.

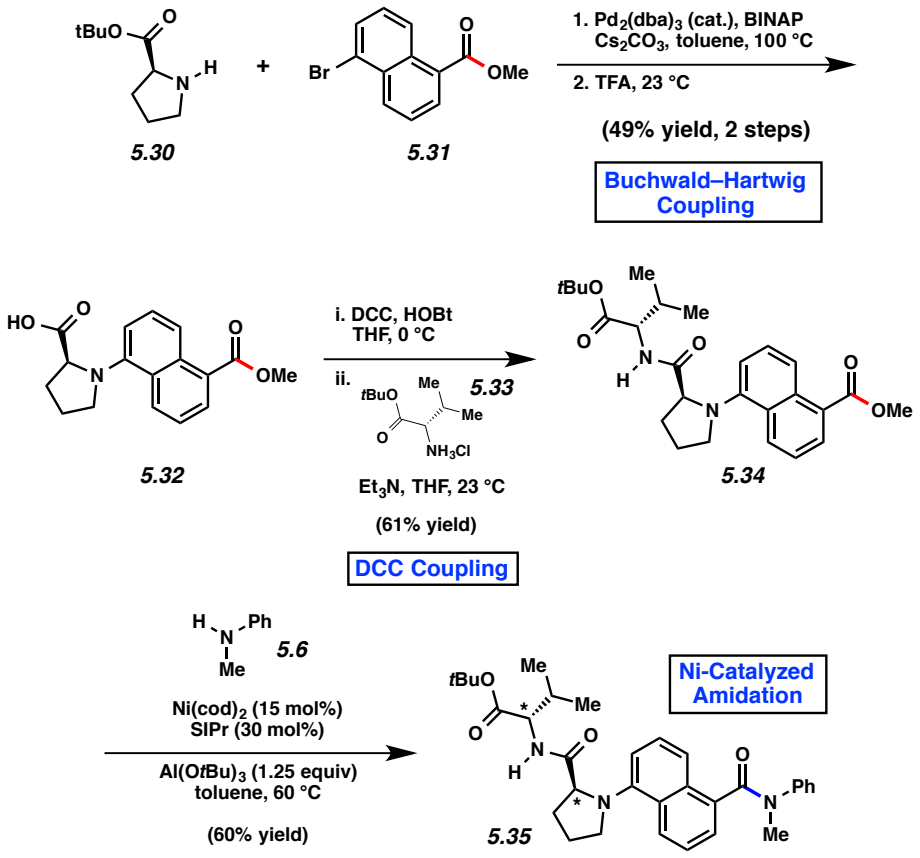

5.8 Conclusion

In summary, this study establishes that the acyl C–O bonds of simple esters may be activated using nickel catalysis. This finding is expected to prompt the further exploration of simple esters in non-decarbonylative cross-coupling processes that rely on non-precious metal catalysis.

5.9 Experimental Section

5.9.1 Materials and Methods

Unless stated otherwise, reactions were conducted in flame-dried glassware under an atmosphere of nitrogen and commercially obtained reagents were used as received. Non-commercially available starting materials were synthesized following protocols specified in Section A in the Experimental Procedures. Toluene was purified by distillation and taken through five freeze-pump-thaw cycles prior to use. Amines were purified by filtration over basic Brockman Grade I 58 Å Al_2O_3 (Activity 1), followed by distillation over calcium hydride, prior to use. $Ni(cod)_2$, $Pd(PPh_3)_4$, $Pd_2(dba)_3$, $Pd(dba)_2$, (±)-BINAP, and SIPr were obtained from Strem Chemicals. Boronic acid **5.38**, amine **5.30**, and L-Valine salt **5.33** were purchased from Combi-Blocks. Morpholine (**5.36**) and 4-fluoro-1-naphthoic acid were purchased from Sigma-Aldrich. Anilines **5.40**, **5.48**, **5.49**, **5.50**, **5.51**, **5.52**, and **5.53** were purchased from Sigma-Aldrich. Methyl 2-naphthoate was purchased from Matrix Scientific. Reaction temperatures were controlled using an IKAmag temperature modulator, and unless stated otherwise, reactions were performed at room temperature (approximately 23 °C). Thin-layer chromatography (TLC) was conducted with EMD gel 60 F254 pre-coated plates (0.25 mm for analytical chromatography and 0.50 mm for preparative chromatography) and visualized using a combination of UV, anisaldehyde, ceric

ammonium molybdate, iodine, vanillin, and potassium permanganate staining techniques. Silicycle Siliaflash P60 (particle size 0.040–0.063 mm) was used for flash column chromatography. ^{1}H NMR spectra were recorded on Bruker spectrometers (at 300, 400, 500, and 600 MHz) and are reported relative to residual solvent signals. Data for ^{1}H NMR spectra are reported as follows: chemical shift (δ ppm), multiplicity, coupling constant (Hz), integration. Data for ^{13}C NMR are reported in terms of chemical shift (at 75 and 125 MHz). IR spectra were recorded on a Perkin-Elmer 100 spectrometer and are reported in terms of frequency absorption (cm^{-1}). High-resolution mass spectra were obtained on Thermo Scientific™ Exactive Mass Spectrometer with DART ID-CUBE. Optical rotations were measured with a Rudolf Autopol III Automatic Polarimeter.

5.9.2 Experimental Procedures

5.9.2.1 Syntheses of Starting Materials

Supporting information for the syntheses of methyl ester substrates (Figures 5.2 and 5.3) have previously been reported: methyl 1-naphthoate,[26] methyl 5-bromo-1-naphthoate,[27] methyl phenanthrene-9-carboxylate,[28] methyl 4-fluoro-1-naphthoate,[29] methyl 6-methoxy-1-naphthoate,[30] and methyl 3-methoxy-2-naphthoate,[31] with the exception of esters **5.37** and **5.39**. Syntheses for these latter compounds and aniline **5.42** are as follows:

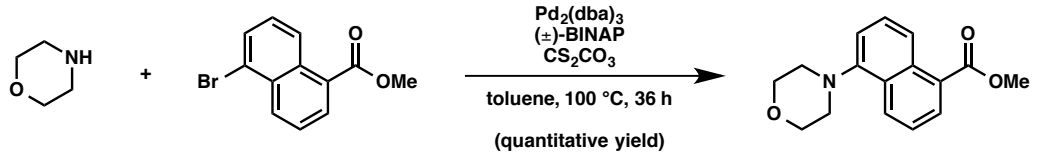

5.36 *5.31* *5.37*

Ester 5.37 (Figure 5.3). To a flask containing bromide **5.31** (0.70 g, 2.64 mmol, 1.0 equiv), $Pd_2(dba)_3$ (0.36 g 0.396 mmol, 15 mol%), (±)-BINAP (0.49 g, 0.792 mmol, 30 mol%), and

Cs_2CO_3 (1.11 g, 3.43 mmol, 1.3 equiv), was added toluene (21 mL, 0.13 M) and morpholine (296 μL, 3.34 mmol, 1.3 equiv). The resulting mixture was stirred at 100 °C for 36 h and then cooled to 23 °C. The reaction mixture was diluted with deionized water (30 mL) and the layers were separated. The aqueous layer was extracted with EtOAc (3 X 50 mL). The combined organic layers were washed with brine (2 X 30 mL), dried over $MgSO_4$, and concentrated under reduced pressure. The crude oil was purified by flash chromatography with (10:1 Hexanes:EtOAc) to yield ester **5.37** (715.0 mg, quantitative yield) as a yellow solid. R_f 0.36 (5:1 Hexanes:EtOAc); ^{1}H NMR: (500 MHz, $CDCl_3$): δ 8.60 (d, *J* = 8.7, 1H), 8.52 (d, *J* = 8.7 , 1H), 8.15 (dd, *J* = 1.3, 7.2, 1H), 7.56 (dq, *J* = 1.2, 7.2, 2H), 7.19 (d, *J* = 7.2, 1H), 4.00–3.98 (m, 7H), 3.11–3.09 (m, 4H); δ; ^{13}C NMR (125 MHz, $CDCl_3$): δ 168.3, 149.8, 132.7, 130.1, 129.5, 128.6, 127.9, 127.7, 124.2, 121.6, 115.4, 67.5, 53.8, 52.3; IR (film): 2962, 2866, 2359, 1720, 1458, 1376, 1260, 1235, 1064, 1031 cm^{-1}; HRMS-ESI (*m/z*) $[M+H]^+$ calcd for $C_{17}H_{15}N_2O$, 263.11844; found 263.11768.

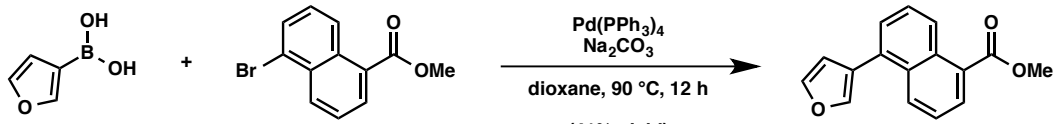

5.38 *5.31* *5.39*

Ester 5.39 (Figure 5.3). To a flask containing bromide **5.31** (1.00 g, 3.78 mmol, 1.0 equiv), boronic acid **5.38** (0.42 g, 3.78 mmol, 1.0 equiv), Na_2CO_3 (1.20 g, 17.01 mmol, 3.0 equiv), and $Pd(PPh_3)_4$ (0.22 g, 0.19 mmol, 5 mol%), was added a solution of dioxane (32 mL) and deionized water (8 mL). The heterogenous mixture was stirred at 90 °C for 12 h and then cooled to 23 °C. The reaction mixture was quenched with 1 M HCl (10 mL) and the layers were separated. the aqueous layer was extracted with EtOAc (3 X 20 mL). The combined organic layers were dried over $MgSO_4$ and concentrated under pressure. The resulting crude oil was purified by flash

chromatography with (10:1 Hexanes:EtOAc) to yield ester **5.39** (0.39 g, 41% yield) as a white solid. R_f 0.36 (10:1 Hexanes:EtOAc); ^{1}H NMR: (500 MHz, $CDCl_3$): δ 8.88 (d, *J* = 8.7, 1H), 8.34–8.32 (m, 1H), 8.18 (dd, *J* = 1.2, 7.2, 1H), 7.64–7.58 (m, 3H), 7.52–7.47 (m, 2H), 4.02 (s, 3H); ^{13}C NMR (125 MHz, $CDCl_3$): δ 168.3, 143.1, 140.6, 132.4, 131.8, 131.4, 130.9, 130.1, 127.8, 127.4, 127.3, 125.6, 124.85, 124.82, 112.7, 52.4; IR (film): 2968, 2867, 2360, 1720, 1509, 1454, 1373, 1268, 1059, 1034, 1019 cm^{-1}; HRMS-ESI (*m/z*) $[M+H]^+$ calcd for $C_{16}H_{13}O_3$, 253.08647; found 253.08577.

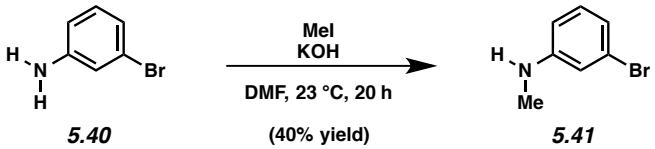

***N*-Methyl-3-bromoaniline (5.41, Figure 5.3)**. To a stirred solution of 3-bromoaniline (**5.40**) (1.26 mL, 11.6 mmol, 1.0 equiv) in DMF (15 mL) was added potassium hydroxide (717.6 mg, 12.8 mmol, 1.1 equiv), then MeI (0.724 mL, 11.6 mmol, 1.0 equiv). After stirring for 20 h at 23 °C, the reaction mixture was quenched with water (15 mL) and extracted with EtOAc (4 x 20 mL). The combined organic layers were washed successively with water (20 mL) and brine (2 x 20 mL), and then dried over $MgSO_4$. The filtered solution was concentrated under reduced pressure and the crude residue was purified by flash chromatography (20:1 Hexanes:EtOAc) to provide *N*-methyl-3-bromoaniline (**5.41**) (873.0 mg, 40% yield) as a pale yellow oil. Spectral data match those previously reported.[32]

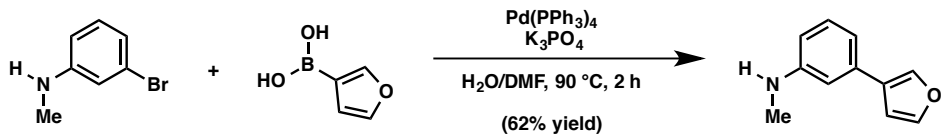

Amine 5.42 (Figure 5.3). To a stirred solution of *N*-methyl-3-bromoaniline (**5.41**) (100.0 mg, 0.54 mmol, 1.0 equiv) in DMF (0.85 mL) and 2.0 M potassium phosphate aqueous solution (0.14 mL) was added boronic acid **5.38** (60.4 mg, 0.54 mmol, 1.0 equiv) and $Pd(PPh_3)_4$ (31.1 mg, 0.027 mmol, 5 mol%). The mixture was heated to 90 °C for 2 h. The mixture was allowed to cool to 23 °C and was then partitioned between water (5 mL) and EtOAc (5 mL). The organic layer was washed with water (5 mL) and brine (5 mL) then dried over $MgSO_4$. The filtered solution was concentrated under reduced pressure and the crude residue was purified by flash chromatography (5:1 Hexanes:EtOAc) to provide amine **5.42** (57.7 mg, 62% yield) as an off-white solid. R_f 0.36 (5:1 Hexanes:EtOAc); ^{1}H NMR: (500 MHz, $CDCl_3$): δ 8.13 (d, *J* = 8.0, 1H), 7.70 (dd, *J* = 1.4, 0.9, 1H), 7.46 (t, *J* = 1.7, 1H), 7.19 (t, *J* = 7.8, 1H), 6.85 (ddd, *J* = 7.6, 2.5, 0.45, 1H), 6.72 (t, *J* = 2.1, 1H), 6.68 (dd, *J* = 1.8, 0.85, 1H), 6.54 (ddd, *J* = 8.1, 2.4, 0.85, 1H), 3.75 (s, 1H), 2.87 (s, 3H); ^{13}C NMR (125 MHz, $CDCl_3$): δ 149.3, 143.6, 138.7, 133.5, 129.8, 126.9, 115.8, 111.9, 110.3, 109.2, 31.2; IR (film): 3417, 2900, 1609, 1517, 1499, 1335, 1245, 1160, 1053, 1016 cm^{-1}; HRMS-ESI (*m/z*) $[M+H]^+$ calcd for $C_{11}H_{12}NO$, 174.09134; found, 174.09115.

*Note: **5.42** was obtained as mixture of rotamers. These data represent empirically observed chemical shifts and coupling constants from the ^{1}H NMR and ^{13}C NMR spectra.*

5.9.2.2 Scope of Methodology

*Representative Procedure (coupling of ester **5.5** and amine **5.6** is used as an example).*

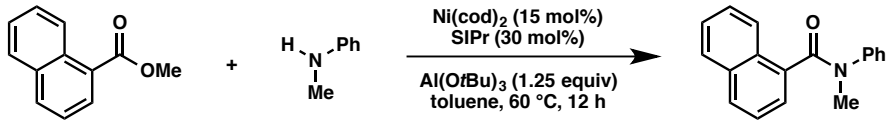

5.5 ***5.6*** ***5.7***

Amide 5.7 (Figure 5.2). A dram vial was charged with ester **5.5** (100.0 mg, 0.54 mmol, 1.0 equiv) and a magnetic stir bar. The vial was brought into a glove box, and then $Al(OtBu)_3$ (165.4 mg, 0.67 mmol, 1.25 equiv), $Ni(cod)_2$ (22.2 mg, 0.081 mmol, 15 mol%), and SIPr (62.9 mg, 0.16 mmol, 30 mol%) were added. Subsequently, toluene (0.54 mL, 1.0 M) and then amine **5.6** (116.3 μL, 1.1 mmol, 2.0 equiv) were added. The vial was sealed with a Teflon-lined screw cap, removed from the glove box, and stirred at 60 °C for 12 h. After cooling to 23 °C, the mixture was diluted with hexanes (0.5 mL) and filtered over a plug of silica gel (10 mL of EtOAc eluent). The volatiles were removed under reduced pressure, and the resulting crude residue was purified by flash chromatography (5:1 Hexanes:EtOAc) to yield ester **5.7** (89% yield, average of two experiments) as a white solid. R_f 0.29 (5:1 Hexanes:EtOAc). Spectral data matched those previously reported.[33]

Any modifications of the conditions shown in the representative procedure above are specified in the following schemes, which depict all of the results from Figures 5.2 and 5.3.

*Note: Amides **5.8–5.13** were obtained as mixtures of rotamers. The tabulated characterization data represent empirically observed chemical shifts and coupling constants from the ^{1}H NMR and ^{13}C NMR spectra.*

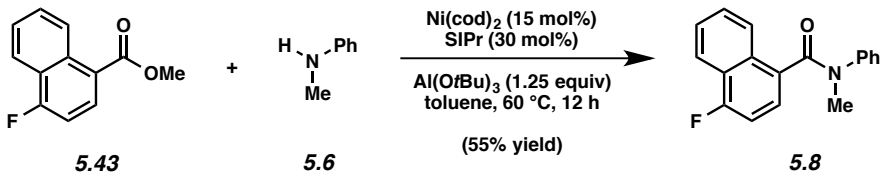

Amide 5.8 (Figure 5.3). Purification by flash chromatography (5:1 Hexanes:EtOAc) generated amide **5.8** (55% yield, average of two experiments) as a white solid. R_f 0.43 (1:1 Hexanes:EtOAc); ^{1}H NMR: (500 MHz, $CDCl_3$): δ 8.14 (d, *J* = 7.9, 1H), 8.05 (d, *J* = 7.9, 1H), 7.62–7.58 (m, 1H), 7.55 (t, *J* = 7.5, 1H), 7.07–6.98 (m, 7H), 3.59 (s, 3H); ^{13}C NMR (125 MHz, $CDCl_3$): δ 170.0, 159.9, 157.9, 144.2, 132.1, 130.64 (d, J_{C-F} = 4.5), 129.1, 127.9, 126.8, 126.6, 126.4, 126.1, 125.4, 123.8, 123.6, 120.94, 120.90, 108 (d, J_{C-F} = 19.8), 37.8; IR (film): 3709, 2868, 2972, 2868, 2843, 2822, 2362, 2341, 2082, 1454, 1055, 1012 cm^{-1}; HRMS-ESI (*m/z*) $[M+H]^+$ calcd for $C_{18}H_{15}FNO$ 280.11377; found, 280.11377.

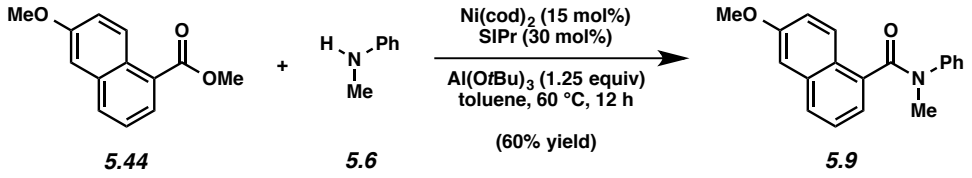

Amide 5.9 (Figure 5.3). Purification by flash chromatography (5:1 → 1:1 Hexanes:EtOAc) generated amide **5.9** (60% yield, average of two experiments) as a white solid. R_f 0.30 (5:1 Hexanes:EtOAc); ^{1}H NMR: (500 MHz, $CDCl_3$): δ 8.00 (d, *J* = 9.0, 1H), 7.55 (br s, 1H), 7.20–7.04 (m, 9H), 3.88 (s, 3H), 3.59 (br s, 3H); ^{13}C NMR (125 MHz, $CDCl_3$): δ 170.7, 157.6, 144.2, 134.7, 134.3, 128.9, 127.9, 127.0, 126.7, 126.3, 125.8, 125.1, 123.6, 119.6, 106.2, 55.3, 37.5; IR (film): 3701, 3680, 2969, 2919, 2865, 2359, 2341, 2075, 2053, 1644, 1454, 1267, 1051, 1016 cm^{-1}; HRMS-ESI (*m/z*) $[M+H]^+$ calcd for $C_{19}H_{18}NO_2$, 292.13375; found, 292.13247.

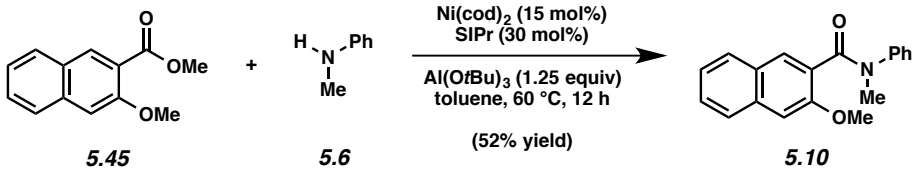

Amide 5.10 (Figure 5.3). Purification by flash chromatography (5:1 → 1:1 Hexanes:EtOAc) generated amide **5.10** (52% yield, average of two experiments) as a white solid. R_f 0.08 (5:1 Hexanes:EtOAc); ^{1}H NMR: (500 MHz, $CDCl_3$): δ 8.07 (d, *J* = 8.5, 1H), 7.75 (d, *J* = 8.5, 1H), 7.66 (d, *J* = 8.0, 1H), 7.53 (d, *J* = 7.5, 1H), 7.50–7.40 (m, 1H), 7.24–6.96 (m, 2H), 6.95–6.47 (m, 3H) 3.93–3.02 (m, 6H); ^{13}C NMR (125 MHz, $CDCl_3$): δ 170.9, 158.0, 137.2, 134.7, 133.5, 130.4, 129.0, 128.4, 127.7, 126.8, 126.2, 125.7, 125.6, 124.6, 114.2, 55.4, 37.9; IR (film): 2935, 1645, 1595, 1496, 1468, 1431, 1371, 1254, 1227, 1033 cm^{-1}; HRMS-ESI (*m/z*) $[M+H]^+$ calcd for $C_{19}H_{18}NO_2$, 292.13321; found, 292.13244.

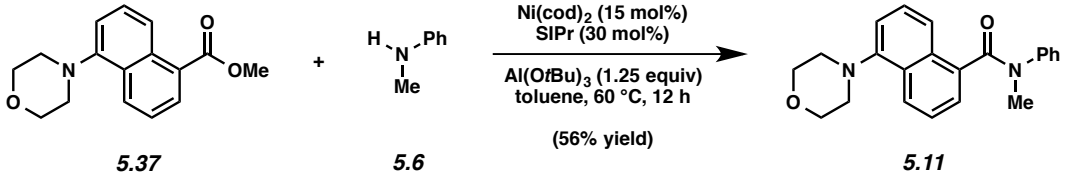

Amide 5.11 (Figure 5.3). Purification by flash chromatography (1:1 Hexanes:EtOAc) generated amide **5.11** (56% yield, average of two experiments) as a white solid. R_f 0.26 (5:1 Hexanes:EtOAc); ^{1}H NMR: (500 MHz, $CDCl_3$): δ 8.08 (br s, 1H), 7.83 (d, *J* = 7.2, 1H); 7.49 (t, *J* = 7.8 ,1H), 7.17–6.99 (m, 8H), 3.93 (br s, 4H), 3.61 (br s, 3H), 3.04 (br s, 4H); ^{13}C NMR (125 MHz, $CDCl_3$): δ 170.8, 149.7, 144.2, 135.0, 131.8, 129.0, 128.9, 126.9, 126.7, 126.4, 125.8, 124.5, 124.1, 121.3, 115.1, 67.5, 53.6, 37.5; IR (film): 3713, 3680, 2972, 2868, 2359, 2341, 1713, 1267, 1051, 1030, 1012 cm^{-1}; HRMS-ESI (*m/z*) $[M+H]^+$ calcd for $C_{22}H_{23}N_2O_2$, 347.17595, found, 347.17595.

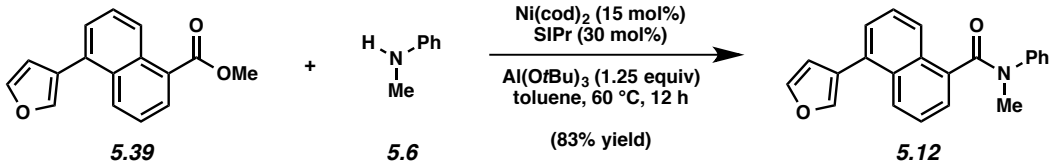

Amide 5.12 (Figure 5.3). Purification by flash chromatography (5:1→1:1 Hexanes:EtOAc) generated amide **5.12** (83% yield, average of two experiments) as a white solid. R_f 0.25 (5:1 Hexanes:EtOAc); ^{1}H NMR: (500 MHz, $CDCl_3$): δ 8.10 (d, *J* = 7.6, 1H), 7.97 (br s, 1H), 7.60–7.45 (m, 5H), 7.17–7.01 (m, 6H), 6.63 (s, 1H), 3.63 (s, 3H) ; ^{13}C NMR (125 MHz, $CDCl_3$): δ 170.7, 144.2, 142.9, 140.5, 134.9, 131.8, 131.2, 130.8, 129.1, 127.2, 126.8, 126.7, 126.4, 125.8, 125.2, 124.6, 112.5, 37.6; IR (film): 3709, 3666, 2969, 2919, 2865, 2362, 2075, 2075, 1713, 1648, 1454, 1264, 1059, 1016 cm^{-1}; HRMS-ESI (*m/z*) $[M+H]^+$ calcd for $C_{22}H_{18}NO_2$, 328.13375; found, 328.13145.

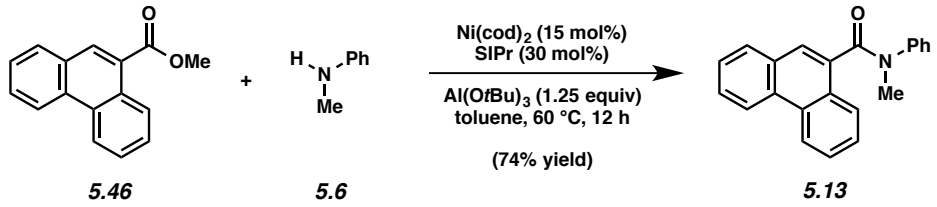

Amide 5.13 (Figure 5.3). Purification by flash chromatography (10:1 → 1:1 Hexanes:EtOAc) generated amide **5.13** (74% yield, average of two experiments) as a white solid. R_f 0.45 (1:1 Hexanes:EtOAc); ^{1}H NMR: (500 MHz, $CDCl_3$): δ 8.62 (d, *J* = 24.3, 2H), 8.15 (br s, 1H), 7.66–7.47 (m, 7H), 7.06–6.93 (m, 4H), 3.66 (s, 3H); ^{13}C NMR (125 MHz, $CDCl_3$): δ 170.5, 144.1, 133.3, 130.4, 130.3, 129.1, 128.9, 127.4, 127.2, 126.9, 126.3, 123.0, 122.5, 37.6; IR (film): 3714, 3677, 2976, 2863, 2364, 1643, 1594, 1365, 1272, 1059, 1030, 1015 cm^{-1}; HRMS-ESI (*m/z*) $[M+H]^+$ calcd for $C_{22}H_{18}NO$, 312.13884, found, 312.13713.

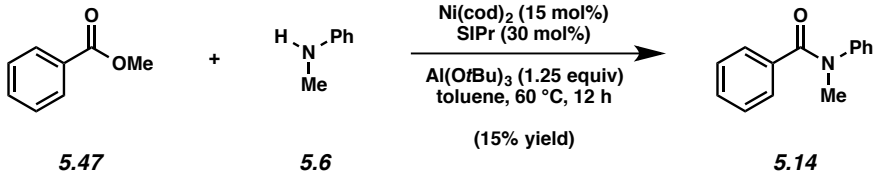

5.47 *5.6* *5.14*

Amide 5.14 (Figure 5.3). Purification by flash chromatography (10:1 → 1:1 Hexanes:EtOAc) generated amide **5.14** (15% yield, average of two experiments) as a white solid. R_f 0.33 (5:1 Hexanes:EtOAc). Spectral data match those previously reported.[34]

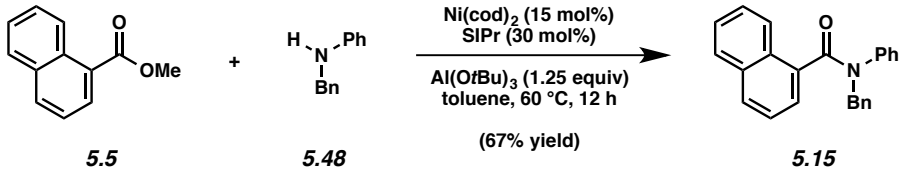

5.5 *5.48* *5.15*

Amide 5.15 (Figure 5.3). Purification by flash chromatography (10:1 Hexanes:EtOAc) generated amide **5.15** (67% yield, average of two experiments) as a clear oil. R_f 0.29 (5:1 Hexanes:EtOAc); ^{1}H NMR: (500 MHz, $CDCl_3$): δ 8.12 (d, *J* = 8.4, 1H), 7.75 (d, *J* = 7.5, 1H), 7.65 (app d, *J* = 5.5, 1H), 7.54 (t, *J* = 7.5, 1H), 7.46 (t, *J* = 7.4, 1H), 7.43–7.37 (m, 2H), 7.37–7.27 (m, 3H), 7.22–7.11 (m, 2H), 6.94 (app s, 3H), 6.82 (app s, 2H), 5.26 (app s, 2H); ^{13}C NMR (125 MHz, $CDCl_3$): δ 170.6, 142.7, 142.7, 137.7, 134.4, 133.5, 130.6, 129.2, 128.9, 128.9, 128.7, 128.4, 127.7, 127.1, 127.0, 126.2, 125.8, 125.5, 124.5, 53.2; IR (film): 3060, 2932, 2323, 1644, 1593, 1494, 1404, 1377, 1259, 1203, 1033 cm^{-1}; HRMS-ESI (*m/z*) $[M+H]^+$ calcd for $C_{24}H_{20}NO$, 338.15394; found, 338.15319.

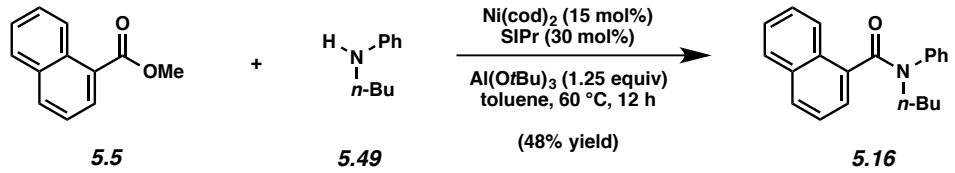

5.5 *5.49* *5.16*

Amide 5.16 (Figure 5.3). Purification by flash chromatography (10:1 Hexanes:EtOAc) generated amide **5.16** (48% yield, average of two experiments) as a white solid. R_f 0.43 (5:1 Hexanes:EtOAc); ^{1}H NMR: (500 MHz, $CDCl_3$): δ 8.10 (d, *J* = 8.2, 1H), 7.75 (d, *J* = 7.6, 1H), 7.64 (d, *J* = 7.2, 1H), 7.55 (app t, *J* = 7.3, 1H), 7.50–7.41 (m, 1H), 7.24–7.08 (m, 2H), 7.08–6.82 (m, 5H), 4.07 (s, 2H), 1.87–1.61 (m, 2H), 1.53–1.32 (m, 2H), 1.10–0.85 (m, 3H); ^{13}C NMR (125 MHz, $CDCl_3$): δ 170.2, 142.9, 134.9, 133.4, 130.5, 128.9, 128.4, 127.6, 126.9, 126.9, 126.1, 125.6, 125.5, 124.5, 49.4, 30.1, 20.4, 14.0; IR (film): 3053, 1646, 1508, 1363, 1218, 1117 cm^{-1}; HRMS-ESI (*m/z*) $[M+H]^+$ calcd for $C_{21}H_{22}NO$, 304.16959; found, 304.17024.

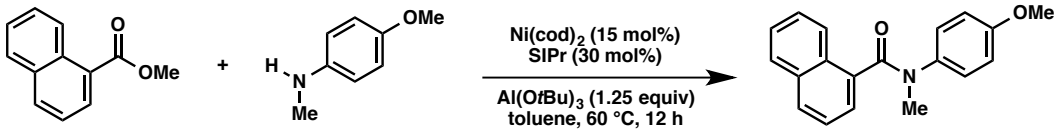

5.5 *5.50* *5.17*

Amide 5.17 (Figure 5.3). Purification by flash chromatography (5:1 Hexanes:EtOAc) generated amide **5.17** (65% yield, average of two experiments) as a white solid. R_f 0.07 (5:1 Hexanes:EtOAc); ^{1}H NMR: (500 MHz, $CDCl_3$): δ 8.07 (d, *J* = 8.4, 1H), 7.76 (d, *J* = 8.2, 1H), 7.66 (d, *J* = 7.9, 1H), 7.53 (app t, *J* = 7.5, 1H), 7.49–7.41 (m, 1H), 7.22–6.95 (m, 2H), 6.95–6.48 (m, 3H), 3.62 (s, 3H), 3.58 (s, 3H); ^{13}C NMR (125 MHz, $CDCl_3$): δ 170.9, 158.0, 137.2, 134.7, 133.5, 130.4, 129.0, 128.4, 127.7, 126.8, 126.2, 125.7, 125.6, 124.6, 114.2, 55.4, 37.9; IR (film): 3711, 2934, 2322, 1643, 1510, 1367, 1247, 1033 cm^{-1}; HRMS-ESI (*m/z*) $[M+H]^+$ calcd for $C_{19}H_{18}NO_2$, 292.13321; found, 292.13234.

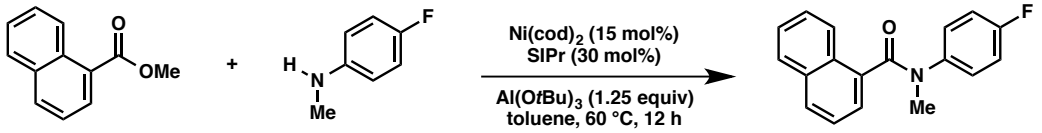

5.5 *5.51* (62% yield) *5.18*

Amide 18 (Figure 3). Purification by flash chromatography (5:1 Hexanes:EtOAc) generated amide **18** (62% yield, average of two experiments) as a clear oil. R_f 0.09 (5:1 Hexanes:EtOAc). Spectral data match those previously reported.[35]

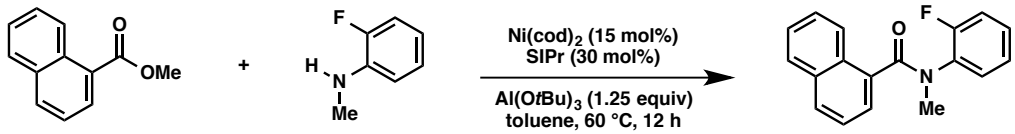

5.5 *5.52* (50% yield) *5.19*

Amide 5.19 (Figure 5.3). Purification by flash chromatography (5:1 Hexanes:EtOAc) generated amide **5.19** (50% yield, average of two experiments) as a clear oil. R_f 0.17 (5:1 Hexanes:EtOAc); ^{1}H NMR: (500 MHz, $CDCl_3$): δ 8.10 (d, *J* = 8.4, 1H), 7.74 (d, *J* = 8.1, 1H), 7.68 (d, *J* = 8.2, 1H), 7.53 (t, *J* = 7.4, 1H), 7.45 (t, *J* = 7.6, 1H), 7.27 (t, *J* = 7.0, 2H), 7.20 (t, *J* = 7.8, 1H), 7.04–6.65 (m, 3H), 3.56 (s, 3H); ^{13}C NMR (125 MHz, $CDCl_3$): δ 171.0, 158.6, 156.6, 134.0, 133.4, 131.9, 130.3, 129.4, 129.2, 128.3, 126.9, 126.2, 125.4, 125.0, 124.4, 124.4, 116.5, 36.8; IR (film): 3048, 2943, 1651, 1501, 1361, 1261, 1101 cm^{-1}; HRMS-ESI (*m/z*) $[M+H]^+$ calcd for $C_{18}H_{15}FNO$, 280.11322; found, 280.11190.

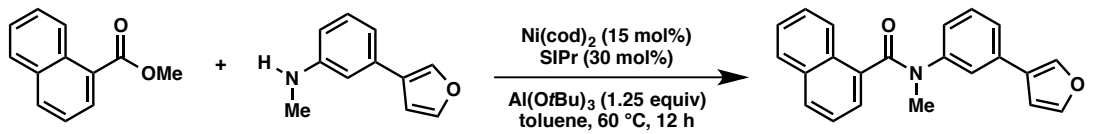

5.5 *5.42* *5.20*

Amide 5.20 (Figure 5.3). Purification by flash chromatography (5:1 Hexanes:EtOAc) generated amide **5.20** (73% yield, average of two experiments) as a clear oil. R_f 0.18 (5:1 Hexanes:EtOAc); ^{1}H NMR: (500 MHz, $CDCl_3$): δ 8.13 (d, *J* = 8.0, 1H), 7.79 (d, *J* = 6.6 , 1H), 7.68 (br s, 1H), 7.59 (ddd, *J* = 15.3, 6.9, 1.3, 1H), 7.50 (t, *J* = 7.4, 1H), 7.35 (s, 1H), 7.20 (br s, 2H), 7.07 (br s, 2H), 7.01 (br s, 1H), 6.92 (s, 1H), 6.21 (br s, 1H), 3.65 (s, 3H); ^{13}C NMR (125 MHz, $CDCl_3$): δ 170.8, 143.8, 138.7, 134.7, 133.4, 133.2, 130.6, 129.5, 129.3, 128.5, 127.0, 126.3, 125.6, 125.4, 124.7, 124.7, 124.4, 124.3, 124.2, 124.0, 108.6, 37.4; IR (film): 3056, 2337, 1644, 1610, 1508, 1366, 1258, 1162, 1121, 1018 cm^{-1}; HRMS-ESI (*m/z*) $[M+H]^+$ calcd for $C_{22}H_{18}NO_2$, 328.13321; found, 328.13238.

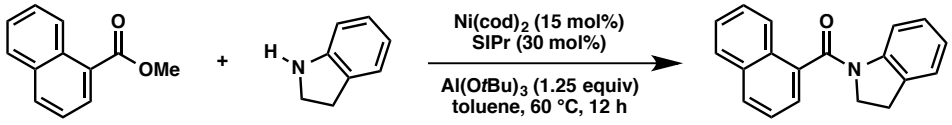

5.5 *5.53* *5.21*

Amide 5.21 (Figure 5.3). Purification by flash chromatography (10:1 Hexanes:EtOAc) generated amide **5.21** (61% yield, average of two experiments) as a white solid. R_f 0.27 (5:1 Hexanes:EtOAc); ^{1}H NMR: (500 MHz, $CDCl_3$): δ 8.48 (d, *J* = 7.9, 1H), 8.03–7.83 (m, 3H), 7.60–7.43 (m, 4H), 7.40–6.49 (m, 3H), 5.48– 3.60 (m, 2H), 3.39–2.86 (m, 2H); ^{13}C NMR (125 MHz, $CDCl_3$): δ 142.8, 135.7, 133.7, 132.2, 129.6, 129.2, 128.6, 128.5, 127.8, 127.4, 126.7, 125.4, 124.9, 124.6, 124.0, 123.9, 117.8, 50.1, 28.3; IR (film): 3046, 2958, 1641, 1593, 1481,

1407, 1382, 1337, 1260, 1155, 1108 cm^{-1}; HRMS-ESI (*m/z*) $[M+H]^+$ calcd for $C_{19}H_{16}NO$, 274.12264; found, 274.12179.

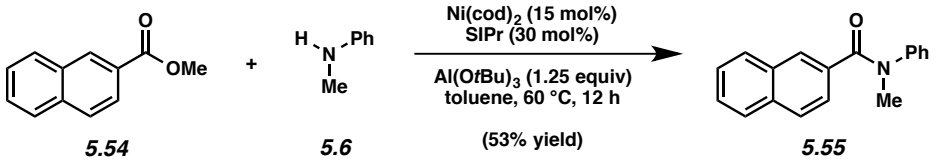

Amide 5.55 (Figure 5.6). Purification by flash chromatography (5:1 Hexanes:EtOAc) generated amide **5.55** (53% yield, average of two experiments) as a white solid. R_f 0.29 (5:1 Hexanes:EtOAc). Spectral data match those previously reported.[36]

5.9.2.3 Sequential Site-Selective C–N Bond Forming Processes

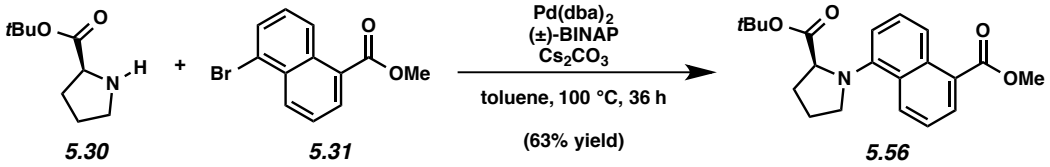

Ester 5.56 (Figure 5.7). A flame-dried Schlenk tube was charged with bromide **5.31** (1.29 g, 4.86 mmol, 1.0 equiv) and amine **5.30** (1.0 g, 5.84 mmol, 1.2 equiv). The reaction vessel was brought into a glove box, and then $Pd(dba)_2$ (0.84 g, 1.46 mmol, 30 mol%), (±)-BINAP (1.36 g, 2.19 mmol, 45 mol%), Cs_2CO_3 (1.66 g, 5.10 mmol, 1.05 equiv), and toluene (9.72 mL, 0.5 M) were added. The vessel was then removed from the glove box, and the heterogenous mixture was heated to 100 °C for 36 h. After cooling to 23 °C, the reaction mixture was diluted with Et_2O (5 mL). The insoluble solids were removed by filtration and the organic filtrate was concentrated under reduced pressure. The resulting crude oil was purified via flash chromatography (Hexanes:EtOAc = 5:1) to give **5.56** as a yellow oil (1.09 g, 63% yield); R_f 0.65 (5:1 Hexanes:EtOAc); ^1H NMR: (500 MHz, $CDCl_3$): δ 8.50 (d, *J* = 8.6, 1H), 8.48 (d, *J* = 8.3, 1H),

8.12 (dd, *J* = 6.2, 8.6, 1H), 7.49–7.45 (m, 2H), 7.17 (d, *J* = 7.5, 1H), 4.38 (dd, *J* = 5.7, 7.8, 1H), 3.98 (s, 3H), 3.86 (app q, *J* = 7.0, 9.0, 1H), 3.13–3.09 (m, 1H), 2.43–2.34 (m, 1H), 2.19–2.10 (m, 1H), 2.05–1.96 (m, 1H), 1.15 (s, 9H); ^{13}C NMR (125 MHz, $CDCl_3$): δ 172.6, 168.5, 146.5, 132.7, 130.0, 129.9, 129.8, 127.6, 127.5, 123.4, 120.4, 115.4, 80.8. 64.6, 53.8, 52.2, 30.0, 27.8, 24.3; IR (film): 2927, 2854, 1719, 1578, 1462, 1406, 1367, 1262, 1151, 1116, 1072, 1040, 1000 cm^{-1}; HRMS-ESI (*m/z*) $[M+H]^+$ calcd for $C_{21}H_{26}NO_4$, 356.18618; found, 356.18552; $[a]^{20.5}_D$ –6.20° (*c* = 1.000, CH_2Cl_2).

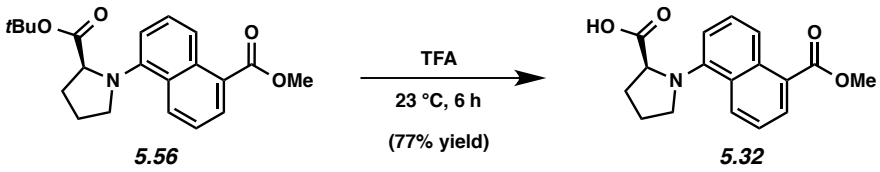

5.56 *5.32*

Carboxylic acid 5.32 (Figure 5.7). To a flask containing ester **5.56** (1.11 g, 3.12 mmol, 1.0 equiv) was added trifluoroacetic acid (13.0 mL, 0.24 M). After stirring for 6 h at 23 °C, the brown mixture was concentrated under reduced pressure. The resulting oil was diluted with CH_2Cl_2 (5 mL) and then concentrated under reduced pressure (repeated with 2 additional iterations). The crude oil was purified via flash chromatography (Hexanes:Et_2O = 1:1) to give carboxylic acid **5.32** as a yellow solid (0.72 g, 77% yield); R_f 0.33 (1:1 Hexanes:Et_2O); ^{1}H NMR: (500 MHz, $CDCl_3$): δ 8.62 (d, *J* = 8.6, 1H), 8.44 (d, *J* = 8.6, 1H), 8.16 (d, *J* = 7.2, 1H), 7.55 (quintet, *J* = 8.1, 1H), 7.22 (d, *J* = 7.4, 1H), 4.51 (dd, *J* = 5.9, 2.2, 1H), 3.91 (s, 3H), 3.91–3.86 (m, 1H), 3.07–3.02 (m, 1H), 2.55–2.51 (m, 1H), 2.31–2.27 (m, 1H), 2.13–2.09 (m, 2H); ^{13}C NMR (125 MHz, $CDCl_3$): δ 175.7, 168.2, 145.8, 132.7, 130.3, 130.1, 128.2, 128.1, 127.7, 124.6, 122.5, 116.3, 64.1, 56.8, 52.4, 30.7, 25.0; IR (film): 3709, 3680, 2972, 2919, 1868, 2359, 2341,

1720, 1271, 1055, 1009 cm^{-1}; HRMS-ESI (*m/z*) $[M+H]^+$ calcd for $C_{17}H_{18}NO_4$, 300.12358; found, 300.12212; $[a]^{27.3}_D$ +25.40° (*c* = 1.000, CH_2Cl_2).

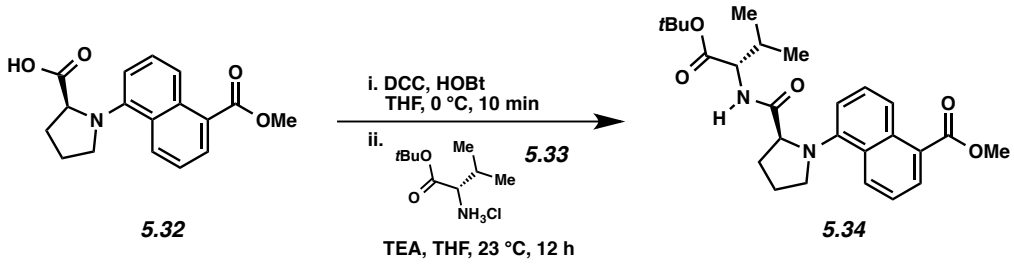

Ester 5.34 (Figure 5.7). To a flask containing L-Valine salt **5.33** (0.40 g, 0.19 mmol, 1.1 equiv) was added triethylamine (0.093 mL) and THF (0.93 mL). The heterogeneous mixture was stirred at 23 °C for 1 h. To another flask containing carboxylic acid **5.32** (0.050 g, 0.17 mmol, 1.0 equiv) and THF (1.85 mL) was added hydroxybenzotriazole (0.025 g, 0.19 mmol, 1.1 equiv) at 0 °C. After stirring for 10 min, the flask was charged with *N*,*N*'-dicyclohexylcarbodiimide (0.035 g, 0.19 mmol, 1.1 equiv) and the mixture containing the L-valine salt **5.33**, triethylamine, and THF. The resulting mixture was stirred at 23 °C for 12 h. The heterogeneous mixture was filtered to remove the precipitate and the organic filtrate was then concentrated under reduced pressure. The resulting yellow oil was dissolved in EtOAc (30 mL) and washed subsequently with saturated sodium bicarbonate solution (20 mL), saturated sodium bisulfate (20 mL), and brine (2 X 20 mL). After drying over Na_2SO_4, the organics were concentrated under reduced pressure. The crude oil was purified via flash chromatography (5:1 Hexanes:EtOAc → 1:1 Hexanes:EtOAc) to give ester **5.34** as a yellow oil (0.047 g, 61% yield); R_f 0.52 (1:1 Hexanes:EtOAc); ^{1}H NMR: (500 MHz, $CDCl_3$): δ 8.53 (d, *J* = 8.1, 1H), 8.14 (d, *J* = 6.8, 1H), 7.55 (t, *J* = 7.7, 1H), 7.48 (t, *J* = 8.2, 1H), 7.30 (d, *J* = 9.0, 1H), 7.21 (d, *J* = 7.4, 1H), 4.39 (t, *J* = 7.2, 1H), 4.24 (dd, *J* = 5.4, 3.6, 1H), 3.99 (s, 3H), 3.94–3.89 (m, 1H), 3.04–2.99 (m, 1H), 2.57–

2.50 (m, 1H), 2.21–2.15 (m, 1H), 2.11–1.95 (m, 3H), 1.02 (s, 9H), 0.88 (t, J = 6.7, 6H); ^{13}C NMR (125 MHz, $CDCl_3$): δ 173.1, 170.0, 168.3, 146.8, 132.8, 130.1, 130.0, 128.7, 128.0, 127.7, 124.1, 121.6, 115.3, 81.5, 65.2, 57.4, 57.2, 52.3, 31.6, 31.4, 27.6, 25.0, 18.9, 17.9; IR (film): 3713, 3694, 3680, 3666, 3001, 2843, 2822, 2362, 2345, 2078, 2255, 1716, 1673, 1580, 1508, 1457, 1343, 1278, 1257, 1051, 1012 cm^{-1}; HRMS-ESI (m/z) $[M+H]^+$ calcd for $C_{26}H_{35}N_2O_5$, 455.25460; found, 455.25109; $[a]^{26.6}_D$ +190.40° (c = 1.000, CH_2Cl_2).

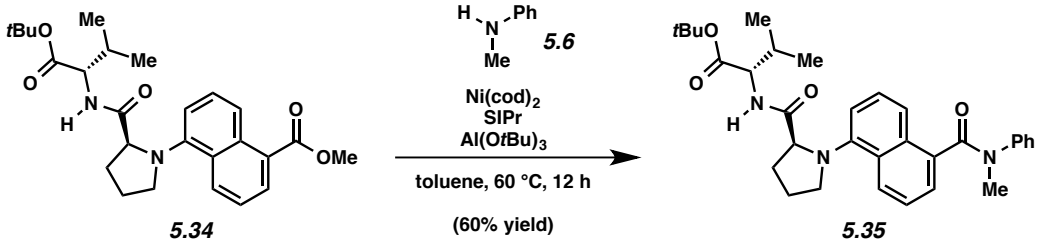

Amide 5.35 (Figure 5.7). A dram vial was charged with ester **5.34** (50.0 mg, 0.11 mmol, 1.0 equiv) and a magnetic stir bar. The reaction vessel was brought into a glove box, and then $Al(OtBu)_3$ (34.5 mg, 0.14 mmol, 1.25 equiv), $Ni(cod)_2$ (5.0 mg, 0.0165 mmol, 15 mol%) and SIPr (13.0 mg, 0.033 mmol, 30 mol%) were added. Subsequently, toluene (0.11 mL, 1.0 M) and then amine **5.6** (24 μL, 0.22 mmol, 2.0 equiv) were added. The vial was sealed with a Teflon-lined screw cap, removed from the glove box, and stirred at 60 °C for 12 h. After cooling to 23 °C, the mixture was diluted with hexanes (0.5 mL) and filtered over a plug of silica gel (10 mL of EtOAc eluent). The volatiles were removed under reduced pressure, and the crude residue was purified by flash chromatography (1:1 Hexanes:EtOAc) to yield amide **5.35** (35.3 mg, 61% yield) as a yellow oil. R_f 0.27 (1:1 Hexanes:EtOAc); ^{1}H NMR: (400 MHz, $CDCl_3$): δ 8.13 (br s, 1H), 7.79 (br s, 1H), 7.43 (t, J = 7.9, 1H), 7.34 (d, J = 8.5, 1H), 7.21–6.00 (m, 8H); 4.35 (apt t, J = 6.4, 1H), 4.24 (dd, J = 5.1, 3.6, 1H), 3.84 (br s, 1H), 3.61 (br s, 3H), 3.01 (br s, 1H), 2.50 (br s,

1H), 2.20–2.13 (m, 1H), 2.08–2.02 (m, 3H), 1.09 (s, 9H), 0.87 (dd, J = 12.0, 6.7, 6H); ^{13}C NMR (125 MHz, $CDCl_3$): δ173.2, 170.6, 170.0, 146.9, 144.2, 135.0, 132.1, 129.4, 129.0, 126.9, 126.7, 126.4, 125.7, 124.8, 124.0, 121.2, 115.0, 81.5, 65.2, 57.4, 57.0, 37.6, 31.4, 31.3, 27.7, 25.0, 18.9, 17.9; IR (film): 3385, 3060, 2966, 2928, 2870, 1730, 1675, 1647, 1586, 1496, 1464, 1407, 1367, 1281, 1214, 1150, 1111 cm^{-1}; HRMS-ESI (m/z) $[M+H]^+$ calcd for $C_{32}H_{40}N_3O_4$ 530.30188; found, 530.30074; $[a]^{20.7}_D$ +326° (c = 1.000, CH_2Cl_2).

Note: Amide ***5.35*** *was obtained as mixture of rotamers. These data represent empirically observed chemical shifts and coupling constants from the ^{1}H NMR and ^{13}C NMR spectra.*

5.9.2.4 Gram Scale Coupling

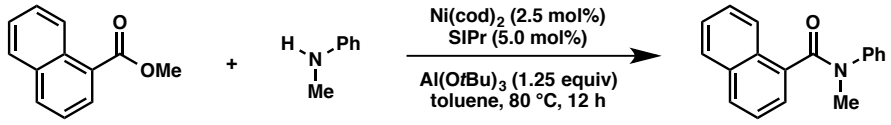

5.5 ***5.6*** ***5.7***

Amide 5.7 (Figure 5.2). A scintillation vial was charged with ester **5.5** (1.0 g, 5.4 mmol, 1.0 equiv) and a magnetic stir bar. The reaction vessel was brought into a glove box, and then $Al(OtBu)_3$ (1.67 g, 6.75 mmol, 1.25 equiv), $Ni(cod)_2$ (37.1 mg, 0.135 mmol, 2.5 mol%), and SIPr (105.5 mg, 0.27 mmol, 5.0 mol%) were added. Subsequently, toluene (5.4 mL, 1.0 M) and then amine **5.6** (1.2 mL, 10.8 mmol, 2.0 equiv) were added. The vial was sealed with a Teflon-lined screw cap, removed from the glove box, and stirred at 80 °C for 12 h. After cooling to 23 °C, the mixture was diluted with hexanes (5.0 mL) and filtered over silica gel (100.0 mL of EtOAc eluent). The volatiles were removed under reduced pressure, and the crude residue was purified by flash chromatography (5:1→1:1 Hexanes:EtOAc) to yield amide **5.7** as a white solid (0.71 g, 50% yield). Spectral data matched those previously reported.[33]

5.9.3 Computational Method

All the calculations were carried out with the Gaussian 09 package. Geometry optimizations were performed with B3LYP.[37] The LANL2DZ basis set[38] with ECP was used for Ni, and the 6-31G (d) basis set[39] was used for other atoms. Frequency analysis was conducted at the same level of theory to verify the stationary points to be minima or saddle points. The single-point energies and solvent effects in toluene were computed with M06[40]/SDD- 6-311+G(d,p) basis sets by using SMD solvation model.[41] Computed structures are illustrated using CYLView.

5.9.3.1 Complete Reference of Gaussian 09

Frisch, M. J.; Trucks, G. W.; Schlegel, H. B.; Scuseria, G. E.; Robb, M. A.; Cheeseman, J. R.; Scalmani, G.; Barone, V.; Mennucci, B.; Petersson, G. A.; Nakatsuji, H.; Caricato, M.; Li, X.; Hratchian, H. P.; Izmaylov, A. F.; Bloino, J.; Zheng, G.; Sonnenberg, J. L.; Hada, M.; Ehara, M.; Toyota, K.; Fukuda, R.; Hasegawa, J.; Ishida, M.; Nakajima, T.; Honda, Y.; Kitao, O.; Nakai, H.; Vreven, T.; Montgomery, Jr., J. A.; Peralta, J. E.; Ogliaro, F.; Bearpark, M.; Heyd, J. J.; Brothers, E.; Kudin, K. N.; Staroverov, V. N.; Keith, T.; Kobayashi, R.; Normand, J.; Raghavachari, K.; Rendell, A.; Burant, J. C.; Iyengar, S. S.; Tomasi, J.; Cossi, M.; Rega, N.; Millam, J. M.; Klene, M.; Knox, J. E.; Cross, J. B.; Bakken, V.; Adamo, C.; Jaramillo, J.; Gomperts, R.; Stratmann, R. E.; Yazyev, O.; Austin, A. J.; Cammi, R.; Pomelli, C.; Ochterski, J. W.; Martin, R. L.; Morokuma, K.; Zakrzewski, V. G.; Voth, G. A.; Salvador, P.; Dannenberg, J. J.; Dapprich, S.; Daniels, A. D.; Farkas, O.; Foresman, J. B.; Ortiz, J. V.; Cioslowski, J.; Fox, D. J. *Gaussian 09, Rev. D.01*; Gaussian, Inc., Wallingford, CT, **2010**.

5.9.3.2 Computed Catalytic Cycle

Figure 5.8. Gibbs Free Energy Changes of the Full Catalytic Cycle of Nickel-Catalyzed Amidation of Methyl 1-Naphthoate. LA = $Al(OMe)_3$ and R = 1-naphthyl.

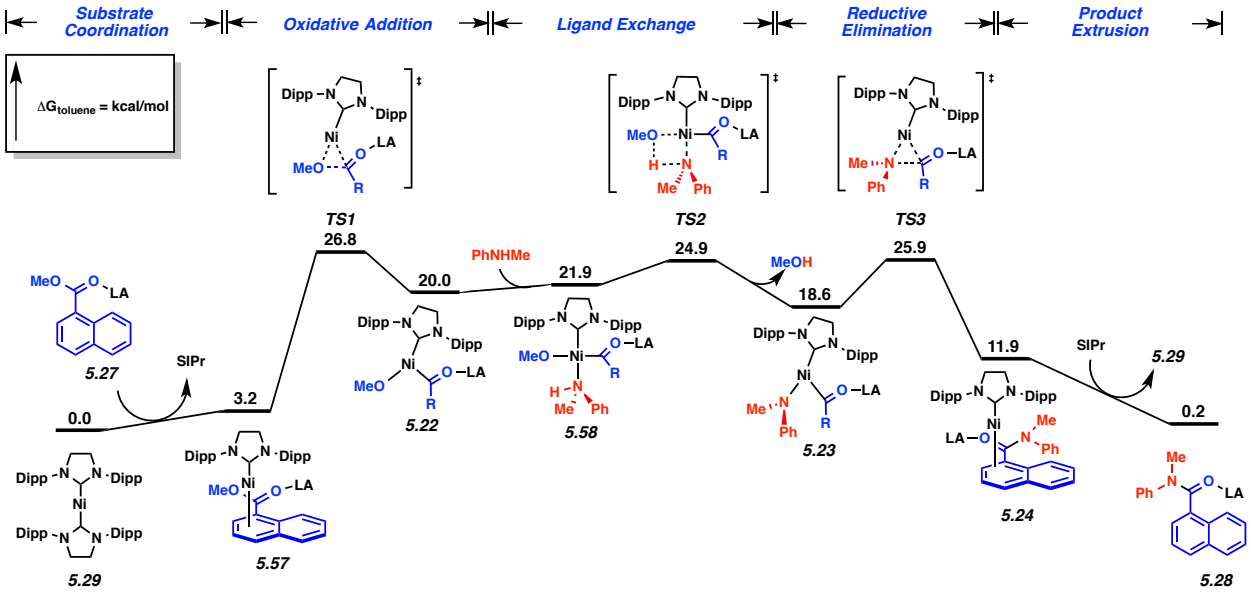

5.9.3.3 Transition States for Decarbonylation Pathways

Figure 5.9. Gibbs Free Energy Changes of Possible Decarbonylation Transition States, the Free Energies are Compared to $[Ni(SIPr)_2]$. LA = $Al(OMe)_3$.

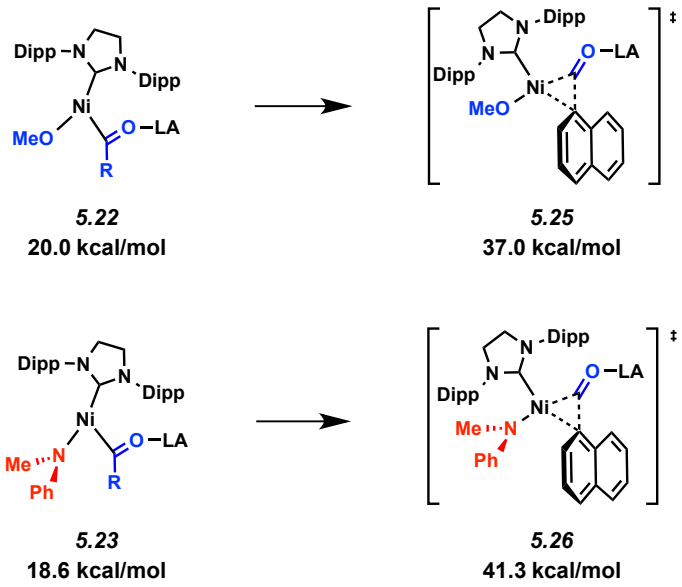

5.9.3.4 Effects of Additive on Ester Complexation

The aluminium additive significantly favors the ester coordination to nickel. The coordination of ester-aluminium complex is 7.3 kcal/mol more favorable as compared to that of ester (Figure 5.10). Applying the distortion/interaction analysis, we found the interaction between the [Ni(SIPr)] and the substrate determines the stability of the Ni-ester complex (**5.57** and **5.59**). The interaction between nickel and substrate is 63.7 kcal/mol in **5.57**, while the similar interaction in **5.59** is only 53.9 kcal/mol. This overrides the penalty of distortion in **5.57** and makes the complexation with ester-aluminium stronger than that with ester only. Since the SIPr is a very strong electron-donating ligand, the d-π* back-donation from nickel to ester contribute significantly to the stabilization of the complex. The addition of $Al(OMe)_3$ favors this d-π* interaction, thus increasing the interaction energy and eventually lead to the energy difference of complexation between **5.57** and **5.59**. This change of d-π* interaction can also be verified through charge distribution. The NBO charge of carbonyl oxygen in methyl 1-naphthoate is -0.614, and the charge changes to -0.642 after the complexation with [Ni(SIPr)]. In the presence of $Al(OMe)_3$, the NBO charge of carbonyl oxygen in the ester- $Al(OMe)_3$ complex is -0.739, and the negative charge increases to -0.787 after the complexation with[Ni(SIPr)]. The change of charge is -0.028 without the additive, and -0.048 with the Lewis acid, supporting the argument that the aluminium favors the d-π* interaction and stabilizes the Ni-ester complex.

Figure 5.10. Distortion/Interaction Analysis of the Complexation Energy between Ni(SIPr) and Ester or Ester-Aluminium Complex.

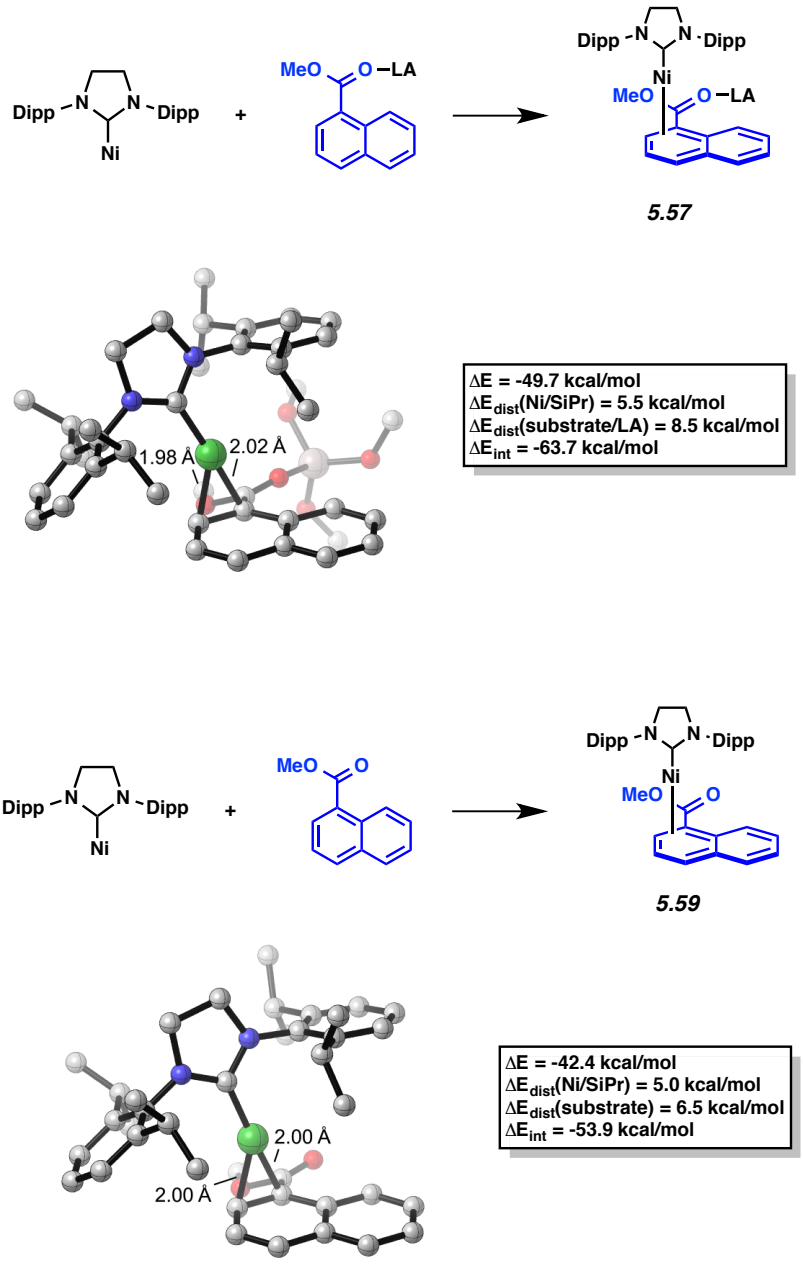

5.9.3.5 Dihedral Angles and Bond Lengths of Selected Esters and Amides

Figure 5.11. Dihedral Angles and Bond Lengths of Selected Esters and Amides.

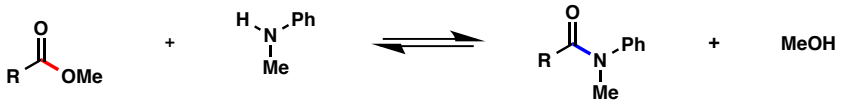

	1-Naphthyl	*2-Naphthyl*	*Phenyl*
Calculated ΔG_{rxn}	**4.8 kcal/mol**	**6.8 kcal/mol**	**6.8 kcal/mol**

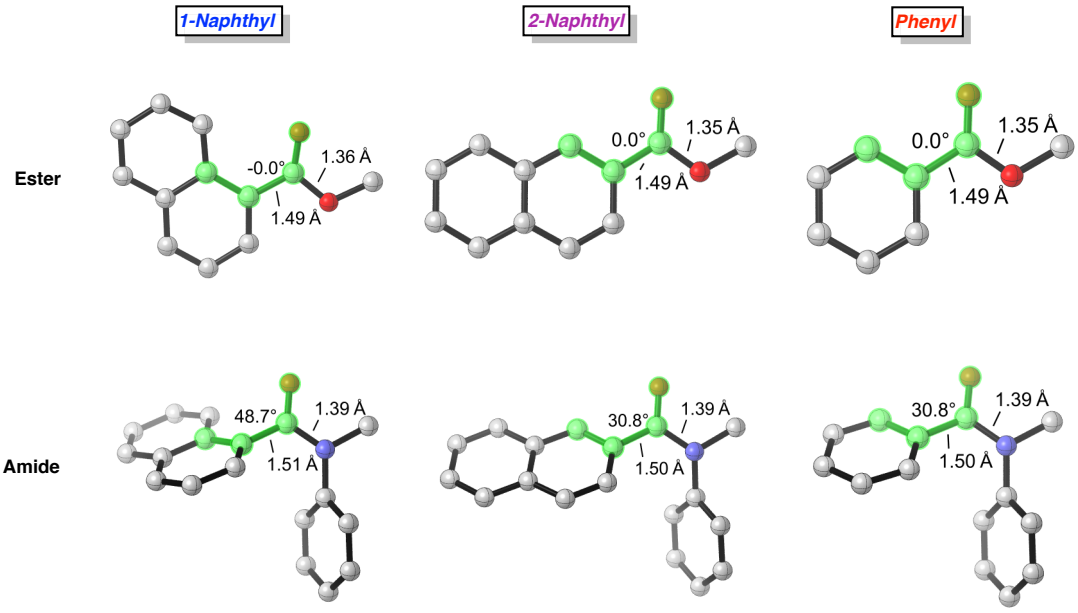

5.9.3.6 Dihedral Angles and Bond Lengths of Selected Esters and Amides with Additive

Figure 5.12. Dihedral Angle and Bond Length of Selected Esters and Amides with Lewis Acid.

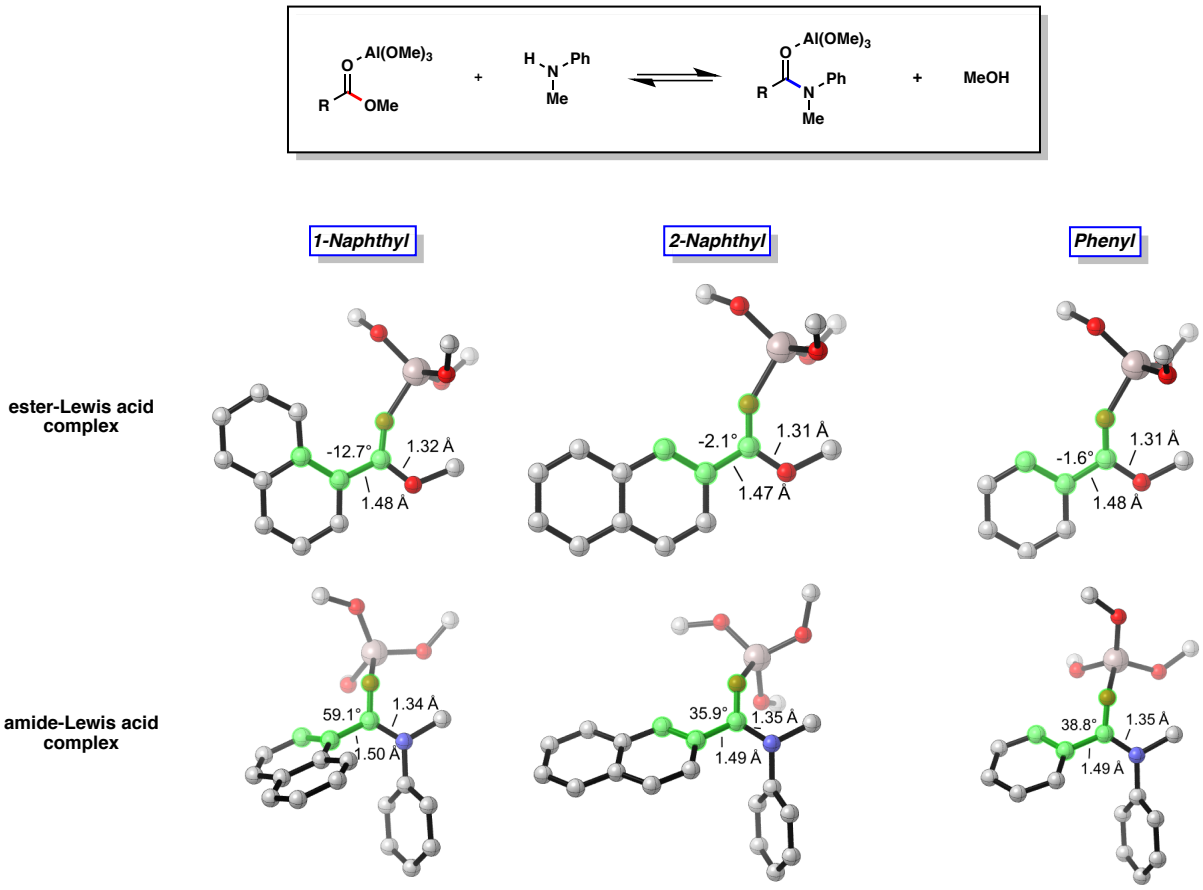

5.9.3.7 Energies and Cartesian Coordinates of the Structures

Energies and Cartesian coordinates of the structures have been published.[42]

Appendix Five: Spectra Relevant to Chapter Five

Nickel-Catalyzed Activation of Acyl C–O Bonds of Methyl Esters

Liana Hie, Noah F. Fine Nathel, Xin Hong, Yun-Fang Yang,
Kendall N. Houk, and Neil K. Garg

Angew. Chem. Int. Ed. **2016**, *55*, 2810–2814.

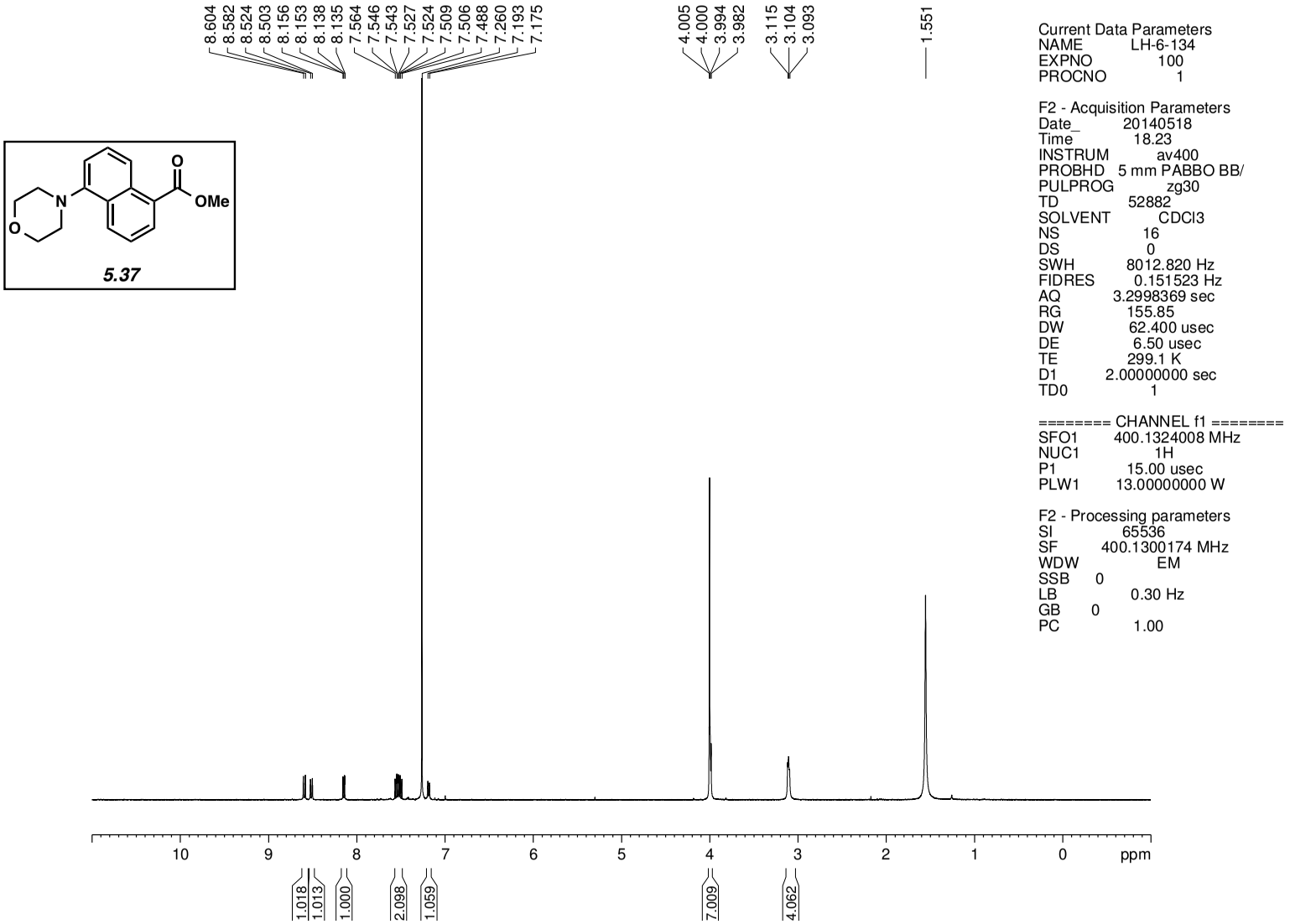

Figure A5.1 ^{1}H NMR (400 MHz, $CDCl_3$) of compound **5.37**.

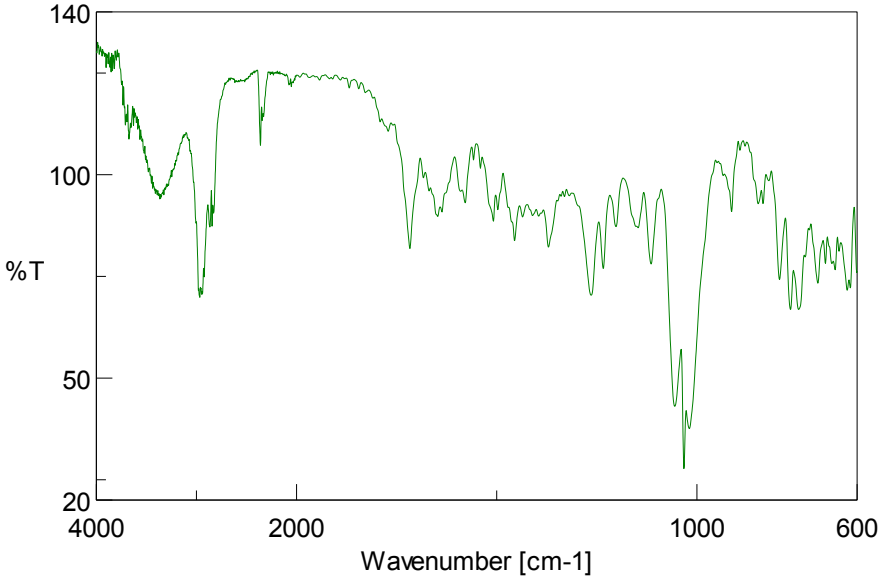

Figure A5.2 Infrared spectrum of compound **5.37**.

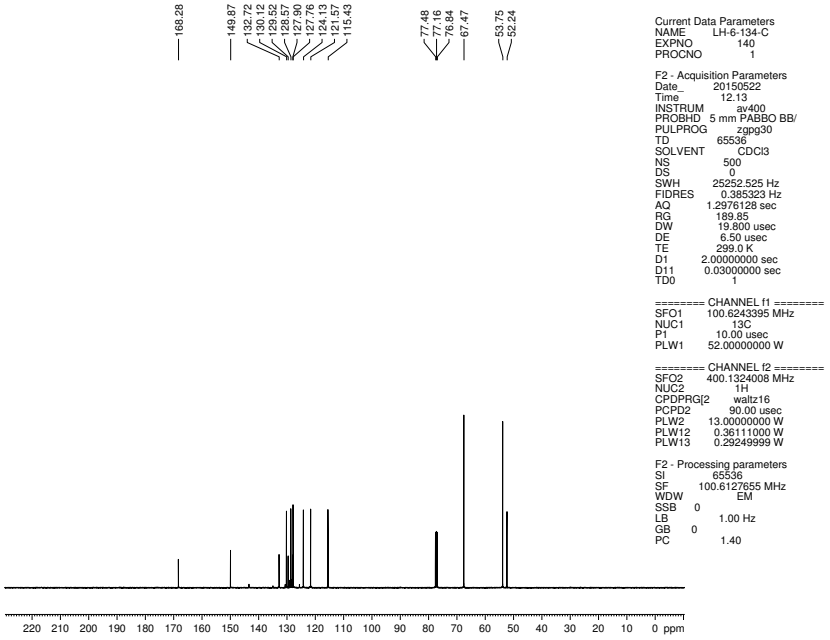

Figure A5.3 ^{13}C NMR (125 MHz, $CDCl_3$) of compound **5.37**.

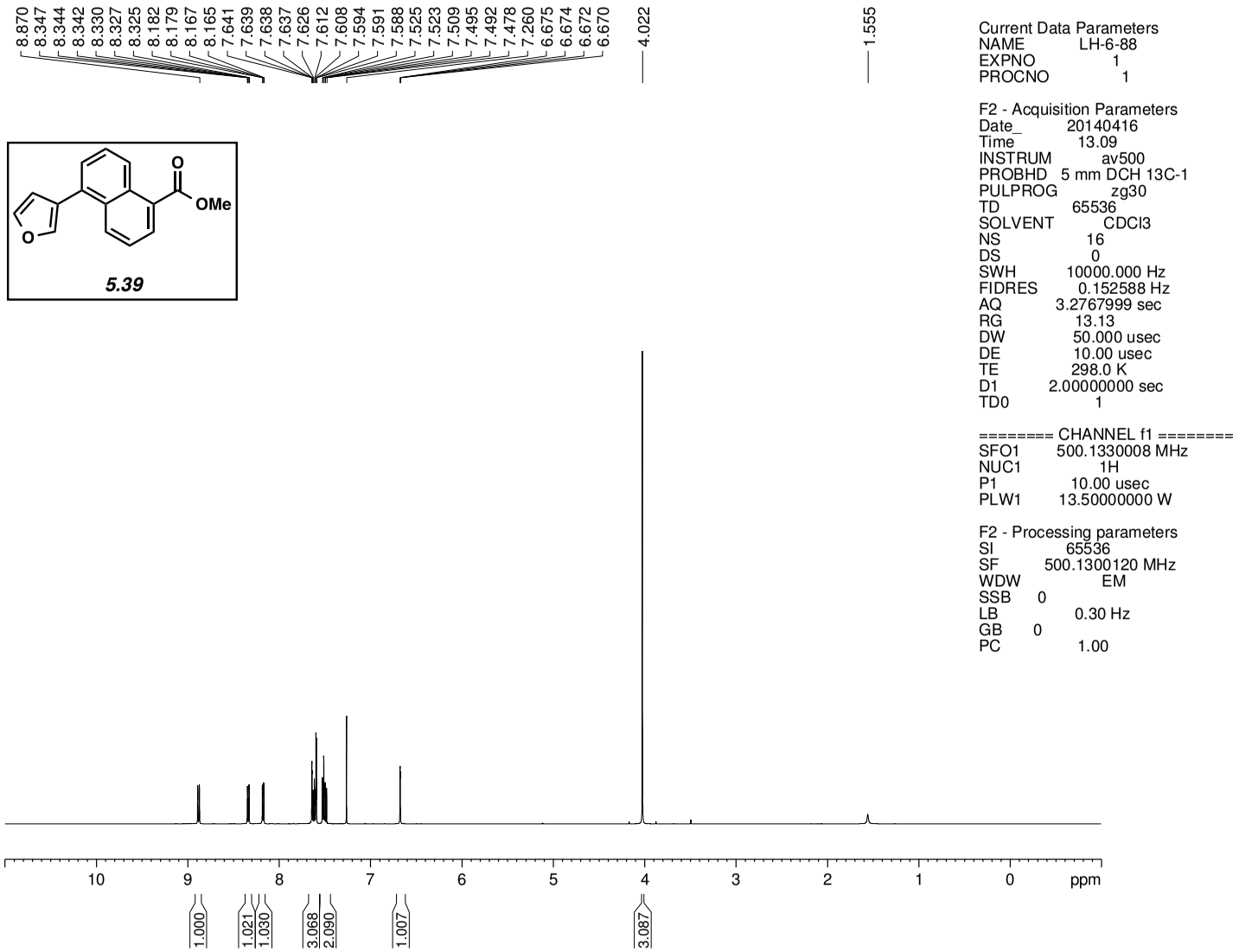

Figure A5.4 ^{1}H NMR (500 MHz, $CDCl_3$) of compound **5.39**.

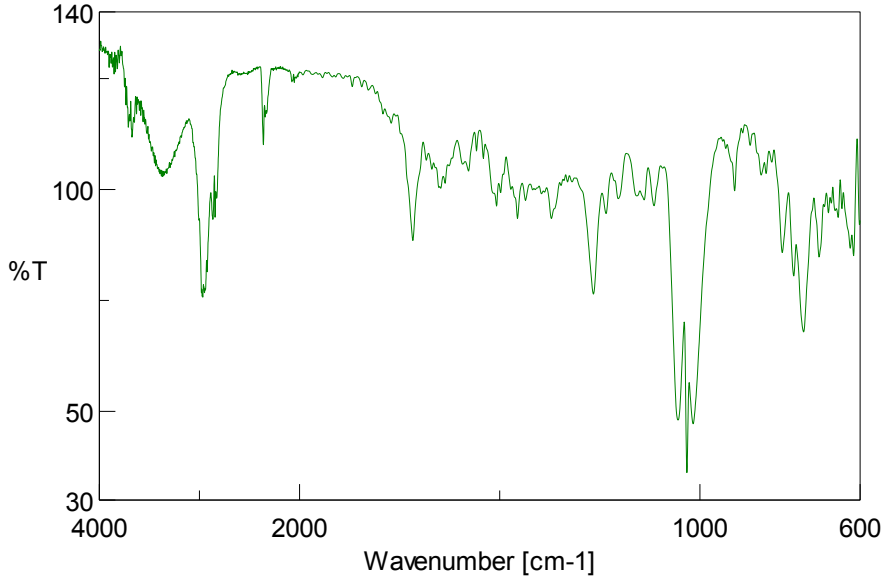

Figure A5.5 Infrared spectrum of compound **5.39**.

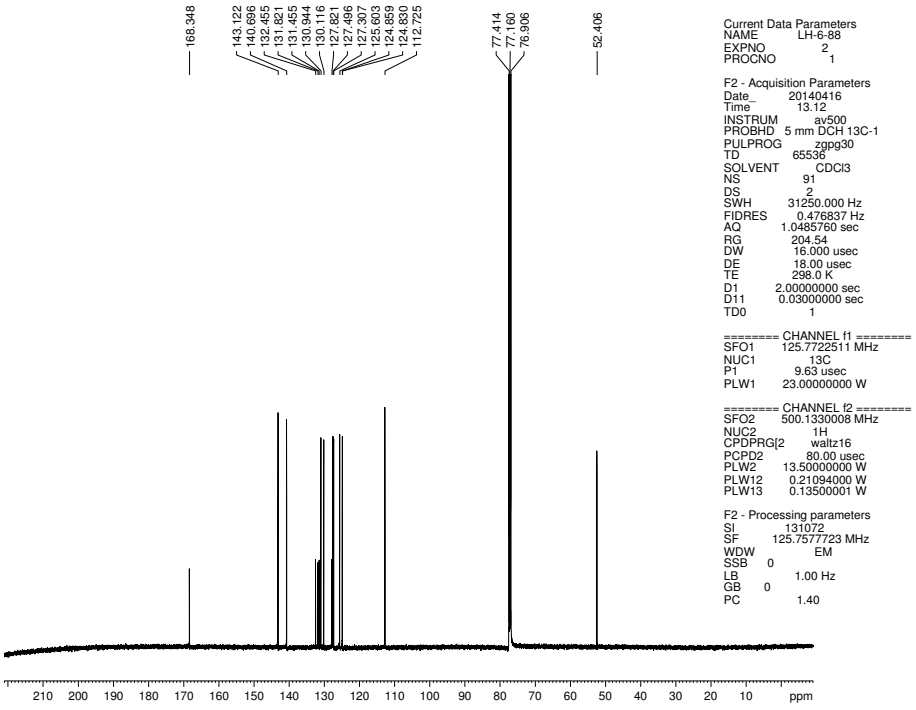

Figure A5.6 ^{13}C NMR (125 MHz, $CDCl_3$) of compound **5.39**.

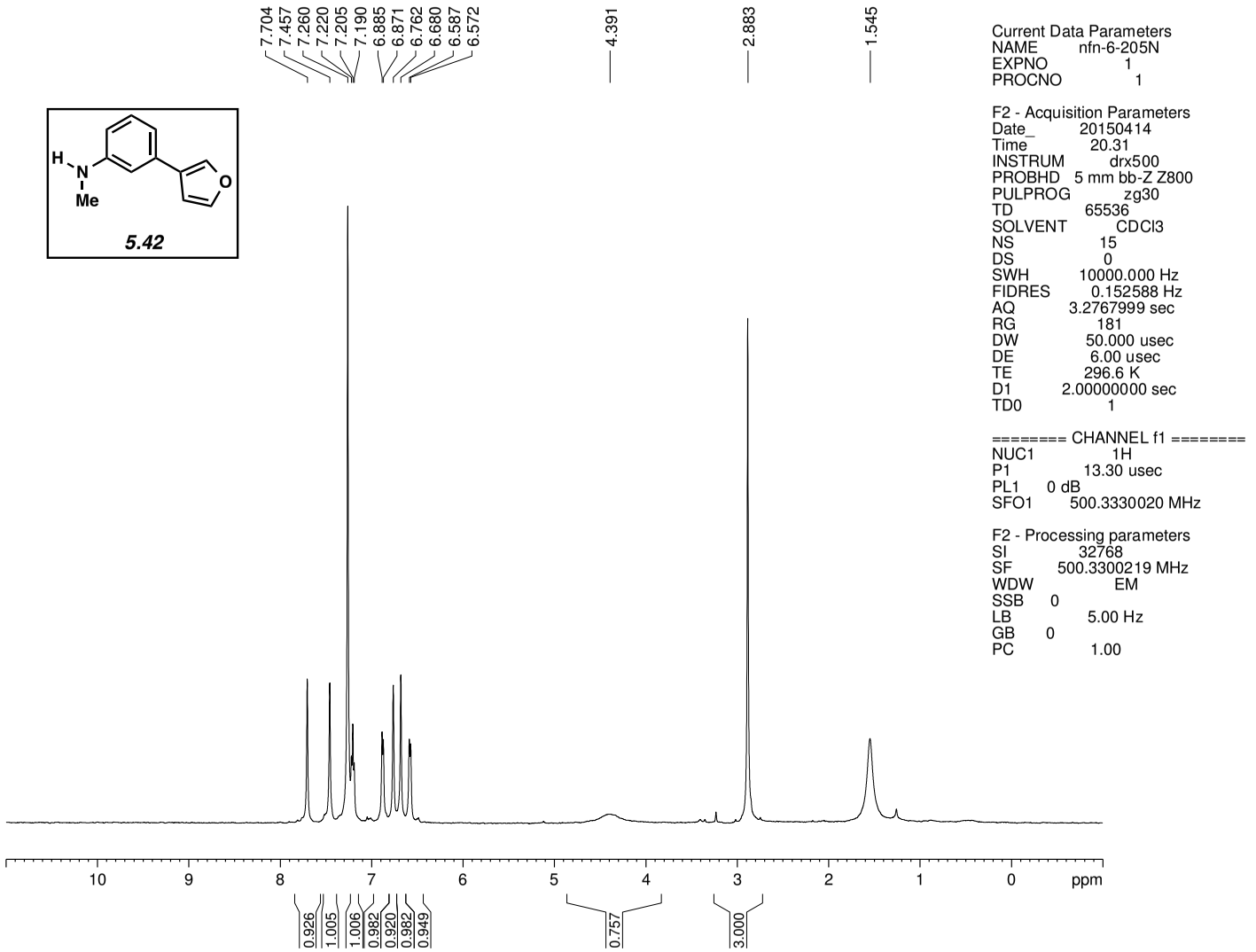

Figure A5.7 ^{1}H NMR (500 MHz, $CDCl_3$) of compound **5.42**.

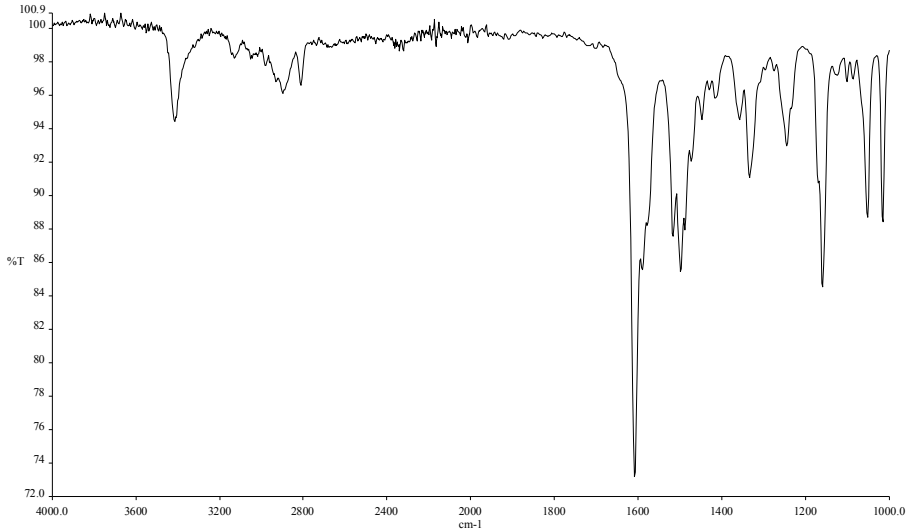

Figure A5.8 Infrared spectrum of compound **5.42**.

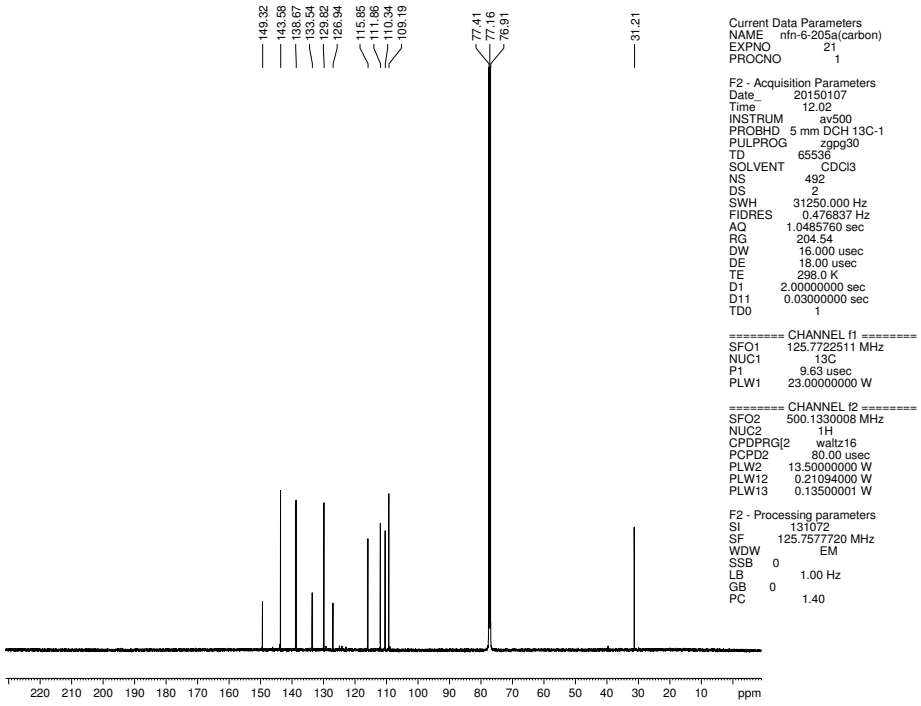

Figure A5.9 ^{13}C NMR (125 MHz, $CDCl_3$) of compound **5.42**.

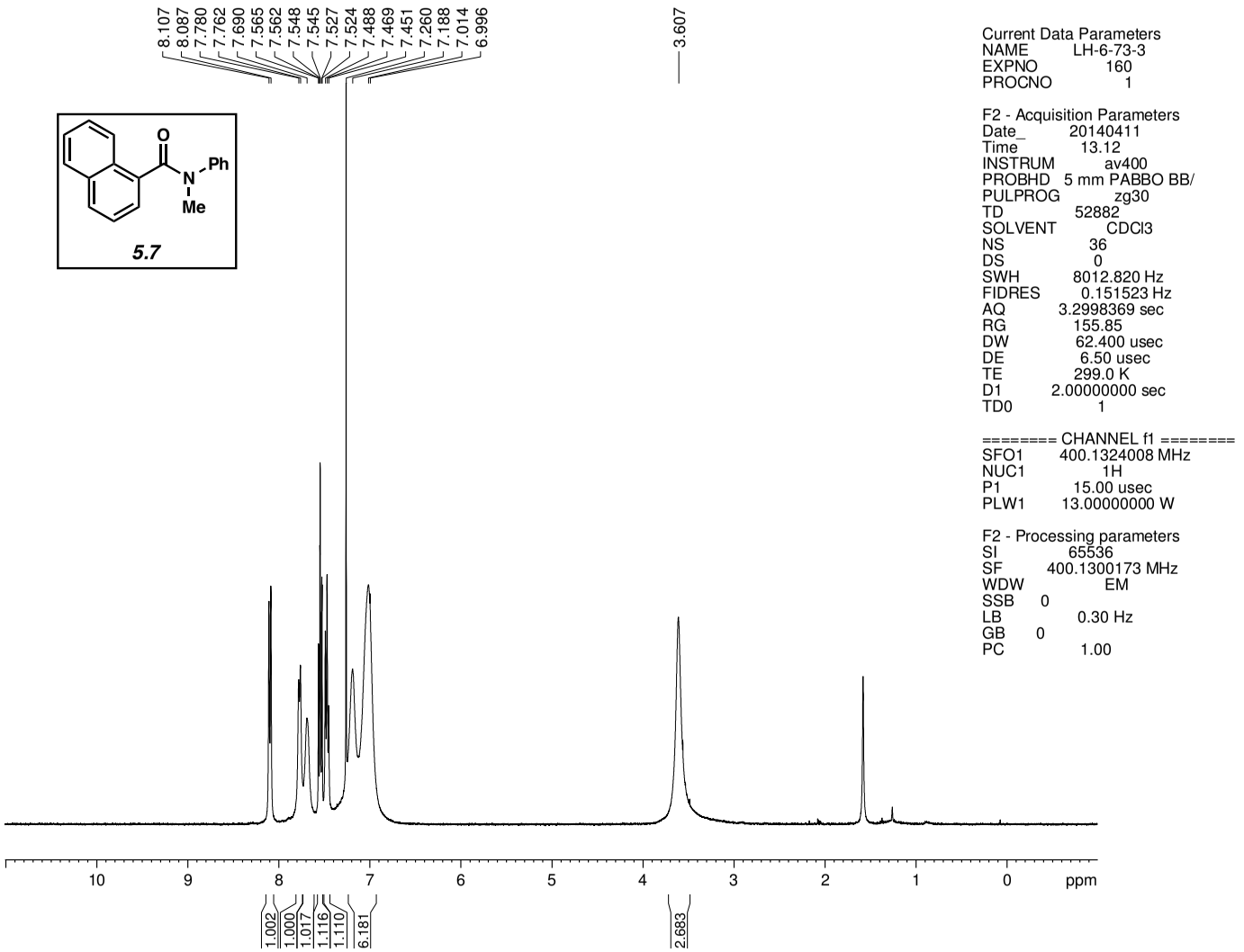

Figure A5.10 ^{1}H NMR (400 MHz, $CDCl_3$) of compound **5.7**.

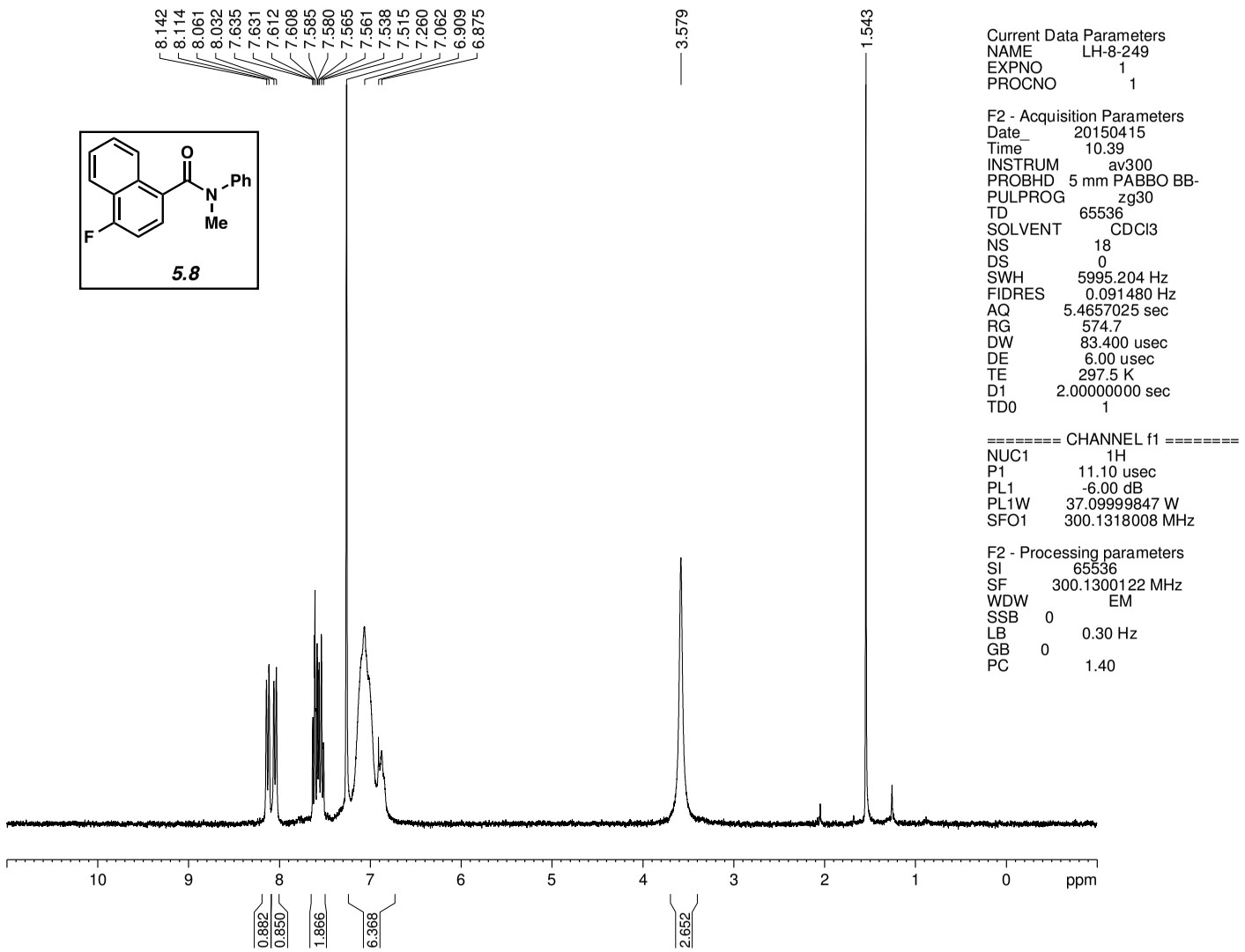

Figure A5.11 ^{1}H NMR (300 MHz, $CDCl_3$) of compound **5.8**.

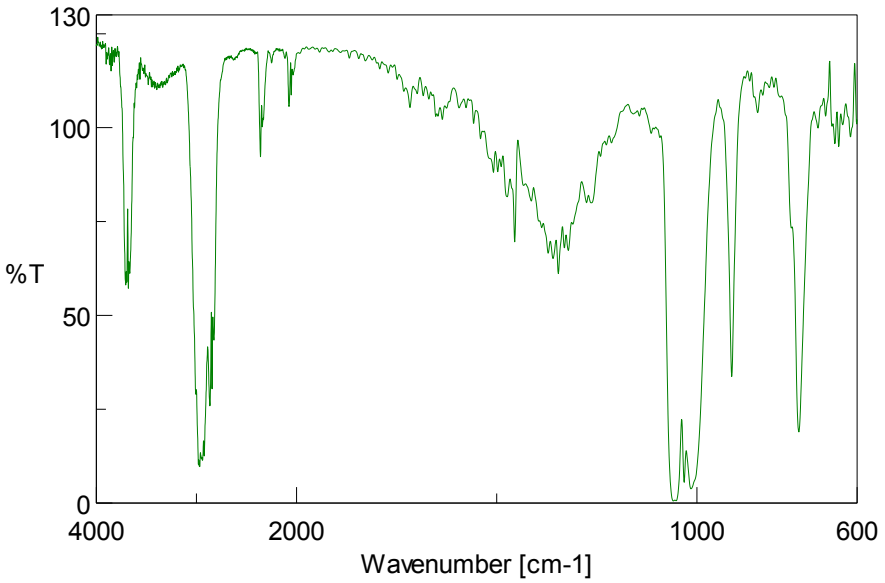

Figure A5.12 Infrared spectrum of compound **5.8**.

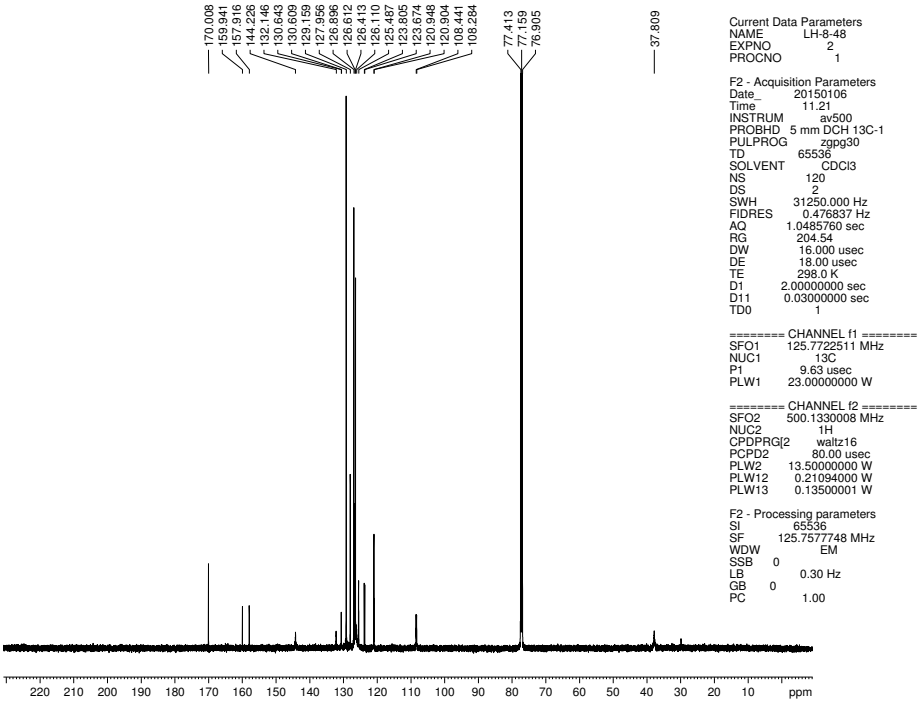

Figure A5.13 ^{13}C NMR (125 MHz, $CDCl_3$) of compound **5.8**.

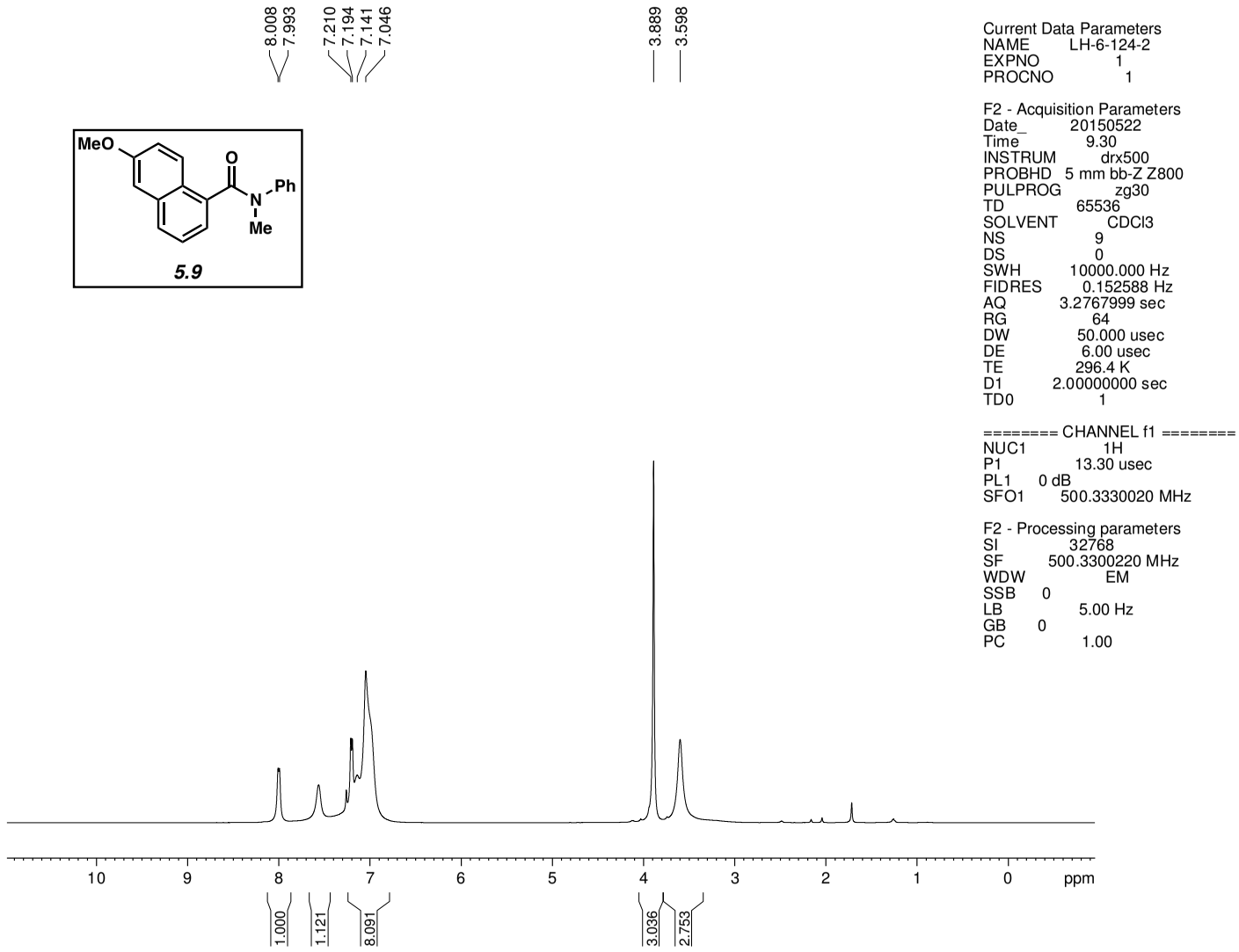

Figure A5.14 ^{1}H NMR (500 MHz, $CDCl_3$) of compound **5.9**.

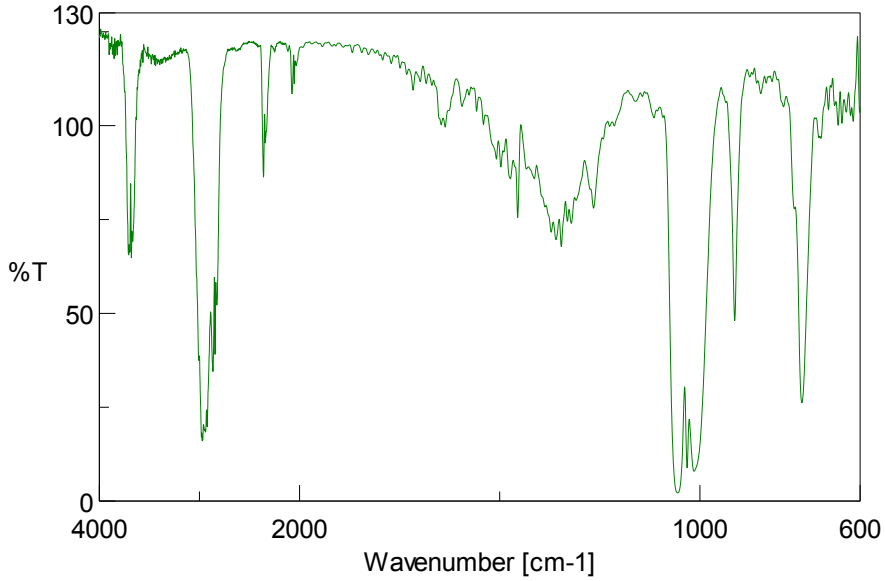

Figure A5.15 Infrared spectrum of compound **5.9**.

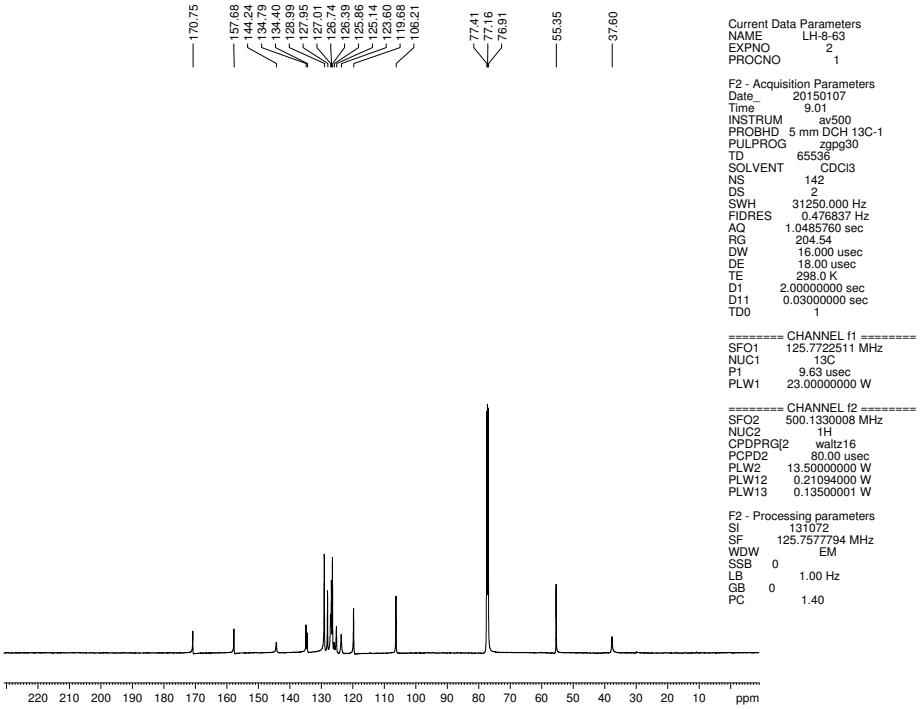

Figure A5.16 ^{13}C NMR (125 MHz, $CDCl_3$) of compound **5.9**.

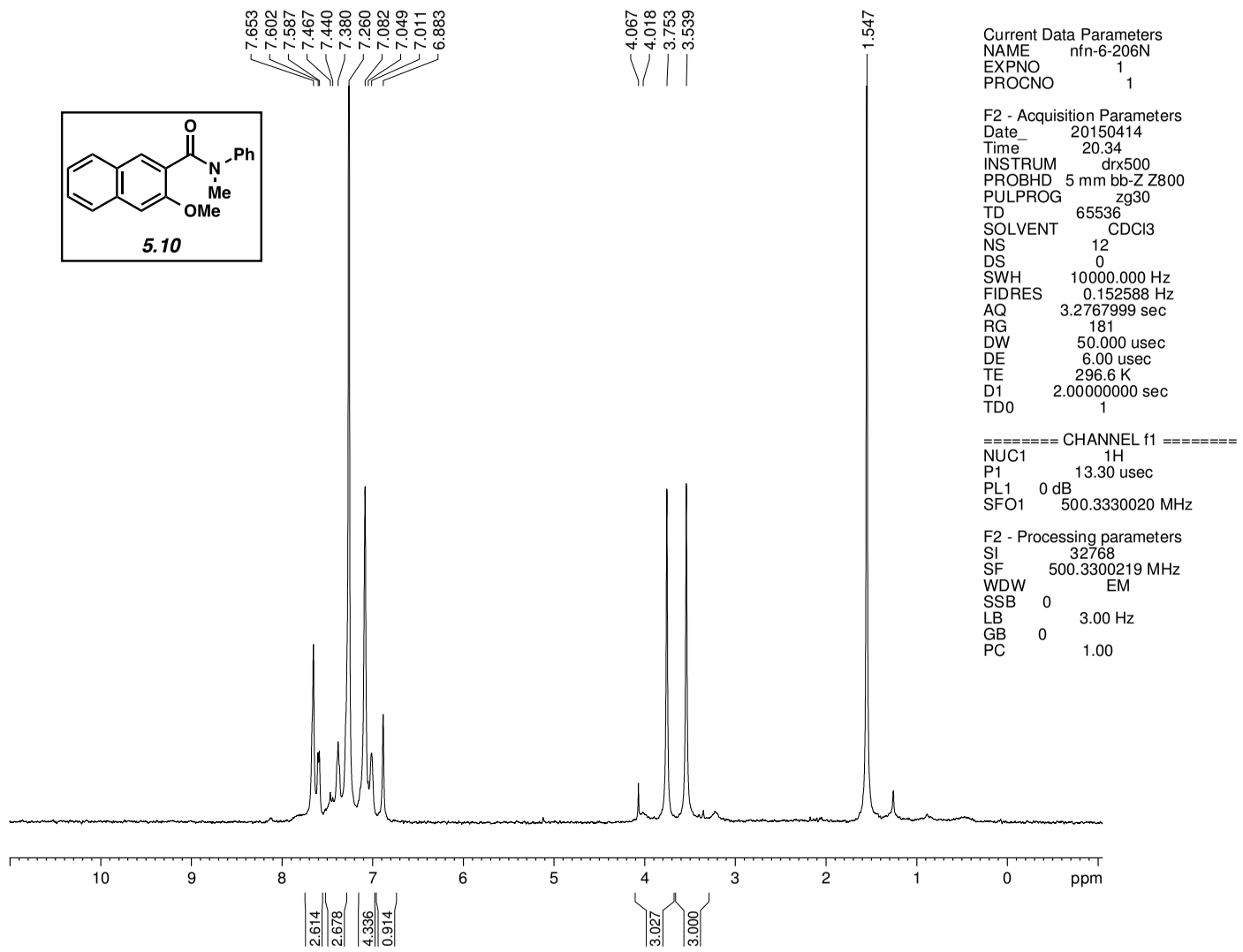

Figure A5.17 ^{1}H NMR (500 MHz, $CDCl_3$) of compound **5.10**.

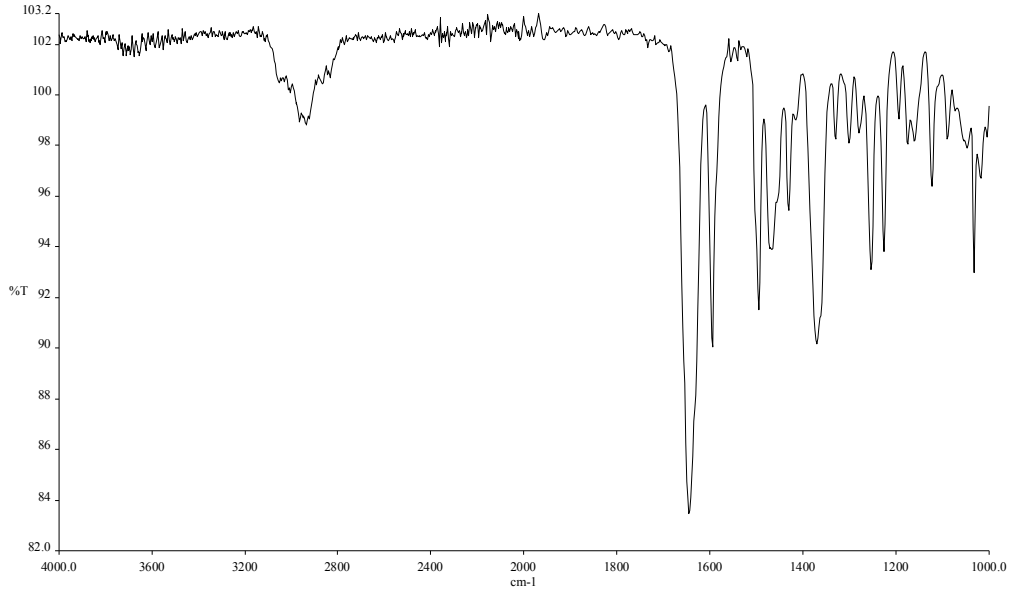

Figure A5.18 Infrared spectrum of compound **5.10**.

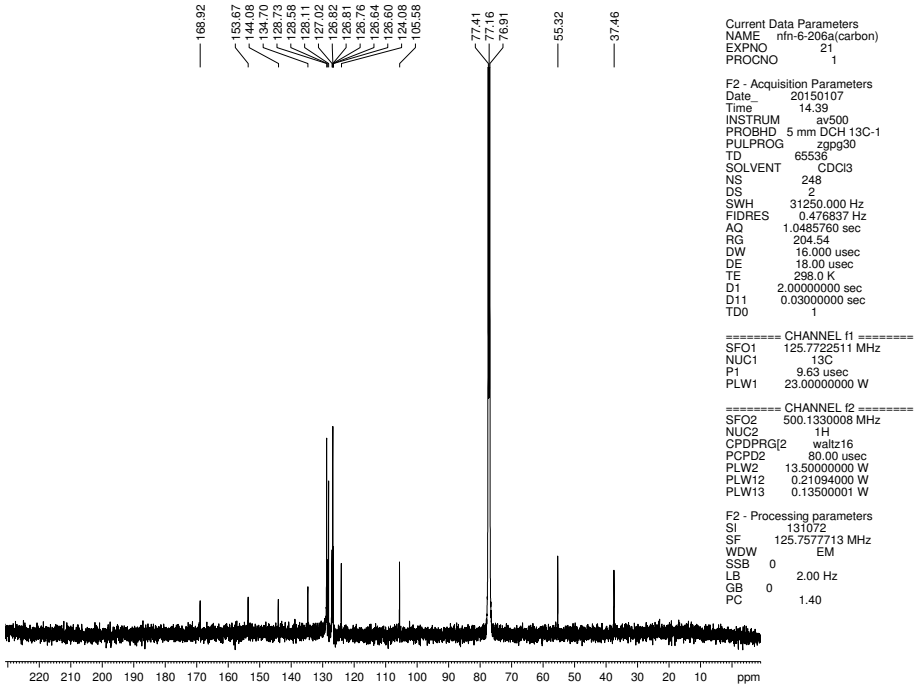

*Figure A5.*19 ^{13}C NMR (125 MHz, $CDCl_3$) of compound **5.10**.

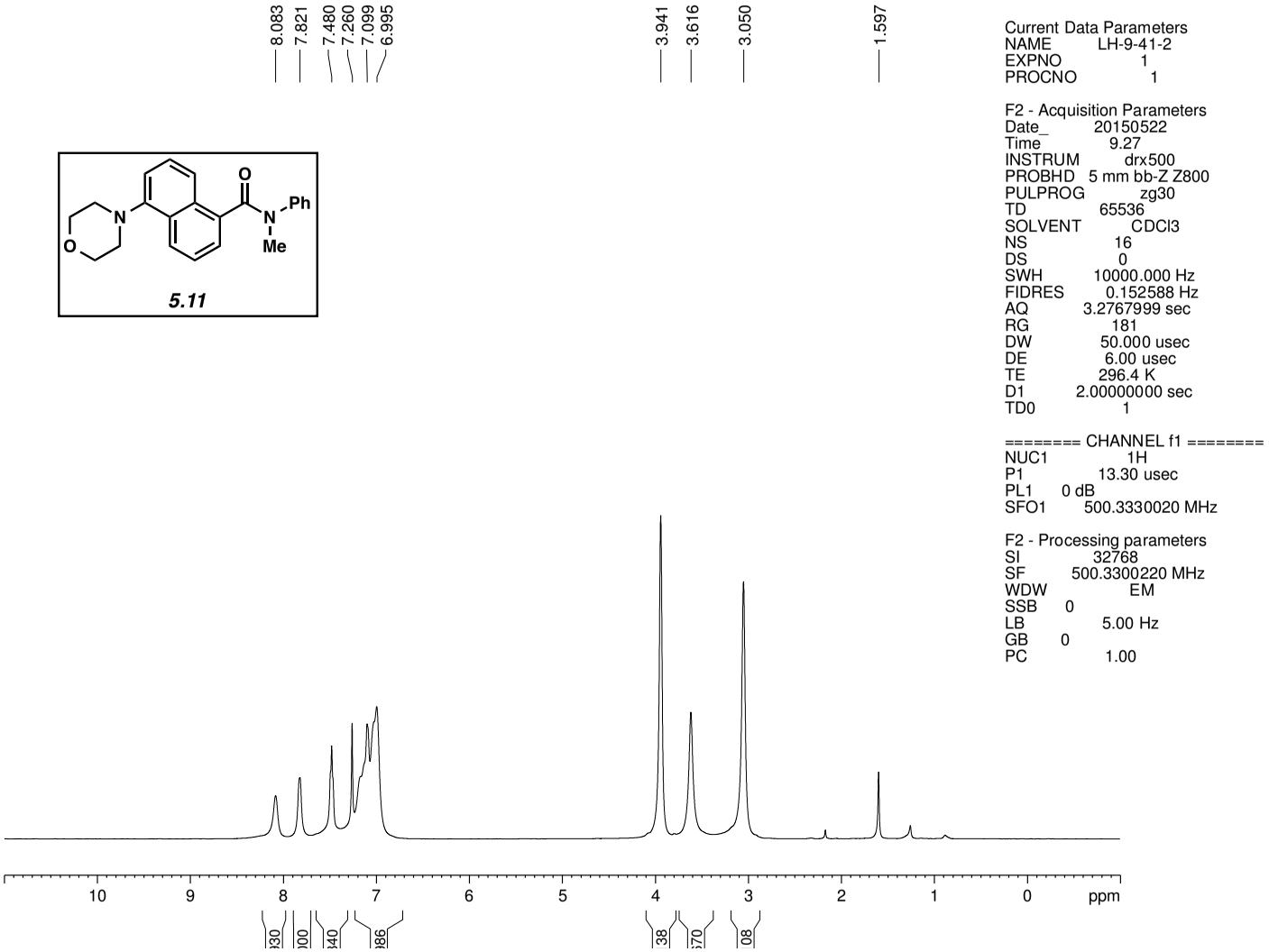

Figure A5.20 ^{1}H NMR (500 MHz, $CDCl_3$) of compound **5.11**.

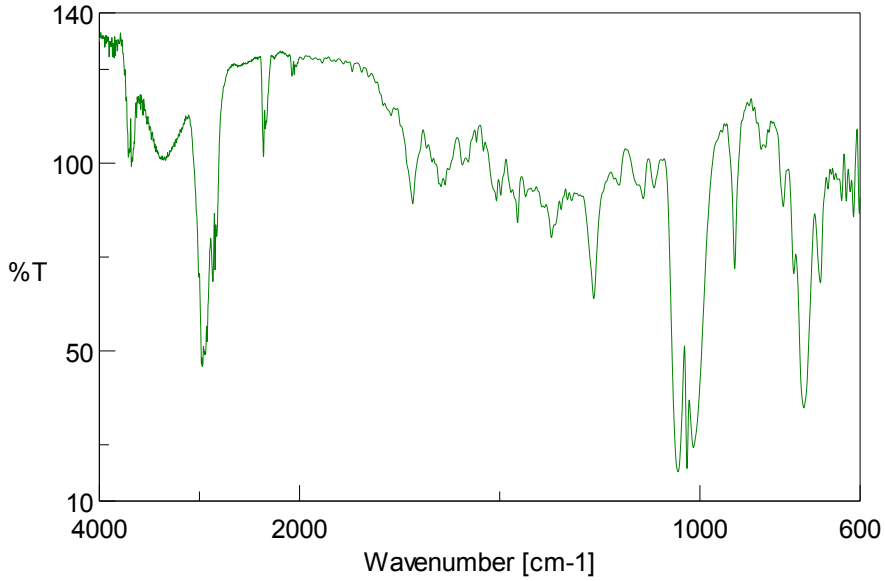

Figure A5.21 Infrared spectrum of compound **5.11**.

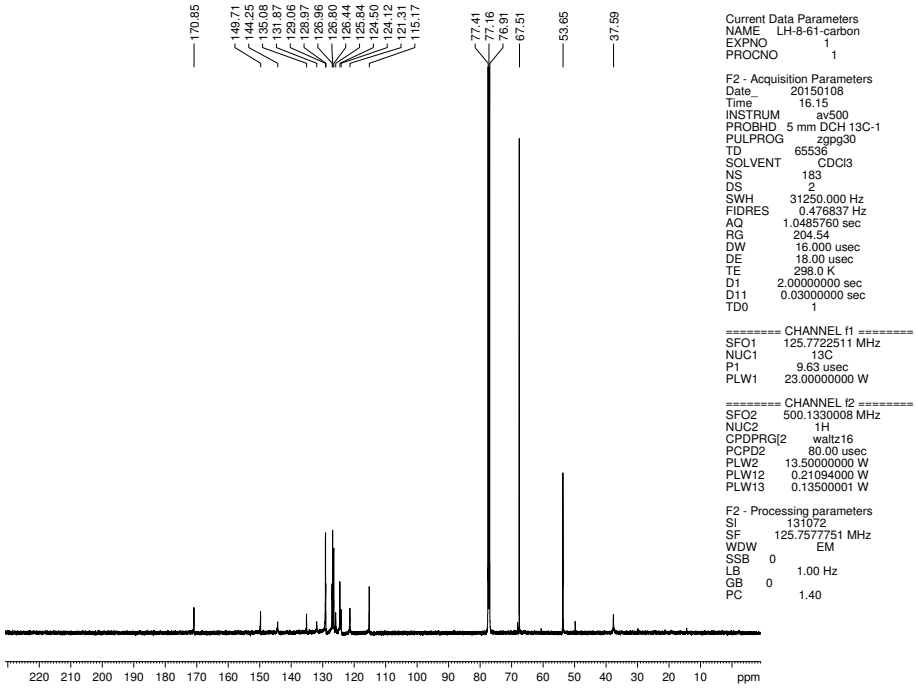

Figure A5.22 ^{13}C NMR (125 MHz, $CDCl_3$) of compound **5.11**.

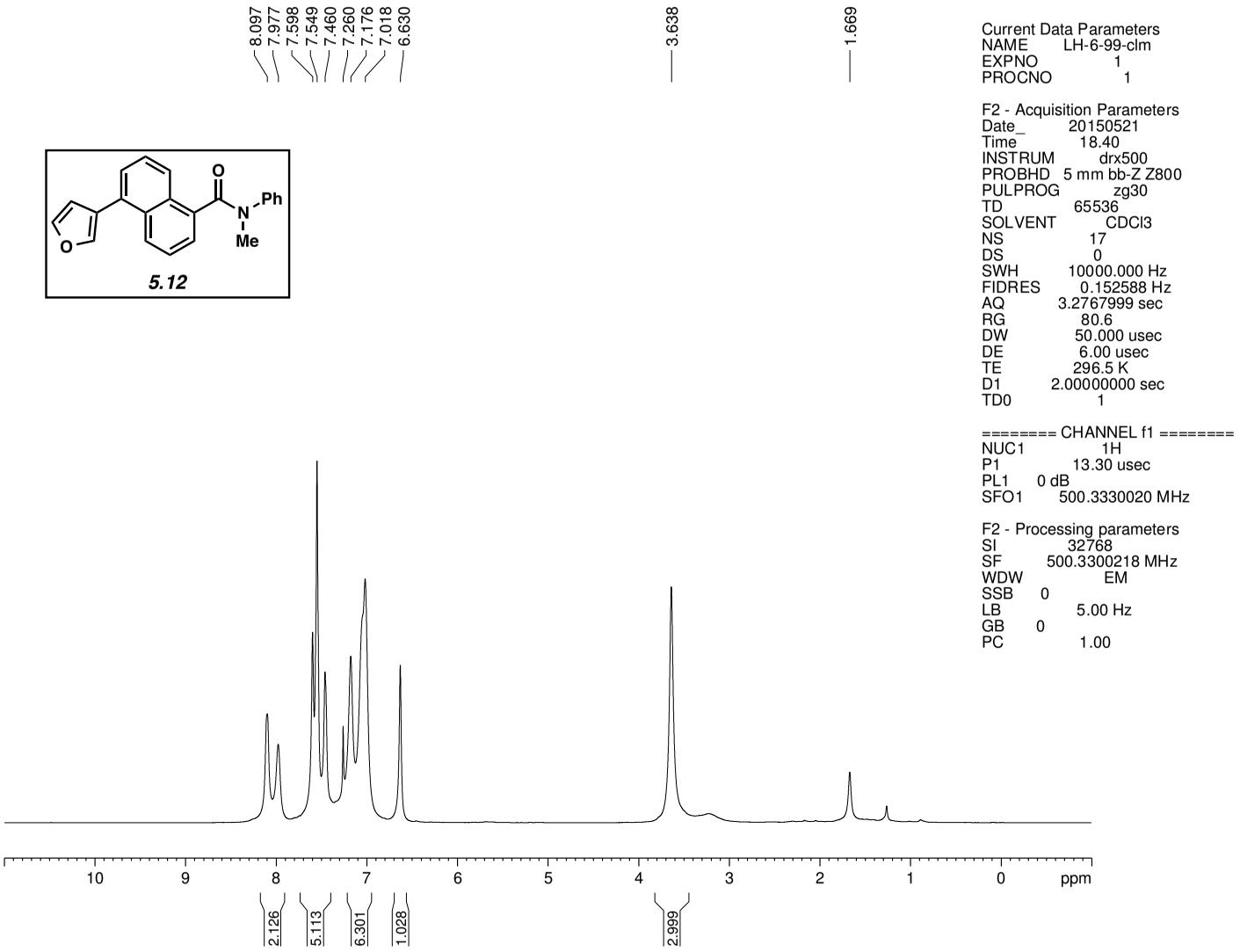

Figure A5.23 ^{1}H NMR (500 MHz, $CDCl_3$) of compound **5.12**.

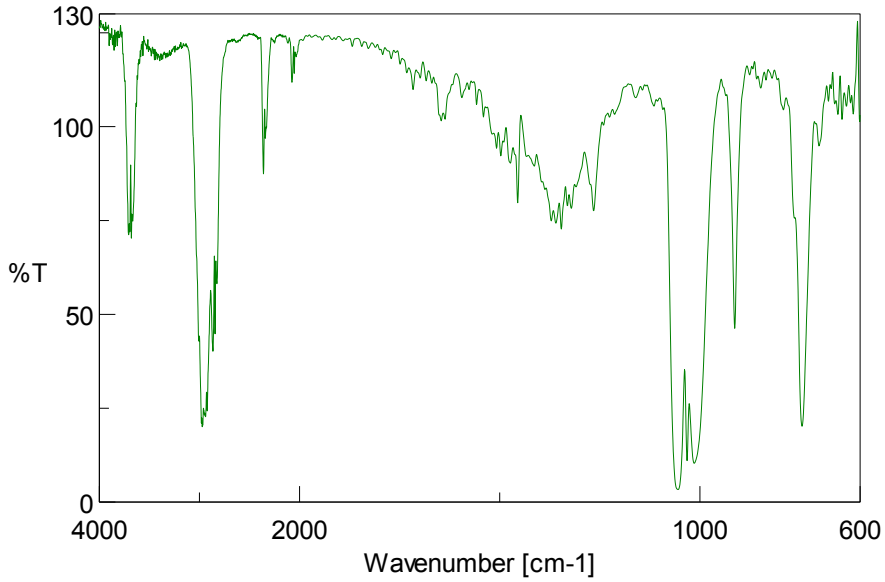

Figure A5.24 Infrared spectrum of compound **5.12**.

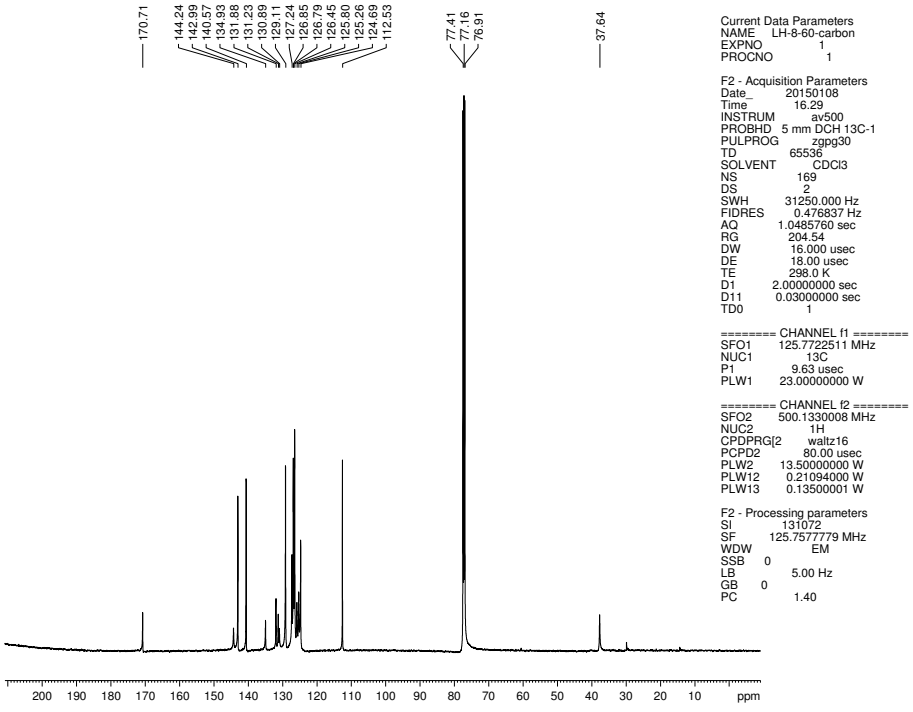

Figure A5.25 ^{13}C NMR (125 MHz, $CDCl_3$) of compound **5.12**.

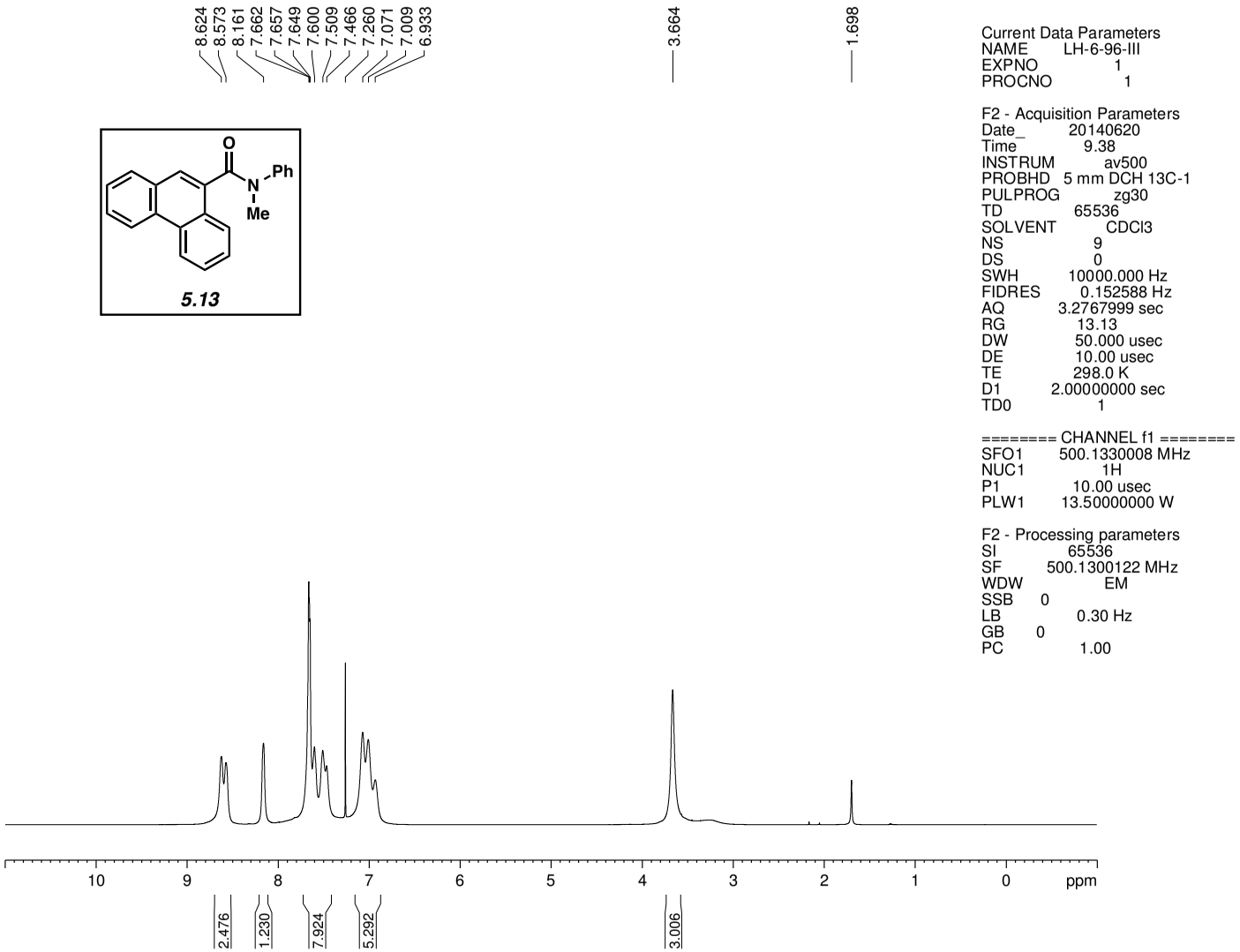

Figure A5.26 ^{1}H NMR (500 MHz, $CDCl_3$) of compound **5.13**.

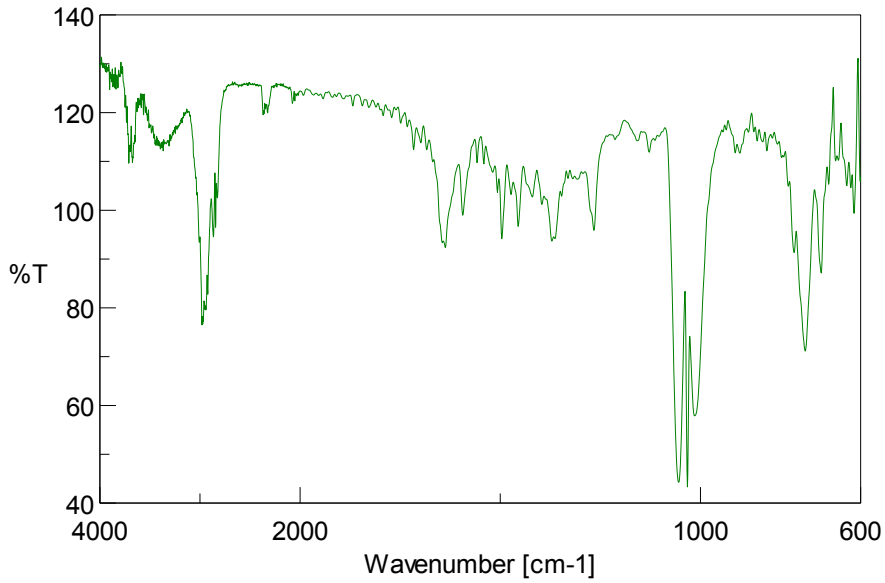

Figure A5.27 Infrared spectrum of compound **5.13**.

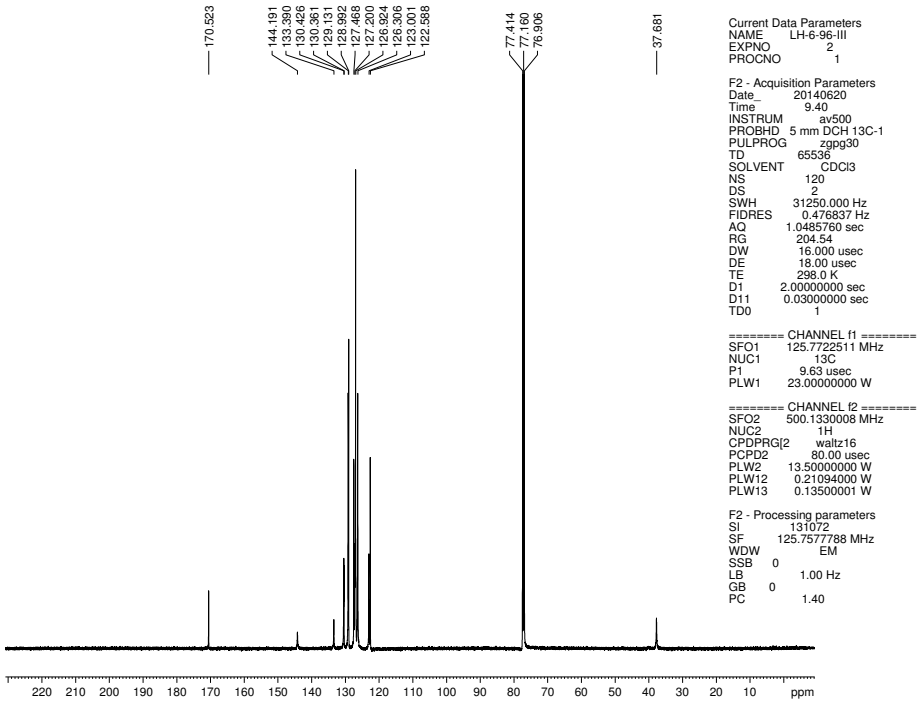

Figure A5.28 ^{13}C NMR (125 MHz, $CDCl_3$) of compound **5.13**.

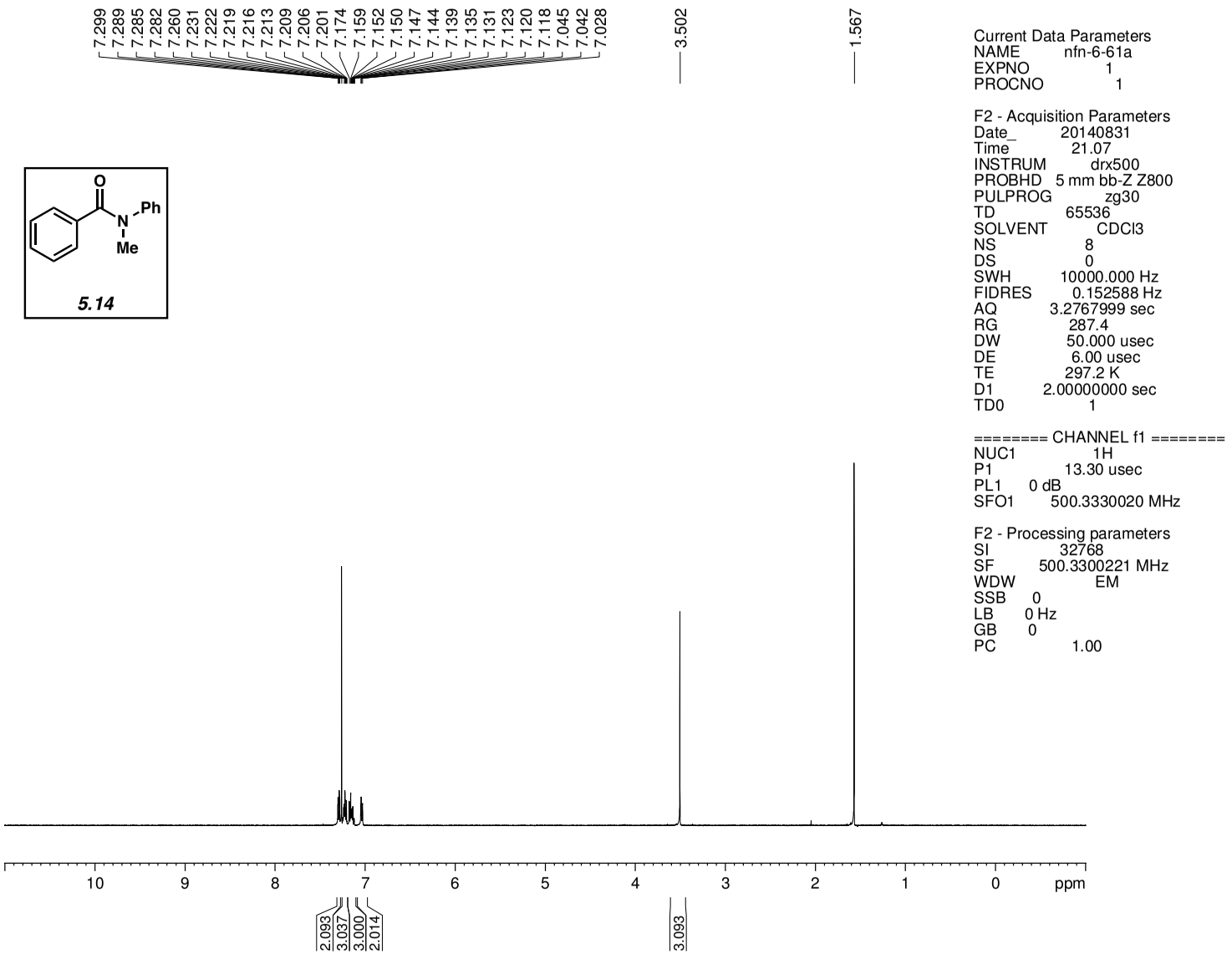

Figure A5.29 ^{1}H NMR (500 MHz, $CDCl_3$) of compound **5.14**.

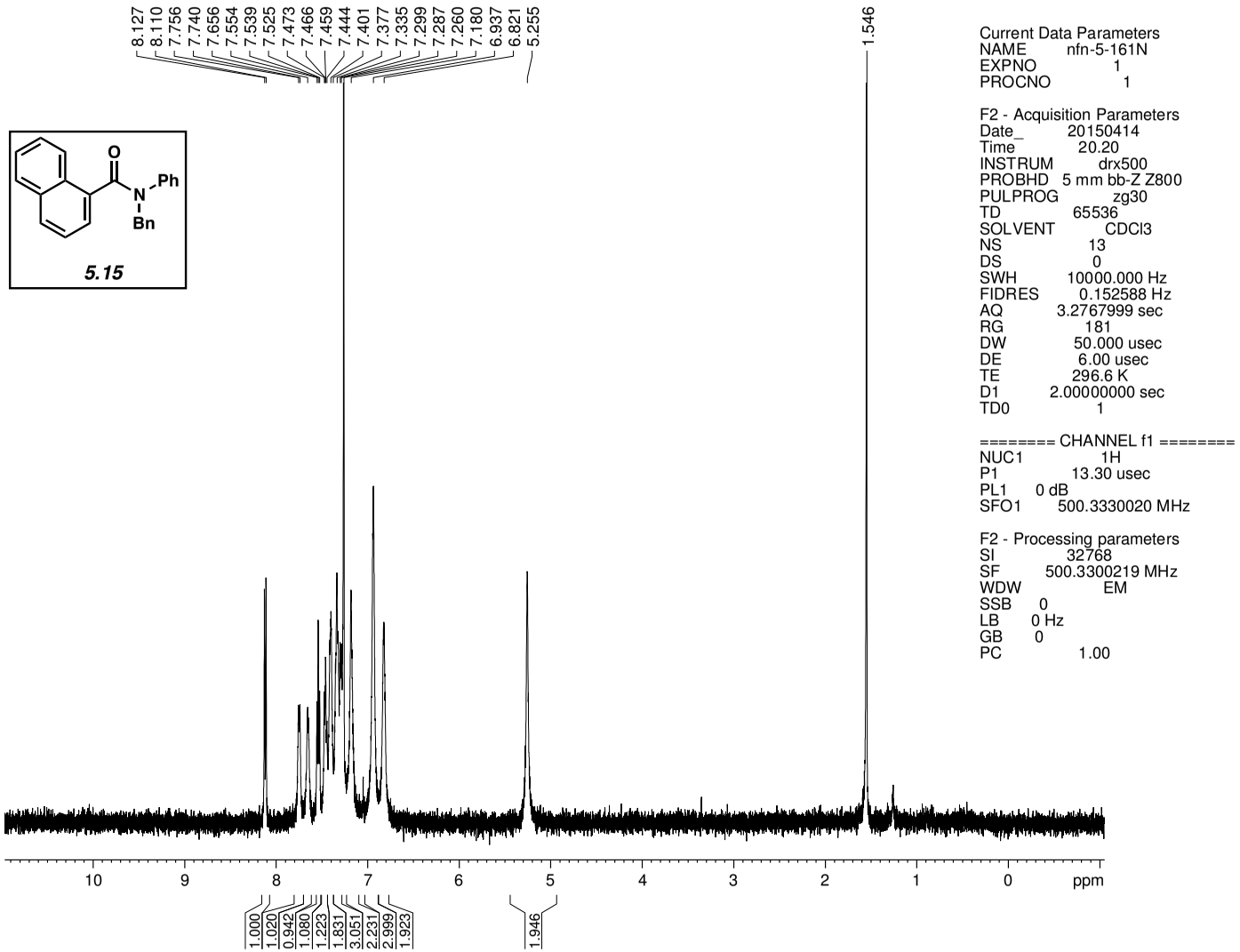

Figure A5.30 ^{1}H NMR (500 MHz, $CDCl_3$) of compound **5.15**.

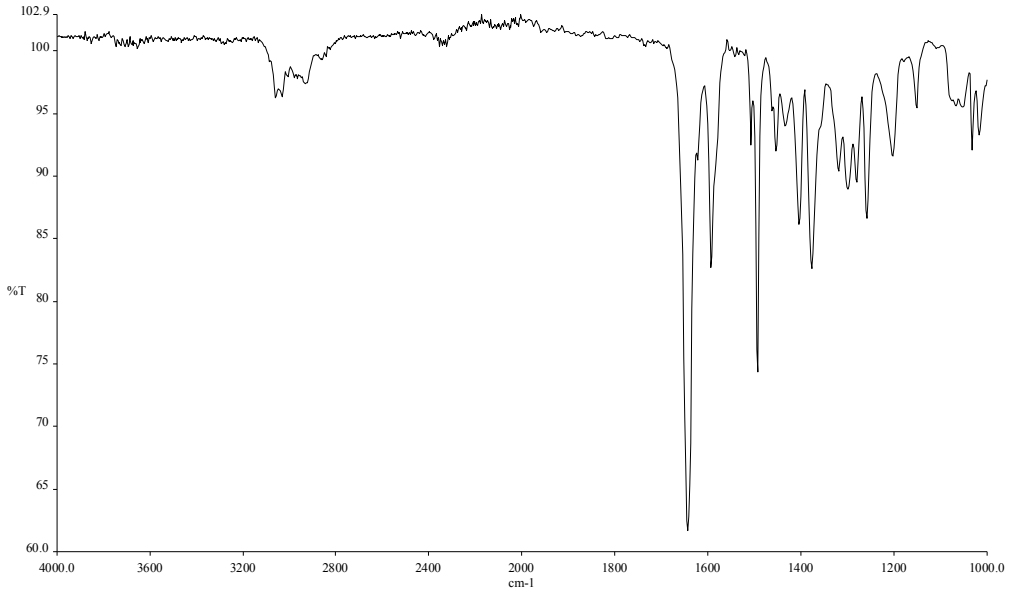

Figure A5.31 Infrared spectrum of compound **5.15**.

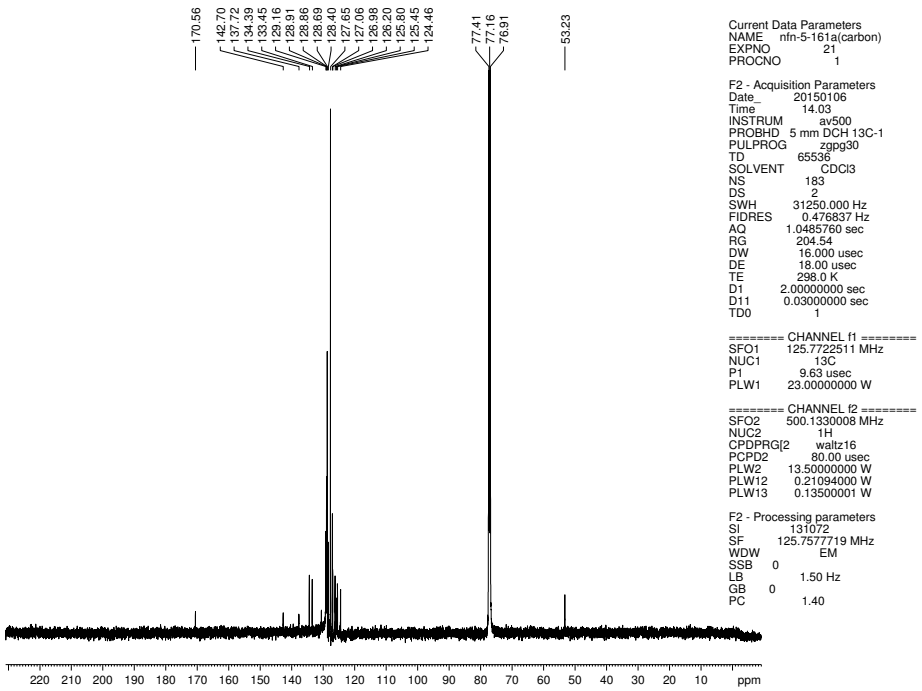

Figure A5.32 ^{13}C NMR (125 MHz, $CDCl_3$) of compound **5.15**.

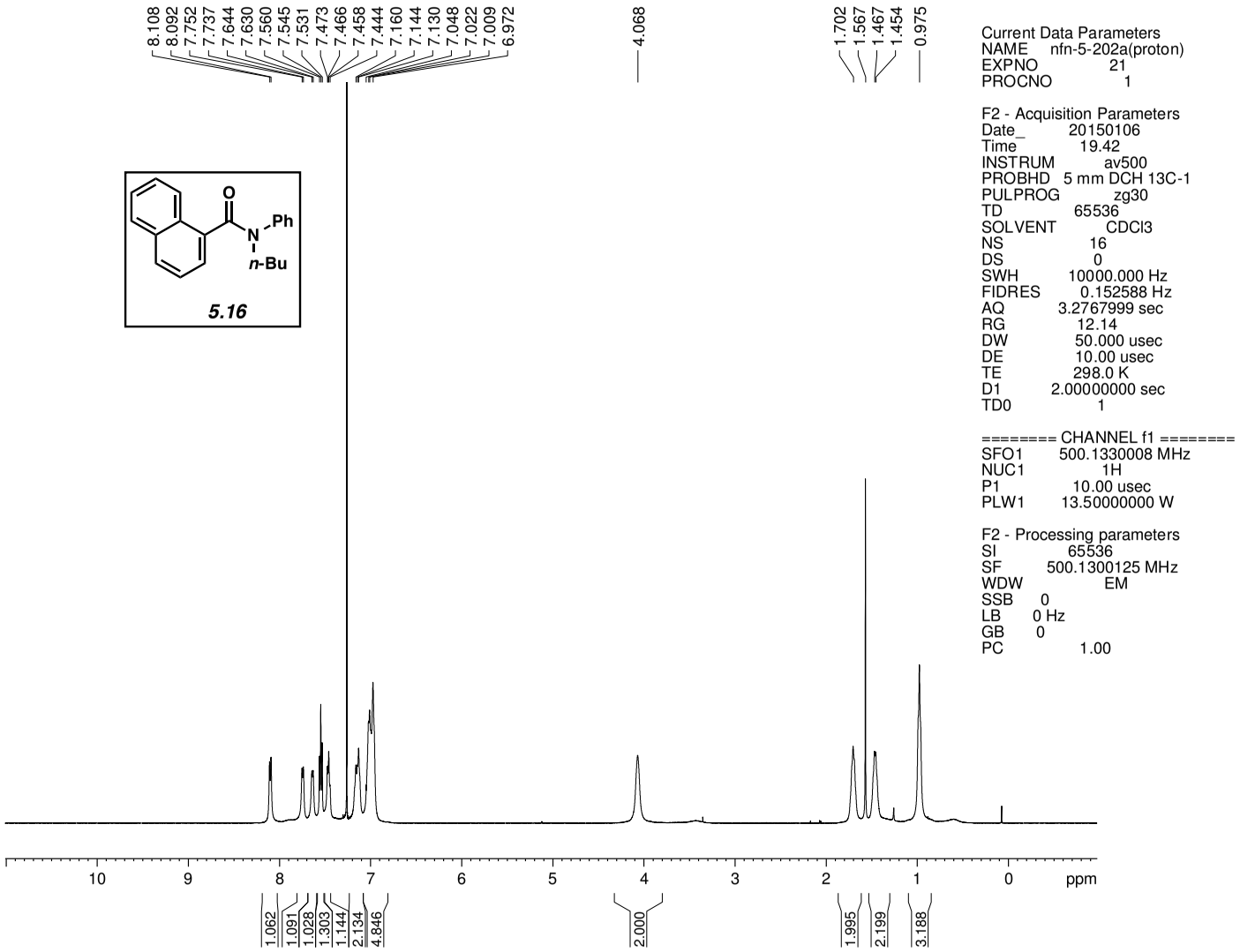

Figure A5.33 ^{1}H NMR (500 MHz, $CDCl_3$) of compound **5.16**.

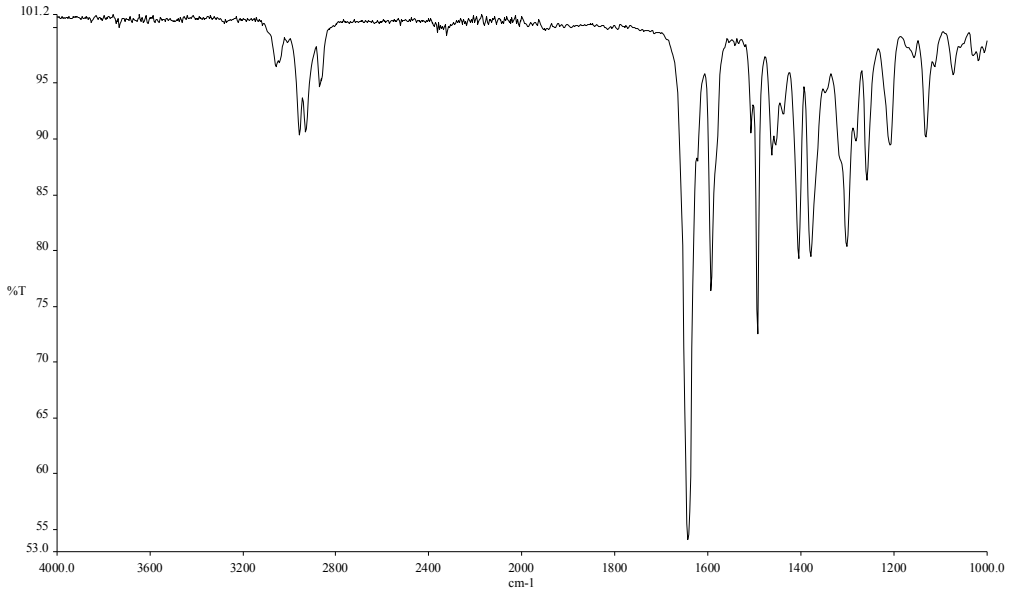

Figure A5.34 Infrared spectrum of compound **5.16**.

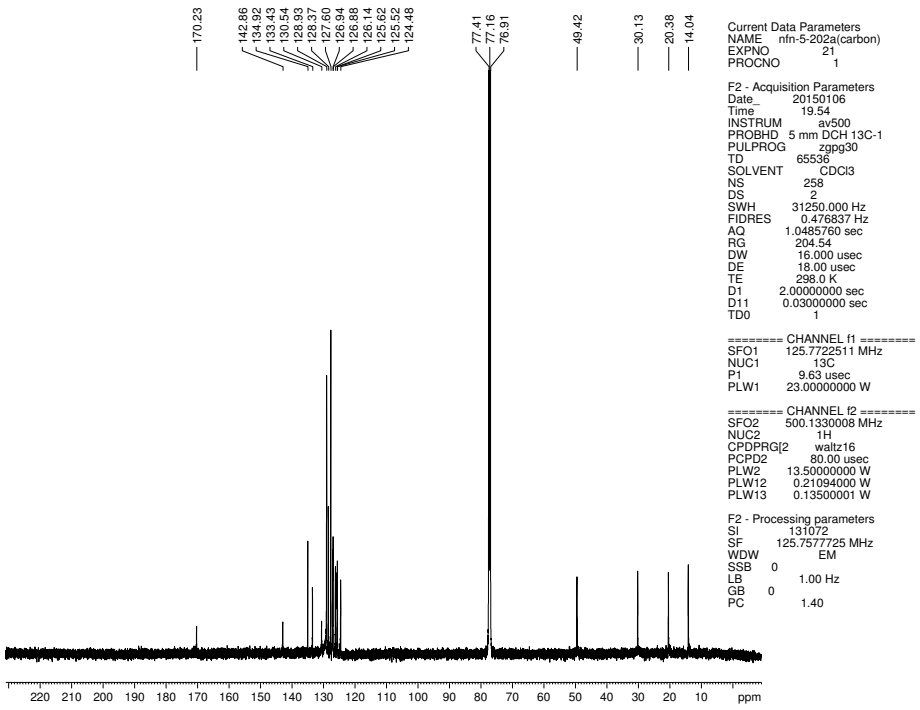

Figure A5.35 ^{13}C NMR (125 MHz, $CDCl_3$) of compound **5.16**.

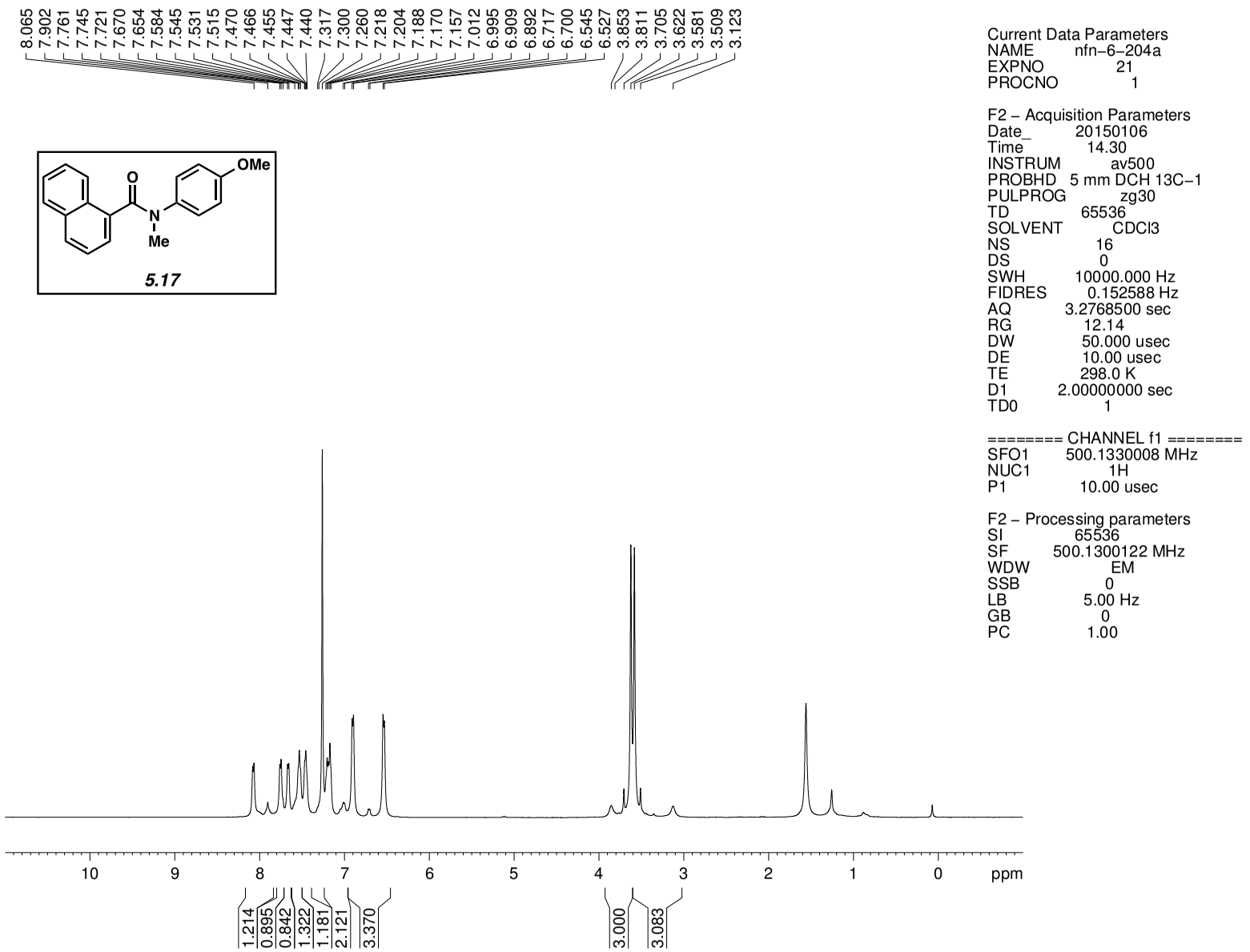

Figure A5.36 ^{1}H NMR (500 MHz, $CDCl_3$) of compound **5.17**.

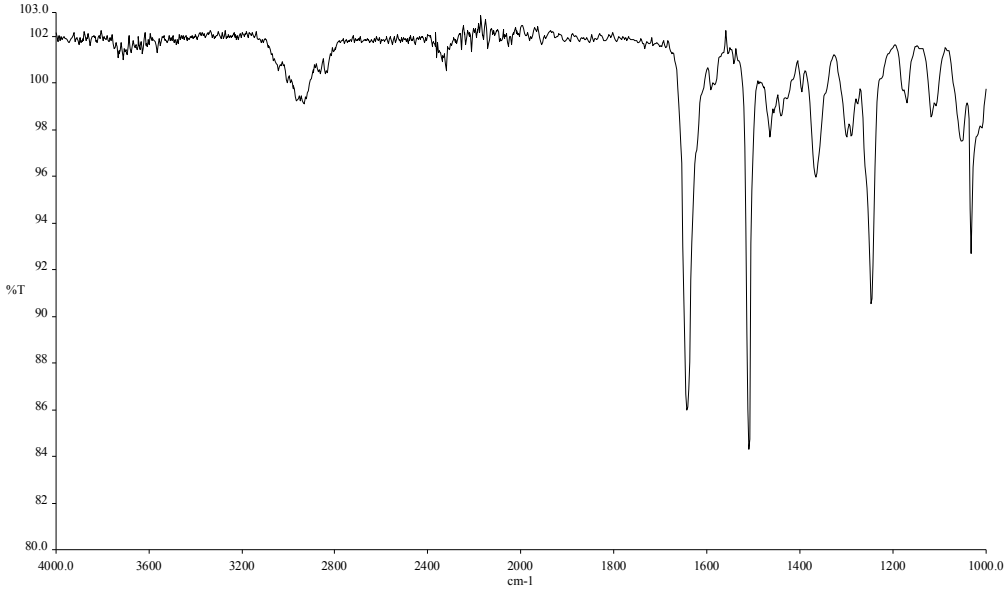

Figure A5.37 Infrared spectrum of compound **5.17**.

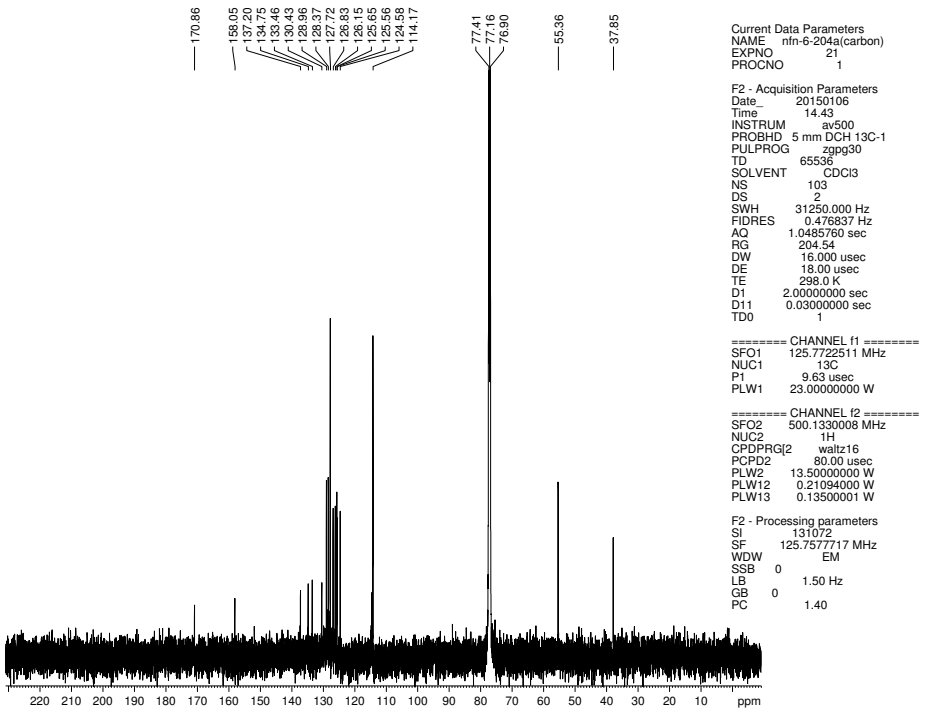

Figure A5.38 ^{13}C NMR (125 MHz, $CDCl_3$) of compound **5.17**.

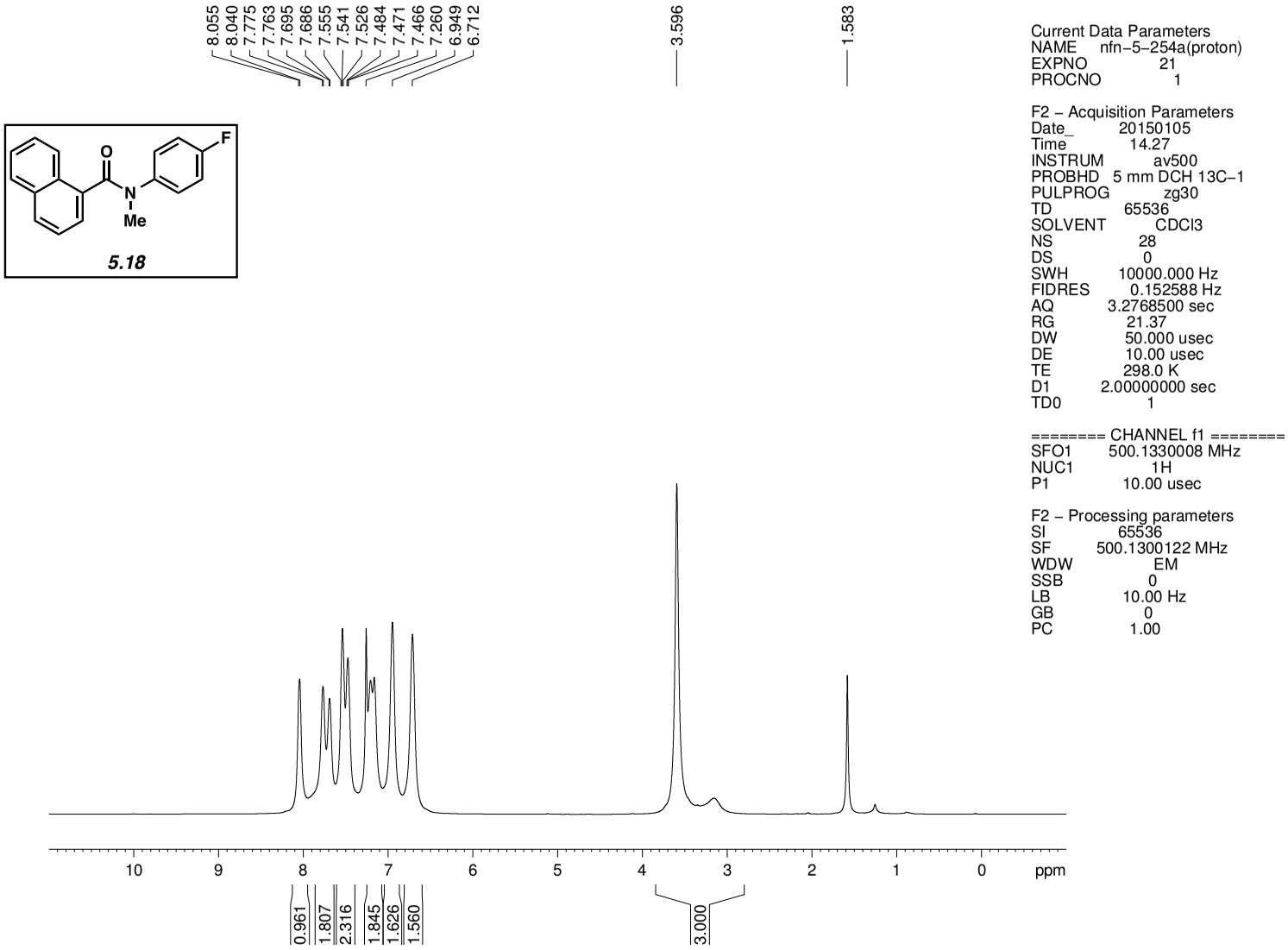

Figure A5.39 ^{1}H NMR (500 MHz, $CDCl_3$) of compound **5.18**.

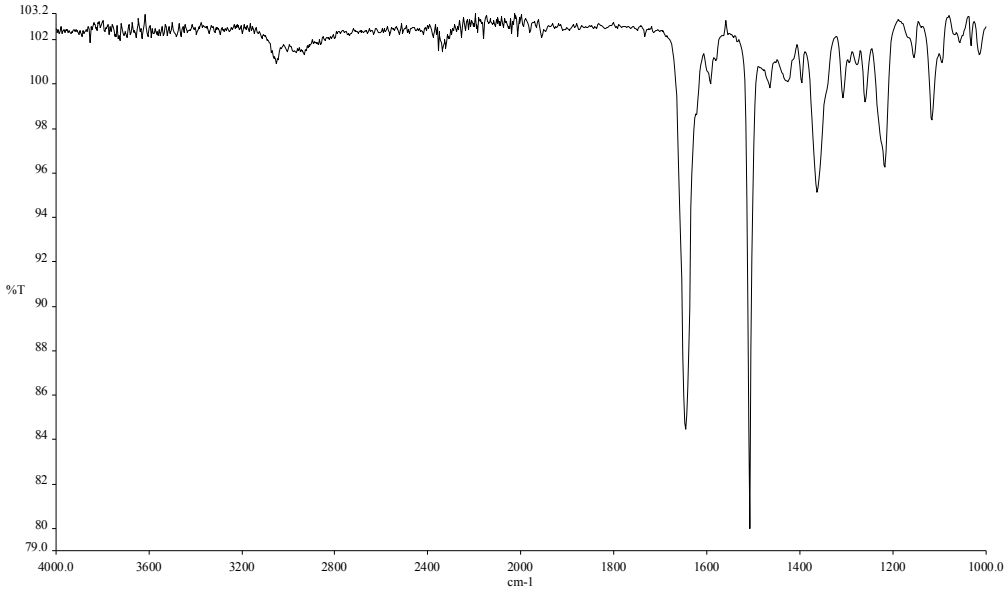

Figure A5.40 Infrared spectrum of compound **5.18**.

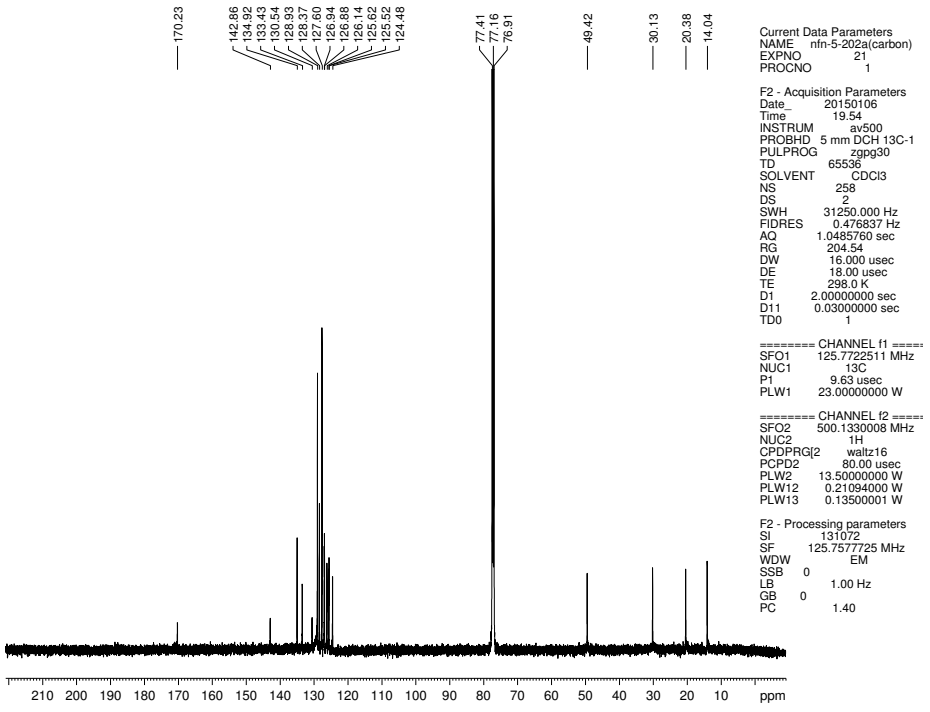

Figure A5.41 ^{13}C NMR (125 MHz, $CDCl_3$) of compound **5.18**.

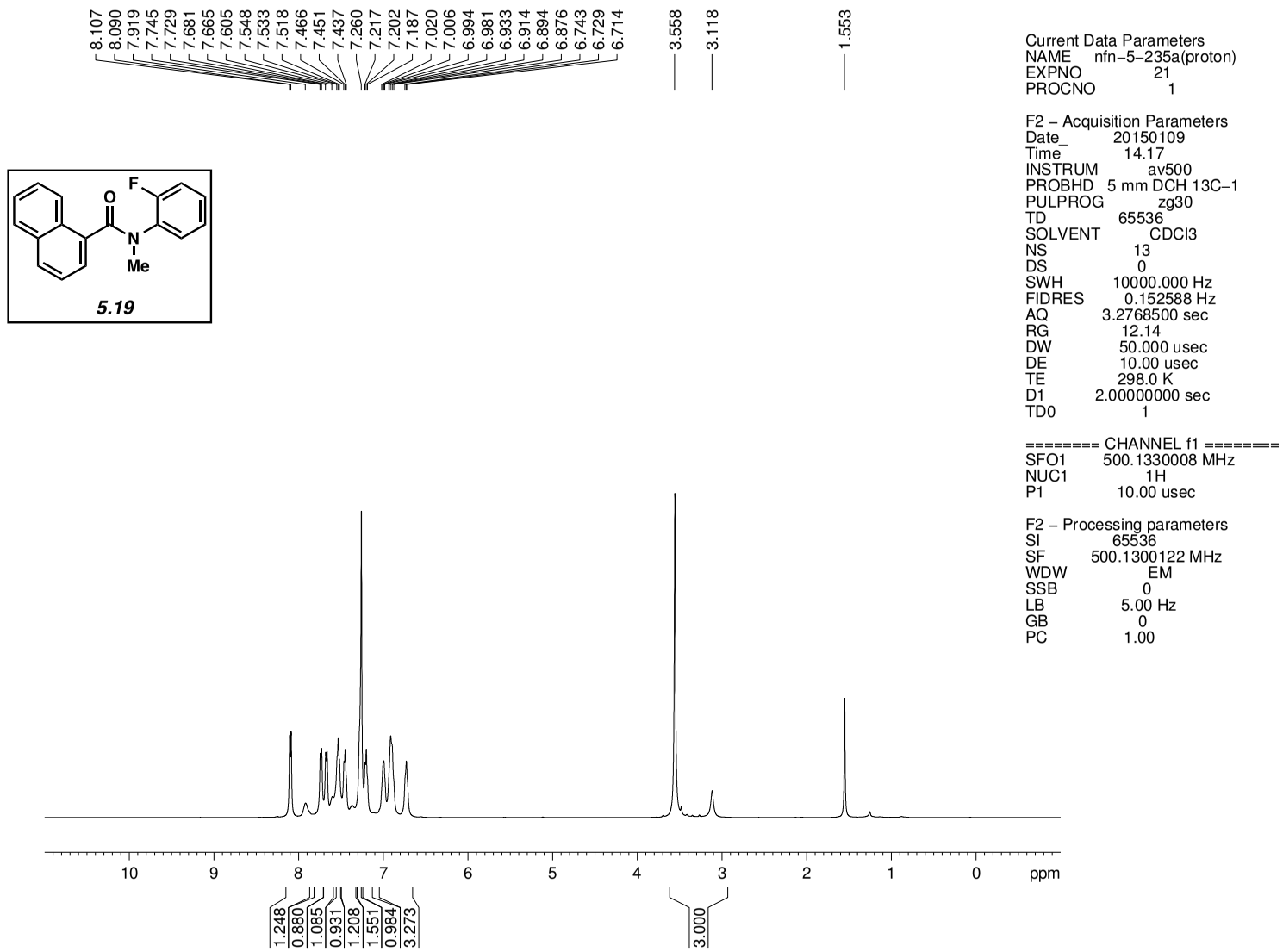

Figure A5.42 ^{1}H NMR (500 MHz, $CDCl_3$) of compound **5.19**.

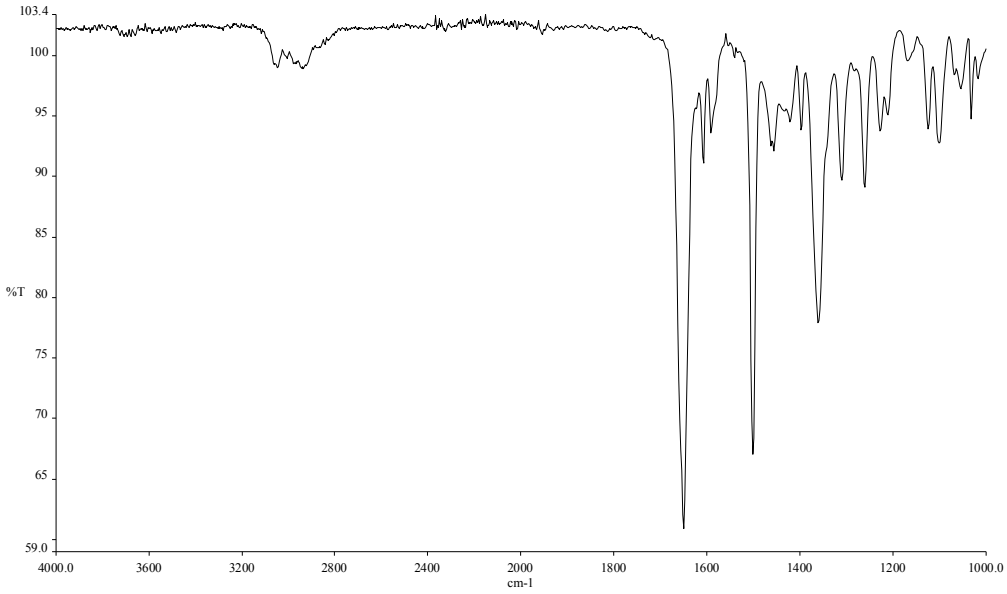

Figure A5.43 Infrared spectrum of compound **5.19**.

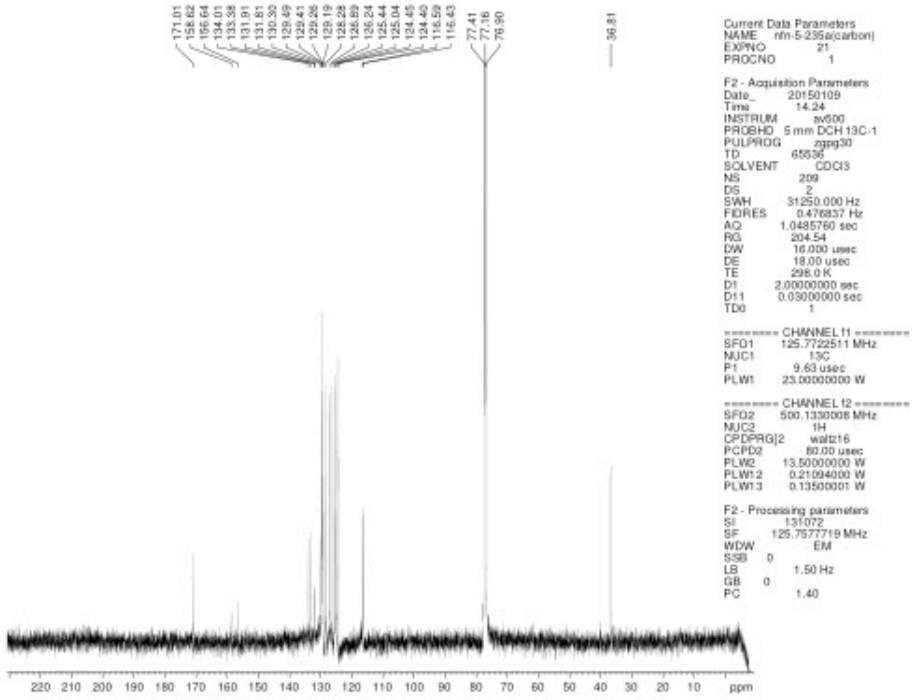

Figure A5.44 ^{13}C NMR (125 MHz, $CDCl_3$) of compound **5.19**.

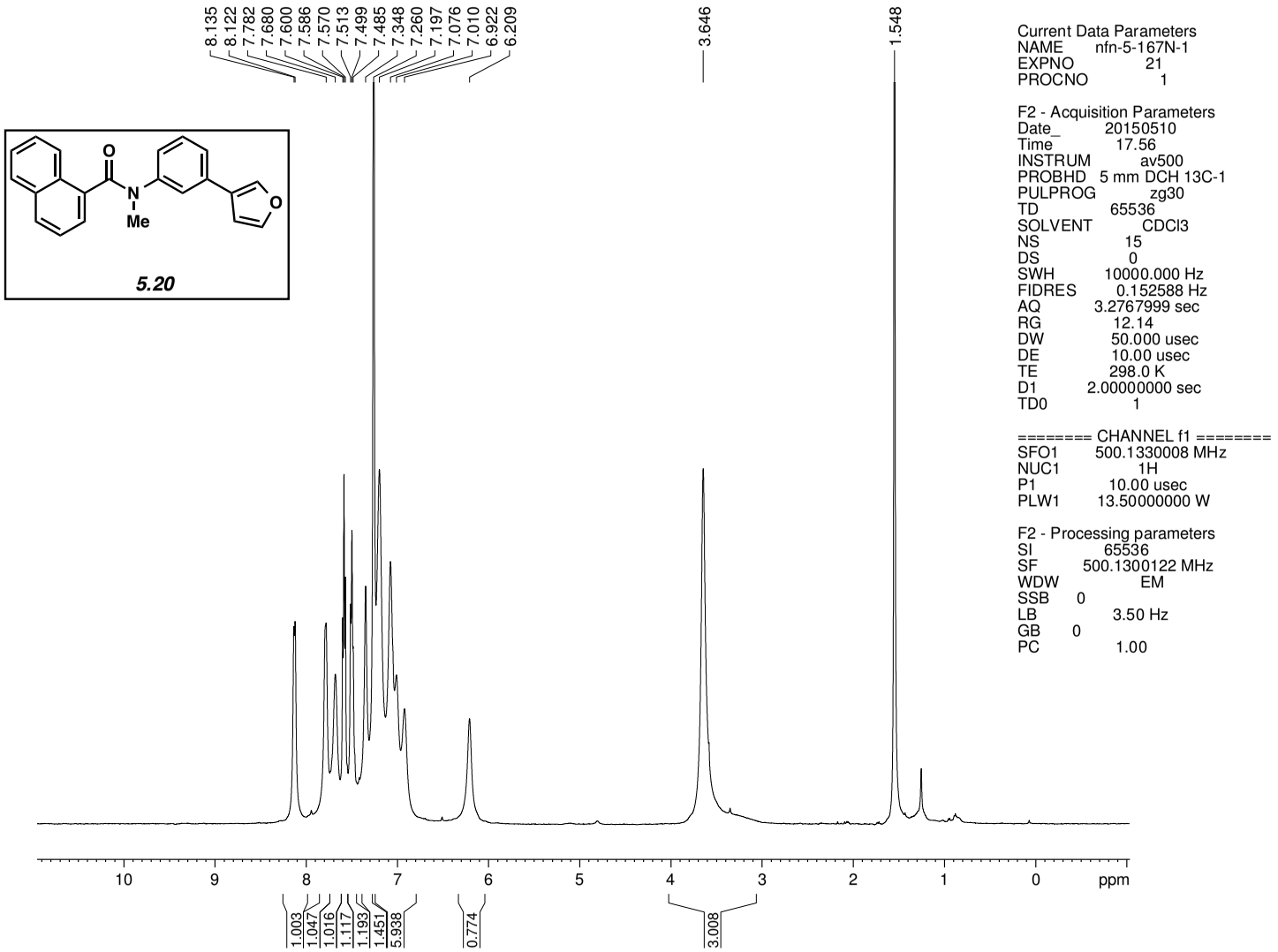

Figure A5.45 ^{1}H NMR (500 MHz, $CDCl_3$) of compound **5.20**.

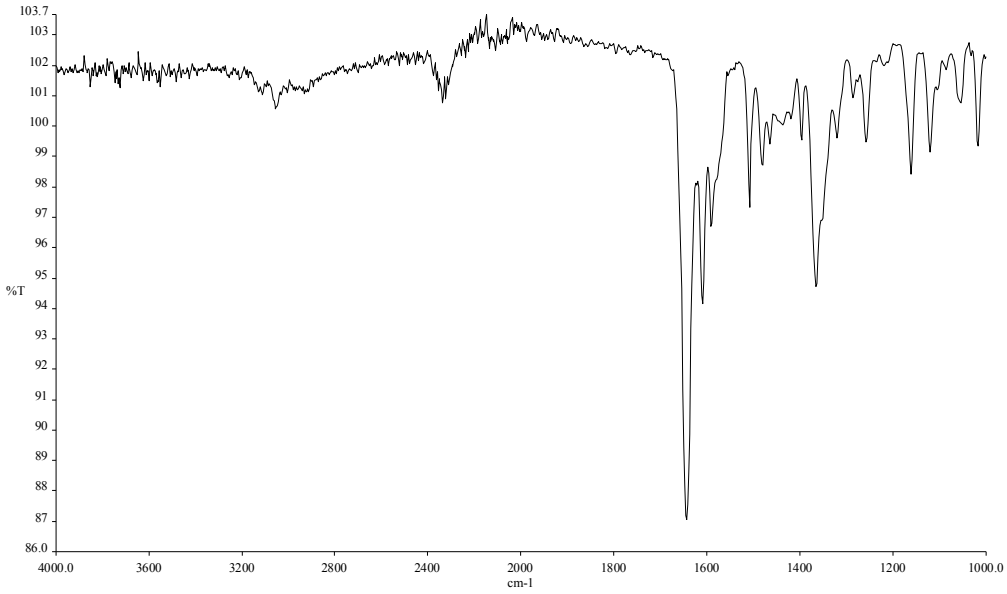

Figure A5.46 Infrared spectrum of compound **5.20**.

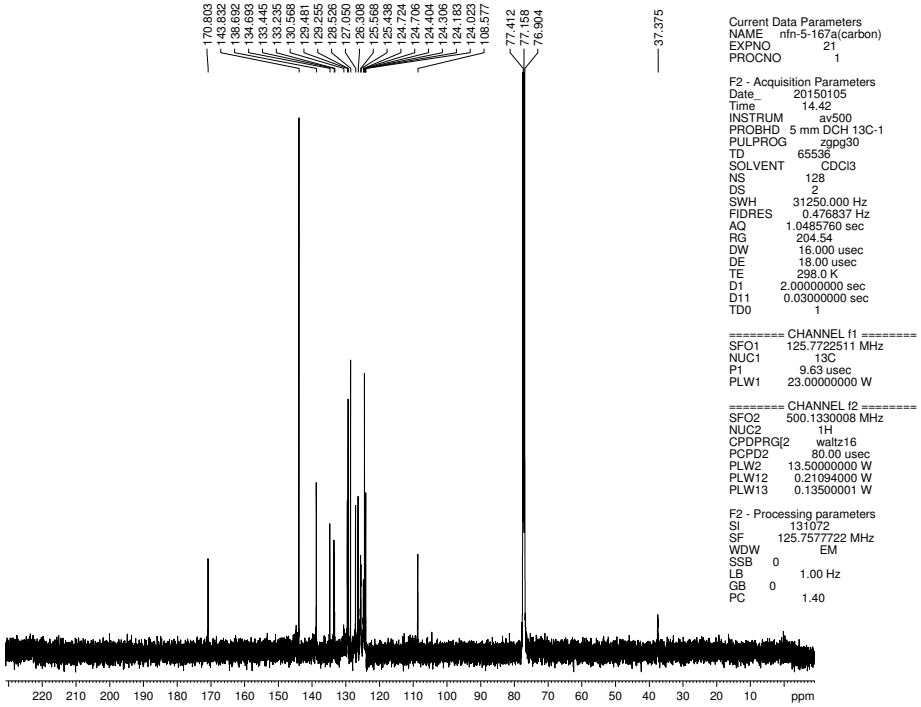

Figure A5.47 ^{13}C NMR (125 MHz, $CDCl_3$) of compound **5.20**.

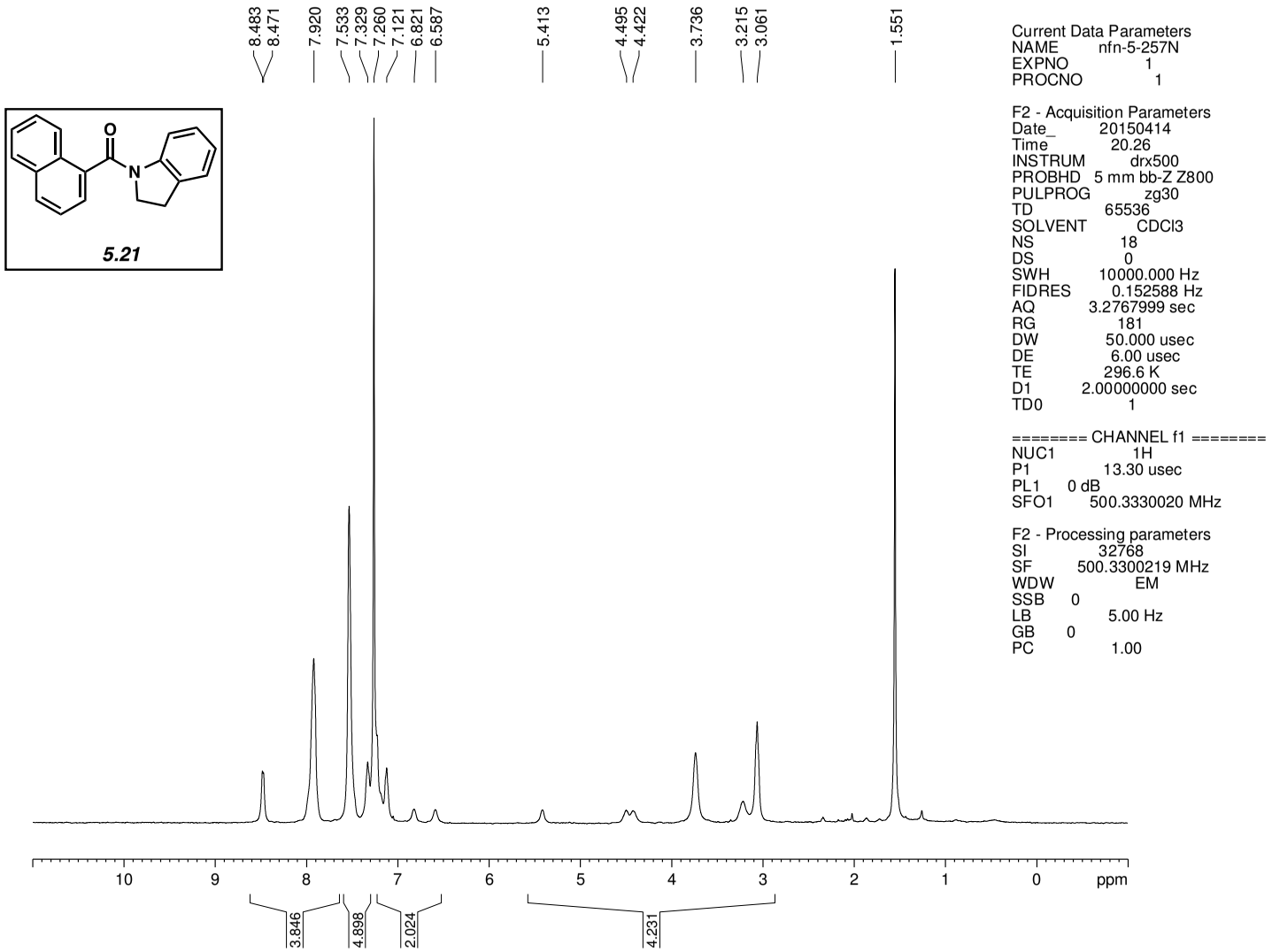

Figure A5.48 ^{1}H NMR (500 MHz, $CDCl_3$) of compound **5.21**.

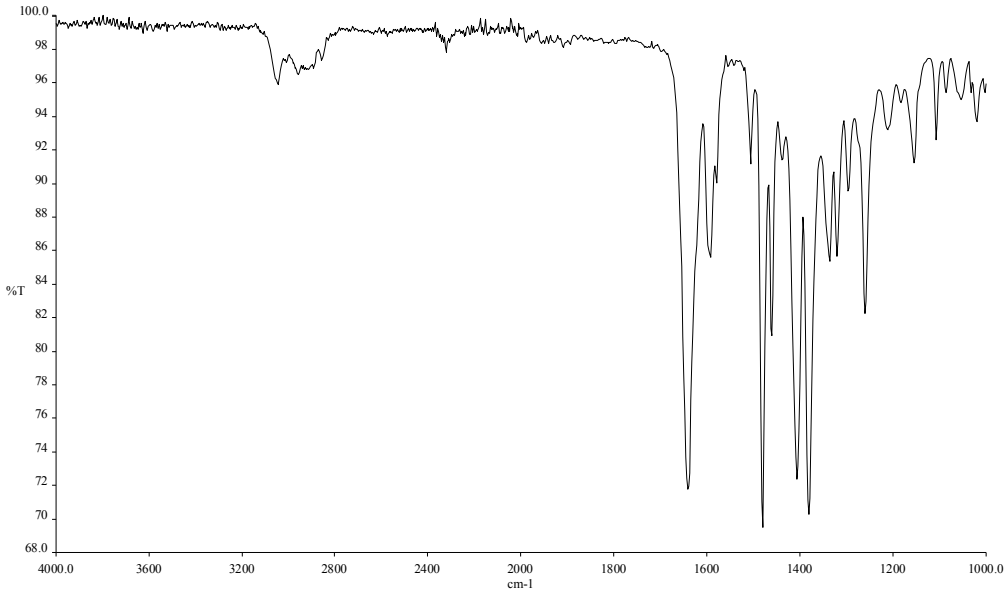

Figure A5.49 Infrared spectrum of compound **5.21**.

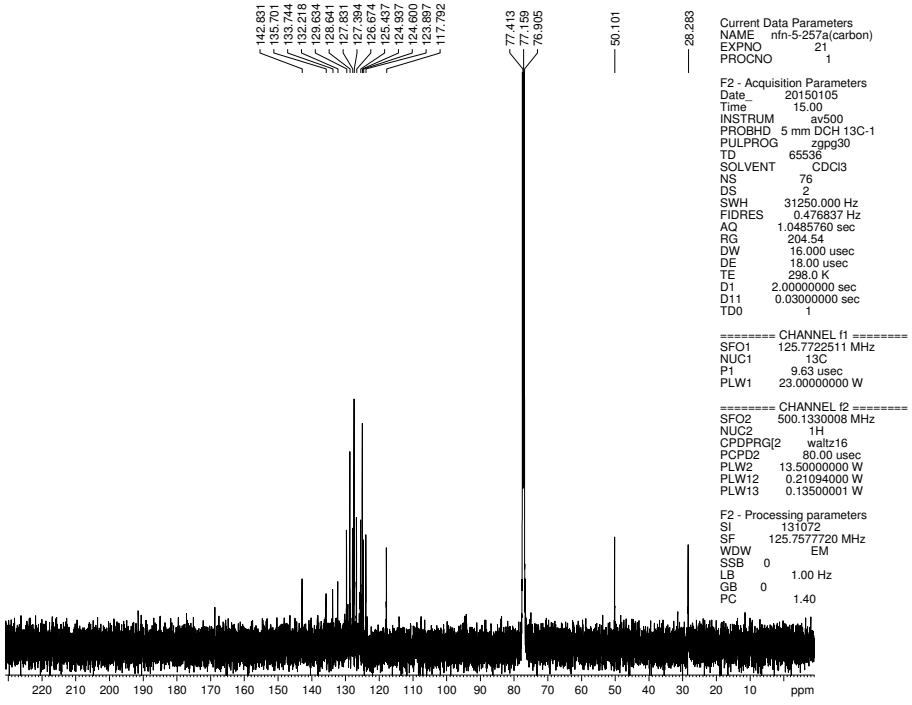

Figure A5.50 ^{13}C NMR (125 MHz, $CDCl_3$) of compound **5.21**.

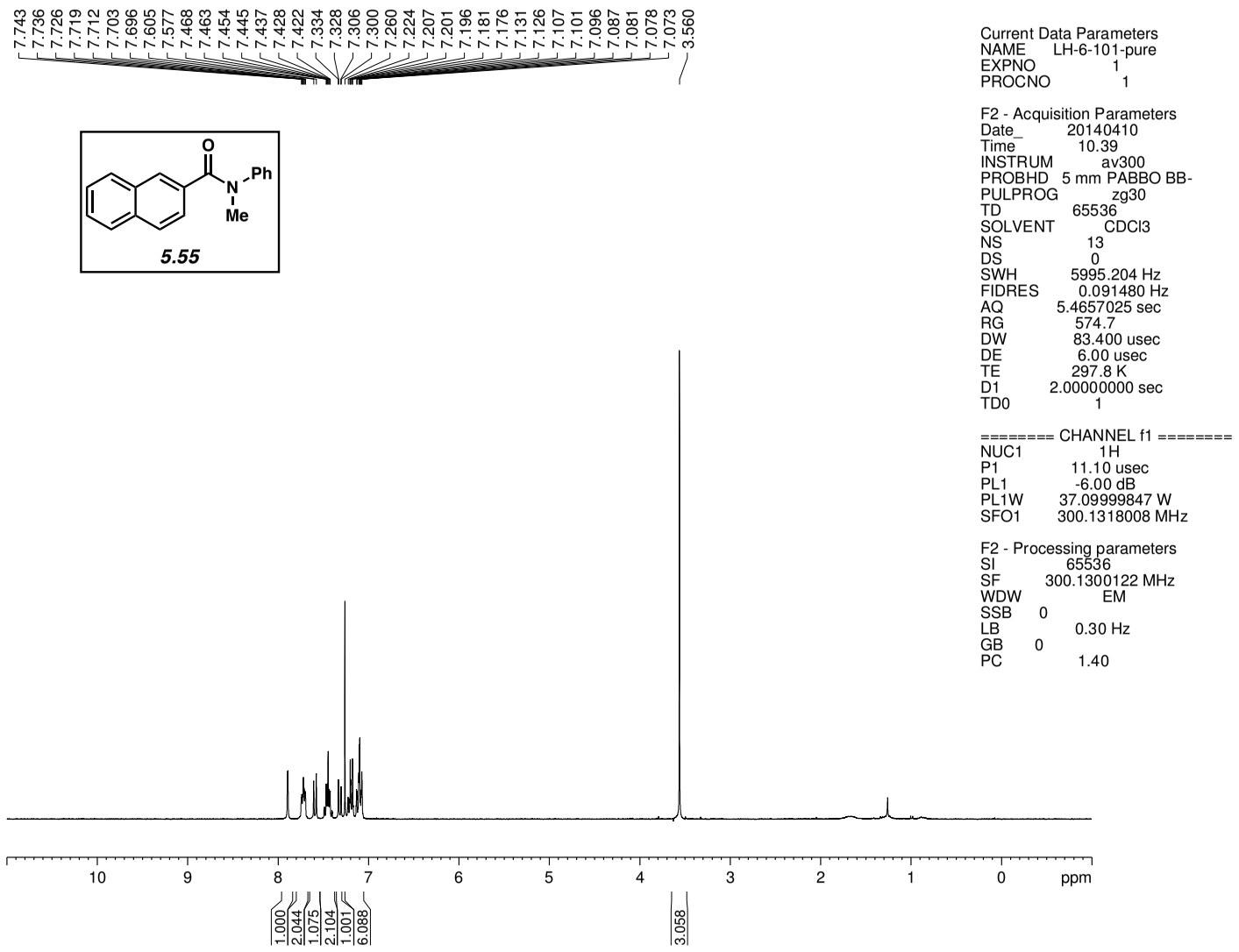

Figure A5.51 ^{1}H NMR (500 MHz, $CDCl_3$) of compound **5.55**.

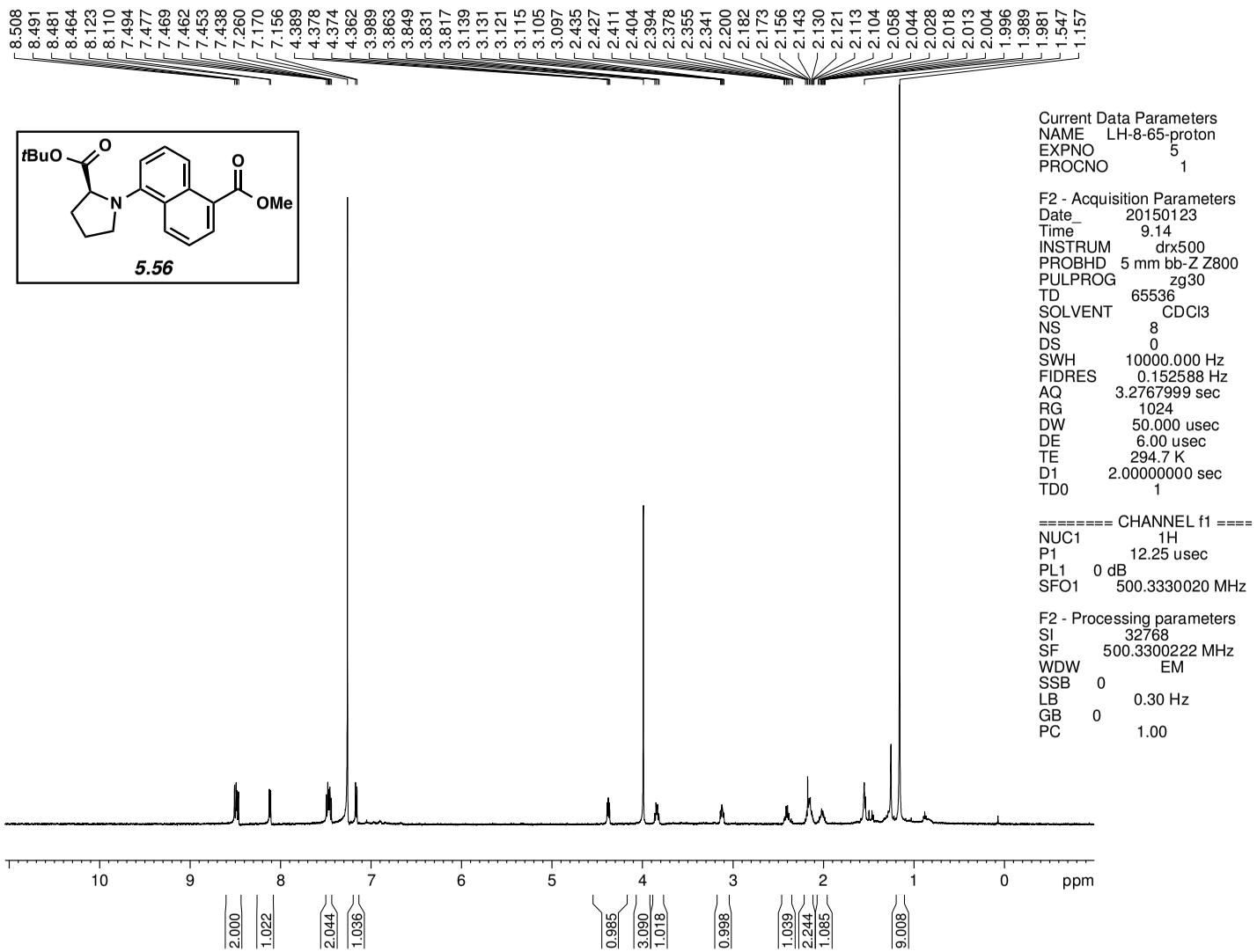

Figure A5.52 ^{1}H NMR (500 MHz, $CDCl_3$) of compound **5.56**.

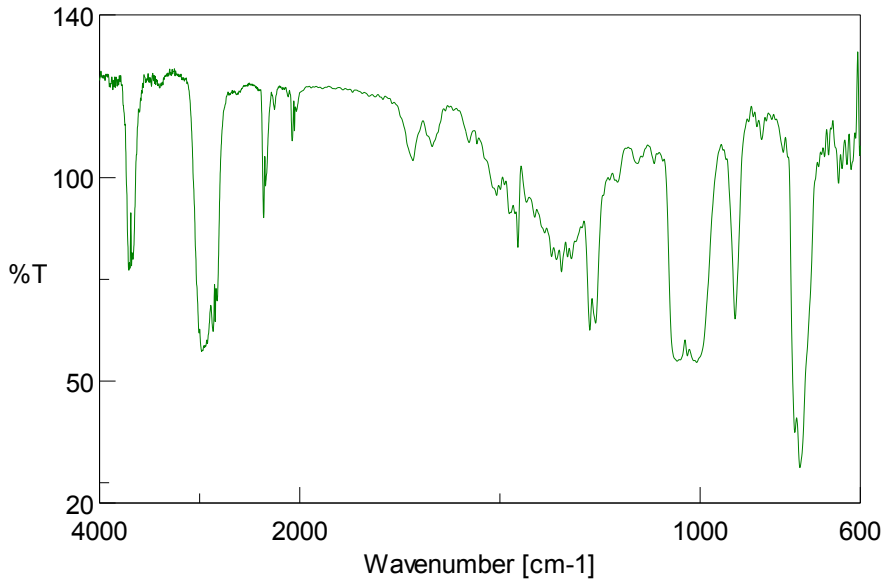

Figure A5.53 Infrared spectrum of compound **5.56**.

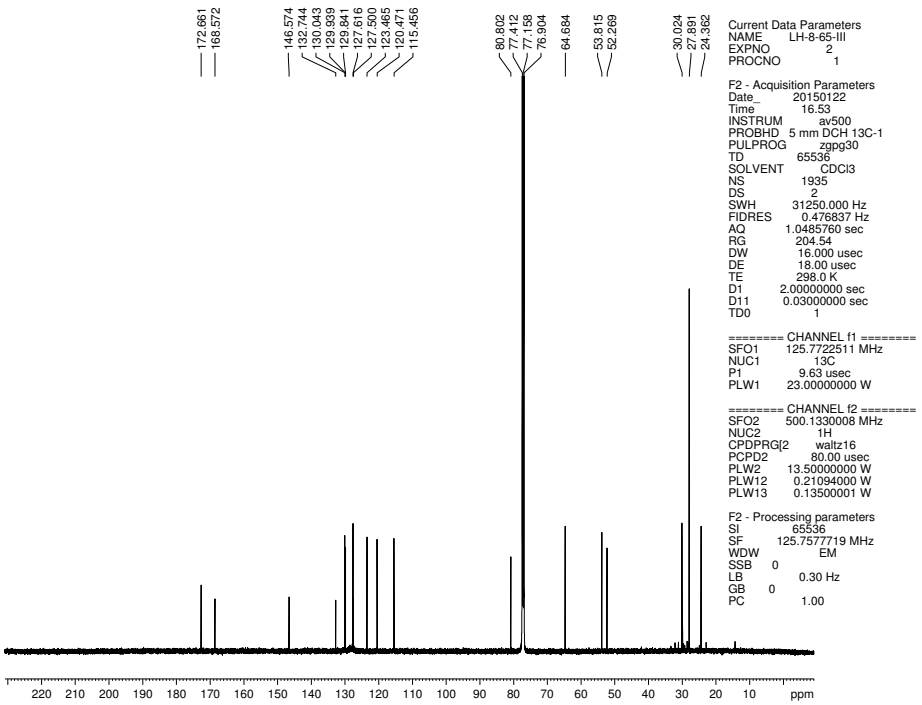

Figure A5.54 ^{13}C NMR (125 MHz, $CDCl_3$) of compound **5.56**.

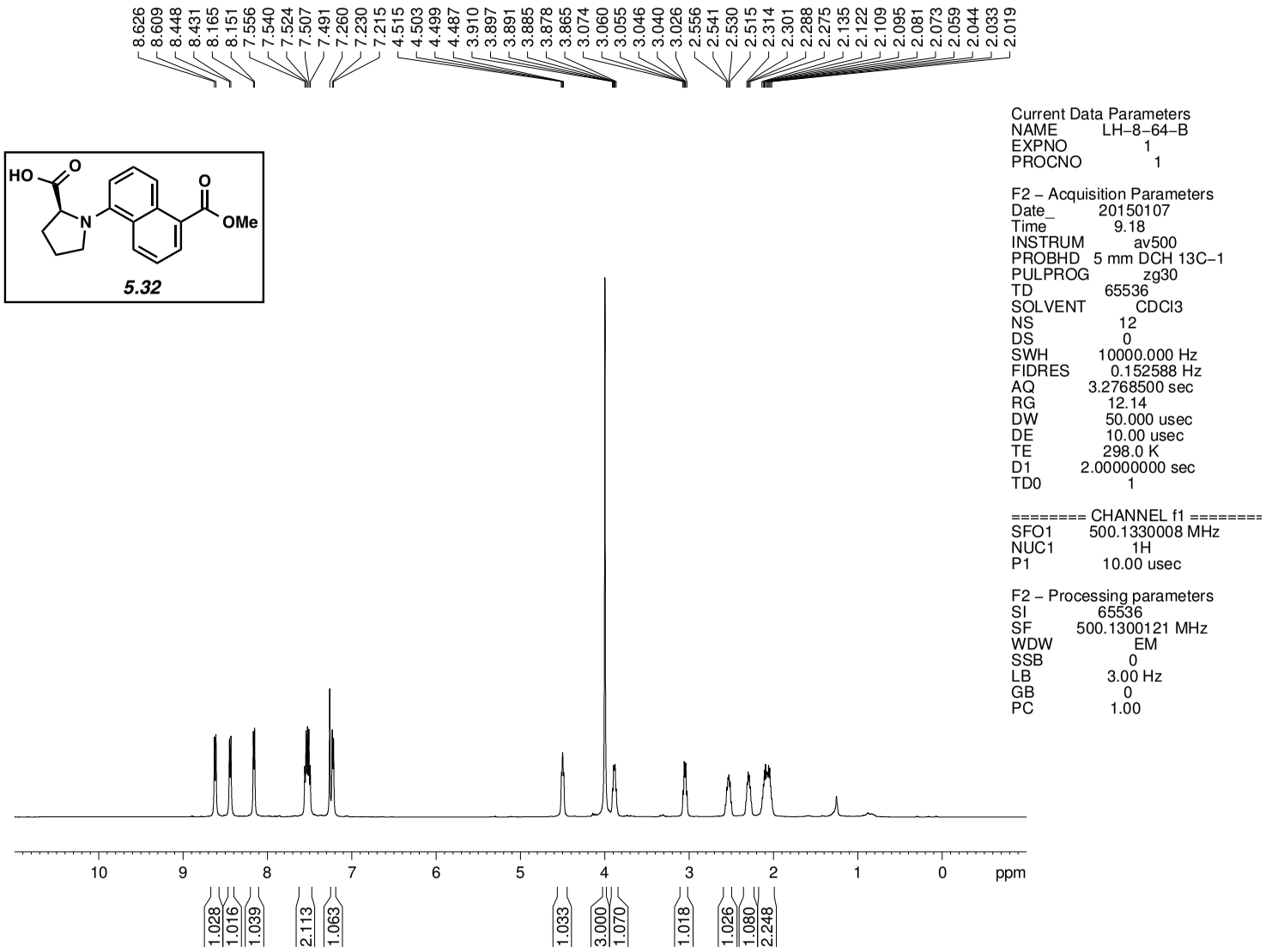

Figure A5.55 ^{1}H NMR (500 MHz, $CDCl_3$) of compound **5.32**.

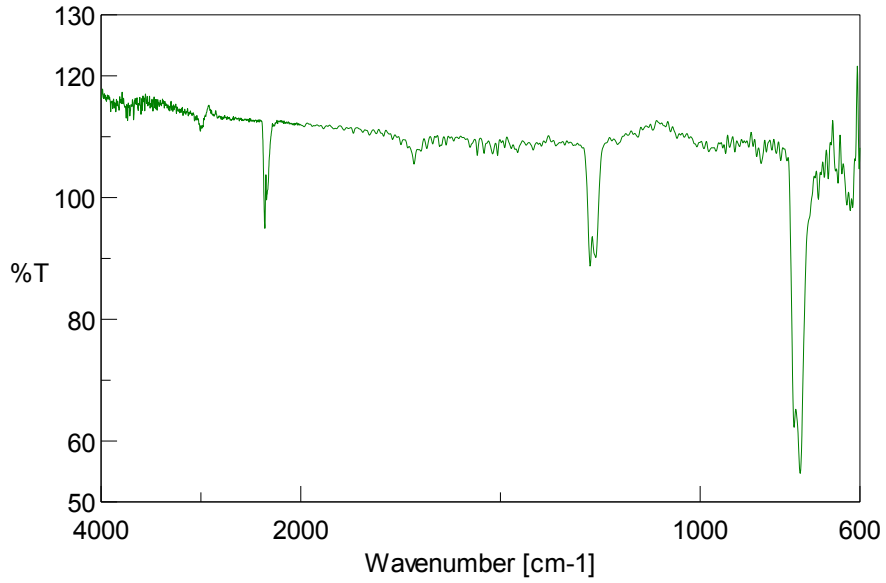

Figure A5.56 Infrared spectrum of compound **5.32**.

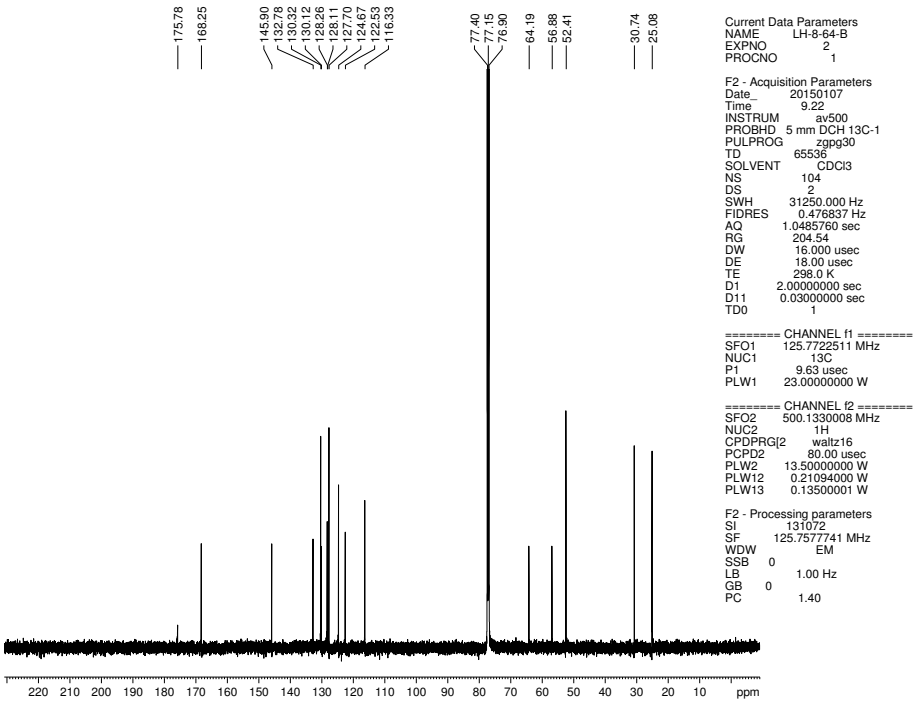

Figure A5.57 ^{13}C NMR (125 MHz, $CDCl_3$) of compound **5.32**.

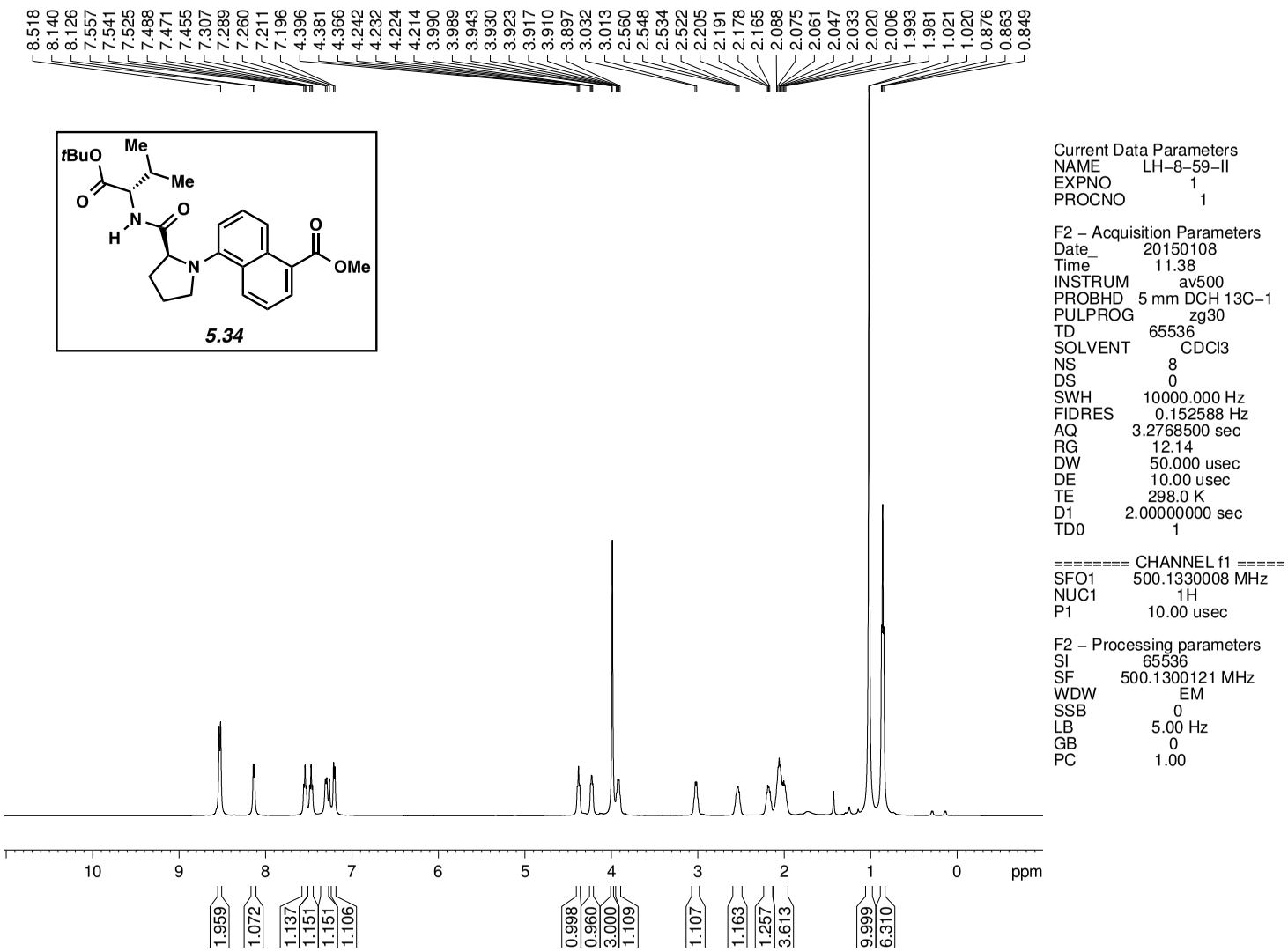

Figure A5.58 ^{1}H NMR (500 MHz, $CDCl_3$) of compound **5.34**.

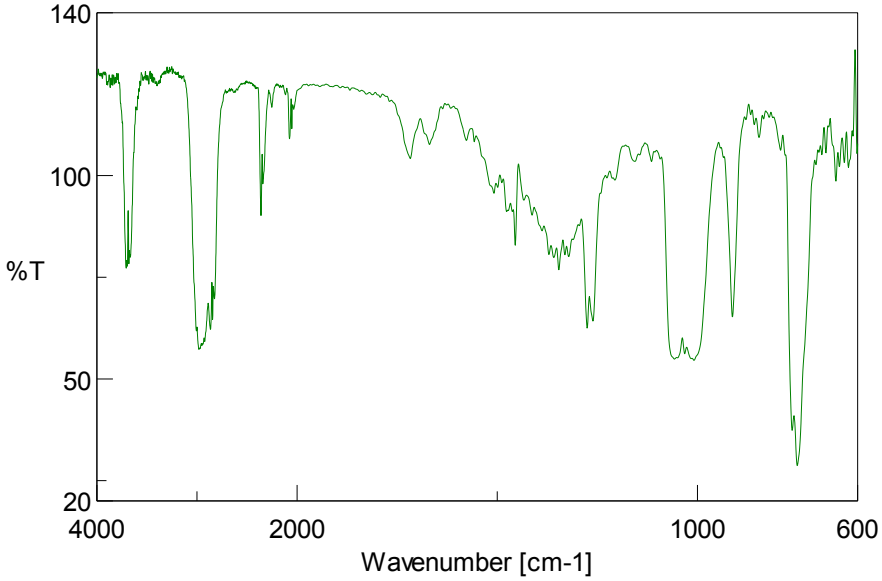

Figure A5.59 Infrared spectrum of compound **5.34**.

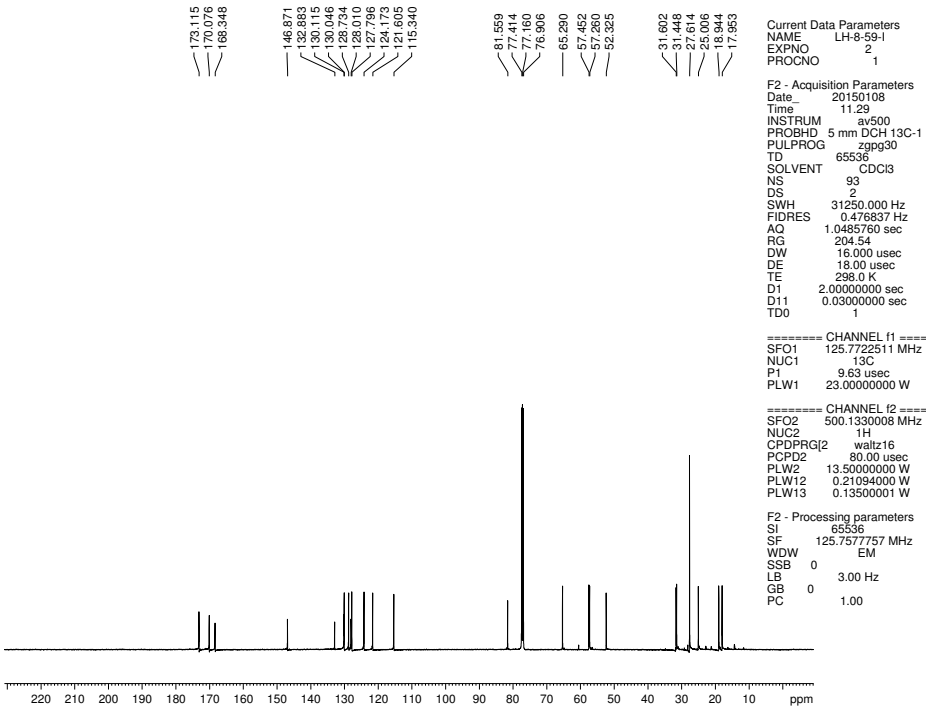

Figure A5.60 ^{13}C NMR (125 MHz, $CDCl_3$) of compound **5.34.**

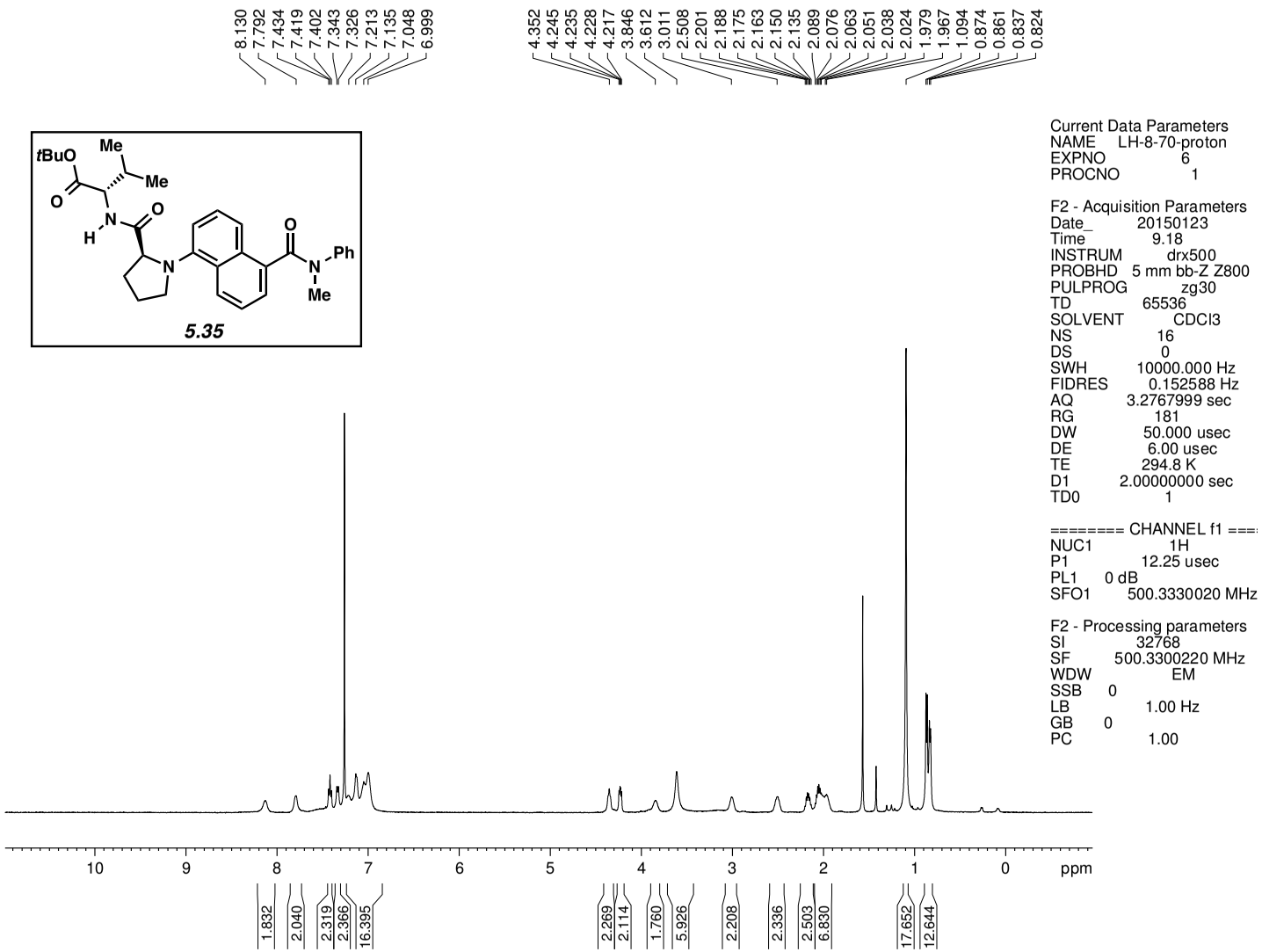

Figure A5.61 ^{1}H NMR (500 MHz, $CDCl_3$) of compound **5.35**.

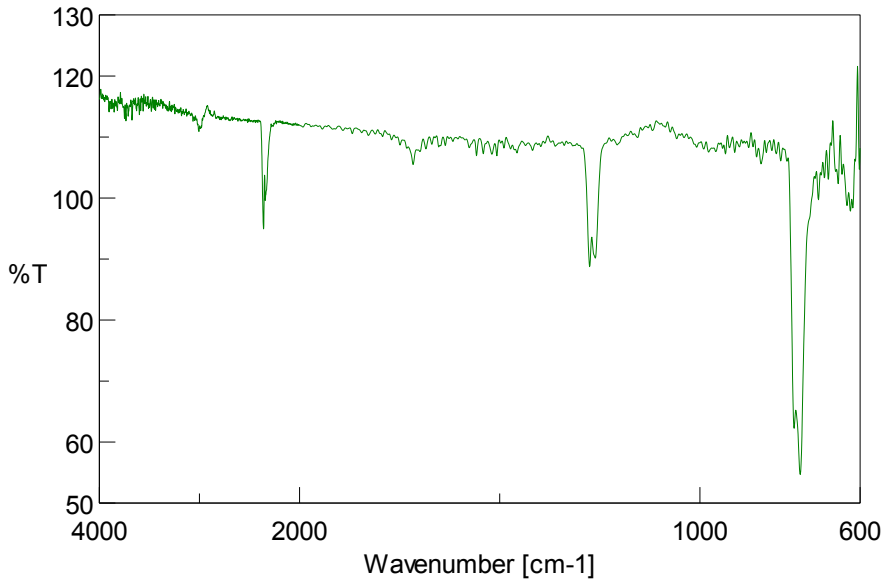

Figure A5.62 Infrared spectrum of compound **5.35**.

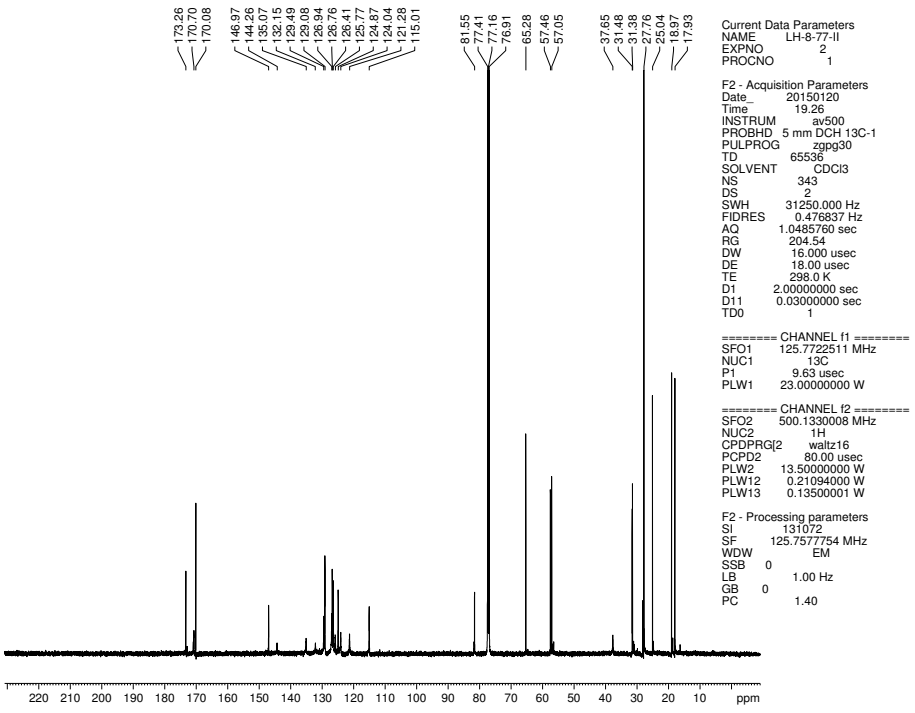

Figure A5.63 ^{13}C NMR (125 MHz, $CDCl_3$) of compound **5.35.**

5.10. Notes and References

[1] (a) Jiang, L.; Buchwald, S. L. In *Metal-Catalyzed Cross-Coupling Reactions*, 2nd ed.; Meijere, A.; Diederich, F., Eds.; Wiley-VCH: Weinheim, 2004; pp 699–760. (b) Shen, H. C. In *Application of Transition Metal Catalysis in Drug Discovery and Development: An Industrial Perspective*;. Crawley, M. L.; Trost, B. M., Eds.; John Wiley & Sons, Inc.: Hoboken, NJ, 2012; pp 25–96.

[2] (a) Tasker, S. Z.; Standley, E. A.; Jamison, T. F. *Nature* **2014**, *509*, 299–309. (b) Mesganaw, T.; Garg, N. K. *Org. Process Res. Dev.* **2013**, *17*, 29–39. (c) Rosen, B. M.; Quasdorf, K. W.; Wilson, D. A.; Zhang, N.; Resmerita, A.-M.; Garg, N. K.; Percec, V. *Chem. Rev.* **2011**, *111*, 1346–1416. (d) Li, B.-J.; Yu, D.-G.; Sun, C.-L.; Shi, Z.-J. *Chem. Eur. J.* **2011**, *17*, 1728–1759.

[3] For initial studies, see: (a) Guan, B.-T.; Wang, Y.; Li, B.-J.; Yu, D.-G.; Shi, Z.-J. *J. Am. Chem. Soc.* **2008**, *130*, 14468–14470. (b) Quasdorf, K. W.; Tian, X.; Garg, N. K. *J. Am. Chem. Soc.* **2008**, *130*, 14422–14423.

[4] Yamamoto, T.; Ishizu, J.; Kohara, T.; Komiya, S.; Yamamoto, A. *J. Am. Chem. Soc.* **1980**, *102*, 3758–3764.

[5] (a) Amaike, K.; Muto, K.; Yamaguchi, J.; Itami, K. *J. Am. Chem. Soc.* **2012**, *134*, 13573–13576. (b) Xu, H.; Muto, K.; Yamaguchi, J.; Zhao, C.; Itami, K.; Musaev, D. G. *J. Am. Chem. Soc.* **2014**, *136*, 14834–14844. (c) Muto, K.; Yamaguchi, J.; Musaev, D. G.; Itami, K. *Nature Commun.* **2015**, 6, 7508–7515.

[6] Tatamidani, H.; Kakiuchi, F.; Chatani, N. *Org. Lett.* **2004**, *6*, 3597–3599.

[7] For a review of amides, see: A. Greenberg, C. M. Breneman, J. F. Liebman, eds. *The Amide Linkage: Structural Significance in Chemistry, Biochemistry, and Materials Science*; Wiley-VCH, 2000.

[8] For reviews regarding amide formation using catalysis, see: (a) Allen, C. L.; Williams, J. M. J. *Chem. Soc. Rev.* **2011**, *40*, 3405–3415. (b) Pattabiraman, V. R.; Bode, J. W. *Nature* **2011**, *480*, 471–479.

[9] The conversion of carboxylic acids to amides is used commonly, but relies on the use of stoichiometric coupling agents that generate waste. Alternatives have been highly sought after as described in the following select examples: (a) Gunanathan, C.; Ben-David, Y.; Milstein, D. *Science* **2007**, *317*, 790–792. (b) Bode, J. W.; Sohn, S. S. *J. Am. Chem. Soc.* **2007**, *129*, 13798–13799. (c) Vora, H. U.; Rovis, T. *J. Am. Chem. Soc.* **2007**, *129*, 13796–13797. (d) Nordstrøm, L. U.; Vogt, H.; Madsen, R. *J. Am. Chem. Soc.* **2008**, *130*, 17672–17673. (e) Al-Zoubi, R. M.; Marion, O.; Hall, D. G. *Angew. Chem. Int. Ed.* **2008**, *47*, 2876–2879.

[10] Hie, L.; Fine Nathel, N. F.; Shah, T. K.; Baker, E. L.; Hong, X.; Yang, Y.-F.; Liu, P.; Houk, K. N.; Garg, N. K. *Nature* **2015**, *524*, 79–83.

[11] As shown in Figure 5.6, theory predicts that substrate **5.5** should prove most fruitful.

[12] On gram-scale, this coupling could be performed with 2.5 mol% of Ni to give amide **5.7** in 50% yield.

[13] The use of other ligands (e.g., mono- and bidentate phosphines, bidentate pyridyl, pybox, and many other *N*-heterocyclic carbenes) in place of SIPr also led to no reaction or low conversions. IPr, however, can be used in place of SIPr to give comparable yields of products.

[14] The mass balance in most reactions is unreacted starting material.

[15] (a) Wisniewska, H. M.; Swift, E. C.; Jarvo, E. R. *J. Am. Chem. Soc.* **2013**, *135*, 9083–9090. (b)

Zhou, Q.; Srinivas, H. D.; Dasgupta, S.; Watson, M. P. *J. Am. Chem. Soc.* **2013**, *135*, 3307–3310. (c) Taylor, B. L. H.; Harris, M. R.; Jarvo, E. R. *Angew. Chem. Int. Ed.* **2012**, *51*, 7790–7793. (d) Yu, D.-G.; Shi, Z.-J. *Angew. Chem. Int. Ed.* **2011**, *50*, 7097–7100. (e) Yu, D. G.; Li, B.-J.; Zheng, S.-F.; Guan, B.-T.; Wang, B.-Q.; Shi, Z.-J. *Angew. Chem. Int. Ed.* **2010**, *49*, 4566–4570. (f) Tobisu, M.; Shimasaki, T.; Chatani, N. *Angew. Chem. Int. Ed.* **2008**, *47*, 4866–4869.

[16] The favorable reactivity seen in π-extended systems may be related to pre-complexation of the nickel catalyst, as well as to the thermodynamic factors discussed here.

[17] The non-catalyzed reaction of anilines with ester **5.5** is sluggish and is not observed under our reaction conditions.

[18] For computational studies of nickel-catalyzed decarbonylative couplings of esters, see refs 5b and 5c and the following: (a) Hong, X.; Liang, Y.; Houk, K. N. *J. Am. Chem. Soc.* **2014**, *136*, 2017–2025. (b) Li, Z.; Zhang, S.-L.; Fu, Y.; Guo, Q.-X.; Liu, L. *J. Am. Chem. Soc.* **2009**, *131*, 8815–8823. (c) Lu, Q.; Yu, H.; Fu, Y. *J. Am. Chem. Soc.* **2014**, *136*, 8252–8260.

[19] Related ligand exchange processes presumably take place in the nickel-catalyzed amination of methyl ethers; see: Tobisu, M.; Yasutome, A.; Yamaka, K.; Shimasaki, T.; Chatani, N. *Tetrahedron* **2012**, *68*, 5157–5161.

[20] The variation between the calculated thermoneutral reaction free energy and the observed yields may partially be attributed to differences between the actual experimental conditions and the DFT calculations.

[21] $Al(O\textit{t}Bu)_3$ may also serve to absorb the methanol being generated, thus promoting the forward reaction. The complexation between $Al(OMe)_3$ and methanol was calculated to be exergonic by 11.0 kcal/mol.

[22] Ni-toluene/NHC complex can also be considered as the resting stage of the catalyst; see: Hoshimoto, Y.; Hayashi, Y.; Suzuki, H.; Ohashi, N.; Ogoshi, S. *Organometallics* **2014**, *33*, 1276–1282.

[23] Distortion of bond lengths was also examined, but found to be insignificant in all cases.

[24] The twisting out of planarity has a minimal effect on the amide–$Al(OR)_3$ stability; rather, electron donation from the amide nitrogen is the primary stabilizing factor.

[25] Wolfe, J. P.; Buchwald, S. L. *Tetrahedron Lett*. **1997**, *38*, 6359–6362.

[26] Hirashima, S.-I.; Nobuta, T.; Tada, N.; Miura, T.; Itoh, A. *Org*. *Lett*. **2010**, *12*, 3645–3647.

[27] Bulgarevich, S. B.; Ivanova, N. A.; Movshovich, D. Ya.; Mannschreck, A.; Kiefl, C. *J*. *Mol*. *Struct*. **1994**, *326*, 17–24.

[28] Xiao, T.; Dong, X.; Tang, Y.; Zhou, L. *Adv*. *Synth*. *Cat*. **2012**, *354*, 3195–3199.

[29] Gaul, M.; Kim, A.; Searle, L. L.; Patch, R.l Rentzperis, D.; Xu, G.; Zhu, X. (Janssen Pharmaceutica N. V.) Substituted Phenoxy Thiazolidinediones as Estrogen Related Receptor-Alpha Modulators. U.S. Patent 2,008,109,727, September 12, 2008.

[30] Kisic, A.; Stephan, M.; Mohar, B. *Org*. *Lett*. **2013**, *15*, 1614–1617.

[31] Ushijima, S.; Moriyama, K.; Togo, H. *Tetrahedron* **2012**, *68*, 4701–4709.

[32] Gonzalez, I.; Mosquera, J.; Guerrero, C.; Rodriguez, R.; Cruces, J. *Org*. *Lett*. **2009**, *11*, 1677–1680.

[33] Fang, W.; Deng, Q.; Xu, M.; Tu, T. *Org*. *Lett*. **2013**, *15*, 3678–3681.

[34] Whittaker, A. M.; Dong, V. M. *Angew*. *Chem*. *Int*. *Ed*. **2015**, *54*, 1312–1315.

[35] Fang, W.; Deng, Q.; Xu, M.; Tu, T. *Org*. *Lett*. **2013**, *15*, 3678–3681.

[36] Baroudi, A.; Alicea, J.; Flack, P.; Kirincich, J.; Alabugin, I. *J*. *Org*. *Chem*. **2011**, *76*, 1521–1537.

[37] (a) Becke, A. D. *J. Chem. Phys.* **1993**, *98*, 5648–5652. (b) Lee, C.; Yang W.; Parr, R. G. *Phys. Rev. B* **1988**, *37*, 785–789. (c) Becke, A. D. *J. Chem. Phys.* **1993**, *98*, 1372–1377. (d) Stephens, P. J.; Devlin, F. J.; Chabalowski, C. F.; Frisch, M. J. *J. Phys. Chem.* **1994**, *98*, 1623–1627.

[38] (a) Hay, P. J.; Wadt, W. R. *J. Chem. Phys.* **1985**, *82*, 299–310. (b) Roy, L. E.; Hay, P. J.; Martin, R. L. *J. Chem. Theory Comput.* **2008**, *4*, 1029–1031. (c) Ehlers, A. W.; Böhme, M.; Dapprich, S.; Gobbi, A.; Höllwarth, A.; Jonas, V.; Köhler, K. F.; Stegmann, R.; Veldkamp, A.; Frenking, G. *Chem. Phys. Lett.* **1993**, *208*, 111–114.

[39] (a) Ditchfield, R.; Hehre, W. J.; Pople, J. A. *J. Chem. Phys.* **1971**, *54*, 724–728. (b) Hehre, W. J.; Ditchfield, R.; Pople, J. A. *J. Chem. Phys.* **1971**, *54*, 2257–2261. (c) Hariharan, P. C.; Pople, J. A. *Theor. Chim. Acta.* **1973**, *28*, 213–222.

[40] Zhao, Y.; Truhlar, D. G. *Theor. Chem. Acc.* **2008**, *120*, 215–241.

[41] Marenich, A. V.; Cramer, C. J.; Truhlar, D. G. *J. Phys. Chem. B* **2009**, *113*, 6378–6396.

[42] Hie, L.; Fine Nathel, N. F.; Hong, X.; Yang, Y.-F.; Houk, K. N.; Garg, N. K. *Angew. Chem. Int. Ed.* **2016**, *55*, 2810–2814.

CHAPTER SIX

Construction of Quaternary Stereocenters via Nickel-Catalyzed Heck Cyclizations

Jean-Nicolas Desrosiers, Liana Hie, Heewon Lee, Nelu Grinberg, Nizar Haddad, Nathan K. Yee, Neil K. Garg, and Chris H. Senanayake

Manuscript Submitted

6.1. Abstract

The nickel-catalyzed Heck cyclization for the construction of quaternary stereocenters is reported. This transformation is demonstrated in the synthesis of 3,3-disubstituted oxindoles, which are prevalent motifs seen in numerous biologically active molecules. The methodology possess a wide substrate scope, proceeds in synthetically useful yields, and provides a rare means to construct stereocomplex frameworks using non-precious metal catalysis.

6.2. Introduction

In recent years, there has been tremendous interest in the development of cross-couplings facilitated by non-precious metal catalysis.[1] Reactions catalyzed by nickel, in particular, have been highly sought after. In comparison to palladium, the metal most frequently used in cross-couplings, nickel is significantly more abundant, much less expensive, and also possesses a lower CO_2 footprint.[1] Efforts toward the development of nickel-catalyzed cross-couplings have primarily focused on traditional processes, such as arylation and amination, with further breakthroughs in sp^2–sp^3 couplings[1a] (Figure 6.1A).

Figure 6.1. (a) Common Ni-Catalyzed Couplings. (b) Present Study of Ni-Catalyzed Heck Cyclization for Quaternary Stereocenter Formation.

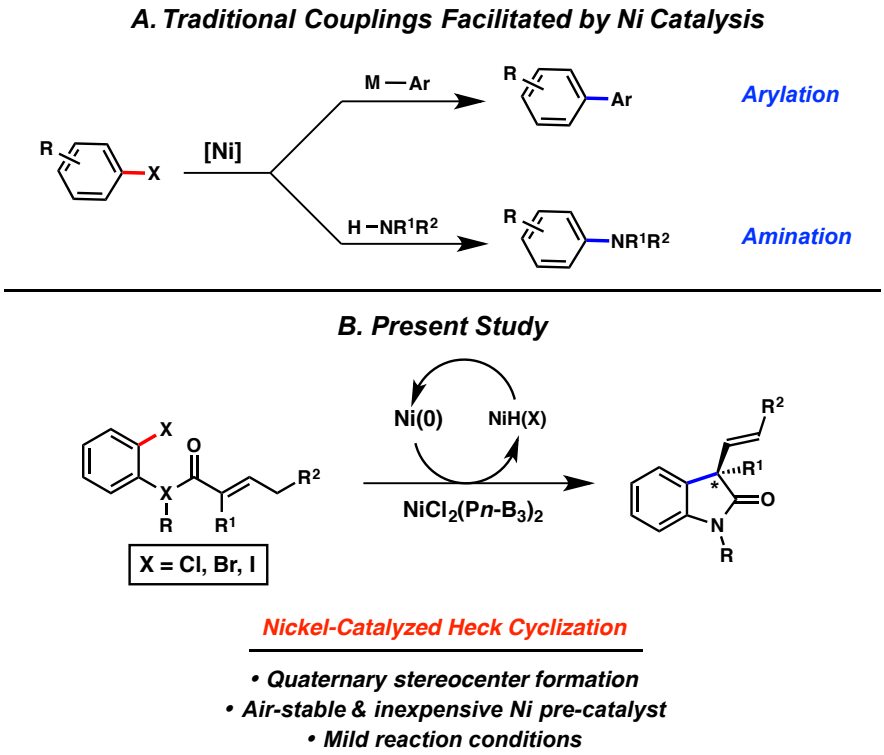

As a part of our efforts to incorporate the use of non-precious metal catalysis in the preparation of active pharmaceutical ingredients, we became interested in the use of nickel catalysis to forge new rings and install quaternary stereocenters. We targeted the Heck cyclization for this task, given the success of the palladium-catalyzed variant.[2,3] Examples of Ni-catalyzed Heck cyclizations have been reported,[4] however, no methodological studies focused on building quaternary stereocenters have been described.[5] In fact, to our knowledge, only a single example of a Ni-catalyzed Heck cyclization to build a quaternary stereocenter is available in the literature, which proceeded in modest yield.[6] Encouraged by the growing demonstrated versatility of nickel,[1] in addition to Jacobsen's aryl cyanation methodology to build quaternary centers,[7] we sought to develop the first nickel-catalyzed Heck cyclization methodology to

construct quaternary stereocenters. We report the success of these efforts, as demonstrated in the synthesis of medicinally privileged 3,3-disubstituted oxindole frameworks[8] (Figure 6.1B). The methodology possesses a wide substrate scope, proceeds in synthetically useful yields, and provides a rare means to construct stereocomplex frameworks using non-precious metal catalysis.

Although analogous to the palladium-catalyzed Heck cyclization, the nickel-catalyzed variant bears less precedent and is complicated by several challenges. First, catalyst regeneration from the nickel (II) hydride species back to Ni(0) is more arduous than in the corresponding palladium-catalyzed system.[9] The nickel (II) hydride resting state species can induce undesired side-reactions, such as over-reduction or isomerization.[10] Second, the β-hydride elimination step for Ni systems have a larger energy barrier compared to palladium systems.[9] The less reactive organo-nickel intermediate can then undergo other transformations, such as protonolysis or dimerization, instead of the productive β-H elimination.[10] In addition to the aforementioned challenges, the nickel-catalyzed Heck reaction for quaternary center formation is presumably difficult, given there is only a single example of such a process in the literature.[6]

6.3. Optimization and Substrate Scope

We selected **6.1** as a substrate for initial testing of the nickel-catalyzed intramolecular Heck reaction[11] for quaternary stereocenter construction and surveyed various bases and reducing agents in the presence of phenanthroline, $NiCl_2$(dme) and DBU (Table 6.1). Preliminary results indicated the base-sensitivity of the starting material (entries 1–3). In these examples, decomposition was observed. The use of carbonate bases, such as K_2CO_3, afforded the desired spiroxindole **6.2** and reduced product **6.3** (entry 4). Also, slight variations of the

nickel/phenanthroline ratio gave non-reproducible results. In order to facilitate the catalyst activation/regeneration and to ensure reproducibility of reaction yields, several external reducing agents[12] were tested. In the presence of those, variying amounts of reduced product **6.3** were observed. When boronic acid derivatives or phenylsilane was used, the spiroxindole **6.2** was not generated (entries 5–7). Triethylsilane provided better conversion, but a large amount of **6.3** was formed (entry 8). Among metallic reductants explored (entry 9–11), manganese was optimal. The combination of manganese and a lower temperature was found to be optimal (entry 12–13).[13]

Table 6.1. Optimization of Reaction Conditions.[a]

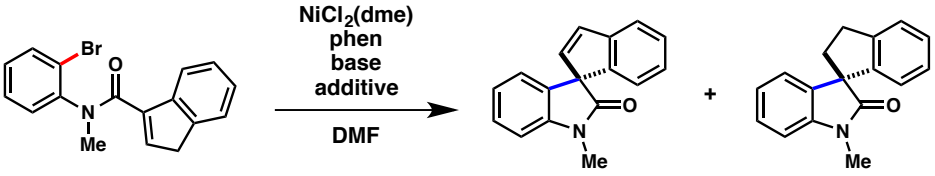

6.1 ***6.2*** ***6.3***

Entry	Base	Additive	Temp (°C)	Yield of 6.2 (%)[b]	Yield of 6.3 (%)[b]
1	DBU	none	120	3	0
2	Et_3N	none	120	0	0
3	KOAc	none	120	0	0
4	K_2CO_3	none	120	10–57	0–15
5	K_2CO_3	Ph–B(OH)$_2$	80	0	0
6	K_2CO_3	Ph–B(pin)	80	0	0
7	K_2CO_3	$PhSiH_3$	80	0	0
8	K_2CO_3	Et_3SiH	80	36	64
9	K_2CO_3	Cr	80	14	0
10	K_2CO_3	Zn	80	53	47
11	K_2CO_3	Mn	80	77	23
12	K_2CO_3	Mn	60	79	12
13	Na_2CO_3	Mn	60	81	6

[a] Reaction conditions: $NiCl_2$(DME)(10 mol%), phen (10 mol%), Additive (3.0 equiv), Base (3.0 equiv), and DMF (0.3 M). [b] Determined by HPLC area %.

An extensive survey of ligands was performed to improve the reaction profile and yields. Selected examples are presented in Figure 6.2. Phenanthroline derivatives were tested, but most of them provided no higher yield than 52% (**L1**–**L7**). Tetramethyl-phenanthroline (**L4**) was the second best ligand of this family and provided spirooxindole **6.2** in 42% yield. The use of the *N*-heterocyclic carbene IPr or SIPr gave poor yields. The desired cyclized product could be obtained in higher yields (entries 6–11) when bis(phosphines) were employed, with the best being dpee (59% yield of **6.2**). The use of mono-phosphine ligands (PPh_3, PCy_3, P*t*-Bu_3, P*n*-Bu_3, PEt_3) demonstrated that electron-rich non-hindered ligands such as P*n*-Bu_3 led to a striking yield improvement to form **6.2** in 90% yield according to ^{1}H NMR assay yield and 85% yield when isolated. Furthermore, it was discovered that the air-stable precatalyst, $NiCl_2$(P*n*-Bu_3)$_2$ could be used in place of $NiCl_2$(dme) and ligand to give **6.2** in a comparable yield.[14]

Figure 6.2. Survey of Ligands.[a]

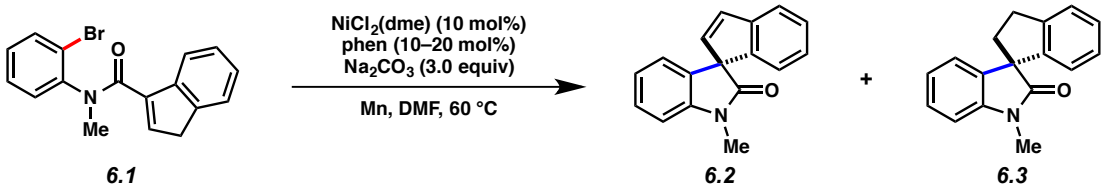

6.1 *6.2* *6.3*

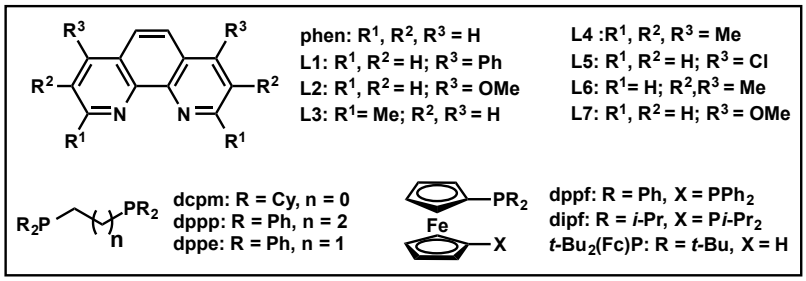

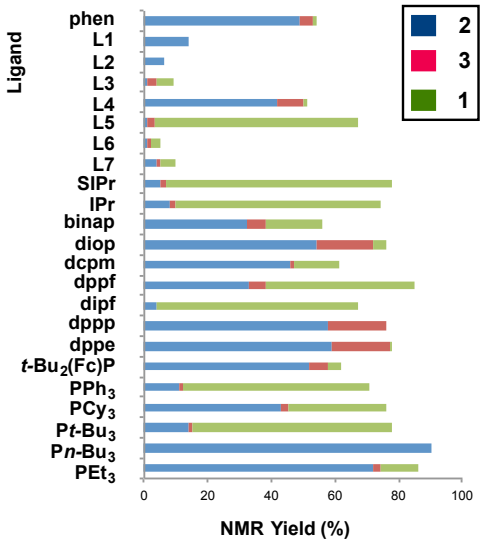

[a] Yields determined by ^{1}H NMR using dimethylfumarate as external standard.

With the optimal conditions in hands,[15] the effects of the electrophile were explored (Figure 6.3). As opposed to the standard palladium-catalyzed system,[3] both aryl bromide **6.1** and chloride **6.4** are competent electrophiles and afforded spirooxindole **6.2** in good yield. However, the cyclization provided either lower yield or no oxindole when iodide **6.5** or methoxide **6.6** was used as the electrophile.

Figure 6.3. Influence of the Source of Aryl Halides.

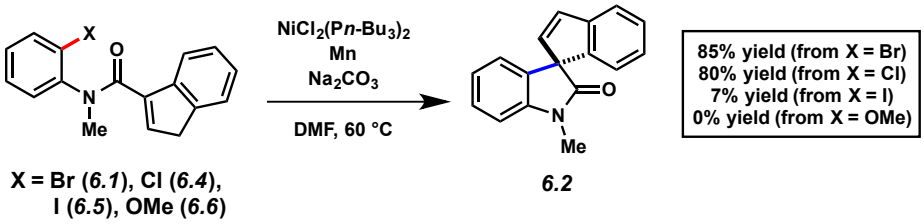

Different substituents on the arene moiety were then tested under the standard reaction conditions (Figure 6.4). Compounds containing electron-donating groups were tolerated as shown by the formation of **6.7** and **6.8** in good yields. Spiroxindoles containing a trifluoromethyl ether (**6.9**) or fluoride (**6.10**), respectively, were also obtained in synthetically useful yields. It should be noted that **6.9** and **6.10** cannot be directly accessed via α-vinylation of oxindoles.

Figure 6.4. Effects of Substituents on the Aryl Ring.[a]

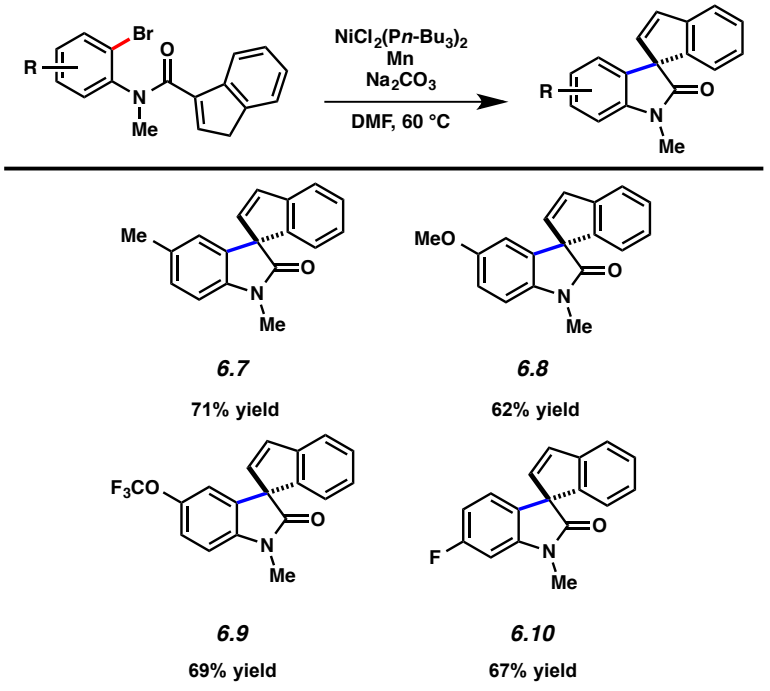

[a] Reaction conditions: substrate (100.0 mg), $NiCl_2(Pn\text{-}Bu_3)_2$ (10 mol%), Mn (3.0 equiv), Na_2CO_3 (3.0 equiv), and DMF (0.3 M) at 60 °C for 12 h. Yields were determined from isolation experiments.

The effect of the alkene stereochemistry on the quaternary center formation was then studied (Figure 6.5). *E*- and Z-Alkenes (**6.11** and **6.12)** afforded oxindole **6.13** in 64 and 66% yield, respectively.

Figure 6.5. Effect of Alkene Geometry.[a]

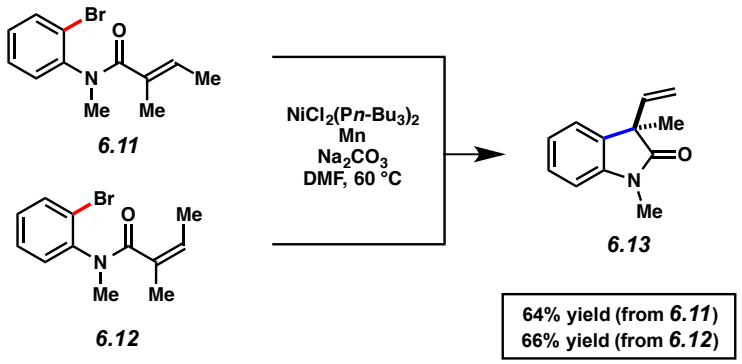

[a] Reaction conditions: substrate (100.0 mg), $NiCl_2(Pn\text{-}Bu_3)_2$ (10 mol%), Mn (3.0 equiv), Na_2CO_3 (3.0 equiv), and DMF (0.3 M) at 60 °C for 12 h. Yields were determined from isolation experiments.

The alkene substitution pattern of the substrate was then examined (Figure 6.6). The chloride variant of substrate **6.12** also provided **6.13** in a comparable yield. When a C6-trifluoromethyl substituent was present, oxindole **6.14** was obtained in 69% yield. High yield was observed for cyclization of the substrate containing a propene side-chain, which gave oxindole **6.15** with exclusive formation of the *E*-alkene. A cyclopentene-derived substrate was also evaluated; intriguingly, this required an iodo-substituted arene in order to generate the desired product **6.16** in 70% yield,[16] while the cyclohexyl based substrate only gave 12% yield of **6.17**. Various protecting groups were also explored under the optimized reaction conditions. A MOM protected aniline gave rise to the desired cyclized product **6.18**. It should be noted that there are only few examples of Ni-catalyzed Heck cyclizations in the presence of basic nitrogens.[17] Additionally, this methodology was found to be compatible with alcohols, nitriles, esters, ketones, and amides via a robustness screening.[18]

Figure 6.6. Evaluation of Alkene Substituents and Protecting Groups.[a]

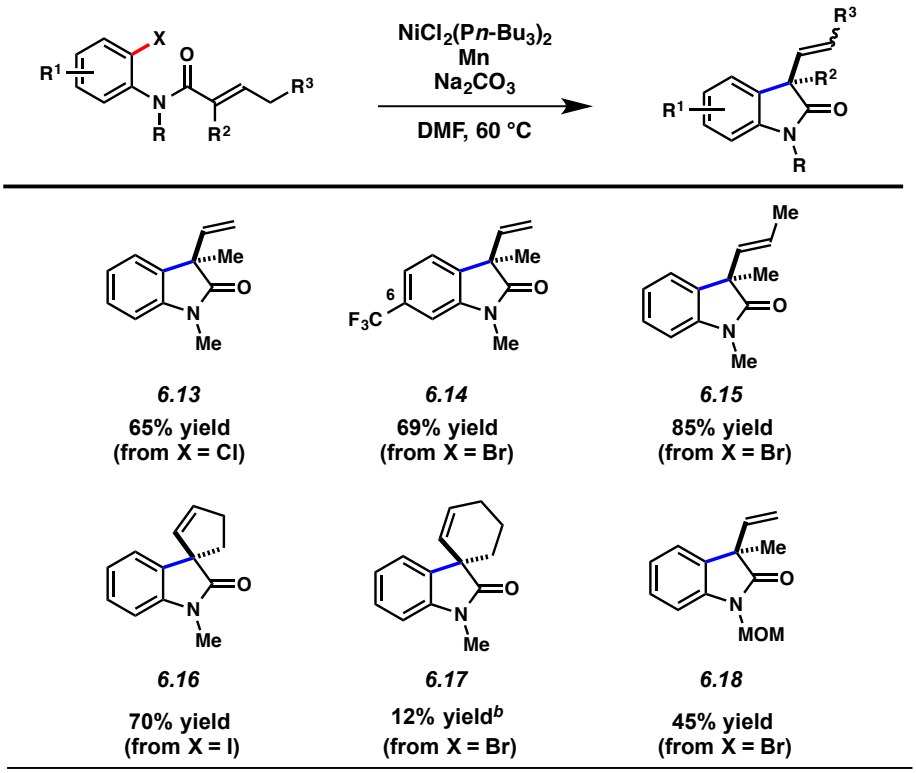

[a] Reaction conditions: substrate (100.0 mg), $NiCl_2(Pn\text{-}Bu_3)_2$ (10 mol%), Mn (3.0 equiv), Na_2CO_3 (3.0 equiv), and DMF (0.3 M) at 60 °C for 12 h. Yields were determined from isolation experiments.

The asymmetric version of the nickel-catalyzed Heck cyclization was also tested. Preliminary results indicated that treatment of substrate **6.1** with ligand catASium KtB containing a binaphthyl chiral backbone could afford enantioenriched oxindole **6.2** in 37% yield with a 70:30 er (Figure 6.7). Despite the modest yield, this results suggests an enantioselective variant may be accessible with further optimization.

Figure 6.7. Preliminary Data on the Asymmetric Variant.

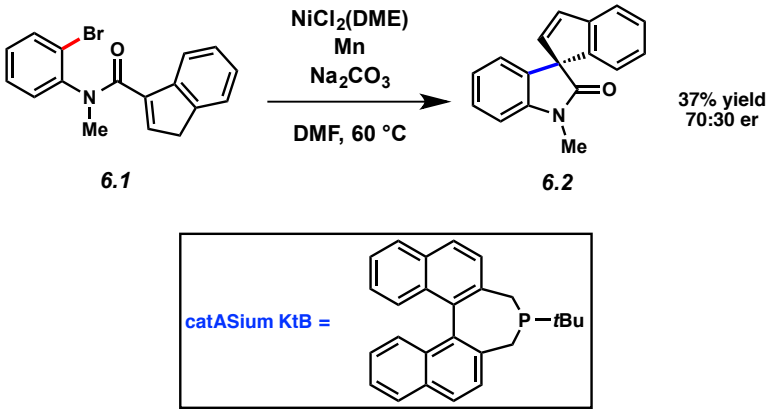

6.4. Conclusion

In conclusion, we have reported a methodological study on the first nickel-catalyzed intramolecular Heck reaction for the synthesis of quaternary stereocenters. The transformation was achieved in the context of 3,3-disubstituted oxindole synthesis and gives products in synthetically useful yields. The use of an air-stable nickel precatalyst provides additional cost-efficiency for this methodology while being experimentally convenient. This method demonstrates the ability of Ni catalysis to construct stereochemically complex polycyclic frameworks. Optimization of the enantioselective version of this transformation using chiral ligands will be the subject of future investigations.

6.5. Experimental Section

6.5.1. Materials and Methods

Unless stated otherwise, reactions were conducted under an atmosphere of nitrogen using standard Schlenk or glove box techniques. Commercially obtained reagents were used as received. 2-Bromo-*N*-methylaniline, 2-chloro-*N*-methylaniline and 2-methoxy-*N*-methylaniline

were purchased from Sigma-Aldrich. 2-Bromo-*N*-methyl-4-(trifluoromethoxy)aniline is commercially available from Oakwood. 2-Bromo-5-fluoro-*N*-methylaniline hydrochloride is commercially available from Combi-Blocks, Inc. (*E*)-2-methylpent-2-enoic acid and 1*H*-indene-3-carboxylic acid were purchased from Sigma-Aldrich. Tiglic acid was purchased from Fluka. Angelic acid was purchased from TCI America. $NiCl_2(P\textit{n}\text{-}Bu_3)_2$, Mn, and Na_2CO_3 were purchased from Sigma-Aldrich. DMF was purchased from Sigma-Aldrich in a Sure-Seal bottle and degassed by sparging with nitrogen prior to use. Aluminium oxide, neutral, Brockmann I (50-200 μm, 60 Å) was purchased from Acros. ^{1}H NMR spectra were recorded on Bruker spectrometers (at 400 and 500 MHz) and are reported relative to residual solvent signals. Data for ^{1}H NMR spectra are reported as follows: chemical shift (δ ppm), multiplicity, coupling constant (Hz), integration and are referenced to the residual solvent peak 7.26 ppm for $CDCl_3$. Data for ^{13}C NMR are reported in terms of chemical shift (at 100 and 125 MHz) and are referenced to the residual solvent peak 77.15 for $CDCl_3$. IR spectra were recorded on a Thermo Nicolet 3700 FT-IR spectrometer and are reported in terms of frequency absorption (cm^{-1}). High resolution mass spectral data were acquired using an Agilent LC/MSD TOF (time-of-flight) mass spectrometer in an electrospray positive ionization mode *via* flow injection. Low-resolution mass spectra were obtained using Waters Xevo TDQ attached to a Waters Acquity UPLC**.** TLC analysis was performed using hexanes/EtOAc as the eluent and visualized using UV light. Flash chromatography was accomplished using a Teledyne CombiFlash Rf (visualizing spirooxindoles at 254 nm) with Silicycle SiliaSep Flash Cartridges (60Å porosity, 40-63 μm).

6.5.2. Experimental Procedure

6.5.2.1. Synthesis of Starting Materials (General Procedure A)

*Representative procedure for the synthesis of substrates **6.1**, **6.4**, **6.6**, **6.24**, **6.26**, **6.28**, and **6.30** (synthesis of bromide **6.1** is used as an example).*

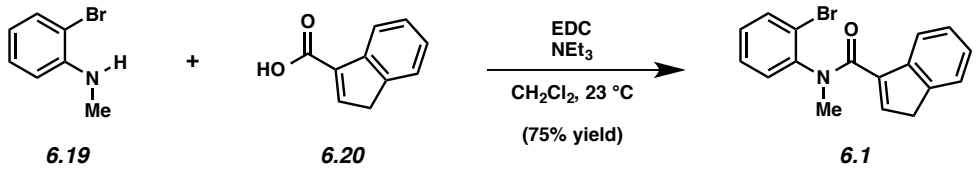

6.19 *6.20* *6.1*

Bromide 6.1 (Table 6.1 & Figures 6.2–6.3). To a solution of 1-ethyl-3-(3-dimethylaminopropyl)carbodiimide (EDC) (5.60 g, 29.1 mmol, 1.5 equiv) in CH_2Cl_2 (65 mL, 0.3 M) was added NEt_3 (4.0 equiv) at 23 °C. To the mixture was then added carboxylic acid **6.20** (3.11 g, 19.4 mmol, 1.0 equiv) and aniline **6.19** (2.5 mL, 21.33 mmol, 1.1 equiv). The resulting heterogeneous mixture was allowed to stir at 23 °C for 12 h and then diluted with CH_2Cl_2 (30 mL). The mixture was then washed with deionized water (30 mL), 1.0 M HCl (30 mL), saturated sodium bicarbonate solution (30 mL), and deionized water (30 mL). The mixture was dried over Na_2SO_4 and the volatiles were removed under reduced pressure. The crude residue was purified via flash chromatography (0 → 25% EtOAc in hexanes) to afford bromide **6.1** as a light orange solid (4.78 g, 75% yield). ^{1}H NMR (500 MHz, $CDCl_3$): δ 7.79–7.77 (m, 1H), 7.57–7.55 (m, 1H), 7.36–7.32 (m, 2H), 7.21 (br s, 3H), 7.11 (br s, 1H), 6.13 (s, 1H), 3.41 (s, 3H), 3.26 (dd, J = 19.0, 24.0, 2H); ^{13}C NMR (125 MHz, $CDCl_3$): δ 166.7, 143.6, 142.7, 138.8, 136.1, 133.7, 129.9, 129.3, 128.6, 126.5, 125.3, 123.5, 123.3, 121.9, 38.7, 36.4; FT-IR (cm^{-1}, neat, ATR): 3067, 2927, 1733, 1641, 1581, 1567, 1475, 1457, 1433, 1416, 1379, 1333, 1299, 1283, 1265, 1131, 1095, 1039, 1027, 963, 804; HRMS-ESI (m/z) $[M+H]^+$ calcd for $C_{17}H_{15}BrNO$, 328.0337; found 328.0305.

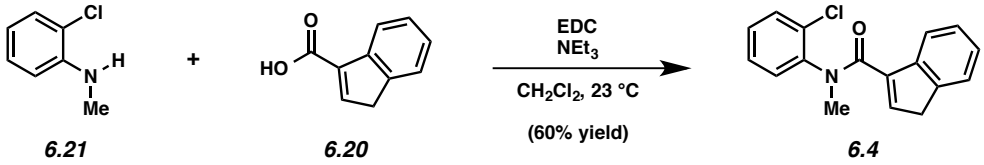

6.21 *6.20* *6.4*

Chloride 6.4 (Figure 6.3). The title compound was prepared according to the General Procedure A from 2-chloro-*N*-methylaniline (**6.21**, 1.0 g, 7.1 mmol, 1.1 equiv) and carboxylic acid **6.20** (1.0 g, 6.4 mmol, 1.0 equiv). Purification by flash chromatography (0 → 25% EtOAc in hexanes) generated chloride **6.4** (1.1 g, 60% yield) as a white solid. ^{1}H NMR (400 MHz, $CDCl_3$): δ 7.76 (d, *J* = 7.5, 1H), 7.38–7.29 (m, 3H), 7.21–7.14 (m, 4H), 6.12 (s, 1H), 3.41 (s, 3H), 3.26 (dd, *J* = 11.0, 24.0, 2H); ^{13}C NMR (100 MHz, $CDCl_3$): δ 166.9, 142.8, 142.1, 138.9, 135.9, 132.8, 130.5, 129.8, 129.1, 127.9, 126.6, 125.4, 123.6, 121.8, 38.6, 36.4; FT-IR (cm^{-1}, neat, ATR): 3064, 3025, 2994, 2928, 2898, 1643, 1606, 1583, 1567, 1479, 1457, 1444, 1414, 1379, 1350, 1332, 1312, 1285, 1268, 1254, 1231, 1202, 1171, 1133, 1098, 1076, 1048, 1031, 1019, 962, 923, 866; HRMS-ESI (m/z) $[M+H]^+$ calcd for $C_{17}H_{15}ClNO$, 284.0842; found 284.0843

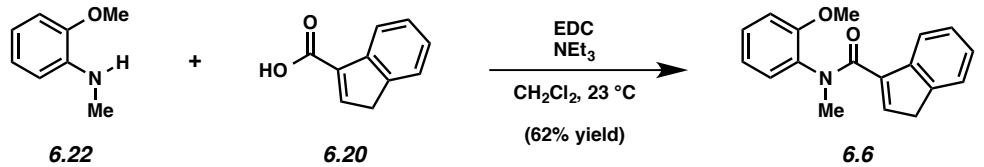

6.22 *6.20* *6.6*

Methoxide 6.6 (Figure 6.3). The title compound was prepared according to the General Procedure A from 2-methoxide-*N*-methylaniline (**6.22**, 0.5 g, 3.6 mmol, 1.1 equiv) and carboxylic acid **6.20** (0.53 g, 3.3 mmol, 1.0 equiv). Purification by flash chromatography (0 → 25% EtOAc in hexanes) generated methoxide **6.6** (0.92 g, 62% yield) as a light orange solid. ^{1}H NMR (400 MHz, $CDCl_3$): δ 7.70 (d, *J* = 7.4, 1H), 7.32–7.29 (m, 2H), 7.16–7.11 (m, 3H), 6.81–6.76 (m, 2H), 6.09 (s, 1H), 3.60 (s, 3H), 3.38 (s, 3H), 3.16 (s, 2H); ^{13}C NMR (100 MHz, $CDCl_3$): δ 167.8, 154.8, 142.9, 142.8, 139.5, 134.9, 133.5, 128.7, 128.6, 126.4, 125.0, 123.4, 121.6, 120.8,

111.7, 55.4, 38.4, 36.4; FT-IR (cm^{-1}, neat, ATR): 3084, 3061, 3003, 2958, 2934, 2905, 1640, 1596, 1583, 1567, 1496, 1457, 1432, 1416, 1379, 1333, 1297, 1271, 1230, 1163, 1119, 1028, 963, 861, 848; HRMS-ESI (m/z) $[M+H]^+$ calcd for $C_{18}H_{18}NO_2$ 280.1338; found 280.1322.

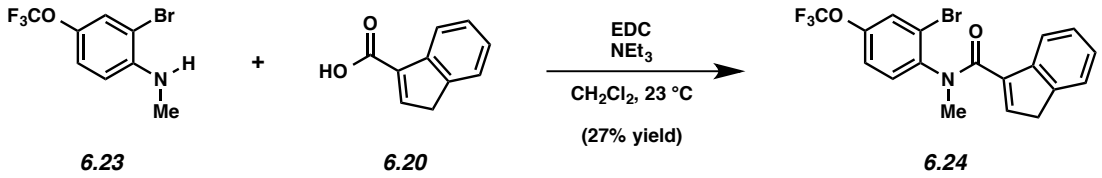

6.23 *6.20* *6.24*

Bromide 6.24. The title compound was prepared according to the General Procedure A from 2-bromo-*N*-methyl-4-(trifluoromethoxy)aniline (**6.23**, 1.8 g, 6.8 mmol, 1.1 equiv) and carboxylic acid **6.20** (1.0 g, 6.2 mmol, 1.0 equiv). Purification by flash chromatography (0 → 25% EtOAc in hexanes) generated bromide **6.24** (0.69 g, 27% yield) as a light brown oil. ^{1}H NMR (500 MHz, $CDCl_3$): δ 7.75–7.74 (m, 1H), 7.45–7.32 (m, 4H), 7.23–7.22 (m, 1H), 7.08 (br s, 1H), 6.13 (s, 1H), 3.40 (s, 3H), 3.29 (dd, J = 23.0, 17.3, 2H); ^{13}C NMR (125 MHz, $CDCl_3$): δ 166.6, 148.3, 142.8, 142.5, 138.8, 136.2, 126.6, 126.1, 125.6, 123.97, 123.7, 121.8, 121.3, 120.9, 119.3, 38.7, 36.5; ^{19}F NMR (376 MHz, $CDCl_3$): δ -58.1; FT-IR (cm^{-1}, neat, ATR): 3074, 3050, 2964, 1653, 1621, 1569, 1487, 1483, 1401, 1376, 1334, 1300, 1130, 1096, 1037, 978, 962, 948, 921, 885; HRMS-ESI (m/z) $[M+H]^+$ calcd for $C_{18}H_{14}BrF_3NO_2$, 412.0160, found 412.1630.

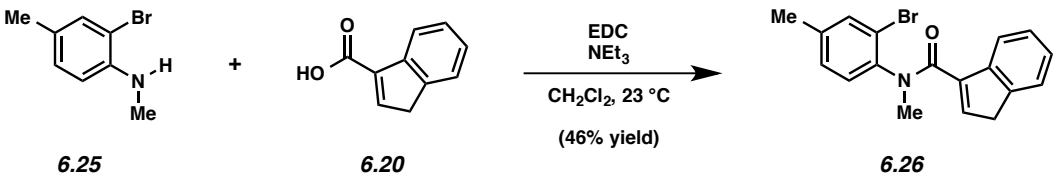

6.25 *6.20* *6.26*

Bromide 6.26. The title compound was prepared according to the General Procedure A from 2-bromo-*N*,4-dimethylaniline[19] (**6.25**, 1.4 g, 6.8 mmol, 1.1 equiv) and carboxylic acid **6.20** (1.0 g,

6.2 mmol, 1.0 equiv). Purification by flash chromatography (0 → 25% EtOAc in hexanes) generated bromide **6.26** (1.0 g, 46% yield) as a light orange solid. ^{1}H NMR (400 MHz, $CDCl_3$): δ 7.78 (d, *J* = 7.8, 1H), 7.34–7.29 (m, 3H), 7.21–7.17 (m, 1H), 7.08 (d, *J* = 7.8, 1H), 6.99–6.77 (m, 1H), 6.14 (s, 1H), 3.38 (s, 3H), 3.27 (dd, *J* = 24.2, 11.0, 2H), 2.29 (s, 3H); ^{13}C NMR (100 MHz, $CDCl_3$): δ 166.9, 142.9, 142.8, 141.0, 139.7, 138.9, 135.9, 134.1, 129.5, 129.3, 126.5, 125.3, 123.5, 122.9, 121.9, 38.7, 36.6, 20.8; FT-IR (cm^{-1}, neat, ATR): 3042, 2957, 2925, 2868, 2766, 1618, 1569, 1493, 1462 1457, 1422, 1392, 1377, 1333, 1301, 1311, 1283, 1262, 1202, 1134, 1101, 1039, 983, 965, 888, 862. HRMS-ESI (m/z) $[M+H]^+$ calcd for $C_{18}H_{17}BrNO$, 342.0494; found 342.0507.

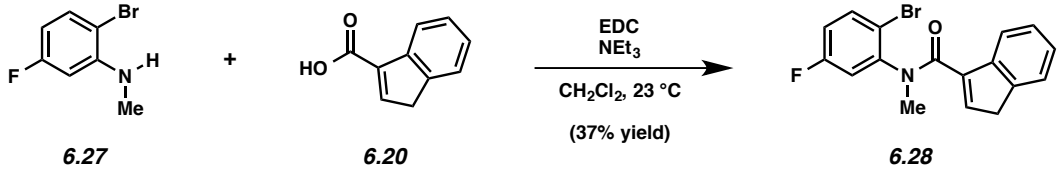

6.27 *6.20* *6.28*

Bromide 6.28. The title compound was prepared according to the General Procedure A from 2-bromo-5-fluoro-*N*-methylaniline (**6.27**, 1.4 g, 6.8 mmol, 1.1 equiv) and carboxylic acid **6.20** (1.0 g, 6.2 mmol, 1.0 equiv). Purification by flash chromatography (0 → 25% EtOAc in hexanes) generated bromide **6.28** (0.78 g, 37% yield) as a white solid. ^{1}H NMR (400 MHz, $CDCl_3$): 7.77–7.52 (m, 1H), 7.54–7.50 (m, 1H), 7.39–7.31 (m, 2H), 7.23–7.19 (m, 1H), 7.02–6.97 (m, 1H), 6.88–6.85 (m, 1H), 6.18 (s, 1H), 3.39 (s, 3H), 3.24 (s, 2H); ^{13}C NMR (125 MHz, $CDCl_3$): 166.5, 162.99, 161.0, 144.9, 142.8, 142.5, 138.7, 136.5, 134.6 (d, *J* = 8.5), 126.6, 125.6, 123.7, 121.9, 117.5 (d, *J* = 22) 116.8 (d, *J* = 22), 38.8; ^{19}F NMR (376 MHz, $CDCl_3$): δ -112.1; FT-IR (cm^{-1}, neat, ATR): 3054, 1696, 1618, 1596, 1577, 1567, 1459, 1412, 1330, 1311, 1197, 1149, 1071, 1032,

996, 972, 925, 905; HRMS-ESI (m/z) $[M+H]^+$ calcd for $C_{17}H_{14}BrFNO$ 346.0243, found 346.0248.

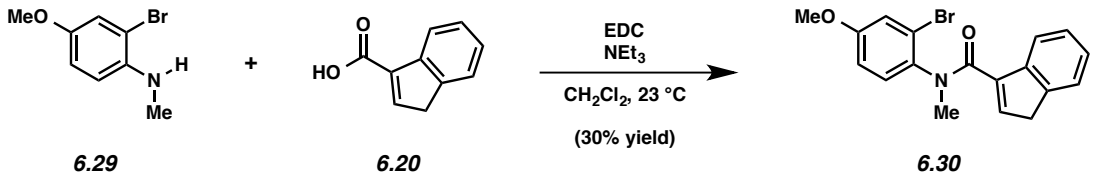

6.29 *6.20* *6.30*

Bromide 6.30 (Figure 6.3). The title compound was prepared according to the General Procedure A from 2-bromo-4-methoxy-*N*-methylaniline[20] (**6.29**, 1.5 g, 6.8 mmol, 1.1 equiv) and carboxylic acid **6.20** (1.0 g, 6.2 mmol, 1.0 equiv). Purification by flash chromatography (0 → 25% EtOAc in hexanes) generated bromide **6.30** (0.67 g, 30% yield) as a light brown oil. ^{1}H NMR (500 MHz, $CDCl_3$): δ 7.77 (d, *J* = 7.4, 1H), 7.37–7.29 (m, 2H), 7.21–7.17 (m, 1H), 7.11–7.07 (m, 2H), 6.72–6.71 (m, 1H), 6.14 (s, 1H), 3.76 (s, 3H), 3.37 (s, 3H), 3.28 (dd, *J* = 24.4, 14.4, 2H); ^{13}C NMR (125 MHz, $CDCl_3$): δ 166.8, 159.1, 142.7, 142.6, 138.7, 136.1, 135.6, 130.0, 126.3, 125.1, 123.5, 123.4, 121.7, 118.3, 114.1, 55.6, 38.5, 36.5; FT-IR (cm^{-1}, neat, ATR): 3042, 2929, 2835, 2760, 1639, 1603, 1587, 1567, 1494, 1462, 1457, 1401, 1379, 1337, 1301, 1315, 1278, 1263, 1228, 1172, 1136, 1099, 1077, 1027, 982, 964, 922, 889.; HRMS-ESI (m/z) $[M+H]^+$ calcd for $C_{18}H_{17}BrNO_2$, 358.0443, found 358.0447.

6.5.2.2 Synthesis of Starting Materials (General Procedure B)

*Representative procedure for the synthesis of substrates **6.11**, **6.12**, **6.33**, **6.35**, **6.37**, **6.39**, and **6.42** (synthesis of bromide **6.11** is used as an example).*

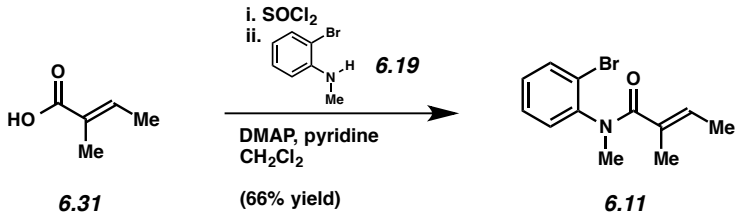

Bromide 6.11 (Figure 6.5). To an oven-dried flask was added (*Z*)-2-methylbut-2-enoic acid (**6.31**, 0.79 g, 7.9 mmol, 1.7 equiv) and thionyl chloride (1.5 g, 12.2 mmol, 2.6 equiv). The resulting mixture was stirred at 60 °C for 1 h. The mixture was concentrated under reduced pressure to remove excess thionyl chloride. The resulting oil was diluted with CH_2Cl_2 (10 mL) and then added to a mixture containing 2-bromo-*N*-methylaniline (**6.19**, 0.87 g, 4.7 mmol, 1.0 equiv), pyridine (0.85 g, 10.8 mmol, 2.3 equiv), DMAP (29.3 mg, 0.24 mmol, 0.05 equiv), and CH_2Cl_2 (50 mL, 0.6 M). The mixture was then allowed to stir at 23 °C. After stirring for 12 h, the mixture was diluted with deionized water (40 mL) and CH_2Cl_2 (30 mL). The layers were separated and the aqueous layer was extracted with CH_2Cl_2 (3 X 40 mL). The organics were dried over Na_2SO_4 and then concentrate under reduced pressure. Purification by flash chromatography (0 → 30% EtOAc in hexanes) generated bromide **6.11** (1.78 g, 66% yield) as a white solid. The preparation of this compound has previously been reported.[21] ^{1}H NMR (500 MHz, $CDCl_3$): δ 7.61 (d, *J* = 8.7, 1H), 7.31–7.27 (m, 1H), 7.16–7.13 (m, 2H), 5.79–5.70 (m, 1H), 3.23 (s, 3H), 1.62 (s, 3H), 1.44 (br s, 3H).

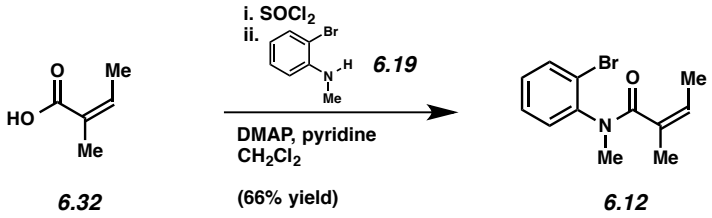

Bromide 6.12 (Figure 6.5). The title compound was prepared according to the General Procedure B using 2-bromo-*N*-methylaniline (**6.19**, 0.97 g, 5.2 mmol, 1.0 equiv) and tiglic acid (**6.32**, 0.79 g, 7.9 mmol, 1.7 equiv). Purification by flash chromatography (0 → 30% EtOAc in hexanes) generated bromide **6.12** (1.78 g, 66% yield) as a white solid. The preparation of this compound has previously been reported.[21]

^{1}H NMR (500 MHz, $CDCl_3$): δ 7.45 (d, *J* = 7.7, 1H), 7.31–7.25 (m, 2H), 7.22–7.18 (m, 1H), 5.24 (q, *J* = 7.0, 1H), 3.28 (s, 3H), 1.67 (d, *J* = 7.0, 3H), 1.61 (br s, 3H).

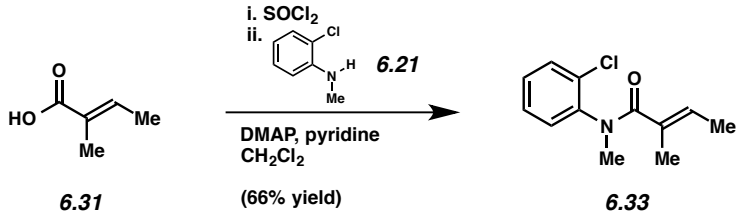

Chloride 6.33 (Figure 6.6). The title compound was prepared according to the General Procedure B using 2-chloro-*N*-methylaniline (**6.21**, 0.74 g, 5.2 mmol, 1.0 equiv) and angelic acid (**6.31**, 0.79 g, 7.9 mmol, 1.7 equiv). Purification by flash chromatography (0 → 30% EtOAc in hexanes) generated chloride **6.23** (1.78 g, 66% yield) as a white solid. ^{1}H NMR (400 MHz, $CDCl_3$): δ 7.42 (d, *J* = 7.4, 1H), 7.27–7.21 (m, 2H), 7.17–7.13 (m, 1H), 5.76–5.68 (m, 1H), 3.24 (s, 3H), 1.63 (s, 3H), 1.45 (br s, 3H); ^{13}C NMR (100 MHz, $CDCl_3$): δ 173.4, 143.3, 132.2, 132.1, 130.4, 129.8, 128.5, 127.6, 122.6, 36.4, 13.7, 13.3; FT-IR (cm^{-1}, neat, ATR): 3061, 2965, 2940,

2897, 1750, 1671, 1643, 1592, 1579, 1485, 1424, 1351, 1278, 1155, 1072, 969, 855; HRMS-ESI (m/z) $[M+H]^+$ calcd for $C_{12}H_{14}ClNO$, 224.0837, found 224.0832.

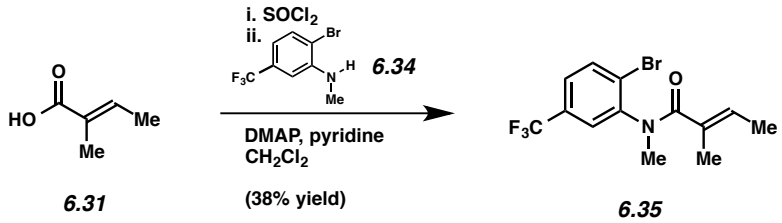

Bromide 6.35. The title compound was prepared according to the General Procedure B using 2-bromo-*N*-methyl-5-(trifluoromethyl)aniline (**6.34**, 1.47 g, 6.0 mmol, 1.0 equiv) and tiglic acid (**6.31**, 1.0 g, 10.0 mmol, 1.7 equiv). Purification by flash chromatography (0 → 25% EtOAc in hexanes) generated bromide **6.35** (0.76 g, 38% yield) as a pale yellow oil. ^{1}H NMR (400 MHz, $CDCl_3$): δ 7.79 (dd, J = 0.61, 8.9, 1H), 7.46–7.40 (m, 2H), 5.75 (br s, 1H), 3.30 (s, 3H), 1.66 (br s, 3H), 1.48 (br s, 3H); ^{13}C NMR (125 MHz, $CDCl_3$): δ 173.3, 134.6, 132.0, 131.3, 131.1, 127.20, 127.17, 127.07, 125.5, 125.4, 124.4, 122.2, 13.9, 13.4; ^{19}F NMR (376 MHz, $CDCl_3$): δ -62.8; FT-IR (cm^{-1}, neat, ATR): 3040, 2925, 2865, 1665, 1644, 1603, 1576, 1481, 1423, 1289, 1256, 1172, 1129, 1078, 1051, 1031, 1003; HRMS-ESI (m/z) $[M+H]^+$ calcd for $C_{13}H_{14}BrF_3NO$, 336.0211, found 336.0194.

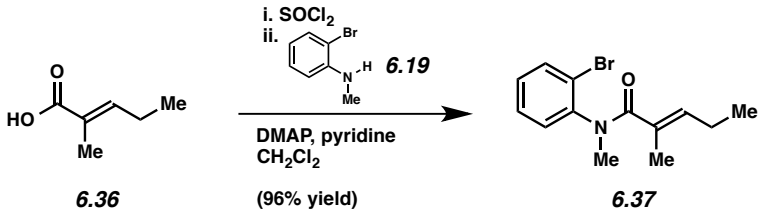

Bromide 6.37 The title compound was prepared according to the General Procedure B using 2-bromo-*N*-methylaniline (**6.19**, 0.97 g, 5.2 mmol, 1.0 equiv) and (*E*)-2-methylpent-2-enoic acid (**6.36**, 1.0 g, 8.8 mmol, 1.7 equiv). Purification by flash chromatography (5 → 25% EtOAc in

hexanes) generated bromide **6.37** (1.4 g, 96% yield) as a pale yellow oil. ^{1}H NMR (400 MHz, $CDCl_3$): δ 7.61 (d, *J* = 7.8, 1H), 7.31–7.29 (m, 1H), 7.16–7.13 (m, 2H), 5.60–5.58 (m, 1H), 3.25 (s, 3H), 1.85–1.80 (m, 2H), 1.53 (s, 3H), 0.65 (br s, 3H); ^{13}C NMR (100 MHz, $CDCl_3$): δ 173.3, 143.9, 136.6, 133.5, 130.1, 129.9, 128.7, 128.2, 122.6, 36.3, 20.7, 13.8, 12.7; FT-IR (cm^{-1}, neat, ATR): 3057, 2963, 2931, 2872, 1707, 1660, 1635, 1583, 1569, 1477, 1435, 1418, 1362, 1341, 1309, 1250, 1194, 1130, 1102, 1051, 1038, 1028, 969, 883, 859; HRMS-ESI (m/z) $[M+H]^+$ calcd for $C_{13}H_{16}BrNO$, 281.0415, found 282.0478.

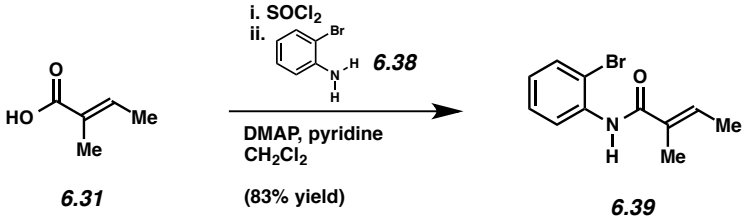

6.31 6.39

Bromide 6.39. The title compound was prepared according to the General Procedure B using aniline (**6.38**, 5.0 g, 29.0 mmol, 1.0 equiv) and tiglic acid (**6.31**, 5.0 g, 50.0 mmol, 1.7 equiv. Purification via flash chromatography (0 to 30% EtOAc in hexanes) to generate secondary amide **6.39** (6.1 g, 83% yield) as a white solid. ^{1}H NMR (400 MHz, $CDCl_3$): δ 8.46–8.44 (m, 1H), 8.04 (s, 1H), 7.55–7.53 (m, 1H), 7.34–7.30 (m, 1H), 6.99–6.95 (m, 1H), 6.69–6.64 (m, 1H), 1.99 (s, 3H), 1.86 (d, *J* = 6.9, 3H); ^{13}C NMR (125 MHz, $CDCl_3$): δ 167.2, 136.1, 132.6, 132.5, 132.2, 128.5, 124.96, 121.8, 113.65, 113.64, 14.4, 12.5; FT-IR (cm^{-1}, neat, ATR): 3406, 3120, 3079, 3058, 3026, 2987, 2916, 2856, 1682, 1633, 1610, 1587, 1577, 1515, 1459, 1433, 1384, 1336, 1300, 1234, 1152, 1072, 1021, 983, 953, 865; HRMS-ESI (m/z) $[M+H]^+$ calcd for $C_{11}H_{13}BrNO$, 254.0181, found 254.0182.

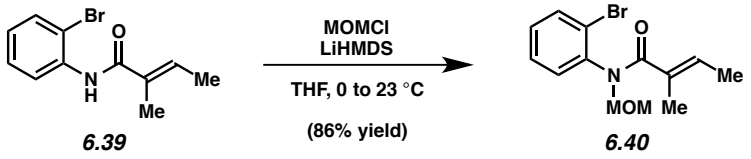

6.39 *6.40*

Bromide 6.40. To a solution of secondary amide **6.39** (1.0 gm 3.9 mmol, 1.0 equiv) and THF (47.0 mL, 0.083 M) was added LiHMDS (5.46 mL, 1.4 equiv) at 0 °C over 15 min. The mixture was gradually warmed to 23 °C. After stirring for 1 h, MOMCl (0.50 mL, 6.63 mL, 1.7 equiv) was added to the mixture. The resulting mixture was stirred at 23 °C for 1 h and then quenched slowly with saturated sodium bicarbonate solution (40 mL). The layers were separated and the aqueous layer was extracted with EtOAc (3 X 50 mL). After drying over Na_2SO_4, the mixture was then concentrated under reduced pressure. The crude oil was purified via flash chromatography (0 → 25% EtOAc in hexanes) to yield **6.40** as a clear oil (1.20 g, 86% yield). ^{1}H NMR (500 MHz, $CDCl_3$): δ 7.62 (d, J = 8.2, 0.8, 1H), 7.34–7.30 (m, 1H), 7.27–7.25 (m, 1H), 7.18–7.15 (m, 1H), 5.81 (br s, 1H), 5.54 (br s, 1H), 4.62 (d, J = 10.0, 1H), 3.43 (s, 3H), 1.70 (br s, 3H), 1.50 (br s, 3H); ^{13}C NMR (125 MHz, $CDCl_3$): δ 173.9, 141.3, 133.7, 131.5, 129.2, 128.3, 123.2, 78.9, 57.0, 13.9, 13.5; FT-IR (cm^{-1}, neat, ATR): 3061, 2987, 2935, 2858, 2825, 1664, 1645, 1584, 1525, 1475, 1444, 1396, 1366, 1291, 1266, 1196, 1181, 1163, 1109, 1078, 1046, 1029, 995, 972, 912, 878; HRMS-ESI (m/z) $[M+H]^+$ calcd for $C_{13}H_{17}BrNO_2$, 298.0443, found 298.0454.

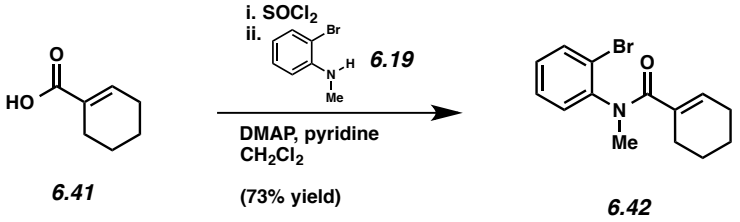

Bromide 6.42. The title compound was prepared according to the General Procedure B using 2-bromo-*N*-methylaniline (**6.19**, 0.97 g, 5.2 mmol, 1.0 equiv) and cyclohex-1-ene-1-carboxylic acid (**6.41**, 1.0 g, 7.9 mmol, 1.7 equiv). Purification by flash chromatography (0 → 30% EtOAc in hexanes) generated bromide **6.42** (1.41 g, 73% yield) as a white solid. Spectral data matched those previously reported.[22]

6.5.2.3 Synthesis of Starting Materials (Miscellaneous)

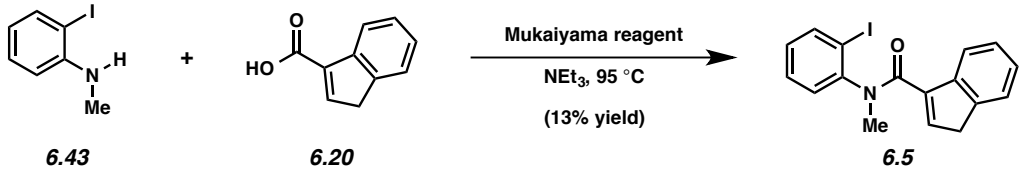

Iodide 6.5 . The title compound was prepared according to the report from Mukaiyama and coworkers.[23] To a solution of the carboxylic acid (**6.20**, 0.60 g, 3.7 mmol, 1.0 equiv), 2-iodo-*N*-methylaniline[24] (**6.43**, 0. 86 g, 3.7 mmol, 1.0 equiv), and NEt_3 (1.03 mL, 7.4 mmol. 2.0 equiv) was added 2-chloro-1-methylpyridinium iodide (1.13 g, 4.44 mmol, 1.2 equiv) at 23 °C. The resulting mixture was stirred at 95 °C for 2 h. After cooling to 23 °C, the mixture was diluted with CH_2Cl_2 (50 mL) and then washed with 2N HCl (30 mL) and deionized water (30 mL). The organics were then concentrated under reduced pressure. The resulting mixture was purified by flash chromatography (0 → 20% EtOAc in hexanes) generated iodide **6.5** (0.18 g, 13% yield) as a light yellow solid. ^{1}H NMR (500 MHz, $CDCl_3$): δ 7.83 (d, J = 7.7, 2H), 7.36–7.31 (m, 2H), 7.24–7.18 (m, 3H), 6.97 (t, J = 7.4, 1H), 6.11 (s, 1H), 3.39 (s, 3H), 3.26 (dd, J = 21, 24, 2H); ^{13}C

NMR (100 MHz, $CDCl_3$): δ 166.5, 147.1, 142.9, 142.7, 140.1, 138.7, 136.4, 129.6, 129.4, 126.5, 125.4, 123.5, 122.2, 99.6, 38.8, 36.9; FT-IR (cm^{-1}, neat, ATR): 2984, 2939, 2909, 1741, 1652, 1465, 1446, 1374, 1300, 1243, 1098, 1047, 919; HRMS-ESI (m/z) $[M+H]^+$ calcd for $C_{17}H_{15}INO$, 376.0198, found 376.0216.

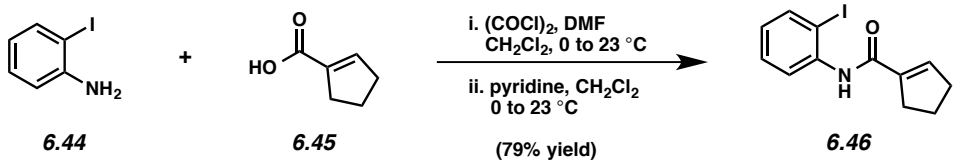

6.44 *6.45* *6.46*

Iodide 6.46. To a suspension of cyclopent-1-ene-1-carboxylic acid (**6.45**, 1.0 g, 8.9 mmol, 1.5 equiv) in CH_2Cl_2 (2.3 mL) was added oxalyl chloride (1.23 g, 9.7 mmol, 1.65 equiv) dropwise at 0 °C. The resulting mixture was stirred at 0 °C for 10 min and then at 23 °C for 1 h. The mixture was diluted with CH_2Cl_2 (3 mL) and added to a solution of 2-iodoaniline (**6.44**, 1.29 g, 5.9 mmol, 1.0 equiv) and pyridine (0.77 g, 9.7 mmol, 1.65 equiv) at 0 °C. After stirring at 23 °C for 1 h, the mixture was diluted with deionized water (5 mL). The layers were separated and the aqueous layer was extracted with EtOAc (3 X 15 mL). After drying over Na_2SO_4, the mixture was concentrated under reduced pressure. Purification by flash chromatography (0 → 30% EtOAc in hexanes) generated bromide **6.46** (1.46 g, 79% yield) as a white solid. Spectral data matched those previously reported.[25]

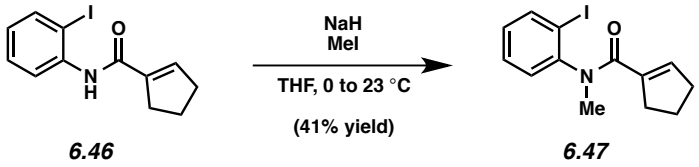

6.46 *6.47*

Iodide 6.47. To a flask containing NaH (60% in oil dispersion, 0.28 g, 7.1 mmol, 1.2 equiv) and THF (20 mL, 0.3M) was added amide **6.46** (1.84 g, 5.9 mmol, 1.0 equiv) at 0 °C. The mixture was stirred at 23 °C for 30 min and then MeI was added (0.44 mL, 7.1 mmol, 1.2 equiv). The resulting mixture was stirred at 23 °C for 12 h and the diluted with deionized water (10 mL). The layers were separated and the aqueous layer was extracted with EtOAc (3 X 20 mL). After drying over Na_2SO_4, the mixture was concentrated under reduced pressure. Purification by flash chromatography (0 → 30% EtOAc in hexanes) generated bromide **6.47** (0.80 g, 41% yield) as a white solid. Spectral data matched those previously reported.[25]

6.5.2.4. Nickel-Catalyzed Heck Cyclization for the Synthesis of Spirooxindoles.

*Representative procedure (cyclization of bromide **6.2** was used as an example).*

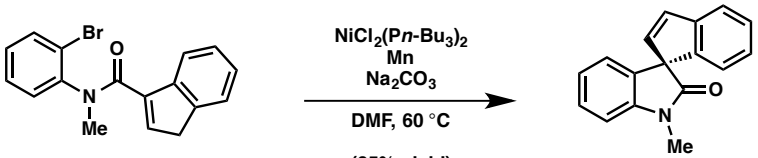

6.1 *6.2*

Bromide 6.2 (Table 6.1 & Figures 6.2–6.3). A reaction vial was charged with the bromide (**6.1**, 100.0 mg, 0.30 mmol, 1.0 equiv), Na_2CO_3 (95.4 mg, 0.90 mmol, 3.0 equiv), Mn (49.4 mg, 0.90 mmol, 3.0 equiv), $NiCl_2(P\textit{n}\text{-}Bu_3)_2$ (16.0 mg, 0.030 mmol, 10 mol%), DMF (1.0 mL, 0.3 M), and a magnetic stir bar in a glove box. The vial was sealed with a PTFE septum, removed from the glove box, and stirred at 23 °C for 1 h. The reaction mixture was then stirred at 60 °C for 12 h. After cooling to 23 °C, the mixture was diluted with EtOAc (2.0 mL) and filtered over a plug of

neutral aluminium oxide (30 mL of EtOAc eluent). The organics were then washed with deionized water (3 X 10 mL), dried over Na_2SO_4, and concentrated under reduced pressure. Purification by flash chromatography (0 → 25% EtOAc in hexanes) generated spirooxindole **6.2** (85% yield) as a light orange solid. ^{1}H NMR (400 MHz, $CDCl_3$): δ 7.42 (d, J = 7.2, 1H), 7.34–7.25 (m, 2H), 7.12–7.09 (m, 2H), 6.97–6.89 (m, 3H), 6.76 (d, J = 6.9, 1H), 6.25 (d, J = 4.7, 1H), 3.33 (s, 3H); ^{13}C NMR (100 MHz, $CDCl_3$): δ 174.9, 145.7, 145.0, 144.8, 135.9, 135.7, 130.0, 128.8, 128.1, 126.4, 123.6, 123.0, 122.4, 122.0, 108.5, 27.1; FT-IR (cm^{-1}, neat, ATR): 3400, 3062, 2932, 1708, 1654, 1608, 1556, 1490, 1467, 1417, 1379, 1365, 1345, 1301, 1263, 1243, 1194, 1169, 1161, 1154, 1124, 1098, 1079, 1030, 1021, 984, 947, 927, 883; HRMS-ESI (m/z) $[M+H]^+$ calcd for $C_{17}H_{13}NO$, 247.0997, found 248.1082.

Any modifications of the conditions shown in the representative procedure above are specified in the following schemes, which depict all of the results from Table 6.1 and Figures 6.2–6.6.

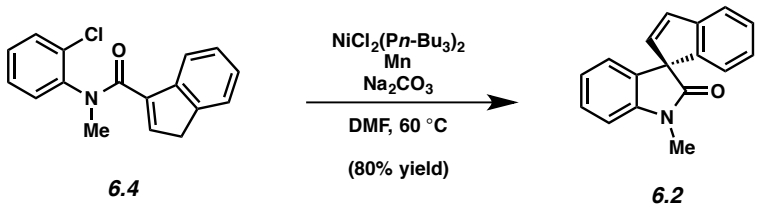

6.4 ***6.2***

Spirooxindole 6.2 (Figure 6.3). Purification by flash chromatography (0 → 25% EtOAc in hexanes) generated spirooxindole **6.2** (80% yield) as a light orange solid. Spectral data of spirooxindole **6.2** matched the characterization data shown in page 416–417.

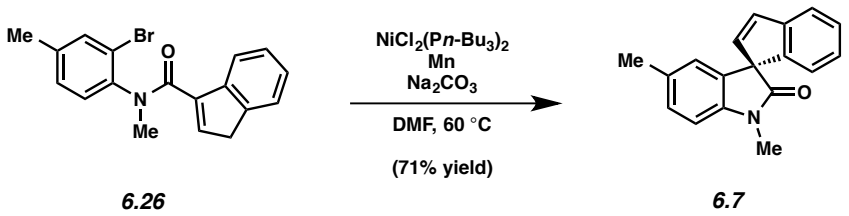

6.26 *6.7*

Spirooxindole 6.7 (Figure 6.4) Purification by flash chromatography (0 → 25% EtOAc in hexanes) generated spirooxindole **6.7** (53.8 mg, 71% yield) as a light pink solid. ^{1}H NMR (400 MHz, $CDCl_3$): δ 7.42–7.41 (m, 1H), 7.31–7.27 (dt, *J* = 1.1, 7.5, 1H), 7.13–7.09 (m, 3H), 6.92–6.90 (m, 1H), 6.86 (d, *J* = 7.9, 1H), 6.57 (br s, 1H), 6.26 (d, *J* = 5.5, 1H), 3.31 (s, 3H), 2.22 (s, 3H); ^{13}C NMR (125 MHz, $CDCl_3$): δ 174.8, 145.8, 144.8, 142.6, 136.2, 135.5, 132.7, 129.0, 128.1, 128.0, 126.4, 124.4, 122.4, 121.97, 108.24, 27.1, 21.0; FT-IR (cm^{-1}, neat, ATR): 3399, 3082, 3063, 2912, 2866, 1700, 1664, 1618, 1499, 1461, 1425, 1358, 1340, 1288, 1270, 1245, 1152, 1104, 1086, 1013, 960, 938, 84, 859, 806, 759, 725, 700; HRMS-ESI (m/z) $[M+H]^+$ calcd for $C_{18}H_{16}NO$, 262.1232; found 262.1229.

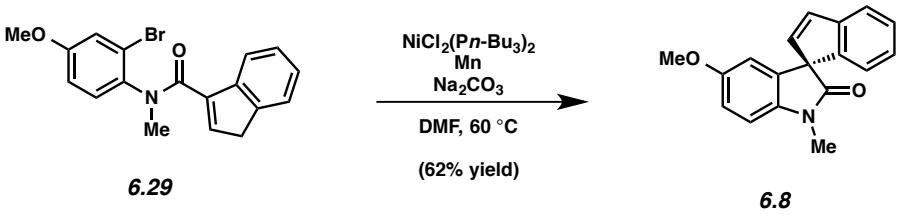

6.29 *6.8*

Spirooxindole 6.8 (Figure 6.4). The title compound was prepared via the general cyclization procedure C using *N*-(2-bromo-4-methoxyphenyl)-*N*-methyl-1*H*-indene-3-carboxamide (**6.22**, 0.10 g, 0.28 mmol, 1.0 equiv). Purification by flash chromatography (0 → 25% EtOAc in hexanes) generated spirooxindole **6.8** (48.1 mg, 62% yield) as a light red solid. ^{1}H NMR (400 MHz, $CDCl_3$): δ 7.43–7.41 (d, *J* = 6.9, 1H), 7.31–7.27 (m, 2H), 7.11 (br, 2H), 6.92–6.83 (m, 2H), 6.37 (s, 1H), 6.26–6.25 (d, *J* = 4.5, 1H), 3.68 (s, 3H), 3.31 (s, H); ^{13}C NMR (125 MHz, $CDCl_3$):

δ 174.5, 156.3, 145.7, 144.7, 138.5, 135.97, 135.7, 129.3, 128.1, 126.4, 122.4, 121.96, 113.54, 110.5, 108.8, 55.8, 27.2; FT-IR (cm^{-1}, neat, ATR): 3403, 3063, 2957, 2832, 1708, 1639, 1599, 1497, 1434, 1345, 1286, 1274, 1238, 1219, 1154, 1134, 1112, 1077, 1033, 1022, 973, 902, 871, 859, 803, 762, 728, 700; HRMS-ESI (m/z) $[M+H]^+$ calcd for $C_{18}H_{16}NO_2$, 278.1181, found 278.1173.

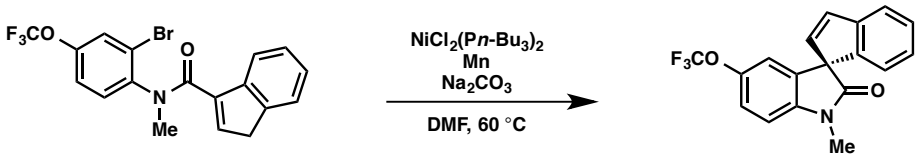

6.23 *6.9*

Spirooxindole 6.9 (Figure 6.4). The title compound was prepared via the general cyclization procedure C using *N*-(2-bromo-4-(trifluoromethoxy)phenyl)-*N*-methyl-1*H*-indene-3-carboxamide (**6.23**, 0.10 g, 0.24 mmol, 1.0 equiv). Purification by flash chromatography (0 → 25% EtOAc in hexanes) generated spirooxindole **6.9** (54.9 mg, 69% yield) as a light red solid. ^1H NMR (400 MHz, $CDCl_3$): δ 7.44–7.42 (m, 1H), 7.34–7.30 (dt, J = 1.1, 7.8, 1H); 7.22–7.19 (m, 1H), 7.15–7.12 (m, 2H), 6.96 (d, J = 8.6, 1H), 6.91–6.89 (m, 1H), 6.65–6.64 (m, 1H), 6.24 (d, J = 5.4, 1H), 3.34 (s, 3H); ^{13}C NMR (125 MHz, $CDCl_3$): δ 174.6, 145.12, 145.11, 144.9, 144.7, 143.7, 136.4, 135.1, 129.78, 128.5, 126.7, 122.4, 122.2, 121.9, 121.6, 119.5, 117.6, 108.8, 27.3; FT-IR (cm^{-1}, neat, ATR): 3075, 2920, 2851, 1709, 1656, 1616, 1496, 1464, 1421, 1367, 1337, 1245, 1147, 114.5 1100, 1081, 1016, 955, 937, 879, 854, 825HRMS-ESI (m/z) $[M+H]^+$ calcd for $C_{18}H_{13}F_3NO_3$, 332.0898, found 332.0882.

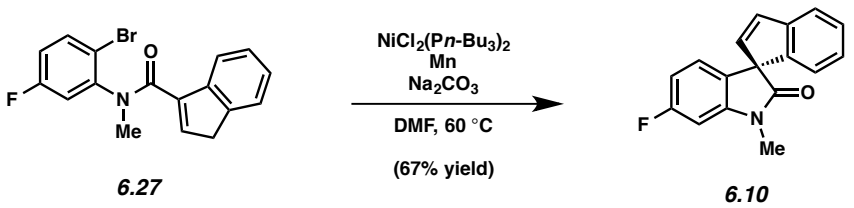

6.27 *6.10*

Spirooxindole 6.10 (Figure 6.4). The title compound was prepared via the general cyclization procedure C using *N*-(2-bromo-5-fluorophenyl)-*N*-methyl-1*H*-indene-3-carboxamide (**6.27**, 0.10 g, 0.29 mmol, 1.0 equiv). Purification by flash chromatography (0 → 25% EtOAc in hexanes) generated spirooxindole **6.10** (51.5 mg, 67% yield) as a light pink solid. ^{1}H NMR (400 MHz, $CDCl_3$): δ 7.42–7.40 (m, 1H), 7.32–7.28 (dt, *J* = 1.1, 7.4, 1H), 7.14–7.11 (m, 2H), 6.90–6.88 (m, 1H), 6.72–6.62 (m, 3H), 6.22 (d, *J* = 5.4, 1H), 3.31 (s, 3H); ^{13}C NMR (125 MHz, $CDCl_3$): δ 175.2, 164.5, 162.6, 146.5, 146.4, 145.4, 144.7, 135.8, 135.7, 128.3, 126.5, 124.8, 124.7, 122.3, 122.1, 109.2, 97.5, 97.3, 27.2; ^{19}F NMR (376 MHz, $CDCl_3$): δ -111.5; FT-IR (cm^{-1}, neat, ATR): 3123, 2953, 1708, 1607, 1502, 1461, 1448, 1368, 1330, 1260, 1122, 1082, 1072, 974, 938, 848, 814, 801, 773, 765, 699; HRMS-ESI (m/z) $[M+H]^+$ calcd for $C_{17}H_{13}FNO$, 266.0981; found 266.0965.

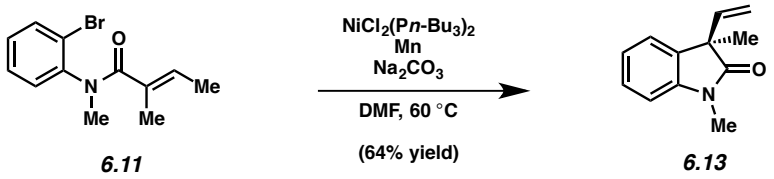

6.11 *6.13*

Spirooxindole 6.13 (Figure 6.5). The title compound was prepared according to the general procedure C using (*E*)-*N*-(2-bromophenyl)-*N*,2-dimethylbut-2-enamide (**6.11**, 100.0 mg, 0.37 mmol, 1.0 equiv). Purification by flash chromatography (10% acetone in hexanes) generated spirooxindole **6.13** (64% yield) as a clear oil. ^{1}H NMR (500 MHz, $CDCl_3$): δ 7.31 (t, *J* = 7.6, 7.4, 1H), 7.20–7.18 (m, 1H), 7.10 (t, *J* = 7.4, 7.2, 1H), 6.88 (d, *J* = 7.6, 1H), 5.98 (dd, *J* = 10.5, 6.7,

1H), 5.16–5.11 (m, 2H), 3.21 (s, 3H) 1.49 (s, 3H); ^{13}C NMR (125 MHz, $CDCl_3$): δ 178.8, 143.1, 138.2, 132.8, 128.2, 123.97, 122.7, 115.4, 108.4, 51.4, 26.5, 22.6. Spectral data matched those previously reported.[26]

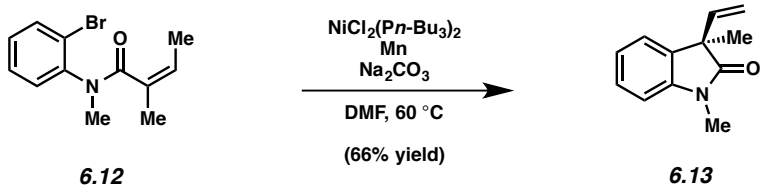

6.12 *6.13*

Spirooxindole 6.13 (Figure 6.5) Purification by flash chromatography (10% acetone in hexanes) generated spirooxindole **6.13** (66% yield) as a clear oil. Spectral data of spirooxindole **6.13** matched the characterization data shown in page 420–421.

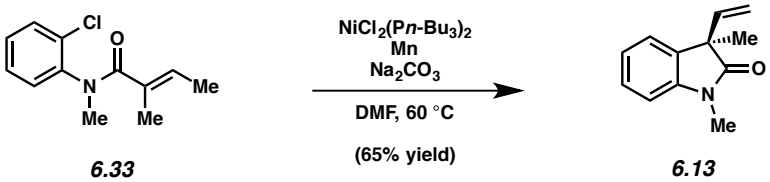

6.33 *6.13*

Spirooxindole 6.13 (Figure 6.6). Purification by flash chromatography (10% acetone in hexanes) generated spirooxindole **6.13** (65% yield) as a clear oil. Spectral data of spirooxindole **6.13** matched the characterization data shown in page 420–421.

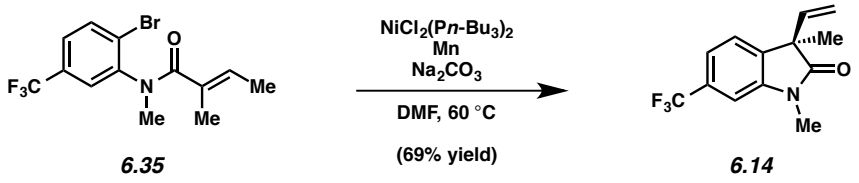

6.35 *6.14*

Spirooxindole 6.14 (Figure 6.6) Purification by flash chromatography (10% acetone in hexanes) generated spirooxindole **6.14** (69% yield) as a clear oil. ^{1}H NMR (500 MHz, $CDCl_3$): δ 7.38–7.35 (m, 2H), 7.07–7.04 (m, 1H), 5.96 (dd, J = 10.0, 6.3, 1H), 5.20 (d, J = 10.0, 2H), 5.13 (d, J =

16.5, 1H), 3.25 (s, 3H), 1.51 (s, 3H); ^{13}C NMR (125 MHz, $CDCl_3$): δ 178.4, 143.7, 137.3, 124.2, 122.8, 119.8, 116.1, 105.1, 51.3, 31.5, 26.7, 22.6; FT-IR (cm^{-1}, neat, ATR): 2970, 2930, 2852, 1722, 1625, 1510, 1460, 1320, 1258, 1167, 1125, 932, 862, 827, 712, 687, 670, 510; HRMS-ESI (m/z) $[M+H]^+$ calcd for $C_{13}H_{13}F_3NO$, 256.0949, found 256.0921.

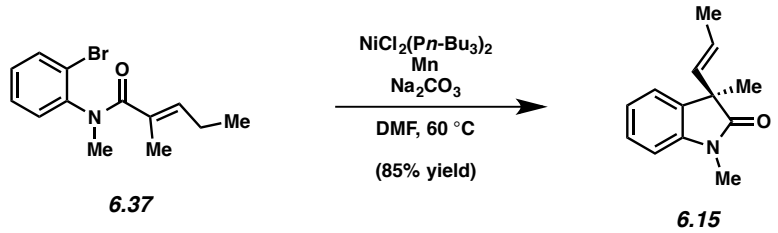

6.37 *6.15*

Spirooxindole 6.15 (Figure 6.6). Purification by flash chromatography (10% acetone in hexanes) generated spirooxindole **6.15** (85% yield) as a colourless oil. ^{1}H NMR (500 MHz, $CDCl_3$): δ 7.29–7.28 (m, 1H), 7.19 (d, J = 7.0, 1H), 7.09 (t, J = 7.4, 1H), 6.86 (d, J = 7.7, 1H), 5.60–5.57 (m, 1H), 5.55–5.49 (m, 1H), 3.20 (s, 3H), 1.67 (d, J = 5.9, 3H), 1.46 (s, 3H); ^{13}C NMR (125 MHz, $CDCl_3$): δ 179.5, 143.1, 133.7, 131.2, 127.99, 126.2, 123.9, 122.6, 108.2, 50.6, 26.4, 23.1, 18.0. Spectral data matched those previously reported.[27]

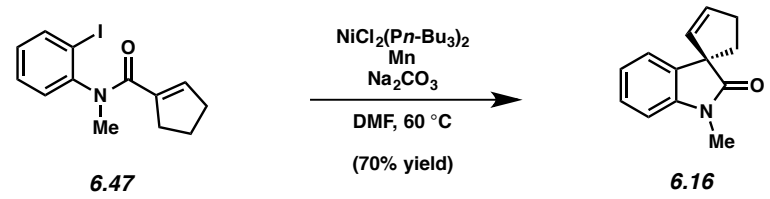

6.47 *6.16*

Spirooxindole 6.16 (Figure 6.6). Purification by flash chromatography (10% acetone in hexanes) generated spirooxindole **6.16** (70% yield) as a clear oil. ^{1}H NMR (500 MHz, $CDCl_3$): δ 7.39–7.35 (m, 2H), 7.32–7.28 (m, 1H), 7.17–7.15 (m, 2H), 5.69–6.68 (m, 1H), 4.96–4.94 (m, 1H), 3.37 (s, 3H), 2.43–2.38 (m, 2H), 2.04–1.96 (m, 1H), 1.88–1.82 (m, 1H); ^{13}C NMR (125

MHz, $CDCl_3$): δ 167.9, 146.3, 144.2, 132.3, 129.5, 127.7, 127.0, 90.3, 37.7, 32.97, 29.8, 27.96. Spectral data matched those previously reported.[28]

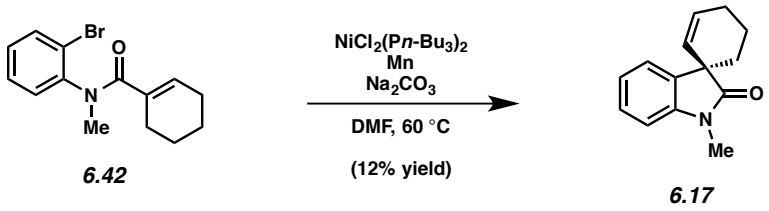

6.42 *6.17*

Spirooxindole 6.17 (Figures 6.6). Purification by flash chromatography (10% acetone in hexanes) generated spirooxindole **6.17** (12% yield) as a clear oil. ^{1}H NMR (500 MHz, $CDCl_3$): δ 7.33 (d, *J* = 7.4, 1H), 7.29 (td, *J* = 7.8, 1.1, 1H), 7.03 (td, *J* = 7.6, 0.8, 1H), 6.87 (d, *J* = 7.8, 1H), 5.94–5.91 (m, 1H), 5.89–5.85 (m, 1H), 3.22 (s, 3H), 2.68 (dq, *J* = 17.7, 2.7, 1H), 2.34–2.32 (m, 2H), 2.09–2.03 (m, 1H), 1.97–1.92 (m, 1H); 1.53–1.50 (m, 1H); ^{13}C NMR (125 MHz, $CDCl_3$): δ 180.9, 142.9, 134.7, 127.8, 126.9, 125.0, 124.1, 122.4, 107.99, 45.99, 31.8, 29.1 26.4, 21.97. Spectral data matched those previously reported.[29]

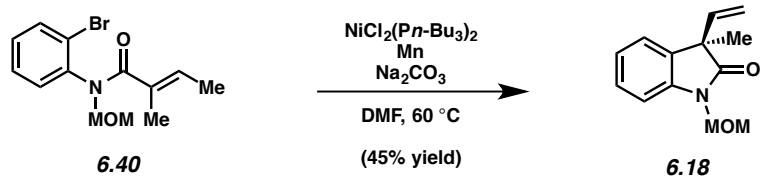

6.40 *6.18*

Spirooxindole 6.18 (Figure 6.6). Purification by flash chromatography (0 → 15% acetone in Hexanes) generated spirooxindole **6.18** (45% yield) as a clear oil. ^{1}H NMR (500 MHz, $CDCl_3$): δ 7.31 (td, *J* = 7.7, 1.1, 1H), 7.22 (d, *J* = 7.3, 1H), 7.14–7.10 (m, 1H), 7.07–7.03 (m, 1H), 6.01 (dd, J = 10.2, 6.8, 1H), 5.18–5.11 (m, 4H), 3.31 (s, 3H), 1.53 (s, 3H); ^{13}C NMR (125 MHz, $CDCl_3$): δ 179.5, 141.3, 138.2, 132.3, 128.3, 124.2, 123.2, 115.7, 109.9, 71.4, 56.2, 51.7, 22.97; FT-IR (cm^{-1}, neat, ATR): 3092, 3060, 2975, 2933, 2825, 1722, 1612, 1488, 1468, 1370, 1290, 1344, 1298,

1227, 1111, 1187, 1084, 916, 762, 707, 640, 535, 487; HRMS-ESI (m/z) $[M+H]^+$ calcd for $C_{13}H_{16}NO_2$, 218.1181, found 218.1173.

6.5.2.5. Enantioselective Nickel-Catalyzed Heck Cyclization

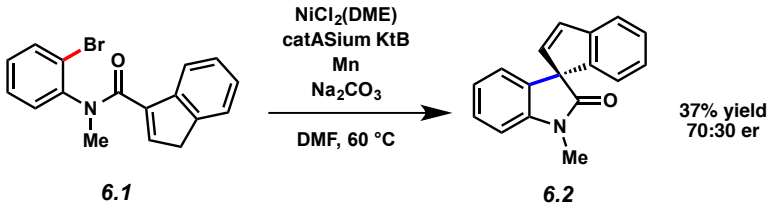

6.1 *6.2*

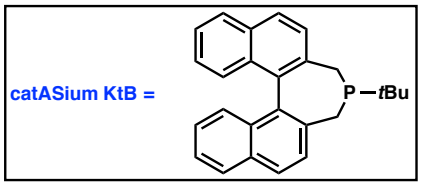

A reaction vial was charged with $NiCl_2(DME)_2$ (6.7 mg, 0.030 mmol, 10 mol%), catASium KtB (22.4mg, 0.061 mmol, 20 mol%), DMF (1.0 mL, 0.3 M), and a magnetic stir bar in a glove box. The mixture was stirred for 30 min. Bromide **6.1** (100.0 mg, 0.30 mmol, 1.0 equiv), Na_2CO_3 (95.4 mg, 0.90 mmol, 3.0 equiv), and Mn (49.4 mg, 0.90 mmol, 3.0 equiv) were then added. The vial was sealed with a cap containing a PTFE septum, removed from the glove box, and stirred at 23 °C for 1 h. The reaction mixture was then stirred at 60 °C for 12 h. After cooling to 23 °C, the mixture was diluted with EtOAc (2.0 mL) and filtered over a plug of neutral aluminum oxide (30 mL of EtOAc eluent). The organics were then washed with deionized water (3 X 10 mL), dried over Na_2SO_4, and concentrated under reduced pressure. Purification by flash chromatography (0 → 25% EtOAc in hexanes) generated spirooxindole **6.2** (37% yield) as a light orange solid. Spectral data of spirooxindole **6.2** matched the characterization data shown in page 416–417. Enantiomeric excess (70:30 er) was determined by HPLC analysis (Amylose-SA, 10% EtOH in heptane, tr (major) 4.5 min, tr (minor) 4.9 min).

6.5.2.6. Robustness Screening

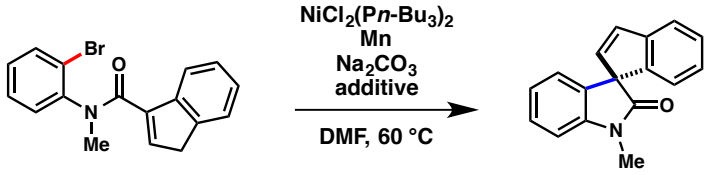

6.1 *6.2*

A reaction vial was charged with the bromide (**6.1**, 100.0 mg, 0.30 mmol, 1.0 equiv), Na_2CO_3 (95.4 mg, 0.90 mmol, 3.0 equiv), Mn (49.4 mg, 0.90 mmol, 3.0 equiv), $NiCl_2(Pn\text{-}Bu_3)_2$ (16.0 mg, 0.030 mmol, 10 mol%), additive (1.0 equiv), DMF (1.0 mL, 0.3 M), and a magnetic stir bar in a glove box. The vial was sealed with a cap containing a PTFE septum, removed from the glove box, and stirred at 23 °C for 1 h. The reaction mixture was then stirred at 60 °C for 12 h. After cooling to 23 °C, the mixture was diluted with EtOAc (2.0 mL) and filtered over a plug of neutral aluminum oxide (30 mL of EtOAc eluent). The organics were then washed with deionized water (3 X 10 mL), dried over Na_2SO_4, and concentrated under reduced pressure. Spectral data of spirooxindole **6.2** matched the characterization data shown in page 416–417.

Additive	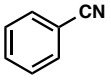	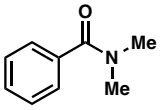	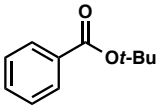	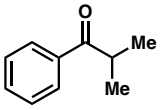	HO*t*-Bu
Yield (%)[a]	84	62	56	72	78
Additive recovery (%)[a]	72	85	99	99	67

[a] Yields were determined by ^{1}H NMR analysis using dimethylfumarate as an internal standard.

6.5.2.7. Glove-Box Free Procedure

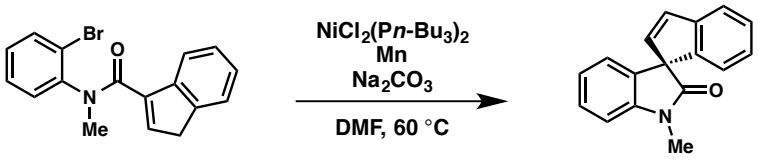

6.1 *6.2*

A reaction vial was charged with the bromide (**6.1**, 200.0 mg, 0.60 mmol, 1.0 equiv), Na_2CO_3 (190.8 mg, 1.80 mmol, 3.0 equiv), Mn (98.8 mg, 1.80 mmol, 3.0 equiv), $NiCl_2(P\textit{n}\text{-}Bu_3)_2$ (32.0 mg, 0.060 mmol, 10 mol%), and a magnetic stir bar on a bench top under air. The vial was sealed with a cap containing a PTFE septum, and underwent three vacuum-nitrogen backfill cycles. Pre-nitrogen-sparged DMF (2.0 mL, 0.3 M) was charged into the vial. The resulting mixture underwent two vacuum-nitrogen backfill cycles and was stirred at 23 °C for 1 h. The reaction mixture was then stirred at 60 °C for 12 h. After cooling to 23 °C, the mixture was diluted with EtOAc (4.0 mL) and filtered over a plug of neutral aluminum oxide (60 mL of EtOAc eluent). The organics were then washed with deionized water (6 X 10 mL), dried over Na_2SO_4, and concentrated under reduced pressure. Purification by flash chromatography (0 → 25% EtOAc in hexanes) generated spirooxindole **6.2** (71% yield) as a light orange solid. Spectral data of spirooxindole **6.2** matched the characterization data shown in page 416–417.

Appendix Six: Spectra Relevant to Chapter Six

Construction of Quaternary Stereocenters via Nickel-Catalyzed Heck Cyclizations

Jean-Nicolas Desrosiers, Liana Hie, Heewon Lee, Nelu Grinberg, Nizar Haddad, Nathan K. Yee, Neil K. Garg, and Chris H. Senanayake

Manuscript Submitted

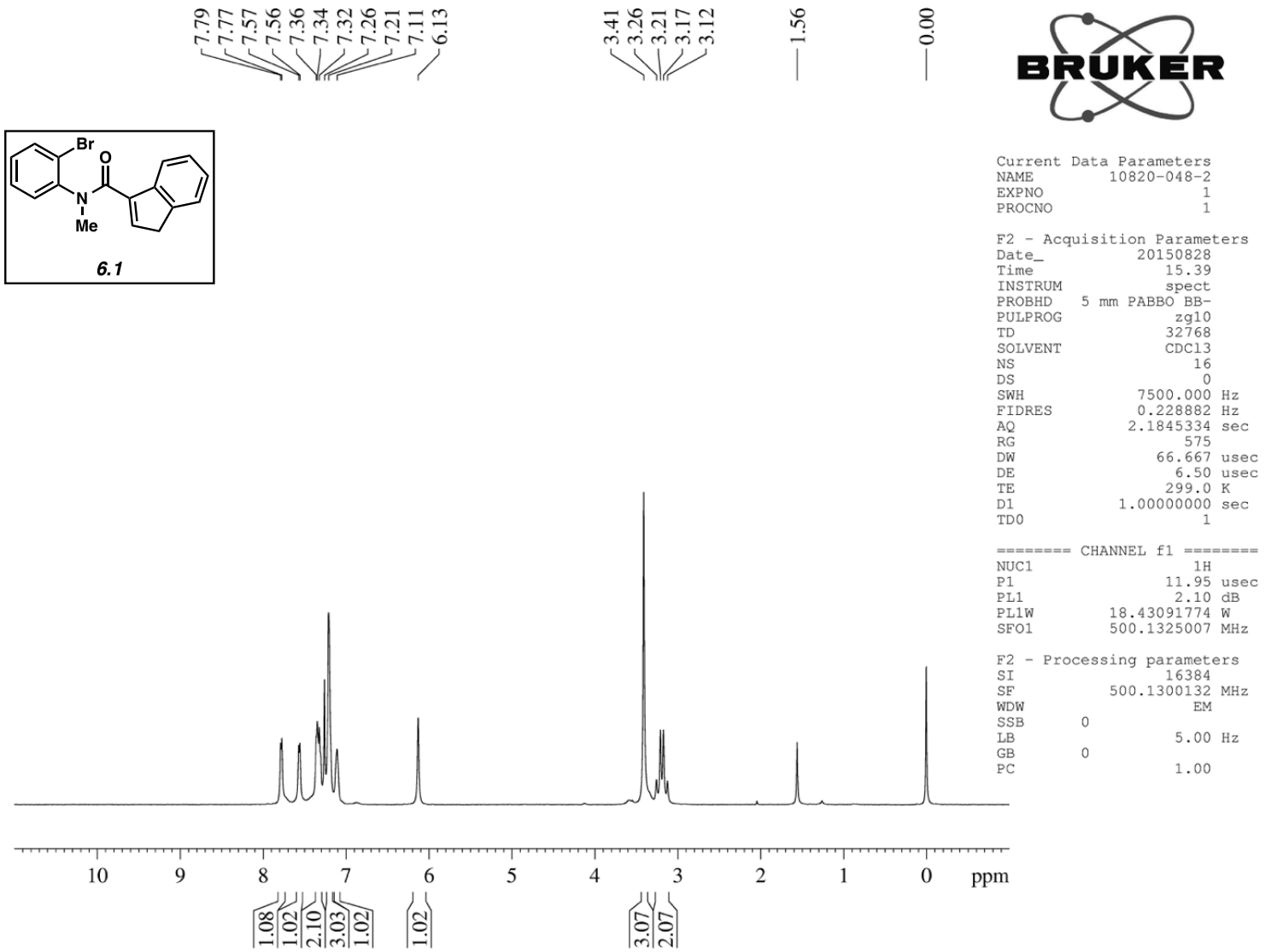

Figure A6.1 ^{1}H NMR (500 MHz, $CDCl_3$) of compound **6.1**.

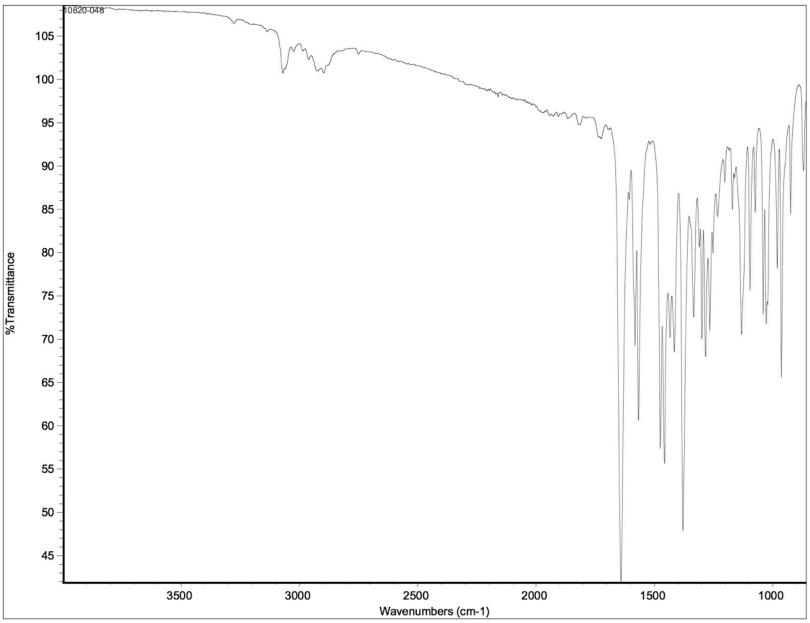

Figure A6.2 Infrared spectrum of compound **6.1**.

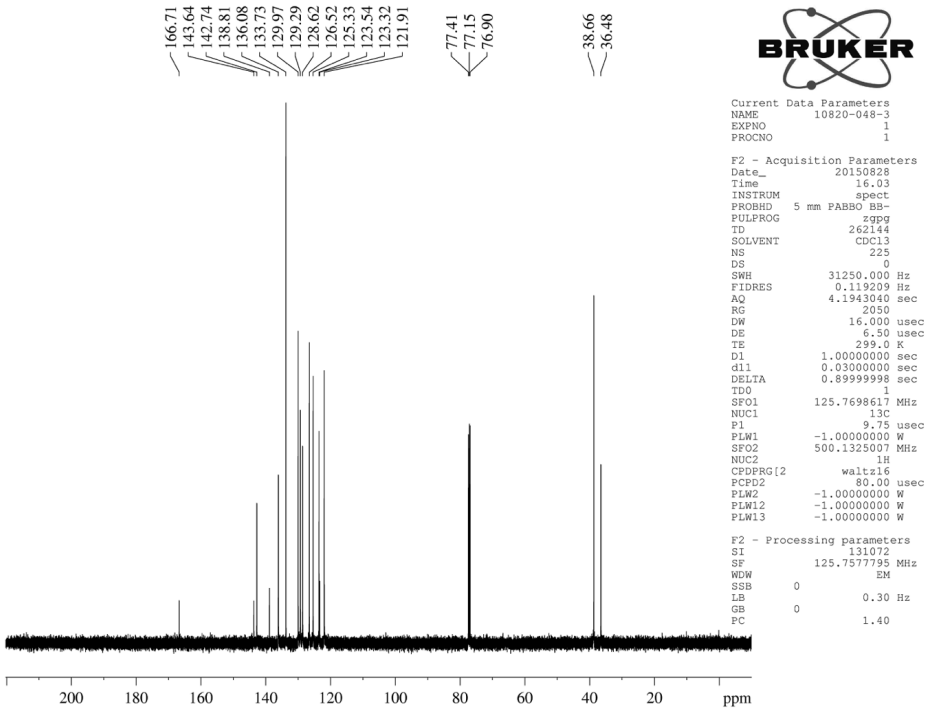

Figure A6.3 ^{13}C NMR (125 MHz, $CDCl_3$) of compound **6.1**.

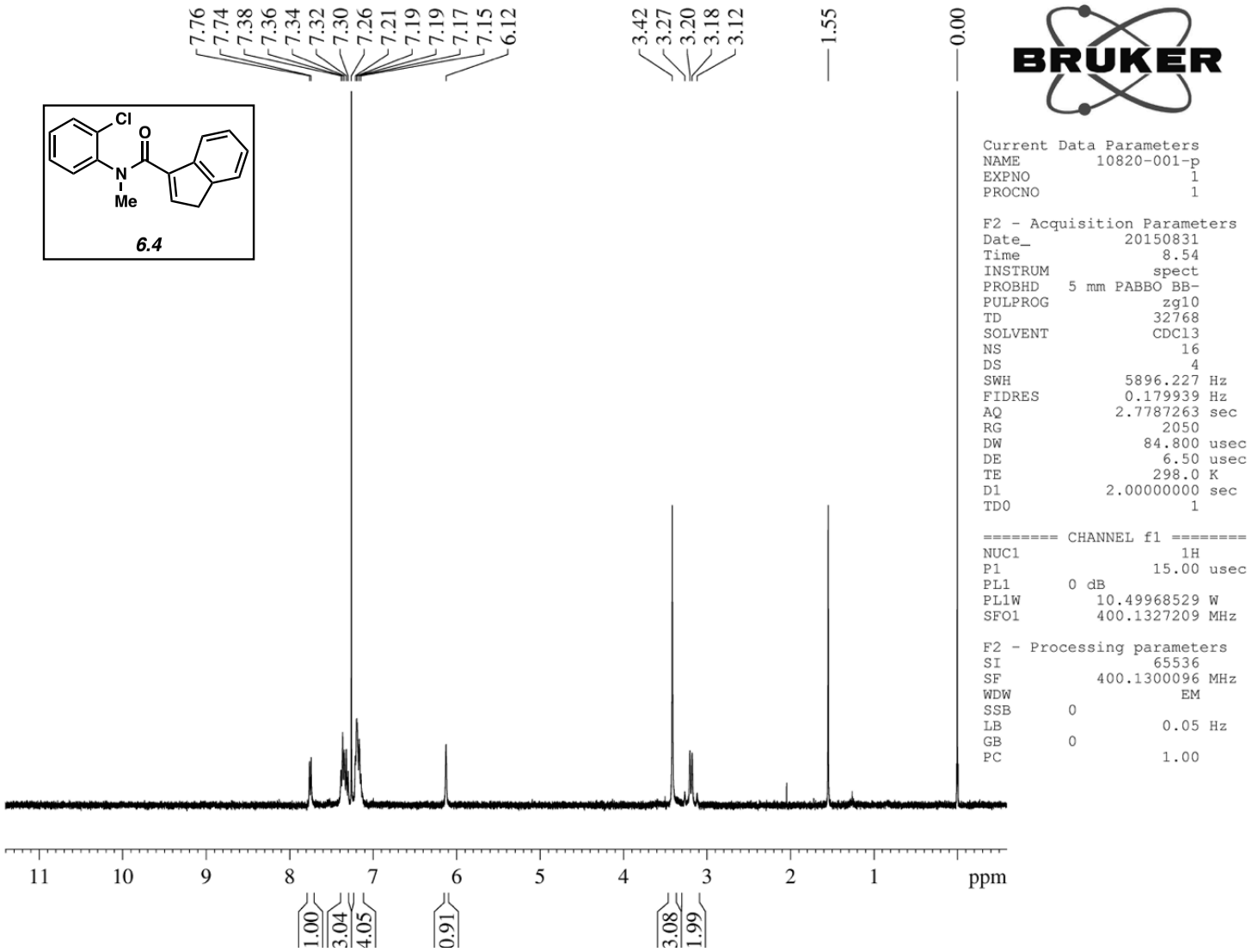

Figure A6.4 ^{1}H NMR (500 MHz, $CDCl_3$) of compound **6.4**.

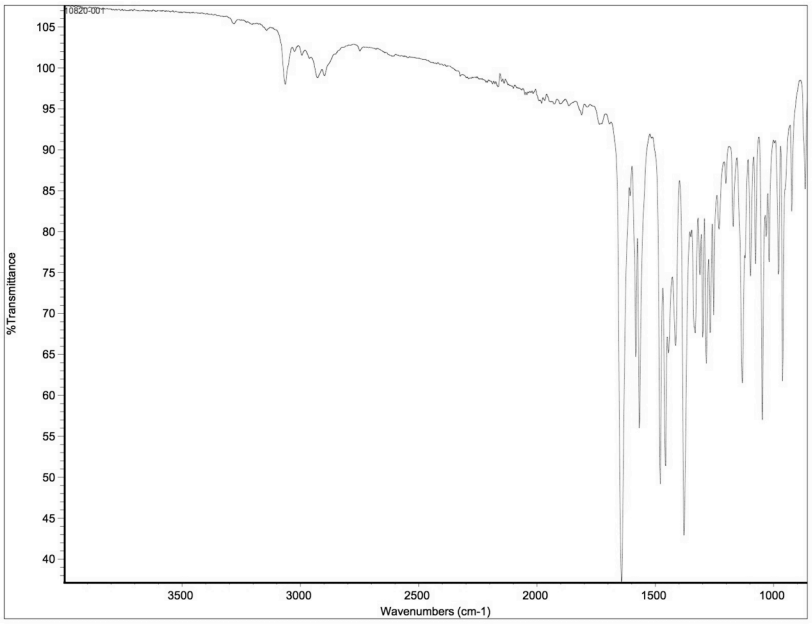

Figure A6.5 Infrared spectrum of compound **6.4**.

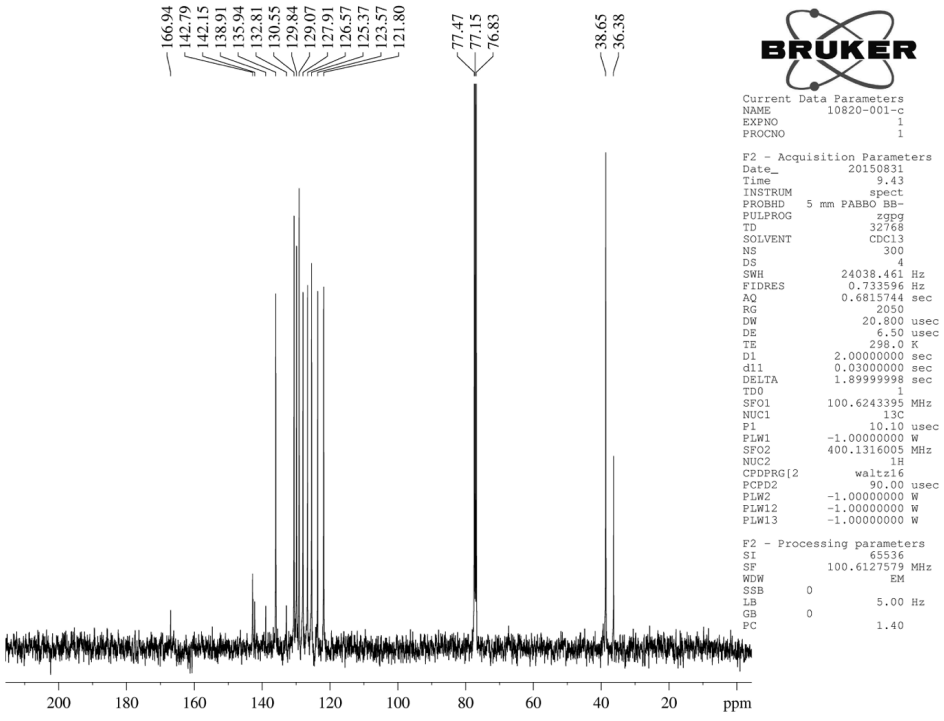

Figure A6.6 ^{13}C NMR (125 MHz, $CDCl_3$) of compound **6.4**.

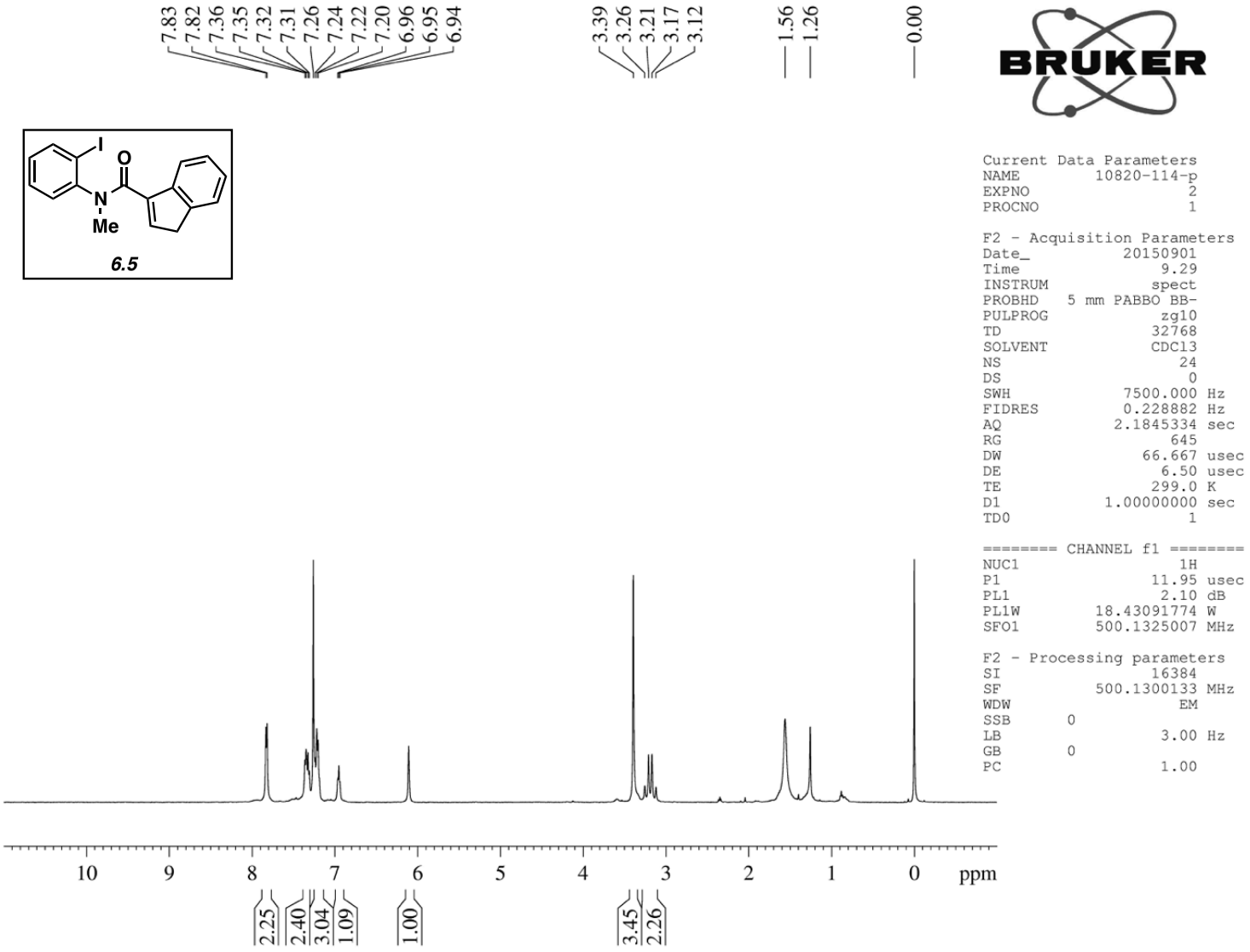

Figure A6.7 ^{1}H NMR (500 MHz, $CDCl_3$) of compound **6.5**.

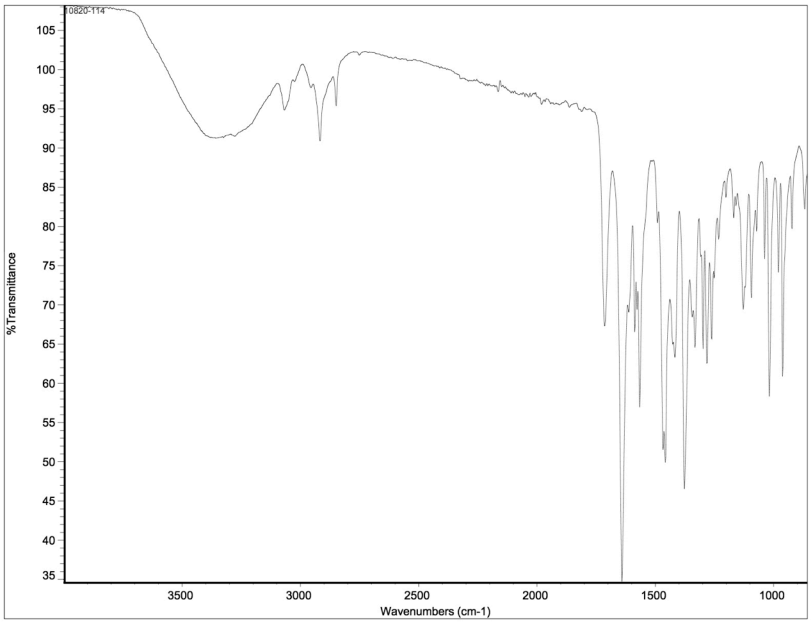

Figure A6.8 Infrared spectrum of compound **6.5**.

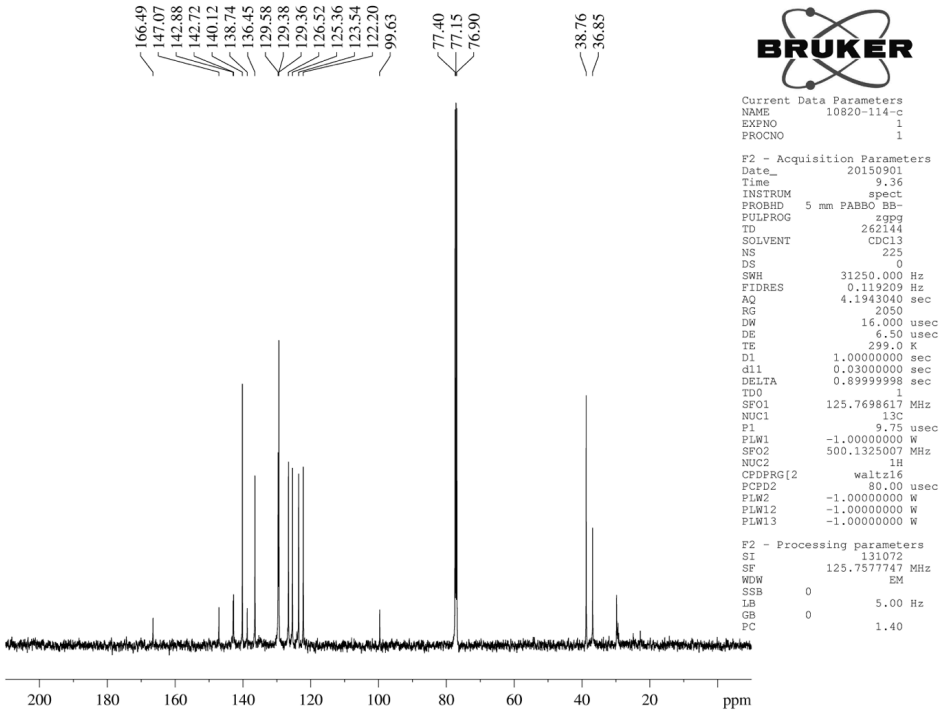

Figure A6.9 ^{13}C NMR (125 MHz, $CDCl_3$) of compound **6.5**.

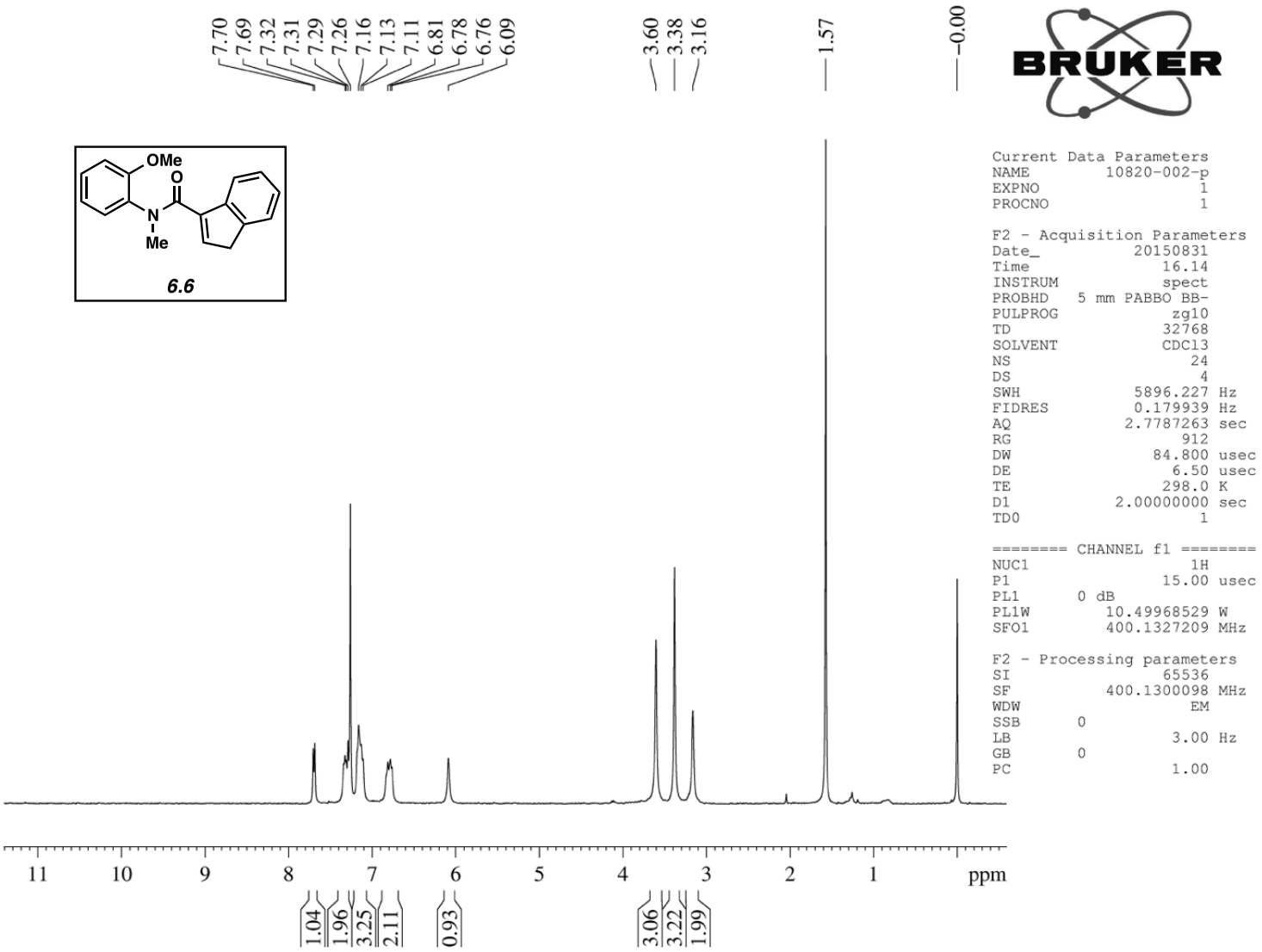

Figure A6.10 ^{1}H NMR (500 MHz, $CDCl_3$) of compound **6.6**.

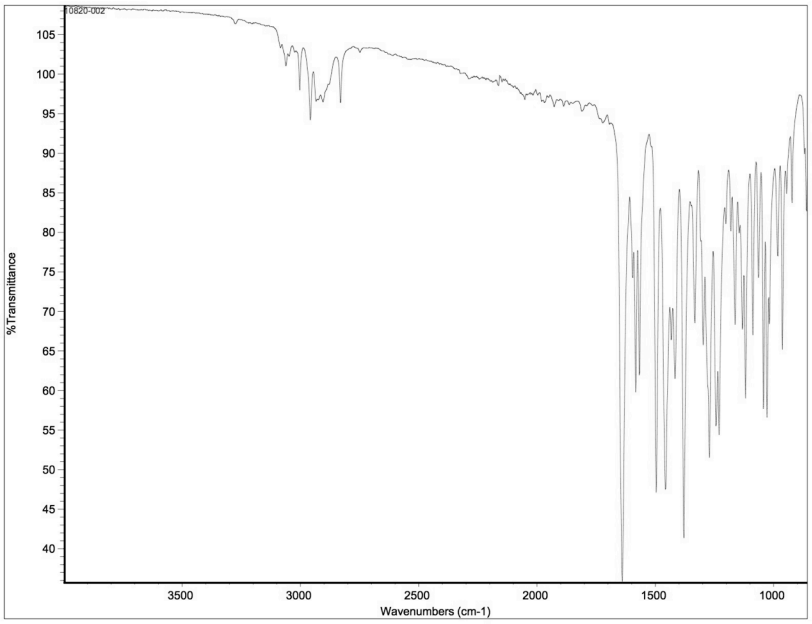

Figure A6.11 Infrared spectrum of compound **6.6**.

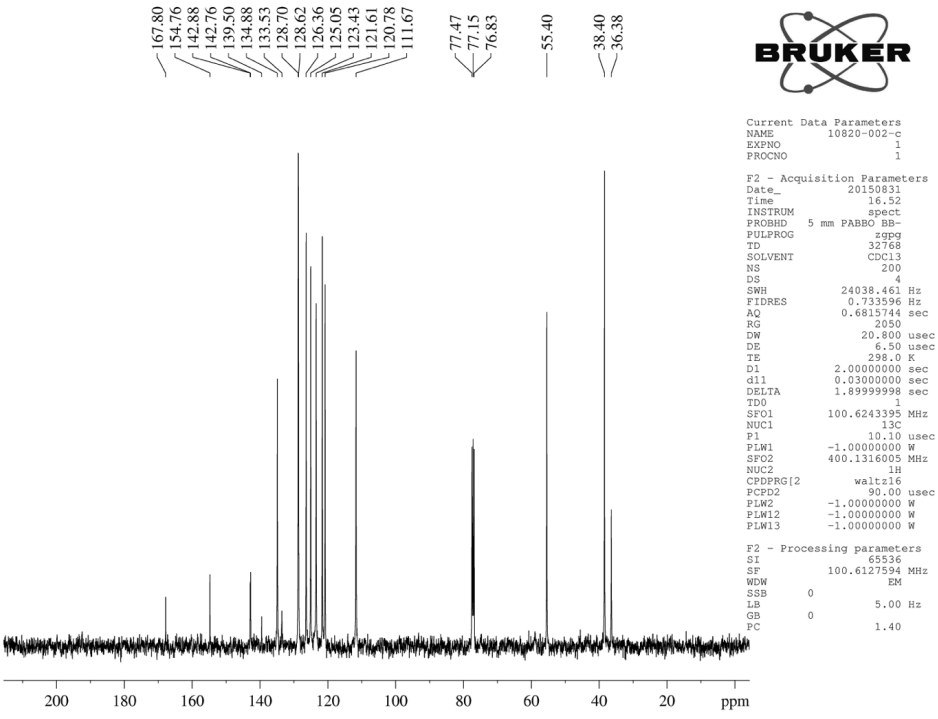

Figure A6.12 ^{13}C NMR (125 MHz, $CDCl_3$) of compound **6.6**.

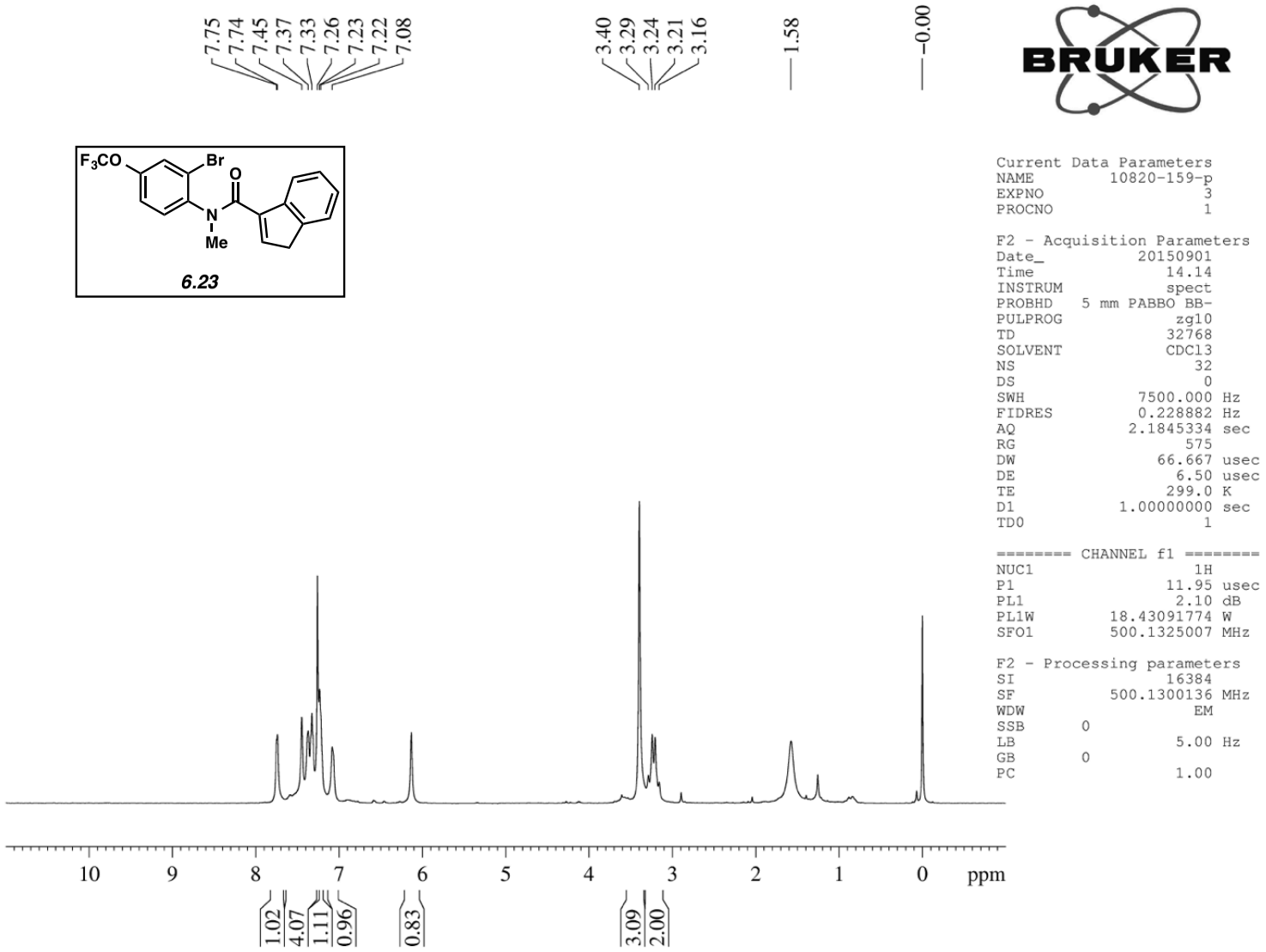

Figure A6.13 ^{1}H NMR (500 MHz, $CDCl_3$) of compound **6.23**.

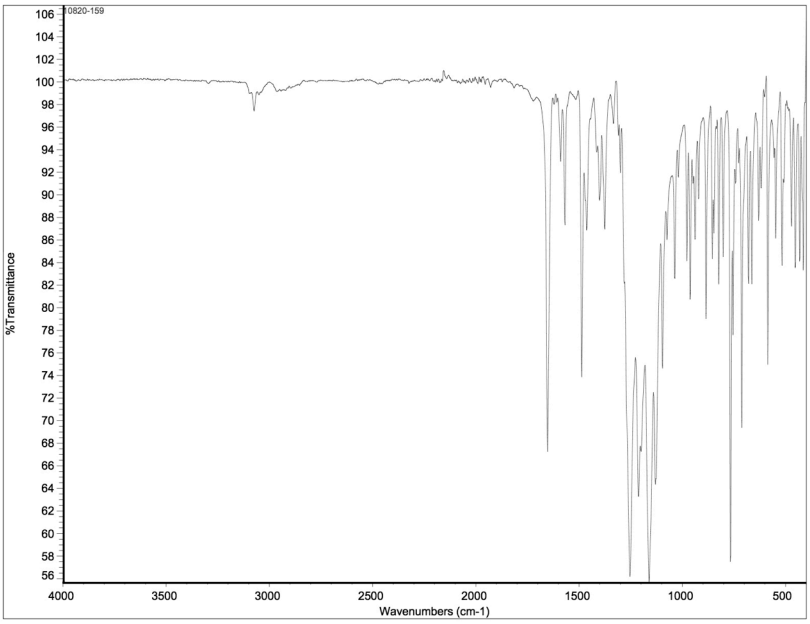

Figure A6.14 Infrared spectrum of compound **6.23**.

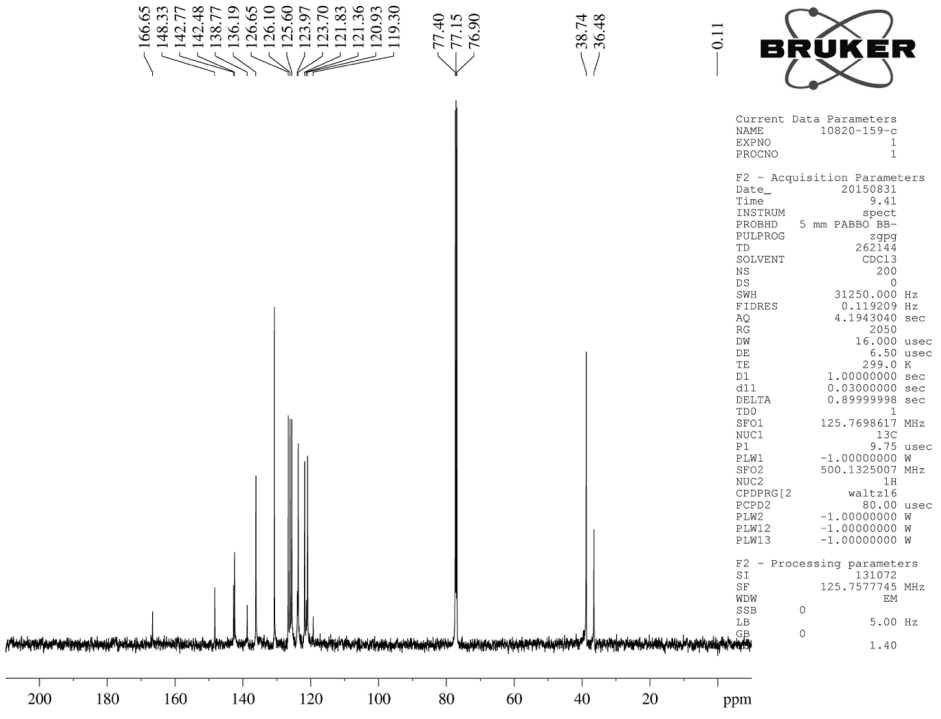

Figure A6.15 ^{13}C NMR (125 MHz, $CDCl_3$) of compound **6.23**.

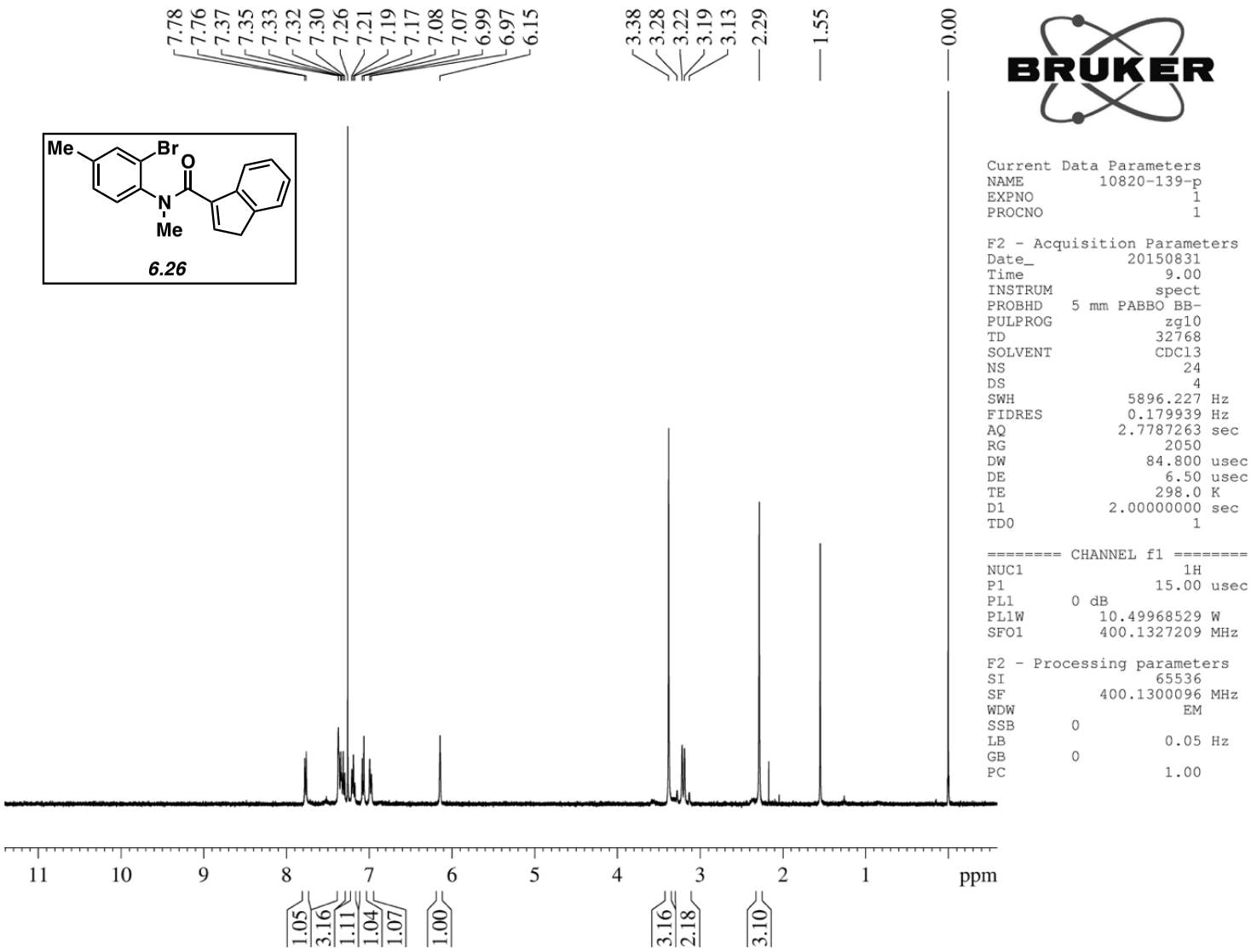

Figure A6.16 ^{1}H NMR (500 MHz, $CDCl_3$) of compound **6.26**.

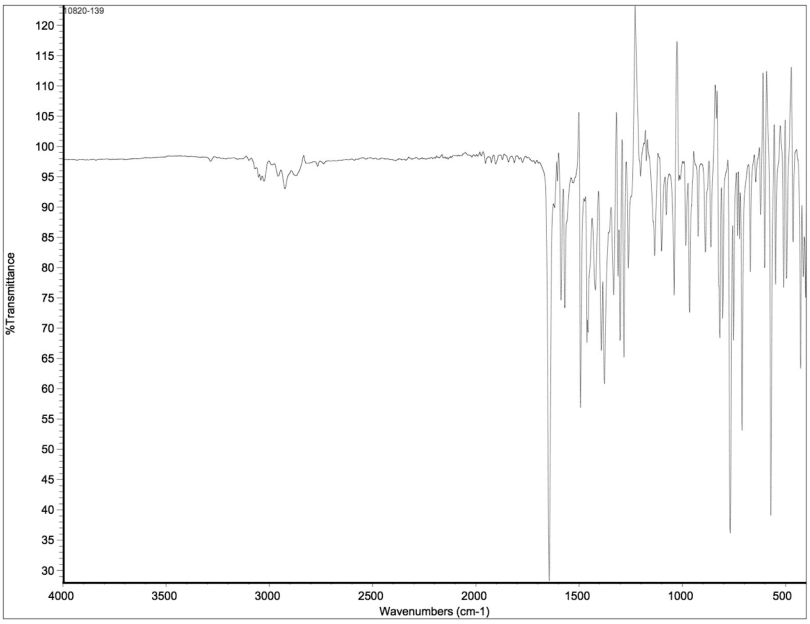

Figure A6.17 Infrared spectrum of compound **6.26**.

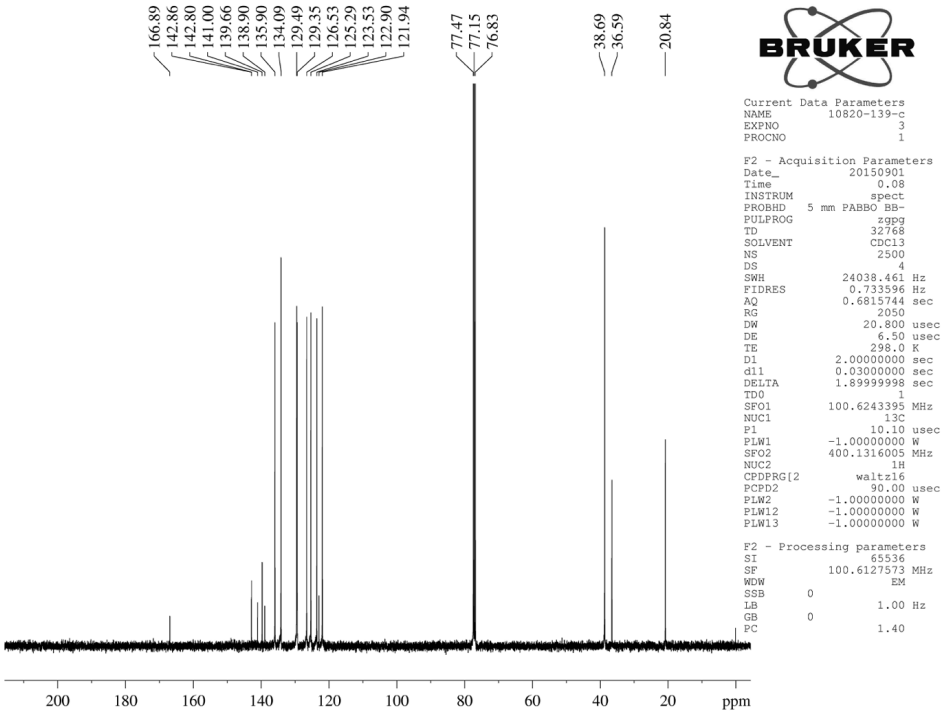

Figure A6.18 ^{13}C NMR (125 MHz, $CDCl_3$) of compound **6.26**.

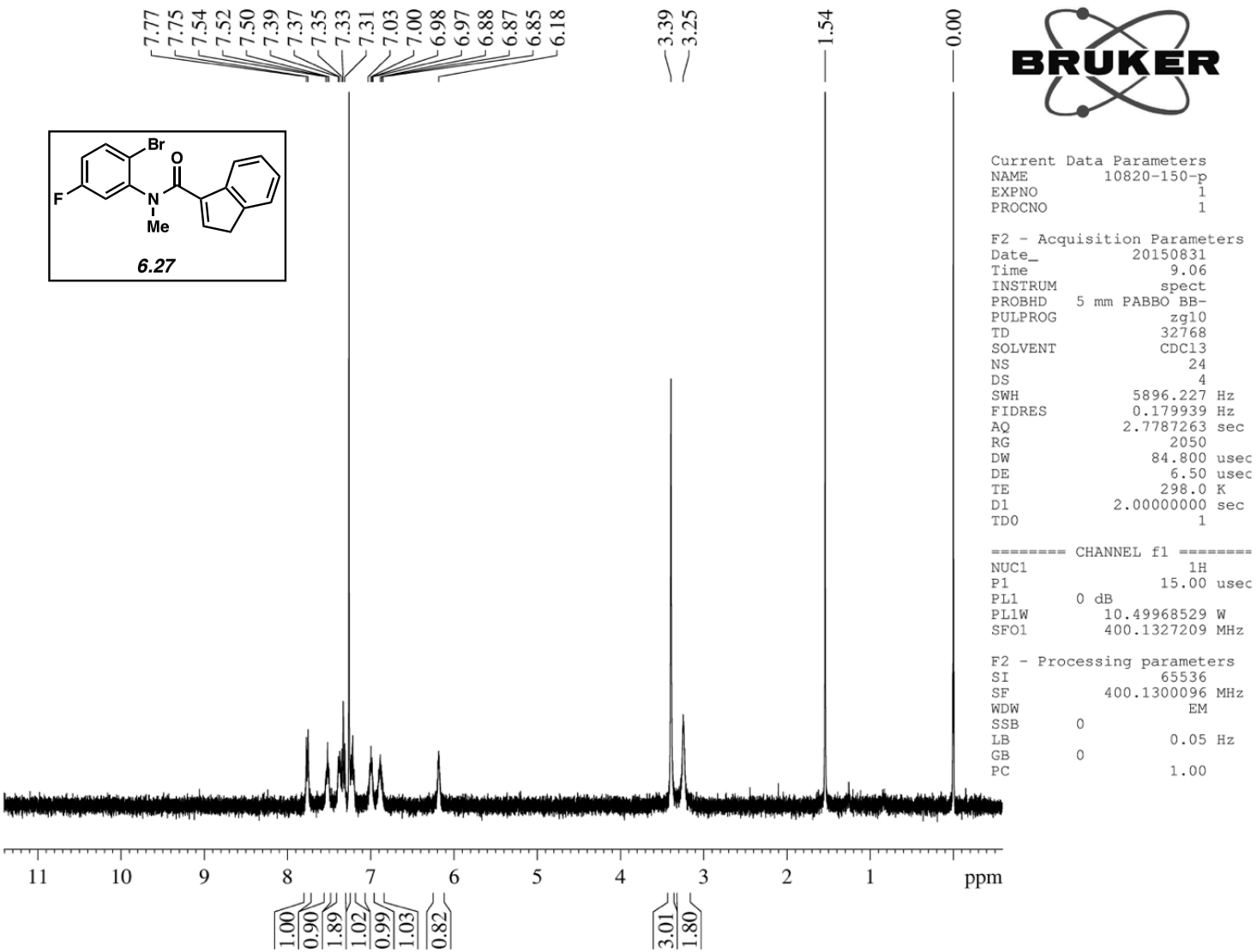

Figure A6.19 ^{1}H NMR (500 MHz, $CDCl_3$) of compound **6.27**.

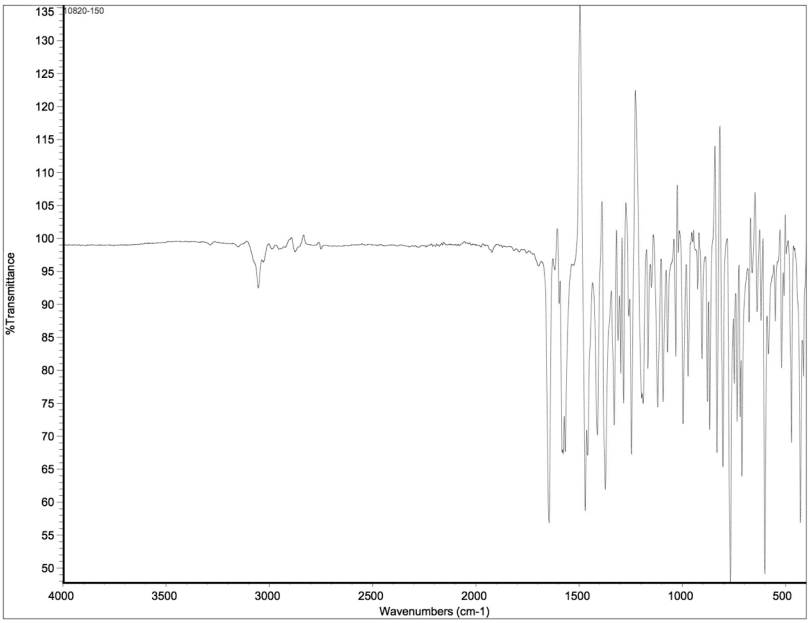

Figure A6.20 Infrared spectrum of compound **6.27**.

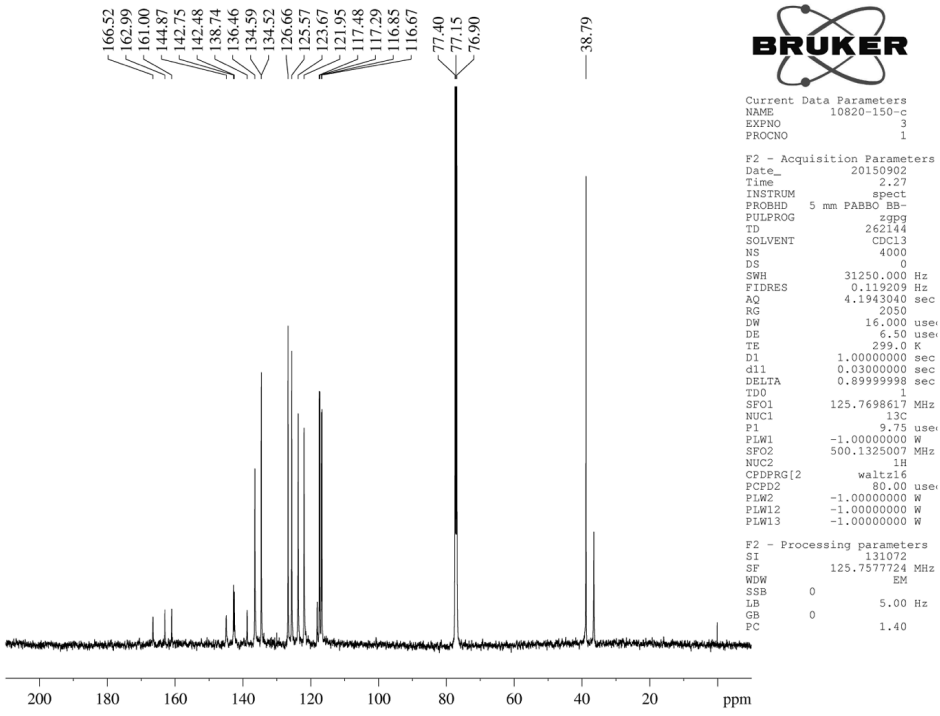

Figure A6.21 ^{13}C NMR (125 MHz, $CDCl_3$) of compound **6.27**.

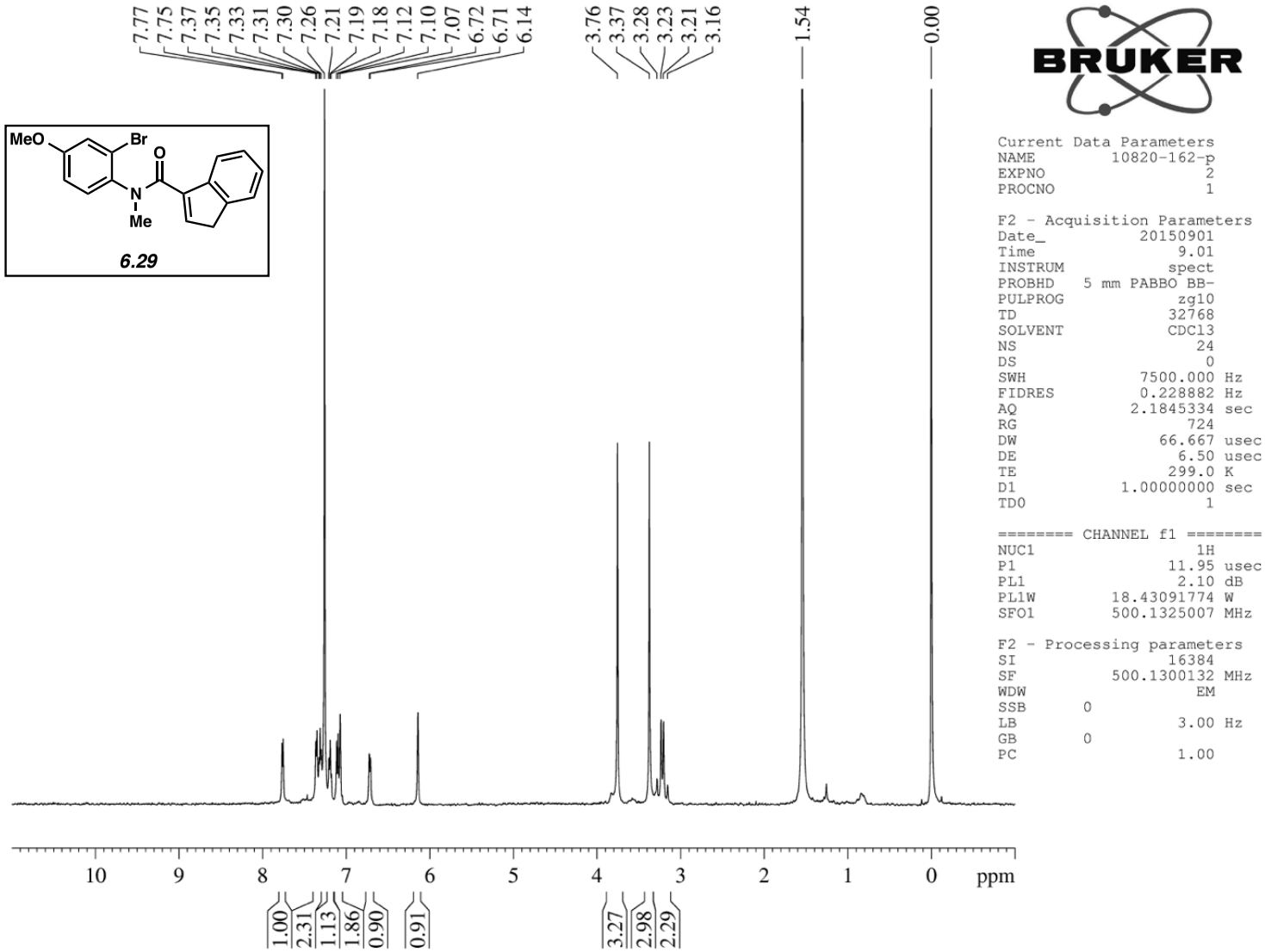

Figure A6.22 ^{1}H NMR (500 MHz, $CDCl_3$) of compound **6.29**.

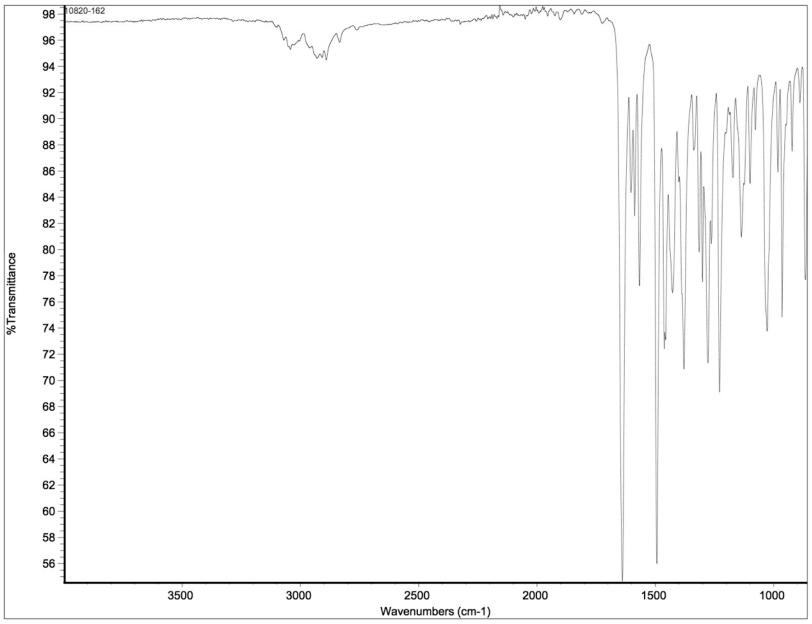

Figure A6.23 Infrared spectrum of compound **6.29**.

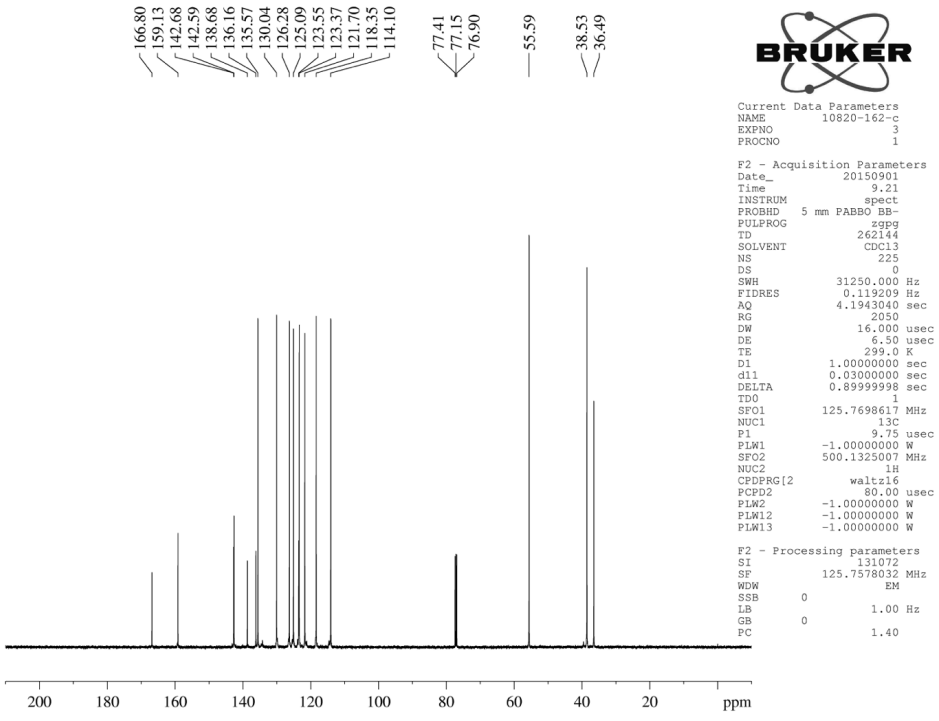

Figure A6.24 ^{13}C NMR (125 MHz, $CDCl_3$) of compound **6.29**.

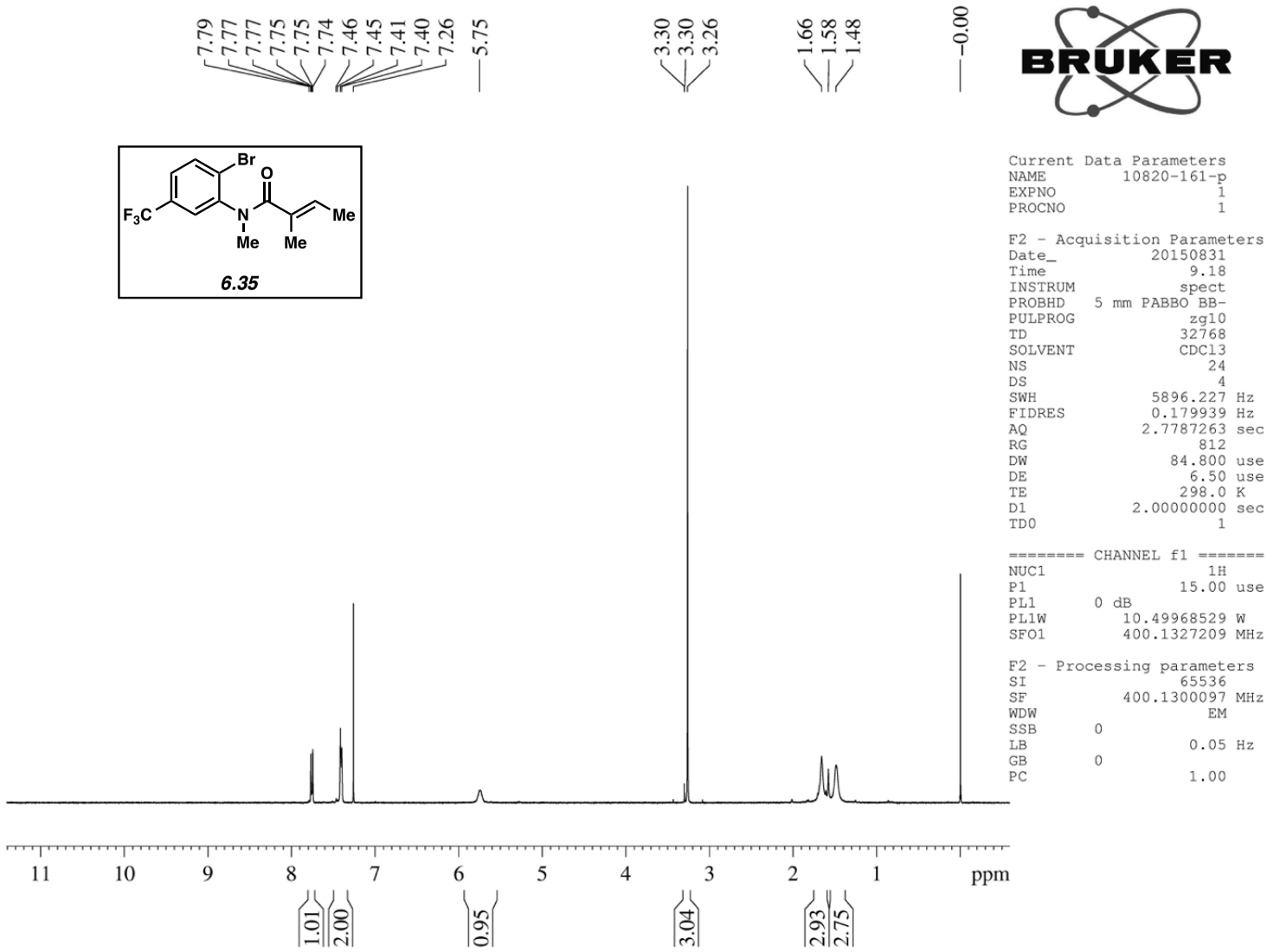

Figure A6.25 ^{1}H NMR (500 MHz, $CDCl_3$) of compound **6.35**.

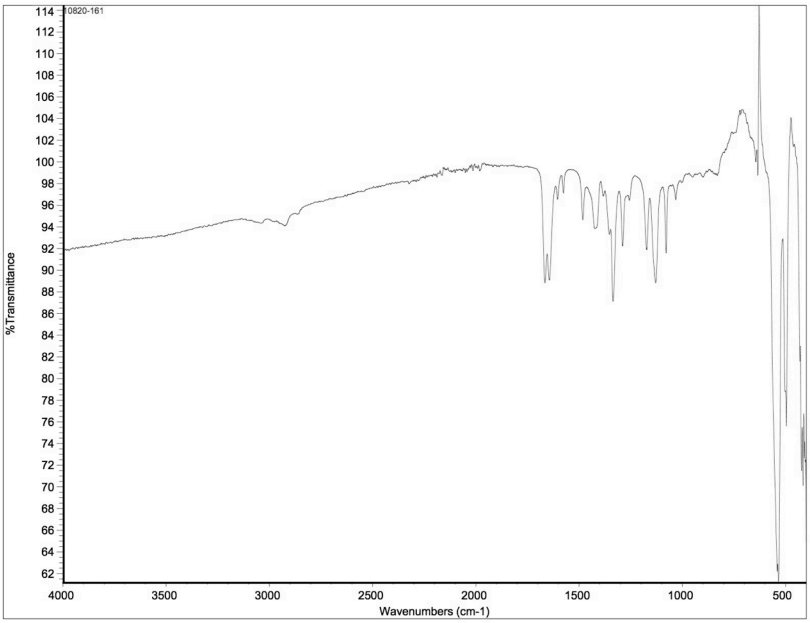

Figure A6.26 Infrared spectrum of compound **6.35**.

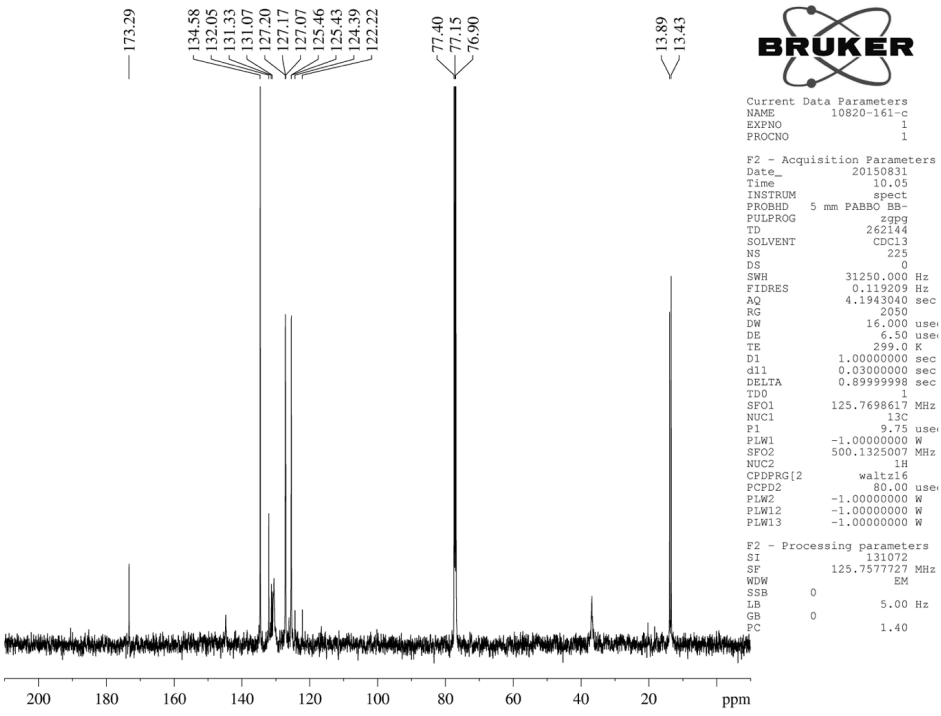

Figure A6.27 ^{13}C NMR (125 MHz, $CDCl_3$) of compound **6.35**.

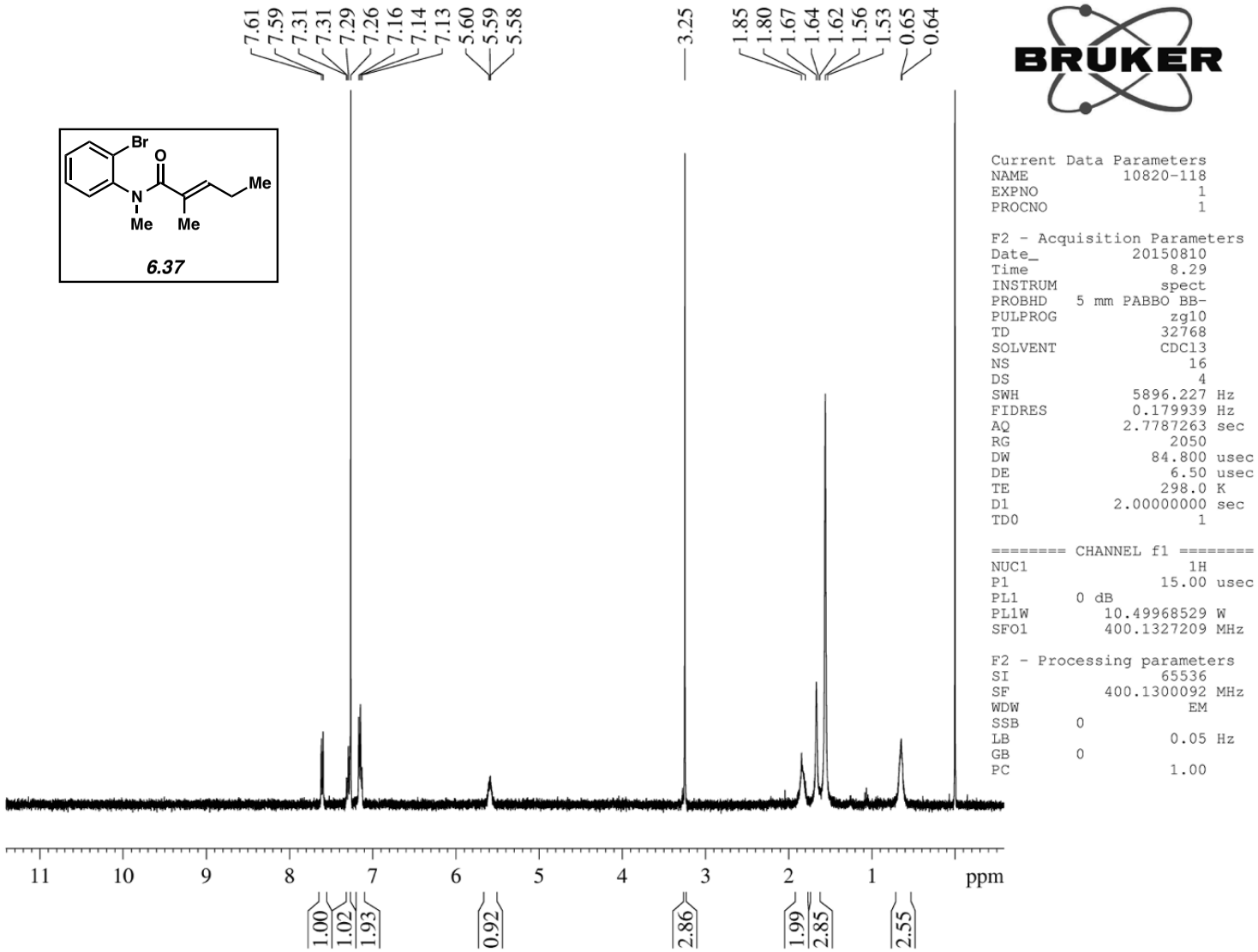

Figure A6.28 ^{1}H NMR (500 MHz, $CDCl_3$) of compound **6.37**.

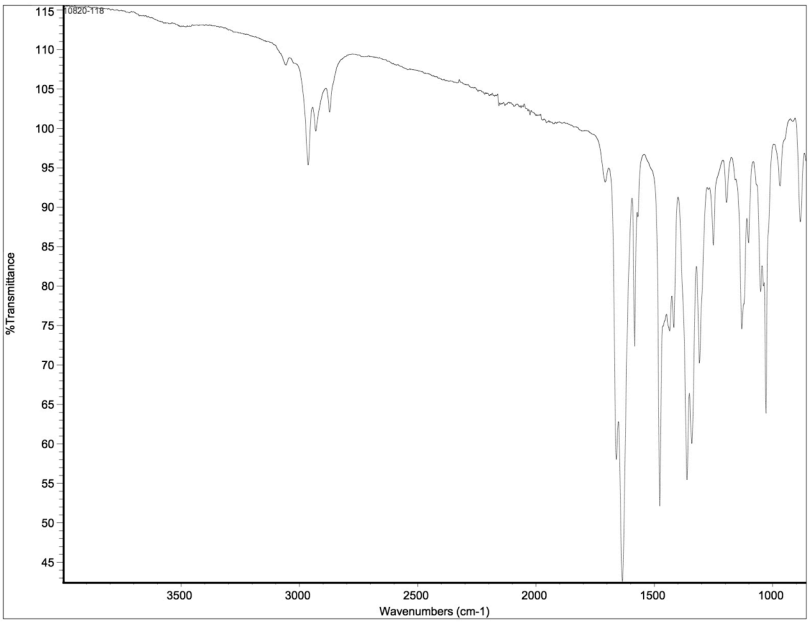

Figure A6.29 Infrared spectrum of compound **6.37**.

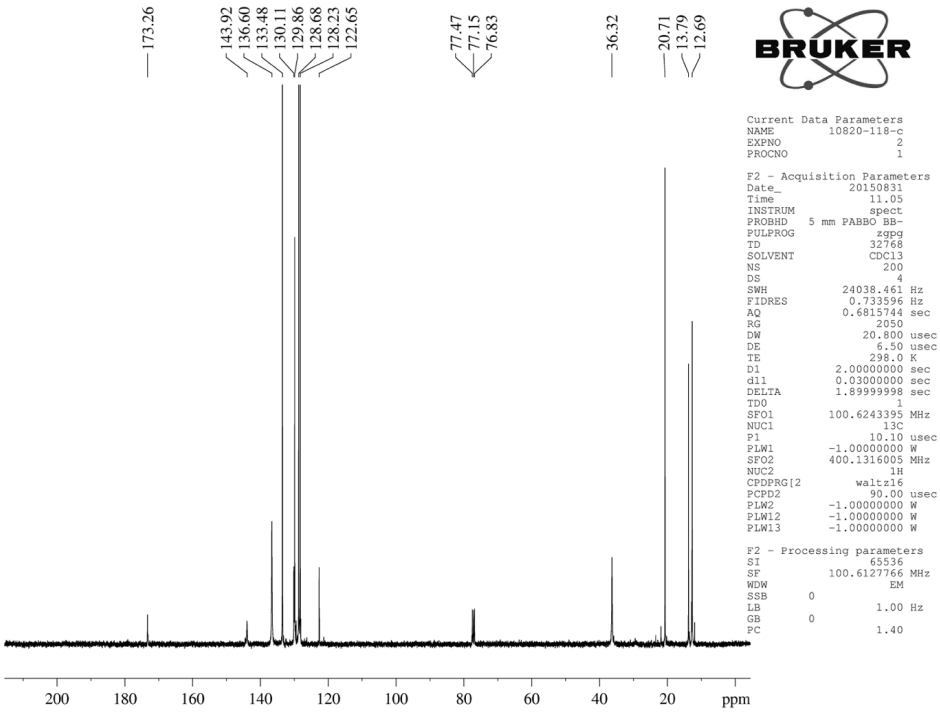

Figure A6.30 ^{13}C NMR (125 MHz, $CDCl_3$) of compound **6.37**.

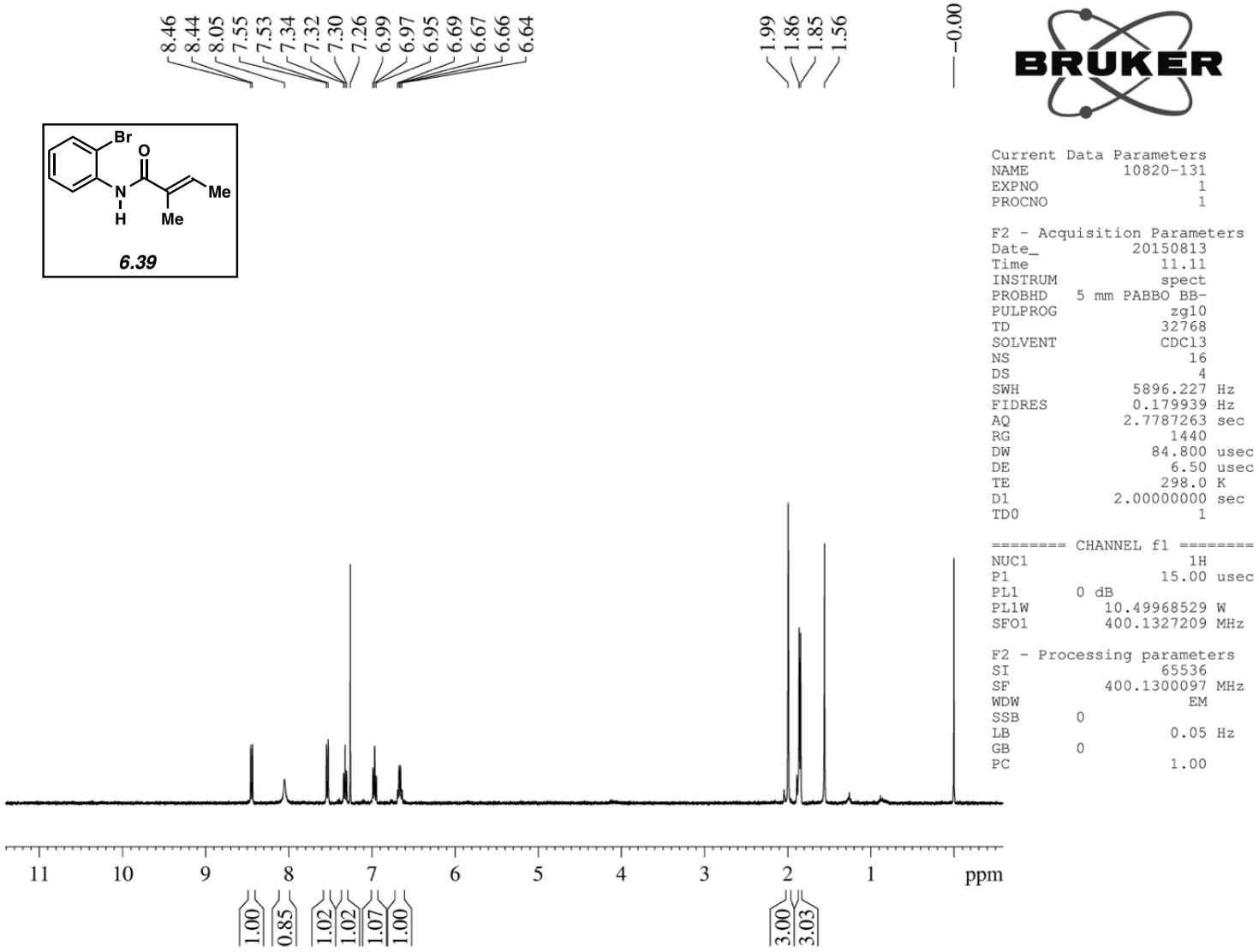

Figure A6.31 ^{1}H NMR (500 MHz, $CDCl_3$) of compound **6.39**.

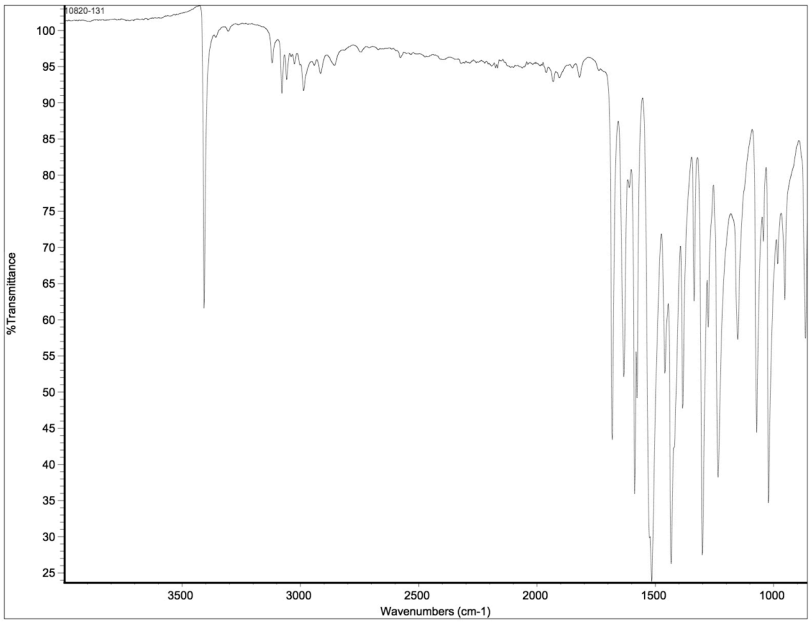

Figure A6.32 Infrared spectrum of compound **6.39**.

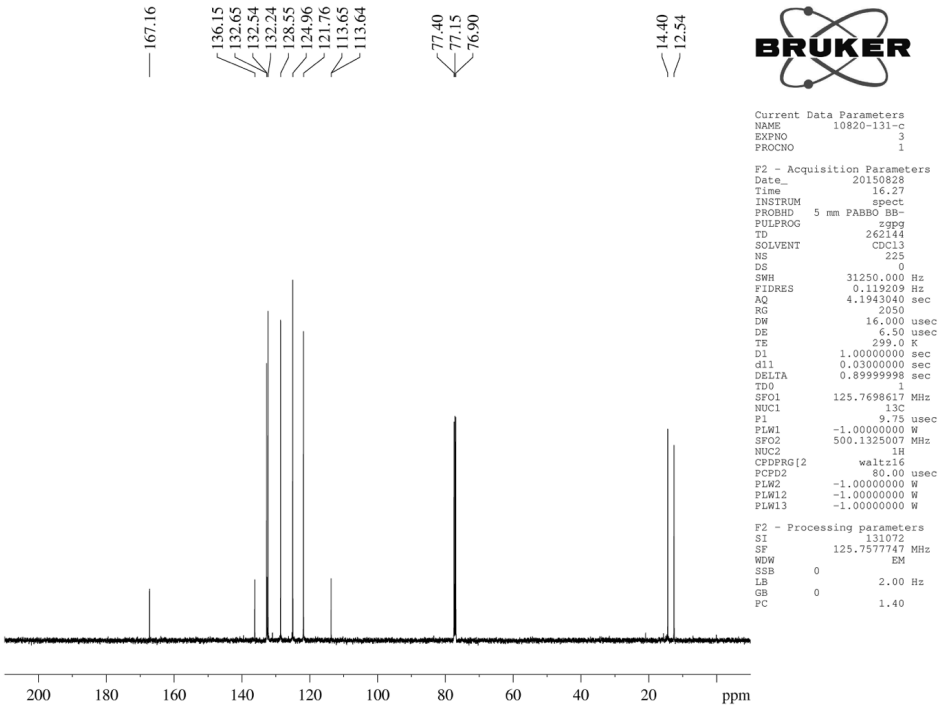

Figure A6.33 ^{13}C NMR (125 MHz, $CDCl_3$) of compound **6.39**.

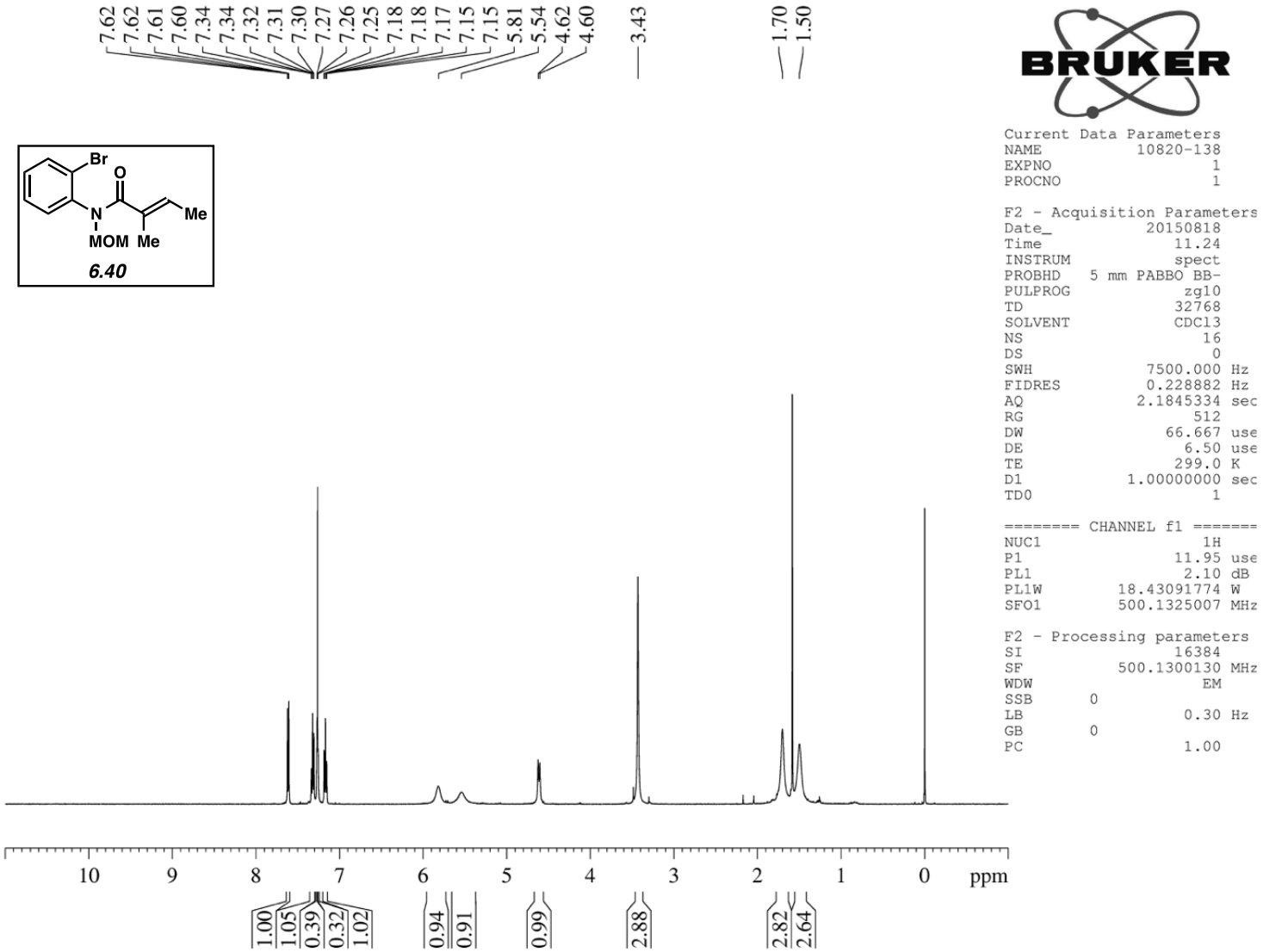

Figure A6.34 ^{1}H NMR (500 MHz, $CDCl_3$) of compound **6.40**.

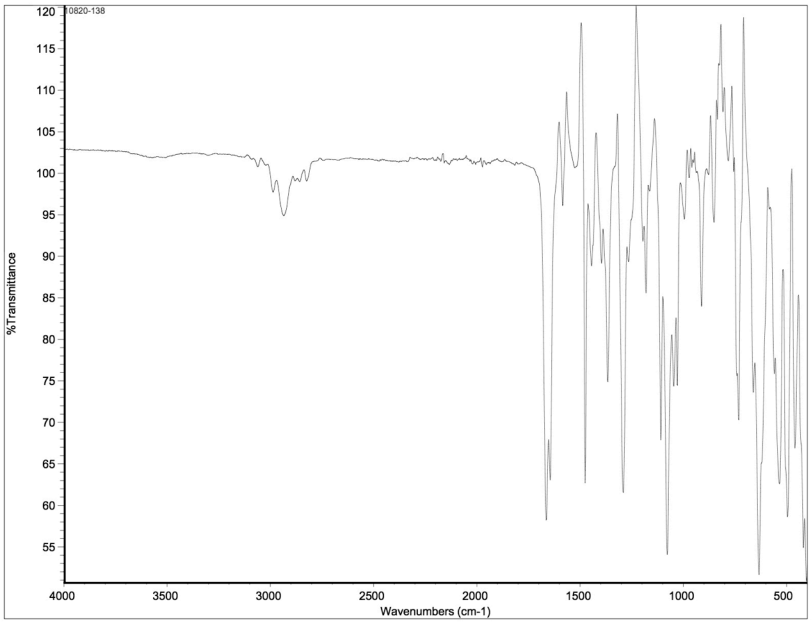

Figure A6.35 Infrared spectrum of compound **6.40**.

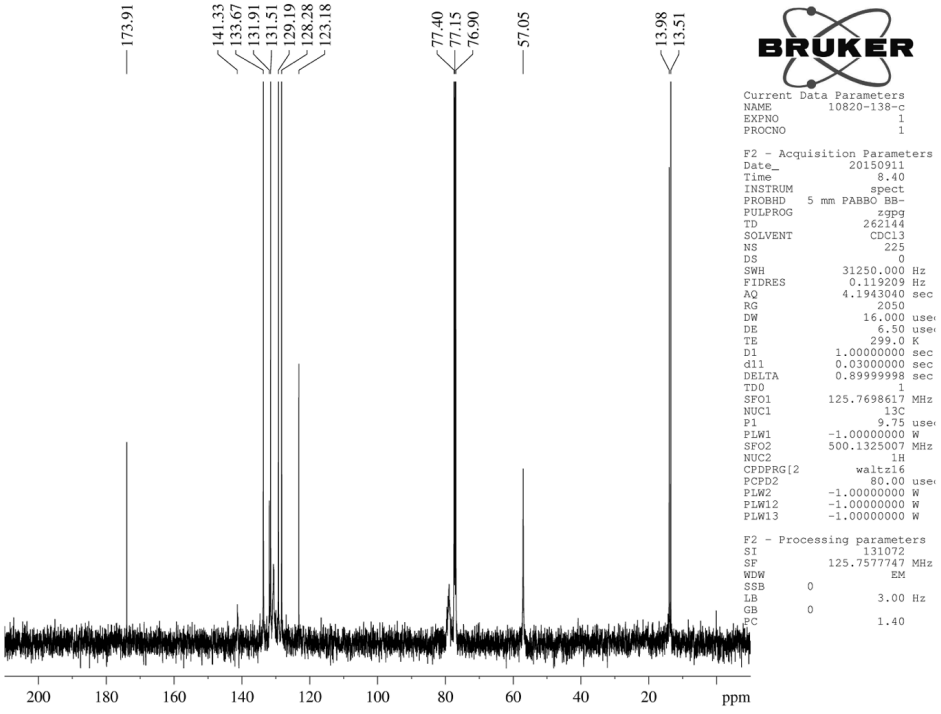

Figure A6.36 ^{13}C NMR (125 MHz, $CDCl_3$) of compound **6.40**.

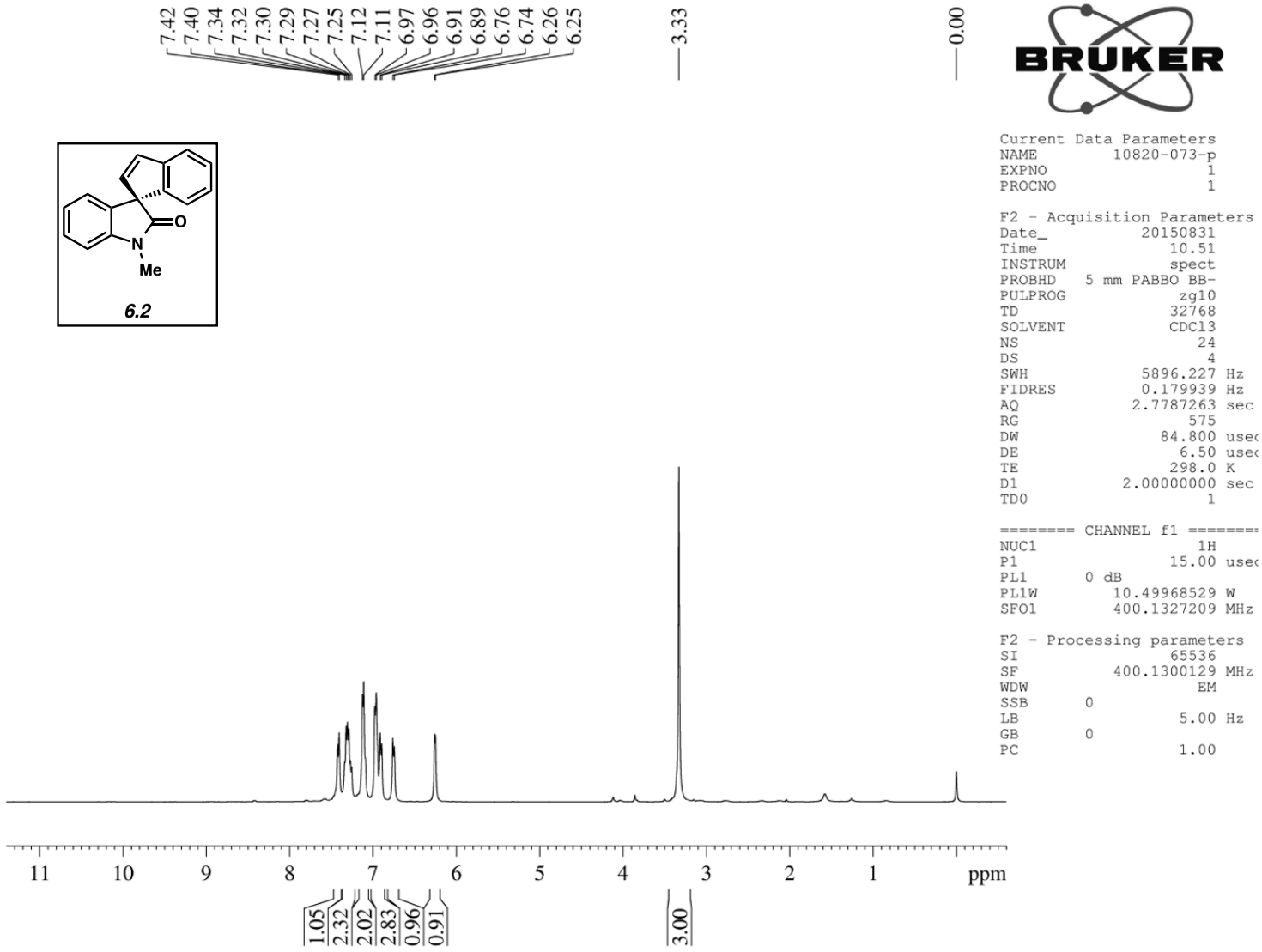

Figure A6.37 ^{1}H NMR (500 MHz, $CDCl_3$) of compound **6.2**.

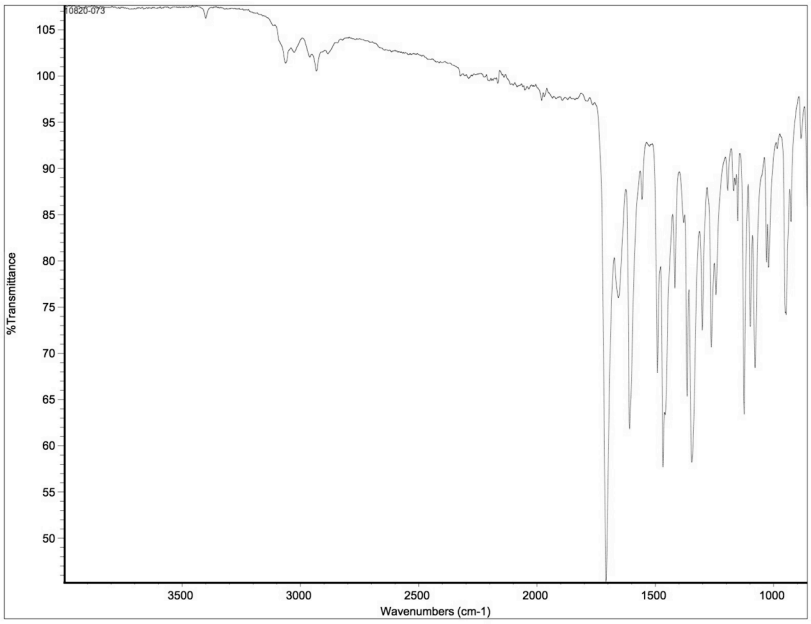

Figure A6.38 Infrared spectrum of compound **6.2**.

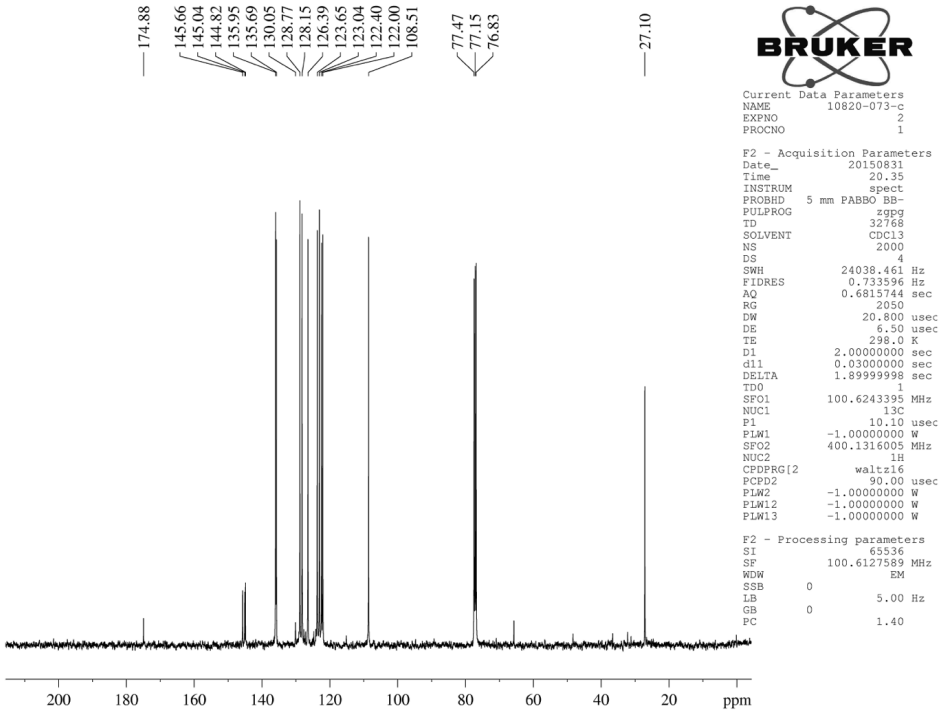

Figure A6.39 ^{13}C NMR (125 MHz, $CDCl_3$) of compound **6.2**.

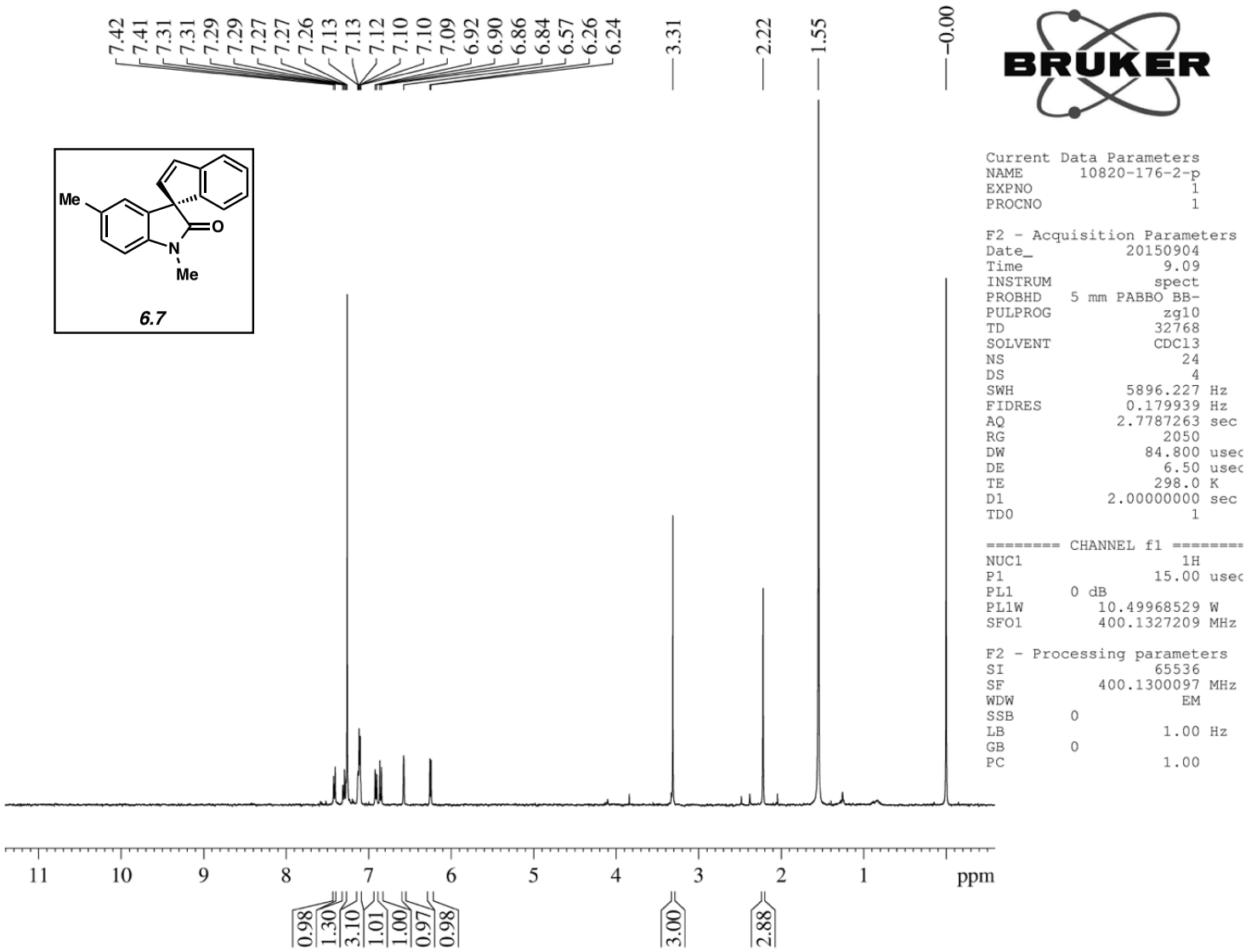

Figure A6.40 ^{1}H NMR (500 MHz, $CDCl_3$) of compound **6.7**.

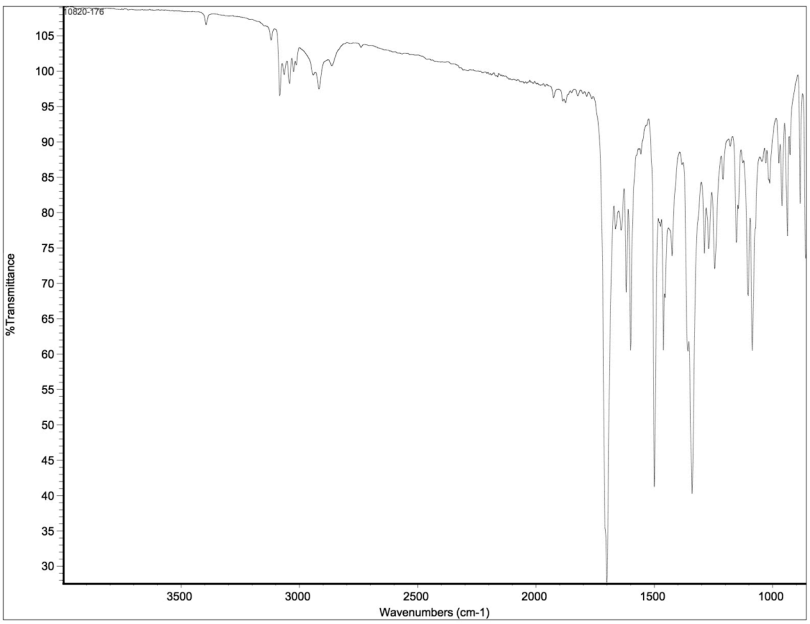

Figure A6.41 Infrared spectrum of compound **6.7**.

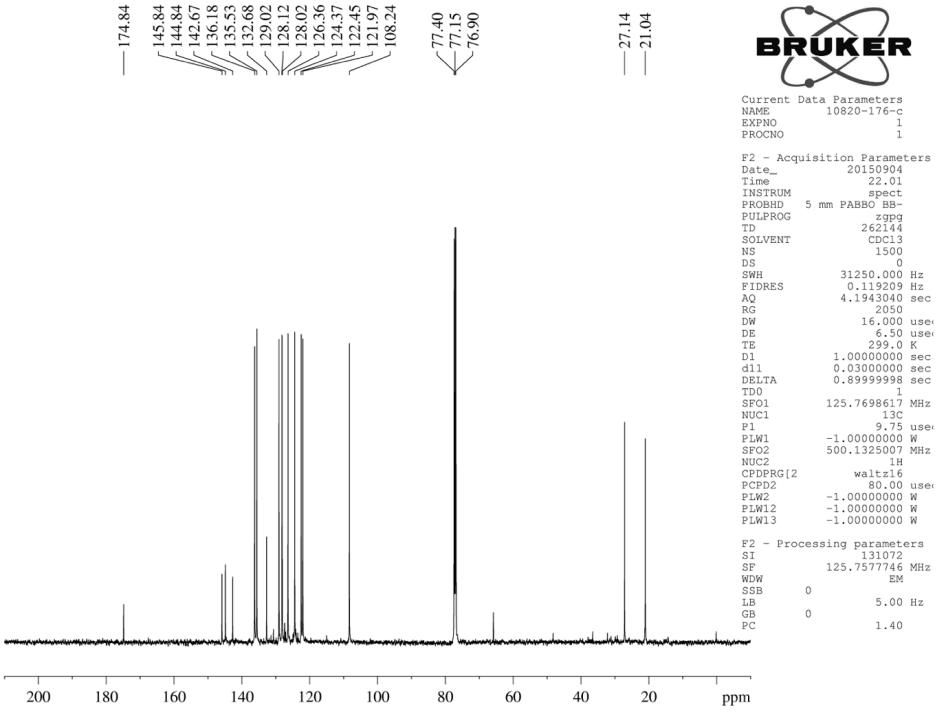

Figure A6.42 ^{13}C NMR (125 MHz, $CDCl_3$) of compound **6.7**.

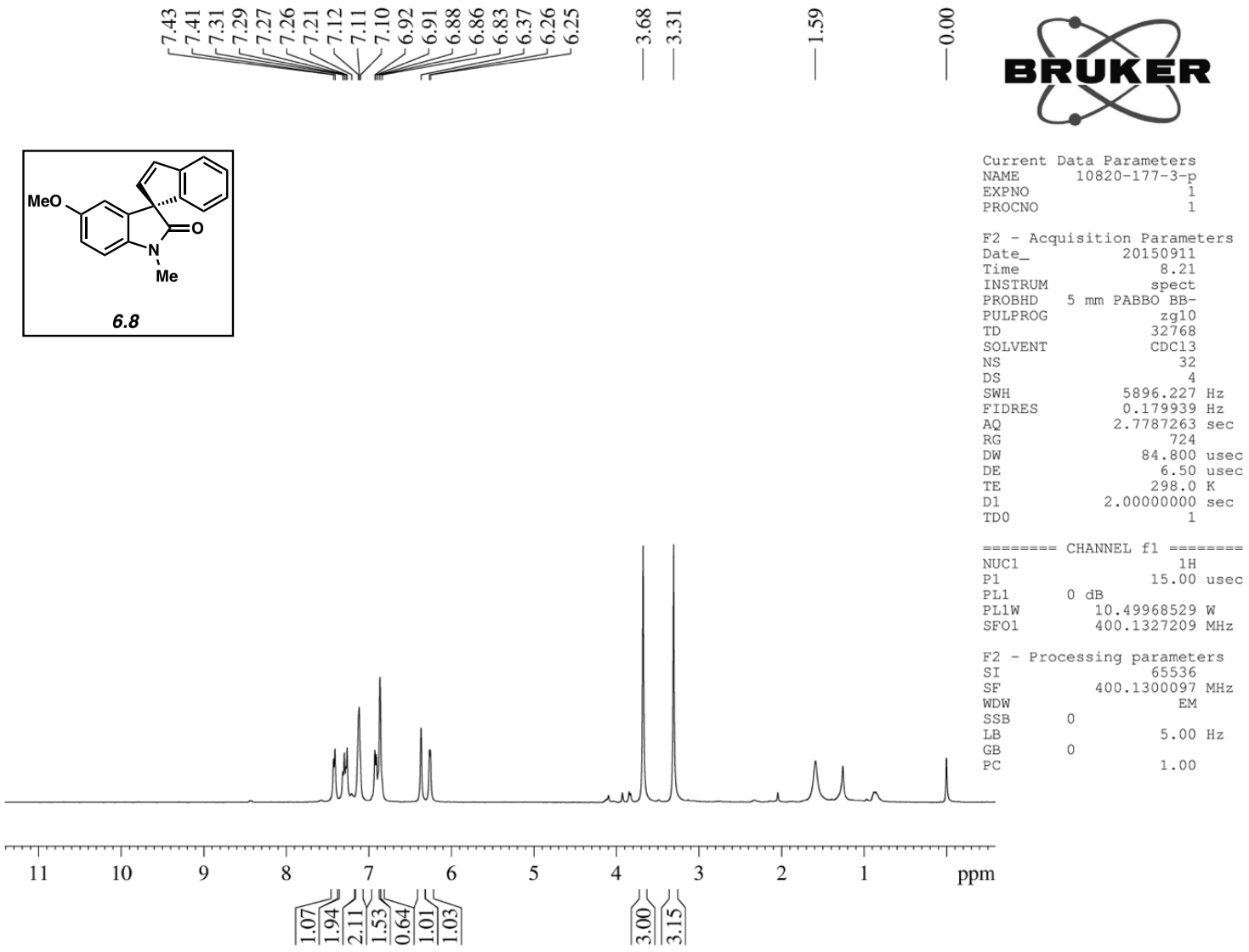

Figure A6.43 ^{1}H NMR (500 MHz, $CDCl_3$) of compound **6.8**.

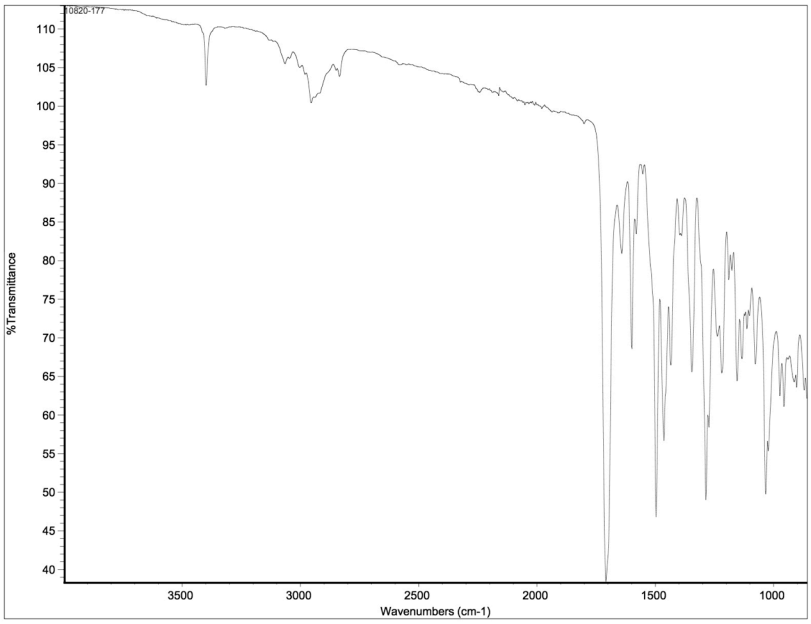

Figure A6.44 Infrared spectrum of compound **6.8**.

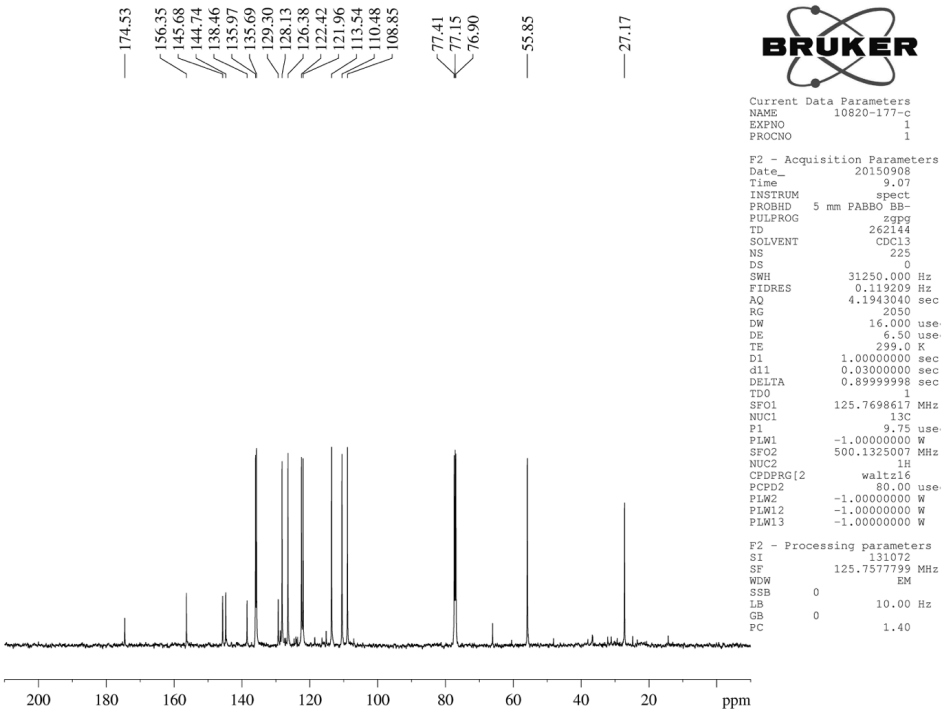

Figure A6.45 ^{13}C NMR (125 MHz, $CDCl_3$) of compound **6.8**.

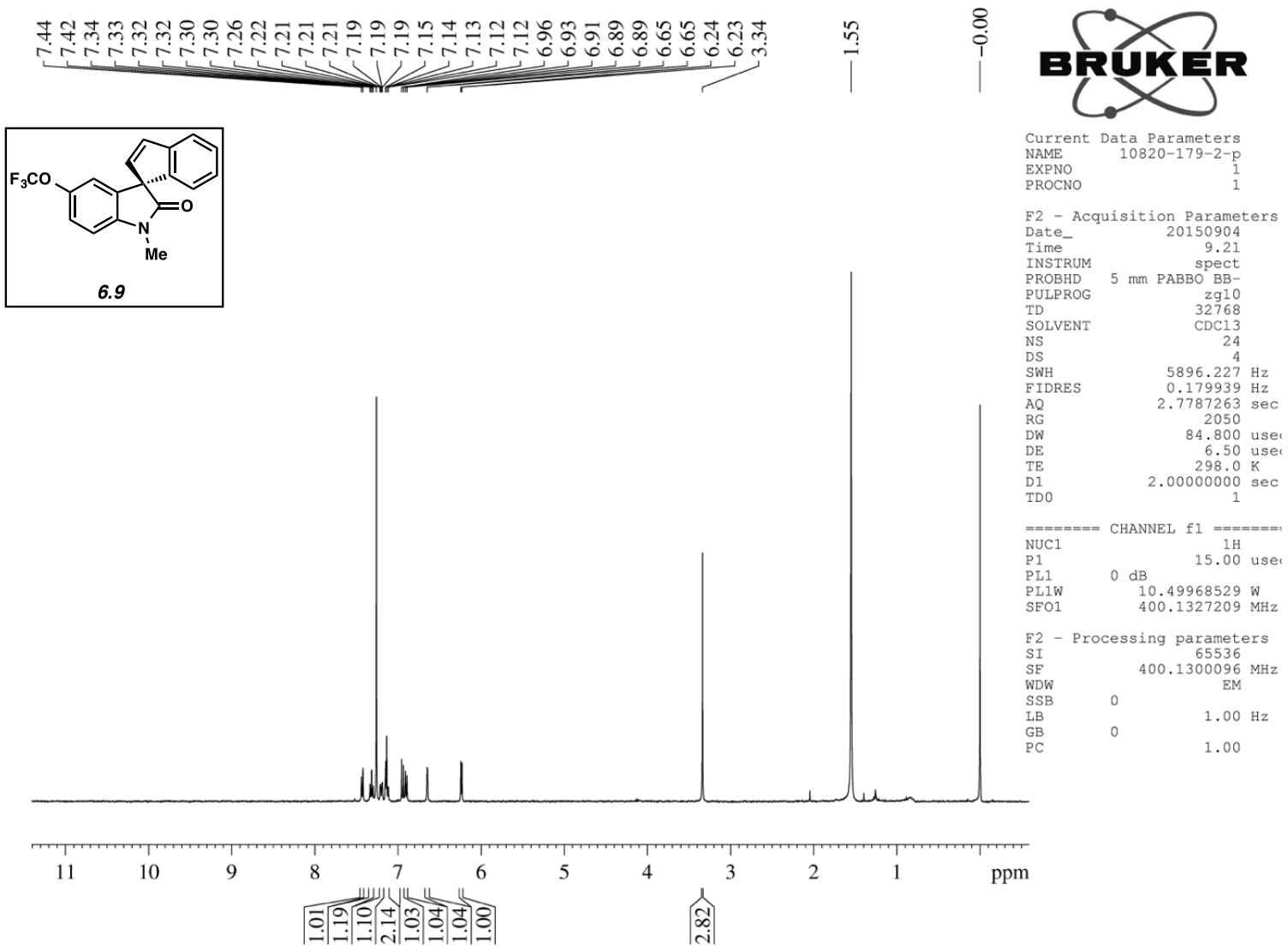

Figure A6.46 ^{1}H NMR (500 MHz, $CDCl_3$) of compound **6.9**.

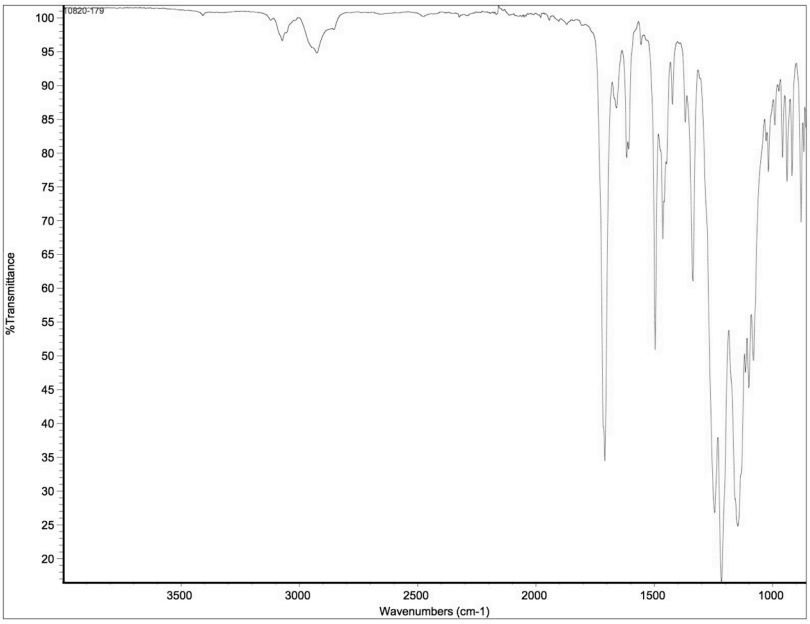

Figure A6.47 Infrared spectrum of compound **6.9**.

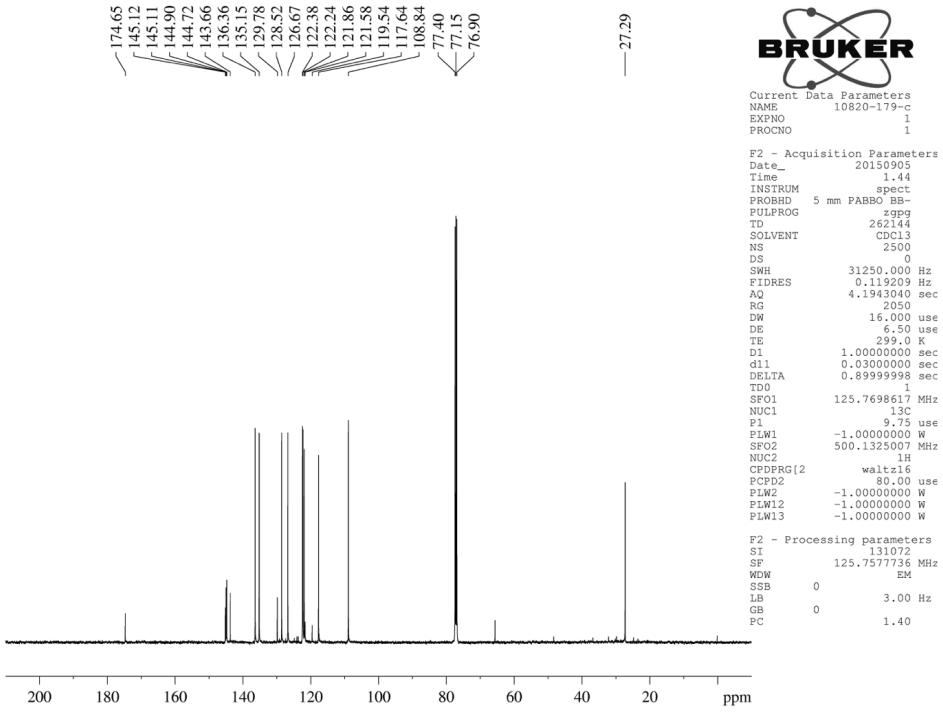

Figure A6.48 ^{13}C NMR (125 MHz, $CDCl_3$) of compound **6.9**.

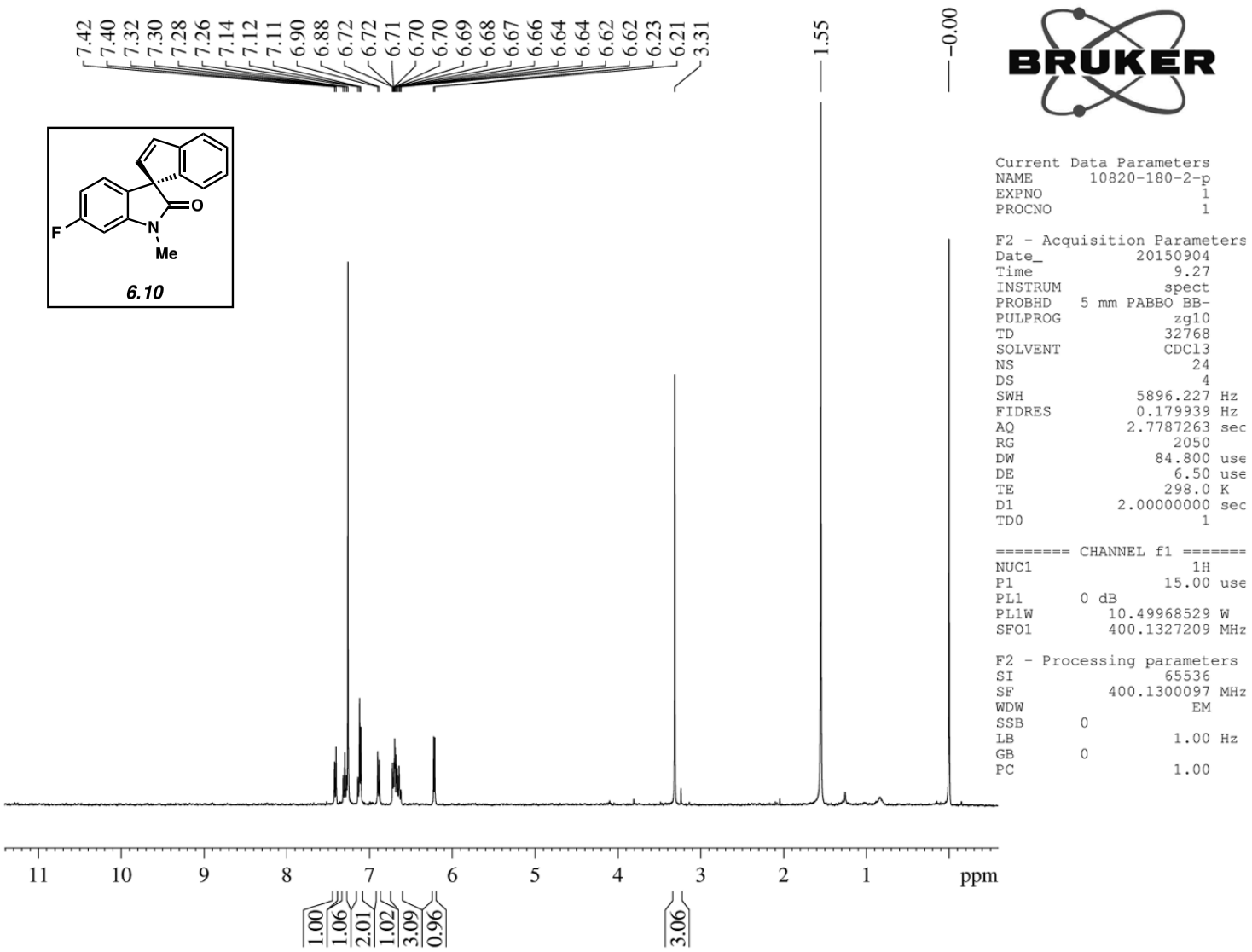

Figure A6.49 ^{1}H NMR (500 MHz, $CDCl_3$) of compound **6.10**.

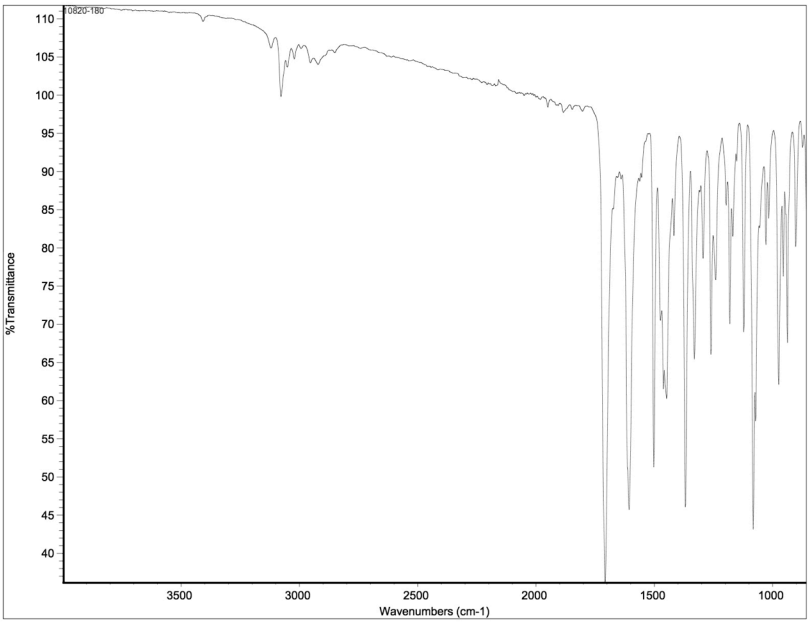

Figure A6.50 Infrared spectrum of compound **6.10**.

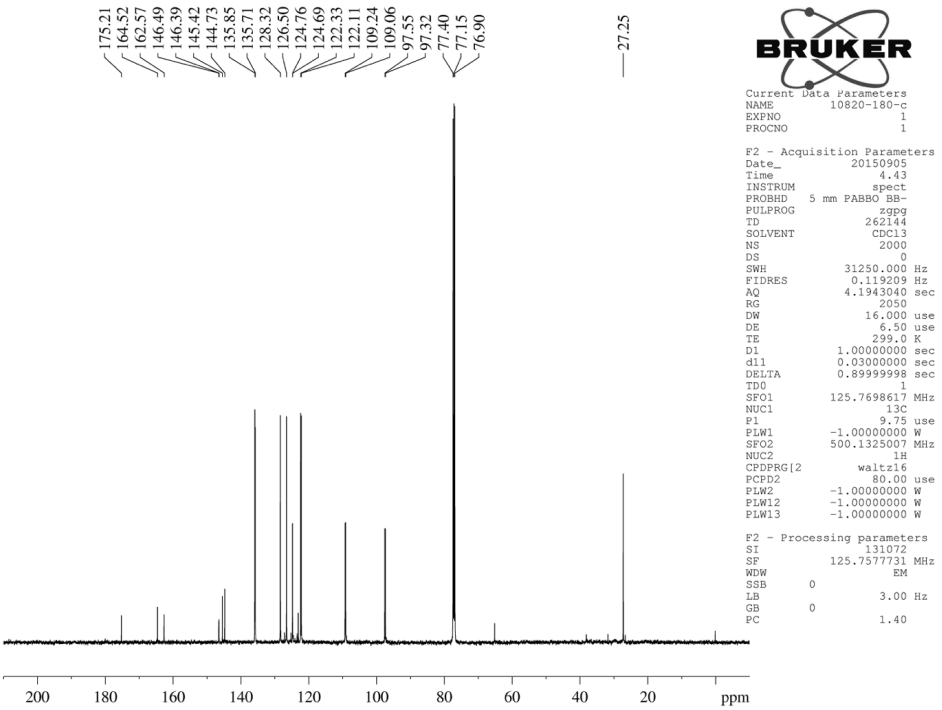

Figure A6.51 ^{13}C NMR (125 MHz, $CDCl_3$) of compound **6.10**.

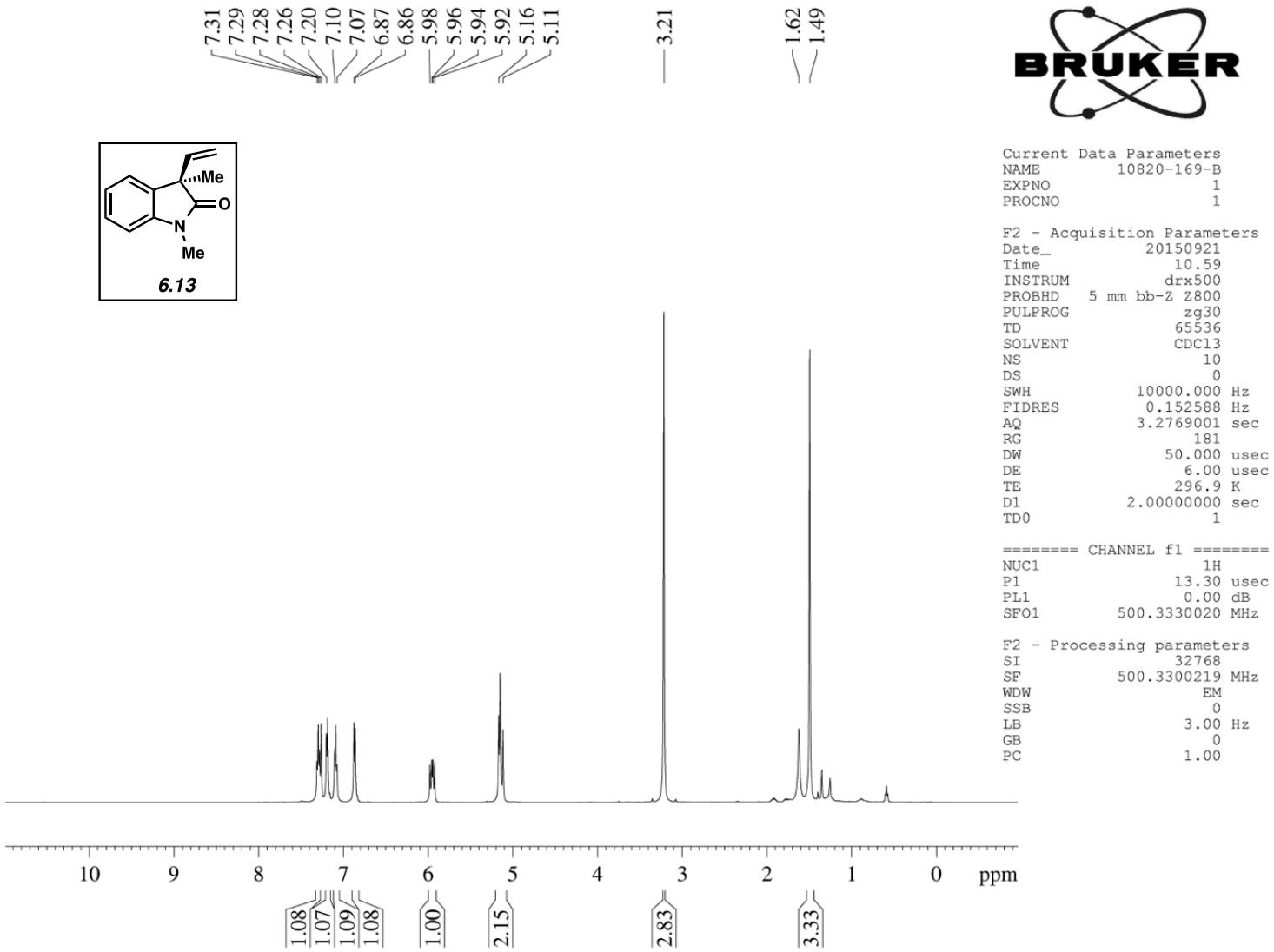

Figure A6.52 ^{1}H NMR (500 MHz, $CDCl_3$) of compound **6.13**.

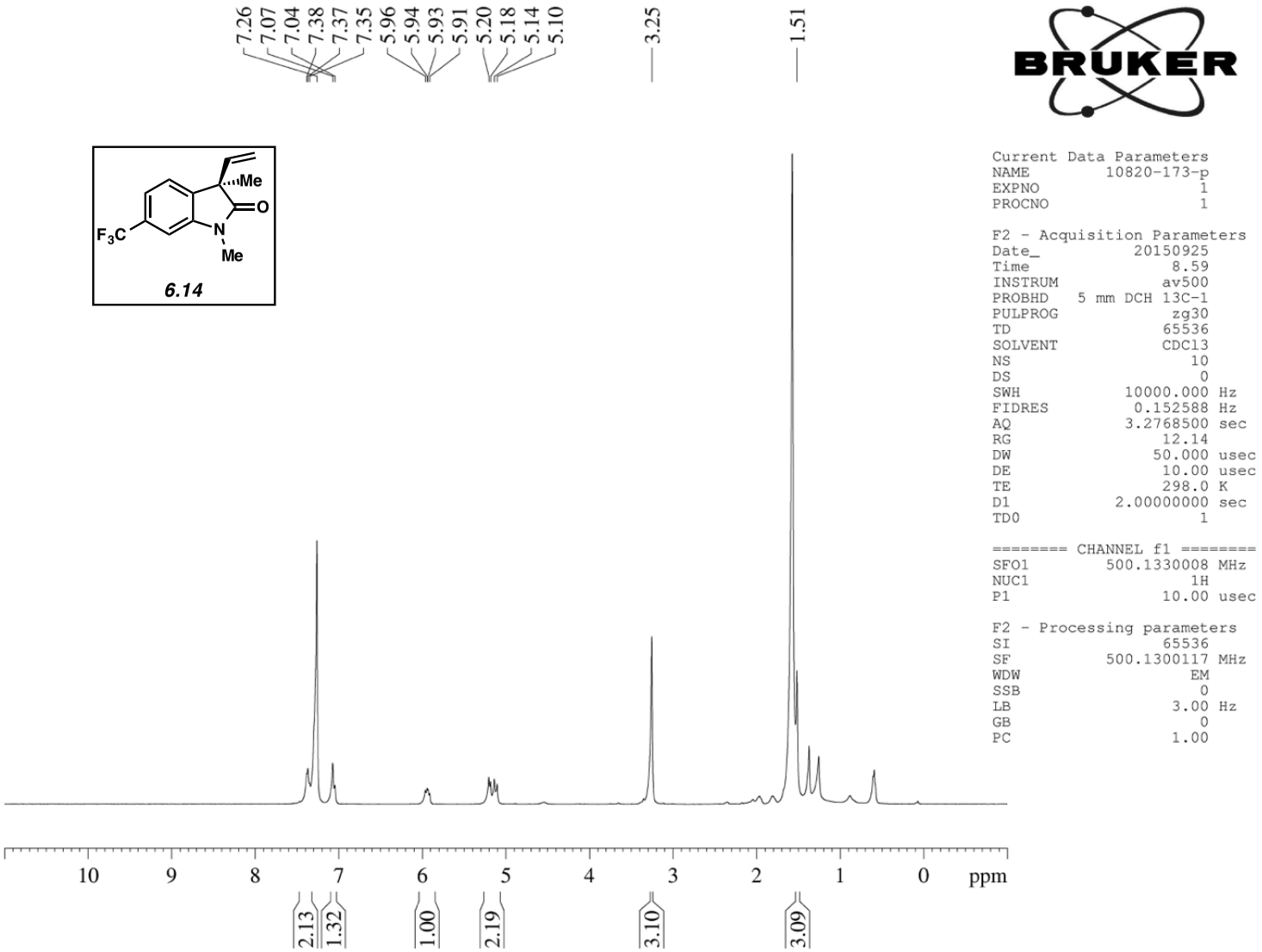

Figure A6.53 ^{1}H NMR (500 MHz, $CDCl_3$) of compound **6.14**.

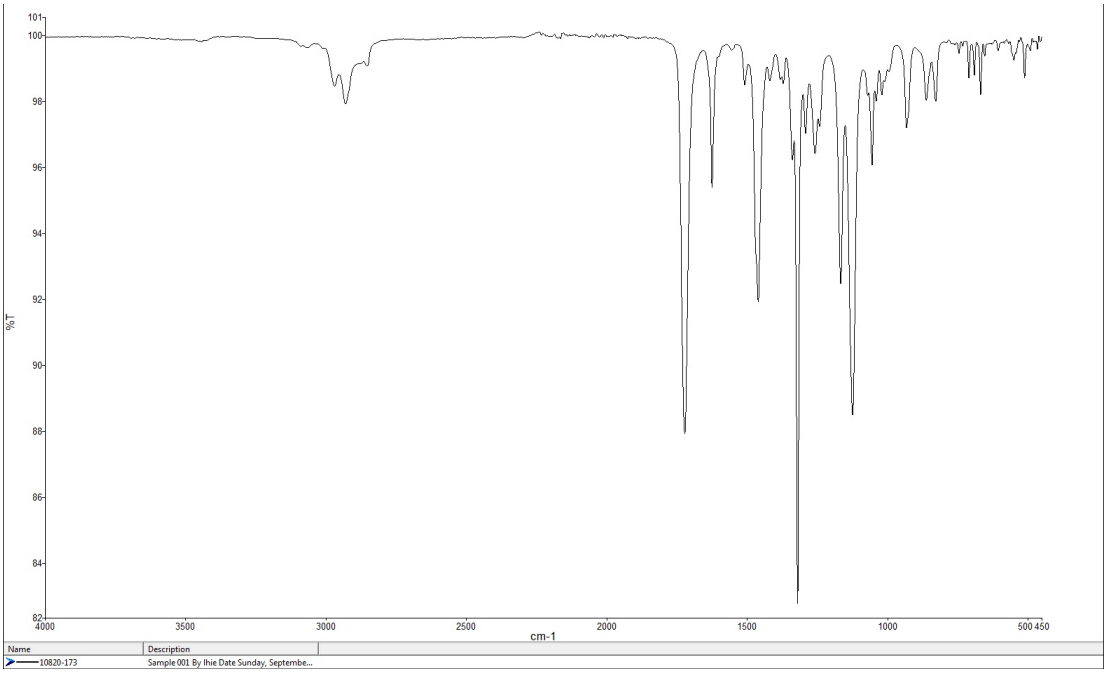

Figure A6.54 Infrared spectrum of compound **6.14**.

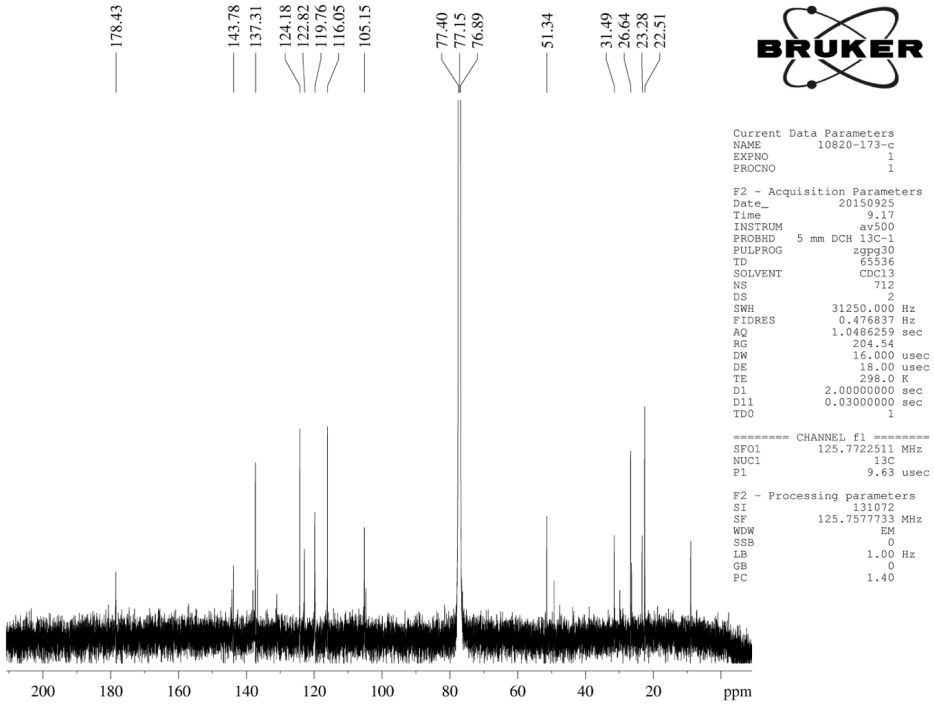

Figure A6.55 ^{13}C NMR (125 MHz, $CDCl_3$) of compound **6.14**.

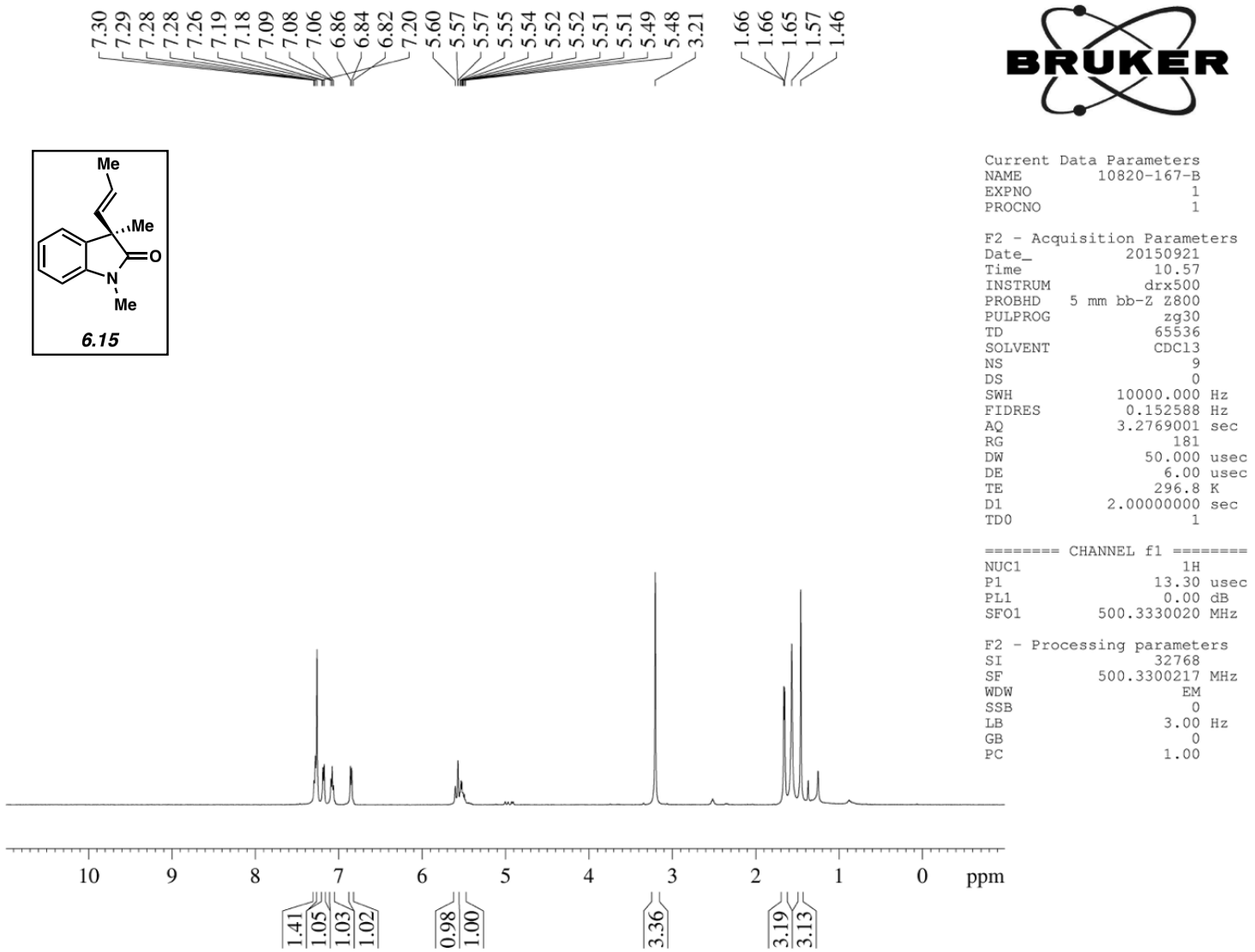

Figure A6.56 ^{1}H NMR (500 MHz, $CDCl_3$) of compound **6.15**.

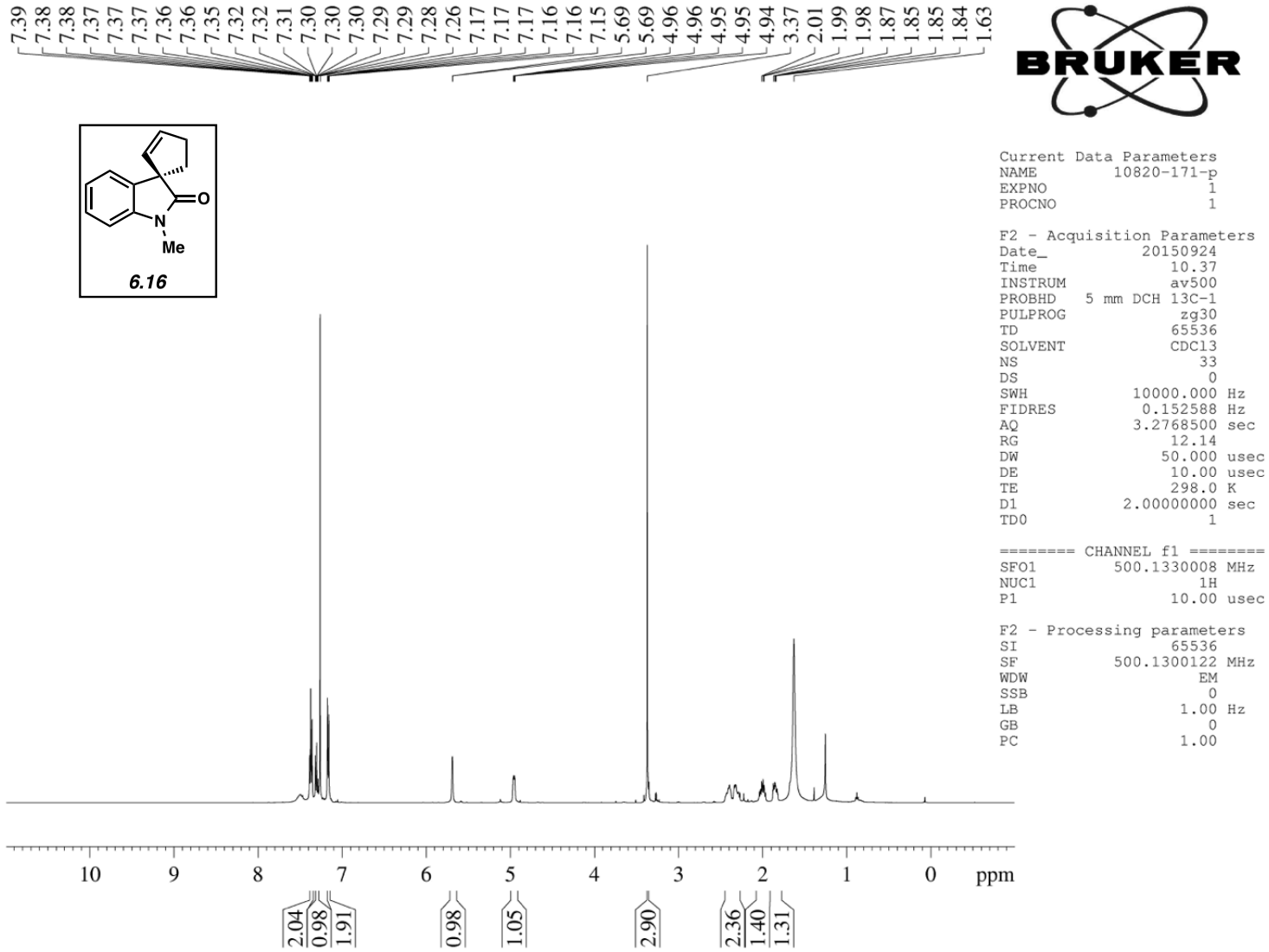

Figure A6.57 ^{1}H NMR (500 MHz, $CDCl_3$) of compound **6.16**.

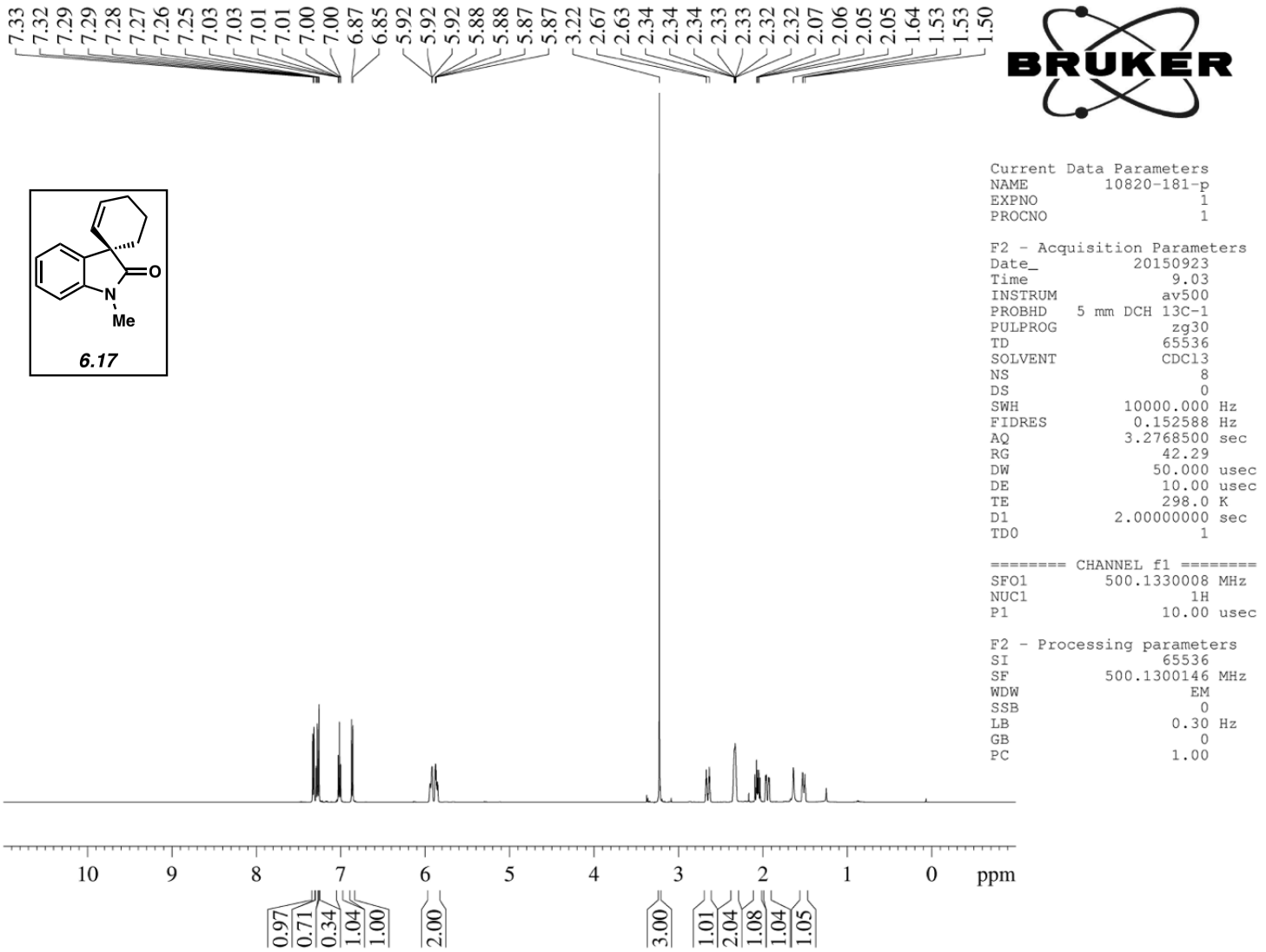

Figure A6.58 ^{1}H NMR (500 MHz, $CDCl_3$) of compound **6.17**.

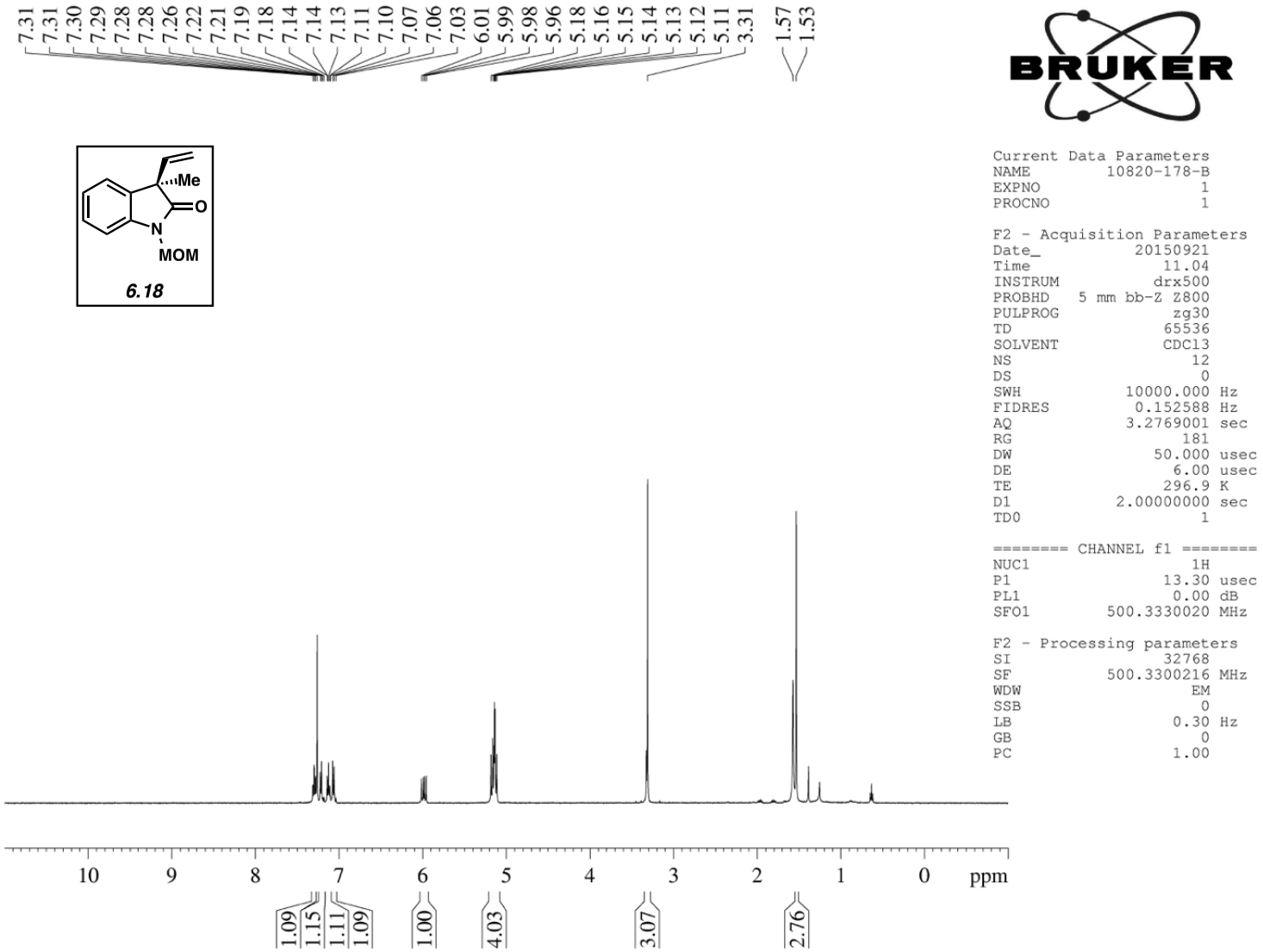

Figure A6.59 ^{1}H NMR (500 MHz, $CDCl_3$) of compound **6.18**.

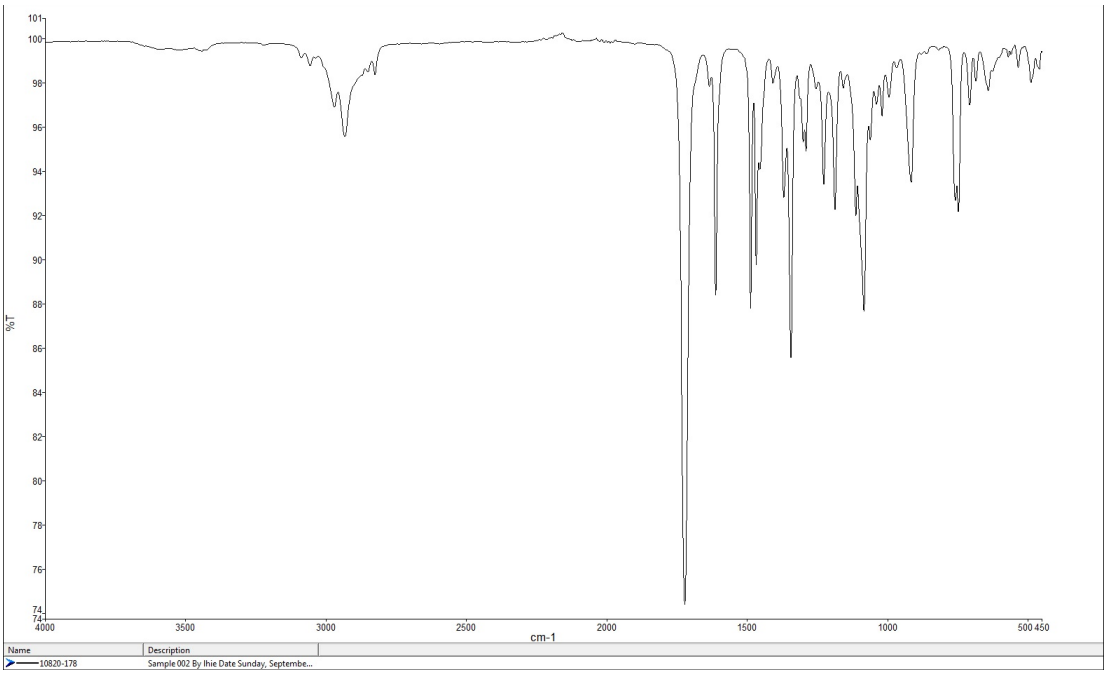

Figure A6.60 Infrared spectrum of compound **6.18**.

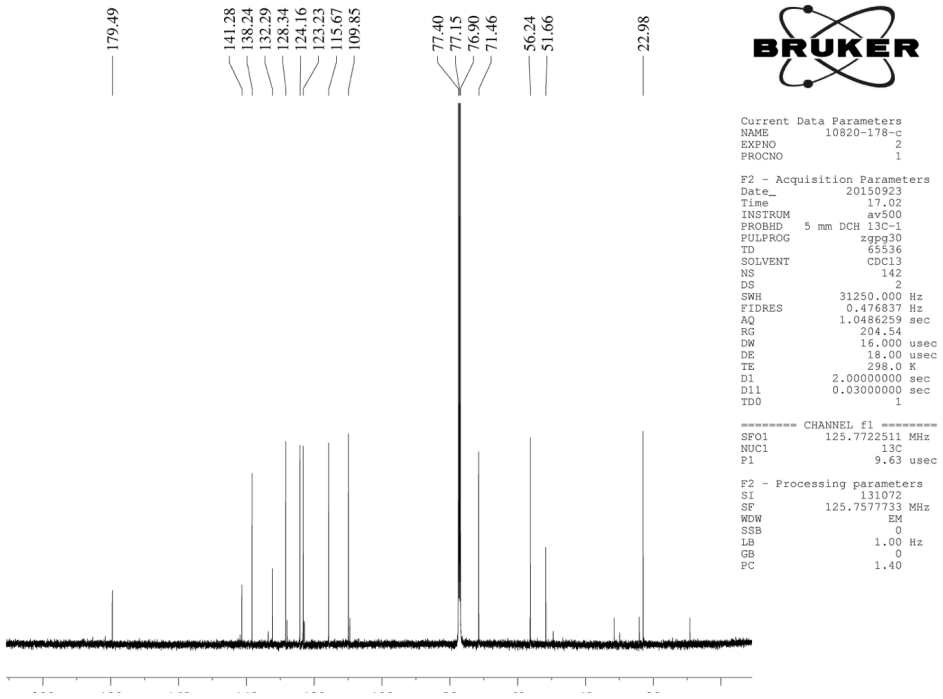

Figure A6.61 ^{13}C NMR (125 MHz, $CDCl_3$) of compound **6.18**.

6.6. Notes and References

[1] (a) Tasker, S. Z.; Standley, E. A.; Jamison, T. F. *Nature* **2014**, *509*, 299–309. (b) Mesganaw, T.; Garg, N. K. *Org. Process Res. Dev.* **2013**, *17*, 29–39. (c) Yu, D.-G.; Li, B.-J.;. Shi, Z.-J *Acc. Chem. Res.* **2010**, *43*, 1486–1495. (d) Rosen, B. M.; Quasdorf, K. W.; Wilson, D. A.; Zhang, N.; Resmerita, A.-M.; Garg, N. K.; Percec, V. *Chem. Rev.* **2011**, *111*, 1346–1416. (e) Li, B.-J.; Yu, D.-G.; Sun, C.-L.; Shi, Z.-J. *Chem.–Eur. J.* **2011**, *17*, 1728–1759.

[2] (a) Mori, M.; Oda, I.; Ban, Y. *Tetrahedron Lett.* **1982**, 5315–5318. (b) Terpko, M. O.; Heck, R. F. *J. Am. Chem. Soc.* **1979**, *101*, 5281–5283. (c) Abelman, M. M.; Oh, T.; Overman, L. E. *J. Org. Chem.* **1987**, *52*, 4130–4133. (d) Early, W. G.; Oh, T.; Overman, L. E. *Tetrahedron Lett.* **1988**, *29,* 3785–3788. (e) Ashimori, A.; Overman, L. E. *J. Org. Chem.* **1992**, *57*, 4571–4572. (f) Madin, A.; Overman, L. E. *Tetrahedron Lett.* **1992**, *33*, 4859–4862. (g) Amengual, R.; Genin, E.; Michelet, V.; Savignac, M.; Genêt, J.-P. *Adv. Synth. Catal.* **2002***, 344*, 393–398. (h) Kiely, D.; Guiry, P. J. *J. Organomet. Chem.* **2003**, *687*, 545–561. (i) Busacca, C. A.; Grossbach, D.; Campbell, S. J.; Dong, Y.; Eriksson, M. C.; Harris, R. E.; Jones, P.-J.; Kim, J.-Y.; Lorenz, J. C.; McKellop, K. B.; O'Brien, E. M.; Qiu, F.; Simpson, R. D.; Smith, L.; So, R. C.; Spinelli, E. M.; Vitous, J.; Zavattaro, C. *J. Org. Chem.* **2004**, *69*, 5187–5195. (j). Busacca, C. A.; Grossbach, D.; So, R. C.; O'Brien, E. M.; Spinelli, E. M. *Org. Lett.* **2003**, *5*, 595–598.

[3] For selected reviews on palladium-catalyzed Heck cyclizations, see: (a) Beletskaya, A. V.; Cheprakov, I. P. *Chem. Rev.* **2000**, *100*, 3009–3066. (b) Zeni, G.; Larock, R. C. *Chem. Rev.* **2006**, *106*, 4644–4680. (c) Nicolaou, K. C.; Bulger, P. G.; Sarlah, D. *Angew. Chem. Int. Ed.* **2005**, *44*, 4442–4489. (d) Dounay, A. B.; Overman, L. E. *Chem. Rev.* **2003**, *103*, 2945–2963. (e) Cacchi, S.; Fabrizi, G. *Chem. Rev.* **2005**, *105*, 2873–2920.

[4] Boldrini, G. P.; Savoia, D.; Tagliavini, E.; Trombinni, C.; Umani Ronchi, A. *J. Organomet. Chem.* **1986**, *301*, C62–64. (b) Lebedev, S. A.; Lopatina, V. S.; Petrow, E. S.; Beletskaya, L. P. *J. Organomet. Chem.* **1988**, *344*, 253–259. (c) Ehle, A. R.; Zhou, Q.; Watson, M. P. *Org. Lett.* **2012**, *14*, 1202–1205. (d) Inamoto, K.; Kuroda, J.-I.; Hiroya, K.; Noda, Y.; Watanabe, M.; Sakamoto, T. *Organometallics* **2006**, *25*, 3095–3098. (e) Sun, L.; Pei, W.; Shen, C. *J. Chem. Res.* **2006**, 388–389. (f) Kelkar, A. A.; Hanaoka, T.; Kubotam, Y.; Sugi, Y. *Cat. Lett.* **1994**, *29*, 69–75. (g) Gøgsig, T. M.; Kleimark, J.; Nilsson Lill, S. O.; Korsager, S.; Lindhardt, A. T.; Norrby, P.-O.; Srydstrup, T. F. *J. Am. Chem. Soc.* **2012**, *134*, 443–452. (h) Tasker, S. Z.; Gutierrez, A. C.; Jamison, T. F. *Angew. Chem. Int. Ed.* **2014**, *53*, 1858–1861. (i) Iyer, S.; Ramesh, C.; Ramani, A. *Tetrahedron Lett.* **1997**, *38*, 8533–8536. (j) Lin, P.-S.; Jeganmohan, M.; Cheng, C.-H. *Chem. Asian J.* **2007**, *2*, 1409–1416. (k) Wang, Z.-X.; Chai, Z.-C. *Eur. J. Inorg. Chem.* **2007**, 4492–4499. (l) Ma, S.; Wang, H.; Gao, K.; Zhao, F. *J. Mol. Cat. A.* **2006**, 17–20. (m) Bhanage, B. M.; Zhao, F.; Shirai, M.; Arai M. *Cat. Lett.* **1998**, *54*, 195–198.

[5] Few nickel-catalyzed methods to build quaternary stereocenters are available; examples include arylcyanation, C–O bond cleavage, Friedel–Crafts alkylation, and Michael addition. For selected examples, see reference 7 and the following: a) Spielvogel, D. J.; Buchwald, S. L. *J. Am. Chem. Soc.* **2002**, *124*, 3500–3501. (b) Zhang, A.; Rajanbabu, T. V. *J. Am. Chem. Soc.* **2006**, *128*, 5620–5621. (c) Zultanski, S. L.; Fu, G. C. *J. Am Chem Soc.* **2013**, *135*, 624–627. (d) Hong, Y. C.; Gandeepan, P.; Mannathan, S.; Lee, W. T.; x. Cheng, W. T. *Org. Lett.* **2014**, *16*, 806–809. (e) Gao, J.-R.; Wu, H.; Xiang, B.; W.-B. Yu, Han, L. *J. Am. Chem. Soc.* **2013**, *135*, 2983–2986. (f) Cornella, J.; Jackson, E. P.; Martin, R. *Angew. Chem. Int. Ed.* **2015**, *54*, 4075–4078. (g) Gao, J.-R.; Wu, H.; Xiang, B.; Yu, W.-B.; Han, L.; Jia, Y.-X. *J. Am. Chem. Soc.* **2013**, *135*, 2983–2986. (h) Nakao, Y.; Ebata, S.; Yada, A.; Hiyama, T.; Ikawa, M.; Ogoshi. S. *J. Am. Chem. Soc.*

2008, *130*, 12874–12875. (i) Clariana, J.; Galvez, N.; Marchi, C.; Moreno-Manas, M.; Vallribera, A.; Molins, E. *Tetrahedron* **1999**, *55*, 7331–7344.

[6] Lhermet, R.; Durandetti, M.; Maddaluno, J. *Beilstein J. Org. Chem.* **2013**, *9*, 710–716.

[7] Watson, M. P.; Jacobsen, E. N. *J. Am. Chem. Soc.* **2008**, *130*, 12594–12595.

[8] (a) Bin Yu, B.; Yu, D. Q.; Liu, H. M. *Eur. J. Med. Chem.* **2015**, *97*, 673–698. (b) Cheng, D.; Ishihara, Y.; Tan, B.; Barbas III, C. F. *ACS Catal.* **2014**, *4*, 743–762. (c) Ziarani, G. M.; Lashgari, N. *Arkivoc* **2012**, 277-320. (d) Zhou, F.; Liu, Y.-L.; Zhou, J. *Adv. Synth. Catal.* **2010**, *352*, 1381–1407.

[9] Lin, B.-L.; Liu, L.; Fu, Y.; Luo, S.-W.; Chen, Q.; Guo, Q.-X. *Organometallics* **2004**, *23*, 2114–2123.

[10] (a) Chakraborty, S.; Zhang, J.; Krause, J. A.; Guan, H. *J. Am. Chem. Soc.* **2010**, *132*, 8872–8873. (b) Lin, S.; Day, M. W.; Agapie, T. *J. Am. Chem. Soc.* **2011**, 133, 3828–3831. (c) Tran, B. L.; Pink, M.; Mindiola, D. J. *Organometallics* **2009**, 28, 2234–2243. (d). Tolman, C. A. *J. Am. Chem. Soc.* **1972**, *94*, 2994–2999.

[11] (a) Sole, D.; Cancho, Y.; Llebaria, A.; Josep, M.; Moréto, J. M.; Delgado, A. J. Org. Chem. **1996**, 61, 5895–5904. (b) Kim, H.; Lee, C. *Org. Lett.* **2011**, *13*, 2050–2053.

[12] For examples discussing the use of external reductants for nickel-catalyzed systems, see: (a) Hie, L.; Ramgren, S. D.; Mesganaw, T.; Garg, N. K. *Org. Lett.* **2012,** *14*, 4782–4185. (b) Colon, I.; Kelsey, D. R. *J. Org. Chem.* **1986,** *51*, 2627–2637.

[13] When the amount of manganese was decreased to 1.0 equivalent, only a slight decrease of yield (71% yield) was obtained. When 0.5 equivalent was used, the yield of the reaction decreased significantly to 13% yield.

[14] This reaction can be set-up outside of a glove-box to afford similar yields.

[15] In the absence of base, the reaction gave oxindole **6.2** in 53% yield and oxindole **6.3** in 18% yield. Additionally, lowering the catalyst loading to 5 mol% of the nickel catalyst decreased the yield of **6.2** to 42% yield.

[16] The corresponding bromide substrate provided oxindole **6.16** in 20% yield at 60 °C and 27% yield at 80 °C.

[17] (a) Iyer, S.; Ramesh, C.; Ramani, A. *Tetrahedron Lett*. **1997**, *38*, 8533–8536. (b) Tasker, S. Z.; Jamison, T. F. *J. Am. Chem. Soc*. **2015**, *137*, 9531–9534. Also see references 11a and 11b.

[18] For the robustness screening concept, see: Collins, K. D.; Glorius, F. *Nature Chem*. **2013**, *5*, 597–601.

[19] Kale, A. P.; Kumar, G. S.; Mangadan, A. R. K.; Kapur, M. *Org. Lett*. **2015**, *17*, 1324–1327.

[20] Groth, U.; Koettgen, P.; Langenbach, P.; Lindermaier, A.; Schuetz, T.; Wiegand, M. *Synlett* **2008**, 1301–1304.

[21] Clark, A. J.; Jones, K. *Tetrahedron Lett*. **1989**, *30*, 5485–5488.

[22] Harayama, T.; Toko, H.; Nishioka, H.; Abe, H. Takeuchi, Y. *Heterocycles* **2003**, *59*, 541–546.

[23] Mukaiyama, T.; Usui, M.; Saigo, K. *Chem. Lett*. **1976**, *5*, 49–50.

[24] Nakamura, I.; Sato, Y.; Konta, S.; Terada, M. *Tetrahedron Lett*. **2009**, *50*, 2075–2077.

[25] Seashore-Ludlow, B.; Somfai, P. *Org. Lett.* **2010**, *12*, 3732–3735.

[26] Amengual, R.; Genin, E.; Michelet, V.; Savignac, M.; Genet, J.-P. *Adv. Synth. Catal*. **2002**, *344*, 393–398.

[27] Taylor, A. M.; Altman, R. A.; Buchwald, S. L. *J. Am. Chem. Soc*. **2009**, *131*, 9900–9901.

[28] Seashore-Ludlow, B.; Danielsson, J.; Somfai, P. *Adv. Synth. Catal*. **2012**, *354*, 205–216.

[29] Abelman, M. M.; Oh, T.; Overman, L. E. *J. Org. Chem*. **1987**, *52*, 4130–4133.

CHAPTER SEVEN

Nickel-Catalyzed Esterification of Aliphatic Amides

Liana Hie, Emma L. Baker, Sarah M. Anthony, Jean-Nicolas Desrosiers,
Chris Senanayake, and Neil K. Garg
Manuscript in preparation

7.1. Abstract

Recent studies have demonstrated that amides can be used in nickel-catalyzed reactions that lead to cleavage of the amide C–N bond, with formation of a C–C or C–heteroatom bond. However, the scope of these methodologies has been restricted to amides where the carbonyl is directly attached to an arene or heteroarene. We now report the catalytic C–N bond activation of amides derived from aliphatic carboxylic acids using nickel catalysis and the commercially available ligand terpyridine. The methodology requires only a slight excess of the alcohol nucleophile and is tolerant of variation in both coupling partners. Moreover, the reaction proceeds readily in the presence of heterocycles, epimerizable stereocenters, and amino acid-derived substrates. These studies are expected to further stimulate the use of amides as synthetic building blocks for C–C and C–heteroatom bond formation.

7.2. Introduction

Amides are prevalent functional groups seen in synthetic intermediates, natural products, proteins, and various other molecules of importance.[1] Accordingly, the development of methods to construct amide C–N bonds has been a popular topic of study for many decades.[1] In contrast,

the ability to harness amides as synthetic building blocks in C–N bond cleavage reactions has remained underdeveloped.[2,3] The low synthetic utility of amides can be attributed to the strength of the amide C–N bond, which benefits from well-known resonance stabilization.[4]

With this longstanding challenge in mind, recent efforts have focused on the metal-catalyzed cleavage of amide C–N bonds, with applications in C–C and C–heteroatom bond formation.[5,6,7] Breakthroughs in this area include palladium-catalyzed decarbonylative[6d] and non-decarbonylative[5,6b,e] C–C bond formations using twisted amides or other activated amide substrates. Additionally, nickel catalysis has been deemed effective for reactions of anilides and Ts- or Boc-activated amide derivatives (Figure 1).[6a,7] In turn, ketones, esters, or even other amides can be readily prepared under mild reaction conditions and in a predictable manner,[6a,7] using attractive non-precious metal catalysis.[8] Despite the promise of these methodologies, a notable drawback has been pervasive in amide activation chemistry: especially within the realm of nickel-catalyzed amide activation, the methodology has required that the amide substrate bear an aromatic (or heteroaromatic) ring attached to the carbonyl. For amide activation methodologies to become generally useful, we sought to overcome this limitation and enable the activation and cross-coupling of amides derived from aliphatic carboxylic acids.

Herein, we show for the first time that amides derived from aliphatic carboxylic acids can indeed be activated using nickel-catalysis, as demonstrated in the conversion of amides to esters. The methodology is tolerant of significant variation in both the amide and alcohol coupling partners, and readily proceeds in the presence of heterocycles, epimerizable stereocenters, and amino acid-derived substrates. These studies not only provide a facile means to convert amides to esters, which itself is a challenging transformation,[9] but should also greatly enable the use of amides as building blocks in chemical synthesis.[2]

Figure 7.1. Nickel-Catalyzed Activation of Benzamides and Derivatives (prior studies) and Nickel-Catalyzed Conversion of Aliphatic Amides to Esters (present study).

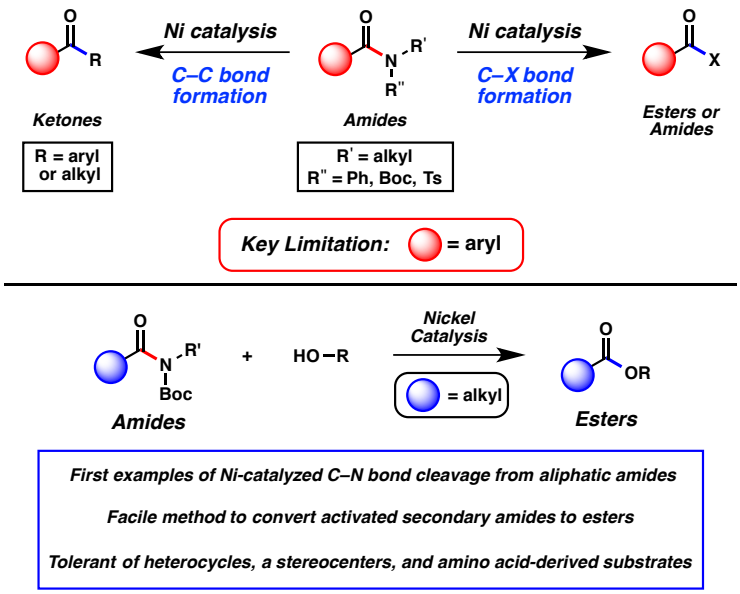

7.3. Optimization and Substrate Scope

We hypothesized that the choice of ligand in the conversion of aliphatic amides to esters could have a dramatic effect on the ease of oxidative addition, which was believed to be the rate-determining step of our proposed catalytic cycle, based on prior computational studies.[7a] Thus, we collaboratively performed an extensive survey of reaction parameters using the Boehringer Ingelheim catalysis screening facility. The screening efforts, which involved the testing of over 100 ligands,[10] were ultimately deemed fruitful and led us to focus on the use of pyridine-type ligands in optimization studies (Table 7.1). The challenging coupling of α-branched amide **7.1** with menthol (**7.2**, 1.2 equiv), a sterically hindered nucleophile, was selected for these efforts. Although the use of bipyridine or phenanthroline led to no appreciable yield of **7.3** (entries 1 and 2), the coupling product was obtained in 24% yield when terpyridine was employed (entry 3). Variations in ligand loading were also tested (entries 4 and 5), but 15 mol% (1:1 Ni to

terpyridine) was found to be ideal. Doubling of the equivalents of **7.2** did not lead to improvements (entry 6). However, it was found that concentration had an effect on the reaction (entries 7 and 8), with higher concentrations giving slightly increased yield of product **7.3**. Finally, we found that increasing the temperature to 100 °C delivered ester **7.3** in 56% yield.[11] As this test transformation allowed for the coupling of two significantly hindered fragments with the remaining mass being only unreacted starting material, we opted to evaluate the scope of our methodology under these reaction conditions.

Table 7.1. Optimization of Reaction Conditions.[a]

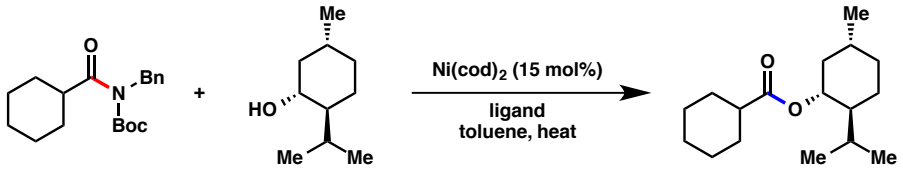

7.1 *7.2* *7.3*

Entry	*Ligand (loading)*	*Equivs of 7.2*	*Time*	*Concentration*	*Temp.*	*Yield*
1	bipyridine (15 mol%)	1.2 equiv	20 h	0.5 M	80 °C	0%
2	phenanthroline (15 mol%)	1.2 equiv	20 h	0.5 M	80 °C	0%
3	terpyridine (15 mol%)	1.2 equiv	20 h	0.5 M	80 °C	24%
4	terpyridine (7.5 mol%)	1.2 equiv	20 h	0.5 M	80 °C	31%
5	terpyridine (30 mol%)	1.2 equiv	20 h	0.5 M	80 °C	31%
6	terpyridine (15 mol%)	2.5 equiv	20 h	0.5 M	80 °C	30%
7	terpyridine (15 mol%)	1.2 equiv	20 h	0.33 M	80 °C	19%
8	terpyridine (15 mol%)	1.2 equiv	20 h	1.0 M	80 °C	35%
9	terpyridine (15 mol%)	1.2 equiv	20 h	1.0 M	100 °C	56%

[a] Yields were determined using hexamethylbenzene as an internal standard.

Having identified suitable reaction conditions, we evaluated the scope of the amide substrate using a slight excess of 1-hexanol as the alcohol coupling partner (Figure 7.2). We were delighted to find that lower catalyst loadings of 5 or 10 mol% nickel could be employed in all cases to give synthetically useful yields of products. Non-α-branched substrates were well tolerated, as deemed by the formation of **7.7**–**7.8**. Of note, the preparation of **7.9** in 92% yield (using 2.5 equivalent of **7.5**), demonstrates the feasibility of converting two amides to esters in the same pot. Although our focus has been on amides derived from aliphatic substrates, it should be noted that vinyl amides can also be employed, as shown by the synthesis of **7.10**. With regard to α-branched aliphatic substrates, amides derived from cyclopentane carboxylic acid and cyclohexane carboxylic acid could be used, as seen by the formation of **7.11** and **7.12**, respectively. The high-yielding preparation of **7.13** and **7.14** further exemplifies the tolerance of our methodology toward α-branching, in addition to olefins and an oxygen-containing heterocycle.

Figure 7.2. Evaluation of Amide Substrate.[a]

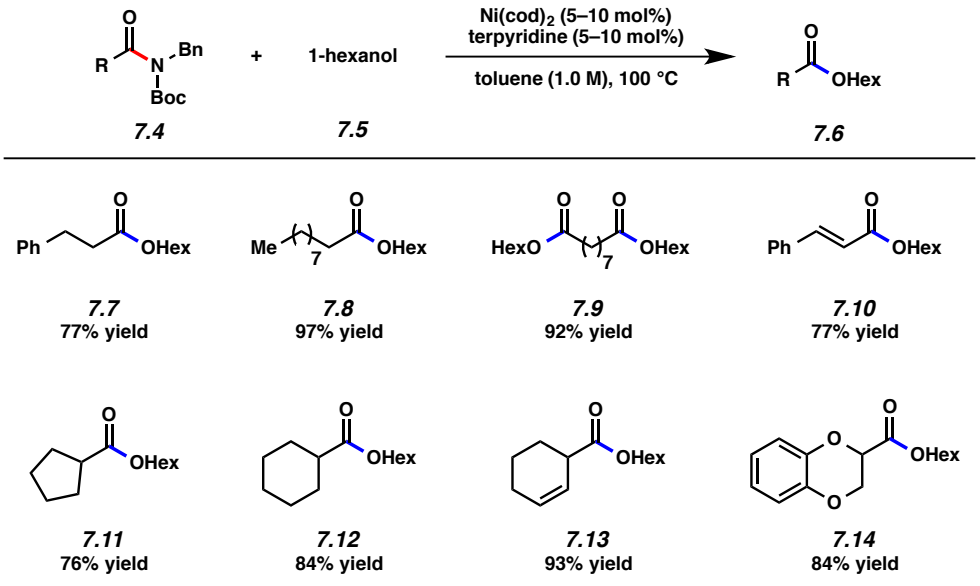

[a] Yields reflect the average of two isolation experiments.

With regard to the alcohol component, the scope of the methodology was found to be quite broad (Figure 7.3). Primary alcohols were well tolerated, including alcohols that bear olefins or ethers, as determined by the formation of **7.18**–**7.20**. In addition to the formation of oxygen-containing heterocyclic esters (**7.21**–**7.22**), we found that sulfur- and nitrogen-containing heterocycles could be employed to give **7.23**–**7.25**. The tolerance of our methodology to furans, thiophenes, indoles, and pyrrolidines bodes well for future applications in natural product and medicinal chemistry. Secondary alcohols also underwent coupling as shown by the formation of esters **7.26**–**7.29**.[12] The fact that this methodology can be used to couple hindered alcohols, such as borneol to give **7.29**, is especially noteworthy.

Figure 7.3. Scope of Alcohol Coupling Partner.[a]

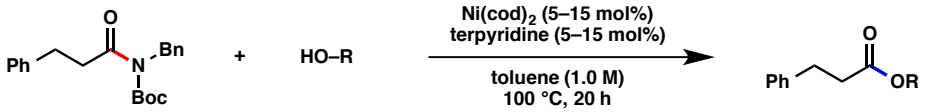

7.15 ***7.16*** ***7.17***

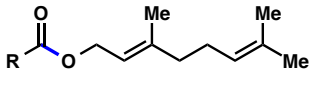

7.18
75% yield

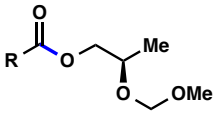

7.19
75% yield

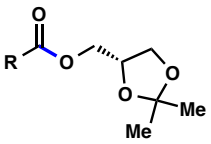

7.20
78% yield

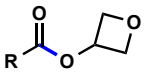

7.21
85% yield

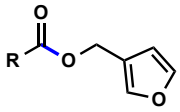

7.22
95% yield

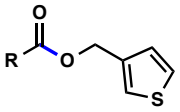

7.23
96% yield

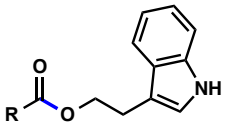

7.24
85% yield

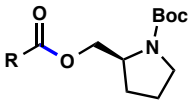

7.25
93% yield

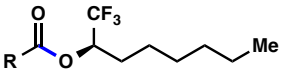

7.26
85% yield

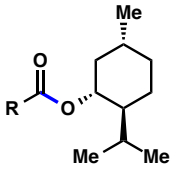

7.27
68% yield

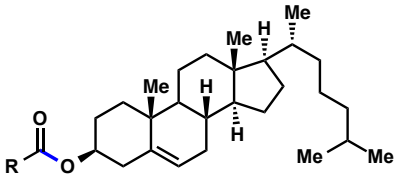

7.28
77% yield

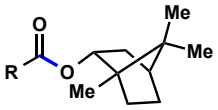

7.29
79% yield

[a] Yields reflect the average of two isolation experiments (R = CH_2CH_2Ph).

In a final test of this methodology, we assessed proline-derived substrates (Figure 7.4). Boc-activated substrates **7.30** and **7.3**1 underwent smooth coupling with 1-hexanol (**7.5**) to provide esters **7.32** and **7.33**, respectively. The mild nature of this methodology bodes well for future applications involving amino acid-derivatives and peptides.

Figure 7.4. Coupling of Proline-Derived Substrates.

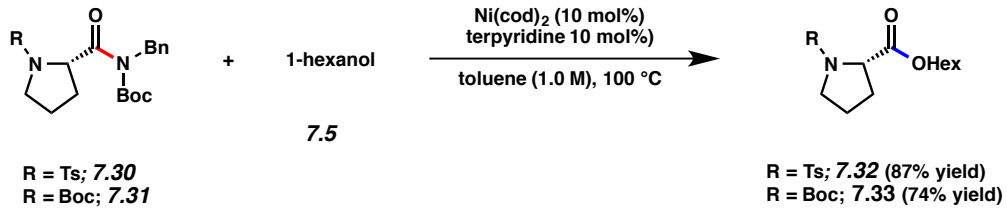

7.4. Conclusion

We have discovered the first nickel-catalyzed activation of amides derived from aliphatic acids, as demonstrated by the esterification of Boc-activated amides. The methodology is tolerant of heterocycles, substrates with epimerizable stereocenters, and amino acid derived-substrates. This study is expected to enable the use of aliphatic amides in other C–C and C–X bond forming reactions.

7.5. Experimental Section

7.5.1. Materials and Methods

Unless stated otherwise, reactions were conducted in flame-dried glassware under an atmosphere of nitrogen and commercially obtained reagents were used as received. Reagents **7.34**–**7.36**, **7.38**, **7.40**, **7.42**, **7.44**, and **7.46** were purchased from Sigma-Aldrich. Reagents **7.48** and **7.49** were purchased from Combi-Blocks, Inc. Alcohols **7.2, 7.5** and **7.59**–**7.70** were

purchased from Sigma-Adrich. Alcohols **7.62** and **7.65** were purchased from Combi-Blocks, Inc. Benzylamine was purchased from Sigma-Aldrich. EDC and HOBt were purchased from Chem-Impex International. DMAP and Boc_2O were purchased from Oakwood Products, Inc. Non-commercially available starting materials were synthesized following protocols specified in Section 7.5.2. Toluene was purified by distillation and taken through five freeze-pump-thaw cycles prior to use. $Ni(cod)_2$ was obtained from Strem Chemicals. Terpyridine was obtained from Sigma-Aldrich. Reaction temperatures were controlled using an IKAmag temperature modulator, and unless stated otherwise, reactions were performed at room temperature (approximately 23 °C). Thin-layer chromatography (TLC) was conducted with EMD gel 60 F254 pre-coated plates (0.25 mm for analytical chromatography and 0.50 mm for preparative chromatography) and visualized using a combination of UV, anisaldehyde, ceric ammonium molybdate, iodine, vanillin, and potassium permanganate staining techniques. Silicycle Siliaflash P60 (particle size 0.040–0.063 mm) was used for flash column chromatography. ^{1}H NMR spectra were recorded on Bruker spectrometers (at 500 MHz) and are reported relative to residual solvent signals. Data for ^{1}H NMR spectra are reported as follows: chemical shift (δ ppm), multiplicity, coupling constant (Hz), and integration. Data for ^{13}C NMR are reported in terms of chemical shift (at 125 MHz). IR spectra were recorded on a Perkin-Elmer 100 spectrometer and are reported in terms of frequency absorption (cm^{-1}). High-resolution mass spectra were obtained on Thermo Scientific™ Exactive Mass Spectrometer with DART ID-CUBE, Waters GST premier, and Waters LCT premier. Optical rotations were measured with a Rudolf Autopol III Automatic Polarimeter.

7.5.2. Experimental Procedure

7.5.2.1. Synthesis of Starting Materials

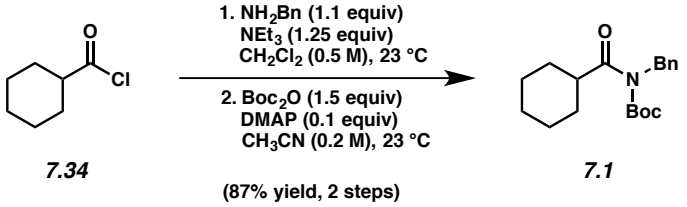

7.34 *7.1*

(87% yield, 2 steps)

Amide 7.1. To a solution of acid chloride **7.34** (2.0 g, 13.64 mmol, 1.0 equiv) and triethylamine (2.40 mL, 17.05 mmol, 1.25 equiv) in dichloromethane (20 mL) was added a solution of benzylamine (1.64 mL, 15.0 mmol, 1.1 equiv) in dichloromethane (7 mL, 0.5 M). The reaction mixture was stirred at 23 °C for 1 h, diluted with CH_2Cl_2 (30 mL), and then washed successively with 1.0 M HCl (25 mL) and brine (25 mL). The organic layer was dried over Na_2SO_4 and concentrated under reduced pressure. The resulting crude solid material was used in the subsequent step without further purification.

To a flask containing the crude material from the previous step was added DMAP (84.3 mg, 0.69 mmol, 0.1 equiv), followed by acetonitrile (35 mL, 0.2 M). Boc_2O (2.26 g, 10.35 mmol, 1.5 equiv) in one portion. The reaction vessel was flushed with N_2, and then the reaction mixture was allowed to stir at 23 °C for 12 h. The reaction mixture was diluted with EtOAc (50 mL), and then washed with 1.0 M HCl (20 mL) and brine (20 mL). The organics were dried over Na_2SO_4 and concentrated under reduced pressure. The resulting crude residue was purified by flash chromatography (20:1 Hexanes:EtOAc) to yield amide **7.1** (1.91 g, 87% yield, over two steps) as a white solid. Amide **7.1**: mp: 45.2–47.1 °C; R_f 0.50 (10:1 Hexanes:EtOAc); ^{1}H NMR (500 MHz, $CDCl_3$): δ 7.30–7.20 (m, 5H), 4.88 (s, 2H), 3.43 (tt, J = 11.4, 3.2, 1H), 1.90–1.87 (m, 2H), 1.80–1.76 (m, 2H), 1.70–1.66 (m, 1H), 1.51–1.43 (m, 1H), 1.47 (s, 9H), 1.37–1.18 (m, 3H); ^{13}C NMR (125 MHz, $CDCl_3$): δ 179.8, 153.3, 138.7, 128.4, 127.6, 127.1, 83.1, 47.8, 44.9, 30.0, 28.0,

26.1, 25.9; IR (film): 2925, 2857, 1732, 1697, 1460, 1363, 1216, 1148, 1074; HRMS-ESI (m/z) $[M + Na]^+$ calcd for $C_{19}H_{27}NO_3Na$ 340.1889; found 340.1881.

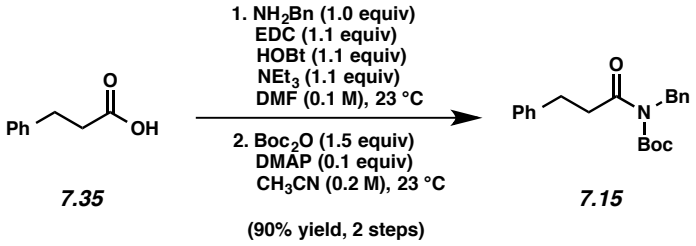

Amide 7.15. To a mixture of carboxylic acid **7.35** (10.50 g, 70.0 mmol, 1.0 equiv), EDC (14.80 g, 77.0 mmol, 1.1 equiv), HOBt (10.4 g, 77.0 mmol, 1.1 equiv), triethylamine (10.7 mL, 77.0 mmol, 1.1 equiv), and DMF (700.0 mL, 0.1 M) was added benzylamine (8.24 g, 77.0 mmol, 1.1 equiv). The resulting mixture was stirred at 23 °C for 12 h, and then diluted with deionized water (500 mL) and EtOAc (500 mL). The layers were separated and the organic layer was washed successively with 1.0 M HCl (300 mL), saturated aqueous $NaHCO_3$ (300 mL), and brine (300 mL). The organics were dried over Na_2SO_4 and concentrated under reduced pressure. The resulting crude solid material was used in the subsequent step without further purification.

To a flask containing the crude material from the previous step was added DMAP (0.86 g, 7.0 mmol, 0.1 equiv) followed by acetonitrile (350 mL, 0.2 M). Boc_2O (22.92 g, 105.0 mmol, 1.5 equiv) was added in one portion and the reaction vessel was flushed with N_2. The reaction mixture was allowed to stir at 23 °C for 12 h. The reaction mixture was diluted with EtOAc (50 mL) and then washed with saturated aqueous $NaHCO_3$ (2 X 100 mL) and brine (100 mL). The organics were dried over Na_2SO_4 and concentrated under reduced pressure. The resulting crude residue was purified by flash chromatography (20:1 Hexanes:EtOAc) to yield amide **7.15** (21.50 g, 90% yield, over two steps) as a white solid. Amide **7.15**: mp: 65.3–67.1 °C; R_f 0.60 (5:1 Hexanes:EtOAc); ^{1}H NMR (500 MHz, $CDCl_3$): δ 7.31–7.27 (m, 4H), 7.25–7.18 (m, 6H), 4.89 (s,

2H), 3.28 (t, J = 7.7 , 2H), 3.03 (t, J = 7.7, 2H), 1.39 (s, 9H); ^{13}C NMR (125 MHz, $CDCl_3$): δ 175.5, 153.2, 141.3, 138.4, 128.7, 128.5, 128.4, 127.6, 127.2, 126.1, 83.3, 47.5, 40.1, 31.3, 28.0; IR (film): 3032, 2979, 1731, 1693, 1373, 1210, 1145, 995; HRMS-ESI (m/z) $[M+Na]^+$ calcd for $C_{21}H_{25}NO_3Na$ 362.1732; found 362.1739.

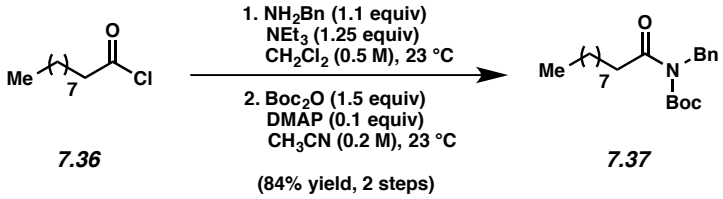

7.36 *7.37*

Amide 7.37. To a solution of acid chloride **7.36** (2.0 g, 10.5 mmol, 1.0 equiv), triethylamine (1.82 mL, 13.13 mmol, 1.25 equiv), and dichloromethane (16 mL), was added a solution of benzylamine (1.26 mL, 11.55 mmol, 1.1 equiv) in dichloromethane (5 mL, 0.5 M). The reaction mixture was stirred at 23 °C for 1 h, diluted with CH_2Cl_2 (30 mL), and then washed successively with 1.0 M HCl (25 mL) and brine (25 mL). The organic layer was dried over Na_2SO_4 and concentrated under reduced pressure. The resulting crude solid material was used in the subsequent step without further purification.

To a flask containing the crude material from the previous step was added DMAP (69.6 mg, 0.57 mmol, 0.1 equiv) followed by acetonitrile (28.5 mL, 0.2 M). Boc_2O (1.87 g, 8.6 mmol, 1.5 equiv) was added in one portion and the reaction vessel was flushed with N_2. The reaction mixture was allowed to stir at 23 °C for 12 h. The reaction mixture was diluted with EtOAc (50 mL), and then washed with 1.0 M HCl (20 mL) and brine (20 mL). The organics were dried over Na_2SO_4 and concentrated under reduced pressure. The resulting crude residue was purified by flash chromatography (20:1 Hexanes:EtOAc) to yield amide **7.37** (1.76 g, 84% yield, over two steps) as a clear oil. Amide **7.37**: R_f 0.48 (10:1 Hexanes:EtOAc); ^{1}H NMR (500 MHz,

$CDCl_3$): δ 7.30–7.27 (m, 2H), 7.25–7.21 (m, 3H), 4.88 (s, 2H), 2.92 (t, *J* = 7.5, 2H), 1.69–1.63 (m, 2H), 1.41 (s, 9H), 1.34–1.26 (m, 12H), 0.89 (t, *J* = 7.0, 3H); ^{13}C NMR (125 MHz, $CDCl_3$): δ 176.4, 153.3, 138.6, 128.4, 127.8, 127.2, 83.2, 47.4, 38.5, 32.0, 29.6, 29.4, 29.3, 28.0, 25.4, 22.8, 14.2; IR (film): 2925, 2857, 1732, 1697, 1460, 1363, 1216, 1148, 1074; HRMS-ESI (m/z) $[M+Na]^+$ calcd for $C_{22}H_{35}NO_3Na$ 384.2515; found 384.2516.

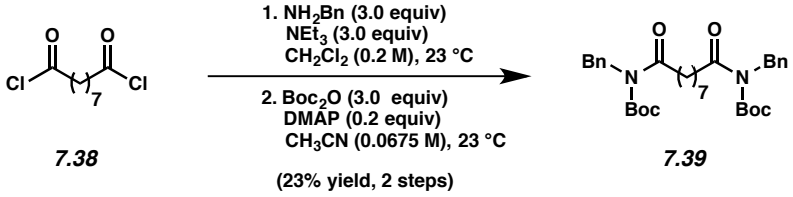

Amide 7.39. To a solution of acid chloride **7.38** (2.0 g, 8.9 mmol, 1.0 equiv), triethylamine (3.72 mL, 26.7 mmol, 3.0 equiv), and dichloromethane (80 mL), was added a solution of benzylamine (2.92 mL, 26.7 mmol, 3.0 equiv) in dichloromethane (10 mL, 0.099 M). The reaction mixture was stirred at 23 °C for 4 h and then filtered over celite. The pad was eluted with CH_2Cl_2 (40 mL). The collected organics were washed successively with 1.0 M HCl (25 mL) and brine (25 mL). The organics were dried over Na_2SO_4 and then concentrated under reduced pressure. The resulting crude solid material was used in the subsequent step without further purification.

To a flask containing the crude material from the previous step was added DMAP (108.7 mg, 0.89 mmol, 0.1 equiv), followed by acetonitrile (44 mL, 0.2 M). Boc_2O (5.83 g, 26.7 mmol, 3.0 equiv) was added in one portion and the reaction vessel was flushed with N_2. The reaction mixture was allowed to stir at 23 °C for 12 h. The reaction mixture was diluted with EtOAc (50 mL) and then washed with deionized water (3 X 50 mL). The organics were dried over Na_2SO_4 and concentrated under reduced pressure. The resulting crude residue was purified by flash chromatography (20:1 → 10:1 Hexanes:EtOAc) to yield amide **7.39** as a white solid (1.16 g,

23% yield). Amide **7.39**: mp: 67.0–69.2 °C; R_f 0.33 (20:1 Hexanes:EtOAc); ^{1}H NMR (500 MHz, $CDCl_3$): δ 7.30–7.27 (m, 4H), 7.25–7.20 (m, 6H), 4.88 (s, 4H), 2.90 (t, J = 7.6, 4H), 1.66–1.63 (m, 4H), 1.40 (s, 18H), 1.34–1.31 (m, 6H); ^{13}C NMR (125 MHz, $CDCl_3$): δ 176.4, 153.3, 138.6, 128.4, 127.7, 127.2, 83.2, 47.4, 38.4, 29.4, 29.3, 28.0, 25.3; IR (film): 3703, 3668, 2977, 2937, 2862, 1732, 1695, 1458, 1373, 1218; HRMS-ESI (m/z) [M+Na]+ calcd for $C_{33}H_{46}N_2O_6Na$ 589.3254; found 589.3254.

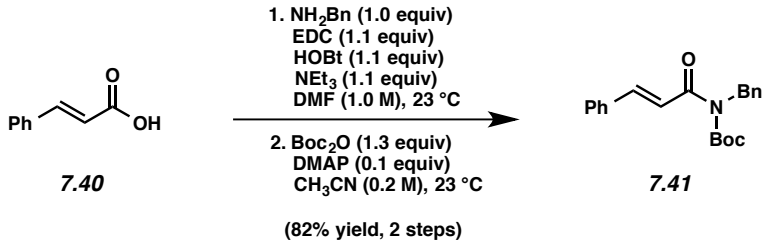

Amide 7.41. To a mixture of carboxylic acid **7.40** (3.0 g, 20.2 mmol, 1.0 equiv), EDC (3.5 g, 22.3 mmol, 1.1 equiv), HOBt (3.4 g, 22.3 mmol, 1.1 equiv) and triethylamine (3.1 mL, 22.3 mmol, 1.1 equiv) in DMF (202 mL, 1.0 M) was added benzylamine (2.4 mL, 22.3 mmol, 1.1 equiv). The resulting mixture was stirred at 23 °C for 17 h, and then diluted with deionized water (100 mL). The mixture was transferred to a separatory funnel with EtOAc (100 mL) and brine (100 mL). The layers were separated. The aqueous layer was extracted with EtOAc (3 x 100 mL). The combined organic layers were washed with deionized water (3 x 100 mL), dried over Na_2SO_4, and concentrated under reduced pressure. The resulting crude material was used in the subsequent step without further purification.

To a flask containing the crude material from the previous step was added DMAP (239 mg, 1.96 mmol, 0.1 equiv) followed by acetonitrile (98 mL, 0.2 M). Boc_2O (5.6 g, 25.5 mmol, 1.3 equiv) was added in one portion and the reaction vessel was flushed with N_2. The reaction mixture was allowed to stir at 23 °C for 19 h. The reaction was quenched by the addition of

saturated aqueous $NaHCO_3$ (75 mL). The mixture was transferred to a separatory funnel with EtOAc (100 mL) and H_2O (50 mL). The aqueous layer was extracted with EtOAc (3 x 100 mL). The combined organic layers were dried over Na_2SO_4 and then concentrated under reduced pressure. The resulting crude residue was purified by flash chromatography (25:1 Hexanes:EtOAc) to yield amide **7.41** (4.2 g, 82% yield, over two steps) as a white solid. Amide **7.41**: mp: 89.1–92.9 ºC; R_f 0.46 (5:1 Hexanes:EtOAc); ^{1}H NMR (500 MHz, $CDCl_3$): δ 7.78–7.71 (m, 1H), 7.60–7.55 (m, 2H), 7.55–7.49 (m, 1H), 7.41–7.34 (m, 3H), 7.33–7.28 (m, 4H), 7.26–7.21 (m, 1H), 4.97 (s, 2H), 1.43 (s, 9H); ^{13}C NMR (125 MHz, $CDCl_3$): δ 169.0, 153.4, 143.7, 138.5, 135.3, 130.1, 128.9, 128.5, 128.3, 127.7, 127.3, 121.4, 83.5, 48.0, 28.1; IR (film): 2980, 2935, 1722, 1667, 1615 cm^{-1}; HRMS-ESI (*m/z*) $[M + H]^+$ calcd for $C_{21}H_{24}NO_3$ 338.1756; found 338.1738.

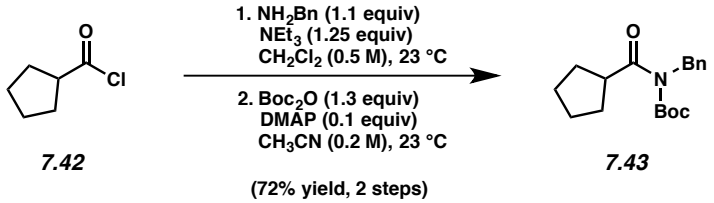

Amide 7.43. To a solution of acid chloride **7.42** (2.0 g, 15.1 mmol, 1.0 equiv) and triethylamine (2.61 mL, 18.9 mmol, 1.25 equiv) in dichloromethane (15.1 mL), was added a solution of benzylamine (1.81 mL, 16.6 mmol, 1.1 equiv) in dichloromethane (15.1 mL, 0.5 M). The reaction mixture was stirred at 23 °C for 15 h. The mixture was diluted with EtOAc (50 mL), and then washed successively with 1.0 M HCl (50 mL) and brine (50 mL). The organic layer was dried over Na_2SO_4 and concentrated under reduced pressure. The resulting crude material was used in the subsequent step without further purification.

To a flask containing the crude material from the previous step was added DMAP (184.0 mg, 1.51 mmol, 0.1 equiv) followed by acetonitrile (76.0 mL, 0.2 M). Boc_2O (4.3 g, 19.6 mmol,

1.3 equiv) was added in one portion and the reaction vessel was flushed with N_2. The reaction mixture was allowed to stir at 23 °C for 24 h. The reaction was quenched by the addition of saturated aqueous $NaHCO_3$ (30 mL), and then transferred to a separatory funnel with EtOAc (50 mL) and H_2O (50 mL). The aqueous layer was extracted with EtOAc (3 x 50 mL). The combined organic layers were dried over Na_2SO_4 and concentrated under reduced pressure. The resulting crude residue was purified by flash chromatography (20:1 Hexanes:EtOAc) to yield amide **7.43** (1.97 g, 72% yield, over two steps) as a clear oil. Amide **7.43**: R_f 0.59 (5:1 Hexanes:EtOAc); ^{1}H NMR (500 MHz, $CDCl_3$): δ 7.32–7.27 (m, 2H), 7.25–7.20 (m, 3H), 4.88 (s, 2H), 3.83–3.72 (m, 1H), 2.01–1.88 (m, 2H), 1.87–1.77 (m, 2H), 1.77–1.66 (m, 2H), 1.64–1.53 (m, 2H), 1.40 (s, 9H); ^{13}C NMR (125 MHz, $CDCl_3$): δ 179.9, 153.3, 138.7, 128.4, 127.5, 127.1, 83.1, 47.8, 45.7, 31.0, 28.0, 26.1; IR (film): 2955, 2867, 1730, 1687, 1453 cm^{-1}; HRMS-ESI (*m/z*) $[M + H]^+$ calcd for $C_{18}H_{26}NO_3$, 304.1913; found 304.1895.

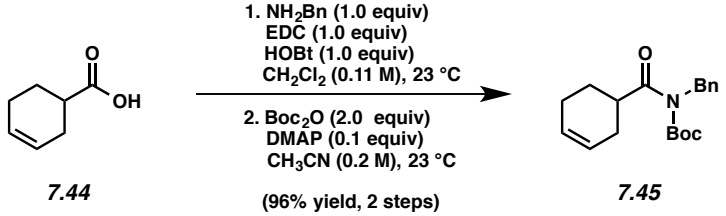

Amide 7.45. To a mixture of carboxylic acid **7.44** (1.0 g, 7.9 mmol, 1.0 equiv), EDC (1.50 g, 7.9 mmol, 1.0 equiv), HOBt (1.1 g, 7.9 mmol, 1.0 equiv), and CH_2Cl_2 (79 mL, 0.1 M) was added benzylamine (0.86 mL, 7.9 mmol, 1.0 equiv). The resulting mixture was stirred at 23 °C for 16 h, and then diluted with CH_2Cl_2 (30 mL). The mixture was washed with 1M HCl (30 mL), saturated aqueous $NaHCO_3$ (30mL), and brine (30 mL). The organics were dried over Na_2SO_4 and then

concentrated under reduced pressure. The resulting crude material was used in the subsequent step without further purification.

To a flask containing the crude material from the previous step was added DMAP (56.7 mg, 0.46 mmol, 0.1 equiv), followed by acetonitrile (23 mL, 0.2 M). Boc_2O (2.03 g, 9.28 mmol, 2.0 equiv) was added in one portion and the reaction vessel was flushed with N_2. The reaction mixture was allowed to stir at 23 °C for 12 h. The mixture was washed with 1.0 M HCl (5 mL) and brine (5 mL). After drying over Na_2SO_4, the organics were concentrated under reduced pressure. The resulting crude residue was purified by flash chromatography (10:1 Hexanes:EtOAc) to yield **7.45** (1.40 g, 96% yield, over two steps) as a clear oil. Amide **7.45**: R_f 0.69 (5:1 Hexanes: EtOAc); ^{1}H NMR (500 MHz, CDCl3): δ 7.31–7.28 (m, 2H), 7.24–7.21 (m, 3H), 5.73–5.67 (m, 2H), 4.88 (d, *J* = 2.9, 2H), 3.66–3.60 (m, 1H), 2.32–2.23 (m, 2H), 2.14–2.10 (m, 2H), 1.98–1.94 (m, 1H), 1.75–1.67 (m, 1H), 1.40 (br s, 9H); ^{13}C NMR (125 MHz, $CDCl_3$): δ179.6, 153.2, 138.6, 128.4, 127.6, 127.2, 126.7, 125.7, 83.3, 47.8, 41.1, 28.6, 28.0, 26.3, 25.1; IR (film): 3030, 2980, 2935, 1730, 1690, 1498, 1455, 1438, 1368, 1343, 1218, 1146, 1074, 1034, 655, HRMS-ESI (m/z) $[M+Na]^+$ calcd for $C_{19}H_{25}NO_3Na$ 338.1732; found 338.1725.

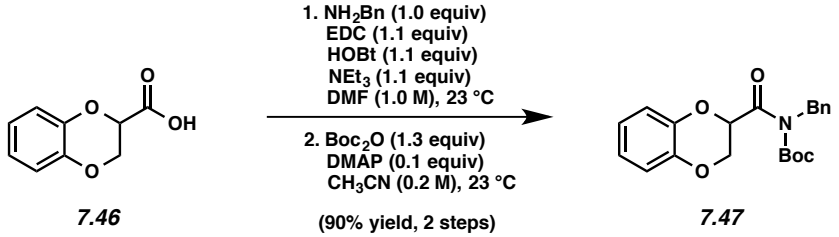

Amide 7.47. To a mixture of carboxylic acid **7.46** (2.0 g, 11.1 mmol, 1.0 equiv), EDC (1.89 g, 12.2 mmol, 1.1 equiv), HOBt (1.87 g, 12.2 mmol, 1.1 equiv), and triethylamine (1.7 mL, 22.3 mmol, 1.1 equiv) in DMF (202 mL, 1.0 M) was added benzylamine (2.4 mL, 12.2 mmol, 1.1

equiv). The resulting mixture was stirred at 23 °C for 18 h, and then diluted with deionized water (100 mL). The mixture was transferred to a separatory funnel with EtOAc (75 mL) and brine (50 mL). The aqueous layer was extracted with EtOAc (3 x 75 mL). The combined organic layers were washed with deionized water (3 x 75 mL), dried over Na_2SO_4, and concentrated under reduced pressure. The resulting crude material was used in the subsequent step without further purification.

To a flask containing the crude material from the previous step was added DMAP (92 mg, 0.78 mmol, 0.1 equiv) followed by acetonitrile (39 mL, 0.2 M). Boc_2O (2.2 g, 10.1 mmol, 1.3 equiv) was added in one portion and the reaction vessel was flushed with N_2. The reaction mixture was allowed to stir at 23 °C for 17 h. The reaction was quenched by the addition of saturated aqueous $NaHCO_3$ (75 mL), and then transferred to a separatory funnel with EtOAc (100 mL) and H_2O (50 mL). The layers were separated. The aqueous layer was extracted with EtOAc (3 x 100 mL). The combined organic layers were dried over Na_2SO_4 and concentrated under reduced pressure. The resulting crude residue was purified by flash chromatography (29:1 → 15:1 Hexanes:EtOAc) to yield amide **7.47** (2.3 g, 90% yield, over two steps) as a white solid. Amide **7.47**: mp: 76.5–78.5 ºC; R_f 0.57 (5:1 Hexanes:EtOAc); ^{1}H NMR (500 MHz, $CDCl_3$): δ 7.33–7.27 (m, 2H), 7.26–7.20 (m, 3H), 7.00–6.94 (m, 1H), 6.92–6.81 (m, 3H), 5.81–5.76 (m, 1H), 4.96–4.80 (m, 2H), 4.50–4.39 (m, 2H), 1.43 (s, 9H), ^{13}C NMR (125 MHz, $CDCl_3$): δ 170.9, 152.9, 143.4, 143.3, 137.5, 128.6, 127.8, 127.5, 122.2, 121.6, 117.2, 117.15, 84.6, 73.9, 65.2, 48.1, 28.0; IR (film): 2980, 2932, 1730, 1710, 1595 cm^{-1}; HRMS-ESI (*m/z*) $[M + H]^+$ calcd for $C_{21}H_{24}NO_5$ 370.1654; found 370.1591.

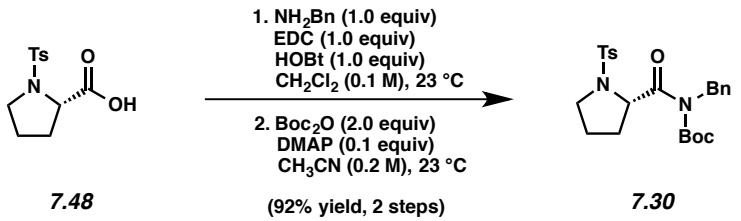

Amide 7.30. To a mixture of carboxylic acid **7.48** (0.50 g, 1.86 mmol, 1.0 equiv), EDC (0.36 g, 1.86 mmol, 1.0 equiv), HOBt (0.25 g, 1.86 mmol, 1.0 equiv), and CH_2Cl_2 (19 mL, 0.1 M) was added benzylamine (0.20 mL, 1.86 mmol, 1.0 equiv). The resulting mixture was stirred at 23 °C for 16 h, and then diluted with CH_2Cl_2 (30 mL). The mixture was washed with deionized water (2 x 20 mL). The organics were dried over Na_2SO_4 and then evaporated under reduced pressure. The resulting crude material was used in the subsequent step without further purification.

To a flask containing the crude material from the previous step was added DMAP (15.9 mg, 0.13 mmol, 0.1 equiv), followed by acetonitrile (6.5 mL, 0.2 M). Boc_2O (0.57 g, 2.6 mmol, 2.0 equiv) was added in one portion and the reaction vessel was flushed with N_2. The reaction mixture was allowed to stir at 23 °C for 12 h. The mixture was washed with 1.0 M HCl (5 mL) and brine (5 mL). After drying over Na_2SO_4, the volatives were evaporated under reduced pressure. The resulting crude residue was purified by flash chromatography (5:1 → 3:1 Hexanes:EtOAc) to yield **7.30** (0.55 g, 92% yield, over two steps) as a white solid. Amide **7.30**: mp: 106.6–107.8 °C; R_f 0.29 (5:1 Hexanes: EtOAc); ^{1}H NMR (500 MHz, $CDCl_3$): δ 7.7 (d, J = 8.1, 2H), 7.32–7.28 (m, 3H), 7.25–7.22 (m, 3H), 5.49 (dd, J = 5.8, 3.0, 1H), 4.99 (d, J = 15, 1H), 4.79 (d, J = 14.8, 1H), 3.54–3.49 (m, 1H), 3.38–3.34 (m, 1H), 2.41 (br s, 3H), 2.24–2.15 (m, 1H), 1.99–1.90 (m, 2H), 1.79–1.73 (m, 1H), 1.41 (s, 9H); ^{13}C NMR (125 MHz, $CDCl_3$): δ 175.4, 153.0, 143.4, 138.1, 135.9, 129.7, 128.5, 127.6, 127.5, 127.3, 83.9, 62.5, 48.6, 47.9, 31.7, 27.9, 24.4, 21.7; IR (film): 2977, 2932, 2855, 1732, 1692, 1453, 1369, 1237, 1148; HRMS-ESI (m/z)

$[M+Na]^+$ calcd for $C_{24}H_{30}N_2O_5SNa$ 481.1773; found 481.1750; $[\alpha]^{23.5}_D$ –1042.0 ° (*c* = 1.00, CH_2Cl_2).

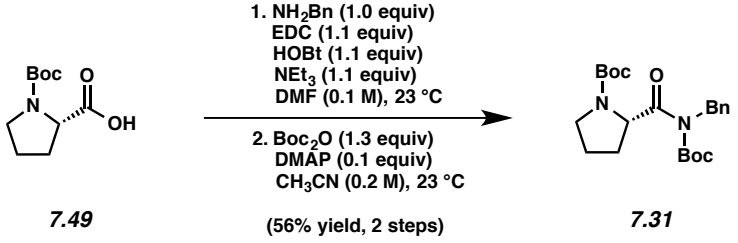

Amide 7.31. To a mixture of carboxylic acid **7.49** (2.0 g, 9.3 mmol, 1.0 equiv), EDC•HCl (1.96 g, 10.23 mmol, 1.1 equiv), HOBt (1.30 g, 10.23 mmol, 1.1 equiv), triethylamine (1.4 mL, 10.23 mmol, 1.1 equiv), and DMF (93 mL, 0.1 M) was added benzylamine (1.12 mL, 10.23 mmol, 1.1 equiv). The resulting mixture was stirred at 23 °C for 16 h, and then diluted with deionized water (50 mL) and EtOAc (30 mL). The layers were separated. The aqueous layer was extracted with EtOAc (3 x 100 mL). The combined organic layers were washed with deionized water (3 x 50 mL), dried over Na_2SO_4 and concentrated under reduced pressure. The resulting crude material was used in the subsequent step without further purification.

To a flask containing the crude material from the previous step was added DMAP (113 mg, 0.93 mmol, 0.1 equiv), followed by acetonitrile (46.5 mL, 0.2 M). Boc_2O (2.64 g, 12.09 mmol, 1.3 equiv) was added in one portion and the reaction vessel was flushed with N_2. The reaction mixture was allowed to stir at 23 °C for 16 h and then quenched by addition of saturated aqueous $NaHCO_3$ (10 mL). The mixture was transferred to a separatory funnel with EtOAc (30 mL) and deionized water (30 mL). The layers were separated. The aqueous layer was extracted with EtOAc (3 x 50 mL). The combined organic layers were dried over Na_2SO_4 and concentrated under reduced pressure. The resulting crude residue was purified by flash chromatography (10:1 Hexanes:EtOAc) to yield **7.31** (1.68 g, 56% yield, over two steps) as a white solid. Amide **7.31**: mp: 81.1–81.8 °C, R_f 0.34 (5:1 Hexanes:EtOAc); ^{1}H NMR (500 MHz, $CDCl_3$): δ 7.32–7.26 (m,

3H), 7.25–7.18 (m, 2H), 5.31–5.2 (m, 1H), 5.09–4.70 (m, 2H), 3.68–3.55 (m, 1H), 3.53–3.39 (m, 1H), 2.41–2.28 (m, 1H), 2.03–1.80 (m, 3H), 1.50–1.30 (m, 18H); ^{13}C NMR (125 MHz, $CDCl_3$): δ 176.3, 176.1, 154.5, 153.7, 152.9, 152.7, 138.3, 138.0, 128.3, 128.3, 127.8, 127.4, 127.3, 127.3, 126.9, 83.6, 83.4, 79.4, 79.3, 61.2, 60.9, 47.6, 47.6, 47.0, 46.7, 31.3, 30.6, 28.5, 28.3, 27.9, 27.9, 23.7, 23.1; IR (film): 2977, 2973, 2932, 2879, 1729, 1697, 1393, 1365, 1146; HRMS-ESI (m/z) HRMS-ESI (m/z) $[M+Na]^+$ calcd for $C_{22}H_{32}N_2O_5Na$ 427.2209; found 427.2195; $[\alpha]^{19.7}_D$ +54.0 ° (*c* = 1.00, CH_2Cl_2).

*Note: Amide **7.31** was obtained as a mixture of rotamers. These data represent empirically observed chemical shifts and coupling constants from the ^{1}H and ^{13}C NMR spectra.*

7.5.2.2. Reaction Discovery

*Representative procedure for pyridine-type ligand screening (coupling of amide **7.15** and menthol (**7.2**) is used as an example).*

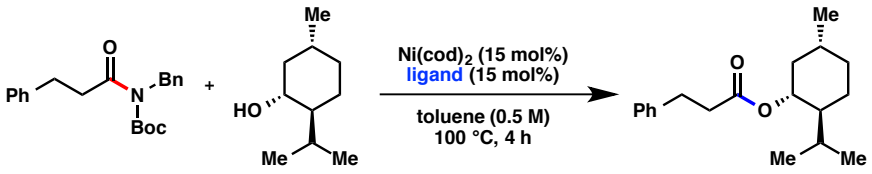

7.15 ***7.2*** ***7.27***

Ester 7.27. A 1-dram vial containing amide **7.15** (50.0 mg, 0.15 mmol, 1.0 equiv), hexamethylbenzene (7.3 mg, 0.045 mmol, 0.3 equiv), and a magnetic stir bar was charged with $Ni(cod)_2$ (6.2 mg, 0.0225 mmol, 15 mol%) and ligand (0.0225 mmol, 15 mol%) in a glove box. Subsequently, toluene (0.15 mL, 1.0 M) and then menthol (**7.2**) (29.3 mg, 0.19 mmol, 1.2 equiv) were added. The vial was sealed with a Teflon-lined screw cap, removed from the glove box, and stirred at 100 °C for 4 h. After cooling to 23 °C, the mixture was diluted with hexanes (0.5 mL) and filtered over a plug of silica gel (10 mL of EtOAc eluent). The volatiles were evaporated under reduced pressure, and the yield was determined by ^1H NMR analysis with hexamethylbenzene as an internal standard.

The representative procedure shown above depicts all of the results shown in Tables 7.1–7.4.

Table 7.2. Evaluation of Pyridine-Type Ligands.[a]

Entry	Ligand	Yield of 7.27	Entry	Ligand	Yield of 7.27
1	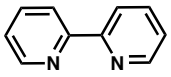	0%	6	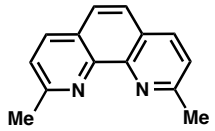	0%
2	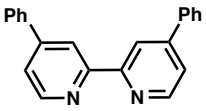	0%	7	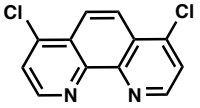	0%
3	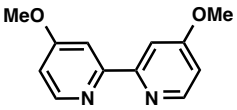	0%	8	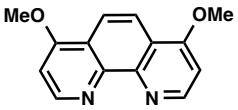	37%
4	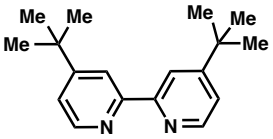	23%	9	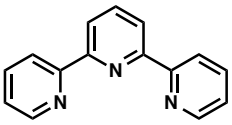	60%
5	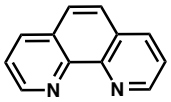	0%	10	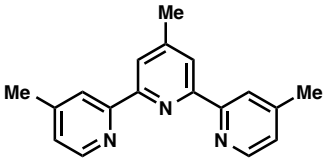	17%

[a] Yields were determined using ^{1}H NMR analysis with hexamethylbenzene as an internal standard.

7.5.2.3. Survey of Amide Substrates

Table 7.3. Survey of Amide Substrates Under the Optimized Reaction Conditions.[a]

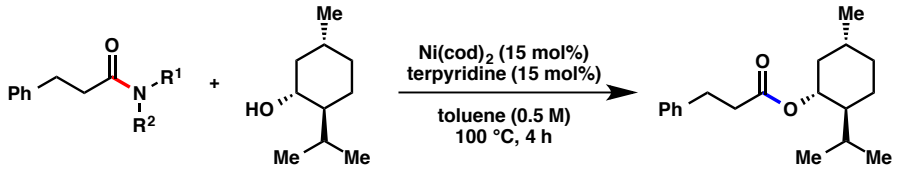

7.2 *7.27*

Entry			*Yield of 7.27*	*Remainder of the mass*
1		*7.50*	0% yield	*7.50*; 100%
2		*7.51*	0% yield	*7.51;* 100%
3		*7.52*	13% yield	*7.52*; 87%
4		*7.15*	60% yield	*7.15*; 40%

[a] Yields were determined using ^{1}H NMR analysis with hexamethylbenzene as an internal standard.

7.5.2.4. Optimization of Reaction Conditions and Relevant Control Experiments

Table 7.4. Optimization of Reaction Conditions.[a]

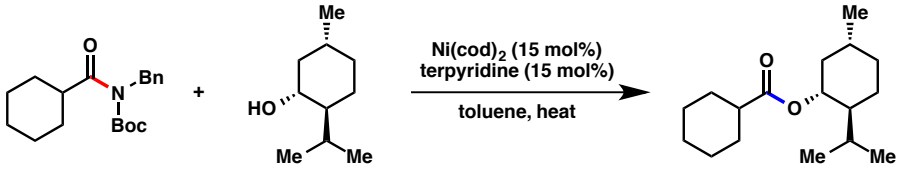

7.1 *7.2* *7.3*

Reaction conditions	*Experimental Results*	
	7.3	*7.1*
$Ni(cod)_2$ (15 mol%), terpyridine (15 mol%), menthol (1.2 equiv), toluene (0.5 M), 80 °C, 20 h	24%	76%
$Ni(cod)_2$ (15 mol%), terpyridine (7.5 mol%), menthol (1.2 equiv), toluene (0.5 M), 80 °C, 20 h	31%	69%
$Ni(cod)_2$ (15 mol%), terpyridine (30 mol%), menthol (1.2 equiv), toluene (0.5 M), 80 °C, 20 h	31%	69%
$Ni(cod)_2$ (15 mol%), terpyridine (15 mol%), menthol (2.5 equiv), toluene (0.5 M), 80 °C, 20 h	30%	70%
$Ni(cod)_2$ (15 mol%), terpyridine (15 mol%), menthol (1.2 equiv), toluene (0.33 M), 80 °C, 20 h	19%	81%
$Ni(cod)_2$ (15 mol%), terpyridine (15 mol%), menthol (1.2 equiv), toluene (1.0 M), 80 °C, 20 h	35%	65%
$Ni(cod)_2$ (15 mol%), terpyridine (15 mol%), menthol (1.2 equiv), toluene (1.0 M), 100 °C, 20 h	56%	44%
Control experiments:		
$Ni(cod)_2$ (15 mol%), menthol (1.2 equiv), toluene (1.0 M), 100 °C, 20 h	0%	100%
Terpyridine (30 mol%), menthol (1.2 equiv), toluene (1.0 M), 100 °C, 20 h	0%	100%
Menthol (1.2 equiv), toluene (1.0 M), 100 °C, 20 h	0%	100%

[a] Yields were determined using ^{1}H NMR analysis with hexamethylbenzene as an internal standard.

7.5.2.5. Scope of Methodology

*Representative Procedure (coupling of amide **7.15** and **7.5** is used as an example).*

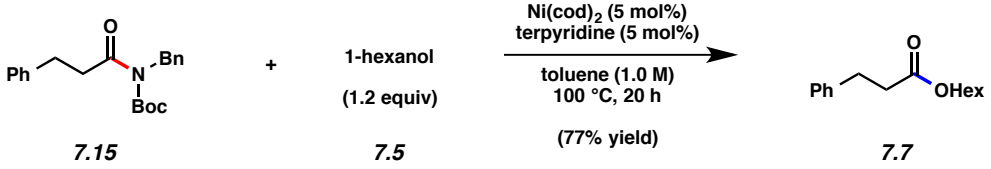

Ester 7.7 (Figure 7.2). A 1-dram vial containing amide **7.15** (71.8 mg, 0.30 mmol, 1.0 equiv) and a magnetic stir bar was charged with $Ni(cod)_2$ (4.1 mg, 0.015 mmol, 5 mol%) and terpyridine (3.5 mg, 0.015 mmol, 5 mol%) in a glove box. Subsequently, toluene (0.30 mL, 1.0 M) and then alcohol **7.5** (38.3 mg, 0.38 mmol, 1.2 equiv) were added. The vial was sealed with a Teflon-lined screw cap, removed from the glove box, and stirred at 100 °C for 20 h. After cooling to 23 °C, the mixture was diluted with hexanes (0.5 mL) and filtered over a plug of silica gel (10 mL of EtOAc eluent). The volatiles were removed under reduced pressure and the crude residue was purified by flash chromatography (50:1 Hexanes:EtOAc) generated ester **7.7** (77% yield, average of two experiments) as a clear oil. Ester **7.7**: R_f 0.52 (20:1 Hexanes:EtOAc). Spectral data match those previously reported.[13]

Any modifications of the conditions shown in the representative procedure above are specified in the following schemes, which depict all of the results shown in Figures 7.2–7.4.

For each of the nickel-catalyzed reactions described herein, control experiments were performed concurrently where $Ni(cod)_2$ and both $Ni(cod)_2$ and terpyridine were omitted from the reactions. In all cases, these control experiments led to the recovery of the amide substrates with no detectable conversion to the corresponding esters.

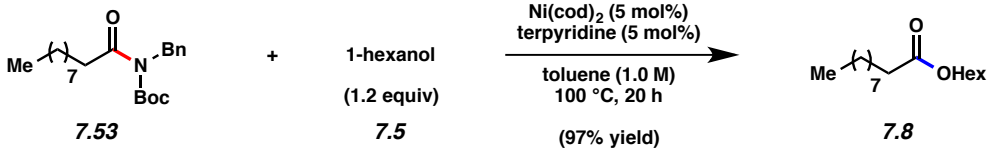

Ester 7.8 (Figure 7.2). Purification by flash chromatography (20:1 Hexanes:EtOAc) generated ester **7.8** (97% yield, average of two experiments) as a clear oil. Ester **7.8**: R_f 0.47 (20:1 Hexanes:EtOAc). Spectral data match those previously reported.[14]

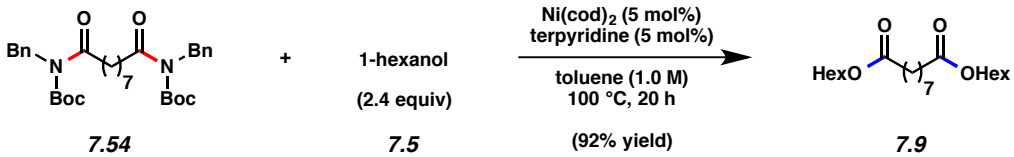

Ester 7.9 (Figure 7.2). Purification by preparative thin layer chromatography (20:1 Hexanes:EtOAc) generated ester **7.9** (92% yield, average of two experiments) as a clear oil. Ester **7.9**: R_f 0.48 (20:1 Hexanes:EtOAc); ^{1}H NMR (500 MHz, $CDCl_3$): 4.06 (t, J = 6.7, 4H), 2.29 (t, J = 7.6, 4H), 1.62–1.57 (m, 8H), 1.35–1.24 (m, 18H), 0.89 (t, J = 6.8, 6H); ^{13}C NMR (125 MHz, $CDCl_3$): δ 174.1, 64.6, 34.5, 31.6, 29.1, 29.05, 28.8, 25.7, 25.1, 22.7, 14.1; IR (film): 2952, 2930, 2857, 1730, 1465, 1248, 1176, 1091, 1011; HRMS-ESI (m/z) $[M+Na]^+$ calcd for $C_{21}H_{40}O_4Na$ 379.2824; found 379.2826.

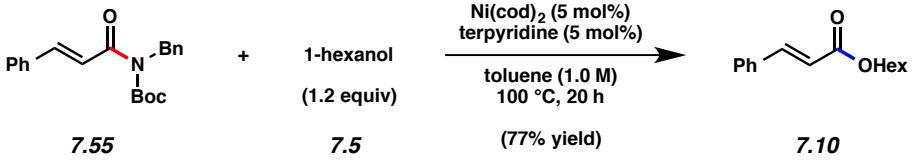

7.55 *7.5* *7.10*

Ester 7.10 (Figure 7.2). Purification by flash chromatography (20:1 Hexanes:EtOAc) generated ester **7.10** (77% yield, average of two experiments) as a clear oil. Ester **7.10**: R_f 0.58 (5:1 Hexanes:EtOAc). Spectral data match those previously reported.[15]

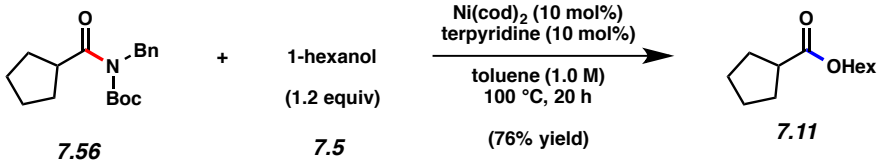

7.56 *7.5* *7.11*

Ester 7.11 (Figure 7.2). Purification by flash chromatography (29:1 Hexanes:EtOAc) generated ester **7.11** (76% yield, average of two experiments) as a clear oil. Ester **7.11**: R_f 0.41 (5:1 Hexanes:EtOAc); ^{1}H NMR (500 MHz, $CDCl_3$): δ 4.05 (t, *J* = 6.7, 2H), 2.71 (quintet, J = 7.9, 8.2, 1H), 1.95–1.83 (m, 2H), 1.83–1.74 (m, 2H), 1.74–1.65 (m, 2H), 1.65–1.51 (m 4H), 1.42–1.22 (m, 6H), 0.95–0.83 (m, 3H); ^{13}C NMR (125 MHz, $CDCl_3$): δ 177.1, 64.6, 44.1, 31.6, 30.2, 28.8, 25.9, 25.7, 22.7, 14.1; IR (film): 2957, 2935, 2870, 1732, 1453 cm^{-1}; HRMS-ESI (*m/z*) $[M+NH_4]^+$ calcd for $C_{12}H_{22}O_2NH_4$, 216.1964; found 216.1958.

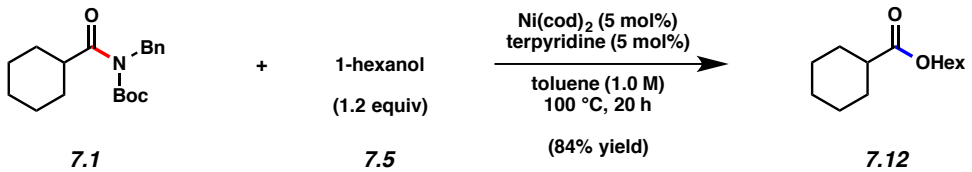

7.1 *7.5* *7.12*

Ester 7.12. Purification by flash chromatography (50:1 Hexanes:EtOAc) generated ester **7.12** (84% yield, average of two experiments) as a clear oil. Ester **7.12**: R_f 0.47 (20:1 Hexanes:EtOAc). Spectral data match those previously reported.[16]

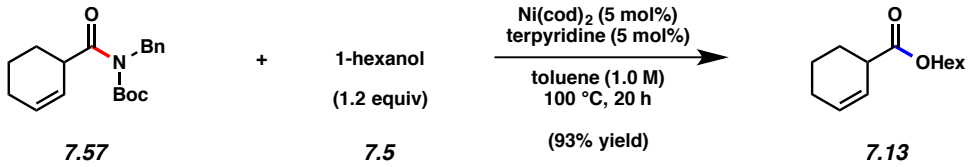

7.57 *7.5* *7.13*

Ester 7.13. Purification by flash chromatography (40:1 Hexanes:EtOAc) generated ester **7.13** (93% yield, average of two experiments) as a clear oil. Ester **7.13**: R_f 0.58 (20:1 Hexanes:EtOAc); ^{1}H NMR (500 MHz, $CDCl_3$): 5.67 (s, 2H), 4.08 (t, J = 6.7, 2H), 2.57–2.51 (m, 1H), 2.25–2.23 (m, 2H), 2.13–1.97 (m, 3H), 1.72–1.58 (m, 3H), 1.36–1.29 (m, 6H), 0.89 (t, J = 6.9, 3H) ^{13}C NMR (125 MHz, $CDCl_3$): δ 176.1, 126.8, 125.4, 64.6, 39.5, 31.6, 28.7, 27.6, 25.7, 25.2, 24.6, 22.7, 14.1; IR (film): 3027, 2977, 2932, 1730, 1690, 1458, 1440, 1366, 1218, 1151, 1074, 1024; HRMS-ESI (m/z) $[M–H]^-$ calcd for $C_{13}H_{21}O_2$ 209.1542; found 209.1535.

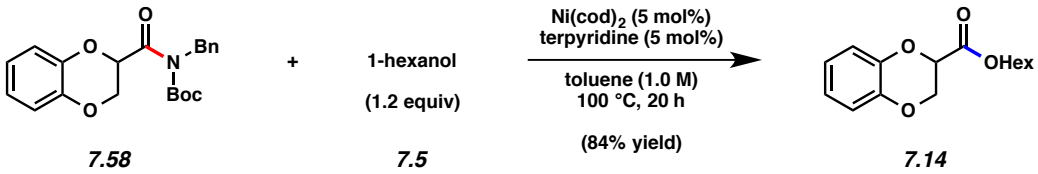

7.58 *7.5* *7.14*

Ester 7.14. Purification by flash chromatography (50:1 Hexanes:EtOAc) generated ester **7.14** (84% yield, average of two experiments) as a clear oil. Ester **7.14**: R_f 0.56 (5:1 Hexanes:EtOAc); ^{1}H NMR (500 MHz, $CDCl_3$): δ 7.02–6.97 (m, 1H), 6.91–6.83 (m, 3H), 4.85–4.81 (m, 1H), 4.44–4.33 (m, 2H), 4.26–4.14 (m, 2H), 1.66–1.57 (m, 2H), 1.33–1.21 (m, 6H), 0.91–0.85 (m, 3H); ^{13}C NMR (125 MHz, $CDCl_3$): δ 168.3, 143.1, 142.5, 122.3, 121.9, 117.5, 117.4, 72.2, 66.2, 65.1, 31.4, 28.6, 25.5, 22.6, 14.1; IR (film): 2957, 2927, 2860, 1760, 1735 cm^{-1}; HRMS-ESI (*m/z*) $[M+Na]^+$ calcd for $C_{15}H_{20}O_4Na$, 287.1259; found 287.1248.

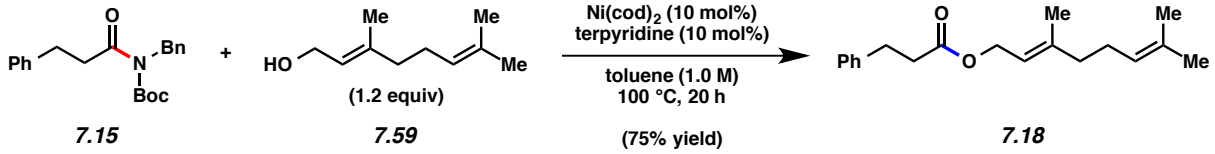

Ester 7.18 (Figure 7.3). Purification by flash chromatography (40:1 Hexanes:EtOAc) generated ester **7.18** (75% yield, average of two experiments) as a clear oil. Ester **7.18**: R_f 0.44 (20:1 Hexanes:EtOAc); ^{1}H NMR (500 MHz, $CDCl_3$): δ 7.30–7.27 (m, 2 H), 7.29–7.18 (m, 3H), 5.33 (td, *J* = 1.2, 1H), 5.10 (tt, *J* = 6.9, 1.3, 1H), 4.60 (d, *J* = 7.2, 2H), 2.97 (apt t, *J* = 8.2, 7.6, 2H), 2.64 (t, *J* = 8.1, 7.5, 2H), 2.12–2.02 (m, 4H), 1.70–1.69 (m, 6H), 1.60 (br s, 3H); ^{13}C NMR (125 MHz, $CDCl_3$): δ 173.1, 142.4, 140.7, 131.99, 128.6, 128.4, 126.3, 123.9, 118.4, 61.5, 39.7, 36.1, 31.1, 26.4, 25.8, 17.8, 16.6; IR (film): 3068, 3026, 2967, 2919, 2857, 1734, 1452, 1379, 1235, 1161; HRMS-ESI (m/z) $[M–H]^-$ calcd for $C_{19}H_{25}O_2$ 285.1855; found 285.1869.

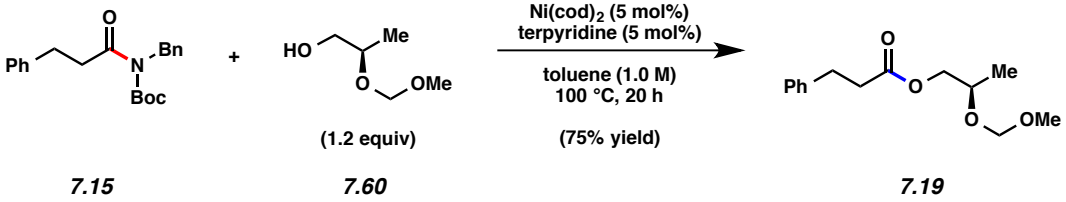

Ester 7.19 (Figure 7.3). Purification by flash chromatography (20:1 → 10:1 Hexanes:EtOAc) generated ester **7.19** (75% yield, average of two experiments) as a clear oil. Ester **7.19**: R_f 0.34 (10:1 Hexanes:EtOAc); ^{1}H NMR (500 MHz, $CDCl_3$): δ 7.32–7.28 (m, 2H), 7.22–7.17 (3H), 4.68 (q, *J* = 6.9, 3.1, 2H), 4.12–4.02 (m, 2H), 3.96–3.86 (m, 1H), 3.36 (br s, 3H), 2.99 (t, *J* = 8.2, 7.4, 2H), 2.69 (apt t, *J* = 8.2, 7.3, 2H), 1.18 (d, *J* = 6.4, 3H); ^{13}C NMR (125 MHz, $CDCl_3$): δ 172.9, 140.6, 128.7, 128.4, 126.4, 95.3, 55.4, 35.9, 31.0, 17.3; IR (film): 3029, 29782934, 2893, 2852, 1734, 1454, 1377, 1142, 1032, 918; HRMS-ESI (m/z) $[M+Na]^+$ calcd for $C_{14}H_{20}O_4Na$ 275.1259; found 275.1263; $[\alpha]^{24.8}_D$ –980.0 ° (*c* = 1.00, CH_2Cl_2).

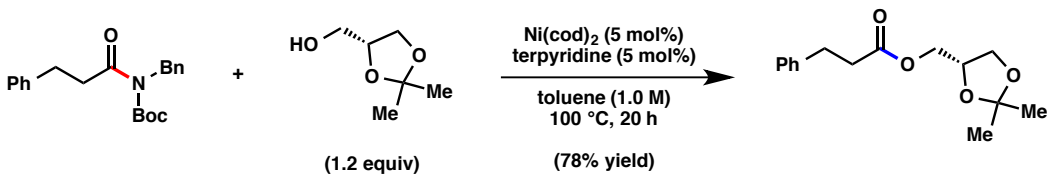

7.15 *7.61* *7.20*

Ester 7.20 (Figure 7.3). Purification by flash chromatography (10:1 Hexanes:EtOAc) generated ester **7.20** (78% yield, average of two experiments) as a clear oil. Ester **7.20**: R_f 0.45 (10:1 Hexanes:EtOAc); ^{1}H NMR (500 MHz, $CDCl_3$): δ 7.30–7.27 (m, 2H), 7.22–7.19 (m, 3H), 4.29–4.24 (m, 1H), 4.17 (dd, *J* = 6.8, 4.8, 1H), 4.10 (dd, *J* = 6.0, 5.5, 1H), 4.04 (dd, *J* = 6.4, 2.0, 1H); 3.69 (dd, *J* = 6.2, 2.3, 1H), 2.98 (t, *J* = 7.8, 2H), 2.69 (apt t, *J* = 8.0, 7.6, 2H), 1.42 (br s, 3H), 1.36 (br s, 3H); ^{13}C NMR (125 MHz, $CDCl_3$): δ 172.8, 140.4, 128.7, 128.4, 126.5, 109.9, 73.7, 66.4, 64.9, 35.8, 31.0, 26.8, 25.5; IR (film): 3030, 2990, 2945, 2892, 1740, 1603, 1495, 1453, 1208, 1154, 1054, 1084; HRMS-ESI (m/z) $[M+Na]^+$ calcd for $C_{15}H_{20}O_4Na$ 287.1259; found 275.1252; $[\alpha]^{25.0}_D$ –990.0 ° (*c* = 1.00, CH_2Cl_2).

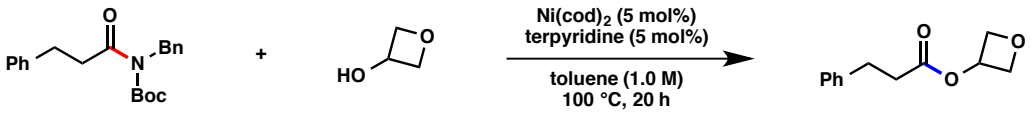

7.15 *7.62* *7.21*

Ester 7.21 (Figure 7.3). Purification by flash chromatography (20:1 → 10:1 Hexanes:EtOAc) generated ester **7.21** (93% yield, average of two experiments) as a clear oil. Ester **7.21**: R_f 0.26 (20:1 Hexanes:EtOAc); ^{1}H NMR (500 MHz, $CDCl_3$): δ 7.31–7.28 (m, 2H), 7.23–7.19 (m, 3H), 5.43–5.40 (m 1H), 4.87–4.84 (m, 2H), 4.59–4.56 (m, 2H), 2.99 (t, *J* =, 2H), 2.70 (apt t, *J* = 8.4, 7.8, 2H); ^{13}C NMR (125 MHz, $CDCl_3$): δ 172.2, 140.1, 128.7, 128.4, 126.5, 77.6, 67.96, 335.6,

30.9; IR (film): 3085, 3066, 3032, 2953, 2882, 1731, 1500, 1455, 1359, 1161, 972; HRMS-ESI (m/z) $[M+Na]^+$ calcd for $C_{12}H_{14}O_3Na$ 229.0841; found 229.0842.

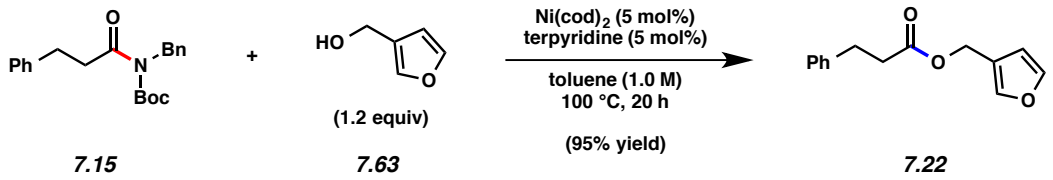

7.15 *7.63* *7.22*

Ester 7.22. Purification by flash chromatography (40:1 → 30:1 Hexanes:EtOAc) generated ester **7.22** (95% yield, average of two experiments) as a clear oil. Ester **7.22**: R_f 0.45 (10:1 Hexanes:EtOAc); ^{1}H NMR (500 MHz, $CDCl_3$): δ 7.423–7.420 (m. 1H), 7.29–7.26 (2H), 7.21–7.17 (m, 3H), 6.39–6.36 (2H), 5.07 (br s, 2H), 2.97 (t, J = 7.7, 2H), 2.68 (t, J = 7.7 , 2H); ^{13}C NMR (125 MHz, $CDCl_3$): δ 172.6, 149.6, 143.4, 140.5, 128.6, 128.4, 126.4, 110.8 110.7, 58.2, 35.9, 30.9; IR (film): 3029, 2935, 1733, 1497, 1454, 1369, 1348, 1145, 1078, 919; HRMS-ESI (m/z) $[M+Na]^+$ calcd for $C_{14}H_{14}O_3Na$ 253.0841; found 253.0763.

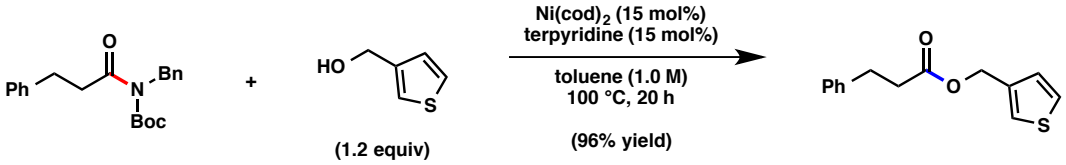

7.15 *7.64* *7.23*

Ester 7.23 (Figure 7.3). Purification by flash chromatography (30:1 Hexanes:EtOAc) generated ester **7.23** (96% yield, average of two experiments) as a clear oil. Ester **7.23**: R_f 0.65 (5:1 Hexanes:EtOAc); ^{1}H NMR (500 MHz, $CDCl_3$): δ 7.34–7.30 (m, 1H), 7.30–7.25 (m, 2H), 7.22–7.16 (m, 3H), 7.10–7.06 (m, 1H), 7.01–6.96 (m, 1H), 5.27 (s, 2H), 2.99–2.93 (m, 2H), 2.70–2.63 (m, 2H); ^{13}C NMR (125 MHz, $CDCl_3$): δ 172.7, 140.5, 138.0, 128.6, 128.4, 128.35, 126.98,

126.96, 126.4, 60.6, 36.0, 31.0; IR (film): 3065, 2955, 1735, 1453, 1146 cm^{-1}; HRMS-ESI (*m/z*) $[M+NH_4]^+$ calcd for $C_{14}H_{14}O_2SNH_4$, 264.1058; found 264.1053.

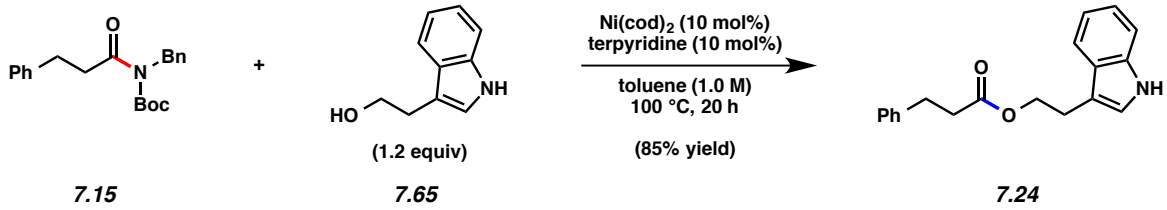

7.15 *7.65* *7.24*

Ester 7.24 (Figure 7.3). Purification by flash chromatography (9:1 Hexanes:EtOAc) generated ester **7.24** (85% yield, average of two experiments) as a bnrow oil. Ester **7.24**: R_f 0.18 (5:1 Hexanes:EtOAc); ^{1}H NMR (500 MHz, $CDCl_3$): δ 7.99 (s, 1H), 7.66–7.60 (m, 1H), 7.40–7.34 (m, 1H), 7.31–7.27 (m, 2H) 7.24–7.17 (m, 4H), 7.17–7.12 (m, 1H), 7.00–6.96 (m, 1H), 4.37 (t, *J* = 7.1, 2H), 3.11–3.06 (m, 2H), 2.98–2.92 (m, 2H), 2.67–2.61 (m, 2H); ^{13}C NMR (125 MHz, $CDCl_3$): δ 173.1, 140.7, 136.3, 128.6, 128.5, 127.6, 126.4, 122.3, 122.1, 119.6, 118.9, 112.2, 111.3, 64.7, 36.1, 31.1, 24.9; IR (film): 3409, 3025, 2920, 1715, 1458 cm^{-1}; HRMS-ESI (*m/z*) $[M+Na]^+$ calcd for $C_{19}H_{19}NO_2Na$, 316.1313; found 316.1304.

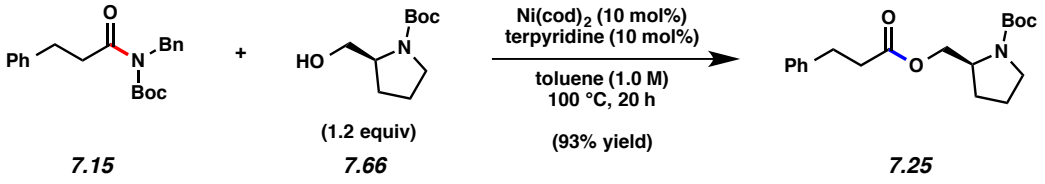

7.15 *7.66* *7.25*

Ester 7.25 (Figure 7.3). Purification by flash chromatography (10:1 → 5:1 Hexanes:EtOAc) generated ester **7.25** (93% yield, average of two experiments) as a clear oil. Ester **7.25**: R_f 0.17 (20:1 Hexanes:EtOAc); ^{1}H NMR (500 MHz, $CDCl_3$): δ 7.30–7.27 (m, 2H), 7.21 (7.18, 3H), 4.17 (dd, *J* = 10.5, 6.9, 1H), 4.06–3.90 (m, 2H), 3.39–3.30 (m, 2H), 2.96 (t, *J* = 7.8, 2H), 2.65 (t, *J* =

7.7, 2H), 1.89–1.65 (m, 5H), (br s, 9H); ^{13}C NMR (125 MHz, $CDCl_3$): δ 172.8, 154.5, 104.5, 128.6, 128.4, 126.4, 79.9, 64.9, 55.6, 46.8, 46.6, 36.0, 31.1, 28.8, 28.6, 27.9, 23.9, 23.1; IR (film): 2974, 1736, 1690, 1454, 1389, 1365, 1248, 1160, 1106, 699; HRMS-ESI (m/z) $[M+Na]^+$ calcd for $C_{19}H_{27}NO_4Na$ 356.1838; found 356.1821; $[\alpha]^{24.7}_D$ –1024.0 ° (*c* = 1.00, CH_2Cl_2).

*Note: Amide **7.25** was obtained as a mixture of rotamers. These data represent empirically observed chemical shifts and coupling constants from the ^{1}H NMR spectrum.*

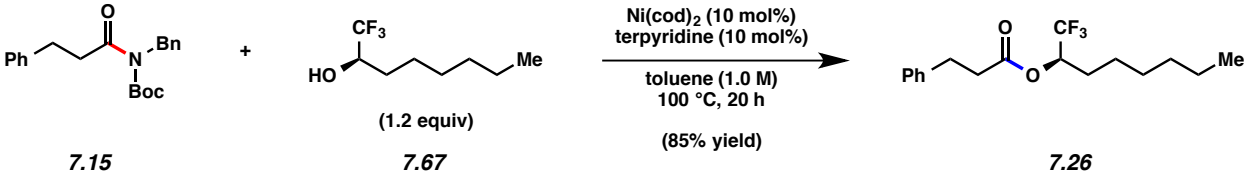

7.15 ***7.67*** ***7.26***

Ester 7.26. Purification by flash chromatography (30:1 Hexanes:EtOAc) generated ester **7.26** (85% yield, average of two experiments) as a clear oil. Ester **7.26**: R_f 0.70 (5:1 Hexanes:EtOAc); ^{1}H NMR (500 MHz, $CDCl_3$): δ 7.31–7.28 (m, 2H), 7.22–7.20 (m, 3H), 5.33–5.26 (m, 1H), 2.99 (t, *J* = 7.7, 2H), 2.78–2.68 (m, 2H), 1.76–1.63 (m, 2H), 1.28–1.24 (m, 6H), 0.89 (t, *J* = 6.8, 3H); ^{13}C NMR (125 MHz, $CDCl_3$): δ 171.6, 140.0, 128.7, 128.4, 126.6, 124.0 (quartet, *J* = 283.5, 562.4), 69.7 (quartet, J = 31.8, 64.8), 35.5, 31.3, 30.9, 27.86, 27.85, 24.2, 22.4, 14.0; ^{19}F NMR (282 MHz, $CDCl_3$): δ –77.2 (d, *J* = 6.9); IR (film): 2957, 2867, 1755, 1278, 1176 cm^{-1}; HRMS-ESI (*m/z*) $[M+NH_4]^+$ calcd for $C_{16}H_{21}F_3O_2NH_4$, 320.1837; found 320.1839; $[\alpha]^{19.8}_D$ +8.80 ° (*c* = 1.00, $CHCl_3$).

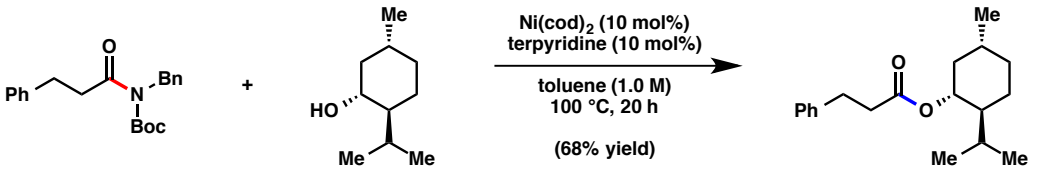

7.15 *7.67* *7.27*

Ester 7.27 (Figure 7.3). Purification by flash chromatography (40:1 Hexanes:EtOAc) generated ester **7.27** (68% yield, average of two experiments) as a clear oil. Ester **7.27**: R_f 0.40 (20:1 Hexanes:EtOAc). Spectral data match those previously reported.[17]

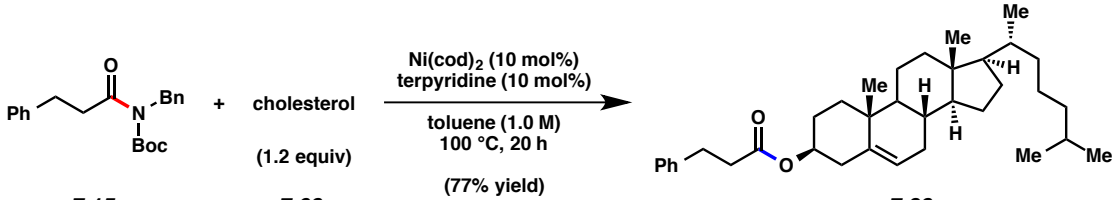

7.15 *7.68* *7.28*

Ester 7.28 (Figure 7.3). Purification by flash chromatography (40:1 Hexanes:EtOAc) generated ester **7.28** (77% yield, average of two experiments) as a white solid. Ester **7.28**: R_f 0.40 (20:1 Hexanes:EtOAc). Spectral data match those previously reported.[18]

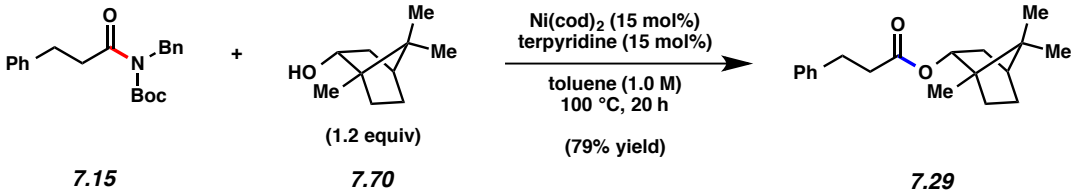

7.15 *7.70* *7.29*

Ester 7.29 (Figure 7.3). Purification by flash chromatography (40:1 Hexanes:EtOAc) generated ester **7.29** (79% yield, average of two experiments) as a clear oil. Ester **7.29**: R_f 0.57 (20:1 Hexanes:EtOAc). Spectral data match those previously reported.[19]

7.5.2.7. Coupling with Amino Acid Derivatives

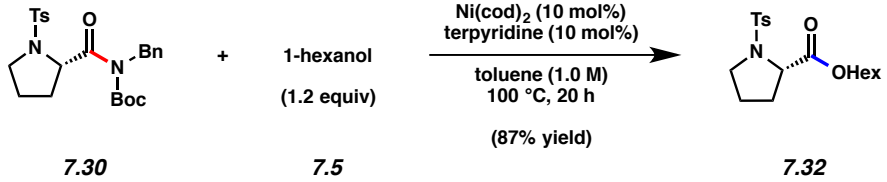

7.30 *7.5* *7.32*

Ester 7.32 (Figure 7.4). Purification by flash chromatography (10:1 → 5:1 Hexanes:EtOAc) generated ester **7.32** (87% yield, average of two experiments) as a clear oil. Ester **7.32**: R_f 0.29 (5:1 Hexanes:EtOAc); ^{1}H NMR (500 MHz, $CDCl_3$): δ 7.76 (d, J = 8.1, 2H), 7.31 (d, J = 8.1, 2H), 4.31–4.28 (m, 1H), 4.13–4.04 (m, 2H), 3.49–3.45 (m, 1H), 3.34–3.29 (m, 1H), 2.42 (s, 3H), 2.06–1.91 (m, 3H), 1.79–1.73 (m, 1H), 1.64–1.58 (m, 2H), 1.35–1.30 (m, 6H), 0.90 (apt t, J = 7.0, 5.6, 3H); ^{13}C NMR (125 MHz, $CDCl_3$): δ 172.3, 143.6, 135.6, 129.7, 127.6, 65.6, 60.6, 48.5, 31.5, 31.1, 28.6, 25.6, 24.8, 22.6, 21.7, 14.1; IR (film): 2957, 2930, 2860, 2875, 1749, 1598, 1455, 1351, 1159, 1094, 1009; HRMS-ESI (m/z) $[M+Na]^+$ calcd for $C_{18}H_{27}NO_4SNa$ 376.1559; found 376.1563; $[\alpha]^{23.5}_D$ –1042.0 ° (c = 1.00, CH_2Cl_2).

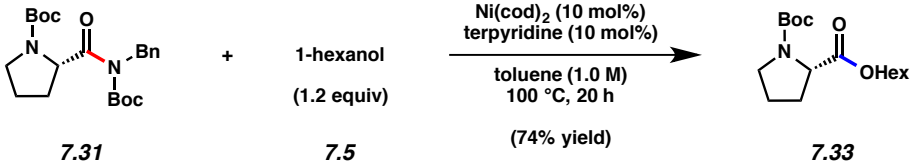

7.31 *7.5* *7.33*

Ester 7.33 (Figure 7.4). Purification via flash chromatography (30:1 → 20:1 → 15:1 Hexanes:EtOAc) yielded ester **7.33** as a clear liquid**.** Ester **7.33**: R_f 0.4 (5:1 Hexanes:EtOAc); ^{1}H NMR (500 MHz, $CDCl_3$): δ 4.38–4.19 (m, 1H), 4.19–4.03 (m, 2H), 3.61–3.31 (m, 2H), 2.30–2.11 (m, 1H), 2.02–1.80 (m, 3H), 1.69–1.58 (m, 2H), 1.50–1.39 (9H), 1.38–1.25 (m, 6H), 0.93–0.83 (m, 3H); ^{13}C NMR (125 MHz, $CDCl_3$): δ 173.5, 173.2, 171.3, 170.8, 169.3, 154.5, 154.0, 147.6, 146.8, 128.8, 127.6, 79.9, 67.5, 66.0, 65.9, 65.2, 62.6, 60.9, 59.3, 59.2, 59.0, 50.6, 49.2,

46.7, 46.4, 46.3, 31.5, 31.5, 31.4, 41.1, 30.4, 30.1, 29.8, 28.7, 28.6, 28.5, 25.7, 25.6, 25.5, 24.4, 24.0, 23.7, 23.6, 22.6, 14.1; IR (film): 2962, 2934, 2872, 2860, 1742, 1699, 1460, 1393, 1363, 1161, 1123; HRMS-ESI (m/z) $[M+Na]^+$ calcd for $C_{16}H_{29}NO_4Na$ 322.1993; found 322.1985; $[\alpha]^{23.4}_D$ –1012.0 ° (*c* = 1.00, CH_2Cl_2).

*Note: Ester **7.33** was obtained as a mixture of rotamers. These data represent empirically observed chemical shifts and coupling constants from the ^1H and ^{13}C NMR spectra.*

Appendix Seven: Spectra Relevant to Chapter Seven

Nickel Catalyzed Esterification of Aliphatic Amides

Liana Hie, Emma L. Baker, Sarah M. Anthony, Jean-Nicolas Desrosiers,
Chris Senanayake, and Neil K. Garg
Manuscript in preparation

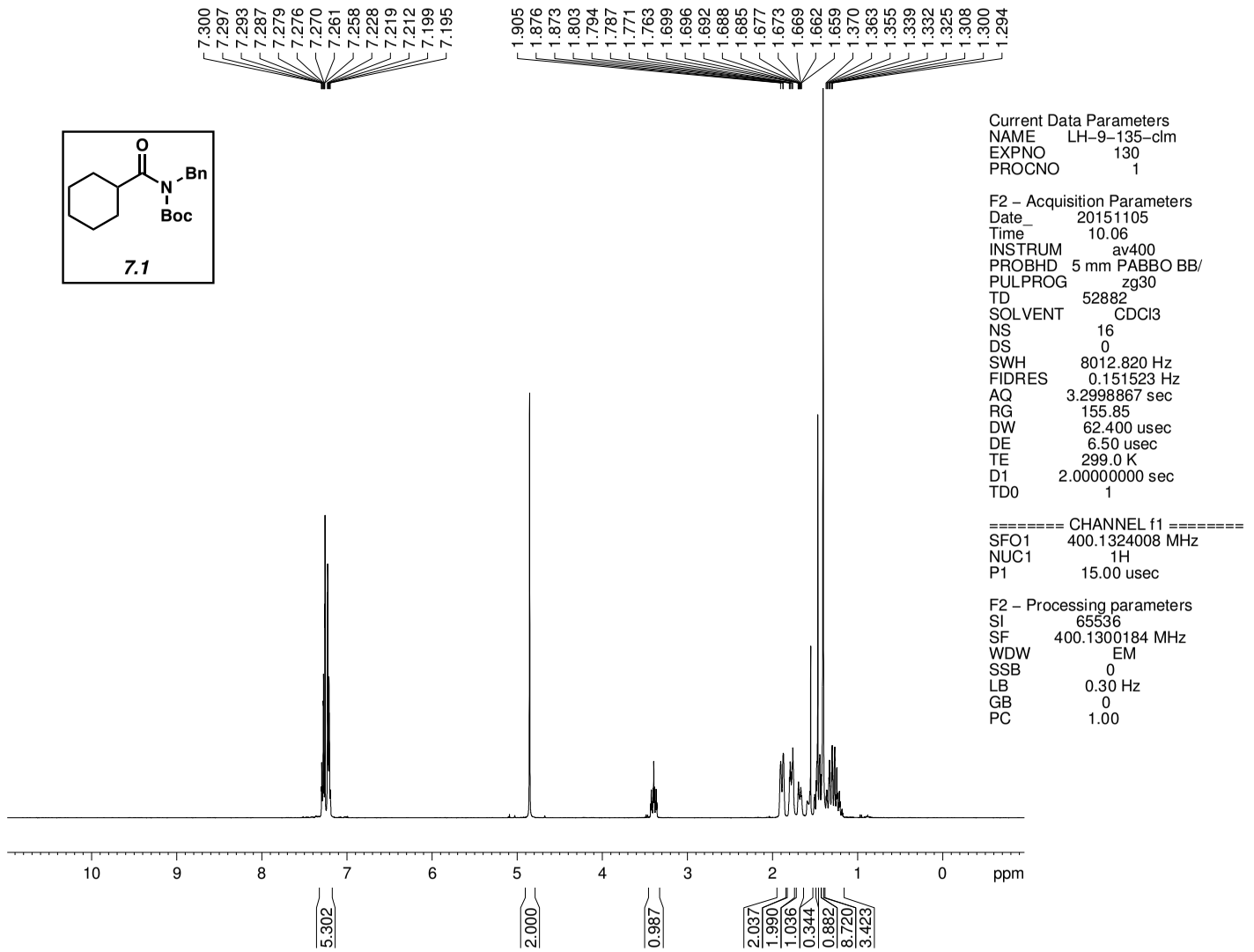

Figure A7.1. ^{1}H NMR (500 MHz, $CDCl_3$) of compound **7.1**

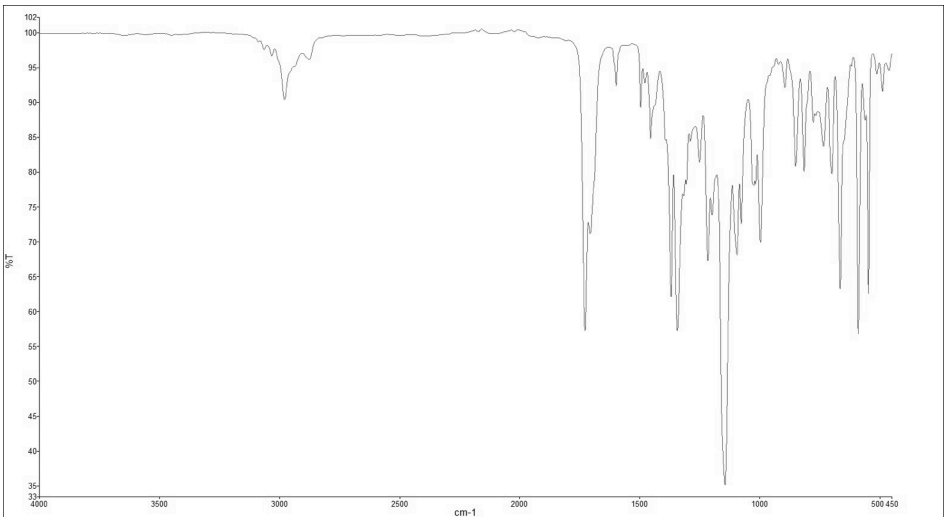

Figure A7.2. Infrared spectrum of compound **7.1**

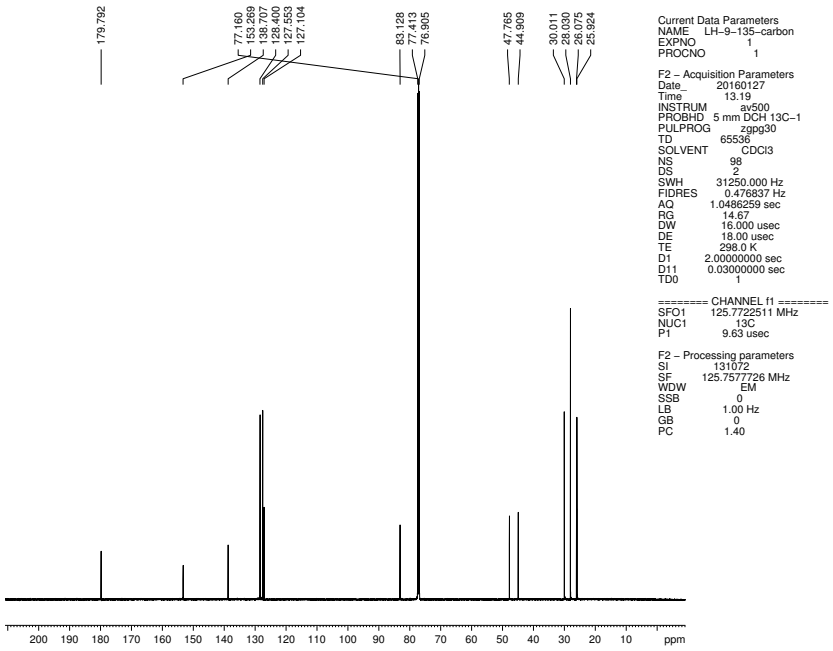

Figure A7.3. ^{13}C NMR (125 MHz, $CDCl_3$) of compound **7.1**

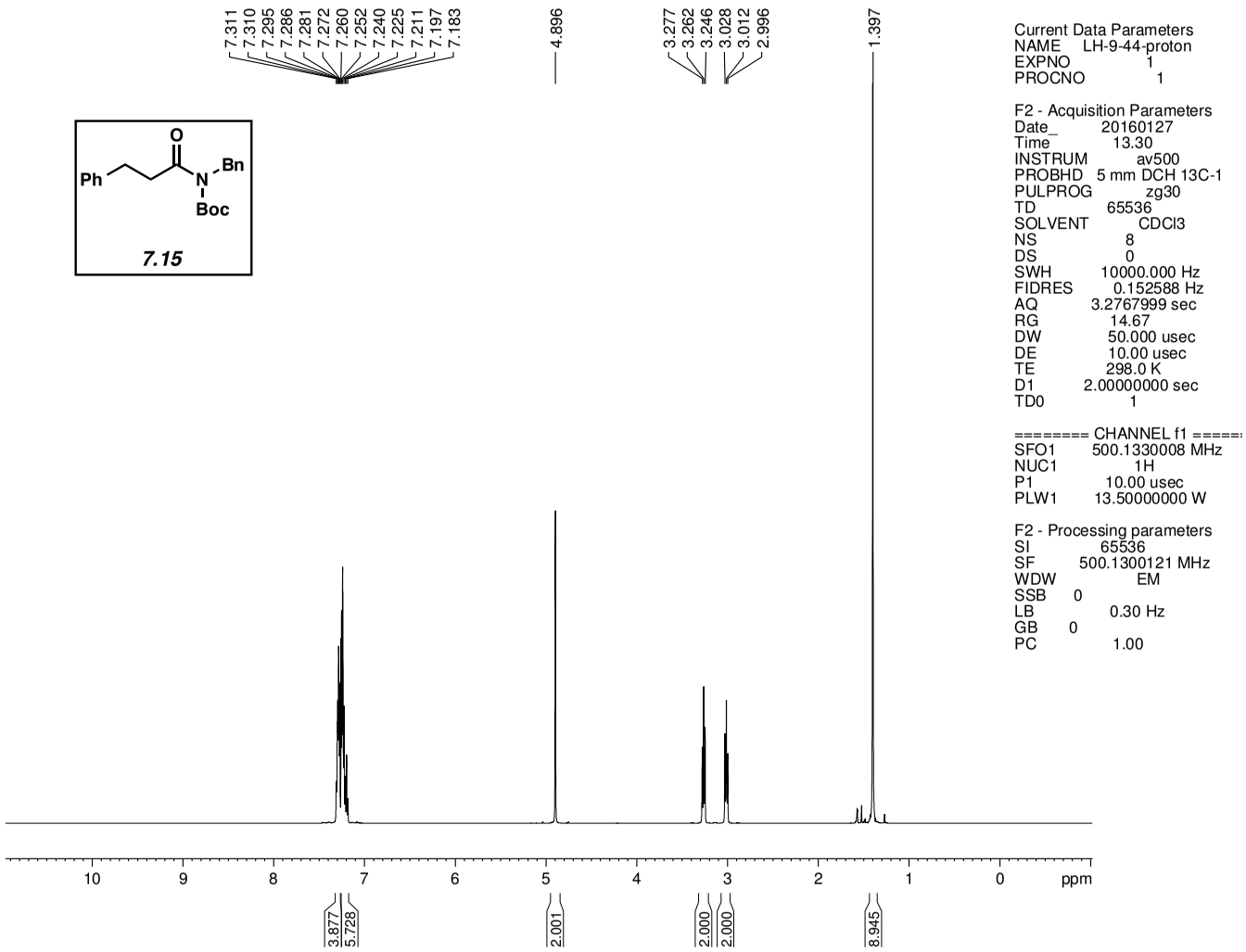

Figure A7.4. ^{1}H NMR (500 MHz, $CDCl_3$) of compound **7.15**

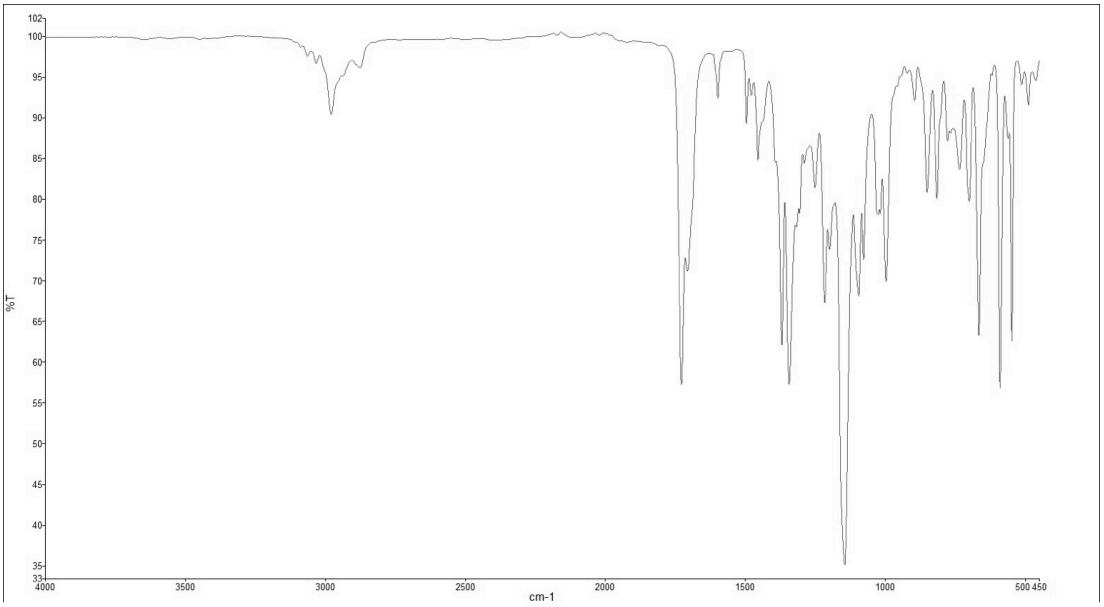

Figure A7.5. Infrared spectrum of compound **7.15**

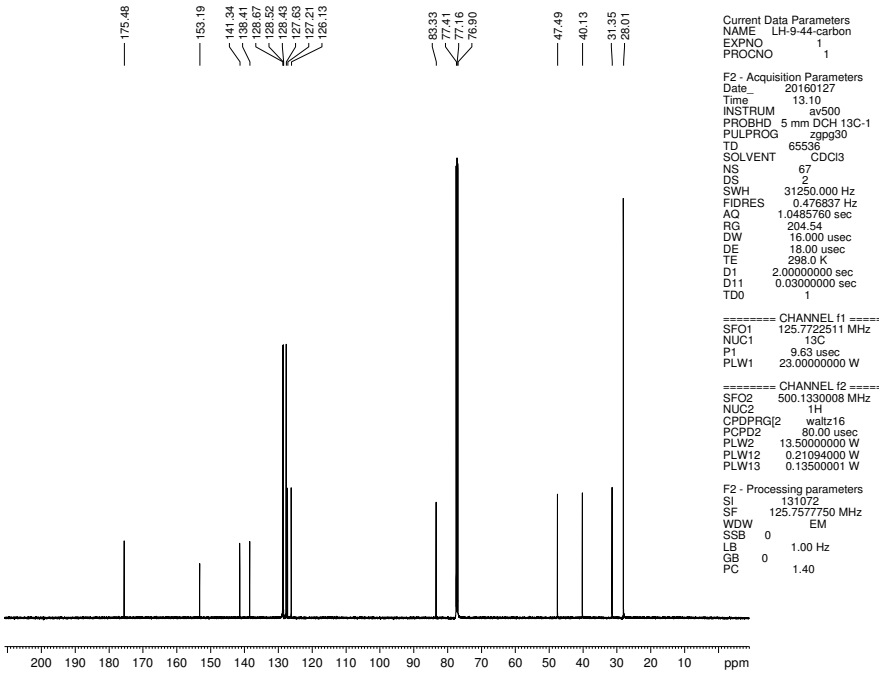

Figure A7.6. ^{13}C NMR (125 MHz, $CDCl_3$) of compound **7.15**

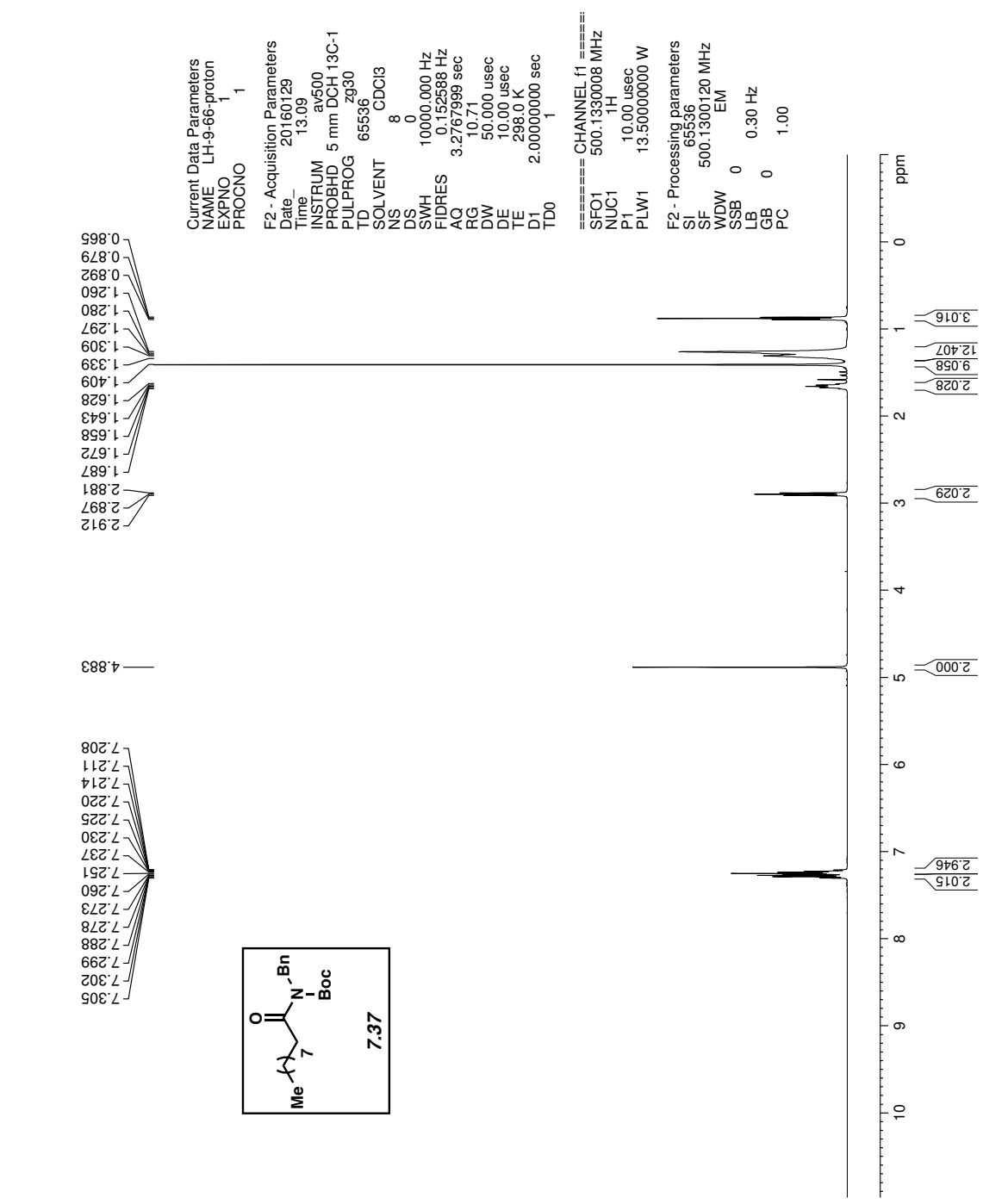

Figure A7.7. ^{1}H NMR (500 MHz, $CDCl_3$) of compound **7.37**

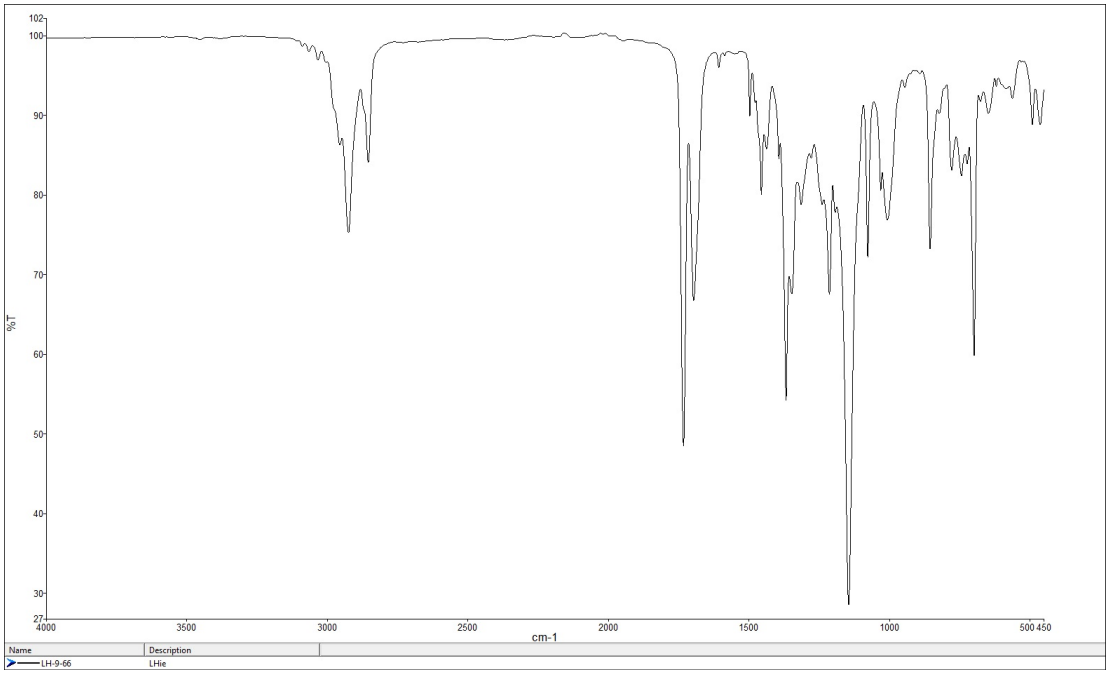

Figure A7.8 Infrared spectrum of compound **7.37**

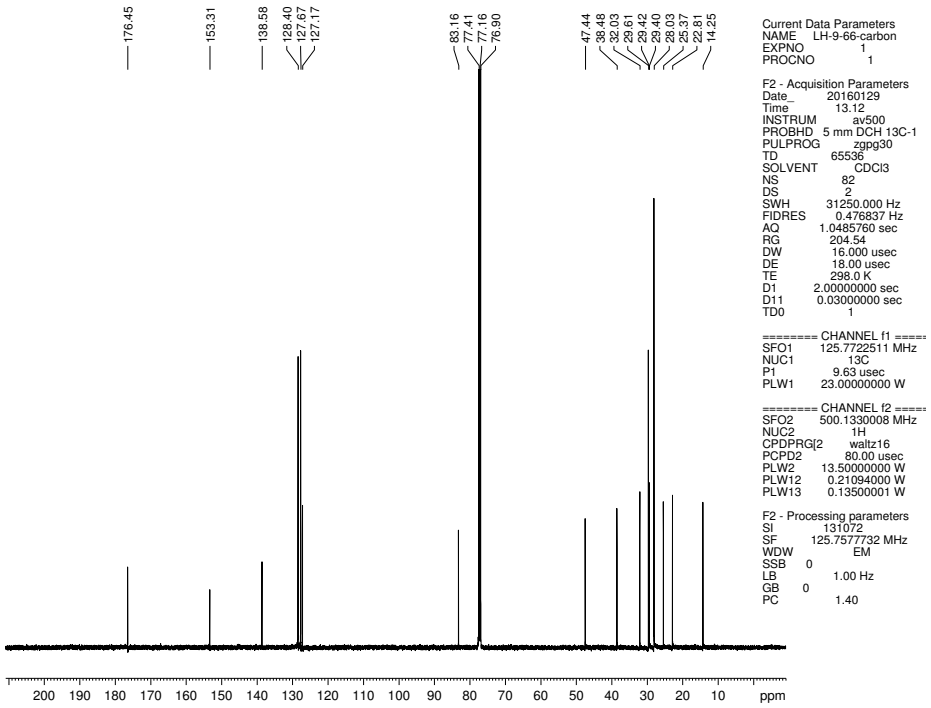

Figure A7.9 ^{13}C NMR (125 MHz, $CDCl_3$) spectrum of compound **7.37**

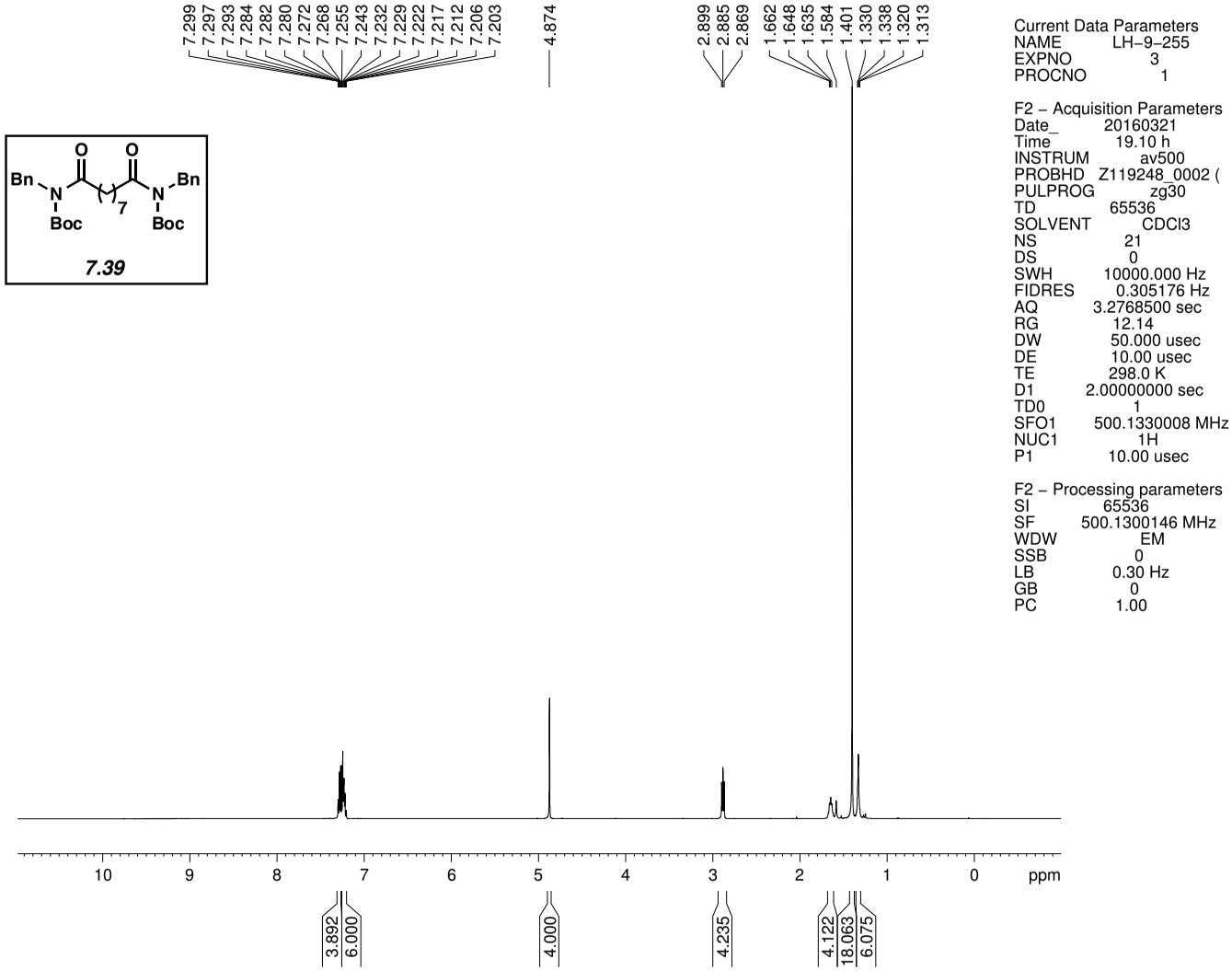

Figure A7.10. ^{1}H NMR (500 MHz, $CDCl_3$) of compound **7.39**

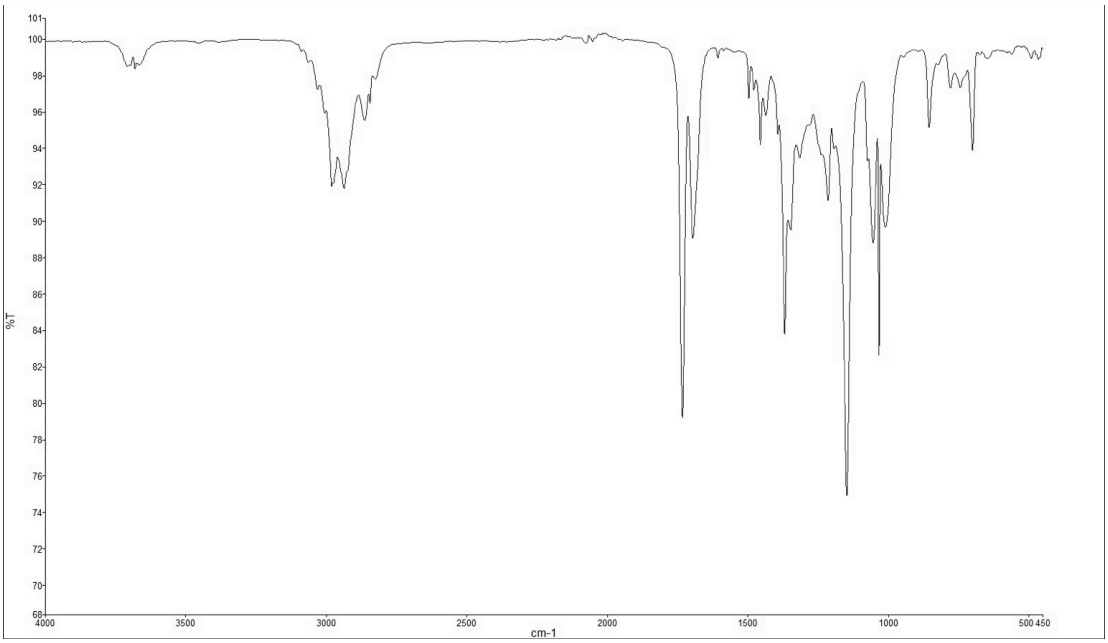

Figure A7.11 Infrared spectrum of compound **7.39**

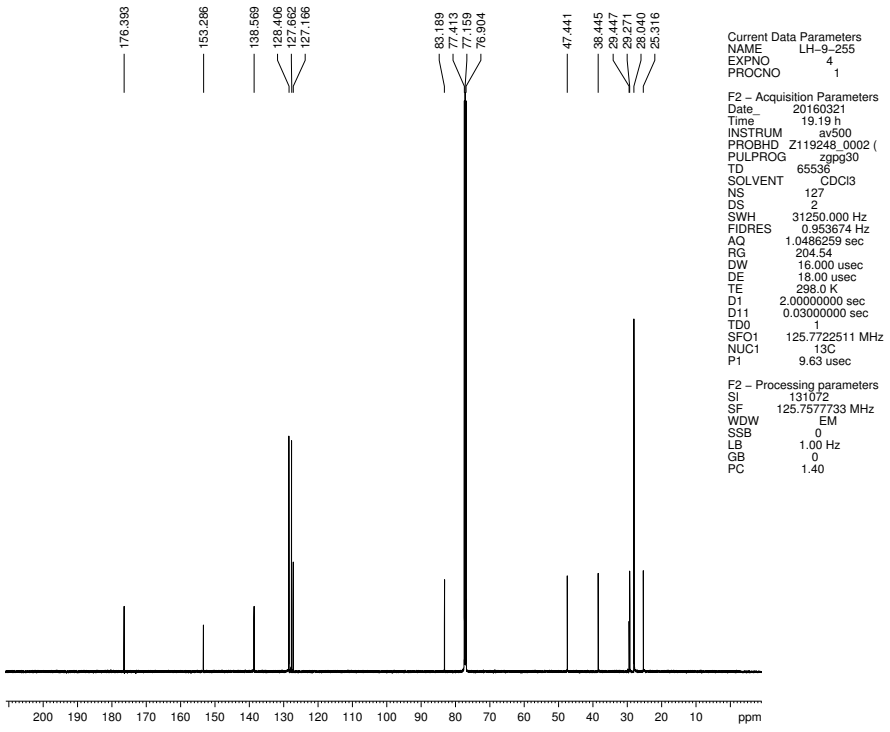

Figure A7.12 ^{13}C NMR (125 MHz, $CDCl_3$) spectrum of compound **7.39**

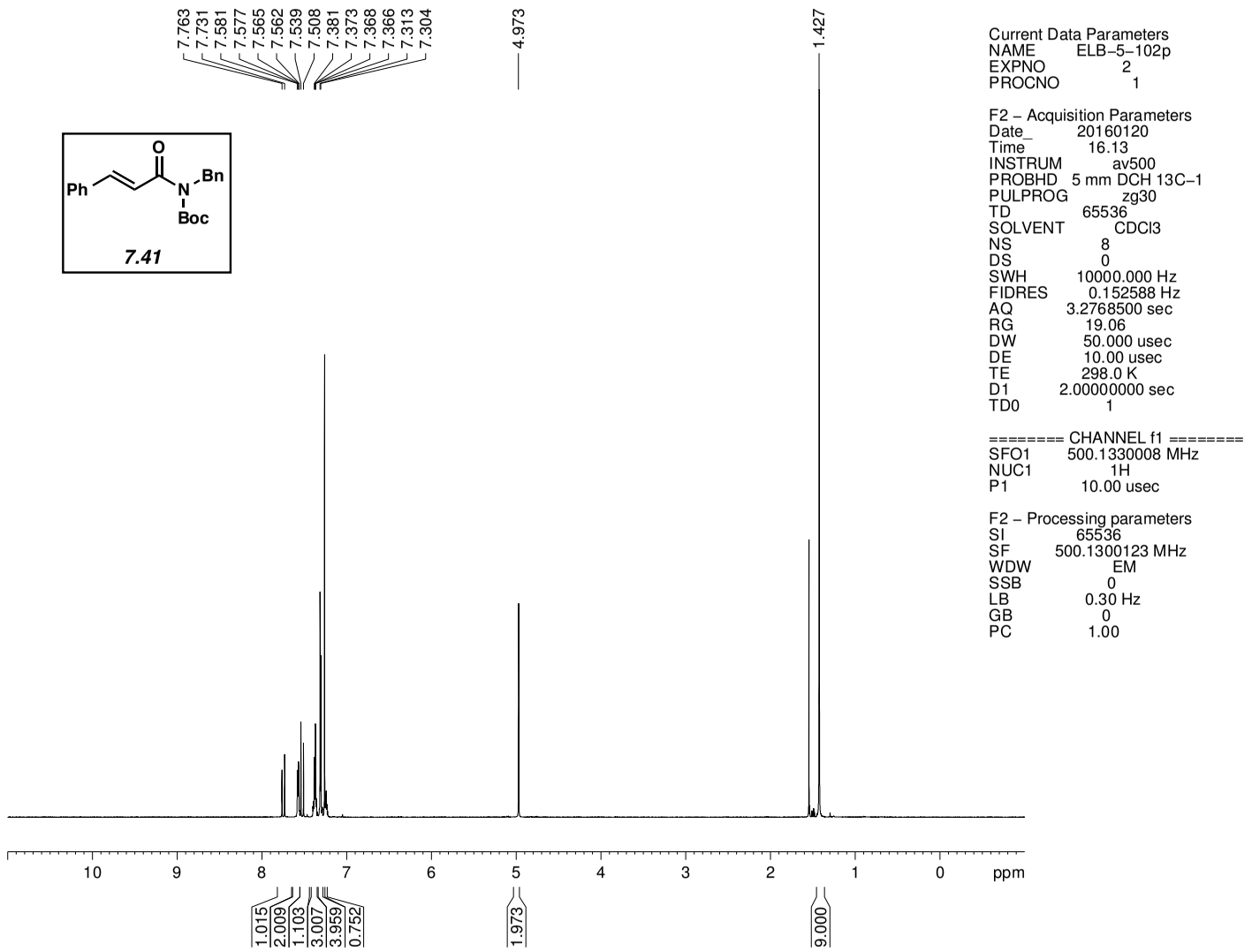

Figure A7.13. ^{1}H NMR (500 MHz, $CDCl_3$) of compound **7.41**

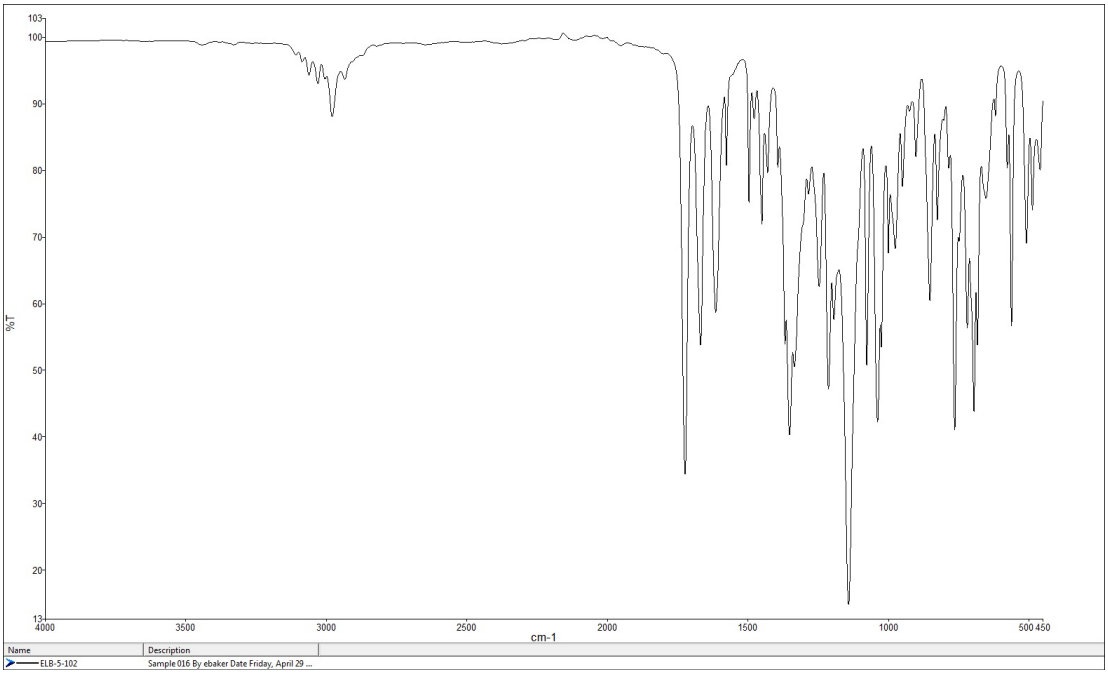

Figure A7.14 Infrared spectrum of compound **7.41**

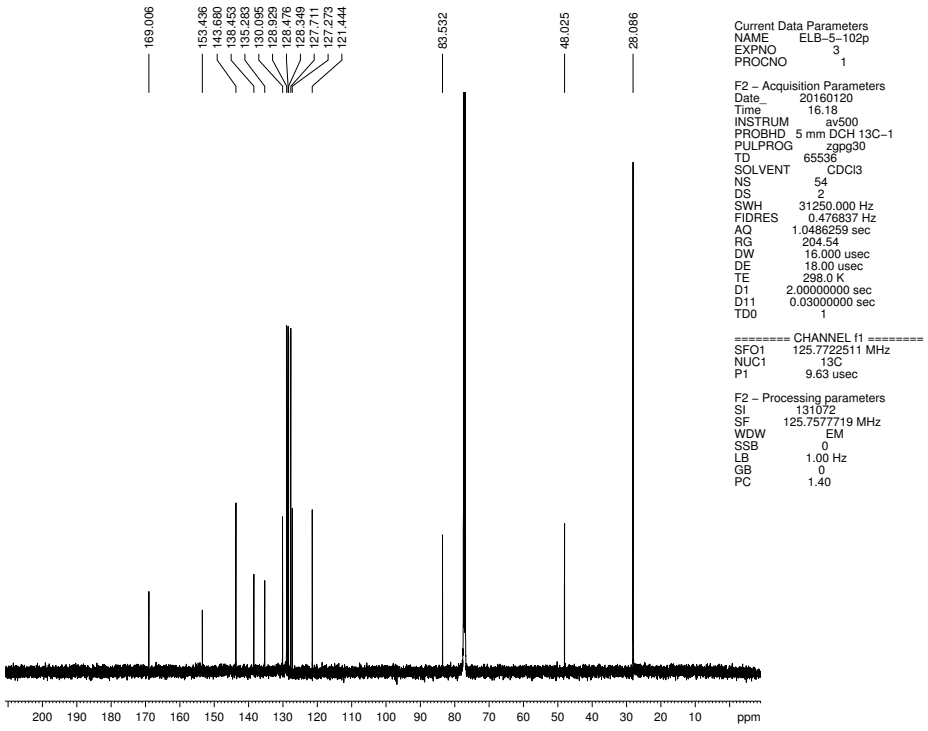

Figure A7.15 ^{13}C NMR (125 MHz, $CDCl_3$) spectrum of compound **7.41**

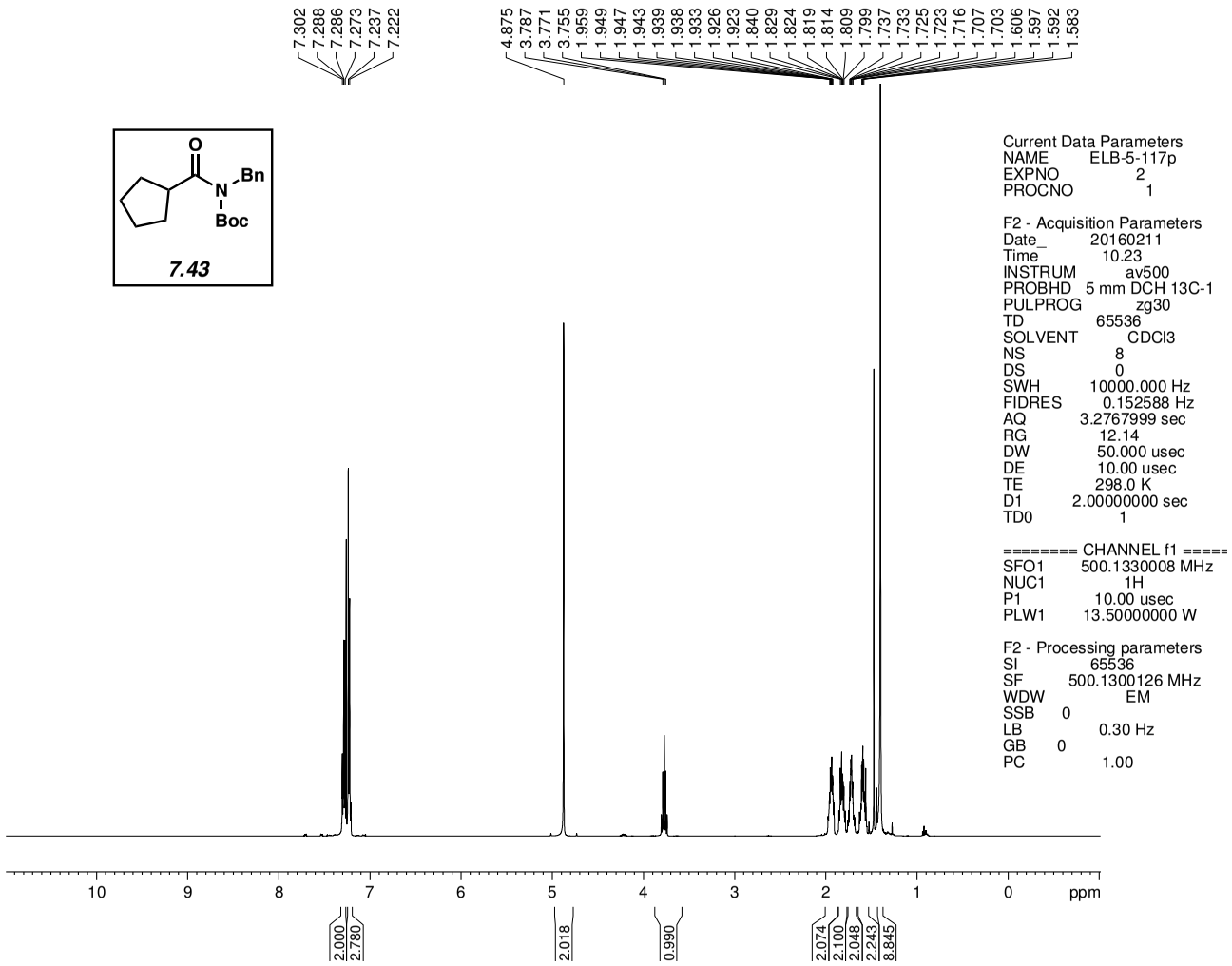

Figure A7.16. ^{1}H NMR (500 MHz, $CDCl_3$) of compound **7.43**

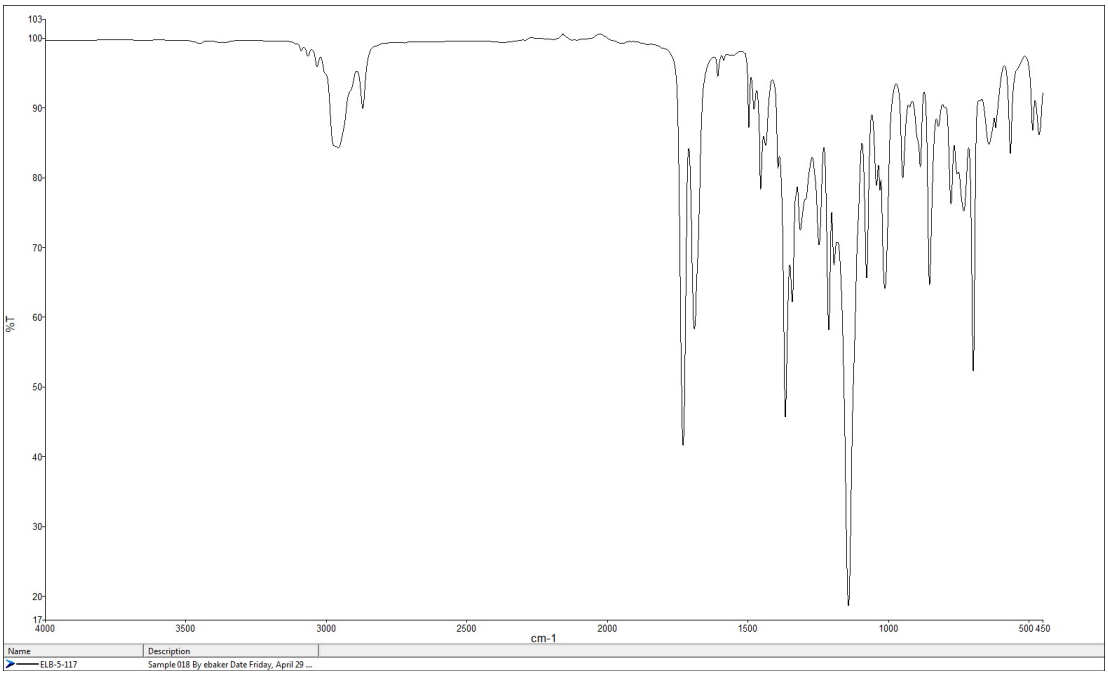

Figure A7.17. Infrared spectrum of compound **7.43**

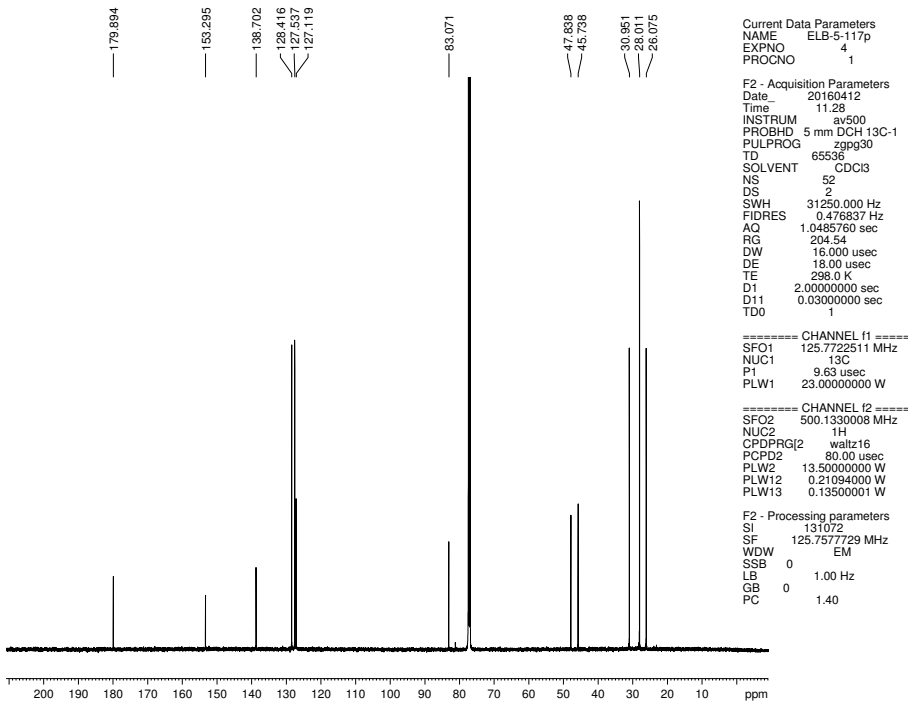

Figure A7.18 ^{13}C NMR (125 MHz, $CDCl_3$) spectrum of compound **7.43**

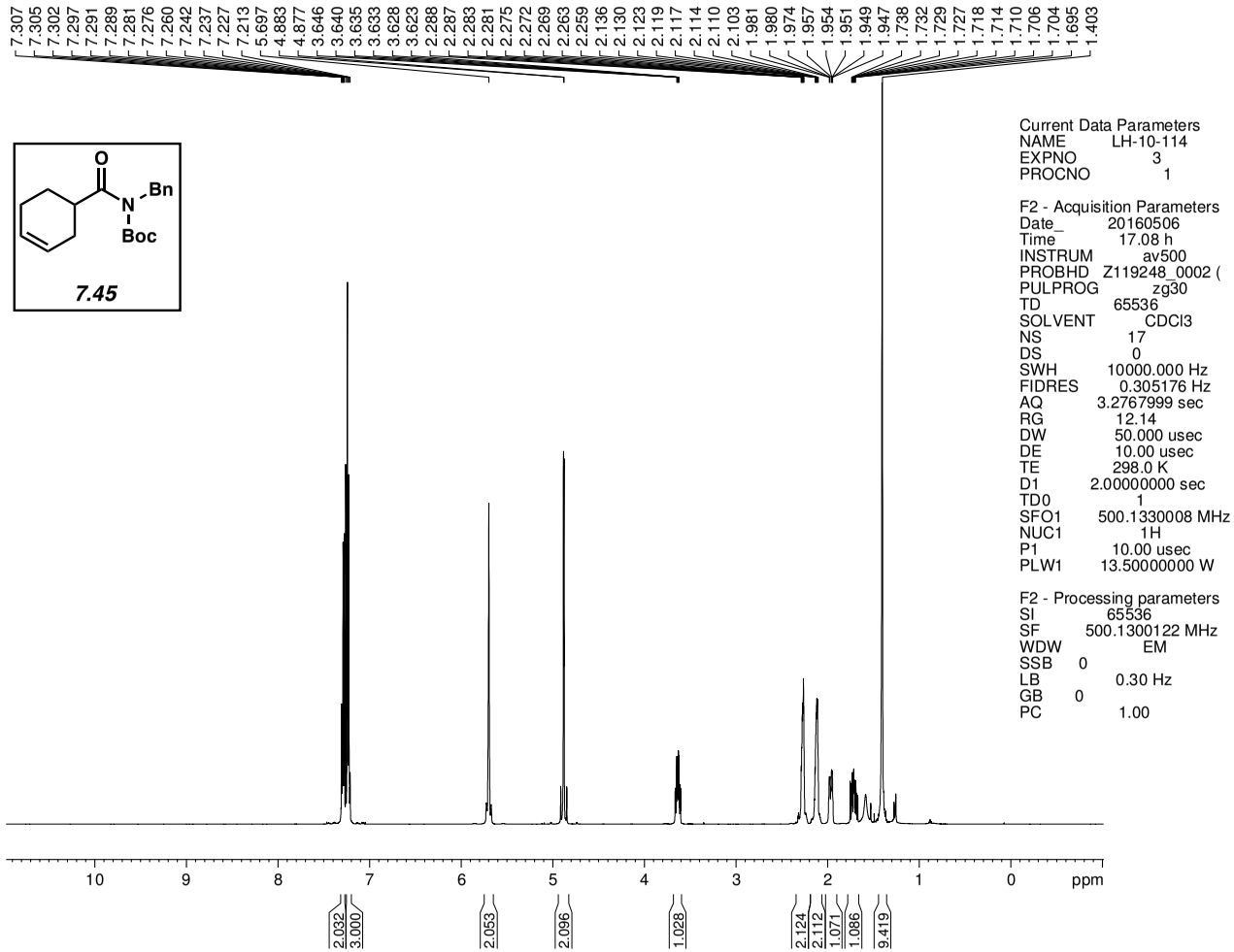

Figure A7.19. ^{1}H NMR (500 MHz, $CDCl_3$) of compound **7.45**

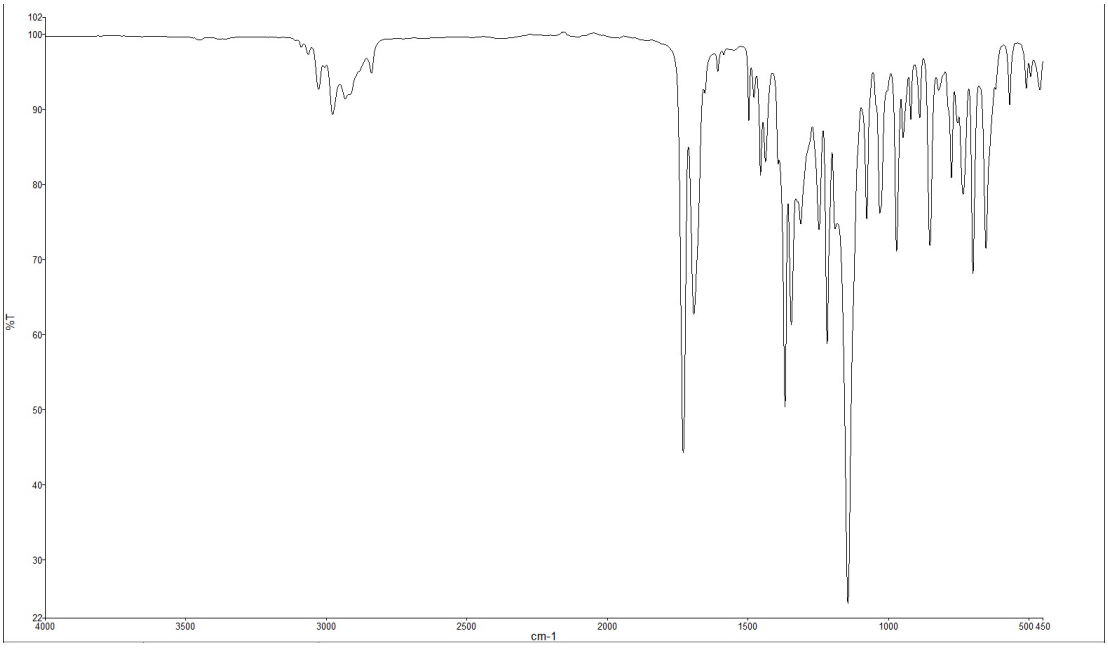

Figure A7.20. Infrared spectrum of compound **7.45**

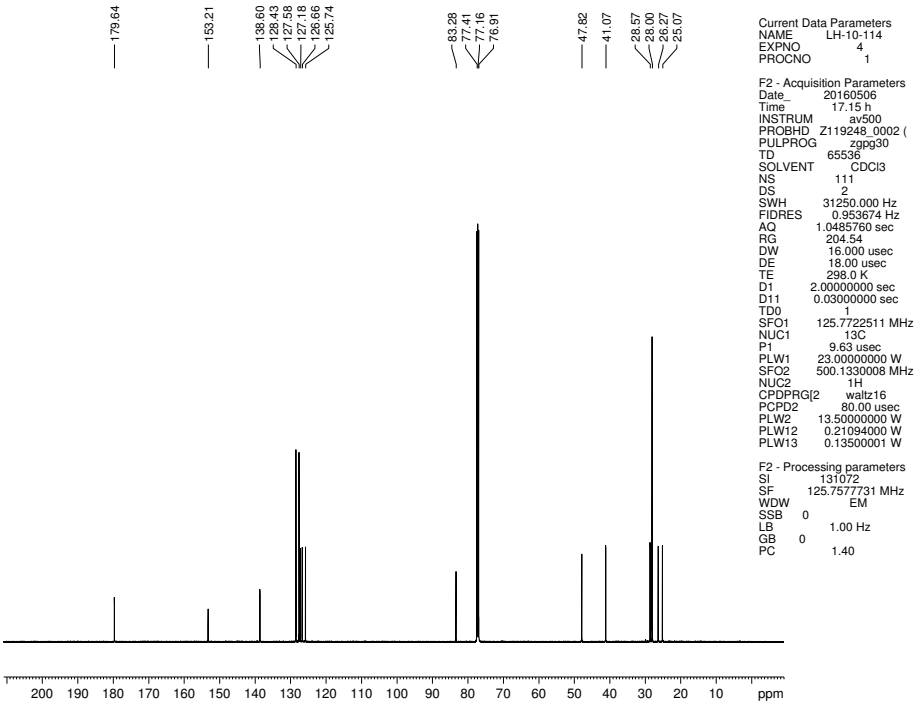

Figure A7.21 ^{13}C NMR (125MHz, $CDCl_3$) spectrum of compound **7.45**

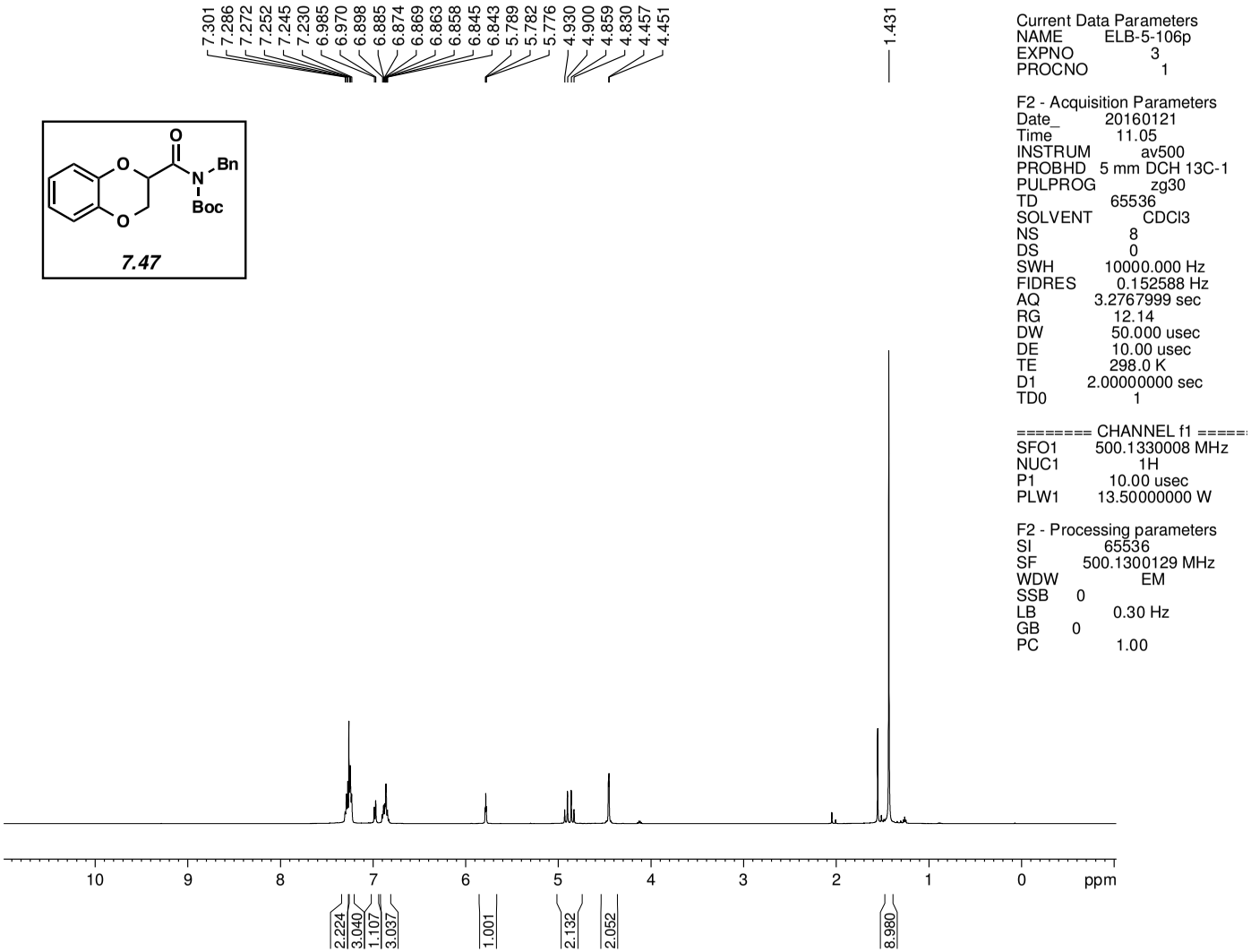

Figure A7.22. ^{1}H NMR (500 MHz, $CDCl_3$) of compound **7.47**

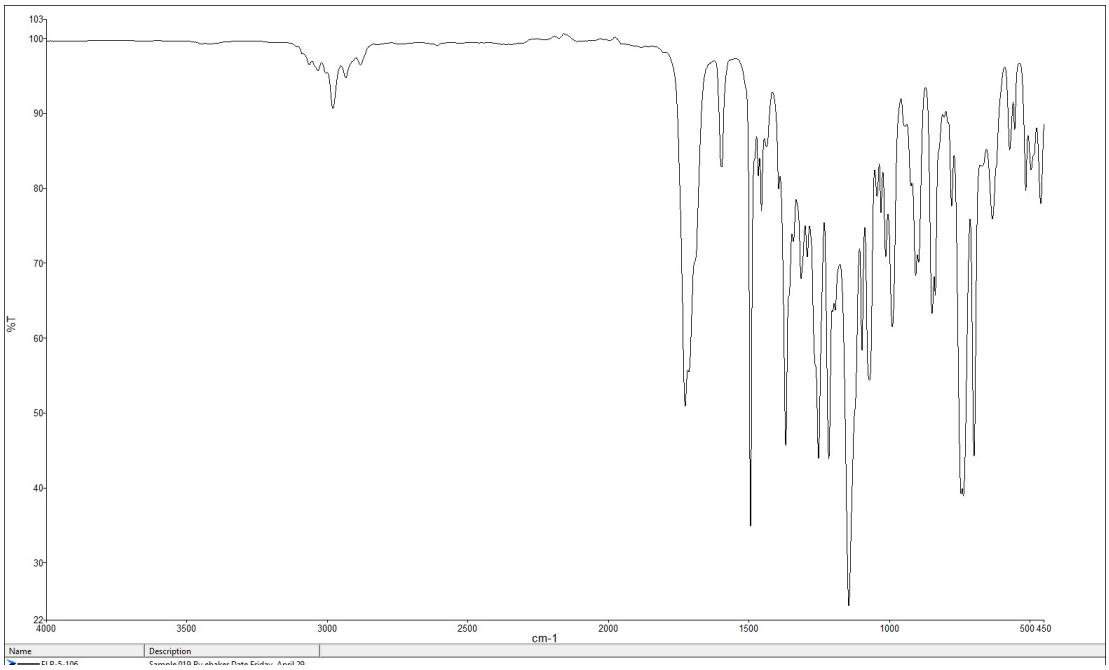

Figure A7.23. Infrared spectrum of compound **7.47**

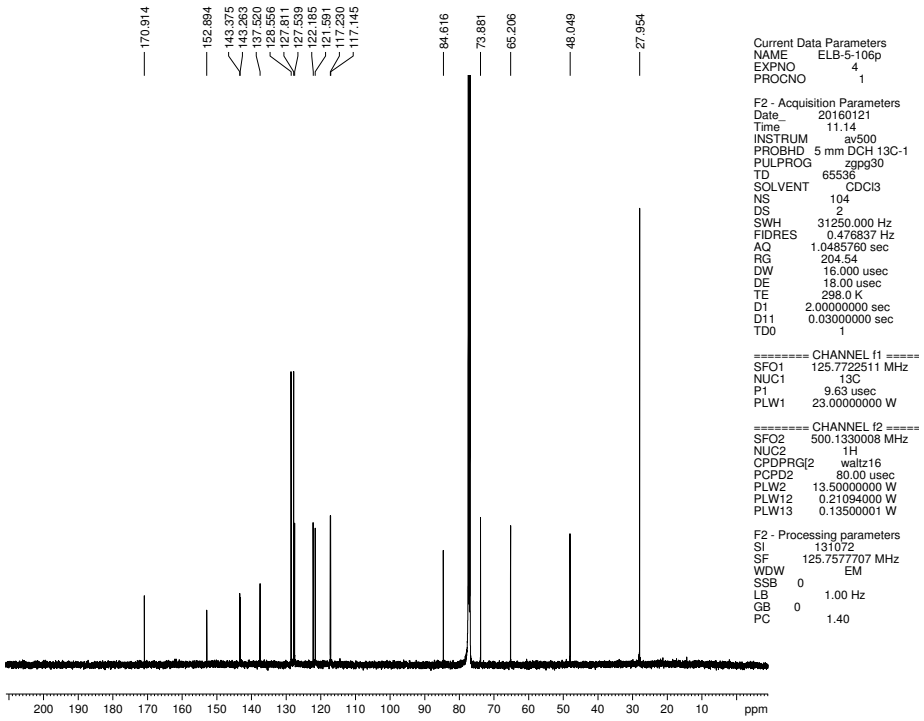

Figure A7.24 ^{13}C NMR (125 MHz, $CDCl_3$) spectrum of compound **7.47**

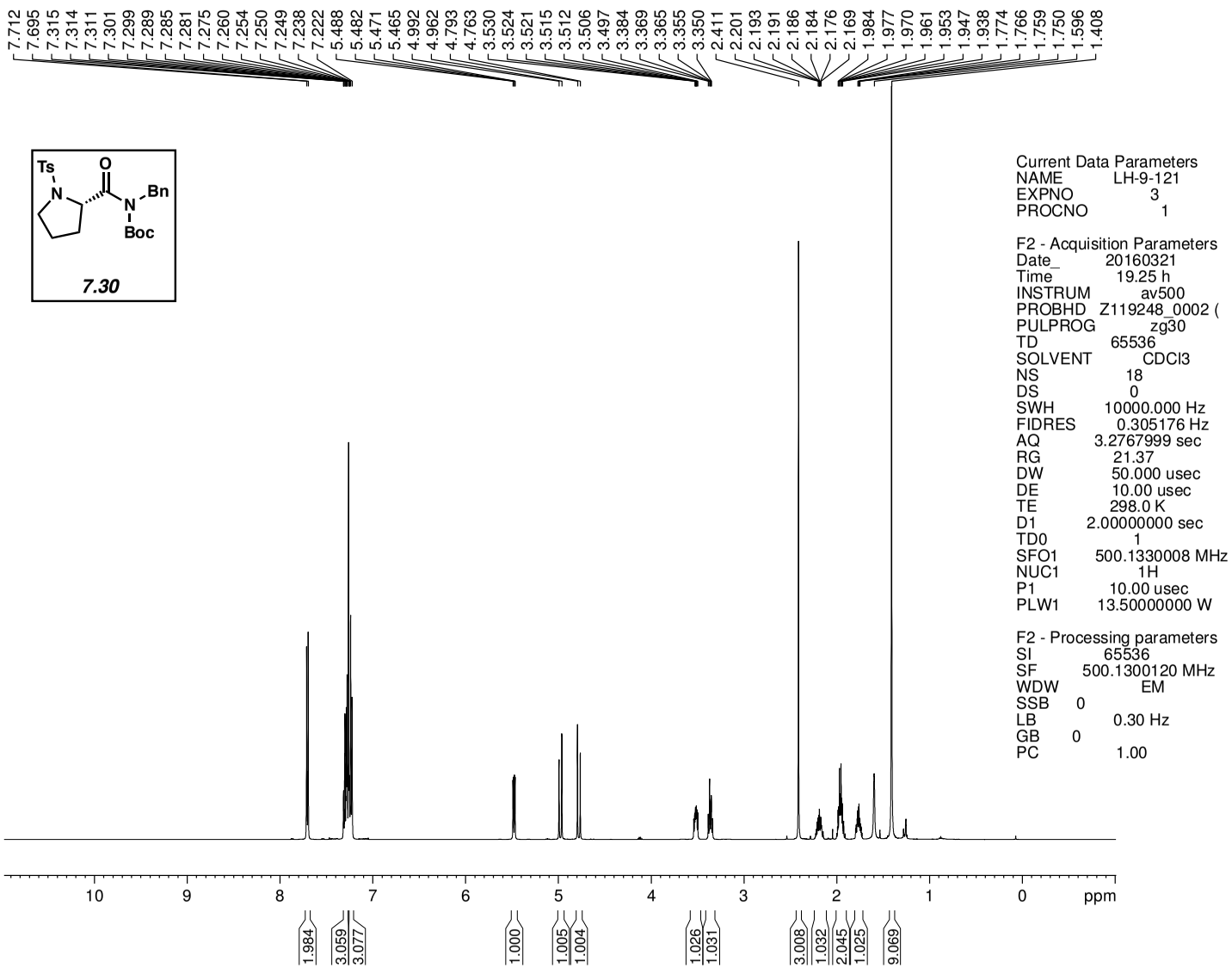

Figure A7.25. ^{1}H NMR (500 MHz, $CDCl_3$) of compound **7.30**

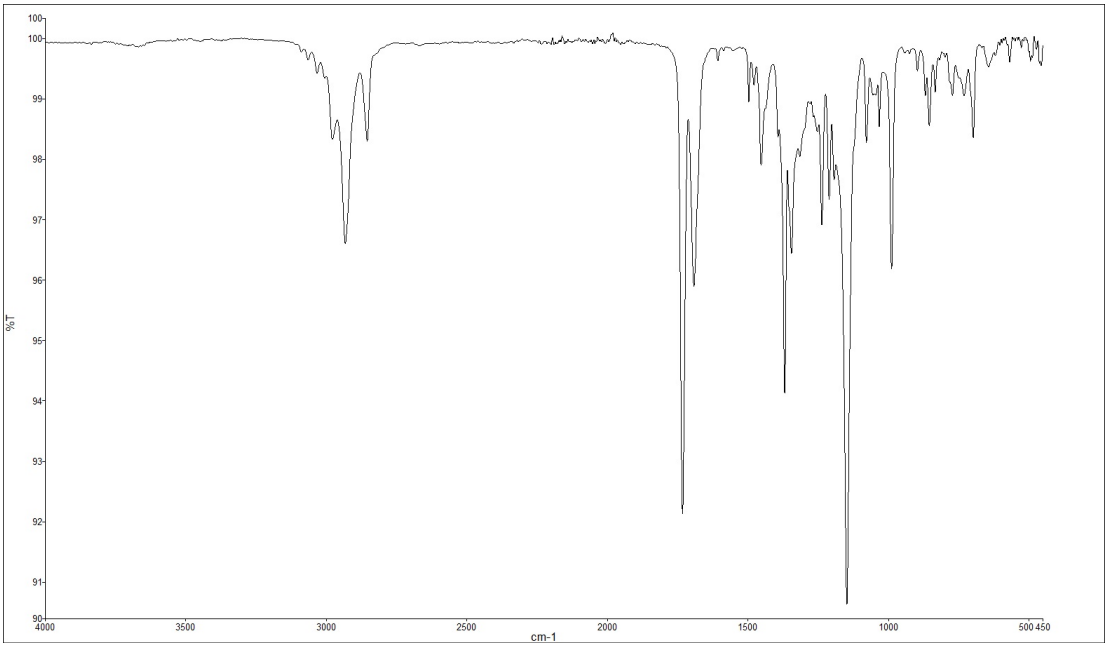

Figure A7.26. Infrared spectrum of compound **7.30**

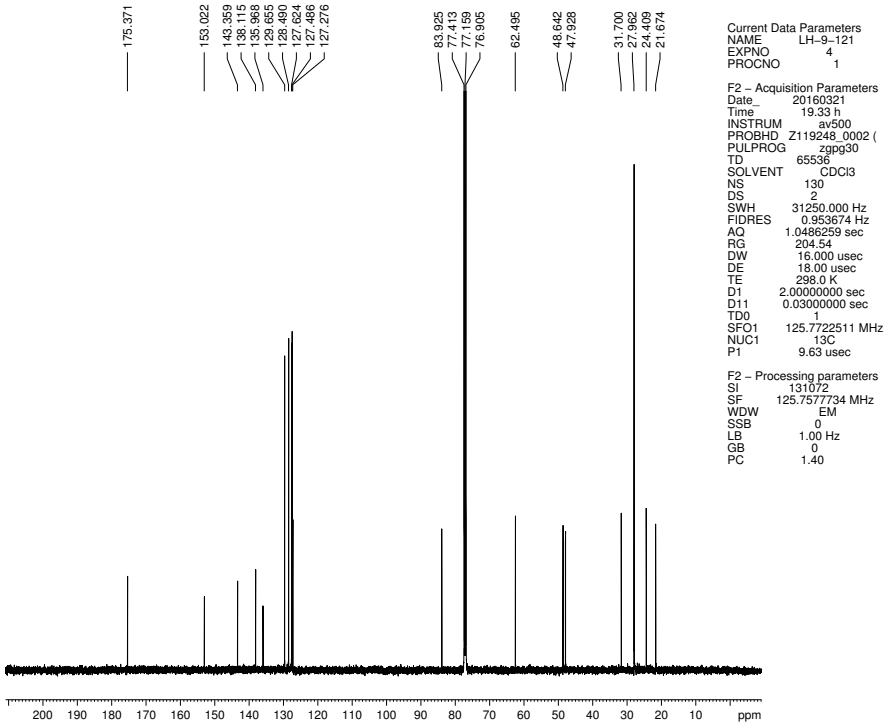

Figure A7.27 ^{13}C NMR (125 MHz, $CDCl_3$) spectrum of compound **7.30**

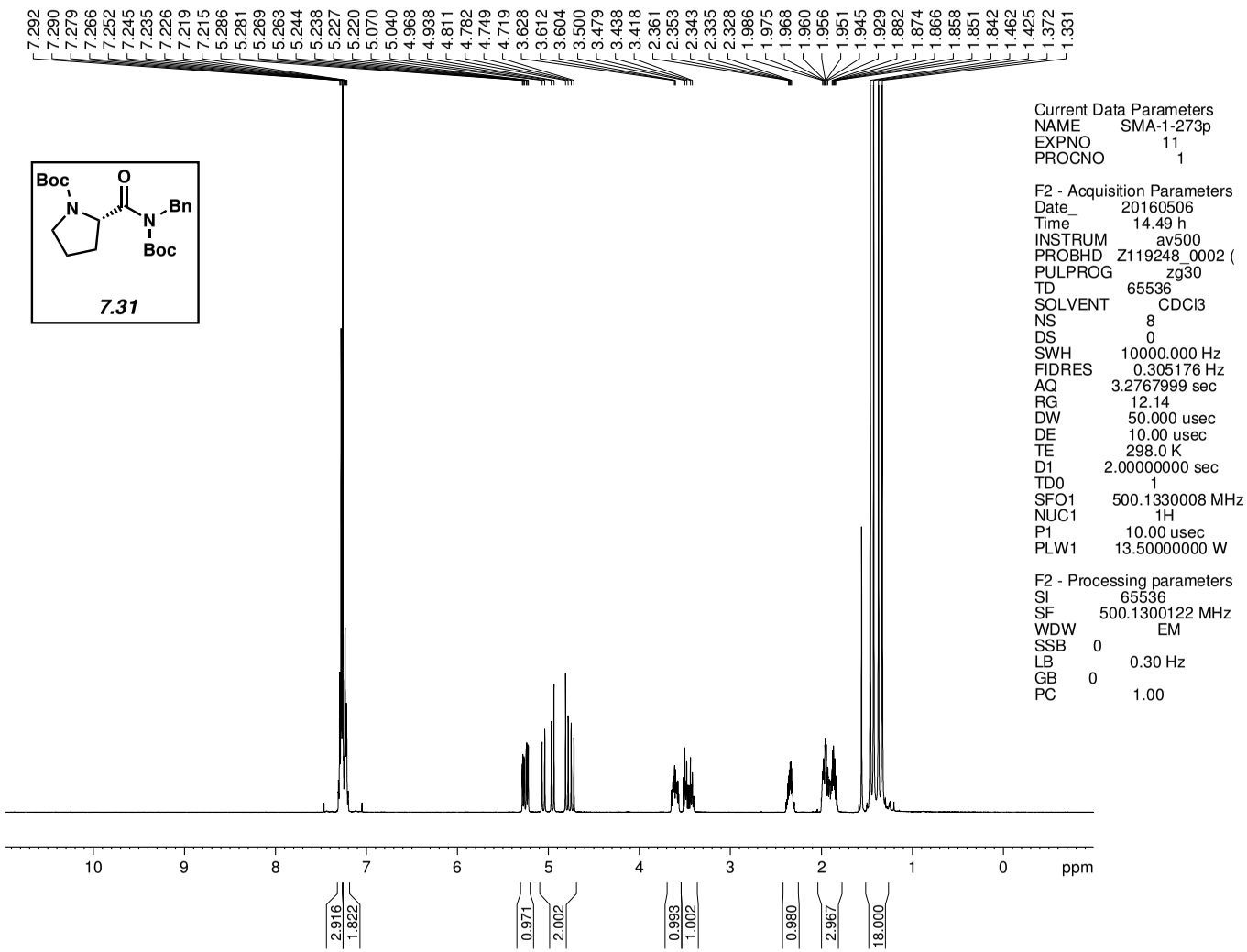

Figure A7.28. ^{1}H NMR (500 MHz, $CDCl_3$) of compound **7.31**

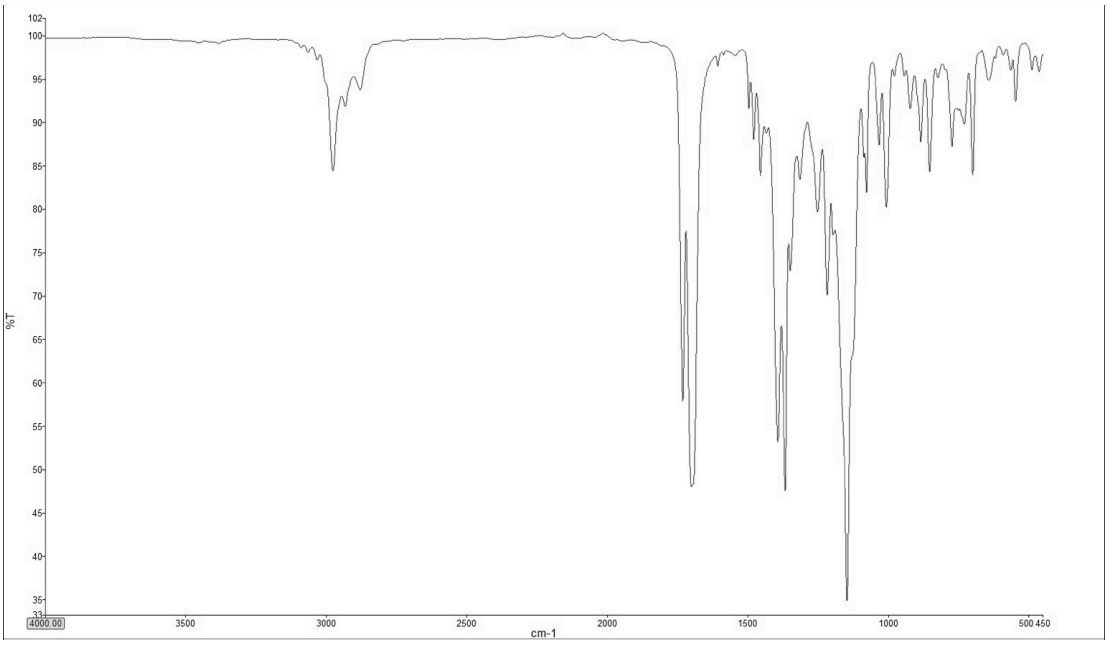

Figure A7.29. Infrared spectrum of compound **7.31**

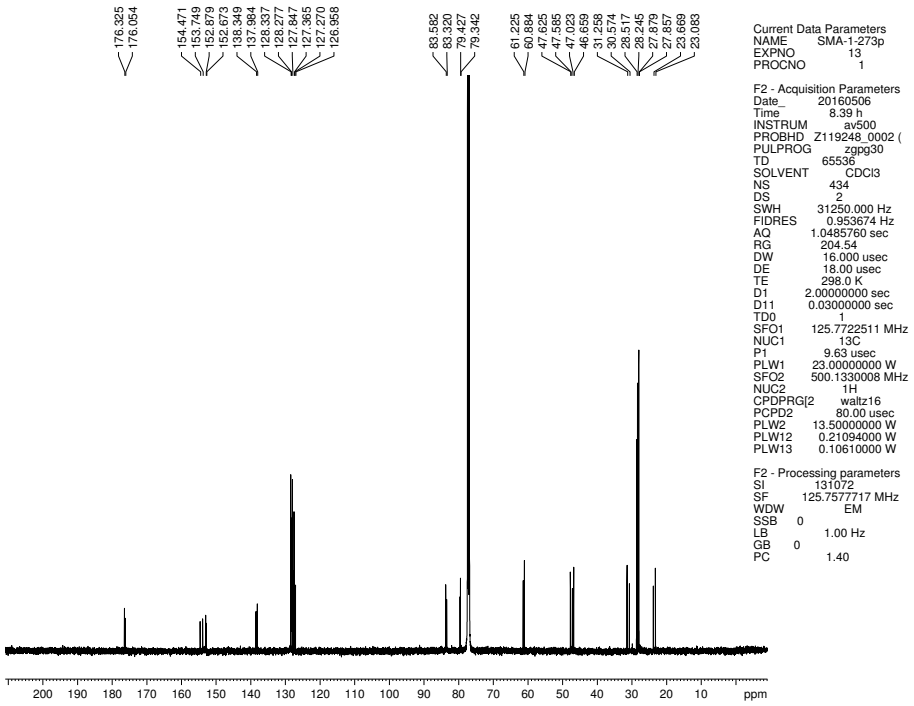

Figure A7.30 ^{13}C NMR (125 MHz, $CDCl_3$) spectrum of compound **7.31**

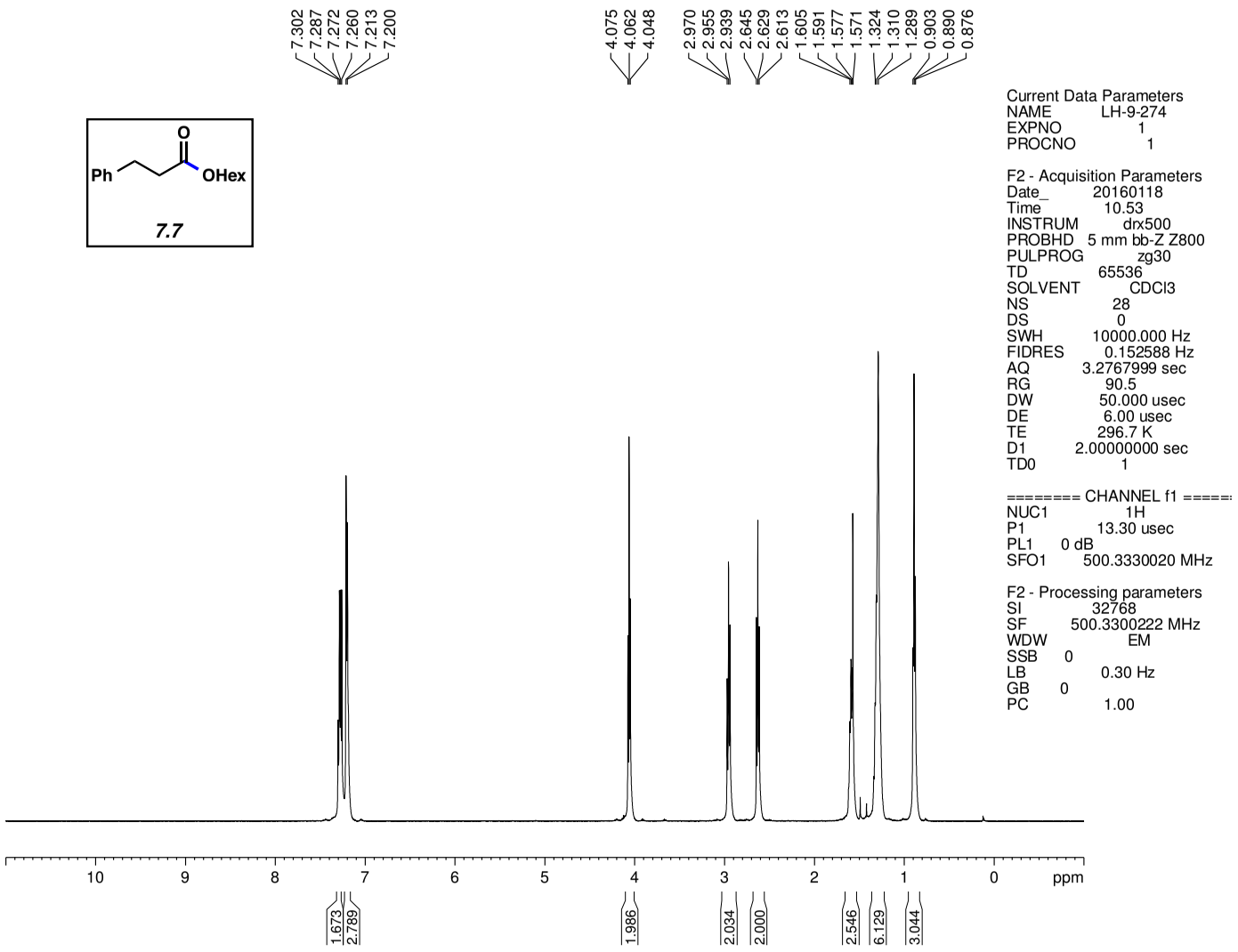

Figure A7.31. ^{1}H NMR (500 MHz, $CDCl_3$) of compound **7.7**

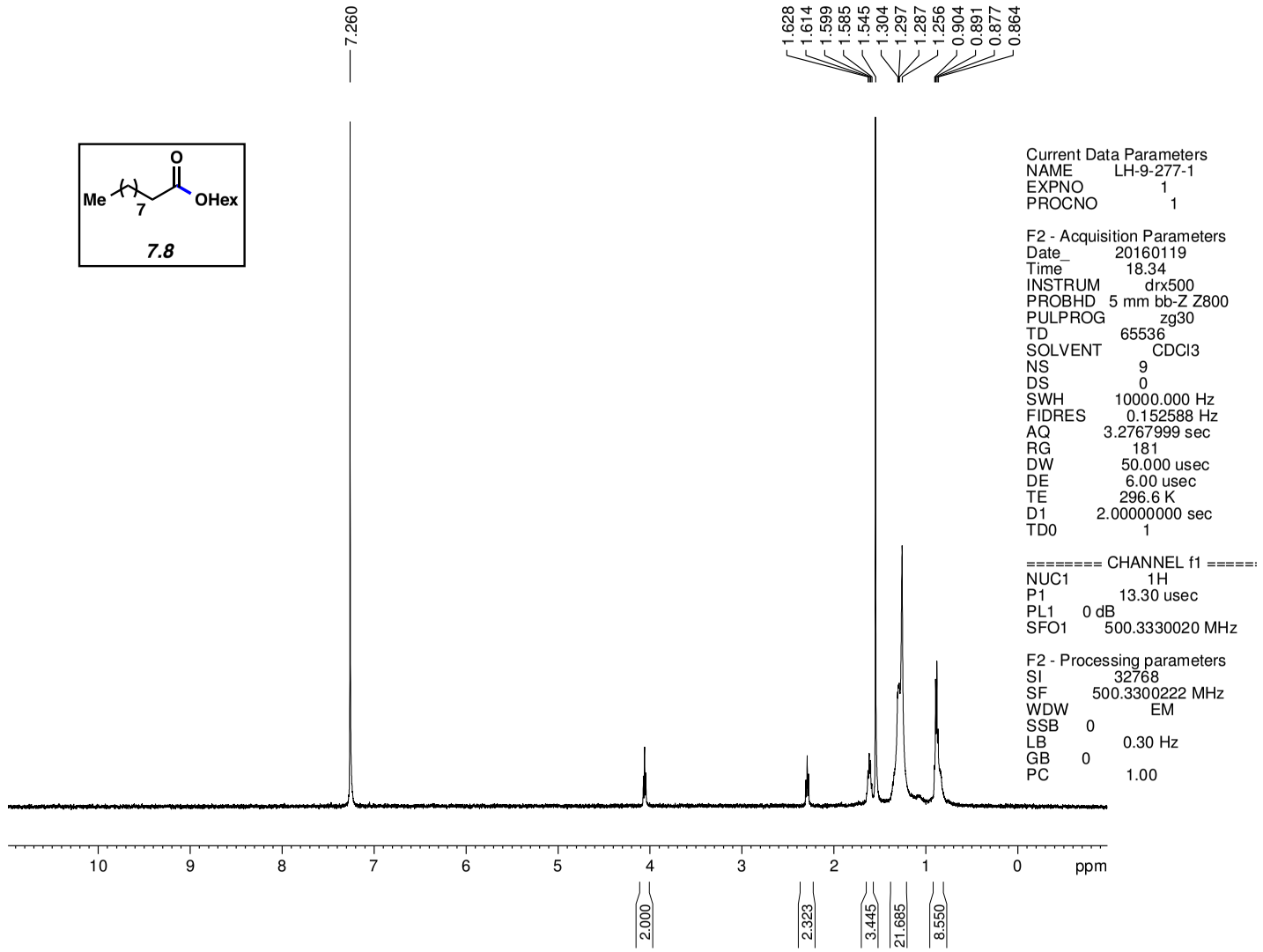

Figure A7.32. ^{1}H NMR (500 MHz, $CDCl_3$) of compound **7.8**

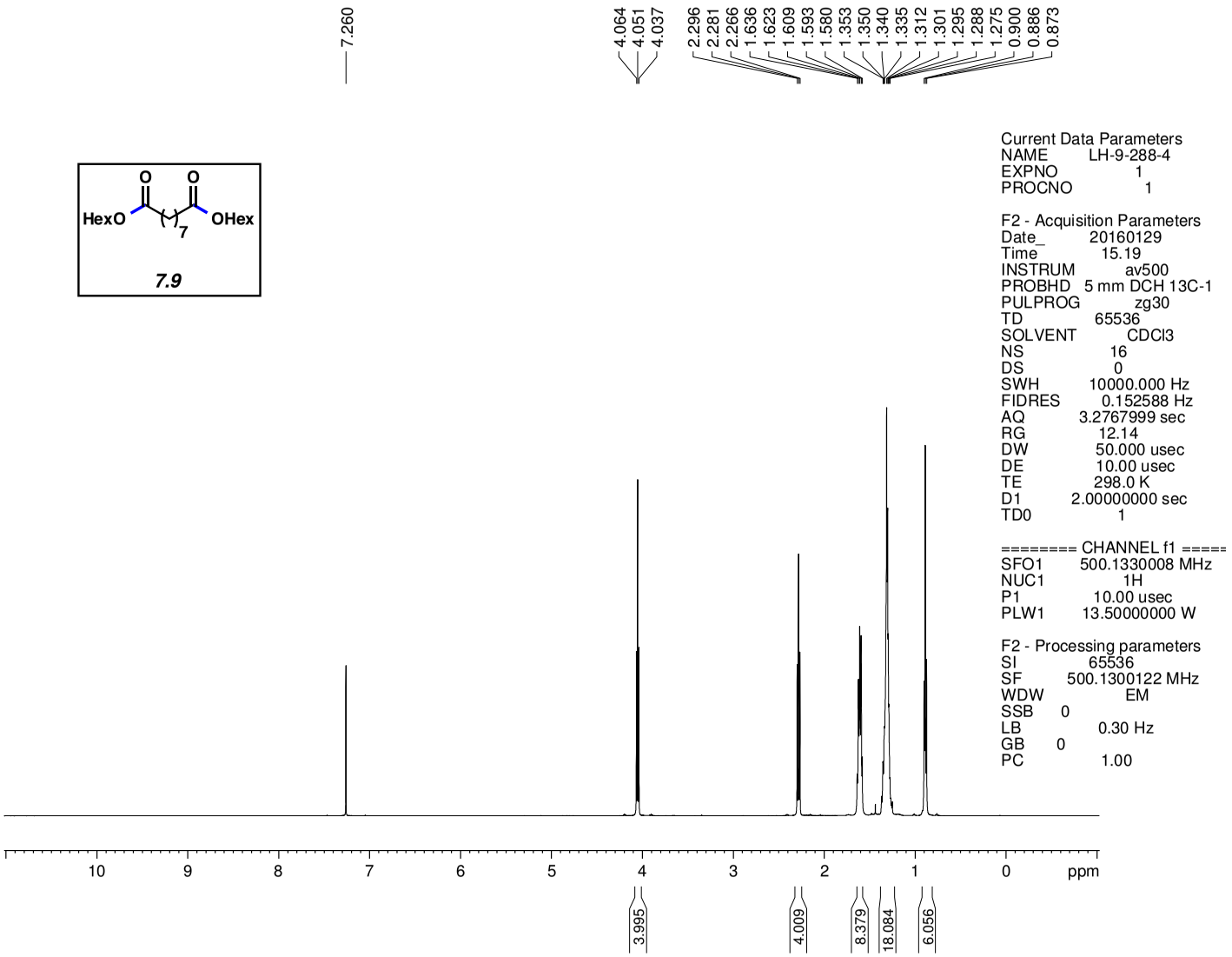

Figure A7.33. ^{1}H NMR (500 MHz, $CDCl_3$) of compound **7.9**

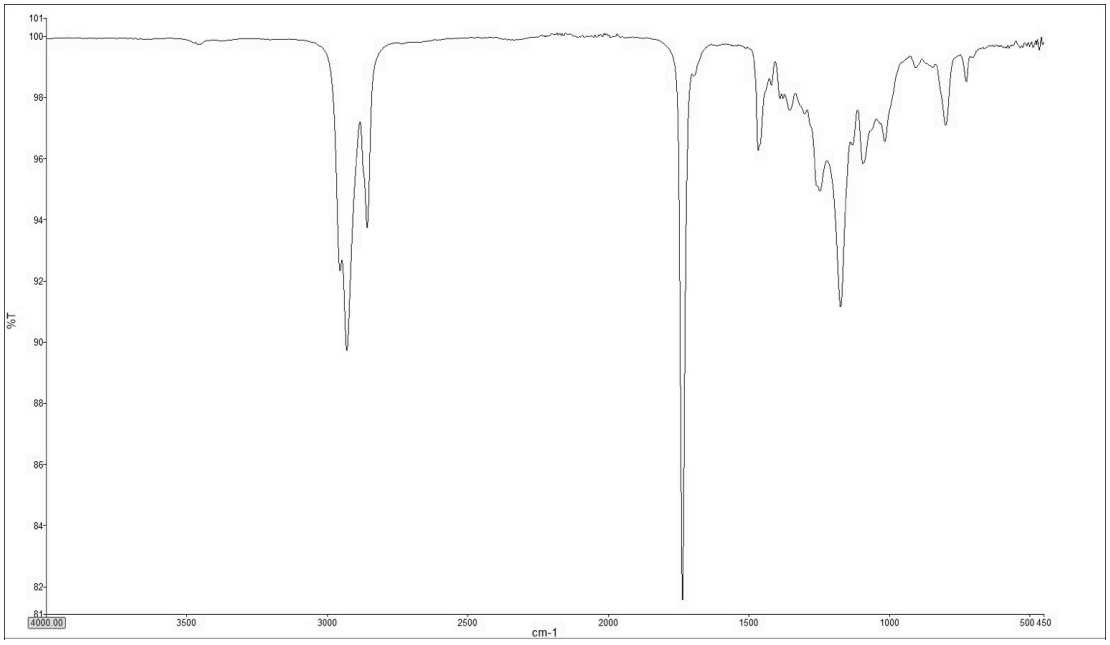

Figure A7.34. Infrared spectrum of compound **7.9**

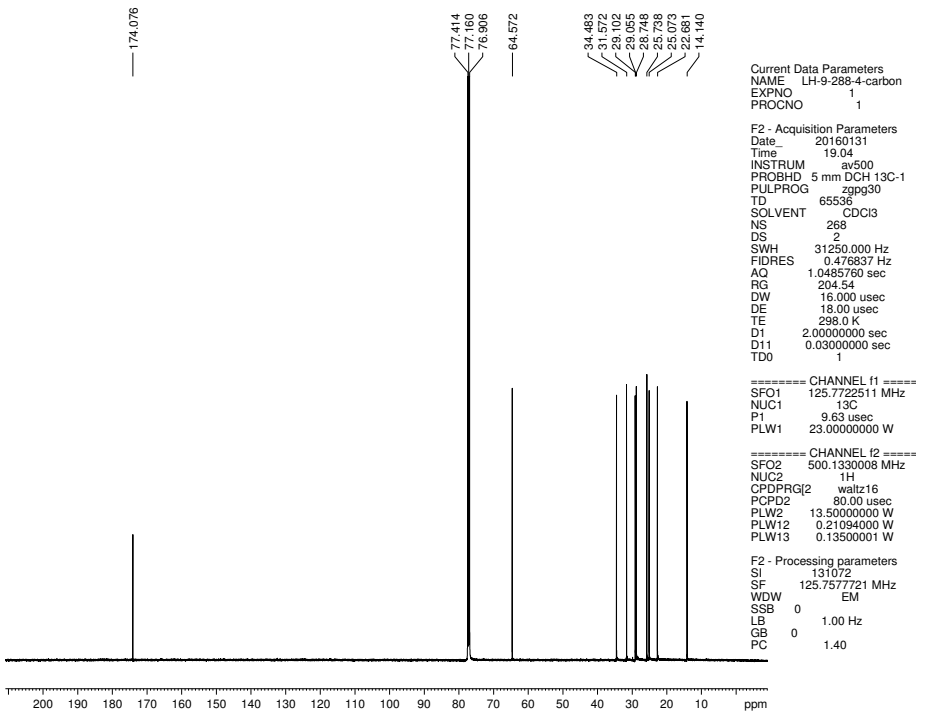

Figure A7.35 ^{13}C NMR (125 MHz, $CDCl_3$) spectrum of compound **7.9**

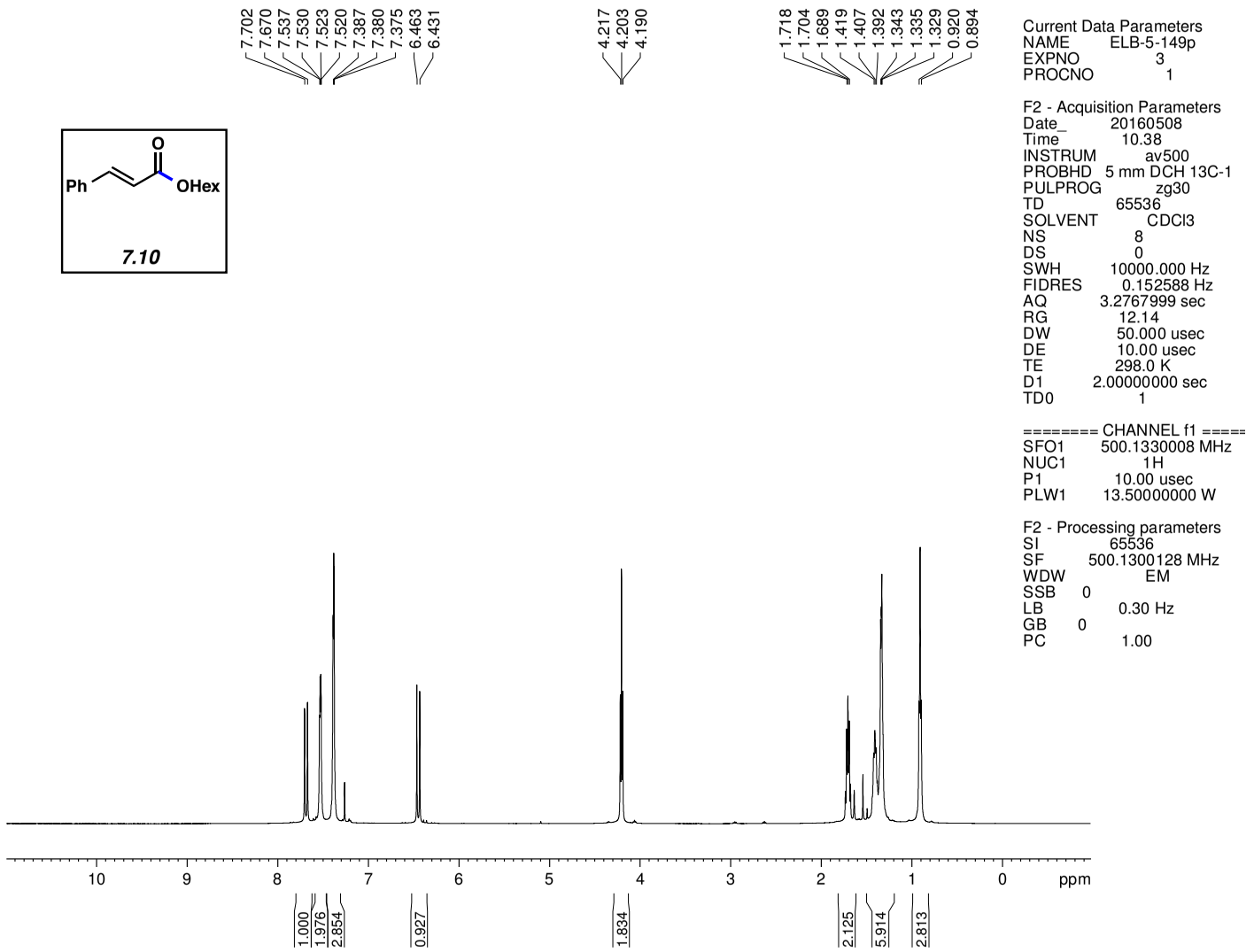

Figure A7.36. ^{1}H NMR (500 MHz, $CDCl_3$) of compound **7.10**

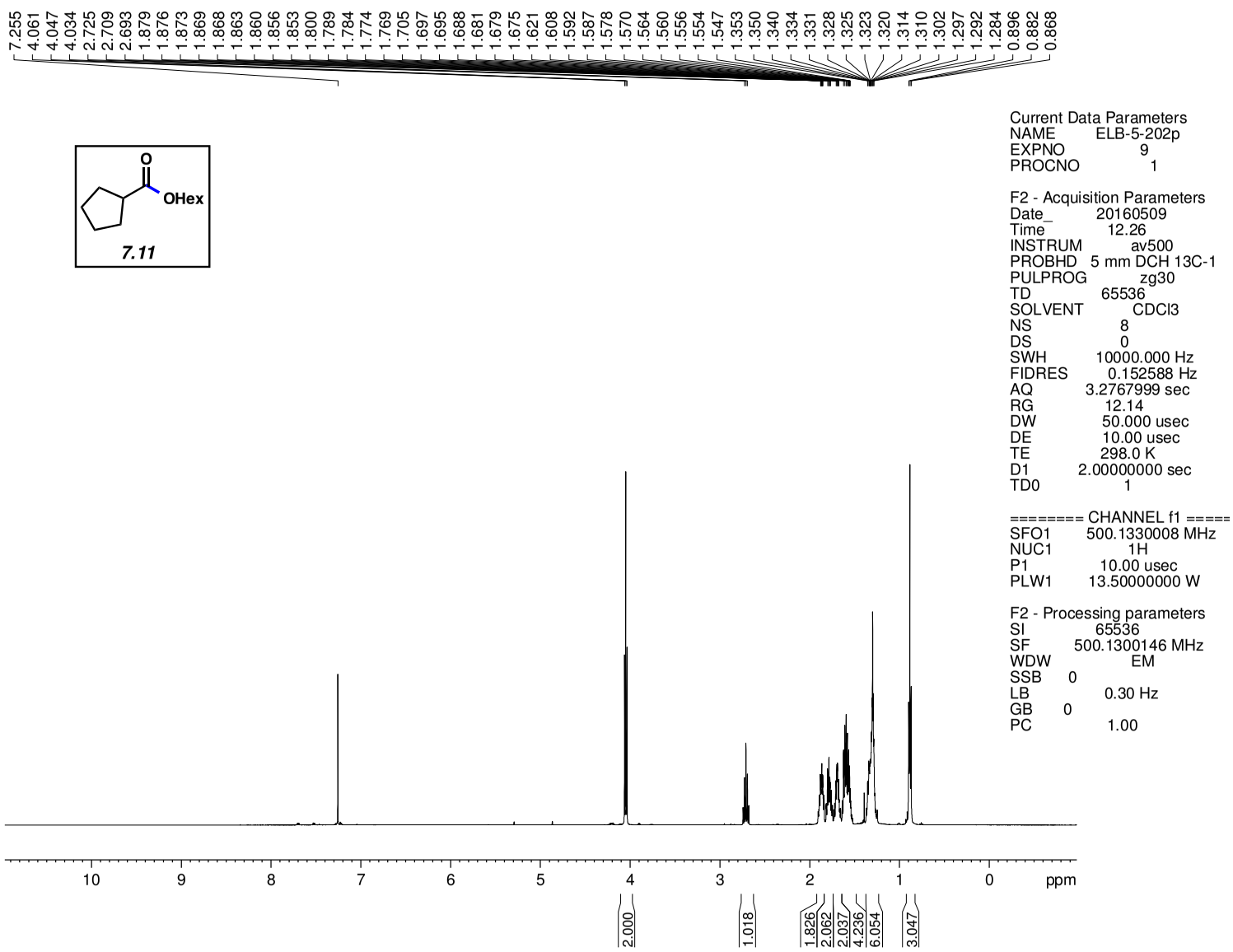

Figure A7.37. ^{1}H NMR (500 MHz, $CDCl_3$) of compound **7.11**

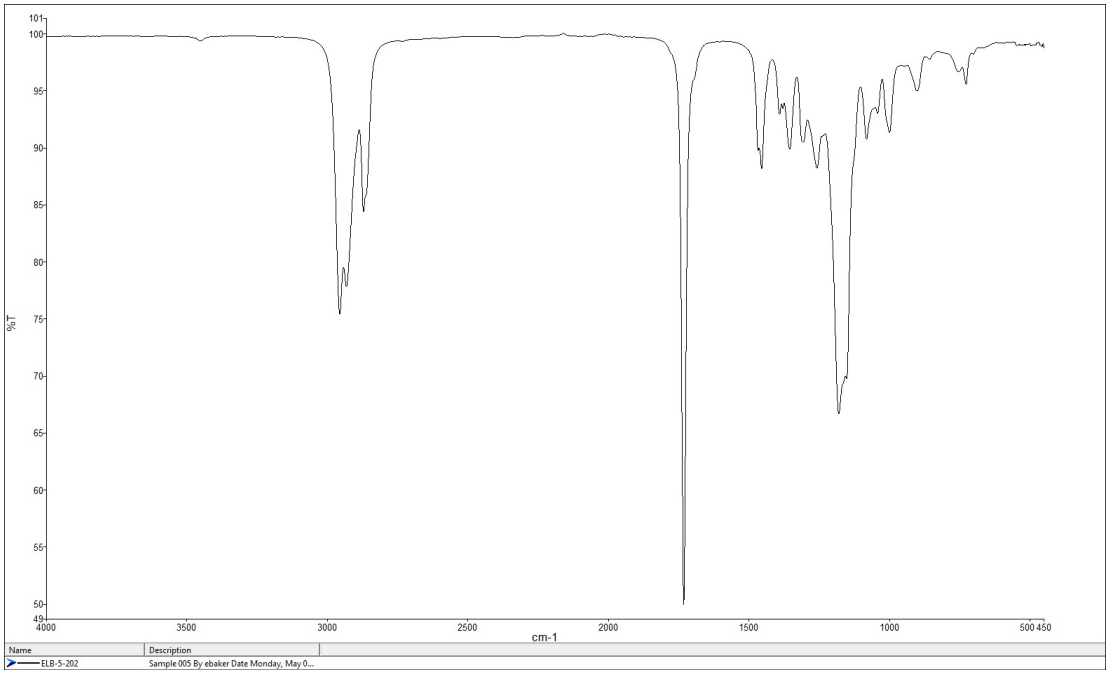

Figure A7.38. Infrared spectrum of compound **7.11**

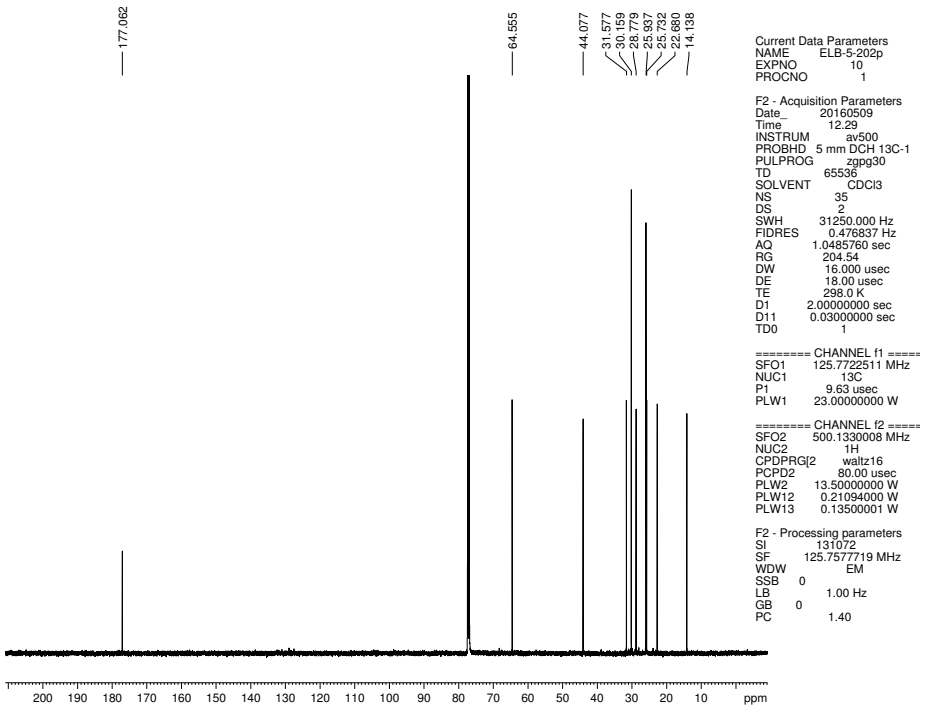

Figure A7.39 ^{13}C NMR (125 MHz, $CDCl_3$) spectrum of compound **7.11**

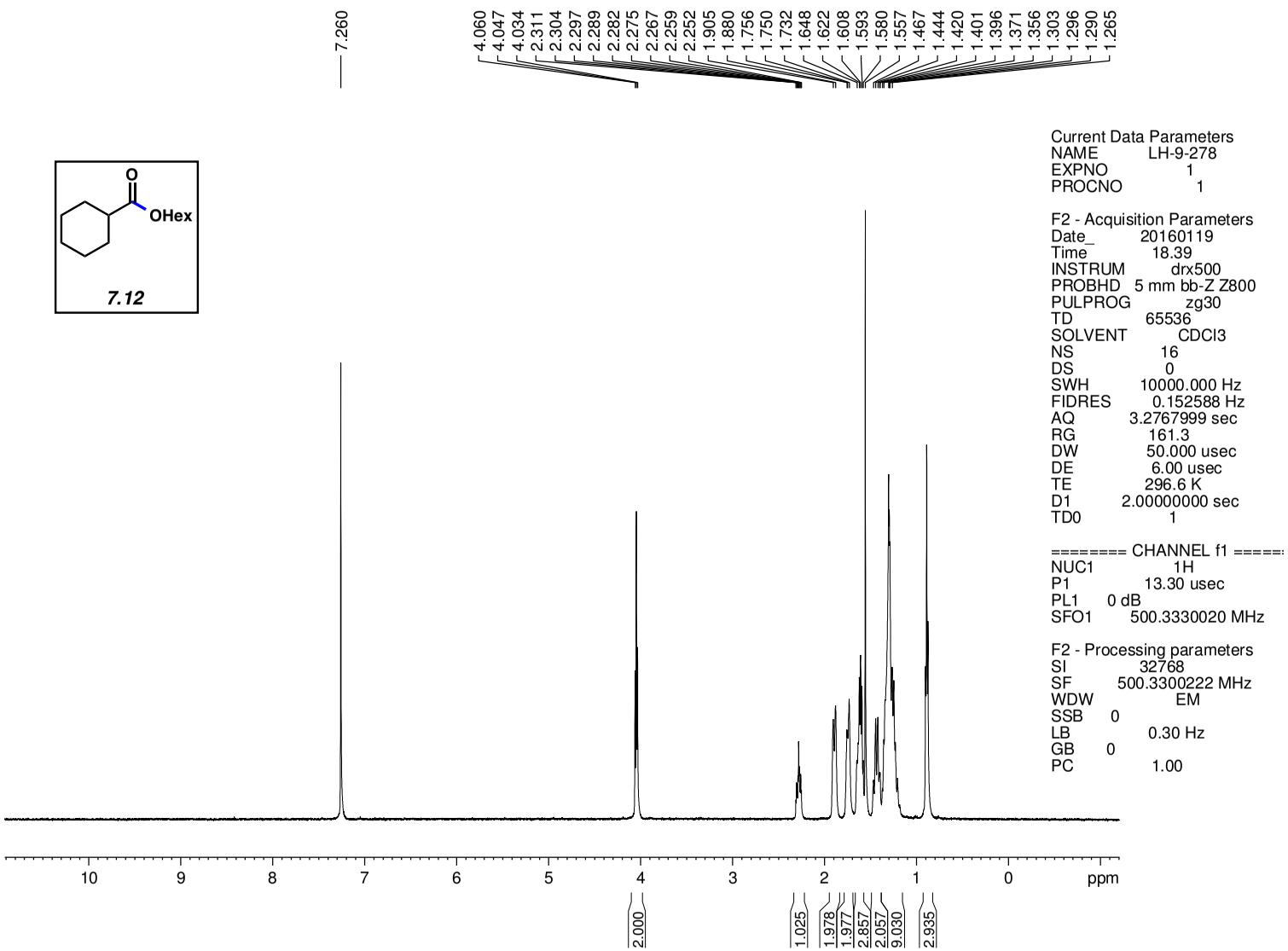

Figure A7.40. ^{1}H NMR (500 MHz, $CDCl_3$) of compound **7.12**

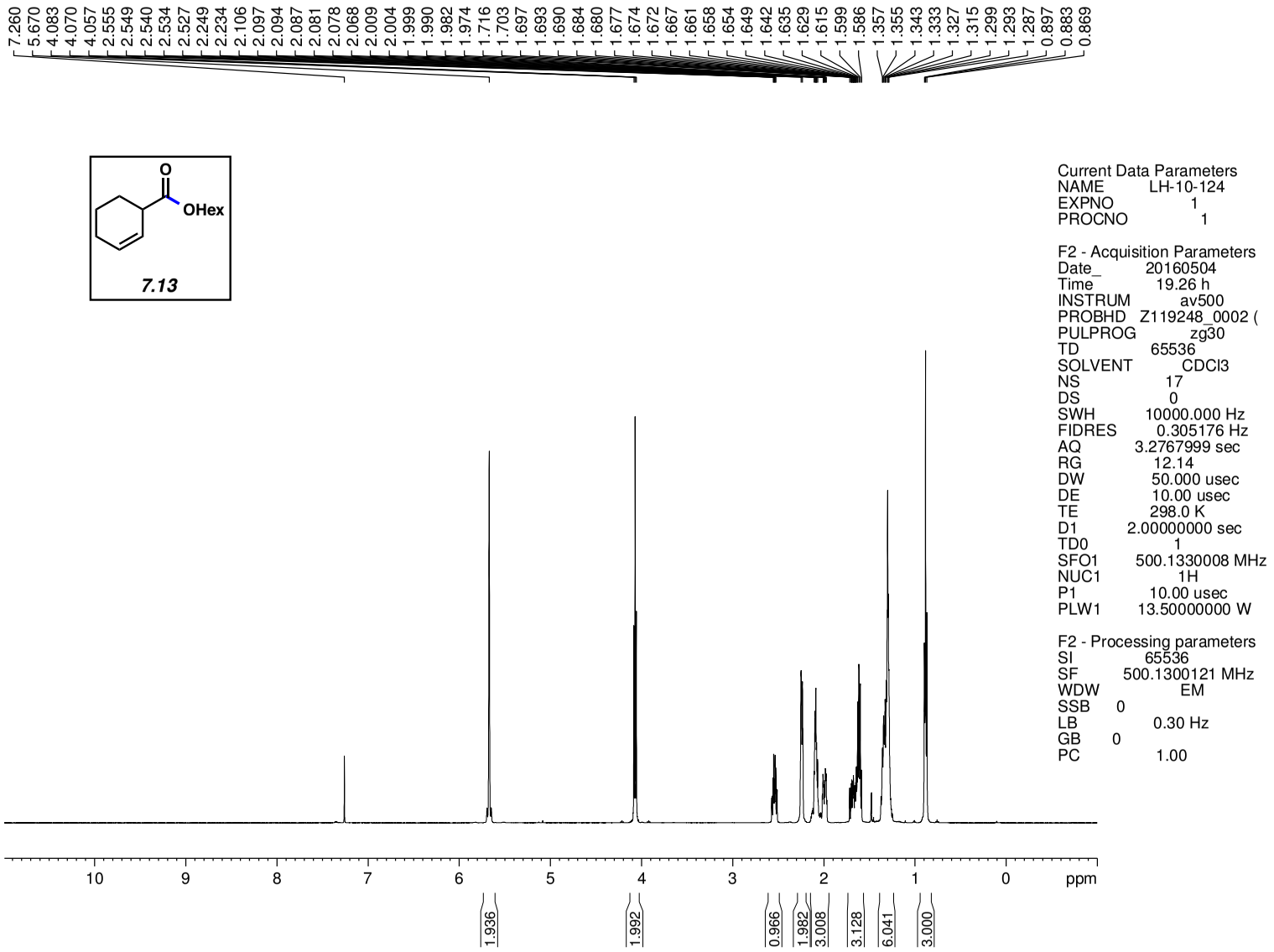

Figure A7.41. ^{1}H NMR (500 MHz, $CDCl_3$) of compound **7.13**

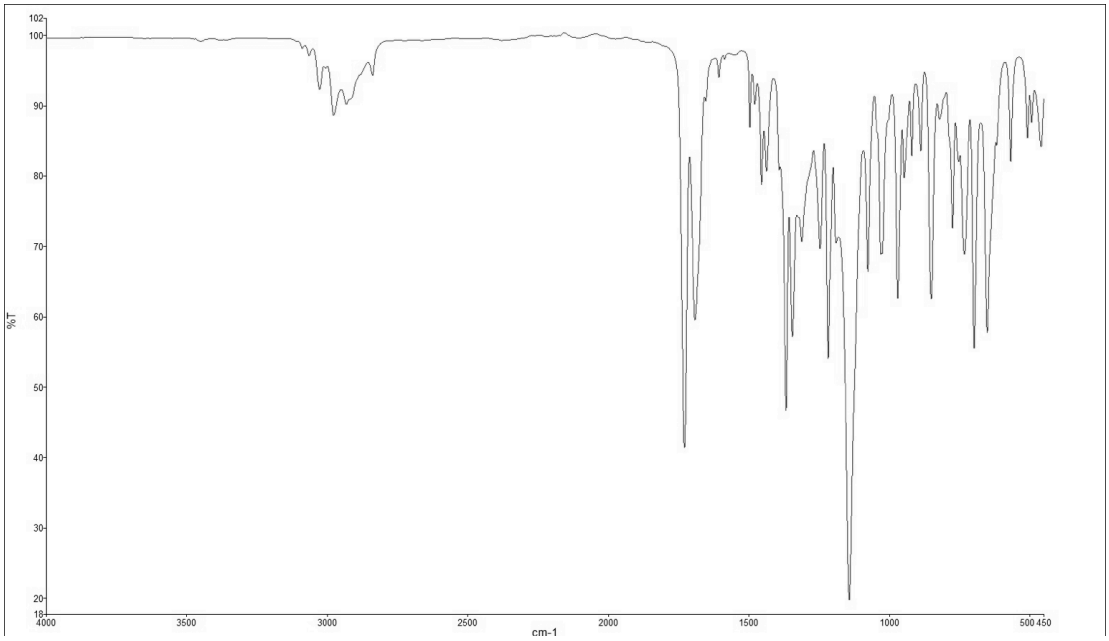

Figure A7.42. Infrared spectrum of compound **7.13**

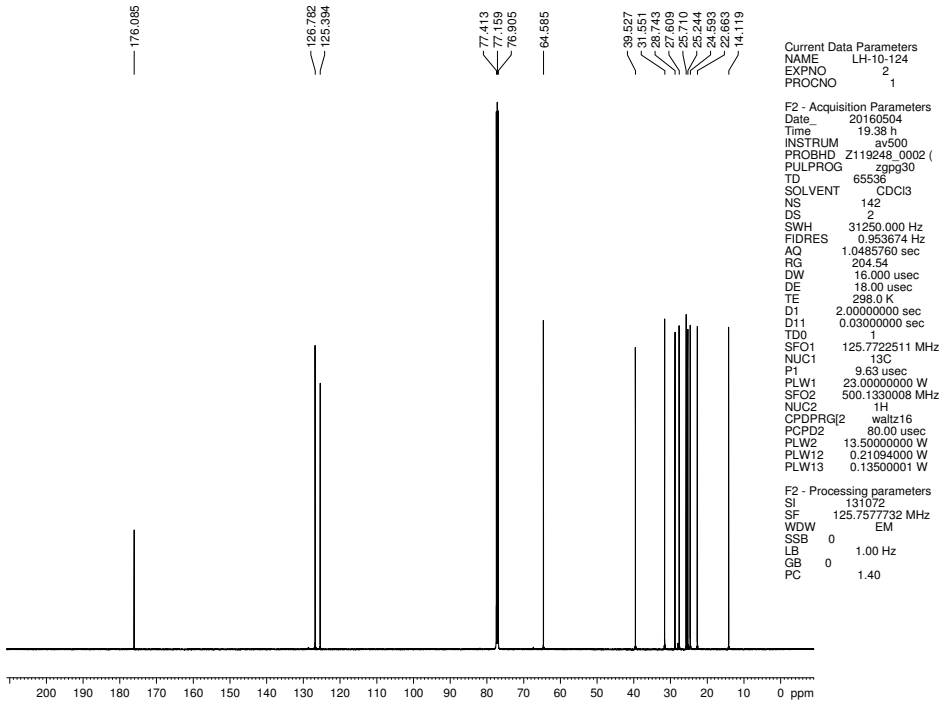

Figure A7.43 ^{13}C NMR (125 MHz, $CDCl_3$) spectrum of compound **7.13**

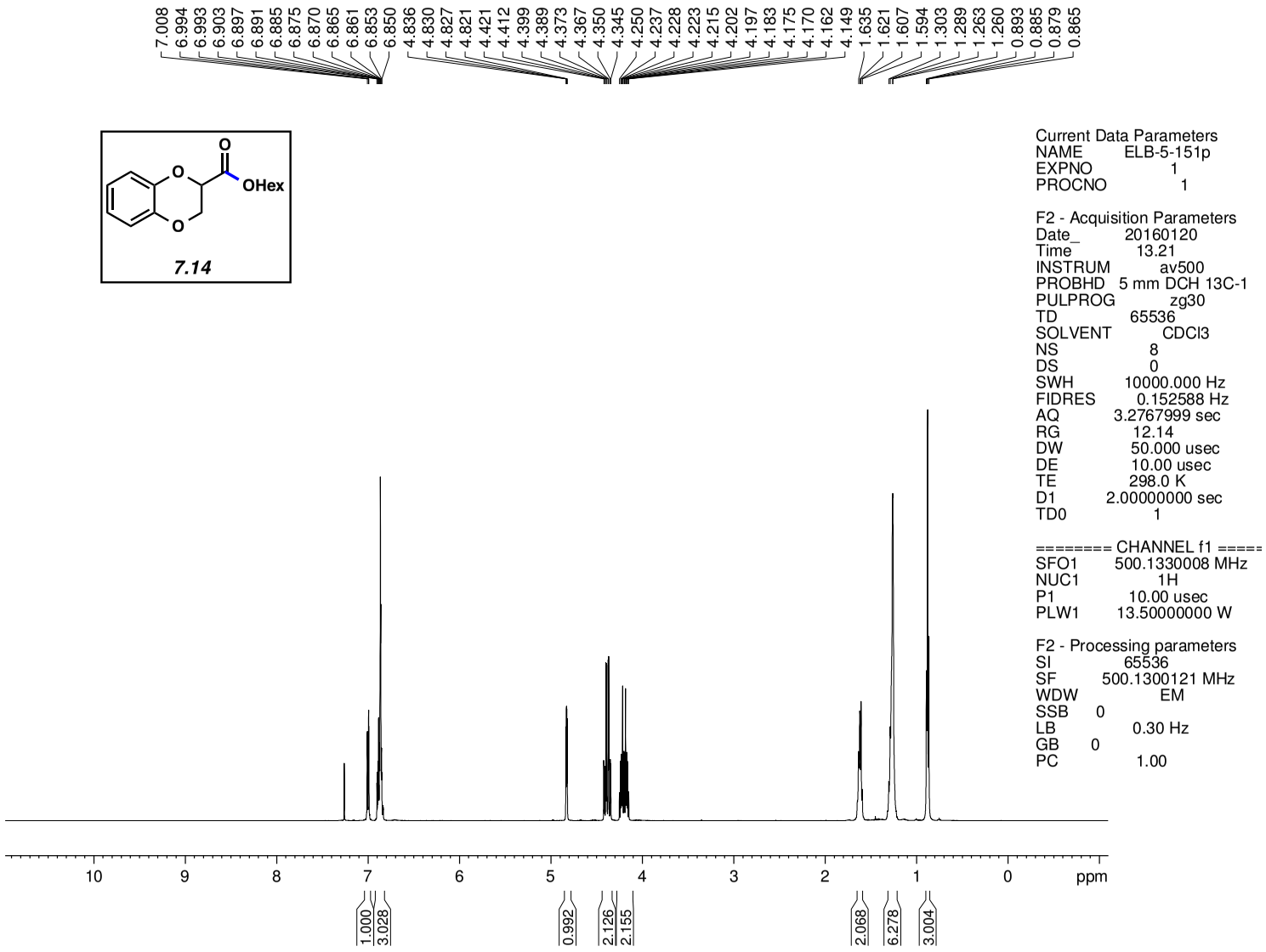

Figure A7.44. ^{1}H NMR (500 MHz, $CDCl_3$) of compound **7.14**

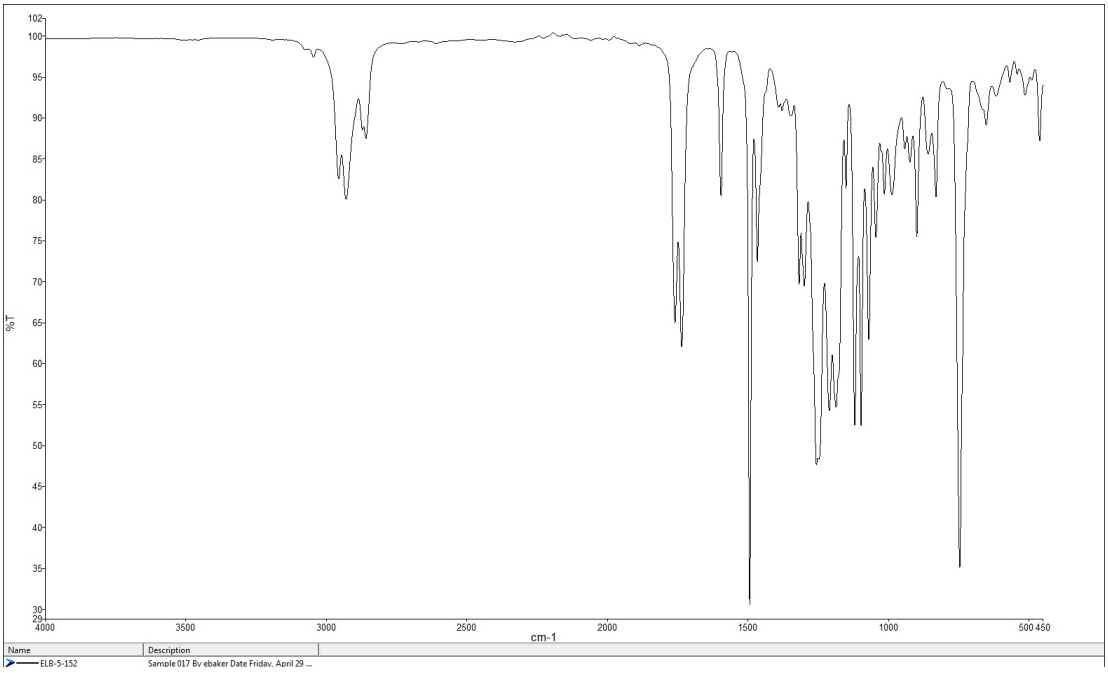

Figure A7.45. Infrared spectrum of compound **7.14**

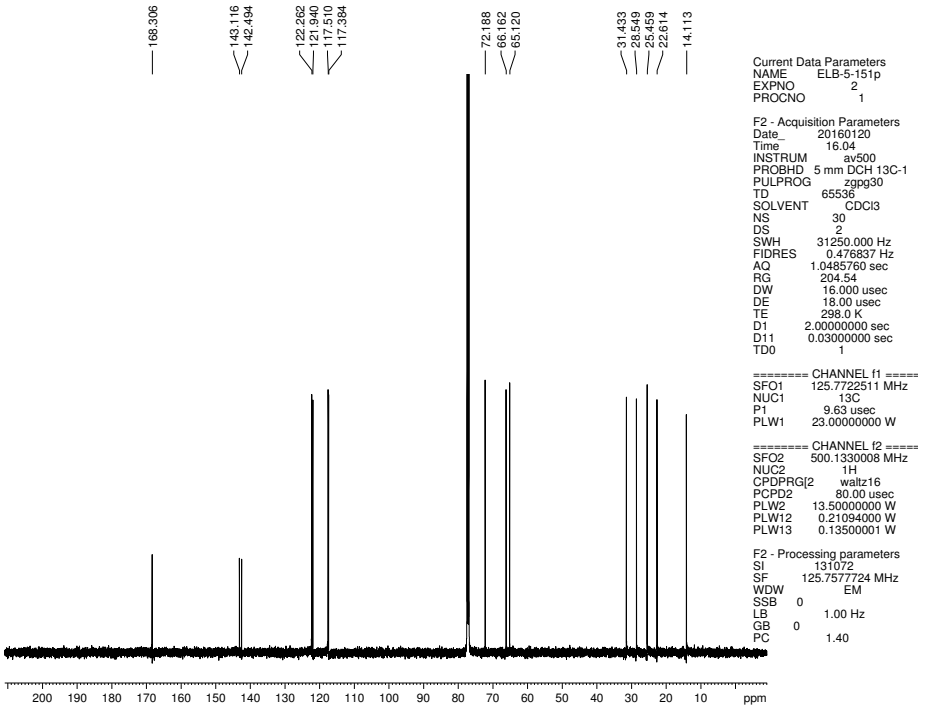

Figure A7.46 ^{13}C NMR (125 MHz, $CDCl_3$) spectrum of compound **7.14**

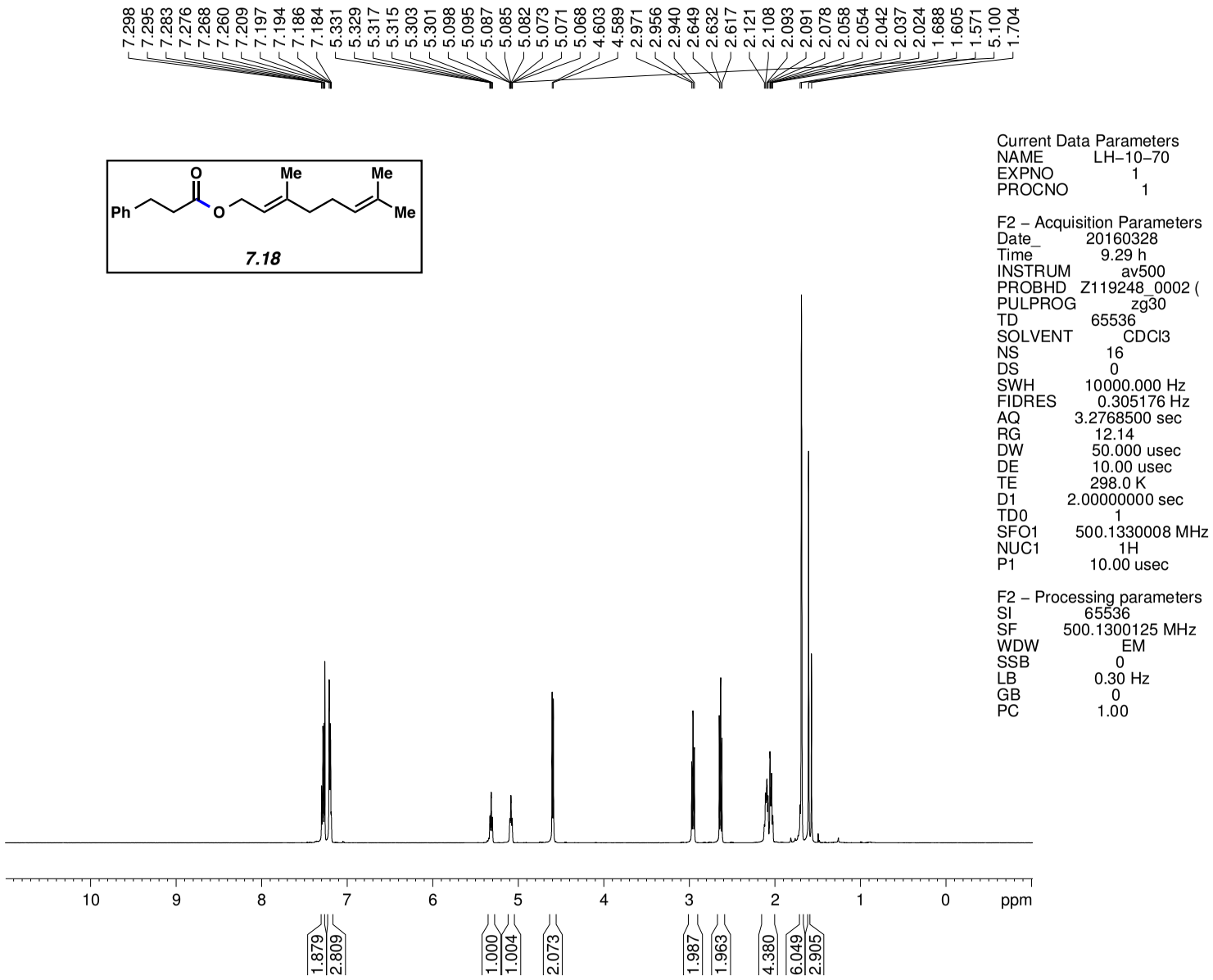

Figure A7.47. ^{1}H NMR (500 MHz, $CDCl_3$) of compound **7.18**

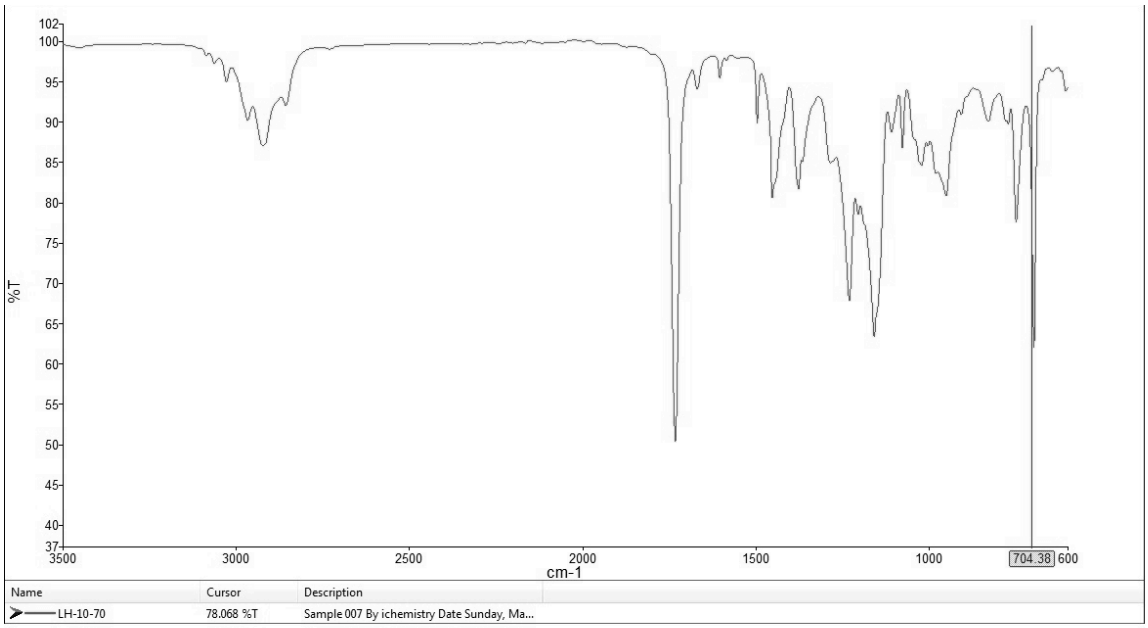

Figure A7.48. Infrared spectrum of compound **7.18**

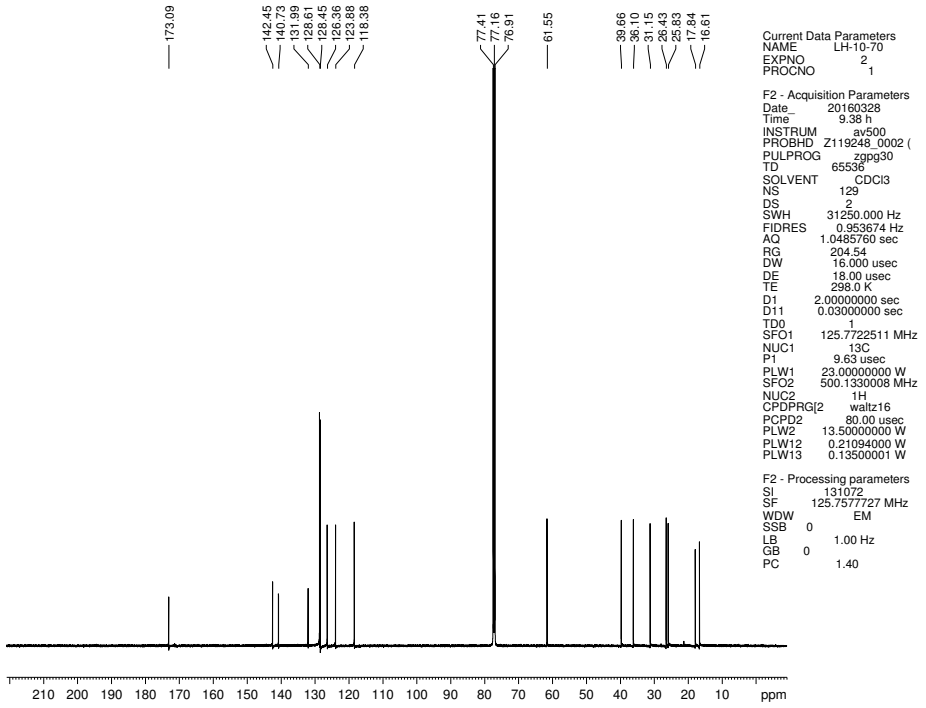

Figure A7.49 ^{13}C NMR (125 MHz, $CDCl_3$) spectrum of compound **7.18**

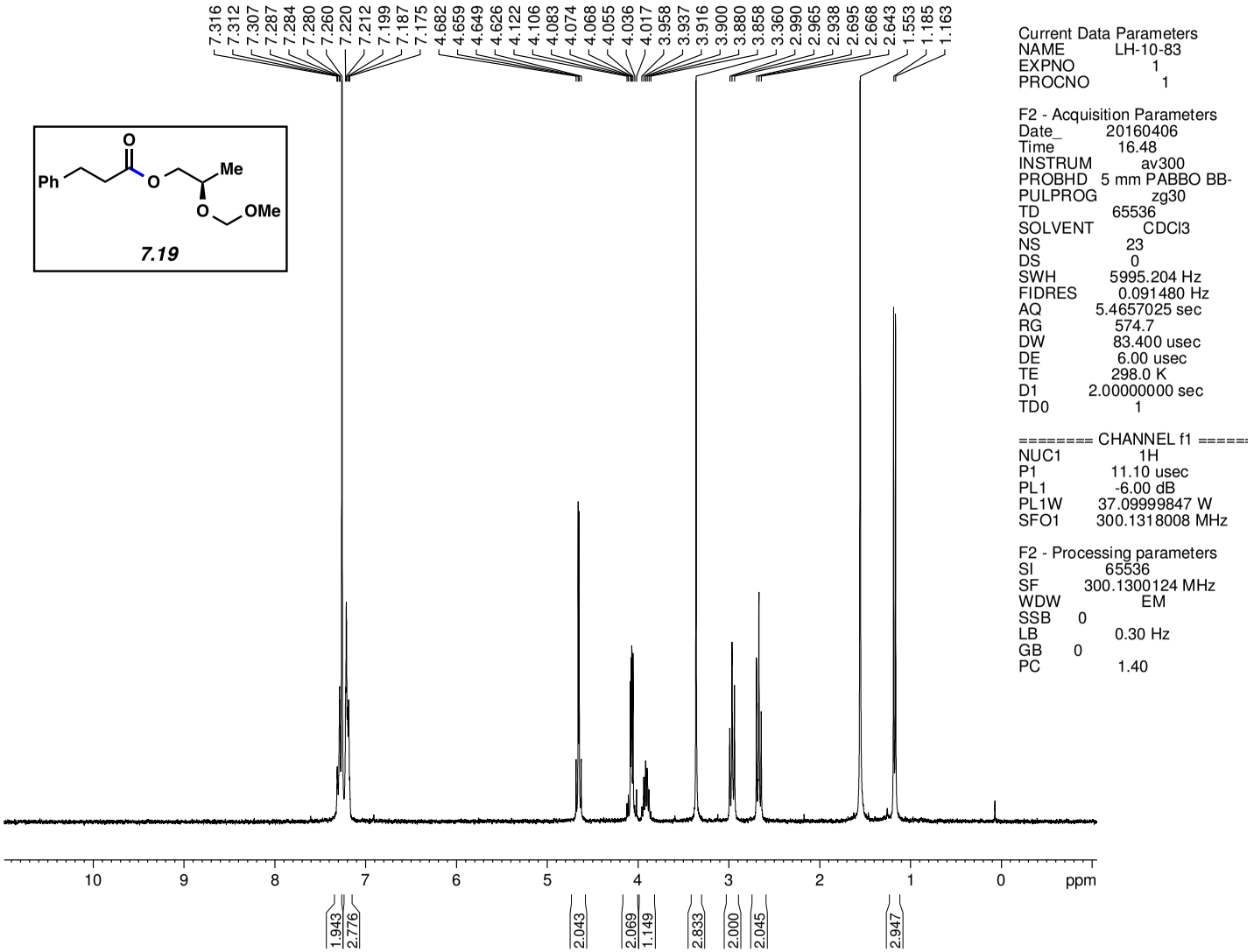

Figure A7.50. ^{1}H NMR (500 MHz, $CDCl_3$) of compound **7.19**

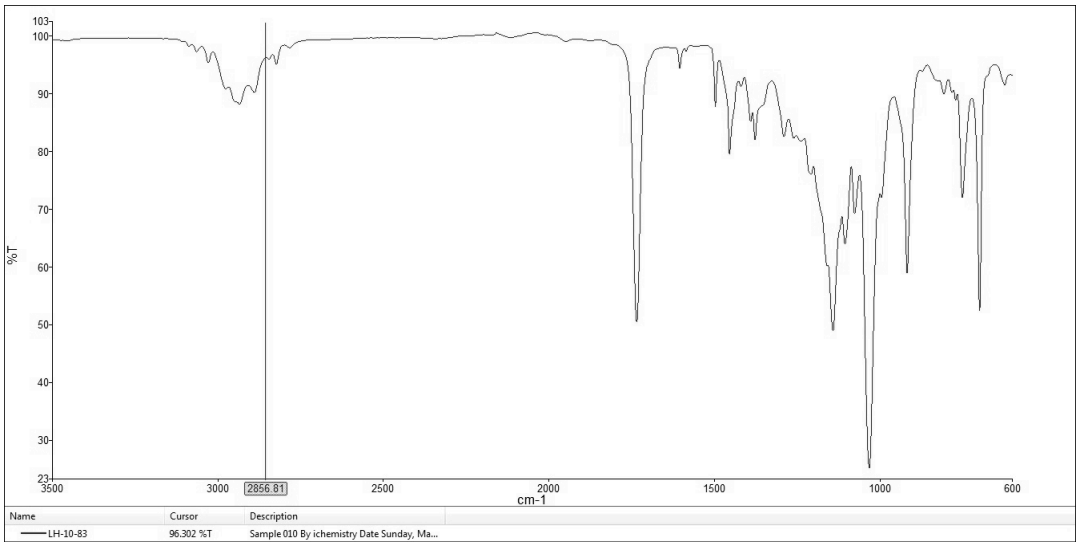

Figure A7.51. Infrared spectrum of compound **7.19**

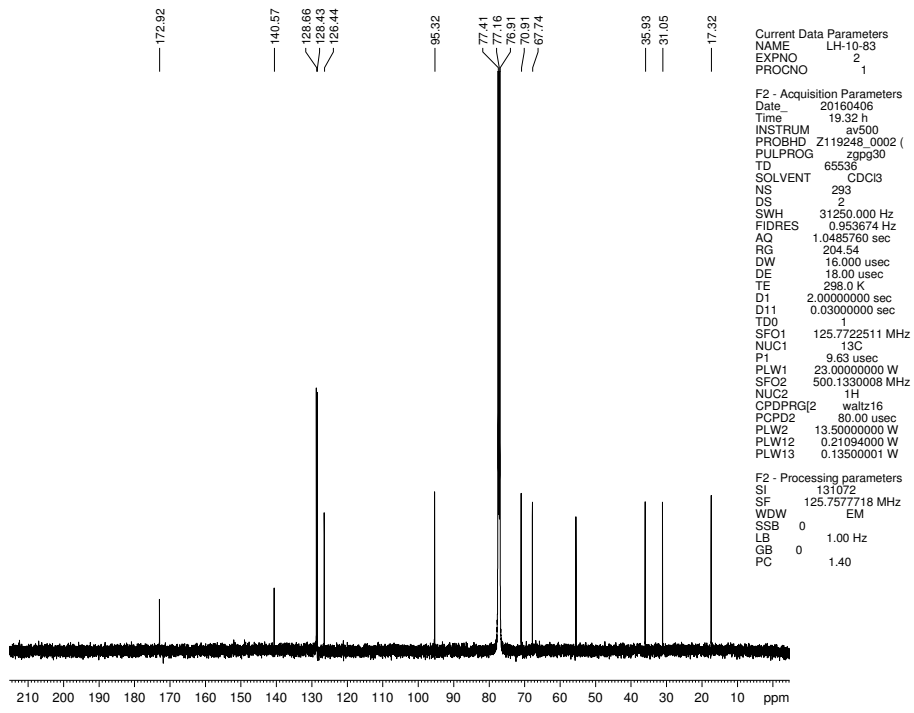

Figure A7.52 ^{13}C NMR (125 MHz, $CDCl_3$) spectrum of compound **7.19**

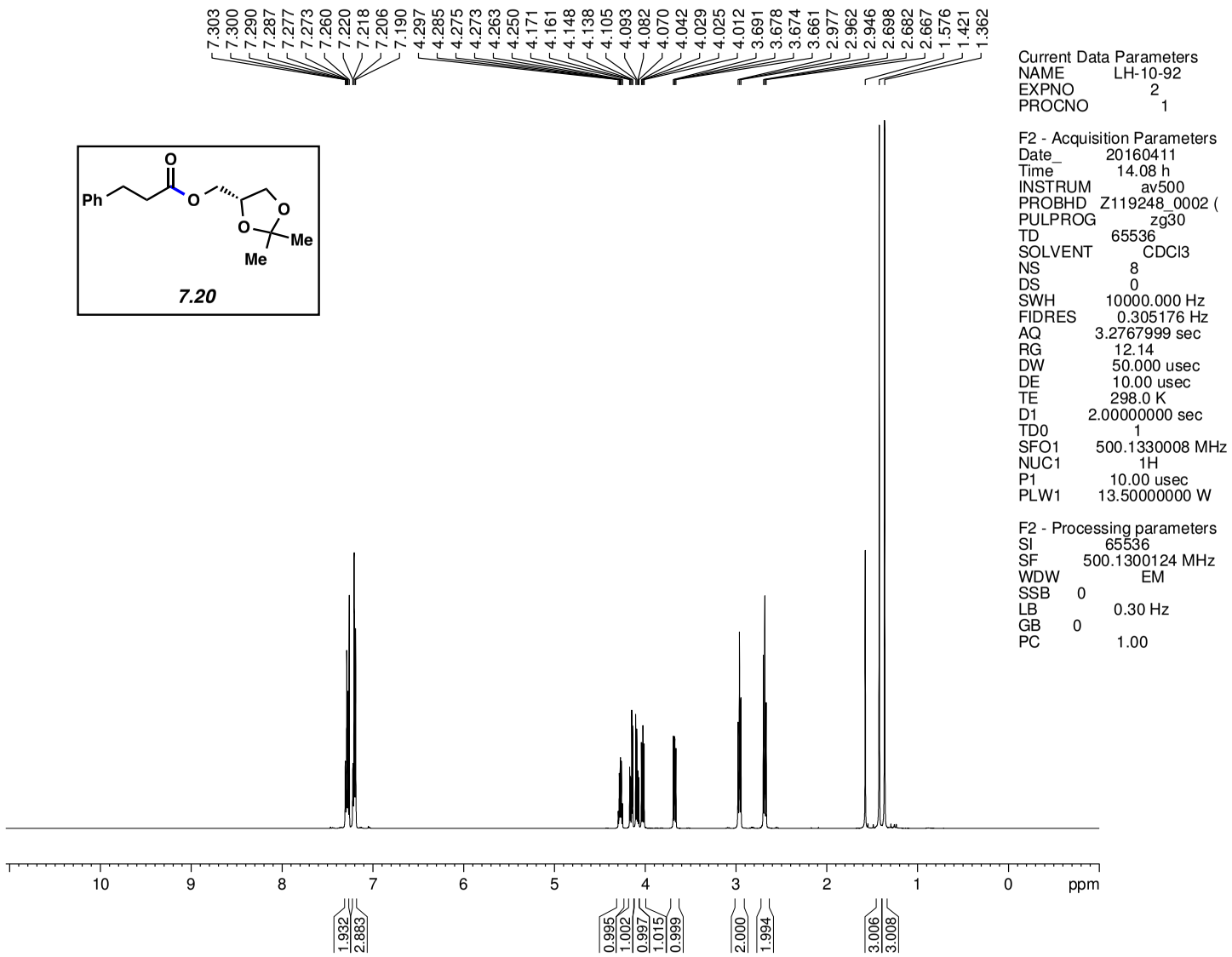

Figure A7.53. ^{1}H NMR (500 MHz, $CDCl_3$) of compound **7.20**

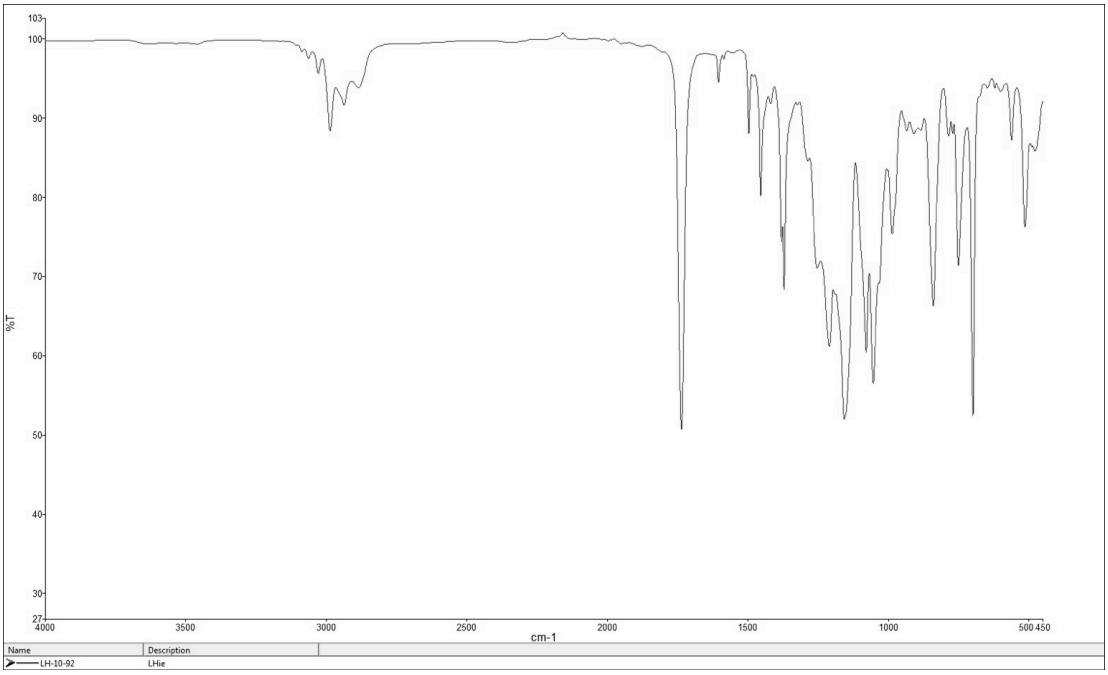

Figure A7.54. Infrared spectrum of compound **7.20**

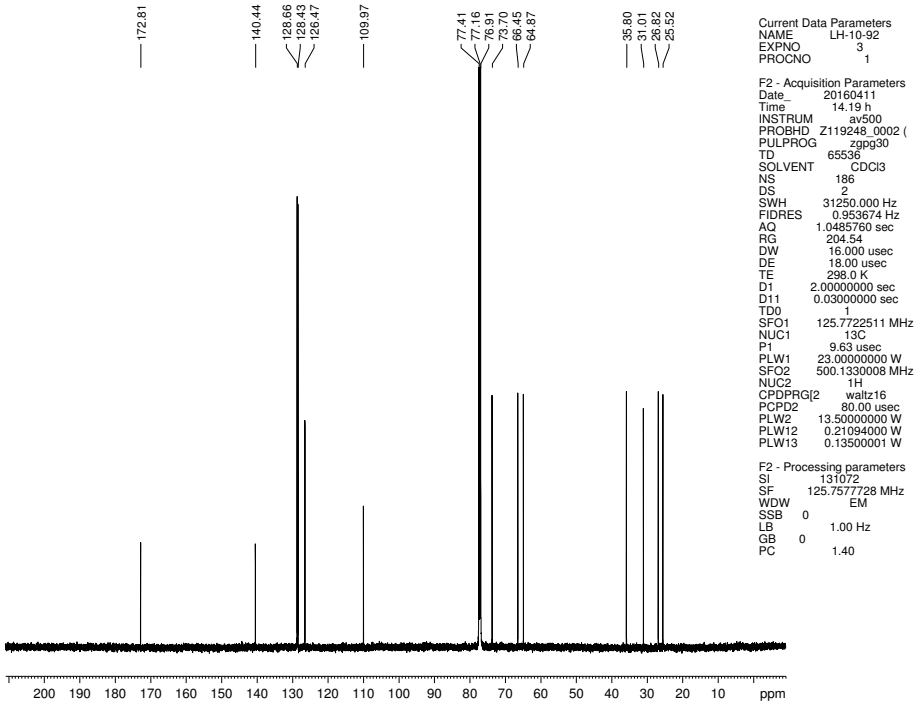

Figure A7.55 ^{13}C NMR (125 MHz, $CDCl_3$) spectrum of compound **7.20**

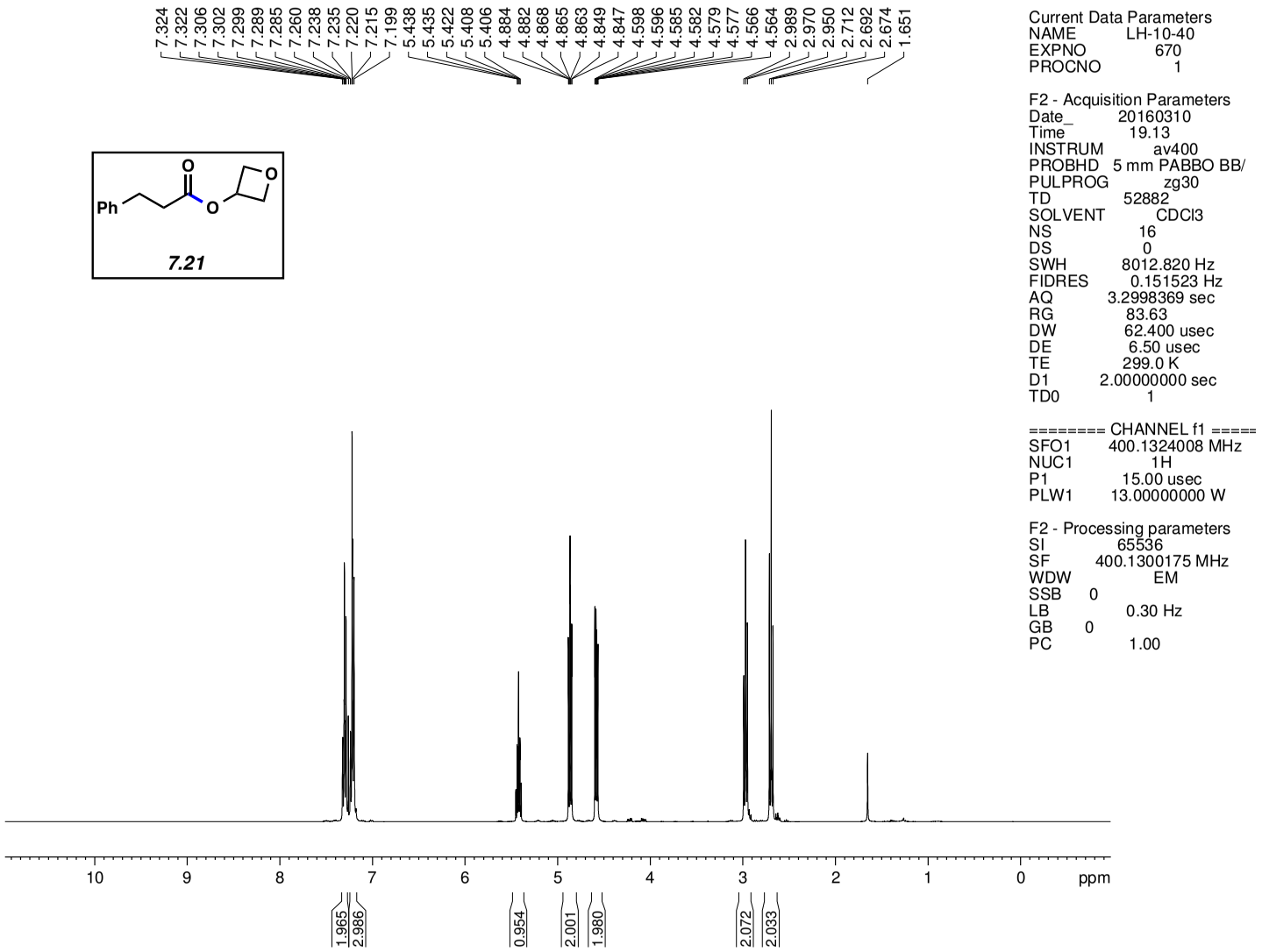

Figure A7.56. ^{1}H NMR (500 MHz, $CDCl_3$) of compound **7.21**

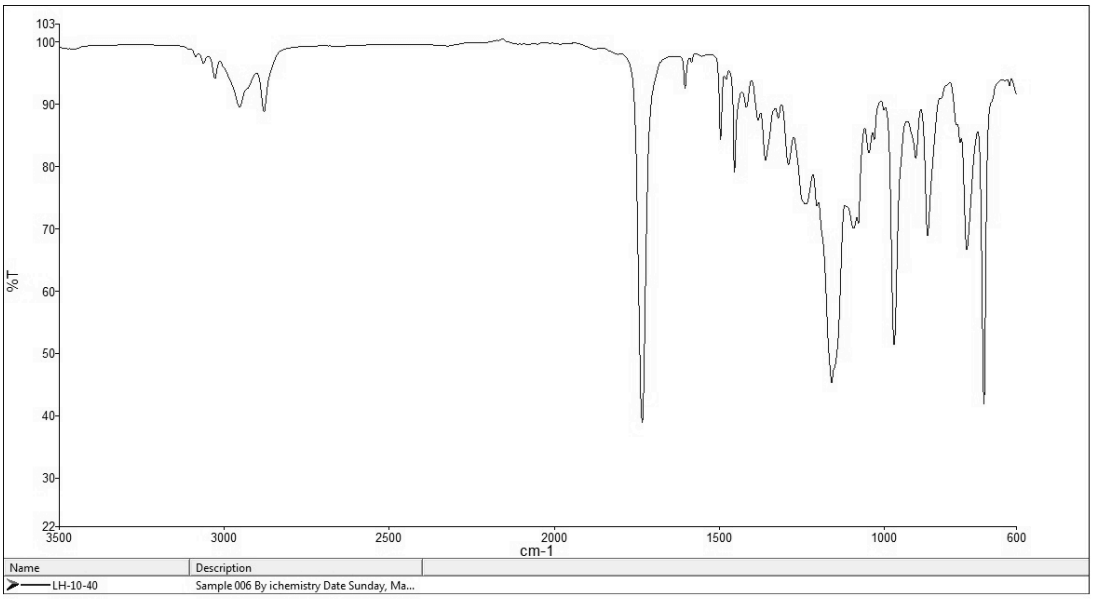

Figure A7.57. Infrared spectrum of compound **7.21**

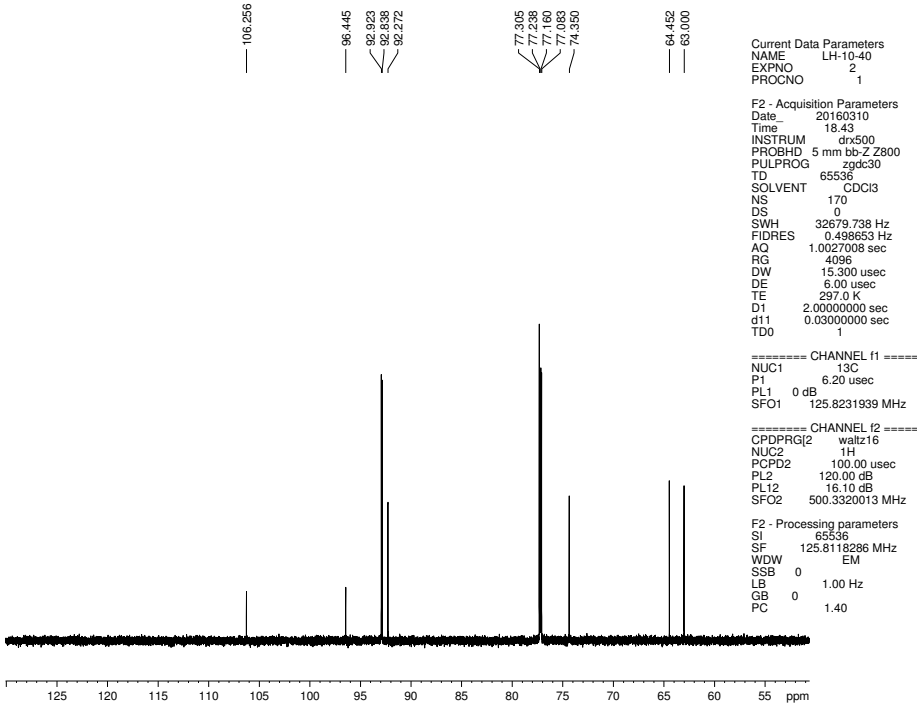

Figure A7.58 ^{13}C NMR (125 MHz, $CDCl_3$) spectrum of compound **7.21**

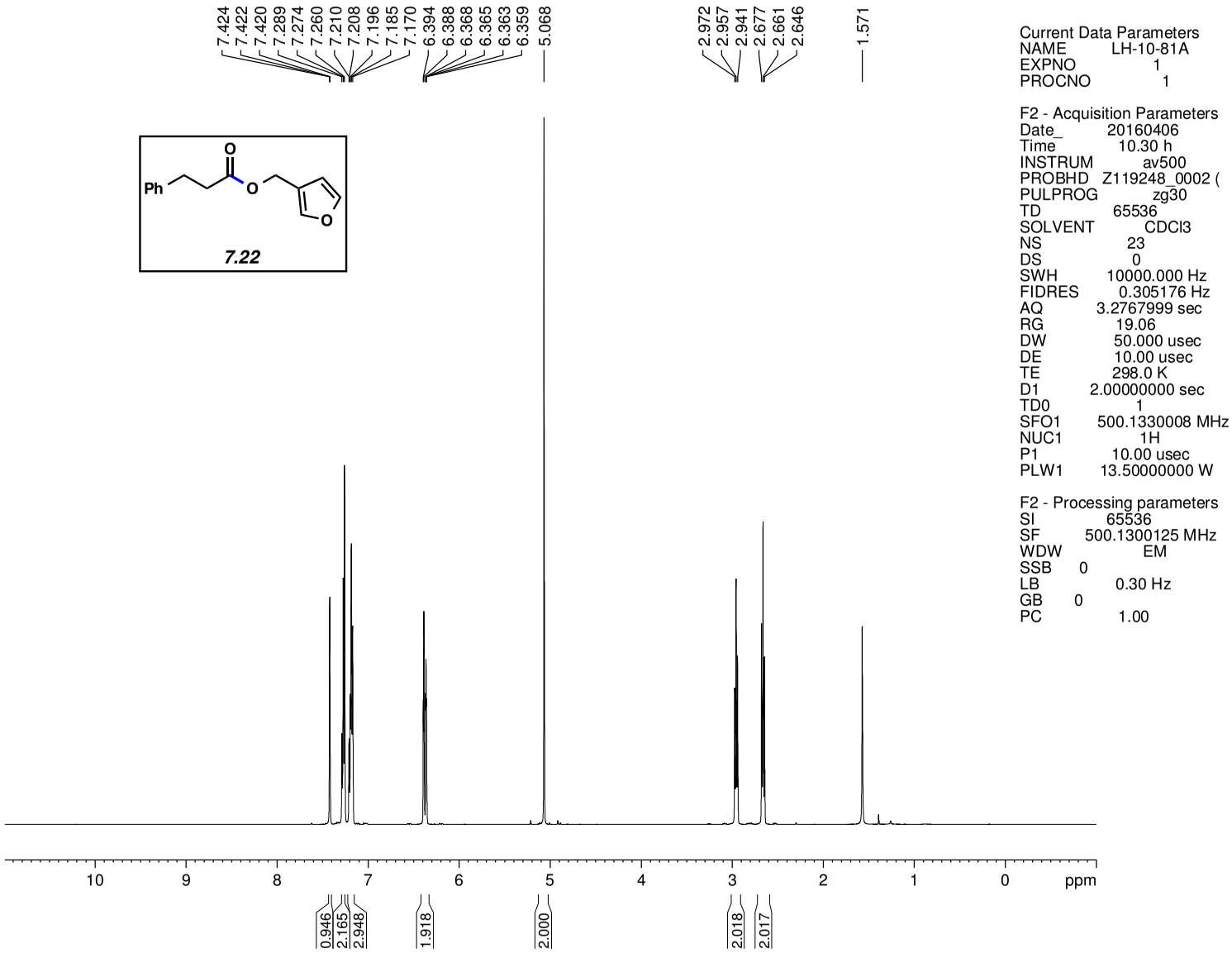

Figure A7.59. ^{1}H NMR (500 MHz, $CDCl_3$) of compound **7.22**

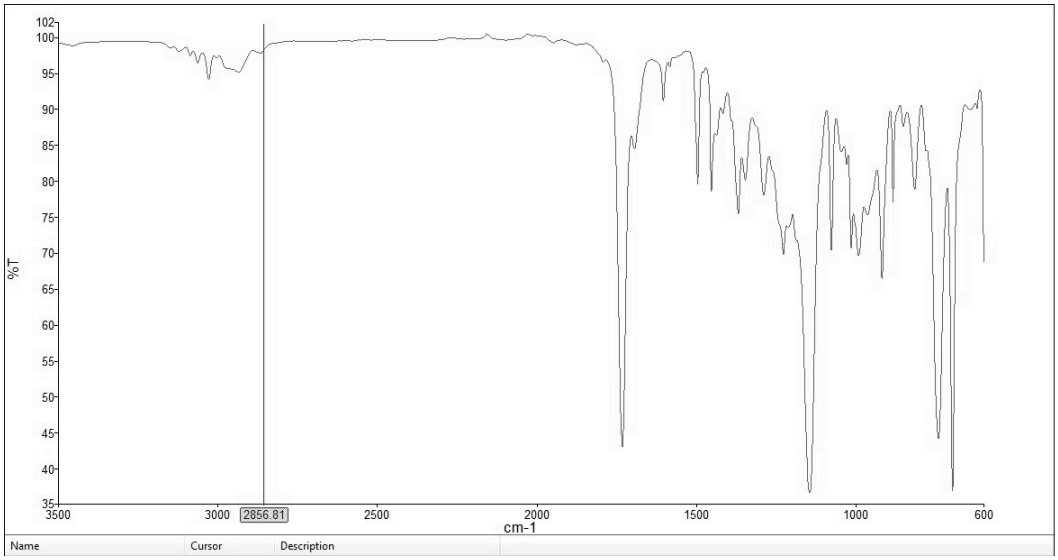

Figure A7.60. Infrared spectrum of compound **7.22**

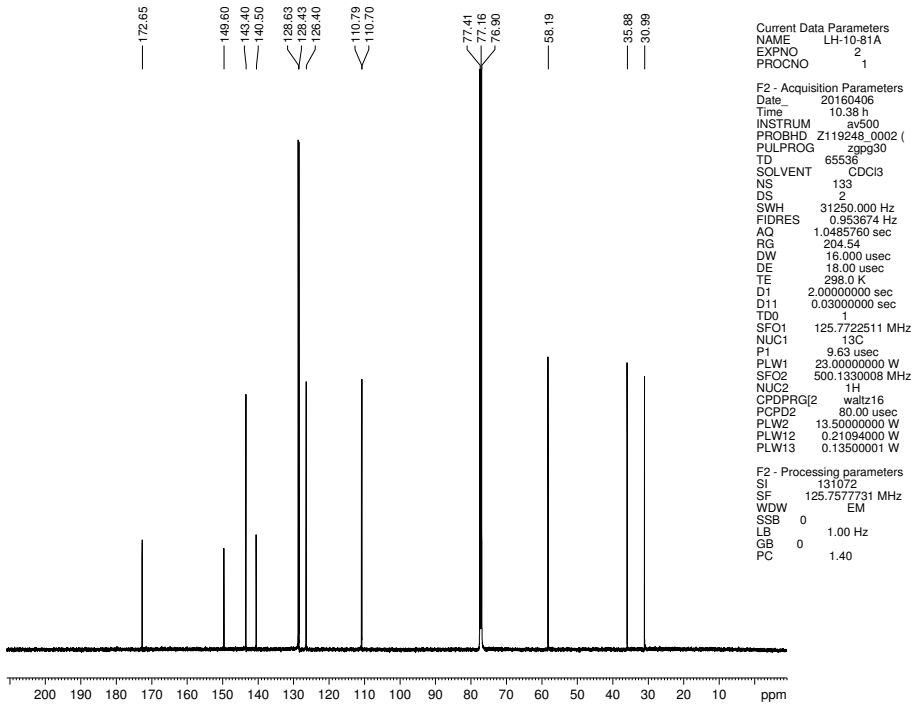

Figure A7.61 ^{13}C NMR (125 MHz, $CDCl_3$) spectrum of compound **7.22**

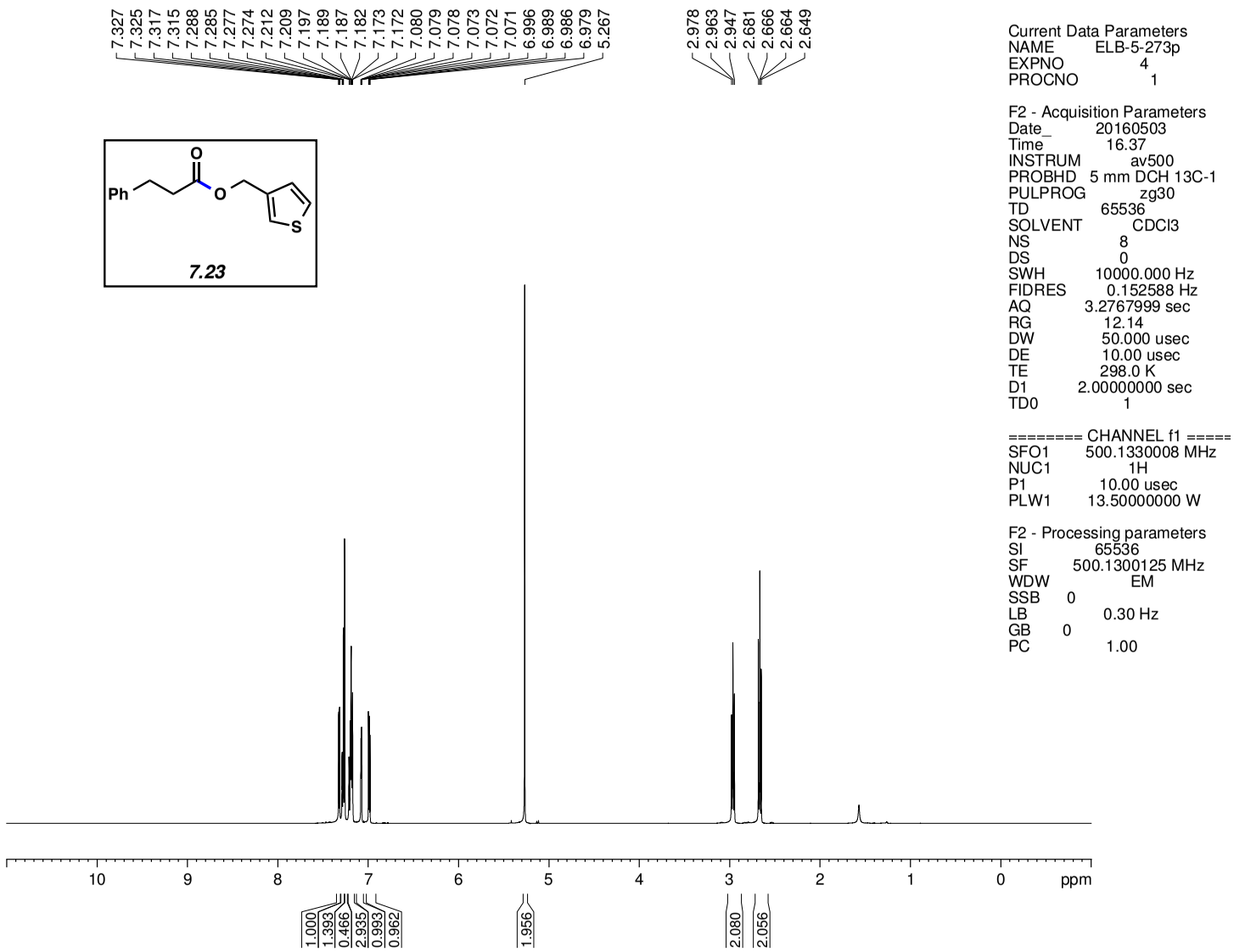

Figure A7.62. ^{1}H NMR (500 MHz, $CDCl_3$) of compound **7.23**

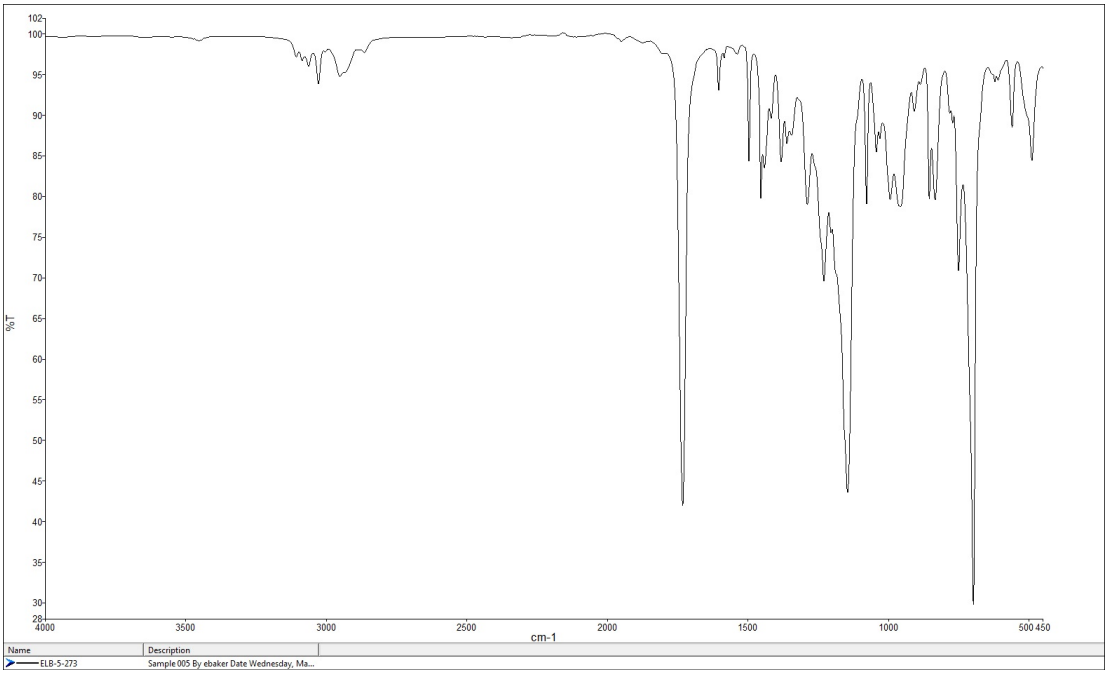

Figure A7.63. Infrared spectrum of compound **7.23**

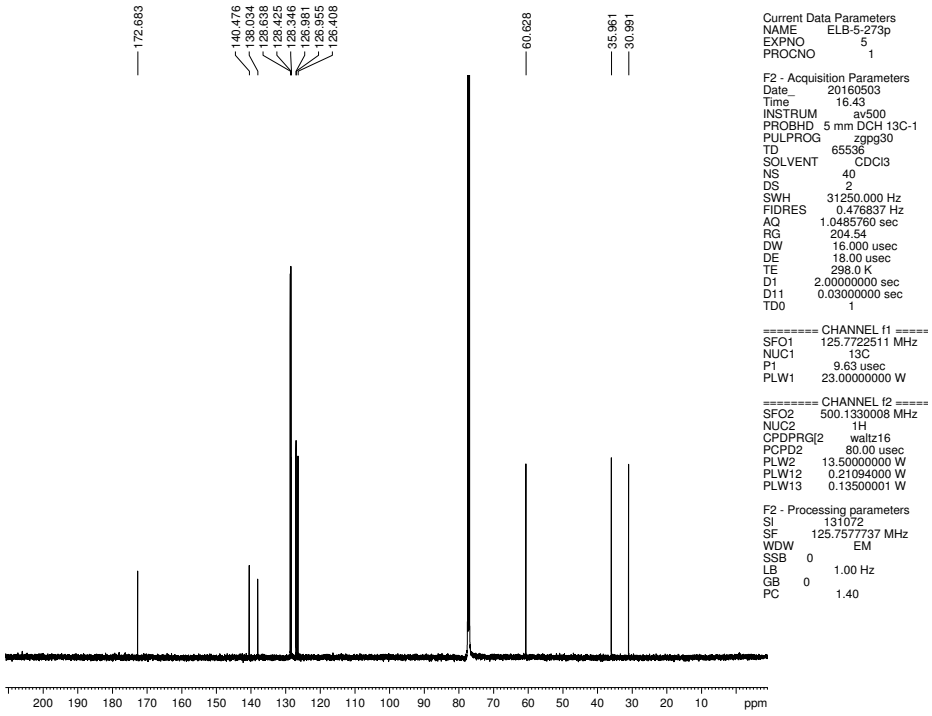

Figure A7.64 ^{13}C NMR (125 MHz, $CDCl_3$) spectrum of compound **7.23**

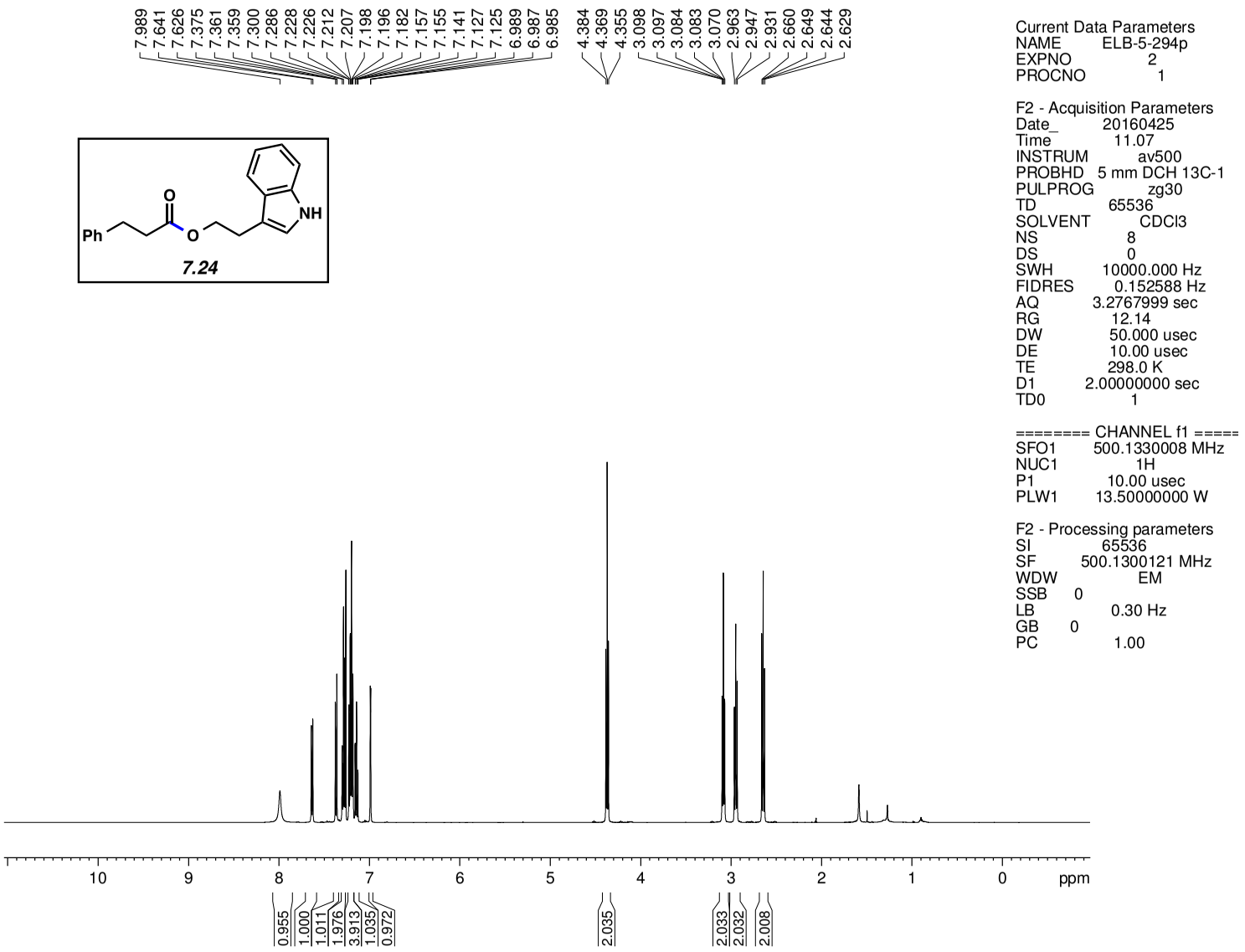

Figure A7.65. ^{1}H NMR (500 MHz, $CDCl_3$) of compound **7.24**

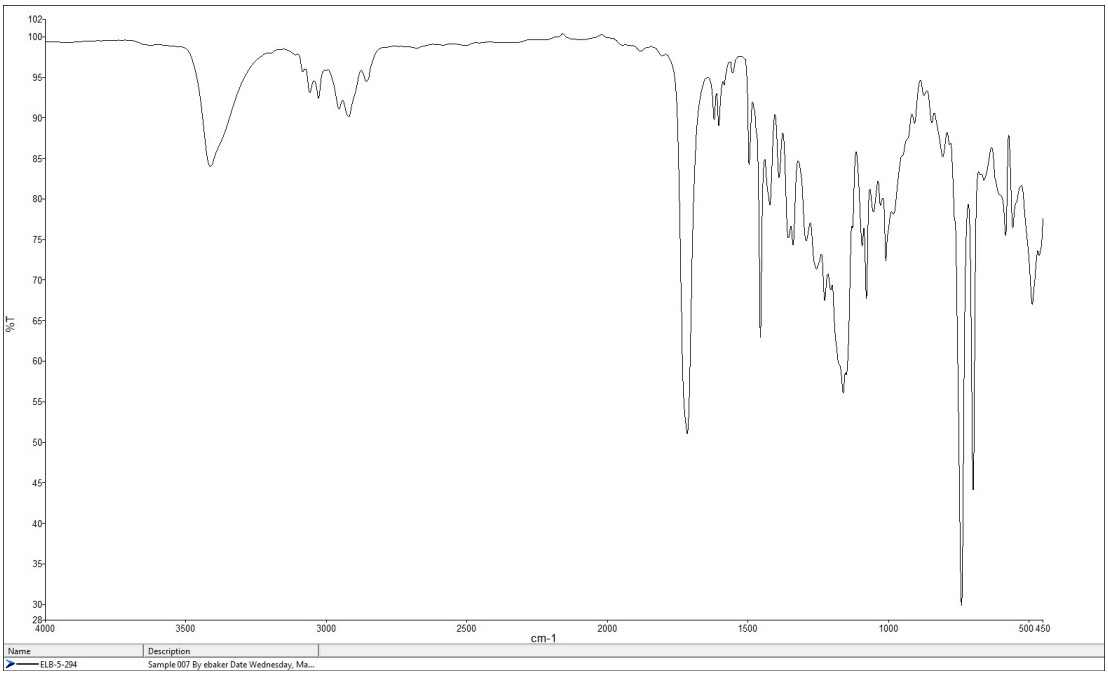

Figure A7.66. Infrared spectrum of compound **7.24**

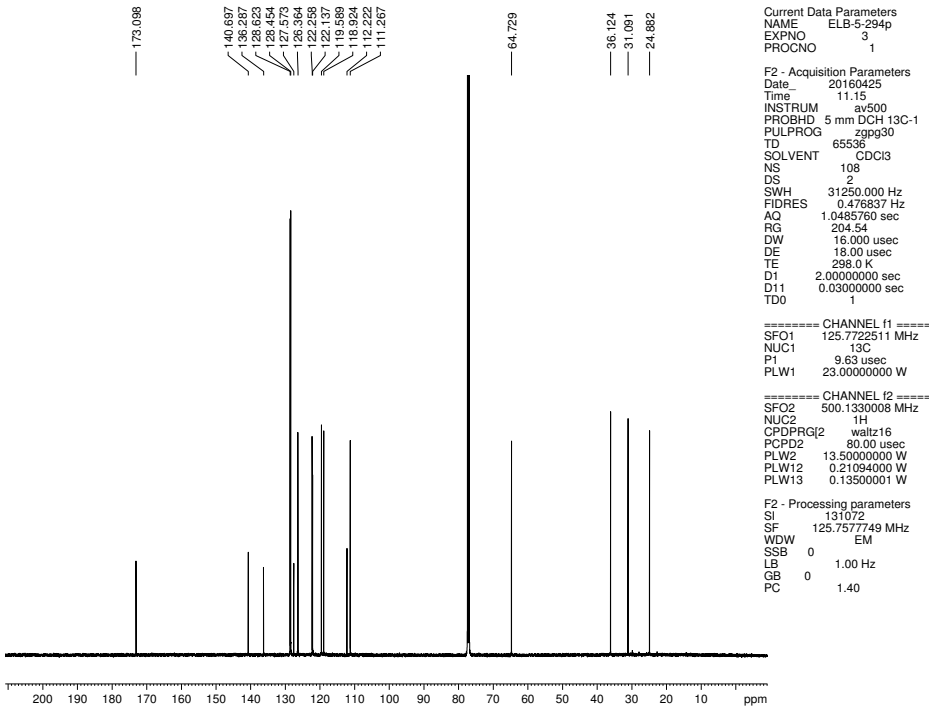

Figure A7.67 ^{13}C NMR (125 MHz, $CDCl_3$) spectrum of compound **7.24**

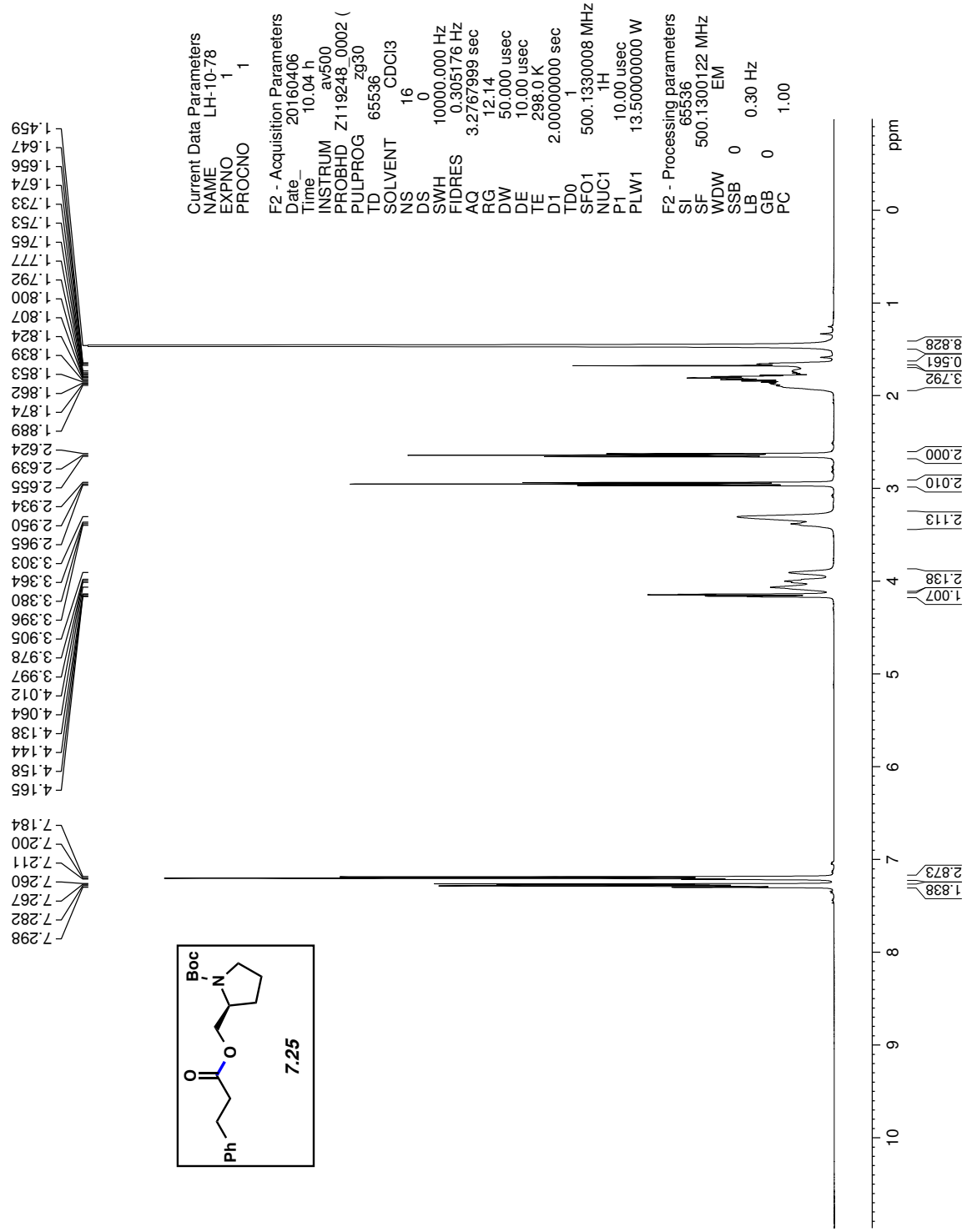

Figure A7.68. ^{1}H NMR (500 MHz, $CDCl_3$) of compound **7.25**

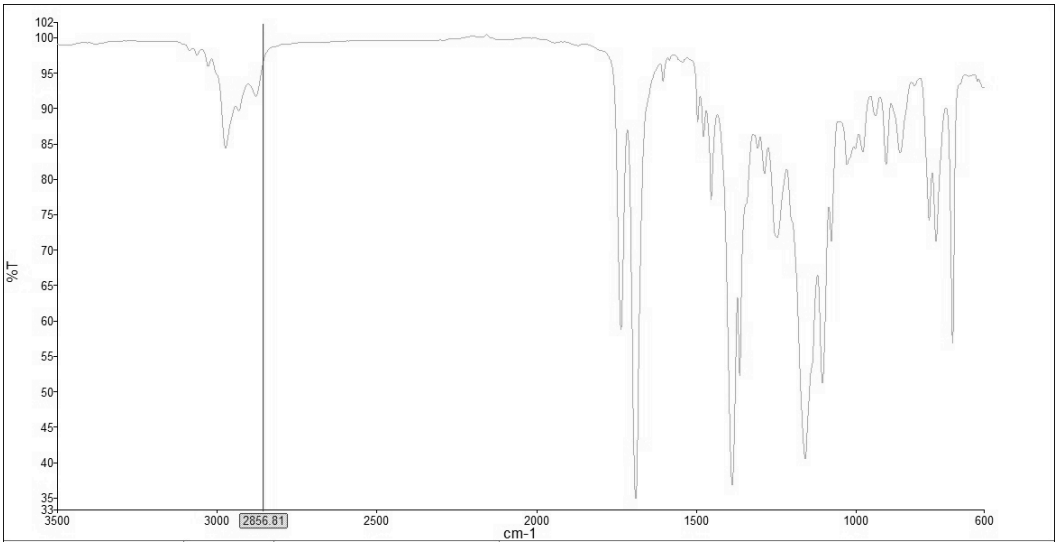

Figure A7.69. Infrared spectrum of compound **7.25**

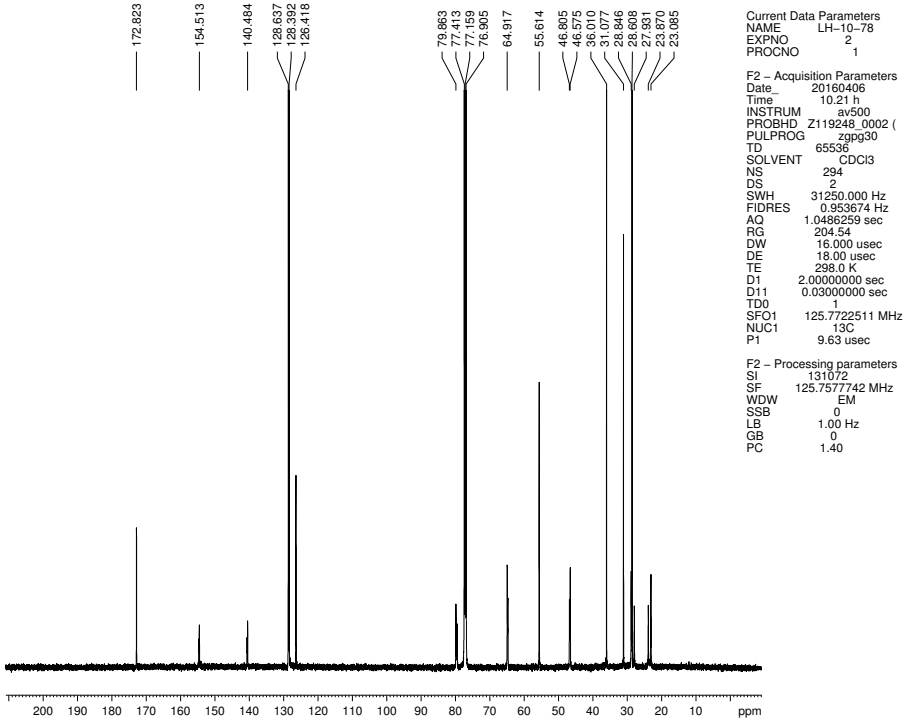

Figure A7.70 ^{13}C NMR (125 MHz, $CDCl_3$) spectrum of compound **7.25**

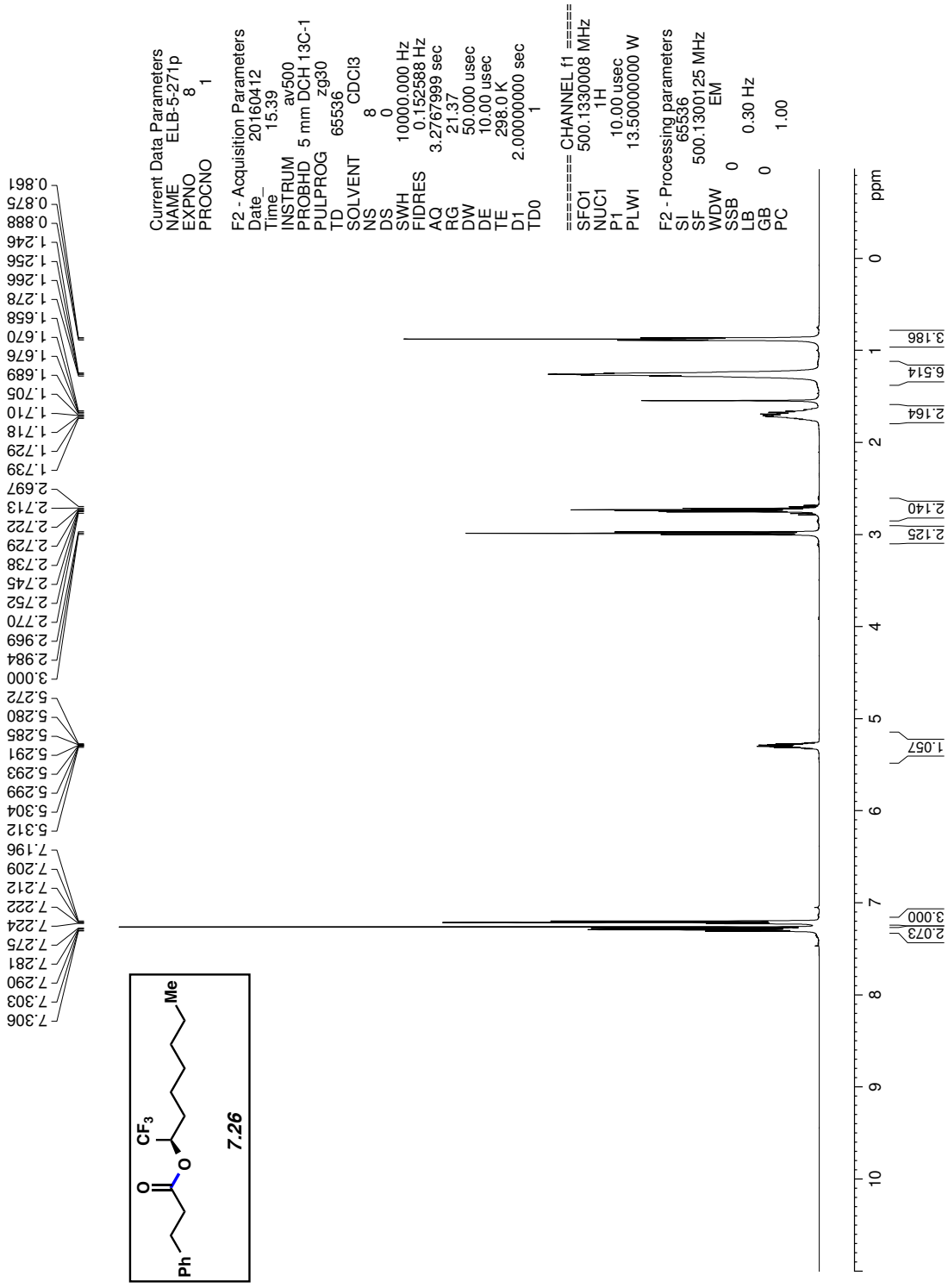

Figure A7.71. ^{1}H NMR (500 MHz, $CDCl_3$) of compound **7.26**

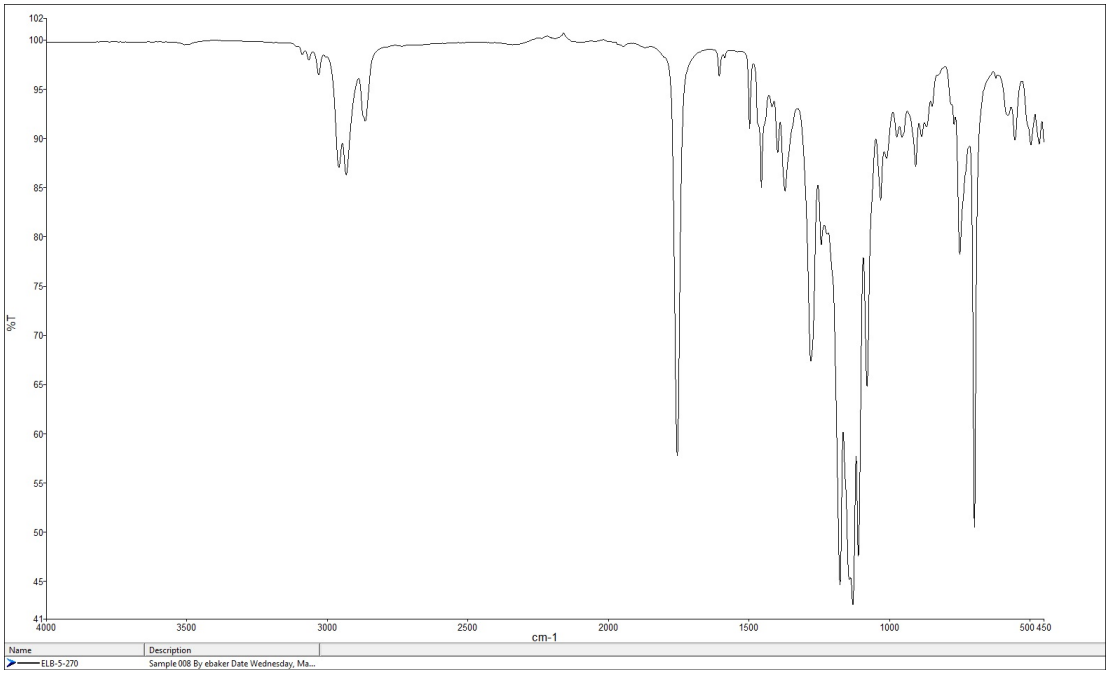

Figure A7.72. Infrared spectrum of compound **7.26**

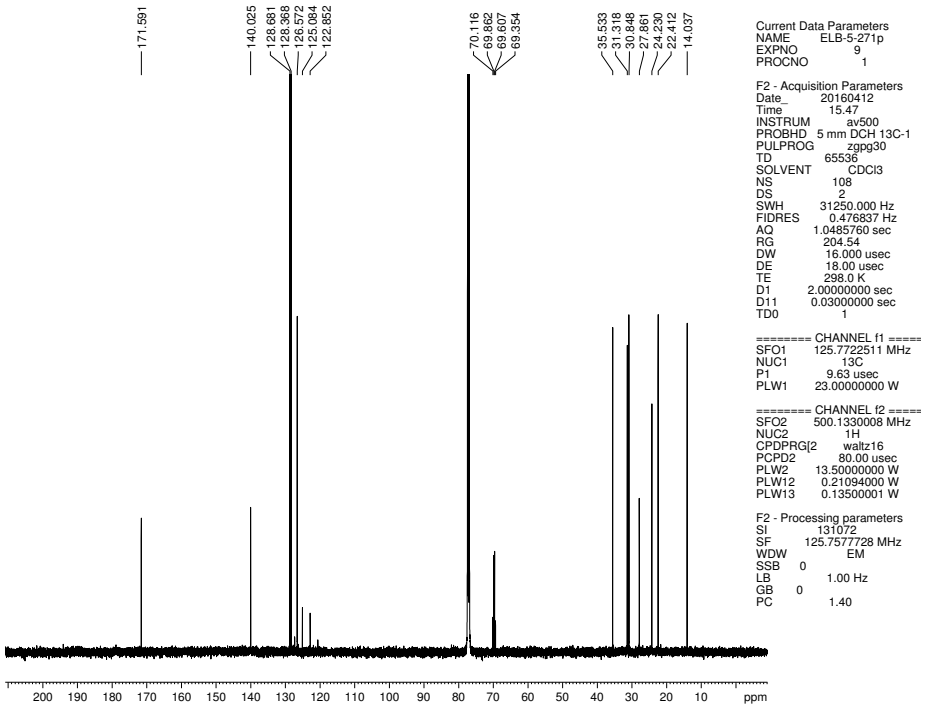

Figure A7.73 ^{13}C NMR (125 MHz, $CDCl_3$) spectrum of compound **7.26**

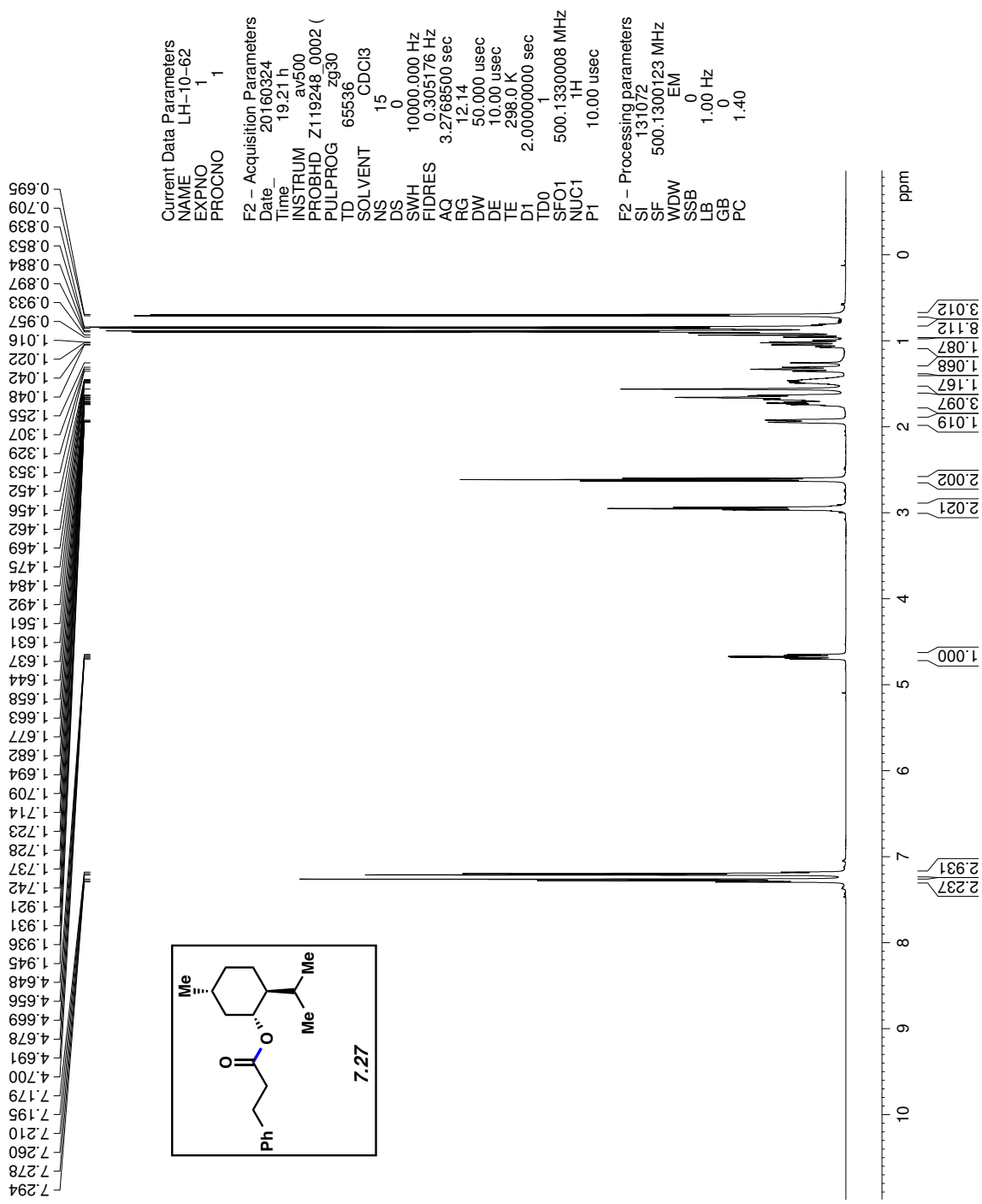

Figure A7.74. ^{1}H NMR (500 MHz, $CDCl_3$) of compound **7.27**

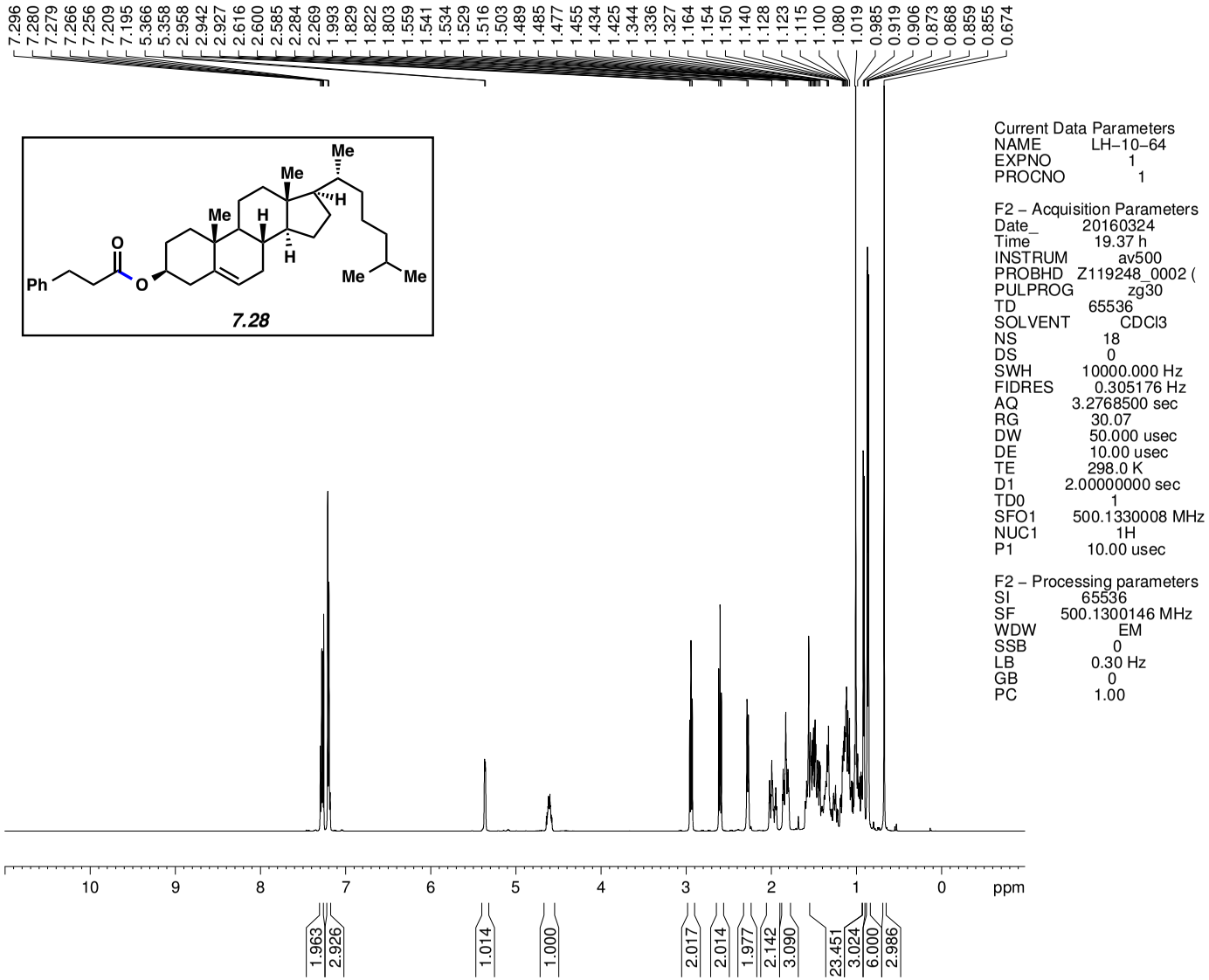

Figure A7.75. ^{1}H NMR (500 MHz, $CDCl_3$) of compound **7.28**

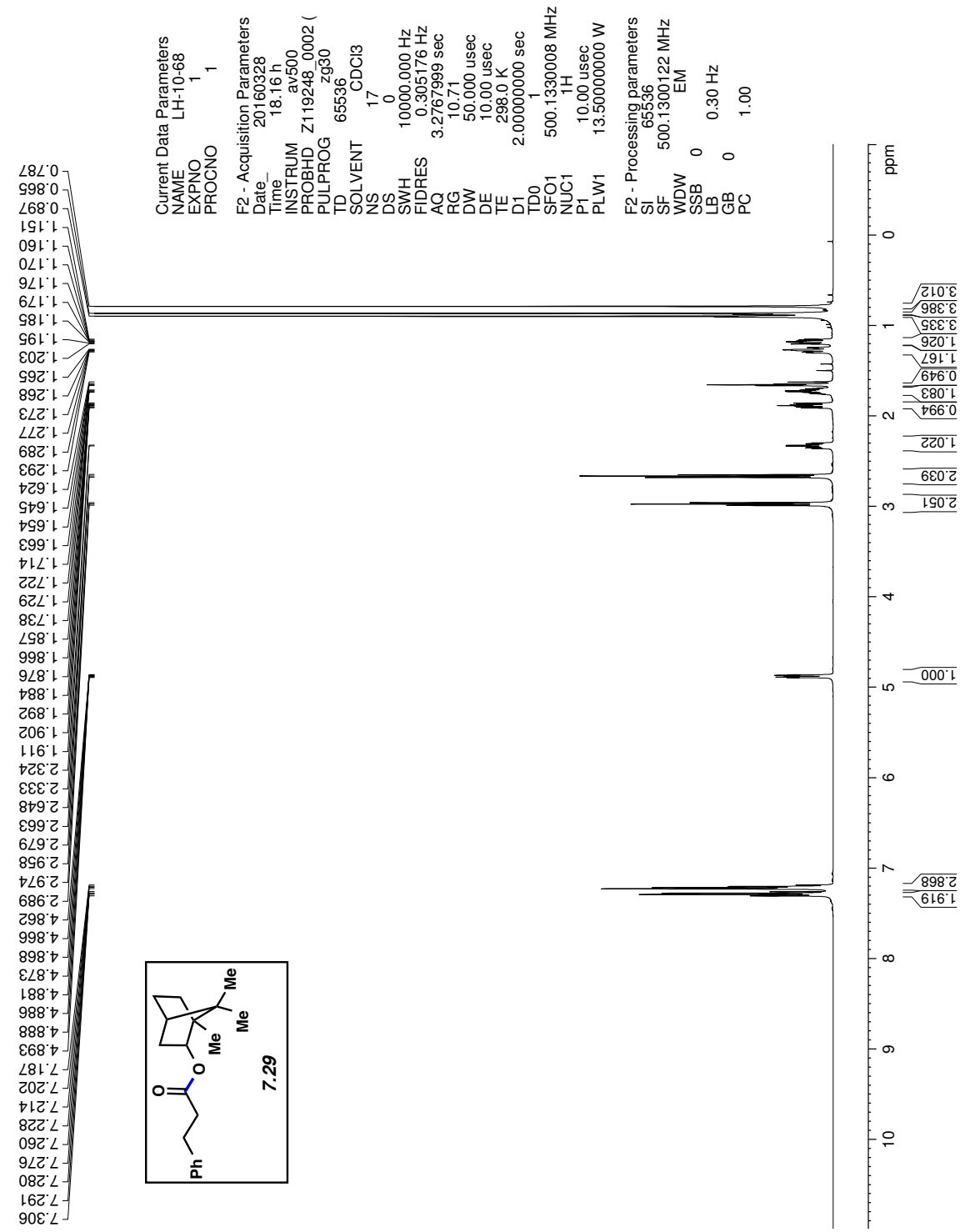

Figure A7.76. ^{1}H NMR (500 MHz, $CDCl_3$) of compound **7.29**

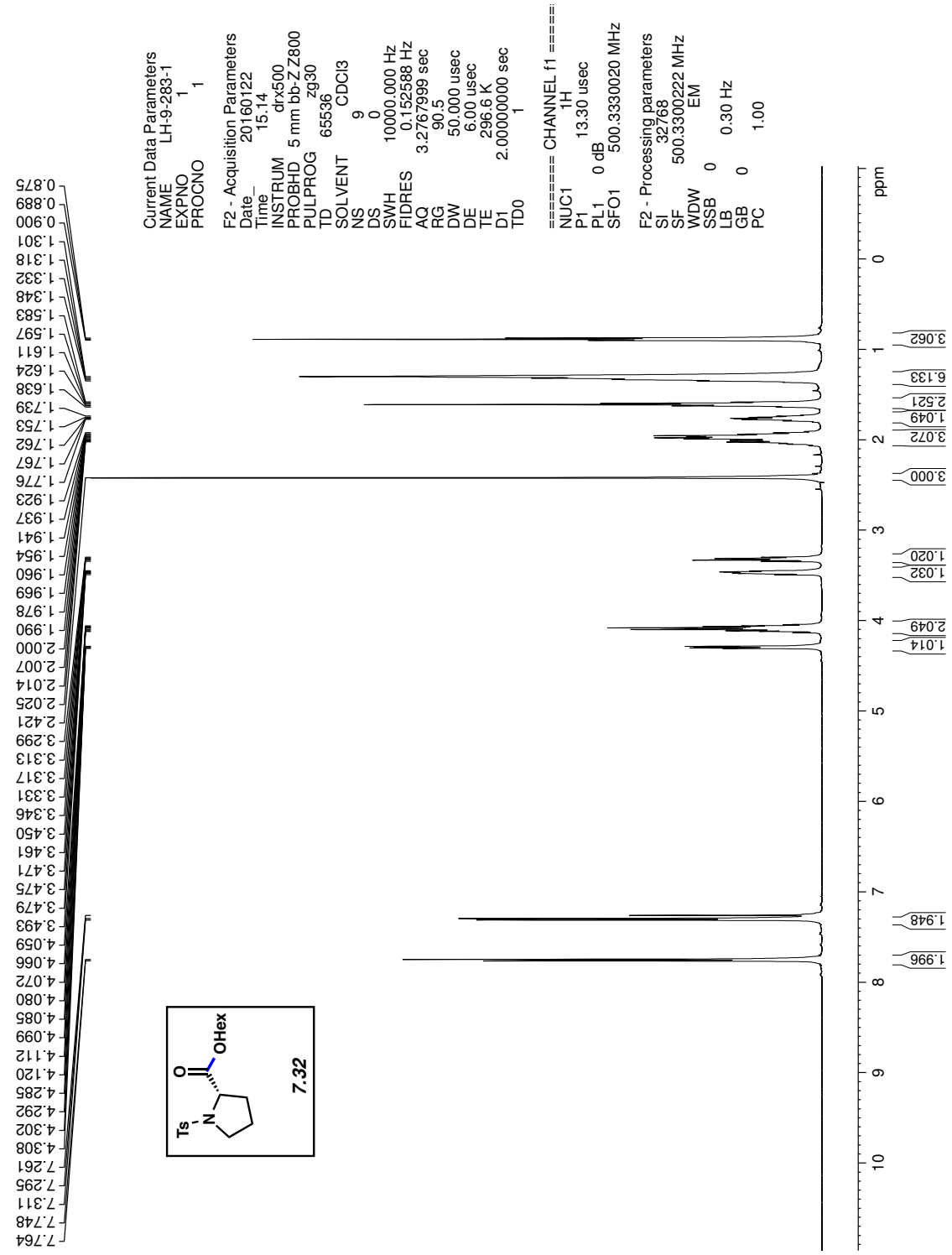

Figure A7.77. ^{1}H NMR (500 MHz, $CDCl_3$) of compound **7.32**

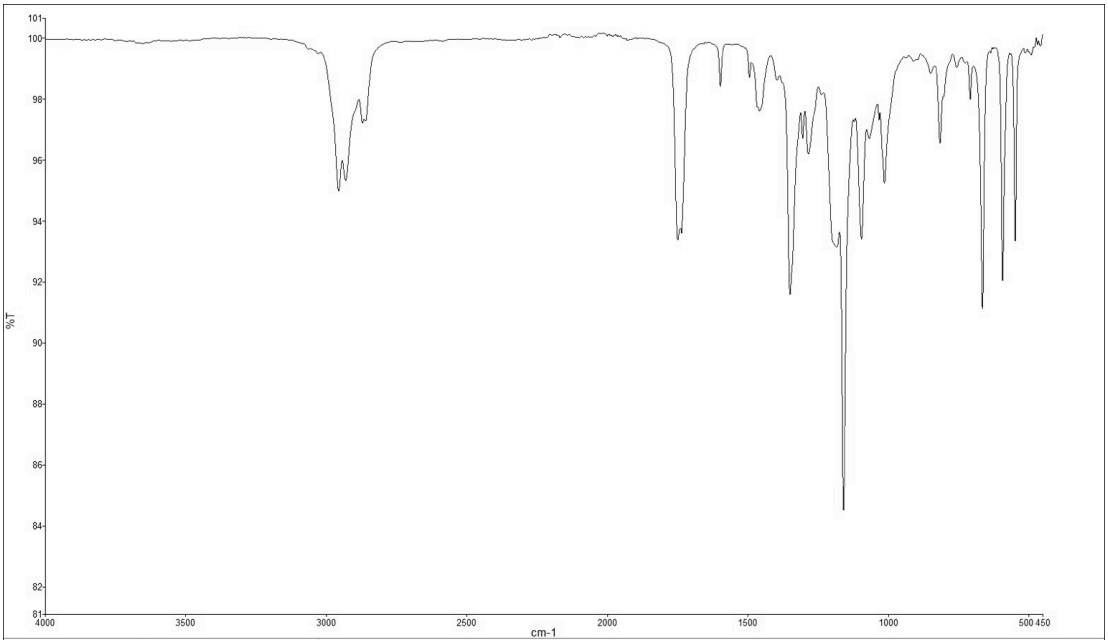

Figure A7.78. Infrared spectrum of compound **7.32**

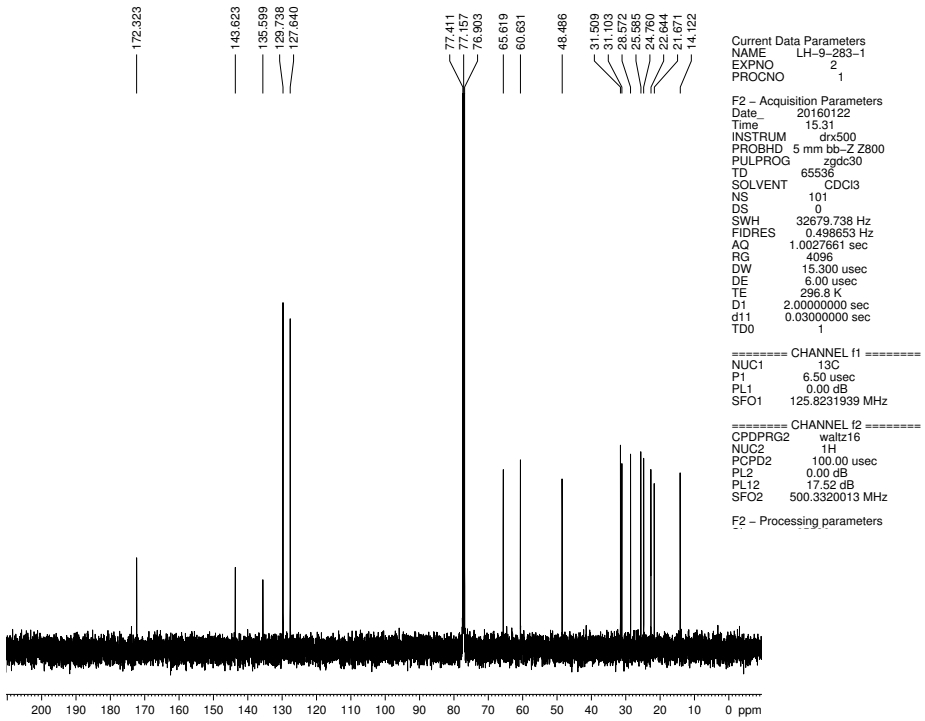

Figure A7.79 ^{13}C NMR (125 MHz, $CDCl_3$) spectrum of compound **7.32**

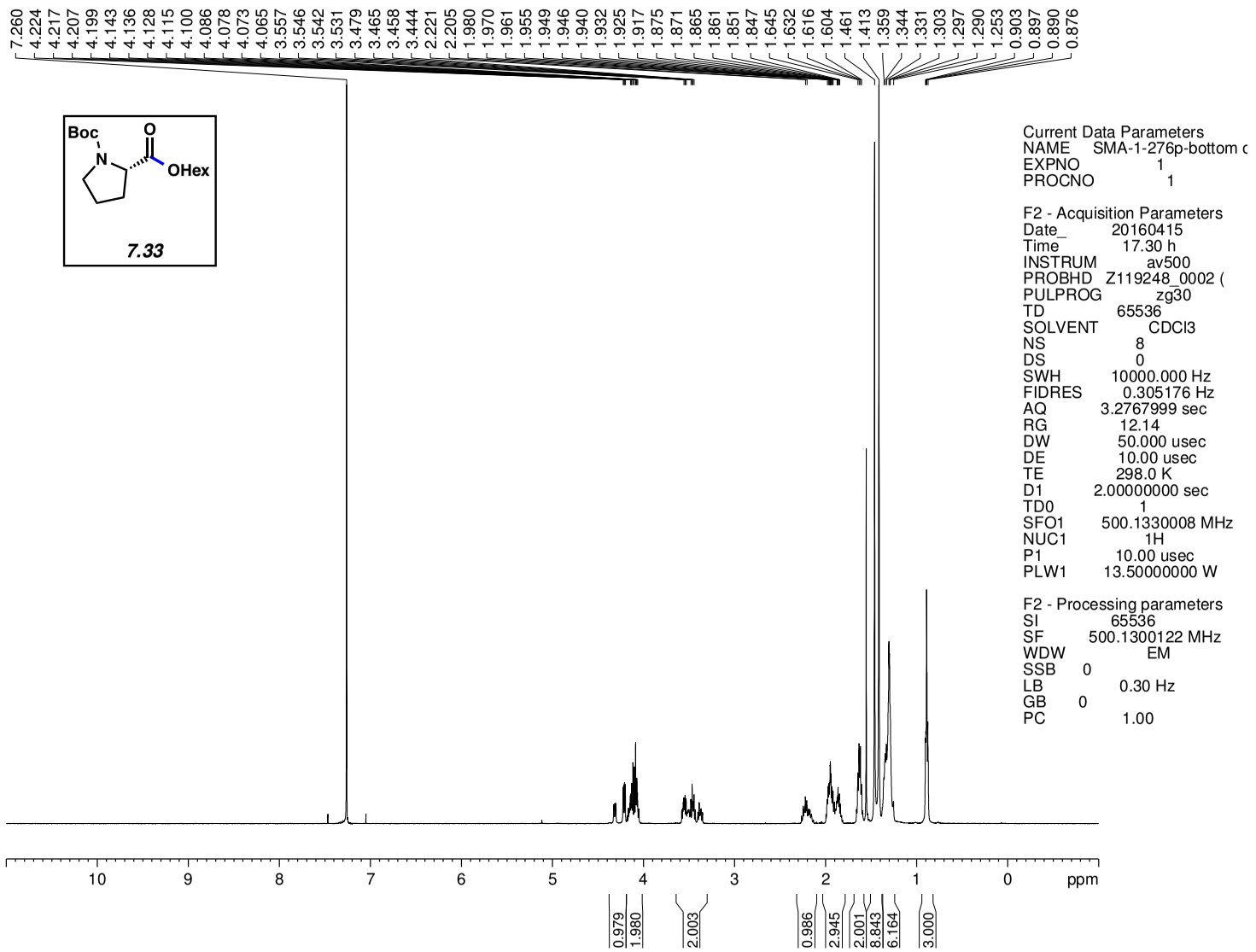

Figure A7.80. ^{1}H NMR (500 MHz, $CDCl_3$) of compound **7.33**

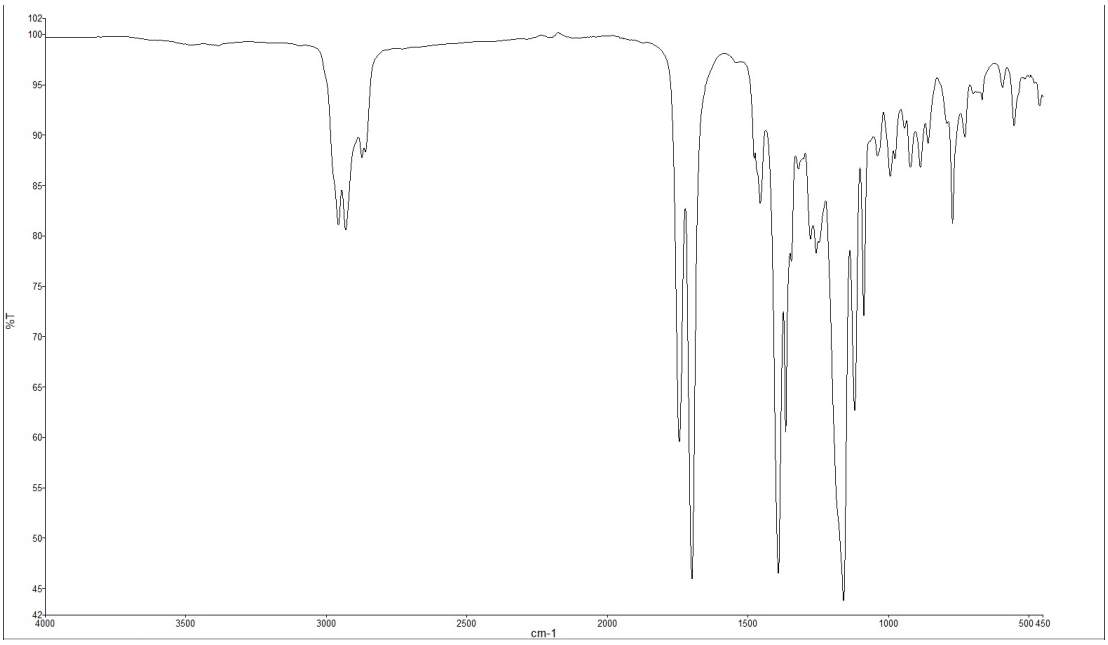

Figure A7.81. Infrared spectrum of compound **7.33**

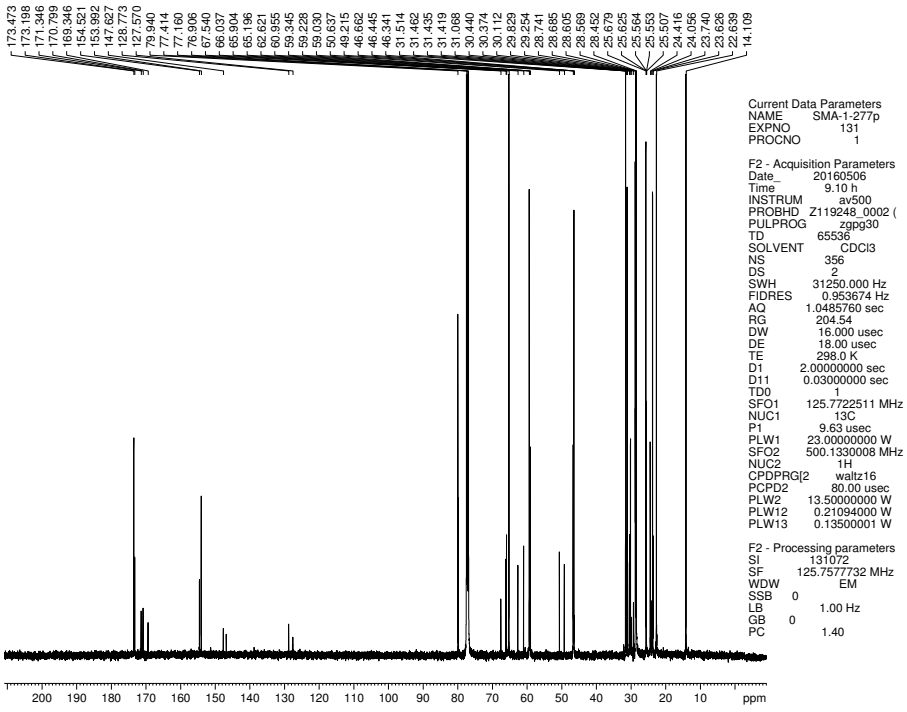

Figure A7.82 ^{13}C NMR (125 MHz, $CDCl_3$) spectrum of compound **7.33**

7.6. Notes and References

[1] Greenberg, A., Breneman, C. M., Liebman, J. F., Eds. *The Amide Linkage: Structural Significance in Chemistry, Biochemistry, and Materials Science*; Wiley-Interscience, 2003.

[2] Amides are considered to be ideally suited for use as synthons in chemical synthesis because of their directing group ability and stability to a variety of reaction conditions. For select recent examples involving amide directing groups in transition metal-catalyzed C–H functionalization methodologies, see: (a) Topczewski, J. J.; Cabrera, P. J.; Saper, N. I.; Sanford, M. S. *Nature* **2016**, *531*, 220–224. (b) He, J.; Jiang, H.; Takise, R.; Zhu, R.-Y.; Chen, G.; Dai, H.-X.; Murali Dhar, T. G.; Shi, J.; Zhang, H.; Cheng, P. T. W.; Yu, J.-Q. *Angew. Chem. Int. Ed*. **2016**, *55*, 785–789. (c) Zhang, X.-G.; Dai, H.-X.; Wasa, M.; Yu, J.-Q. *J. Am. Chem. Soc*. **2012**, *134*, 11948–11951. (d) Shang, R.; Ilies, L.; Nakamura, E. *J. Am. Chem. Soc.* **2015**, *137*, 7660–7663. (e) Matsubara, T.; Ilies, L.; Nakamura, E. *Chem. Asian J*. **2016**, *11*, 380–384. (f) Yokota, A.; Aihara, Y.; Chatani, N. *J. Org. Chem*. **2014**, *79*, 11922–11932. (g) Fruchey, E. R.; Monks, B.M.; Cook, S. P. *J. Am. Chem. Soc*. **2014**, *136*, 13130–13133. (h) Roane, J.; Daugulis, O. *Org. Lett*. **2013**, *15*, 5842–5845. (i) Nishino, M.; Hirano, K.; Satoh, T.; Miura, M. *Angew. Chem. Int. Ed*. **2013**, *52*, 4457–4461.

[3] For select reviews on amides as directing groups in ortho-metalation, see: (a) Whisler, M. C.; MacNeil, S. Snieckus, V.; Beak, P. *Angew. Chem. Int. Ed*. **2004**, *43*, 2206–2225. (b) Snieckus, V. *Chem. Rev*. **1990**, *90*, 879–933. (c) Beak, P.; Snieckus, V. *Acc. Chem. Res*. **1982**, *15*, 306–312.

[4] Pauling, L.; Corey, R. B.; Branson, H. R. *Proc. Natl Acad. Sci. USA* **1951**, *37*, 205–211.

[5] (a) Li, X.; Zou, G. *Chem. Commun.* **2015**, *51*, 5089–5092. (b) Li, X.; Zou, G. *J. Organomet. Chem*. **2015**, *794*, 136–145.

[6] (a) Shi, S.; Meng, G.; Szostak, M. *Angew. Chem. Int. Ed*. **2016**, DOI: 10.1002/anie.201601914. (b) Meng, G.; Szostak, M. *Org. Biomol. Chem*. **2016**, DOI: 10.1039/C6OB00084C. (c) Meng, G.; Szostak, M. *Org. Lett*. **2016**, *18*, 769–799. (d) Meng, G.; Szotak, M. *Angew. Chem. Int. Ed*. **2015**, *54*, 14518–14522. (e) Meng, G.; Szostak, M. *Org. Lett*. **2015**, *17*, 4364–4367.

[7] (a) Simmons, B. J.; Weires, N. A.; Dander, J. E.; Garg, N. K. *ACS Catal*. **2016**, *6*, 3176–3179. (b) Weires, N. A.; Baker, E. L.; Garg, N. K. *Nat*. *Chem*. **2016**, *8*, 75–79. (c) Hie, L.; Fine Nathel, N. F.; Shah, T.; Baker, E. L.; Hong, X.; Yang, Y.-F.; Liu, P.; Houk, K. N.; Garg, N. K. *Nature* **2015**, *524*, 79–83. (d) Baker, E. L.; Yamano, M. M.; Zhou, S.; Anthony, S. M.; Garg, N. K. *Nat. Comun*. **2016**, *in press*.

[8] Nickel catalysis is considered to be attractive because nickel is less expensive, more abundant, and displays a smaller CO_2 footprint, compared to its precious metal counterpart, palladium. For pertinent reviews, see: (a) Rosen, B. M.; Quasdorf, K. W.; Wilson, D. A.; Zhang, N.; Resmerita, A.-M.; Garg, N. K.; Percec, V. *Chem. Rev*. **2011**, *111*, 1346−1416. (b) Tasker, S. Z.; Standley, E. A.; Jamison, T. F. *Nature* **2014**, *509*, 299−309. (c) Mesganaw, T.; Garg, N. K. *Org. Process Res. Dev.* **2013**, *17*, 29−39. (d) Ananikov, V. P. *ACS Catal*. **2015**, *5*, 1964−1971.

[9] The conversion of amides to esters typically requires harshly acidic or basic reaction conditions. For Keck's mild, albeit limited, approach for converting amides to methyl esters, see: Keck, G. E.; McLaws, M. D.; Wager, T. T. *Tetrahedron* **2000**, *56*, 9875–9883.

[10] The use of mono(oxazolines), bis(oxazolines), pyridinebis(oxazolines), *N*-heterocyclic carbenes, *N*-heterocyclic bis(carbenes), mono- and bidentate phosphines, Buchwald-type phosphines, BI-DIME type, and BI-BOP type ligands led either to no reaction or very low conversions.

[11] Heating beyond 100 °C led to diminished yields, whereas increased reaction times led to minimal change in conversion.

[12] Coupling of *t*-butanol with **7.15** under the standard reaction conditions did not lead to product formation.

[13] Guo, L.; Ma, X.; Fang, H.; Jia, X.; Huang, Z. *Angew. Chem. Int. Ed*. **2015**, *54*, 4023–4027.

[14] Henry, C.; Bolien, D.; Ibanescu, B.; Bloodworth, S.; Harrowven, D. C.; Zhang, X.; Craven, A.; Sneddon, H. F.; Whitby, R. J. *Eur. J. Org. Chem*. **2015**, 1491–1499.

[15] Liu, C.; Tang, S.; Zheng, L.; Liu, D.; Zhang, H.; Lei, A. *Angew*. *Chem*. *Int*. *Ed*. **2012**, *51*, 5662–5666.

[16] Won, J.-E.; Kim, H.-K.; Kim, J.-J.; Yim, H.-S.; Kim, M.-J.; Kang, S.-B.; Chung, H.-A.; Lee, S.-G.; Yoon, Y.-J. *Tetrahedron* **2007**, *63*, 12720–12730.

[17] Chakraborti, A. K.; Singh, B.; Chankeshwara, S. V.; Patel, A. R. *J. Org. Chem*. **2009**, *74*, 5967–5974.

[18] Shiina, I.; Kubota, M.; Oshiumi, H.; Hashizume, M. *J. Org. Chem*. **2004**, *69*, 1822–1830.

[19] Glaser, J.; Schultheis, M.; Hazra, B.; Moll, H.; Schurigt, U.; Holzgrabe, U. *Molecules* **2014**, *19*, 1394–1410.